THE GENESIS OF NATROCARBONATITES: CONSTRAINTS FROM EXPERIMENTAL PETROLOGY AND TRACE ELEMENT PARTITIONING

CAROLINE MARIE PETIBON

INFORMATION TO USERS

This manuscript has been reproduced from the microfilm master. UMI films the text directly from the original or copy submitted. Thus, some thesis and dissertation copies are in typewriter face, while others may be from any type of computer printer.

The quality of this reproduction is dependent upon the quality of the copy submitted. Broken or indistinct print, colored or poor quality illustrations and photographs, print bleedthrough, substandard margins, and improper alignment can adversely affect reproduction.

In the unlikely event that the author did not send UMI a complete manuscript and there are missing pages, these will be noted. Also, if unauthorized copyright material had to be removed, a note will indicate the deletion.

Oversize materials (e.g., maps, drawings, charts) are reproduced by sectioning the original, beginning at the upper left-hand corner and continuing from left to right in equal sections with small overlaps.

Photographs included in the original manuscript have been reproduced xerographically in this copy. Higher quality 6" x 9" black and white photographic prints are available for any photographs or illustrations appearing in this copy for an additional charge. Contact UMI directly to order.

Bell & Howell Information and Learning
300 North Zeeb Road, Ann Arbor, MI 48106-1346 USA
800-521-0600

UMI®

THE GENESIS OF NATROCARBONATITES: CONSTRAINTS FROM EXPERIMENTAL PETROLOGY AND TRACE ELEMENT PARTITIONING

by

© Caroline Marie Petibon
Memorial University of Newfoundland

A thesis submitted to the
School of Graduate Studies
in partial fulfilment of the
requirements for the degree of Ph.D. of Science

Department of Earth Sciences
Memorial University of Newfoundland

November 1999

St John's Newfoundland

ABSTRACT

Carbonatites have been widely studied because of their unusual composition and as a key to understanding the geochemical evolution of the mantle. Natrocarbonatites from Oldoinyo Lengai (Tanzania) received special attention because this is the only active carbonatite volcano. Although carbonatites from Oldoinyo Lengai are exceptionally sodic compared to others, many authors have tried to include these lavas in a broader framework of carbonatite petrogenesis which explains the majority of carbonatites.

Various aspects of the petrogenesis of natrocarbonatites from Oldoinyo Lengai have been previously studied. However, previous experimental studies provided little trace element partitioning data between silicate and carbonate liquids at conditions suitable for a comparison with the natural lavas. Moreover, no study has been done on the crystallisation of natrocarbonatites once exsolved.

The aim of this study was two-fold. The first part was to demonstrate that silicate-bearing natrocarbonatites fractionate to silicate-free natrocarbonatites. The second part focussed on how liquid immiscibility produces silicate-bearing, not silicate-free, natrocarbonatites, and on constraining the conditions of liquid immiscibility between silicate-bearing natrocarbonatite and conjugate wollastonite nephelinite.

The experiments were prepared using natural lavas as starting materials. The comparison between phase assemblages, and major and trace element data on natural lavas and on experimental run products was used to constrain the conditions of formation of the natural lavas. The fractionation of the silicate-bearing natrocarbonatite to produce silicate-free natrocarbonatite was studied using experiments at 100 and 20 MPa, 550-900 °C. Results showed that silicate-free natrocarbonatites could be the product of *in situ* crystallisation of silicate-bearing natrocarbonatites at ~ 20 MPa, 600 °C. Liquid immiscibility between silicate-bearing natrocarbonatites and wollastonite nephelinites was studied using experiments prepared with different mixtures of natrocarbonatite and nephelinite at 20-200 MPa, 700-900 °C. Silicate-bearing natrocarbonatites were suggested to exsolve from wollastonite nephelinite at ~ 100 MPa, 750 °C.

The degree of polymerisation of the silicate melt is important in describing the liquid immiscibility process. Therefore, major and trace element partitioning between immiscible liquids was discussed as a function of the structure of the silicate liquid. However, it was shown that the formation of carbonato- and halogen-complexes in both liquids makes the determination of the role of each liquid difficult.

Natrocarbonatites or their parental magma (melilite nephelinite) are more likely not to reach the surface than calciocarbonatites or their parental magma (olivine nephelinite). Consequently, they must be widespread in the lithospheric mantle as efficient metasomatic agents.

ACKNOWLEDGEMENTS

I would like to thank Drs. G.A. Jenner and B.A. Kjarsgaard for suggesting and supervising this project, and Dr. Mark Wilson for advice. I would also like to thank Drs. Simon Jackson, Henry Longerich, Lance Forsythe and Ingo Horn who introduced me to the LAM-ICP-MS laboratory, with special thanks to Dr. Lance Forsythe who spent a lot of time teaching me about electron microprobe, LAM-ICP-MS and experimental petrology at the beginning of my Ph.D. Thanks also go to Drs. Gabor Dobosi and Tony Peterson for the useful discussions. Thanks to the members of staff at Memorial University and at the Geological Survey (Ottawa). Thank you to Drs. Tony Peterson and Keith Bell for providing the samples.

I would like to thank Bruce and Ingrid Kjarsgaard, Kate MacLachlan, Tony Peterson, Sue Roddick for providing me accomodation in Ottawa.

Financial support for this thesis came from: NSERC Operating Grant to Dr. G.A. Jenner; an NSERC-IOR grant jointly with VG; a Memorial University scholarship; and the Geological Survey of Canada for experimental studies.

TABLE OF CONTENTS

LIST OF TABLES

LIST OF FIGURES

LIST OF ABBREVIATIONS AND SYMBOLS

Ne: nepheline.
Cpx: clinopyroxene.
Mela: melanite garnet (Gt).
Wo: wollastonite.
Meli: melilite.
NY: nyerereite; $(Na, K)_2Ca(CO_3)_2$, with substitution of Ca by Sr and Na, and of $(CO_3)^{2-}$ by $(SO_4)^{2-}$, $(PO_4)^{3-}$, F^- and Cl^- (Keller and Krafft, 1990; Dawson et al., 1995b).
GRE: gregoryite; $(Na_{0.78}K_{0.05})_2Ca_{0.17}(CO_3)$, with substitution of Ca by Sr and Na, and of $(CO_3)^{2-}$ by $(SO_4)^{2-}$, $(PO_4)^{3-}$, F^- and Cl^- (Keller and Krafft, 1990; Dawson et al., 1995b).
Ks: kalsilite.
Qz: quartz.
Ne: nepheline component.
SEM: Scanning electron microscope
EMP: Electron microprobe
EDS: energy dispersive spectrometry
WDS: wavelength dispersive spectrometry
LAM-ICP-MS: laser ablation microprobe – inductively coupled plasma – mass spectrometry
GSC: Geological Survey of Canada
cps: counts per second
PM: primitive mantle
NaG: sodium-rich gregoryite
gm/gmass: groundmass
WR: whole rock
LC: carbonate liquid
LS: silicate liquid
REE: Rare earth elements
HFSE: High field strength elements
LFSE: Low field strength elements
NBO/T: number of non-bridging oxygens per tetrahedra
av.: average
D_{equ}: equilibrium partition coefficient.
D_{eff}: effective partition coefficient.
K_D: exchange coefficient.

LIST OF APPENDICES

CHAPTER 1: INTRODUCTION

1.1 - Carbonatites

1.1.1: Opening statement

Carbonatites first received interest because of their exotic chemistry and mineralogy, and later because they may be a key to understanding the geochemical evolution of the mantle. Carbonatites are characterised by an enrichment in volatile elements such as C, F and Cl, and in incompatible elements such as rare earth elements and high field strength elements. They may provide information in fields such as degassing and metasomatic heterogeneity of the mantle, and recycling of the crust. Although it is now accepted that carbonatites are igneous rocks of primary mantle origin, there is still an ongoing debate concerning their genesis. In 1998, an entire Journal of Petrology volume was dedicated to carbonatites (*Carbonatites – Into the twenty-first century*). In the preface to this volume, Bell et al. (1998) summarise the most outstanding current problems in carbonatite research:

> *"1) Are the parental melts to carbonatites derived from the lithosphere or asthenosphere, or do they represent mixtures of both? 2) Are carbonatites generated as partial melts derived directly from the mantle, or are they the products of magmatic differentiation of carbonated silicate melts? 3) How easily can such parental melts migrate through the mantle, and how do such melts affect upper-mantle chemistry and mineralogy (modal and cryptic metasomatism); 4) What is the relationship among the silicate rocks, such as melilitite, nephelinite, ijolite, syenite, and phonolite, and spatially associated carbonatites? 5) How do carbonatite magmas fractionate and evolve?".*

1.1.2: Definition and nomenclature

Carbonatites are magmatic rocks containing more than 50 modal % carbonate minerals (Woolley and Kempe, 1989; Woolley et al., 1995). Most of the 330 carbonatites known world-wide are calciocarbonatites, magnesiocarbonatites and ferrocarbonatites,

i.e., are mainly constituted by calcium-, magnesium- and iron- carbonates. Woolley and Kempe (1989) showed that many carbonatites contain at least two carbonate species which might not always be easy to distinguish because of crystal intergrowths, and that there appears to be a complete solid solution series from dolomite through ferroan dolomite to ankerites. Alkali-rich carbonatite (natrocarbonatite) is retained for carbonatite composed of the sodium-potassium-calcium carbonates nyerereite and gregoryite (see formulae in list of symbols), and is known only at Oldoinyo Lengai.

1.1.3: Petrologic association

Most carbonatite complexes are characterised by a strongly bimodal, silicate/carbonate compositional distribution (*e.g.*, LeBas, 1977; 1987; see Tab. 1.1). Carbonatites usually represent ~ 10 volume % of the igneous complexes, and generally occur late in the formation of the complex (Barker, 1989). The silicate rocks associated with carbonatites are silica-undersaturated, peralkaline rocks, usually of melilititic-nephelinitic-phonolitic affinity. They are mostly comprised of evolved (Mg # < 40) silica-undersaturated, mildly peralkaline nephelinites ((Na+K)/Al < 1.30). Phonolites also occur, and these probably represent more evolved activity and are commonly contaminated by continental crust. Ijolites and syenites may represent plutonic equivalents of nephelinites and phonolites, respectively. Rocks such as olivine-melilitite and olivine-nephelinite, with more primitive compositions (Mg # > 60), are less common than nephelinites, but do occur in small volumes. LeBas (1987) pointed out that the lack of olivine and xenoliths in nephelinites associated with carbonatites may indicate that the magma is arrested and fractionated in some deep (unexposed) reservoir.

Carbonatites can also be spatially related to ultramafic lamprophyres (*e.g.* Alnö, Sweden; Kandalaksha, Russia), and to kimberlites (Premier, South Africa; see Tab. 1.1). Carbonate bodies in kimberlites commonly grade in composition into their hosts (Barker, 1989), *i.e.*, they lack the bimodal distribution exhibited by carbonatite/nephelinite complexes.

Moreover, around 10 % of the carbonatites occur in isolation (*e.g.* Fort Portal, Uganda; see Tab. 1.1). Unlike carbonatites associated with silicate rocks which are mainly calcitic, carbonatites occurring in isolation are usually dolomitic (Tab. 1.1).

Another important feature of most carbonatite complexes is the occurrence of fenites, an invasive metasomatic alteration of country rocks apparently emanating from the intrusion of both carbonatite and silicate magmas (Morogan, 1994). Much emphasis has been placed on the alkali-rich nature of this alteration and its implications for the original alkali content of the adjacent carbonatite magma. Ijolites, syenites and phonolites have also been interpreted as resulting from the fenitisation of country rocks by fluids emanating from the carbonatite magma (Kramm, 1994; Kramm and Sindern, 1998).

1.1.4: Petrogenesis of carbonatites

The importance of carbonatites in understanding mantle chemistry has lead to numerous studies, but despite the abundance of information, their origin is still controversial. Not only is it difficult to determine the relative contribution of lithosphere and asthenosphere in the formation of the parental (or primary) magmas, but the genetic link between carbonatites and the SiO_2-undersaturated silicate rocks they are often associated with is also unclear.

1.1.4.1: Isotopic constraints

The majority of carbonatites are found in rift-related, continental settings, and carbonatite occurrences related to collision-type tectonic activity on a global scale are scarce (Bell et al., 1998). Carbonatites are commonly located on major lithospheric domes or are related to major lineaments, or both (Woolley, 1989). Half of the known carbonatites occur in Africa, with the majority concentrated in, or close to, the East African Rift (Woolley, 1989; Bailey, 1993). In many areas, there has been repetition of carbonatitic activity with time, suggesting a lithospheric control (Woolley, 1989). Several workers have suggested that carbonatites are related to plume activity (*e.g.*, Gerlach et al., 1988; Bell and Simonetti, 1996). However, there is still a debate on the

relative involvement of lithosphere and asthenosphere components in the genesis of the parental magmas.

The neodymium and strontium isotopic compositions of carbonatites have been reported by Bell and Blenkinsop (1989). On an $\varepsilon_{Nd}(T)$ vs. $\varepsilon_{Sr}(T)$ plot, young carbonatites (< 40 Ma old) plot very close to the compositional field for oceanic island basalts (OIB's), although with slightly lower ε_{Nd} and ε_{Sr} values. This was interpreted by Bell and Blenkinsop (1989) as an indication of the mantle origin of carbonatites, although they could not use the Sr and Nd isotopic data to distinguish between a lithospheric or asthenospheric origin. More recently, Tilton and Bell (1994) confirmed that complexes < 200 Ma old have signatures that clearly indicate a mantle origin. Kwon et al. (1989) also concluded that carbonatites are of a mantle origin on the basis of Pb isotopic compositions. They showed that Pb isotopic data for < 100 Ma old complexes are within the compositional fields of present-day oceanic volcanic rocks as defined by MORB and OIB on $^{207}Pb/^{204}Pb$-$^{206}Pb/^{204}Pb$ and $^{208}Pb/^{204}Pb$-$^{206}Pb/^{204}Pb$ diagrams. Stable isotopic compositions of unfractionated and unaltered carbonatites lie in a restricted range that also indicate a mantle origin (see Taylor et al., 1967).

In summary, the isotopic compositions of Sr, Nd, Pb, O and C of carbonatites indicate that they are ultimately of mantle origin. Moreover, Sr, Nd and Pb isotopic compositions of carbonatites indicate that more than one mantle source needs to be invoked for generating the parental melts to carbonatite. The relationship between plume activity and carbonatitic magmatism is strongly supported by Nd, Pb and Sr isotope data obtained from Indian carbonatites (Simonetti et al., 1998; Veena et al., 1998). The plume carries heat and volatiles, and this might trigger the formation of small degrees of carbonated melts from the mantle. The heat from the plume increases the local geotherm, and the volatiles lower the solidus of the peridotite and may provide major constituents of carbonatites (and parental silicate magmas). Bell et al. (1998) showed that metasomatism is restricted only to the lithosphere, which traps fluid or melt incursions generated from the convecting asthenosphere. According to

Jones (1989), the metasomatised lithosphere is the ultimate source of the magmas. Note also that the isotopic compositions of the primary SiO_2-undersaturated silicate rocks are usually similar to the carbonatites they are associated with, which indicates that they are from a similar/same source.

1.1.4.2: Genesis

Evidence from phase equilibrium experiments has shown that carbonatite melts could be generated by primary mantle melting and by the differentiation of carbonated silicate melts. Three hypotheses have commonly been proposed for their genesis:

a) Primary origin from the mantle, with independent production of the silicate magma from a similar/same source (Eckerman, 1948; Holmes, 1952; Dawson, 1962a; 1966; Koster van Groos, 1975; Eggler, 1975; 1978; Wallace and Green. 1988; Bailey, 1989; Gittins, 1989; Falloon and Green, 1990; Odezynskyj, 1990; Thibault et al., 1992; Dalton, 1993; Dalton and Wood, 1993 a and b; Harmer and Gittins, 1998);

b) Crystal fractionation from a SiO_2-undersaturated silicate magma derived from the mantle (King, 1949; King and Sutherland, 1966; Watkinson and Wyllie, 1971; Wyllie, 1987; Lee and Wyllie, 1994);

c) Liquid immiscibility from a mantle-derived SiO_2-undersaturated, carbonated silicate magma (Eckermann, 1961; 1966; Ferguson & Currie, 1971; Rankin & LeBas, 1974; King, 1965; Koster van Groos and Wyllie, 1963; 1966; 1968; 1973; LeBas, 1977; 1981; 1989; Romanchev & Sokolov, 1979; Hamilton et al., 1979; Freestone and Hamilton, 1980; Wyllie, 1989; Brooker and Hamilton, 1990; Kjarsgaard and Hamilton, 1988, 1989; Kjarsgaard, 1990; Kjarsgaard and Peterson, 1991; Pyle et al., 1991; Macdonald et al., 1993; Hamilton and Kjarsgaard, 1993; Lee and Wyllie, 1994; 1996; 1997a; 1997b; 1998; Kjarsgaard et al., 1995; Church & Jones, 1995; Kjarsgaard, 1998; Wyllie and Lee, 1998; Veksler et al., 1998b).

1.1.4.2.a: Primary origin from the mantle

Experimental studies have been made by Huang and Wyllie (1976), Eggler (1978), Wallace and Green (1988), Wyllie (1989) and Falloon and Green (1990) to

investigate the composition of a primary carbonatite melt in the mantle for various degrees of fluid saturation and CO_2/H_2O ratios (see Fig. 1.1). They concluded that primary, sodic dolomitic carbonatites can be produced by direct partial melting of a carbonated, fertile amphibole-peridotite. More recent studies by Wyllie and Lee (1998) and Lee and Wyllie (1998) confirmed this finding. Wyllie and Lee (1998) observed that the composition of carbonatitic melts in equilibrium with lherzolite mineral assemblages will invariably be dolomitic, with Ca/(Ca + Mg) ratios of 0.5-0.7 at pressures from 2 GPa to at least 7 GPa. Moreover, Lee and Wyllie (1998) studied the system CaO-$(MgO + FeO^*)$-$(Na_2O + K_2O)$-$(SiO_2 + Al_2O_3 + TiO_2)$-$CO_2$ at 1.0 and 2.5 GPa, and showed that calciocarbonatites and natrocarbonatites are excluded as candidates for primary magmas from the mantle.

The production of carbonatite magmas by near-solidus melting of synthetic carbonated peridotite has been studied recently at 3 GPa by Moore and Wood (1998) and at 6 GPa by Dalton and Presnall (1998). Dalton and Presnall (1998) showed that equilibrium melting of a model lherzolite containing 0.15 wt. % CO_2 produced liquids at 6 GPa which demonstrate a systematic compositional variation with increasing temperature (*i.e.*, increasing degree of partial melting). This compositional variation spans a continuum of rock compositions, ranging from the near-solidus dolomitic carbonatites through ultramafic lamprophyres. At lower pressure (3 GPa), however, Moore and Wood (1998) illustrated that there is a sharp compositional break from carbonatite to carbonated silicate liquid over a 50 °C heating interval.

The 10 % of erupted carbonatites that occur in isolation are usually dolomitic and probably represent primary carbonatites originated directly by partial melting of a peridotite (see Tab. 1.1). The fact that isolated, primary carbonatites are scarce compared to carbonatites associated with silicate rocks probably reflects their difficulty to erupt, since they represent small volumes of melt that is highly reactive with the surrounding mantle. If primary carbonatite melts produced by partial melting of the mantle do not find a conduit to the surface, they will undergo thermal and chemical death (Bell et al., 1998) as they rise and meet the solidus ledge at lower

pressures (see Fig. 1.1). This later fate is compatible with the scarcity of erupted, primary carbonatites, and the importance of mantle metasomatism by carbonatite melts (Green and Wallace, 1988; Yaxley et al., 1991; Rudnick et al., 1993).

Some authors (*e.g.* Harmer and Gittins, 1997, 1998; Dalton and Wood, 1993a) consider that carbonatites other than the isolated dolomitic carbonatites represent primary carbonatites (Tab. 1.1). Harmer and Gittins (1998) suggested that most carbonatites are of primary mantle derivation and that the divergent Nd and Sr isotopic compositions of the associated silicate rocks reflect different mantle source regions. Harmer and Gittins (1997) showed that in ancient shields such as Canada and southern Africa, many carbonatite complexes are dolomite-ankerite carbonatites rather than calciocarbonatites. They showed that both types of carbonatites can be derived from a magnesian carbonatite melt produced by partial melting in the mantle, and that the bimodality observed between calcio- and magnesio-carbonatites does not require different parent magmas. According to them, the production of calcitic or dolomitic carbonatites from a magnesian magma depends on the stability of the dolomite in the crust, *i.e.*, calcite precipitates at higher temperature than dolomite. This view disagrees with the general view that Mg- and Fe-rich carbonatites are late-stage fractionation products from calciocarbonatites (see LeBas, 1989).

Dalton and Wood (1993a) performed experiments to study the compositions of primary carbonate melts and their evolution through wallrock reaction in the mantle. They showed that the composition of near-solidus melts from depleted lherzolite at pressures greater than 2.5 GPa are carbonatitic with low alkali contents and Ca/(Ca + Mg) ratios of 0.72-0.74; and primary carbonate melts from fertile mantle are more sodic with Ca/(Ca + Mg + Fe + Na) of 0.52 and Na/(Na + Ca + Mg + Fe) up to 0.15. Wallrock reaction of primary melts with harzburgite at pressures < 2.5 GPa can produce calciocarbonatites. They also showed that melts richer in Na_2CO_3 can be produced by wallrock reaction of primary carbonate melts with lherzolite, and that these melts are possible parental magmas of natrocarbonatites.

1.1.4.2.b: Crystal fractionation from an SiO_2-undersaturated silicate magma

The study of Watkinson and Wyllie (1971) on the system $NaAlSiO_4$-$CaCO_3$ (+ 25 % H_2O) illustrated that silica-undersaturated melts can eventually yield liquids which precipitate calcite (see Fig. 1.2). Wyllie and Lee (1998) and Lee and Wyllie (1998) examined carbonated silicate liquid differentiation. They suggested that one potential residual liquid path involves reaching the silicate-carbonate liquidus boundary, resulting in the precipitation of silicate and carbonate phases, which could form calciocarbonatites.

The formation of carbonatites by crystal fractionation, shown to be possible by experimental studies, is observed in nature in a few instances, *e.g.*, the Salmgorskii ring complex, Kola peninsula, Russia (Korobeinikov et al., 1998), Kovdor (Veksler et al., 1998a) and Premier, South Africa and Blue Hills, Namibia (Kjarsgaard, 1998). For these three localities, carbonatites formed by crystal fractionation from parental, silicate magmas, *e.g.*, carbonated melanephelinite (Kovdor) and kimberlites or alkali ultrabasic magmas (Premier and Blue Hills).

1.1.4.2.c: Liquid immiscibility from an SiO_2-undersaturated, carbonated silicate magma formed in the mantle

Liquid immiscibility between silicate and carbonate magmas is compatible with the bimodal distribution of rock types commonly observed in alkali-silicate/carbonatite complexes. At Shombole, the occurrence of carbonate globules in the nephelinites supports the liquid immiscibility hypothesis (Kjarsgaard and Peterson, 1991).

Experimental evidence for silicate/carbonate liquid immiscibility in synthetic, geologically relevant systems was first demonstrated by Koster van Groos and Wyllie (1963, 1966, 1968, 1973) and Wendlandt and Harrison (1979). Selected data from pre-1988 studies, which have been reviewed in Kjarsgaard and Hamilton (1988), are presented in Figure 1.3. The findings of Koster van Groos and Wyllie are, chronologically: 1963 – presence of a miscibility gap in the system albite-Na_2CO_3 (+ 10 wt. % H_2O) at 100 MPa; 1966 – large miscibility gap between an albite-rich aluminosilicate liquid and a sodium carbonate liquid, at 100 MPa and over a range of

temperature down to 870 °C; 1968 – shrinkage of the miscibility gap (see Fig. 1.3; evolution from A to A") with addition of more than 10 wt. % of H_2O; 1973 – shrinkage of the miscibility gap with increasing anorthite content, in the system plagioclase-Na_2CO_3 (+ 10 wt. % H_2O). Koster van Groos (1975) prepared an experiment at 1 GPa and 725 °C in a complex synthetic system with 16 wt. % H_2O, and produced a carbonate liquid with 75 wt. % $CaCO_3$ that was interpreted by Kjarsgaard and Hamilton (1988) as being an immiscible liquid. Kjarsgaard and Hamilton (1988, 1989) studied the system SiO_2-Al_2O_3-CaO-Na_2O-CO_2 at 500 and 200 MPa, 1250 °C (see Fig. 1.4). They showed that both natrocarbonatites and calciocarbonatites can be exsolved from a peralkaline silicate liquid at crustal pressures. All these experimental studies showed that at crustal pressures the size of the two liquid field increases with increasing pressure and decreasing temperature.

Lee et al. (1994) studied the system CaO-SiO_2-CO_2 at 2.5 GPa. They found rounded calcite crystals, which had previously been interpreted as carbonate liquid (see Kjarsgaard and Hamilton, 1988), and suggested that there is no immiscibility between quartz or calcium silicates and calcite. This has been used in Figure 1.4 to modify data presented by Kjarsgaard and Hamilton (1988) and Kjarsgaard (1990).

Lee and Wyllie (1994, 1996, 1997a, 1997b) studied the system SiO_2-Al_2O_3-CaO-Na_2O-CO_2 at pressures up to 2.5 GPa, and showed that liquid immiscibility occurs at least until this pressure, although the immiscibility field is smaller at high pressure. However, in 1998, they studied the system CaO-(MgO + FeO*)-(Na_2O + K_2O)-(SiO_2 + Al_2O_3 + TiO_2)-CO_2 at 1.0 and 2.5 GPa and showed that immiscible carbonate-rich magmas have maximum $CaCO_3$ contents of 75-80 wt. %, and that the formation of (equilibrium) carbonate-rich liquids immiscible with silicate magma is unlikely in the mantle because the miscibility gap is much narrower at 2.5 GPa than at crustal pressures. Brooker (1998) argued against this last point on the basis that undersaturation of CO_2 in the experiments by Lee and Wyllie inhibits liquid immiscibility. He demonstrated that a wide two-liquid field does exist at mantle pressures (2.5 GPa).

Kjarsgaard (1998) examined the sub-liquidus phase assemblages of an exsolved, carbonated high-CaO nephelinite at 0.2 and 0.5 GPa, and found two-liquid plus melilite phase assemblages in 0.2 GPa experiments, that suggested a potential genetic link between sövites and coexisting melilite nephelinites. On the basis of his experimental results, he also showed that sövites could represent cumulates from an immiscible carbonate liquid conjugate to low peralkalinity wollastonite nephelinite.

Relatively few studies have examined the partitioning behaviour of trace elements between immiscible silicate and carbonate liquids (*e.g.*, Freestone and Hamilton, 1980; Hamilton et al., 1989; Jones et al., 1995). The most recent two-liquid partitioning study was done by Veksler et al. (1998b). This later study was done in a system relevant for lavas from Oldoinyo Lengai and provided data on a wide range of trace elements, including rare earth elements, high field strength elements and other elements.

1.1.4.3: Conclusion

Bell et al. (1998) showed that because almost all carbonatites are associated with alkali silicate rocks, usually of nephelinitic or melilitic affinity or their plutonic equivalents, it is difficult to divorce the origin of one from the origin of the other. They also showed that relationships between carbonatites and their associated silicate rocks are complex and are still not completely understood, and that one of the most fundamental problems in carbonatite petrogenesis is to determine whether both melts were generated from the same parental magma, or whether both were generated independent of one another.

Petrological studies support all of three mechanisms outlined above for the generation of carbonatitic melts, *i.e.*, primary melts and melts fractionated from carbonated silicate melts, by crystal fractionation and liquid immiscibility. Although an origin by direct melting from the mantle is preferred for isolated, dolomitic carbonatites, this hypothesis is not favoured for the carbonatites associated with silicate rocks. The author agrees with Bell et al. (1998) that because of the minor volumetric proportion of carbonatite in most complexes and its late emplacement, it is

more likely, in general, to have separated from a relatively evolved or even residual silicate magma.

1.2 - Carbonatites from Oldoinyo Lengai

1.2.1: Field observations and laboratory measurements

Oldoinyo Lengai is located on the Gregory Rift Valley in Tanzania (see Fig. 1.5). Oldoinyo Lengai has received much interest since: 1) it is the only active carbonatite volcano; 2) some nephelinites, and all natrocarbonatites are unusually high in alkalis; and 3) previous workers considered that natrocarbonatites could be the precursors of calciocarbonatites (Dawson, 1962a, LeBas, 1977, 1987). However, natrocarbonatites are highly fractionated (Peterson and Kjarsgaard, 1995; Kjarsgaard et al., 1995; Mitchell, 1997; Gittins and Jago, 1998) and have an exotic mineralogy characterised by the presence of nyerereite and gregoryite. Two types of natrocarbonatites occur at Oldoinyo Lengai: silicate-bearing and silicate-free natrocarbonatites. They have very low viscosities (Norton and Pinkerton, 1997) despite very low temperatures of eruption, between 500 and 600 °C (Krafft and Keller, 1989; Pinkerton et al., 1995). The petrography of peralkaline nephelinites, and silicate-bearing natrocarbonatites from Oldoinyo Lengai is described in Chapter 2.

The eruption history of the Oldoinyo Lengai volcano has been described in detail by Dawson (1962a, 1989) and Dawson et al. (1995a). Dawson (1962a) established the following stratigraphic sequence: (VI) Very recent lavas of the active crater; (V) Variegated tuffs of the active crater; soda deposits of the summit area; black and grey ashes; (IV) Melanephelinite extrusions; (III) Black nephelinite tuffs and agglomerates; (II) Grey tuff and agglomerates of the adventive cones, craters and tuff rings; and (I) Yellow ijolitic tuffs and agglomerates with interbedded lavas.

Peterson and Kjarsgaard (1995) showed that Oldoinyo Lengai has erupted silicate and carbonate magmas in two phases. During the early, most voluminous phase, nephelinites and phonolites of low peralkalinity [$(Na+K) \leq 1.3$] were erupted, together with ijolite and syenite blocks from the underlying intrusive complex. In the very recent

phase, strongly peralkaline nephelinites (but no phonolites) with rare mineral assemblages (wollastonite, combeite) were erupted together with natrocarbonatite.

Although silicate rocks represent ~ 99 % of the volcano (Donaldson et al., 1987), carbonatites have been mainly erupted this century. From 1960 until early August 1966, silicate-free lavas containing nyerereite and gregoryite phenocrysts, nyerereite microphenocrysts and a (Mn, Fe, Pb) sulphide, set in fine-grained matrix (Dawson et al., 1990) were erupted. In late August 1966, the volcano went into a phase of explosive eruption of mixed silicate-carbonate ash containing ~ 25 wt. % SiO_2 (Dawson et al., 1992). After this violent eruption, the volcano became dormant until 1983, when silicate-free lavas similar to the 1960 lavas erupted. Eruptions of silicate-free natrocarbonatites occurred again in 1988 and 1992 (Dawson et al., 1995a and b), but in June 1993, extremely viscous lavas containing ~ 3 wt. % SiO_2 characterised the Chaos Crags flow (Simonetti et al., 1997).

Lavas from Oldoinyo Lengai have been previously described by Gittins and McKie (1980), Donaldson et al. (1987), Peterson (1989a), Dawson (1989), Dawson et al. (1989, 1990, 1992, 1994a, 1995 b and c, 1996), Peterson (1990), Keller and Krafft (1990) and Church and Jones (1995). An entire volume on natrocarbonatites from Oldoinyo Lengai (*Carbonatite volcanism: Oldoinyo Lengai and the petrogenesis of natrocarbonatites*) was edited by Bell and Keller (1995). This volume documents the volcanic history (Dawson et al., 1995a) and volcanological field observations at Oldoinyo Lengai, including field measurements of physical properties of carbonatite lavas (Pinkerton et al., 1995; Pyle et al., 1995). Analytical data obtained from both carbonatite and silicate lavas of Oldoinyo Lengai are also documented in this volume, which include studies on petrology (Koberski and Keller, 1995; Dawson et al., 1995b), major and trace element chemistry (Dawson et al., 1995b; Keller and Spettel, 1995), and radiogenic and stable isotopes (Bell and Dawson, 1995; Pyle, 1995; Keller and Hoefs, 1995). Few publications on natural lavas from Oldoinyo Lengai followed the text edited by Bell and Keller (1995). Mitchell (1997) showed that porphyritic natrocarbonatites erupted in 1995 differ from previously studied lavas in that they preserve textures indicative of groundmass carbonate-carbonate

immiscibility. Gittins and Harmer (1997) described a sample of calciocarbonatite that they interpreted as being of primary igneous origin, *i.e.* not affected by fenitisation. Gittins and Jago (1998) studied the major element composition of silicate-free carbonatites from Oldoinyo Lengai, and showed that the aphyric compositions represent more evolved compositions than the porphyritic ones. More recently, Kramm and Sindern (1998) interpreted ijolites, syenites and phonolites as products of fenitisation of country rocks by fluids emanating from the carbonatite magma. Moreover, Dawson (1998) suggested that alkalis, Sr, Ba and halogens are enriched in combeite nephelinite compared to wollastonite nephelinite, because of the absence of exsolved natrocarbonatite into which these elements would normally partition.

1.2.2: Genesis of Oldoinyo Lengai lavas: constraints from the natural lavas and experiments

The eruption of silicate and carbonate magmas at the same volcano and their bimodal distribution indicate that immiscibility is the most probable origin for the natrocarbonatites of Oldoinyo Lengai. Experimental work by Kjarsgaard et al. (1995) also supports the liquid immiscibility hypothesis. Sweeney et al. (1995a) preferred an origin by direct partial melting from the mantle, based on an experimental study. Morogan and Martin (1985) viewed the natrocarbonatite as a partial melt of fenitised lower crust, and Milton (1968) and Peterson and Marsh (1986) proposed that silicate magmas assimilate trona ($Na_2CO_3.NaHCO_3.2H_2O$) deposits and then exsolve natrocarbonatite melt. However, these latter hypotheses have not received as much attention as the liquid immiscibility hypothesis.

Bell and Dawson (1995) and Bell & Simonetti (1996) determined the Nd, Sr and Pb isotopic signatures of natrocarbonatites and silicate rocks. Bell and Dawson (1995) showed that for Nd and Sr isotopes, Oldoinyo Lengai carbonatites plot on the East African Carbonatite Line (EACL) and do not show any evidence for interaction with lower crustal granulites. Bell and Simonetti (1996) refuted the involvement of trona in the genesis of natrocarbonatites on the basis of their lead isotopic data.

Since field observations at Oldoinyo Lengai and isotopic data obtained on the lavas are most supportive of an origin of the silicate-bearing natrocarbonatites by liquid immiscibility, most experimental studies have been constructed in order to test this hypothesis (Koster Van Groos and Wyllie, 1966, 1968, 1973; Hamilton et al., 1979; Freestone and Hamilton, 1980; Kjarsgaard and Hamilton, 1988, 1989; Kjarsgaard et al., 1995). Experimental studies on trace element partitioning between the immiscible liquids have also been made to constrain the origin of carbonatites (Wendlandt and Harrison, 1979; Hamilton et al., 1989; Jones et al., 1995; Veksler et al., 1998b).

Details of previous studies relevant to the liquid immiscibility process at Oldoinyo Lengai are given in the appropriate chapters, and are compared with results of the present study. Two important findings need to be presented here since they justify the choice of the experimental conditions and the outline of the thesis. These are: 1) examination of the major element compositions of carbonate liquids from immiscibility experiments by Kjarsgaard et al. (1995) suggests that liquid immiscibility from wollastonite nephelinites produces silicate-bearing, not silicate-free natrocarbonatites; and 2) the conditions of liquid immiscibility of natrocarbonatites from peralkaline wollastonite nephelinite have been estimated to be about 100 MPa and 750 °C by Kjarsgaard et al. (1995).

1.3 - Aim and outline of the thesis

The aim of this study is to provide further understanding on the origin of silicate-free and -bearing natrocarbonatites at Oldoinyo Lengai. This will be done by comparing natural rocks from Oldoinyo Lengai to experiments which were made using erupted lavas from Oldoinyo Lengai as starting materials, *i.e.* silicate-bearing natrocarbonatite OL5 and wollastonite nephelinite HOL14. The experiments can be divided in two different sets: 1) those which contain only silicate-bearing natrocarbonatite lava OL5 as the starting material, which will be called OL5-experiments; and 2) the remaining experiments, which were prepared with mixtures of silicate-bearing natrocarbonatite OL5 and wollastonite nephelinite HOL14, or with wollastonite nephelinite HOL14 only.

Fractionation of silicate-bearing natrocarbonatites to produce silicate-free natrocarbonatites will be studied by comparing the mineralogy and major and trace

element chemistry of different phases in natrocarbonatites from Oldoinyo Lengai to those produced in OL5-experiments at 20 and 100 MPa, 550-900 °C (Chapter 3 to 5). Subsequently (Chapters 6 and 7), phase assemblages, and major and trace element data on quenched liquids and on crystals from the second set of experiments, prepared at conditions (P = 20 - 200 MPa and T = 700 - 900 °C) close to those suggested for liquid immiscibility at Oldoinyo Lengai, will be compared to results obtained from natural lavas - in order to test the liquid immiscibility hypothesis.

Experimental and analytical methods are presented in Chapter 2. In Chapter 3, phase assemblages and major element compositions of crystals and carbonate liquid produced in OL5-experiments are compared to those of erupted silicate-bearing natrocarbonatite OL5, in order to constrain the crystallisation of silicate-bearing natrocarbonatite OL5. In Chapter 4, the effects of different parameters (*e.g.*, pressure, temperature, crystal structure) on trace element compositions of crystals and carbonate liquid are discussed, and trace element partition coefficients are calculated for crystal-carbonate liquid pairs. In Chapter 5, the trace element results presented in Chapter 4 are used to further constrain the crystallisation of silicate-bearing natrocarbonatite and the formation of silicate-free natrocarbonatites. Chapter 6 presents the phase assemblages and major element data on crystals and liquids (silicate and carbonate) from the second set of experiments (*i.e.*, experiments prepared using some wollastonite nephelinite HOL14 in the starting mixture ± silicate-bearing natrocarbonatite OL5). The compositions of crystals and liquids are compared between experimental and natural samples. However, the focus in Chapter 6 is on comparing two-liquid major element distribution between experiments and natural lavas, in order to constrain the conditions of liquid immiscibility at Oldoinyo Lengai, and the mechanisms of liquid immiscibility and of distribution of major elements between immiscible liquids are also assessed in detail in this chapter. In Chapter 7, all trace element data collected on crystals and liquids from the second set of experiments are presented. Discussion of the controls of different parameters on trace element partitioning between silicate and carbonate liquids is also made in Chapter 7. Then, emphasis is made on comparing trace element data, especially two-liquid trace element partitioning,

between relevant two-liquid experiments and natural lavas, in order to confirm the P-T conditions of liquid immiscibility determined in Chapter 6. In Chapter 8, the role of volatiles in the petrogenesis and evolution of carbonatites, especially those from Oldoinyo Lengai, is examined in detail, and the relevance of natrocarbonatites to the more common calciocarbonatites is also examined. To facilitate examination of the thesis, tables and figures and are located at the end of each chapter.

Table 1.1: Characteristics of the different types of carbonatites.

Association	Isolated	With nephelinite/phonolite/melilitite		With lamprophyre*/ kimberlite**
		Peralkaline	Extremely peralkaline	
Example	Fort Portal, Uganda (Barker and Nixon, 1989), Newania, India (Viladkar and Wimmenauer, 1986), Kangankunde, Malawi (Buckley and Woolley, 1990), Rufunsa, Zambia (Bailey, 1989)	Shombole, Kenya (Kjarsgaard and Peterson, 1991)	Oldoinyo Lengai, Tanzania (Kjarsgaard et al., 1995)	Alnö*, Sweden (Brueckner and Rex, 1980), Kandalaksha*, Russia (Ivanikov et al., 1998), Frederikshåbs Isblink*, Greenland (Hansen, 1980), Sarfartôq*,**, Greenland (Secher and Larsen, 1980), Premier**, South Africa and Blue Hills*, Namibia (Kjarsgaard, 1998)
Type of carbonatite	Mg-, Fe-rich (dolomitic) carbonatites	Calciocarbonatite (± late-stage Mg-, Fe-rich carbonatites)	Natrocarbonatite	- Kandalaksha, Alnö, Premier and Blue Hills: calciocarbonatite (± Mg); - Frederikshåbs Isblink and Sarfartôq: dolomitic-ankeritic carbonatites
Setting	Rift-related, continental settings, located on major lithospheric domes and/or related to major lineaments. Can also be linked with orogenic activity.			
Trace elements	Carbonatites contain the highest contents of REE (total REE ~ 1 wt. %) and the highest LREE:HREE ratios (La_{pm}/Lu_{pm} = 100-1000) of any igneous rocks. The (late-stage) ferrocarbonatites are, on the whole, richer in REE, although the characteristic enrichment in the LREE is common to all carbonatites (Woolley and Kempe, 1989). Four main stages of mineralisation associated with (late-stage) ferrocarbonatite are: (1) REE, (2) fluorite, (3) baryte and (4) U-Th commonly accompanied by silicification (LeBas, 1989).			

Isotopic composition	Mantle like isotopic compositions, involving more than one component, maybe the lithosphere and the asthenosphere: - $\varepsilon_{Nd}(T)$ vs. $\varepsilon_{Sr}(T)$ of carbonatites < 200 Ma old plot very close to the compositional field for oceanic island basalts (OIB's) (Bell and Blenkinsop, 1989; Tilton and Bell, 1994); - Pb isotopic data for 100 Ma old complexes are within the compositional fields of present-day oceanic volcanic rocks as defined by MORB and OIB on $^{207}Pb/^{204}Pb$-$^{206}Pb/^{204}Pb$ and $^{208}Pb/^{204}Pb$-$^{206}Pb/^{204}Pb$ diagrams (Kwon et al., 1989); - Stable isotopic compositions of unfractionated and unaltered carbonatites lie in a restricted range that also indicate a mantle origin (see Taylor et al., 1967).		
Suggested genesis	Primary melts produced by direct partial melting of a carbonated, fertile amphibole-peridotite (*e.g.* Falloon and Green, 1990; see text)	Three interpretations (see text): - Liquid immiscibility (Peterson and Kjarsgaard, 1995); - Primary melts produced by partial melting of a peridotite, converted to CaO- or Na_2O-rich carbonatite melts by interaction with the lithosphere (Dalton and Wood, 1993a). See also Harmer and Gittins (1998); - Crystal fractionation from parental, silicate magmas (Korobeinikov et al., 1998; Veksler et al., 1998b).	- Liquid immiscibility - conjugate carbonatites and lamprophyres (Frederikshåbs Isblink; Hansen, 1980); - Primary melts from the mantle (Sarfartôq; Secher and Larsen, 1980); - Crystal fractionation from primitive, highly undersaturated kimberlite and alkali ultrabasic magmas (Premier and Blue Hills; Kjarsgaard, 1998).

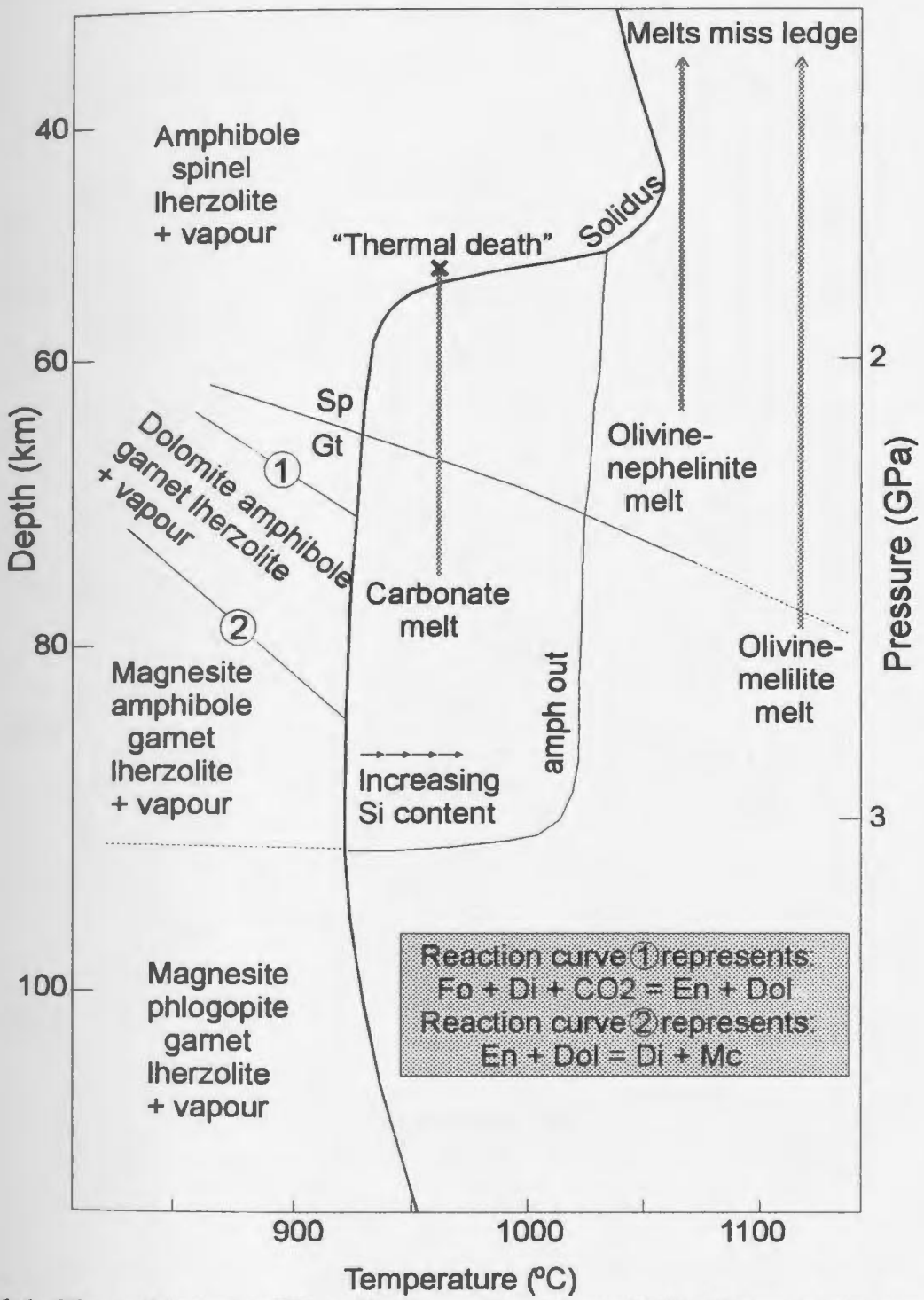

Figure 1.1: The solidus of a "Hawaiian" pyrolite minus 40 % olivine in the presence of CO_2 + H_2O. The CO_2 + H_2O saturated solidus is reproduced (in bold) to show the "thermal death" concept of a rising carbonate melt at approximately 950 °C. Higher temperature melts do not intersect the solidus as they rise. Adapted from Falloon and Green (1990). Abbreviations used: Sp, spinel; Gt, garnet; amph, amphibole; Fo, forsterite; Di, diopside; En, enstatite; Dol, dolomite; Mc, magnesite.

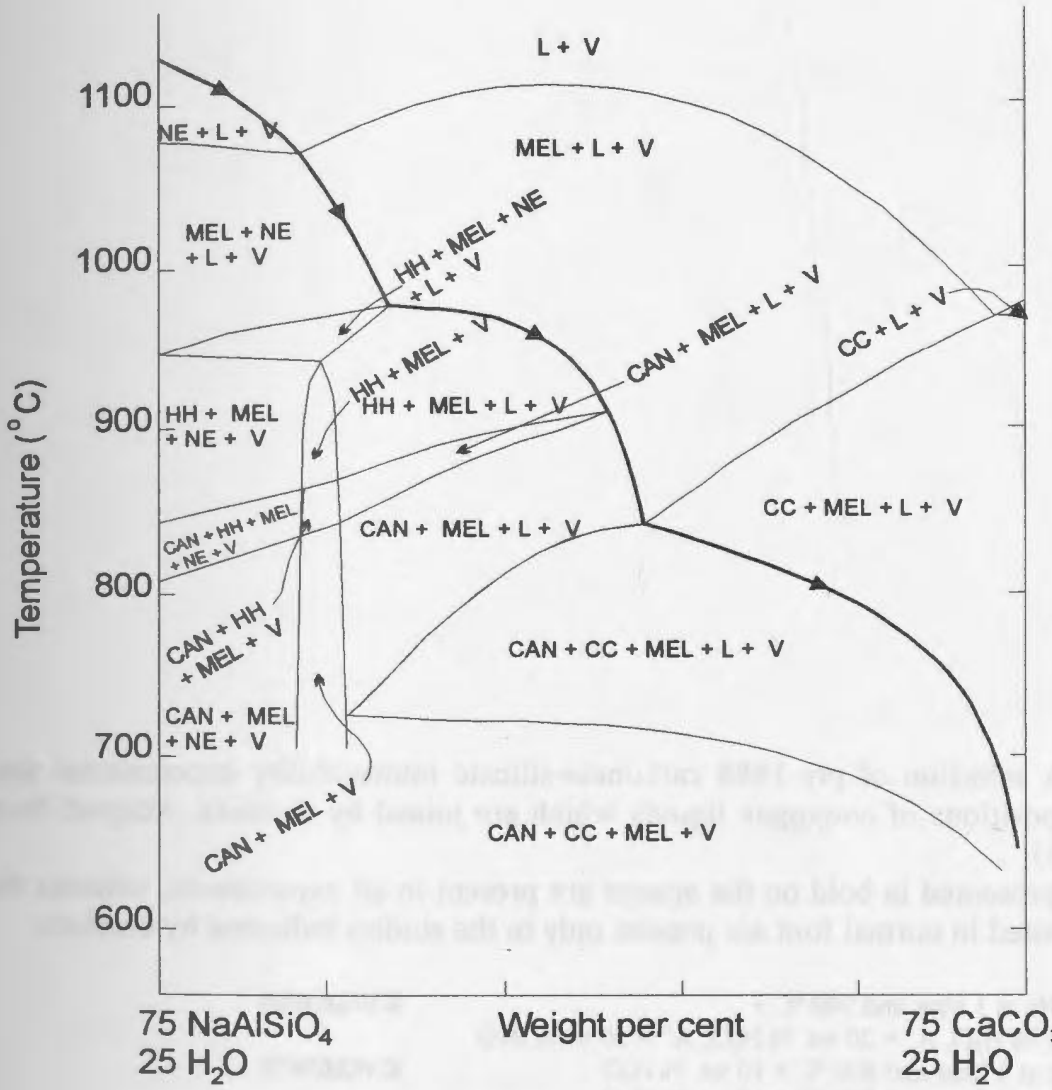

Figure 1.2: The proposed fractionation path (denoted by arrows) of Watkinson and Wyllie (1971) from a low CO_2 silicate magma to a late carbonate precipitating melt, at P = 1 kbar (100 MPa). Abbreviations used: NE, nepheline; MEL, melilite; HH, hydroxyhauyne; CC, calcite; CAN, cancrinite; L, liquid; V, vapour.

Figure 1.3: A selection of pre-1988 carbonate-silicate immiscibility experimental data showing compositions of conjugate liquids which are joined by tie-lines. Adapted from Brooker (1995).
The oxides represented in bold on the apexes are present in all experiments, whereas the oxides represented in normal font are present only in the studies indicated by brackets.

A, A', A" = Ab-Nc at 1 kbar and 900 °C +	KVG&W68
A = 0, 5 & 10 wt. % H_2O, A' = 20 wt. % H_2O, A" = 50 wt% H_2O	
B = $Ab_{80}An_{10}$-Nc at 1 kbar and 800 °C + 10 wt. % H_2O	KVG&W73
C = $Ab_{50}An_{50}$-Nc at 1 kbar and 800 °C + 10 wt. % H_2O	
D = Carbonated MgO and CaO enriched pantellerite at 10 kbar and 725 °C	KVG75
E = Nephelinite-carbonatite extrapolated to 1 kbar and 1100 °C	F&H80
'E = Phonolite-natrocarbonatite extrapolated to 1 kbar and 1100 °C	
F = Sanidine-Kc at 5 kbar and 1300 °C estimated	W&H79
G = Synthetic ijolite-carbonatite at 2 kbar and 900 °C	V78

Ab, albite; An, anorthite; Nc, sodium carbonate; Kc, potassium carbonate; KVG&W68, Koster van Groos & Wyllie (1968); KVG&W73, Koster van Groos & Wyllie (1973); KVG75, Koster van Groos 1975; F&H80, Freestone & Hamilton (1980); W&H79, Wendlandt & Harrison (1979); V78, Verwoerd (1978).

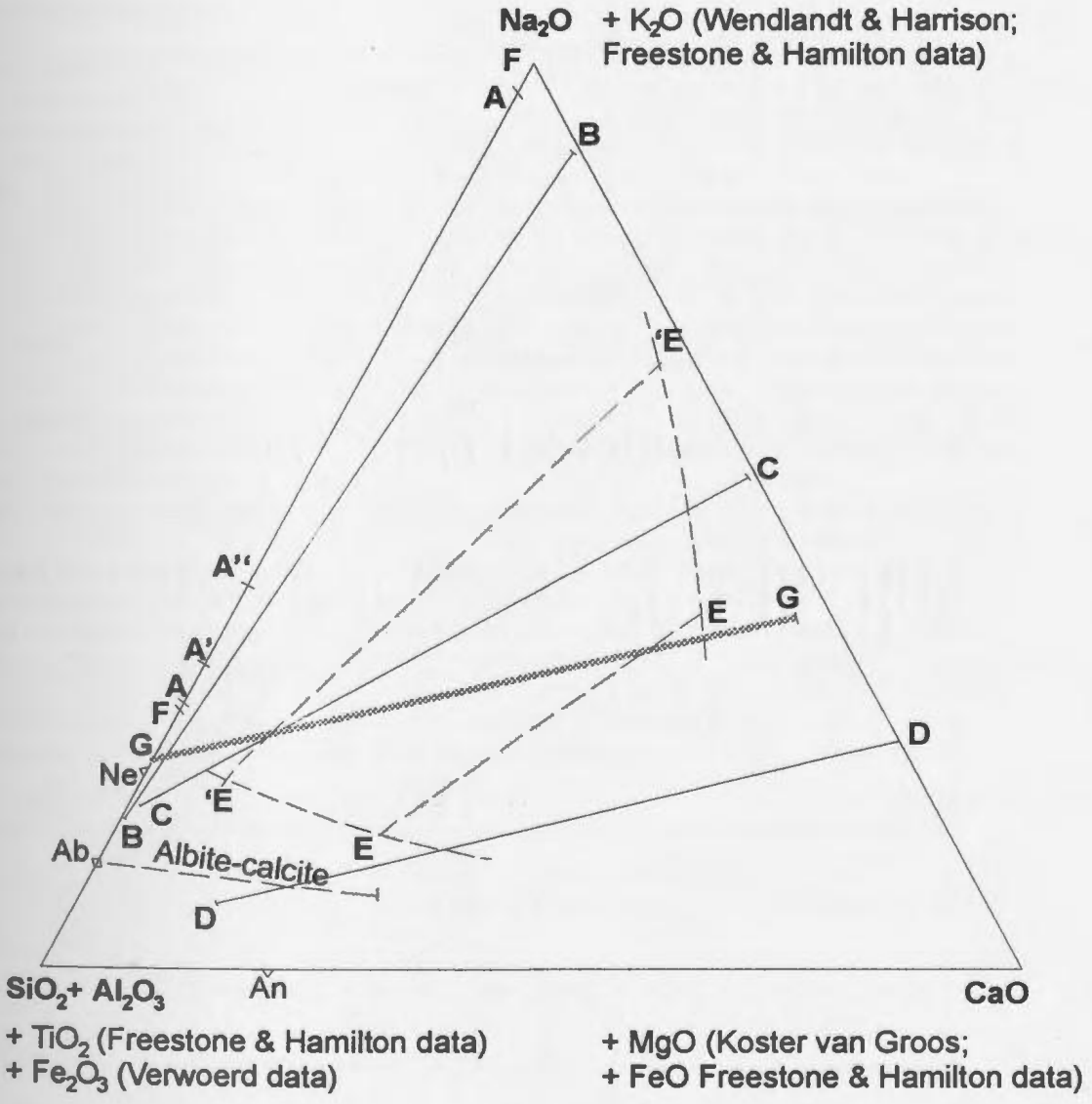
Na_2O + K_2O (Wendlandt & Harrison;
Freestone & Hamilton data)
F
A
B
'E
C
A''
A'
A
F
G
Ne
'E
C
B
Ab
Albite-calcite
E
D
E
G
D
SiO_2+ Al_2O_3
An
CaO
+ TiO_2 (Freestone & Hamilton data)
+ Fe_2O_3 (Verwoerd data)
+ MgO (Koster van Groos;
+ FeO Freestone & Hamilton data)

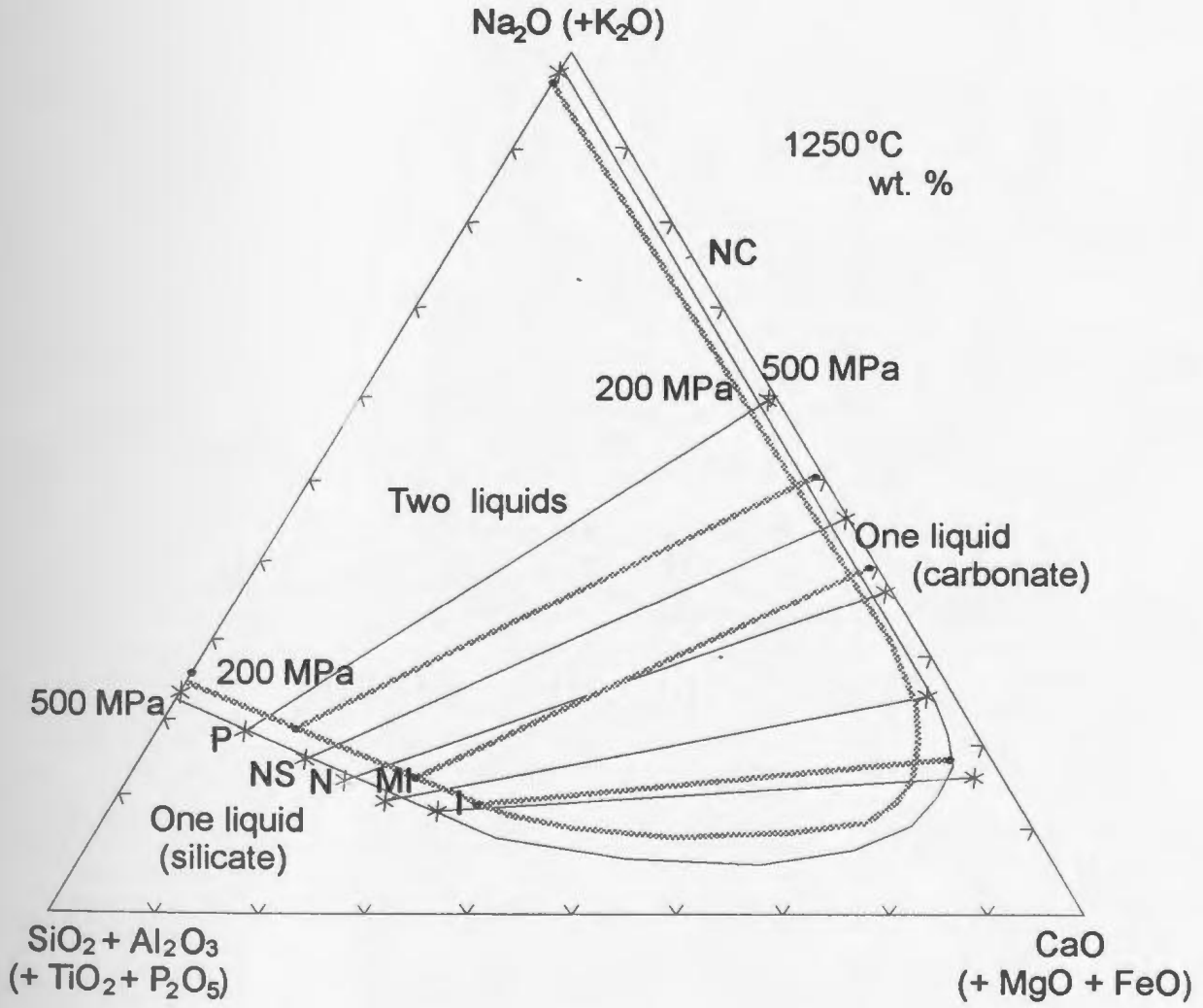

Figure 1.4: Experimental results for the system SiO_2-Al_2O_3-CaO-Na_2O-CO_2 at 1250 °C and 2 and 5 kbar (200 and 500 MPa), modified from Kjarsgaard and Hamilton (1988) and Kjarsgaard (1990). Only a selection of representative tie lines have been included. Natural rock compositions are shown by including additional components in brackets at the apexes of the diagram. P, phonolite; NS, nepheline-syenite; N, nephelinite; MI, microijolite; I, ijolite; NC, natrocarbonatite.

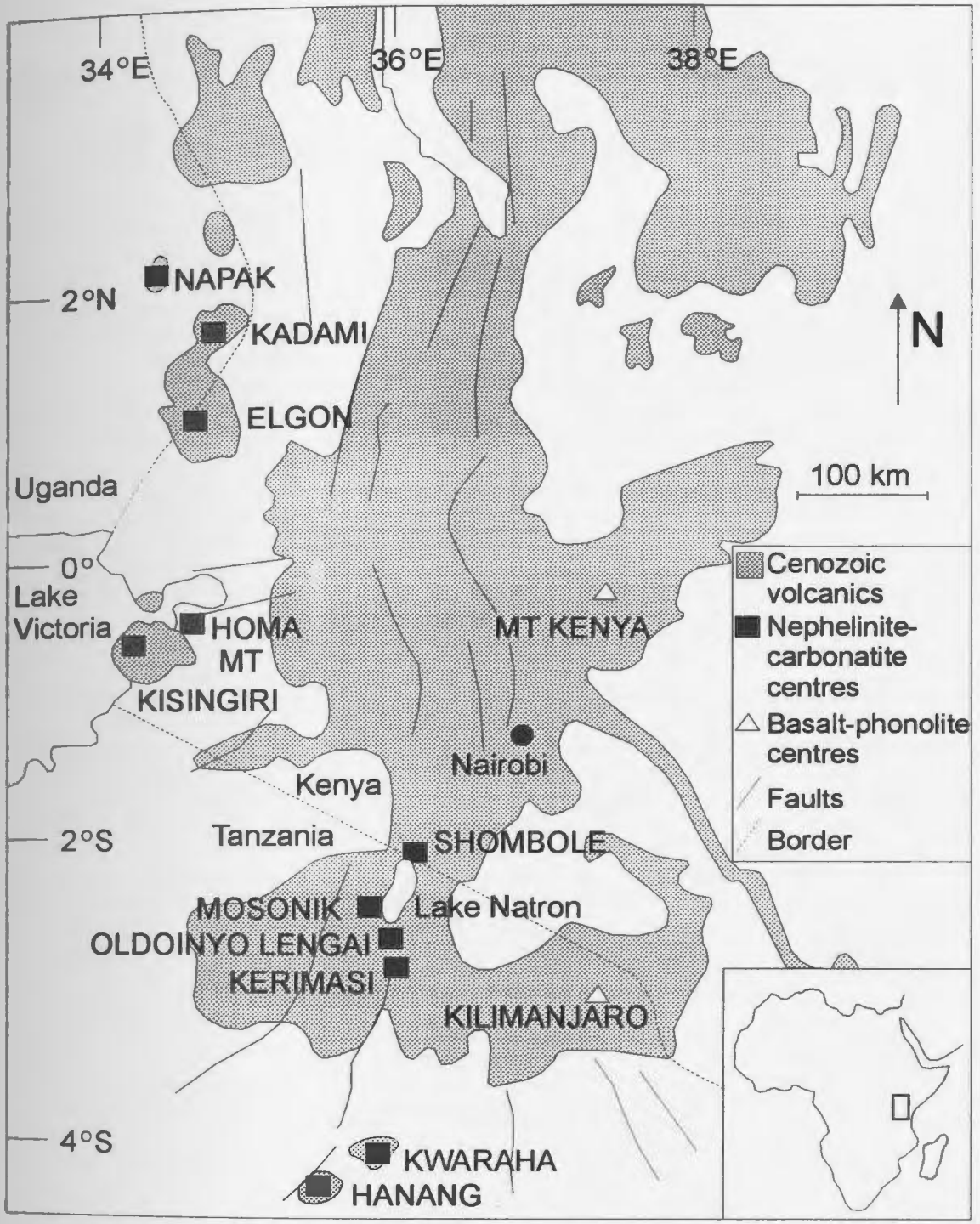

Figure 1.5: Locations of major Cenozoic nephelinite-carbonatite eruptive centres of the East African Rift. After Peterson (1989a).

CHAPTER 2: EXPERIMENTAL AND ANALYTICAL METHODS

The purpose of this chapter is to describe the materials used to prepare the experiments, the experimental methods and the analytical techniques used in obtaining data. Because of the nature of the material used or obtained (*i.e.* alkali-rich carbonate showing quenched overgrowths), and the fine-grained nature of the experimental run products, the analytical techniques were often used at or near their limits. A discussion of the problems and limitations of the techniques used is, therefore, also presented.

2.1 - Analytical methods

2.1.1: Scanning electron microscope (SEM)

Samples were first studied using SEM (Cambridge S200 and S360 at the Geological Survey of Canada, Ottawa; Hitachi S570 at Memorial University of Newfoundland, St John's). This was done in order to make preliminary identifications of the different phases and to obtain back-scattered (BSE) images. The BSE images were used to locate sites for electron microprobe (EMP) and laser ablation – inductively coupled plasma – mass spectrometry (LAM-ICP-MS) analyses.

2.1.2: EMP

Major element composition of the different phases was determined using two Cameca SX50 electron microprobes. Samples were analysed at the GSC (Ottawa), using wavelength dispersive spectrometers (WDS), and at Memorial University of Newfoundland (MUN), using energy dispersive spectrometry (EDS) for most elements, wavelength dispersive spectrometry (WDS) for F, and combined WDS/EDS for Ti. All analyses were made using an accelerating potential of 15 kV and a beam current of 10 nA. Crystals were analysed with a slightly defocused beam (10 μm), silicate liquids with a defocused beam (25 μm), and quenched carbonate liquids with a 40 μm * 50 μm rastered beam.

At the GSC (Ottawa), all the analyses were performed for 10 s on the peak. At MUN, EDS analyses were 100 s long, and standards were calibrated against Co. F was

analysed for 15 s on the background and 30 s on the peak; whereas Ti was analysed for 20 s on the background and 40 s on the peak. The standards used for calibration are reported in Table 2.1. Raw data were corrected using a ZAF procedure (MUN; see Reed, 1996) and PAP procedure (Ottawa).

For the analyses performed at MUN, detection limits are typically ~ 0.1 wt. %, except for TiO_2 (< 0.05 wt. %). Analyses of standards were made at the beginning of the runs, and analyses were performed when the stoichiometry was accurate to 3 %, even though the totals of the analyses might be in the range from 98 to 103 wt. %. To determine the precision, a run of 20 analyses of periclase, corundum, wollastonite and hematite was performed, indicating relative standard deviations of 0.4 % to 0.7 % for Mg, Al, Si, Ca and Fe.

2.1.3: LAM-ICP-MS

2.1.3.1: Apparatus

Figure 2.1 presents a schematic illustration of the LAM-ICP-MS assembly at MUN. The laser ablation sampling device consists of a Q-switched Nd:YAG laser operating at a fundamental wavelength of 1064 nm (Jackson et al., 1992). The laser has been modified by the introduction of frequency-quadrupling hardware, to produce UV radiation (266 nm) (Jenner et al., 1993). The laser beam path is manipulated from the laser via mirrors to the phototube of a petrographic microscope and is focused onto the sample through a silica window into the sample cell (see Fig. 2.1a). Beam diameters as small as 10 μm were used for the analysis of crystals. Pit diameters were on the order of 60 to 80 μm for the analysis of the silicate glass and the quenched carbonate liquid. The ablated material is carried in an Ar gas flow to the ICP-MS (Fisons©, VG-PQII + "S"), where it is dissociated and ionised in the plasma (Fryer et al., 1995). The instrument is optimised so that the sensitivity of the LREE is high (Fig. 2.2).

2.1.3.2: Data acquisition and calculation

For calibration, NIST 610 glass (see Pearce et al., 1997) was analysed twice before, and twice after, analyses of the samples, and the runs consisted of a maximum of 20 analyses (including analyses of NIST 610). Calculation of the concentrations requires the abundance of an internal standard element to be known for each sample. In this study, Ca was used as the internal standard element for most phases. Unlike EMP which is essentially a surface analysis, the signal acquired during LAM-ICP-MS analysis (usually 40-60 seconds) includes a significant depth component as ablation occurs through the sample. Time resolved data acquisition is used for LAM-ICP-MS analysis, *e.g.*, the interval of time that is used in the calculations is selectable, and need not represent the whole ablation interval. This allows the ablation signal to be monitored in order to detect inclusions and heterogeneities in the samples.

Figure 2.3a presents a typical signal recorded when analysing a fairly small pocket of quenched silicate liquid (beam diameter ~ 50 μm) from an experiment. For each isotope, the signal strength is represented by the counts per second versus time (cps vs. time). The background is recorded for ~ 60 s prior to sample analysis. The time resolved signal allows an operator to know when the laser beam has ablated through the silicate liquid and into the sample mounting material underneath. For this example, when the laser starts to ablate the carbonate liquid underneath, the signal for Ca, Rb and Sr increases while it decreases for Mg, Al, Si, Ti, Zr and Nb. Only the signal representing the quenched silicate liquid is selected. Figure 2.3b presents the signal for a large pocket quenched liquid (beam diameter ~ 100 μm). For this sample, the laser did not ablate through the sample and a ~ 60 s interval of sample signal could be selected. Figure 2.4 represents a typical signal for quenched carbonate liquid (~ 100 μm in diameter). The intensity of the signal tends to decrease fairly rapidly with time. The signal is often spiky due to the inherent heterogeneity of the quenched carbonate liquid.

Once the signal interval is selected, and the value of the internal standard specified, final elemental concentrations are calculated using the LAMTRACE

program developed in-house at MUN. The concentrations are then plotted either as chondrite- or primitive mantle- normalised patterns (McDonough and Sun, 1995). Precision and accuracy have been measured on NIST 612, which is a synthetic glass that has been spiked with 61 elements at a nominal concentration of 50 ppm, and on BCR-2G, which is a glass reference material that contains more V, Rb, Sr, Zr, Ba, but less Nb, Hf, Ta, Th, U, MREE and HREE than NIST 612 (Lahaye et al., 1997). Average precision and accuracy estimates based on replicate analyses of these two glasses are below 10 % for most elements. This is comparable with the accuracy and precision reported by Lahaye et al. (1997) for the same materials.

Figure 2.5 presents the chondrite normalised concentrations for quenched silicate liquid from an experiment and Figure 2.6 presents the chondrite normalised concentrations of the reference material BCR-2G. For these two examples, the normalised elemental abundances are several orders of magnitude greater than the detection limits. The agreement between the measured composition of BCR-2G with the reference values attests to the accuracy of the LAM-ICP-MS (Fig. 2.6) for samples having concentrations significantly higher than detection limits.

Detection limits depend on the amount of material that is ablated, which depends on the pit volume and the counting time. Therefore, they are different for each analysis and must be calculated for each individual acquisition. The first step in the calculation is to find the standard deviation of an individual sample count rates in the selected background interval, and the limit of detection must then be normalised to the amount of sample ablated (Longerich et al., 1996). From Figures 2.5 and 2.6 it can be calculated that for a large amount of material ablated (laser beam defocused by 100-300 μm), typical detection limits are in the range of 2-40 ppb for REE, < 50 ppb for HFSE, whereas they are higher for Sr (~ 2 ppm), Ba (~ 0.1 ppm) and Rb (~ 0.2 ppm). The fact that there is achievable reproducibility on the standards shows that for the silicate and carbonate liquids that contain significant amounts of trace elements and for which large volumes of material are ablated, there is confidence in the data that are collected, and differences of > 10 % between different analyses are thought to

be real. On the other hand, small volumes were ablated for the crystals from the experiments because pit diameters were limited by their small size. Small volumes of ablated material led to higher detection limits. For analyses of small crystals of nepheline in the experiments, pit diameter of ~ 10 μm were used, and the detection limits are typically 1-5 ppm for all trace elements and as high as 1000 ppm for Sr (see later in Chapter 4). In conclusion, for each individual analysis, one must examine what the limits of detection are, in order to evaluate what level of confidence to have in the data.

2.2 - Experimental apparatus and methods

The experimental runs were made using cold-seal (Tuttle-type) vessels. A schematic of the apparatus is presented in Figure 2.7 (after Holloway and Wood, 1988). The vessel is a rod of a superalloy (Rene-41), with a 0.64 cm hole drilled almost through to make a test-tube shape. The end of the vessel with the pressure seal is outside the furnace, hence "cold seal", and is formed by a simple cone seal (see inset in Fig. 2.7). The furnaces use Pt-Rh windings with type K furnace thermocouples. Temperature is measured with a type K thermocouple located in a well at the base of the vessel. Pressure is measured using a bourdon tube gauge (Astrogauge), calibrated against a Heise lab standard gauge. The Tuttle vessels used are housed in the laboratory of Dr. Bruce Kjarsgaard at the Geological Survey of Canada (GSC) in Ottawa.

Approximately 0.07 g of sample powder was loaded into gold tubes (2.5 mm OD, 20 mm length) which were sealed by arc welding. The experimental charges were run at pressures of 20, 40, 100 and 200 MPa over the temperature interval 550 – 900 °C. Argon was used as a pressure medium for the unbuffered runs, and methane for the C/CH_4 buffered runs (together with graphite surrounding the capsules). Run times varied from 4 to 618 hours. Samples were quenched at the end of the run by a jet of compressed air. Quenching rates were on average 300 °C/min for the first minute. A temperature correction was employed based on previous calibrations with an internal thermocouple. Reported temperatures are believed to be accurate to ± 5 °C. Pressure is thought to be accurate to ± 2 MPa. No reversal experiments were attempted because of problems with

nucleation of metastable, high-Ti clinopyroxene crystals (see Kjarsgaard et al., 1995). The liquidus was not determined as it lies above the safe operating conditions of the experimental apparatus.

After the run, capsules were weighed to check for weight loss or gain, then punctured and weighed again. Loss of weight after puncturing indicated the presence of a coexisting vapour phase. After observation with a binocular microscope, the run products were mounted in epoxy, polished in liquid paraffin and cleaned in acetone. The latter two steps were taken in order to avoid any contact with water or alcohol that tends to dissolve alkali-bearing carbonates and salts.

2.3 - Starting materials for the experiments

2.3.1: Silicate-bearing natrocarbonatite OL5

A sample of lava OL5 was provided by Dr. Keith Bell (Carleton University). A SEM back scattered image of OL5 is presented in Figure 2.8 and major and trace element concentrations are reported in Table 2.2. OL5 is a porphyritic, silicate-bearing natrocarbonatite lava erupted in 1993 as part of the extremely blocky Chaos Crags flow (Simonetti et al., 1997). Phenocrysts and silicate spheroids are set in a groundmass that consists mainly of intergrowths of coarser grained nyerereite and finer grained sylvite and Na-rich gregoryite (NaG, < 20 μm in diameter). The groundmass also contains grains of Mn, Fe and K, Fe sulphides, barite and witherite ($BaCO_3$) (Dawson et al., 1996). In addition, the groundmass of silicate-bearing natrocarbonatites from the June 1993 eruption also contain patches of a Ca-silicate compositionally similar to tilleyite ($Ca_3[Si_2O_7].2CaCO_3$), and minute crystals of nepheline in association with fluorite/NaG intergrowths. Phenocrysts present in OL5 include nyerereite, gregoryite, clinopyroxene, wollastonite, nepheline, melanite garnet, melilite, apatite, and pyrrhotite.

Silicate spheroids represent ~ 8-10 % volume of the lava (Simonetti et al., 1997). The spheroids have cores comprised of single phenocrysts, or glomeroporphyritic phenocryst clusters. Mineral phases in the spheroids include clinopyroxene, melanite garnet, wollastonite and nepheline, which commonly have mutual inclusion relationships,

suggesting that the liquidus was multiply saturated (Fig. 2.8). A single phenocryst of melilite was observed in a spheroid, which also included nepheline and melanite garnet phenocrysts. The spheroid cores are rimmed by a siliceous mesostasis that also contain microphenocrysts of nepheline, wollastonite, clinopyroxene, melanite garnet and a carbonatitic component in the form of rounded or ovoid globules (Dawson et al., 1996). Dawson et al. (1996) showed that the smaller carbonatitic bodies (up to 100-150 μm) commonly consist of single grains of gregoryite, often with tiny included grains of sylvite, and MnFe, FeK, or Fe sulphides, whereas the larger (up to 250 μm) aggregates, in which gregoryite is always the dominant phase, consist of gregoryite, nyerereite, sylvite, MnFe sulphide, and, less commonly, PbS. They also pointed out that unlike gregoryite, nyerereite does not occur as single grains in the spheroid matrix.

Porphyritic, silicate-bearing natrocarbonatite samples similar to OL5 have been described previously by Dawson et al. (1994a, 1996) and Church & Jones (1995). Dawson et al. (1996) also reported rare titanite phenocrysts in the spheroids, and melilite, titanite, pyrrhotite, perovskite and Ti-magnetite microphenocrysts in the matrix.

2.3.2: Wollastonite nephelinite HOL14

A sample of lava HOL14 was provided by Dr. Tony Peterson (Geological Survey of Canada, Ottawa). A SEM back scattered image of lava HOL14 is presented in Figure 2.9, and major and trace element concentrations are reported in Table 2.2. The petrography of wollastonite nephelinite HOL14 has been described in detail in Peterson (1989a).

Wollastonite nephelinites at Oldoinyo Lengai contain euhedral phenocrysts of wollastonite and are strongly peralkaline with [Na+K]/Al ~ 1.5 (Peterson, 1989a). They are extremely fresh with unaltered, grass-green glass and numerous zeolite-carbonate globules which have been interpreted as immiscible segregations by Peterson (1989a). They contain the phenocryst assemblage nepheline + clinopyroxene + sodalite + melanite + titanite + wollastonite; combeite and leucite appear as microphenocrysts. Cancrinite and vishnevite were found by Donaldson et al. (1987) but were not recognised in Peterson's suite. Mutual inclusion relationships amongst crystal phases suggest that the liquidus was multiply saturated (Fig. 2.9).

2.4 - Run products

A list of the experiments that were performed is provided in Appendix A2 (Tab. A2.1), in which the bulk composition and the pressure and temperature conditions are given for each experiment. A description of the run products is presented in detail in Chapter 3 and 6. They typically consist of one or two quenched liquid(s) plus crystals (mainly nepheline, clinopyroxene, wollastonite, melanite garnet, melilite, nyerereite and gregoryite), with a coexisting vapour (fluid) phase. Minor crystal phases observed include combeite, perovskite, titanite, apatite, vishnevite, sodalite, feldspar, pyrrhotite and spinel (Ti-magnetite).

Experiments prepared at high temperature (≥ 800 °C) are more suitable for EMP and LAM-ICP-MS analyses than those produced in low temperature because they are less crystallised. Experiments prepared using high carbonatite content (≥ 30 wt. % OL5) in the bulk composition contain large pockets of quenched carbonate liquid that can be more easily analysed than in the experiments using lower carbonatite content in the bulk composition. Conversely, experiments prepared using high nephelinite content (≥ 30 wt. % HOL14) in the bulk composition contain large pockets of silicate glass (if they are not highly crystallised, *i.e.* if the temperature is high enough) that can be more easily analysed than in the experiments using lower nephelinite content in the bulk composition.

Figures 2.10, 2.11 and 2.12 present experiments that have textures suitable for EMP and LAM-ICP-MS analyses. These experiments include those made using only OL5 as starting material, for example CP45 that was prepared at 20 MPa, 850 °C (Fig. 2.10). Experiment CP43 was prepared at 20 MPa, 850 °C, using 70 wt. % wollastonite nephelinite HOL14 and 30 wt. % silicate-bearing natrocarbonatite OL5 in the starting composition (Fig. 2.11). Note that the size of the laser ablation spots for experiment CP43 varied depending on the phase analysed. A SEM picture of experiment CP22, which was prepared at 20 MPa, 900 °C, using 50 wt. % wollastonite nephelinite HOL14 and 50 wt. % silicate-bearing natrocarbonatite OL5 in the starting composition, is presented in Figure 2.12. Note that in this experiment, melilite crystals criss-cross the two conjugate liquids, suggesting that equilibrium between liquids and crystals was achieved.

2.5 - Experimental and analytical problems

2.5.1: Small size of the liquid pockets and of the crystals

Some experiments have textures which are not suitable for EMP and LAM-ICP-MS analyses. These include low temperature (< 800 °C) experiments that are highly crystallised and experiments prepared with a low weight fraction of carbonatite in the starting composition (< 20 wt. % OL5).

Examples of these experiments are presented in Figures 2.13, 2.14 and 2.15. Experiment CP8 was prepared at 100 MPa, 700 °C, using 90 wt. % wollastonite nephelinite HOL14 and 10 wt. % silicate-bearing natrocarbonatite OL5 in the starting composition. Its fine texture (Fig. 2.13) makes the analyses by electron microprobe and by LAM-ICP-MS difficult to perform. Experiment CP109 was prepared at 200 MPa, 750 °C, using 80 wt. % wollastonite nephelinite HOL14 and 20 wt. % silicate-bearing natrocarbonatite OL5 in the starting composition. It contains a large carbonate globule that could be analysed easily, but the silicate liquid could not be analysed because of the high crystallinity of the experiment (Fig. 2.14). Experiment CP19 was prepared at 40 MPa, 900 °C, using 90 wt. % wollastonite nephelinite HOL14 and 10 wt. % silicate-bearing natrocarbonatite OL5 in the starting composition. Since it is a high-temperature experiment, it is not highly crystallised and the silicate liquid could be analysed. However, due to the low weight fraction of OL5 in the starting composition, the carbonate liquid is not readily analysed because only small pockets were found (Fig. 2.15).

The optimal size of the electron microprobe beam is 25 μm in diameter for the silicate glass and a 40 μm * 50 μm raster for the quenched carbonate liquid. The optimal size for the laser beam is 100 μm in diameter for the silicate glass and for the quenched carbonate liquid. The problem with analysing small pockets of silicate glass and quenched carbonate liquid with electron microprobe is that the smaller the size of the beam, the higher the alkali-volatilisation. The problem with analysing small pockets of silicate glass and quenched carbonate liquid with LAM-ICP-MS is that the smaller the size of the beam, the smaller the volume ablated and the higher the detection limits.

The SEM photographs of the runs products also illustrate that the size of the crystals is typically 20 to 30 μm in diameter, and is often less. This can be a limit for the LAM-ICP-MS analyses because the laser beam cannot be less then 10 μm in diameter.

2.5.2: Carbonate liquid quenched texture

The carbonate liquid does not quench to glass. Instead it is characterised by an intergrowth of coarser grained nyerereite with a finer grained mixture of gregoryite, salts and various other quenched products (see Fig. 2.10). Genge et al. (1995) showed that the formation of glasses in carbonatitic systems was problematic because they are unpolymerised, ionic materials that are unable to form the rigid three-dimensional network structures demonstrated by most glass-forming materials. Additionally, the low viscosities and densities of carbonate melts (Janz et al., 1979; Dawson et al., 1990) and the high mobilities of their component species (Spedding and Mills, 1965) are unfavourable to glass formation since they facilitate spontaneous crystallisation.

2.5.2.1: Polishing problems

Polishing problems arose because of the differential hardness of alkali salts and carbonate solids. The presence of sodium-rich carbonates and salts prevented the use of water or alcohol at any stage of the polishing. Therefore polishing oil was used, with acetone for cleaning between the different stages. Two different methods of polishing were used at MUN and at the GSC. At MUN, polishing laps (30 μm, 9 μm) were used for the first two steps; whereas in Ottawa, aluminium powder (400 grit, 800 grit) was used. The final stages were the same at MUN and in Ottawa (6 μm and 1 μm diamond powder on TEXMET© 2000 polishing cloth).

Another polishing problem associated with the quenched texture of carbonate liquid is that interstitial, finer grained material between coarse grained nyerereite tends to pluck during polishing. In order to limit the plucking, polishing with coarse grit was limited to the removal of the superficial epoxy.

2.5.2.2: Difficulty in obtaining a representative analysis

The quenched texture also produces problems with respect to the analysis of a representative sample by EMP and LAM-ICP-MS. The carbonate liquid is highly heterogeneous because of its quenched texture; therefore as many analyses as possible have to be made in order to provide a representative analysis of the sample.

The aim of this section is to present the variety of quenching styles that may be developed by carbonate liquid in different experiments, and the impact that the quenching style has on the facility or the difficulty in acquiring a representative analysis of the carbonate liquid. First, generalities about nucleation and crystal growth will be presented (see Dowty, 1980; Lofgren, 1980), followed by a presentation of the styles of quenching that may be observed in carbonate liquids in the experiments of this study. Subsequently a discussion will be made of how representative the analyses may be according to the quenching style, and how this can be evaluated (and corrected in a few instances) when processing the data in Chapter 3 and 4.

A rapid quench can bring a physical system into a metastable state which is characterised by a prolonged lifetime (Abraham, 1974; Debenedetti, 1996). The latter is determined by the intensity of nucleation and growth of the phase(s) (Shneidman, 1999). An enormous variety of nucleation models (both "classical" or "nonclassical") are used to explain or predict the observed behaviour (Shneidman, 1999).

Dowty (1980) showed that nucleation can be classified as either homogeneous, if it arises entirely through random thermal fluctuations in the liquid, or heterogeneous, if the presence of another phase in contact with the liquids facilitates the process. This other phase may be a pre-existing crystal (*i.e.* stable before the quench) or the capsule wall, whose smoothness might vary in space. A nucleus larger than the "critical nucleus" will grow spontaneously, but any smaller nucleus is unstable and prone to dissolution. Lofgren (1980) defined the incubation period as the time required for nucleation to occur once a melt is lowered to a crystallisation temperature, and showed that this parameter can be an especially important variable in cooling experiments.

Dowty (1980) showed that in high-supercooling regimes, the volume diffusion (transport within the liquid) has the main control on the growth rate of crystals. Not only transport in the liquid controls the growth rate (of crystals), but also limited diffusion might produce diffusion gradients in the liquid, which causes the composition at the interface to differ from that in the main body of the liquid, away from the crystals. In this case, if the element in question is partitioned into the liquid, its concentration in the crystals is greater than would be predicted from the bulk liquid composition, and if it is partitioned into the crystal, its concentration is less.

The occurrence of adsorption adds further complications. Elements adsorbed on the surface of a crystal may interfere with the uptake of the crystal constituents, thus slowing or poisoning growth. In addition to slowing the growth in some cases, adsorbed foreign atoms may be incorporated into the crystal. The occurrence of sector zoning in igneous minerals seems to demonstrate that adsorption has some effect, and at least the majority of sector-zoning models assume the importance of adsorption (Dowty, 1980).

For this study, two different types of crystals that may form during the quench will be distinguished. The first type of crystals, termed "quenched crystals", are new phases that grow from new nuclei, and not on pre-existing crystals. The second type of crystals, termed "quenched overgrowths", are phases that crystallise on pre-existing crystals that were present before the quench. Although the quench overgrowth is the same mineral as the crystal around which it grows, the composition of the overgrowth (rim) is not necessarily the same as the composition of the pre-existing crystal (core) because during quench, there is surface equilibrium only.

Lofgren (1980) showed that while cooling is an obvious factor in controlling texture, the interaction of cooling with the nucleation kinetics, oxygen fugacity, precooling melt history, and volatiles is important. He also showed that the incubation time varies with cooling rate, and therefore, nucleation does not take place at the same temperature in different experiments conducted on the same liquid cooled at a given rate. In general, the nucleation temperature is depressed as the cooling rate increases.

Nucleation, however, is a random, statistical process, and even for the same cooling rate, nucleation may not occur at the same temperature or rate. In conclusion, the quenching style may vary significantly from sample to sample because it is affected by many parameters, and because of the randomness of nucleation.

Depending on the quenching style, the individual major (and trace) element compositions of the quenched liquid can be somewhat variable. If no quench overgrowths form on pre-existing crystals or capsule wall (homogeneous nucleation), the major element composition of the carbonate liquid will not be modified during the quenching process (case 1). If quench phases are evenly distributed throughout the liquid (at the scale of the microprobe or laser beam), the compositions of individual analyses of the liquid will be close to the expected composition of the carbonate liquid (case 1a). If quench phases are not evenly distributed throughout the liquid, then scatter may be expected for the analyses of the liquid (case 1b). If quench overgrowths do form on pre-existing crystals or if crystals form on capsule wall (heterogeneous nucleation), the major element composition of the carbonate liquid will be modified during the quench (case 2). Moreover, remaining quench phases within the carbonate liquid may be distributed evenly (case 2a) or not (case 2b).

The reason why some phases may not be evenly distributed can be: 1) some quenched crystals might form preferentially close to pre-existing crystals, even if they are not overgrowths; and 2) crystals might settle down within the capsule. The SEM photographs indicate that both quenched crystals and quenched overgrowths (zoned crystals) form in the experiments of this study. Quenched phases in the carbonate liquid may have an extremely exotic mineralogy. Scattered, bright crystals are visible on SEM pictures, that can be disseminated randomly or as clusters in the liquid, or form preferentially close to pre-existing crystals. If nyerereite needles form at an early stage of the quench and connect each other, then the interstitial liquid might not be able to circulate and the carbonate liquid is not expected to be heterogeneous at the scale of the needle. On the other hand, if exotic crystals form first, they can affect the composition of the liquid significantly over a larger scale.

Quenched crystals (and to a lesser degree quenched overgrowths) may contain significant amounts of some elements, especially trace elements (*e.g.* REE, Nb, Ta, Zr, Hf, U and Th). The presence of these crystals may lead to a difficulty in obtaining representative analyses of the carbonate liquid that may be more or less heterogeneous. Therefore, the effect of the quenching on liquid compositions will be evaluated in Chapter 3 and 4, when presenting major and trace element data on the experiments.

2.5.3: Difficulties in analysing carbonate phases

Difficulties arose when analysing carbonate phases, especially crystal phases (nyerereite and gregoryite). In order to quantify this analytical problem and to determine its relation to the analytical conditions, carbonate phases from the silicate-free natrocarbonatite CML5 (donated by Dr. Tony Peterson) were analysed at MUN and also at Harvard University (by Joy Reid) for comparison. The analyses are reported in Table 2.3, together with EMP analyses of the same phases, performed at Berkeley by Dr. Tony Peterson (see Peterson, 1990). Individual analyses of phases from silicate-free natrocarbonatite CML5 are given in Table A2.2 (Appendix A2). Moreover, carbonate phases from selected experiments were analysed at MUN and also at Harvard University by Joy Reid. The analyses are compared in Table 2.4.

There is a fairly good agreement between the analyses of the CML5 groundmass performed at MUN and those performed at Harvard and Berkeley (Tab. 2.3). The concentrations of major elements determined at MUN are usually intermediate between those determined in the two other laboratories. Note, however, that the total of the analysis performed at Harvard is low (79.3 wt. %). Table 2.4 shows that analyses of carbonate liquid from experiments CP117 and CP108 performed at MUN and at Harvard are in good agreement with each other. Figure 2.16 also shows that during the first 60 s of an analysis of an OL5-experiment, no Na or Cl loss was noticed. Slight loss of these two elements occurred after 60 s, whereas the signal of F, on the other hand, tended to increase during data collection.

Examination of Table 2.3 shows that for nyerereite from lava CML5, data acquired at Harvard and at Berkeley are in good agreement with each other, whereas those acquired at MUN show low concentrations of Na_2O, SO_3, F and Cl, and high concentrations of the remaining elements. Figure 2.17 shows that at MUN, the signal for Na decreased during data acquisition (sodium volatilisation), whereas the signals for K and Ca increased. On the other hand, the signals for Na and K at Harvard did not vary significantly during acquisition. Because of the Na volatilisation problem encountered at MUN (but not at Harvard or Berkeley), the data acquired on nyerereite of CML5 were used to calculate a correction factor for most elements (in Tab. 2.3). The correction factor is the ratio between the concentrations in Peterson (1990) and the concentrations measured at MUN. The correction factor is applied to the raw analyses of nyerereite analysed at MUN. Table 2.4 illustrates that the analyses of nyerereite from experiment CP108 show a discrepancy between MUN and Harvard similar to that noted on nyerereite from lava CML5.

Examination of Table 2.3 shows that for gregoryite from lava CML5, data acquired at MUN and at Berkeley are in general good agreement with each other, although, the concentrations obtained at MUN are higher for CaO, SrO, BaO, K_2O, P_2O_5, SO_3 and Cl, and lower for Na_2O and F. Concentrations of most elements are lower when determined at Harvard, even though the signals of Na and K increase with time (Fig. 2.18). They are especially low for Na_2O and CO_2, hence the low total (75.6 wt. %) compared to the total from Berkeley (97.2 wt. %). The reason why the data from MUN are in better agreement with the data collected at Berkeley might be the increasing signal during the acquisition which prevents low totals (Fig. 2.18). The reason why the signal for all elements increases, especially Na, is not understood (but might occur because of CO_2 volatilisation). The data acquired on gregoryite of CML5 were used to calculated a correction factor for most elements (in Tab. 2.3), in a similar way as for nyerereite. Table 2.4 illustrates that the analyses of gregoryite from experiment CP112 show a discrepancy between MUN and Harvard similar to that noted on nyerereite from CML5.

The discrepancies between the data collected in three different laboratories are due to different running conditions used: spectrometry (WDS at Berkeley and Harvard, EDS at MUN), counting time, standardisation (more appropriate standards used by Peterson, 1990), current (15 nA at Berkeley and Harvard, 10 nA at MUN), beam diameter (20 μm at Berkeley, 10 μm at MUN and 100 μm x 100 μm raster at Harvard).

2.5.4: Error bars

Due to the experimental and analytical difficulties, the standard deviation for most elements in liquid and crystal phases is often fairly high. In order not to overload the plots, error bars are not plotted on many figures. However, details on the calculation of standard deviation for concentration and partitioning plots are given in Appendix A2.

2.5.5: Reversal experiments

No reversal experiments could be made to check for equilibrium because of nucleation of metastable, high-Ti clinopyroxene crystals (see, Kjarsgaard et al., 1995). However, equilibrium is thought to have been achieved in most experiments for the following reasons: 1) the melilite crystals criss-cross the two conjugate liquids in experiments CP14 and CP22 (Fig. 2.12); and 2) the experimental charge CP16 and its duplicate CP65 were run, respectively, for 166 and 476 hours. They have similar phase assemblages (see Tab. 3.1 in next chapter), which suggests that equilibrium was achieved after 166 hours.

Tab 2.1: Standards used for electron microprobe analyses.

	MUN	GSC
Na	NaBePO	NaCl
Sr	celestite	strontianite
Mg	periclase	periclase
Al	corundum	topaz
Si	quartz	topaz
S	$BaSO_4$	ZnS
K	microcline	KBr
Ca	wollastonite	wollastonite
Mn	$MnTiO_3$	Mn
Fe	hematite	Fe
P	apatite	apatite
Ba	barite	SANBI
Cl	tugtupite	NaCl
F	fluorite	topaz
Ti	ilmenite	Ti

Table 2.2: Major and trace element analyses of starting materials (wollastonite nephelinite HOL14 and silicate-bearing natrocarbonatite OL5), and major and trace element compositions of the starting mixtures shown as proportions of HOL14/OL5 (in wt. %).

	HOL14	OL5	95/5	90/10	80/20	70/30	50/50	40/60	30/70	20/80	10/90
wt%											
SiO2	45.70	3.20	43.6	41.5	37.2	33.0	24.5	20.2	16.0	11.7	7.45
TiO2	0.97	0.10	0.93	0.88	0.80	0.71	0.54	0.45	0.36	0.27	0.19
Al2O3	15.90	0.90	15.2	14.4	12.9	11.4	8.40	6.90	5.40	3.90	2.40
Fe2O3	5.10	1.44	4.92	4.73	4.37	4.00	3.27	2.90	2.54	2.17	1.81
FeO	3.10	n.d.	2.95	2.79	2.48	2.17	1.55	1.24	0.93	0.62	0.31
MnO	0.30	0.35	0.30	0.31	0.31	0.32	0.33	0.33	0.34	0.34	0.35
MgO	0.78	0.40	0.76	0.74	0.70	0.67	0.59	0.55	0.51	0.48	0.44
CaO	5.94	15.4	6.41	6.89	7.83	8.78	10.7	11.6	12.6	13.5	14.5
Na2O	11.40	28.3	12.2	13.1	14.8	16.5	19.9	21.5	23.2	24.9	26.6
K2O	4.99	6.13	5.05	5.10	5.22	5.33	5.56	5.67	5.79	5.90	6.02
P2O5	0.28	1.07	0.32	0.36	0.44	0.52	0.68	0.75	0.83	0.91	0.99
H2Ot	3.40	b.d.	3.23	3.06	2.72	2.38	1.70	1.36	1.02	0.68	0.34
CO2	0.80	30.4	2.28	3.76	6.72	9.68	15.6	18.6	21.5	24.5	27.4
F	0.22	1.64	0.29	0.36	0.51	0.65	0.93	1.07	1.21	1.36	1.50
Cl	0.29	2.54	0.40	0.51	0.74	0.96	1.41	1.64	1.86	2.09	2.31
SO3	0.31	2.55	0.42	0.53	0.76	0.98	1.43	1.65	1.88	2.10	2.33
Total	99.48	94.42	99.23	98.97	98.47	97.96	96.95	96.44	95.94	95.43	94.93
ppm											
V	160	129	158	157	154	151	145	141	138	135	132
Rb	102	151	104	107	112	116	126	131	136	141	146
Sr	2127	9465	2493	2860	3594	4328	5796	6530	7263	7997	8731
Ba	1653	8390	1990	2327	3001	3674	5022	5695	6369	7043	7716
Y	37.6	14.9	36.4	35.3	33.0	30.8	26.2	24.0	21.7	19.4	17.2
La	89.4	430	106	123	158	192	260	294	328	362	396
Ce	121	512	141	160	199	238	317	356	395	434	473
Nd	36.4	104	39.8	43.2	49.9	56.7	70.2	77.0	83.7	90.5	97.2
Sm	6.59	9.4	6.73	6.87	7.15	7.43	7.99	8.28	8.56	8.84	9.12
Eu	2.13	2.3	2.14	2.15	2.17	2.18	2.22	2.23	2.25	2.27	2.28
Gd	6.31	4.6	6.22	6.14	5.97	5.79	5.45	5.28	5.11	4.94	4.77
Dy	5.74	2.2	5.56	5.39	5.03	4.68	3.97	3.62	3.26	2.91	2.55
Er	3.26	1.1	3.15	3.04	2.83	2.61	2.18	1.96	1.75	1.53	1.32
Yb	3.09	0.1	2.94	2.79	2.50	2.20	1.60	1.30	1.00	0.70	0.40
Lu	0.44	0.05	0.42	0.40	0.36	0.32	0.24	0.20	0.17	0.13	0.09
Zr	929	55	885	841	754	666	492	404	317	230	142
Hf	15.2	0.8	14.5	13.7	12.3	10.9	7.99	6.55	5.11	3.68	2.24
Nb	280	75.2	270	260	239	219	178	157	137	116	95.7
Ta	2.93	0.21	2.79	2.66	2.38	2.11	1.57	1.30	1.03	0.75	0.48
Th	8.30	9.4	8.36	8.41	8.52	8.63	8.85	8.96	9.07	9.18	9.29
U	6.92	9.7	7.05	7.19	7.47	7.75	8.31	8.59	8.86	9.14	9.42

Note: Major element composition of HOL14 determined by XRF (from Peterson, 1989a). Major element composition of OL5 determined by ICPES (Belanger), except for F, Cl, CO2, H2O and SO3 performed by Analytical Chemistry, GSC Ottawa.
Trace element composition of HOL14 determined by solution ICP-MS at MUN (except for V, from Peterson, 1989a). Trace element composition of OL5 determined by solution ICP-MS by Simonetti et al. (1997), except for V determined by XRF on fused glass disks and for Ba determined by INNA (from Simonetti et al., 1997).

Table 2.3: Microprobe analyses from three different institutions (Harvard, Berkeley, MUN) of groundmass, nyerereite and gregoryite from sample CML5. For some elements, the calculation of a correction factor (C.F.) was done by ratioing the concentrations measured at Berkeley with those obtained at MUN

Groundmass CML5				Nyerereite CML5					Gregoryite CML5				
	Harvard	Berkeley	MUN		Harvard	Berkeley	MUN	C.F.		Harvard	Berkeley	MUN	C.F.
FeO	0.25	0.21	n.d.	FeO	0.01	0.02	n.d.	n.c.	FeO	0.04	0.04	b.d.	n.c.
MnO	0.30	0.21	0.48	MnO	0.06	0.05	n.d.	n.c.	MnO	0.06	0.06	n.d.	n.c.
MgO	0.17	0.54	0.66	MgO	0.04	0.09	b.d.	n.c.	MgO	0.03	0.13	n.d.	n.c.
CaO	9.10	12.66	11.73	CaO	24.35	24.43	32.55	0.7504	CaO	5.45	8.67	9.94	0.8720
SrO	0.90	1.66	1.57	SrO	2.01	2.24	3.06	0.7324	SrO	0.43	0.79	0.90	0.8778
BaO	1.07	1.63	2.05	BaO	0.63	0.58	0.89	0.6891	BaO	0.32	0.28	0.50	0.5600
Na2O	27.64	34.59	27.83	Na2O	22.18	23.53	14.42	1.6321	Na2O	33.55	43.16	37.47	1.1518
K2O	6.33	9.76	7.44	K2O	7.71	7.87	9.64	0.8166	K2O	3.14	4.11	4.96	0.8291
CO2 stoi	26.14	27.48	n.d.	CO2 stoi	38.57	39.35	n.d.		CO2 stoi	27.2	33.01	n.d.	
P2O5	0.50	0.68	0.60	P2O5	0.53	0.37	0.53	0.6938	P2O5	1.35	2.04	2.78	0.7342
SO3	2.65	3.24	2.75	SO3	1.15	1.12	1.12	1.0030	SO3	3.50	4.24	4.86	0.8729
F	0.96	4.42	2.05	F	0.05	0.27	0.20	1.3500	F	0.09	0.40	0.20	1.9753
Cl	3.33	6.04	3.73	Cl	0.26	0.25	0.19	1.3187	Cl	0.46	0.55	0.56	0.9872
Total	79.33	100.00		Total	97.54	99.98			Total	75.62	97.19		

Note: Analyses at Harvard University by Joy Reid and at Berkeley by Tony Peterson (see Peterson, 1990).
** Note that for nyerereite and gregoryite analysed at Berkeley, the analysis is for the average of CML5 and CML9, a similar silicate-free natrocarbonatite. CO2 stoi = CO2 calculated for perfect stoichiometry.
Abbreviations used are: n.d.: not determined; b.d.: below detection; n.c.: not corrected.

Table 2.4: Electron microprobe analyses of nyerereite, gregoryite and carbonate liquid (LC) from selected experiments. Comparison between data from Harvard University (by Joy Reid) and data from MUN.

Phase	Nyerereite	Nyerereite	Gregoryite	Gregoryite	LC	LC	LC	LC
Experiment	CP108	CP108	CP112	CP112	CP117	CP117	CP108	CP108
Institution	Harvard	MUN	Harvard	MUN	Harvard	MUN	Harvard	MUN
FeO	0.03	0.20	0.15	b.d.	1.41	1.61	0.32	0.52
MnO	0.08	b.d.	0.12	b.d.	0.33	0.33	0.34	0.41
MgO	0.02	b.d.	0.03	b.d.	0.27	0.36	0.17	0.30
CaO	25.26	33.10	7.22	11.25	13.70	13.65	11.81	13.22
SrO	1.56	2.40	0.52	0.85	1.03	1.17	1.12	1.53
BaO	0.36	0.50	0.16	0.40	0.80	0.63	1.10	1.21
Na2O	23.56	16.45	39.36	36.95	22.09	23.97	27.95	28.87
K2O	5.70	7.27	2.27	4.10	5.21	4.53	7.85	6.78
Al2O3	0.01	b.d.	b.d.	b.d.	2.30	2.65	0.02	0.20
SiO2	0.03	0.20	b.d.	b.d.	6.06	5.51	0.23	0.50
TiO2	0.03	0.03	b.d.	b.d.	0.13	0.12	0.01	0.03
CO2	41.25	n.a.	44.13	n.a.	39.94	n.a.	35.38	n.a.
P2O5	0.78	0.77	1.66	2.60	1.03	1.04	0.75	0.89
SO3	1.12	1.13	3.83	5.10	2.39	2.25	3.28	3.06
F	0.06	b.d.	0.21	0.55	2.06	1.06	4.36	4.44
Cl	0.14	0.08	0.33	0.25	1.23	1.01	5.31	2.83
Total	100.00	61.80	100.00	61.80	100.00	59.56	100.00	64.33

Note: b.d.: below detection; n.a.: not analyzed. Note that the analyses from Harvard were calculated for a total of 100 wt. %. Note also that the data obtained at MUN are not filtered or corrected, and therefore, may differ from the data that will be presented in the next chapters.

Figure 2.1: Schematic of the laser ablation microprobe solid sample introduction system (a) and of the ICP-MS (b). a). The ablated sample is carried from the sample cell to the ICP by the Ar nebulizer gas using 1-2 m of flexible tubing. M1 is a beam sample, M2 and M3 are mirrors, P is a half wave plate, and PM is the power meter (from Jackson et al., 1992). b) schematic diagram of the PlasmaQuad ICP-MS.

a

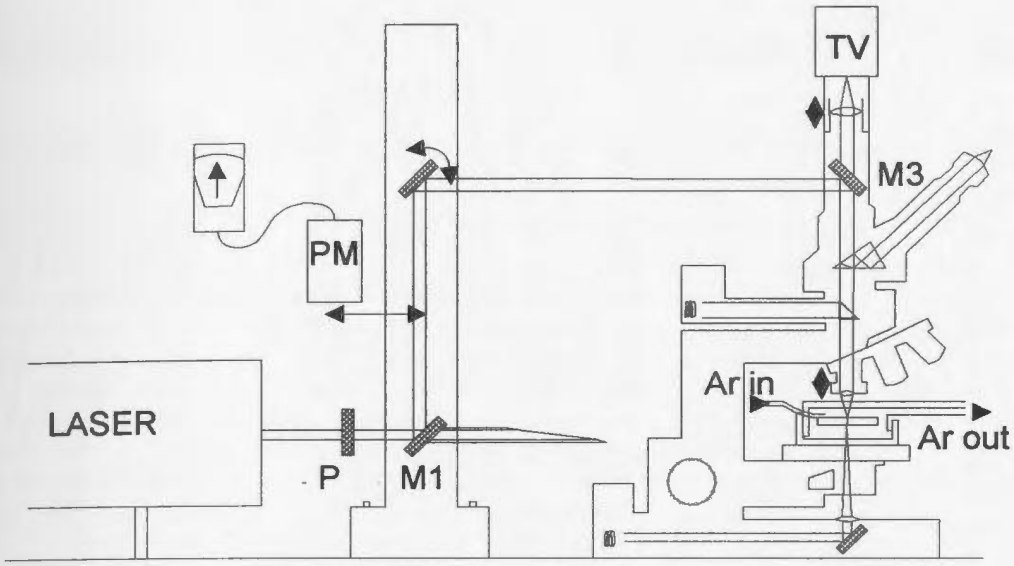
TV
M3
PM
LASER
P
M1
Ar in
Ar out

b

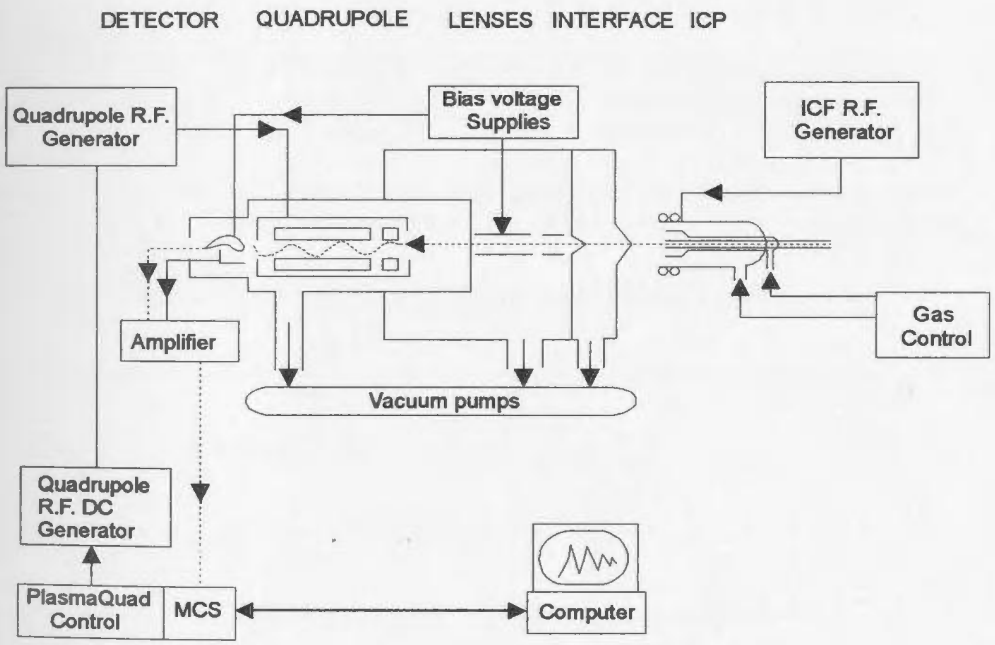
DETECTOR
QUADRUPOLE
LENSES
INTERFACE
ICP
Quadrupole R.F. Generator
Bias voltage Supplies
ICF R.F. Generator
Amplifier
Gas Control
Vacuum pumps
Quadrupole R.F. DC Generator
PlasmaQuad Control
MCS
Computer

Figure 2.2: Average sensitivity (in cps/ppm) of the LAM-ICP-MS determined for glass NIST 610, normalised to the abundance.

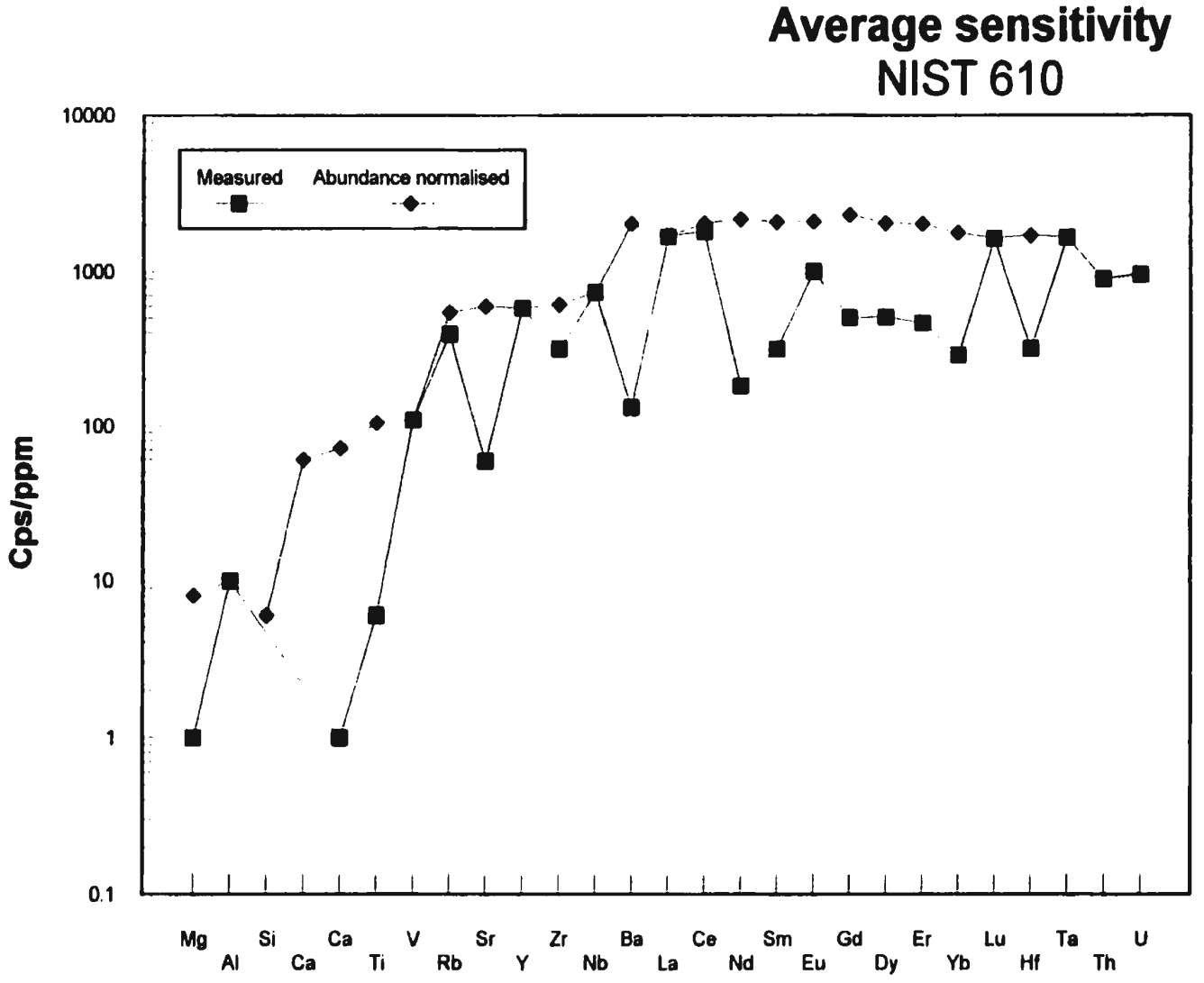
Average sensitivity
NIST 610
Measured
Abundance normalised
Cps/ppm
10000
1000
100
10
1
0.1
Mg
Al
Si
Ca
Ca
Ti
V
Rb
Sr
Y
Zr
Nb
Ba
La
Ce
Nd
Sm
Eu
Gd
Dy
Er
Yb
Lu
Hf
Ta
Th
U

Figure 2.3a: Signal acquired during an analysis of quenched silicate liquid (beam diameter is ~ 50 μm). The background is recorded for > 50 s, and the signal is selected for < 10 s. At t ~ 70 s, the increase of the Ca, Rb and Sr relative to other signals indicates that the laser has ablated through the sample and was ablating quenched carbonate liquid.

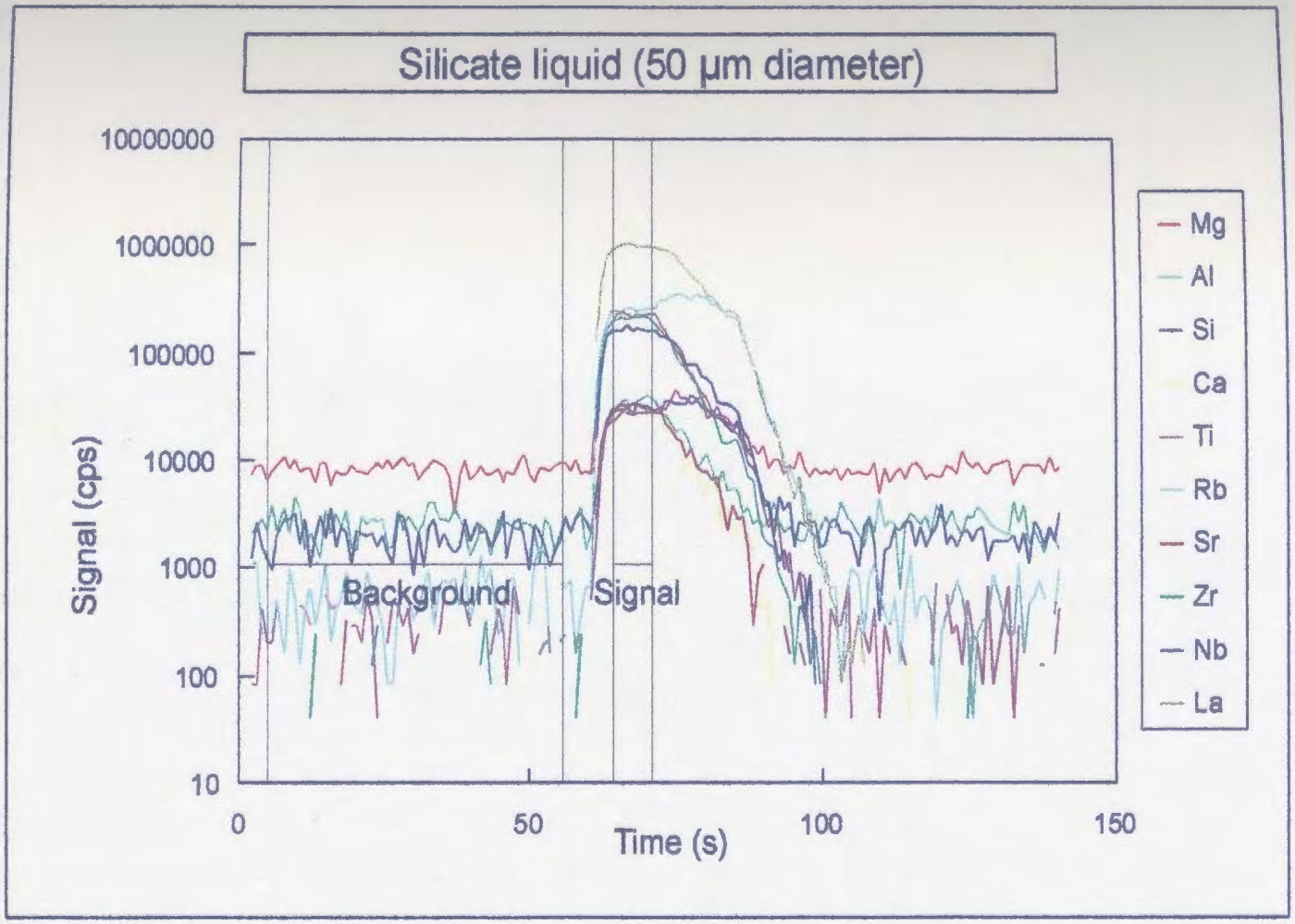
Silicate liquid (50 µm diameter)
10000000
1000000
100000
10000
1000
100
10
Signal (cps)
Background
Signal
0
50
100
150
Time (s)
Mg
Al
Si
Ca
Ti
Rb
Sr
Zr
Nb
La

Figure 2.3b: Signal acquired during an analysis of quenched silicate liquid (beam diameter is ~ 100 μm), for which all elements behave consistently, allowing the signal to be integrated for ~ 60 s.

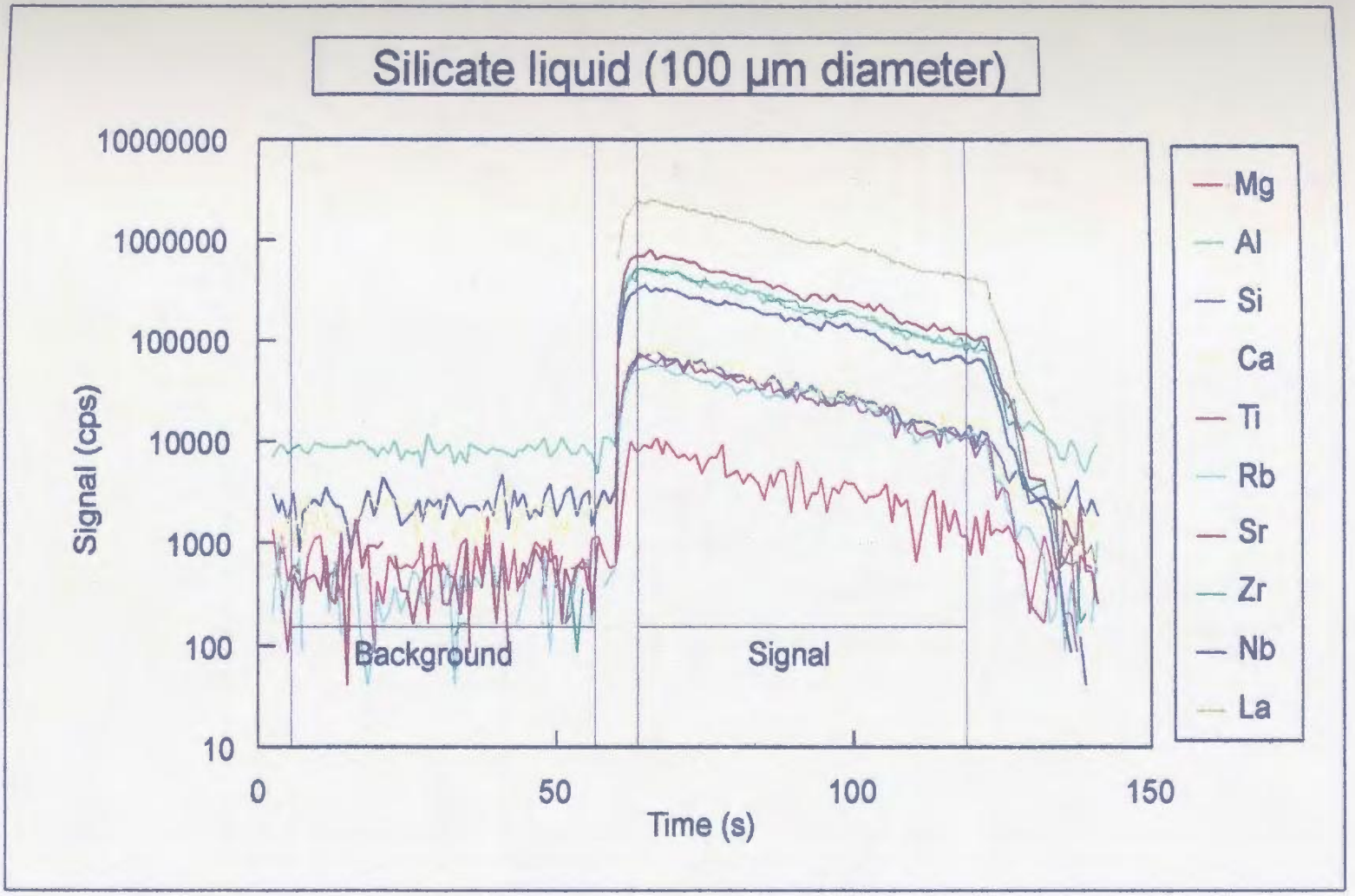
Silicate liquid (100 µm diameter)
10000000
1000000
100000
10000
1000
100
10
Signal (cps)
0
50
100
150
Time (s)
Background
Signal
Mg
Al
Si
Ca
Ti
Rb
Sr
Zr
Nb
La

Figure 2.4: Signal acquired during an analysis of quenched carbonate liquid (beam diameter is ~ 100 μm), for which the signal was integrated for ~ 50 s.

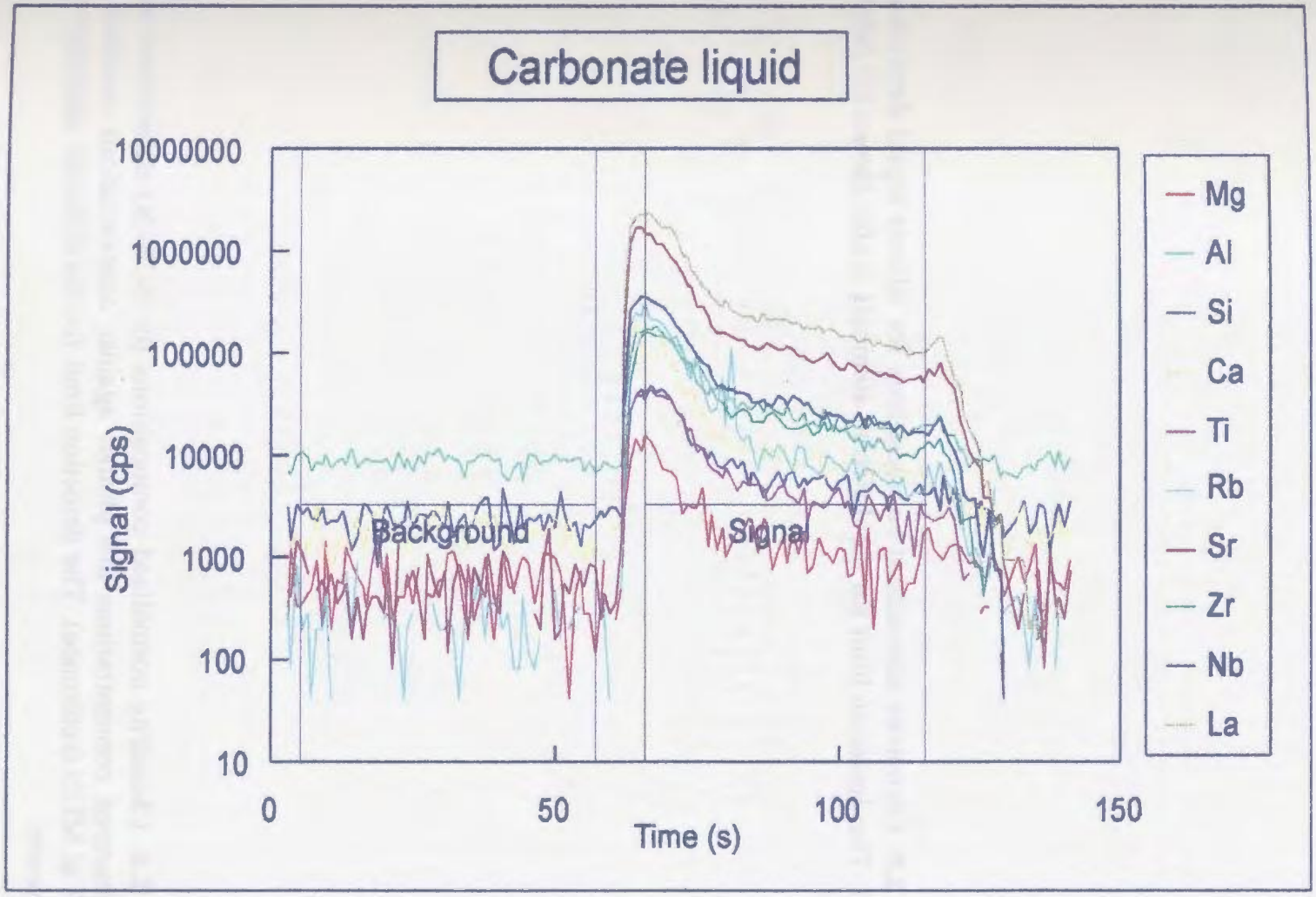
Carbonate liquid
10000000
1000000
100000
10000
1000
100
10
Signal (cps)
Background
Signal
0
50
100
150
Time (s)
Mg
Al
Si
Ca
Ti
Rb
Sr
Zr
Nb
La

Figure 2.5: Chondrite normalised compositions for silicate liquid determined by LAM-ICP-MS. The detection limit for the different elements is also shown for reference.

Figure 2.6: Chondrite normalised compositions for BCR-2G determined by LAM-ICP-MS. Measured concentrations are plotted against concentrations obtained by solution ICP-MS at MUN (reference). The detection limit for the different elements is also shown for reference.

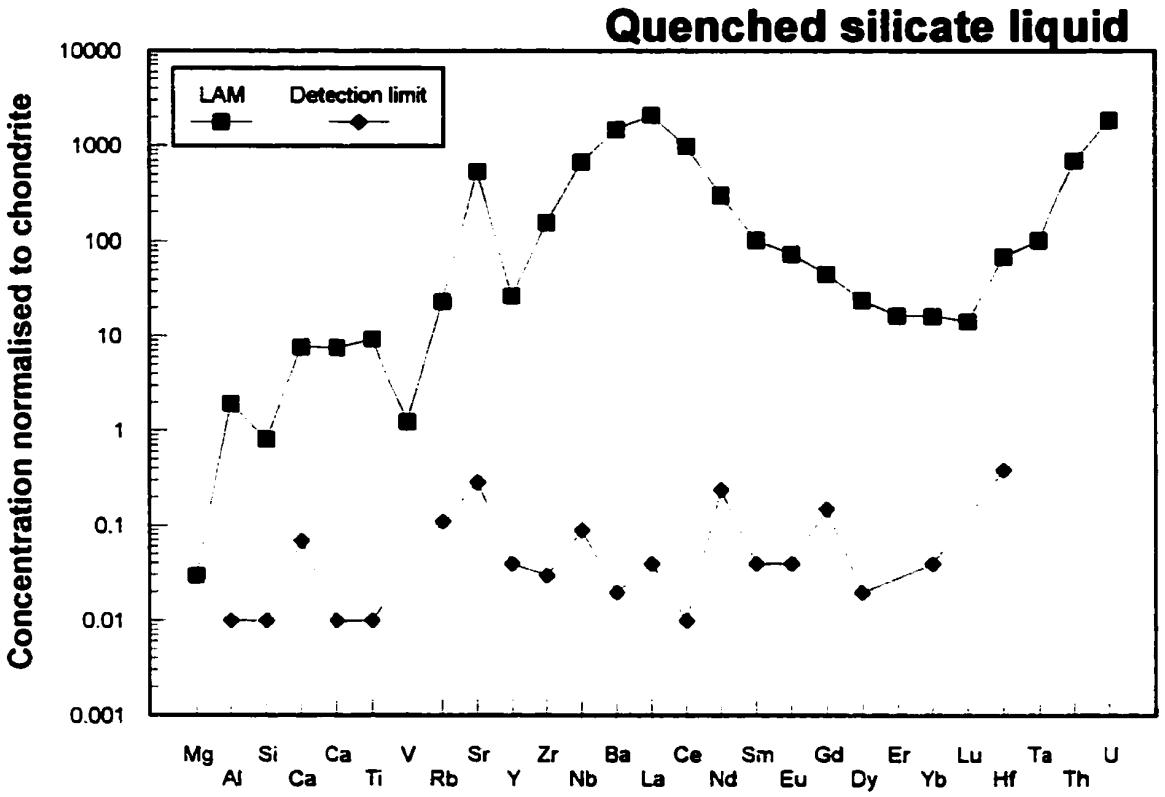
Quenched silicate liquid
LAM
Detection limit
Concentration normalised to chondrite
10000
1000
100
10
1
0.1
0.01
0.001
Mg Al Si Ca Ca Ti V Rb Sr Y Zr Nb Ba La Ce Nd Sm Eu Gd Dy Er Yb Lu Hf Ta Th U

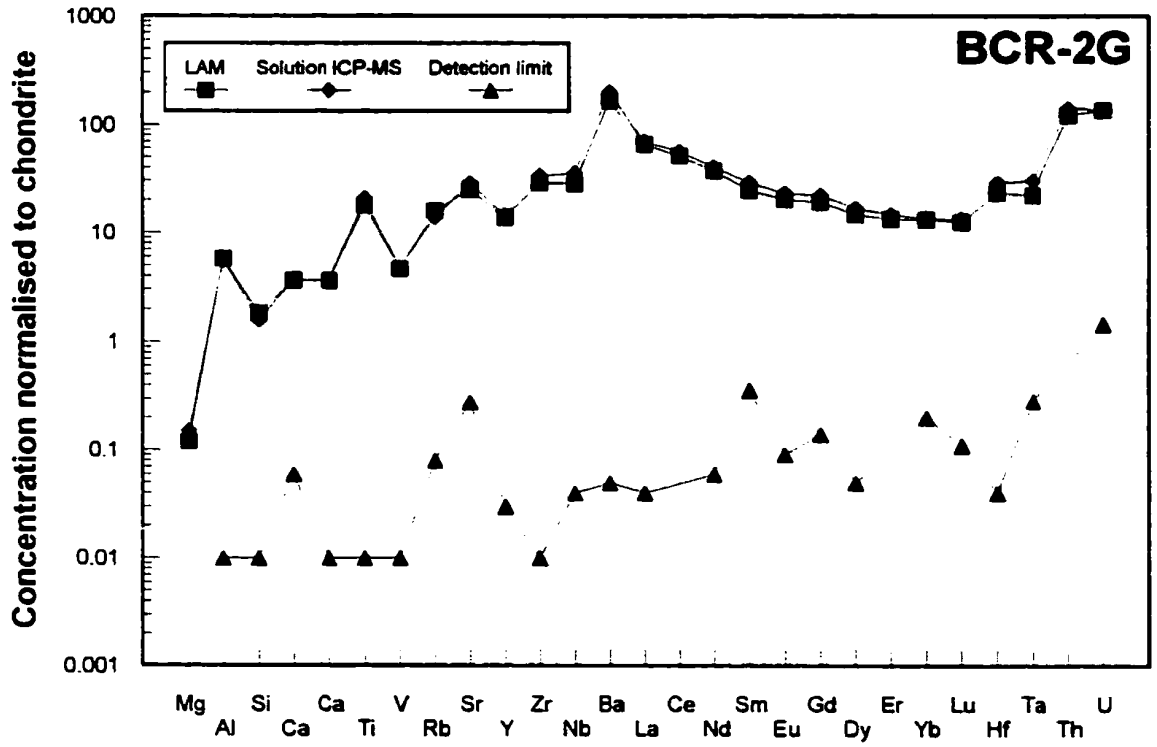
BCR-2G
LAM
Solution ICP-MS
Detection limit
Concentration normalised to chondrite
1000
100
10
1
0.1
0.01
0.001
Mg Al Si Ca Ca Ti V Rb Sr Y Zr Nb Ba La Ce Nd Sm Eu Gd Dy Er Yb Lu Hf Ta Th U

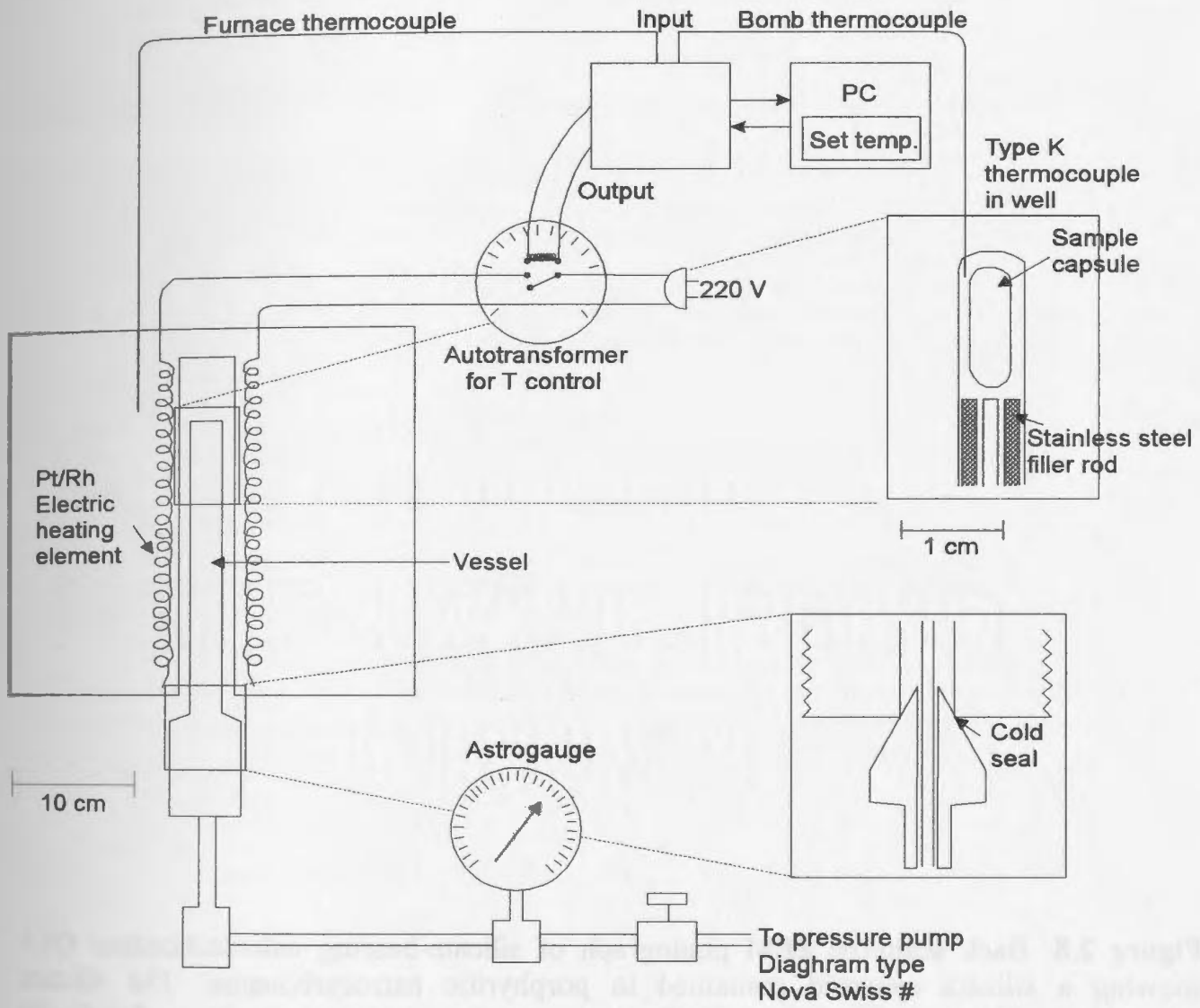

Figure 2.7: Schematic of the experimental apparatus used for the preparation of the samples. From Holloway and Wood (1988).

Figure 2.8: Back scattered SEM photograph of silicate-bearing natrocarbonatite OL5 showing a silicate spheroid contained in porphyritic natrocarbonatite. The silicate spheroid is cored by a phenocryst of clinopyroxene that contains inclusions of melanite garnet and nepheline. One laser pit is visible in the melanite garnet, and two in the clinopyroxene. Microphenocrysts in the groundmass of the spheroid are nepheline, clinopyroxene, melanite garnet, wollastonite and Na-rich gregoryite. The groundmass of the spheroids is of wollastonite nephelinite composition. The surrounding porphyritic natrocarbonatite consists of phenocrysts of nyerereite and gregoryite in a groundmass composed of nyerereite, gregoryite, sylvite and other phases. An isolated phenocryst of wollastonite is also present in the natrocarbonatite. The following abbreviations are used: Wo, wollastonite; Cpx, clinopyroxene; Gt, melanite garnet; Ne, nepheline; NY, nyerereite; GRE, gregoryite.

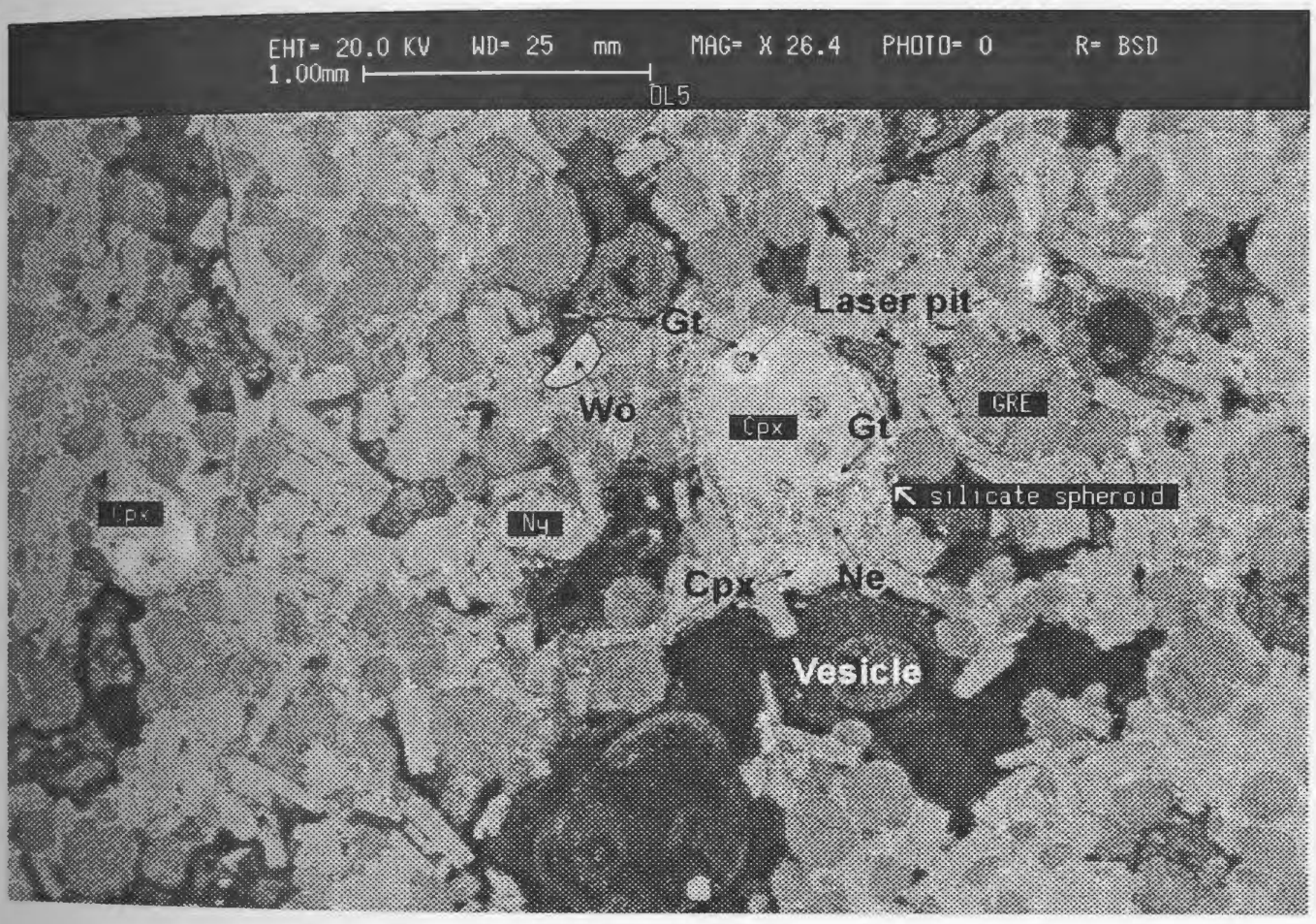
EHT= 20.0 KV WD= 25 mm MAG= X 26.4 PHOTO= 0 R= BSD
1.00mm
DL5
Gt
Laser pit
Wo
Cpx
Gt
GRE
silicate spheroid
Cpx
N4
Cpx
Ne
Vesicle

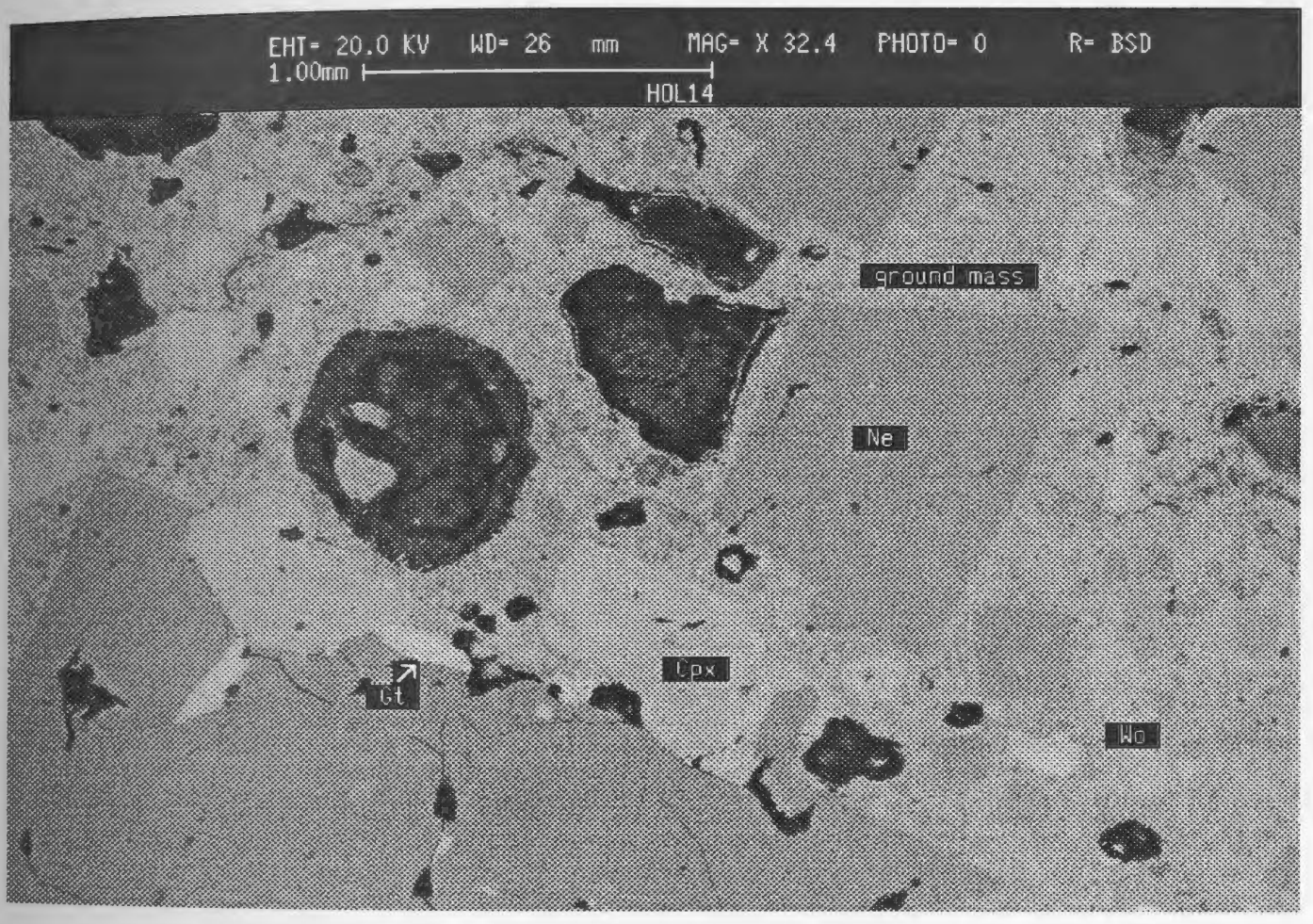

Figure 2.9: Back scattered SEM photograph of wollastonite nephelinite HOL14 showing crystals of nepheline, clinopyroxene, melanite garnet and wollastonite set in a matrix of wollastonite nephelinite composition. The following abbreviations are used: Wo, wollastonite; Cpx, clinopyroxene; Gt, melanite garnet; Ne, nepheline.

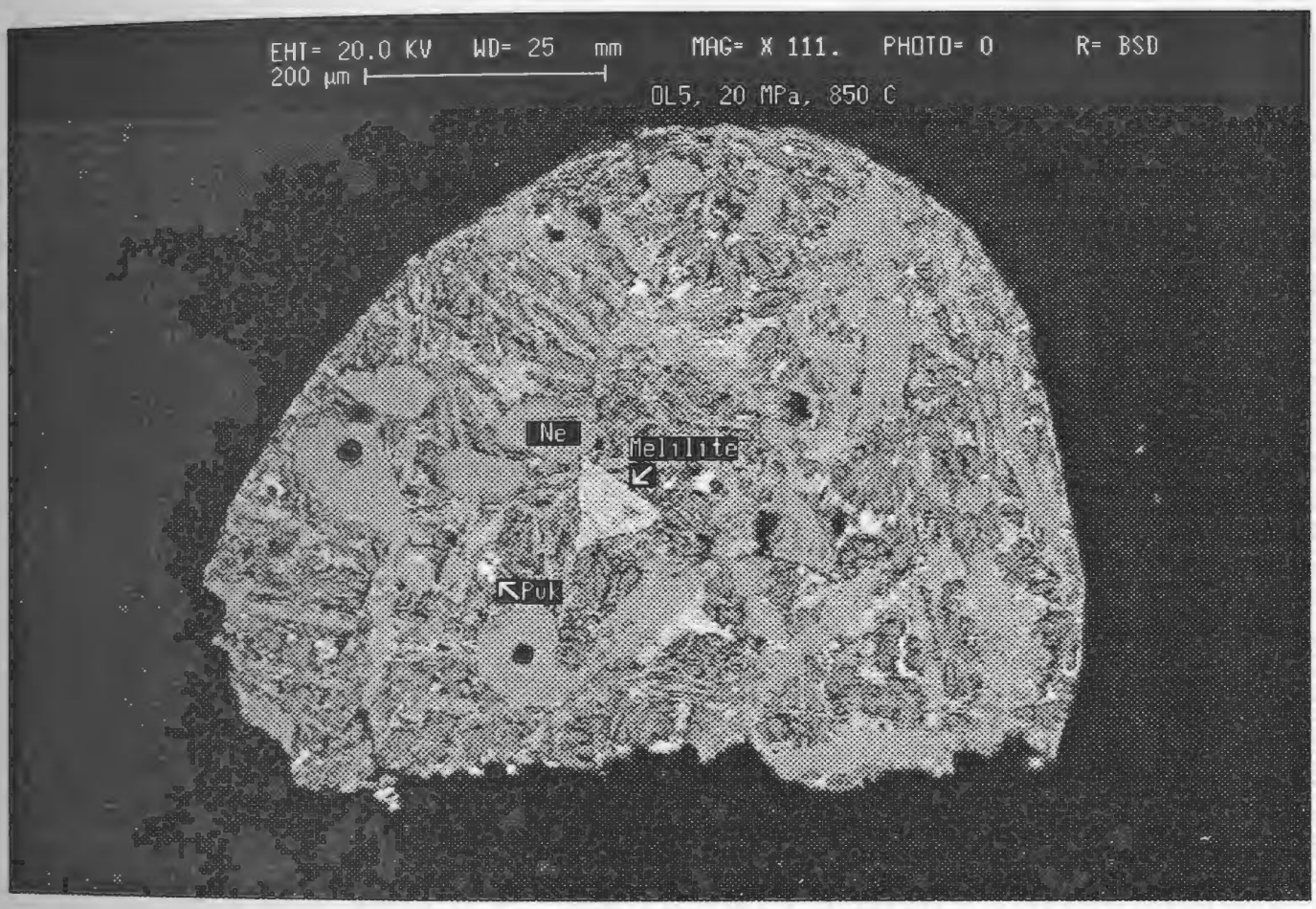

Figure 2.10: Back scattered SEM photograph of experimental charge CP45, prepared at 20 MPa and 850 °C, using 100 wt. % silicate-bearing natrocarbonatite OL5 in the starting composition. Large crystals of melilite and nepheline and smaller crystals of perovskite are set in the quenched carbonate liquid. Laser pits are visible in the nepheline crystals. The following abbreviations are used: Ne, nepheline; Pvk, perovskite.

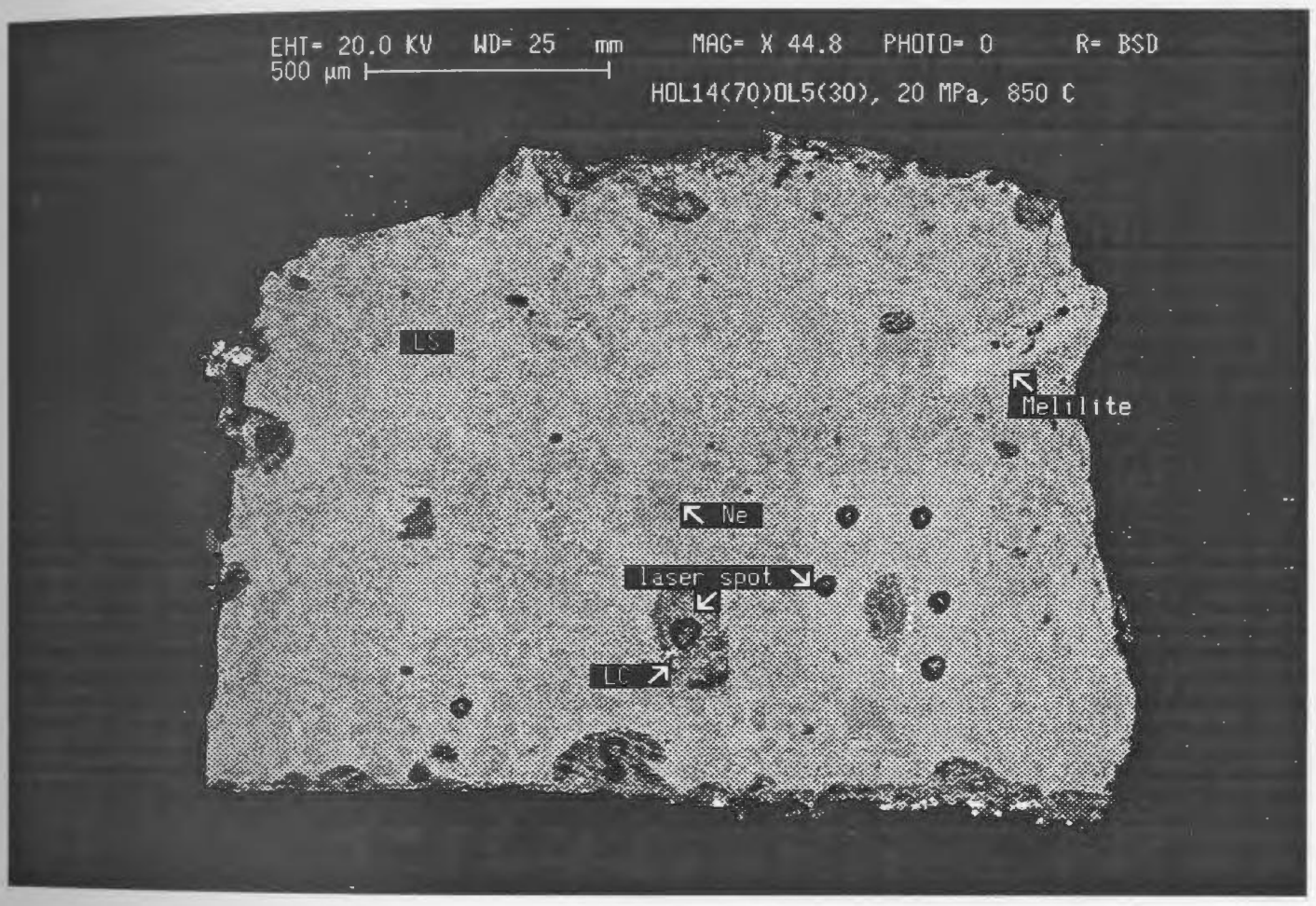

Figure 2.11: Back scattered SEM photograph of experimental charge CP43, prepared at 20 MPa, 850 °C, using 70 wt. % wollastonite nephelinite HOL14 and 30 wt. % silicate-bearing natrocarbonatite OL5 in the starting composition. Large crystals of melilite and nepheline are set in the silicate liquid. Large laser pits are visible in the silicate and carbonate liquids. The following abbreviations are used: Ne, nepheline; LC, carbonate liquid; LS, silicate liquid.

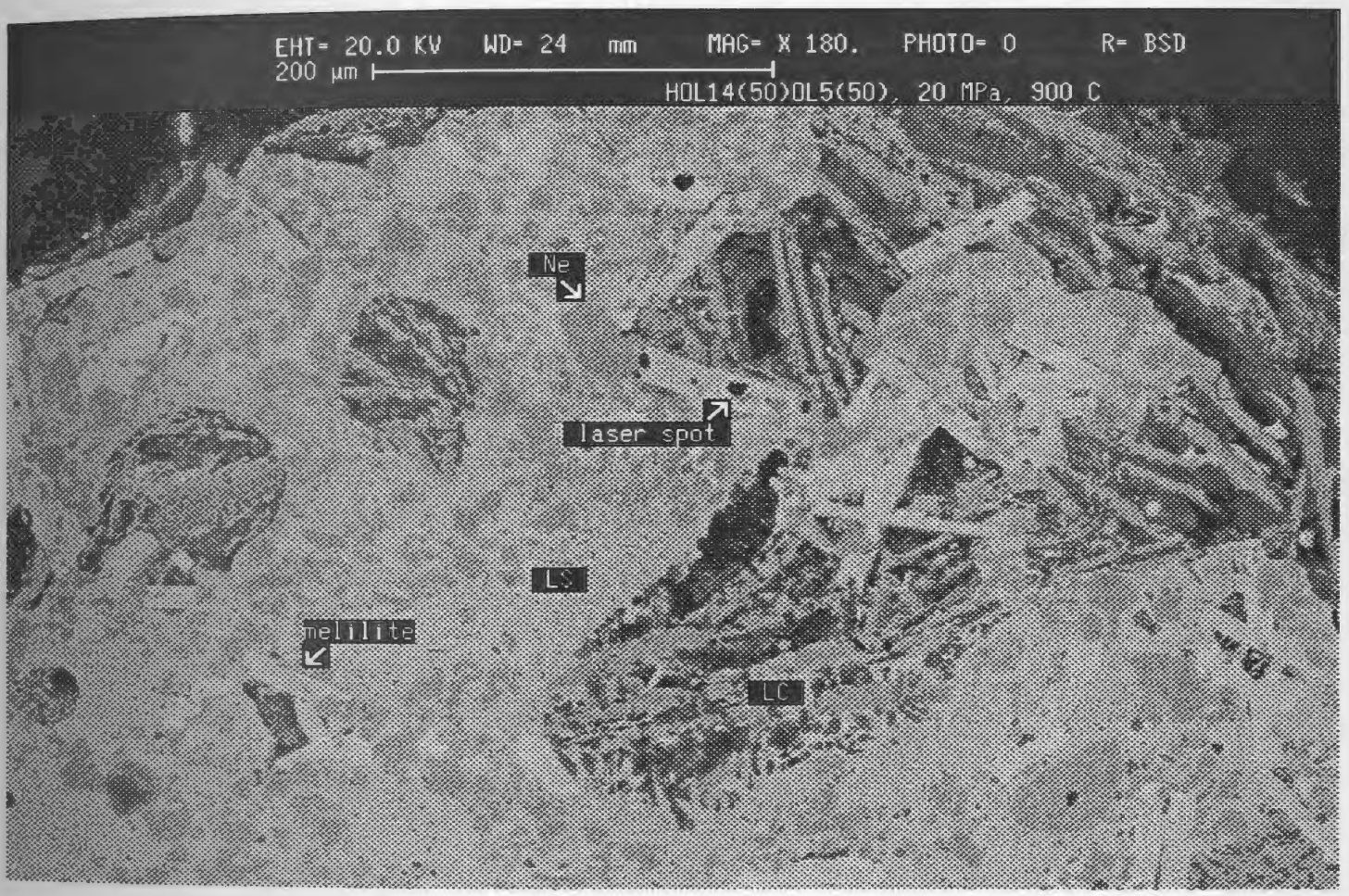

Figure 2.12: Back scattered SEM photograph of experimental charge CP22, prepared at 20 MPa, 900 °C, using 50 wt. % wollastonite nephelinite HOL14 and 50 wt. % silicate-bearing natrocarbonatite OL5 in the starting composition. Crystals of melilite criss-cross the silicate and the carbonate liquids. Large laser pits are visible in the melilite. The following abbreviations are used: Ne, nepheline; LC, carbonate liquid; LS, silicate liquid.

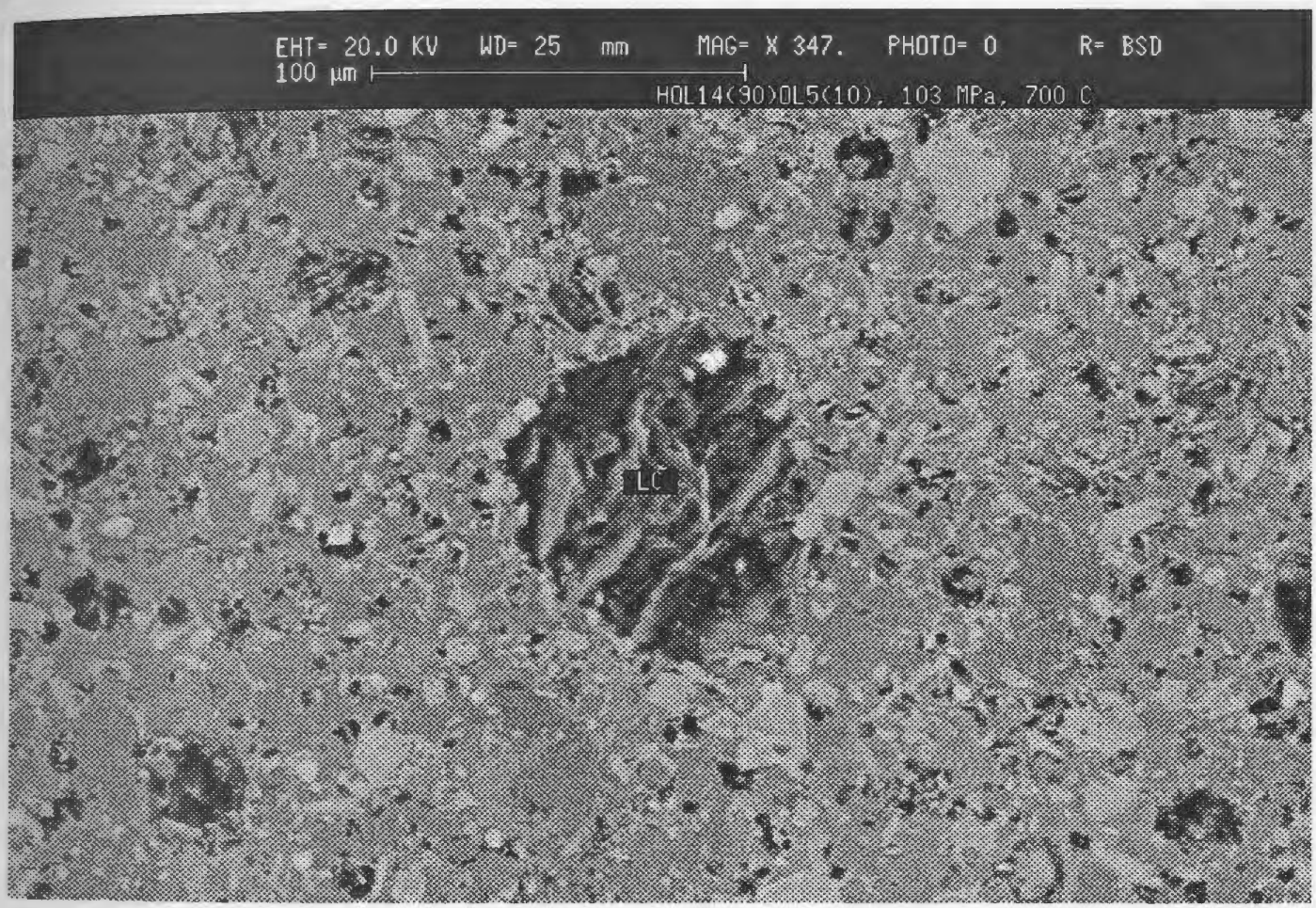

Figure 2.13: Back scattered SEM photograph of experimental charge CP8, prepared at 103 MPa, 700 °C, using 90 wt. % wollastonite nephelinite HOL14 and 10 wt. % silicate-bearing natrocarbonatite OL5 in the starting composition. In this experiment, prepared at low temperature and low weight fraction of OL5 in the starting composition, the carbonate globules are very small (and scarce), and the silicate liquid is too highly crystallised to be analysed by LAM-ICP-MS. The following abbreviation is used: LC, carbonate liquid.

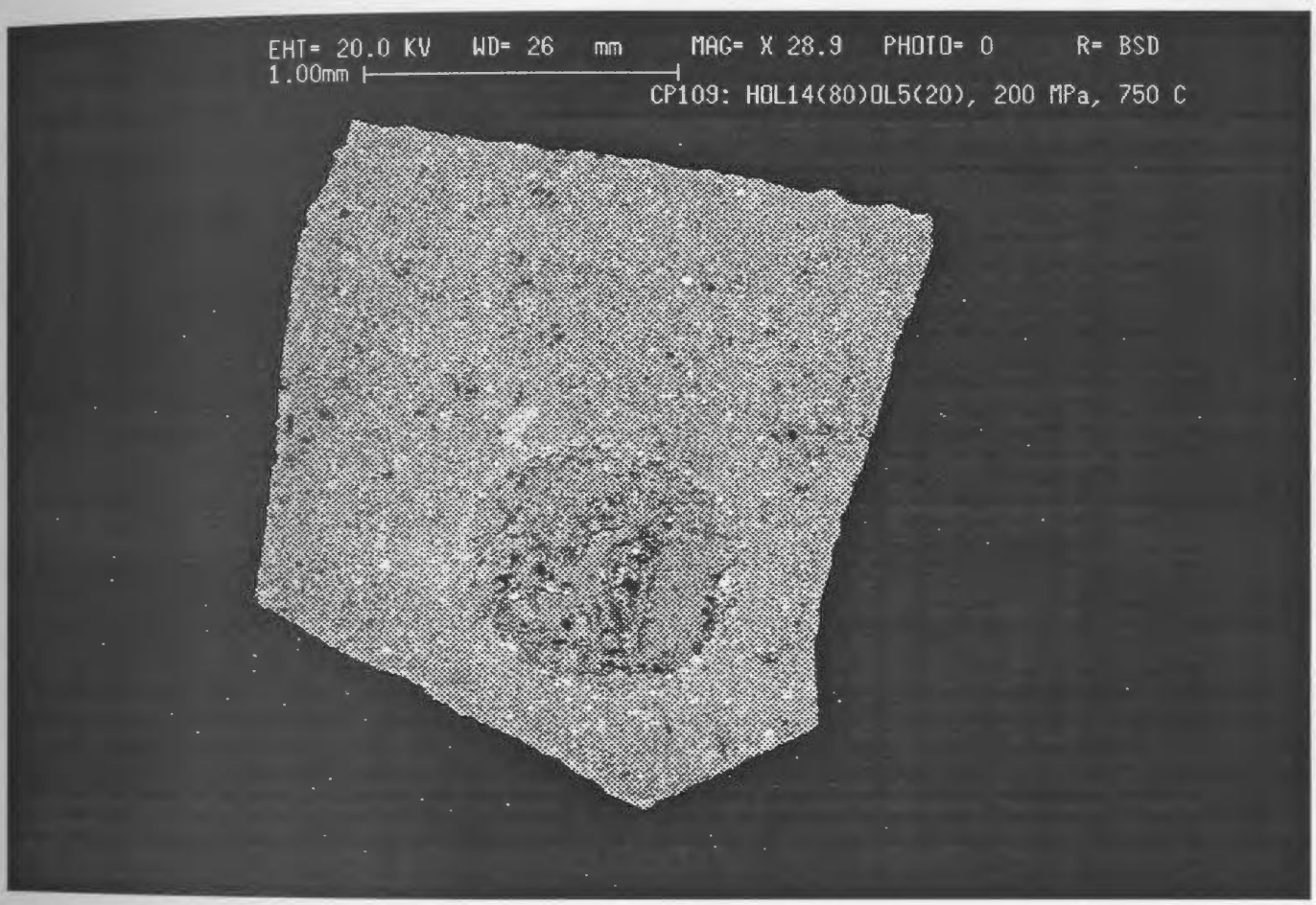

Figure 2.14: Back scattered SEM photograph of experimental charge CP109, prepared at 200 MPa, 750 °C, with 80 wt. % wollastonite nephelinite HOL14 and 20 wt. % silicate-bearing natrocarbonatite OL5 in the starting composition. In this experiment, prepared at low temperature and fairly high weight fraction of OL5 in the starting composition, a large carbonate globule is present, but large silicate liquid pockets are absent (silicate liquid highly crystallised).

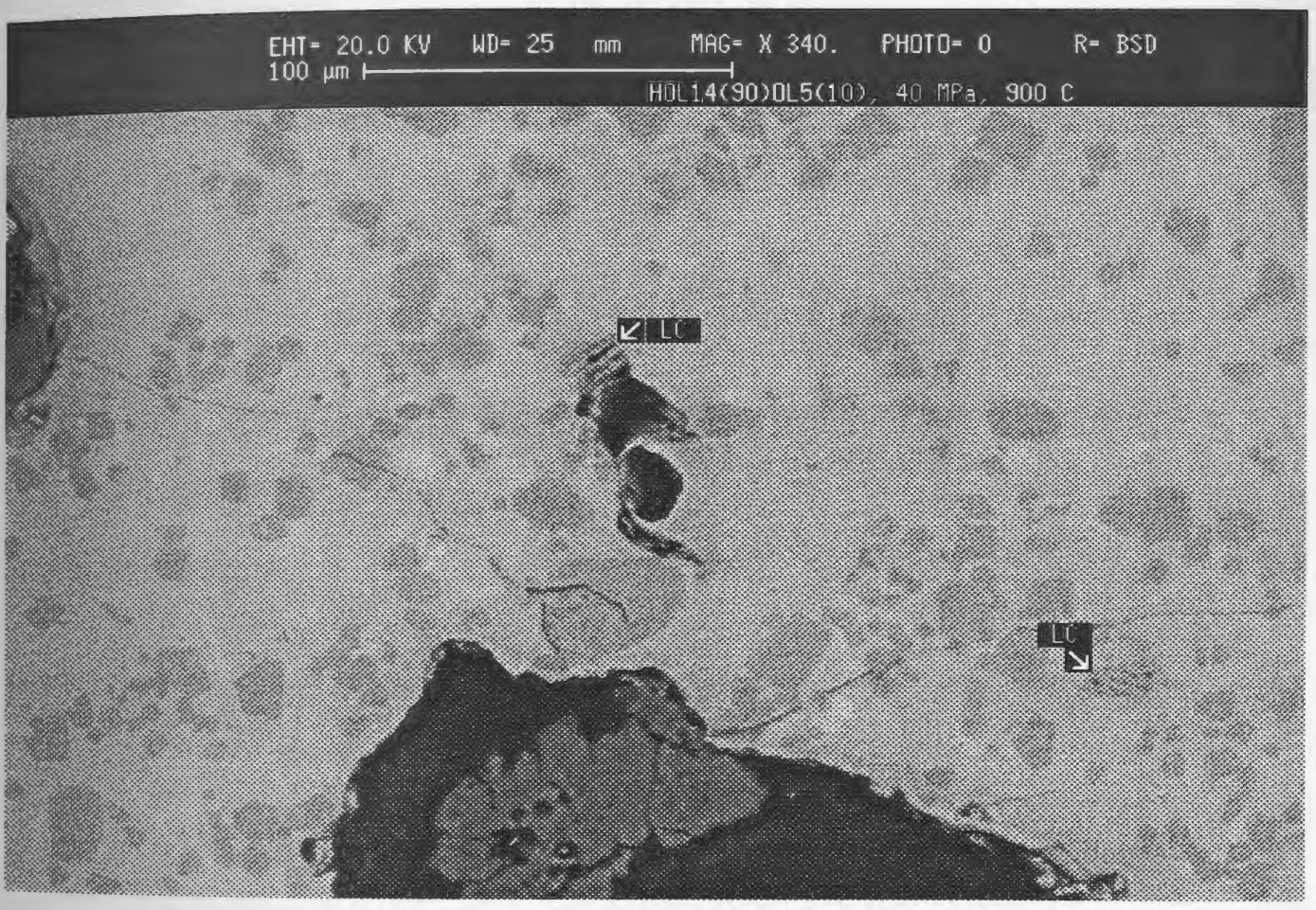

Figure 2.15: Back scattered SEM photograph of experimental charge CP19, prepared at 40 MPa, 900 °C, with 90 wt. % wollastonite nephelinite HOL14 and 10 wt. % silicate-bearing natrocarbonatite OL5 in the starting composition. In this experiment, prepared at high temperature and low weight fraction of OL5 in the starting composition, the silicate liquid forms quite large areas free of nepheline crystals, but the carbonate globules are very small and scarce. The following abbreviation is used: LC, carbonate liquid.

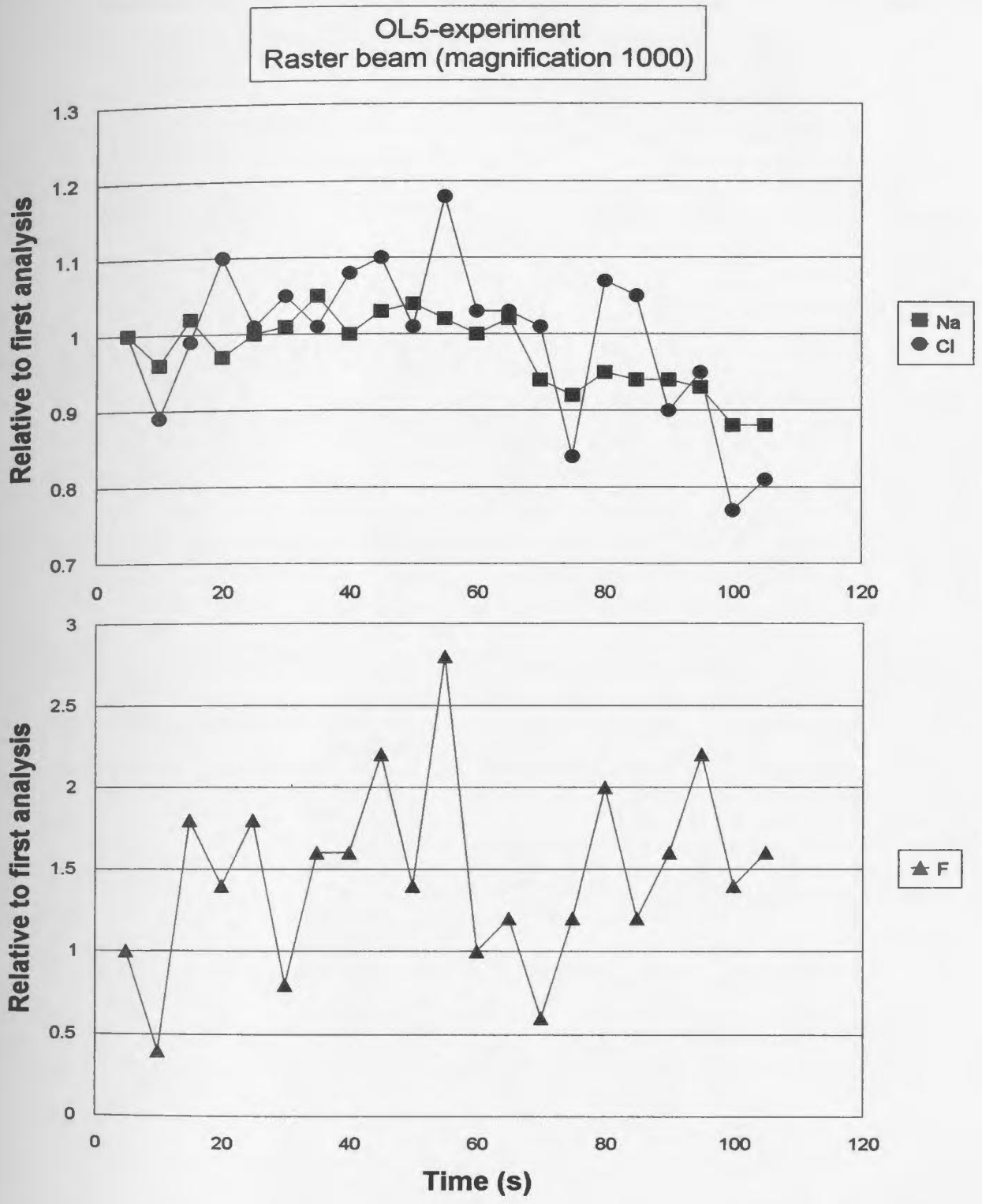

Figure 2.16: Ratio of Na, Cl and F signals (in cps) relatively to the first analysis over a 105 s interval, for carbonate liquid of an experiment prepared using OL5 as the starting composition. Data obtained by electron microprobe at MUN, using a raster beam.

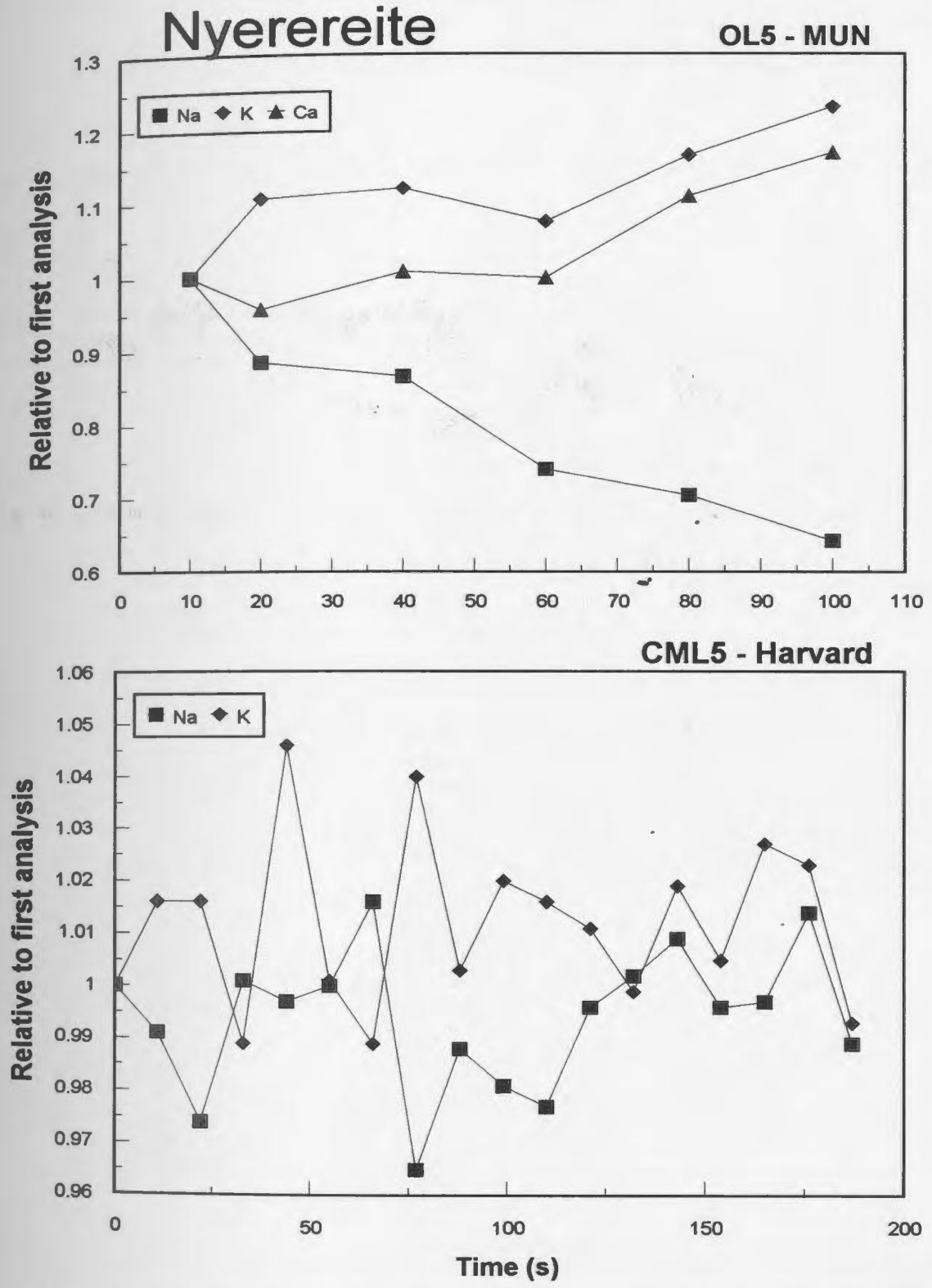

Figure 2.17: Ratio of Na, K and Ca signals (in cps) relatively to the first analysis, for nyerereite from silicate-bearing natrocarbonatite OL5 (at MUN), and ratio of Na and K signals (in cps) relatively to the first analysis for nyerereite from silicate-free natrocarbonatite CML5 (at Harvard; analyst: Joy Reid).

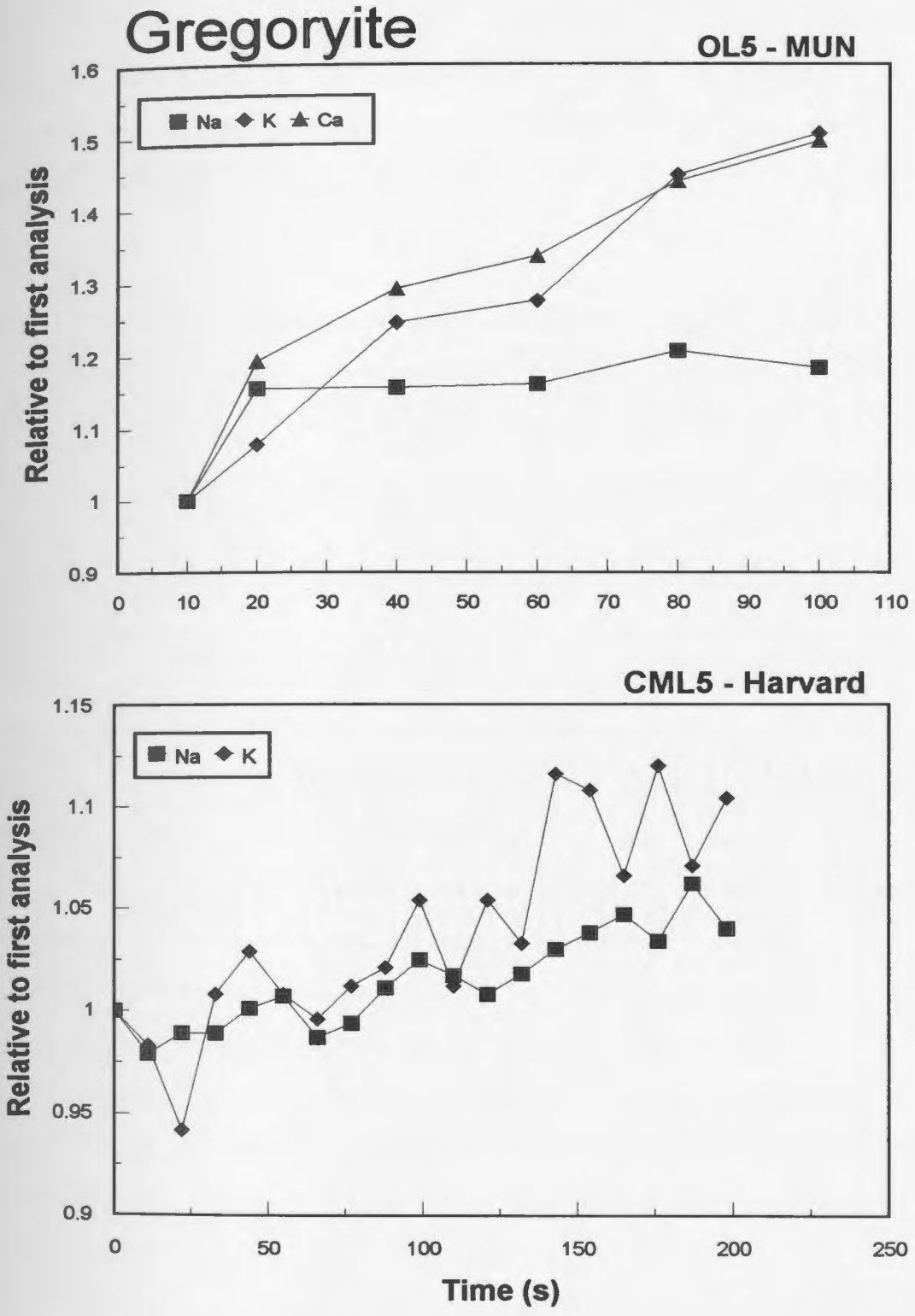

Figure 2.18: Ratio of Na, K and Ca signals (in cps) relatively to the first analysis, for gregoryite from silicate-bearing natrocarbonatite OL5 (at MUN), and ratio of Na and K signals (in cps) relatively to the first analysis for gregoryite from silicate-free natrocarbonatite CML5 (at Harvard; analyst: Joy Reid).

CHAPTER 3 – CRYSTALLISATION OF SILICATE-BEARING NATROCARBONATITES AND FORMATION OF SILICATE-FREE NATROCARBONATITES – PART I: CONSTRAINTS FROM PHASE EQUILIBRIA AND MAJOR ELEMENTS.

3.1 - Introduction

The origin of many carbonatites, and of natrocarbonatites from Oldoinyo Lengai in particular, remains problematic. Two models are commonly proposed to explain the origin of carbonatites: (1) immiscible carbonate liquids exsolved from parental CO_2-bearing silicate melts (melilitite or nephelinite), that are of mantle derivation; or, (2) primary carbonate melts derived directly by partial melting of the mantle. Recent experimental work supports the model that, at Oldoinyo Lengai, natrocarbonatite magmas are exsolved from highly peralkaline wollastonite nephelinite magmas (Kjarsgaard et al., 1995). It has been suggested, however, that natrocarbonatite at Oldoinyo Lengai might be derived from a primary sodic dolomitic carbonatite parent magma by fractional crystallisation and wall-rock interaction (Sweeney et al., 1995a). Complementing these experimental studies, Bell and Simonetti (1996) determined the Nd, Sr and Pb isotopic signature of the natrocarbonatites, but could not use these data to distinguish between a primary mantle origin for natrocarbonatites and an origin by liquid immiscibility. However, the coherence of multiple lines of evidence supports the hypothesis that natrocarbonatites are exsolved from highly peralkaline nephelinites (see Bell and Keller, 1995).

There are two distinct types of natrocarbonatite at Oldoinyo Lengai: silicate-bearing and silicate-free. The latter type accounts for 70 % of all the available analyses of natrocarbonatites from Oldoinyo Lengai (Fig. 3.1). Silicate-free natrocarbonatites are defined as natrocarbonatites containing less than 0.5 wt. % SiO_2 and are dominated by phenocrysts of nyerereite and gregoryite, with extremely rare silicate phases (see Peterson, 1990; Keller and Krafft, 1990; Dawson et al., 1995b; Mitchell, 1997; Gittins and Jago, 1998). Silicate-bearing natrocarbonatites contain > 0.5 wt. % SiO_2, with most having 1.0

– 4.0 wt. % SiO_2 (Fig. 3.1). These natrocarbonatites contain silicate phenocrysts (nepheline, clinopyroxene, melanite garnet, melilite and wollastonite) in addition to nyerereite and gregoryite. Moreover, they contain silicate spheroids (see petrographic description of silicate-bearing natrocarbonatite OL5 in Chapter 2, and major element composition in Table 2.2).

Immiscible natrocarbonate liquids exsolved from wollastonite nephelinite melts in the experiments of Kjarsgaard et al. (1995) contained between 1.3 and 5.2 wt. % SiO_2. Importantly, note that this SiO_2 content is part of the "silicate component" which is completely in solution in the natrocarbonatite liquid. Moreover, previous experiments (at $P < 400$ MPa, $T < 1000$ °C) on silicate-carbonate liquid immiscibility all demonstrated that exsolved carbonate liquids that contained > 25 wt. % $Na_2O + K_2O$ also contained > 1 wt. % SiO_2 (*e.g.* Koster Van Groos and Wyllie, 1973; Freestone and Hamilton, 1980; Hamilton et al., 1989; Kjarsgaard and Hamilton, 1989). These observations indicate that exsolved parental natrocarbonatite melts are likely to be silica-rich (> 1 wt. % SiO_2) for the estimated P-T-X conditions of exsolution at Oldoinyo Lengai (*i.e.* 100 MPa, 750 °C; see Kjarsgaard et al., 1995). Thus a dichotomy exists between the predominance of silicate-free natrocarbonatite lavas at Oldoinyo Lengai and the compositions of parental natrocarbonate liquids suggested by experimental work (Fig. 3.1).

Two-liquid plus solid phase experiments have demonstrated that exsolved natrocarbonate melts are in equilibrium (saturated) with (ferromagnesian) silicate phases (Kjarsgaard et al., 1995). These authors suggested that if exsolved natrocarbonatite melts separate from their silicate host, further precipitation and fractionation of these solid phases would produce a halogen-rich and SiO_2-, TiO_2-, Al_2O_3-, MgO- and FeO-depleted natrocarbonatite magma (*i.e.* a silicate-free natrocarbonatite). Complementary experimental studies in model silicate-carbonate systems have demonstrated that an immiscible carbonate melt that separates from its conjugate silicate liquid will first precipitate silicate minerals on cooling (Lee and Wyllie, 1998).

To further examine silicate mineral fractionation in carbonate melts, and the relationship between silicate-bearing and silicate-free natrocarbonatite, a low pressure phase equilibrium study was undertaken on a natural silicate-bearing natrocarbonatite (OL5) from Oldoinyo Lengai. Phase relationships, and mineral and liquid compositions observed in the experiments and in naturally occurring natrocarbonatites are used together to provide a model for natrocarbonatite magma differentiation at Oldoinyo Lengai.

3.2 - Experimental rationale

The use of liquidus studies in establishing relationships between magmas is well established (see Wyllie, 1984); nonetheless it is useful to reiterate some of the fundamentals. First, the experiments should reproduce or be consistent with the sequence and composition of the phases appearing in the natural rocks. This establishes that the P-T-volatile conditions used are comparable with those occurring in nature. Second, liquidus studies are by their very nature an examination of bulk, equilibrium crystallisation. Subsequent comparison with natural rocks must take into account that far more complicated mechanisms may have been operative (*i.e.*, crystal fractionation; mixing). One potential pitfall in doing liquidus studies is that the starting composition may be incorrectly chosen (*e.g.* does not represent a parent magma and/or a liquid composition). Nonetheless, coherence in mineral composition and crystallisation order between that observed in the experiments and in the natural rocks may eliminate the need for more complicated petrogenetic models.

3.3 - Results

3.3.1: Run products – Comparison with erupted lava OL5

Details of the experimental conditions (P, T, t) and the phase assemblage present in each run are listed in Table 3.1. Run products consist of quench carbonate liquid ± crystals of nepheline, melanite garnet, clinopyroxene, apatite, wollastonite, melilite, nyerereite, gregoryite and a co-existing vapour (fluid) phase (see Fig. 2.10; Fig. 3.2). Minor crystal

phases observed include perovskite, sodalite, K-feldspar and Fe-rich spinel. A P-T diagram constructed from the experimental data is presented in Figure 3.3. Experiments indicate that pressure has a significant effect on mineral stability. In the temperature range studied, nepheline, clinopyroxene and nyerereite are present in both 20 and 100 MPa experiments, whereas melanite garnet, melilite, wollastonite and gregoryite are present only at 20 MPa (Tab. 3.1 and Fig. 3.3). At 100 MPa, nyerereite first precipitates between 600 and 625 °C. In contrast, at 20 MPa nyerereite precipitates at slightly higher temperature (625 to 650 °C; Fig. 3.3). Gregoryite first crystallises between 600 and 625 °C in the 20 MPa experiments (Fig. 3.3). Decreasing pressure (20 vs. 100 MPa) raises the temperature at which silicate phases first precipitate, with the exception of clinopyroxene, which first crystallises at a higher temperature in the 100 MPa experiments (Fig. 3.3).

The liquidus temperature of natrocarbonatite OL5 was not determined experimentally because of temperature limits of the externally heated pressure vessel. The very low modal proportion of nepheline in the experimental charge at 900 °C and 100 MPa suggests that the liquidus temperature may be only slightly higher (~ 925 °C). At 20 MPa and 900 °C, however, there is an increased modal proportion of nepheline in the experimental charge, suggesting a higher liquidus temperature at 20 MPa than at 100 MPa.

Some minor phases are present in the experimental run products which were not observed in the erupted lava OL5. These include perovskite, Fe-rich spinel, K-feldspar and sodalite. The absence of these phases in erupted lava OL5 is suggested to be due to their P-T dependent stability. Typical silicate-free natrocarbonatite eruption temperatures of 590 °C have been recorded by Norton and Pinkerton (1997). Perovskite and Fe-rich spinel crystals precipitate at low pressure and high temperature and are not observed in runs at T < 750 °C. K-feldspar was observed in only one experiment, at 100 MPa and 700 °C. Similarly, sodalite was observed in only one run at 20 MPa and 550 °C. The absence of these minor phases in lava OL5 is consistent with recorded eruption temperatures and the phase assemblages produced in the experiments of this study. It should be noted that

pyrrhotite exists in lava OL5, but was not observed in the experiments. This is suggested to be a consequence of a different sulphur fugacity in the experiments.

The comparison between phase assemblages in experiments and in natural lava OL5 shows that if the lone melilite-bearing spheroid in lava OL5 is ignored (see later in the discussion), then the phase assemblage of lava OL5, *i.e.* nepheline, wollastonite, melanite, clinopyroxene, nyerereite, apatite and gregoryite, is replicated at ~ 615 °C and 20 MPa (Fig. 3.3).

3.3.2: Comparison of solid phase compositions in experimental run products and in erupted lava OL5

In the present chapter, average major element compositions of the different phases are given in the tables, and the number of analyses used to calculate the averages are also reported (individual analyses are given in Appendix A3). The compositions of isolated phenocrysts and of phenocrysts in spheroids are presented separately, in order to assess whether or not they formed at similar P-T-X conditions. The compositions of microphenocrysts in spheroids are also presented separately. Microphenocrysts are likely to form at lower temperature and pressure than phenocrysts. Since their composition may be significantly affected by a higher cooling rate, limited interpretation will be made of their P-T conditions of formation. Since the phase assemblage of natural erupted silicate-bearing natrocarbonatite OL5 is replicated at ~ 615 °C and 20 MPa, special attention is paid to comparing the major element compositions of phenocrysts in lava OL5 to the crystal phases in the experimental runs at 20 MPa, 600 and 625 °C.

3.3.2.1: Nepheline

Major element compositions of nepheline are reported in Table 3.2, together with the proportion of the different end-members calculated utilising the method of Peterson (1989a). For each crystal, the proportion of nepheline (Ne), quartz (Qz) and kalsilite (Ks) has been plotted on a Ne-Qz-Ks ternary diagram (Fig. 3.4). Nepheline compositions in 100 MPa experiments are temperature dependent. Over a 300 °C

cooling interval (900 - 600 °C), there is an increase in K_2O content (from 5.8 to 6.9 wt. %). In contrast, Na_2O in nepheline initially decreases from 17.1 to 16.4 wt. % over the temperature interval 900 - 700 °C and then remains at near-constant concentration to 550 °C.

Nepheline in the experiments at 20 MPa exhibits a different compositional trend with decreasing temperature (Tab. 3.2). At 20 MPa, K_2O increases from 6.0 to 6.9 wt. % over the temperature interval 900 - 775 °C, and from 6.3 to 7.4 wt. % over the temperature interval 750 - 575 °C. Similarly, Na_2O increases from 16.4 to 16.6 wt. % over the temperature interval 900 - 775 °C, and from 15.9 to 16.3 wt. % over the temperature interval 750 - 575 °C. The compositional variations of Na_2O, however, are not significant given the uncertainty of the measurements. Over the temperature interval 775 to 625 °C, Al_2O_3 decreases from 32.7 to 31.2 wt. % while Fe_2O_3 increases from 1.3 to 2.6 wt. % (increasing substitution of Fe^{3+} for Al^{3+}). From 625 to 575 °C, Al_2O_3 increases from 31.2 to 32.5 wt. % while Fe_2O_3 decreases from 2.6 to 1.6 wt. %.

The variation of major element compositions at 100 MPa leads to a decreasing nepheline end-member component of the solid solution from 850 to 625 °C, and an increasing kalsilite component from 900 to 750 °C. At 20 MPa, kalsilite and nepheline end-member components increase from 900 to 775 °C, while the quartz component decreases. At both pressures, nepheline from lower temperature experiments tends to be the richest in kalsilite component (see Fig. 3.4). With pressure decreasing from 100 to 20 MPa, Al_2O_3 and Na_2O (and Ne component) tend to decrease, whereas Fe_2O_3, K_2O (and Ks and Qz components) tend to increase.

The isolated nepheline phenocrysts and the nepheline phenocrysts within the silicate spheroids in natural lava OL5 have similar compositions, with core compositions respectively of $Ne_{77.6}Ks_{20.9}Qz_{1.5}$ and $Ne_{78.1}Ks_{20.5}Qz_{1.4}$. Compared to nepheline in experiment CP129 (20 MPa, 625 °C), they contain more Al_2O_3 (~ 32.4 vs. 31.2 wt. %) and Na_2O (~ 16.7 vs. 16.2 wt. %), and less Fe_2O_3 (~ 1.7 vs. 2.6 wt. %) and K_2O (~ 6.5 vs. 6.9 wt. %). Comparison between nepheline from experiments

CP129 (625 °C) and CP126 (575 °C) indicates that Al_2O_3, Na_2O and K_2O increase and Fe_2O_3 decreases at T < 625 °C. Higher Al_2O_3 and lower Fe_2O_3 contents of nepheline in natural OL5 compared to nepheline in the experiment at 625 °C supports its formation at T < 625 °C, *e.g.* 615 °C. However, high Na_2O and low K_2O contents do not support these conditions of formation.

Individual analyses of nepheline in 20 MPa-, low temperature- experiments as well as nepheline phenocrysts in natural lava OL5 are plotted on a Ne-Qz-Ks ternary diagram (Fig. 3.5). The compositional range exhibited by phenocrysts from natural OL5 does not overlap that of nepheline from the experiments. Nepheline phenocrysts in lava OL5 are more enriched in the Ne end-member component compared to nepheline in the experiments. Figure 3.4 shows that nepheline phenocrysts from lava OL5 have higher Ne values than those from experiments at 20 MPa, 625 and 575 °C, closer in composition to nepheline in higher pressure and temperature experiments.

In lava OL5, nepheline microphenocrysts in the spheroid groundmass contain more SiO_2, Fe_2O_3 and K_2O, and less Al_2O_3 and Na_2O than do phenocrysts. Microphenocrysts are more enriched in kalsilite and quartz components and more depleted in the nepheline end-member component compared to the phenocrysts, and best resemble nepheline analyses from the 20 MPa, 625 °C experiment.

In natural lava OL5, zoning of nepheline phenocrysts from spheroids was examined based on 28 rim and 35 core analyses on 8 crystals. Nepheline crystals were observed to have Fe-rich and Na-poor rims. This is consistent with the work of Church and Jones (1995) and Dawson et al. (1996), who showed that some nepheline crystals are zoned with Fe-rich rims. Nepheline microphenocrysts in the groundmass of spheroids from lava OL5 also exhibit zoning with Fe-rich rims ($Ne_{69.0}Ks_{22.3}Qz_{8.7}$) compared to cores ($Ne_{74.0}Ks_{22.6}Qz_{3.4}$), although only one rim and three core analyses were obtained. Rims of microphenocrysts are also Na-poor compared to cores.

3.3.2.2: Clinopyroxene

Major element compositions of clinopyroxene are reported in Table 3.3. They are mainly low-Al, low-Ti diopside-hedenbergite-aegirine solid solutions. The proportion of Mg, (Fe^{2+} + Mn), and Na end-members is reported in Table 3.3, corresponding to the proportion of the end-members diopside ($CaMgSi_2O_6$), hedenbergite ($CaFeSi_2O_6$) and aegirine ($NaFe^{3+}Si_2O_6$) respectively. Data are illustrated in Figure 3.6 for each crystal. Structural formulae based on 12 oxygens are also reported (Tab. 3.3), as well as Mg number (Mg #), which represents $Mg/(Mg+Fe^{2+})$ x 100 (mole proportions). Analyses with CaO lower than 19 wt. % are thought to represent quenched, aegirine-rich clinopyroxene overgrowths. Quench overgrowths on clinopyroxene have been observed in most experiments containing clinopyroxene. All clinopyroxene analyses obtained are reported in Appendix A3. Representative analyses are presented in Table 3.3.

For the 100 MPa runs, with cooling from 625 to 550 °C, clinopyroxene crystals exhibit enrichment in MgO (*i.e.*, diopside component) and Fe_2O_3 (without concomitant enrichment in Na_2O expected for an increase in aegirine component) and depletion in Al_2O_3, TiO_2, CaO and FeO+MnO (*i.e.*, hedenbergite component). Over the cooling interval from 625 to 550 °C, Mg # increases from 57 to 87. At 20 MPa, from 625 to 550 °C, there is a depletion in Na_2O and Fe_2O_3 (*i.e.*, aegirine component) with enrichment in CaO and FeO+MnO (*i.e.*, hedenbergite component). From 600 to 550 °C, there is a depletion in Al_2O_3 and TiO_2 and an enrichment in MgO. Mg # is fairly constant at 20 MPa, in the range from 62 to 66. In low temperature experiments ($T \leq$ 600 °C), there is an increase of TiO_2, Al_2O_3, FeO and CaO and a decrease of Fe_2O_3, MgO and Na_2O with pressure decreasing from 100 to 20 MPa.

Clinopyroxene crystals from different environments in natural erupted OL5 (isolated phenocrysts, phenocrysts in spheroids and microphenocrysts in spheroids) demonstrate a similar compositional range as those from the experiments (Tab. 3.3; Fig. 3.6). Clinopyroxene phenocrysts have fairly consistent compositions whether they

are isolated ($Di_{52.9}He_{31.4}Ae_{15.7}$) or in spheroids ($Di_{52.7}He_{31.6}Ae_{15.6}$). Mg # are similar for clinopyroxene phenocrysts in erupted lava OL5 and in experiments at 20 MPa.

Individual analyses of clinopyroxene in 20 MPa-, low temperature- experiments as well as clinopyroxene phenocrysts in lava OL5 are plotted in Figure 3.7. Phenocrysts from erupted lava OL5 show a wide compositional range (variability in diopside component). However, their compositional range overlaps that of clinopyroxene from the experiment at 600 °C. Their average major element composition is very similar to that of clinopyroxene produced in experiment CP108 at 20 MPa, 600 °C (Tab. 3.3). Clinopyroxene in this experiment has a combination of high TiO_2 and Al_2O_3 and low Fe_2O_3 and Na_2O, which makes it the best analogue to clinopyroxene phenocrysts in natural lava OL5. By comparing the composition of clinopyroxene in the experiment at 625 °C to that at 600 °C, one might infer that the composition of clinopyroxene in an experiment at 615 °C would be similar to that in natural OL5 for most major elements, except for slightly lower CaO and higher Fe_2O_3 and Na_2O.

Compared to the phenocrysts in natural OL5, the clinopyroxene microphenocrysts in the spheroid groundmass contain more Fe_2O_3, MnO and Na_2O, and less TiO_2, Al_2O_3, MgO and CaO (*i.e.*, they are more aegirine-rich, and diopside-poor), and have slightly lower Mg # (62 versus 64). In natural lava OL5, isolated phenocrysts do not show evidence of zoning (see Tab. 3.3). There is no evidence of zoning in phenocrysts in spheroids, based on 16 analyses of rim and 34 analyses of core on 6 different crystals. The absence of zoning in clinopyroxene differs from results reported by Church and Jones (1995) who showed that many clinopyroxene crystals display reversed zoning with more Fe-Na-rich cores, and that others display normal zoning. Dawson et al. (1996) reported that some clinopyroxene crystals were not zoned but that some have Ti-augite cores and aegirine-rich rims. Nine core and seven rim analyses of clinopyroxene microphenocrysts in spheroids show that it is slightly zoned, with core composition of $Di_{47.7}He_{30.7}Ae_{21.6}$, and rim composition of

$Di_{53.3}He_{27.4}Ae_{19.3}$. Compared to the core, the rim contains less Fe_2O_3, FeO, MnO and Na_2O, and more TiO_2, Al_2O_3, MgO and CaO (*i.e.*, they are more aegirine- and hedenbergite-poor, and more diopside- rich). They have higher Mg # (67 versus 62), with Mg enrichment indicating reverse zoning.

3.3.2.3: Melanite garnet

Major element compositions of melanite garnet are reported in Table 3.4. For plotting purposes, all Fe was arbitrarily recast as Fe^{3+} since recalculation and assignment of cations by charge balance is problematic since both Fe and Ti occur in two valence states (Kjarsgaard et al., 1995). The proportion of Fe^{3+}, Al and Ti is reported in Table 3.4 and used to represent the composition of melanite garnet in Figure 3.8. In Figure 3.8, all average analyses from experiments and from natural lava OL5 are plotted, whereas in Figure 3.9, all individual analyses of melanite garnet in 20 MPa-, low temperature- experiments as well as melanite garnet phenocrysts in erupted lava OL5 are plotted.

Melanite garnet has a relatively wide compositional variation with TiO_2 abundances ranging from 8.6 to 12.9 wt. % (Tab. 3.4, Fig. 3.8). Melanite garnets from the experiments have compositions varying from $Fe_{73.1}Al_{2.8}Ti_{24.1}$ to $Fe_{62.1}Al_{4.0}Ti_{33.9}$. Figures 3.8 and 3.9 illustrate that the compositions of melanite garnet show a fairly large scatter. However, Figure 3.8 illustrates that the composition of melanite from the experiments overlaps that of phenocrysts in natural lava OL5 and that the latter have fairly consistent compositions whether they are isolated ($Fe_{63.7}Al_{3.0}Ti_{33.3}$) or in silicate spheroids ($Fe_{64.8}Al_{3.9}Ti_{31.3}$). Moreover, Figure 3.9 illustrates that individual analyses of phenocrysts cluster together, and that they plot close to the composition of melanite garnet in the experiment at 600 °C, for which three analyses were obtained. The only available analysis of melanite garnet at 625 °C shows that it is much more depleted in Ti compared to phenocrysts in natural OL5 and melanite garnet in experiments at 600 °C (Fig. 3.9). The melanite garnet at 625 °C has the lowest TiO_2 content among all

garnets (see Tab. 3.4). It is possible that the equilibrium melanite garnet at 625 °C contains more TiO_2 than the one analysed. Because it is suspicious, the data for melanite garnet in the experiment at 625 °C were not used for comparison with melanite garnet in natural lava OL5. However, the similarity between the major element composition of melanite garnet in lava OL5 (phenocrysts) and in the experiment at 600 °C (Tab. 3.4) suggests that a temperature of crystallisation of the phenocrysts at ~ 600 °C (*e.g.* 615 °C) is reasonable.

In natural lava OL5, 5 core analyses and 5 rim analyses of one isolated garnet showed that the rim is Fe-rich and Ti-poor compared to the core, in agreement with Church and Jones (1995). Five qualitative analyses of the rim and 6 analyses of the core of a single phenocryst in a spheroid showed no zoning, which agrees with Dawson et al. (1996) who showed that some melanite garnets are uniform in composition. Compared to the phenocrysts, the melanite garnet microphenocryst in the groundmass of spheroids ($Fe_{70.1}Al_{2.8}Ti_{27.1}$) contains lower TiO_2, consistent with the observations of Dawson et al. (1996), and also lower Al_2O_3, MgO, and higher Fe_2O_3 and MnO.

3.3.2.4: Melilite

Major element compositions of melilite crystals are reported in Table 3.5. Structural formulae based on 7 oxygens are also reported, as well as Mg number (Mg #). Compositions are plotted on an Fe-åkermanite ($Ca_2Fe^{2+}Si_2O_7$) – Na-melilite ($CaNaAlSi_2O_7$) – Mg-åkermanite ($Ca_2MgSi_2O_7$) triangular diagram (Fig. 3.10). In the åkermanite – Fe-åkermanite - Na-melilite series the iron is assumed to be present mainly as Fe^{2+}, whereas in iron-gehlenite, iron is substituting for Al and is present as Fe^{3+} (Deer et al., 1992). Because other authors (*e.g.* Donaldson and Dawson, 1978; Dawson et al., 1996) report all Fe as Fe^{2+} for melilites in lavas from Oldoinyo Lengai, all iron was reported as FeO_t. Determination of FeO and Fe_2O_3 by the method of Droop (1987) would lead to 1/3 to 2/3's iron as Fe^{3+} in melilites for the present study

as well as for the study by Dawson et al. (1996). However, in order to simplify comparison with the published data, this calculation is not carried out. With all iron reported as Fe^{2+}, the number of cations based on 7 oxygens in the present study is 5.03-5.08. This result is comparable to results from studies by Donaldson and Dawson (1978) and Dawson et al. (1996), with values as high as 5.11 for a melilite by Dawson et al. (1996).

Melilite crystals from the experiments have a range of major element compositions which overlap the composition of the single melilite phenocryst observed (in mutual association with nepheline and melanite garnet in a silicate spheroid) and analysed in lava OL5 (Tab. 3.5). In melilite crystals from the experiments, CaO and SrO decrease and Na_2O increases with temperature decreasing from 850 to 775 °C. Increase of Na-melilite is therefore noted with decreasing temperature, whereas Mg # is more variable. Melilite in natural OL5 ($Na_{47.1}Mg_{25.6}Fe_{27.3}$) has a major element composition close to that of the melilite from experiments at 800 and 775 °C, and to the melilite phenocryst in a spheroid in silicate-bearing natrocarbonatite BD4413 ($Na_{46.5}Mg_{20.4}Fe_{33.1}$; see Dawson et al., 1996).

3.3.2.5: Nyerereite

Major element compositions of nyerereite are reported in Table 3.6. The different end-members were calculated using the method of Peterson (1990). They are defined as Nc = Na/2, Kc = K/2, and Cc = Ca + Fe + Mn + Mg + Sr + Ba (molar proportion).

Examination of nyerereite compositions in Table 3.6 shows that at 100 MPa, with temperature decreasing from 600 to 550 °C, P_2O_5 decreases, whereas SrO increases in the nyerereite from the experiments. At 20 MPa, with temperature decreasing from 625 to 550 °C, P_2O_5 decreases, whereas K_2O and SrO increase. Nyerereite crystals from the 20 MPa experiments contain less CaO and SO_3 and more K_2O (and Kc component) and SrO (and possibly F and Cl) than nyerereite crystals from the 100 MPa experiments, and have compositions more similar to nyerereite

phenocrysts from erupted lava OL5, although these contain even more K_2O ($Cc_{50.2}Nc_{41.3}Kc_{8.5}$). Note that nyerereite from lava OL5 contains less Na_2O and SO_3 and more K_2O, F, Cl, BaO and SrO than any nyerereite from the experiments.

The average composition of nyerereite phenocrysts from experiments and silicate-bearing natrocarbonatite OL5 is plotted in Figure 3.11, whereas in Figure 3.12, all individual analyses of nyerereite in 20 MPa experiments as well as nyerereite phenocrysts in natural OL5 are plotted (molecular Nc-Kc-Cc). Nyerereite crystals have restricted compositions within a single experiment, and at 20 MPa, all nyerereite analyses except for those at 575 °C cluster together (Fig. 3.12). The three analyses of nyerereite phenocrysts in natural lava OL5 also cluster together, but at higher Kc than nyerereite from the experiments. The lower CaO, P_2O_5 and SO_3 and higher K_2O, SrO and Cl content in nyerereite from lava OL5 compared to those in the experiments at 20 MPa, 625 and 600 °C (see Tab. 3.6) could be explained by a pressure of crystallisation of < 20 MPa, based on the compositional trends that are observed on nyerereite from the experiments with pressure decreasing from 100 to 20 MPa (see Tab. 3.6).

3.3.2.6: Gregoryite

Major element compositions of gregoryite are reported in Table 3.6 and plotted in Figure 3.11. Examination of gregoryite compositions in Table 3.6 shows that with temperature decreasing from 600 to 550 °C, K_2O, F, Cl, SO_3 and SrO contents increase whereas CaO, Na_2O and P_2O_5 contents decrease in gregoryite from the experiments. Moreover, the Nc component decreases from 74.3 to 73.0 mol. %, whereas both Kc and Cc components increase, from 4.0 to 4.5 mol. % and from 21.7 to 22.6 mol. %, respectively. However, these variations are not significant, and gregoryite crystals from the experiments at 600 and 550 °C plot close together on the Nc-Kc-Cc ternary diagram (Fig. 3.11).

Not many analyses of gregoryite are available from the experiments, mainly because gregoryite is only present in 20 MPa-, low temperature- experiments.

However, comparison between the composition of gregoryite phenocrysts from silicate-bearing natrocarbonatite lava OL5 and the experiments shows a better agreement for experiments at 600 °C than at 550 °C. Gregoryite in natural OL5 has higher P_2O_5 and lower F and SO_3 compared to gregoryite in the experiment at 600 °C. These trends suggest that gregoryite in natural OL5 could have crystallised at T > 600 °C.

Gregoryite microphenocrysts in the groundmass of spheroids in natural OL5 ($Cc_{15.7}Nc_{81.2}Kc_{3.0}$) contain more sodium than the phenocrysts ($Cc_{20.9}Nc_{74.8}Kc_{4.3}$), although not as much as the sodium-rich gregoryite ($Cc_{8.3}Nc_{89.5}Kc_{2.3}$) reported by Dawson et al. (1996) as a discrete phase and as intergrowths with fluorite in the groundmass of silicate-bearing natrocarbonatite BD4403. In natural lava OL5, microphenocrysts contain less CaO, K_2O, P_2O_5 and SrO, and more Na_2O, F, Cl and SO_3 compared to phenocrysts.

3.3.2.7: Wollastonite

Wollastonite crystals in experiment CP129 (20 MPa, 625 °C) contain neither FeO nor MgO, but significant MnO (0.84 wt. %) (Tab. 3.7). In contrast, wollastonite crystals in natural lava OL5 contain significant FeO (0.85-0.95 wt. %), MgO (0.23-0.30 wt. %) and less MnO (0.38-0.44 wt. %), similar to compositions reported by Dawson et al. (1996). Isolated phenocrysts, and phenocrysts and microphenocrysts in the silicate spheroids in lava OL5 have similar compositions. These compositions do not overlap that of wollastonite in the experiment CP129 (based on a single analysis).

3.3.2.8: Apatite

Apatite was observed in the experiments at temperatures ≤ 625 °C. The major element composition is broadly similar to that in natural OL5 (Tab. 3.7). Both contain significant fluorine (2.6 wt. % in apatite from lava OL5; > 3 wt. % in apatite from the experiments). In the unit cell of fluorapatite ($Ca_{10}P_6O_{24}F_2$; Hogarth, 1989), Na

substitutes for Ca ($Ca^{2+} + Ca^{2+} \rightarrow Na^{+} + REE^{3+}$) and Si for P ($Ca^{2+} + P^{5+} \rightarrow REE^{3+} + Si^{4+}$). There is minor substitution of Si noted both in apatite from lava OL5 and from experiments (britholite end-member). Na_2O is present in apatite from lava OL5 (= 0.35 wt.%) as well as in apatite from experiment CP107 (100 MPa, 600 °C) at 0.3 wt. %. Dawson et al. (1995b) reported apatite from silicate-free natrocarbonatites erupted in November 1988 which contains much higher Na_2O (7.9 wt. %), SiO_2 (2.5 wt. %), and higher F (4.5 wt. %).

3.3.2.9: Others

Perovskite was identified in only one experiment (CP45: 20 MPa, 850 °C). Its composition is reported in Table 3.7. It contains high concentrations of La (La_2O_3 = 4.7 wt. %) and Ce (Ce_2O_3 = 8.2 wt. %). The other rare earth elements, Nb and Zr were not analysed, hence the low total (Tab. 3.7). Chakhmouradian and Mitchell (1997) showed evolutionary trends from perovskite *sensus stricto* toward $NaNbO_3$ (lueshite trend) and toward $NaREEO_3$ (loparite trend) for perovskite-group minerals from the Kola province (Russia). Chakhmouradian and Mitchell (1998) also showed that perovskite-group minerals from the Khibina alkaline complex, Kola Peninsula of Russia, are primarily members of the lueshite-perovskite-loparite-(Ce) solid solution series. Nickel and McAdam (1963) proposed that minor element variations within perovskite crystals are due to two sets of substitutions: $Ca^{2+}Ti^{4+}$ - $Na^{+}Nb^{5+}$ and $Ca^{2+}Ti^{4+}$ - (0.5 Na, 0.5 Ce)Ti^{4+}. These substitutions might explain the amount of Na_2O (1.6 wt. %) found in perovskite from experiment CP45.

The composition of isolated phenocrysts of pyrrhotite in silicate-bearing natrocarbonatite OL5 is reported in Table 3.7. It was not observed in the experimental run charges. Pyrrhotite in natural OL5 has a similar composition to that in wollastonitite BD127 (Dawson et al., 1995c) though it contains even more K_2O (11.3 wt. % vs. 7.4 wt. %). Pyrrhotite from other silicate intrusive rocks (nepheline syenite,

nepheline-wollastonitite-glass veins) do not contain as much K (see Table 13 in Dawson et al., 1995c).

The major element composition of spinel in experiment CP80 (20 MPa, 775 °C) is reported in Table 3.8. It is mainly represented by magnetite, and it contains a significant amount of Ti (TiO_2 = 4.0 wt. %) (ulvospinel end-member). Small amounts of Al substitute for Fe^{3+}, and Ca, Mn and Mg replace Fe^{2+}. Minor SiO_2 and Na_2O are also present in the analysis.

Sodalite $Na_8(Al_6Si_6O_{24})Cl_2$ occurs as a replacement of nepheline in the lowest P-T experiments due to the high Cl content of the carbonate liquid. It contains 1.7 wt. % Fe_2O_3 (Fe^{3+} in replacement of Al^{3+}), 2.6 wt. % K_2O (K substitutes for Na), and 0.8 wt. % SO_4 (SO_4 substitutes for Cl).

One K-feldspar analysis is reported in Table 3.8. It contains 1.6 wt. % Na_2O and 0.8 wt. % Fe_2O_3 (Fe^{3+} in replacement of Al^{3+}). An unidentified (Si,Al)(Ca,Na,Fe)F – bearing phase, encountered once as an isolated phenocryst in lava OL5, has not been analysed in previous studies of rocks from Oldoinyo Lengai.

3.3.2.10: Summary

The phenocrysts present in erupted silicate-bearing natrocarbonatite OL5 include nepheline, clinopyroxene, melanite garnet, wollastonite, apatite, nyerereite and gregoryite. Moreover, one single melilite phenocryst was observed in a silicate spheroid, and minor pyrrhotite is also present. The phase assemblage of natural OL5 would be best duplicated by an experiment at 20 MPa, 615 °C, although pyrrhotite is absent from the experimental run products, and melilite is not present at 615 °C.

Clinopyroxene and gregoryite phenocrysts have similar major element compositions in silicate-bearing natrocarbonatite OL5 and in the experiments at 20 MPa, 600-625 °C. Moreover, clinopyroxene and gregoryite in experiments prepared at P-T conditions different than 20 MPa, 600-625 °C, do not have compositions matching those in natural lava OL5, which further suggests that 20 MPa, 615 °C are the

conditions at which these crystals formed in lava OL5. The composition of melanite garnet in silicate-bearing natrocarbonatite OL5 is also comparable to that in the experiment at 20 MPa, 600 °C. However, because of the scatter in the data, the comparison does not tightly constrain the P-T conditions, as compared to clinopyroxene and gregoryite.

Nepheline in natural lava OL5 contains more Na_2O and less K_2O compared to what is expected at 20 MPa, 615 °C by comparison with the experiments. Conversely, the three nyerereite phenocrysts which have been analysed contain less Na_2O and more K_2O than in the experiments at 20 MPa.

3.3.3: Major element composition of carbonate liquid from the experiments

3.3.3.1: Calculation of the composition of carbonate liquid

In Chapter 2, it was shown that representative analyses of carbonate liquid are difficult to obtain, mainly because of its inherent heterogeneity (due to its quenched texture), and also because of alkali volatilisation during electron microprobe analysis. For each experiment, in order to obtain the best representative composition of carbonate liquid as possible, individual analyses are compared to a calculated, hypothetical compositional range of residual liquid. The composition of the residual liquid is calculated by removing the appropriate proportion of crystals from the starting composition (bulk composition = OL5; see Tab. 2.2). Details of the calculation are given in Appendix A3.

For each experiment, the composition of the residual liquid can be calculated because the phase proportions, crystal phase compositions, and bulk starting composition are known. The composition of the residual liquid so calculated is only approximate, mainly because the phase proportions are not rigorously constrained. However, it is possible to determine in which direction the composition of the calculated, residual liquid would evolve with changing crystal phase proportions and/or

compositions. This allows the determination of a range of possible compositions of the calculated, residual liquid. The calculated composition of the residual liquid is then used to constrain the selection of the individual analyses measured for carbonate liquid in experiments, so that the average composition can be determined.

Phase proportions were determined by examining the SEM photographs for each experiment. However, some phases were not observed in the experiments even though they are expected to be present, as indicated by the phase diagram and/or by mass balance calculations (Tab. 3.9). Note that the proportion of nepheline in experiments CP118 (100 MPa, 625 °C) and CP80 (20 MPa, 775 °C) are slightly too low, based on strict petrological criteria. However, since these proportions are based on the observation of the experimental run products, they were not increased for the calculations.

For each experiment, variation diagrams using different elements versus SiO_2 were examined in order to optimise the selection of individual analyses of the carbonate liquid. The choice of SiO_2 was made because: 1) carbonate liquid does not contain a large amount of SiO_2 compared to the silicate crystals present in the experiments, therefore its SiO_2 concentration can be significantly affected by small amounts of crystallisation; and 2) SiO_2 concentration is used to distinguish between silicate-bearing and silicate-free natrocarbonatites.

Variation diagrams have been examined for each element of each experiment. In this chapter, three examples have been chosen to illustrate how the selection of individual analyses of the carbonate liquid is made: CP106 (100 MPa, 850 °C; see Fig. 3.13), CP129 (20 MPa, 625 °C; see Fig. 3.14) and CP108 (20 MPa, 600 °C; see Fig. 3.15). For experiment CP106, variation diagrams are presented for selected major elements only, whereas for experiments CP129 and CP108, all major elements are presented because the data for these two experiments are extensively used in the discussion. These figures illustrate the variability among the carbonate liquid analyses

within a single experiment, which is due to the carbonate liquids not quenching to homogeneous glasses.

In Chapter 2, it was shown that the type of quenching can be very variable among the experiments because nucleation is a random process that depends on numerous parameters. The degree of heterogeneity of the carbonate liquid depends on whether quench overgrowths form on pre-existing crystals, whether nucleation occurs on the wall of the capsules, whether crystal settling occurs within the capsule, whether nyerereite needles are connected, and whether nuclei are numerous or not in the remaining liquid.

Depending on the type of quenching, the individual major (and trace) element compositions of the quenched liquid can be somewhat variable. The different possibilities for the quenching types suggest that it may be appropriate in certain cases to reject individual analyses of the quenched carbonate liquid. In this study, there was generally a small number of analyses determined for individual experiments (see Chapter 3 and 4), therefore, the results did not merit a rigorous statistical approach for rejecting individual analyses from the calculation of the composition of the carbonate liquid. A general approach was adopted in which the largest number of analyses was retained, such that the average of the individual analyses compared reasonably well to the calculated composition (= OL5 minus crystals) as denoted by the residual liquid vector (RL) shown in Figures 3.13, 3.14 and 3.15.

The silica content of the calculated, residual liquid was used as the primary criteria for selecting the results. Analyses of quenched liquids that deviated widely from the calculated value were excluded. After the first selection based on silica content, the results were further scrutinised, *i.e.*, for each element. While results for individual elements might have been rejected, this did not entail rejecting the whole analysis, as opposed to SiO_2. This is illustrated in Figure 3.14j. Among the four analyses of the carbonate liquid that have a high SO_3 content compared to the SO_3 concentration of the calculated, residual liquid, only the one having the highest value

has been rejected. The three remaining analyses have been kept because the measured composition of the carbonate liquid is closer to the composition of the calculated, residual liquid when these are included in the calculation. Similarly, the two analyses that have the lowest SO_3 content have been rejected, though they are not outliers, since the measured composition of the carbonate liquid is closer to the composition of the calculated, residual liquid when these are excluded from the calculation.

Figures 3.13, 3.14 and 3.15 show that the individual analyses for CaO, SO_3, BaO, SrO and MnO are in general agreement with the concentrations in the calculated, residual liquid, although there might be some scatter, especially for MnO. The good agreement is due to the fact that on average, these elements are present in similar amounts in the quenched carbonate liquid and in its two main constituents, *i.e.* nyerereite and gregoryite. Concentrations are more variable for Na_2O and K_2O because these two elements are volatile and may partition into the vesicles (as salts). The scatter exhibited by P_2O_5, Cl and F can also be explained by partitioning into minor phases (in vesicles or not), and also by the fact that these elements are in concentrations close to limits of detection. In general, FeO and MgO do not show a good agreement with the calculated concentrations of the carbonate liquid because they may be preferentially incorporated by some phase that is not well represented in the analyses (see later in section 3.3.3.2).

3.3.3.2: Composition of carbonate liquid from the experiments - Results

The concentrations of major elements determined for carbonate liquids from experiments at different pressure and temperature are given in Table 3.10 and plotted in Figure 3.16 and Figure 3.17, for experiments at 100 and 20 MPa, respectively. Standard deviations (1 σ) for each element are calculated using the different analyses of carbonate liquid that were selected from an experiment (Tab. 3.10). Standard deviations represent mainly the heterogeneity of the carbonate liquid (hence their high values), but also the analytical precision ("analytical σ" is usually significantly lower).

For each experiment, the average composition of all analyses (before rejection) is also reported in Table 3.10, together with the standard deviations. The composition of the residual liquid calculated by mass balance is also reported in Table 3.10. Measured compositions (after and before rejection) are in general agreement with the calculated composition of carbonate liquid calculated by mass balance (OL5 minus crystals). In general, the standard deviation is significantly smaller after applying the rejection process.

The measured and calculated compositions of the carbonate liquid are generally similar within one standard deviation, both at 100 and 20 MPa (Figs. 3.16 and 3.17). However, there are, in some cases, discrepancies between the compositions of measured and calculated, residual carbonate liquid. When there is a significant discrepancy between measured and calculated concentrations, it is usually the measured concentration that is lower. This usually indicates that (at least) one phase was not analysed in the carbonate liquid. One must determine whether this "missing phase" is a quenched phase or a stable phase. If it is a quench phase that was not analysed, then the carbonate liquid composition that is measured is not representative of the carbonate liquid, and the calculated composition better represents the liquid composition. On the other hand, if it is a stable phase that was not analysed, then the carbonate liquid composition that is measured is representative of the carbonate liquid, and the calculated composition is erroneous because it has not taken that stable phase into account in the calculation. It is not straightforward to determine whether the "missing phase" is a quenched or a stable phase. This is especially important for trace elements which can be significantly affected by the fractionation of minor phases. Therefore, this problem will be examined in more details in the appropriate sections (*e.g.* Chapter 4).

3.3.3.2.a: 100 MPa

Are compositional changes of carbonate liquid at 100 MPa consistent with changes in the phase assemblages with temperature? Crystal phases present in the experiments at 100 MPa are shown in Figure 3.16. Above 700 °C, nepheline is the only crystal phase present in the 100 MPa-experiments (apart from minor K-feldspar at 700 °C). Precipitation of nepheline should lead to decreasing SiO_2 and Al_2O_3, similar K_2O and FeO, and increasing CaO, Na_2O and all other elements with decreasing temperature. This is indeed the case, but because nepheline is present in such low amounts in the experiments (2 % maximum), only SiO_2 and Al_2O_3, which are significantly more concentrated in nepheline compared to the carbonate liquid, show a significant concentration change with decreasing temperature.

At 625 °C, nepheline is joined by clinopyroxene (1 % each). The carbonate liquid at 625 °C differs from the carbonate liquid at 700 °C mainly by having a higher content of Al_2O_3 because of its lower amount of nepheline, and by having a lower content of FeO, MnO and MgO because of the precipitation of clinopyroxene.

Below 600 °C, nyerereite and apatite are present in addition to the higher-temperature crystal phases nepheline and clinopyroxene (see Fig. 3.3). The concentration of CaO decreases significantly in carbonate liquid with decreasing temperature because it partitions into three crystallising phases (clinopyroxene, nyerereite and apatite) compared to carbonate liquid. Because nyerereite is present in high proportion (12-30 vol. %), and because it contains low SiO_2, Al_2O_3, FeO, MnO, MgO, F, Cl and BaO compared to the carbonate liquid, it serves as the main control of these elements whose concentration tends to increase in the carbonate liquid at low temperature. The increase of K_2O in carbonate liquid at low temperature is not as pronounced as these other elements because the K_2O content in nyerereite is not significantly low relative to the carbonate liquid. Since nyerereite contains more SrO than carbonate liquid, especially at low temperature, SrO concentration decreases in the carbonate liquid with decreasing temperature. Although apatite crystallises at low

temperature, P_2O_5 concentration increases in the carbonate liquid because its concentration is controlled by the other more abundant phases which do not contain much P_2O_5 relative to the carbonate liquid, *i.e.* clinopyroxene, nyerereite and nepheline. There is a discrepancy between the measured and calculated concentrations of TiO_2 and FeO in carbonate liquid at low temperature, probably because some Ti-magnetite must have precipitated at these conditions, that was not observed during the SEM work. It is not known whether this magnetite is a stable or a quench phase, therefore whether it is the measured or the calculated TiO_2 and FeO concentrations that are more representative of the carbonate liquid.

Note that the data for MnO are fairly inconsistent at 100 MPa. This can be partly explained by the fact that MnO content in the carbonate liquid is close to detection limits. Therefore, no attempt was made to interpret the MnO data as a function of phases under- or over-represented in the analyses.

Note also that the scale used in some of the figures accentuates the discrepancies between measured and calculated concentrations. Compared to the calculated concentrations, the measured concentrations for the carbonate liquid in the experiment CP79 (800 °C) are low for FeO (1.10 vs. 1.29 wt. %), MnO (0.30 vs. 0.36 wt. %), MgO (0.30 vs. 0.41 wt. %) and high for SrO (1.53 vs. 1.33 wt. %). Because of the scale used for the figures, the experiment CP79 looks like a "bad run". However, based on the fact that the data for SiO_2, TiO_2, K_2O, CaO, Na_2O, K_2O, P_2O_5, F, Cl and SO_3 are in good agreement, and that the discrepancies for the remaining elements are reasonable, this experiment was not rejected.

3.3.3.2.b: 20 MPa

Are compositional changes of carbonate liquid at 20 MPa consistent with the changes in phase assemblages with temperature? Crystal phases present in the experiments at 20 MPa are shown in Figure 3.17. At 20 MPa, there are more crystal phases present in the experiments (*e.g.* spinel, melilite, wollastonite and gregoryite) than at 100 MPa,

and they appear at higher temperature (nepheline always co-precipitates with other phases). Consequently, at 20 MPa the carbonate liquid exhibits compositional trends which are more irregular, both for the measured and calculated liquid (Fig. 3.17).

From 900 to 700 °C, the general trends for compositional changes in calculated, residual carbonate liquid with decreasing temperature are: (1) increasing concentrations of Na_2O, K_2O, F, Cl, SO_3, BaO, SrO and P_2O_5; (2) decreasing concentrations of SiO_2, TiO_2 and CaO; (3) FeO, MgO and Al_2O_3 show more complicated trends. FeO concentration decreases from 900 to 775 °C because of the presence of spinel (and melilite). At T < 775 °C, the proportion of melilite decreases with decreasing temperature, leading to increasing FeO in the carbonate liquid. MnO and MgO show similar trends as FeO. At 625 °C, with the appearance of clinopyroxene, nyerereite and apatite, the concentration of many elements decreases in the carbonate liquid (*e.g.* MgO compatible in clinopyroxene, P_2O_5 in apatite, SrO in nyerereite); whereas, Na_2O, K_2O, MnO, F, Cl, SO_3 and BaO have concentrations that increase between 700 and 625 °C because they are less concentrated in the crystal assemblage than in the carbonate liquid. At low temperature, due to the large amount of carbonate crystals, the concentration of CaO, Na_2O and SrO decreases in the carbonate liquid, while the concentration of remaining elements tends to increase. At 20 MPa, there is a discrepancy between the measured and calculated concentrations of TiO_2, FeO, MnO, MgO and Al_2O_3 at low temperature because some Ti-magnetite must have precipitated at these conditions, that was not observed during the SEM work. Like at 100 MPa, it is not straightforward to determine whether this magnetite is a stable or a quenched phase.

At low pressure and temperature, more crystal phases are present in the experimental charges, and carbonate liquid analyses generally show higher scatter. Moreover, the calculation of the composition of the residual liquid can be significantly affected by the proportion and composition of the crystal phases, and is therefore more sensitive at low pressure and temperature where more crystal phases are present.

Experiments CP126 (20 MPa, 575 °C) and CP112 (20 MPa, 550 °C) illustrate the difficulty in obtaining analyses and in calculating the composition of the residual liquid at low pressure and temperature (see Fig. 3.17).

Because of the crystallisation of various silicate minerals over the whole temperature range, and the larger amounts of carbonate crystals at low temperature, the trends of composition of the calculated, residual carbonate liquid at 20 MPa are quite different than at 100 MPa. One important difference between the two pressures is that the average SiO_2 concentration is lower at 20 than at 100 MPa because silicate crystals are present in higher proportions. Importantly, it is at 625-600 °C that SiO_2 concentration is the lowest, *i.e.* 0.43-0.76 wt. %. This will have implications for the discussion related to the formation of silicate-free natrocarbonatites.

3.4 - Discussion

3.4.1: Equilibrium cooling history of natural lava OL5

The phenocrysts present in silicate-bearing natrocarbonatite OL5 include nyerereite, gregoryite, nepheline, clinopyroxene, wollastonite, melanite garnet, melilite, apatite and pyrrhotite. In the 100 MPa experiments, melanite garnet, melilite and gregoryite did not precipitate. The phenocryst minerals noted in lava OL5, however, precipitate in the 20 MPa experiments.

The mineral assemblage of natural OL5 cannot be exactly duplicated at 20 MPa because of the absence of pyrrhotite in the experiments (suggested to be related to control of sulphur fugacity). However, it is suggested that OL5 mostly records a silicate-bearing natrocarbonatite magma undergoing bulk equilibrium cooling at ~ 20 MPa, 615 °C. The solitary (relict?) silicate spheroid in lava OL5 that contains melilite, nepheline and melanite phenocrysts represents a temperature of 775 °C at 20 MPa. Phenocrysts of melanite, wollastonite and nepheline in natural OL5 are equivalent to the co-precipitating phase assemblage in 20 MPa experiments observed over the temperature interval from 750 to 635 °C. However, if the lone melilite-bearing spheroid is ignored (as a high temperature

relict), then the phase assemblage of OL5, *i.e.* nepheline, wollastonite, melanite, clinopyroxene, nyerereite, apatite and gregoryite, is replicated at 615 °C and 20 MPa (Fig. 3.3). Moreover, clinopyroxene, melanite garnet and gregoryite have similar major element compositions for phenocrysts in natural OL5 and in the experiments at 20 MPa, 600-625 °C. In conclusion, the comparison of crystal assemblages and compositions between natural and experimental samples suggests that natural lava OL5 mostly recorded a bulk equilibrium crystallisation history at 20 MPa, 615 °C.

The proportions of different phases in an (hypothetical) experiment at 20 MPa, 615 °C, and in natural lava OL5 are compared in Table 3.11 and in Figure 3.18. No actual experimental charge was prepared at 20 MPa, 615 °C. Therefore, the phase proportions of the (hypothetical) experiment at these P-T conditions were estimated by averaging the phase proportions in the 20 MPa-experiments at 600 and 625 °C (see Tab. 3.9). The results of this interpolation show that at 20 MPa, 615 °C, an experiment would contain: ~ 2 vol. % nepheline, 3 vol. % clinopyroxene, 0.7 vol. % melanite garnet, 0.05 vol. % wollastonite, 10 vol. % nyerereite, 2.5 vol. % gregoryite, 0.3 vol. % apatite and the remaining material (= 81.45 vol. %) would be represented by quenched carbonate liquid (Tab. 3.11). Observation of SEM photographs show that natural lava OL5 contains: ~ 8 vol. % silicate crystals and spheroids (+ apatite phenocrysts), 19 vol. % groundmass, and ~ equal amounts of nyerereite and gregoryite. Therefore, although natural lava OL5 has the same phase assemblage as in a hypothetical experiment at 20 MPa and 615 °C, it is highly crystallised compared to the experiment; especially, it contains a significantly higher proportions of carbonate crystals (see Fig. 3.18). The similarity of phase assemblages between the natural and experimental samples suggests that the natural lava OL5 underwent bulk equilibrium crystallisation at ~ 20 MPa, 615 °C, but the higher crystallinity of the natural lava suggests that the carbonate melt in lava OL5 underwent more extensive crystallisation during cooling than the carbonate liquid in the experiments did (see Fig. 3.18).

This indicates that the equivalent of the carbonate liquid from the hypothetical experiment at 20 MPa, 615 °C is not the groundmass of the natural lava OL5, but the groundmass plus the crystals that precipitated during cooling, before quench (Fig. 3.18). An estimation of the phases in lava OL5 whose sum is equivalent to the carbonate liquid from the experiment at 20 MPa, 615 °C is presented in Table 3.11 and in Figure 3.18. This model "liquid" will be termed calculated equivalent liquid (CEL). The calculation is based on the assumption that the phenocryst assemblage (at equilibrium, before cooling) is the same in natural lava OL5 as in the experiment at 20 MPa, 615 °C (see Tab. 3.11). The proportion of siliceous mesostasis (1.7 vol. %) is such that when added to the 6.05 vol. % consisting of silicate crystals and apatite from the phenocryst assemblage, it gives a total of 7.75 vol. %, in agreement with the fact that silicate crystals and spheroids (+ apatite phenocrysts) represent ~ 8 vol. % of natural lava OL5. The proportions of microphenocrysts in spheroids in natural lava OL5 (nepheline, wollastonite, clinopyroxene, melanite garnet and gregogryite) have been arbitrarily estimated to be 0.1 vol. % (see Tab. 3.11). The proportions of nyerereite and gregoryite have been calculated so that when adding the proportions of carbonate crystals from the phenocryst assemblage and from the CEL, nyerereite and gregoryite are in similar amounts (*i.e.*, ~ 37 vol. %).

In summary, the equivalent of the carbonate liquid from a hypothetical experiment at 20 MPa, 615 °C is represented by a combination of groundmass + carbonate crystals + siliceous mesostasis in lava OL5, *i.e.* the phases which are not the equivalent of the phenocrysts from the experiments (see Tab. 3.11). The calculation shows that CEL in natural OL5 is represented by groundmass (19 vol. %), plus 27 vol. % nyerereite, plus 33.85 vol. % gregoryite, plus 1.7 vol. % siliceous mesostasis (see Tab. 3.11 for proportion of different phases within siliceous mesostasis of the spheroids).

The composition of the groundmass and of the CEL of silicate-bearing natrocarbonatite OL5 is presented in Table 3.12. They are plotted in Figure 3.19 together with the composition of carbonate liquid in experiments at 20 MPa, 600 and 625 °C. Figure 3.19 illustrates that the groundmass of natural OL5 has a very different major

element composition compared to carbonate liquid in experiments at 20 MPa, 600 and 625 °C, indicating that it does not represent the liquid from which the phenocrysts formed. It also shows that the CEL for natural lava OL5 has a very similar composition as carbonate liquid from the experiments at 600 and 625 °C, given the experimental and analytical errors. The higher SiO_2 content of CEL for OL5 compared to that for carbonate liquid in experimental runs (1.48 versus ~ 0.6 wt. %) can be partly attributed to using too high of a proportion of siliceous mesostasis in the calculation. Since groundmass represents a high proportion of the CEL, the composition of the CEL is very sensitive to the composition of the groundmass which is very heterogeneous (see individual analyses in Tab. A3.2).

3.4.2: Does OL5 represent a silicate-bearing natrocarbonatite parent magma?

Silicate-bearing natrocarbonatite OL5 was obtained from the Chaos Crags flow erupted in June 1993. The lavas from this flow are very thick and viscous, and contain ~ 3 wt. % SiO_2. The silica is mainly represented by silicate phenocrysts (both isolated and in the spheroids), and also by the siliceous mesostasis of the spheroids and by the groundmass. Nepheline, melanite, clinopyroxene and wollastonite crystals in natural lava OL5 are euhedral and not corroded, suggesting they are in equilibrium with the surrounding natrocarbonatite melt. Silicate phenocrysts in the spheroids also do not show any evidence of corrosion, even when they protrude from the spheroids into the carbonatite. The gregoryite crystals in the wollastonite-nepheline melt occur as small round crystals that have no apparent reaction textures, therefore the wollastonite-nepheline material cannot be the product of reaction between natrocarbonatite host and the silicate phenocrysts (see Church and Jones, 1995). Melilite from OL5 (and other silicate-bearing natrocarbonatites; *e.g.*, Dawson et al., 1996) differ in composition compared to those from the 1966 eruption (Dawson et al., 1992; Fig. 3.10). The very explosive 1966 eruption has been shown to be the product of physical mixing between natrocarbonatite and silicate magmas (Dawson et al., 1992), and pyroclastic deposits contain up to 25 wt. % SiO_2. Silicate minerals in the pyroclastic rocks from the 1966

eruption have disequilibrium textures with the host natrocarbonatite, *e.g.* corroded crystals of wollastonite and clinopyroxene are surrounded by coronas containing combeite, melilite and Ca-silicates (Dawson et al., 1992). In silicate-bearing natrocarbonatites from the Chaos Crag flow, on the other hand, all the evidence listed above shows an absence of disequilibrium reactions between the silicate phases and the surrounding natrocarbonatite melt.

Textural observations by Dawson et al. (1996) on silicate-bearing natrocarbonatites suggested that the matrix of the silicate spheroids was liquid or plastic when they were in contact with the carbonatitic melt, *i.e.*, the spheroids are not accidental clasts ('xenoliths') eroded from the vent walls. In lava OL5, the major element compositions of the phenocrysts in the spheroids are not significantly different from isolated phenocrysts in the natrocarbonatite. These observations suggest that both types of phenocrysts are in equilibrium with natrocarbonatite melt, and are not xenoliths. This is consistent with the observation by Bell and Simonetti (1996) that the spheroids have similar Sr and Nd isotopic signatures as their natrocarbonatite host. As the isolated phenocrysts and the phenocryst assemblages of the silicate spheroids are here considered to be stable crystallising phases in a silicate-bearing natrocarbonatite magma, this in turn indicates that the SiO_2 content of OL5 (3.20 wt. %) is probably the original, or close to the original, level of SiO_2 in the parent magma. Hence it is suggested that SiO_2 of 2 - 5 wt. % in silicate-bearing natrocarbonatite are best interpreted as a primary feature of parental natrocarbonatite magma, even though silicate-bearing natrocarbonatites contribute only to a small proportion of the erupted natrocarbonatites at Oldoinyo Lengai (see Fig. 3.1).

3.4.3: Origin of the silicate spheroids

The silicate spheroids in silicate-bearing natrocarbonatite have been previously interpreted as immiscible silicate liquids (Church and Jones, 1995), and as the result of mixing between natrocarbonatite and wollastonite nephelinite (Dawson et al., 1996). Phase relationships presented in this Chapter indicate that the starting composition of

silicate-bearing natrocarbonatite OL5 does not intersect the two liquid field (Fig. 3.3). Absence of an immiscibility relationship is consistent with the previous observations that the silicate - carbonate two liquid field decreases in width with decreasing pressure (Koster van Groos and Wyllie, 1966; see Chapter 5). It is therefore difficult to reconcile an origin for the spheroids by immiscibility (*e.g.* Church and Jones, 1995), as already pointed out by Dawson et al. (1996).

The experimental observation that silicate-bearing natrocarbonatite parental magmas have nepheline appearing on the liquidus first, with an extensive interval of silicate mineral co-precipitation, removes the requirement of adding silicate phases from a wollastonite nephelinite to a silicate-free natrocarbonatite (Dawson et al., 1996). The silicate spheroids are suggested to form from the agglomeration of silicate crystals that precipitated in equilibrium with natrocarbonatite magma (see Fig. 3.18). The homogeneous compositions of the silicate phenocrysts in lava OL5 suggests this occurred over a restricted temperature interval.

In section 3.4.1 it was suggested that the equivalent of the carbonate liquid from the experiments at 20 MPa, 615 °C is groundmass + carbonate crystals + siliceous mesostasis in natural lava OL5, in the proportions shown in Table 3.11. Typical eruption temperatures of natrocarbonatite lavas at Oldoinyo Lengai are 590 ± 10 °C. During the temperature interval 615-590 °C, carbonate crystals may precipitate extensively. Growth rate for nyerereite and gregoryite is high, *i.e.* 2.5 * 10^{-10} cm/s according to Peterson (1990), and increases rapidly with undercooling (Kirkpatrick et al., 1976). Dawson et al. (1990) showed that for the 1988 eruption of Oldoinyo Lengai, gas loss could cause undercooling and consequent crystal growth. Crystallisation of late-stage carbonate crystals in large amounts is supported by the observation that in the experiments at 20 MPa, the proportion of carbonate crystals increases dramatically at low temperature (*e.g.* 45 vol. % nyerereite and 25 vol. % gregoryite at 550 °C).

It is therefore proposed that during ascent of the magma (before the quench), nyerereite and gregoryite crystallise extensively, which explains the high crystallinity and

low proportion of groundmass in OL5 compared to experiments at 20 MPa, 625 – 600 °C. Consequently, the residual liquid becomes enriched in silica. Microphenocrysts of silicate crystals (and gregoryite) precipitate from this silica-rich residual liquid and clump around the phenocrysts which themselves tend to clump together (glomeroporphyritic assemblages). The residual liquid after the precipitation of the microphenocrysts is still silica-rich; it is represented by the groundmass of OL5, which contains 4.08 wt. % SiO_2. Microphenocrysts in spheroids have different compositions compared to phenocrysts because they crystallise at higher cooling rate, from a more evolved liquid, probably at lower pressure and temperature. However, no attempt was made here to interpret their composition in terms of P-T-X conditions because too many parameters interplay, and because of the high cooling rate which can significantly modify the major element compositions of crystals compared to what is expected during equilibrium conditions. Note however that for nepheline and melanite garnet, enrichment in iron in microphenocrysts compared to phenocrysts (in spheroids and isolated, respectively), and in rim compared to core, might reflect enrichment in iron of the carbonate liquid during crystallisation. Moreover, enrichment in kalsilite and quartz components and depletion in nepheline end-member component in nepheline microphenocrysts compared to phenocrysts might reflect lower P-T conditions of formation.

3.4.4: Formation of natrocarbonatites

Silicate-bearing natrocarbonatite OL5 was shown to have undergone bulk equilibrium crystallisation at 20 MPa, 615 °C. Crystallisation of silicate-bearing natrocarbonatites at these conditions is dominated by ferromagnesian silicates and nepheline. This indicates that silicate-free natrocarbonatite lavas are likely to be differentiates from silicate-bearing natrocarbonatites, probably at $P \leq 20$ MPa and $T \leq 615$ °C.

Bulk equilibrium crystallisation of silicate-bearing natrocarbonatite at 20 MPa was shown to produce residual carbonate liquid relatively depleted in SiO_2 due to crystallisation of various silicate crystals over the whole temperature range (see Fig. 3.17

and Tab. 3.10), unlike at 100 MPa. Importantly, it is at 625-600 °C that the SiO_2 content in the carbonate liquid is the lowest, *i.e.* 0.43-0.76 wt. %. It increases to 1.60 wt. % at 550 °C. Therefore, at 20 MPa, 600-625 °C is the temperature range at which the carbonate liquid is the most depleted in SiO_2 and the point at which silicate-free natrocarbonatites could be produced by bulk equilibrium crystallisation of silicate-bearing natrocarbonatites. Rayleigh fractionation could produce even lower SiO_2 contents, more similar to SiO_2 in silicate-free natrocarbonatites.

However, major elements are not as sensitive as trace elements for solving whether bulk equilibrium crystallisation or Rayleigh fractionation produces silicate-free natrocarbonatites from silicate-bearing natrocarbonatites. Therefore, these processes will be discussed in more detail in Chapter 5, when comparing trace element data between the natural lavas and the experiments. However, it can already be noted that the predominance of evolved magmas (silicate-free) compared to parental magmas (silicate-bearing) suggests that convective fractionation is the process operating in the magma chamber.

3.5 - Conclusions

Comparison of the results obtained by petrological and experimental studies on silicate-bearing natrocarbonatite OL5 indicates that this sample is a suitable candidate for a natrocarbonatite parent magma having undergone bulk equilibrium crystallisation at 20 MPa, 600-625 °C. This is demonstrated by the coherence between phase assemblages and phase compositions in natural lava OL5 and in experiments at 20 MPa, 615 °C. A critical feature of the experimental phase relationships for OL5 is that nepheline crystallises first, and a variety of silicate minerals co-precipitate over a protracted cooling interval. Crystallisation at 20 MPa is dominated by ferromagnesian silicates and nepheline down to 635 °C. Silicate-free natrocarbonatite lavas are the typical product at Oldoinyo Lengai and are likely to be differentiates from silicate-bearing natrocarbonatites. Details of the processes producing silicate-free natrocarbonatites from silicate-bearing natrocarbonatites

will be discussed in detail in Chapter 5 by comparing trace element compositions between experiments and natural lavas.

Table 3.1: Experimental run products of OL5-experiments at different pressure (P) and temperature (T). Run times (in hours) are also shown.

Sample number	P (MPa)	T (C)	Time (h)	Phase assemblage
CP88	100	900	4:30	LC+Ne+F
CP106	100	850	20	LC+Ne+F
CP79	100	800	116	LC+Ne+F
CP96	100	750	382	LC+Ne+F
CP98	100	700	161	LC+Ne+K-Fd+F
CP118	100	625	87	LC+Ne+Cpx+F
CP107	100	600	114	LC+Ne+Cpx+NY+Ap+F
CP128	100	575	255	LC+Ne+Cpx+NY+Ap+F
CP127	100	550	114	LC+Ne+Cpx+NY+Ap+F
CP90	20	900	4	LC+Ne+Fe-spinel+F
CP45	20	850	46	LC+Ne+Melilite+Perovskite+Fe-spinel+F
CP61	20	800	109	LC+Ne+Melilite+Fe-Mn-spinel+F
CP80	20	775	65	LC+Ne+Mela+Melilite+Fe-spinel+F
CP51	20	750	116	LC+Ne+Mela+Wo+Melilite+F
CP57	20	700	164	LC+Ne+Mela+Wo+F
CP129	20	625	236	LC+Ne+Cpx+Mela+Wo+NY+Ap+F
CP108	20	600	114	LC+Ne+Cpx+Mela+NY+GRE+Ap+F
CP126	20	575	114	LC+Ne+Cpx+Mela+NY+GRE+Ap+F
CP112	20	550	88	LC+Cpx+Mela+NY+GRE+sodalite+Ap+F

Abbreviations used are: LC: carbonate liquid; F: fluid (CO_2/H_2O mixture, CO_2-rich); Ne: nepheline; K-Fd: potassic feldspar; Cpx: clinopyroxene; Mela: melanite garnet; NY: nyerereite; Ap: apatite; Wo: wollastonite; GRE: gregoryite.

Table 3.2: Major element microprobe analyses of nepheline from OL5-experimental run products and from natural erupted silicate-bearing natrocarbonatite OL5.

SAMPLE	CP88	CP106	CP79	CP96	CP98	CP118	CP107	CP128	CP127	CP90
# of analyses	1	2	3	2	3	1	2	1	2	1
Pressure	100	100	100	100	100	100	100	100	100	20
Temperature	900	850	800	750	700	625	600	575	550	900
SiO2	43.06	42.38	42.70	42.25	42.61	42.32	42.69	42.77	42.48	43.46
Al2O3	32.32	32.43	32.40	32.42	32.46	31.96	32.56	32.50	32.53	30.77
Fe2O3	1.75	1.63	1.60	1.87	1.73	2.34	1.45	1.42	1.54	2.89
CaO	b.d.	0.49	0.20	b.d.	0.20	0.25	b.d.	0.22	b.d.	0.50
Na2O	17.05	17.02	16.91	16.86	16.43	16.40	16.44	16.43	16.47	16.39
K2O	5.81	6.05	6.18	6.60	6.57	6.75	6.87	6.67	6.98	5.99
Ks	17.9	18.7	19.1	20.5	20.4	21.0	21.3	20.6	21.6	18.6
Nf	3.2	3.0	2.9	3.4	3.2	4.3	2.7	2.6	2.8	5.3
Ne	76.7	77.1	76.6	76.1	74.1	73.2	74.7	74.7	74.8	71.8
An	0.0	2.5	1.0	0.0	1.0	1.3	0.0	1.1	0.0	2.6
Cn	-1.0	-2.1	-1.6	-1.4	-1.0	-1.4	-1.1	-1.3	-1.2	-1.9
Qz	3.1	0.8	1.9	1.4	2.4	1.7	2.5	2.4	2.0	3.6

SAMPLE	CP45	CP80	CP51	CP57	CP129	CP126	OL5	OL5	OL5	OL5
# of analyses	2	2	2	1	1	1	10	4	2	1
Pressure	20	20	20	20	20	20	Ph-c.	Ph-c. sph.	mph-c. sph.	mph-r. sph.
Temperature	850	775	750	700	625	575				
SiO2	43.15	42.26	43.76	42.54	43.24	42.33	42.42	42.50	43.11	44.33
Al2O3	32.39	32.67	31.84	32.05	31.17	32.48	32.42	32.37	32.00	31.42
Fe2O3	1.50	1.31	1.88	2.13	2.56	1.56	1.72	1.63	1.89	2.57
CaO	0.19	0.25	0.33	b.d.	b.d.	b.d.	0.27	0.42	0.29	0.19
Na2O	16.57	16.58	15.87	16.33	16.15	16.25	16.65	16.67	15.98	14.74
K2O	6.20	6.94	6.32	6.95	6.88	7.38	6.53	6.40	6.72	6.75
Ks	19.1	21.5	19.5	21.6	21.3	22.9	20.2	19.8	20.8	20.8
Nf	2.7	2.4	3.4	3.9	4.7	2.9	3.1	3.0	3.5	4.7
Ne	74.9	75.8	70.9	73.1	71.5	73.9	75.3	75.5	71.6	64.3
An	1.0	1.3	1.7	0.0	0.0	0.0	1.4	2.2	1.5	1.0
Cn	-1.0	-1.9	-0.5	-1.1	-1.3	-1.4	-1.5	-1.8	-0.9	1.2
Qz	3.3	0.9	5.1	2.4	3.8	1.7	1.5	1.3	3.6	8.1

Note: Pressure is in MPa, temperature in oC. Analyses are recalculated to 100 wt. %.
Normative abundance of end-members determined by the method of Peterson (1989a).
Abbreviations used are: Ks: kalsilite; Nf: Na2Fe2Si2O8; Ne: nepheline; An: anorthite; Cn: corundum; Qz: quartz; b.d.: below detection; Ph: phenocryst; mph: microphenocryst; c: core; r: rim.

Table 3.3: Major element microprobe analyses and structural formulae of clinopyroxene from OL5-experimental run products and from natural erupted silicate-bearing natrocarbonatite OL5.

SAMPLE	CP118	CP107	CP127	CP129	CP108	CP112	OL5	OL5	OL5	OL5
# of analyses	1	3	1	1	3	3	6	7	9	7
Pressure	100	100	100	20	20	20	Ph-c.	Ph-c. sph.	mph-c. sph.	mph-r. sph.
Temperature	625	600	550	625	600	550				
SiO2	49.77	51.59	52.55	51.92	50.91	51.03	50.40	51.11	50.74	50.82
TiO2	0.60	0.47	0.13	0.20	0.68	0.53	0.95	0.59	0.54	0.61
Al2O3	1.41	0.60	b.d.	0.56	1.11	0.89	1.65	0.92	0.83	1.12
Fe2O3	7.95	6.90	9.69	7.97	6.16	5.39	5.99	6.00	8.50	7.78
FeO	9.93	8.39	2.72	7.91	9.52	9.62	8.91	9.03	8.56	7.69
MnO	0.51	0.43	1.80	0.42	0.46	0.50	0.42	0.52	0.56	0.45
MgO	7.50	8.84	10.16	8.75	8.58	8.95	8.83	8.94	7.94	8.90
CaO	20.08	20.30	19.71	19.35	20.39	21.35	20.83	20.85	19.55	20.15
Na2O	2.27	2.48	3.24	2.92	2.17	1.74	2.02	2.04	2.77	2.48
	Structural formula for O = 12.									
Si	3.84	3.93	3.96	3.95	3.89	3.90	3.85	3.90	3.89	3.88
Al	0.13	0.05	0.00	0.05	0.10	0.08	0.15	0.08	0.08	0.10
Al	0.00	0.00	0.00	0.00	0.00	0.00	0.00	0.00	0.00	0.00
Fe3+	0.46	0.40	0.55	0.46	0.36	0.31	0.34	0.35	0.49	0.45
Ti	0.04	0.03	0.01	0.01	0.04	0.03	0.06	0.03	0.03	0.04
Mg	0.86	1.01	1.14	0.99	0.98	1.02	1.01	1.02	0.91	1.01
Fe2+	0.64	0.54	0.17	0.50	0.61	0.62	0.57	0.58	0.55	0.49
Mn	0.03	0.03	0.12	0.03	0.03	0.03	0.03	0.03	0.04	0.03
Ca	1.66	1.66	1.59	1.58	1.67	1.75	1.70	1.71	1.61	1.65
Na	0.34	0.37	0.47	0.43	0.32	0.26	0.30	0.30	0.41	0.37
Mg	46.0	51.9	60.0	50.8	50.5	53.0	52.9	52.7	47.7	53.3
(Fe2+)+Mn	35.9	29.1	15.1	27.2	33.0	33.7	31.4	31.6	30.7	27.4
Na	18.1	19.0	24.9	22.1	16.6	13.4	15.7	15.6	21.6	19.3
Mg#	57.4	65.2	87.0	66.3	61.6	62.4	63.9	63.8	62.3	67.4

Note: Pressure is in MPa, temperature in oC. Analyses are recalculated to 100 wt. %.
Mg # = 100*Mg/(Mg+Fe2+). Numbers of ions on the basis of 12 oxygens.
FeO and Fe2O3 determined by stoichiometry utilising the method of Droop (1987). Mg, (Fe2+)+Mn and Na are normalised molar proportions. Abbreviations used are: b.d.: below detection; Ph: phenocryst; mph: microphenocryst; sph.: spheroid; c: core; r: rim; Mg #: Mg number.

Table 3.4: Major element microprobe analyses and structural formulae of melanite garnet from OL5-experimental run products and from natural erupted silicate-bearing natrocarbonatite OL5.

SAMPLE	CP80	CP51	CP57	CP129	CP108	CP126	CP112	OL5	OL5	OL5
# of analyses	1	2	2	1	3	2	1	4	3	2
Pressure	20	20	20	20	20	20	20	Ph-c.	Ph-c. sph.	mph-c. sph.
Temperature	775	750	700	625	600	575	550			
SiO2	29.40	30.20	29.04	31.75	29.61	31.58	30.53	29.78	30.23	30.83
TiO2	10.20	12.32	12.77	8.63	12.87	9.30	11.47	12.60	11.73	9.74
Al2O3	0.71	0.58	0.75	0.63	0.98	0.90	0.59	0.73	0.92	0.65
Fe2O3	27.06	24.59	24.01	26.19	23.62	25.44	25.08	24.05	24.23	25.16
MnO	0.30	0.34	0.30	b.d.	0.47	0.40	b.d.	0.35	0.35	0.50
MgO	0.51	0.54	0.60	0.56	0.62	0.40	0.39	0.63	0.56	0.45
CaO	31.62	30.85	32.18	31.74	31.13	31.68	31.24	31.27	31.45	31.53
Na2O	b.d.	0.58	0.35	0.49	0.69	0.30	0.70	0.60	0.53	1.15
K2O	0.20	b.d.	b.d.	b.d.	b.d.	b.d.	b.d.	b.d.	b.d.	b.d.
	Structural formula for O = 12.									
Si	2.50	2.55	2.46	2.67	2.50	2.66	2.57	2.51	2.55	2.61
Al	0.07	0.06	0.08	0.06	0.10	0.09	0.06	0.07	0.09	0.07
Ti	0.43	0.40	0.47	0.26	0.41	0.25	0.37	0.42	0.36	0.33
Fe3+	1.73	1.56	1.53	1.66	1.50	1.61	1.59	1.53	1.54	1.60
Ti	0.23	0.38	0.35	0.28	0.41	0.33	0.36	0.38	0.38	0.29
Mg	0.06	0.07	0.08	0.07	0.08	0.05	0.05	0.08	0.07	0.06
Mn	0.02	0.02	0.02	0.00	0.03	0.03	0.00	0.03	0.03	0.04
Ca	2.88	2.79	2.92	2.86	2.81	2.86	2.82	2.83	2.84	2.86
Na	0.00	0.10	0.06	0.08	0.11	0.05	0.11	0.10	0.09	0.19
K	0.02	0.00	0.00	0.00	0.00	0.00	0.00	0.00	0.00	0.00
Fe3+	70.5	65.0	63.3	73.1	62.1	70.4	66.9	63.7	64.8	70.1
Al	2.9	2.4	3.1	2.8	4.0	3.9	2.5	3.0	3.9	2.8
Ti	26.6	32.6	33.6	24.1	33.9	25.7	30.6	33.3	31.3	27.1

Note: Pressure is in MPa, temperature in oC. Analyses are recalculated to 100 wt. %.
Numbers of ions on the basis of 12 oxygens. Fe3+, Al and Ti are normalised molar proportions.
Abbreviations used are: b.d.: below detection; Ph: phenocryst; mph: microphenocryst; sph.: spheroid; c: core.

Table 3.5: Major element microprobe analyses and structural formulae of melilite from OL5-experimental run products and from natural erupted silicate-bearing natrocarbonatite OL5.

SAMPLE	CP45	CP61	CP80	OL5
# of analyses	2	2	3	1
Pressure	20	20	20	Ph-c. sph.
Temperature	850	800	775	
SiO2	43.03	42.71	43.37	43.75
Al2O3	7.34	6.63	7.24	7.96
FeOt	6.40	6.98	6.49	7.26
MnO	0.68	0.90	0.89	b.d.
MgO	4.60	4.32	4.38	4.33
CaO	30.20	30.30	29.47	30.95
Na2O	4.98	5.53	5.76	5.75
K2O	0.20	0.25	0.10	b.d.
SrO	2.57	2.36	2.30	
	Structural formula for O = 7.			
Si	2.00	2.00	2.01	2.00
Al	0.40	0.37	0.40	0.43
Mg	0.32	0.30	0.30	0.30
Fe2+	0.25	0.27	0.25	0.28
Mn	0.03	0.04	0.04	0.00
Na	0.45	0.50	0.52	0.51
Ca	1.50	1.52	1.47	1.52
K	0.01	0.02	0.01	0.00
Sr	0.07	0.06	0.06	
Na	44.2	46.6	48.3	47.1
Fe2+	24.5	25.4	23.5	25.6
Mg	31.4	28.0	28.2	27.3
Mg #	56.2	52.4	54.6	51.6

Note: Pressure is in MPa, temperature in oC.
Analyses are recalculated to 100 wt. %, with all iron as Fe2+ (see text). Numbers of ions on the basis of 7 oxygens.
Mg # = 100*Mg/(Mg+Fe2+).
Abbreviations used are: b.d.: below detection;
Ph.: Phenocryst; sph. spheroid; c: core.

Table 3.6: Major element microprobe analyses of carbonate crystals from OL5-experimental run products and from natural erupted silicate-bearing natrocarbonatite OL5.

Sample	CP107	CP128	CP127	CP129	CP108	CP126	CP112	CP108	CP112	OL5	OL5	OL5
Phase	NY	NY	NY	NY	NY	NY	NY	GRE	GRE	NY	GRE	GRE
# of analyses	7	4	3	2	6	3	2	3	1	3	1	2
Pressure	100	100	100	20	20	20	20	20	20	Ph-c.	Ph-c.	mph. sph.
Temperature	600	575	550	625	600	575	550	600	550			
FeO	b.d.	b.d.	b.d.	b.d.	0.20	b.d.	b.d.	b.d.	b.d.	b.d.	b.d.	0.4
MnO	0.20	0.30	0.20	b.d.	b.d.	b.d.	0.20	0.20	b.d.	b.d.	b.d.	b.d.
MgO	b.d.	b.d.	b.d.	b.d.	b.d.	b.d.	b.d.	b.d.	b.d.	b.d.	b.d.	0.4
CaO	25.61	25.46	25.44	25.39	24.84	24.89	24.16	10.61	10.46	24.56	9.85	6.63
Na2O	26.81	25.38	25.84	27.55	26.85	23.58	26.77	42.46	39.39	22.85	41.35	46.07
K2O	4.70	4.57	4.68	5.88	5.93	6.21	6.49	3.48	3.65	7.73	3.57	2.61
P2O5	0.65	0.45	0.37	0.63	0.53	0.50	0.35	2.62	1.98	0.49	3.52	2.42
F	b.d.	0.20	b.d.	b.d.	b.d.	0.27	b.d.	0.53	1.58	0.41	0.20	0.4
Cl	0.11	0.13	b.d.	0.15	0.11	0.18	0.12	0.27	0.29	0.26	0.59	0.84
SO3	1.20	1.20	1.17	1.10	1.14	1.19	1.10	3.70	4.89	0.94	2.88	3.58
BaO	0.36	0.28	0.39	0.45	0.34	0.38	0.34	b.d.	0.22	0.55	0.39	0.36
SrO	1.59	1.68	1.78	1.73	1.76	1.91	1.94	0.79	0.88	2.22	0.88	0.83
Total	61.23	59.65	59.87	62.88	61.70	59.11	61.47	64.66	63.34	60.01	63.23	64.54
CaF2	0.00	0.01	0.00	0.00	0.00	0.01	0.00	0.02	0.05	0.01	0.01	0.01
Na2Cl2	0.00	0.00	0.00	0.00	0.00	0.00	0.00	0.00	0.00	0.00	0.01	0.01
CaSO4	0.02	0.02	0.02	0.01	0.01	0.02	0.01	0.05	0.07	0.01	0.04	0.05
Na2P2O6	0.00	0.00	0.00	0.00	0.00	0.00	0.00	0.02	0.02	0.00	0.03	0.02
FeCO3	0.00	0.00	0.00	0.00	0.00	0.00	0.00	0.00	0.00	0.00	0.00	0.01
SrCO3	0.02	0.02	0.02	0.02	0.02	0.02	0.02	0.01	0.01	0.02	0.01	0.01
BaCO3	0.00	0.00	0.00	0.00	0.00	0.00	0.00	0.00	0.00	0.00	0.00	0.00
CaCO3	0.46	0.46	0.47	0.45	0.45	0.46	0.44	0.14	0.10	0.45	0.15	0.07
Na2CO3	0.44	0.43	0.44	0.45	0.45	0.41	0.45	0.72	0.71	0.40	0.71	0.79
K2CO3	0.05	0.05	0.05	0.06	0.07	0.07	0.07	0.04	0.04	0.09	0.04	0.03

Note: Pressure is in MPa, temperature in oC.
Values are corrected according to correction factors determined in Chapter 2 (Tab. 2.3).
Normative abundance of end-members determined by the method of Peterson (1990).
Abbreviations used: NY: nyerereite; GRE: gregoryite; Ph.: phenocryst; mph: microphenocryst; sph.: spheroid; c: core; b.d.: below detection.

Table 3.7: Major element microprobe analyses of miscellaneous minerals from experimental run products and from natural erupted silicate-bearing natrocarbonatite OL5.

	Wo	Pvk	Ap	Ap	Ap	Wo	Wo	Wo	Ap	Py**	Unidentified phase
Sample	CP129	CP45	CP107	CP129	CP112	Ph-c.	Ph-c. sph.	mph. sph.	Ph.	Ph.	Ph.
# of analyses	1	3	1	1	1	7	4	2	9	1	1
Pressure	20	20	100	20	20						
Temperature	625	850	600	625	550						
SiO2	50.10	2.07	0.9	0.39	0.69	51.94	52.15	52.80	0.87	0.7	36.3
TiO2		39.80									0.6
Al2O3											12.5
FeOt	b.d.	5.33				0.93	0.95	0.85		44.9**	4.4
MnO	0.84					0.44	0.38	0.40		2.9	b.d.
MgO						0.24	0.23	0.30			0.8
CaO	46.14	27.97	54.0	53.73	53.34	46.94	47.05	47.15	54.43	0.2	28.1
Na2O	0.87	1.57	0.3	b.d.	b.d.	0.30	b.d.	0.35	0.35	3.8	8.5
K2O										11.3	3.6
P2O5			42.1	43.26	42.39				42.02		b.d.
F			3.0	3.61	4.01				2.60		5.7
Cl											0.1
SO3										34.3 **	b.d.
BaO											b.d.
SrO		2.00	b.d.	1.07	0.71						0.7
La2O3		4.67									
Ce2O3		8.23									
Total	97.95	91.63	100.3	102.06	101.14	100.79	100.76	101.85	100.27	98.10	101.25

Note: Pressure is in MPa, temperature in oC.
**FeO and SO3 recalculated as Fe and S for pyrrhotite. Abbreviations used are:
Wo: wollastonite; Pvk: perovskite; Ap: apatite; Py: pyrrhotite; Ph: phenocryst; mph: microphenocryst; sph: spheroid; c: core; b.d.: below detection.

Table 3.8: Major element microprobe analyses of miscellaneous minerals from OL5-experimental run products.

	Fe-sp	K-Fd	Sod
Sample	CP80	CP98	CP112
# of analyses	5	1	2
Pressure	20	100	20
Temperature	775	700	550
SiO2	0.42	64.7	38.15
TiO2	4.04		
Al2O3	0.30	18.1	29.69
Fe2O3	62.61	0.78	1.67
FeO	29.42		
MnO	2.92		
MgO	0.76		
CaO	0.24	b.d.	b.d.
Na2O	0.45	1.6	22.66
K2O		15.0	2.55
Cl			6.33
SO4			0.84
Total	101.16	100.18	101.87
Total-O=Cl			100.44

Note: Pressure is in MPa, temperature in oC.
Abbreviations used are: Fe-sp: Fe-spinel; K-Fd: K-feldspar; Sod: sodalite. FeO and Fe2O3 in spinel determined by stoichiometry utilising the method of Droop (1987).

Table 3.9: Proportions of crystal phases in equilibrium with carbonate liquid in the experiments based on analyses of SEM photographs.

Sample	P (MPa)	T (°C)	Phase proportions
CP88	100	900	1 % Ne
CP106	100	850	1.5 % Ne
CP79	100	800	2 % Ne
CP96	100	750	2 % Ne
CP98	100	700	2 % Ne, 0.3 % K-Fd
CP118	100	625	1 % Ne, 1 % Cpx
CP107	100	600	0.5 % Ne, 1.5 % Cpx, 12 % NY, 0.01 % Ap
CP128	100	575	0.3 % Ne, 1.5 % Cpx, 25 % NY, 0.02 % Ap
CP127	100	550	0.3 % Ne, 0.4 % Cpx, 30 % NY, 0.02 % Ap
CP90	20	900	2 % Ne, 0.4 % Sp
CP45	20	850	2.5 % Ne, 0.5 % Meli, 0.4 % Sp, 0.05 % Pvk
CP61	20	800	2.5 % Ne, 1 % Meli, 0.5 % Sp, (0.2 % Pvk)
CP80	20	775	2 % Ne, 0.5 % Mela, 2.5 % Meli, 0.5 % Sp
CP51	20	750	2.5 % Ne, 0.5 % Mela, 1 % Wo, 0.5 % Meli, (0.5 % Sp)
CP57	20	700	2.5 % Ne, 0.6 % Mela, 3 % Wo, (0.5 % Sp)
CP129	20	625	2 % Ne, 3 % Cpx, 1 % Mela, 0.1 % Wo, 5 % NY, 0.3 % Ap
CP108	20	600	2 % Ne, 3 % Cpx, 0.4 % Mela, 15 % NY, 5 % GRE, 0.3 % Ap
CP126	20	575	2 % Ne, 3 % Cpx, 0.4 % Mela, 30 % NY, 15 % GRE, 0.3 % Ap
CP112	20	550	2.5 % Sod, 3 % Cpx, 0.4 % Mela, 45 % NY, 25 % GRE, 0.5 % Ap

In brackets: phases not observed but thought to be present in the experiments, according to mass balance calculations.
Abbreviations used are: Ne: nepheline; K-Fd: K-feldspar; Cpx: clinopyroxene; NY: nyerereite; Ap: apatite; Sp: spinel; Meli: melilite; Pvk: perovskite; Mela: melanite garnet; Wo: wollastonite; GRE: gregoryite; Sod: sodalite.

Table 3 10 Major element microprobe analyses of carbonate liquids from the OL5-experimental run products (in wt %)
Comparison between the best representative analyses, the average of all analyses, and the expected composition calculated from mass balance

Sample	CP88		ALL		Expected	CP106		ALL		Expected	CP79		ALL		Expected
P (MPa)	100					100					100				
T (oC)	900					850					800				
# an	5		7			15		21			3		11		
SiO2	2 96	± 0 76	3 30	± 1 90	2 79	2 69	± 0 25	2 81	± 1 17	2 59	2 33	± 0 12	2 30	± 0 53	2 38
TiO2	0 09	± 0 03	0 09	± 0 02	0 10	0 10	± 0 02	0 11	± 0 03	0 10	0 11	± 0 02	0 09	± 0 02	0 10
Al2O3	0 40	± 0 20	1 13	± 1 81	0 58	0 29	± 0 06	0 55	± 1 06	0 41	0 25	± 0 07	1 12	± 0 05	0 24
FeOt	1 30	± 0 22	1 24	± 0 21	1 29	1 29	± 0 16	1 24	± 0 23	1 29	1 10	± 0 10	0 75	± 0 25	1 29
MnO	0 38	± 0 04	0 37	± 0 05	0 35	0 35	± 0 07	0 37	± 0 08	0 36	0 30	± 0 00	0 23	± 0 05	0 36
MgO	0 40	± 0 08	0 33	± 0 12	0 40	0 39	± 0 07	0 39	± 0 07	0 41	0 30	± 0 00	0 25	± 0 04	0 41
CaO	15 46	± 0 61	15 26	± 1 54	15 56	15 62	± 1 06	15 63	± 2 26	15 63	16 05	± 0 92	12 92	± 3 33	15 72
Na2O	27 25	± 1 35	26 34	± 1 33	28 41	28 49	± 1 70	27 63	± 1 86	28 48	28 03	± 1 03	21 59	± 2 57	28 54
K2O	4 89	± 0 34	4 77	± 0 35	6 13	6 08	± 0 51	6 69	± 0 98	6 13	6 06	± 0 00	4 21	± 0 84	6 13
P2O5	1 02	± 0 13	1 04	± 0 13	1 08	1 25	± 0 08	1 24	± 0 12	1 09	1 20	± 0 00	0 94	± 0 12	1 09
F	1 58	± 0 10	1 67	± 0 38	1 66	1 48	± 0 37	1 52	± 0 58	1 67	1 71	± 0 18	1 62	± 1 13	1 67
Cl	2 01	± 1 19	1 30	± 0 96	2 57	2 73	± 0 72	3 83	± 1 94	2 58	2 68	± 0 00	1 41	± 0 61	2 59
SO3	2 30	± 0 24	2 21	± 0 23	2 58	2 50	± 0 28	2 33	± 0 33	2 59	2 60	± 0 53	2 02	± 0 51	2 60
BaO	0 90	± 0 18	0 89	± 0 22	0 91	0 96	± 0 12	0 98	± 0 20	0 92	0 87	± 0 06	0 71	± 0 15	0 92
SrO	1 34	± 0 07	1 31	± 0 08	1 31	1 35	± 0 07	1 34	± 0 15	1 32	1 53	± 0 10	1 11	± 0 23	1 33
Total	62 30					65 56					65 12				
Mg/(Mg+Fe)	0 35					0 35					0 33				

Sample	CP96		ALL		Expected	CP98		ALL		Expected	CP118		ALL		Expected
P (MPa)	100					100					100				
T (oC)	750					700					625				
# an	6		18			4		11			12		16		
SiO2	2 25	± 0 49	2 22	± 1 17	2 39	1 95	± 0 13	1 72	± 0 77	2 20	2 16	± 1 50	2 22	± 1 61	2 31
TiO2	0 10	± 0 01	0 08	± 0 02	0 10	0 10	± 0 03	0 10	± 0 03	0 10	0 09	± 0 03	0 07	± 0 03	0 10
Al2O3	0 23	± 0 06	0 62	± 1 10	0 25	0 20	± 0 00	0 53	± 0 38	0 20	0 63	± 0 34	0 70	± 0 43	0 57
FeOt	1 23	± 0 06	0 87	± 0 31	1 29	1 30	± 0 18	1 12	± 0 27	1 29	1 04	± 0 07	1 02	± 0 25	1 12
MnO	0 32	± 0 04	0 29	± 0 07	0 36	0 40	± 0 00	0 37	± 0 10	0 36	0 33	± 0 05	0 31	± 0 06	0 35
MgO	0 40	± 0 00	0 36	± 0 10	0 41	0 40	± 0 00	0 33	± 0 08	0 41	0 34	± 0 05	0 36	± 0 09	0 33
CaO	15 53	± 1 44	15 67	± 3 04	15 72	15 57	± 0 96	16 49	± 2 22	15 76	15 74	± 0 63	15 15	± 2 21	15 51
Na2O	25 34	± 0 45	22 50	± 2 96	28 54	29 36	± 1 68	28 96	± 1 78	28 63	29 03	± 1 59	28 68	± 3 42	28 69
K2O	5 90	± 1 02	4 92	± 0 81	6 12	5 84	± 0 86	5 47	± 0 76	6 09	5 95	± 0 84	5 51	± 1 73	6 19
P2O5	1 08	± 0 24	1 07	± 0 22	1 09	1 17	± 0 15	1 25	± 0 23	1 10	1 10	± 0 45	1 04	± 0 42	1 09
F	1 66	± 0 34	1 45	± 0 97	1 67	2 13	± 0 60	1 81	± 0 66	1 68	1 33	± 0 39	1 60	± 1 02	1 67
Cl	0 91	± 0 36	0 92	± 0 36	2 59	2 49	± 1 16	1 92	± 0 89	2 60	2 31	± 1 06	2 82	± 2 46	2 59
SO3	2 55	± 1 07	2 17	± 0 84	2 60	2 53	± 0 40	2 33	± 0 30	2 61	2 50	± 0 31	2 31	± 0 40	2 60
BaO	1 10	± 0 17	0 99	± 0 36	0 92	0 90	± 0 10	1 07	± 0 20	0 93	0 92	± 0 10	0 93	± 0 18	0 92
SrO	1 27	± 0 05	1 34	± 0 24	1 33	1 39	± 0 14	1 49	± 0 19	1 33	1 36	± 0 17	1 29	± 0 22	1 33
Total	59 87					65 72					64 84				
Mg/(Mg+Fe)	0 37					0 35					0 37				

Data for best representative analyses and for average of all analyses are from Table A3 xxx in Appendix A3 Abbreviations used are b d below detection, n d not determined, # an number of analyses Raw data have been corrected for the five following elements Na2O (0 86), K2O (0 91), F (1 46), Cl (0 43) and SrO (1 13)
The raw data have been divided by the correction factors in brackets One sigma errors are calculated between individual analyses of carbonate liquid within an experiment, for best representative average analyses and average of all analyses

Table 3 10 (suite)

Sample	CP107		ALL		Expected	CP128		ALL		Expected	CP127		ALL		Expected
P (MPa)	100					100					100				
T (oC)	600					575					550				
# an	12		17			9		19			5		18		
SiO2	2 69	± 1 57	3 96	± 2 74	2 57	3 37	± 1 14	4 28	± 1 62	3 13	4 46	± 1 23	4 35	± 1 96	4 12
TiO2	0 09	± 0 05	0 09	± 0 04	0 11	0 08	± 0 04	0 10	± 0 09	0 13	0 09	± 0 09	0 07	± 0 06	0 14
Al2O3	0 82	± 0 46	1 73	± 1 69	0 85	1 11	± 0 20	1 37	± 0 72	1 08	1 24	± 0 58	1 34	± 0 71	1 16
FeOt	1 21	± 0 45	1 06	± 0 47	1 25	1 37	± 0 24	1 17	± 0 36	1 46	1 36	± 0 65	1 21	± 0 45	1 80
MnO	0 35	± 0 08	0 34	± 0 10	0 37	0 35	± 0 09	0 38	± 0 13	0 37	0 40	± 0 00	0 46	± 0 09	0 41
MgO	0 33	± 0 05	0 29	± 0 08	0 31	0 40	± 0 11	0 41	± 0 11	0 36	0 48	± 0 13	0 39	± 0 15	0 52
CaO	14 43	± 2 20	14 63	± 3 88	14 00	11 95	± 1 19	10 89	± 2 08	11 90	8 24	± 2 45	8 43	± 2 50	11 08
Na2O	29 00	± 0 94	27 71	± 1 75	29 08	27 45	± 2 50	23 94	± 3 75	29 85	23 25	± 1 79	21 87	± 4 91	29 55
K2O	5 61	± 0 61	6 08	± 1 23	6 44	6 72	± 0 87	6 28	± 1 32	6 78	6 95	± 2 03	6 02	± 2 05	6 79
P2O5	1 10	± 0 24	1 56	± 0 94	1 15	1 35	± 0 32	1 60	± 0 47	1 30	1 40	± 0 42	1 76	± 0 69	1 37
F	1 68	± 0 72	1 24	± 0 70	1 91	2 03	± 0 55	2 54	± 1 73	2 17	3 88	± 0 63	3 30	± 2 88	2 37
Cl	2 85	± 1 49	3 65	± 2 34	2 94	3 50	± 0 58	5 22	± 3 02	3 42	4 18	± 3 16	4 16	± 3 65	3 66
SO3	2 36	± 0 23	2 22	± 0 57	2 80	2 50	± 0 37	2 22	± 0 46	3 07	2 65	± 0 78	2 27	± 0 84	3 17
BaO	1 01	± 0 18	0 93	± 0 20	1 00	1 13	± 0 24	1 03	± 0 27	1 14	1 08	± 0 19	0 97	± 0 21	1 14
SrO	1 34	± 0 19	1 27	± 0 26	1 29	1 07	± 0 13	1 01	± 0 17	1 20	1 11	± 0 06	0 86	± 0 23	1 11
Total	64 88					64 37					60 76				
Mg/(Mg+Fe)	0 32					0 34					0 38				

Table 3 10 (suite)

Sample	CP80		ALL		Calculated	CP45		ALL		Calculated	CP61		ALL		Calculated
P (MPa)	20					20					20				
T (oC)	900					850					800				
# an	13		20			7		12			10		17		
SiO2	2 48	± 0 19	2 52	± 0 32	2 38	2 01	± 0 23	1 69	± 0 48	2 17	1 44	± 0 62	1 22	± 0 63	1 74
TiO2	0 10	± 0 01	0 10	± 0 02	0 09	0 07	± 0 02	0 08	± 0 02	0 07	b d	± 0 00	b d	± n d	0 00
Al2O3	0 23	± 0 05	0 24	± 0 05	0 29	0 19	± 0 00	0 22	± 0 05	0 05	b d	± 0 00	b d	± n d.	0 01
FeO	0 78	± 0 08	0 81	± 0 18	0 92	1 05	± 0 23	0 90	± 0 36	0 91	0 70	± 0 44	0 70	± 0 39	0 79
MnO	0 33	± 0 05	0 32	± 0 08	0 35	0 34	± 0 08	0 32	± 0 09	0 35	0 41	± 0 17	0 51	± 0 24	0 34
MgO	0 39	± 0 05	0 40	± 0 11	0 41	0 38	± 0 07	0 39	± 0 12	0 39	0 37	± 0 12	0 45	± 0 19	0 36
CaO	16 40	± 1 10	16 54	± 1 37	15 76	15 89	± 1 83	15 99	± 1 96	15 77	15 62	± 2 47	13 26	± 4 49	15.89
Na2O	29 23	± 1 33	27 41	± 3 53	28 65	27 84	± 2 70	27 76	± 2 77	28 65	33 88	± 3 43	33 49	± 4 88	29 03
K2O	6 74	± 0 94	7 17	± 1 36	6 16	5 78	± 1 37	5 75	± 1 20	6 19	6 41	± 1 00	6 17	± 2.16	6 23
P2O5	1 14	± 0 28	1 20	± 0 40	1 10	1 13	± 0 22	1 43	± 0 34	1 11	1 07	± 0 32	1 02	± 0 37	1 12
F	1 85	± 0 25	2 51	± 1 10	1 68	1 88	± 0 63	2 16	± 1 00	1 70	1 91	± 1 02	3 16	± 2 83	1 71
Cl	2 87	± 0 88	3 47	± 1 70	2 60	2 38	± 0 99	2 61	± 2 49	2 63	2 89	± 1 80	6 02	± 6 17	2 65
SO3	2 62	± 0 45	2 79	± 0 83	2 61	2 74	± 0 52	2 81	± 0 55	2 64	2 89	± 0 43	2 86	± 0 76	2 66
BaO	0 94	± 0 26	1 05	± 0 34	0 93	0 99	± 0 18	1 17	± 0 37	0 94	0 98	± 0 30	0 96	± 0 36	0 94
SrO	1 38	± 0 13	1.43	± 0 17	1 33	1 32	± 0 11	1 31	± 0 13	1 33	1 26	± 0 16	1 23	± 0 22	1.33
Total	67 49					64 00					69 82				
Mg/(Mg+Fe)	0 47					0 39					0 48				

Sample	CP80		ALL		Calculated	CP51		ALL		Calculated	CP57		ALL		Calculated
P (MPa)	20					20					20				
T (oC)	775					750					700				
# an	24		24			10		14			8		14		
SiO2	1 15	± 0 17	1 15	± 0 17	1 16	1 13	± 0 99	1 04	± 0 89	1 29	0 43	± 0 24	1 05	± 0 99	0 50
TiO2	0 04	± 0 01	0 04	± 0 01	0 03	0 04	± 0 00	0 06	± 0 01	0 02	b d	± 0 00	0 09	± 0 00	0 00
Al2O3	0 20	± 0 00	0 25	± 0 07	0 05	n d	± 0 00	1 75	± 0 00	0 06	n d	± 0 00	1 07	± 1 16	0 11
FeO	0 48	± 0 11	0 48	± 0 11	0 59	0 66	± 0 53	0 65	± 0 46	0 72	0 50	± 0 20	0 78	± 0 54	0 74
MnO	0 30	± 0 07	0 30	± 0 07	0 33	0 37	± 0 20	0 38	± 0 20	0 34	0 34	± 0 15	0 39	± 0 20	0.33
MgO	0 32	± 0 07	0 32	± 0 07	0 30	0 36	± 0 13	0 46	± 0 24	0 39	0 40	± 0 14	0 55	± 0 27	0 42
CaO	15 96	± 1 20	16 38	± 1 79	15 34	15 43	± 3 26	13 73	± 3 81	15 39	14 78	± 2 57	13 35	± 3 09	14.77
Na2O	29 67	± 1 08	29 62	± 1 52	29 44	29 34	± 3 31	29 75	± 5 18	29 32	30 39	± 2 53	30 79	± 3 74	29.81
K2O	6 03	± 0 38	5 77	± 0 50	6 33	5 89	± 1 64	7 64	± 3 22	6 28	6 60	± 0 93	7 41	± 2 52	6 37
P2O5	1 20	± 0 09	1 30	± 0 17	1 13	1 06	± 0 25	1 19	± 0 47	1 13	1 12	± 0 28	0 96	± 0 39	1 14
F	1 90	± 0 46	2 08	± 0 67	1 74	1 72	± 0 95	3 07	± 2 58	1 73	1 90	± 0 89	2 67	± 1 95	1.75
Cl	2 53	± 0 45	1 31	± 0 45	2 69	2 30	± 1 18	7 18	± 7 97	2 67	3 24	± 1 00	6 43	± 3 78	2 72
SO3	2 73	± 0 27	2 88	± 0 35	2 70	2 74	± 0 68	2 92	± 0 78	2 66	2 30	± 0 37	2 67	± 1 74	2 73
BaO	1 04	± 0 13	1 05	± 0 15	0 96	0 97	± 0 25	1 07	± 0 43	0 95	0 90	± 0 24	0 86	± 0 30	0 97
SrO	1 37	± 0 13	1 43	± 0 15	1 32	1 30	± 0 10	1 21	± 0 39	1 36	1 31	± 0 13	1 19	± 0 17	1 39
Total	64 94					63 34					64 21				
Mg/(Mg+Fe)	n d					0 50					0 59				

Table 3.10 (suite)

Sample	CP129		ALL		Calculated	CP108		ALL		Calculated	CP126		ALL		Calculated
P (MPa)	20					20					20				
T (oC)	625					600					575				
# an	25		25			8		20			4		7		
SiO2	0.43	± 0.20	0.43	± 0.20	0.43	0.76	± 0.34	0.52	± 0.33	0.92	1.33	± 1.26	0.91	± 1.03	1.31
TiO2	b.d.	± 0.00	b.d.	± n.d.	0.01	b.d.	± 0.00	0.03	± 0.00	0.04	n.d.	± 0.00	0.04	± 0.01	0.08
Al2O3	b.d.	± 0.00	b.d.	± n.d.	0.28	0.20	± 0.00	0.20	± 0.00	0.30	0.40	± 0.00	0.35	± 0.07	0.40
FeO	0.55	± 0.07	0.40	± 0.09	0.63	0.73	± 0.05	0.53	± 0.18	0.92	0.73	± 0.46	0.57	± 0.38	1.43
MnO	0.35	± 0.11	0.35	± 0.11	0.38	0.43	± 0.08	0.43	± 0.14	0.44	0.58	± 0.10	0.49	± 0.13	0.60
MgO	0.20	± 0.00	0.37	± 0.14	0.15	0.20	± 0.00	0.33	± 0.11	0.16	0.33	± 0.23	0.33	± 0.19	0.27
CaO	15.04	± 2.75	15.33	± 3.54	14.72	13.45	± 2.20	12.73	± 2.50	13.77	7.15	± 0.70	6.76	± 0.83	10.80
Na2O	31.04	± 2.07	31.94	± 3.07	29.97	30.57	± 0.33	33.71	± 2.11	29.28	27.65	± 2.89	25.36	± 3.52	28.73
K2O	6.77	± 0.97	7.40	± 1.53	6.44	6.91	± 1.13	7.63	± 1.87	6.63	7.44	± 0.86	8.49	± 2.30	7.14
P2O5	1.01	± 0.11	0.94	± 0.17	1.03	0.93	± 0.27	0.89	± 0.26	0.99	0.43	± 0.05	0.40	± 0.06	0.80
F	1.82	± 0.83	2.40	± 1.39	1.84	2.24	± 0.53	3.34	± 1.42	2.16	3.46	± 1.12	4.84	± 1.75	2.92
Cl	2.97	± 1.45	4.83	± 3.56	2.86	3.41	± 0.83	7.52	± 4.18	3.38	6.70	± 1.66	11.42	± 4.39	4.66
SO3	2.82	± 0.79	2.83	± 0.98	2.82	2.91	± 0.35	3.12	± 0.41	2.95	3.05	± 0.44	2.99	± 0.34	3.26
BaO	1.00	± 0.29	1.03	± 0.30	1.00	1.13	± 0.25	1.23	± 0.34	1.15	1.60	± 0.52	1.69	± 0.38	1.57
SrO	1.45	± 0.23	1.47	± 0.27	1.37	1.36	± 0.12	1.32	± 0.17	1.34	0.93	± 0.11	0.88	± 0.10	1.21
Total	65.44					65.24					63.96				
Mg/(Mg+Fe)	0.39					0.33					0.45				

Sample	CP112		ALL		Calculated
P (MPa)	20				
T (oC)	550				
# an	1		5		
SiO2	1.60	± 0.00	3.62	± 3.92	2.32
TiO2	0.05	± 0.00	0.25	± 0.29	0.15
Al2O3	0.40	± 0.00	1.23	± 0.85	0.52
FeO	1.10	± 0.00	1.74	± 1.19	2.96
MnO	0.50	± 0.00	0.46	± 0.11	1.00
MgO	0.40	± 0.00	0.61	± 0.30	0.52
CaO	10.50	± 0.00	9.51	± 2.99	3.55
Na2O	24.67	± 0.00	26.36	± 6.57	23.57
K2O	6.50	± 0.00	8.29	± 3.75	9.10
P2O5	1.20	± 0.00	1.12	± 0.44	0.84
F	2.40	± 0.00	4.45	± 2.76	4.99
Cl	5.05	± 0.00	7.09	± 4.13	9.19
SO3	3.60	± 0.00	5.06	± 3.56	3.32
BaO	1.50	± 0.00	1.74	± 0.37	2.84
SrO	1.24	± 0.00	1.03	± 0.29	0.83
Total	60.71				
Mg/(Mg+Fe)	0.39				

Table 3.11: Comparison of phases (in vol. %) between erupted lava OL5 and a hypothetical experiment at 20 MPa and 615 °C representing the estimate of the likely P-T conditions of formation of natural OL5.

Experiment (20 MPa and 615 °C)	**Silicate-bearing natrocarbonatite lava OL5**
PHENOCRYSTS	PHENOCRYST ASSEMBLAGE (isolated + in spheroids)
2 vol. % Nepheline	2 vol. % Nepheline
3 vol. % Clinopyroxene	3 vol. % Clinopyroxene → 6.05 vol. % silicate crystals and apatite in phenocryst assemblage
0.7 vol. % Melanite garnet	0.7 vol. % Melanite garnet
0.05 vol. % Wollastonite	0.05 vol. % Wollastonite
0.3 vol. % Apatite	0.3 vol. % Apatite
10 vol. % Nyerereite	10 vol. % Nyerereite
2.5 vol. % Gregoryite	2.5 vol. % Gregoryite
QUENCHED CARBONATE LIQUID	CALCULATED EQUIVALENT LIQUID (CEL)
81.45 vol. %	Groundmass = 19 vol. % (contains 4.08 wt. % SiO_2)
	Nyerereite = 27 vol. %
	Gregoryite = 33.75 vol. %
	Siliceous mesostasis of the silicate spheroids = 1.7 vol. %, including: - 1.2 vol. % groundmass - 0.1 vol. % nepheline - 0.1 vol. % wollastonite - 0.1 vol. % clinopyroxene - 0.1 vol. % melanite garnet - 0.1 vol. % gregoryite

Note that the fluid phase (in experiments) and vesicles (in OL5) are not taken into account.
Phase proportions in hypothetical experiment at 20 MPa and 615 °C were determined by interpolation of phase assemblages of experiments at 600 and 625 °C.
Phase proportions in natural OL5 were calculated by assuming that the phenocryst assemblage is the same as in the experiment, and by taking into account that: 1) the groundmass represents 19 vol. %,

Table 3.12: Major element microprobe analyses of the groundmass of natural lava OL5 and of the groundmass of the silicate spheroids in erupted lava OL5, and calculated composition of the carbonate liquid in a hypothetical experiment at 20 MPa, 615 °C.

	Groundmass	Groundmass spheroids	LC @ 615 °C (calculated)
SiO_2	4.08	30.5	1.48
TiO_2	0.18	0.40	0.06
Al_2O_3	0.36	5.93	0.19
FeO_t	3.23	5.23	0.85
MnO	0.93	0.50	0.22
MgO	0.50	0.45	0.13
CaO	17.0	24.2	16.45
Na_2O	31.7	15.5	31.99
K_2O	8.13	3.58	5.94
P_2O_5	0.72	0.60	1.78
F	3.82	2.08	1.13
Cl	11.7	0.79	3.05
SO_3	3.54	2.30	2.33
BaO	1.03	b.d.	0.58
SrO	1.01	0.60	1.33
Total	87.97	92.61	67.51

The major element composition of the groundmass was corrected using the same correction factors as for carbonate liquid from the experiments (see Tab. 3.10). The composition of the carbonate liquid (LC) in the hypothetical experiment at 20 MPa, 615 °C was calculated using the proportions shown in Table 3.11.

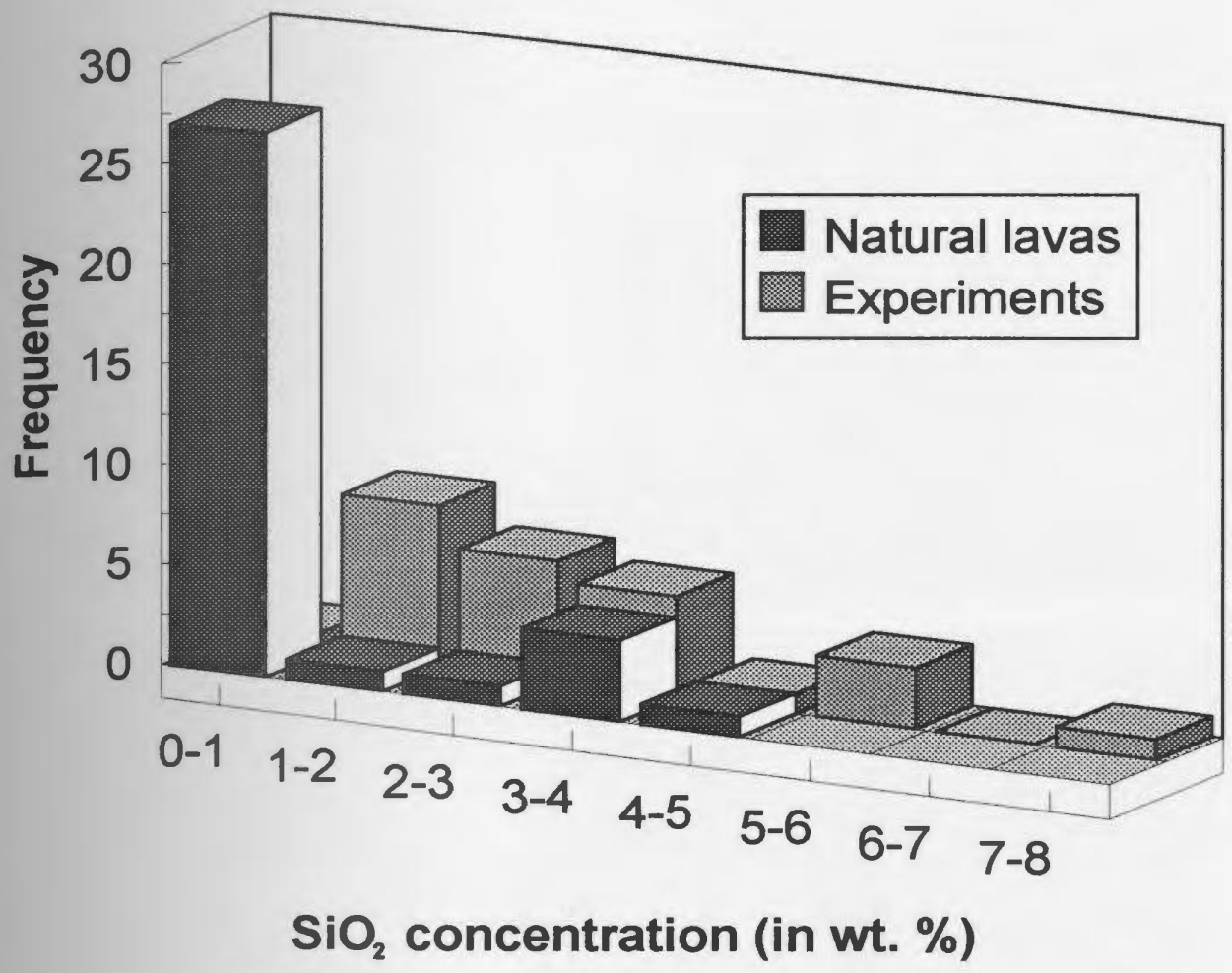

Figure 3.1: Frequency-SiO_2 diagram for natrocarbonatites, illustrating a bimodal distribution, with a high- and low-SiO_2 population. Sources of data: Keller and Krafft (1990), Church and Jones (1995), Dawson et al. (1995b, 1996), Keller and Hoefs (1995), and Simonetti et al. (1997). For comparison, the SiO_2 concentrations from the immiscibility experiments (see Chapter 6) are also shown.

Figure 3.2: A) Back-scattered electron image (BSE) of OL5-experiment CP107 (100 MPa, 600 °C) showing crystals of nepheline (Ne), clinopyroxene (Cpx) and nyerereite (NY) in quenched carbonate liquid. It should be noted that the size and shape of the nyerereite phenocrysts are readily distinguished from the blade- and needle-shaped nyerereite quenched crystals. B) BSE image of OL5-experiment CP108 (20 MPa, 600 °C) showing crystals of clinopyroxene, melanite garnet (Gt), nyerereite and gregoryite (GRE) in quenched carbonate liquid.

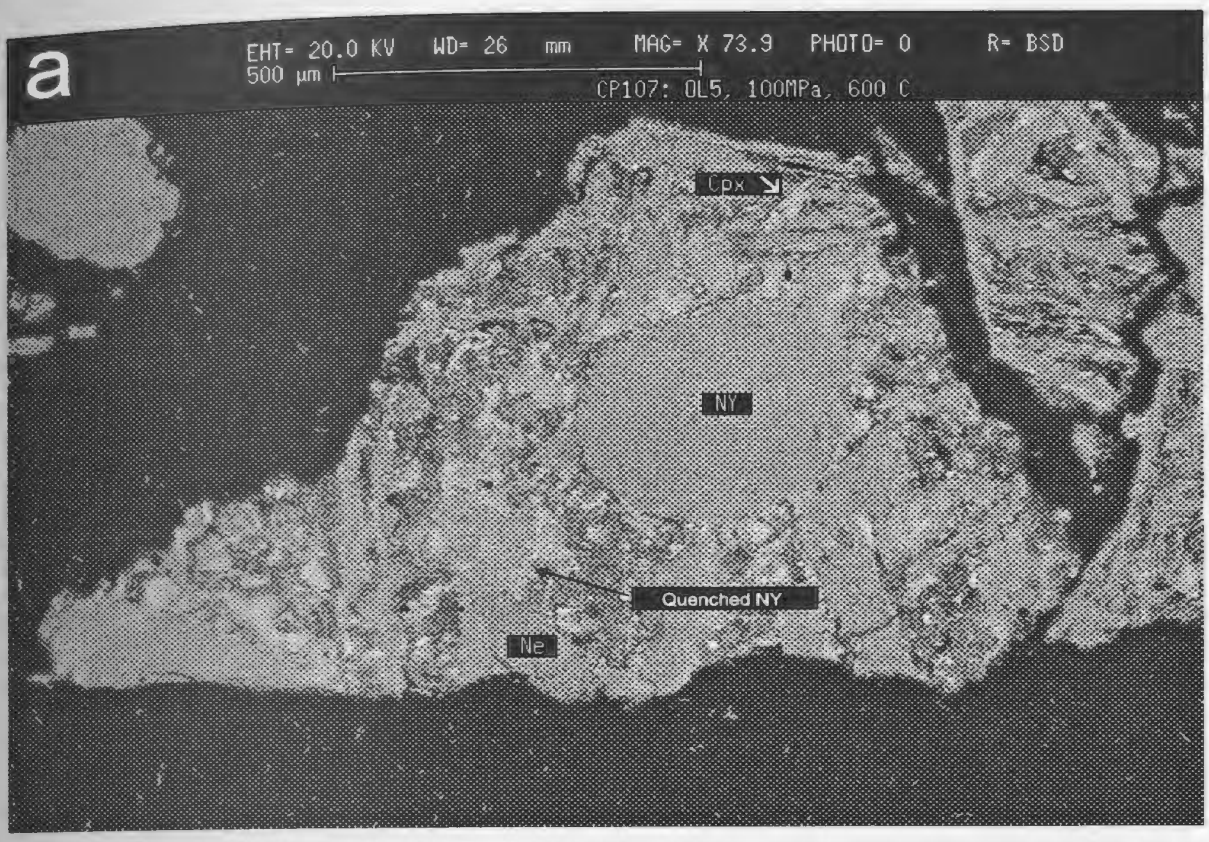
a
EHT= 20.0 KV WD= 26 mm MAG= X 73.9 PHOTO= 0 R= BSD
500 µm
CP107: OL5, 100MPa, 600 C
Cpx
NY
Quenched NY
Ne

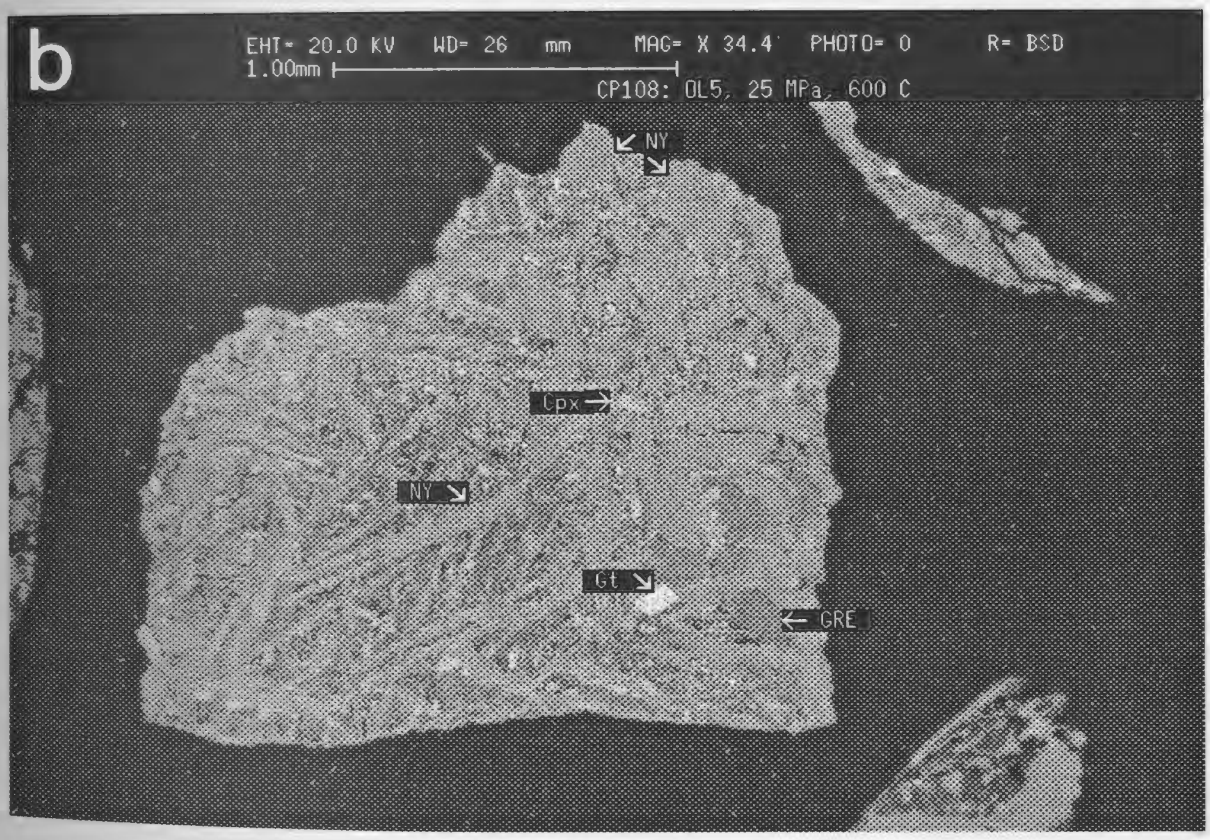
b
EHT= 20.0 KV WD= 26 mm MAG= X 34.4 PHOTO= 0 R= BSD
1.00mm
CP108: OL5, 25 MPa, 600 C
NY
Cpx
NY
Gt
GRE

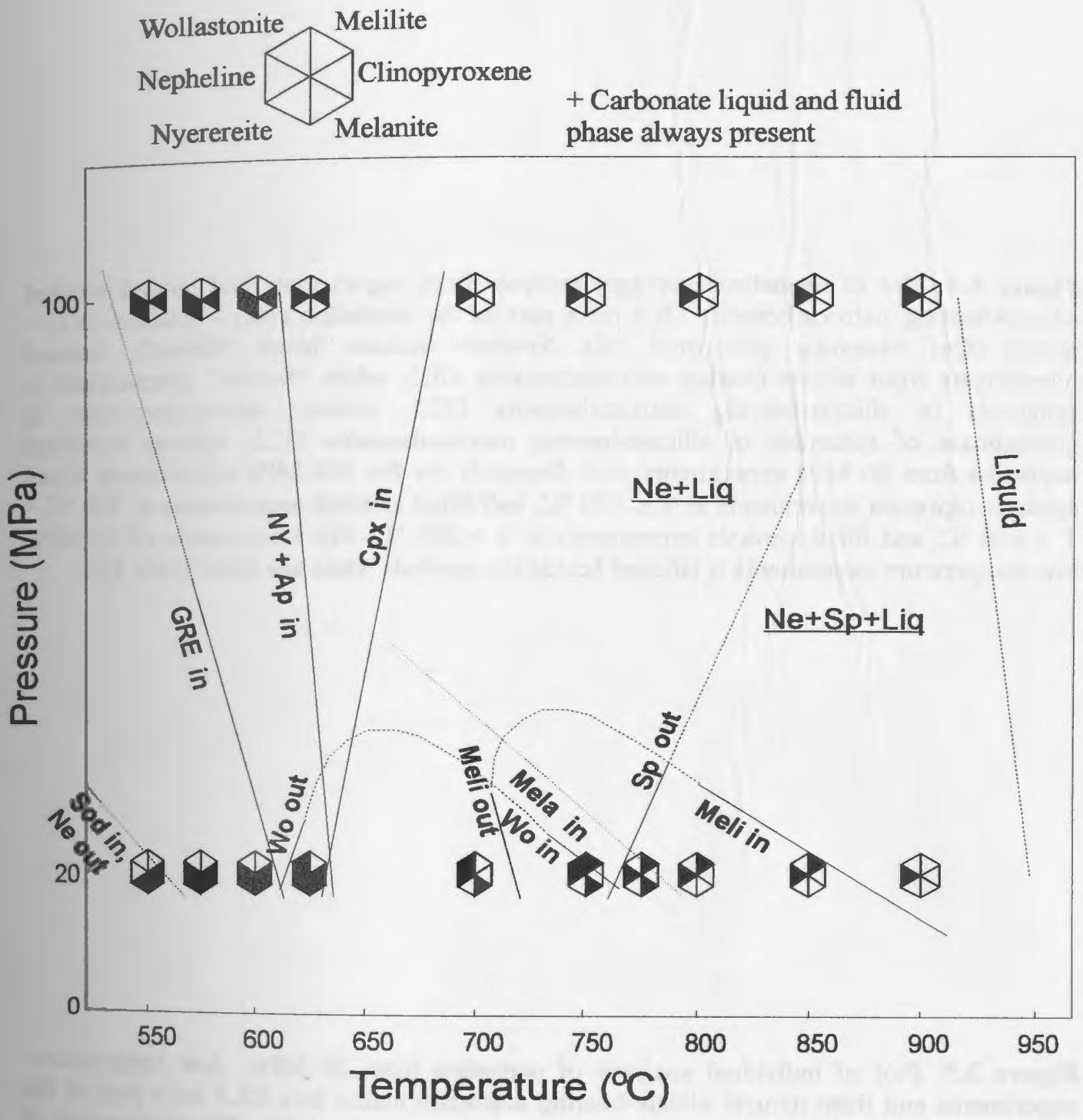

Figure 3.3: Pressure-temperature diagram for silicate-bearing natrocarbonatite OL5 experiments at 100 and 20 MPa over the temperature range 900-550 °C. Shaded portions of the hexagonal symbols indicate which phases were present. Abbreviations used are: Liq: liquid; Ne: nepheline; Sp: spinel; Meli: melilite; Cpx: clinopyroxene; Wo: wollastonite; Mela: melanite garnet; NY: nyerereite; GRE: gregoryite; Sod: sodalite; Ap: apatite.

Figure 3.4: Plot of nepheline (average) analyses from experiments and natural erupted silicate-bearing natrocarbonatite OL5 on a part of the nepheline (Ne) – kalsilite (Ks) – quartz (Qz) triangular plot (mol. %). Symbols include: black "flower", isolated phenocrysts from silicate-bearing natrocarbonatite OL5; white "flower", phenocrysts in spheroids of silicate-bearing natrocarbonatite OL5; circles, microphenocrysts in groundmass of spheroids of silicate-bearing natrocarbonatite OL5; squares represent nepheline from 20 MPa experiments, and diamonds are for 100 MPa experiments. Open symbols represent experiments at $T \leq 700$ °C, half-filled symbols experiments at 700 °C $< T \leq 800$ °C, and filled symbols experiments at $T > 800$ °C. The temperature of 20 MPa, low-temperature experiments is labelled beside the symbols. Data are from Table 3.2.

Figure 3.5: Plot of individual analyses of nepheline from 20 MPa-, low temperature-experiments and from natural silicate-bearing natrocarbonatite lava OL5 on a part of the nepheline (Ne) – kalsilite (Ks) – quartz (Qz) triangular plot (mol. %). The temperature of the experiments is labelled beside the symbols. Data are from Tables A3.1 and A3.2 in Appendix A3.

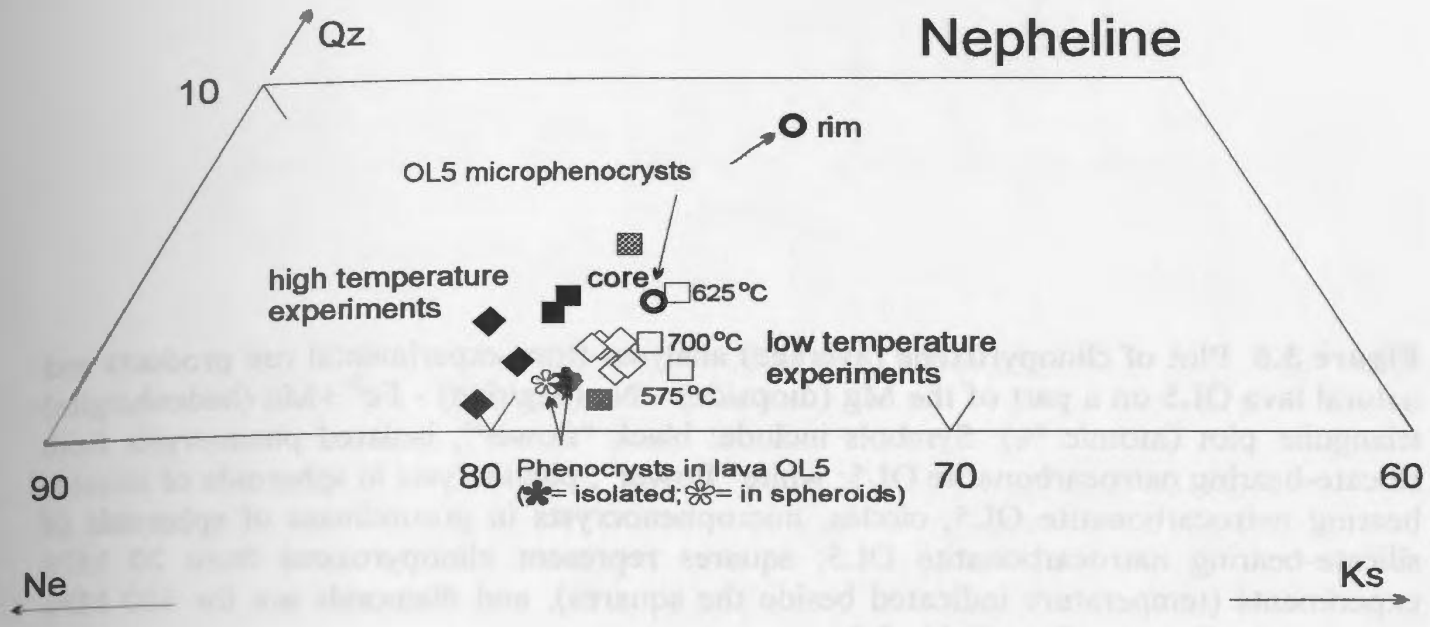
Qz
Nepheline
10
rim
OL5 microphenocrysts
high temperature
experiments
core
625 °C
700 °C
low temperature
experiments
575 °C
90
80
Phenocrysts in lava OL5
(✱= isolated; ❀= in spheroids)
70
60
Ne
Ks

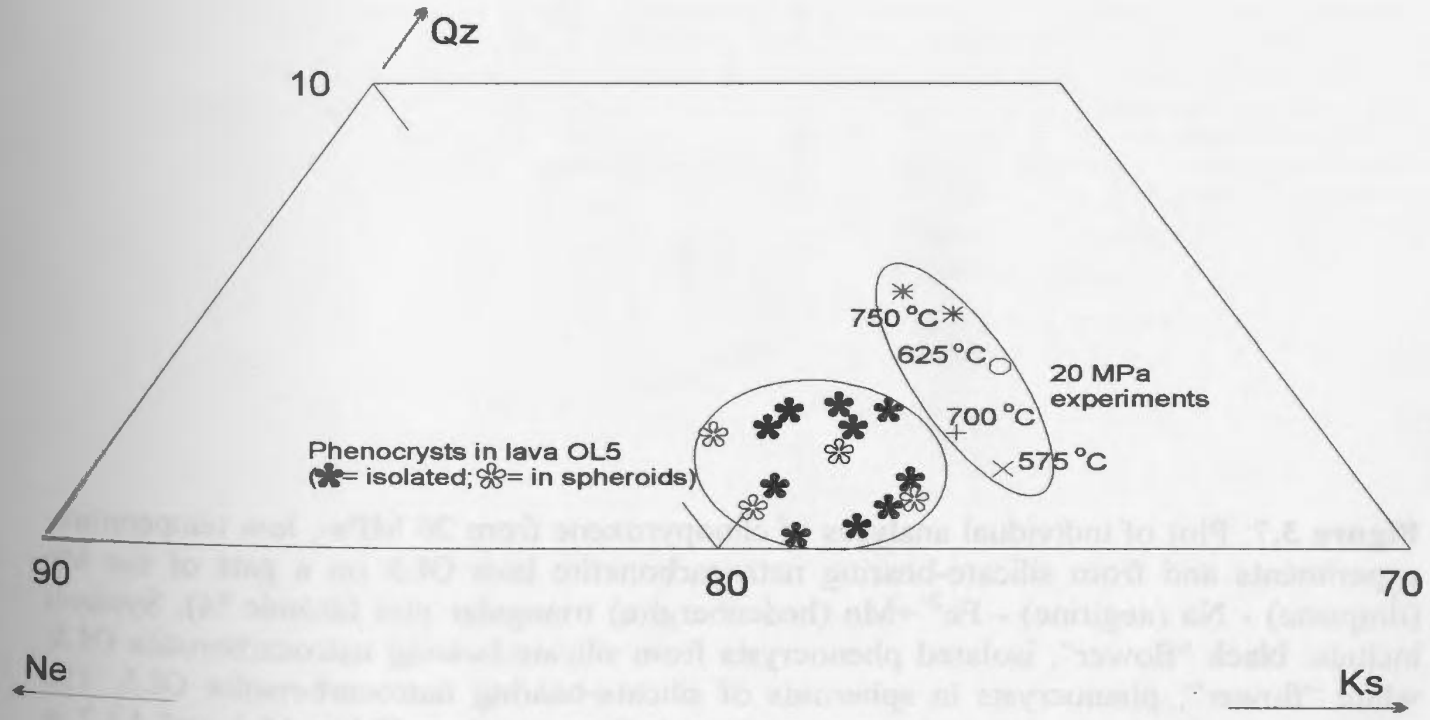
Qz
10
750 °C
625 °C
20 MPa
experiments
700 °C
575 °C
Phenocrysts in lava OL5
(✱= isolated; ❀= in spheroids)
90
80
70
Ne
Ks

Figure 3.6: Plot of clinopyroxene (average) analyses from experimental run products and natural lava OL5 on a part of the Mg (diopside) - Na (aegirine) - Fe^{2+}+Mn (hedenbergite) triangular plot (atomic %). Symbols include: black "flower", isolated phenocrysts from silicate-bearing natrocarbonatite OL5; white "flower", phenocrysts in spheroids of silicate-bearing natrocarbonatite OL5; circles, microphenocrysts in groundmass of spheroids of silicate-bearing natrocarbonatite OL5; squares represent clinopyroxene from 20 MPa experiments (temperature indicated beside the squares), and diamonds are for 100 MPa experiments. Data are from Table 3.3.

Figure 3.7: Plot of individual analyses of clinopyroxene from 20 MPa-, low temperature-experiments and from silicate-bearing natrocarbonatite lava OL5 on a part of the Mg (diopside) - Na (aegirine) - Fe^{2+}+Mn (hedenbergite) triangular plot (atomic %). Symbols include: black "flower", isolated phenocrysts from silicate-bearing natrocarbonatite OL5; white "flower", phenocrysts in spheroids of silicate-bearing natrocarbonatite OL5. The temperature of the experimental data is indicated. Data are from Table A3.1 and A3.2 in Appendix A3.

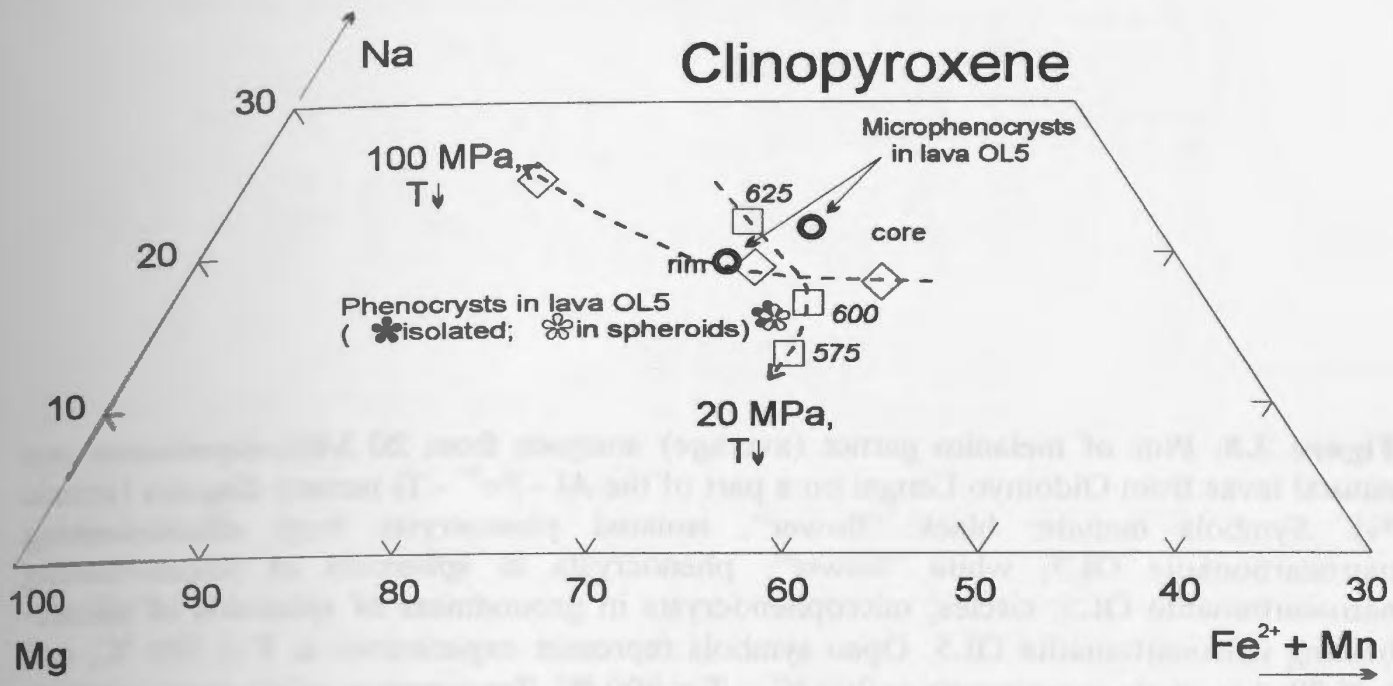
Clinopyroxene
Na
30
20
10
100 MPa,
T↓
Microphenocrysts
in lava OL5
625
core
rim
Phenocrysts in lava OL5
(isolated; in spheroids)
600
575
20 MPa,
T↓
100
90
80
70
60
50
40
30
Mg
Fe2+ + Mn

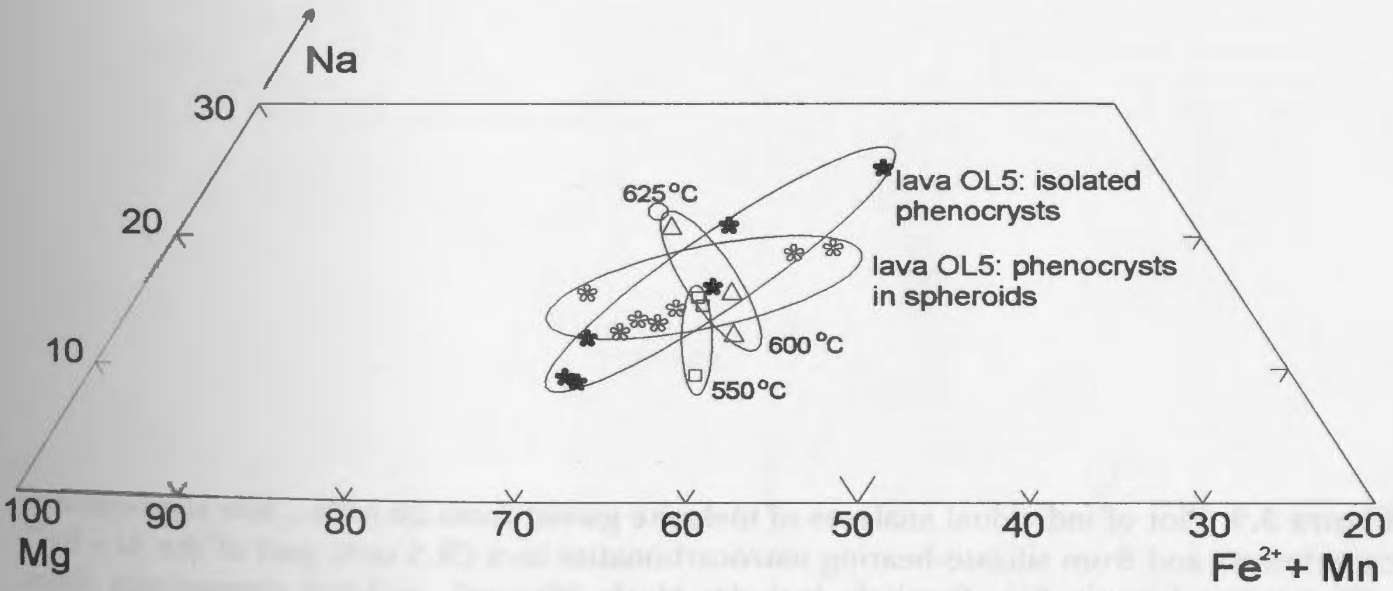
Na
30
20
10
625°C
lava OL5: isolated
phenocrysts
lava OL5: phenocrysts
in spheroids
600°C
550°C
100
90
80
70
60
50
40
30
20
Mg
Fe2+ + Mn

Figure 3.8: Plot of melanite garnet (average) analyses from 20 MPa-experiments and natural lavas from Oldoinyo Lengai on a part of the Al - Fe^{3+} - Ti ternary diagram (atomic %). Symbols include: black "flower", isolated phenocrysts from silicate-bearing natrocarbonatite OL5; white "flower", phenocrysts in spheroids of silicate-bearing natrocarbonatite OL5; circles, microphenocrysts in groundmass of spheroids of silicate-bearing natrocarbonatite OL5. Open symbols represent experiments at $T \leq 700$ °C, and half-filled symbols experiments at 700 °C $< T \leq 800$ °C. Temperature of the experiments is indicated beside the symbols. Data are from Table 3.4.

Figure 3.9: Plot of individual analyses of melanite garnet from 20 MPa-, low temperature-experiments and from silicate-bearing natrocarbonatite lava OL5 onto part of the Al - Fe^{3+} - Ti ternary (atomic %). Symbols include: black "flower", isolated phenocrysts from silicate-bearing natrocarbonatite OL5; white "flower", phenocrysts in spheroids of silicate-bearing natrocarbonatite OL5. Temperature of the experiments is indicated. Data are from Tables A3.1 and A3.2 in Appendix A3.

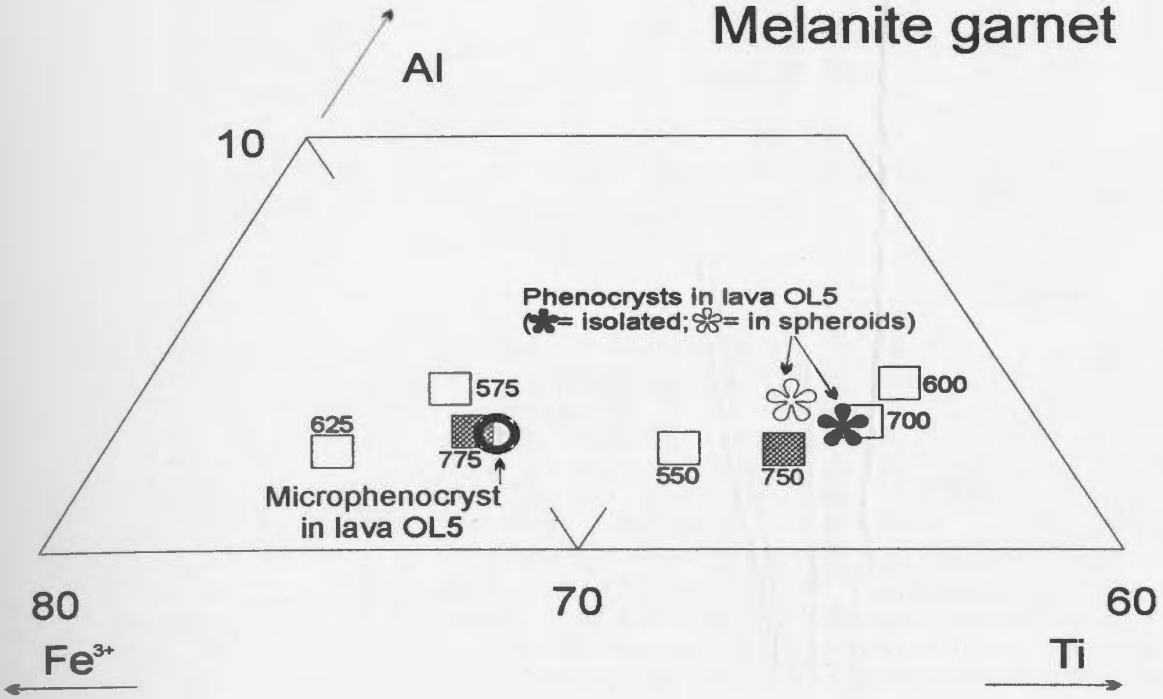
Melanite garnet
Al
10
Phenocrysts in lava OL5
(✱= isolated; ❀= in spheroids)
575
600
625
700
775
550
750
Microphenocryst
in lava OL5
80
70
60
Fe3+
Ti

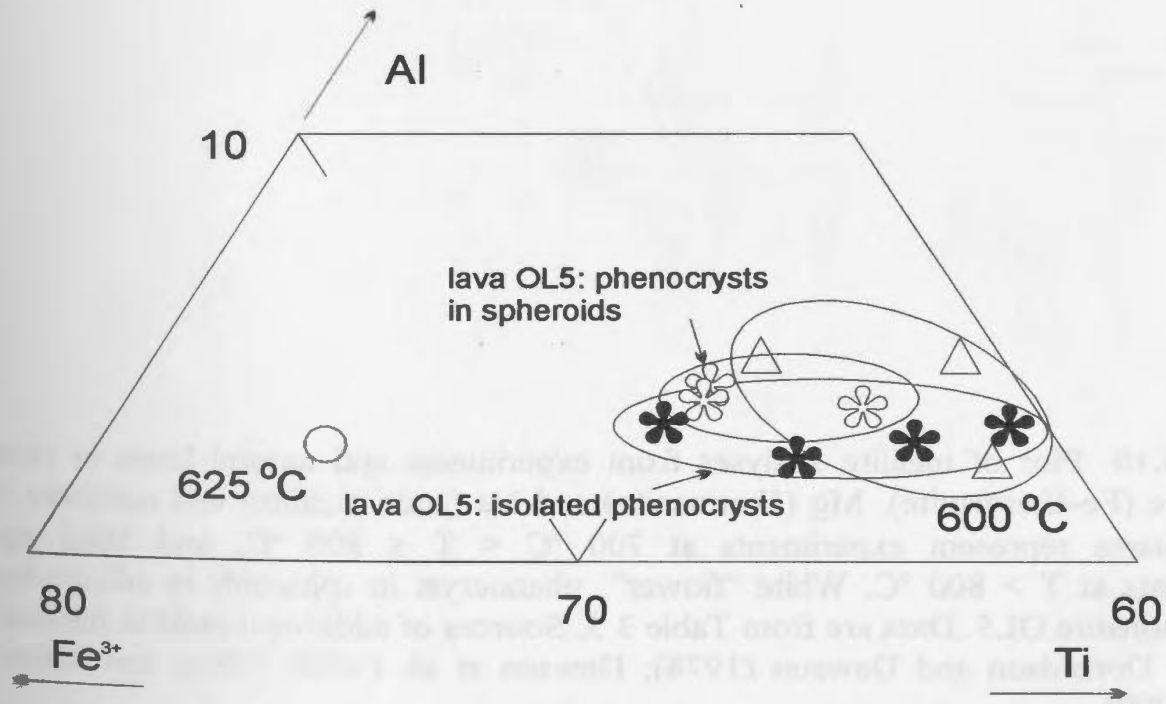
Al
10
lava OL5: phenocrysts
in spheroids
625 °C
lava OL5: isolated phenocrysts
600 °C
80
70
60
Fe3+
Ti

Figure 3.10: Plot of melilite analyses from experiments and natural lavas in terms of ternary Fe (Fe-åkermanite), Mg (åkermanite) and Na (soda melilite) end members. Half-filled squares represent experiments at 700 °C < T ≤ 800 °C, and filled squares experiments at T > 800 °C. White "flower", phenocryst in spheroids in silicate-bearing natrocarbonatite OL5. Data are from Table 3.5. Sources of additional melilite mineral data are from Donaldson and Dawson (1978); Dawson et al. (1989, 1996) and Keller and Krafft (1990).

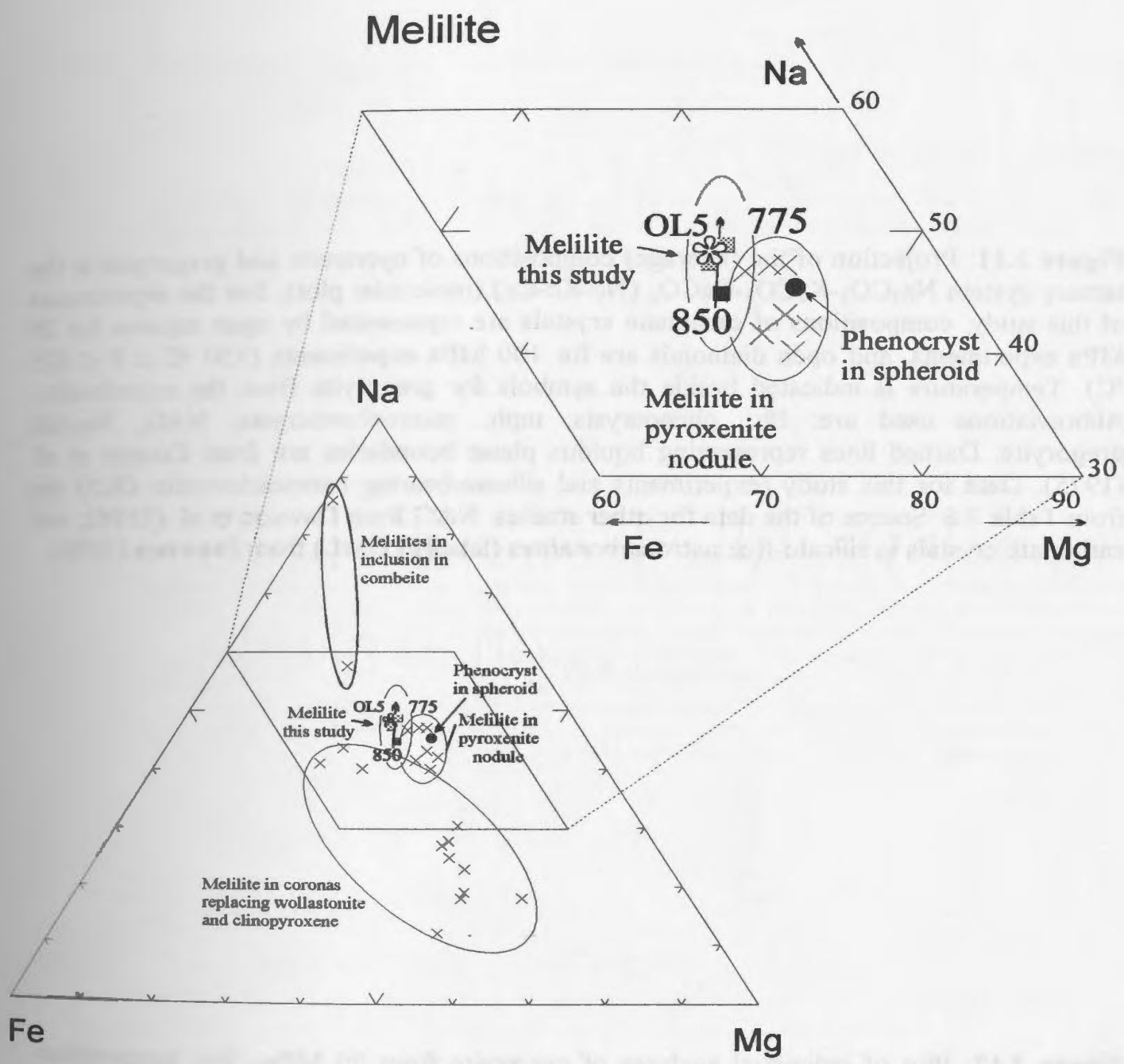
Melilite
Na
60
50
40
30
OL5
775
850
Melilite
this study
Phenocryst
in spheroid
Melilite in
pyroxenite
nodule
60
70
80
90
Fe
Mg
Na
Melilites in
inclusion in
combeite
Phenocryst
in spheroid
Melilite
this study
OL5
775
850
Melilite in
pyroxenite
nodule
Melilite in coronas
replacing wollastonite
and clinopyroxene
Fe
Mg

Figure 3.11: Projection of the (average) compositions of nyerereite and gregoryite in the ternary system Na_2CO_3-K_2CO_3-$CaCO_3$ (Nc-Kc-Cc) (molecular plot). For the experiments of this study, compositions of carbonate crystals are represented by open squares for 20 MPa experiments, and open diamonds are for 100 MPa experiments (550 °C ≤ T ≤ 625 °C). Temperature is indicated beside the symbols for gregoryite from the experiments. Abbreviations used are: Ph., phenocrysts; mph., microphenocrysts; NAG, Na-rich gregoryite. Dashed lines representing liquidus phase boundaries are from Cooper et al. (1975). Data for this study (experiments and silicate-bearing natrocarbonatite OL5) are from Table 3.6. Source of the data for other studies: NAG from Dawson et al. (1996), and carbonate crystals in silicate-free natrocarbonatites (labelled CML) from Peterson (1990).

Figure 3.12: Plot of individual analyses of nyerereite from 20 MPa-, low temperature-experiments and from silicate-bearing natrocarbonatite lava OL5 in the ternary system Na_2CO_3-K_2CO_3-$CaCO_3$ (Nc-Kc-Cc) (molecular plot). Symbols include: filled diamonds, isolated phenocrysts from lava OL5; o, experiments at 625 °C; Δ, experiments at 600 °C; x, experiments at 575 °C; □, experiments at 550 °C. The temperature of the experiments is indicated beside the symbol. Dashed lines representing liquidus phase boundaries are from Cooper et al. (1975). Data are from Tables A3.1 and A3.2 in Appendix A3.

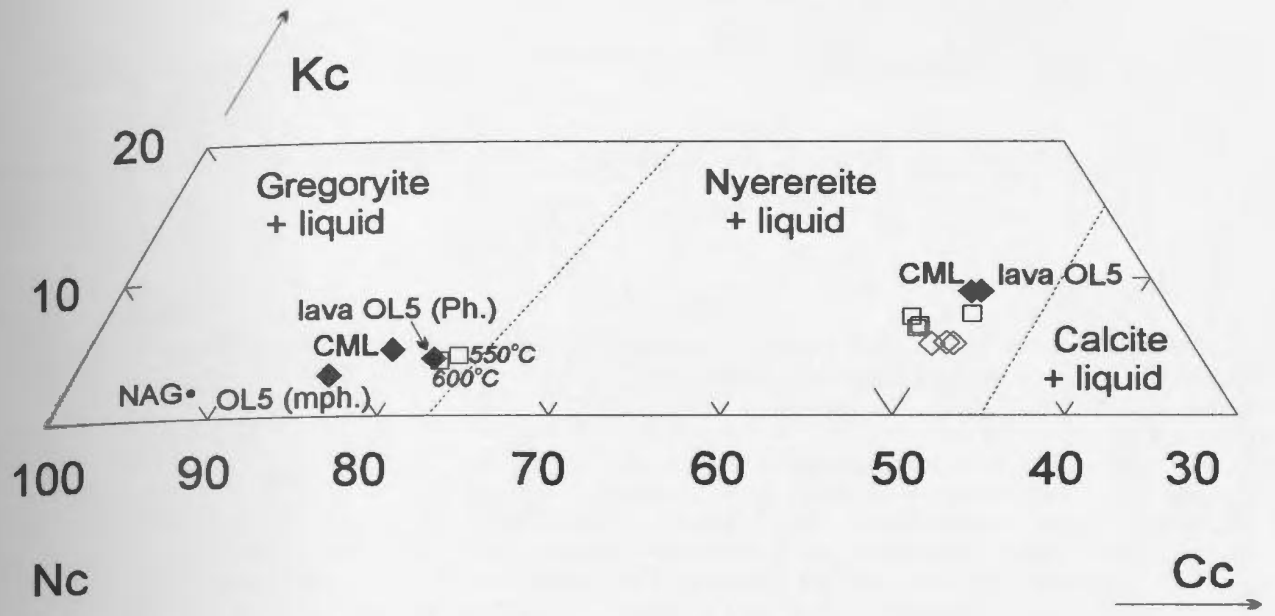
Kc
20
10
Gregoryite
+ liquid
Nyerereite
+ liquid
CML
lava OL5
lava OL5 (Ph.)
CML
550°C
600°C
NAG
OL5 (mph.)
Calcite
+ liquid
100
90
80
70
60
50
40
30
Nc
Cc

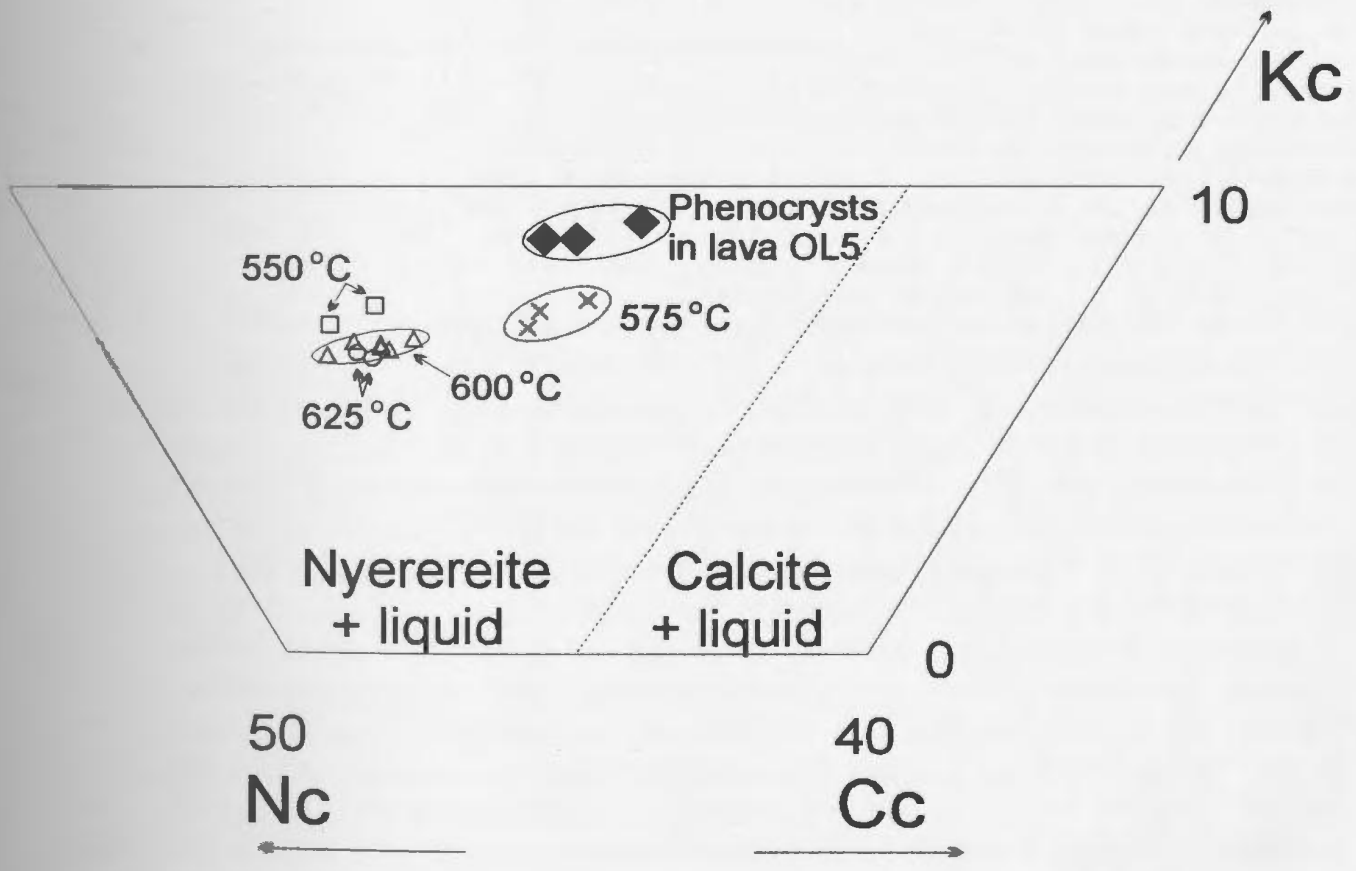
Kc
10
Phenocrysts
in lava OL5
550 °C
575 °C
600 °C
625 °C
Nyerereite
+ liquid
Calcite
+ liquid
0
50
40
Nc
Cc

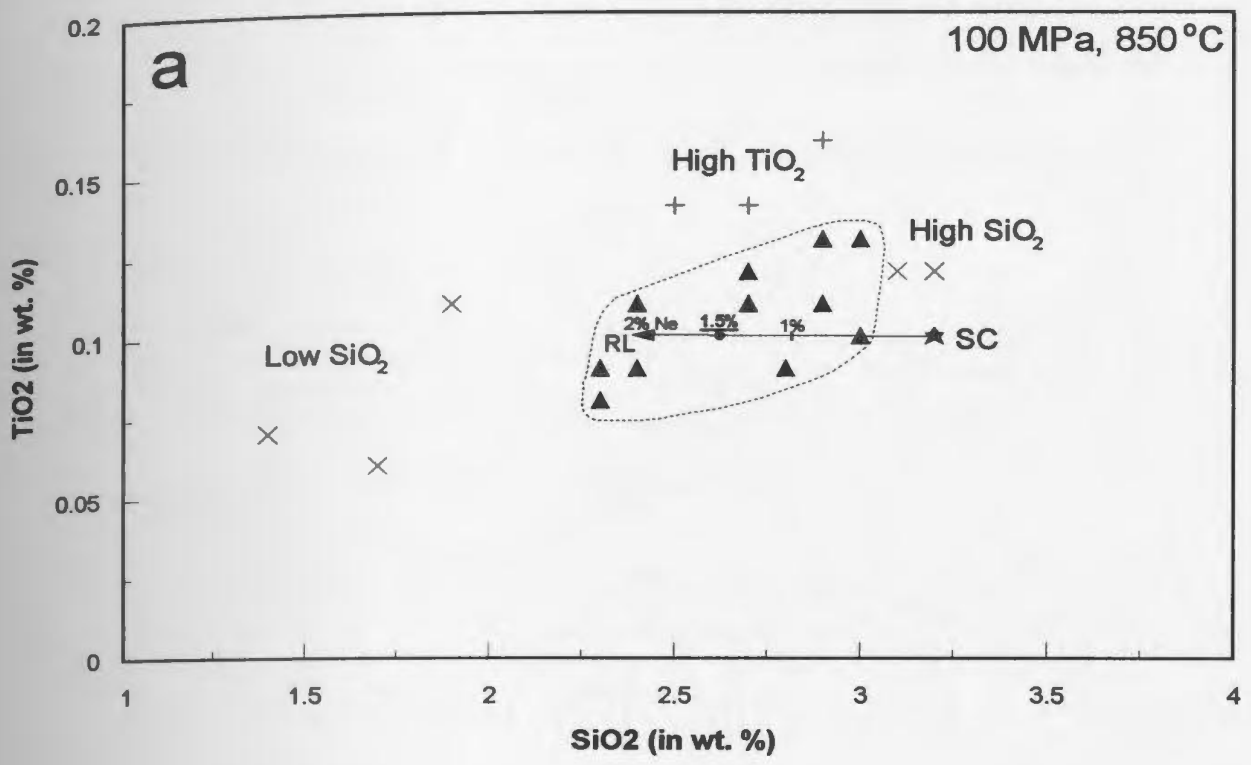

Figure 3.13: Variation diagrams for selected major elements versus SiO_2 for carbonate liquid from experiment CP106 (100 MPa, 850 °C). Elements plotted versus SiO_2 are: (a) TiO_2; (b) Al_2O_3; (c) CaO; (d) K_2O; (e) P_2O_5; (f) Cl and (g) SO_3. The arrow represents the direction toward which the composition of the calculated, residual liquid (RL) evolves when nepheline is subtracted from the starting composition (SC). The proportion of subtracted nepheline (Ne) is labelled (in wt. %) beside the arrow. The dot represents the calculated, residual liquid for 1.5 % nepheline (proportion suggested to be present in CP106 based on SEM work) subtracted from the starting composition. Individual analyses which have been rejected for having too high or too low of a SiO_2 content compared to that of the calculated, residual liquid are represented by a cross (x). Individual analyses which have been rejected for having too high or too low concentration of the element plotted on the y-axis compared to that of the calculated, residual liquid are represented by a cross (+). Individual analyses used to calculate the average liquid composition are represented by a filled triangle and are within the area denoted by a dotted line. Individual analyses of carbonate liquid are from Table A3.3 in Appendix 3, and calculated composition of the residual liquid is from Table 3.10.

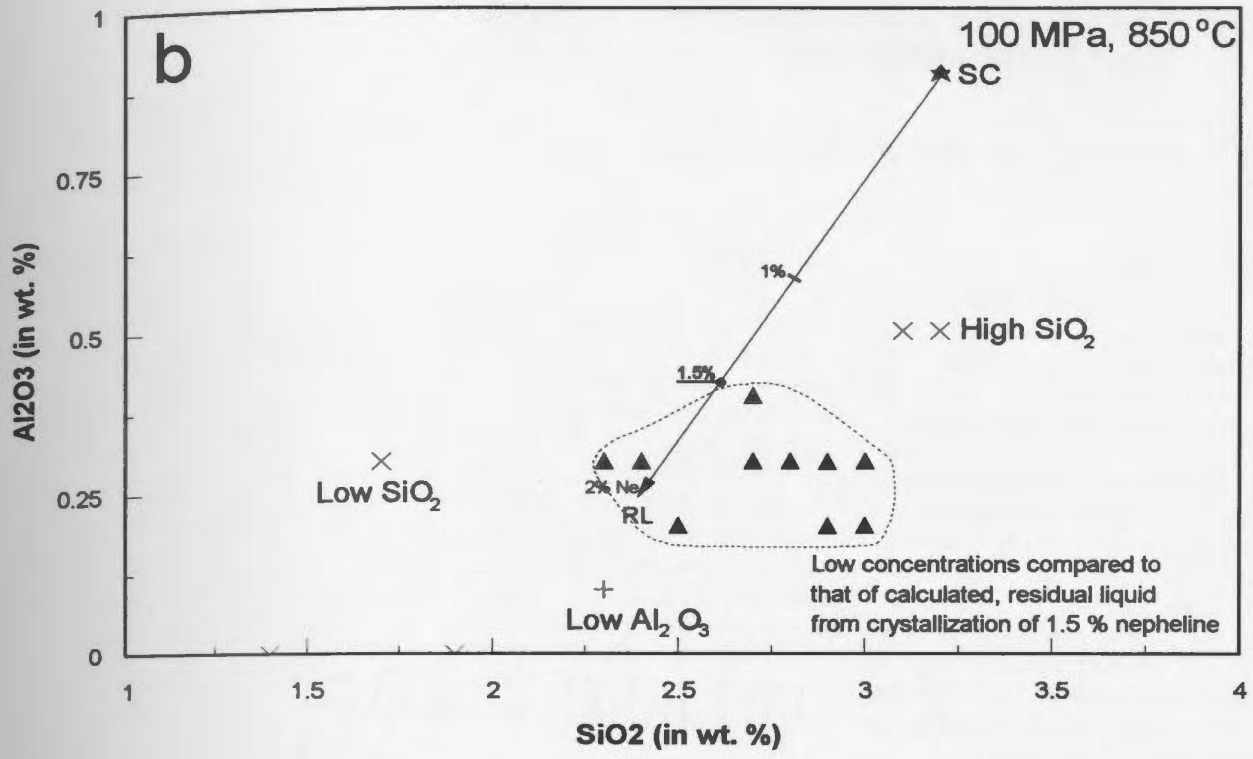
b
100 MPa, 850°C
SC
1%
1.5%
High SiO2
Low SiO2
2% Ne
RL
Low concentrations compared to
that of calculated, residual liquid
from crystallization of 1.5 % nepheline
Low Al2 O3
Al2O3 (in wt. %)
SiO2 (in wt. %)
0
0.25
0.5
0.75
1
1
1.5
2
2.5
3
3.5
4

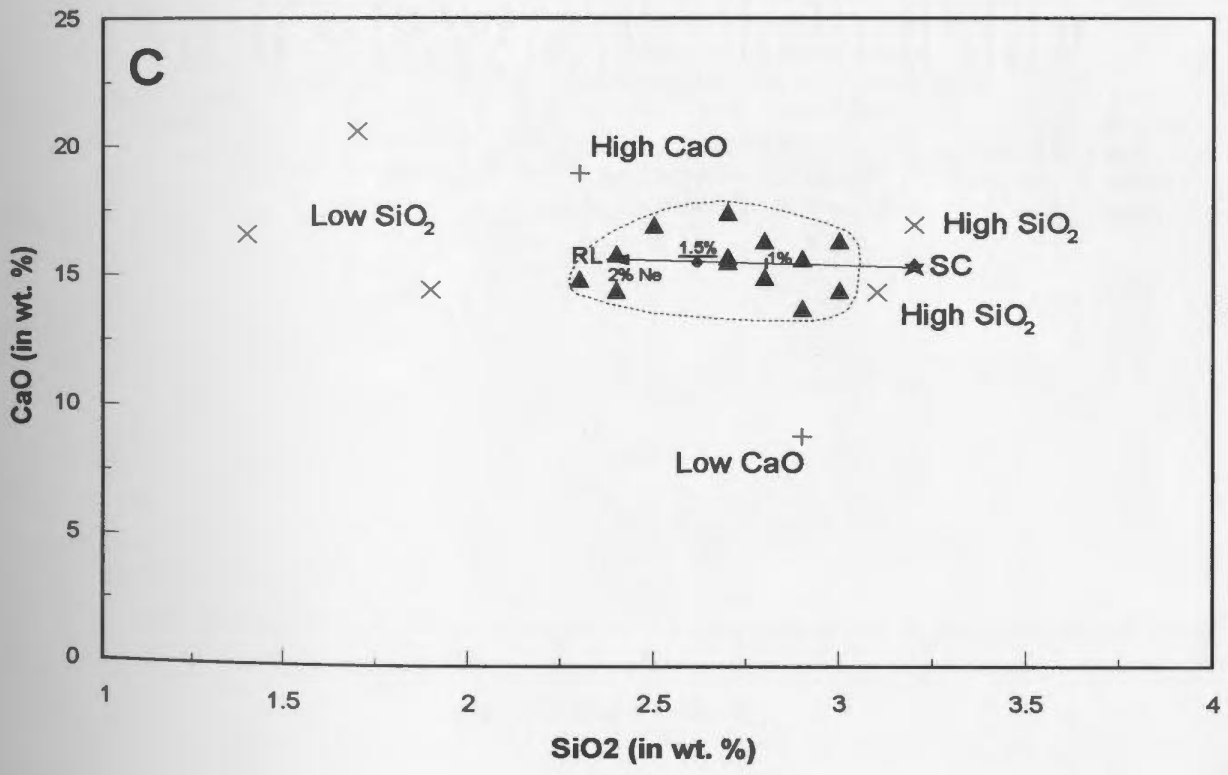
c
High CaO
Low SiO2
High SiO2
RL
1.5%
1%
2% Ne
SC
High SiO2
Low CaO
CaO (in wt. %)
SiO2 (in wt. %)
0
5
10
15
20
25
1
1.5
2
2.5
3
3.5
4

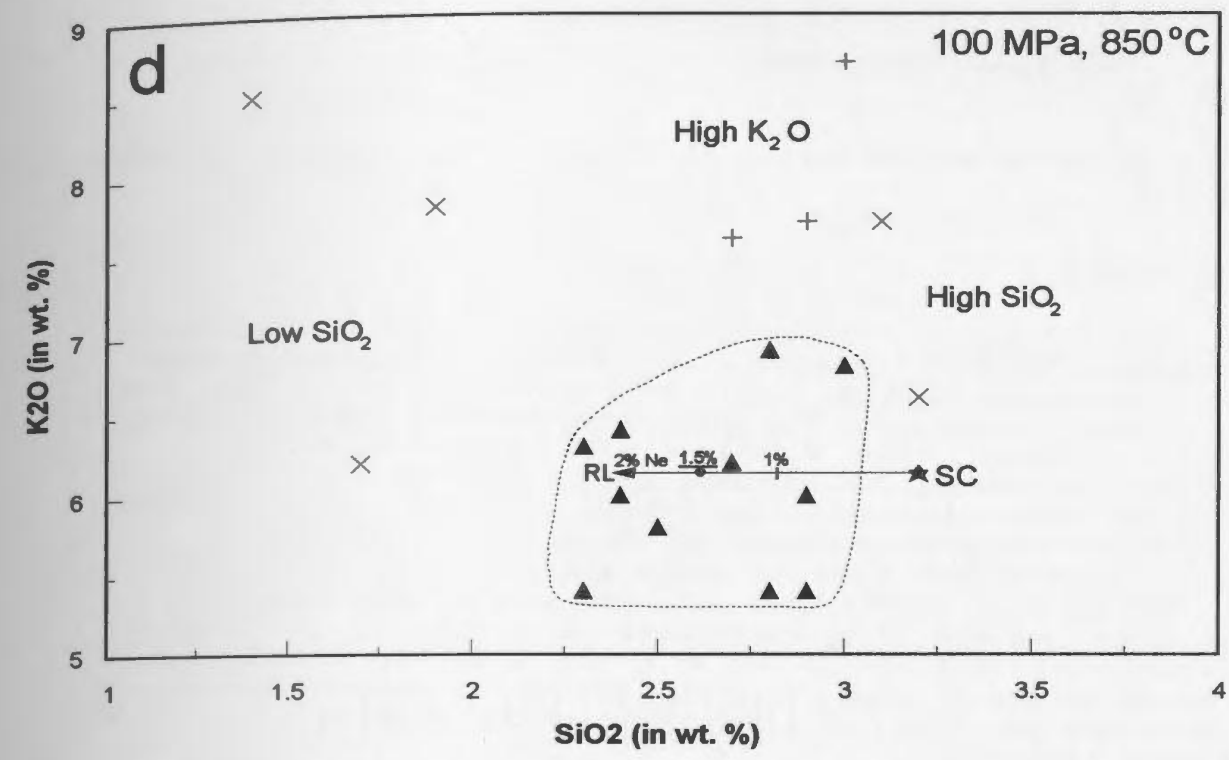
d
100 MPa, 850 °C
High K_2O
High SiO_2
Low SiO_2
RL
2% Ne
1.5%
1%
SC
K2O (in wt. %)
SiO2 (in wt. %)
9
8
7
6
5
1
1.5
2
2.5
3
3.5
4

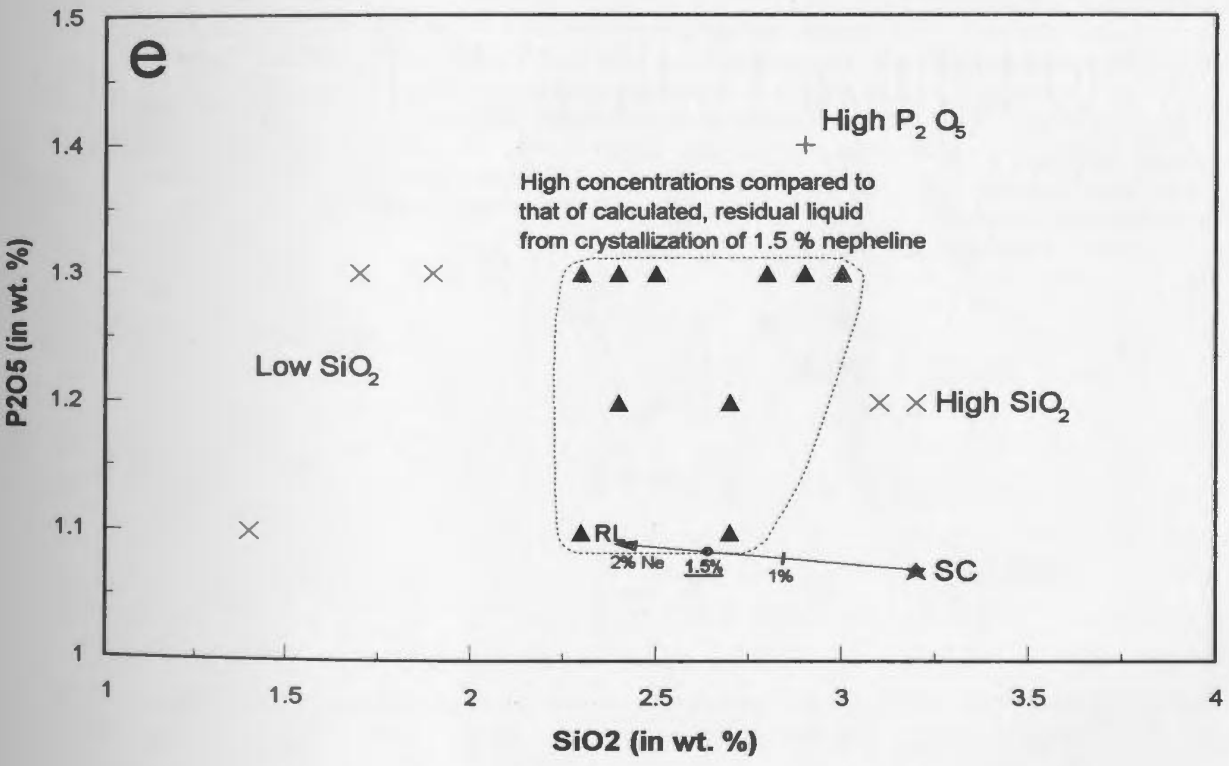
e
High P_2O_5
High concentrations compared to
that of calculated, residual liquid
from crystallization of 1.5 % nepheline
Low SiO_2
High SiO_2
RL
2% Ne
1.5%
1%
SC
P2O5 (in wt. %)
SiO2 (in wt. %)
1.5
1.4
1.3
1.2
1.1
1
1
1.5
2
2.5
3
3.5
4

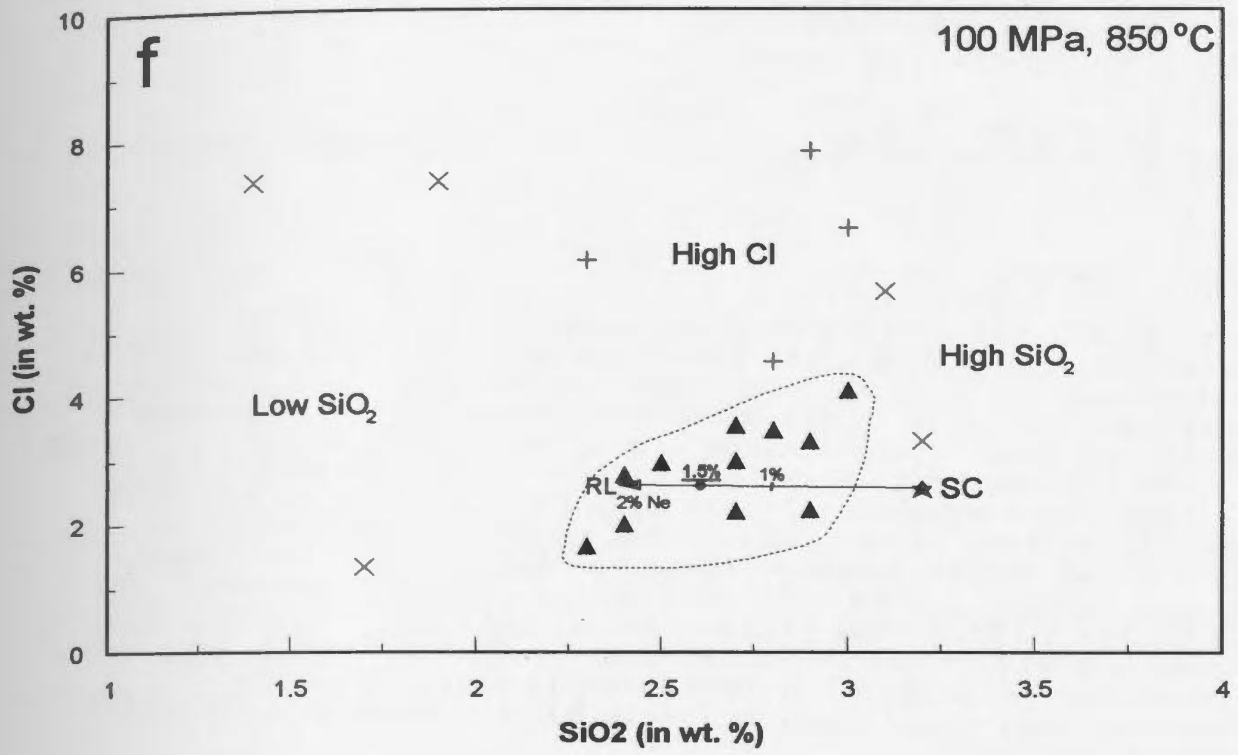
f
100 MPa, 850 °C
High Cl
High SiO2
Low SiO2
RL
2% Ne
1.5%
1%
SC
Cl (in wt. %)
SiO2 (in wt. %)
0
2
4
6
8
10
1
1.5
2
2.5
3
3.5
4

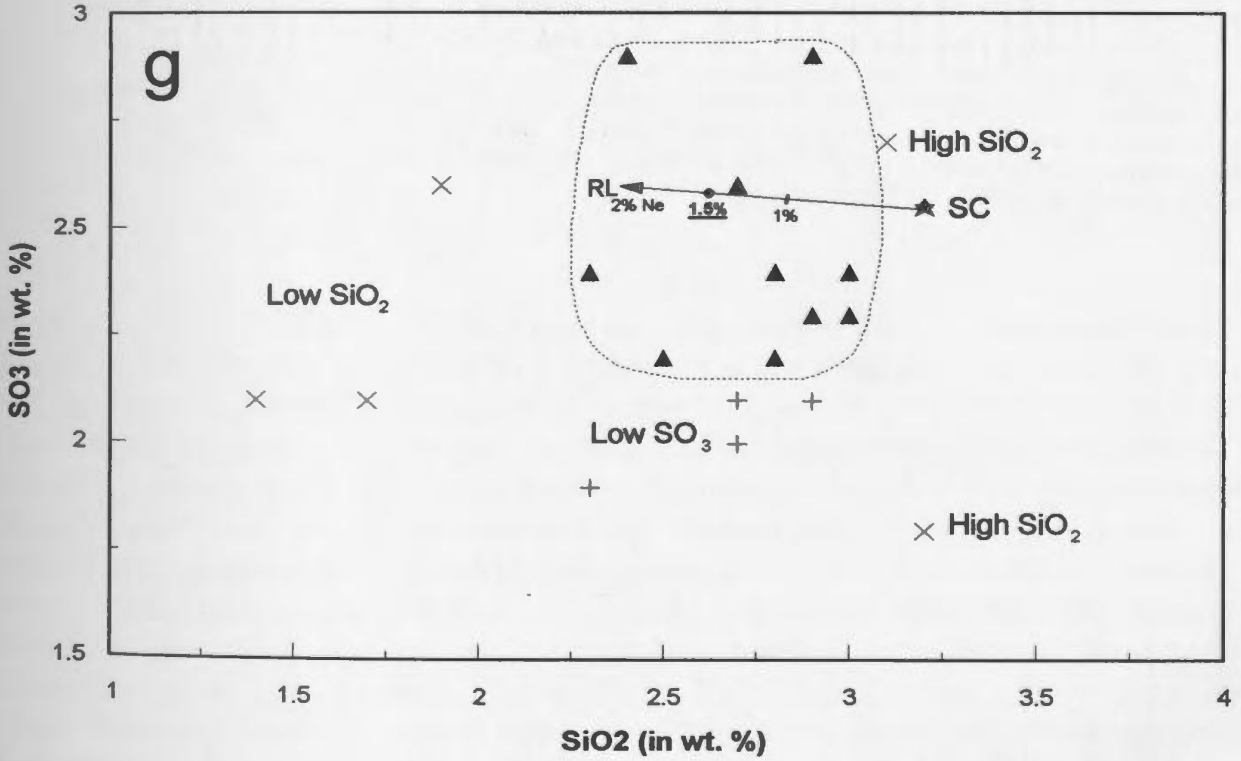
g
High SiO2
RL
2% Ne
1.5%
1%
SC
Low SiO2
Low SO3
High SiO2
SO3 (in wt. %)
SiO2 (in wt. %)
1.5
2
2.5
3
1
1.5
2
2.5
3
3.5
4

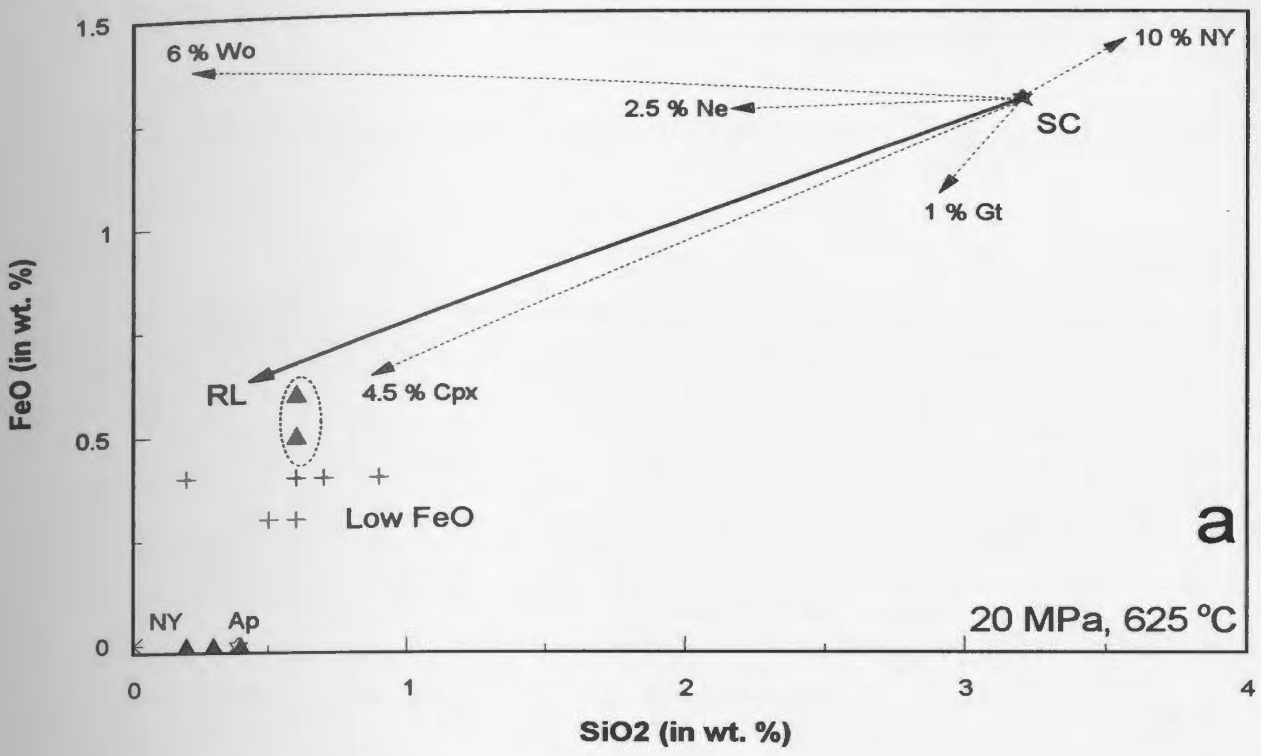

Figure 3.14: Variation diagrams for major elements versus SiO_2 for carbonate liquid from experiment CP129 (20 MPa, 625 °C). Elements plotted versus SiO_2 are: (a) FeO; (b) MnO; (c) MgO; (d) CaO; (e) Na_2O; (f) K_2O; (g) P_2O_5; (h) F; (i) Cl; (j) SO_3; (k) BaO; and (l) SrO. The bold dark arrow represents the direction toward which the composition of the calculated, residual liquid (RL) evolves when crystals present in CP129 (see proportions in Tab. 3.9) are subtracted from the starting composition (SC). Other dotted arrows represent the direction toward which the composition of the calculated, residual liquid evolves when each crystal phase is individually subtracted from the bulk composition (proportion of crystals used for the calculation is labelled at the end of the arrow). See caption of Figure 3.13 for remaining symbols. Note that the composition of individual crystals is plotted when they occur within the scale of the graph. Abbreviations used are: Ne, nepheline; Cpx, clinopyroxene; Gt, melanite garnet; Wo, wollastonite; NY, nyerereite; Ap, apatite. Individual analyses of carbonate liquid are from Table A3.3 in Appendix 3, and calculated composition of the residual liquid is from Table 3.10.

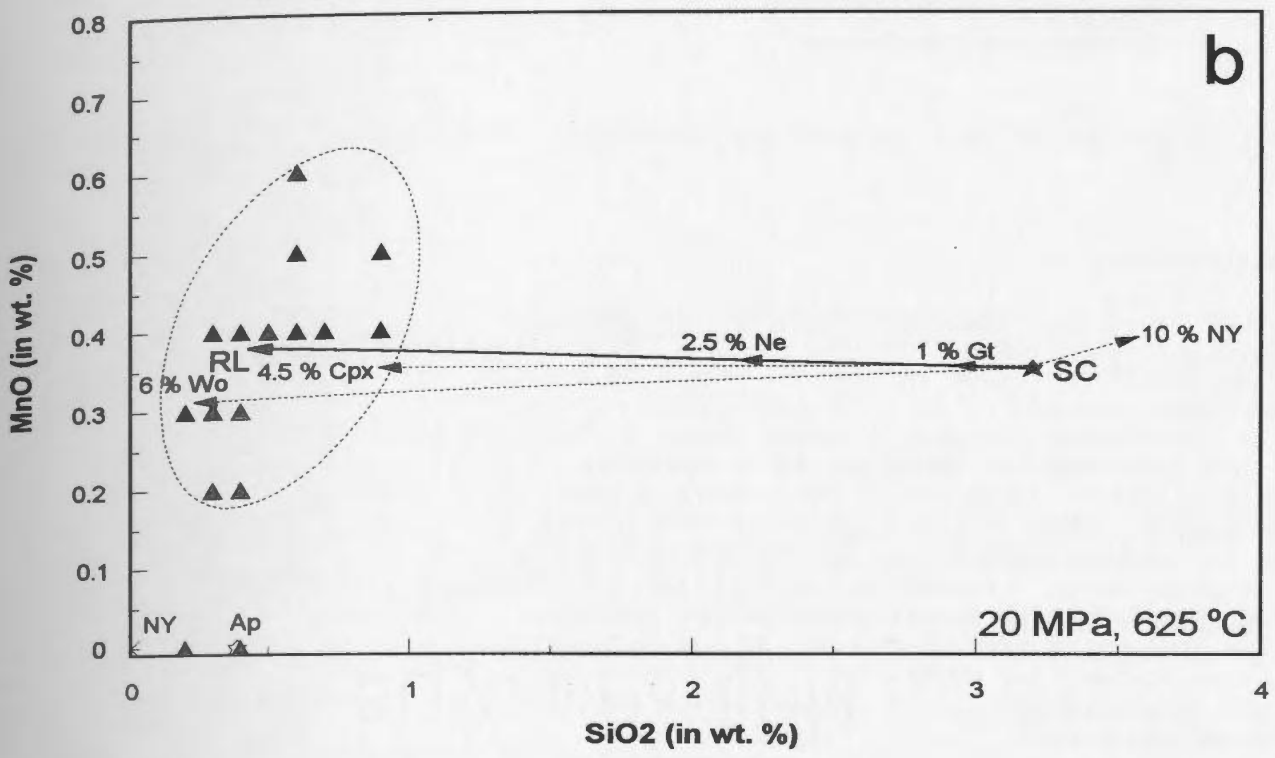
b
MnO (in wt. %)
SiO2 (in wt. %)
RL
6 % Wo
4.5 % Cpx
2.5 % Ne
1 % Gt
SC
10 % NY
NY
Ap
20 MPa, 625 °C

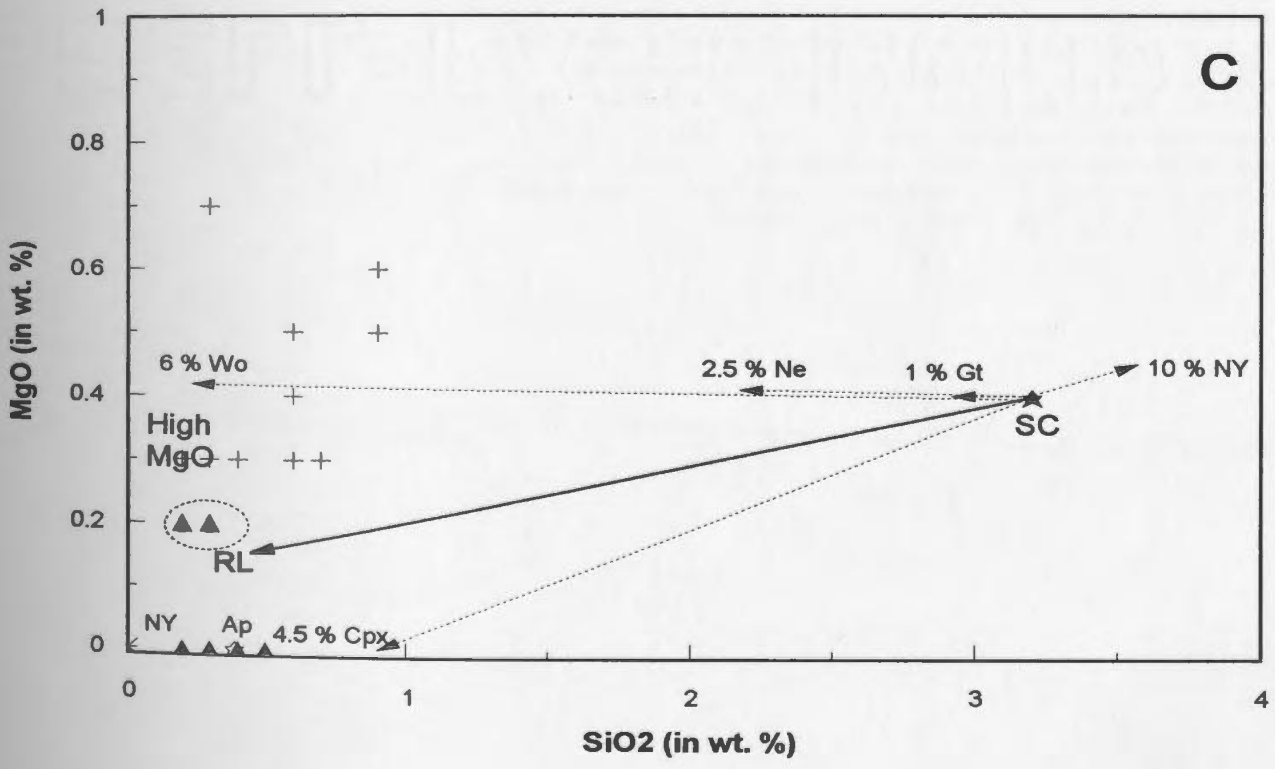
C
MgO (in wt. %)
SiO2 (in wt. %)
6 % Wo
2.5 % Ne
1 % Gt
10 % NY
SC
High MgO
RL
NY
Ap
4.5 % Cpx

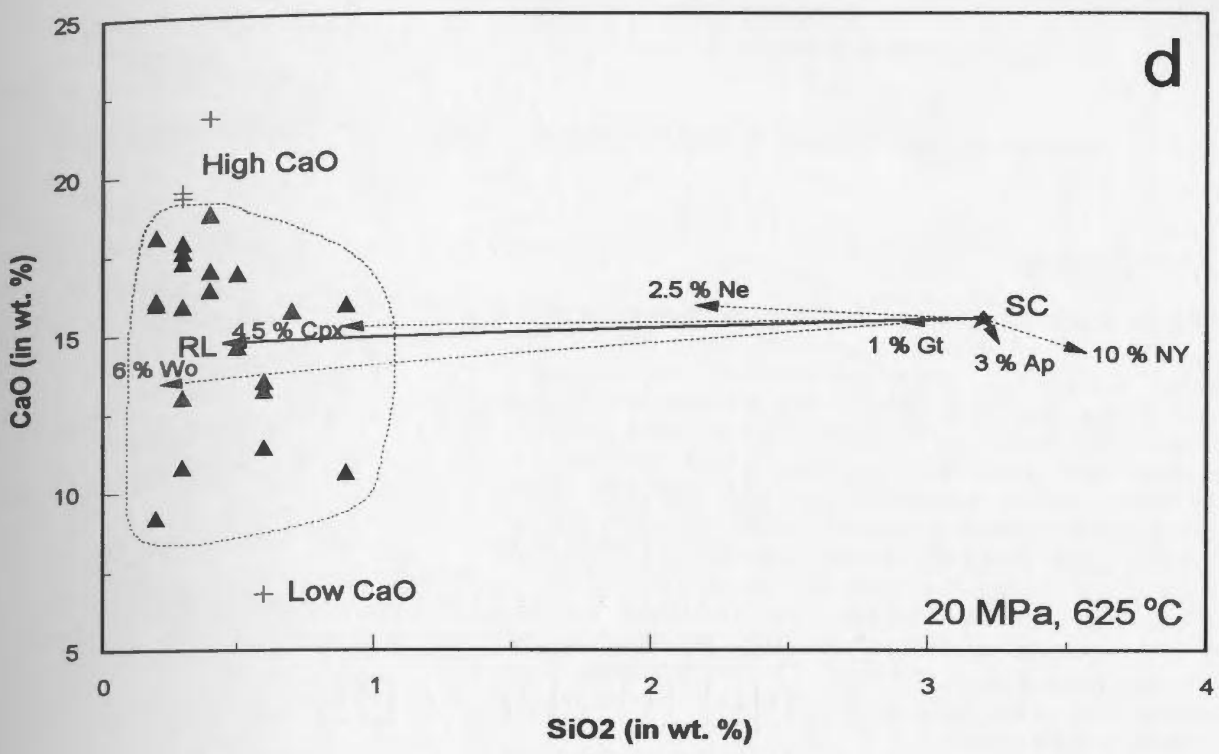
d
High CaO
Low CaO
RL
6 % Wo
4.5 % Cpx
2.5 % Ne
1 % Gt
3 % Ap
SC
10 % NY
20 MPa, 625 °C
CaO (in wt. %)
SiO2 (in wt. %)
25
20
15
10
5
0
1
2
3
4

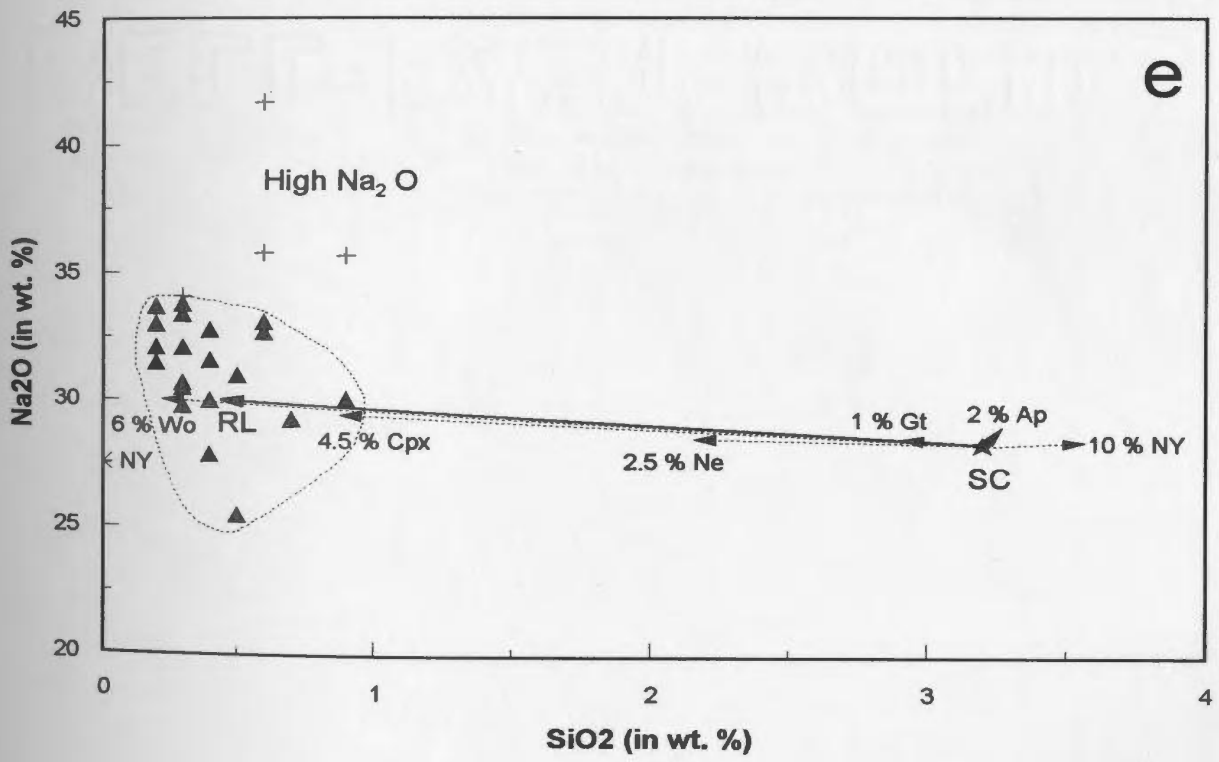
e
High Na2 O
6 % Wo
RL
4.5 % Cpx
2.5 % Ne
1 % Gt
2 % Ap
SC
10 % NY
NY
Na2O (in wt. %)
SiO2 (in wt. %)
45
40
35
30
25
20
0
1
2
3
4

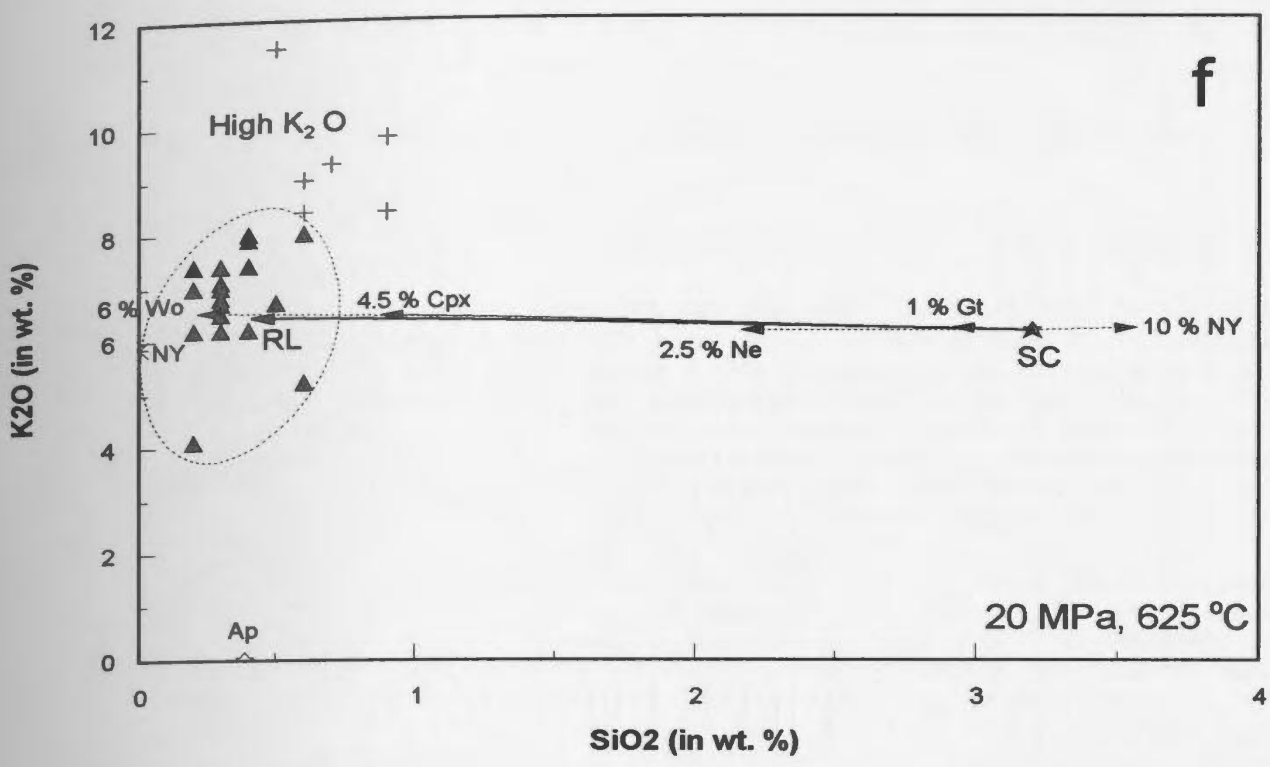
f
High K_2O
6 % Wo
NY
RL
4.5 % Cpx
2.5 % Ne
1 % Gt
SC
10 % NY
Ap
20 MPa, 625 °C
K2O (in wt. %)
SiO2 (in wt. %)
0
2
4
6
8
10
12
1
3

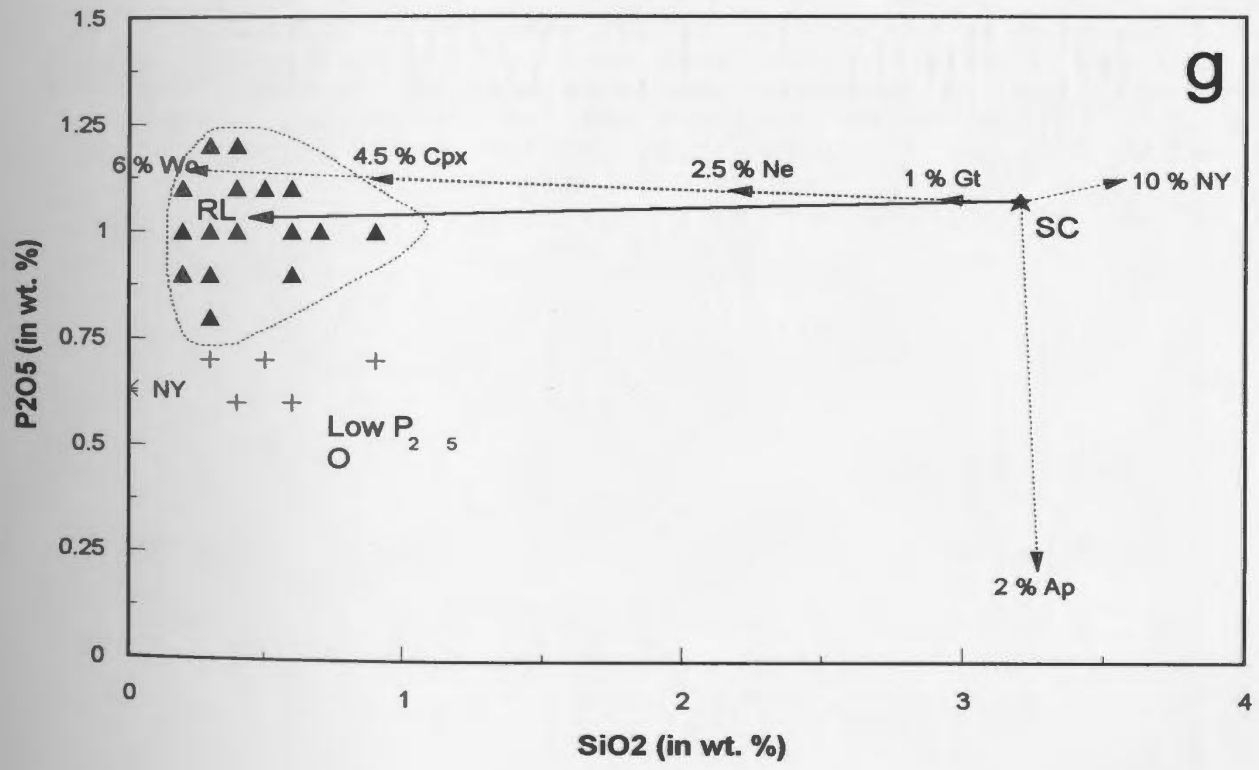
g
6 % Wo
4.5 % Cpx
2.5 % Ne
1 % Gt
10 % NY
RL
SC
NY
Low P_2O_5
2 % Ap
P2O5 (in wt. %)
SiO2 (in wt. %)
0
0.25
0.5
0.75
1
1.25
1.5
1
2
3
4

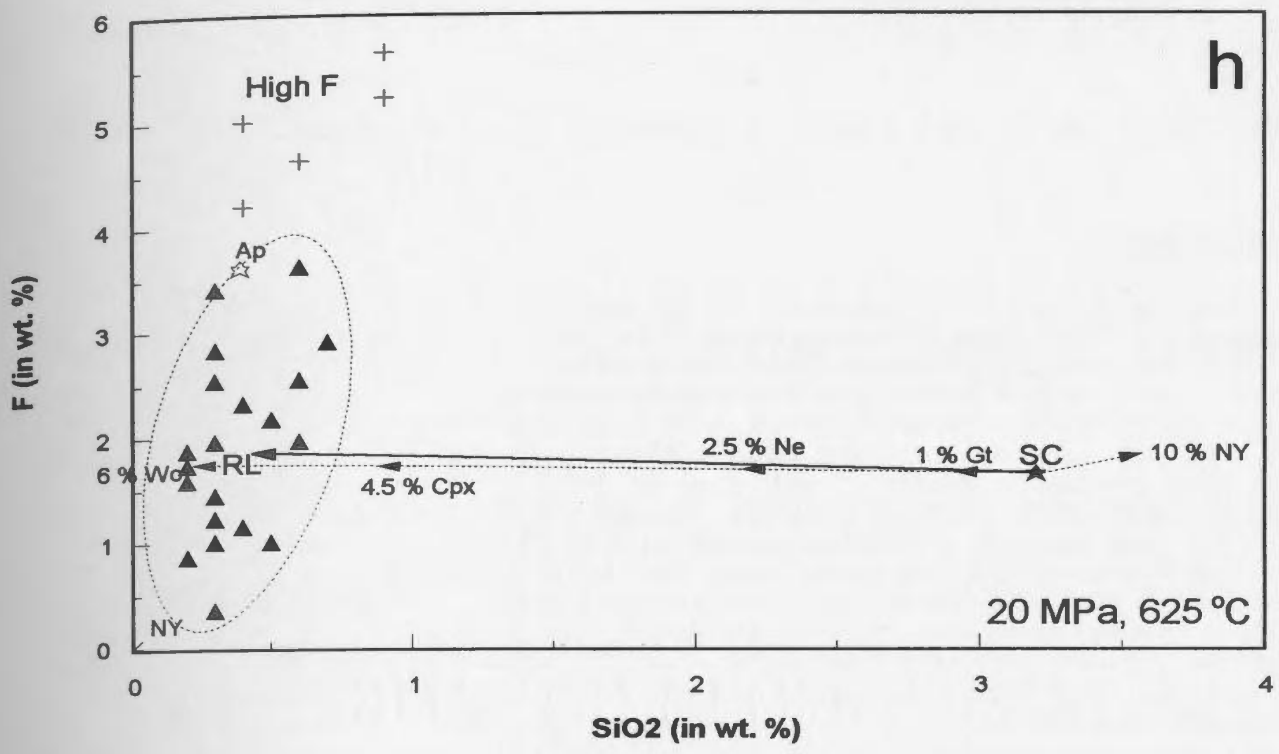
h
High F
Ap
RL
6 % Wo
NY
2.5 % Ne
1 % Gt
SC
10 % NY
4.5 % Cpx
20 MPa, 625 °C
F (in wt. %)
SiO2 (in wt. %)
0
1
2
3
4
5
6

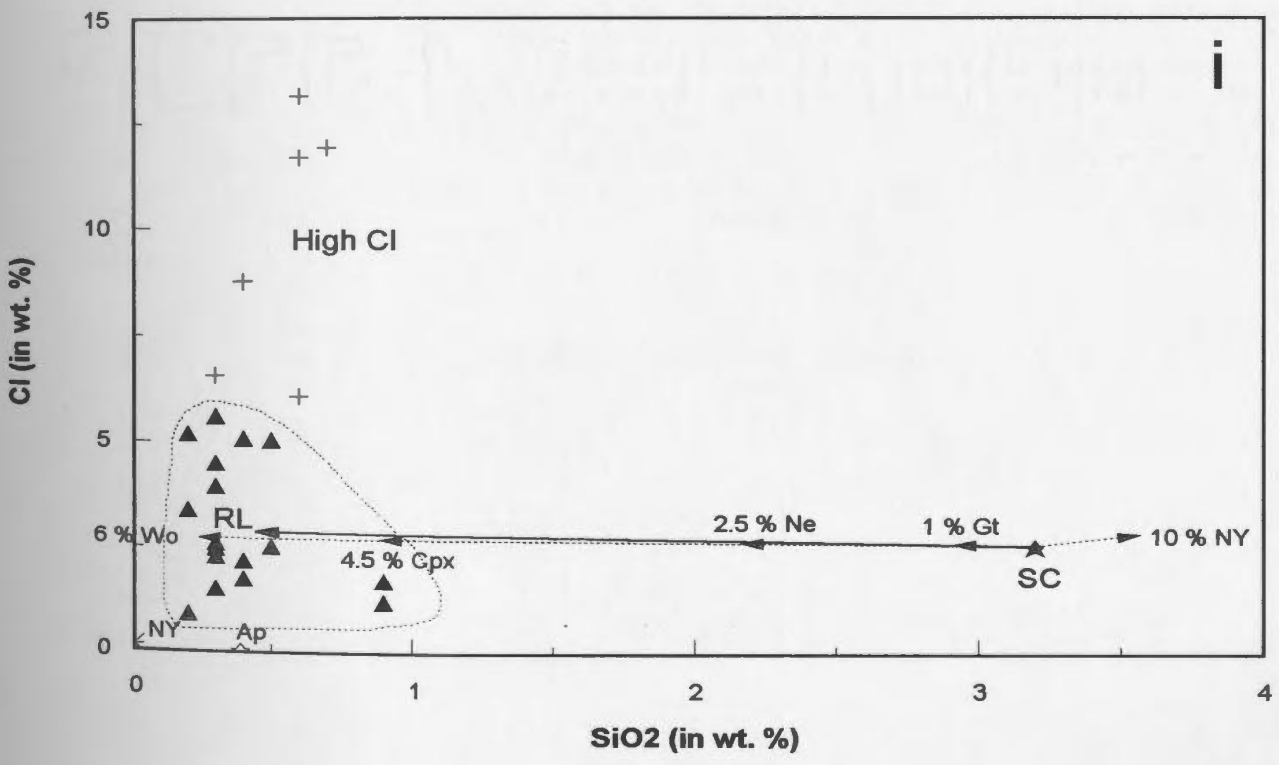
i
High Cl
RL
6 % Wo
NY
Ap
2.5 % Ne
1 % Gt
SC
10 % NY
4.5 % Cpx
Cl (in wt. %)
SiO2 (in wt. %)
0
1
2
3
4
5
6
10
15

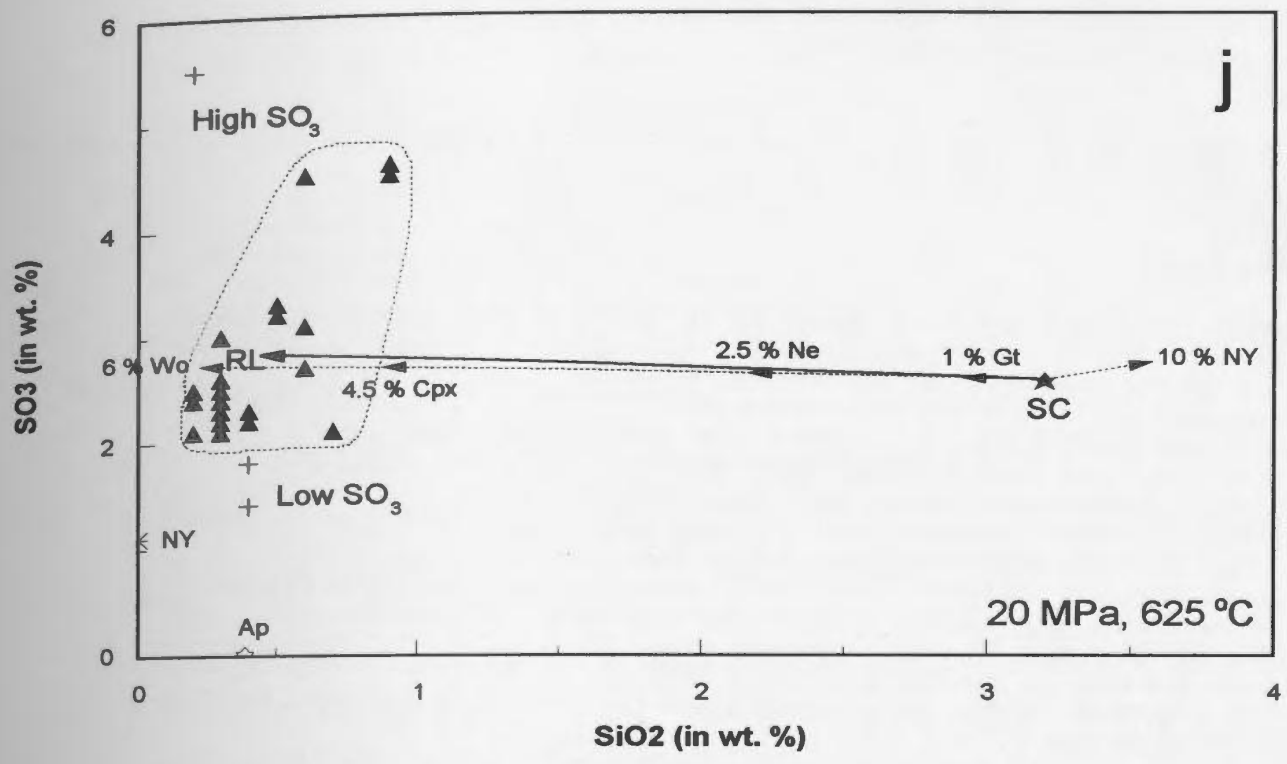
j
High SO_3
Low SO_3
RL
6 % Wo
2.5 % Ne
1 % Gt
10 % NY
4.5 % Cpx
SC
NY
Ap
20 MPa, 625 °C
SO3 (in wt. %)
SiO2 (in wt. %)
0
2
4
6
0
1
2
3
4

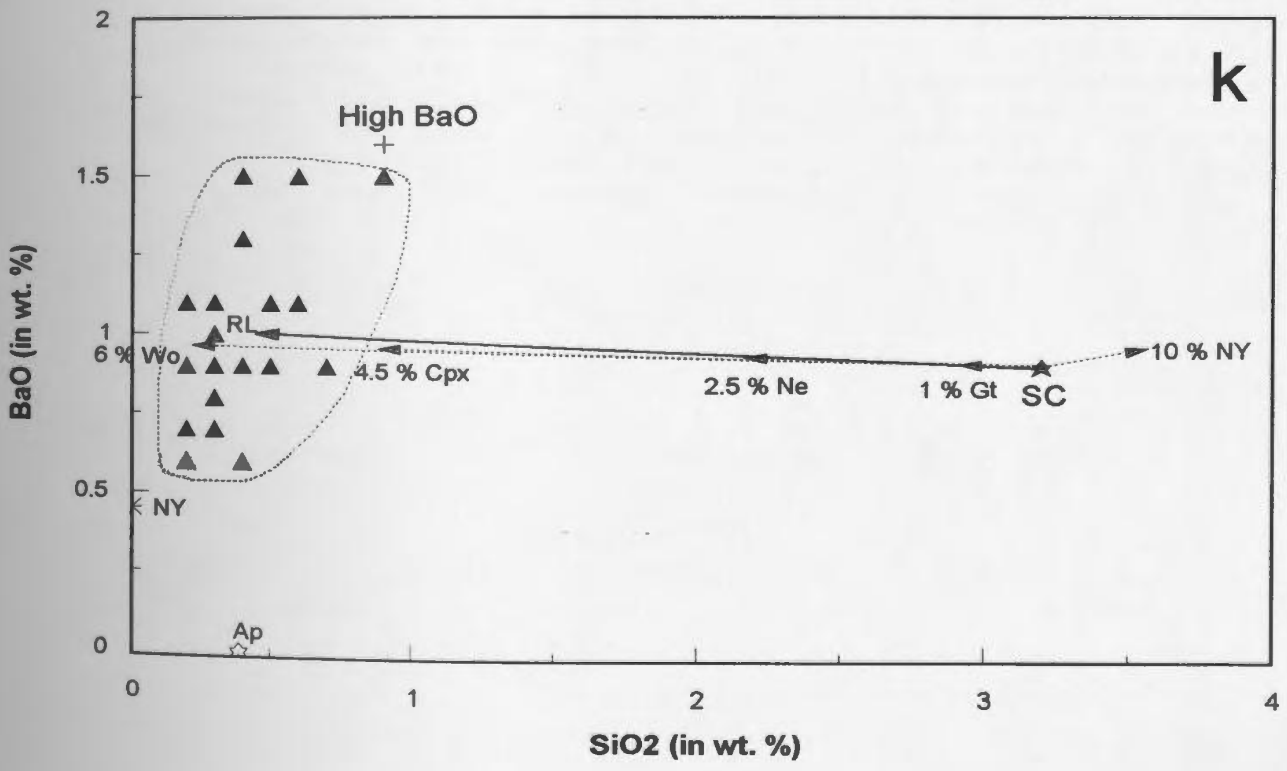
k
High BaO
RL
6 % Wo
4.5 % Cpx
2.5 % Ne
1 % Gt
SC
10 % NY
NY
Ap
BaO (in wt. %)
SiO2 (in wt. %)
0
0.5
1
1.5
2
0
1
2
3
4

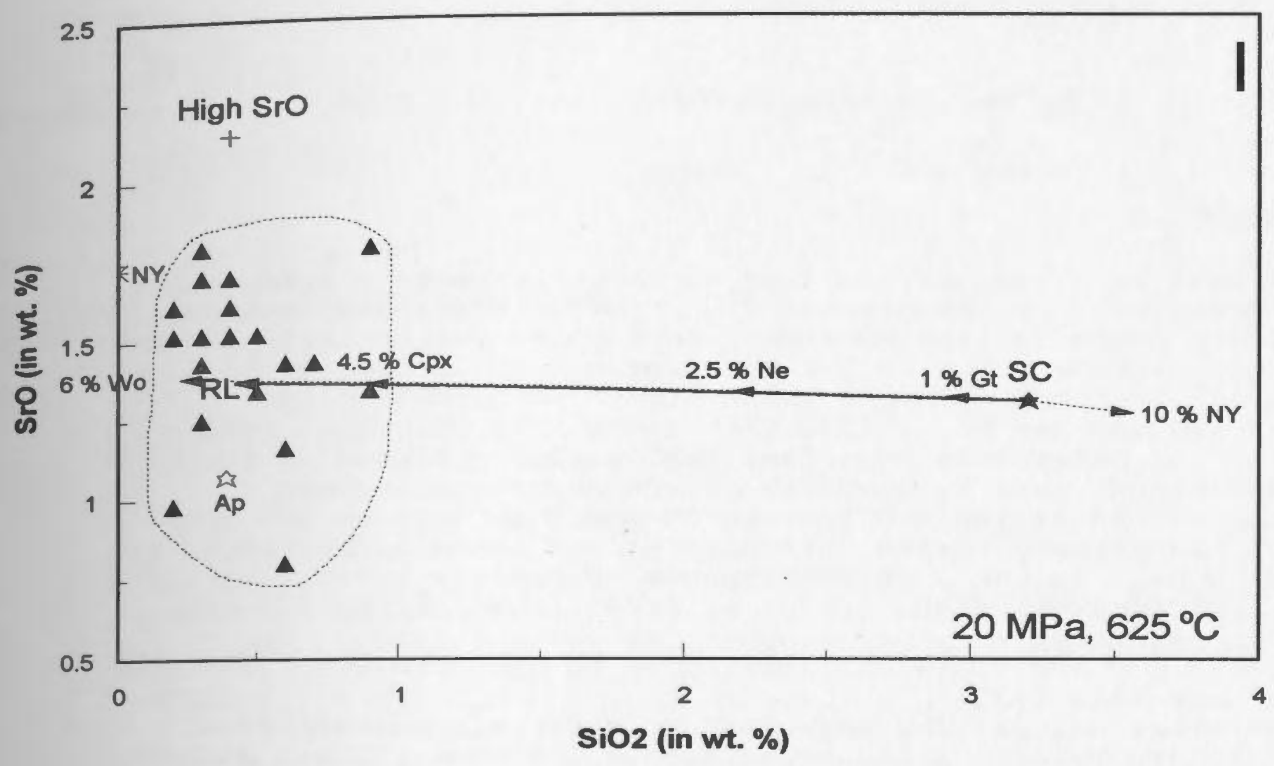
2.5
2
1.5
1
0.5
SrO (in wt. %)
High SrO
NY
6 % Wo
RL
4.5 % Cpx
2.5 % Ne
1 % Gt
SC
10 % NY
Ap
20 MPa, 625 °C
0
1
2
3
4
SiO2 (in wt. %)

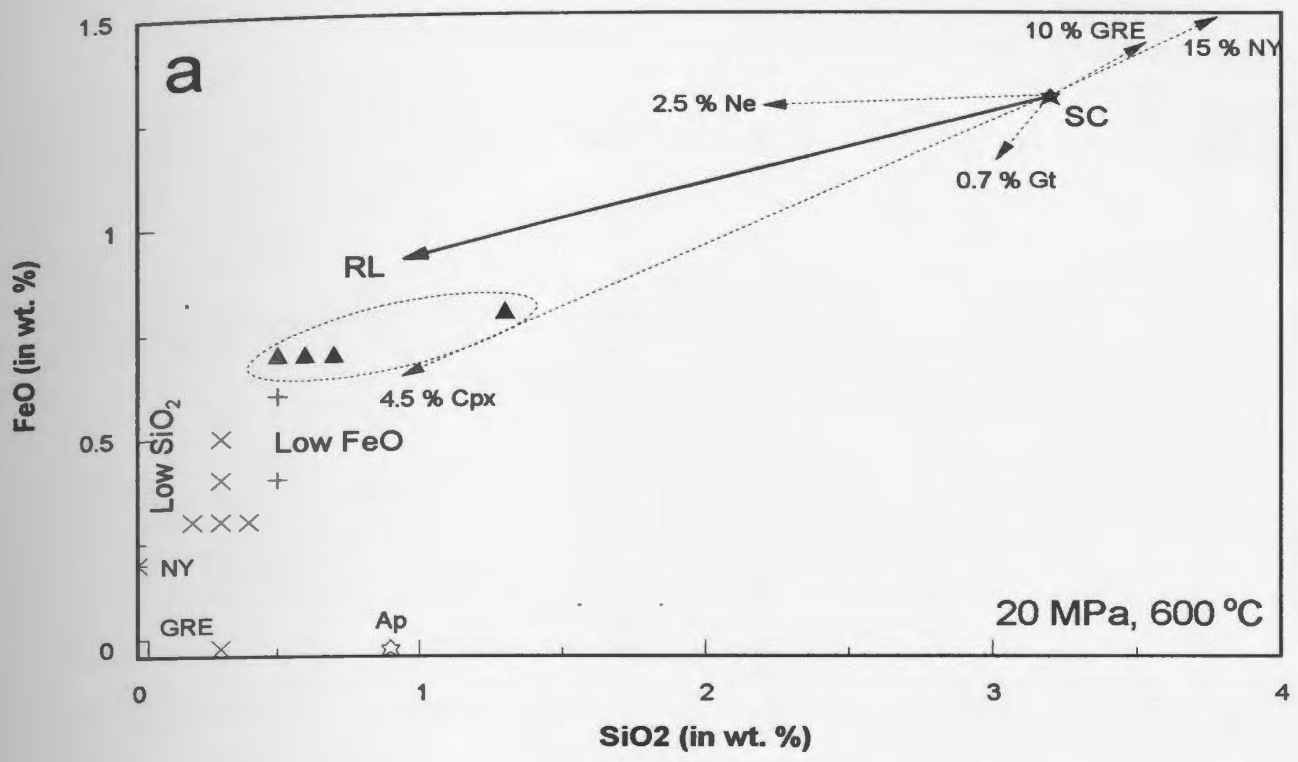

Figure 3.15: Variation diagrams for major elements versus SiO_2 for carbonate liquid from experiment CP108 (20 MPa, 600 °C). Elements plotted versus SiO_2 are: (a) FeO; (b) MnO; (c) MgO; (d) CaO; (e) Na_2O; (f) K_2O; (g) P_2O_5; (h) F; (i) Cl; (j) SO_3; (k) BaO; and (l) SrO. The bold dark arrow represents the direction toward which the composition of the calculated, residual liquid (RL) evolves when crystals present in CP108 (see proportions in Tab. 3.9) are subtracted from the starting composition (SC). Other dotted arrows represent the direction toward which the composition of the carbonate liquid evolves when each crystal is subtracted from the bulk composition (proportion of crystals used for the calculation labelled at the end of the arrow). GRE, gregoryite. See caption of Figure 3.14 for remaining abbreviations and symbols. Individual analyses of carbonate liquid are from Table A3.3 in Appendix 3, and calculated composition of the residual liquid is from Table 3.10.

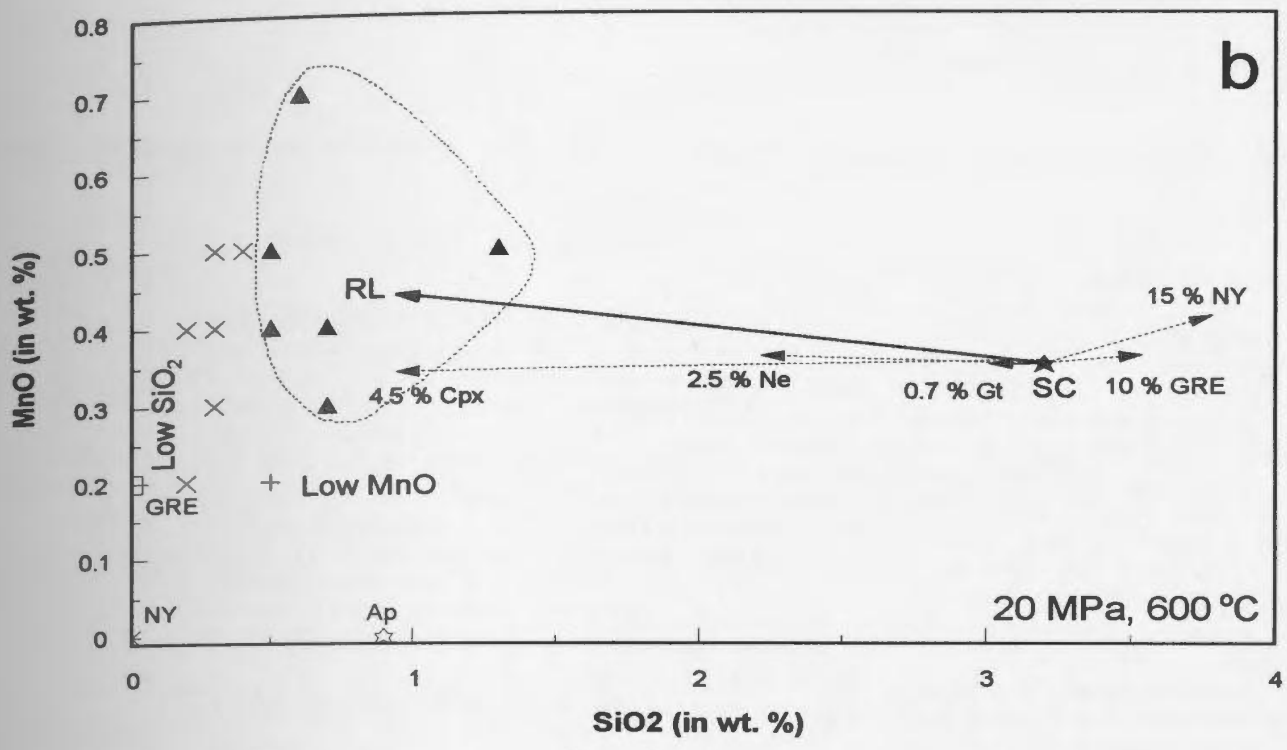
b
MnO (in wt. %)
SiO2 (in wt. %)
RL
15 % NY
2.5 % Ne
0.7 % Gt
SC
10 % GRE
4.5 % Cpx
Low SiO2
Low MnO
GRE
NY
Ap
20 MPa, 600 °C

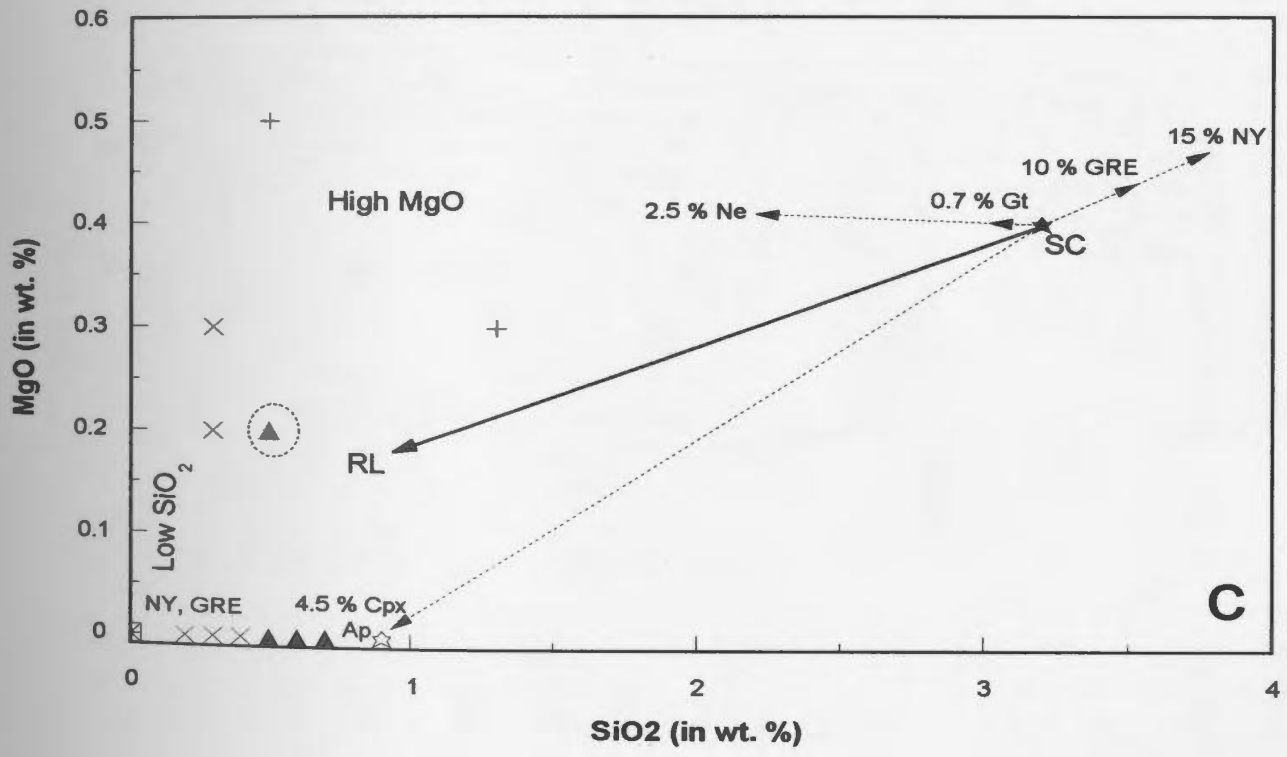
c
MgO (in wt. %)
SiO2 (in wt. %)
High MgO
15 % NY
10 % GRE
2.5 % Ne
0.7 % Gt
SC
RL
Low SiO2
NY, GRE
4.5 % Cpx
Ap

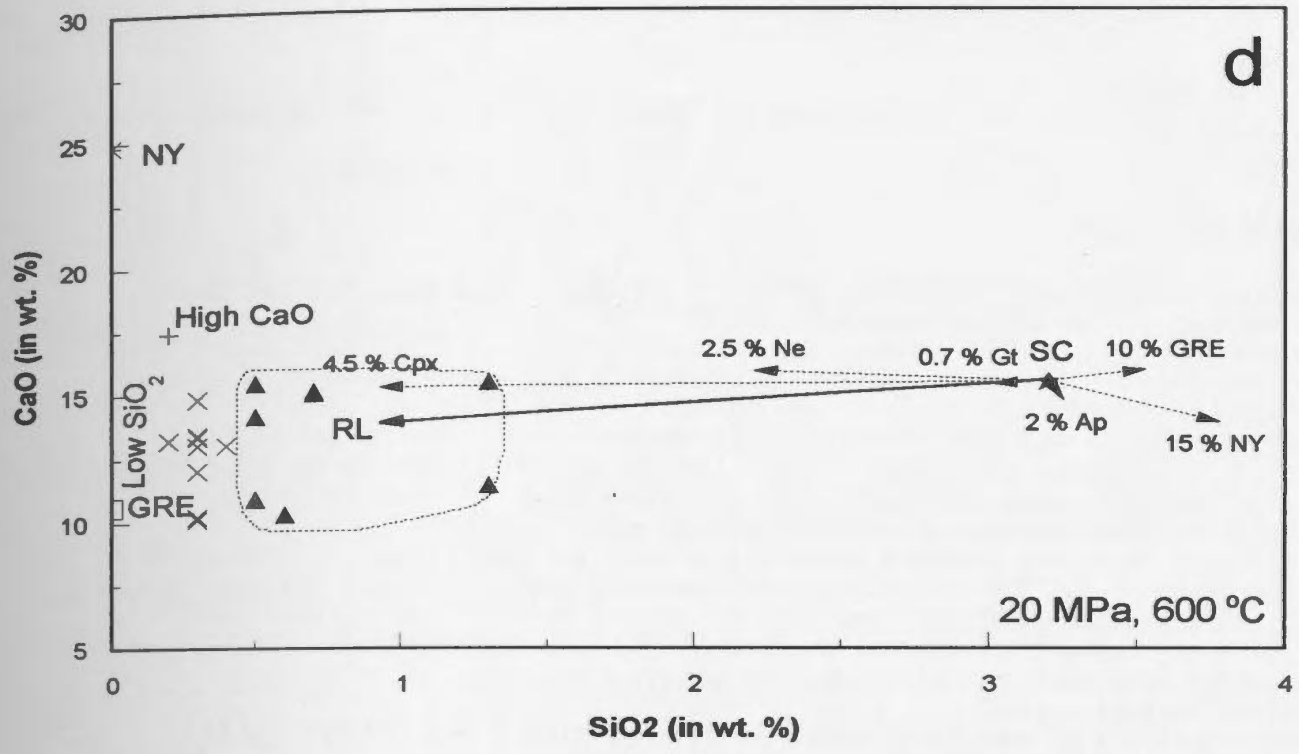
d
NY
High CaO
Low SiO2
GRE
4.5 % Cpx
RL
2.5 % Ne
0.7 % Gt
SC
10 % GRE
2 % Ap
15 % NY
20 MPa, 600 °C
CaO (in wt. %)
SiO2 (in wt. %)

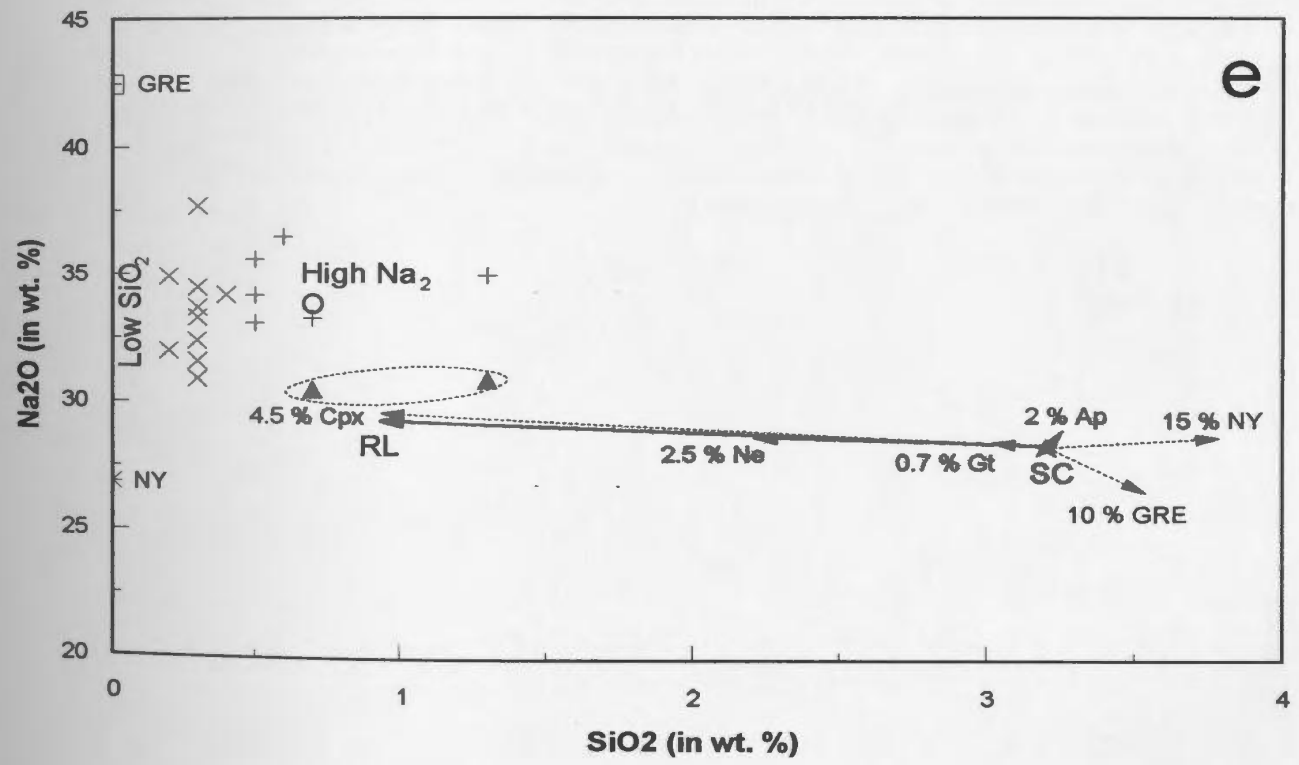
e
GRE
High Na2O
Low SiO2
4.5 % Cpx
RL
2.5 % Ne
0.7 % Gt
SC
2 % Ap
15 % NY
10 % GRE
NY
Na2O (in wt. %)
SiO2 (in wt. %)

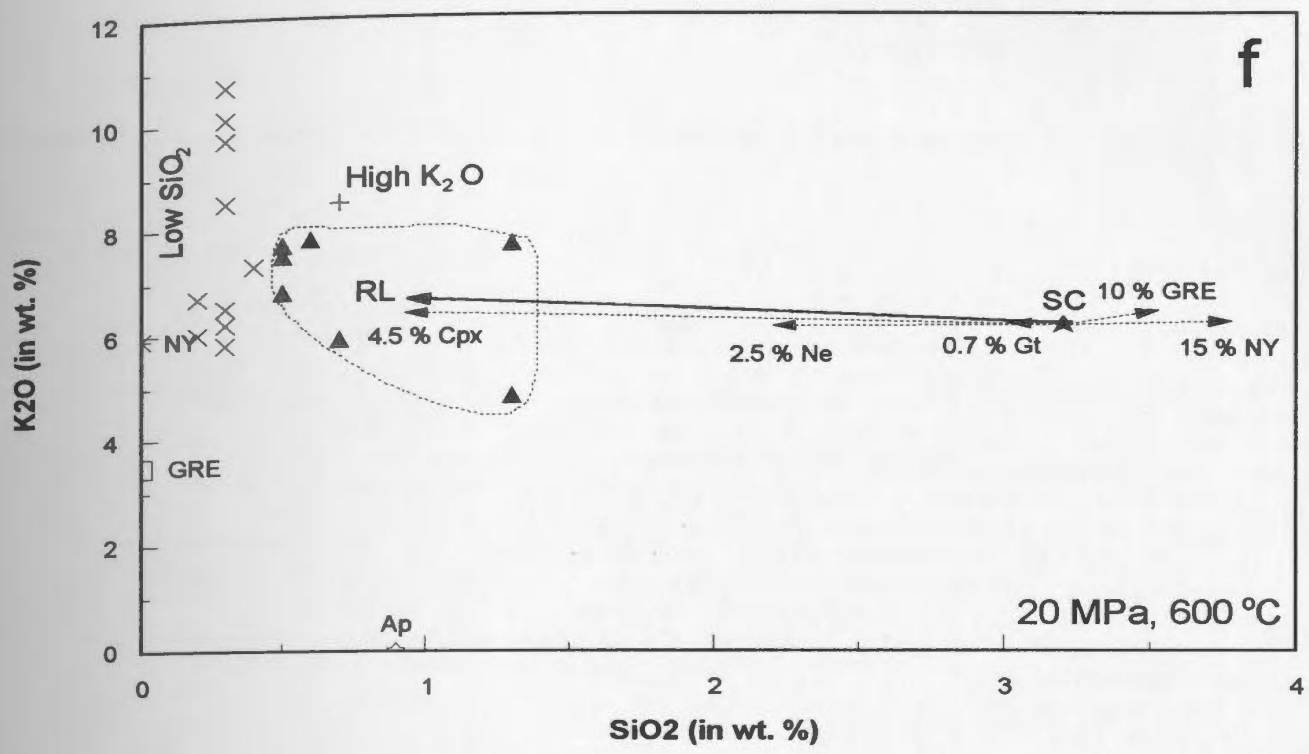
f
High K_2O
Low SiO_2
RL
SC
10 % GRE
4.5 % Cpx
2.5 % Ne
0.7 % Gt
15 % NY
NY
GRE
Ap
20 MPa, 600 °C
K2O (in wt. %)
SiO2 (in wt. %)

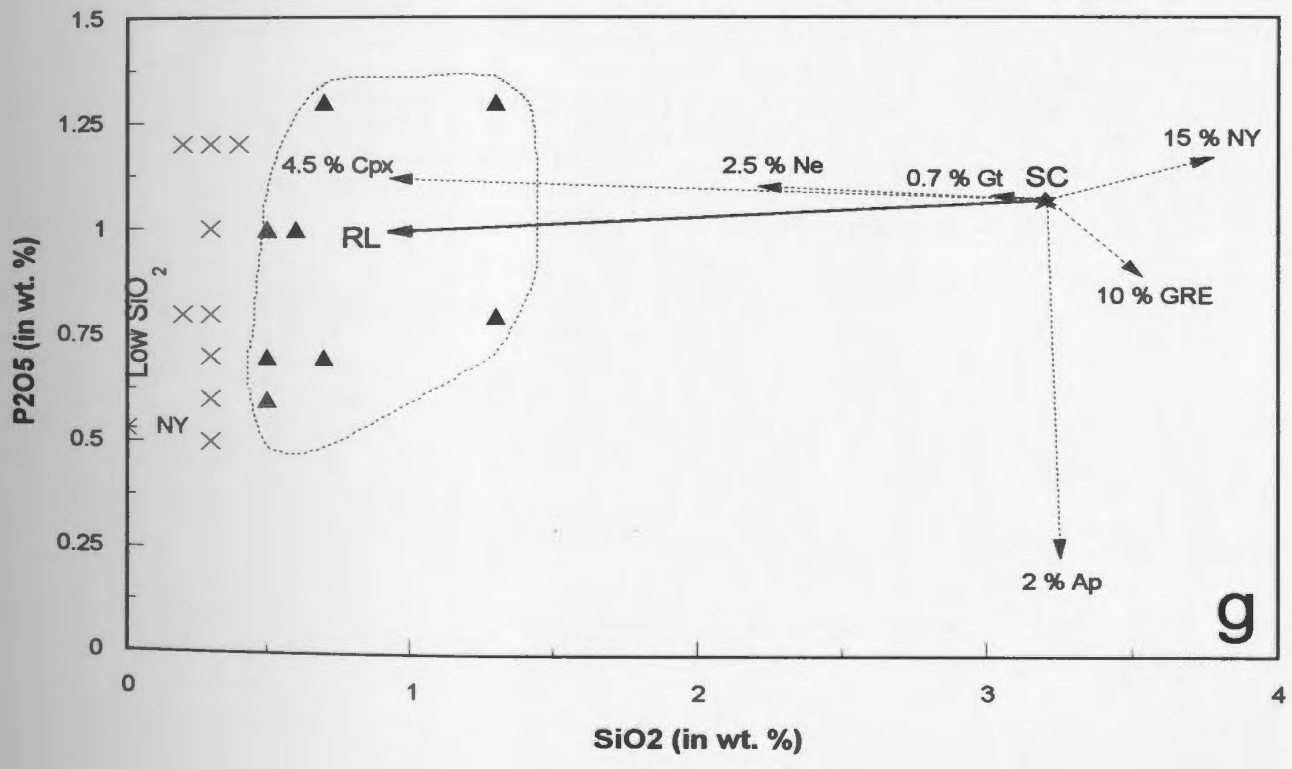
g
4.5 % Cpx
2.5 % Ne
0.7 % Gt
SC
15 % NY
RL
10 % GRE
Low SiO_2
NY
2 % Ap
P2O5 (in wt. %)
SiO2 (in wt. %)

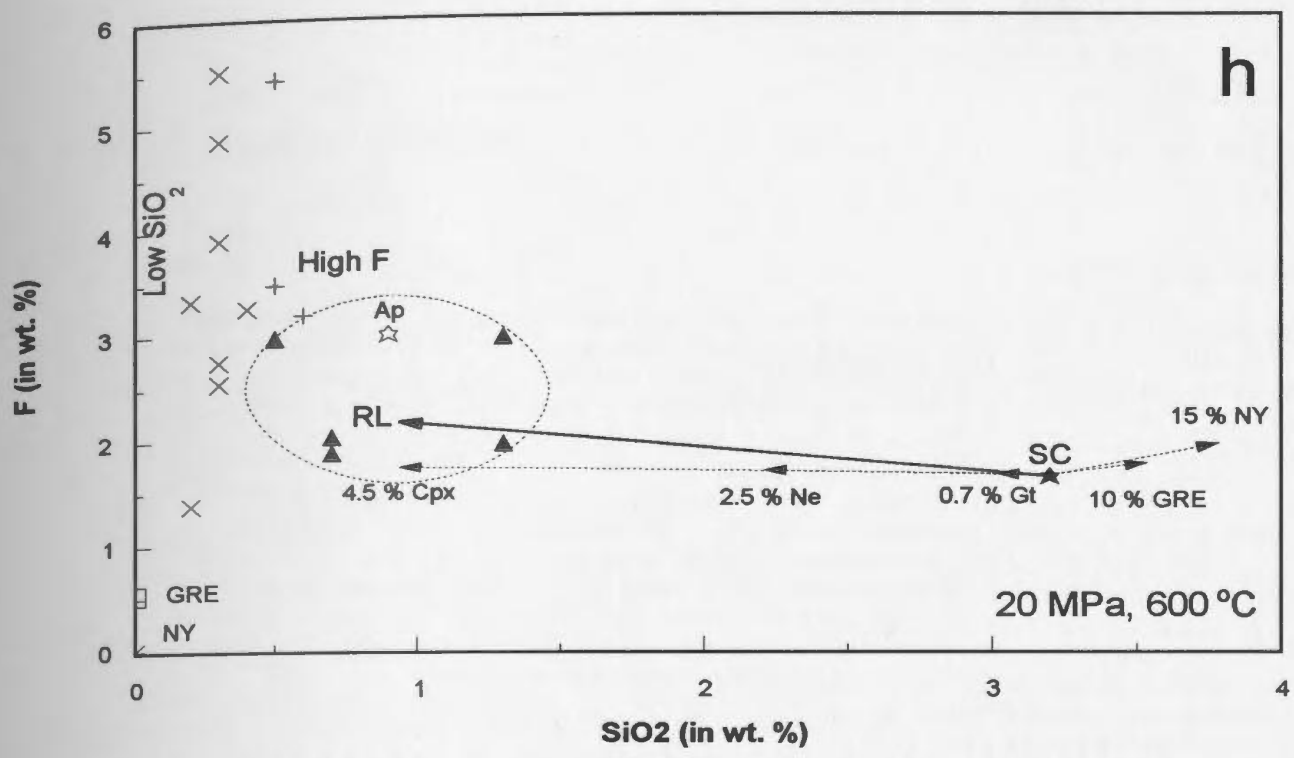
h
F (in wt. %)
SiO2 (in wt. %)
Low SiO2
High F
Ap
RL
SC
15 % NY
4.5 % Cpx
2.5 % Ne
0.7 % Gt
10 % GRE
GRE
NY
20 MPa, 600 °C

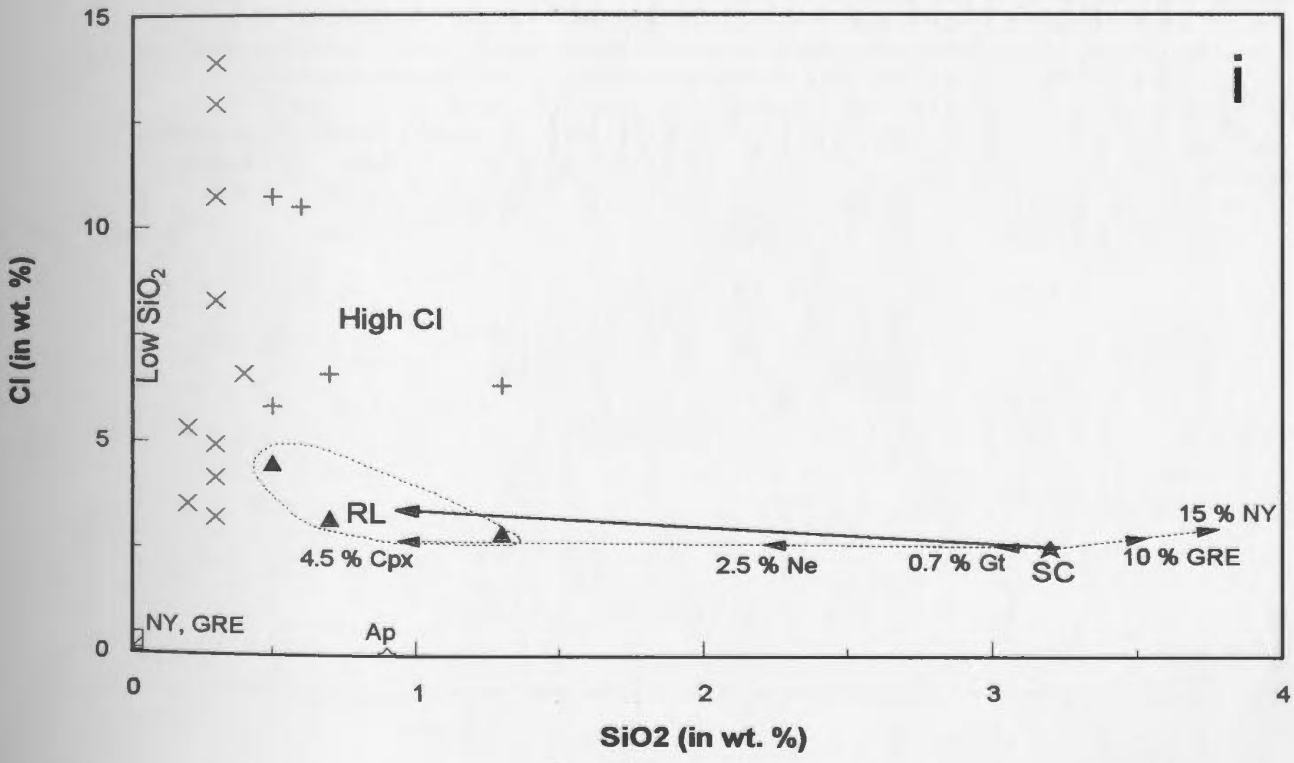
i
Cl (in wt. %)
SiO2 (in wt. %)
Low SiO2
High Cl
RL
15 % NY
4.5 % Cpx
2.5 % Ne
0.7 % Gt
SC
10 % GRE
NY, GRE
Ap

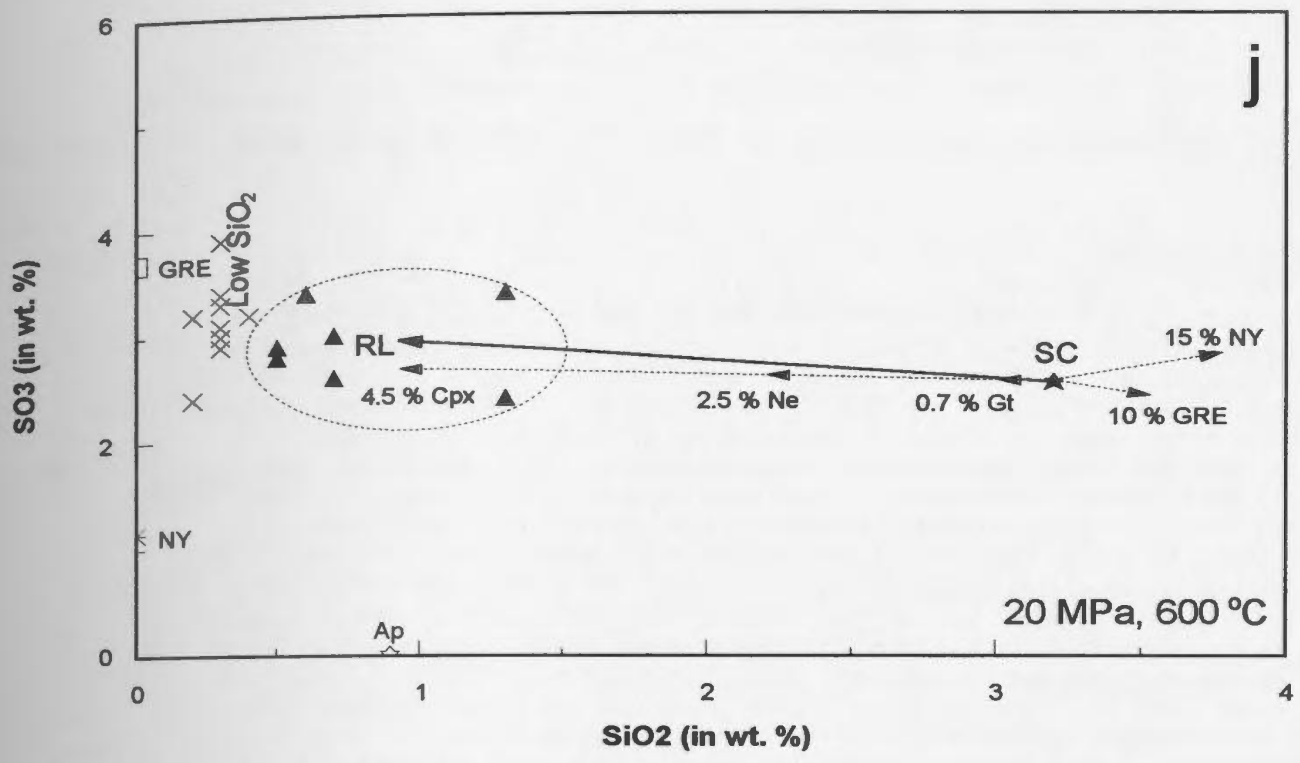
j
SO3 (in wt. %)
SiO2 (in wt. %)
Low SiO2
GRE
NY
Ap
RL
SC
4.5 % Cpx
2.5 % Ne
0.7 % Gt
15 % NY
10 % GRE
20 MPa, 600 °C
0
1
2
3
4
0
2
4
6

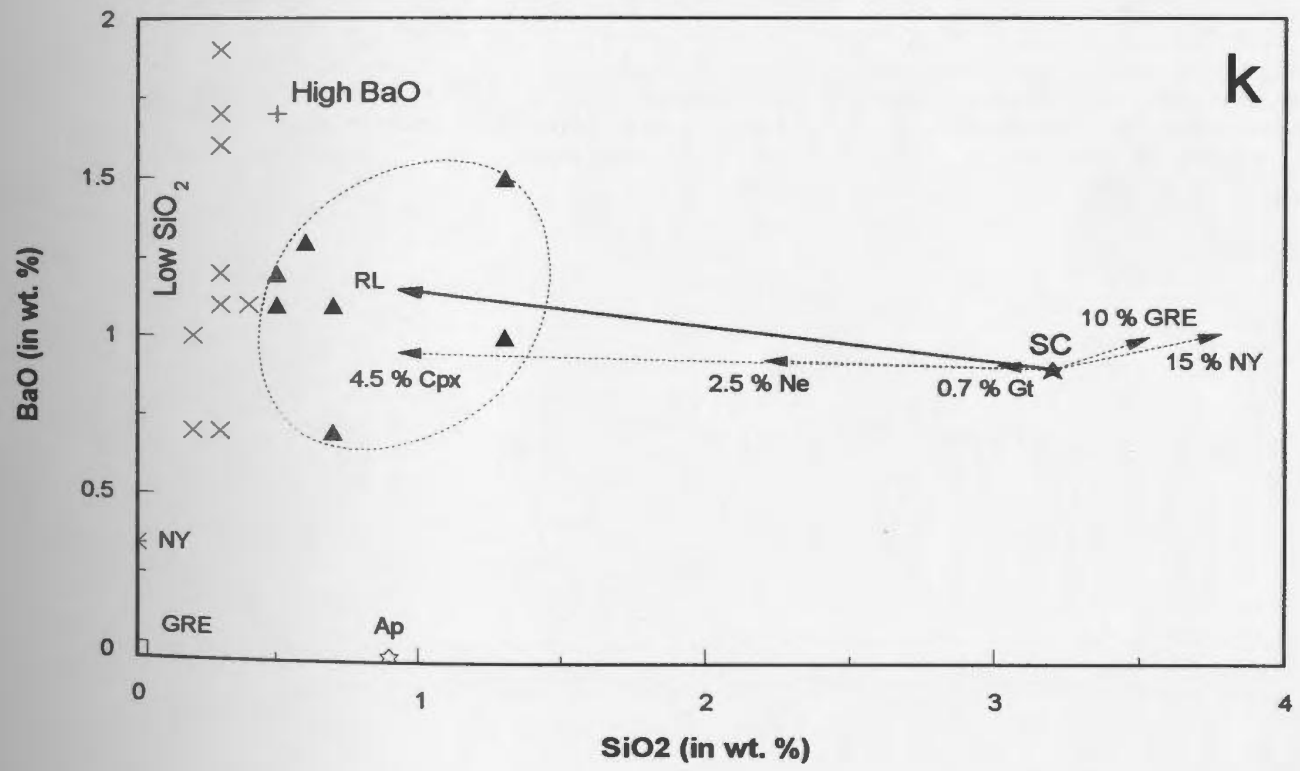
k
BaO (in wt. %)
SiO2 (in wt. %)
High BaO
Low SiO2
GRE
NY
Ap
RL
SC
4.5 % Cpx
2.5 % Ne
0.7 % Gt
10 % GRE
15 % NY
0
1
2
3
4
0
0.5
1
1.5
2

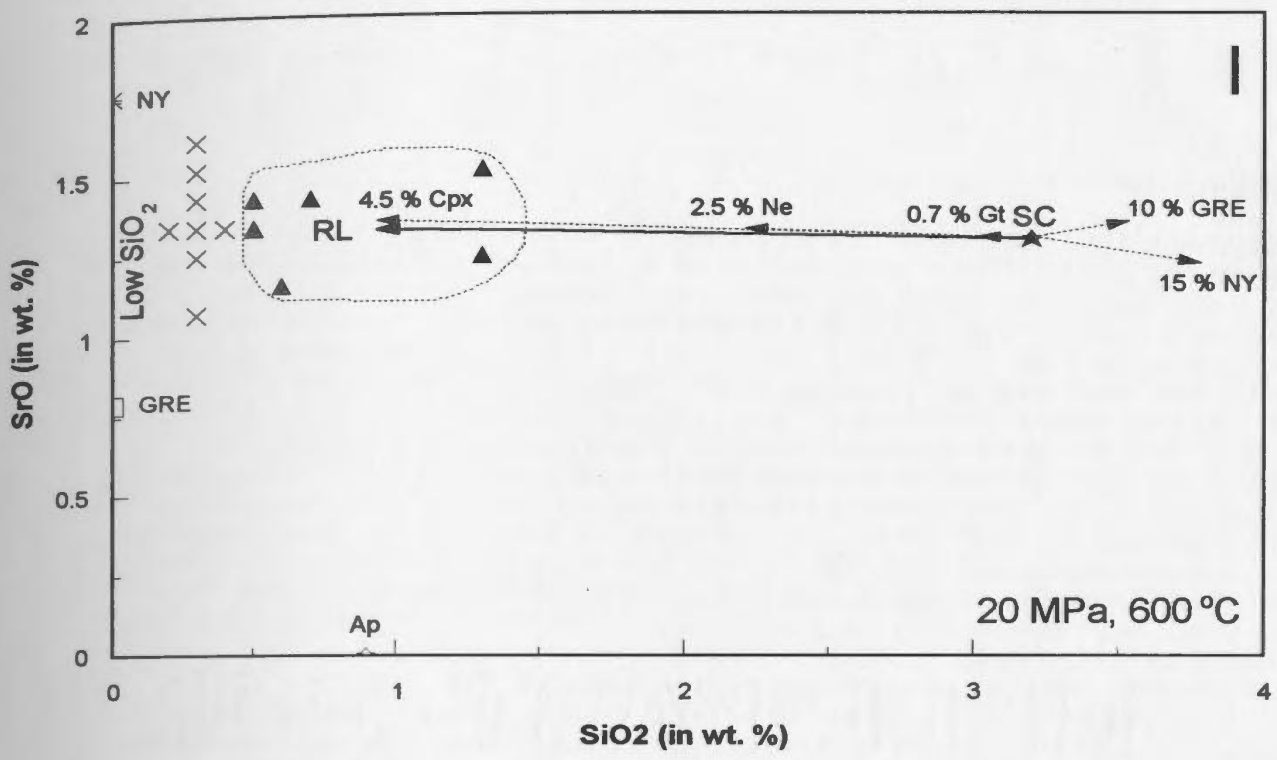
NY
Low SiO2
RL
4.5 % Cpx
2.5 % Ne
0.7 % Gt SC
10 % GRE
15 % NY
GRE
Ap
20 MPa, 600 °C
SrO (in wt. %)
SiO2 (in wt. %)
0
0.5
1
1.5
2
0
1
2
3
4

Figure 3.16: Concentration of different major elements in carbonate liquid (LC) from experiments at 100 MPa, as a function of temperature. "Measured LC" represents the average composition of the carbonate liquid as per the criteria outlined in the text and on Figures 3.14, 3.15 and 3.16. The shaded area represents one sigma (where σ represents the standard deviation between the different analyses of an experiment); it is interpolated between different experiments in a few cases. For comparison, the concentration of different elements in natural silicate-bearing natrocarbonatite OL5 and in the calculated carbonate liquid (= OL5 minus crystals) are also plotted. The bars above the graphs represent the temperature range over which the crystals are present in the experimental charges. (a) SiO_2; (b) TiO_2; (c) Al_2O_3; (d) FeO; (e) MnO; (f) MgO; (g) CaO; (h) Na_2O; (i) K_2O; (j) P_2O_5; (k) F; (l) Cl; (m) SO_3; (n) BaO; and (o) SrO. Data are from Table 3.10 for the experiments, and from Table 2.2 for natural silicate-bearing natrocarbonatite OL5.

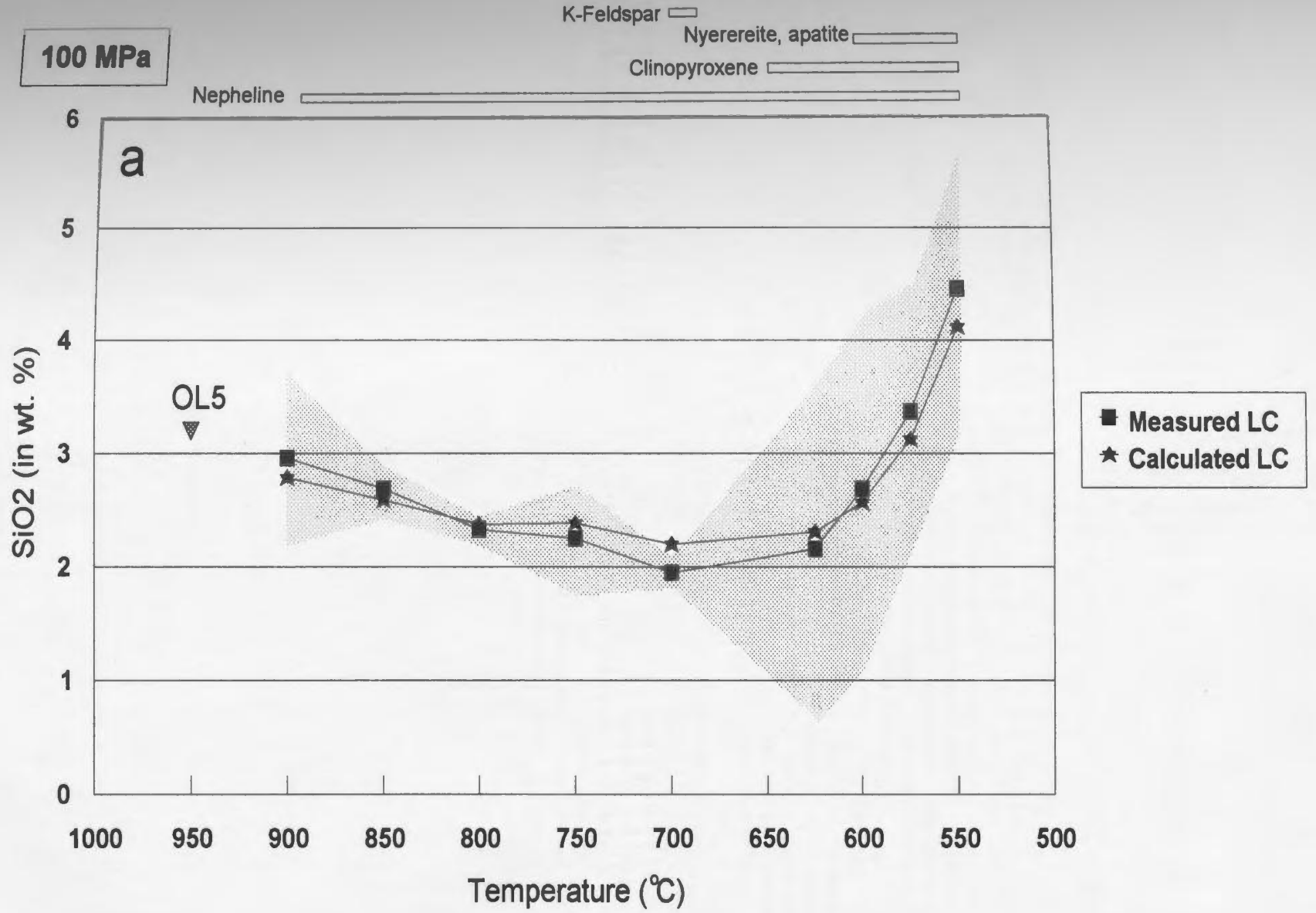
100 MPa
K-Feldspar
Nyerereite, apatite
Clinopyroxene
Nepheline
a
OL5
SiO2 (in wt. %)
Temperature (℃)
Measured LC
Calculated LC
6
5
4
3
2
1
0
1000
950
900
850
800
750
700
650
600
550
500

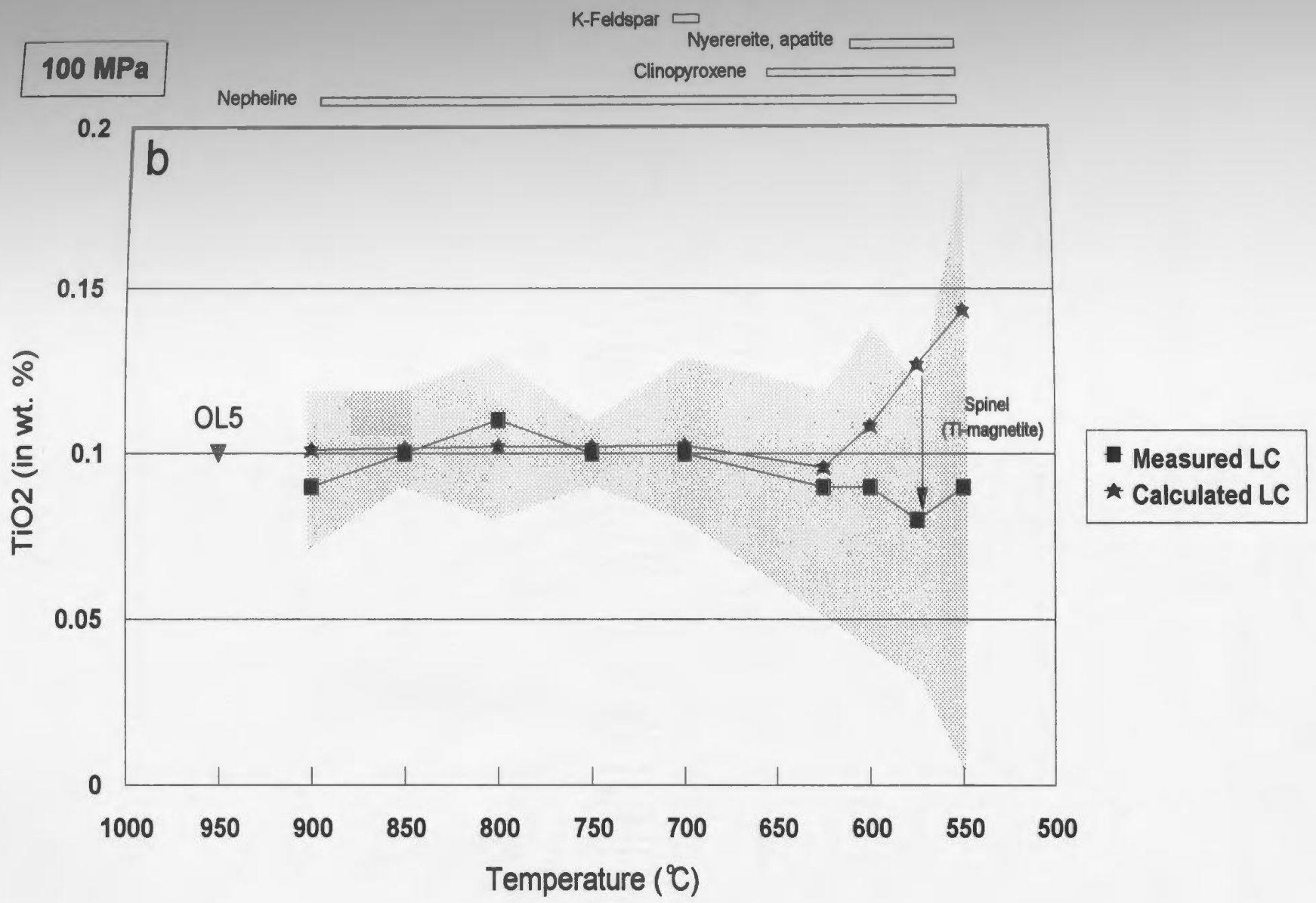
100 MPa
K-Feldspar
Nyerereite, apatite
Clinopyroxene
Nepheline
b
0.2
0.15
0.1
0.05
0
TiO2 (in wt. %)
OL5
Spinel
(Ti-magnetite)
Measured LC
Calculated LC
1000
950
900
850
800
750
700
650
600
550
500
Temperature (℃)

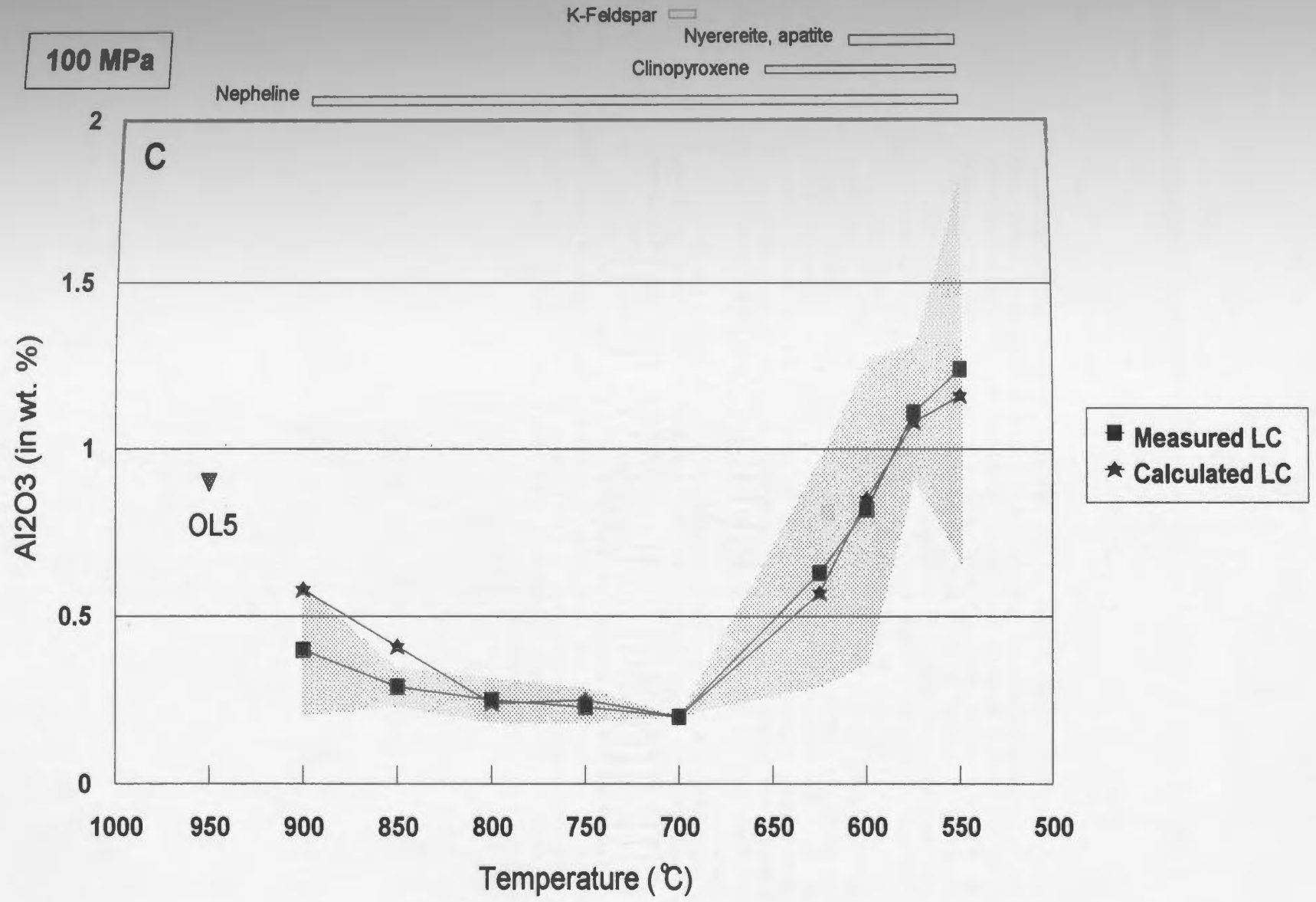
100 MPa
K-Feldspar
Nyerereite, apatite
Clinopyroxene
Nepheline
C
OL5
Al2O3 (in wt. %)
2
1.5
1
0.5
0
1000
950
900
850
800
750
700
650
600
550
500
Temperature (℃)
Measured LC
Calculated LC

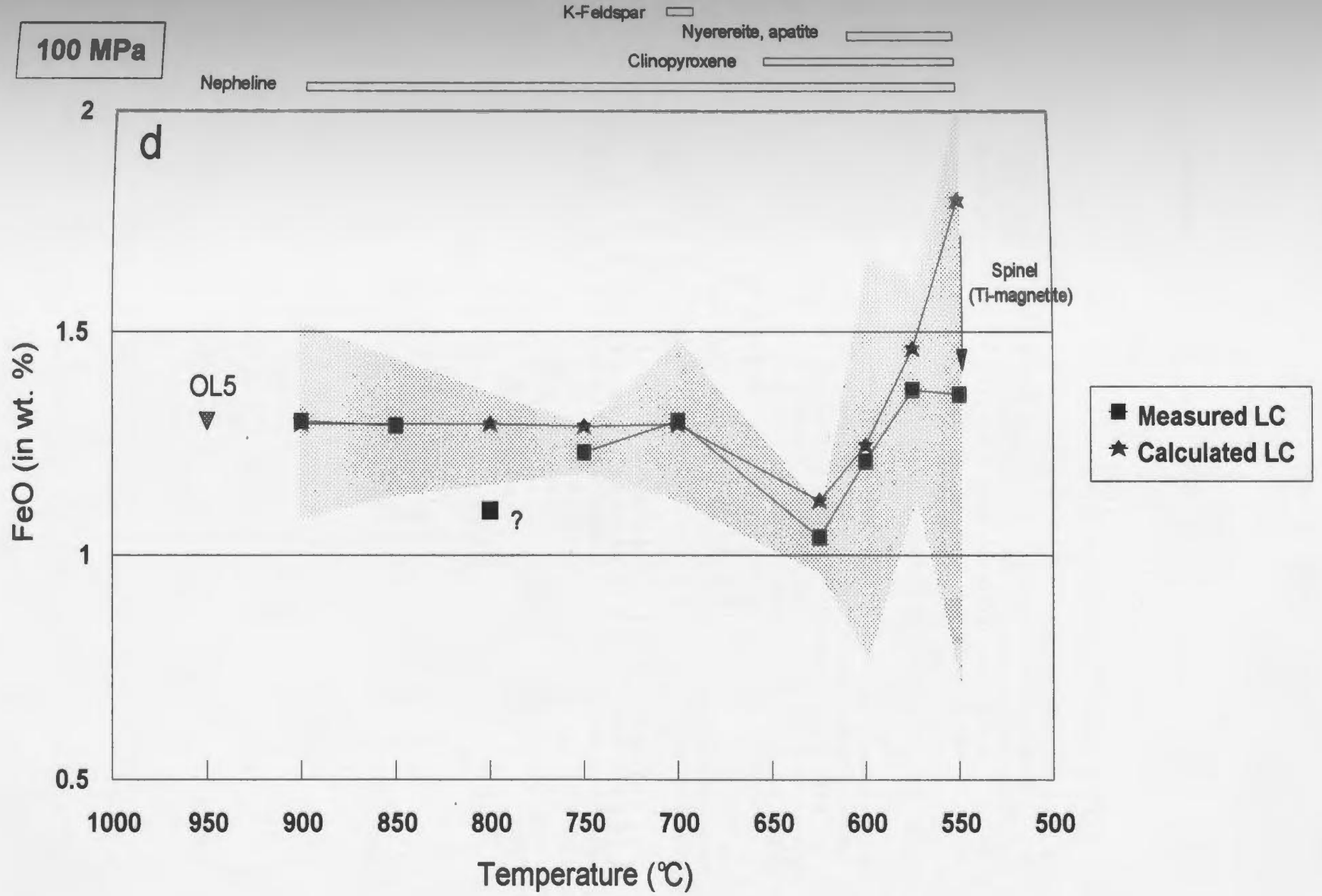
100 MPa
K-Feldspar
Nyerereite, apatite
Clinopyroxene
Nepheline
d
Spinel
(Ti-magnetite)
OL5
?
Measured LC
Calculated LC
FeO (in wt. %)
2
1.5
1
0.5
1000
950
900
850
800
750
700
650
600
550
500
Temperature (°C)

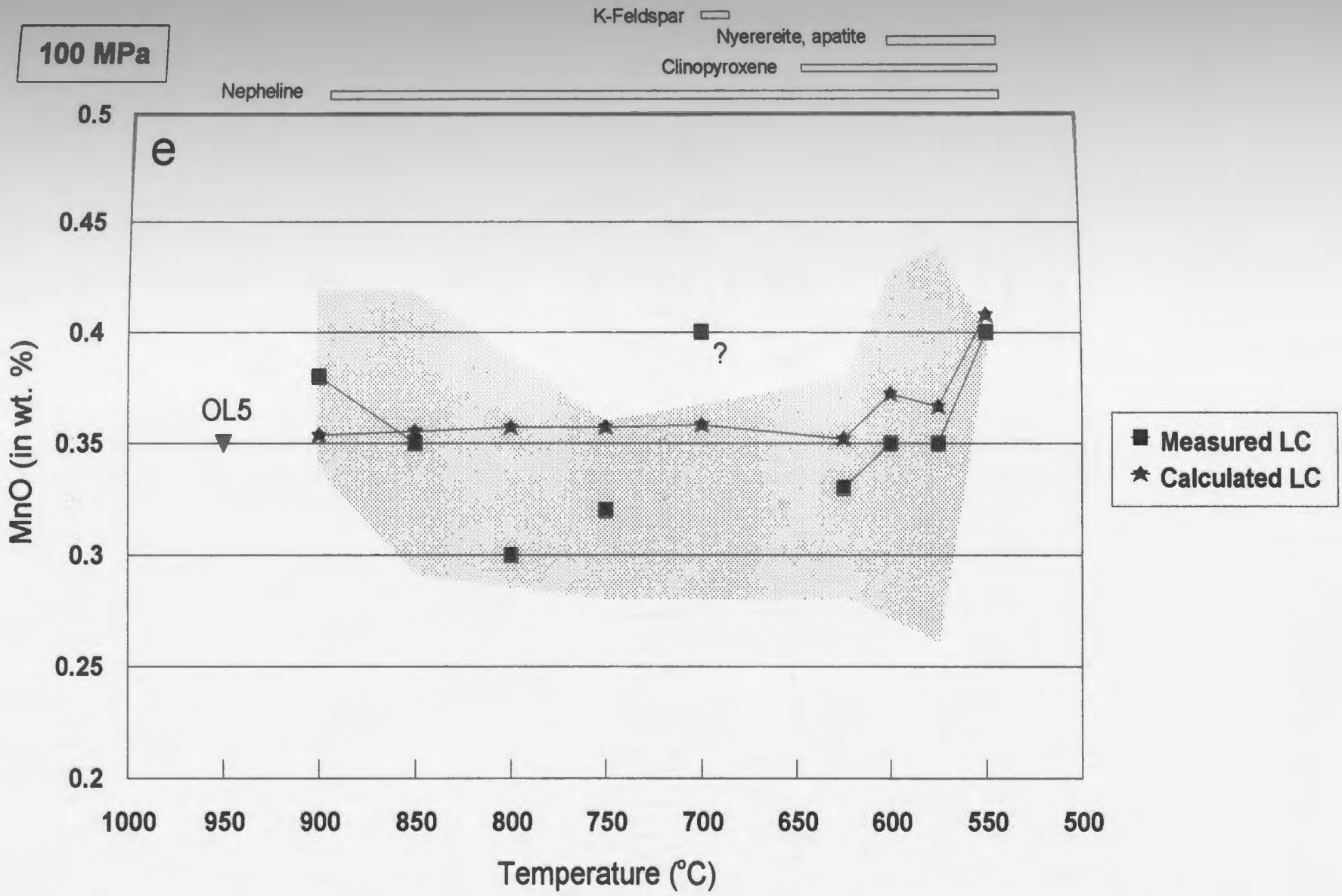
100 MPa
K-Feldspar
Nyerereite, apatite
Clinopyroxene
Nepheline
e
OL5
?
MnO (in wt. %)
0.5
0.45
0.4
0.35
0.3
0.25
0.2
1000
950
900
850
800
750
700
650
600
550
500
Temperature (°C)
Measured LC
Calculated LC

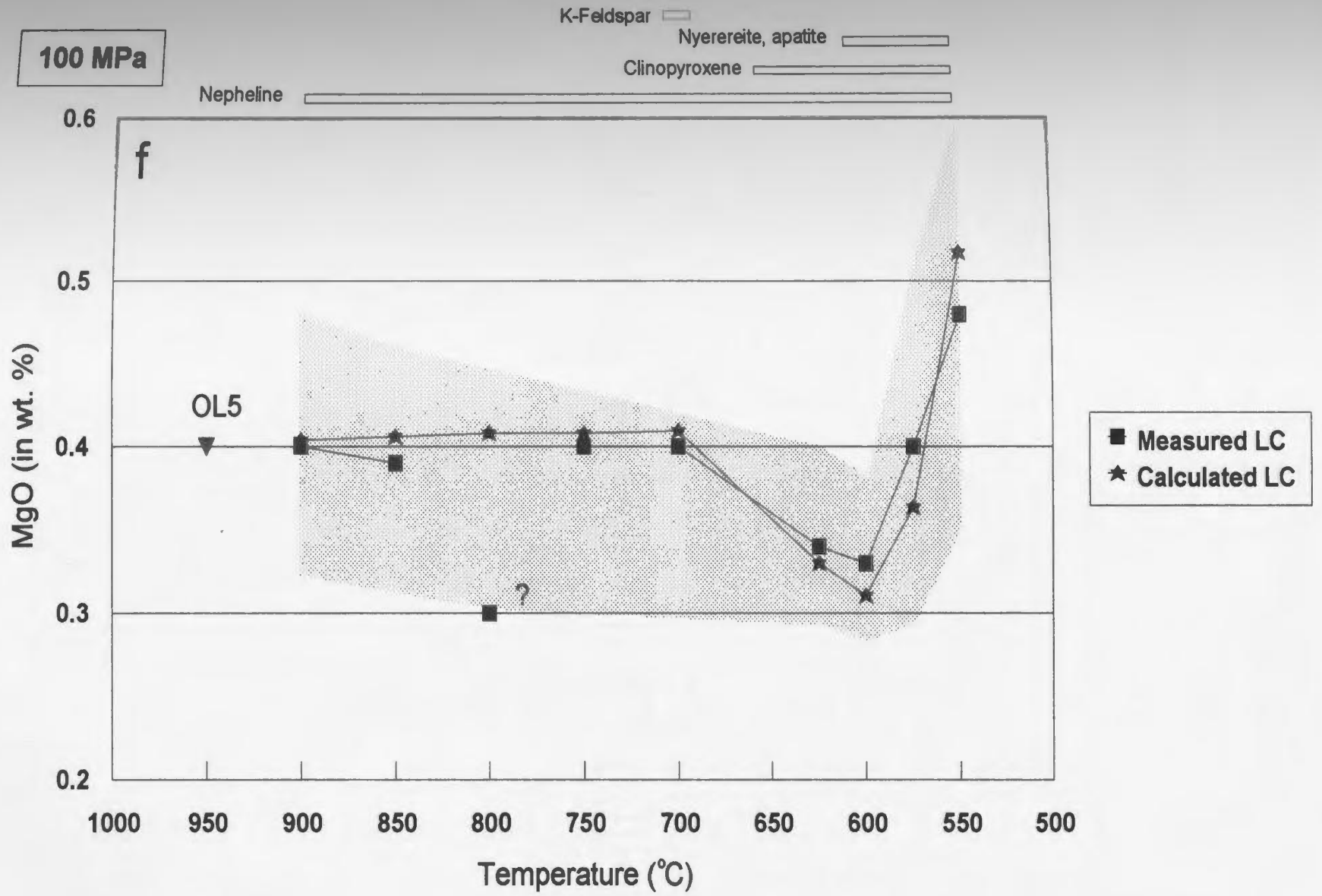
100 MPa
K-Feldspar
Nyerereite, apatite
Clinopyroxene
Nepheline
f
OL5
?
MgO (in wt. %)
0.6
0.5
0.4
0.3
0.2
1000
950
900
850
800
750
700
650
600
550
500
Temperature (°C)
Measured LC
Calculated LC

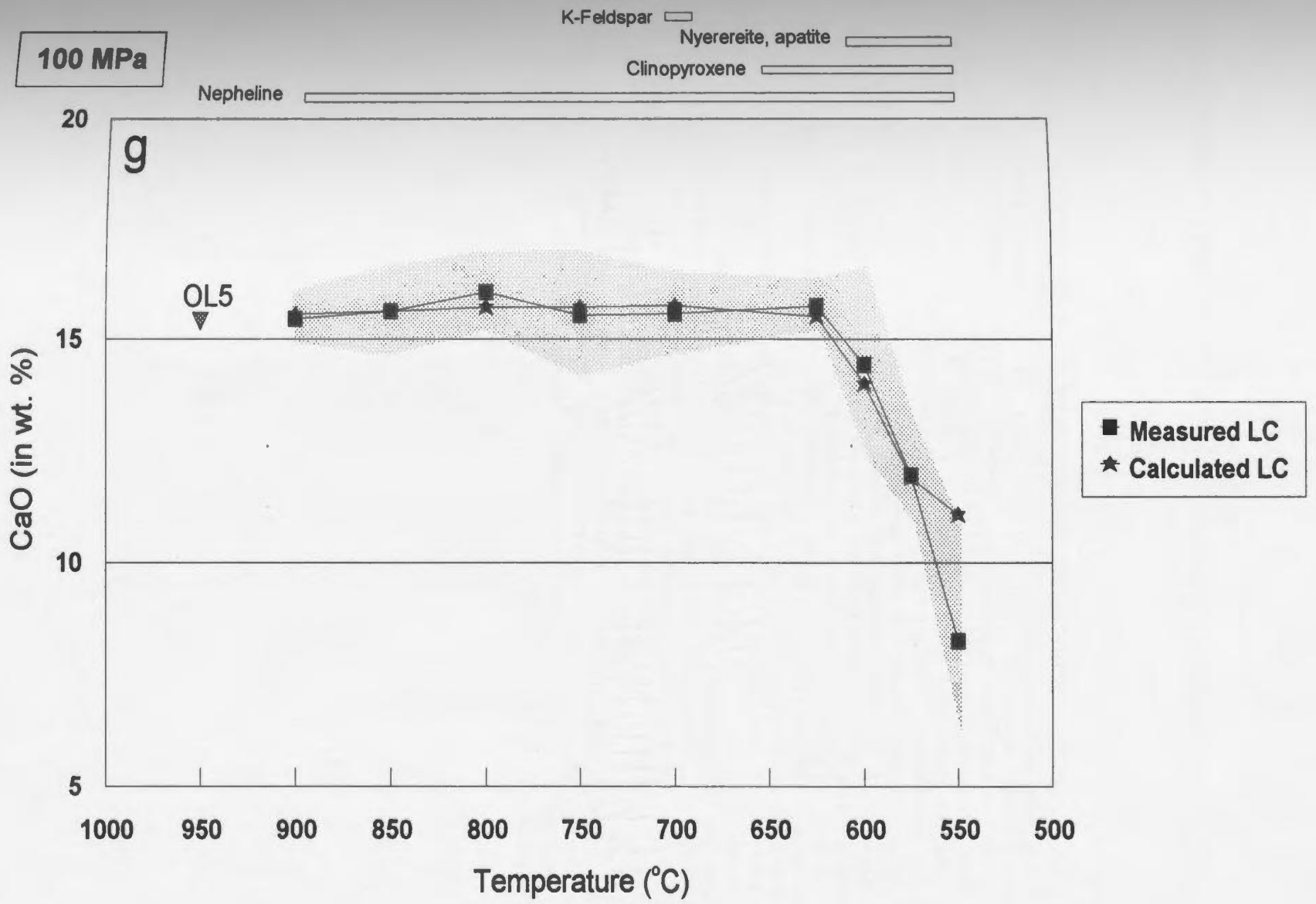
100 MPa
K-Feldspar
Nyerereite, apatite
Clinopyroxene
Nepheline
g
OL5
CaO (in wt. %)
20
15
10
5
1000
950
900
850
800
750
700
650
600
550
500
Temperature (°C)
Measured LC
Calculated LC

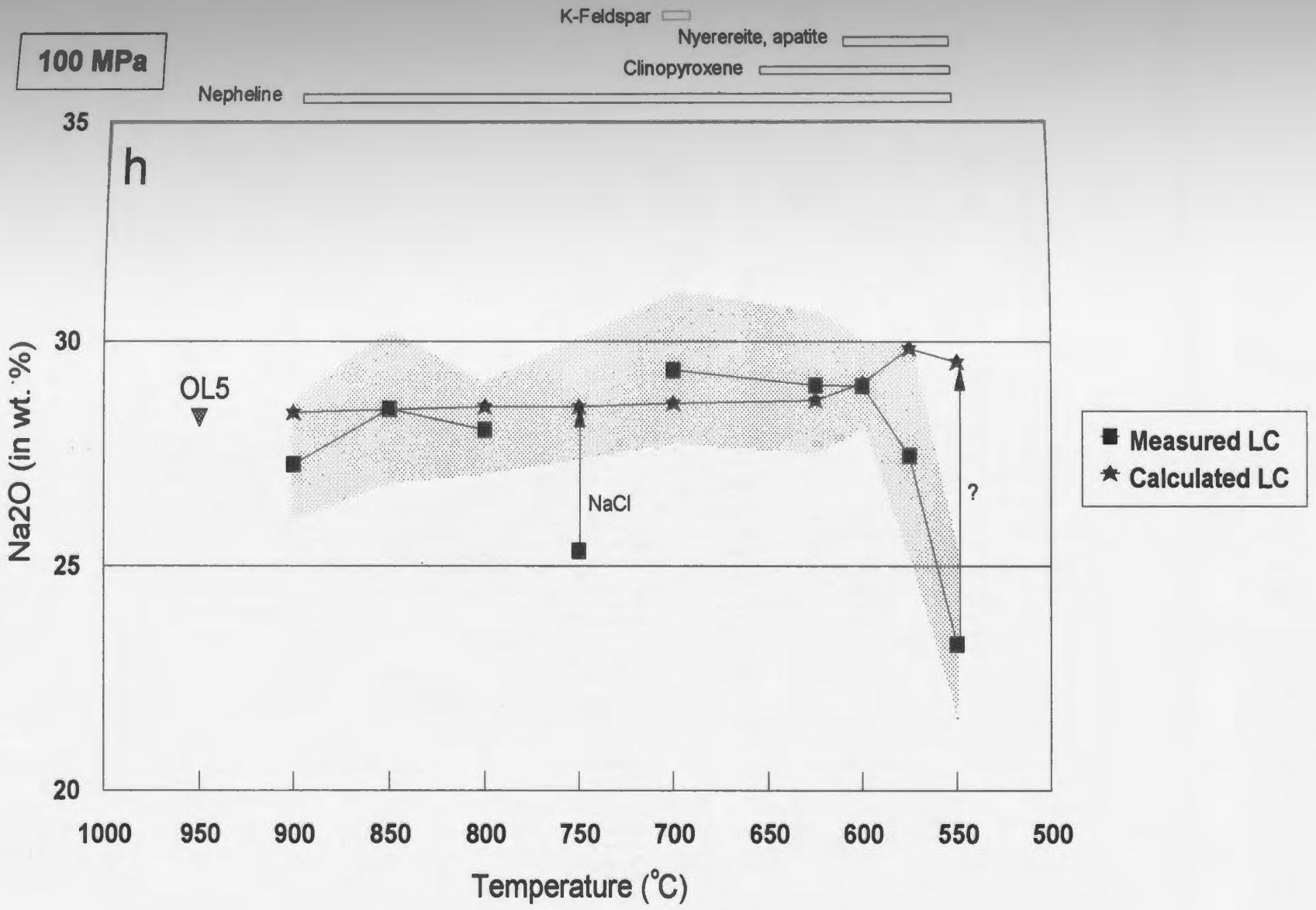
100 MPa
K-Feldspar
Nyerereite, apatite
Clinopyroxene
Nepheline
h
OL5
NaCl
?
Measured LC
Calculated LC
Na2O (in wt. %)
35
30
25
20
1000
950
900
850
800
750
700
650
600
550
500
Temperature (°C)

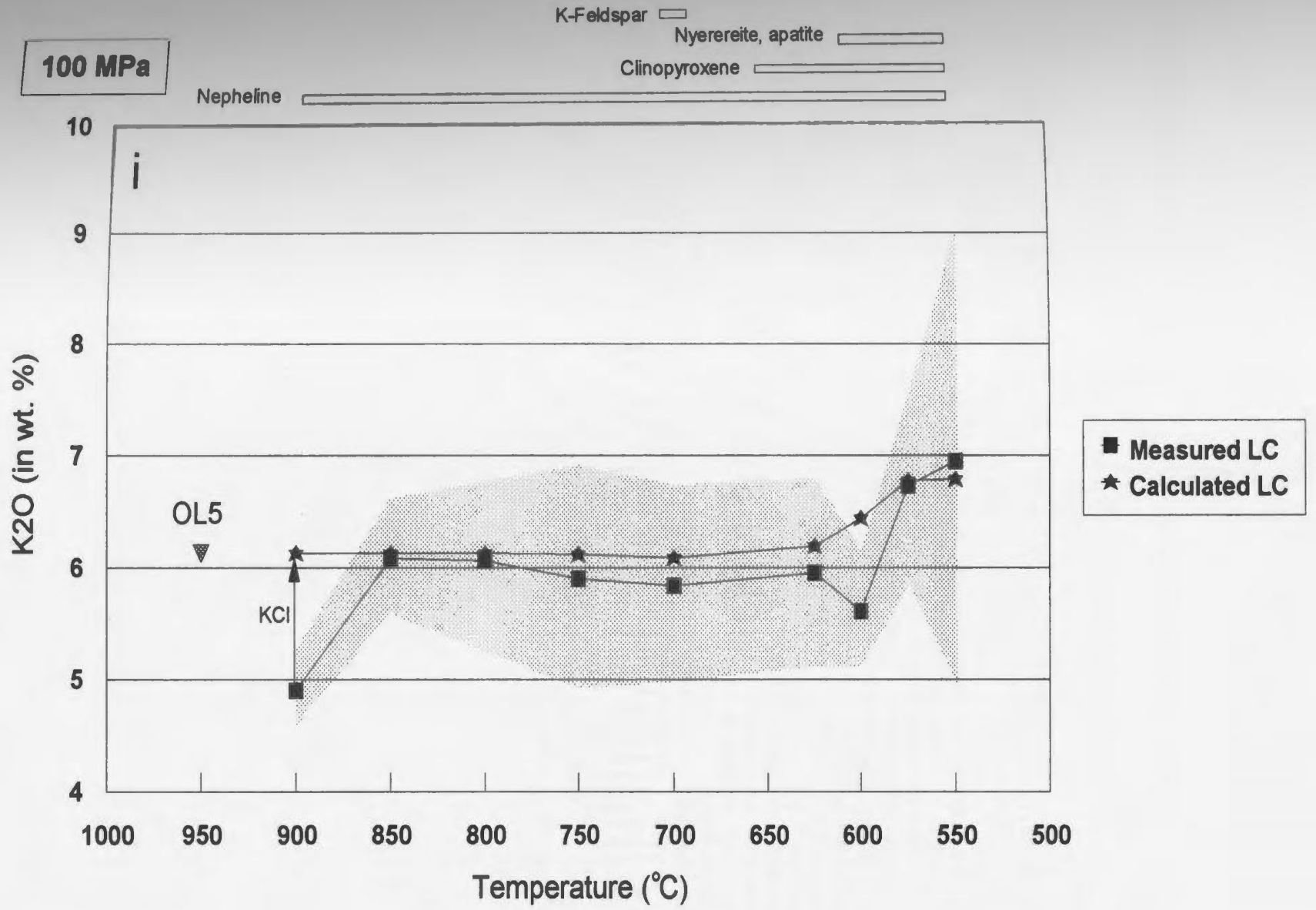
100 MPa
K-Feldspar
Nyerereite, apatite
Clinopyroxene
Nepheline
i
OL5
KCl
K2O (in wt. %)
10
9
8
7
6
5
4
1000
950
900
850
800
750
700
650
600
550
500
Temperature (°C)
Measured LC
Calculated LC

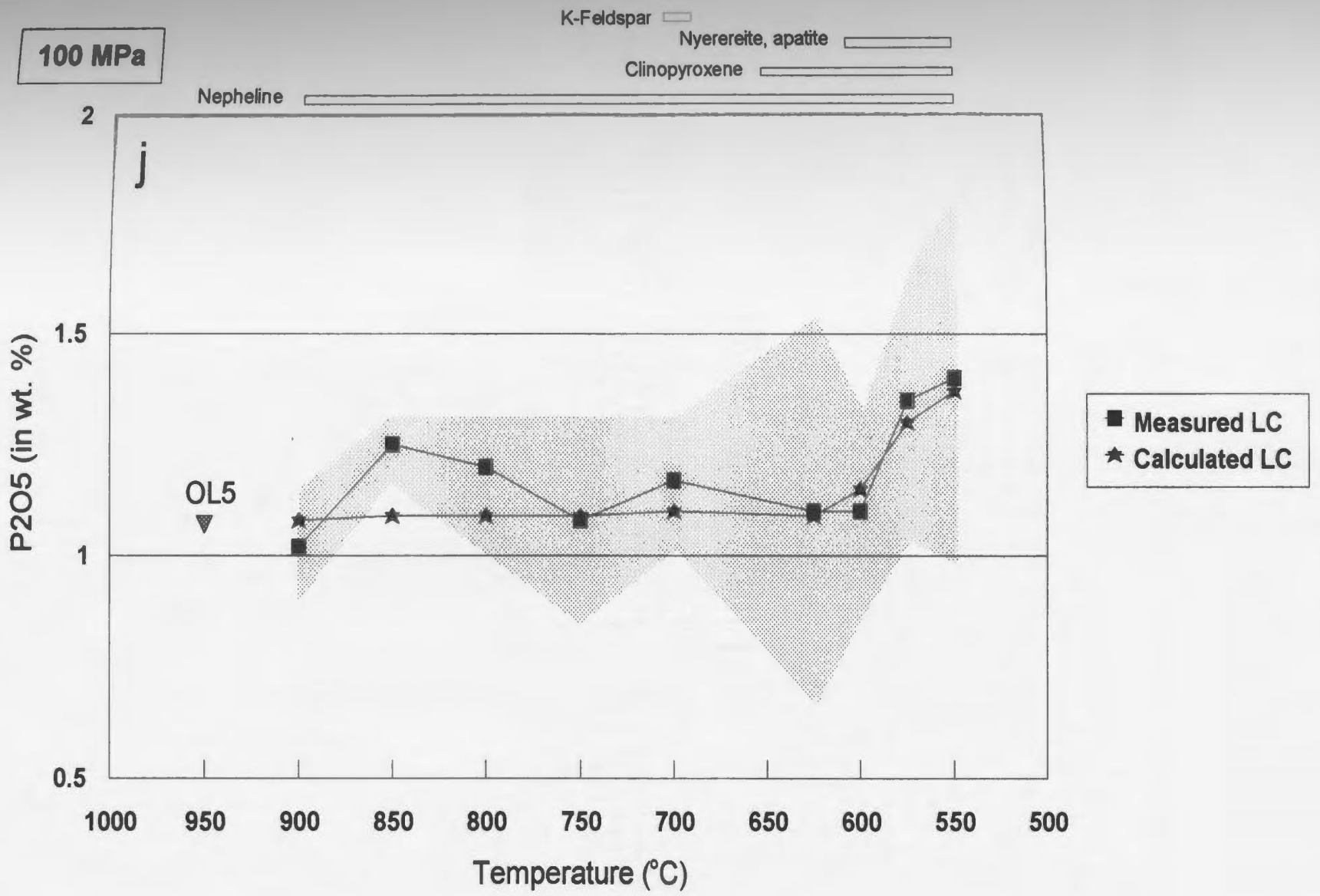
100 MPa
K-Feldspar
Nyerereite, apatite
Clinopyroxene
Nepheline
j
OL5
P2O5 (in wt. %)
2
1.5
1
0.5
1000
950
900
850
800
750
700
650
600
550
500
Temperature (°C)
Measured LC
Calculated LC

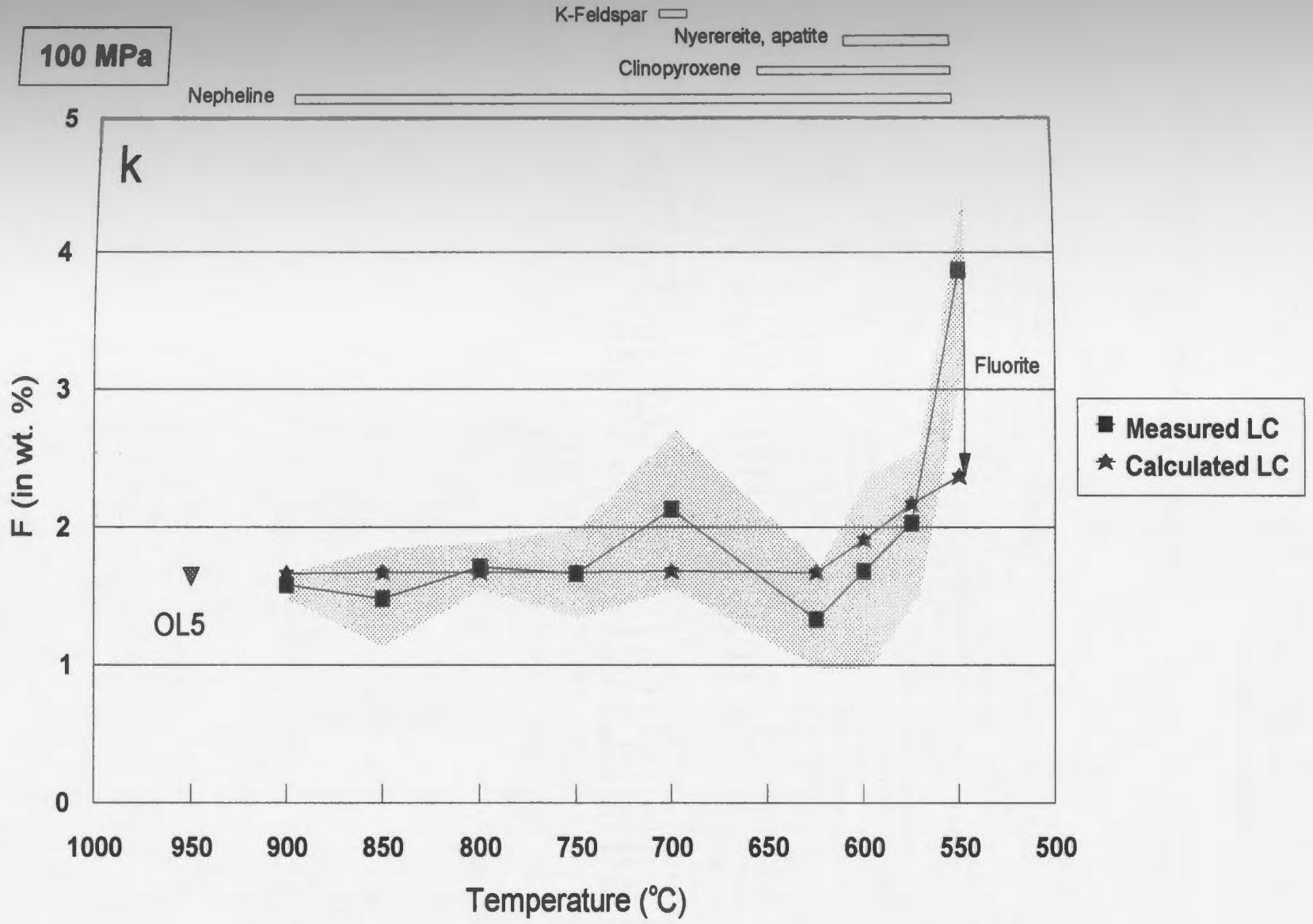
100 MPa
K-Feldspar
Nyerereite, apatite
Clinopyroxene
Nepheline
k
5
4
3
2
1
0
F (in wt. %)
Fluorite
OL5
Measured LC
Calculated LC
1000
950
900
850
800
750
700
650
600
550
500
Temperature (°C)

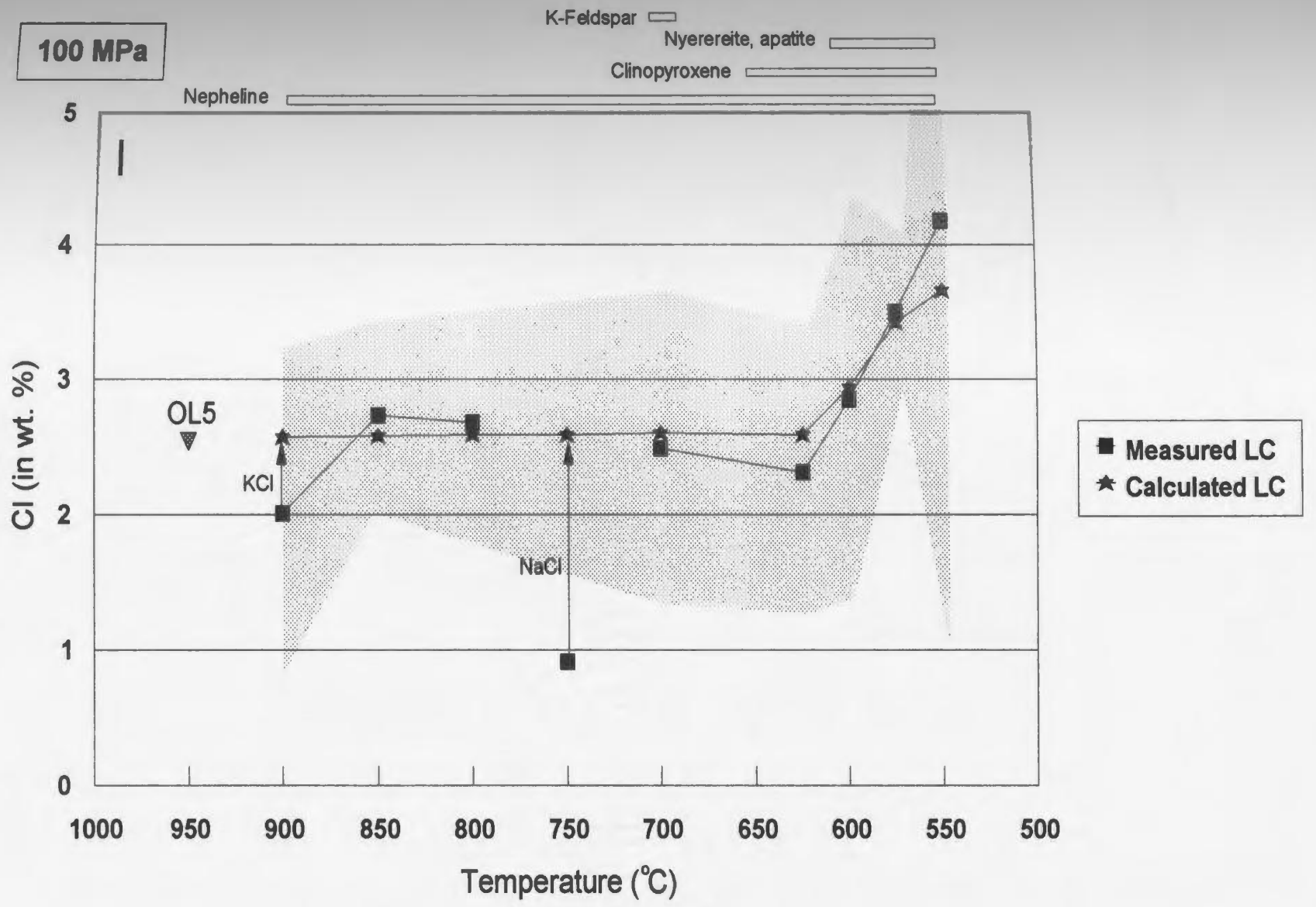
100 MPa
K-Feldspar
Nyerereite, apatite
Clinopyroxene
Nepheline
OL5
KCl
NaCl
Cl (in wt. %)
Temperature (°C)
Measured LC
Calculated LC
5
4
3
2
1
0
1000
950
900
850
800
750
700
650
600
550
500

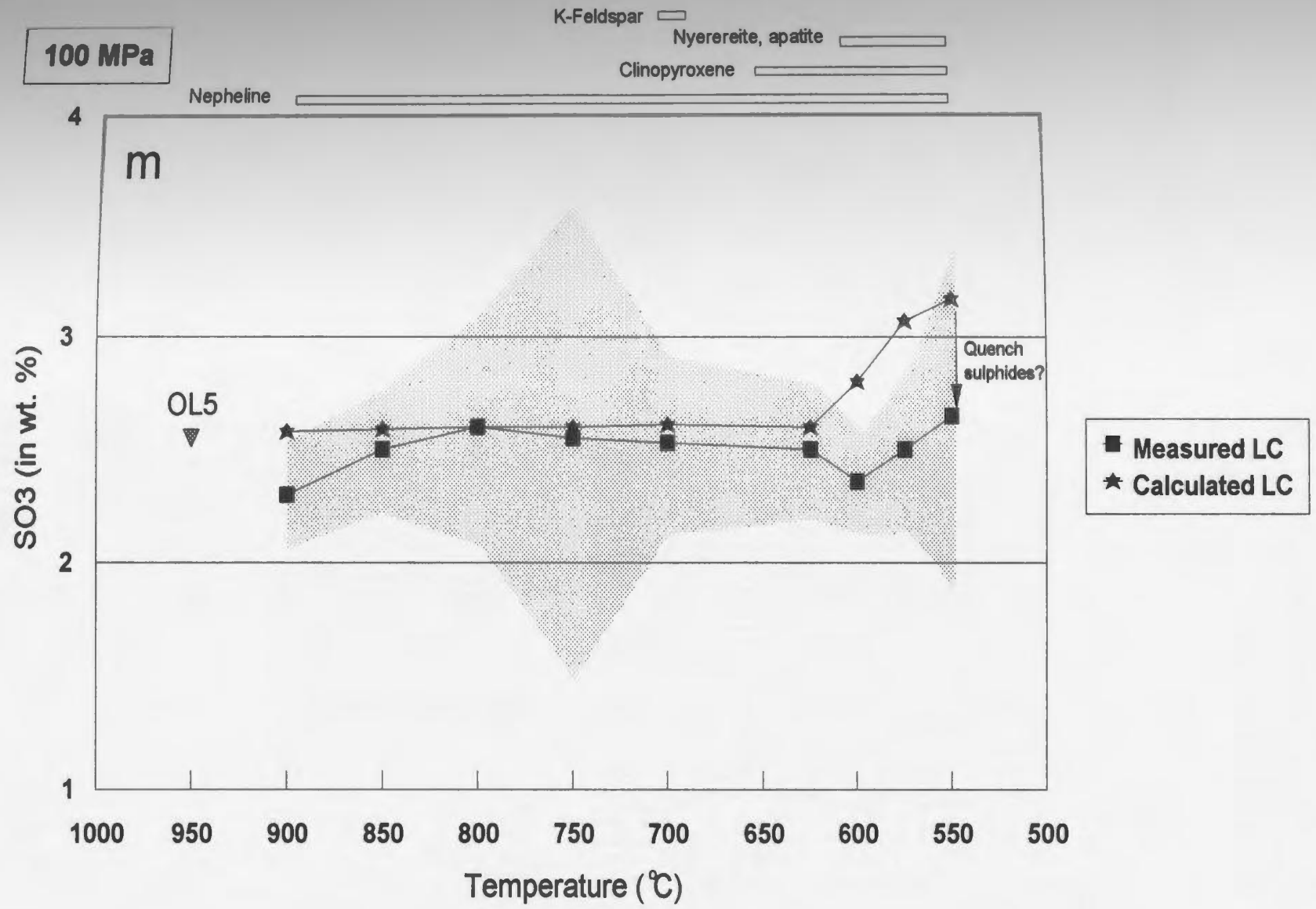
100 MPa
K-Feldspar
Nyerereite, apatite
Clinopyroxene
Nepheline
m
OL5
Quench sulphides?
SO3 (in wt. %)
4
3
2
1
1000
950
900
850
800
750
700
650
600
550
500
Temperature (°C)
Measured LC
Calculated LC

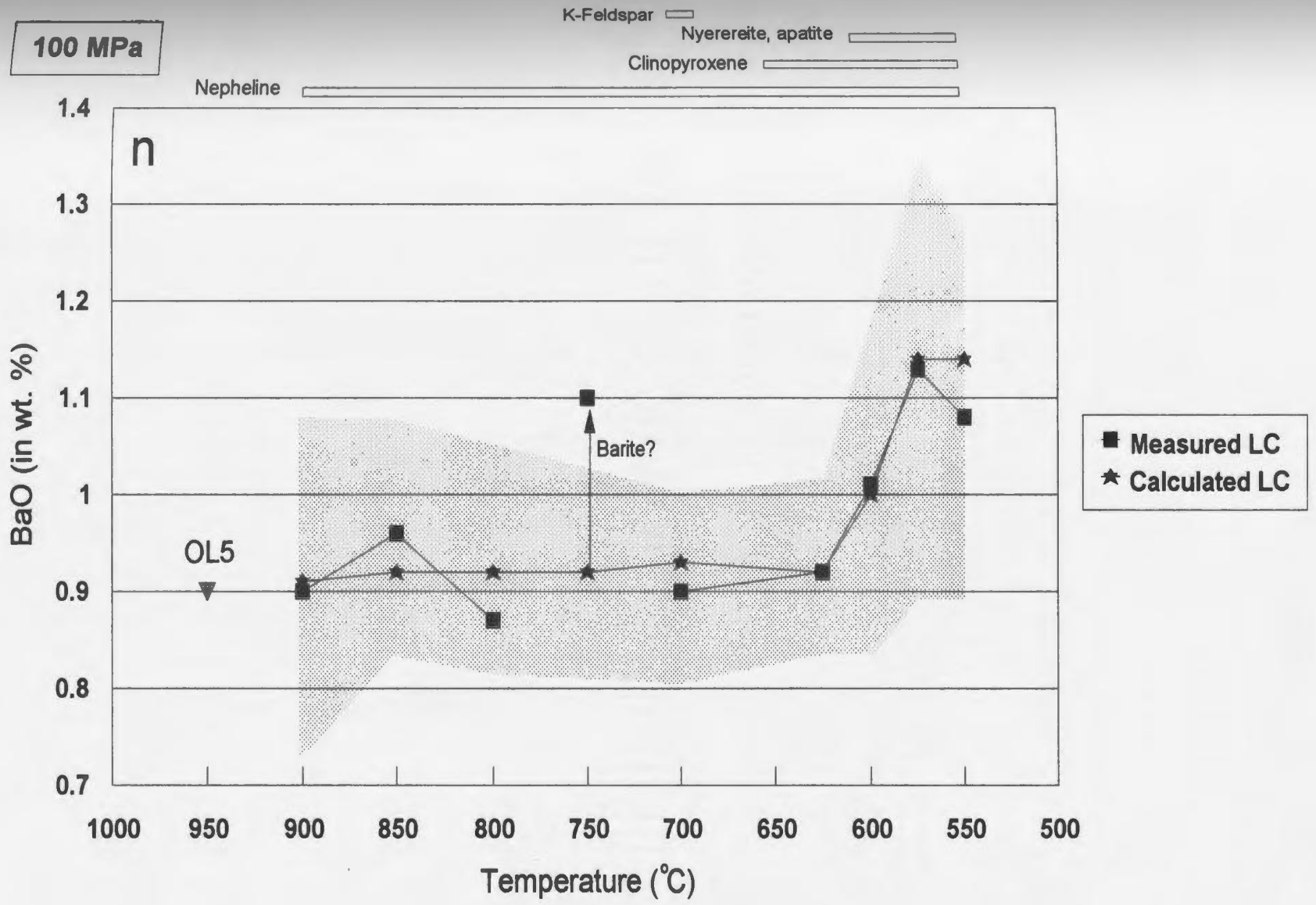
100 MPa
K-Feldspar
Nyerereite, apatite
Clinopyroxene
Nepheline
n
BaO (in wt. %)
1.4
1.3
1.2
1.1
1
0.9
0.8
0.7
OL5
Barite?
Measured LC
Calculated LC
1000
950
900
850
800
750
700
650
600
550
500
Temperature (°C)

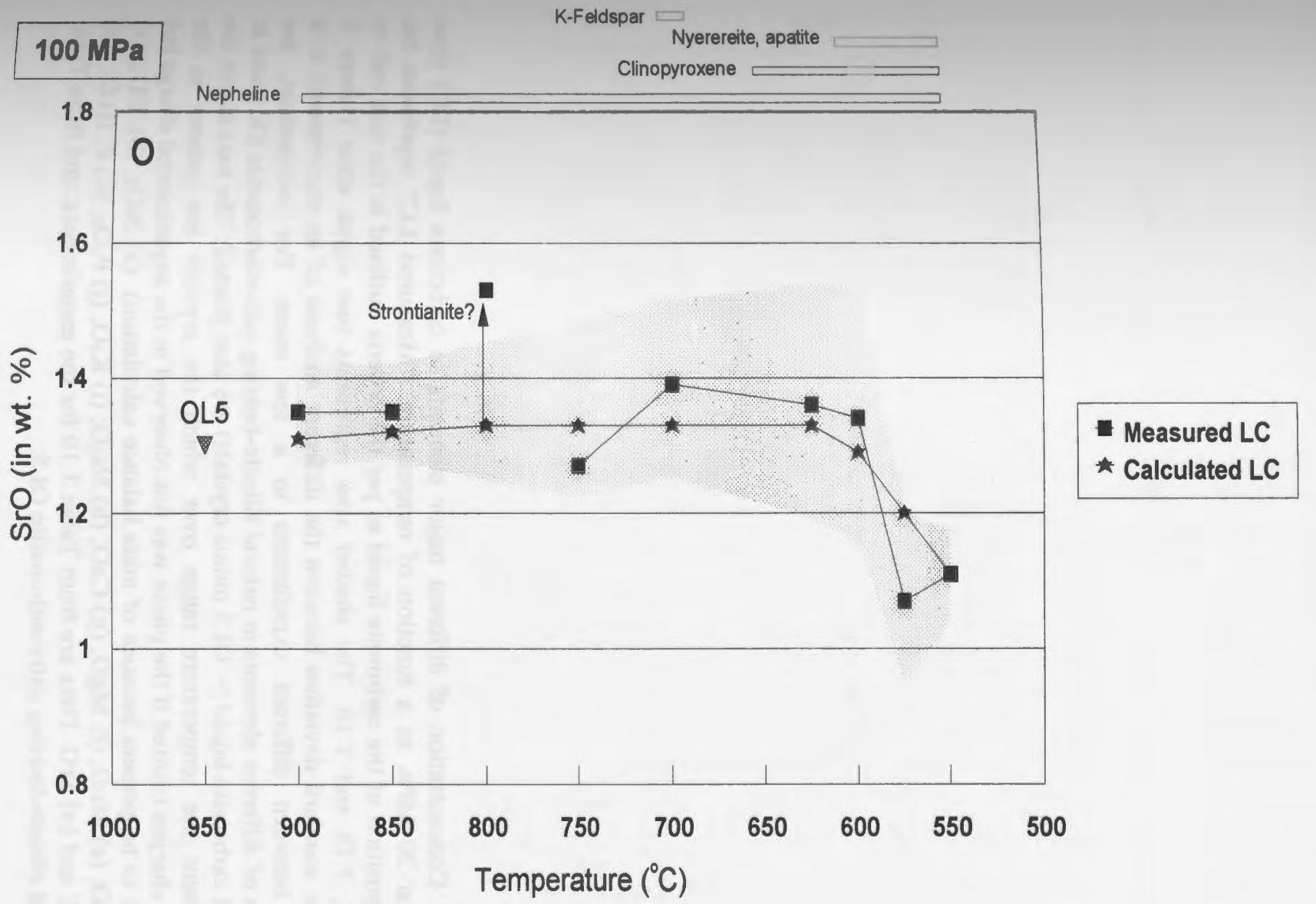
100 MPa
K-Feldspar
Nyerereite, apatite
Clinopyroxene
Nepheline
O
Strontianite?
OL5
SrO (in wt. %)
1.8
1.6
1.4
1.2
1
0.8
1000
950
900
850
800
750
700
650
600
550
500
Temperature (°C)
Measured LC
Calculated LC

Figure 3.17: Concentration of different major elements in carbonate liquid (LC) from experiments at 20 MPa, as a function of temperature. "Measured LC" represents the average composition of the carbonate liquid as per the criteria outlined in the text and on Figures 3.14, 3.15 and 3.16. The shaded area represents one sigma error (where σ represents the standard deviation between the different analyses of an experiment); it is interpolated between different experiments in a few cases. For comparison, the concentration of different elements in natural silicate-bearing natrocarbonatite OL5 and in the calculated carbonate liquid (= OL5 minus crystals) are also plotted. The bars above the graphs represent the temperature range over which the crystals are present in the experimental charges (dotted if the phase was not observed in the experimental charge but was expected to be present because of mass balance calculation). (a) SiO_2; (b) TiO_2; (c) Al_2O_3; (d) FeO; (e) MnO; (f) MgO; (g) CaO; (h) Na_2O; (i) K_2O; (j) P_2O_5; (k) F; (l) Cl; (m) SO_3; (n) BaO; and (o) SrO. Data are from Table 3.10 for the experiments, and from Table 2.2 for natural silicate-bearing natrocarbonatite OL5.

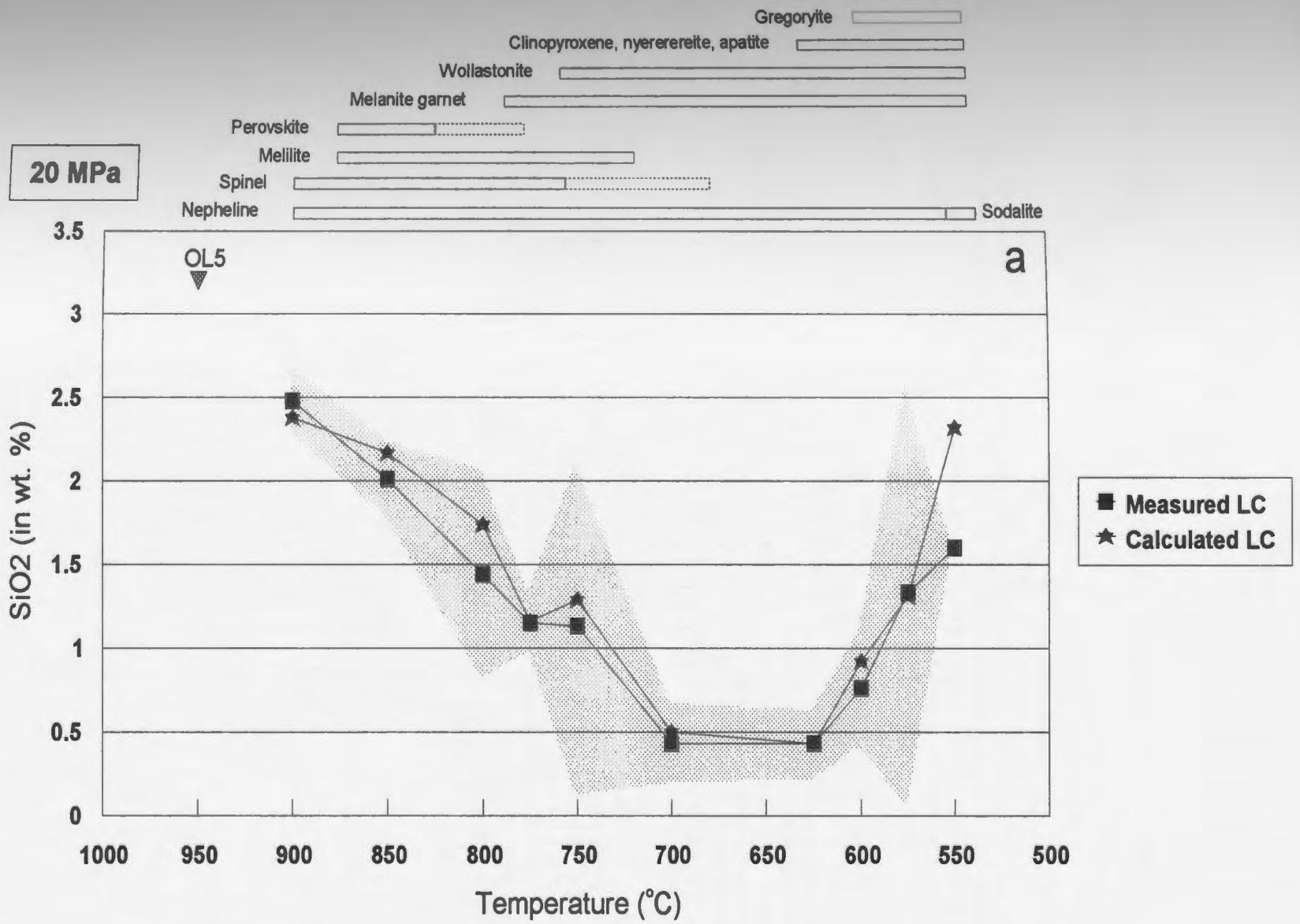
Gregoryite
Clinopyroxene, nyerereite, apatite
Wollastonite
Melanite garnet
Perovskite
Melilite
Spinel
Nepheline
Sodalite
20 MPa
OL5
a
3.5
3
2.5
2
1.5
1
0.5
0
SiO2 (in wt. %)
1000
950
900
850
800
750
700
650
600
550
500
Temperature (°C)
Measured LC
Calculated LC

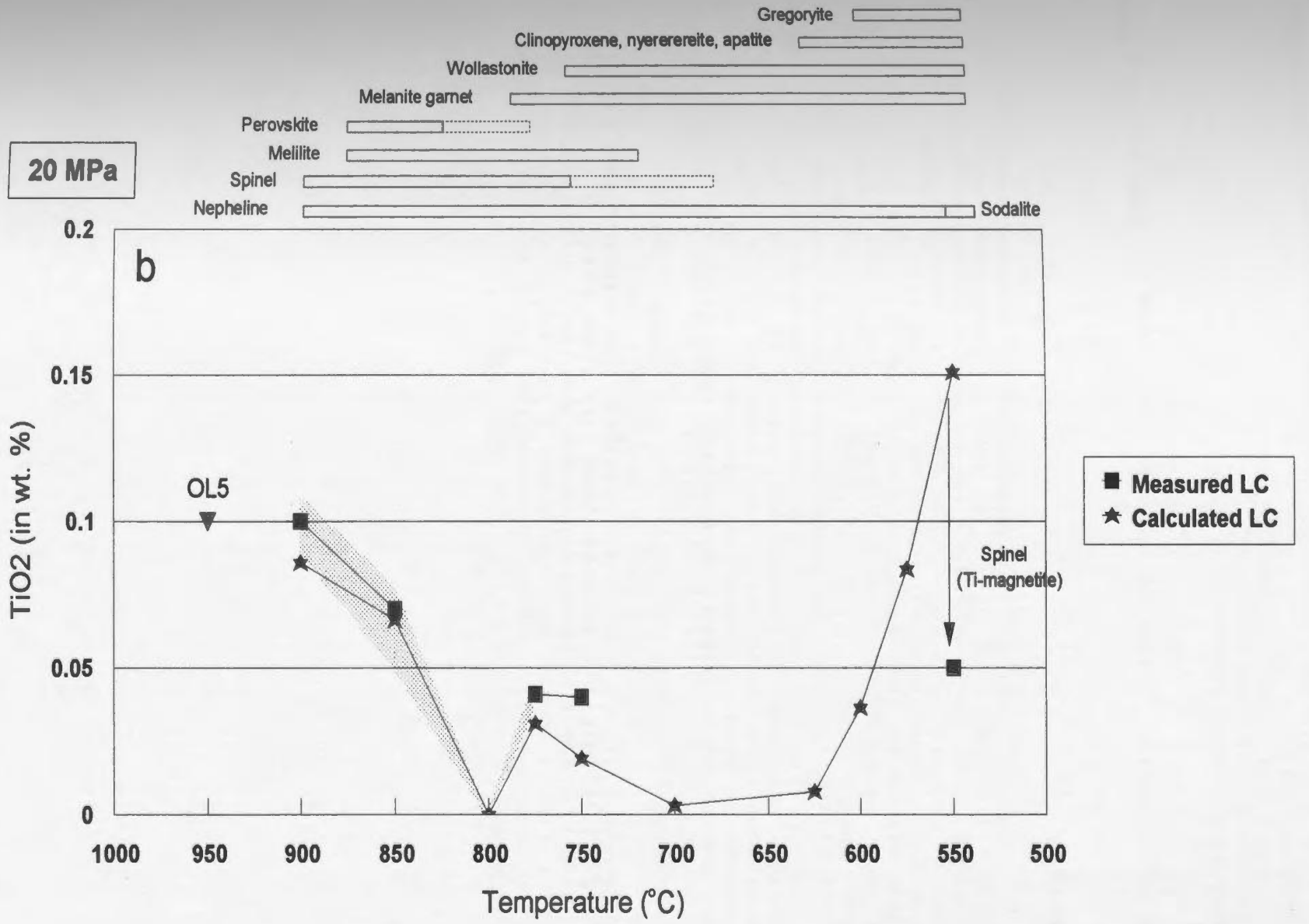
Gregoryite
Clinopyroxene, nyerereite, apatite
Wollastonite
Melanite garnet
Perovskite
Melilite
Spinel
Nepheline
Sodalite
20 MPa
b
OL5
Spinel
(Ti-magnetite)
Measured LC
Calculated LC
TiO2 (in wt. %)
Temperature (°C)
0.2
0.15
0.1
0.05
0
1000
950
900
850
800
750
700
650
600
550
500

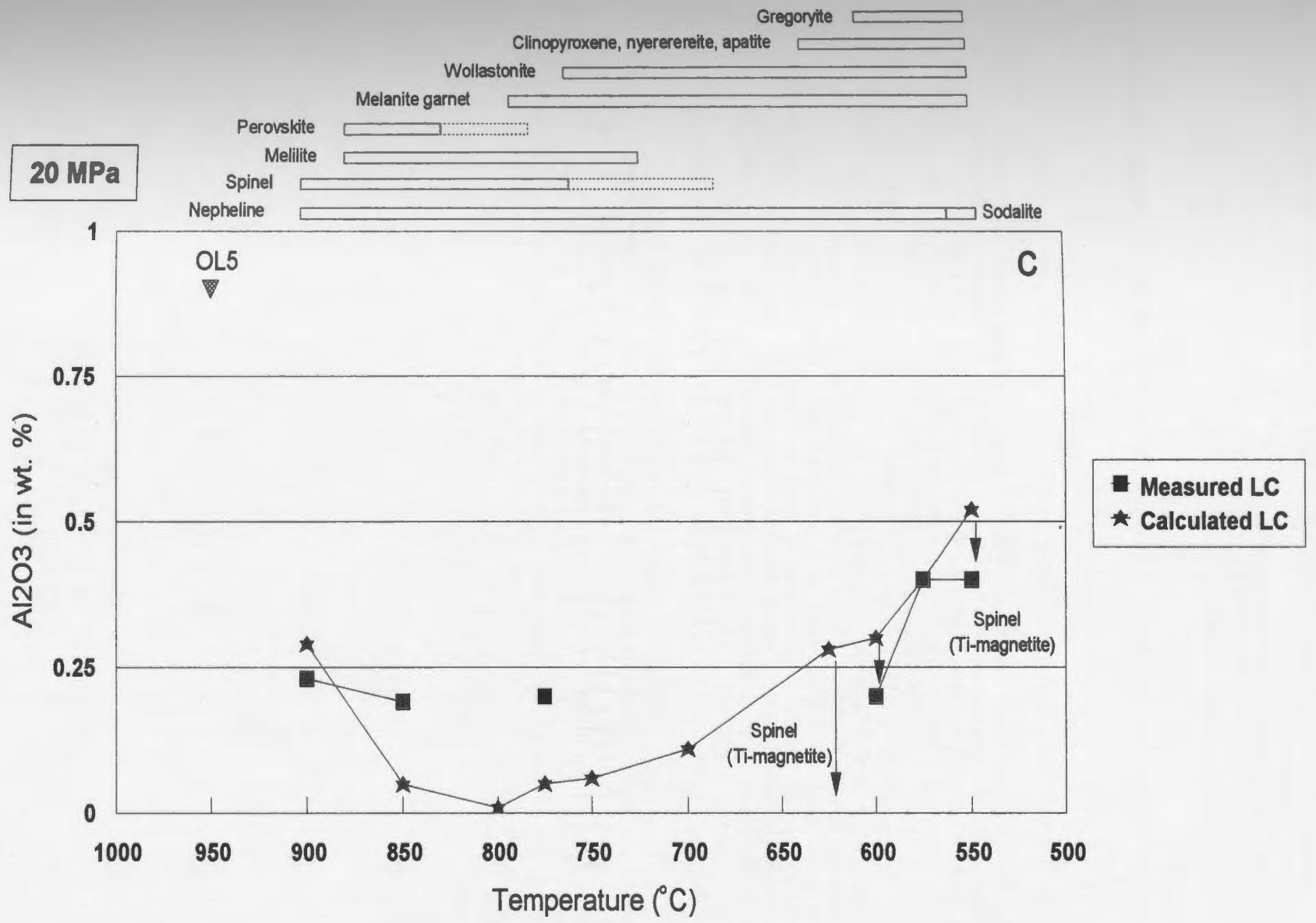
Gregoryite
Clinopyroxene, nyerereite, apatite
Wollastonite
Melanite garnet
Perovskite
Melilite
Spinel
Nepheline
Sodalite
20 MPa
OL5
C
1
0.75
0.5
0.25
0
Al2O3 (in wt. %)
Measured LC
Calculated LC
Spinel
(Ti-magnetite)
Spinel
(Ti-magnetite)
1000
950
900
850
800
750
700
650
600
550
500
Temperature (°C)

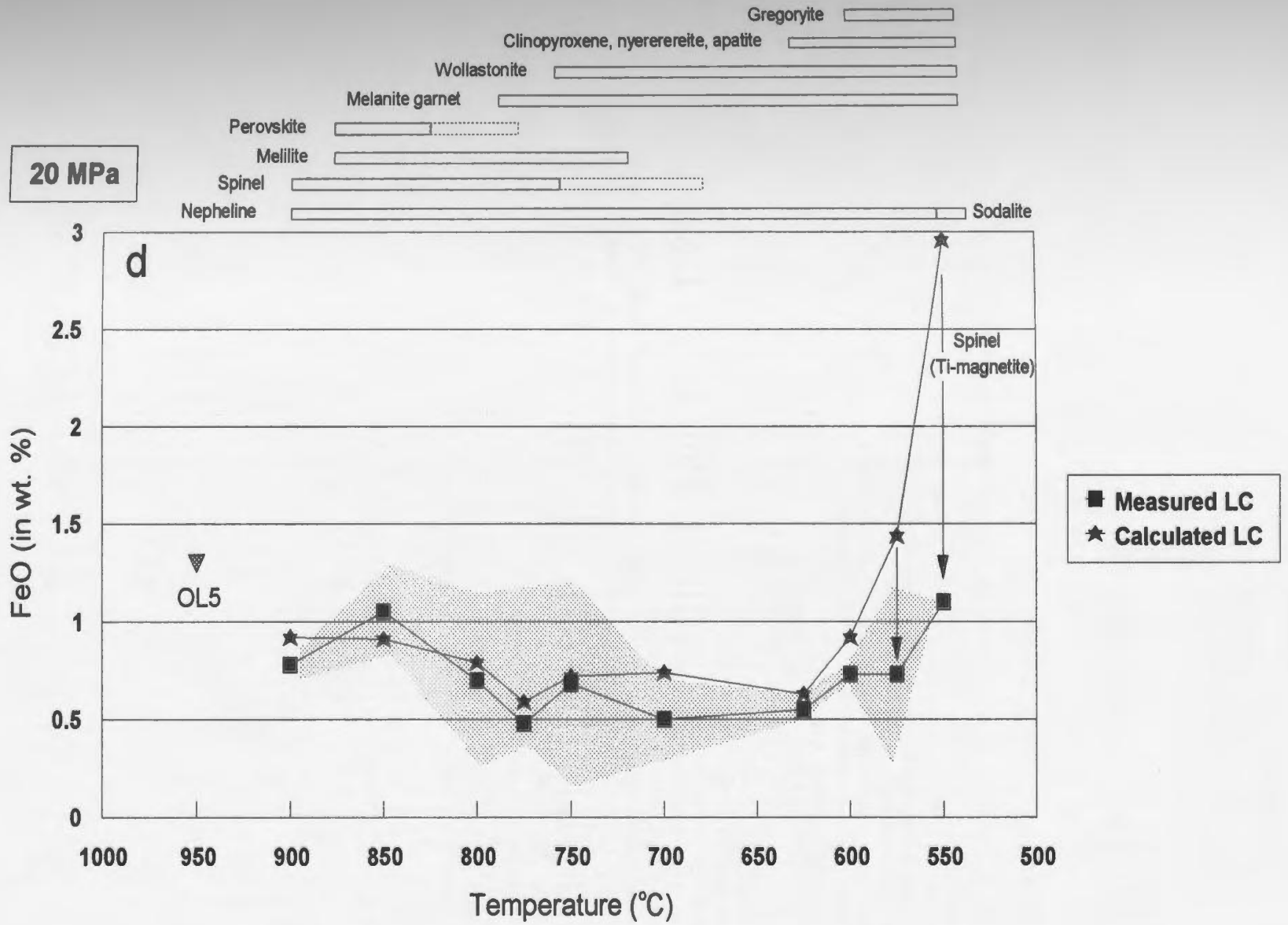
Gregoryite
Clinopyroxene, nyerereite, apatite
Wollastonite
Melanite garnet
Perovskite
Melilite
Spinel
Nepheline
Sodalite
20 MPa
d
Spinel
(Ti-magnetite)
OL5
Measured LC
Calculated LC
FeO (in wt. %)
Temperature (°C)
3
2.5
2
1.5
1
0.5
0
1000
950
900
850
800
750
700
650
600
550
500

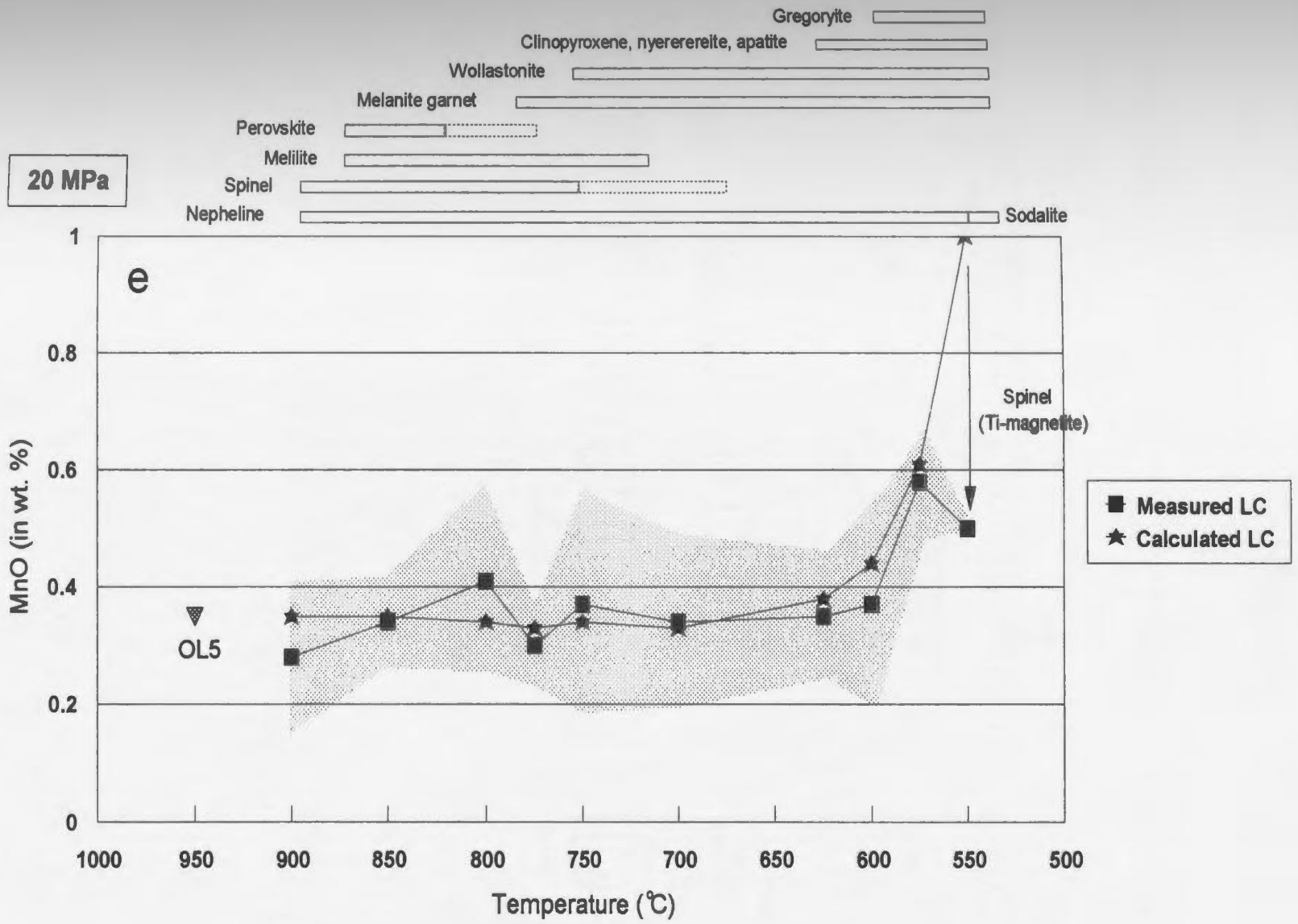
Gregoryite
Clinopyroxene, nyerereite, apatite
Wollastonite
Melanite garnet
Perovskite
Melilite
Spinel
Nepheline
Sodalite
20 MPa
e
1
0.8
0.6
0.4
0.2
0
MnO (in wt. %)
OL5
Spinel
(Ti-magnetite)
Measured LC
Calculated LC
1000
950
900
850
800
750
700
650
600
550
500
Temperature (℃)

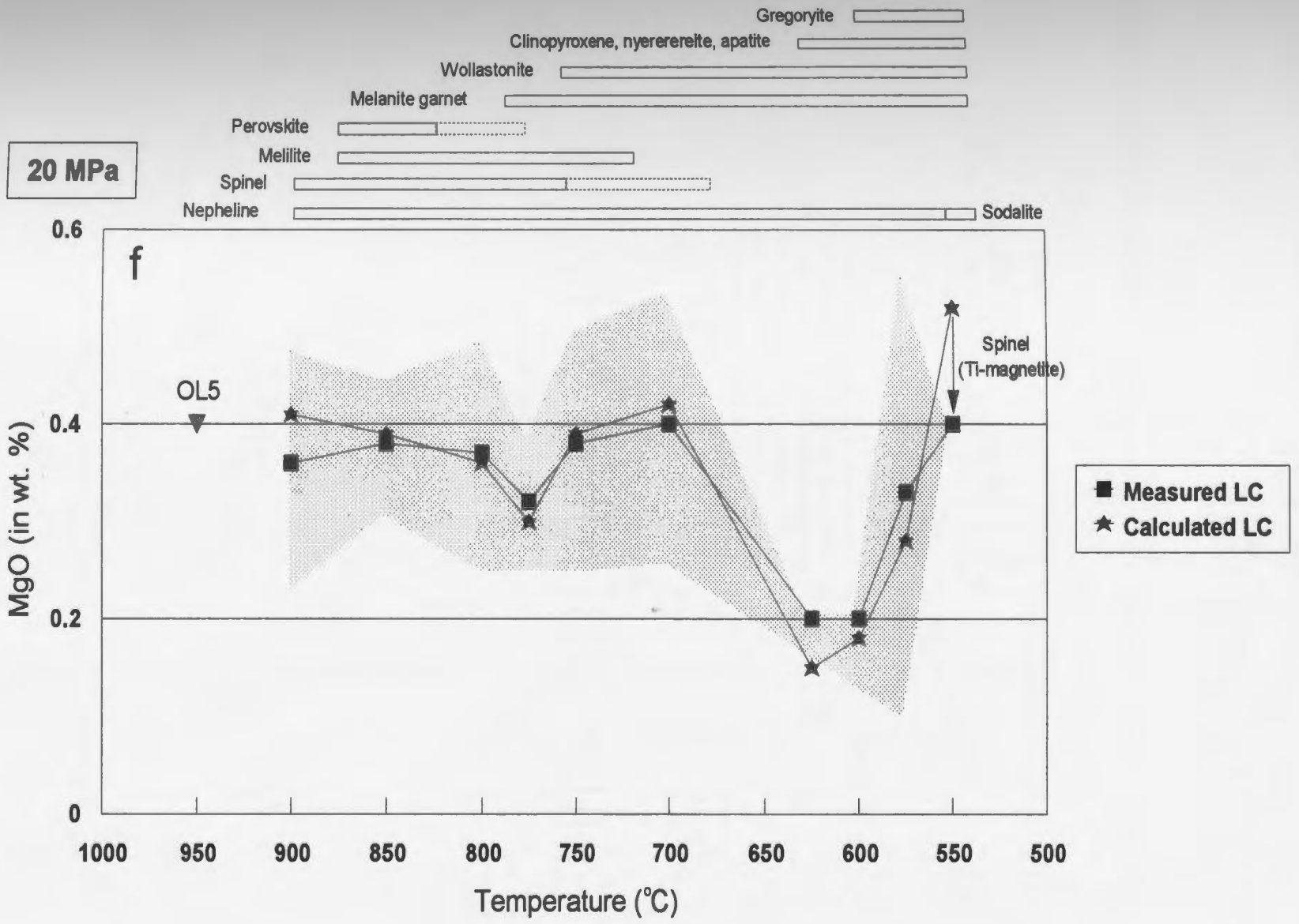
Gregoryite
Clinopyroxene, nyerereite, apatite
Wollastonite
Melanite garnet
Perovskite
Melilite
Spinel
Nepheline
Sodalite
20 MPa
f
OL5
Spinel
(Ti-magnetite)
Measured LC
Calculated LC
MgO (in wt. %)
0.6
0.4
0.2
0
1000
950
900
850
800
750
700
650
600
550
500
Temperature (°C)

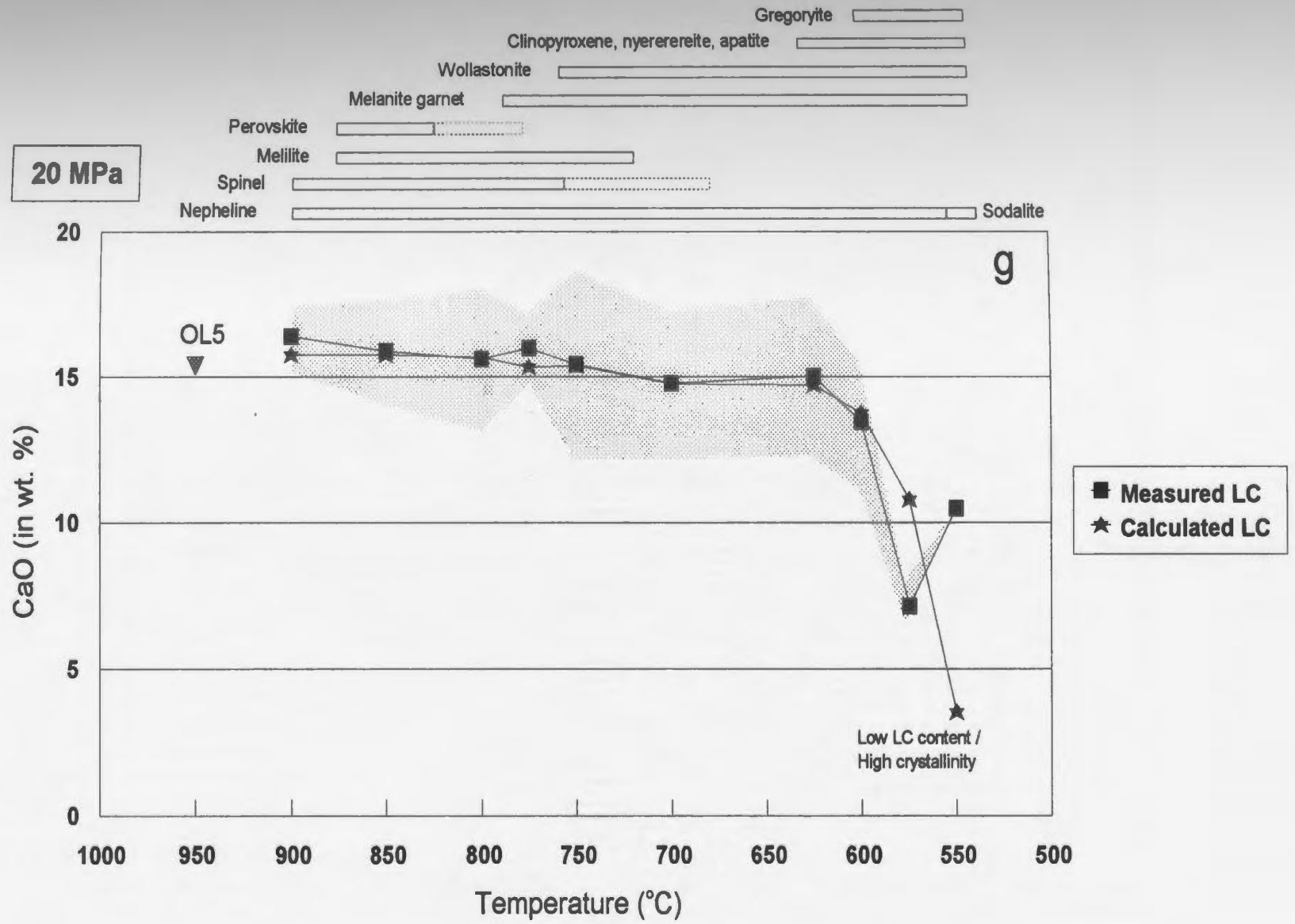
Gregoryite
Clinopyroxene, nyerereite, apatite
Wollastonite
Melanite garnet
Perovskite
Melilite
Spinel
Nepheline
Sodalite
20 MPa
g
OL5
Low LC content /
High crystallinity
Measured LC
Calculated LC
CaO (in wt. %)
Temperature (°C)
20
15
10
5
0
1000
950
900
850
800
750
700
650
600
550
500

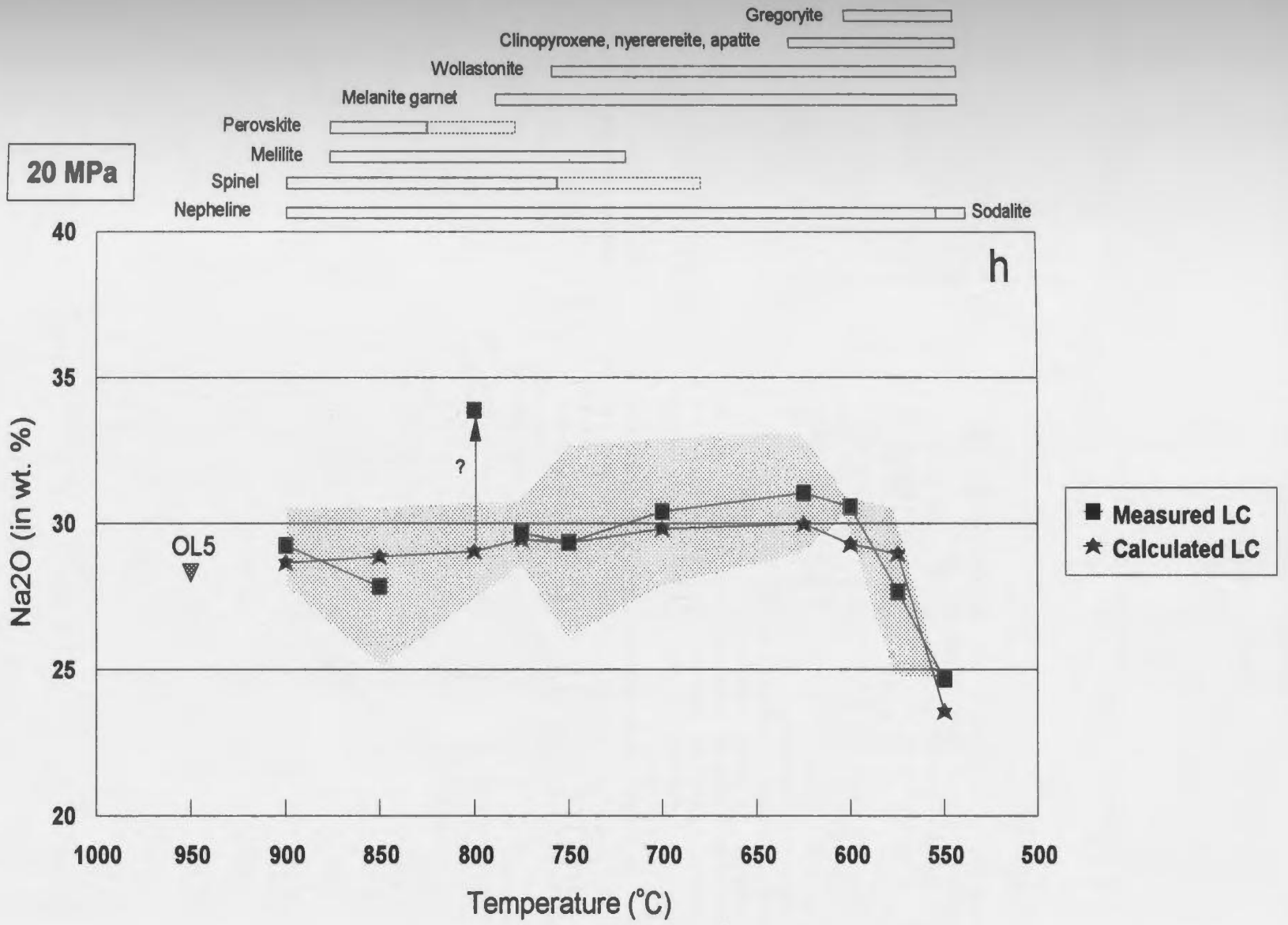
Gregoryite
Clinopyroxene, nyerereite, apatite
Wollastonite
Melanite garnet
Perovskite
Melilite
Spinel
Nepheline
Sodalite
20 MPa
h
40
35
30
25
20
Na2O (in wt. %)
?
OL5
1000
950
900
850
800
750
700
650
600
550
500
Temperature (°C)
Measured LC
Calculated LC

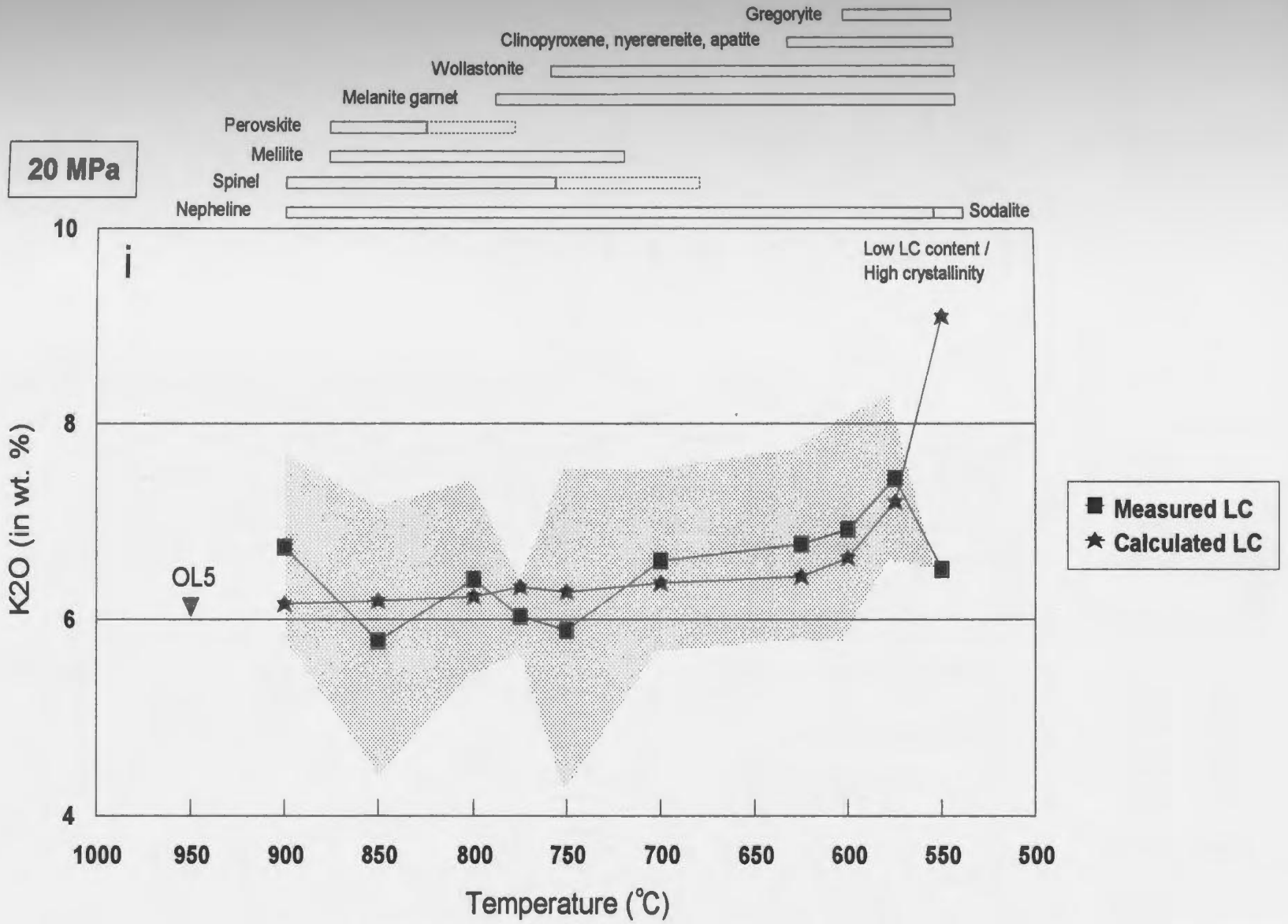
Gregoryite
Clinopyroxene, nyerereereite, apatite
Wollastonite
Melanite garnet
Perovskite
Melilite
Spinel
Nepheline
Sodalite
20 MPa
i
Low LC content /
High crystallinity
OL5
K2O (in wt. %)
10
8
6
4
1000
950
900
850
800
750
700
650
600
550
500
Temperature (°C)
Measured LC
Calculated LC

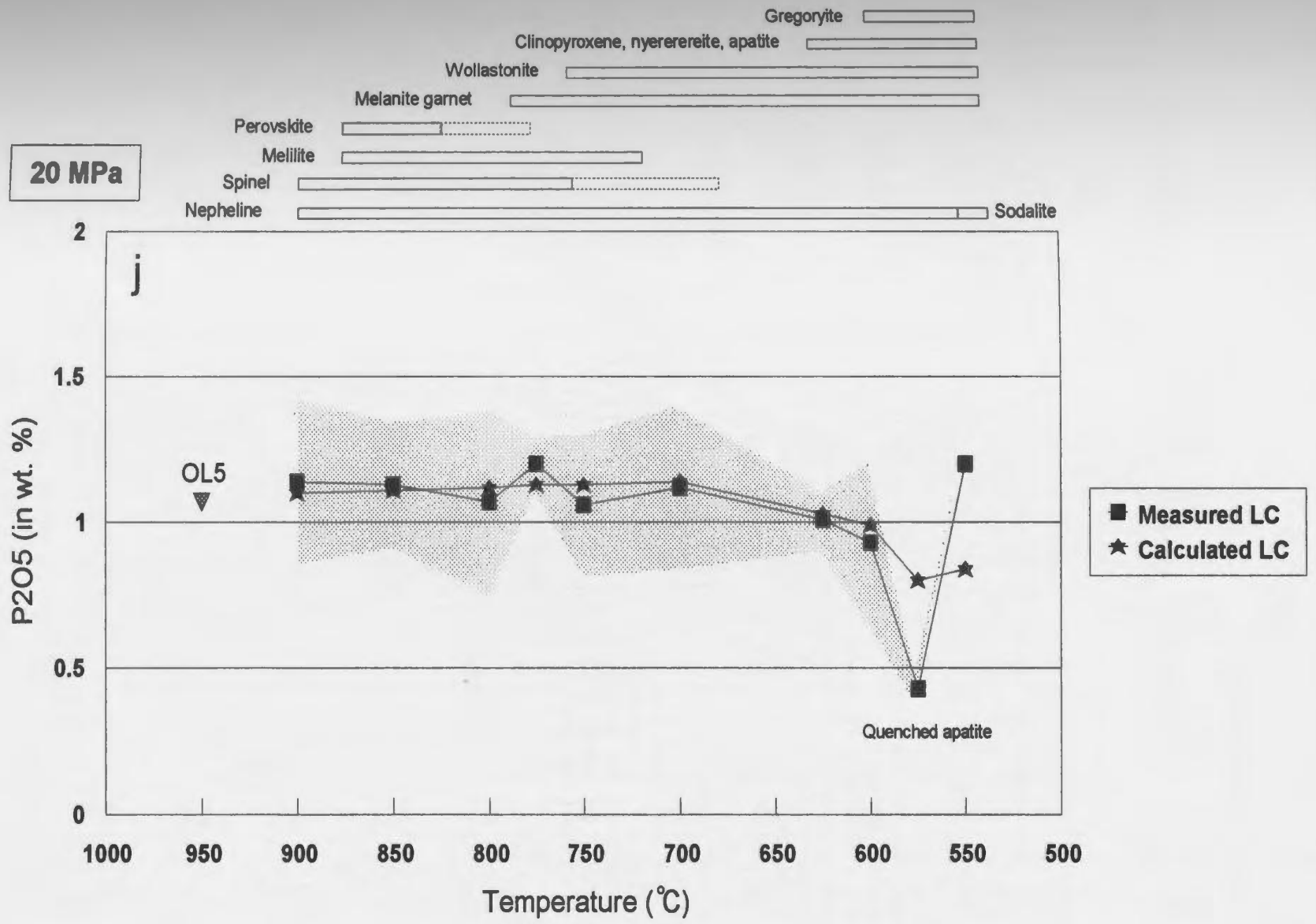
Gregoryite
Clinopyroxene, nyerereite, apatite
Wollastonite
Melanite garnet
Perovskite
Melilite
Spinel
Nepheline
Sodalite
20 MPa
j
OL5
Quenched apatite
Measured LC
Calculated LC
P2O5 (in wt. %)
Temperature (℃)
2
1.5
1
0.5
0
1000
950
900
850
800
750
700
650
600
550
500

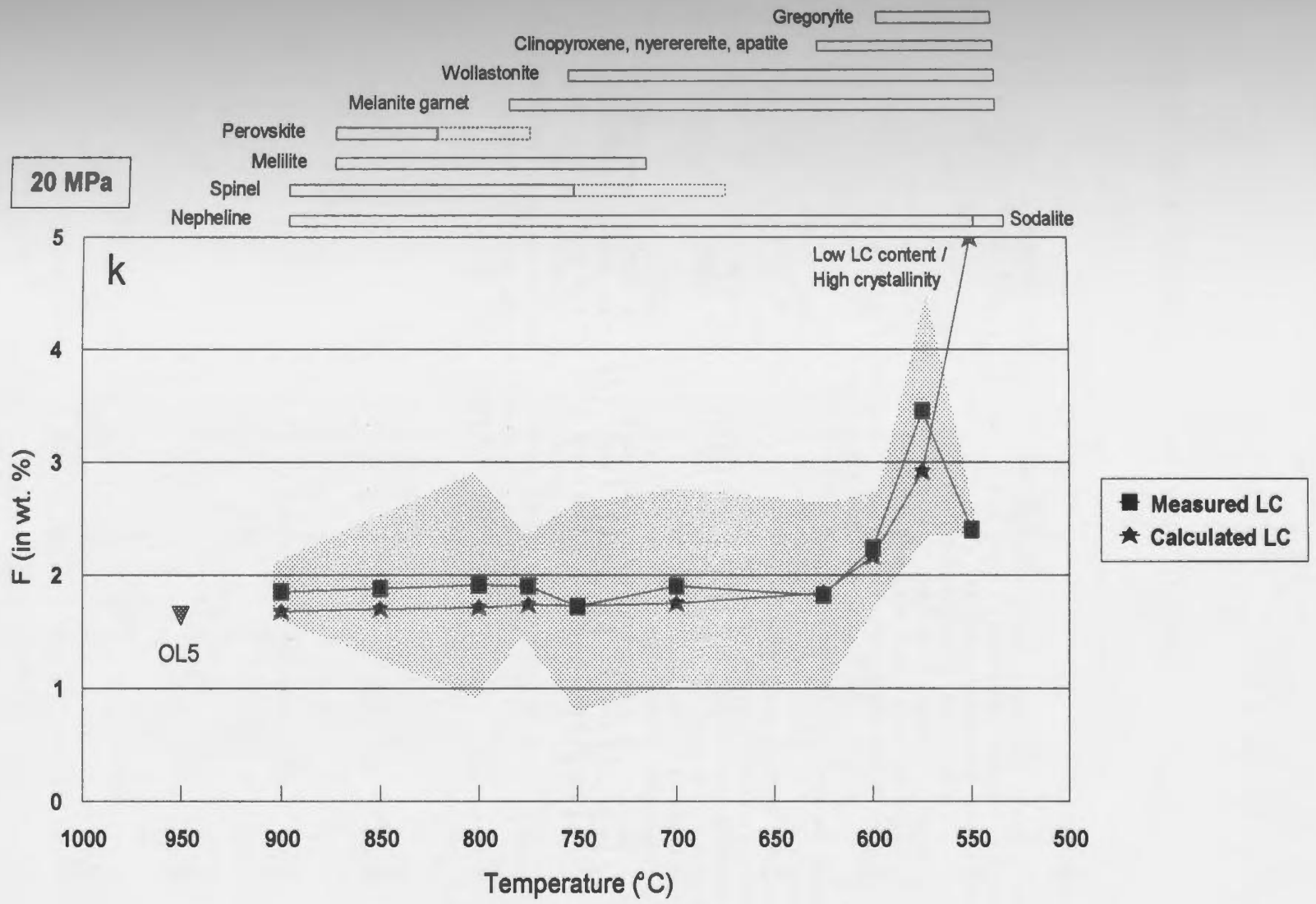
Gregoryite
Clinopyroxene, nyerereite, apatite
Wollastonite
Melanite garnet
Perovskite
Melilite
Spinel
Nepheline
Sodalite
20 MPa
k
Low LC content /
High crystallinity
OL5
F (in wt. %)
Temperature (°C)
Measured LC
Calculated LC

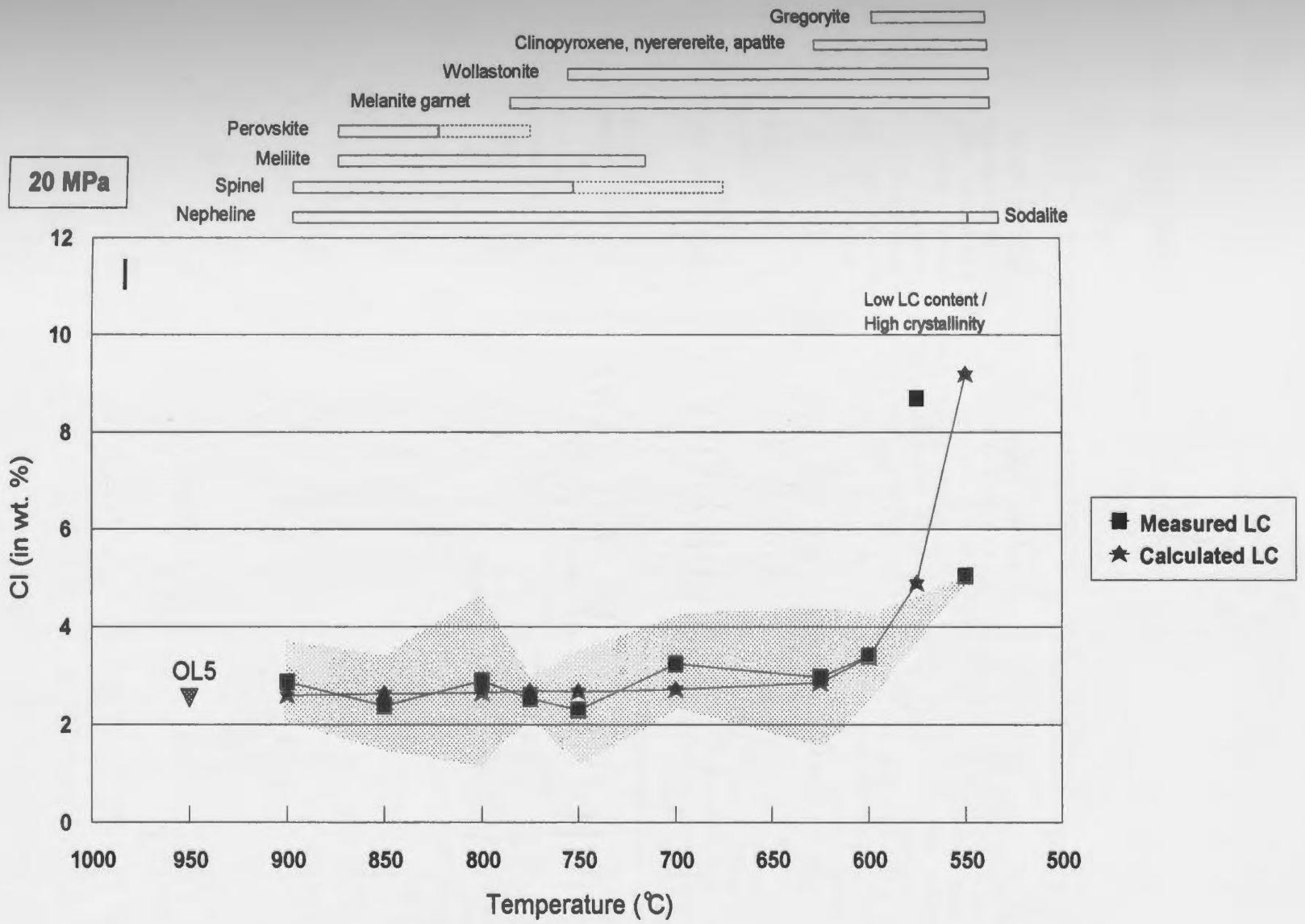
Gregoryite
Clinopyroxene, nyerereite, apatite
Wollastonite
Melanite garnet
Perovskite
Melilite
Spinel
Nepheline
Sodalite
20 MPa
Low LC content /
High crystallinity
OL5
Cl (in wt. %)
Temperature (℃)
Measured LC
Calculated LC
12
10
8
6
4
2
0
1000
950
900
850
800
750
700
650
600
550
500

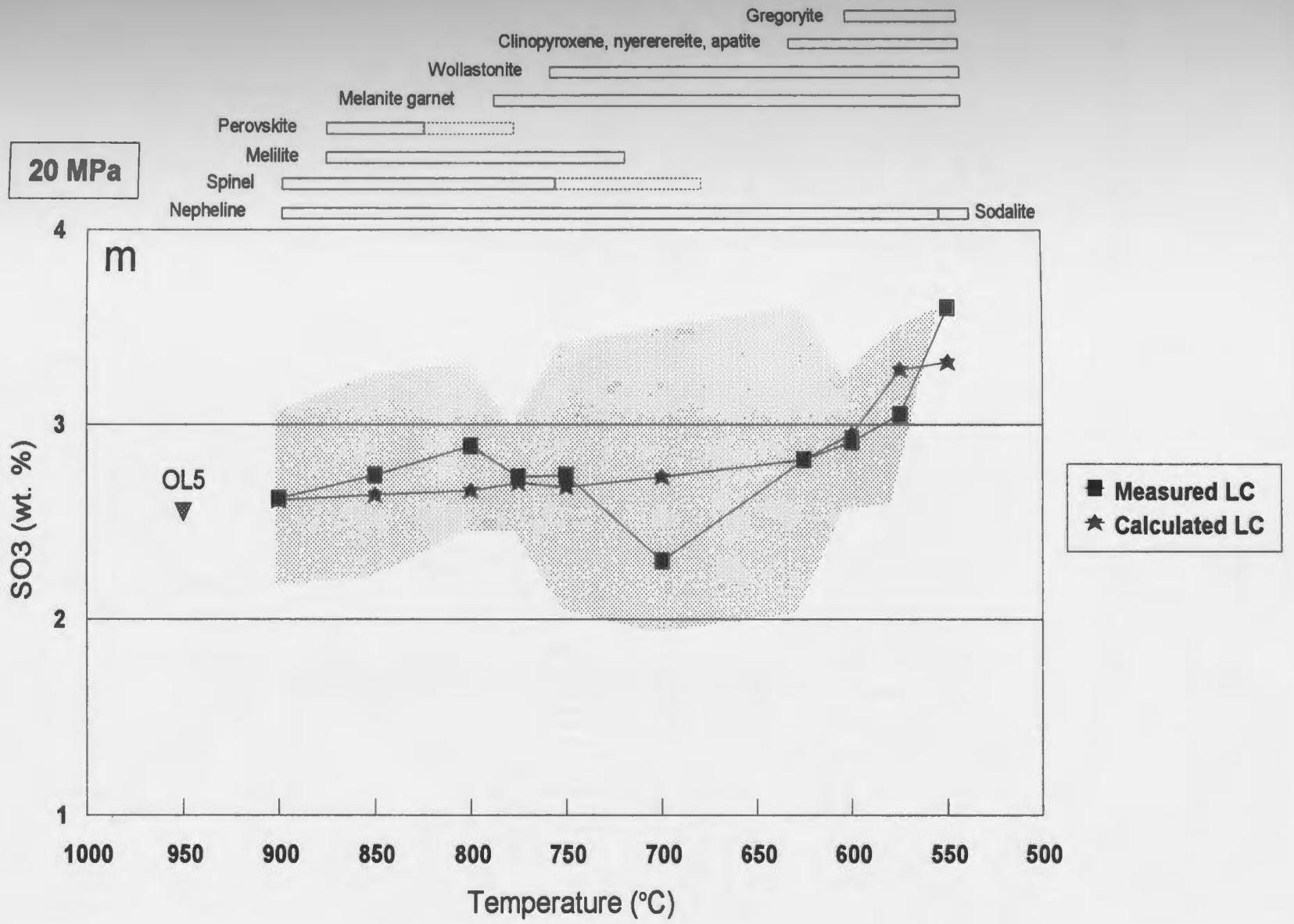
Gregoryite
Clinopyroxene, nyerereite, apatite
Wollastonite
Melanite garnet
Perovskite
Melilite
Spinel
Nepheline
Sodalite
20 MPa
m
OL5
SO3 (wt. %)
4
3
2
1
1000
950
900
850
800
750
700
650
600
550
500
Temperature (°C)
Measured LC
Calculated LC

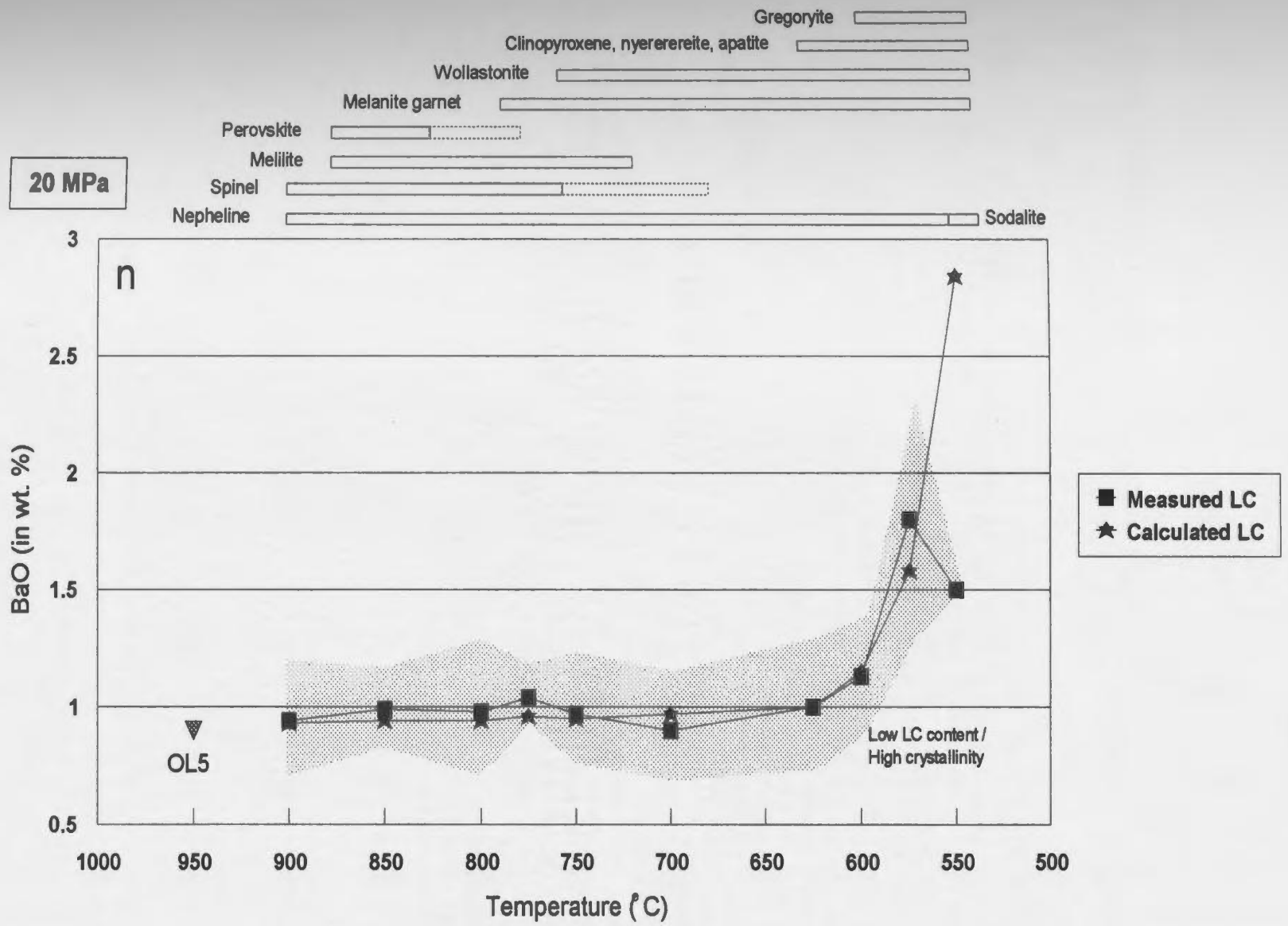
Gregoryite
Clinopyroxene, nyerereite, apatite
Wollastonite
Melanite garnet
Perovskite
Melilite
Spinel
Nepheline
Sodalite
20 MPa
n
BaO (in wt. %)
3
2.5
2
1.5
1
0.5
OL5
Low LC content /
High crystallinity
Measured LC
Calculated LC
1000
950
900
850
800
750
700
650
600
550
500
Temperature (°C)

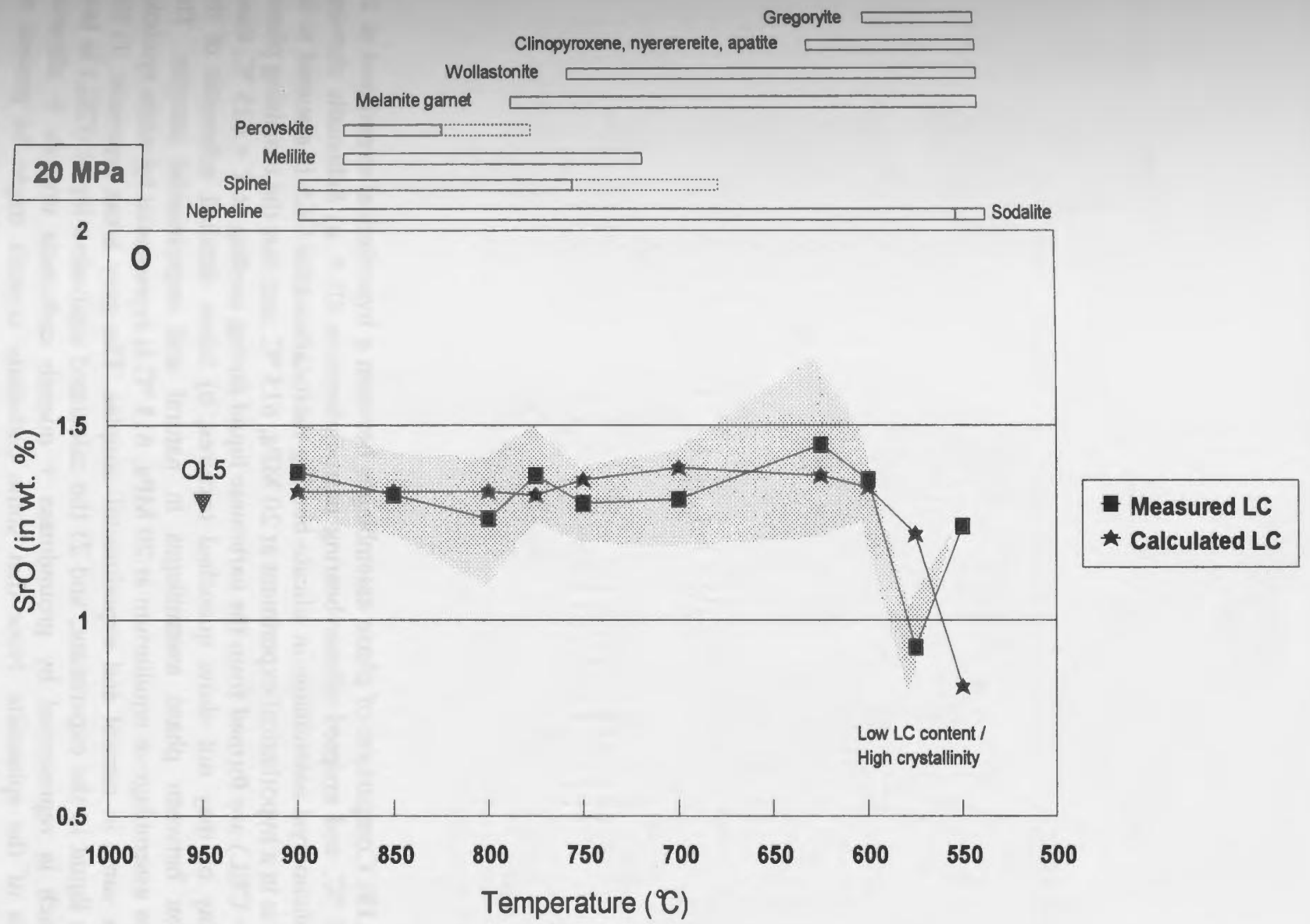
Gregoryite
Clinopyroxene, nyerereite, apatite
Wollastonite
Melanite garnet
Perovskite
Melilite
Spinel
Nepheline
Sodalite
20 MPa
O
OL5
SrO (in wt. %)
2
1.5
1
0.5
1000
950
900
850
800
750
700
650
600
550
500
Temperature (℃)
Low LC content /
High crystallinity
Measured LC
Calculated LC

Figure 3.18: Comparison of phase assemblages between a hypothetical experiment at 20 MPa, 615 °C, and erupted silicate-bearing natrocarbonatite OL5. a) Schematic showing that the phenocryst assemblage in silicate-bearing natrocarbonatite OL5 is assumed to be the same as in a hypothetical experiment at 20 MPa, 615 °C, and that the remaining phases in OL5 (= CEL) are formed from the carbonate liquid during cooling at T < 615 °C; these phases may or may not show quenched textures; b) More detailed schematic of the comparison between phase assemblages in natural and experimental samples. The phenocryst assemblage at equilibrium at 20 MPa, 615 °C is represented by white symbols, and is the same in natural and experimental samples. The grey areas represent: 1) the carbonate liquid in the experiment; and 2) the calculated equivalent liquid (CEL) in lava OL5, which is represented by groundmass + quench carbonate crystals + siliceous mesostasis of the spheroids. Note that some carbonate crystals might be present as overgrowths on preexisting crystals. See text for the details on the calculations.

a

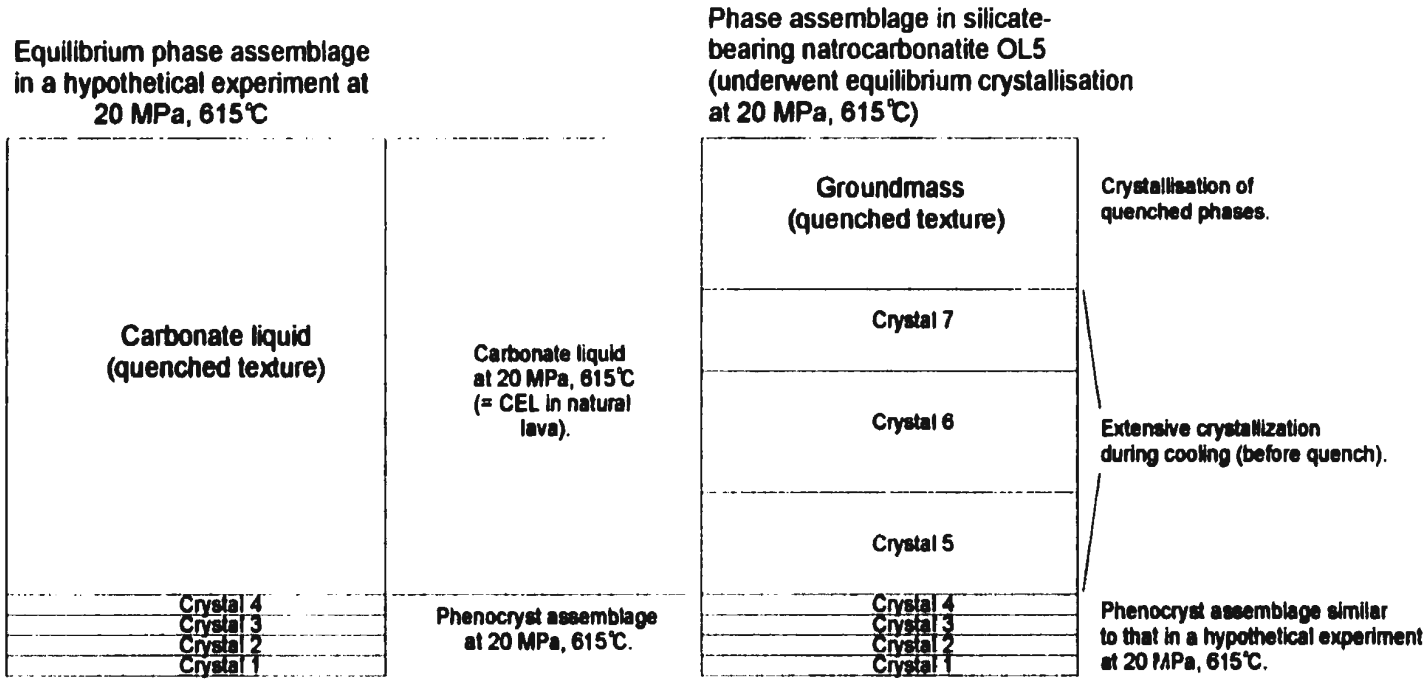
Equilibrium phase assemblage in a hypothetical experiment at 20 MPa, 615°C
Carbonate liquid (quenched texture)
Crystal 4
Crystal 3
Crystal 2
Crystal 1
Carbonate liquid at 20 MPa, 615°C (= CEL in natural lava).
Phenocryst assemblage at 20 MPa, 615°C.
Phase assemblage in silicate-bearing natrocarbonatite OL5 (underwent equilibrium crystallisation at 20 MPa, 615°C)
Groundmass (quenched texture)
Crystal 7
Crystal 6
Crystal 5
Crystal 4
Crystal 3
Crystal 2
Crystal 1
Crystallisation of quenched phases.
Extensive crystallization during cooling (before quench).
Phenocryst assemblage similar to that in a hypothetical experiment at 20 MPa, 615°C.

b

Silicate-bearing natrocarbonatite OL5

Equilibrium modal proportions of phases in a hypothetical experiment at 20 MPa, 615°C

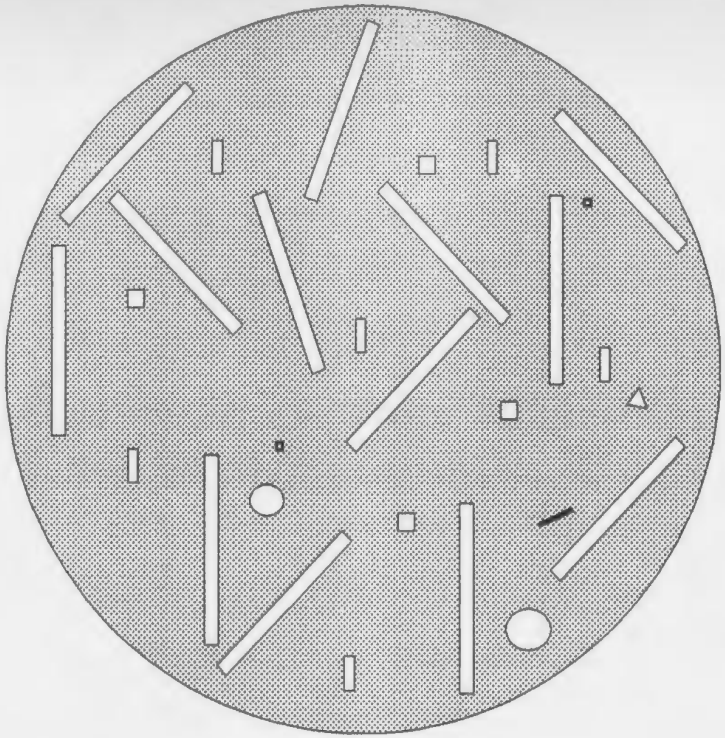

Phenocryst assemblage at 20 MPa, 615°C (white)

Same in experiment and in OL5

- 2 % Nepheline
- 3 % Clinopyroxene
- 0.7 % Melanite
- 0.05 % Wollastonite
- 0.3 % Apatite
- 10 % Nyerereite
- 2.5 % Gregoryite

Liquid (grey)

- In the experiment: 81.45 % carbonate liquid

- In OL5: calculated equivalent liquid (CEL)=

  - 19 % groundmass
  - 27 % nyerereite
  - 33.75 % gregoryite
  - 1.7 % siliceous mesostasis

  including:
  - 1.2 % groundmass
  - 0.1 % Nepheline
  - 0.1 % Clinopyroxene
  - 0.1 % Melanite
  - 0.1 % Wollastonite
  - 0.1 % Gregoryite

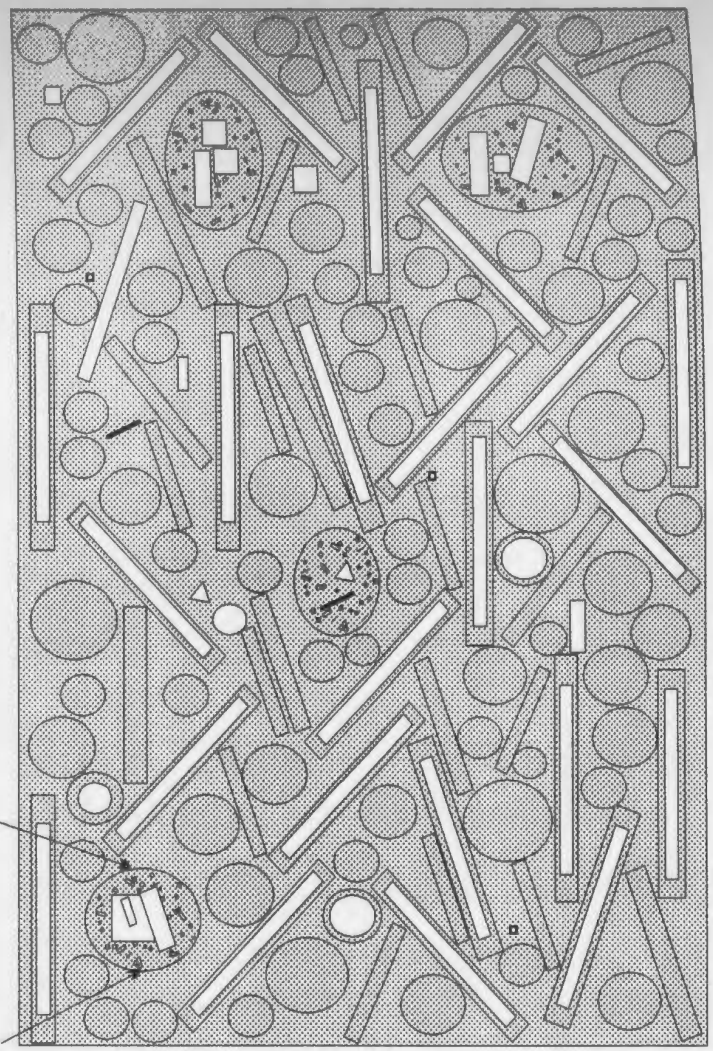

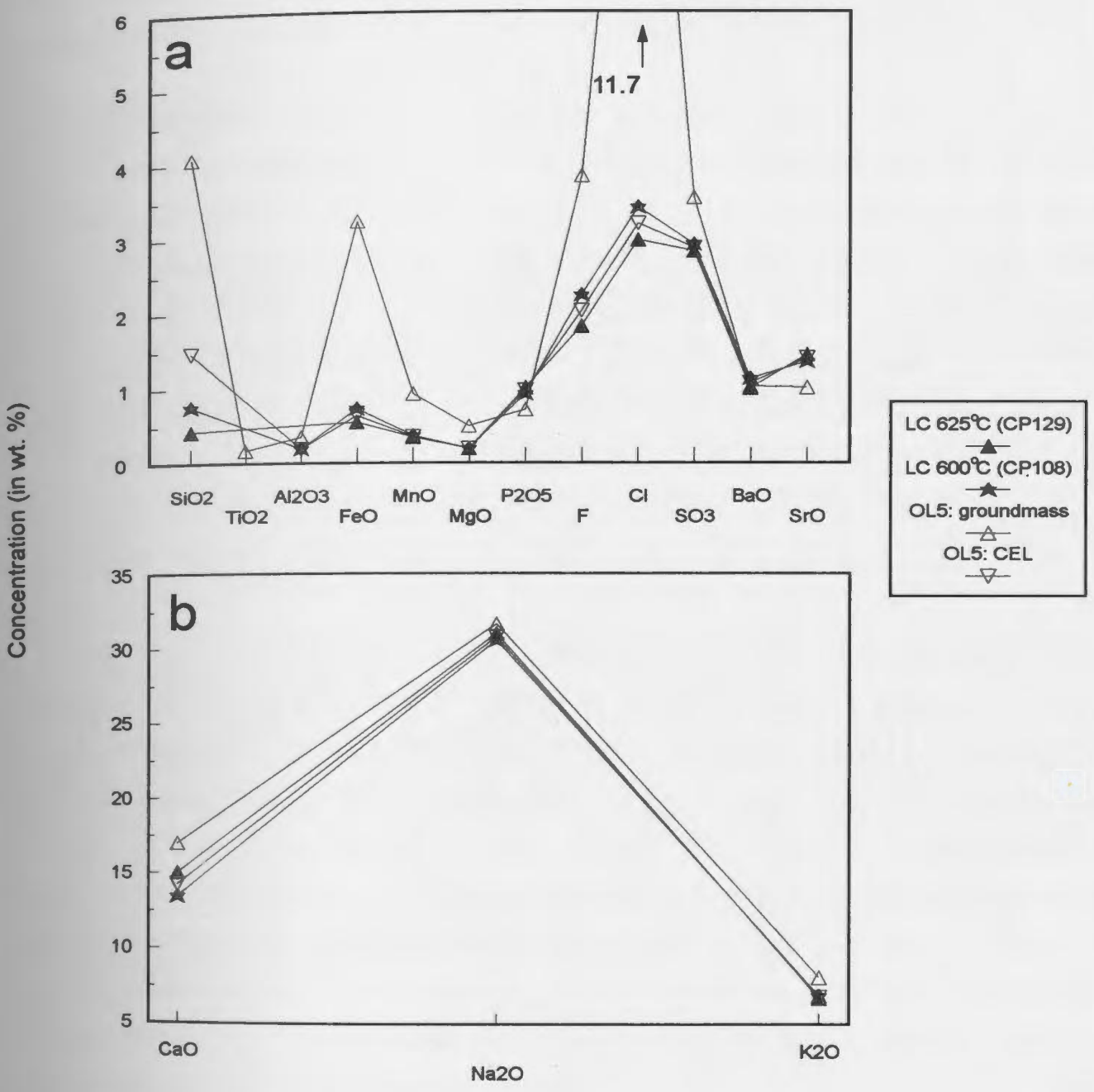

Figure 3.19: Major element composition of carbonate liquid (LC) in experiments at 20 MPa, 600 and 625 °C (experiments CP129 and CP108, respectively), and of calculated equivalent liquid (CEL), and groundmass in silicate-bearing natrocarbonatite lava OL5 (see text for discussion). The definition of calculated equivalent liquid (CEL) is shown in Table 3.11. (a) Elements with lowest concentrations; (b) Elements with highest concentrations. Data are from Tables 3.10 and 3.12.

CHAPTER 4 – TRACE ELEMENT DATA: COMPARISON BETWEEN EXPERIMENTAL RUN PRODUCTS AND NATURAL LAVAS.

4.1 - Introduction

Results of LAM-ICP-MS trace element analyses obtained on experimental run products are compared to those obtained on natural silicate-bearing and silicate-free natrocarbonatites from Oldoinyo Lengai. The aim is to determine which parameters can explain the differences and/or similarities that occur among phases of different samples. Once the effect of quenching is separated from the effect of other parameters, the calculated partition coefficients between crystals and liquid can be better understood and examined as a function of pressure, temperature and composition, and also of crystal structure. Data from this chapter will be used in Chapter 5 to examine the crystallisation of silicate-bearing natrocarbonatite OL5 and the formation of silicate-free natrocarbonatites.

No data are available from previous studies of partition coefficients between silicate minerals and carbonatite liquid at crustal conditions. Dawson et al. (1994b) presented partitioning for perovskite, apatite and titanite in silicate rocks from Oldoinyo Lengai, but only on crystal-crystal pairs. All of the experimental data are at mantle conditions because of the growing interest in mantle metasomatism related to carbonatites and the need to determine D-values for trace elements between major mantle minerals and carbonatite liquids (Brenan and Watson, 1991; Green et al., 1992; Sweeney et al., 1992, 1995b; Walker et al., 1992; Jones et al., 1995; and Klemme et al. 1995). The results of this chapter are the first available trace element data for crystal-carbonate liquid pairs determined by experiments at crustal pressures.

In this study, a range of different elements for all phases were determined including: low field strength elements (LFSE) - Ba, Sr, Rb, Th and U; high field strength elements (HFSE) - Zr, Nb, Hf and Ta; rare earth elements (REE); plus yttrium (Y) and vanadium (V). Concentrations are presented plotted on primitive mantle (PM) normalised plots, divided into 2 groups: 1) REE; and 2) LFSE, Y, V, and HFSE. This division of the data

has been made to facilitate comparison of elements which usually behave as coherent pairs, *i.e.*, elements which usually partition similarly, namely, U-Th, Nb-Ta and Zr-Hf. Yttrium is not a lanthanide so it has been grouped with the remaining elements for simplicity.

4.2 - Results

Average analyses for each phase are presented, with the number of analyses used to calculate the average values indicated in the tables. Complete data sets and the relative standard deviation (RSD) are given in Appendix A4. The data typically display a wide range of values (high RSD) for results on both crystals and carbonate liquid.

A number of factors contributed to the high RSD's. For crystals, surface contamination by a "spray" of condensed ablated material was commonly observed. As a consequence some analyses could not be taken into account in the final compilation. In some cases, small crystal size limited the volume of material that could be ablated and, therefore, detection limits are high. This in part explains some of the difficulty in obtaining the data, especially for elements at low concentration levels.

The method for calculating trace element compositions of crystals is iterative. The first step is to exclude some entire individual analyses from the average when a particular analysis is significantly different. This usually reflects extreme surface contamination or ablation of more than one phase. The second step is to exclude the elements which produce high relative standard deviation (RSD) or which are internally inconsistent for some individual analyses (marked by an asterix in appendix tables). Analyses of the cores of crystals are used to calculate average compositions since the composition of the rims can be affected by high growth rate during quench, although the small size of many of the crystals in the experiments may preclude any other choice. The presence of trace element zoning could not be defined in this LAM-ICP-MS study.

The textural heterogeneity of the quenched carbonate liquid explains the wide ranges recorded for trace element data on the liquids. To minimise the effects of these problems, a data evaluation process similar to that used in the previous chapter was used.

Examination of each individual analysis compared to the calculated composition of the residual liquid (= starting composition OL5 minus crystals) was used to decide which carbonate liquid analyses were kept or rejected, as was done in Chapter 3 for the major elements.

4.2.1: Composition of major crystal phases in OL5-experiments

Trace element compositions of the major crystal phases in the experiments are presented below. No trace element data are available for some minor, small crystal phases (*e.g.* apatite and perovskite) on which attempts to collect data were unsuccessful.

4.2.1.1: Nepheline

Data for nepheline are reported in Table 4.1, and normalised concentrations are illustrated in Figure 4.1. Detection limits, which vary for different experiments, are also given in Table 4.1. The concentration of most elements in nepheline are close to the detection limit and it is difficult to obtain reliable sets of data. For most elements, the range between highest and lowest value is one order of magnitude or higher, and almost certainly reflects scatter due to analytical problems, primarily ablation of associated quenched carbonate liquid. The lowest values probably represent the "best" or most accurate levels, but these values are closer to detection limit, and not precise.

Rubidium has the most consistent concentration level among nepheline crystals from different experiments, in the range 68-115 ppm (av. 90 ppm). Barium and uranium also have fairly consistent concentrations among nepheline crystals from different experiments. Barium has concentrations varying from 8.1 to 68 ppm (av. 27 ppm). If nepheline from experiment CP79 (100 MPa, 800 °C) is excluded, U shows consistent concentrations varying from 0.48 to 1.04 ppm. The remaining trace elements have concentrations which are below detection limits in nepheline from most experiments. However, despite the scarcity of the data, the REE data are fairly consistent with one another.

4.2.1.2: Clinopyroxene

Trace element analyses of clinopyroxene crystals from the experiments are reported in Table 4.2 and illustrated in Figure 4.2. There is more confidence in the results for clinopyroxene from experiment CP107 (100 MPa, 600 °C), for which most of the data have been kept. The REE pattern is concave up ($La_{pm} > 10$, $Er_{pm} < 2.50$ and $Lu_{pm} \sim 8$). High field strength elements in clinopyroxene are abundant, with Nb in the range of 12-33 ppm and Zr in the range of 233-388 ppm. No effect of pressure or temperature on the trace element compositions of clinopyroxene can be deduced from this small set of data.

4.2.1.3: Melanite garnet

Trace element analyses of melanite garnet from the experiments are reported in Table 4.3 and normalised concentrations plotted in Figure 4.3. Trace element data for garnet are easier to obtain, compared to nepheline and clinopyroxene, because of their higher trace element concentrations.

For experiments CP51 (20 MPa, 750 °C), CP57 (20 MPa, 700 °C) and CP108 (20 MPa, 600 °C), REE patterns are convex up, with normalised concentrations of Nd (181-311) higher than those of La (53-89) and Lu (57-81). Thorium, U and HFSE have the highest normalised concentrations (>100). Niobium has concentrations in the range of 390 - 953 ppm and Zr has concentrations in the range of 3158 - 3536 ppm. No systematic effect of temperature on the trace element composition of melanite garnets from 20 MPa-experiments is indicated by comparing trace element data from experiments CP51, CP57 and CP108 (respectively at 750, 700 and 600 °C).

4.2.1.4: Wollastonite

Analyses of trace elements in wollastonite from experiment CP51 (20 MPa, 750 °C) are reported in Table 4.4, and illustrated in Figure 4.4. Concentrations of La and Lu are, respectively, 31.5 and 0.93 ppm. The REE-pattern is slightly irregular, with $La_{pm}/Lu_{pm} = 3.5$.

4.2.1.5: Melilite

Trace element composition of melilite from experiment CP51 (20 MPa, 750 °C) is reported in Table 4.5 and plotted in Figure 4.5. Strontium is the element showing the highest concentration (15482 ppm); this value is equivalent to 1.84 wt. % SrO, and compares fairly well with the SrO content determined on melilite crystals from OL5-experiments by electron microprobe (= 2.3 – 2.6 wt. %; see Tab. 3.5). Ce, La and Ba also have fairly high concentrations of 638, 462 and 278 ppm, respectively. HREE could not be analysed because of their low concentrations; however available analyses of LREE and MREE show that the slope of the normalised REE pattern is fairly steep (La_{pm}/Gd_{pm} = 100).

4.2.1.6: Nyerereite

Trace element analyses of nyerereite from the experiments are reported in Table 4.6, and shown in Figure 4.6. There is a fairly wide range in the trace element data of nyerereite at different P-T conditions. Light REE, MREE, Ba, Sr, Rb and Y show a (relatively) narrow concentration range between the nyerereite crystals from different experiments, with less than one order of magnitude between highest and lowest values; whereas, the remaining elements show a more significant range. Barium and Sr have very high concentrations, in the range of 2696-25784 ppm (*i.e.*, 0.30 to 2.88 wt. % BaO) and 10643-26189 ppm (*i.e.*, 1.27 to 3.10 wt. % SrO), respectively. These values are in agreement with the values determined on nyerereite crystals from OL5-experiments by electron microprobe, *i.e.* BaO in the range of 0.28 to 0.45 wt. %, and SrO in the range of 1.59 to 1.94 wt. % (see Tab. 3.6), although the highest Ba concentrations determined by LAM-ICP-MS are significantly higher than any value determined by electron microprobe. Concentrations of La and Lu are in the range of 137-1138 and 0.04-0.58 ppm, respectively. The slope of the normalised REE patterns is fairly steep (La_{pm}/Lu_{pm} = 204-536). At 100 MPa, trace element concentrations decrease in nyerereite with decreasing temperature from 600 to 550 °C; whereas, at

20 MPa trace element concentrations increase with decreasing temperature from 600 to 550 °C.

4.2.1.7: Gregoryite

Trace elements analyses of gregoryite from the experiments are reported in Table 4.7, and normalised concentrations plotted in Figure 4.7. Barium (1021-3742 ppm) and Sr (4354-5994 ppm) have very high concentrations, equivalent to 0.11-0.42 wt. % BaO and 0.51-0.65 wt. % SrO. These values are in agreement with the values obtained by electron microprobe on gregoryite crystals from OL5-experiments, *i.e.*, 0.22 wt. % for BaO and 0.79-0.88 wt. % for SrO (see Tab. 3.6). Concentrations of La and Gd are in the range of 56-221 and 1.00-1.51 ppm, respectively. The slope of the normalised REE patterns is fairly steep (La_{pm}/Lu_{pm} = 65-446). The quite wide range in the trace element data of gregoryite from different experiments suggests a temperature dependence. At 20 MPa, the concentration of many trace elements increase with decreasing temperature.

4.2.1.8: Titanite

One quenched titanite crystal was analysed in experiment CP107 (100 MPa, 600 °C). Trace element concentrations are reported in Table 4.8, and illustrated in Figure 4.8. High field strength elements have the highest concentrations, especially Zr (12549 ppm) and Nb (12369 ppm); Ta and Hf have concentrations of 530 ppm and 120 ppm, respectively. The REE -pattern is not very steep (La_{pm}/Yb_{pm} ~ 10).

4.2.2: Phase compositions in silicate-bearing natrocarbonatite OL5 and in silicate-free natrocarbonatites

In this section the trace element composition of crystal phases and of groundmass in silicate-bearing natrocarbonatite lava OL5 and in silicate-free natrocarbonatites CML5, CML9 and BD4169 are presented. Porphyritic, silicate-free natrocarbonatites CML5 and CML9 were erupted in 1963; the samples were donated by Dr. Tony Peterson and are described in Peterson (1990). Porphyritic, silicate-free natrocarbonatite BD4169 was

erupted in November 1988; the sample was donated by Dr. Barry Dawson and is described in Dawson et al. (1990).

In silicate-bearing natrocarbonatite OL5, isolated phenocrysts and phenocrysts from the spheroids have similar trace element compositions and are therefore presented together, with the exception of wollastonite. The trace element composition of microphenocrysts is presented separately. Despite the larger size of the crystals in natural lavas compared to experimental charges, the standard deviations can be fairly high for analyses of crystals (there can be one order of magnitude between highest and lowest values for these crystals analysed in OL5). However, RSD are not plotted in order to avoid confusing the plots.

4.2.2.1: Nepheline

Trace element concentrations of nepheline in silicate-bearing natrocarbonatite OL5 are reported in Table 4.9 and plotted in Figure 4.9. Microphenocrysts in lava OL5 have concentrations for most elements which are consistently one order of magnitude higher than in phenocrysts. Only Rb has a similar concentration in microphenocrysts and in phenocrysts (89.8 and 79.1 ppm, respectively). Nepheline phenocrysts and microphenocrysts have a shallow REE-pattern with La_{pm}/Yb_{pm} ~ 5-10. They both show a positive Eu-anomaly. A positive Eu-anomaly has also been noted by Eby (1975) in urtite at Oka.

4.2.2.2: Clinopyroxene

Trace element concentrations of clinopyroxene from silicate-bearing natrocarbonatite OL5 are reported in Table 4.9 and plotted in Figure 4.10. Phenocrysts and microphenocrysts have very similar REE-patterns with $10 < La_{pm} < 20$, Dy_{pm} ~ 1.35 and Lu_{pm} ~ 5 (concave up).

Microphenocrysts in OL5 have similar trace element concentrations as phenocrysts for Sr (567 vs. 628 ppm), Y (5.4 vs. 5.0 ppm), V (196 vs. 239 ppm), Zr (344 vs. 458 ppm) and Hf (8.2 vs. 10.1 ppm), but they have significantly higher

concentrations for Ba (17.5 vs. 2.4 ppm), Rb (5.4 vs. 0.4 ppm), U (0.24 vs. 0.12 ppm), Th (0.55 vs. 0.02 ppm), Nb (3.2 vs. 0.7 ppm) and Ta (0.12 vs. 0.05 ppm).

4.2.2.3: Melanite garnet

Trace element concentrations of melanite garnet from silicate-bearing natrocarbonatite OL5 are reported in Table 4.9 and plotted in Figure 4.11. An inclusion of melanite garnet in a clinopyroxene phenocryst of a spheroid is considered part of the phenocryst assemblage.

Phenocrysts and microphenocrysts of melanite garnet in lava OL5 have similar trace element concentrations, except for Ba (0.8 vs. 4.7 ppm) and Sr (156 vs. 87 ppm). Microphenocryst inclusions in phenocrysts are considered part of the phenocryst assemblage and have a similar composition. REE patterns are convex up, with normalised concentrations of Sm (~ 250-300) higher than those of La (~ 50-70) and Lu (~ 80). Thorium, U and HFSE have the highest normalised concentrations (> 100). Niobium has concentrations in the range of 325 - 484 ppm and Zr has concentrations in the range of 4101 - 4159 ppm.

4.2.2.4: Wollastonite

Trace element concentrations of wollastonite from silicate-bearing natrocarbonatite OL5 are reported in Table 4.9 and plotted in Figure 4.12. The three types of wollastonite (*i.e.*, isolated phenocrysts, phenocrysts in spheroids and microphenocrysts in spheroids) have been plotted separately. The average composition has been calculated by averaging 4 analyses for isolated phenocrysts, 5 analyses for phenocrysts in spheroids and 3 analyses for microphenocrysts in spheroids. Trace element concentrations of the three types of wollastonite in OL5 are similar for REE (La in the range of 24-27 ppm; Lu in the range of 0.91-0.97 ppm), Ba (7.9-11 ppm), Sr (895-955 ppm), Rb (2.2-4.7 ppm) and Y (63-72 ppm). But for V, U, Th and HFSE, the values for the different types of crystals vary. The compositional range (in ppm) exhibited by these elements is as follows: V: 6.9-33; U: 0.04-0.51; Th:

0.09-0.14; Nb: 0.33-8.6; Ta: 0.02-0.25; Zr: 4.9-45; and Hf: 0.25-0.89. Isolated phenocrysts have the highest concentrations for most of these elements, whereas phenocrysts in the spheroids have the lowest concentrations.

4.2.2.5: Nyerereite

Trace element concentrations in nyerereite from silicate-bearing natrocarbonatite OL5 are reported in Table 4.9 and plotted in Figure 4.13. LREE and LFSE have high concentrations of 227 ppm for La, 5769 ppm for Ba (= 0.64 wt. % BaO), 15601 ppm for Sr (= 1.84 wt. % SrO) and 115 ppm for Rb. The BaO and SrO contents determined by LAM-ICP-MS are similar to those determined by electron microprobe, *i.e.* 0.55 wt. % BaO and 2.22 wt. % SrO (see Tab. 3.6). The REE-pattern is steep and smooth with La_{pm}/Lu_{pm} ~ 1000. For comparison, trace element concentrations of nyerereite from silicate-free natrocarbonatites CML5, CML9 and BD4169 are also reported in Table 4.9 and plotted in Figure 4.13. Trace element concentrations of nyerereite from carbonatite OL102, which is a porphyritic silicate-free natrocarbonatite erupted in June 1988, are also plotted in Figure 4.13 (data from Keller and Spettel, 1995). Nyerereite crystals in silicate-free natrocarbonatites have very similar trace element compositions as these in OL5, except for lava OL102 which contains higher REE.

4.2.2.6: Gregoryite

Trace element concentrations of gregoryite in silicate-bearing natrocarbonatite OL5 are reported in Table 4.9 and plotted in Figure 4.14. Light REE and LFSE have high concentrations, *e.g.* 70.7 ppm for La, 3269 ppm for Ba (= 0.36 wt. % BaO), 6638 ppm for Sr (= 0.78 wt. % SrO) and 61.5 ppm for Rb. The BaO and SrO contents determined by LAM-ICP-MS are very similar to those determined by electron microprobe, *i.e.* 0.39 wt. % BaO and 0.88 wt. % SrO (see Tab. 3.6). The REE-pattern is steep and smooth with La_{pm}/Lu_{pm} ~ 1000. For comparison, trace element concentrations of gregoryite from silicate-free natrocarbonatites CML5, CML9 and BD4169 and OL102 (Keller and Spettel, 1995) are also reported in Table 4.9 and

plotted in Figure 4.14. Gregoryite crystals in silicate-free natrocarbonatites have very similar trace element compositions as those in OL5, except for lava OL102 which contains higher REE, U and Th.

4.2.2.7: Apatite

Trace element concentrations of apatite in silicate-bearing natrocarbonatite OL5 are given in Table 4.9 and are represented in Figure 4.15. Apatite has high concentrations of La (1789 ppm) and the REE-pattern is steep (La_{pm}/Lu_{pm} ~ 224). Apatite is characterised by high concentrations of U and Th with values of 7.5 and 71.2 ppm, respectively.

4.2.2.8: Groundmass

Trace element concentrations of the groundmass, and the groundmass of the silicate spheroids, in silicate-bearing natrocarbonatite OL5 are given in Table 4.9 and are represented in Figure 4.16. In OL5 groundmass, LREE and LFSE have high concentrations of 783 ppm for La, 9566 ppm for Ba (= 1.13 wt. % BaO), 10708 ppm for Sr (= 1.20 wt. % SrO) and 185 ppm for Rb. The concentrations of BaO and SrO determined for the groundmass by LAM-ICP-MS are in very good agreement with those determined by electron microprobe, *i.e.* 1.03 wt. % for BaO and 1.01 wt. % for SrO (see Tab. 3.12). The REE-pattern is steep and smooth, with La_{pm}/Lu_{pm} ~ 500. The groundmass in the spheroids has similar concentrations relative to OL5 groundmass of some LFSE, LREE and Lu; approximately 2 times higher concentrations of remaining REE, Th and Nb; and about an order of magnitude higher concentrations of Ta, Zr and Hf.

For comparison, trace element concentrations of groundmass in silicate-free natrocarbonatites CML5, CML9 and BD4169 are also reported in Table 4.9 and plotted in Figure 4.16. The groundmass in silicate-free natrocarbonatites from the 1963 eruption (*i.e.*, CML5 and CML9) have concentrations of MREE, HREE, Th, Nb and Zr that are significantly lower than those in OL5 (the difference varies from a

factor of 3 to two orders of magnitude for Zr). The REE-pattern for groundmass of these silicate-free natrocarbonatites is steeper than that for silicate-bearing natrocarbonatites. Trace elements concentrations in silicate-free natrocarbonatite BD4169 (November 1988) are intermediate between those in OL5 and in CML5 (and CML9), or similar to those in CML5 and CML9.

4.2.3: Trace element composition of carbonate liquid from the experiments

Determining the composition of the carbonate liquid in the experimental run products is not a simple process. The inherent heterogeneity of the quenched carbonate liquid necessitates using an iterative process to determine its trace element composition, along the lines followed for the determination of the major element compositions in the last chapter. Variation diagrams have been examined for each element of each experiment. In this chapter, five examples have been chosen to illustrate how the selection of analyses was made: CP88 (100 MPa, 900 °C; see Fig. 4.17), CP118 (100 MPa, 625 °C; see Fig. 4.18), CP57 (20 MPa, 700 °C; see Fig. 4.19), CP129 (20 MPa, 625 °C; see Fig. 4.20) and CP108 (20 MPa, 600 °C; see Fig. 4.21). Only one representative element is presented for elements which have similar behaviour. These are: Rb for alkalis; Ba for alkaline earths; Ce for LREE, Gd for MREE, Yb for HREE, U for U-Th pair, Nb for Nb-Ta pair and Zr for Zr-Hf pair. These figures illustrate the variability amongst the carbonate liquid analyses within a single experiment, which is due in large part to quenching effects (see Chapter 2). As was the case for the major elements, because there can be a discrepancy between measured and calculated, residual carbonate liquid compositions, both are plotted.

4.2.3.1: Calculation of the composition of the carbonate liquid

In order to calculate the trace element composition of carbonate liquid from the experiments, the same approach was used as for the major elements. Variation diagrams with TiO_2 on the x-axis (when possible), and trace elements on the y-axis were used to optimise the selection of individual analyses used to calculate the

average carbonate liquid composition. Individual analyses are compared to the calculated, theoretical composition of the carbonate liquid for each experiment. This calculated composition is represented by the composition of the starting composition (OL5) minus crystals (see proportions in Chapter 3, Table 3.9). The composition of the residual liquid so calculated is approximate, mainly because the phase proportions and trace element compositions for individual phases are not thoroughly constrained. When the concentration of TiO_2 is too low, SiO_2 or Sr is used. TiO_2 and SiO_2 have been analysed by electron microprobe, but are also analysed by LAM-ICP-MS together with the trace elements.

Experiment CP88 (100 MPa, 900 °C) contains only 1 % nepheline. Since nepheline does not concentrate trace elements, and because it is present in very low abundance (1 volume %), the carbonate liquid in this experiment is expected to have a very similar trace element composition to the starting material, *i.e.*, silicate-bearing natrocarbonatite OL5. Individual analyses of carbonate liquid in experiment CP88 are presented in Figure 4.17. Four analyses have been rejected for having significantly higher TiO_2 content than that measured by electron microprobe (= 0.09 wt. %; see Table 3.10) or by XRF (= 0.1 wt. %; Simonetti et al., 1997). Six analyses have been selected to calculate the average analysis of carbonate liquid in experiment CP88. The calculated TiO_2 content of 0.13 wt. % is reasonably close to the TiO_2 content reported by other methods. Figure 4.17 illustrates that most trace element concentrations so calculated are fairly similar to those reported by Simonetti et al. (1997). Note that there is a systematic bias between the data from this study and the data given in Simonetti et al. (1997). To avoid any confusion this might introduce, the calculated residual liquid compositions utilise the trace element data from experiment CP88 as a proxy for OL5 whole rock data (Tab. 4.10), rather than the data from Simonetti et al. (1997) presented in Table 2.2. The trace elements concentrations of lava OL5 are calculated by multiplying the concentrations measured on the carbonate liquid of experiment CP88 by 0.99, in order to take into account the presence of 1 % nepheline in the experimental charge (see Tab. 4.10). Advantages of using the trace element

composition of OL5 so calculated are that there are no uncertainties due to dissolution problems and all trace element concentrations are determined by the same technique.

Individual analyses of carbonate liquid in experiment CP118 (100 MPa, 625 °C) are presented in Figure 4.18. Five analyses out of ten were rejected for having too high of a concentration of TiO_2 compared to that in the calculated, residual liquid (RL). The average composition of the five remaining analyses is usually close to that in the calculated, residual liquid, except for Zr which shows significantly lower concentrations in the measured compared to the calculated value.

Individual analyses of carbonate liquid in experiment CP57 (20 MPa, 700 °C) are presented on a variation diagram, in which the concentration of different trace elements are plotted against SiO_2 (Fig. 4.19). Only three analyses have been performed, and many data were rejected for the calculation of the average composition.

Individual analyses of carbonate liquid in experiment CP129 (20 MPa, 625 °C) are presented on a variation diagram in which the concentration of different trace elements are plotted against Sr (Fig. 4.20). Seven analyses out of ten were rejected for having too high or too low of a Sr value compared to that of the calculated, residual liquid (RL). The average composition of the three remaining analyses is usually close to that of the calculated, residual liquid, except for Nb and Zr which show significantly lower concentrations in the measured compared to the calculated value.

Individual analyses of carbonate liquid in experiment CP108 (20 MPa, 600 °C) are presented on a variation diagram in which the concentration of different trace elements are plotted against Sr (Fig. 4.21). Eight analyses out of eleven were rejected for having too high or too low of a Sr value compared to that of the calculated, residual liquid (RL). The average composition of the three remaining analyses is usually close to that of the calculated, residual liquid, except for Nb and Zr which show significantly lower concentrations in the measured compared to the calculated value.

In summary, these variation diagrams illustrate that it is usually possible to obtain representative analytical data for carbonate liquid from the experiments. However, Figures 4.20 and 4.21 also illustrate that for 20 MPa-experiments CP129 and CP108 (respectively 625 and 600 °C), the concentration of HFSE is much lower in all measured composition compared to the calculated composition. These discrepancies are due to some phase(s) not being analysed in the carbonate liquid. Depending on whether the "missing phases" are stable or quenched phases, the measured concentrations of these elements in the liquid might be appropriate, or not (see Chapter 3).

4.2.3.2: Composition of the carbonate liquid - Results

The concentrations of trace elements determined for carbonate liquids from experiments at different pressure and temperature are given in Table 4.10 and plotted in Figure 4.22 and Figure 4.23, for experiments at 100 and 20 MPa, respectively. The calculated composition of the residual liquid (starting composition OL5 minus crystals) is also plotted for comparison (the data are given in Appendix A4). As was the case for major elements, the standard deviation presented reflects mainly the heterogeneity of the carbonate liquid (hence its high value), as well as the analytical precision ("analytical σ" is significantly lower). When only one analysis is taken into account, the analytical standard deviation is plotted, which is assumed to be 5 % for all elements.

Figure 4.22 and Figure 4.23 illustrate that most of the measured compositions for the carbonate liquid from the experiments are similar to the calculated compositions (within 1 σ, which can be fairly high). However, there are some exceptions, mainly U, Th and HFSE whose concentrations can be significantly lower than the calculated concentrations.

Are compositional changes of carbonate liquid at 100 MPa explained by changes of phase assemblages with temperature (Fig. 4.22)? At 100 MPa, from 900 down to 700 °C, nepheline is the only precipitating phase. It contains lower concentrations of

trace elements than the carbonate liquid, and therefore, the concentration of all trace elements increases in the calculated, residual carbonate liquid. However, because the maximum amount of nepheline which crystallises is 2 volume %, the compositional variation is not important. At 625 °C, nepheline is joined by clinopyroxene (1 volume % each). The concentration of Ba, Sr, Rb, La and Ce is lower in combined clinopyroxene + nepheline than in carbonate liquid, and therefore the trace element concentrations increase in the carbonate liquid with precipitation of these phases. The concentration of Y, V, MREE, HREE is higher in combined clinopyroxene + nepheline than in carbonate liquid, and therefore decreases in the carbonate liquid with precipitation of these phases. The concentration of U, Th, Nb and Ta in the carbonate liquid at 625 °C should not significantly decrease compared to the case at 750 °C. Zr and Hf have significantly higher concentrations in clinopyroxene compared to the carbonate liquid, therefore their concentrations in the carbonate liquid should decrease with decreasing temperature. Figure 4.22 (g, h and i) shows that the measured concentrations of U, Nb and Zr are much lower than what is calculated for the carbonate liquid. At temperatures lower than 625 °C, the phase assemblage includes nyerereite plus apatite plus nepheline and clinopyroxene. The variation of trace element concentrations with decreasing temperature is very irregular, both for measured and calculated compositions, and the measured concentrations are usually lower than the calculated concentrations.

Are compositional changes of carbonate liquid at 20 MPa explained by changes of phase assemblages with temperature (Fig. 4.23)? At 20 MPa, more crystal phases are present than in 100 MPa-experiments. Compositional trends exhibited by carbonate liquid as a function of temperature are more irregular than at 100 MPa. From 900 down to 800 °C, the concentration of most trace elements varies significantly, *e.g.* REE, Th, HFSE, whose concentrations decrease with the presence of perovskite at 850 °C. At 800 °C HFSE have very low concentrations compared to those of calculated, residual liquid. At 700 °C, the concentration of MREE, HREE and HFSE is lower than at 800 °C. This can be attributed to the presence of melanite

garnet in which these elements are concentrated compared to the carbonate liquid. At temperatures lower than 625 °C, and the concentration of most trace elements decreases in the carbonate liquid because the weighted sum of the crystallising phases (clinopyroxene, nyerereite, apatite and gregoryite) contains more trace elements than the carbonate liquid.

Figures 4.22 and 4.23 show that at both pressures, the curves of calculated liquid compositions are highly variable at low temperature. This is due to a significant variation in the proportion of carbonate crystals between different experiments. This makes the composition of the carbonate liquid very difficult to calculate at low temperature because there are less constraints on the calculated composition than at higher temperature. At 20 MPa, 550 °C, both measured and calculated concentrations are unreliable. The calculated concentrations of the carbonate liquid are negative for most trace element. This is attributed to concentrations that are too high for nyerereite as measured in experiment CP112.

At 100 MPa and T ≤ 625 °C, measured concentrations of U, Nb and Zr are significantly lower than calculated values (see Fig. 4.22 g, h and i, respectively), and at 20 MPa and T ≤ 800 °C, measured concentrations of Nb and Zr are significantly lower than calculated values (see Fig. 4.23 h and i, respectively). These low values can be attributed to the precipitation of phases in which these elements (U, Th, HFSE) are highly concentrated, but which may be under-represented in the analyses for the following reasons: 1) because they are scarce, quenched phases (*e.g.* perovskite, titanite) which are under-represented in the analyses; 2) because they are quenched overgrowths on pre-existing crystals (*e.g.*, clinopyroxene at low temperature); 3) because they are concentrated in the fluid phase (material in vesicles that has not been analysed); and/or 4) because there is a stable phase (*e.g.* perovskite, titanite, Ti-magnetite) that was not observed in the experimental run products. Similar processes can explain the low concentrations of MREE at 700 and 625 °C and of HREE at 700 °C compared to the calculated concentrations. At 20 MPa, measured concentrations of

Y and MREE are significantly higher than calculated values at 900 and 850 °C, and measured concentrations of HREE are significantly higher than calculated values at 850 °C. These high concentrations could be explained by the fact that the carbonate liquid is heterogeneous, and that the analyses over-represent MREE and HREE (apatite over-represented; see high P_2O_5 in Fig. 3.16j).

It is not straightforward to determine whether the missing phase(s) is (are) stable or quenched phases, and therefore whether measured or calculated composition are better representative of the composition of the carbonate liquid. For the previously presented cases 1, 2 and 3, the calculated composition is expected to better represent the composition of the carbonate liquid, whereas in case 4 it is the measured composition which is a better representative. Before investigating whether the missing phases are stable or quenched, the nature of these phases must be determined. Calculations were made in an attempt to reconcile major and trace element data. These calculations showed that: 1) subtracting perovskite, titanite or melanite garnet from bulk composition OL5 in large enough amounts to fix trace element data is not possible because it leads to negative TiO_2 in the calculated composition of the residual liquid; 2) subtracting Ti-magnetite (which was suggested as a missing phase in Chapter 3) cannot explain all the discrepancies between trace element of measured and calculated compositions of carbonate liquid. Ti-magnetite may contain large amounts of some trace elements (REE, HFSE, U, Th) but does not contain as much TiO_2 as perovskite, titanite or melanite garnet (*e.g.*, Nielsen et al., 1994; Schock, 1979). Therefore, this phase was thought to be a good candidate to explain the discrepancies between the trace elements of both liquids. However, at 20 MPa and high temperature (900-800 °C), despite the fact that 0.4-0.5 % Ti-magnetite is present in the capsules, and that the calculation of the residual liquid was made assuming trace element concentrations of 0 ppm in spinel, the measured concentrations of U, Th and HFSE are similar to the calculated concentrations (see Fig. 4.23). If the presence of 0.5 % spinel led to extreme depletion of trace elements in the residual liquid, then the measured concentrations would be significantly lower than the calculated

concentrations: this is not the case at high temperature (see Fig. 4.23). This suggests that if Ti-magnetite was the missing phase that produced the low HFSE concentrations at lower temperature, it would require either much higher amounts of precipitation than 0.5 % (which is not possible otherwise the calculated iron concentration in the residual liquid would become negative), or it would require an extreme dependence of $D_{Magnetite/LC}$ with temperature which does not seem reasonable; 3) (an) unknown phase(s), rich in some trace elements but poor in TiO_2 and FeO, precipitated and was under-represented in the analyses. Although it is known from mass balance calculations that such a phase is needed to explain the trace element data, its nature is not known, *i.e.*, its composition, and whether it is quenched or stable phase. However, the comparison between trace element partitioning data (presented later in section 4.3.3) with previous experimental studies (see Appendix A4), and the comparison between trace element data of the carbonate liquid from the experiments with data from natural lavas (see later in Chapter 5) are better explained if the calculated, not the measured compositions, are chosen to represent the carbonate liquid from the experiments. Therefore, it is proposed that the missing phase(s) is (are) quenched phase(s), not stable phase(s), and that the composition of the calculated, residual liquid is preferred to the measured composition when there is a discrepancy between the two.

In conclusion, trace element compositions measured on carbonate liquid in OL5-experiments are usually in agreement with the compositions calculated by mass balance calculation. Quenched crystal phases (or fluid phases) are thought to account for most of the compositional differences.

4.3 - Discussion

4.3.1: Comparison of solid phase compositions in experiments and in lava OL5

Trace element compositions of different phases in silicate-bearing natrocarbonatite OL5 are compared to the corresponding phases in the experiments. Isolated phenocrysts

and phenocrysts from the spheroids in silicate-bearing natrocarbonatite OL5 have similar trace element compositions and are therefore presented together, with the exception of wollastonite. This is based on the observation that the silicate phenocryst phases have previously been shown to form at similar P-T conditions whether they are isolated or in aggregates (see Chapter 3).

The trace element compositions of microphenocrysts in the natural rocks are plotted separately since there are a number of different parameters involved in their formation. Especially, kinetic effects may be dramatic on trace element concentrations of microphenocrysts, compared to concentrations at equilibrium, and superimpose on (and even hide) the compositional trends due to crystallisation of the microphenocrysts at lower P-T compared to phenocrysts. In Chapter 2 it was claimed that two factors can affect trace element compositions (and to a lesser extent, major compositions) of crystals and liquid during the quench: 1) adsorption/desorption of elements on crystals, that is dependent on the charge/radius ratio of the element (see Shimizu, 1981); and 2) diffusion in the melt (see Dowty, 1980).

4.3.1.1: Nepheline

Normalised concentration of trace elements from nepheline phenocrysts and microphenocrysts in silicate-bearing natrocarbonatite OL5 are plotted in Figure 4.24. For comparison, the range of concentrations for nepheline crystals from the experiments are also plotted. Trace element concentrations of nepheline in OL5-experiments are within the range exhibited by nepheline phenocrysts and microphenocrysts from silicate-bearing natrocarbonatite OL5. Nepheline phenocrysts from silicate-bearing natrocarbonatite OL5 have trace element patterns parallel to those of nepheline from the experiments, although at lower concentrations for most elements. Nepheline microphenocrysts from silicate-bearing natrocarbonatite OL5 also have trace element patterns parallel to those of nepheline from the experiments, but many elements (Sr, Y, V, Th, Zr, La, Ce, Eu, Dy) have slightly higher concentrations.

The data from the experiments are too scattered to give information on the P-T conditions of formation of phenocrysts in natural OL5. The higher trace element concentrations in nepheline from both experiments and microphenocrysts in OL5 compared to phenocrysts in OL5 could be a consequence of the quenching. The fact that the trace element patterns are parallel to each other suggests that trace elements are not selectively enriched as a function of z/r^2 (Coulomb interaction). This suggests that the enrichment is not due to adsorption/desorption processes (see Shimizu, 1981). Most trace elements are in low concentrations in nepheline and are expelled into the surrounding carbonate liquid when nepheline crystallises. Because of their increasing concentrations in the surrounding liquid, trace elements may be incorporated in nepheline during further crystallisation, despite their incompatibility (Dowty, 1980). This enrichment process explains the trace element patterns exhibited by the nepheline crystals of lava OL5 better, *i.e.* the fact that the trace element patterns of different nepheline crystals are parallel to each other.

4.3.1.2: Clinopyroxene

Normalised concentrations of trace elements from clinopyroxene phenocrysts and microphenocrysts in silicate-bearing natrocarbonatite OL5 are plotted in Figure 4.25. For comparison, trace element concentrations for clinopyroxene from the experiments are also plotted.

Phenocrysts and microphenocrysts have identical REE-patterns with one another and with those produced in the experiments. Among the other trace elements that have been analysed, Y, V. Zr and Hf have similar trace element concentrations in both the phenocrysts of lava OL5 and those produced in the experiments. The concentration of the remaining trace elements (Ba, Sr, Rb, U, Th, Nb and Ta) is consistently lower in phenocrysts of OL5 compared to clinopyroxene in the experiments, by approximately one order of magnitude. Phenocrysts and microphenocrysts in lava OL5 have similar trace element concentrations for Sr, Y, V, Zr and Hf, but microphenocrysts have higher concentrations than phenocrysts for Ba,

Rb, U, Th, Nb and Ta (by one order of magnitude for Ba, Rb and Th), and are more similar to the clinopyroxene from the experiments for Ba, Rb, U, Th, Nb and Ta.

Following the work of Van Orman et al. (1998), the explanation for these observations may be slow diffusion of U and Th, and high adsorption/low desorption of HFSE in fast grown clinopyroxene crystals compared to phenocrysts. Enrichment of Zr and Hf in fast grown clinopyroxene crystals compared to phenocrysts is not observed, because these elements are compatible in clinopyroxene and become depleted in the surrounding carbonate liquid during fast growth. High concentrations of Ba and Rb in fast grown clinopyroxene crystals compared to phenocrysts can be explained by the fact that they are incompatible in clinopyroxene, and therefore become enriched in the surrounding carbonate liquid during fast growth of the crystal.

4.3.1.3: Melanite garnet

Normalised concentrations of trace elements from melanite garnet phenocrysts and microphenocrysts in silicate-bearing natrocarbonatite OL5 are plotted in Figure 4.26. Normalised values are similar for phenocrysts and microphenocrysts in OL5 except for slightly lower Ba and slightly higher Sr in microphenocrysts than in phenocrysts. Trace element concentrations of melanite garnet from the experiments are also plotted, and compare very well to those in OL5. All melanite garnet crystals have a REE pattern that is convex up, with MREE showing the highest normalised values. The fact that all crystals of melanite garnet that have been analysed are within a narrow compositional range indicates that their composition is controlled by site chemistry rather than pressure, temperature, composition and are not affected by high growth rate.

4.3.1.4: Wollastonite

Normalised concentration of trace elements from wollastonite phenocrysts (isolated and in spheroids) and microphenocrysts in silicate-bearing natrocarbonatite OL5 are plotted in Figure 4.27. For comparison, trace element concentrations of wollastonite

in experiment CP51 (20 MPa, 750 °C) are also plotted. The REE-patterns are fairly flat, with La_{pm}/Lu_{pm} ~ 3. Trace element concentrations are similar for isolated phenocrysts, phenocrysts and microphenocrysts in spheroids of OL5 for REE, Ba, Sr, Rb, Y. For all of these elements except Ba, they have identical concentration to those in wollastonite produced in the experiments. However, the concentrations V, U, Th and HFSE are very different for the different crystal types. The observation that trace element concentrations in isolated phenocrysts are different from those in spheroids, and higher than in the microphenocrysts is unexpected.

4.3.1.5: Nyerereite

Normalised concentration of trace elements from nyerereite phenocrysts in silicate-bearing natrocarbonatite OL5 are plotted in Figure 4.28, along with data from the experiments. It was shown earlier that at 100 MPa, trace element concentrations decrease with temperature decreasing from 600 to 550 °C, whereas at 20 MPa, trace element concentrations increase with temperature decreasing from 600 to 550 °C. Mass balance calculations (section 4.2.3.2) showed that the trace element concentrations that have been measured on nyerereite from experiment CP112 (20 MPa, 550 °C) (see Fig. 4.6) are probably too high. Therefore trace element concentrations of nyerereite from experiment CP112 (20 MPa, 550 °C) are not presented in Figure 4.28.

Nyerereite from natural lava OL5 has trace element concentrations within the range exhibited by nyerereite crystals from the experiments for Ba, Sr, Rb, V, U, Th and HFSE; it also has LREE, MREE and Y concentrations similar to the less enriched nyerereite crystals from experiments.

4.3.1.6: Gregoryite

Normalised concentrations of trace elements from gregoryite phenocrysts in silicate-bearing natrocarbonatite OL5 are plotted in Figure 4.29, with data from the

experiments. Same as in nyerereite at 20 MPa, the concentration of trace elements increases in gregoryite with decreasing temperature, except for Sr, U, Nb, and HREE.

Gregoryite in natural lava OL5 has very similar trace element concentrations to those found in experiments at 600 and 575 °C, except for slightly lower MREE and HREE values. However, the fact that trace element patterns are parallel to subparallel in gregoryite from natural lava OL5 and from the experiments attests to the validity of the data.

4.3.1.7: Summary

Despite the wide compositional range exhibited by crystals from the experiments, it is possible to be confident in the data because of the general consistency observed between the experimental and natural systems. The difference in trace element compositions among crystals in different samples can usually be explained by differences of pressure and temperature (*e.g.*, nyerereite and gregoryite for which P-T effects were noted), or differences in growth rate (*e.g.*, nepheline and clinopyroxene). Note that for clinopyroxene, it is only U, Th, Nb and Ta whose concentrations are affected by a high growth rate.

4.3.2: Trace element partition coefficients - background and terminology

Trace elements, because of their low concentrations, generally do not form individual phases but instead are accommodated as minor components in mineral solid solutions, in melts or in other fluid phases (Wood and Fraser, 1976). If equilibrium is achieved, trace elements are incorporated in crystals: 1) mostly as interstitial defects if their concentration is very low; or 2) as solid solutions substituting for atoms of the host phase if their concentration is high enough. In the first case, partition coefficients of trace elements between the two phases are dependent on trace element concentration (Henry's law is not obeyed); in the second case, trace element partition coefficients are independent of their concentration (Henry's law is obeyed). If there is disequilibrium due to rapid growth, then trace elements are incorporated in occluded zones. The terminology

of Beattie et al. (1993) is used for this study, where D is defined as the ratio of the concentration of a component in two phases.

If the concentrations of some trace elements in the crystals and/or in the liquid are affected by quenching, trace element partition coefficients between crystals and liquid are effective D's (D_{eff}), and are a function of crystal structure and protosite configurations, rate of crystal growth, face normal diffusivities of components, growth mechanism and diffusive lag within the growth medium (Bouch et al., 1997). In the case of achievement of equilibrium, trace element partition coefficients between crystals and liquid are equilibrium D's (D_{equ}), and are a function of pressure, temperature, composition and structure of crystal and liquid phases, and oxygen fugacity. All these parameters are interrelated and it is difficult to separate their individual effects and to determine their relative importance. However, experimental studies can allow the investigation of the effects of different parameters.

Pressure, temperature and starting composition are the experimental conditions, *i.e.* they are the intensive parameters which are set at the beginning of the run. Other variables are not as straightforward because they can vary without being controlled at the start of the run, for example, the composition and structure of crystal and liquid phases, and oxygen fugacity. Previous studies have showed that these variables may have a significant effect on trace element partitioning. Vicenzi et al. (1994) showed the importance of oxygen fugacity in controlling trace element partition coefficients. A number of experimental studies designed to characterise mineral-liquid element partitioning [*e.g.* Watson (1977), Ryerson and Hess (1978), Hart and Davis (1978), Leeman and Lindstrom (1978), Takahashi (1978), Mysen and Virgo (1980), and Kohn and Schofield (1994)] have shown that one of the most important factors influencing the distribution of trace and minor elements between phenocrysts and silicate liquid is the composition and, hence, the structure of the melt phase. The control of silicate melt structure and composition on trace element partitioning has been confirmed by Vicenzi et al. (1994) who studied the trace element partitioning between immiscible silicate liquids, and by Lesher (1986) who reported the effect of silicate liquid composition trace element

partitioning from Soret studies. In the present Chapter, D's are measured between crystals and carbonate liquid, and are not expected to be affected by the composition and structure of the liquid because carbonate liquid can be considered a highly depolymerized liquid.

Trace element partitioning between crystals and liquid is often well described by the structure of crystals (see Onuma et al., 1968; Jensen, 1973). Trace elements substitute for major elements according to their charge and radius, and the ability of a crystalline or melt phase to incorporate a given trace element into its structure is controlled by the size of the available crystallographic sites and the ability of the phases to charge balance the incorporated cation (Gaetani and Grove, 1995). These controls are well illustrated by Onuma diagrams, on which partition coefficients are plotted as a function of the cation radii of different elements. Onuma et al. (1968) first plotted mineral/lava partition coefficients against ionic radii and drew curves through all elements of the same valency, producing a family of curves, one univalent, one divalent, one trivalent, etc..., where peaks correspond to crystallographic sites. Blundy and Wood (1994) suggested that the maxima of the curves corresponds to the size of the crystal lattice site(s) on which substitution occurs.

The interplay between the different parameters affecting trace element partitioning can be complex. Pressure and temperature can affect the size of the site where trace elements substitute. For solids, changes of volume can be expressed as a function of temperature and pressure by the coefficients α (thermal expansion) and β (compressibility): $V = V_{1bar,\ 298K} + \alpha\ (T-298) + \beta\ (P-1)$. Pressure can also affect the coordination number of the cations, and therefore the volume of the site. Oxygen fugacity can affect the charge of altervalent elements (*e.g.*, Fe, Eu, Ce), hence their radius and partitioning behaviour.

4.3.3: Trace element partition coefficients between crystals and carbonate liquid from experiments and from silicate-bearing natrocarbonatite OL5

In the present study, the calculation of the partition coefficients between crystals and carbonate liquid from the experiments is not always straightforward because the trace

element compositions of carbonate liquid (and in some cases of crystals) may have been modified during quenching. It has previously been shown that in some experiments, trace element concentrations of the carbonate liquid are lower than expected from calculation and this can be attributed to the presence of quench phases. Crystals growing at a fast rate also can have trace element concentrations which are not those at equilibrium. Therefore when calculating D's between crystals and liquid, it must be determined if they are equilibrium D's (D_{equ}) or effective D's (D_{eff}).

For the experiments, when the concentration of a trace element in the carbonate liquid is similar to the calculated value, partition coefficients between crystal and liquid are calculated using the measured composition of the carbonate liquid. On the other hand, when the measured concentration of an element in the carbonate liquid is significantly lower than its calculated value, as a consequence of the precipitation of a quench phase, the appropriate partition coefficient between crystal and liquid is calculated using the calculated composition of the carbonate liquid (= OL5 minus crystals). In this calculation, the trace element composition of crystals which equilibrated with the carbonate liquid before the quench is presumed to be preserved. On the other hand, some crystals form during the quench (quench overgrowths of clinopyroxene, and maybe nepheline, carbonate crystals) and their trace element composition may therefore be affected by the quench.

For silicate-bearing natrocarbonatite OL5, the trace element partition coefficients have to be calculated between the crystals and what is thought to represent the liquid from which they crystallised. This liquid is not represented by the groundmass, but by groundmass plus carbonate crystals plus siliceous mesostasis (calculated equivalent liquid or CEL, see Chapter 3).

Trace element compositions of liquid that were used for the calculation of crystal/liquid trace element partitioning are presented in Table 4.11, for the carbonate liquid in the experiments at different P-T conditions, and for CEL in natural lava OL5. Trace element partition coefficients calculated between crystals and carbonate liquid for the experiments, and between crystals and CEL for natural lava OL5 are presented in

Table 4.12. Trace element partition coefficients are discussed mainly as a function of the crystal structure, but also of pressure and temperature when possible.

4.3.3.1: Nepheline

Trace element partition coefficients between nepheline and carbonate liquid from OL5-experiments and from silicate-bearing natrocarbonatite OL5 are plotted in Figure 4.30. All elements analysed are incompatible in nepheline ($D < 1$) compared to carbonate liquid (except for Zr, Er and Yb which are slightly compatible in microphenocrysts of natural lava OL5). Rubidium is the trace element which shows the most consistent value of partition coefficients between nepheline and carbonate liquid from the experiments, between 0.41 and 0.95. It is also the element for which D's are similar in the experiments and in OL5 (both for phenocrysts and microphenocryts). Barium, U, Th, Nb, La and Ce are the elements which show the lowest D values between phenocrysts and CEL in OL5, *i.e.* < 0.005. Heavy REE ($D \sim 1$) are more compatible than LREE ($D \sim 0.001 - 0.01$). The irregularity of D-patterns is caused by trace element concentrations being close to detection limits in nepheline.

Partition coefficients between nepheline crystals and carbonate liquid in the experiments have similar values to partition coefficients between phenocrysts and CEL in silicate-bearing natrocarbonatite OL5. Partition coefficients between microphenocrysts and CEL in silicate-bearing natrocarbonatite OL5 have higher values. In section 4.3.1.1, it was suggested that nepheline microphenocrysts in silicate-bearing natrocarbonatite OL5 and possibly nepheline crystals in experiments owe their high trace element concentrations compared to those in phenocrysts in lava OL5 to a high cooling rate. In fact, the similarity between D's determined on phenocryst/liquid (in lava OL5) and crystal/carbonate liquid (in the experiments) shows that they are equilibrium D's, whereas D's determined on microphenocryst/liquid (in lava OL5) are effective D's.

Deer et al. (1992) described the structure of nepheline group minerals as being a three-dimensional framework of SiO_4 and AlO_4 tetrahedra with Na,K(Ca) as

interstitial charge-balancing cations. They showed that the common excess of Si over Al in nepheline crystals is balanced by vacancies in (Na,K,Ca) sites. Rubidium has a large radius and has the same charge as K. Therefore it substitutes for K in the large cavities, hence its relatively high partition coefficient compared to other elements. Uranium, Th, Ba and Sr also have a large radius, but they have a higher charge than K and do not substitute for K as Rb does, hence their lower D-values. Other cations are too small and have too high a charge to substitute for K.

4.3.3.2: Clinopyroxene

Trace element partition coefficients between clinopyroxene and carbonate liquid from OL5-experiments and from silicate-bearing natrocarbonatite OL5 are plotted in Figure 4.31. Most elements analysed are incompatible ($D < 1$), except for Zr, Hf and HREE which are slightly to significantly compatible ($1 < D < 10$). Elements showing the lowest partition coefficients between clinopyroxene and carbonate liquid are Ba ($D < 0.01$) and La (~ 0.01). Heavy REE are more compatible than LREE in clinopyroxene, and the REE-D-pattern is fairly smooth. Thorium partitions into clinopyroxene more than U does, in agreement with the findings of LaTourrette and Burnett (1992) and of Hauri et al. (1994) on clinopyroxene / basaltic melt pairs. The fact that curves cross cut each other shows that no systematic effect of pressure or temperature can be determined. The higher D-values of Ba, Rb, Th, Nb and Ta between clinopyroxene and carbonate liquid for experiments and microphenocrysts in lava OL5 compared to phenocrysts in lava OL5 are due to their higher concentration acquired during quenching. For these elements, partition coefficients are equilibrium D's for phenocrysts-CEL pair in OL5, but they are effective D's for microphenocrysts-CEL (in OL5) and crystal-carbonate liquid (in experiments) pairs, respectively.

Deer et al. (1992) showed that the pyroxene formula may, in structural terms, be expressed as $M2M1T_2O_6$. T refers to tetrahedrally coordinated cations (Si^{4+} and Al^{3+}). For the clinopyroxene crystals of this study, $M1$ is occupied by Ti^{4+}, Fe^{3+}, Fe^{2+}, Mg^{2+} and Mn^{2+}. All Al^{3+} is in the tetrahedral site (see Tab. 3.3) and none is available for the

*M*1 site. Cations in *M*1 are in octahedral coordination. Ca^{2+} and Na^{+} occupy the *M*2 site, and are in 8-fold coordination.

The Onuma diagram for clinopyroxene produced in experiment CP107 (100 MPa, 600 °C) and for a clinopyroxene in silicate-bearing natrocarbonatite OL5 are presented in Figure 4.32 and Figure 4.33, respectively. $D_{clinopyroxene/carbonate\ liquid}$ are plotted against cation radius for trace elements. Partition coefficients have also been plotted for some of the main cations occupying the sites *M*2 and *M*1. Partition coefficients for Ca, Na and Ti are plotted, whereas the partition coefficients for Fe^{3+}, Mg^{2+}, Fe^{2+} and Mn^{2+} are not plotted on both Onuma diagrams. The reason for not plotting partition coefficients for Fe^{3+} and Fe^{2+} is that their ratio is not constrained for the carbonate liquid (and may be poorly constrained in the clinopyroxene); the reason for not plotting partition coefficients for Mg^{2+} and Mn^{2+} is that their concentration is low in the carbonate liquid (for both elements) and in clinopyroxene (for Mn), and therefore partition coefficients are not accurately determined. For the major elements whose partition coefficients have not been plotted on the Onuma diagrams (*i.e.* Fe^{3+}, Mg^{2+}, Fe^{2+} and Mn^{2+}), cation radii have been indicated on the plots.

Ionic radii are from Shannon (1976). A series of curves can be drawn on these diagrams which show that: 1) large mono-, di- and tri-valent cations substitute for Ca and Na on the *M*2 site; 2) smaller tetravalent Zr and Hf and pentavalent Nb and Ta substitute in the *M*1 site, for Fe^{3+}, Fe^{2+}, Ti^{4+}, Mg^{2+} and Mn^{2+}; 3) Th and U, although tetravalent, fall way off the Ti-Zr-Hf regression, which indicates that their ionic radii are too large for incorporation in the *M*1 site. They are incorporated in the *M*2 site (see Lundstrom et al., 1998). For the *M*2 site, peaks for low valency cations are broader than for high valency cations. The peak of the 4+ curve falls at ~ 0.66 Å, which is close to the radius of Fe^{3+}, Ti^{4+} and Mg^{2+}, whereas the peak for the *M*2 site falls at ~ 0.98 Å, which is much lower than the radius of Ca^{2+} (1.12 Å). A possible explanation for this is found in Purton et al. (1997), who showed that for pure clinopyroxene, the calculated solution energies always show a minimum at a radius

corresponding to that of the host cation, whereas for impure clinopyroxene (with <1 Ca per formula unit) the optimum cation radius varies with composition.

Note that for the Onuma diagram for clinopyroxene in silicate-bearing natrocarbonatite OL5 (Fig. 4.33), two different curves appear for the *M*2 site. The first one, defined by LREE and some MREE, by monovalent and divalent cations, and by U and Th, has a peak at 1.05 Å. The second one, defined by HREE has a peak at 0.98 Å. Deer et al. (1992) previously showed that the *M*2 site coordination is irregular and varies according to the atom present, six-fold for Mg and eight-fold for Ca and Na. Although the stoichiometry of the clinopyroxene in lava OL5 indicates only Ca and Na present in the *M*2 site (see Tab. 3.3), it is possible that its coordination number is variable (maybe some minor Mg present), which would explain the presence of two different peaks.

Substitutions can be straightforward, as exemplified by the substitution of divalent cations Sr^{2+} and Ba^{2+} for Ca^{2+}. But substitutions of tri- and tetra-valent cations for Ca^{2+}, of tetravalent cations for Fe^{3+}, or of pentavalent cations for Ti^{4+} have to be charge balanced. Charge balancing of tri-, tetra- and penta-valent cations in the *M*1 and *M*2 sites is usually done by coupled substitution involving the replacement of Al^{3+} for Si^{4+} in the tetrahedral site. The substitution of U^{4+} and Th^{4+} into the *M*2 site requires two tetrahedral Al ions in close proximity to satisfy local charge balance constraints (Lundstrom et al., 1998).

4.3.3.3: Melanite garnet

Trace element partition coefficients for melanite garnet from OL5-experiments and from silicate-bearing natrocarbonatite OL5 are plotted in Figure 4.34. D-values between garnet and carbonate liquid determined on experiments and on lava OL5 are extremely similar. This confirms that all of the D's which are calculated are equilibrium, not effective D's. No effect of temperature on partition coefficients is measurable. Most elements are compatible in garnet compared to carbonate liquid (except for Ba, Sr, U, La and Ce). REE-D-patterns are convex up and flatten towards

HREE (D ~ 50 - 100 for HREE). Heavy REE and HFSE have the highest D-values, with D's as high as 100 in some cases. Melanite garnet retains Th preferentially over U, opposite to garnet in high-Al basalt (Hauri et al., 1994).

The structure of garnet has been described in Deer et al. (1992). The unit cell of garnet contains eight $X_3Y_2Z_3O_{12}$ units. It consists of alternating ZO_4 tetrahedra (Z = Si, Al, Ti) and YO_6 octahedra (in melanite, Y = Fe^{3+}, Ti, with Fe^{3+} > Ti) which share corners to form a three-dimensional network. Within this network there are cavities that can be described as distorted cubes of eight oxygens which are coordinated with the divalent, X cations (Ca^{2+}, Mg^{2+}, Fe^{2+} or Mn^{2+}).

Onuma diagrams for data from experiment CP51 (20 MPa, 750 °C) and for silicate-bearing natrocarbonatite OL5 are presented in Figure 4.35 and Figure 4.36, respectively. $D_{garnet/carbonate\ liquid}$ are plotted against cation radius for the trace elements. D's are also plotted for Ca and Ti which occupy the sites X and Y, respectively. D's have not been plotted for some major or minor elements, *i.e.* Na^{+}, Mg^{2+}, Mn^{2+} (because of their low concentration in garnet and/or in carbonate liquid), and Fe^{3+} and Fe^{2+} (because of the poor knowledge of their ratio, both in garnet and in carbonate liquid). A series of curves can be drawn on these diagrams which show that: 1) large mono-, di- and tri-valent cations substitute for Ca on the X site; 2) smaller tetravalent Zr and Hf and pentavalent Nb and Ta substitute in the Y site; 3) Th and U, although being tetravalent, fall way off the Ti-Zr-Hf regression, which indicates that their ionic radii are too large for incorporation into the Y site, and that they are incorporated in the X site. The peak of the 4+ curve falls at ~ 0.66 Å, which is close to the radius of Fe^{3+}, Ti^{4+} and Mg^{2+}, and the peak for the X site falls at ~ 1.03 Å, which is slightly smaller than the radius of Ca^{2+} (1.12 Å).

As in clinopyroxene, substitutions in garnet can be straightforward (*e.g.* substitution of Sr^{2+} and Ba^{2+} for Ca^{2+}), or coupled (charge balancing of tri-, tetra- and penta-valent cations in the Y and X sites coupled with substitution of Al^{3+} for Si^{4+} in the Z site).

4.3.3.4: Wollastonite

Trace element partition coefficients for wollastonite from OL5-experiments and from silicate-bearing natrocarbonatite OL5 are plotted in Figure 4.37. Strontium, Y and REE have very similar D-values in experimental and natural samples. Yttrium, MREE and HREE are compatible ($1 < D < 7$) in wollastonite, whereas the remaining elements are incompatible ($0.001 < D < 1$). The REE-D-pattern flattens towards HREE (D ~ 9-17 for HREE). Experimental data most closely agree with those of the phenocrysts in the spheroids of lava OL5.

The structure of wollastonite, as described by Klein and Hurlbut (1993), consists of infinite chains, parallel to the *c*-axis, with a unit repeat of three twisted tetrahedra, and with Ca in irregular octahedral coordination linking the SiO_3 chains. In wollastonite ($CaSiO_3$), REE^{3+} (and Y^{3+}) substitute for Ca^{2+}. However, because of the size difference within the rare earth elements, HREE substitute more strongly than LREE for Ca. Sr^{2+} and Ba^{2+}, although having the appropriate charge to replace Ca^{2+}, have a much larger radius, and therefore substitute less easily than MREE and HREE, hence their lower D-values.

Wollastonite from experiment CP129 (20 MPa, 625) contains 0.13 wt % Na_2O and wollastonite from silicate-bearing natrocarbonatite OL5 contains 0.30 wt. % Na_2O (see Tab. 3.7). This indicates that substitution of Na^{+} for Ca^{2+} could charge balance substitutions of tri-, tetra- and penta-valent cations for Ca^{2+}.

4.3.3.5: Melilite

Trace element partition coefficients for melilite from OL5-experiment CP51 (20 MPa, 750 °C) are plotted in Figure 4.38. The gaps in the extended pattern indicate that the elements which are not reported (Rb, V, HREE, U and Ta) are below detection limit, *i.e.*, probably incompatible in melilite. Melilite shows fairly flat REE-D-patterns, with $D_{melilite/Carbonate\ liquid} \sim 1$. All analysed elements are incompatible in melilite compared to carbonate liquid, except for Sr, Nd, Sm and Gd which are slightly compatible ($D_{melilite/Carbonate\ liquid} < 1.4$). Nb, Ba, Zr and Hf have D-values < 0.1.

The structure of melilite group minerals has been described by Deer et al. (1992). It is based on a tetragonal lattice which in äkermanite has Mg atoms located at the corner face centers of the unit cell. The Mg atoms are in tetrahedra of oxygens, all four of which are shared by adjacent SiO_4 tetrahedra, which themselves are linked in pairs to form Si_2O_7 groups. The linkage of Mg and Si tetrahedra forms five-membered rings and these are linked to form corrugated sheets parallel to (001), the sheets being held together by Ca-O bonds. Al^{3+} substitutes for Si^{4+} in the T2 site, and Al^{3+} substitutes for Mg^{2+} in the T1 site.

In melilite crystals of the present study, Si alone occupies the T2 site, and all Al^{3+} is in the T1 site, together with Mg^{2+}, Fe^{2+} and Mn^{2+}; Ca^{2+}, Na^{+}, K^{+} and Sr^{2+} occupy the larger site (see Tab. 3.5). Large mono-, di-, and tri-valent (and probably U, Th) cations substitute for Ca and K in the large site (M1 site according to nomenclature in Beckett et al., 1990), whereas small tetra- and penta-valent cations substitute into the smaller T1 site. Divalent cations also substitute into the T1 site (Beckett et al., 1990).

4.3.3.6: Nyerereite

Trace element partition coefficients between nyerereite and carbonate liquid from OL5-experiments and from silicate-bearing natrocarbonatite OL5 are plotted in Figure 4.39. For Ba, Sr, Rb, Y and REE, most of the D-values are around 1 (between 0.5 and 5), and REE-D-patterns are fairly flat. For the remaining elements (V, U, Th and HFSE), there is a lot of scatter in the D-values (more than 2 orders of magnitude between highest and lowest values), which reflects the scatter in the composition of the nyerereite crystals (see Fig. 4.6). V, Yb, Lu, U, Th and HFSE can have very low D-values ($D < 0.1$ or even < 0.001).

At 100 MPa, D's for REE do not vary systematically with decreasing temperature, but for V, U, Th and HFSE, they decrease with decreasing temperature. At 20 MPa, D's increase with temperature decreasing from 600 to 575 °C for most of the trace elements.

McKie and Frankis (1977) reported an idealised composition $(Na_{0.82}K_{0.18})_2Ca(CO_3)_2$ for nyerereite, with significant minor substitution of $(SO_4)^{2-}$, $(PO_4)^{3-}$ and F^- for $(CO_3)^{2-}$; Keller and Krafft (1990) report the composition as $(Na_{0.82}K_{0.19})_2(Ca,Sr,Ba)_{0.975}(CO_3)_2$, with complex substitution of $(CO_3)^{2-}$ by $(SO_4)^{2-}$, $(PO_4)^{3-}$, F^- and Cl^-; and Peterson (1990) reported average composition $Nc_{41}Kc_9Cc_{50}$ (neglecting F, Cl, P_2O_5, and SO_3) where Nc = Na_2CO_3, Kc = K_2CO_3, and Cc = $(Ca,Sr)CO_3$.

The coordination number of Ca^{2+} and other cations in nyerereite is inferred below by analogy with the calcite/aragonite structure. Klein and Hurlbut (1993) showed that when the (CO_3) group of calcite is combined with large divalent cations (ionic radii greater than 1.0 Å: Ba, Sr), the radius ratios generally do not permit stable 6-fold coordination and orthorhombic structures result (aragonite structure type). Because nyerereite has significant amounts of K, Rb and Sr (large cations), and because it has been shown by McKie and Frankis (1977) to be an orthorhombic mineral (like aragonite and unlike calcite which is rhombohedric), cations are expected to be in 9-fold coordination.

An Onuma diagram for silicate-bearing natrocarbonatite OL5 is presented in Figure 4.40. $D_{nyerereite/carbonate\ liquid}$ are plotted against cation radius for the trace elements, and also for Ca, Na and K which are the main cations in nyerereite. Monovalent cation Rb^+ substitutes for K^+, divalent cations Sr, Ba substitute for Ca^{2+}, and so do REE^{3+}. The peak of the curves falls at ~ 1.20 Å, which is slightly larger than the radius of Ca^{2+} (1.18 Å). Cherniak (1998) showed that in calcite, REE are incorporated on the Ca^{2+} site, likely charge compensated by Na^+ (if present in the system, *i.e.* in the present case), or through the substitution $2\ REE^{3+} + \square \rightarrow 3\ Ca^{2+}$, where $\square$ represents a vacancy. In nyerereite, where large amounts of Na are present, the first substitution scheme is expected to be prevalent. Because of the large amount of K also present, it is likely that substitution of REE for the Ca^{2+} site is also charge balanced by K^+ for Ca^{2+}.

4.3.3.7: Gregoryite

Trace element partition coefficients between gregoryite and carbonate liquid from OL5-experiments and from silicate-bearing natrocarbonatite OL5 are plotted in Figure 4.41. Most D-values are between 0.1 and 1, and REE-D-patterns are fairly flat. The exceptions for this are V, U, Th and HFSE which can have much lower D-values ($D < 0.1$ or even < 0.01). At 20 MPa, D's tend to increase with decreasing temperature for many trace elements (Ba, Sr, Rb, Y, V, Th, Zr, LREE).

The composition of gregoryite reported by Keller and Krafft (1990) is: $Na_{1.74}K_{0.1}(Ca,Sr,Ba)_{0.16}(CO_3)_2$, with complex substitution of $(CO_3)^{2-}$ by $(SO_4)^{2-}$, $(PO_4)^{3-}$, F^- and Cl^-. Peterson (1990) reported average composition $Nc_{77}Kc_5Cc_{18}$ (neglecting F, Cl, P_2O_5, and SO_3) where Nc = Na_2CO_3, Kc = K_2CO_3, and Cc = $(Ca,Sr)CO_3$. Gregoryite is expected to have a similar structure to nyerereite.

An Onuma diagram for silicate-bearing natrocarbonatite OL5 is presented in Figure 4.42. $D_{gregoryite/carbonate\ liquid}$ are plotted against cation radius for the trace elements, and also for Ca, Na and K which are the main cations in gregoryite. Monovalent cation Rb^+ substitutes for K^+, divalent cations Mg, Mn, Sr, Ba substitute for Ca^{2+}, and so do REE. It is difficult to define a peak for the curves because these are fairly flat. However, like nyerereite, the peak of the curves appears to fall at ~ 1.20 Å, which is slightly higher than the radius of Ca^{2+} (1.18 Å).

4.3.3.8: Apatite

Trace element partition coefficients between apatite and CEL from silicate-bearing natrocarbonatite OL5 are plotted in Figure 4.43. Y, Th, and REE are compatible in apatite compared to carbonate liquid, especially Y, Th, MREE and HREE which have D-values in the range of 10-34. All trace elements have D values > 0.01. The REE D-pattern is convex up, with $D_{Apatite/Carbonate\ liquid}$ = ~ 6 for La, ~ 34 for Dy and ~ 14 for Lu.

The structure of apatite has been described by Deer et al. (1992). Each F atom is surrounded by three atoms at one level and, in addition, Ca-O columns are linked with

PO_4 groups forming a hexagonal network. The different sizes of the monovalent anions lead to a variation in the cell parameters.

An Onuma diagram for apatite in silicate-bearing natrocarbonatite OL5 is presented in Figure 4.44. $D_{apatite/carbonate\ liquid}$ are plotted against cation radius for the trace elements. D's for Ca and Na are also plotted. Kay et al. (1964) found that the Ca ion occupied two distinctly different sites in apatite, a larger one surrounded by nine O anions and a smaller site surrounded by one F^- (or Cl^-, or OH^-) and six O anions. A coordination number of 7 was used for the determination of cation radii. The peak of the curve for mono-, di- and trivalent cations falls at ~ 0.98 Å, which is close to the radius of Ca^{2+} (1.06 Å). The trivalent REE apparently replace Ca^{2+}, and the substitution is coupled to offset the excess position charge introduced by the REE^{3+} ions. The substitution of $REE^{3+} + Si^{4+} \rightarrow Ca^{2+} + P^{5+}$ has been shown to be the most common substitution (see Watson and Green, 1981; Cesbron, 1989), and the significant amounts of SiO_2 in apatite of OL5 (0.87 wt. %, see Tab. 3.7) confirms that this substitution is important for the apatite studied here. Cesbron (1989) also showed that other substitutions such as $2Ca^{2+} \rightarrow REE^{3+} + Na^+$ play a minor role. This substitution is supported by the detection of significant amounts of Na_2O in apatite (0.35 wt. %, see Tab. 3.7).

4.3.3.9: Titanite

Trace element partition coefficients between titanite and carbonate liquid from experiment CP107 (100 MPa, 600 °C) are plotted in Figure 4.45. Because the titanite is a quench crystal, its trace element composition was probably affected by rapid cooling and partition coefficients are effective D's. Among the trace elements which have been analysed, only Ba, Rb and La are incompatible in titanite compared to carbonate liquid (D-values respectively of 0.04, 0.22 and 0.57). The REE-D-pattern is smooth, with increase of D-values with increasing atomic number. The D value for La is 0.57 and Yb it is 26.7. High field strength elements have the highest D-values (> 112, and as high as 991 for Ta).

The structure of titanite has been described by Deer et al. (1992). They showed that the dominant structural units in titanite are chains or corner-sharing TiO_6 octahedra running parallel to the x axis, and that these chains are cross-linked by the SiO_4 tetrahedra sharing the remaining oxygen. This produces a $[TiOSiO_4]^{2-}$ framework with large cavities enclosing Ca atoms in irregular seven-coordination polyhedra.

An Onuma diagram for experiment CP107 (100 MPa, 600 °C) is presented in Figure 4.46. $D_{titanite/carbonate\ liquid}$ are plotted against cation radius for the trace elements. D's are also plotted for Ca and Ti which are the main site occupants. The peak of the 3+ curve is at a radius lower than that of Ca or for the curve for 4+ cations. Because the titanite is quenched, HREE might be adsorbed more efficiently than LREE because of their higher charge/size (z/r) ratio, hence the shift of the curve towards lower values of cation radius.

Bouch et al. (1997) showed that many elements are able to substitute into the titanite complex structure through the operation of a range of possible coupled substitution schemes. The three substitution schemes are:

1 - (Deer et al., 1992) $^{VI}(Al,Fe)^{3+} + F^- = {}^{VI}Ti^{4+} + O^{2-}$.

2 - (Russel et al., 1994): $^{VI}(P,Nb)^{5+} + {}^{VI}(Al,Fe)^{3+} = 2\ {}^{VI}Ti^{4+}$,

and 3 - (Green and Pearson, 1986): $^{VII}(REE,Y)^{3+} + {}^{VI}(Al,Fe)^{3+} = {}^{VII}Ca^{2+} + {}^{VI}Ti^{4+}$. The major element composition of the quench titanite found in experiment CP107 (analysed by LAM-ICP-MS for trace elements) has not been determined by electron microprobe. Therefore it is not possible to determine which substitution scheme is prevalent.

4.3.3.10: Summary

Most elements are incompatible in nepheline, melilite, and gregoryite compared to carbonate liquid. On the other hand, some elements are compatible in other crystal phases compared to carbonate liquid: Y, V, MREE, HREE and HFSE are compatible in melanite garnet; Zr, Hf and HREE are compatible in clinopyroxene; most REE (especially HREE) and Y are compatible in wollastonite; Y, REE (especially MREE)

and Th are compatible in apatite; most trace elements (not Ba, Rb or La) are compatible in titanite, especially HFSE. For nyerereite, it is more variable between different experiments. Note that perovskite in experiment CP45 (20 MPa, 850 °C) was analysed by electron microprobe (see Tab. 3.7 in Chapter 3). It had a La_2O_3 content of 4.7 wt. % (La = 39820 ppm) and Ce_2O_3 content of 8.2 wt. % (Ce = 70265 ppm) which produce partition coefficients between perovskite and carbonate liquid (in experiment CP45) of 65 and 91 respectively.

4.4 - Conclusions

Trace element compositions of crystal phases in the experimental run products and in the erupted natrocarbonatites at Oldoinyo Lengai are generally consistent with each other, and variations can usually be attributed to differences in pressure, temperature and crystal structure (and in some case, quenching). Generally, trace element compositions of carbonate liquid in the experimental run products are also consistent with the calculated values (= bulk composition OL5 minus crystals).

After the effect of the quench on the compositions of crystals and liquids is investigated, the aim is: 1) to keep the data that are not affected by the quench (*e.g.* core of the crystals, most elements in the carbonate liquid) and to correct for the data that have been affected by the quench, when possible (*e.g.* by using calculated, not measured composition of the liquid), and 2) to use these data to calculate partition coefficients on crystal/liquid pairs. Note that the concentrations of most elements in most phases are not affected significantly by the quench.

Partition coefficients determined for crystals and carbonate liquid pairs are in good agreement between natural and experimental samples. Table 4.13 summarises which specific phases preferentially incorporate different trace elements and reports the average D-values. In summary, REE are mostly present in perovskite, apatite, melanite garnet, titanite, nyerereite and gregoryite, HFSE in titanite, perovskite and garnet, Ba and Sr in nyerereite, and Rb in nepheline and nyerereite.

The effect of pressure and temperature on D's has been constrained for a few crystals (nyerereite, gregoryite), but partition coefficients were mostly investigated as a function of the structure of the crystals. Onuma diagrams show that at given P-T conditions, it is the crystal structure that controls the partition behaviour of the trace elements.

Table 4.1: Trace element LAM-ICP-MS analyses of nepheline in OL5-experimental run products (in ppm).

Experiment	P	T	# an.	Ba	Sr	Rb	Y	V	U	Th	Nb	Ta	Zr	Hf
CP88	100	900	1	33.5	<238	74.9	<0.59	<8.60	<0.48	<0.69	<0.77		<0.69	<3.40
CP106	100	850	5	19.9	<854	99.6	0.82	<18.1	0.78	<0.20	<0.44	<1.49	1.40	<1.62
CP79	100	800	5	11.4	<239	107	0.07	<0.78	0.04	0.04	0.26	<0.28	3.30	<0.43
CP96	100	750	1	<1.37	<569	68.5	<1.44	<3.62	<0.95		<0.44	<0.97	<1.97	<3.00
CP118	100	625	6	32.1	<1293	88.2	3.14	<14.0	<5.37	<1.28	<1.19	<0.19	<2.77	<3.16
CP107	100	600	9	38.3	<1057	105	0.40	<9.30	0.62	0.26	<0.86	0.30	<1.03	<1.64
CP90	20	900	1	26.7	<1121	70.3	<2.31	<9.79			<1.39		<2.07	<9.33
CP45	20	850	6	23.1	219	97.6	<0.33	2.19	0.48	<0.12	0.46	<0.29	<0.43	0.31
CP57	20	700	5	8.31	<1229	115	<0.86	<20.0	<2.83	<3.10	<2.71	<0.73	<1.48	<3.95
CP108	20	600	2	8.08	<852	68.3	<1.51	<22.7	0.78	0.30	<0.91		<2.25	<1.37
CP112	20	550	1	67.9	<1872		<1.10	<44.3	1.04	<0.33	14.0	0.27	24.7	<5.71

Experiment	P	T	# an.	La	Ce	Nd	Sm	Eu	Gd	Dy	Er	Yb	Lu
CP88	100	900	1	<0.45	0.60	<2.35	<1.31	0.07	<1.44	<0.84	<0.92	<1.43	<0.35
CP106	100	850	5	0.55	0.71	<2.31	<4.82	0.32	<0.40	0.45	<0.30	<0.42	<0.15
CP79	100	800	5	<0.12	0.36	<1.40	<1.68	<2.34	<0.17	<0.85	0.12	<9.20	<0.20
CP96	100	750	1	0.54	<0.79			<1.92	<3.92				
CP118	100	625	6	4.57	4.93	<13.3	<5.20	<2.14	<1.46	<3.49	<6.87		<0.60
CP107	100	600	9	1.36	2.27	1.29	<5.20	<0.62	<2.95	0.29	1.32	<1.71	<0.16
CP90	20	900	1	0.49	0.76		<10.2			0.29			
CP45	20	850	6	0.66	<2.45	<1.24	<0.78	0.09	<0.46	<0.31	<0.50	0.65	<0.53
CP57	20	700	5	<0.28			<5.14	<0.75	<6.85	<2.44	<2.06		<0.19
CP108	20	600	2					<1.95	<0.46	<3.11	<1.58		<0.09
CP112	20	550	1	7.23	9.10	10.4	1.18			<1.62	0.38	<8.89	

Note: #an.: number of analyses. Pressure (P) is in MPa; temperature (T) is in C. Detection limits are given in ppm.

Table 4.2: Trace element LAM-ICP-MS analyses of clinopyroxene in OL5-experimental run products (in ppm).

Sample	P	T	# an.	La	Ce	Nd	Sm	Eu	Gd	Dy	Er	Yb	Lu
CP107	100	600	10	7.94	19.8	9.76	1.89	0.43	1.66	0.70	1.00	1.29	0.56
CP127	100	550	1	5.28	23.9		b.d.	b.d.	b.d		b.d.	b.d.	b.d.
CP108	20	600	4	5.48	18.8				1.34	0.95	0.76		0.43

Sample	Ba	Sr	Rb	Y	V	U	Th	Nb	Ta	Zr	Hf
CP107	33.0	2416	4.58	2.91	319	1.16	0.72	14.6	1.13	388	7.93
CP127	49.2	b.d.	b.d.	3.40	411	b.d.	5.58	12.0	b.d.	233	8.49
CP108	3.35	b.d.	b.d.	5.28	217	0.74	3.73	33.1	0.66	340	5.30

Note: # an.: number of analyses; b.d.: below detection. Pressure (P) is in MPa; temperature (T) is in C.

Table 4.3: Trace element LAM-ICP-MS analyses of melanite garnet in OL5-experimental run products (in ppm).

Sample	P	T	# an.	La	Ce	Nd	Sm	Eu	Gd	Dy	Er	Yb	Lu
CP51	20	750	2	57.9	298	389	126	45.2	115	107	52.9	38.8	4.84
CP57	20	700	7	57.3	325	380	109	38.2	94.2	83.8	38.7	30.9	3.82
CP108	20	600	3	34.2	195	227	97.0	35.4	111	112	58.2	45.9	5.48

Sample	Ba	Sr	Rb	Y	V	U	Th	Nb	Ta	Zr	Hf
CP51	9.84	109	b.d.	482	628	8.75	24.1	488	31.2	3304	57.7
CP57	7.09	223	b.d.	406	941	9.23	44.9	953	16.9	3158	59.6
CP108		b.d.	b.d.	520	1343	6.82	9.06	390	16.1	3536	57.5

Note: # an.: number of analyses; b.d.: below detection. Pressure (P) is in MPa; temperature (T) is in C.

Table 4.4: Trace element LAM-ICP-MS analyses of wollastonite in OL5-experiment CP51 (20 MPa, 750 C) (in ppm).

Sample	# an.	La	Ce	Nd	Sm	Eu	Gd	Dy	Er	Yb	Lu
CP51	1	31.5	89.6	44.2	10.5	3.85	10.2	11.2			0.93

Sample	Ba	Sr	Rb	Y	V	U	Th	Nb	Ta	Zr	Hf
CP51	68.3	865	b.d.	62.7	2.62	b.d.	b.d.	1.03	0.03	3.77	b.d.

Note: # an.: number of analyses; b.d.: below detection.

Table 4.5: Trace element LAM-ICP-MS analyses of melilite in OL5-experiment CP51 (20 MPa, 750 C) (in ppm).

Sample	# an.	La	Ce	Nd	Sm	Eu	Gd	Dy	Er	Yb	Lu
CP51	1	462	638	147	9.38	1.98	3.90	b.d.	b.d.	b.d.	b.d.

Sample	Ba	Sr	Rb	Y	V	U	Th	Nb	Ta	Zr	Hf
CP51	278	15482	b.d.	4.14	b.d.	b.d.	7.01	0.81	b.d.	4.54	0.10

Note: # an.: number of analyses; b.d.: below detection.

Table 4.6: Trace element LAM-ICP-MS analyses of nyerereite in OL5-experimental run products (in ppm).

Sample	P	T	# an.	La	Ce	Nd	Sm	Eu	Gd	Dy	Er	Yb	Lu
CP107	100	600	11	626	887	167	140	3.74	5.65	4.21	1.47	1.31	0.20
CP128	100	575	2	206	366	82.9	5.80	1.09	1.98	1.59	0.71		0.04
CP127	100	550	3	234	373	85.8	7.37	2.11	3.93	1.31	0.56		
CP108	20	600	3	137	308	62.5	4.92	1.27	1.34	1.00	b.d.	b.d.	b.d.
CP126	20	575	4	308	471	92.6	8.90	1.89	4.19	0.99	0.54	0.72	0.13
CP112	20	550	2	1138	1457	276	16.3	6.55	8.47	5.46	1.52	2.05	0.58

Sample	Ba	Sr	Rb	Y	V	U	Th	Nb	Ta	Zr	Hf
CP107	11795	16486	287	20.7	206	22.7	26.1	62.9	0.12	21.2	0.88
CP128	2880	10643	57.7	7.31	3.11	0.71	0.46	5.10	b.d.	1.64	b.d.
CP127	3391	12738	80.6	6.92	1.05	0.03	0.21	0.16	b.d.	0.06	0.06
CP108	2696	10705	99.8	4.28	b.d.	b.d.	b.d.	1.63	b.d.		
CP126	4924	14679	205	8.40	73.1	1.35	1.30	15.7	0.18	7.45	0.29
CP112	25784	26189	434	24.5	277	27.8	34.3	107	0.33	34.9	b.d.

Note: # an.: number of analyses; b.d.: below detection; pressure (P) is in MPa; temperature (T) is in C.

Table 4.7: Trace element LAM-ICP-MS analyses of gregoryite in OL5-experimental run products (in ppm).

Sample	P	T	# an.	La	Ce	Nd	Sm	Eu	Gd	Dy	Er	Yb	Lu
CP108	20	600	5	55.8	74.7	15.3	1.20	0.31	1.08	b.d.	b.d.	b.d.	0.09
CP126	20	575	7	85.7	119	21.8	1.42	0.33	1.00	0.67	0.20	0.15	0.02
CP112	20	550	3	221	247	37.7	3.24	0.86	1.51	0.64	0.27	0.54	b.d.

Sample	Ba	Sr	Rb	Y	V	U	Th	Nb	Ta	Zr	Hf
CP108	1021	4354	23.8	1.20	13.0	0.27	0.27	0.59	b.d	b.d.	0.52
CP126	1599	5994	36.9	2.18	16.0	0.14	0.41	0.34	b.d.	0.32	b.d.
CP112	3742	5483	61.5	5.64	59.5	4.30	3.16	8.92	0.10	1.67	0.44

Note: # an : number of analyses; b.d.: below detection; pressure (P) is in MPa; temperature (T) is in C.

Table 4.8: Trace element LAM-ICP-MS analysis of quenched titanite in OL5-experiment CP107 (100 MPa, 600 C) (in ppm).

Sample	# an.	La	Ce	Nd	Sm	Eu	Gd	Dy	Er	Yb	Lu
CP107	1	256	729	380	58.1	13.0	37.6	26.2	<5.29	16.4	<0.35

Sample	Ba	Sr	Rb	Y	V	U	Th	Nb	Ta	Zr	Hf
CP107	346	<2871	26.8	90.9	240	26.4	30.8	12369	530	12549	120

Note: # an.: number of analyses.

Table 4.9a: Concentration of rare earth elements of different phases in silicate-bearing natrocarbonatite OL5 and in silicate-free natrocarbonatites CML5, CML9 and BD4169 (in ppm)

Sample	Environment	#an.	La	Ce	Nd	Sm	Eu	Gd	Dy	Er	Yb	Lu
OL5												
Nepheline	Ph.	14	0.42	0.95	0.32	0.21	0.13	0.09	0.12	0.05	0.04	0.03
Nepheline	mph. sph.	1	14.0	33.7	10.1	0.93	0.80	0.63	1.04	0.91	0.78	b.d.
Clinopyroxene	Ph.	16	8.06	20.8	12.4	2.28	0.59	1.25	0.89	0.80	1.55	0.36
Clinopyroxene	mph. sph.	8	10.5	25.6	11.3	2.15	0.54	1.67	0.93	0.82	1.41	0.33
Melanite garnet	Ph.	15	44.6	249	334	124	45.6	127	125	57.9	41.1	4.95
Melanite garnet	mph.	1	35.8	198	297	109	40.5	121	116	58.2	40.6	5.32
Wollastonite	iso. Ph.	4	33.4	77.7	46.2	10.6	3.80	9.42	9.71	5.36	5.63	0.91
Wollastonite	Ph. sph.	5	24.2	74.0	41.3	9.93	3.56	10.1	9.79	5.93	5.92	0.87
Wollastonite	mph. sph.	3	27.4	77.9	42.1	12.0	3.75	9.00	10.7	6.85	5.99	0.97
Apatite	Ph.	4	1789	3129	1225	162	48.5	103	51.1	15.5	7.23	0.83
Nyerereite	Ph.	5	227	253	51.4	3.41	0.73	1.25	0.34	0.09	0.04	0.02
Gregoryite	Ph.	4	70.7	67.4	11.4	0.76	0.13	0.35	0.12	0.05	0.06	0.01
Groundmass		10	783	920	211	19.2	4.83	9.19	4.56	1.70	1.07	0.15
Groundmass sph.		16	827	1104	288	30.6	7.88	15.8	8.29	3.62	2.44	0.33
BD4169												
Nyerereite	Ph.	3	253	294	50.1	3.40	0.80	1.23	0.44	b.d.	b.d.	b.d.
Gregoryite	Ph.	4	70.9	82.3	14.8	1.02	0.21	0.41	0.15	0.03	0.02	0.01
Groundmass		5	986	872	132	9.41	2.27	3.80	1.55	0.68	0.50	0.10
CML5												
Nyerereite	Ph.	5	281	388	59.9	3.74	0.66	0.81	0.26	0.20	b.d.	b.d.
Gregoryite	Ph	5	83.1	89.5	13.1	0.81	0.13	0.24	0.09	0.05	0.03	0.01
Groundmass		7	512	523	71.6	4.27	0.85	1.17	0.39	0.13	0.09	0.02
CML9												
Nyerereite	Ph.	6	257	382	52.8	2.64	0.59	0.96	0.20	0.07	0.05	0.01
Gregoryite	Ph.	5	93.6	113	13.0	0.82	0.16	0.27	0.09	b.d.	0.03	0.02
Groundmass		7	482	498	59.7	3.60	0.78	1.17	0.41	0.15	0.19	0.02

Note: # an.: number of analyses; b.d.: below detection; iso : isolated; Ph . phenocryst; mph.: microphenocryst; sph. spheroid.

Table 4.9b: Concentration of trace elements other than REE of different phases in silicate-bearing natrocarbonatite OL5 and in silicate-free natrocarbonatites CML5, CML9 and BD4169 (in ppm).

Sample	Environment	#an.	Ba	Sr	Rb	Y	V	U	Th	Nb	Ta	Zr	Hf
OL5													
Nepheline	Ph.	14	20.0	105	79.1	0.30	2.30	0.04	0.07	0.53	0.07	3.46	0.24
Nepheline	mph. sph.	1	71.8	481	89.8	7.88	45.9	b.d.	0.90	7.30	b.d.	71.9	b.d.
Clinopyroxene	Ph.	16	2.44	628	0.41	5.02	239	0.12	0.02	0.73	0.05	458	10.1
Clinopyroxene	mph. sph.	8	17.5	567	5.42	5.37	196	0.24	0.55	3.15	0.12	344	8.18
Melanite garnet	Ph.	15	4.73	86.9	0.89	534	848	8.75	13.8	484	31.1	4101	74.2
Melanite garnet	mph.	1	0.95	156	b.d.	517	693	6.14	12.9	325	25.4	4159	77.9
Wollastonite	iso. Ph.	4	9.11	895	2.75	63.1	27.5	0.51	0.14	8.55	0.25	45.2	0.89
Wollastonite	Ph. sph.	5	7.86	955	2.16	62.5	6.91	0.06	b.d.	0.33	0.02	4.86	0.25
Wollastonite	mph. sph.	3	10.9	920	4.73	71.6	33.4	0.04	0.09	2.56	0.02	29.9	0.49
Apatite	Ph.	4	190	7100	5.28	209	96.6	7.49	71.2	1.83	0.05	9.51	b.d.
Nyerereite	Ph.	5	5769	15601	115	3.02	9.26	0.53	0.62	4.54	0.03	2.18	0.14
Gregoryite	Ph.	4	3269	6638	61.5	0.85	56.6	0.10	0.20	0.52	0.11	0.79	0.07
Groundmass		10	9566	10708	185	30.3	194	20.3	23.2	153	0.72	71.9	0.89
Groundmass sph.		16	3666	8365	224	51.7	178	17.1	43.4	347	3.55	599	7.98
BD4169													
Nyerereite	Ph.	3	5297	17248	140	2.63	7.60	0.33	0.22	0.96	2.16	1.14	0.08
Gregoryite	Ph.	4	1830	5925	69.5	0.83	39.7	0.15	0.15	0.26	0.04	0.06	0.04
Groundmass		5	23081	15600	366	11.3	340	7.51	2.95	5.56	0.45	0.48	0.34
CML5													
Nyerereite	Ph.	5	6141	16770	120	1.43	8.93	1.19	0.22	2.53	0.59	b.d.	b.d.
Gregoryite	Ph.	5	2286	5443	62.9	0.45	51.9	0.58	0.06	0.71	0.12	0.05	b.d.
Groundmass		7	9481	11047	338	2.49	178	4.69	0.69	7.28	0.20	0.17	0.08
CML9													
Nyerereite	Ph.	6	5785	14706	170	1.01	8.60	0.36	0.13	1.29	0.08	0.30	0.12
Gregoryite	Ph.	5	2021	5557	70.1	0.51	38.8	0.29	0.05	1.78	0.23	0.31	0.04
Groundmass		7	13020	10964	213	3.04	229	4.55	0.61	7.22	0.70	0.65	0.10

Note: # an.: number of analyses; b.d.: below detection; iso.: isolated; Ph.: phenocryst, mph.: microphenocryst; sph. spherold.

Table 4 10a Concentration of rare earth elements in silicate-bearing natrocarbonatite lava OL5 and in carbonate liquid from OL5-experimental run products (in ppm)

Experiment	P	T	# an	La	Ce	Nd	Sm	Eu
OL5				468	564	114	10 0	2 56
CP88	100	900	6	473 ± 77 9	570 ± 92 4	115 ± 15 2	10 1 ± 1 18	2 58 ± 0 42
CP79	100	800	6	462 ± 84 8	526 ± 84 4	110 ± 16 4	9 71 ± 1 25	2 44 ± 0 34
CP96	100	750	8	446 ± 127	506 ± 117	109 ± 19 4	9 87 ± 1 61	2 42 ± 0 43
CP118	100	625	5	420 ± 84 8	515 ± 81 6	105 ± 18 9	9 47 ± 1 64	2 36 ± 0 45
CP107	100	600	2	450 ± 32 8	535 ± 33 2	107 ± 5 33	9 58 ± 0 55	2 31 ± 0 12
CP128	100	575	8	507 ± 89 9	598 ± 89 6	112 ± 11 0	9 95 ± 1 08	2 60 ± 0 39
CP127	100	550	13	357 ± 81 4	394 ± 88 7	72 6 ± 15 4	6 30 ± 1 74	1 56 ± 0 44
CP90	20	900	7	634 ± 64 4	692 ± 70 1	151 ± 16 1	13 4 ± 1 37	3 41 ± 0 40
CP45	20	850	3	611 ± 90 2	769 ± 130	150 ± 21 9	14 4 ± 2 46	3 65 ± 0 51
CP61	20	800	4	604 ± 83 5	746 ± 90 4	136 ± 19 1	11 4 ± 0 93	2 61 ± 0 25
CP57	20	700	3	459 ± 22 9	558 ± 27 9	127 ± 38 5	6 59 ± 1 24	1 34 ± 0 27
CP129	20	625	3	589 ± 69 3	613 ± 46 7	101 ± 6 76	6 03 ± 0 66	1 34 ± 0 09
CP108	20	600	3	514 ± 96 6	582 ± 96 4	104 ± 14 1	9 04 ± 1 48	2 21 ± 0 35
CP126	20	575	5	694 ± 173	730 ± 170	128 ± 26 6	12 0 ± 1 83	3 02 ± 0 18
CP112	20	550	6	407 ± 200	457 ± 185	80 7 ± 26 7	6 35 ± 1 35	1 92 ± 0 59

Experiment	P	T	# an	Gd	Dy	Er	Yb	Lu
OL5				4 63	2 34	0 91	0 790	0 110
CP88	100	900	6	4 68 ± 0 59	2 37 ± 0 36	0 92 ± 0 18	0 800 ± 0 24	0 110 ± 0 03
CP79	100	800	6	4 56 ± 0 73	2 45 ± 0 39	1 00 ± 0 17	0 827 ± 0 15	0 095 ± 0 02
CP96	100	750	8	4 54 ± 0 84	2 32 ± 0 52	1 00 ± 0 30	0 882 ± 0 24	0 093 ± 0 01
CP118	100	625	5	4 31 ± 0 93	1 95 ± 0 43	0 78 ± 0 25	0 606 ± 0 11	0 077 ± 0 01
CP107	100	600	2	4 42 ± 0 22	2 17 ± 0 11	0 81 ± 0 04	0 615 ± 0 03	0 086 ± 0 004
CP128	100	575	8	4 68 ± 0 68	2 72 ± 0 46	1 07 ± 0 22	0 882 ± 0 10	0 111 ± 0 01
CP127	100	550	13	3 28 ± 0 84	1 75 ± 0 48	0 66 ± 0 22	0 625 ± 0 21	0 083 ± 0 04
CP90	20	900	7	6 60 ± 0 73	3 40 ± 0 38	1 28 ± 0 17	1 05 ± 0 15	0 126 ± 0 03
CP45	20	850	3	7 34 ± 1 04	4 11 ± 0 62	1 63 ± 0 14	0 93 ± 0 05	0 152 ± 0 02
CP61	20	800	4	4 58 ± 0 31	2 10 ± 0 10	0 79 ± 0 04	0 69 ± 0 09	0 086 ± 0 004
CP57	20	700	3	2 21 ± 0 28	0 65 ± 0 09	0 19 ± 0 04	0 21 ± 0 01	0 024 ± 0 01
CP129	20	625	3	2 23 ± 0 11	0 61 ± 0 05	0 22 ± 0 03	0 22 ± 0 08	0 033 ± 0 01
CP108	20	600	3	3 89 ± 0 38	2 06 ± 0 12	0 84 ± 0 17	0 57 ± 0 17	0 102 ± 0 01
CP126	20	575	5	5 16 ± 1 95	2 31 ± 1 29	0 94 ± 0 60	0 82 ± 0 45	0 107 ± 0 06
CP112	20	550	6	2 94 ± 0 76	1 75 ± 0 72	0 57 ± 0 14	0 52 ± 0 29	0 084 ± 0 01

Note # an number of analyses, pressure (P) in MPa, temperature (T) in C
Concentrations are presented +/- 1 standard deviation (1 sigma) Values of 1 sigma in normal font represent experimental standard deviation, and values underlined represent analytical standard deviation (= 5 % of the concentration, i e calculated for a relative standard deviation of 5 %) The concentrations of trace elements in OL5 are calculated as 0 99 * the concentration of the elements in CP88, in order to correct for the 1 % nepheline present in the experiment CP88

Table 4 10b Concentration of trace elements other than REE in silicate-bearing natrocarbonatite lava OL5 and in carbonate liquid from OL5-experimental run products (in ppm)

Experiment	P	T	# an	Ba	Sr	Rb	Y	V
OL5				9213	10905	139	13 8	196
CP88	100	900	6	9306 ± 1602	11015 ± 735	140 ± 33 0	13 9 ± 2 94	198 ± 33 2
CP79	100	800	6	7731 ± 1415	9981 ± 816	112 ± 12 3	15 3 ± 2 72	189 ± 26 9
CP96	100	750	8	7645 ± 1696	10292 ± 885	140 ± 42 7	14 2 ± 4 66	211 ± 97 6
CP118	100	625	5	8451 ± 1184	11008 ± 550	198 ± 41 5	11 2 ± 2 49	227 ± 70 4
CP107	100	600	2	8589 ± 1073	10443 ± 522	124 ± 21 5	13 6 ± 0 68	134 ± 20 4
CP128	100	575	8	9435 ± 1045	9584 ± 1221	149 ± 40 4	14 3 ± 3 06	161 ± 37 1
CP127	100	550	13	6992 ± 2024	6847 ± 1047	123 ± 47 8	12 0 ± 2 85	137 ± 57 9
CP90	20	900	7	9384 ± 1173	11449 ± 572	145 ± 38 0	20 7 ± 2 30	176 ± 35 1
CP45	20	850	3	8837 ± 447	10277 ± 514	144 ± 26 2	25 9 ± 4 18	147 ± 23 8
CP61	20	800	4	10258 ± 654	11021 ± 551	162 ± 31 0	16 0 ± 1 40	215 ± 10 7
CP57	20	700	3	10162 ± 2381	11320 ± 1389	147 ± 53 6	6 42 ± 1 11	249 ± 12 5
CP129	20	625	3	12109 ± 675	11916 ± 596	145 ± 16 1	5 67 ± 0 28	267 ± 34 8
CP108	20	600	3	9601 ± 480	11780 ± 589	168 ± 18 3	17 0 ± 5 52	397 ± 49 8
CP126	20	575	5	9303 ± 5071	6005 ± 1463	112 ± 63 9	14 6 ± 7 05	130 ± 78
CP112	20	550	6	5358 ± 1606	6403 ± 1043	93 7 ± 27 6	12 6 ± 4 73	97 4 ± 40 2

Experiment	P	T	# an	U	Th	Nb	Ta	Zr	Hf
OL5				13 8	12 94	108	0 500	65 9	1.02
CP88	100	900	6	14 0 ± 3 01	13 10 ± 2 74	109 ± 23 6	0 500 ± 0 14	66 5 ± 23.20	1.03 ± 0 39
CP79	100	800	6	12 9 ± 1.75	12.95 ± 2.19	105 ± 12 2	0 541 ± 0 05	87 6 ± 19 23	1 40 ± 0.31
CP96	100	750	8	13 6 ± 4 44	12 42 ± 3 71	131 ± 30 9	0 564 ± 0 09	88 0 ± 4 52	1 22 ± 0 07
CP118	100	625	5	10 6 ± 1 42	11 74 ± 3 99	79 2 ± 15 6	0 038 ± 0 04	13 3 ± 9 04	0 28 ± 0 21
CP107	100	600	2	9 21 ± 0 46	10 12 ± 1 07	74 8 ± 3 89	0 162 ± 0 01	74 1 ± 53 60	1 00 ± 0 69
CP128	100	575	8	10 0 ± 2 37	12 56 ± 2 04	91 7 ± 26 8	0 155 ± 0 09	21 5 ± 8 77	0 36 ± 0 19
CP127	100	550	13	5 88 ± 2 30	11 61 ± 4 93	72 9 ± 18 1	0 065 ± 0 04	6 30 ± 8 44	0 61 ± 0 76
CP90	20	900	7	13 1 ± 1 55	14 0 ± 2 16	104 ± 12 6	0 49 ± 0 08	75 9 ± 11 38	1 17 ± 0 23
CP45	20	850	3	16 3 ± 2 71	9 51 ± 2 08	94 9 ± 10 9	0 23 ± 0 05	79 9 ± 19 69	0 91 ± 0 14
CP61	20	800	4	17 8 ± 1 04	15 1 ± 0.76	89 0 ± 15 7	0 19 ± 0 03	3 08 ± 0 74	0 14 ± 0 12
CP57	20	700	3	18 4 ± 0.92	12 0 ± 0.60	9 64 ± 2 37	0 03 ± 0 01	7 43 ± 0.37	0 12 ± 0 04
CP129	20	625	3	17 3 ± 1 58	7 34 ± 0.37	7 23 ± 0 46	b d ± n.d.	0 93 ± 0.05	0 10 ± 0.005
CP108	20	600	3	21 0 ± 3 17	13 0 ± 1 58	59 0 ± 15 2	0 02 ± 0 01	1 62 ± 0 61	0 15 ± 0 06
CP126	20	575	5	8 9 ± 4 25	12 0 ± 4 51	84 8 ± 33 2	0 21 ± 0 18	33 6 ± 22 5	0 63 ± 0 37
CP112	20	550	6	6 62 ± 0 84	9 72 ± 2 30	72 2 ± 16 7	0 22 ± 0 06	40 2 ± 13 0	0 60 ± 0 07

Note: # an = number of analyses, pressure (P) in MPa, temperature (T) in C
Concentrations are presented +/- 1 standard deviation (1 sigma) Values of 1 sigma in normal font represent experimental standard deviation, and values underlined represent analytical standard deviation (= 5 % of the concentration, i e calculated for a relative standard deviation of 5 %) The concentrations of trace elements in OL5 are calculated as 0 99 * the concentration of the elements in CP88, in order to correct for the 1 % nepheline present in the experiment CP88

Table 4.11 Trace element concentrations of carbonate liquid in OL5-experiments and of calculated equivalent liquid (CEL) in silicate-bearing natrocarbonatite OL5, that have been used for calculation of partition coefficients between crystals and liquid.

Sample	Ba	Sr	Rb	Y	V	U	Th	Nb	Ta	Zr	Hf
Experiments - 100 MPa											
CP88	9306	11015	140	13.9	198	14.0	13.1	109	0.50	66.5	1.03
CP79	7731	9981	112	15.3	189	12.9	13.0	105	0.54	87.6	1.40
CP96	7645	10292	140	14.2	211	13.6	12.4	131	0.56	88.0	1.22
CP118	8451	11008	198	11.2	227	14.1	11.7	110	0.51	62.6	0.94
CP107	8589	10443	124	13.6	134	12.2	10.1	111	0.53	74.1	1.00
CP128	9435	9584	149	14.3	161	18.6	17.5	145	0.68	80.0	1.19
CP127	6992	6847	123	12.0	137	19.9	18.6	155	0.72	92.4	1.39
Experiments - 20 MPa											
CP90	9384	11449	145	20.7	176	13.1	14.0	104	0.49	75.9	1.17
CP45	8837	10277	144	25.9	147	16.3	9.51	94.9	0.23	79.9	0.91
CP61	10258	11021	162	16.0	215	17.8	15.1	89.0	0.45	68.4	1.06
CP51	10210	11171	154	11.2	232	18.1	13.6	99.1	0.44	59.2	0.89
CP57	10162	11320	147	6.42	249	18.4	12.0	109	0.42	50.0	0.71
CP129	12109	11916	145	5.67	267	17.3	7.34	117	0.38	18.9	0.16
CP108	9601	11780	168	17.0	397	21.0	13.0	143	0.58	51.1	0.62
CP126	9303	6005	112	14.6	130	26.5	24.3	202	0.75	70.9	0.80
CP112	5358	6403	93.7	12.6	97.4	6.62	9.72	228	1.06	88.9	1.55
CEL - OL5	5554	10549	110	9.91	75.6	5.22	6.34	42.8	0.31	32.3	0.51

Sample	La	Ce	Nd	Sm	Eu	Gd	Dy	Er	Yb	Lu
Experiments - 100 MPa										
CP88	473	570	115	10.11	2.58	4.68	2.37	0.92	0.80	0.11
CP79	462	526	110	9.71	2.44	4.56	2.45	1.00	0.83	0.10
CP96	446	506	109	9.87	2.42	4.54	2.32	1.00	0.88	0.09
CP118	420	515	105	9.47	2.38	4.31	1.95	0.76	0.61	0.08
CP107	450	535	107	9.58	2.31	4.42	2.17	0.81	0.62	0.09
CP128	507	598	112	9.95	2.60	4.68	2.72	1.07	0.88	0.11
CP127	357	394	72.6	6.30	1.56	3.28	1.75	0.66	0.62	0.08
Experiments - 20 MPa										
CP90	634	692	151	13.4	3.41	6.60	3.40	1.28	1.05	0.13
CP45	611	769	150	14.4	3.65	7.34	4.11	1.63	0.93	0.15
CP61	604	746	136	11.4	2.61	4.58	2.10	0.79	0.69	0.09
CP51	531	652	131	8.99	1.97	3.40	1.37	0.49	0.45	0.05
CP57	459	558	127	6.59	1.34	2.21	0.65	0.19	0.21	0.02
CP129	589	613	101	6.03	1.34	2.23	0.61	0.22	0.22	0.03
CP108	514	582	104	9.04	2.21	3.89	2.06	0.84	0.57	0.10
CP126	694	730	128	12.0	3.02	5.16	2.31	0.94	0.82	0.11
CP112	407	457	80.7	6.35	1.92	2.94	1.75	0.57	0.52	0.08
CEL - OL5	299	343	75.6	6.53	1.59	3.09	1.51	0.58	0.38	0.06

Note: For the experiments, values in normal font are those that have been measured, and values underlined are those that have been calculated (= residual liquid calculated by mass balance).
The trace element composition of CEL was calculated using the trace element compositions of different phases in silicate-bearing natrocarbonatite OL5, according to their proportions presented in Table 3.11.

Table 4.12a: Partition coefficients of REE between crystals and carbonate liquid in OL5-experiments and between crystals and calculated equivalent liquid (CEL) in silicate-bearing natrocarbonatite OL5.

Sample	La	Ce	Nd	Sm	Eu	Gd	Dy	Er	Yb	Lu
Nepheline										
CP88		0.0011			0.027					
CP79		0.0007						0.12		
CP96	0.0012									
CP118	0.011	0.0096								
CP107	0.0030	0.0042	0.012				0.13	1.63		
CP90	0.0008	0.0011					0.085			
CP45	0.0011				0.025				0.70	
CP57										
CP108										
CP112	0.018	0.020	0.13	0.19				0.67		
Average exp	0.0058	0.0061	0.071	0.19	0.026		0.11	0.81	0.70	
OL5 - Ph-c	0.0014	0.0028	0.0042	0.032	0.082	0.028	0.079	0.077	0.10	0.57
OL5 - mph. sph.	0.047	0.10	0.13	0.14	0.50	0.20	0.69	1.56	2.03	
Clinopyroxene										
CP107	0.018	0.037	0.092	0.20	0.19	0.38	0.32	1.23	2.09	6.52
CP127	0.015	0.061								
CP108	0.011	0.032				0.34	0.46	0.90		4.23
OL5 - Ph-c	0.027	0.061	0.16	0.35	0.37	0.40	0.59	1.37	4.05	6.06
OL5 - mph. sph.	0.035	0.075	0.15	0.33	0.34	0.54	0.62	1.40	3.67	5.52
Melanite garnet										
CP51	0.11	0.46	2.96	14.0	22.9	34.0	77.9	108	85.6	88.1
CP57	0.13	0.58	3.01	16.5	28.6	42.6	129	205	146	162
CP108	0.066	0.34	2.18	10.7	16.0	28.5	54.2	68.9	80.1	53.9
OL5 - Ph-c	0.15	0.73	4.42	19.0	28.6	41.1	82.9	99.1	107	84.0
OL5 - mph.	0.12	0.58	3.93	16.7	25.4	39.1	77.1	99.6	106	90.3
Wollastonite										
CP51	0.059	0.14	0.34	1.17	1.95	2.99	8.15	16.2	16.1	16.9
OL5 - Ph-c	0.11	0.23	0.61	1.62	2.38	3.04	6.45	9.18	14.7	15.4
OL5 - Ph-c sph.	0.081	0.22	0.55	1.52	2.23	3.25	6.50	10.2	15.4	14.8
OL5 - mph. sph.	0.092	0.23	0.56	1.84	2.35	2.91	7.13	11.7	15.6	16.4
Melilite										
CP51	0.87	0.98	1.12	1.04	1.00	1.15				
Nyererelte										
CP107	1.39	1.66	1.57	1.46	1.62	1.28	1.94	1.81	2.13	2.33
CP128	0.41	0.61	0.74	0.58	0.42	0.42	0.59	0.67		0.36
CP127	0.66	0.95	1.18	1.17	1.35	1.20	0.75	0.85		
CP108	0.27	0.53	0.60	0.54	0.57	0.34	0.48			
CP126	0.44	0.65	0.72	0.74	0.63	0.81	0.43	0.58	0.88	1.22
OL5 - Ph-c	0.76	0.74	0.68	0.52	0.46	0.40	0.22	0.15	0.10	0.40
Gregoryite										
CP108	0.11	0.13	0.15	0.13	0.14	0.28				0.88
CP126	0.12	0.16	0.17	0.12	0.11	0.19	0.29	0.21	0.18	0.19
CP112	0.54	0.54	0.47	0.51	0.45	0.51	0.37	0.47	1.04	
OL5 - Ph-c	0.24	0.20	0.15	0.12	0.082	0.11	0.080	0.086	0.16	0.17
Apatite										
OL5 - Ph-c	5.98	9.13	16.2	24.8	30.4	33.3	33.9	26.5	18.8	14.1
Titanite										
CP107	0.57	1.36	3.57	6.07	5.65	8.52	12.0		26.7	

Abbreviations used are: Ph., phenocryst; c., core; mph., microphenocryst; sph., spheroid.

Table 4.12b. Partition coefficients of trace elements other than REE between crystals and carbonate liquid in OL5-experiments and between crystals and calculated equivalent liquid (CEL) in silicate-bearing natrocarbonatite OL5.

Sample	Ba	Sr	Rb	Y	V	U	Th	Nb	Ta	Zr	Hf
Nepheline											
CP88	0.0036		0.54								
CP79	0.0015		0.95	0.0046		0.0031	0.0031	0.0025		0.038	
CP96			0.49								
CP118	0.0038		0.45	0.28							
CP107	0.0045		0.85	0.030		0.051	0.026		0.56		
CP90	0.0028		0.48								
CP45	0.0026	0.021	0.68		0.015	0.029		0.0048			0.34
CP57	0.0008		0.79								
CP108	0.0008		0.41			0.037	0.023				
CP112	0.013					0.16		0.062	0.25	0.28	
Average exp	0.0037	0.021	0.63	0.10	0.015	0.056	0.017	0.023	0.41	0.16	0.34
OL5 - Ph-c	0 0036	0.010	0.72	0.030	0.030	0.008	0.010	0.012	0.22	0.11	0.47
OL5 - mph spn	0.013	0.046	0.82	0.79	0.61		0.14	0.17		2.23	
Clinopyroxene											
CP107	0 0038	0.23	0 037	0.21	2.39	0.095	0.071	0.13	2.11	5.24	7.96
CP127	0.0070			0 28	3 00		0 30	0.077		2.52	6.10
CP108	0 0003			0 31	0.55	0.035	0.29	0.23	1.13	6.66	8.49
OL5 - Ph-c	0 0004	0 059	0.0037	0 51	3.17	0.024	0.0037	0.017	0.17	14.2	19 9
OL5 - mph spn	0 0032	0.054	0.049	0.54	2.59	0.046	0.086	0.074	0.39	10.7	16.2
Melanite garnet											
CP51	0 0010	0.010		43.1	2.71	0.48	1.78	4 93	71.4	55 8	65.1
CP57	0 0007	0.020		63.3	3.78	0.50	3 74	8 74	39 7	63.1	83.8
CP108				30.6	3.38	0.32	0.70	2.74	27 5	69 2	92.1
OL5 - Ph-c	0.0009	0 008	0 008	53.9	11.2	1.68	2.18	11.3	101	127	147
OL5 - mph	0 0002	0.015		52.1	9 16	1.18	2.04	7 58	82.6	129	154
Wollastonite											
CP51	0 0067	0 077		5 60	0 011			0 010	0 069	0 064	
OL5 - Ph-c	0 0016	0 085	0.025	6.37	0 36	0.10	0 022	0.20	0 80	1 40	1.75
OL5 - Ph-c spn	0 0014	0 091	0 020	6 30	0.09	0.012		0.0076	0.049	0.15	0.49
OL5 - mph spn	0 0020	0 087	0.043	7 22	0.44	0.0077	0.014	0.060	0.065	0.93	0.97
Melilite											
CP51	0 027	1 39		0.37			0.52	0 0082		0 077	0 11
Nyererite											
CP107	1.37	1 58	2 32	1.52	1.54	1.86	2.58	0.57	0.22	0.29	0.88
CP128	0.31	1 11	0.39	0.51	0.019	0.038	0.026	0.035		0.021	
CP127	0 48	1 86	0.66	0.58	0.0077	0.0015	0 011	0.0010		0.0006	0.043
CP108	0 28	0 91	0.60	0.25				0.011			
CP126	0.53	2.44	1.82	0 58	0.56	0.051	0.053	0.078	0.24	0.11	0.36
OL5 - Ph-c	1 04	1 48	1 05	0 30	0 12	0.10	0.10	0.11	0.10	0.068	0.28
Gregoryite											
CP108	0 11	0.37	0.14	0.071	0.033	0.013	0.021	0.0041			0.83
CP126	0.17	1 00	0.33	0.15	0.12	0.0053	0.017	0.0017		0.005	
CP112	0.70	0.86	0.66	0.45	0.61	0.65	0.33	0.039	0.094	0.019	0.28
OL5 - Ph-c.	0.59	0.63	0.56	0.086	0.75	0.019	0.032	0.012	0.36	0.024	0.14
Apatite											
OL5 - Ph-c	0.034	0.67	0.048	21.1	1.28	1.44	11.2	0.043	0.16	0.29	
Titanite											
CP107	0 040		0.22	6.67	1.79	2.16	3.04	112	991	169	121

Table 4.13: Crystal phases into which the different elements are preferentially incorporated. Average partition coefficients (D) between crystals and carbonate liquid are indicated in brackets.

Elements	Phase 1	Phase 2	Phase 3	Phase 4	Phase 5	Phase 6
LREE	Pvk (D ~ 20)	Ap (D ~ 8)	NY (D ~ 1)	GRE (D ~ 0.5)		
MREE	Pvk (D ~ 50)	Ap (D ~ 34)	Mela (D ~ 30)	Tit (D ~ 8)	Wo (D ~ 2.5)	NY (D ~ 1)
HREE	Mela (D ~ 100)	Tit (D ~ 25)	Ap (D ~ 20)	Wo (D ~ 15)	Cpx (D ~ 5)	NY (D ~ 2)
U, Th	Ap (D_{Th} = 10)	NY (D ~ 2)	Tit (D ~ 2-3)			
Nb, Ta	Tit (D_{Nb} ~ 100; D_{Ta} ~ 1000)	Pvk (D_{Nb} ~ 60)	Mela (D_{Nb} ~ 5; D_{Ta} ~ 50)			
Zr, Hf	Tit (D ~ 150)	Mela (D ~ 50)	Cpx (D ~ 5-10)	Pvk (D_{Zr} ~ 5)		
Ba, Sr	NY (D ~ 1-2)					
Rb	NY (D ~ 1-2)	Ne (D ~ 1)				

Abbreviations used are: Ap: apatite; NY: nyerereite; GRE: gregoryite; Mela: melanite garnet; Tit: titanite; Wo: wollastonite; Cpx: clinopyroxene; Ne: nepheline; Pvk: perovskite.

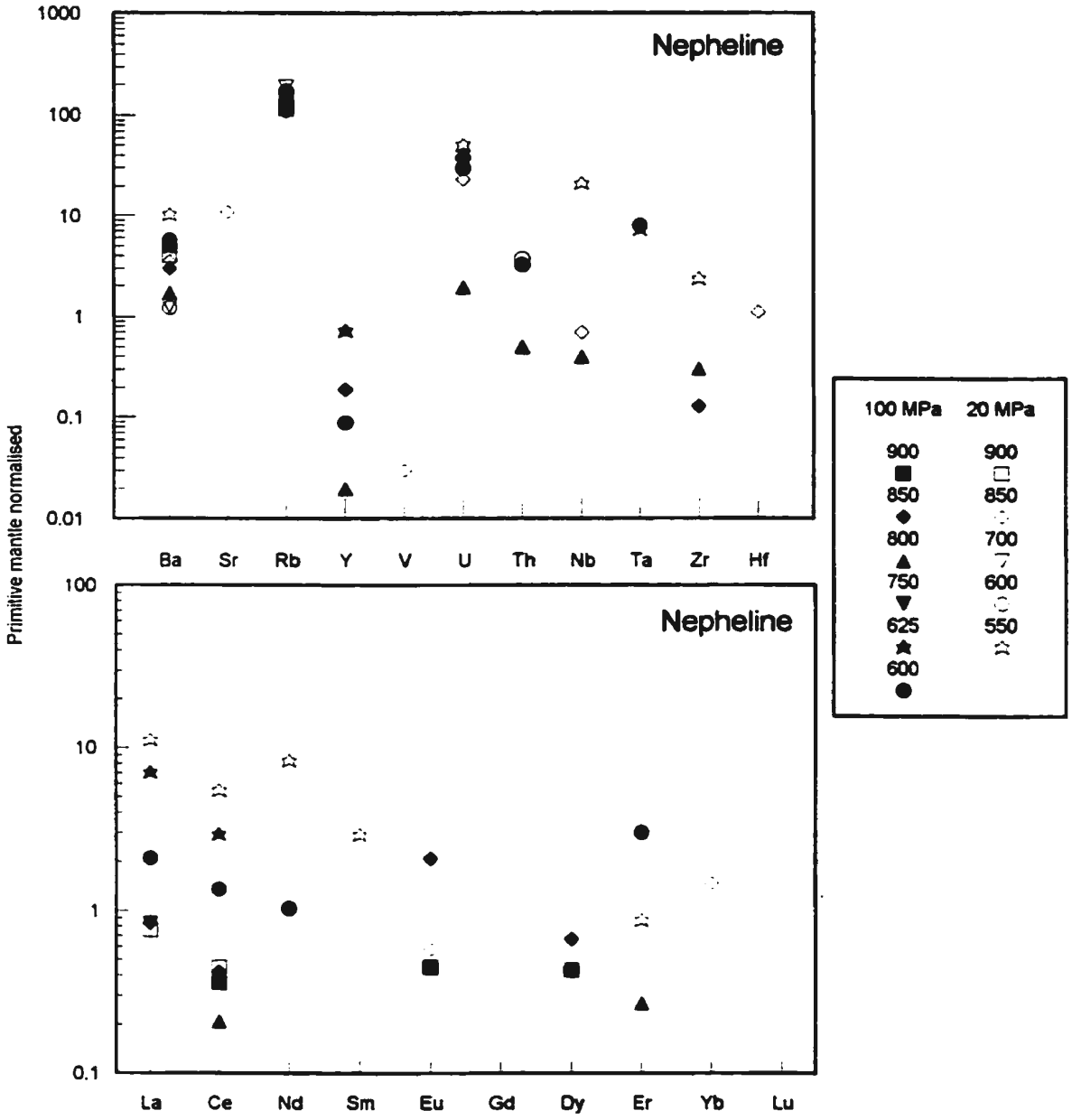

Figure 4.1: Trace element concentrations normalised to primitive mantle for nepheline from OL5-experiments. Filled symbols represent experiments at 100 MPa, and open symbols represent experiments at 20 MPa. Temperature (in °C) is shown beside symbols in legend. Data are from Table 4.1; primitive mantle normalising values are from McDonough and Sun (1995).

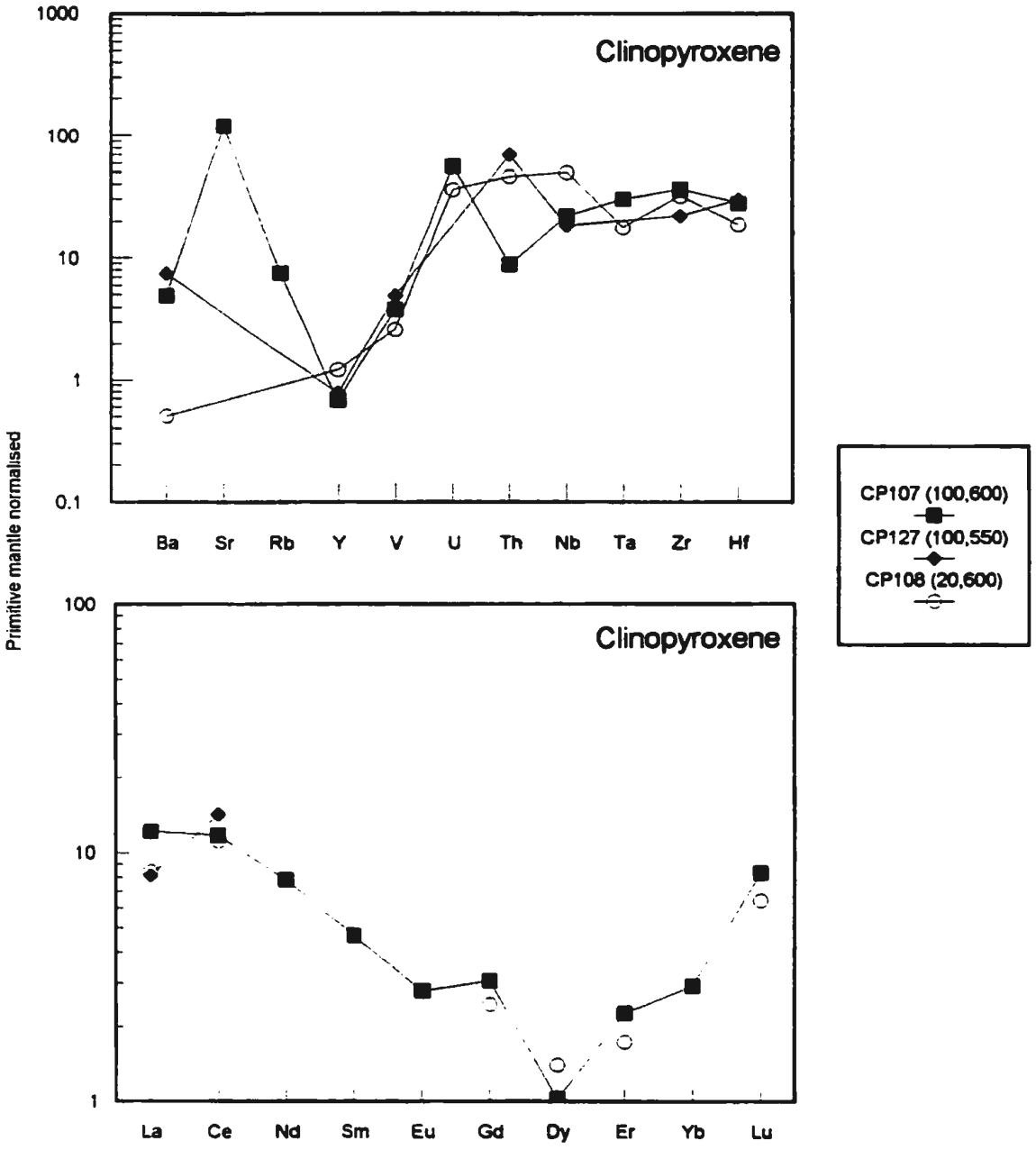

Figure 4.2: Trace element concentrations normalised to primitive mantle for clinopyroxene from OL5-experiments. Pressure (in MPa) and temperature (in °C) are shown in brackets beside experiment number (labelled as CPxx) in legend. Data are from Table 4.2; primitive mantle normalising values are from McDonough and Sun (1995).

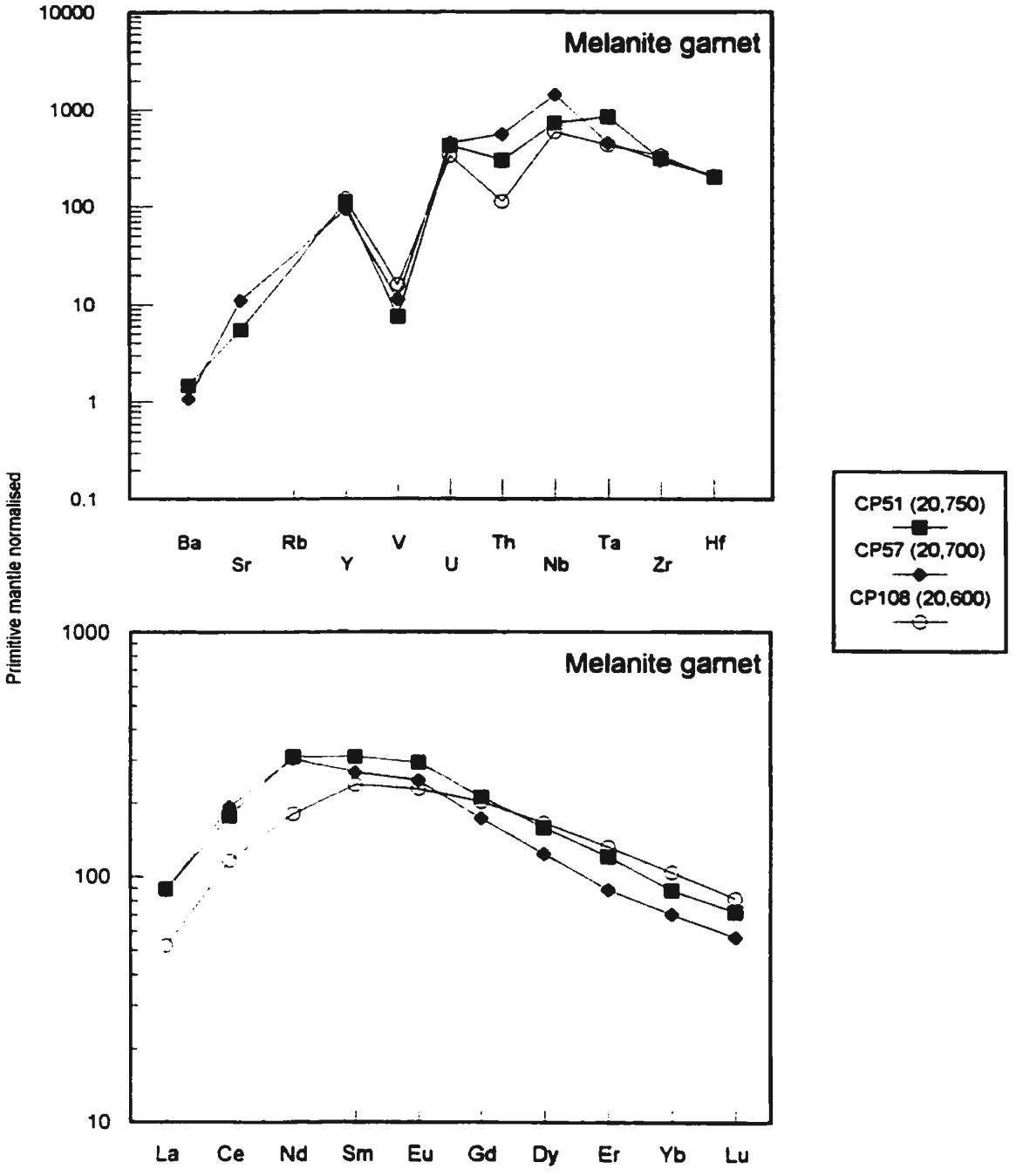

Figure 4.3: Trace element concentrations normalised to primitive mantle for melanite garnet from OL5-experiments. Pressure (in MPa) and temperature (in °C) are shown in brackets beside experiment number (labelled as CPxx) in legend. Data are from Table 4.3; primitive mantle normalising values are from McDonough and Sun (1995).

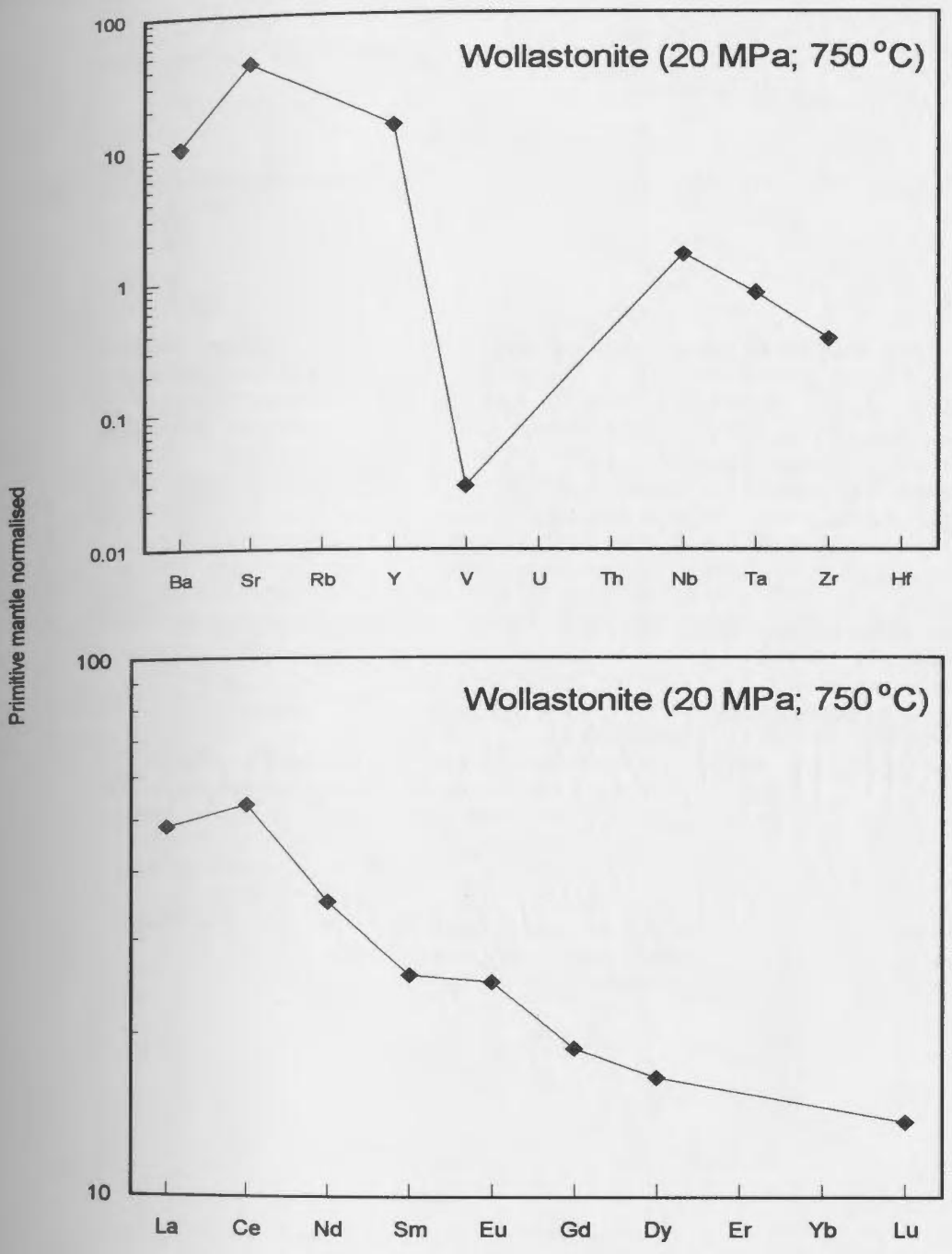

Figure 4.4: Trace element concentrations normalised to primitive mantle for wollastonite in experiment CP51 (20 MPa, 750 °C). Data are from Table 4.4; primitive mantle normalising values are from McDonough and Sun (1995).

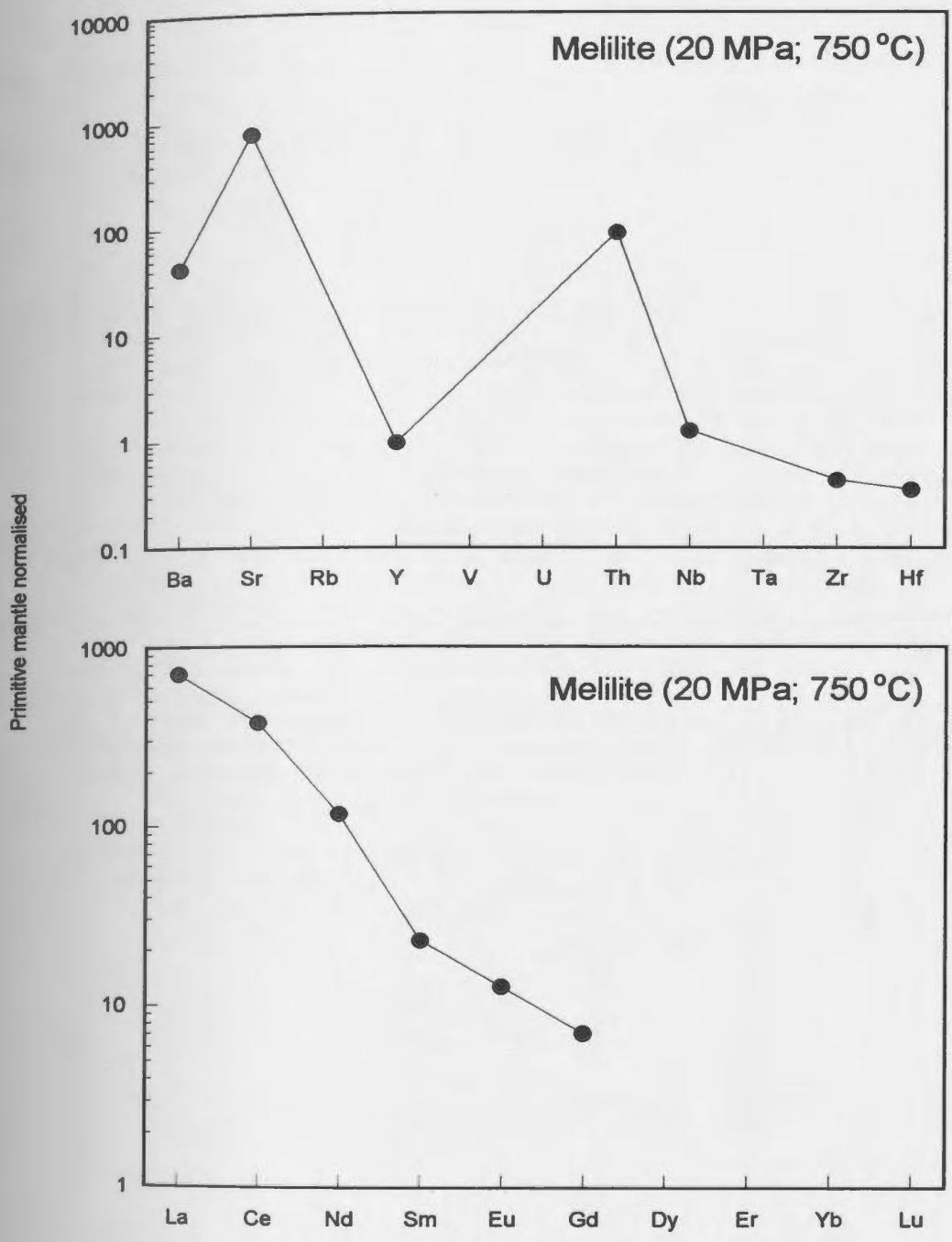

Figure 4.5: Trace element concentrations normalised to primitive mantle for melilite from experiment CP51 (20 MPa, 750 °C). Data are from Table 4.5; primitive mantle normalising values are from McDonough and Sun (1995).

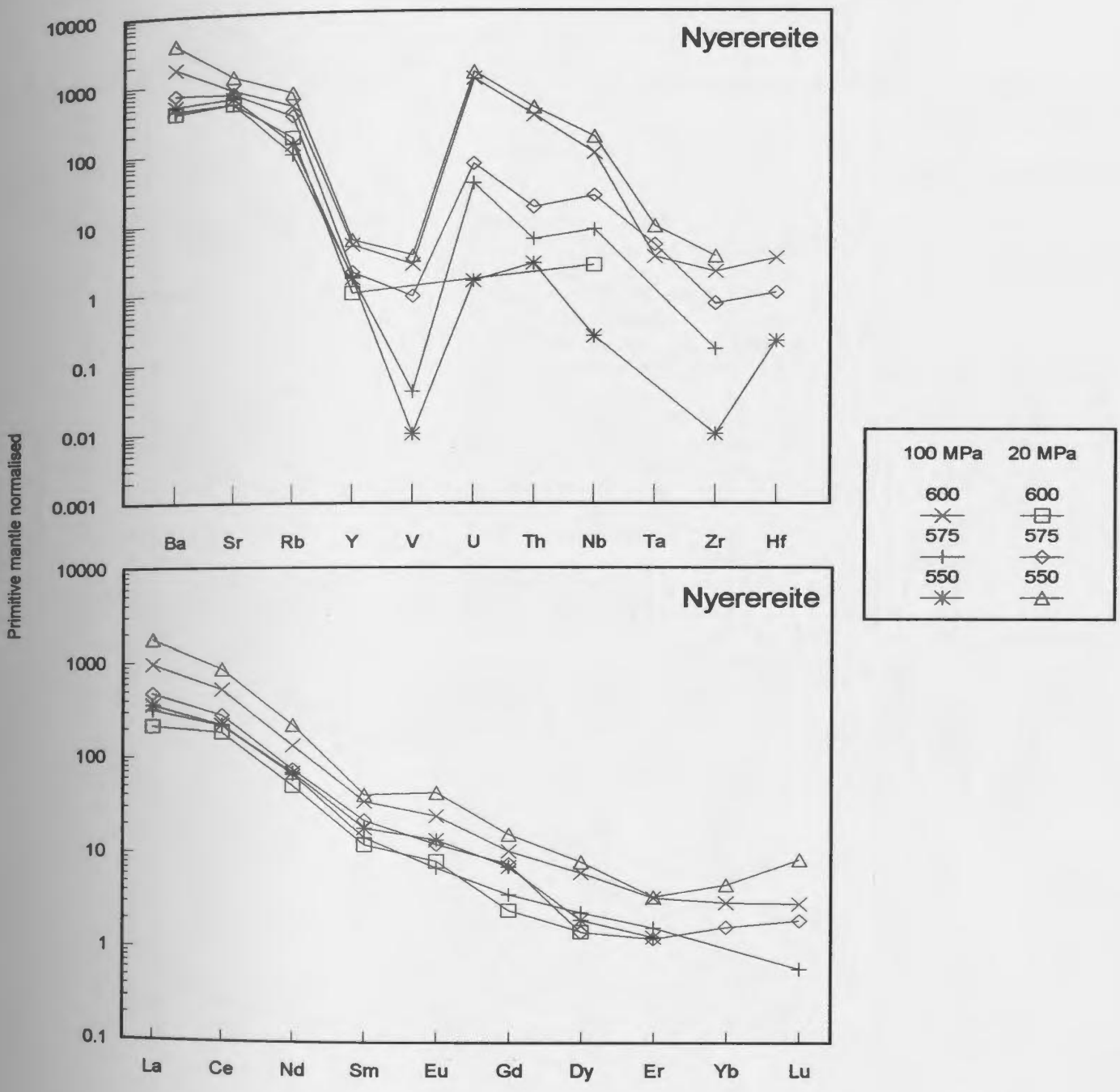

Figure 4.6: Trace element concentrations normalised to primitive mantle for nyerereite in OL5-experiments. Temperature (in °C) is shown beside symbols in legend. Data are from Table 4.6; primitive mantle normalising values are from McDonough and Sun (1995).

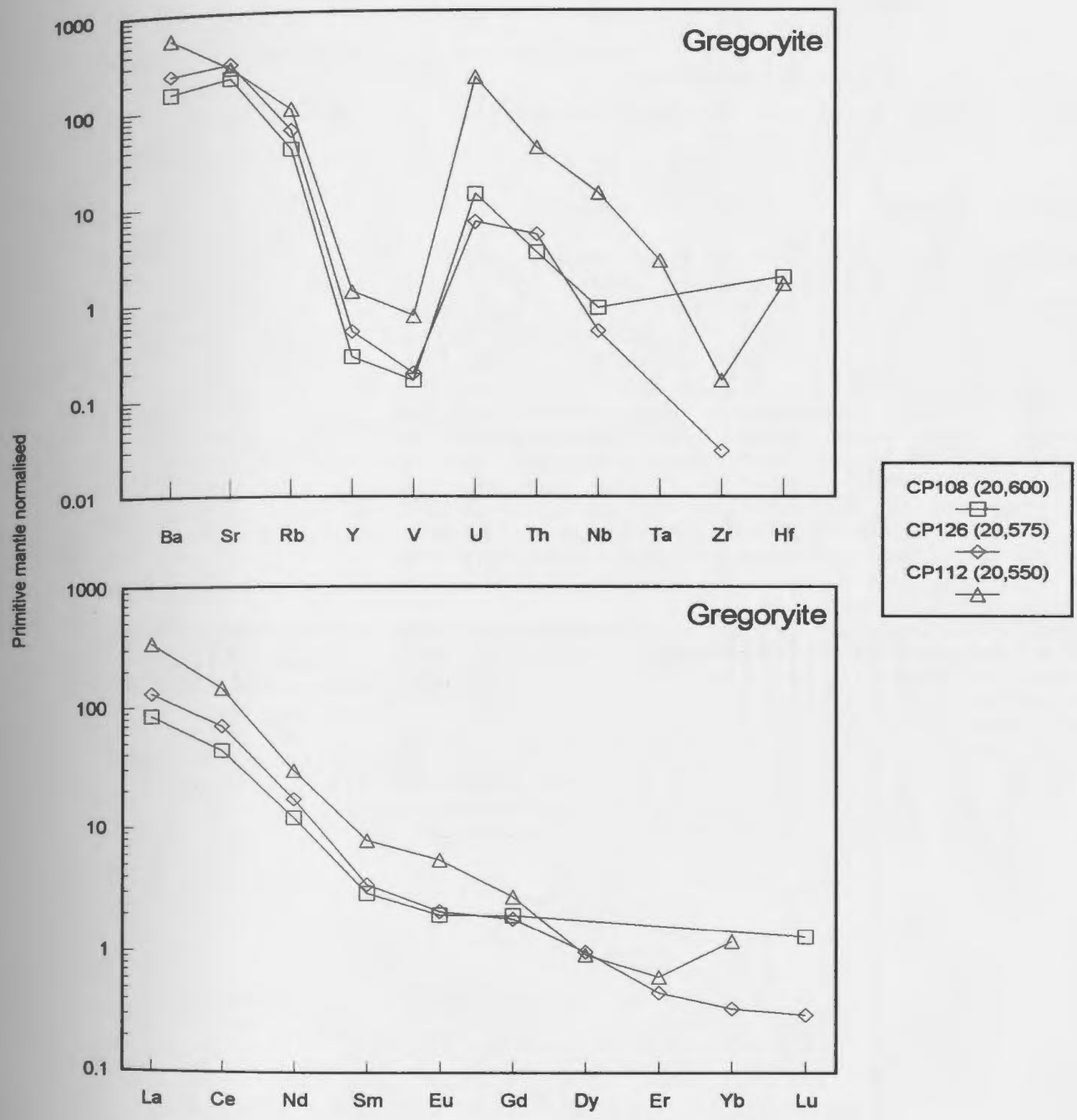

Figure 4.7: Trace element concentrations normalised to primitive mantle for gregoryite from the OL5-experiments. Pressure (in MPa) and temperature (in °C) are shown in brackets beside experiment number (labelled as CPxx) in legend. Data are from Table 4.7; primitive mantle normalising values are from McDonough and Sun (1995).

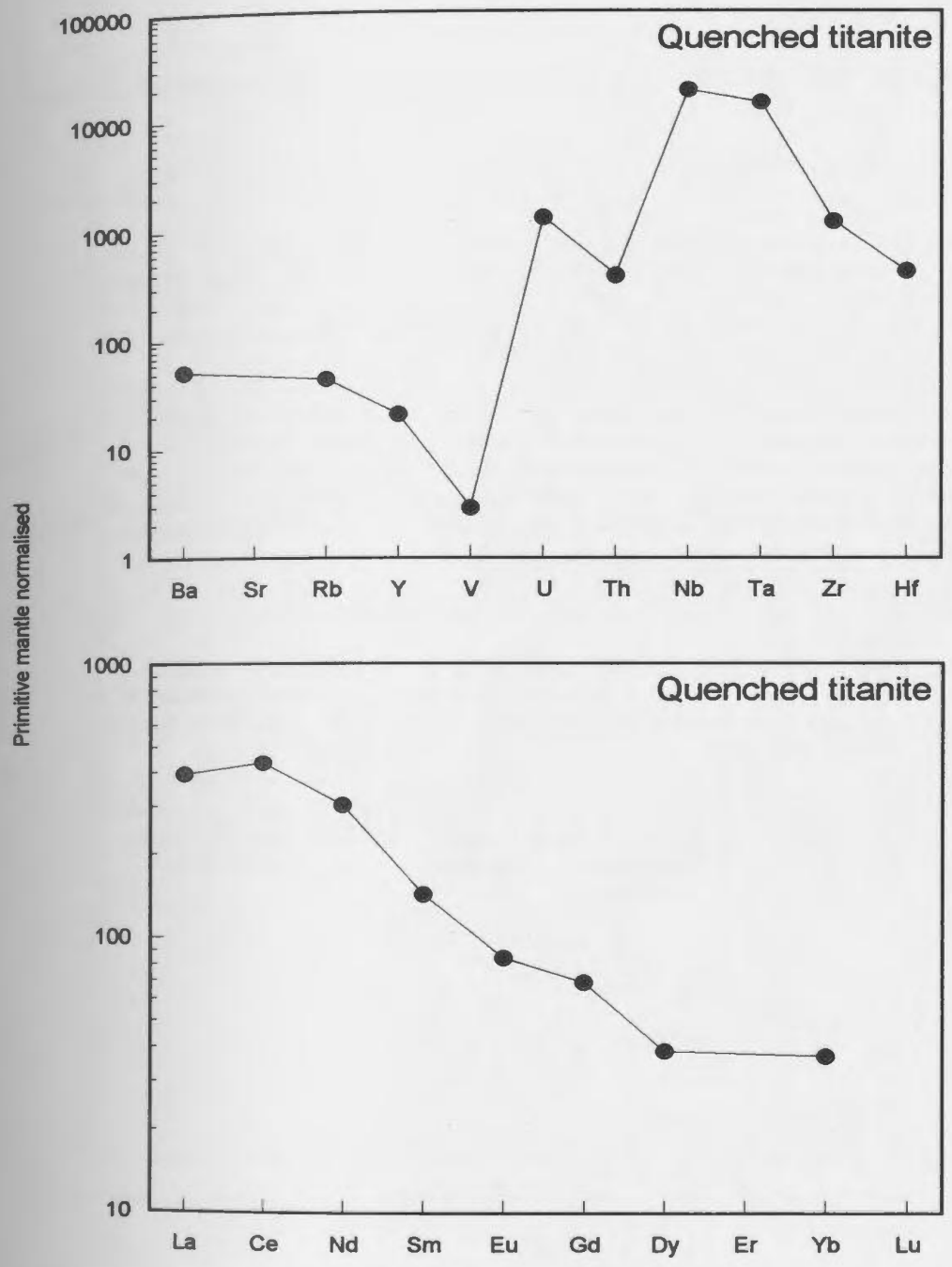

Figure 4.8: Trace element concentrations normalised to primitive mantle for titanite from experiment CP107 (100 MPa, 700 °C). Data are from Table 4.8; primitive mantle normalising values are from McDonough and Sun (1995).

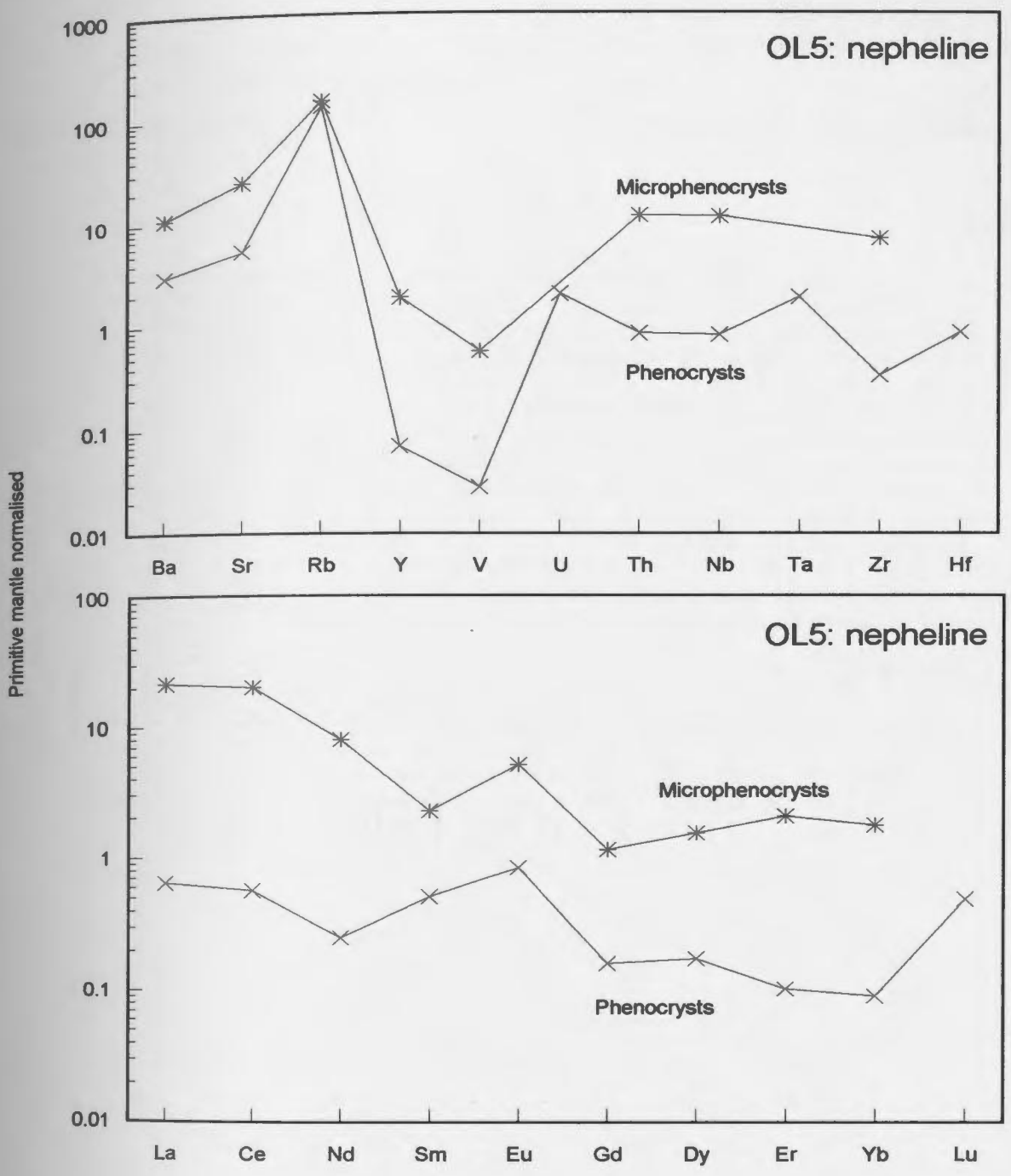

Figure 4.9: Trace element concentrations normalised to primitive mantle of nepheline phenocrysts and microphenocrysts in silicate-bearing natrocarbonatite OL5. Phenocrysts are set in the groundmass, and microphenocrysts are set in the groundmass of the silicate spheroids. Data are from Table 4.9; primitive mantle normalising values are from McDonough and Sun (1995).

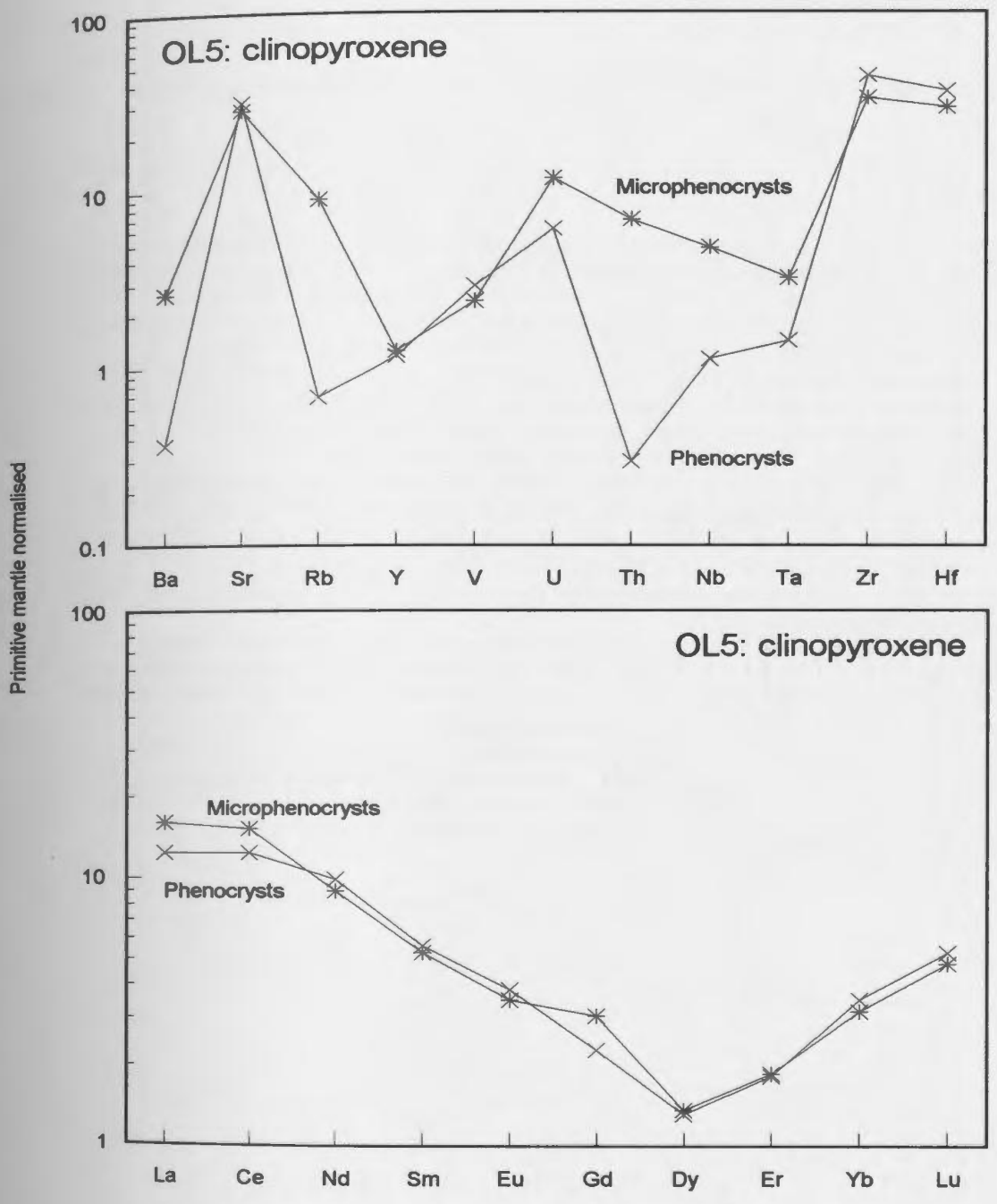

Figure 4.10: Trace element concentrations normalised to primitive mantle for clinopyroxene phenocrysts and microphenocrysts in silicate-bearing natrocarbonatite OL5. Phenocrysts are set in the groundmass, and microphenocrysts are set in the groundmass of the silicate spheroids. Data are from Table 4.9; primitive mantle normalising values are from McDonough and Sun (1995).

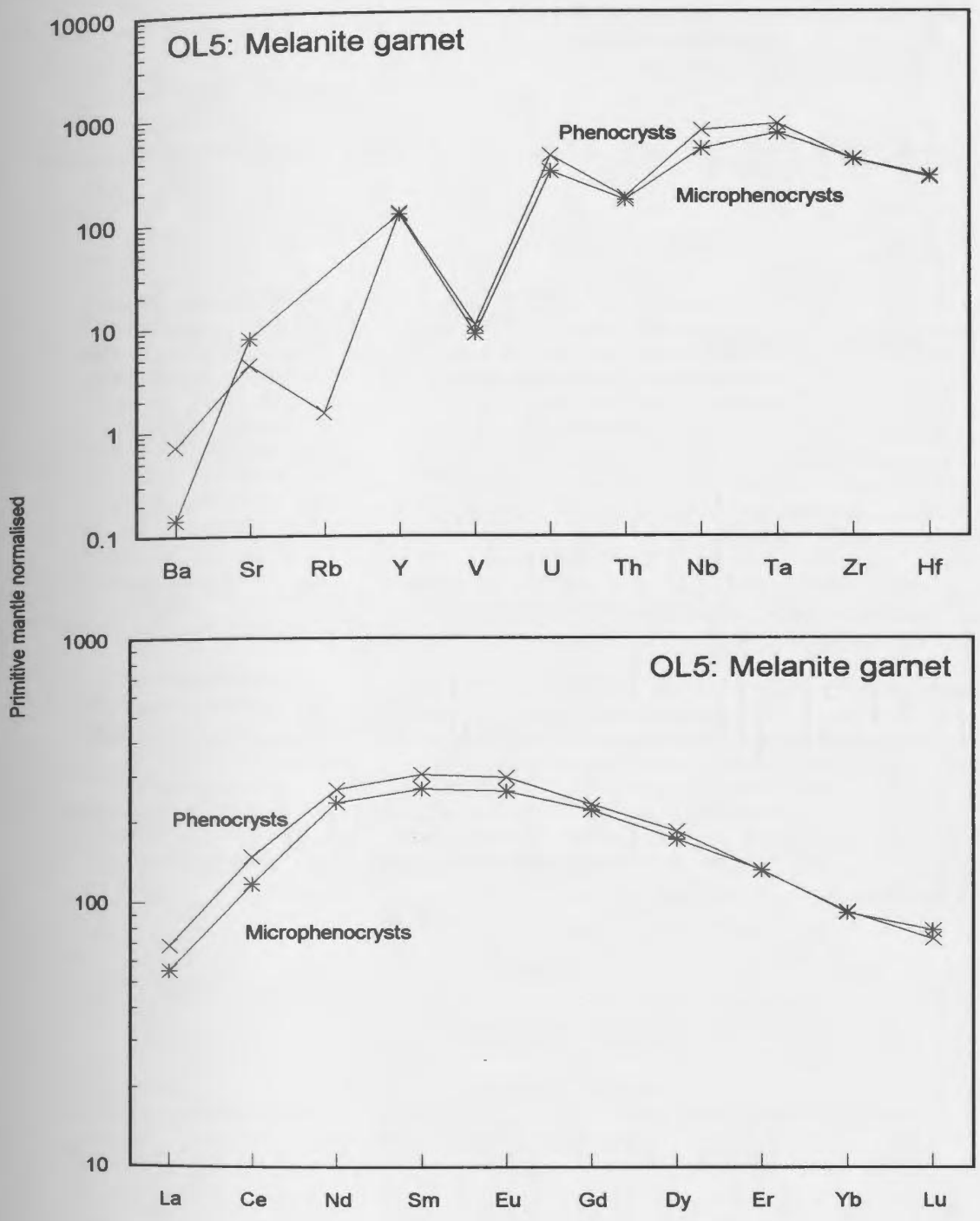

Figure 4.11: Trace element concentrations normalised to primitive mantle for melanite garnet phenocrysts and microphenocrysts in silicate-bearing natrocarbonatite OL5. Phenocrysts are set in the groundmass, and microphenocrysts are in inclusion in a clinopyroxene in a silicate spheroid. Data are from Table 4.9; primitive mantle normalising values are from McDonough and Sun (1995).

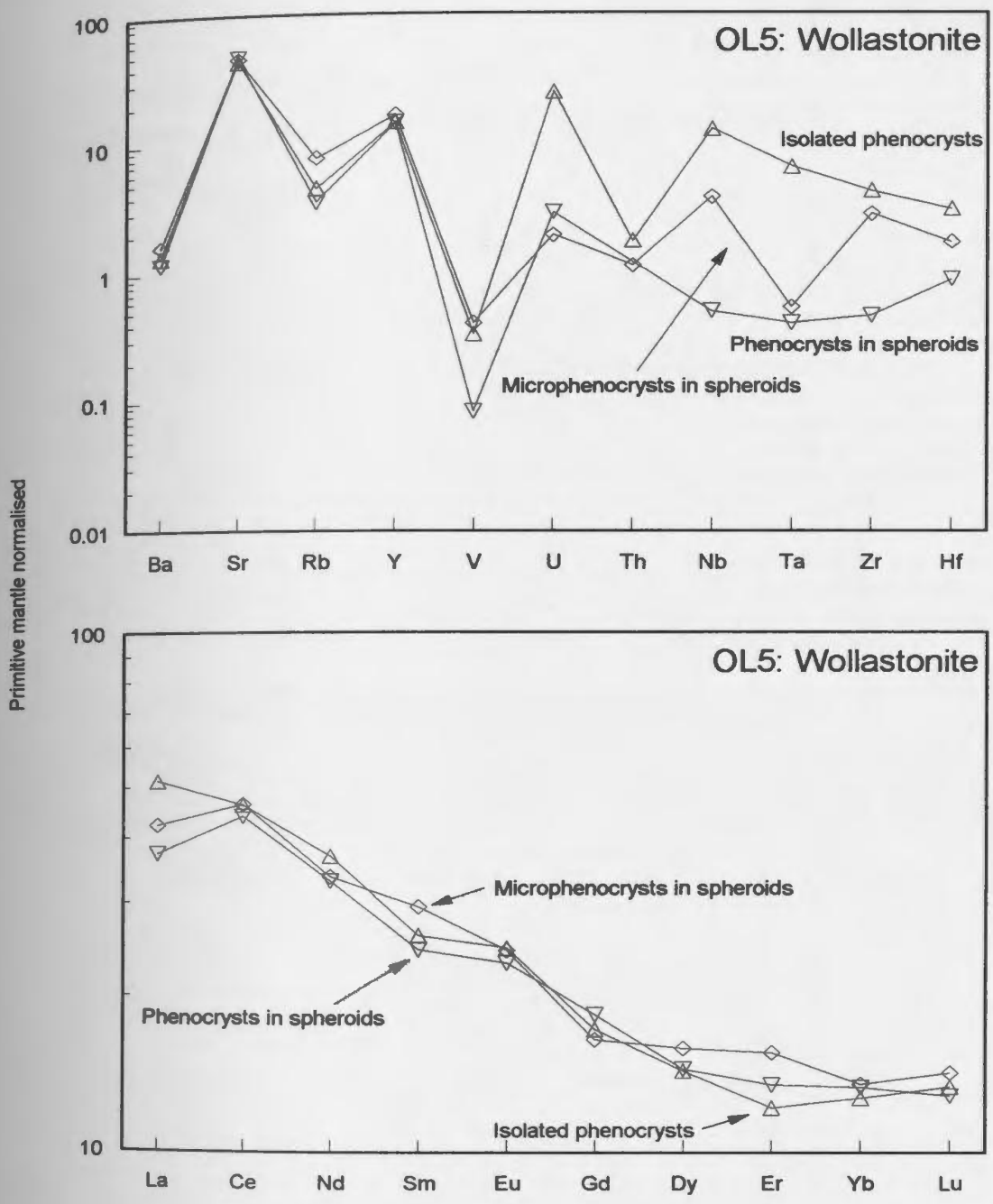

Figure 4.12: Trace element concentrations normalised to primitive mantle for wollastonite in silicate-bearing natrocarbonatite OL5. Isolated phenocrysts (triangles), phenocrysts in spheroids (reverse triangles) and microphenocrysts in spheroids (diamonds) are plotted separately. Data are from Table 4.9; primitive mantle normalising values are from McDonough and Sun (1995).

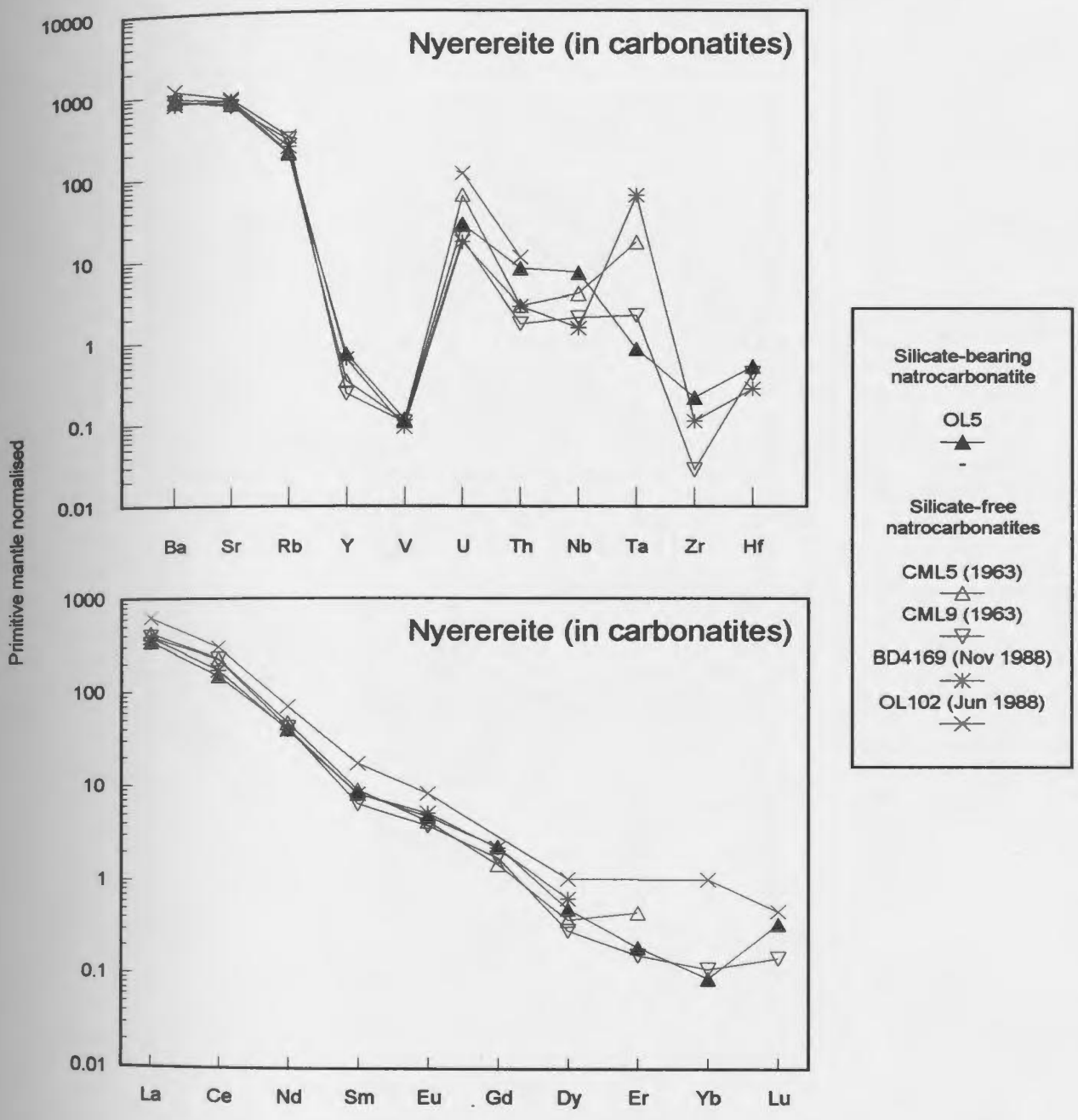

Figure 4.13: Trace element concentrations normalised to primitive mantle for nyerereite in silicate-bearing natrocarbonatite OL5 and in silicate-free natrocarbonatites CML5, CML9, BD4169 and OL102. Data are from Table 4.9; additional data (OL102) are from Keller and Spettel (1995); primitive mantle normalising values are from McDonough and Sun (1995).

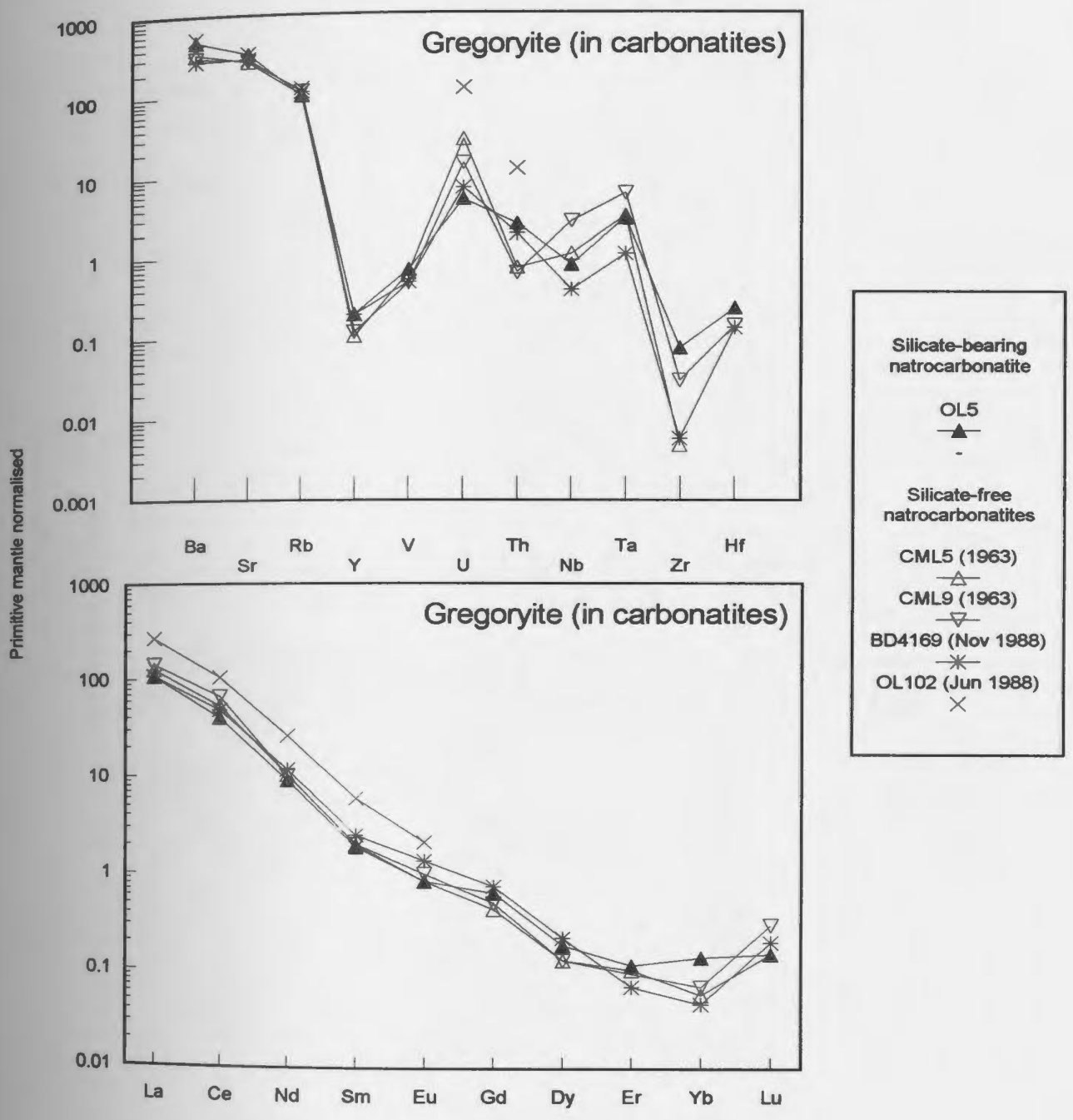

Figure 4.14: Trace element concentrations normalised to primitive mantle for gregoryite in silicate-bearing natrocarbonatite OL5 and in silicate-free natrocarbonatites CML5, CML9, BD4169 and OL102. Data are from Table 4.9; additional data (OL102) are from Keller and Spettel (1995); primitive mantle normalising values are from McDonough and Sun (1995).

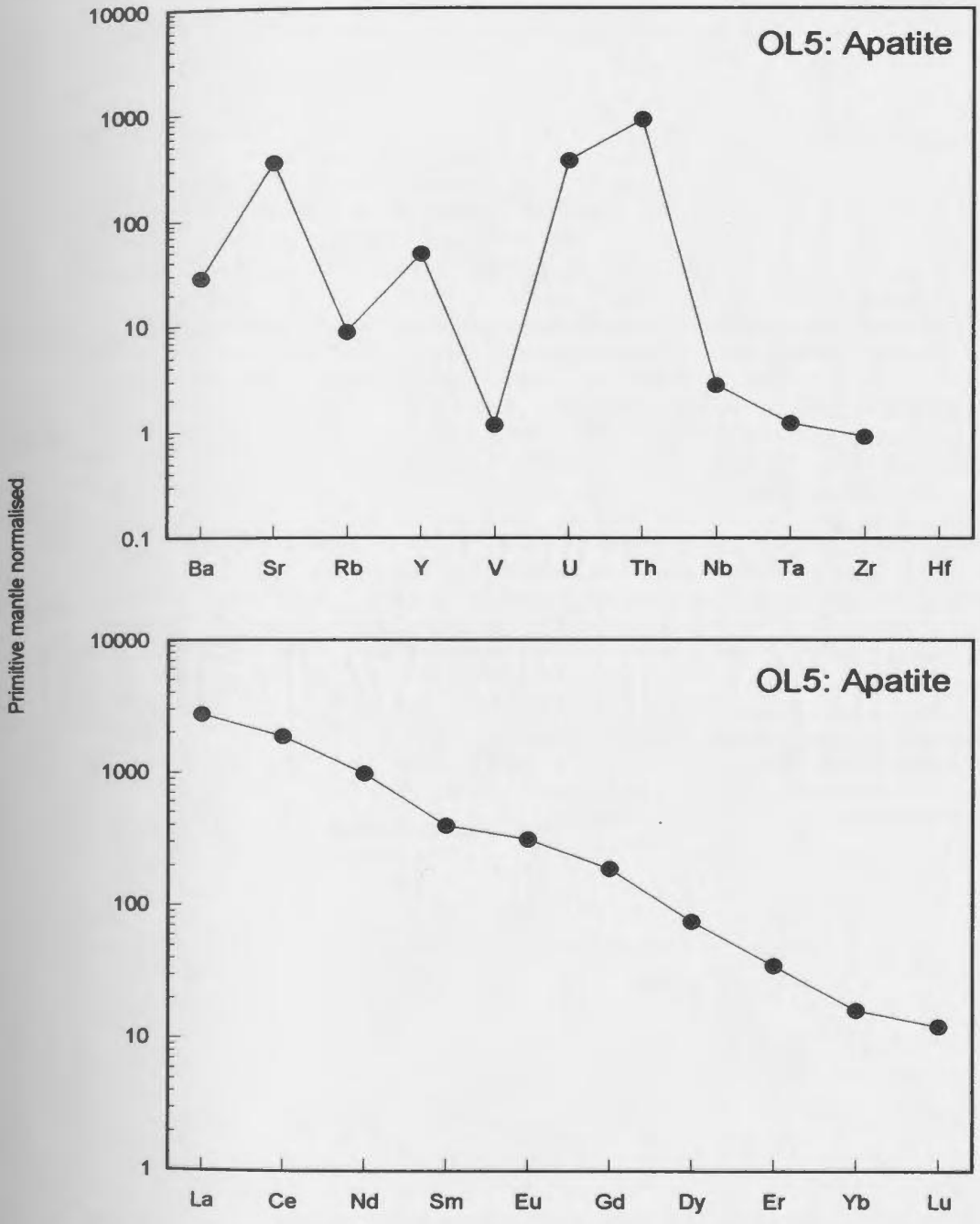

Figure 4.15: Trace element concentrations normalised to primitive mantle for apatite from silicate-bearing natrocarbonatite OL5. Data are from Table 4.9; primitive mantle normalising values are from McDonough and Sun (1995).

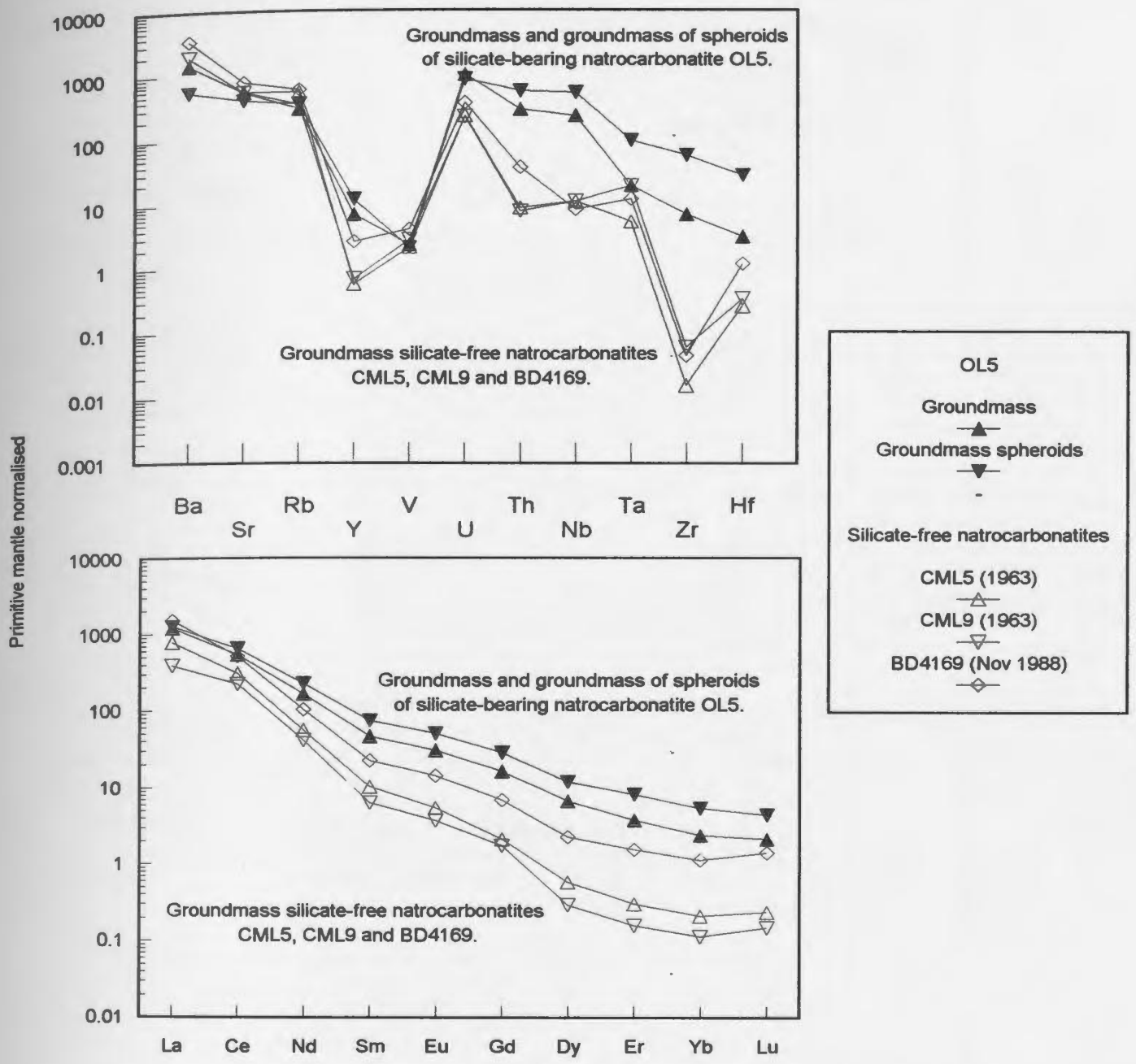

Figure 4.16: Trace element concentrations normalised to primitive mantle for groundmass and groundmass of silicate spheroids in silicate-bearing natrocarbonatite OL5, and of groundmass in silicate-free natrocarbonatites CML5, CML9 and BD4169. Data are from Table 4.9; primitive mantle normalising values are from McDonough and Sun (1995).

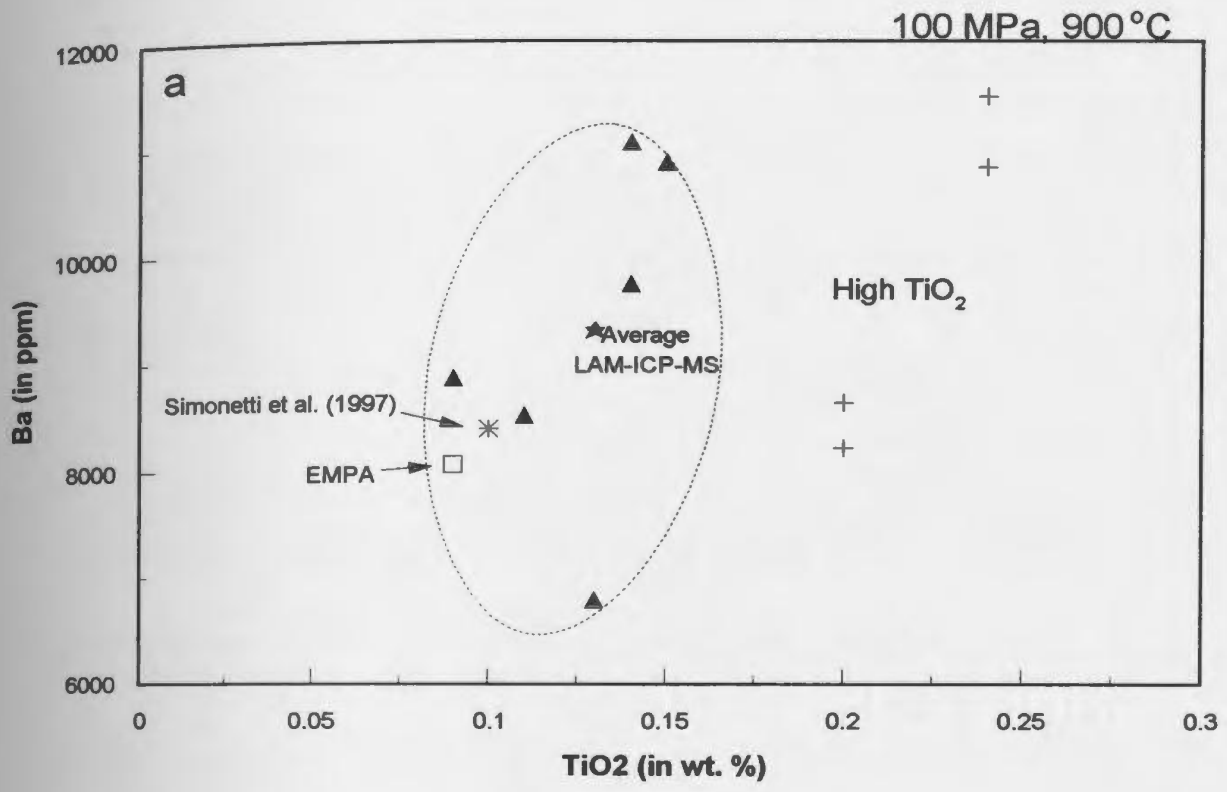

Figure 4.17: Variation diagram for selected trace elements versus TiO_2 for carbonate liquid from experiment CP88 (100 MPa, 900 °C). Elements plotted versus TiO_2 are: (a) Ba; (b) Rb; (c) V; (d) Ce; (e) Gd; (f) Yb; (g) U; (h) Nb; and (i) Zr. Individual analyses which have been rejected for having too high a value of TiO_2 compared to that of the electron microprobe value (= 0.09 wt. %) are represented by a cross (+). Individual analyses used to calculate the average composition of the carbonate liquid are represented by a filled triangle (▲) and are within the area denoted by a dotted line. The average value of these selected analyses is denoted by a star (★). For comparison, data from Simonetti et al. (1997) are also plotted (✳), as well as data obtained by electron microprobe (□) on Figure 4.17a. Individual analyses for the carbonate liquid are from Table A4.2 in Appendix A4, and average analyses are from Table 4.10.

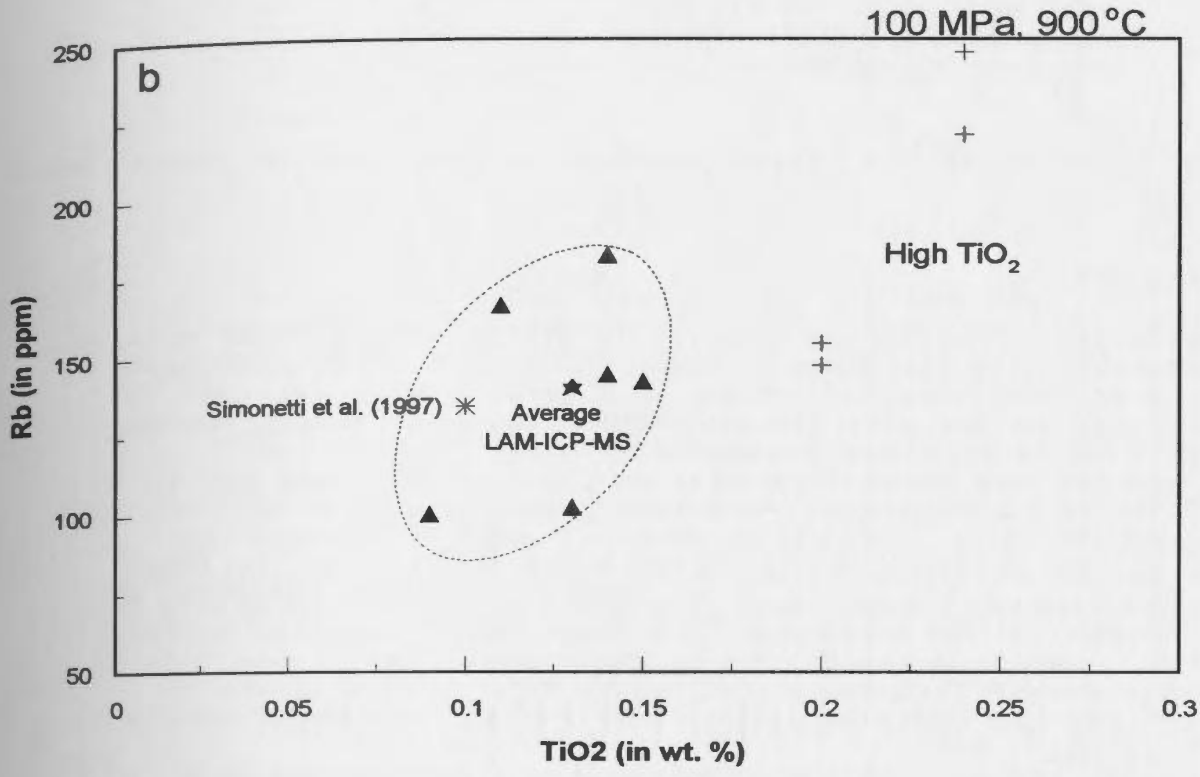
100 MPa, 900 °C
b
High TiO_2
Simonetti et al. (1997)
Average
LAM-ICP-MS
Rb (in ppm)
TiO2 (in wt. %)
250
200
150
100
50
0
0.05
0.1
0.15
0.2
0.25
0.3

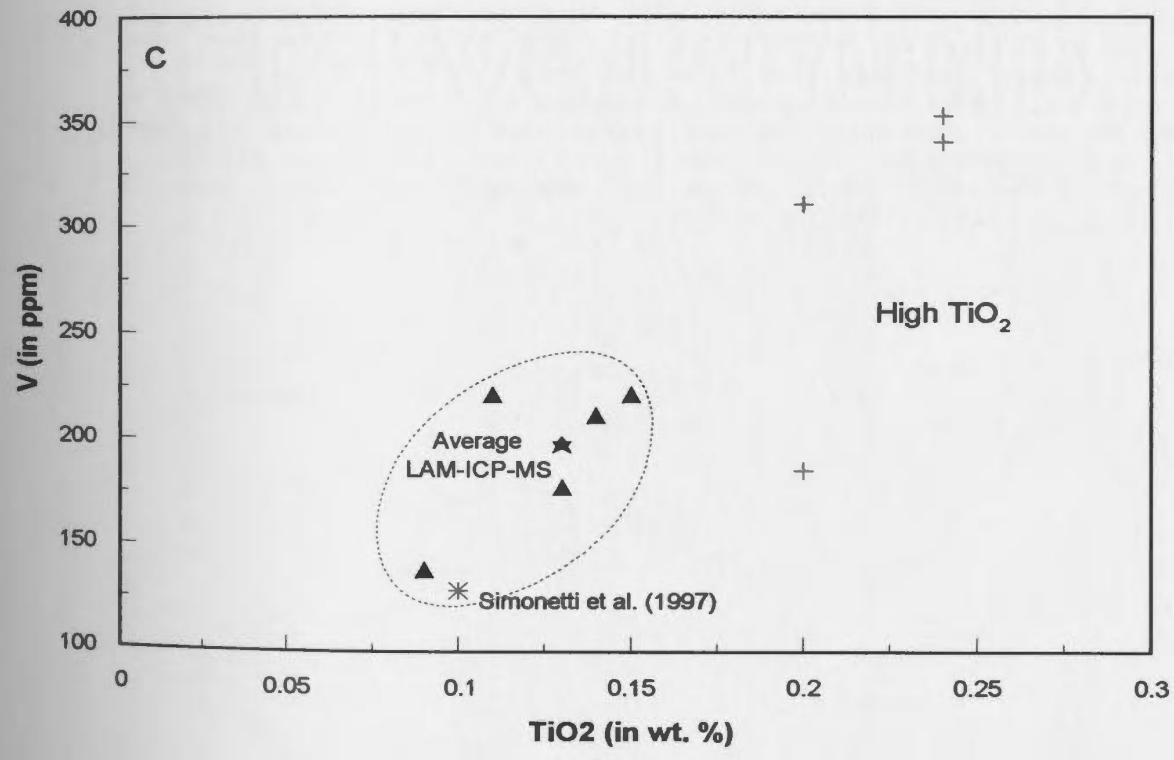
C
High TiO_2
Average
LAM-ICP-MS
Simonetti et al. (1997)
V (in ppm)
TiO2 (in wt. %)
400
350
300
250
200
150
100
0
0.05
0.1
0.15
0.2
0.25
0.3

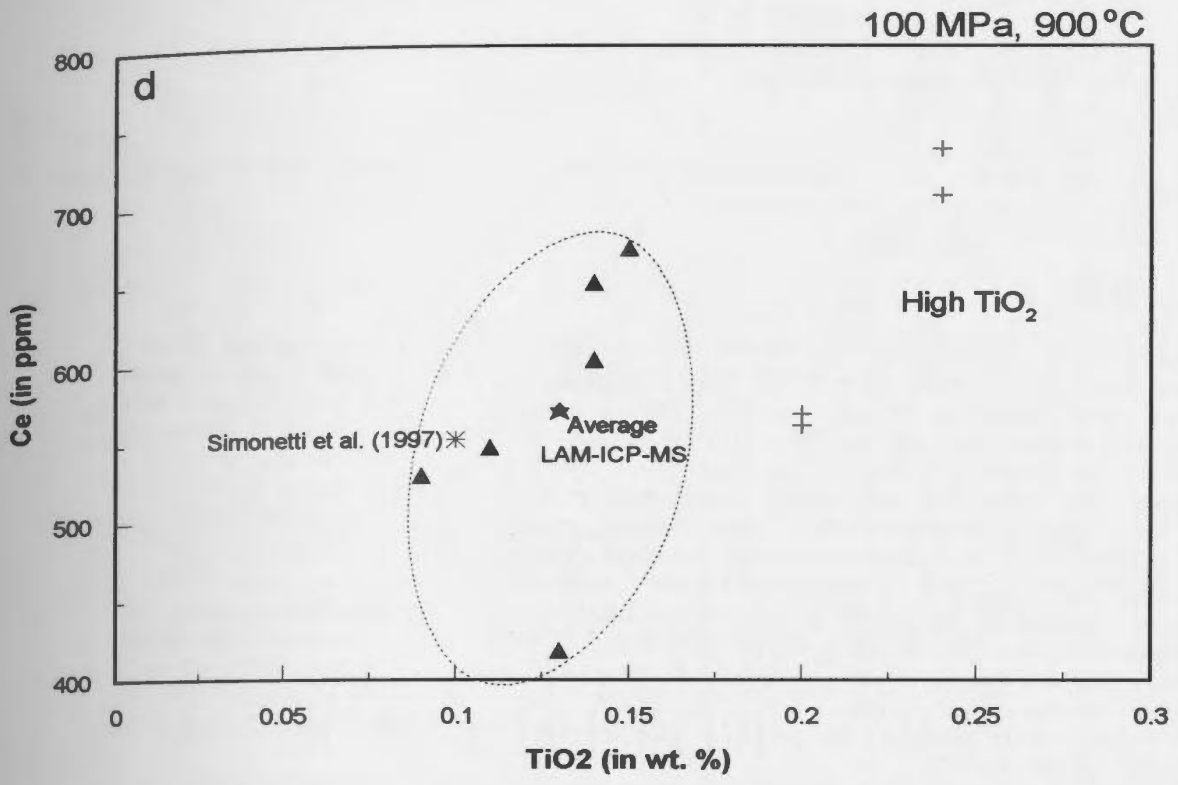
100 MPa, 900 °C
d
800
700
600
500
400
Ce (in ppm)
High TiO2
Simonetti et al. (1997)
Average
LAM-ICP-MS
0
0.05
0.1
0.15
0.2
0.25
0.3
TiO2 (in wt. %)

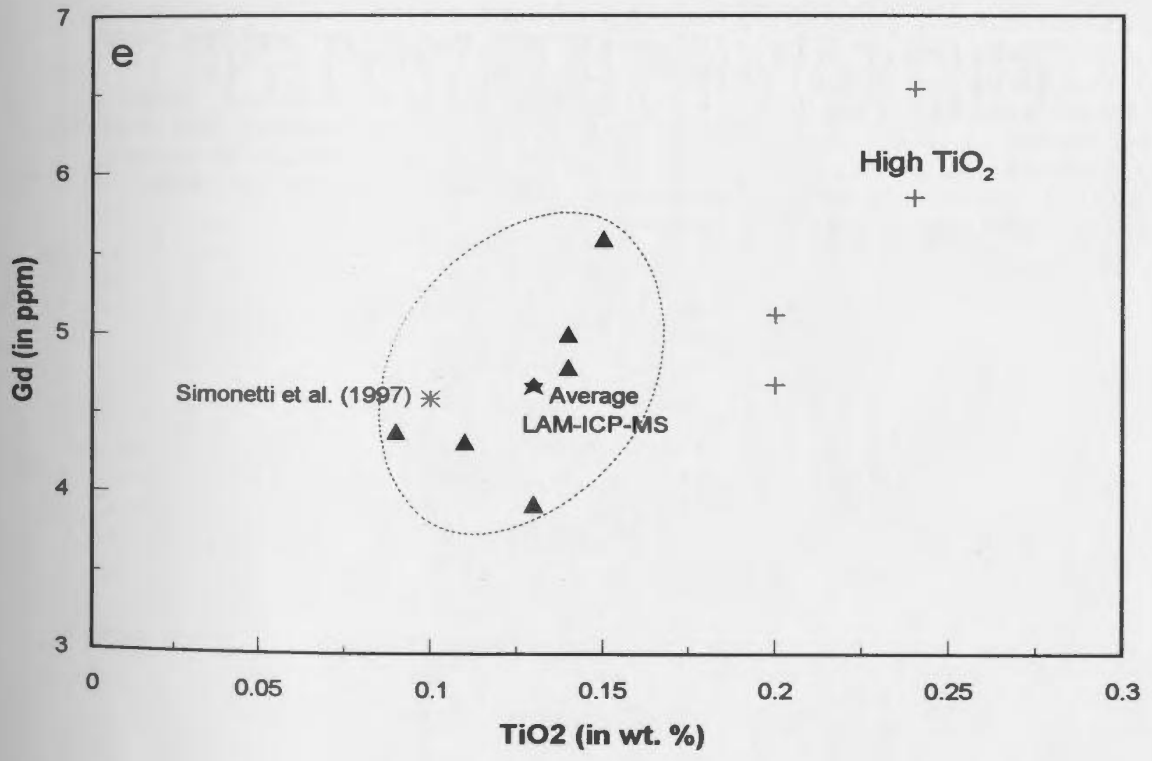
e
7
6
5
4
3
Gd (in ppm)
High TiO2
Simonetti et al. (1997)
Average
LAM-ICP-MS
0
0.05
0.1
0.15
0.2
0.25
0.3
TiO2 (in wt. %)

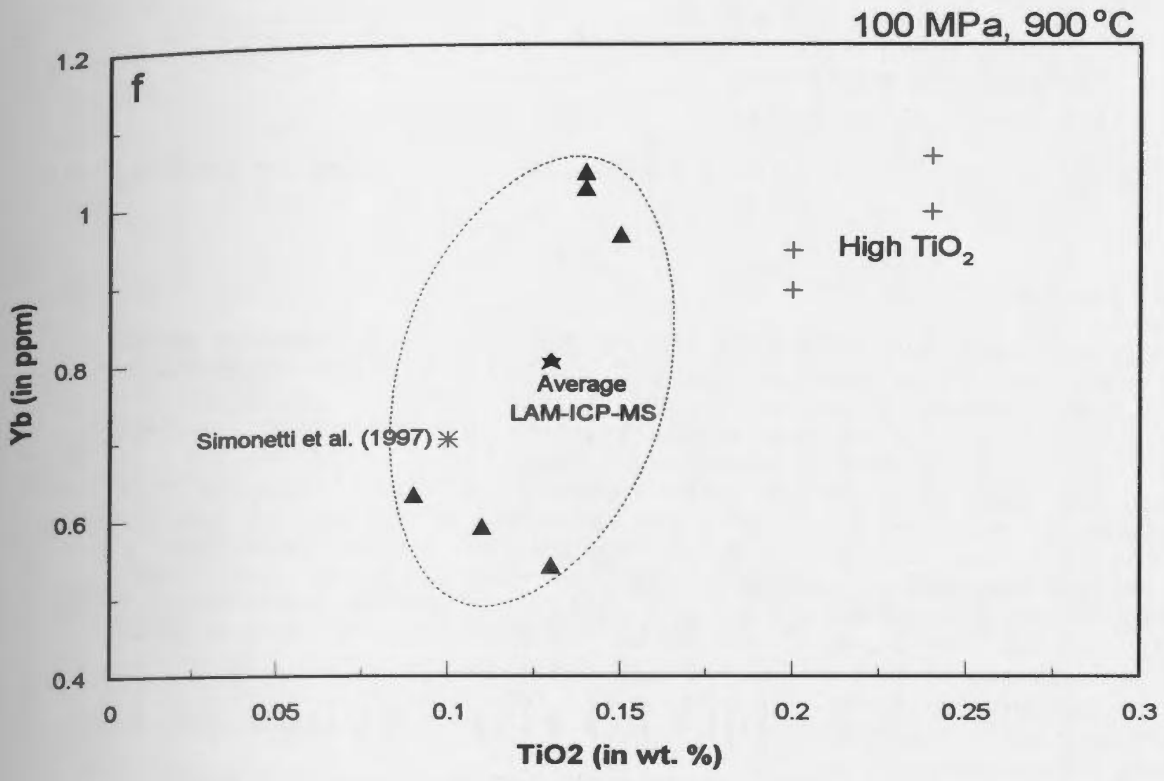
100 MPa, 900 °C
f
1.2
1
0.8
0.6
0.4
Yb (in ppm)
High TiO2
Average
LAM-ICP-MS
Simonetti et al. (1997)
0
0.05
0.1
0.15
0.2
0.25
0.3
TiO2 (in wt. %)

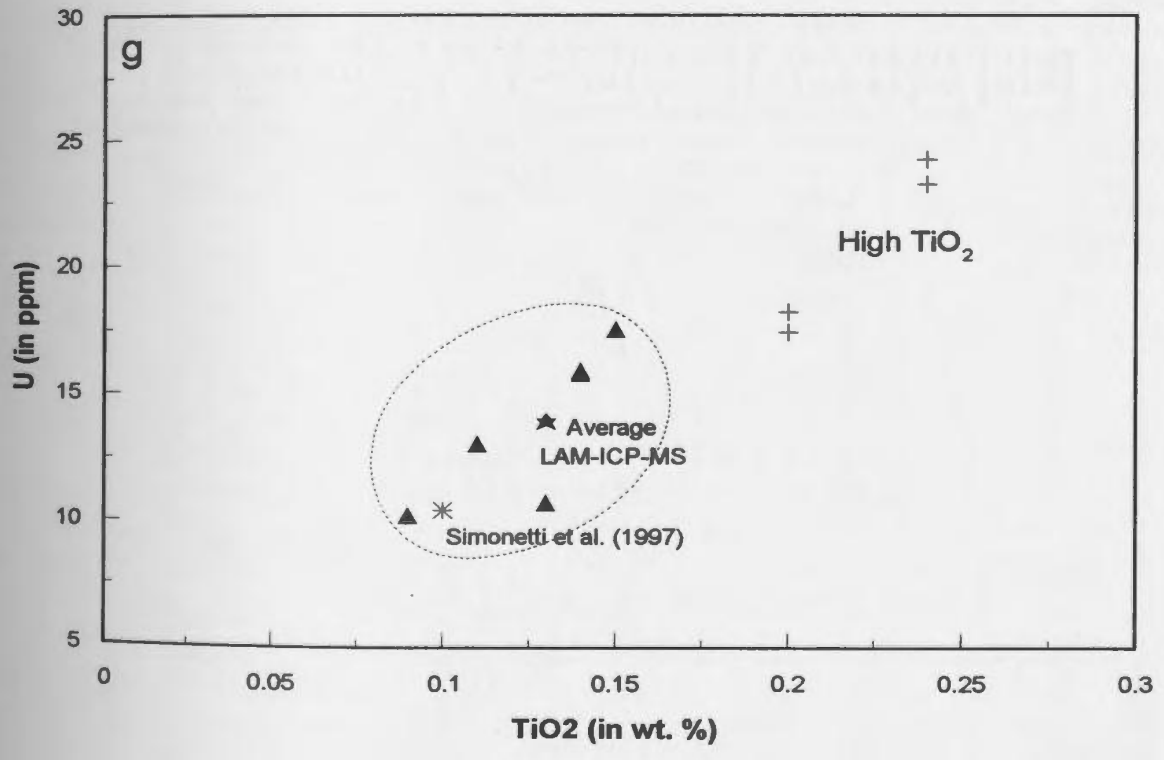
g
30
25
20
15
10
5
U (in ppm)
High TiO2
Average
LAM-ICP-MS
Simonetti et al. (1997)
0
0.05
0.1
0.15
0.2
0.25
0.3
TiO2 (in wt. %)

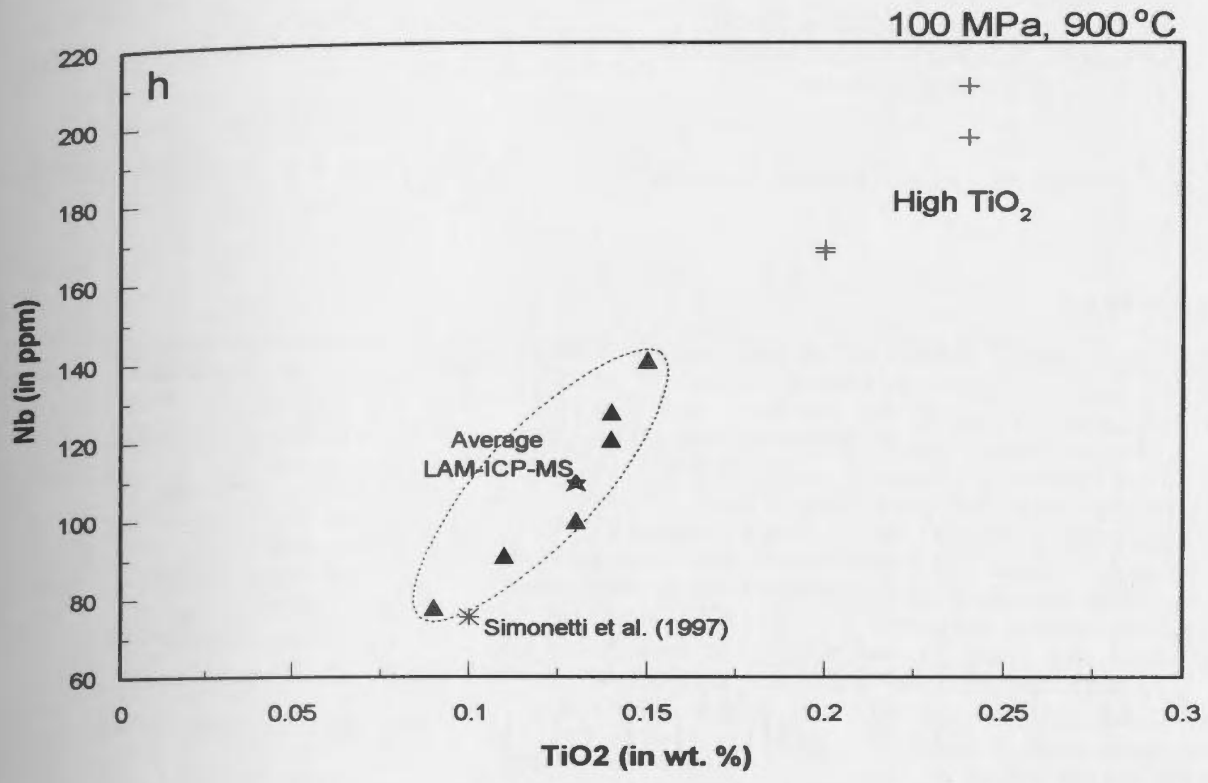
100 MPa, 900 °C
h
High TiO_2
Average
LAM-ICP-MS
Simonetti et al. (1997)
Nb (in ppm)
TiO2 (in wt. %)
220
200
180
160
140
120
100
80
60
0
0.05
0.1
0.15
0.2
0.25
0.3

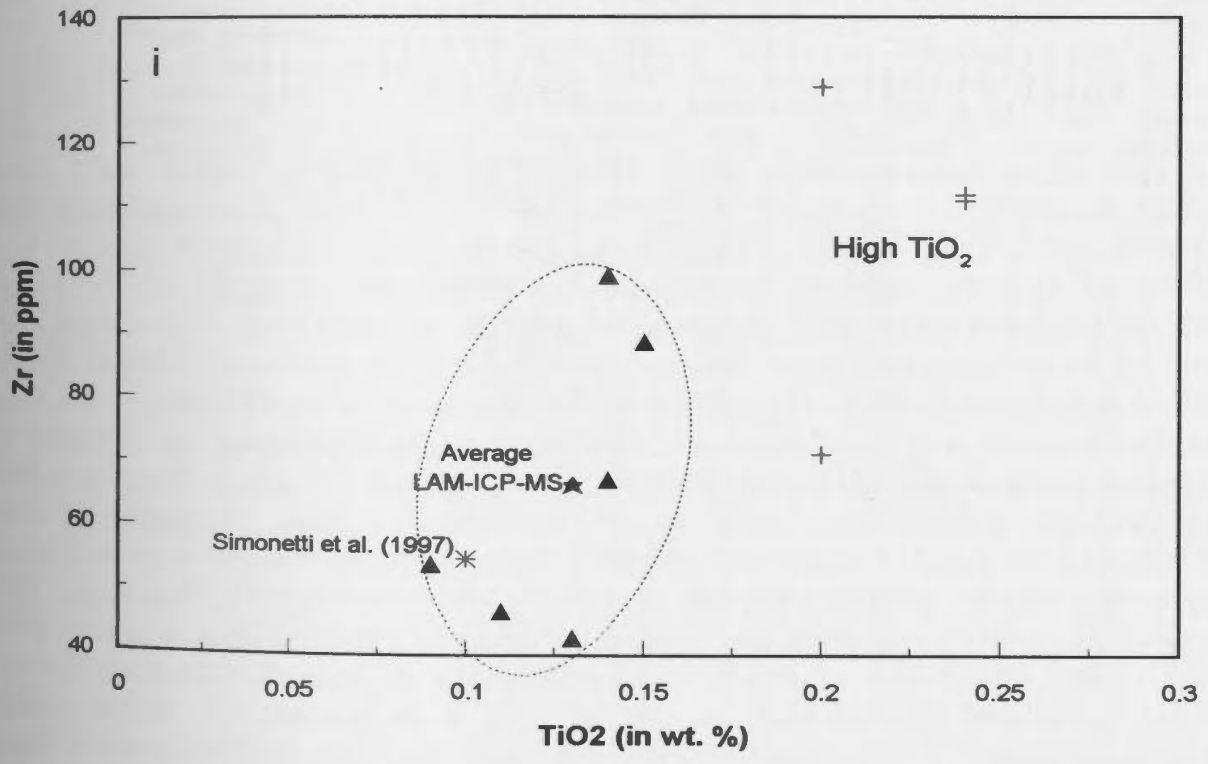
i
High TiO_2
Average
LAM-ICP-MS
Simonetti et al. (1997)
Zr (in ppm)
TiO2 (in wt. %)
140
120
100
80
60
40
0
0.05
0.1
0.15
0.2
0.25
0.3

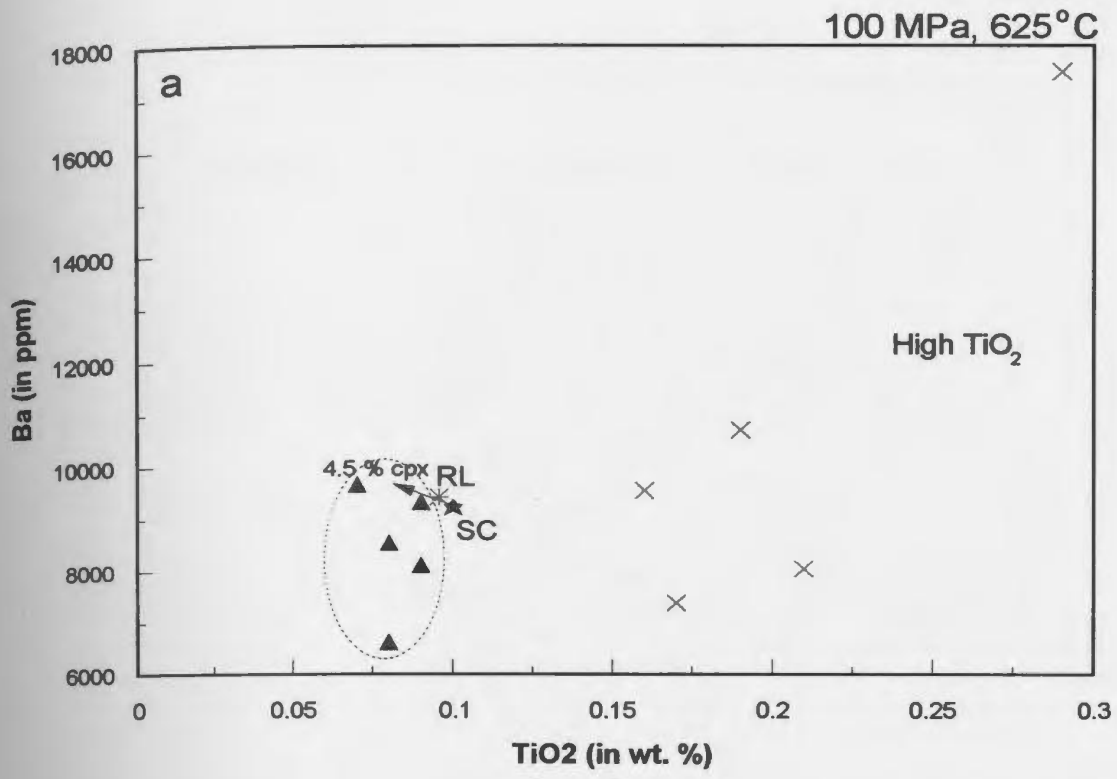

Figure 4.18: Variation diagram for selected trace elements versus TiO_2 for carbonate liquid from experiment CP118 (100 MPa, 625 °C). Elements plotted versus TiO_2 are: (a) Ba; (b) Rb; (c) V; (d) Ce; (e) Gd; (f) Yb; (g) U; (h) Nb; and (i) Zr. The composition of the residual liquid (RL) is calculated by subtracting crystals present in CP118 (see proportions in Tab. 3.9) from the starting composition (SC, represented by ★). Individual analyses which have been rejected for having too high TiO_2 compared to that of the calculated, residual liquid are represented by a cross (x). Individual analyses which have been rejected for having too high or too low concentration of the element plotted on the y-axis compared to that of the calculated, residual liquid are represented by a cross (+). Individual analyses used to calculate the average composition of the liquid are represented by a filled triangle (▲) and are within the area denoted by a dotted line. The arrow represents the direction toward which the composition of the carbonate liquid evolves when 4.5 % clinopyroxene (cpx) is removed from the starting composition (4.5 % is the maximum amount of clinopyroxene that can be subtracted from OL5; higher amounts would lead to negative TiO_2 in the residual liquid). No arrow is drawn to represent the calculated, residual liquid from crystallisation of 2 % nepheline or from the phase assemblage in experiment CP118 because the compositional variation is too small. Individual analyses for the carbonate liquid are from Table A4.2 in Appendix A4, and the calculated concentrations of the residual liquid are given in Table A4.4 in Appendix A4.

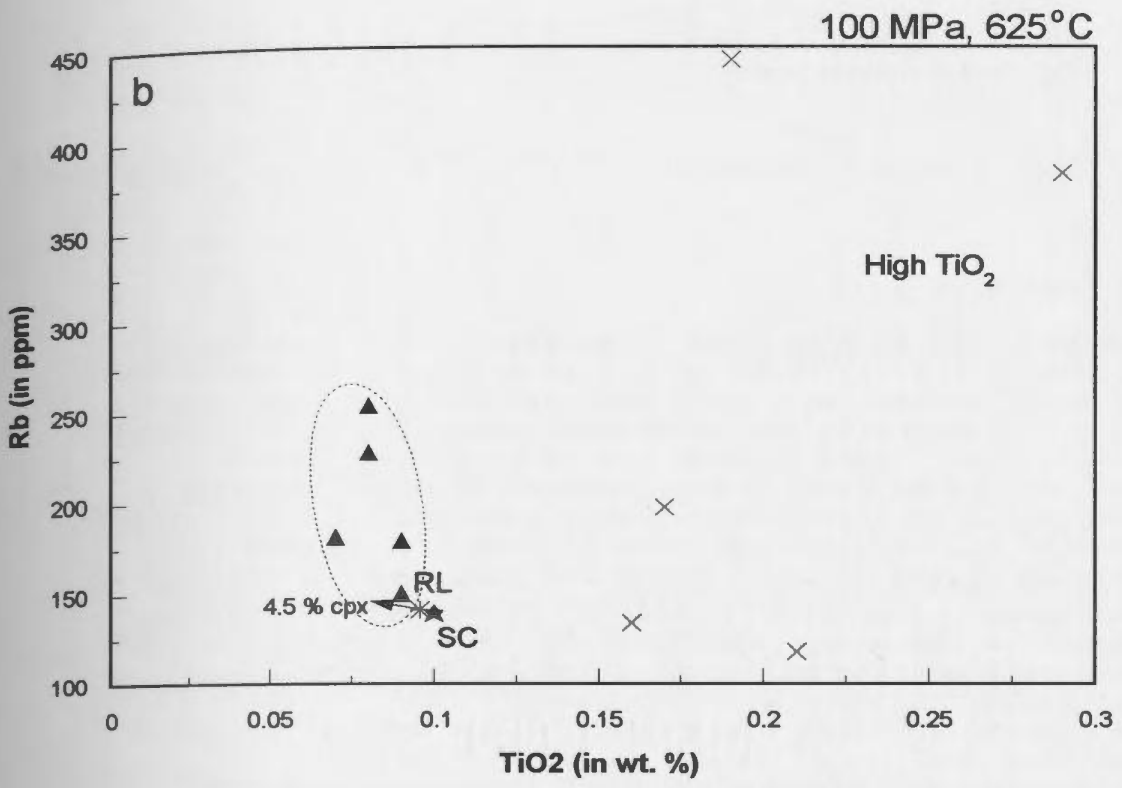
100 MPa, 625°C
b
High TiO2
Rb (in ppm)
TiO2 (in wt. %)
RL
4.5 % cpx
SC
450
400
350
300
250
200
150
100
0
0.05
0.1
0.15
0.2
0.25
0.3

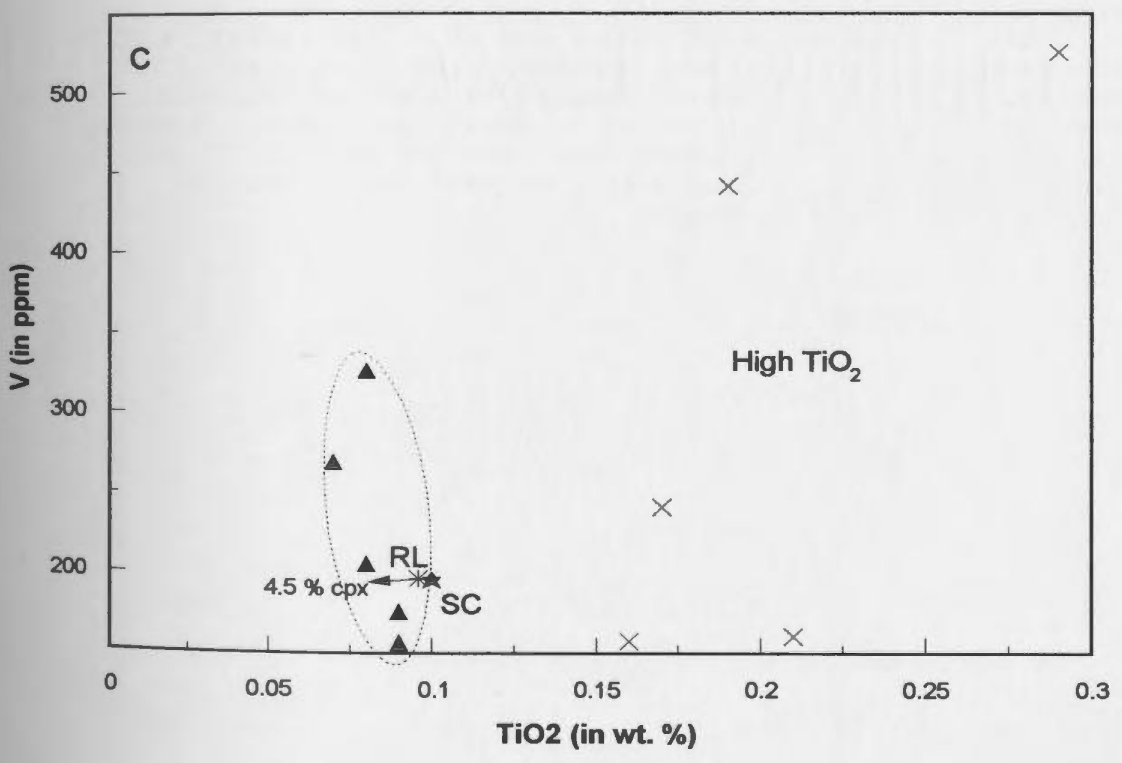
c
High TiO2
V (in ppm)
TiO2 (in wt. %)
RL
4.5 % cpx
SC
500
400
300
200
0
0.05
0.1
0.15
0.2
0.25
0.3

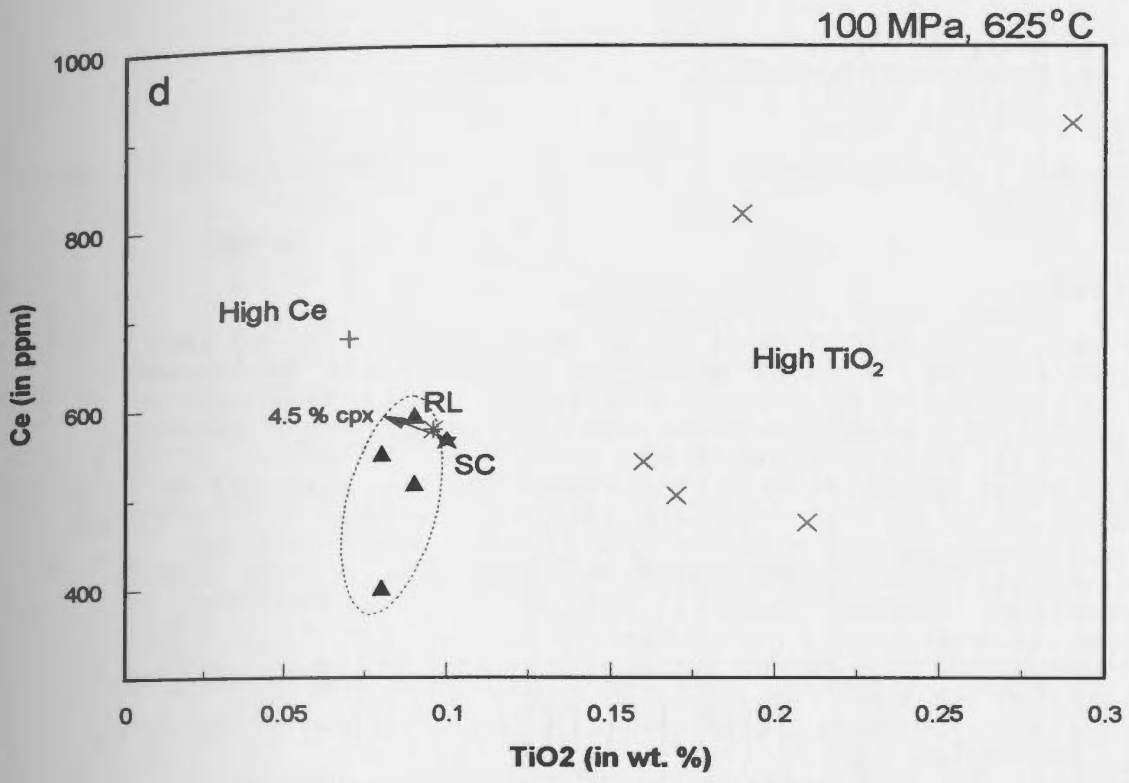
100 MPa, 625°C
d
1000
800
600
400
Ce (in ppm)
High Ce
High TiO2
4.5 % cpx
RL
SC
0
0.05
0.1
0.15
0.2
0.25
0.3
TiO2 (in wt. %)

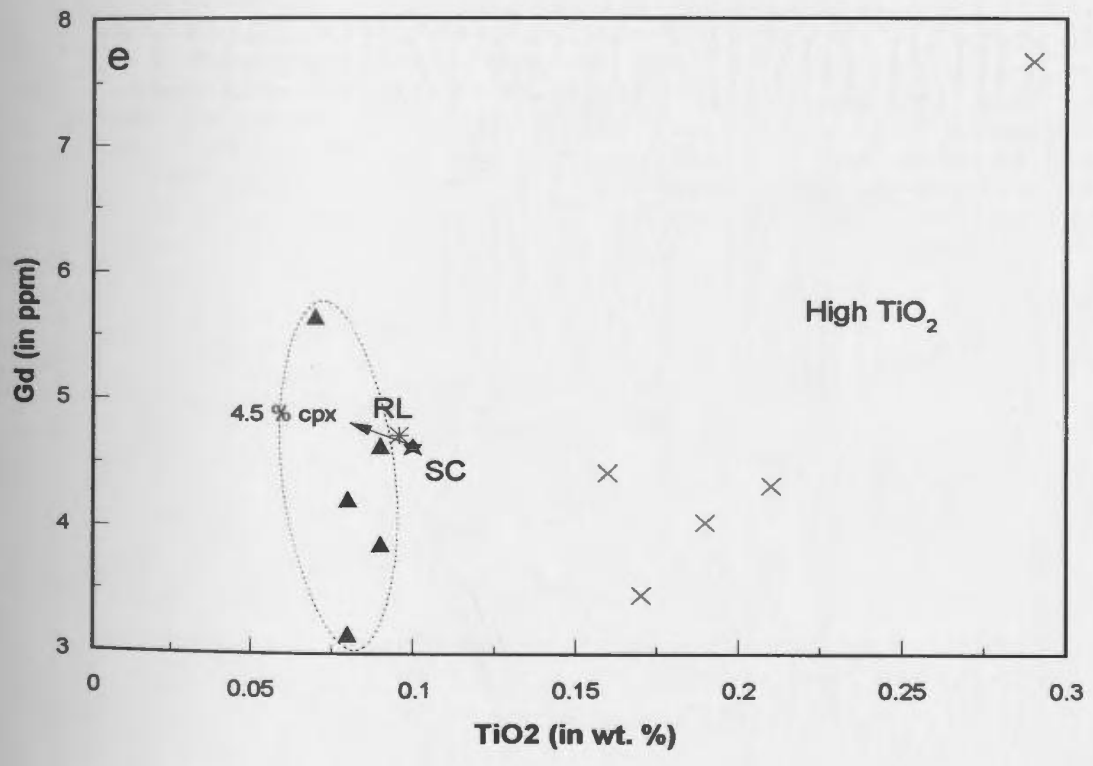
e
8
7
6
5
4
3
Gd (in ppm)
High TiO2
4.5 % cpx
RL
SC
0
0.05
0.1
0.15
0.2
0.25
0.3
TiO2 (in wt. %)

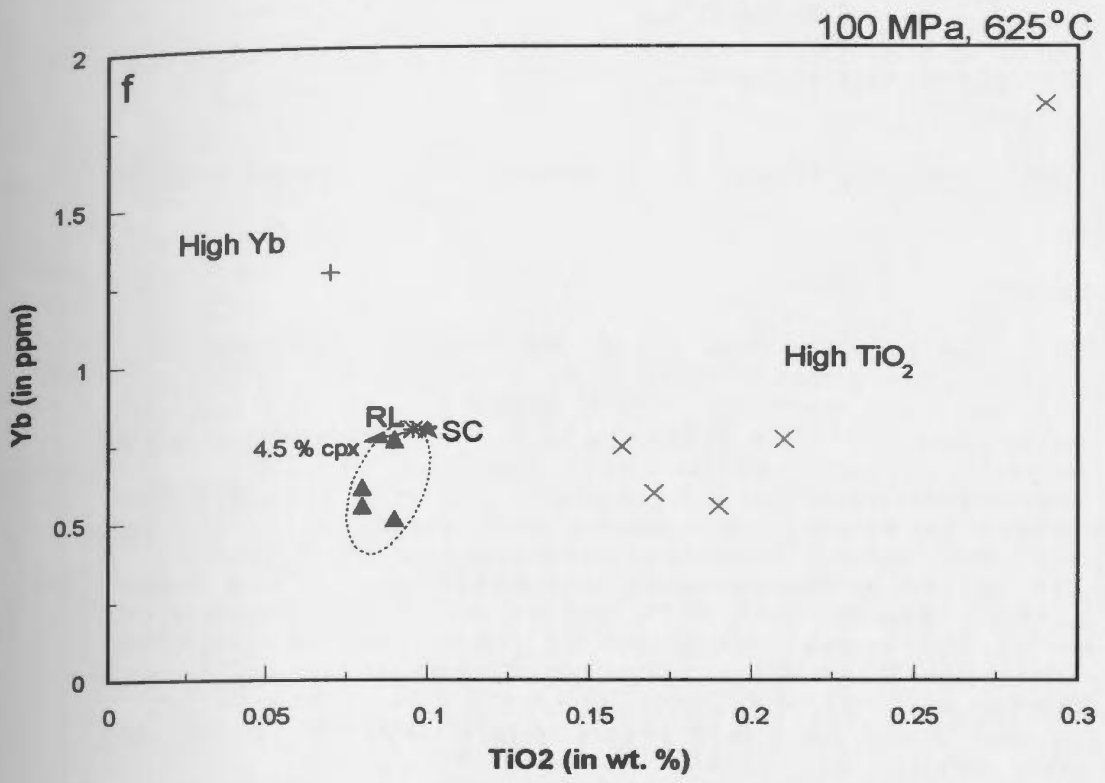
100 MPa, 625°C
f
High Yb
High TiO2
RL
SC
4.5 % cpx
Yb (in ppm)
TiO2 (in wt. %)
0
0.5
1
1.5
2
0.05
0.1
0.15
0.2
0.25
0.3

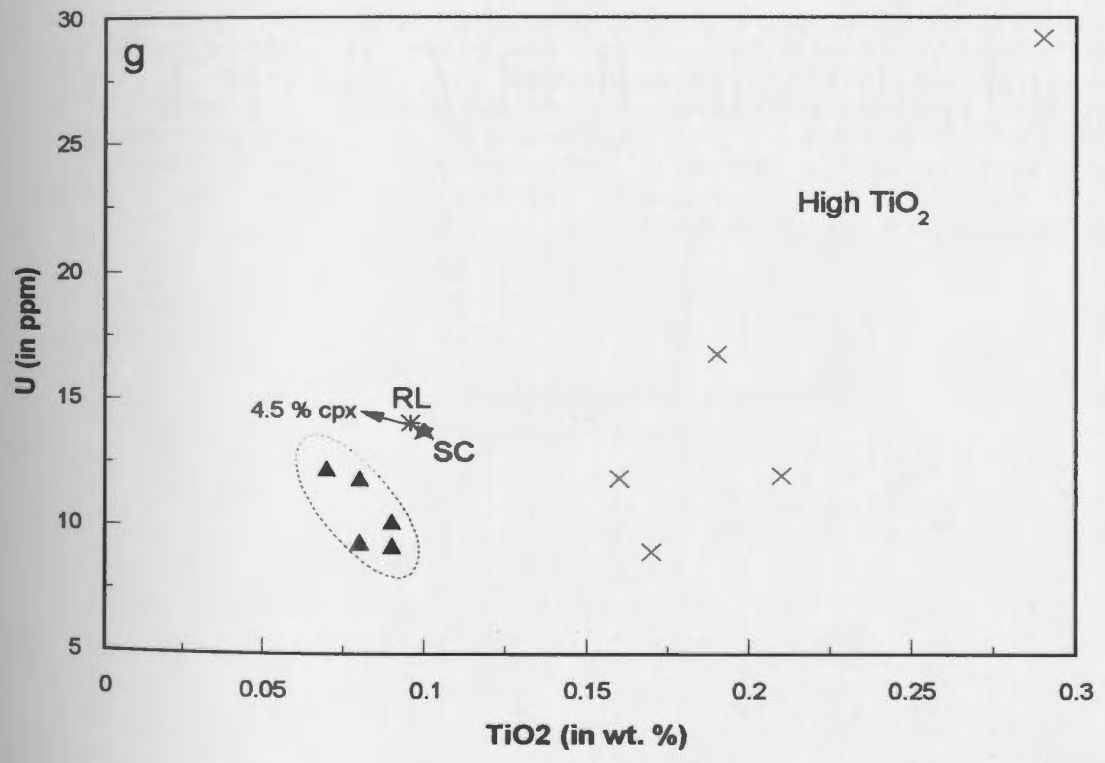
g
High TiO2
RL
SC
4.5 % cpx
U (in ppm)
TiO2 (in wt. %)
5
10
15
20
25
30
0
0.05
0.1
0.15
0.2
0.25
0.3

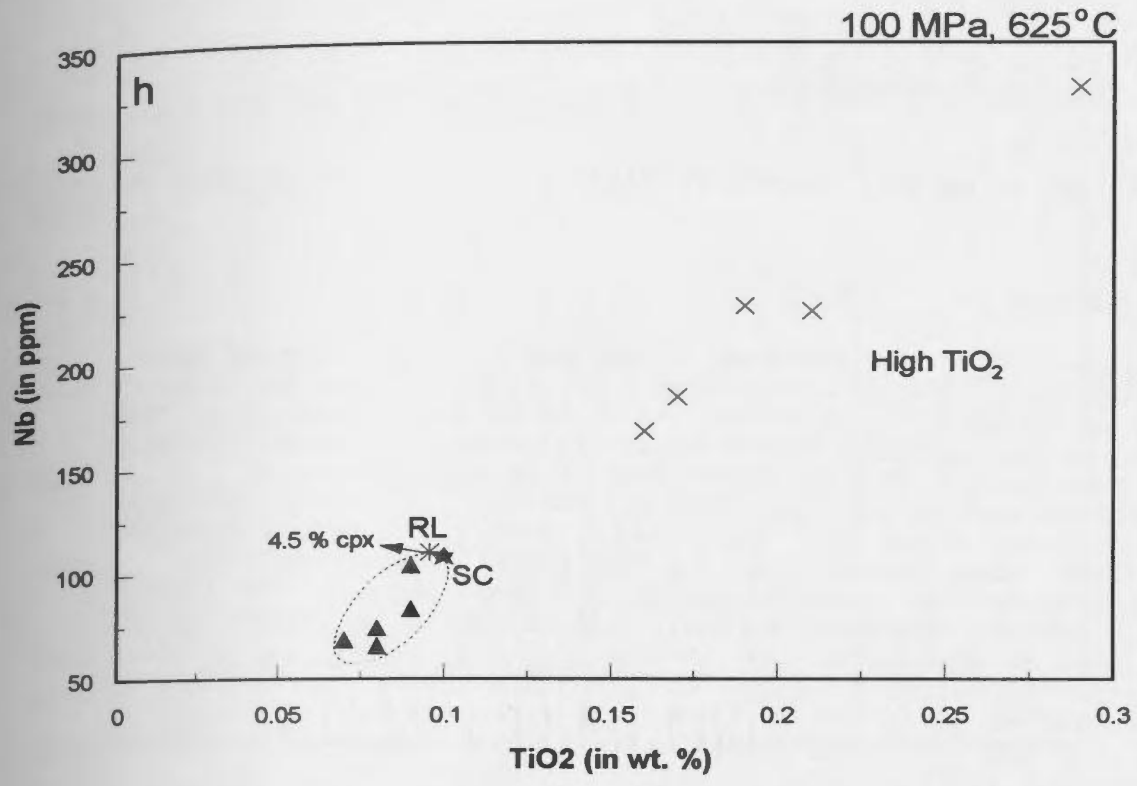
100 MPa, 625°C
h
Nb (in ppm)
TiO2 (in wt. %)
High TiO2
4.5 % cpx
RL
SC
350
300
250
200
150
100
50
0
0.05
0.1
0.15
0.2
0.25
0.3

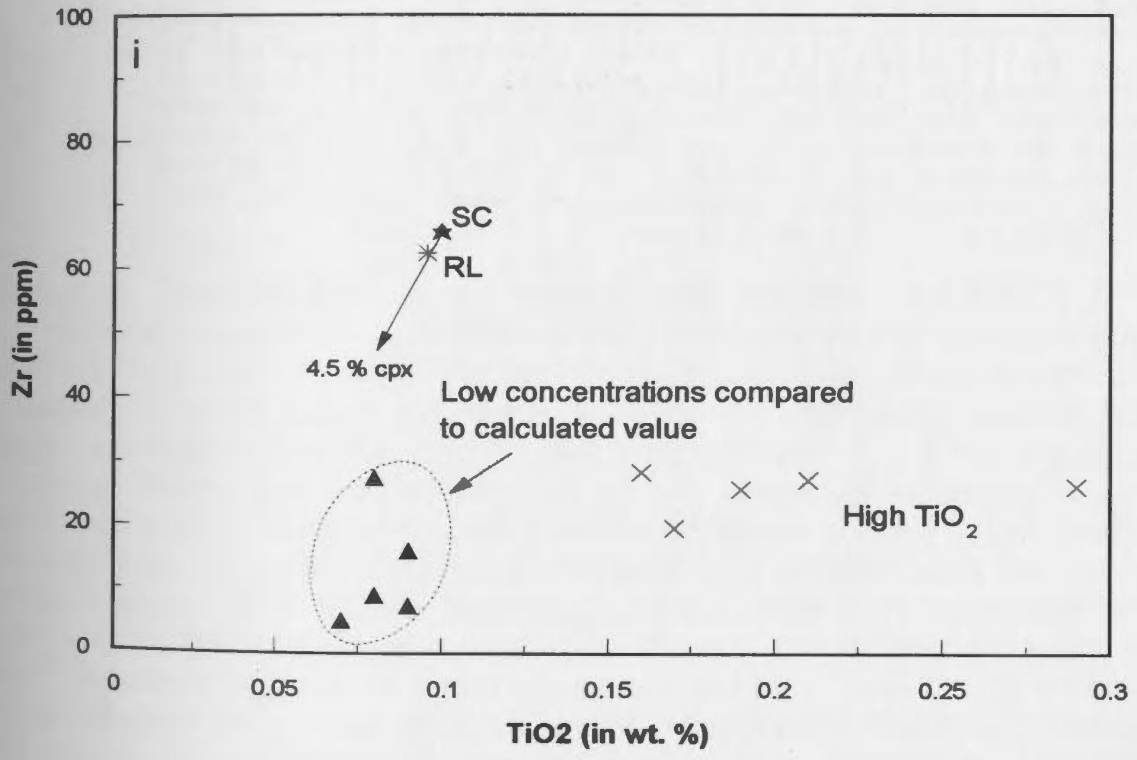
i
Zr (in ppm)
TiO2 (in wt. %)
SC
RL
4.5 % cpx
Low concentrations compared
to calculated value
High TiO2
100
80
60
40
20
0
0
0.05
0.1
0.15
0.2
0.25
0.3

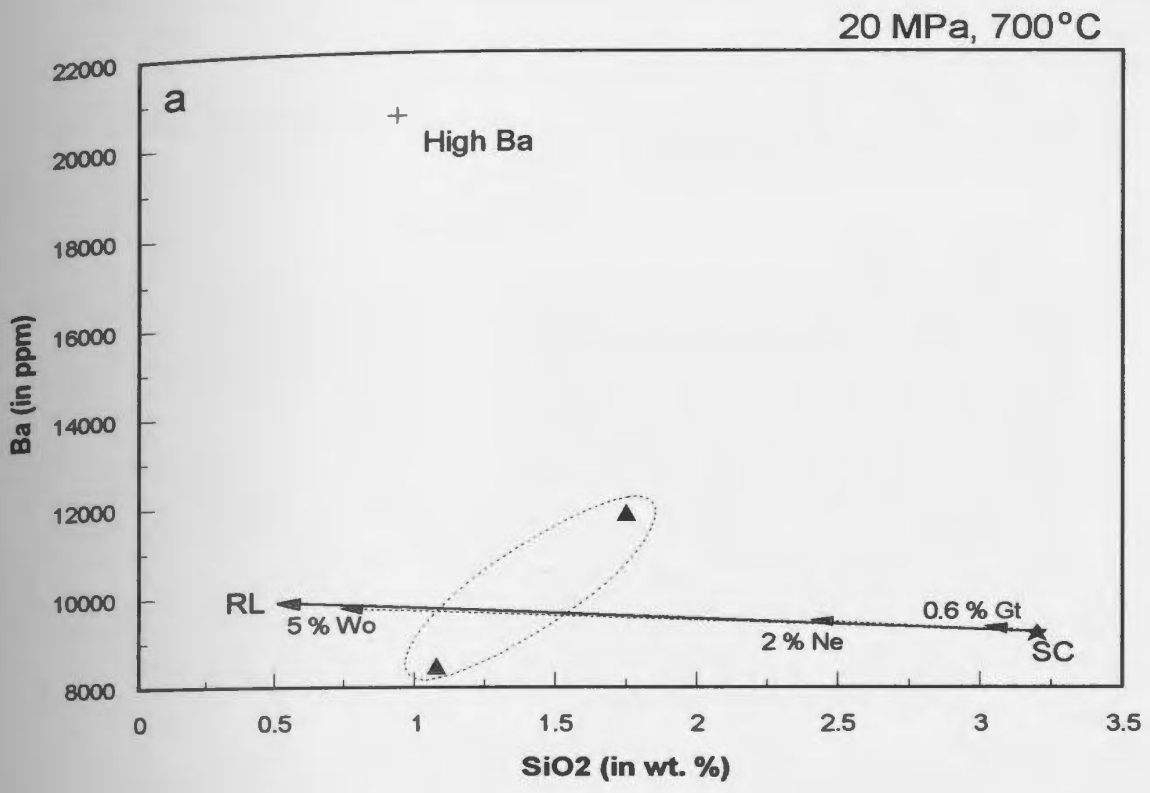

Figure 4.19: Variation diagram for selected trace elements versus SiO_2 for carbonate liquid from experiment CP57 (20 MPa, 700 °C). Elements plotted versus SiO_2 are: (a) Ba; (b) Rb; (c) V; (d) Ce; (e) Gd; (f) Yb; (g) U; (h) Nb; and (i) Zr. The thick arrow represents the direction toward which the composition of the calculated, residual liquid (RL) evolves when crystals present in CP57 (see proportions in Tab. 3.9) are subtracted from the starting composition (SC, represented by ★). Other arrows represent the direction toward which the composition of the carbonate liquid evolves when each crystal is subtracted from the bulk composition (proportion of crystals used for the calculation labelled at the end of the arrow). Individual analyses which have been rejected for having too high or too low of a concentration of the element plotted on the y-axis compared to that of the calculated, residual liquid are represented by a cross (+). Individual analyses used to calculate the average composition of the carbonate liquid are represented by a filled triangle (▲) and are within the area denoted by a dotted line. Abbreviation used are: Ne: nepheline; Gt: melanite garnet; Wo: wollastonite. Individual analyses for the carbonate liquid are from Table A4.2 in Appendix A4, and the calculated concentrations of the residual liquid are given in Table A4.4 in Appendix A4.

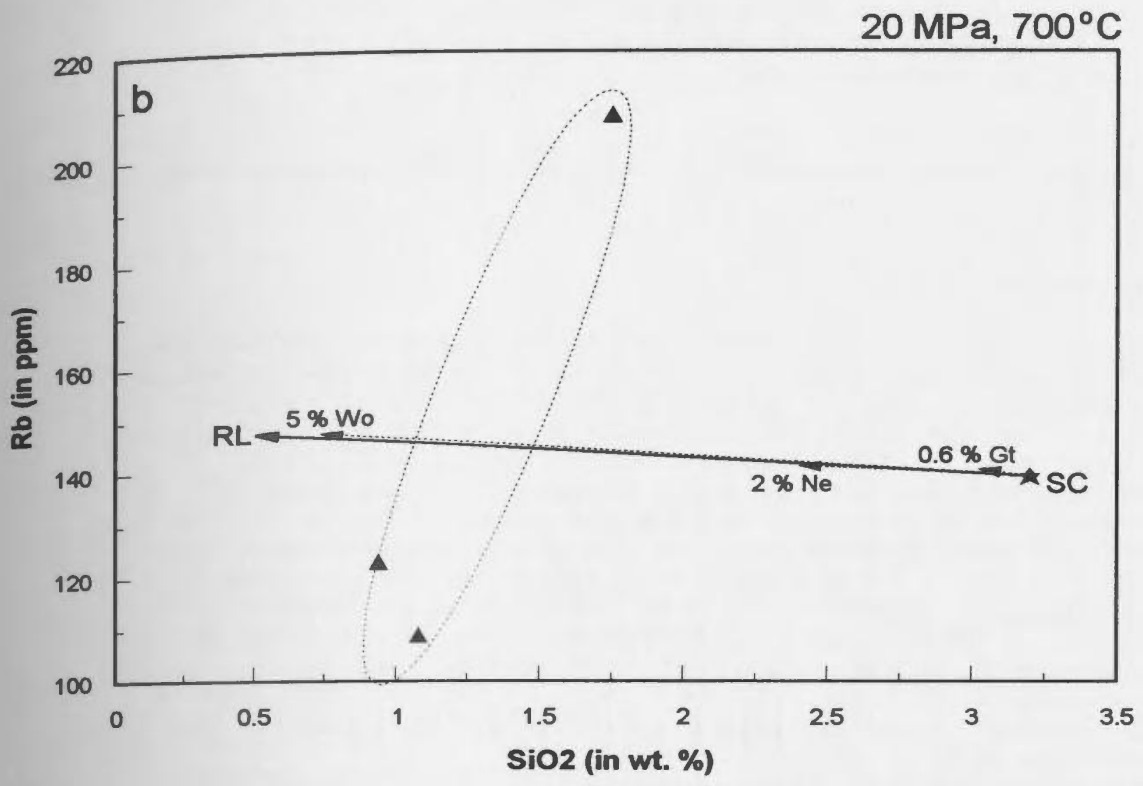
20 MPa, 700°C
b
Rb (in ppm)
SiO2 (in wt. %)
RL
5 % Wo
2 % Ne
0.6 % Gt
SC
220
200
180
160
140
120
100
0
0.5
1
1.5
2
2.5
3
3.5

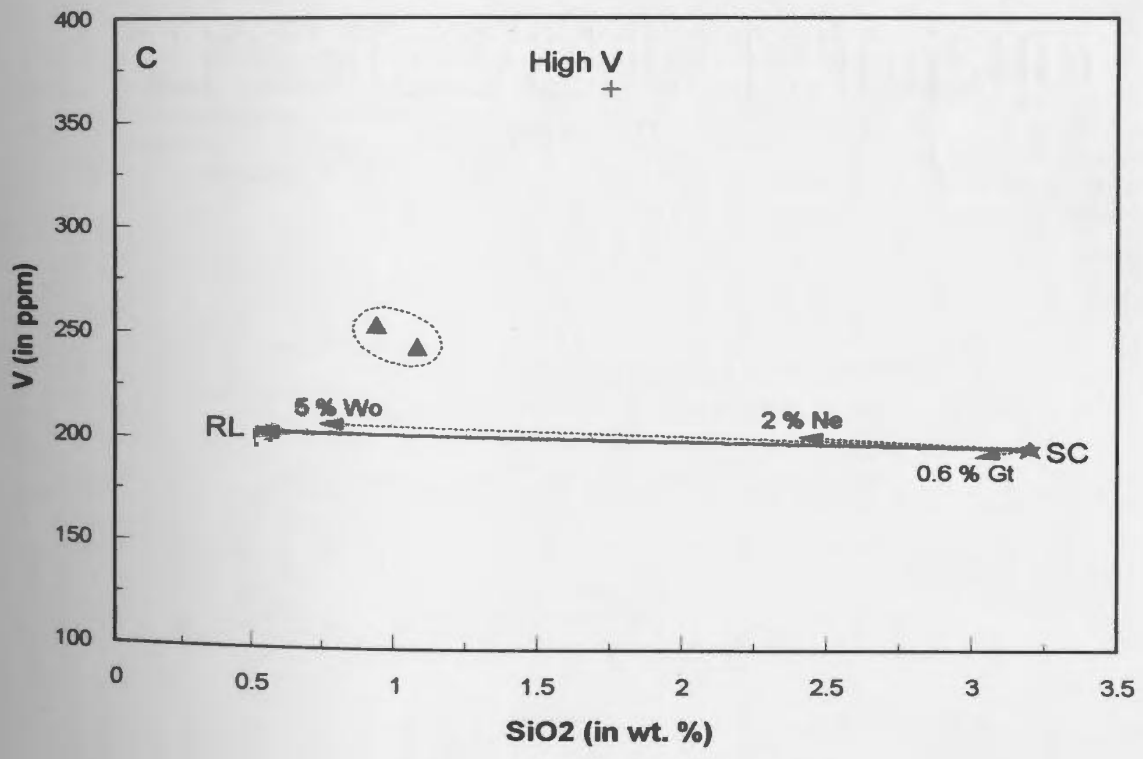
C
High V
V (in ppm)
SiO2 (in wt. %)
RL
5 % Wo
2 % Ne
0.6 % Gt
SC
400
350
300
250
200
150
100
0
0.5
1
1.5
2
2.5
3
3.5

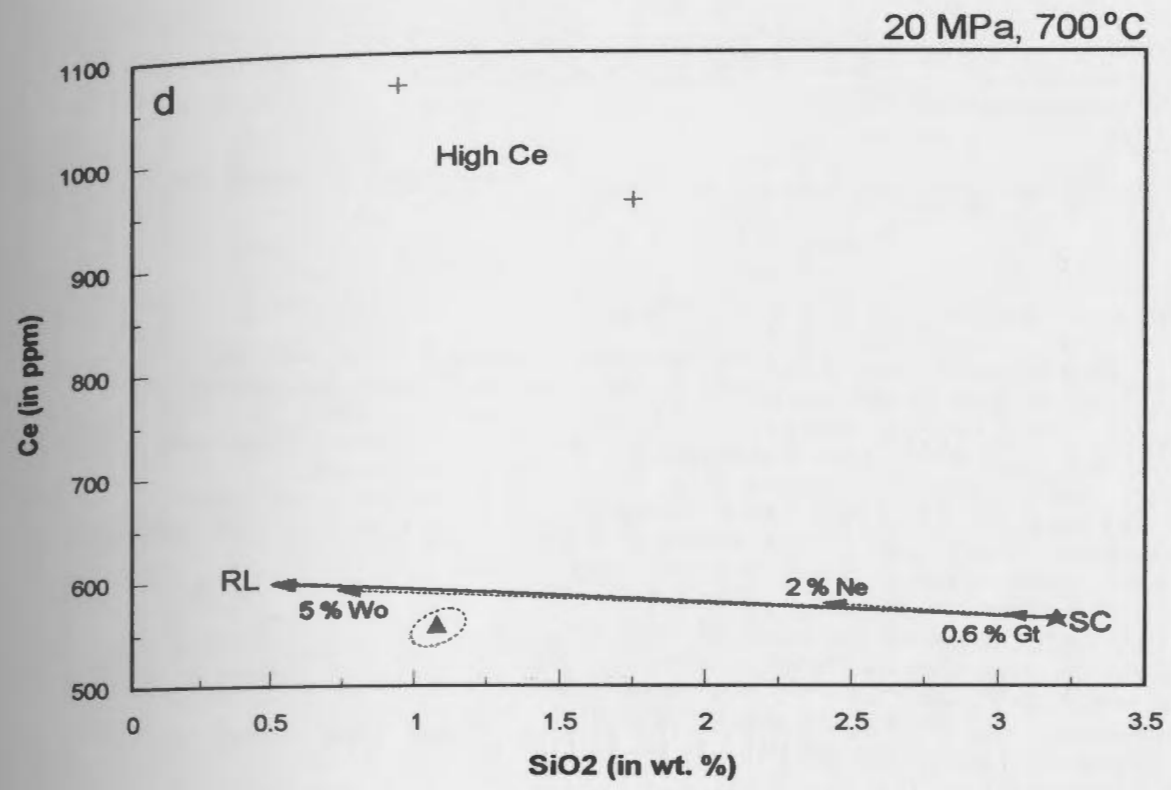
20 MPa, 700 °C
d
High Ce
RL
5 % Wo
2 % Ne
0.6 % Gt
SC
Ce (in ppm)
SiO2 (in wt. %)

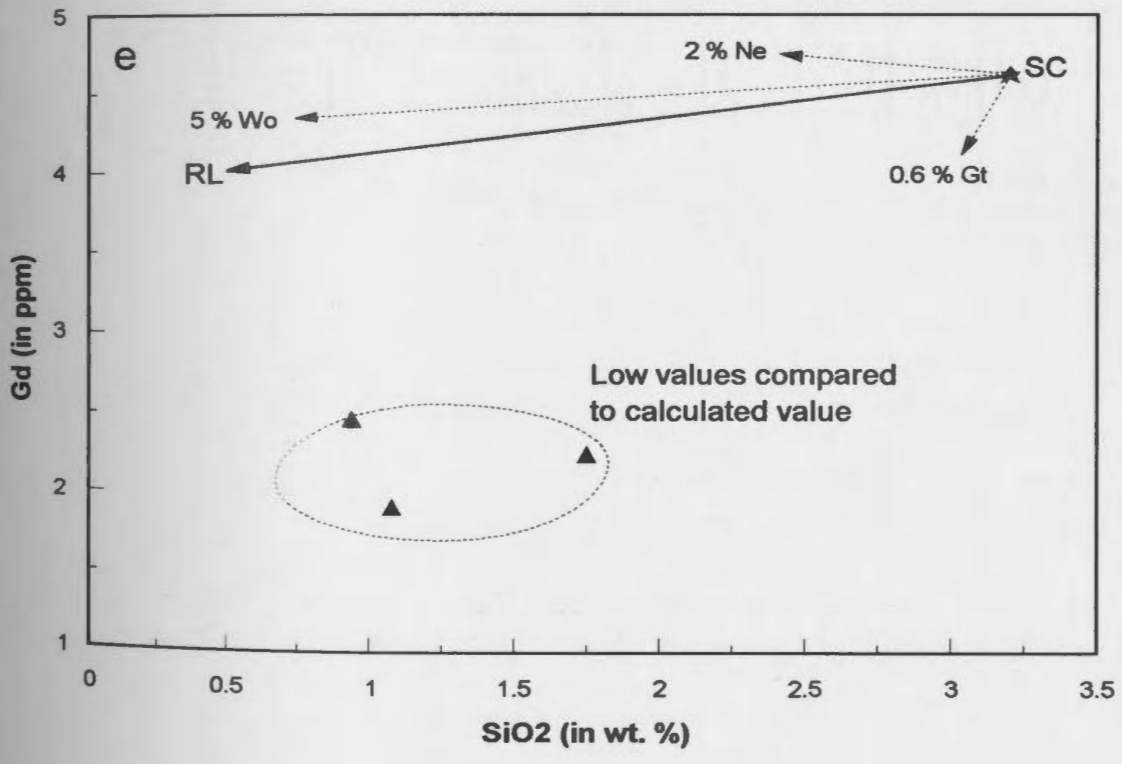
e
2 % Ne
SC
5 % Wo
RL
0.6 % Gt
Low values compared
to calculated value
Gd (in ppm)
SiO2 (in wt. %)

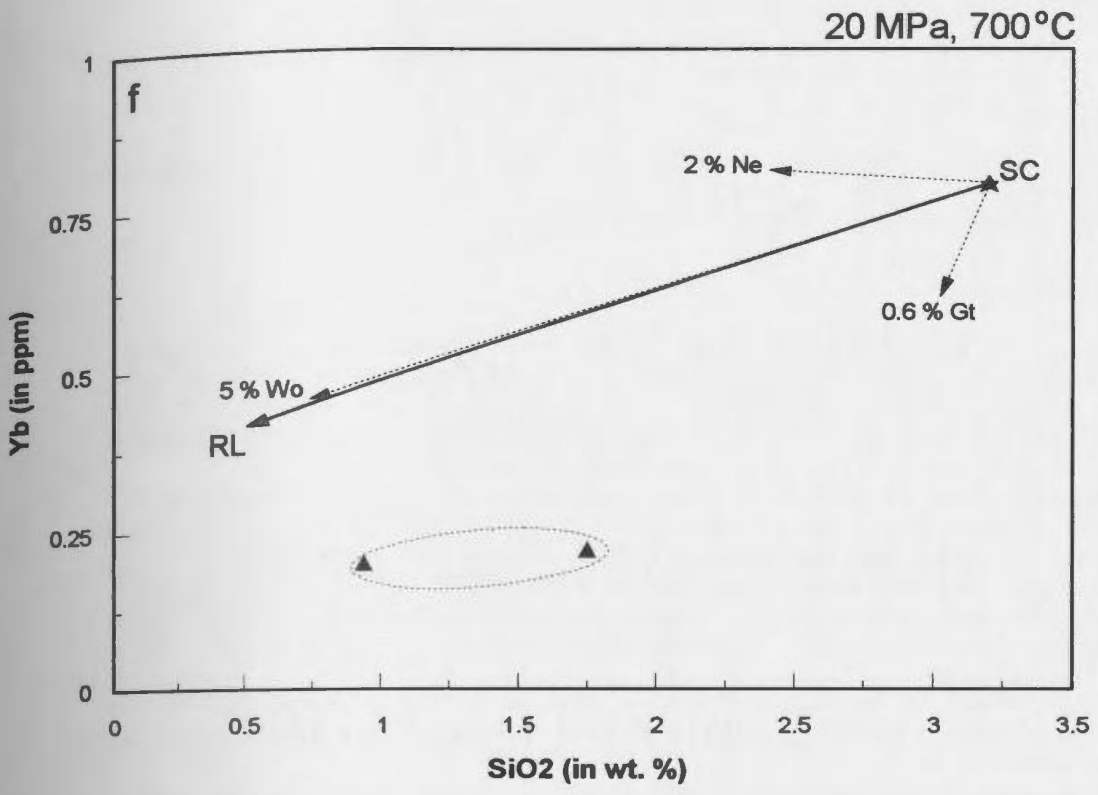
20 MPa, 700°C
f
2 % Ne
SC
0.6 % Gt
5 % Wo
RL
Yb (in ppm)
SiO2 (in wt. %)
1
0.75
0.5
0.25
0
0
0.5
1
1.5
2
2.5
3
3.5

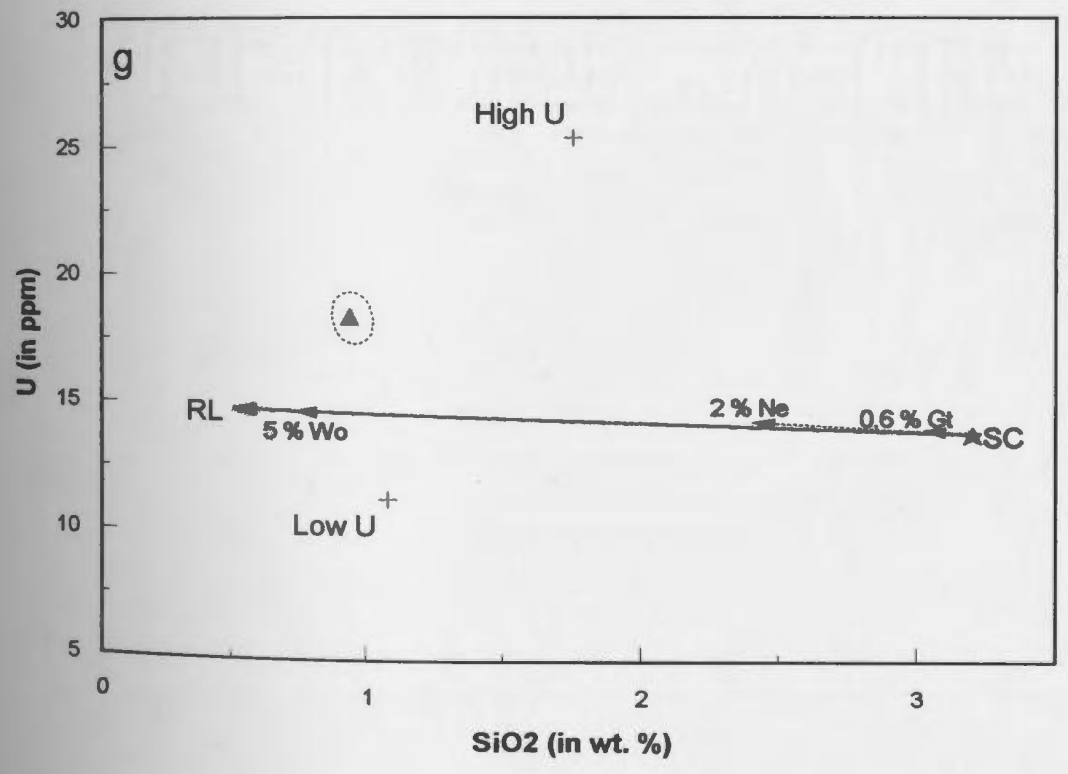
g
High U
RL
5 % Wo
2 % Ne
0.6 % Gt
SC
Low U
U (in ppm)
SiO2 (in wt. %)
30
25
20
15
10
5
0
1
2
3

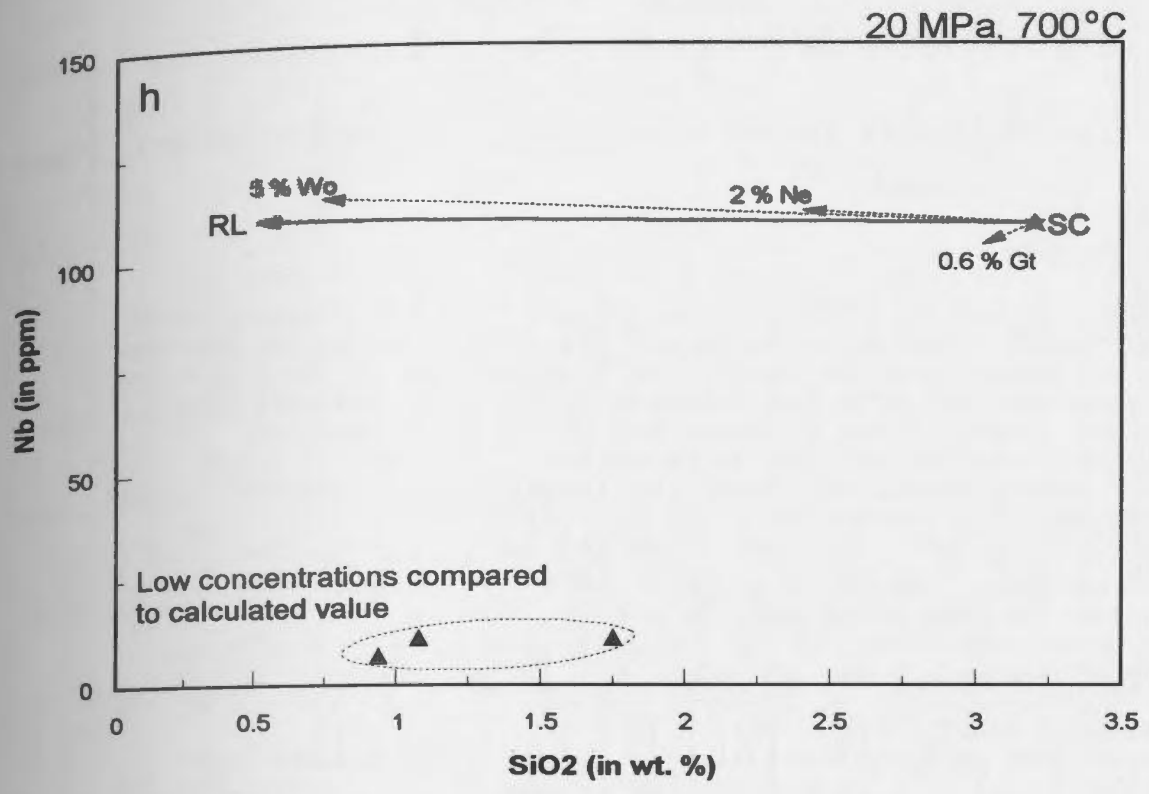
20 MPa, 700°C
h
5 % Wo
2 % Ne
RL
SC
0.6 % Gt
Low concentrations compared
to calculated value
Nb (in ppm)
SiO2 (in wt. %)
150
100
50
0
0
0.5
1
1.5
2
2.5
3
3.5

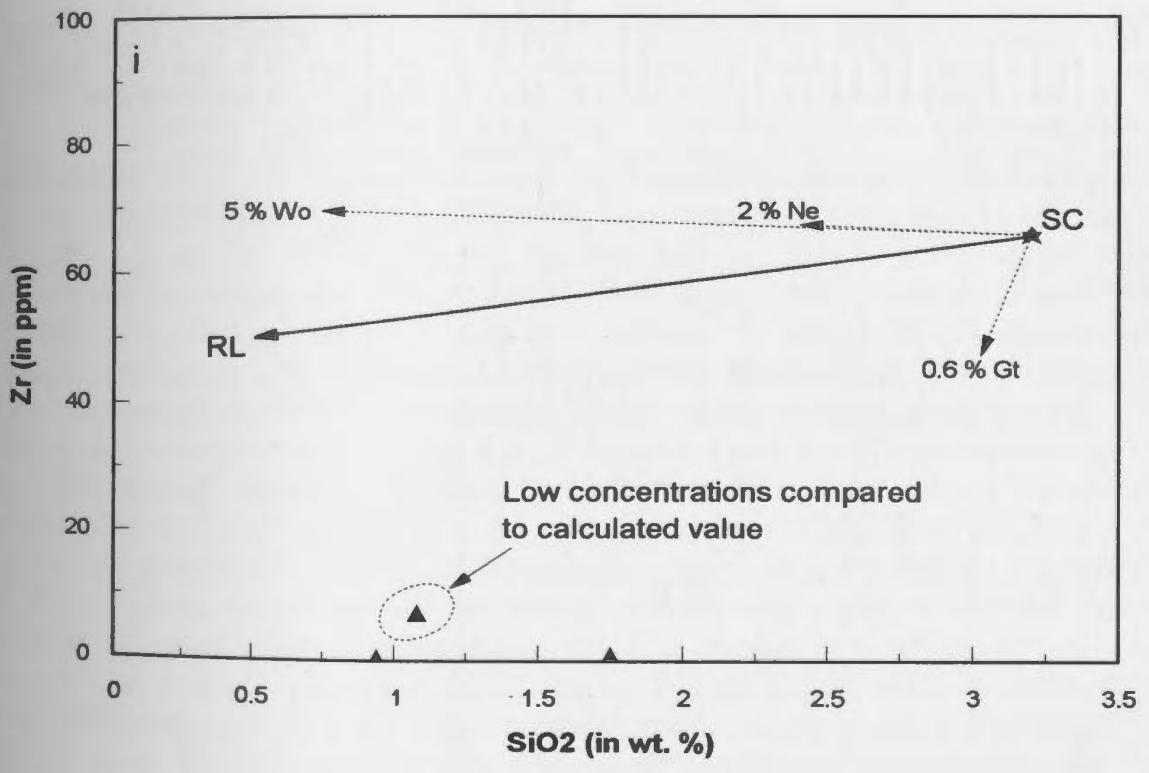
i
5 % Wo
2 % Ne
SC
RL
0.6 % Gt
Low concentrations compared
to calculated value
Zr (in ppm)
SiO2 (in wt. %)
100
80
60
40
20
0
0
0.5
1
1.5
2
2.5
3
3.5

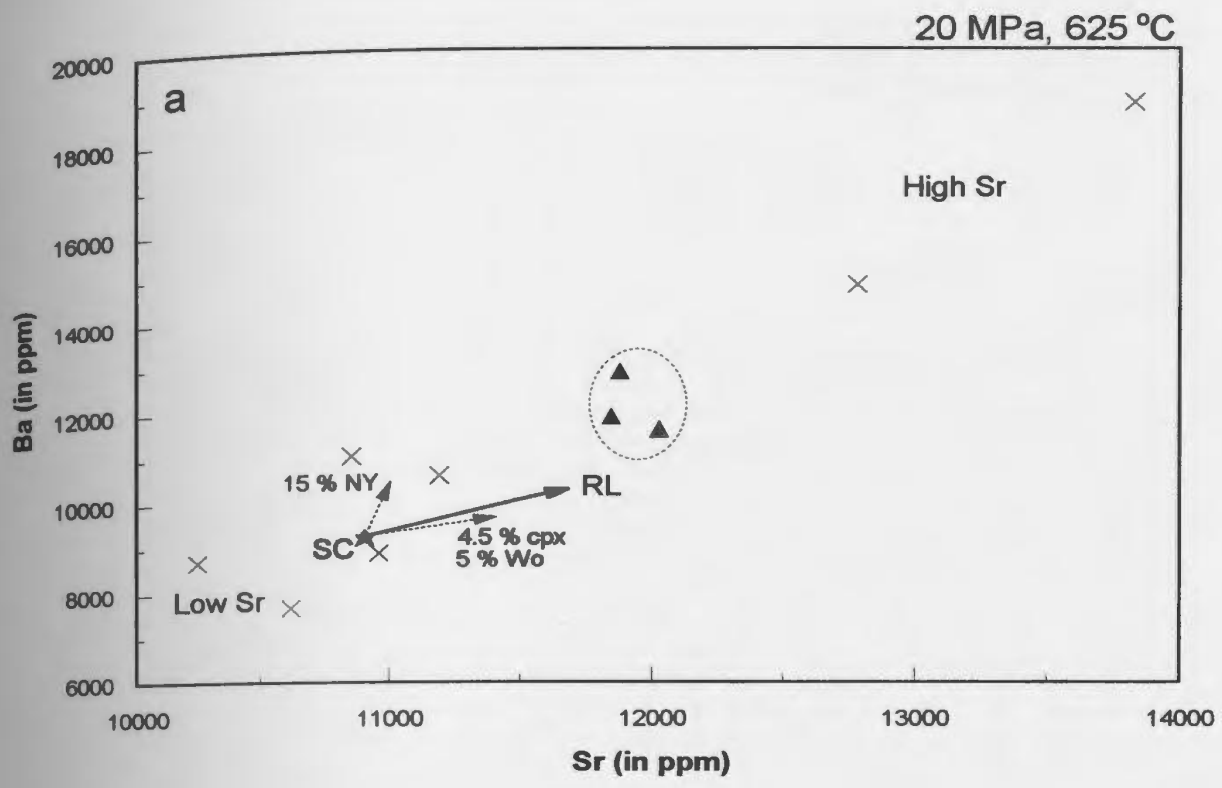

Figure 4.20: Variation diagram for selected trace elements versus Sr for carbonate liquid from experiment CP129 (20 MPa, 625 °C). Elements plotted versus Sr are: (a) Ba; (b) Rb; (c) V; (d) Ce; (e) Gd; (f) Yb; (g) U; (h) Nb; and (i) Zr. The thick arrow represents the direction toward which the composition of the calculated, residual liquid (RL) evolves when crystals present in CP129 (see proportions in Tab. 3.9) are subtracted from the starting composition (SC, represented by ★). Other arrows represent the direction toward which the composition of the carbonate liquid evolves when each crystal is subtracted from the bulk composition (proportion of crystals used for the calculation labelled at the end of the arrow). Individual analyses which have been rejected for having too high or too low of a Sr value compared to that of the calculated, residual liquid are represented by a cross (x). Individual analyses which have been rejected for having too high or too low of a concentration of the element plotted on the y-axis compared to that of the calculated, residual liquid are represented by a cross (+). Individual analyses used to calculate the average composition of the carbonate liquid are represented by a filled triangle (▲) and are within the area denoted by a dotted line. Abbreviation used are: Cpx: clinopyroxene; Gt: melanite garnet; Wo: wollastonite; NY: nyerereite; Ap: apatite; tit: titanite; pvk: perovskite. Individual analyses for the carbonate liquid are from Table A4.2 in Appendix A4, and the calculated concentrations of the residual liquid are given in Table A4.4 in Appendix A4.

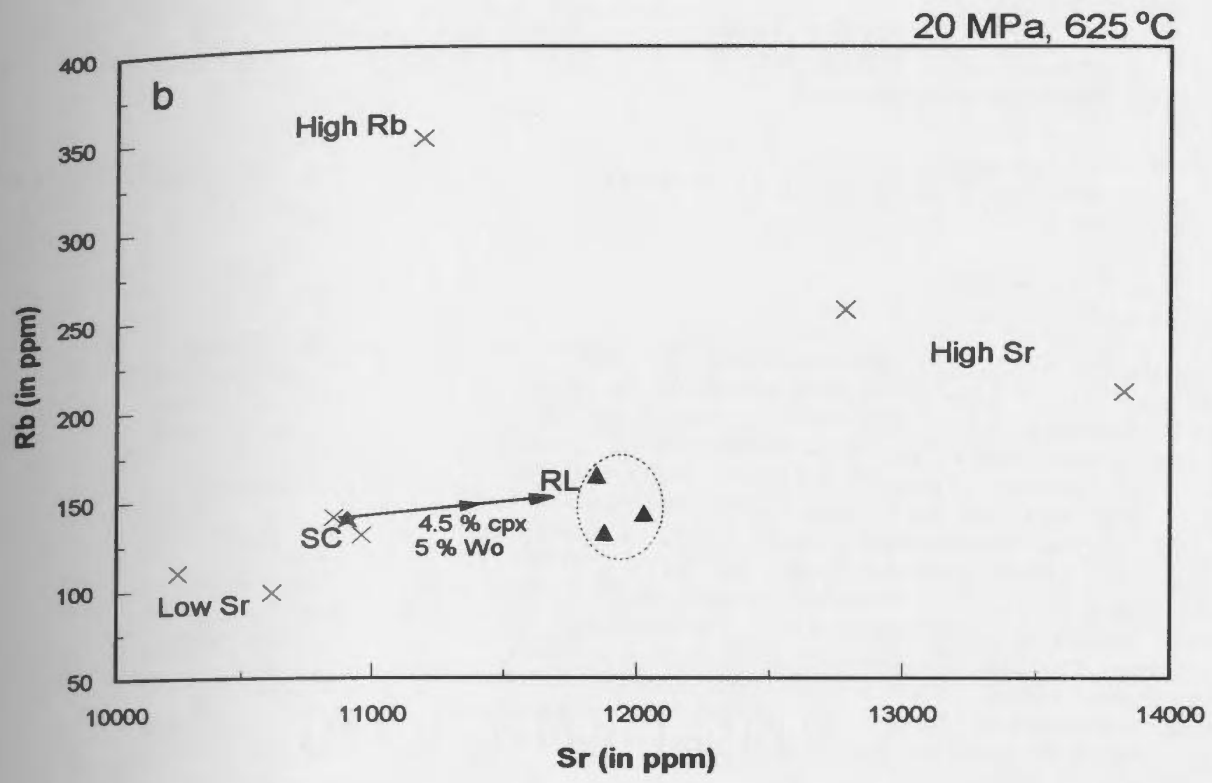
20 MPa, 625 °C
b
High Rb
High Sr
Low Sr
RL
SC
4.5 % cpx
5 % Wo
Rb (in ppm)
Sr (in ppm)
400
350
300
250
200
150
100
50
10000
11000
12000
13000
14000

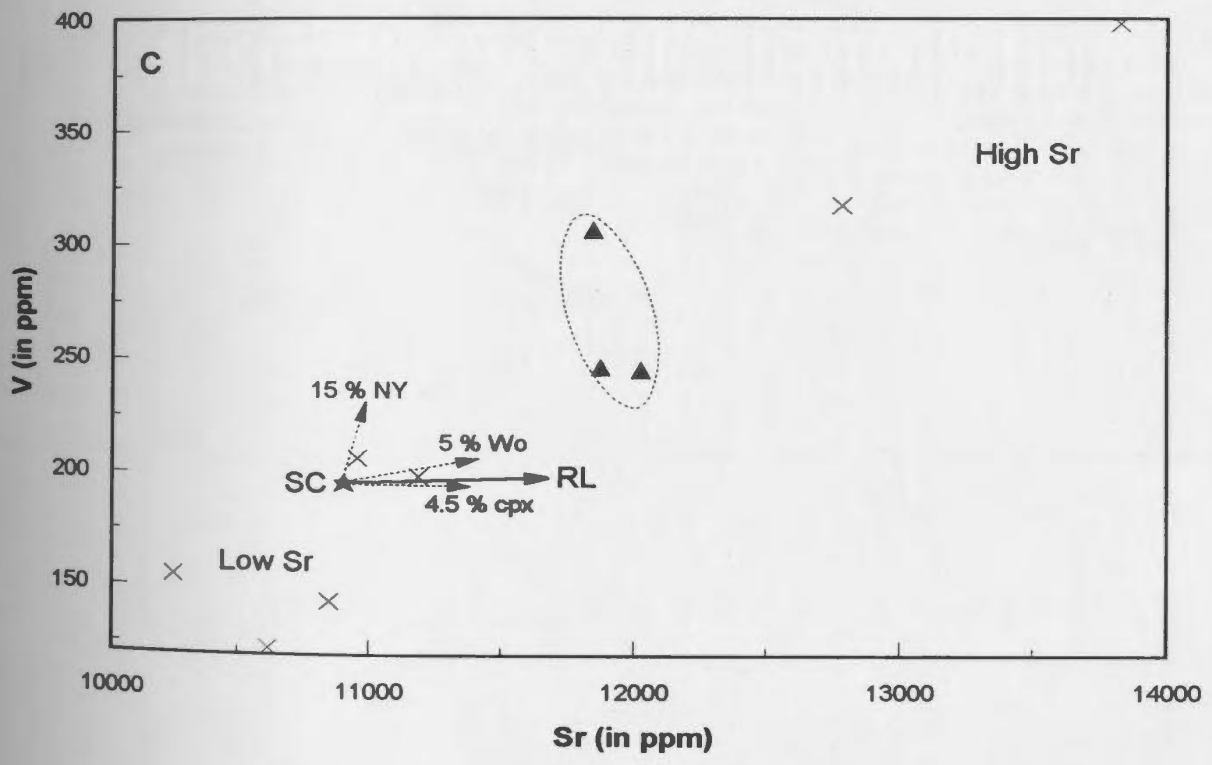
c
High Sr
Low Sr
15 % NY
5 % Wo
SC
RL
4.5 % cpx
V (in ppm)
Sr (in ppm)
400
350
300
250
200
150
10000
11000
12000
13000
14000

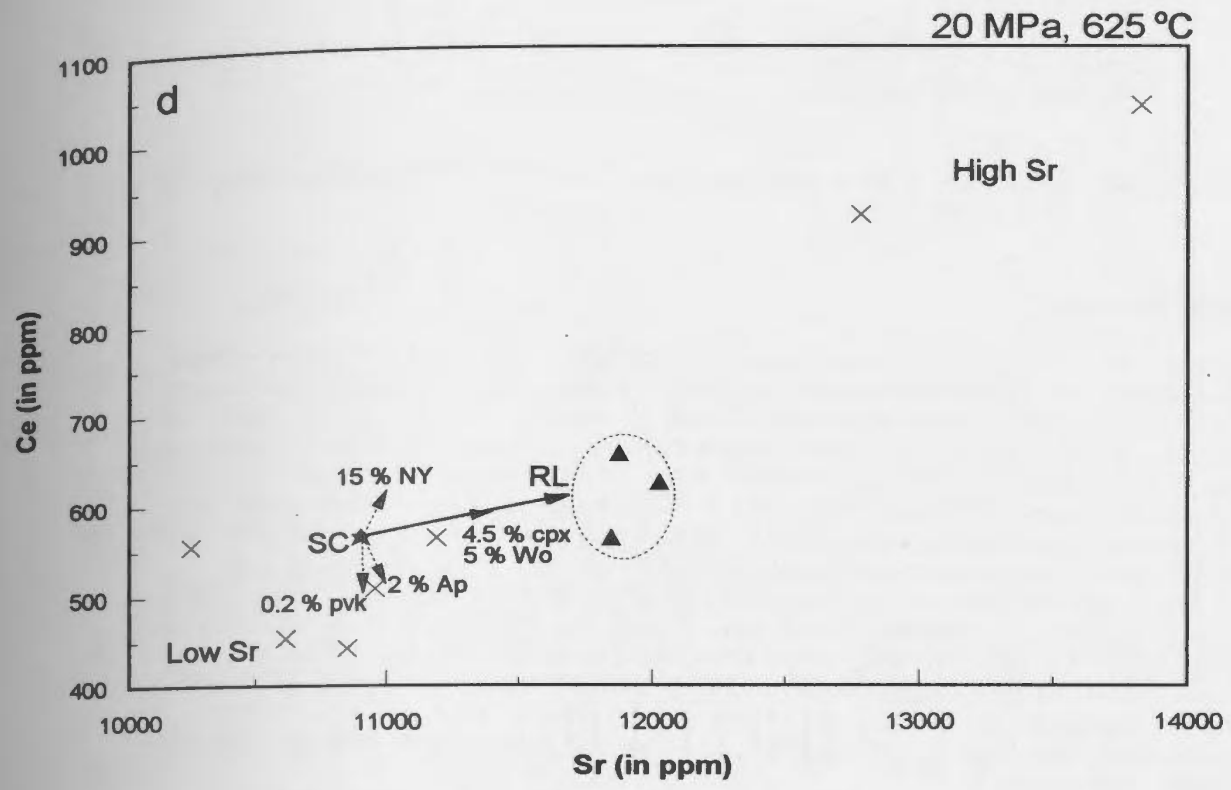
20 MPa, 625 °C
d
High Sr
Low Sr
15 % NY
RL
SC
4.5 % cpx
5 % Wo
2 % Ap
0.2 % pvk
Ce (in ppm)
Sr (in ppm)
1100
1000
900
800
700
600
500
400
10000
11000
12000
13000
14000

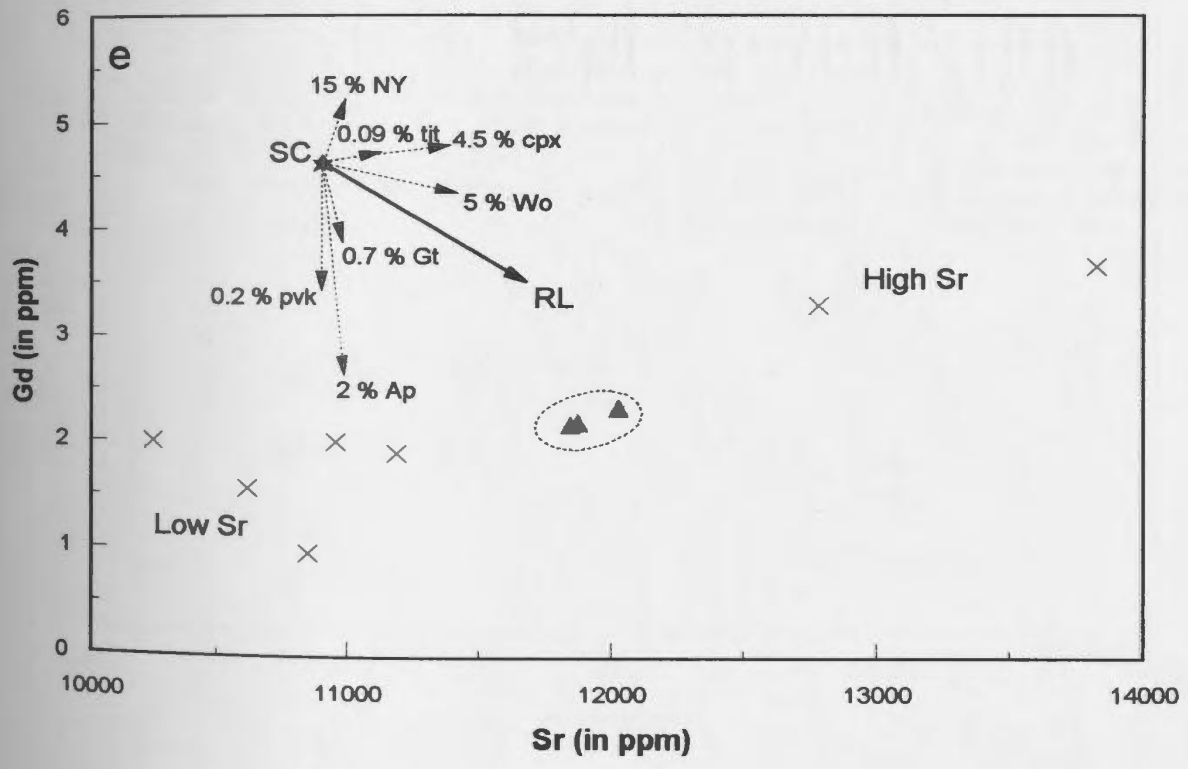
e
15 % NY
0.09 % tit
4.5 % cpx
SC
5 % Wo
0.7 % Gt
0.2 % pvk
RL
High Sr
2 % Ap
Low Sr
Gd (in ppm)
Sr (in ppm)
6
5
4
3
2
1
0
10000
11000
12000
13000
14000

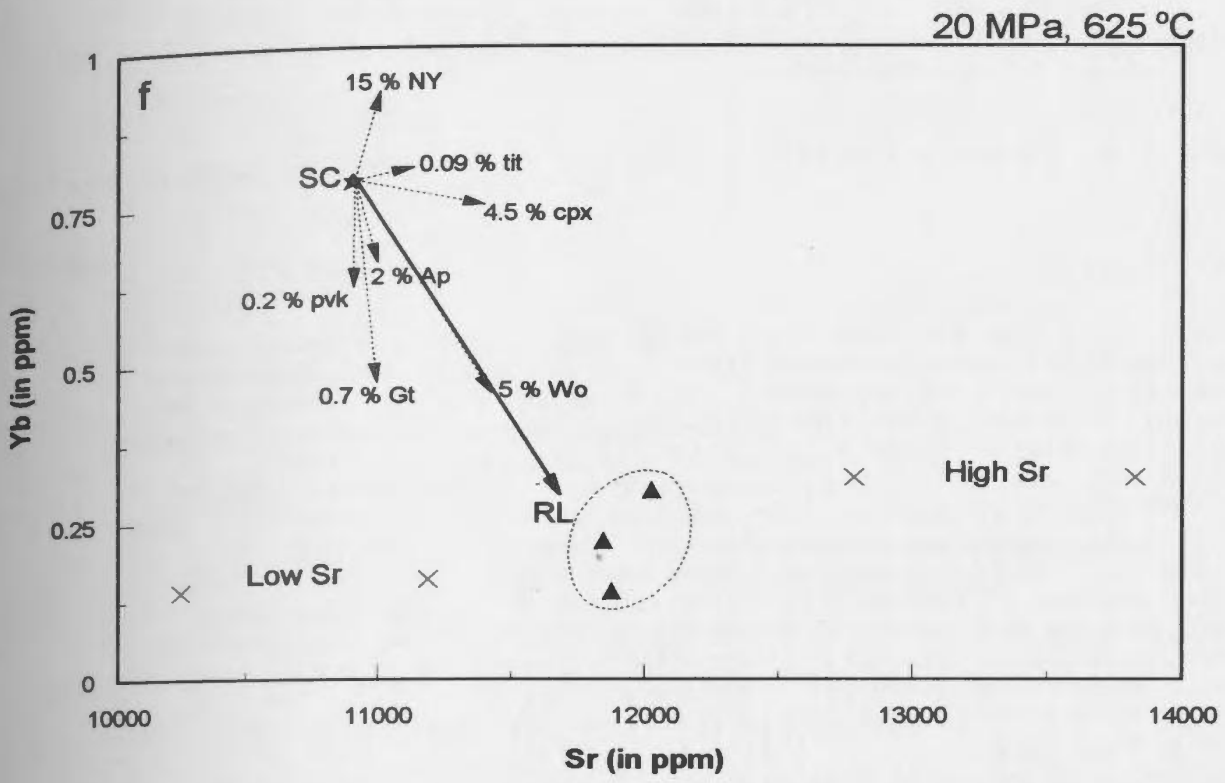
20 MPa, 625 °C
f
15 % NY
SC
0.09 % tit
4.5 % cpx
2 % Ap
0.2 % pvk
0.7 % Gt
5 % Wo
RL
High Sr
Low Sr
Yb (in ppm)
Sr (in ppm)
1
0.75
0.5
0.25
0
10000
11000
12000
13000
14000

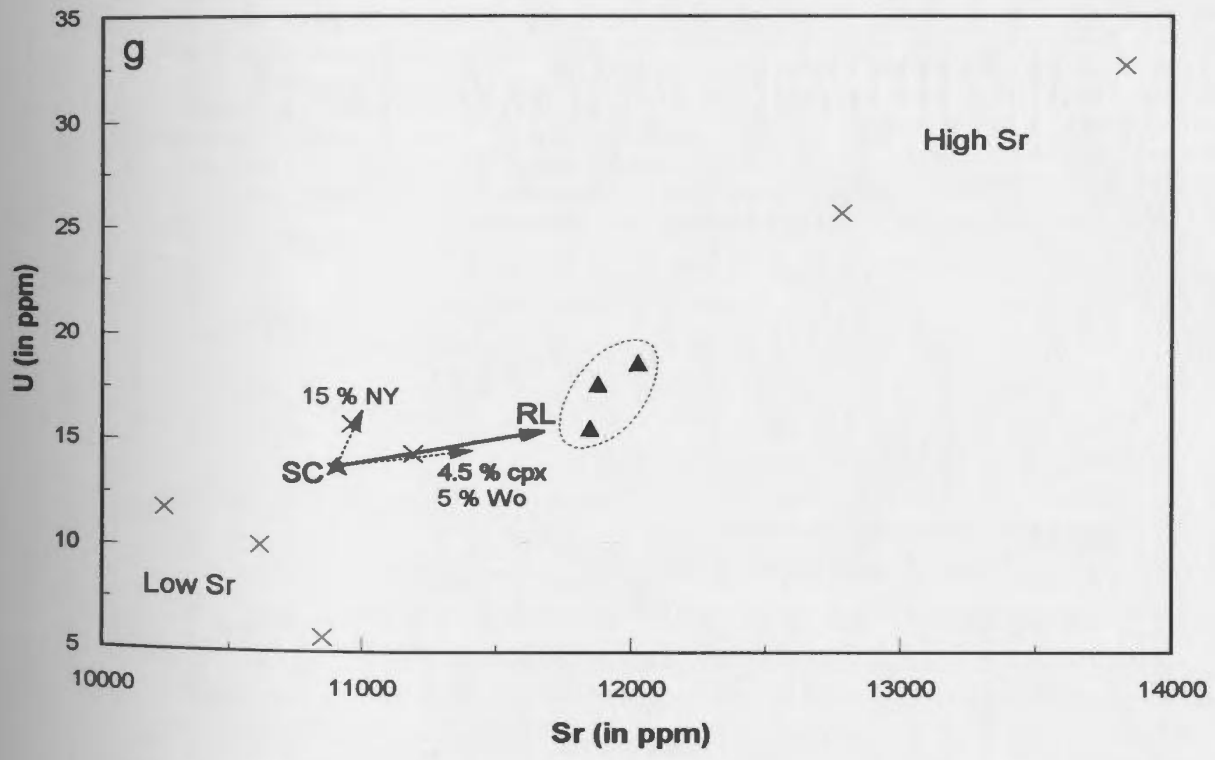
g
High Sr
15 % NY
RL
SC
4.5 % cpx
5 % Wo
Low Sr
U (in ppm)
Sr (in ppm)
35
30
25
20
15
10
5
10000
11000
12000
13000
14000

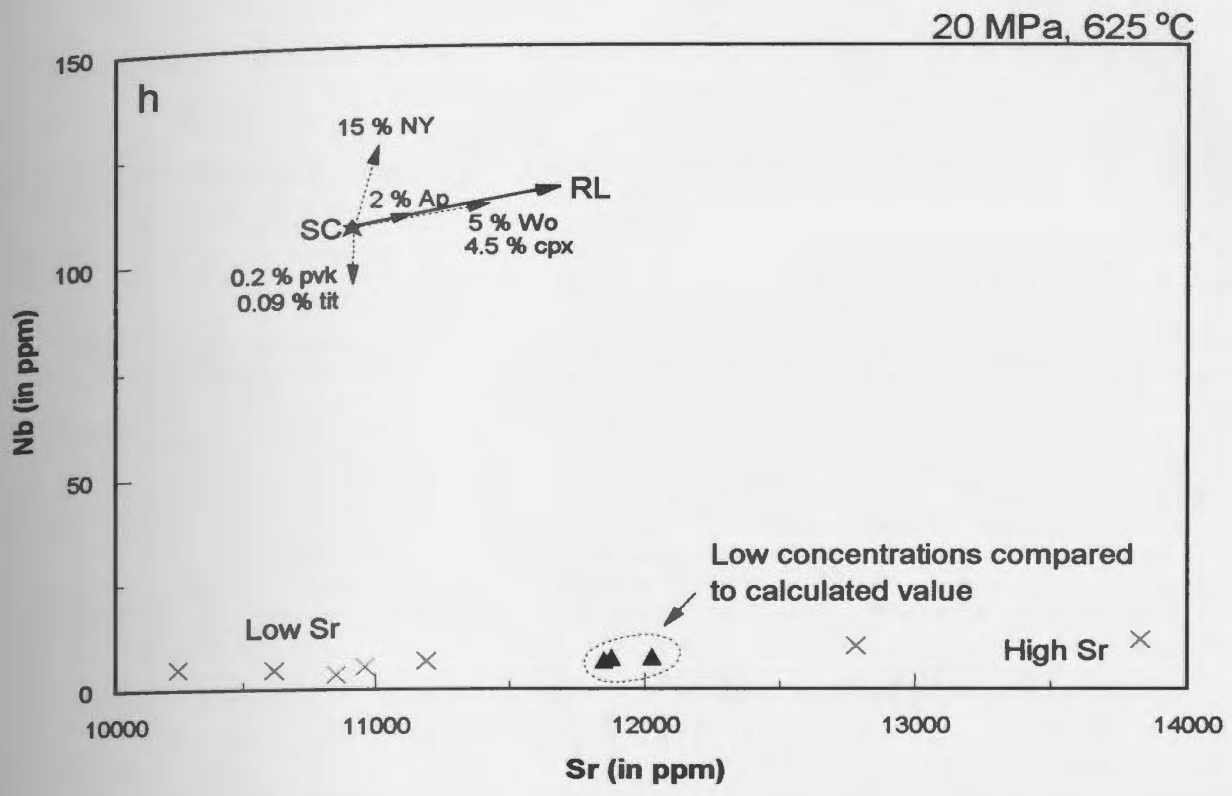
20 MPa, 625 °C
h
15 % NY
2 % Ap
RL
SC
5 % Wo
4.5 % cpx
0.2 % pvk
0.09 % tit
Low concentrations compared
to calculated value
Low Sr
High Sr
Nb (in ppm)
Sr (in ppm)
150
100
50
0
10000
11000
12000
13000
14000

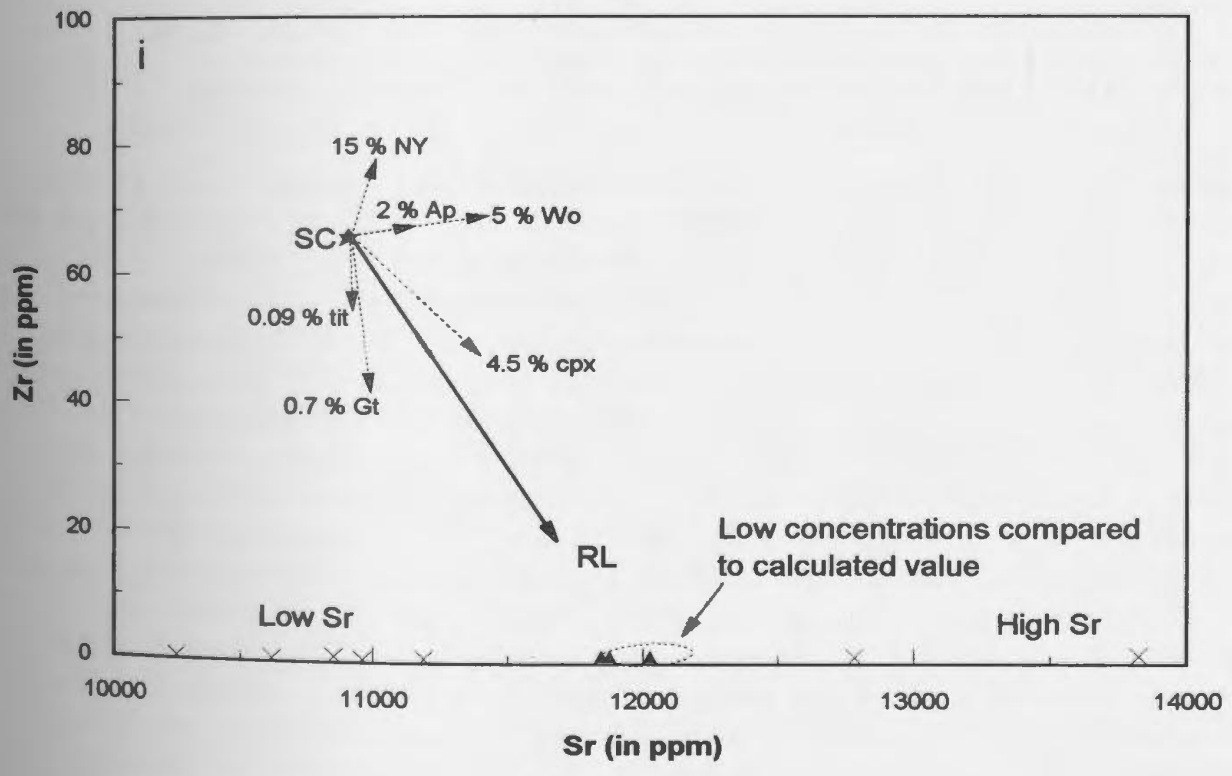
i
15 % NY
2 % Ap
5 % Wo
SC
0.09 % tit
4.5 % cpx
0.7 % Gt
RL
Low concentrations compared
to calculated value
Low Sr
High Sr
Zr (in ppm)
Sr (in ppm)
100
80
60
40
20
0
10000
11000
12000
13000
14000

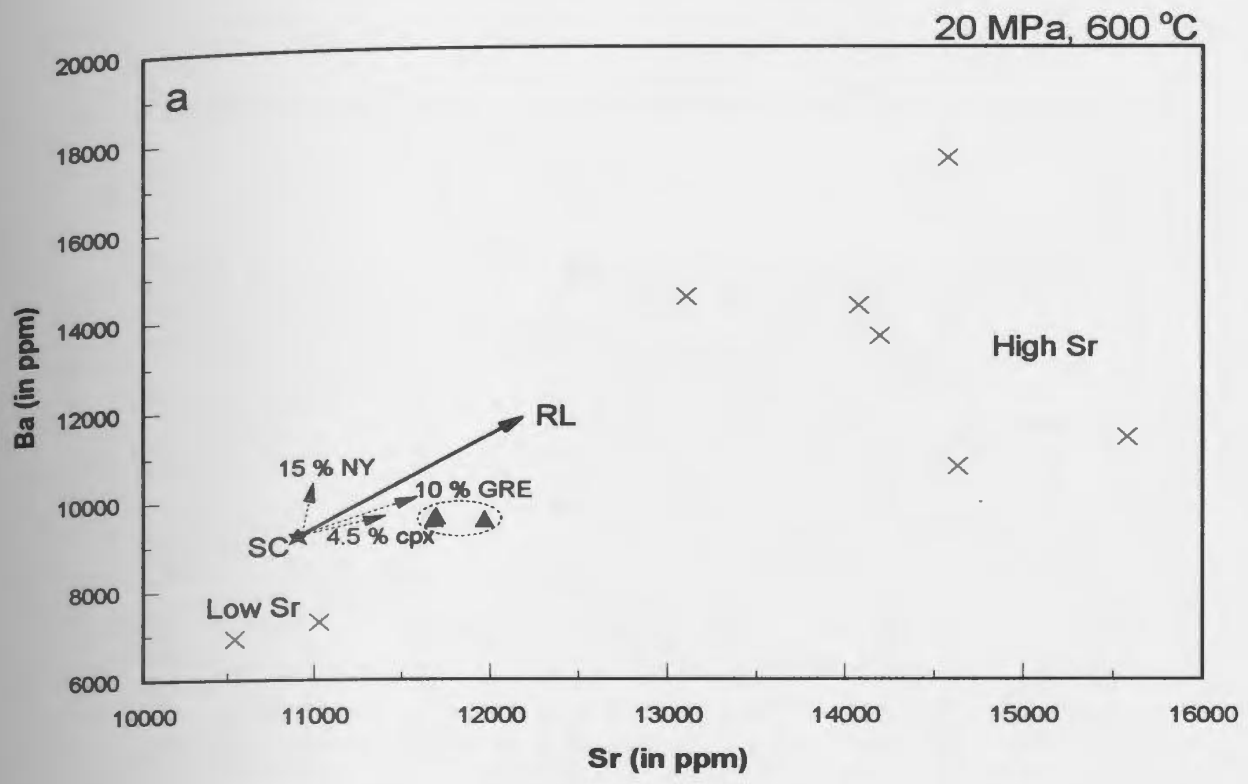

Figure 4.21: Variation diagram for selected trace elements versus Sr for carbonate liquid from experiment CP108 (20 MPa, 600 °C). Elements plotted versus Sr are: (a) Ba; (b) Rb; (c) V; (d) Ce; (e) Gd; (f) Yb; (g) U; (h) Nb; and (i) Zr. The thick arrow represents the direction toward which the composition of the calculated, residual liquid (RL) evolves when crystals present in CP108 (see proportions in Tab. 3.9) are subtracted from the starting composition (SC, represented by ★). Other arrows represent the direction toward which the composition of the carbonate liquid evolves when each crystal is subtracted from the bulk composition (proportion of crystals used for the calculation labelled at the end of the arrow). Individual analyses which have been rejected for having too high or too low of a Sr value compared to that of the calculated, residual liquid are represented by a cross (x). Individual analyses which have been rejected for having too high or too low of a concentration of the element plotted on the y-axis compared to that of the calculated, residual liquid are represented by a cross (+). Individual analyses used to calculate the average composition of the carbonate liquid are represented by a filled triangle (▲) and are within the area denoted by a dotted line. Abbreviation used are: Cpx: clinopyroxene; Gt: melanite garnet; NY: nyerereite; Ap: apatite; GRE: gregoryite; tit: titanite; pvk: perovskite. Individual analyses for the carbonate liquid are from Table A4.2 in Appendix A4, and the calculated concentrations of the residual liquid are given in Table A4.4 in Appendix A4.

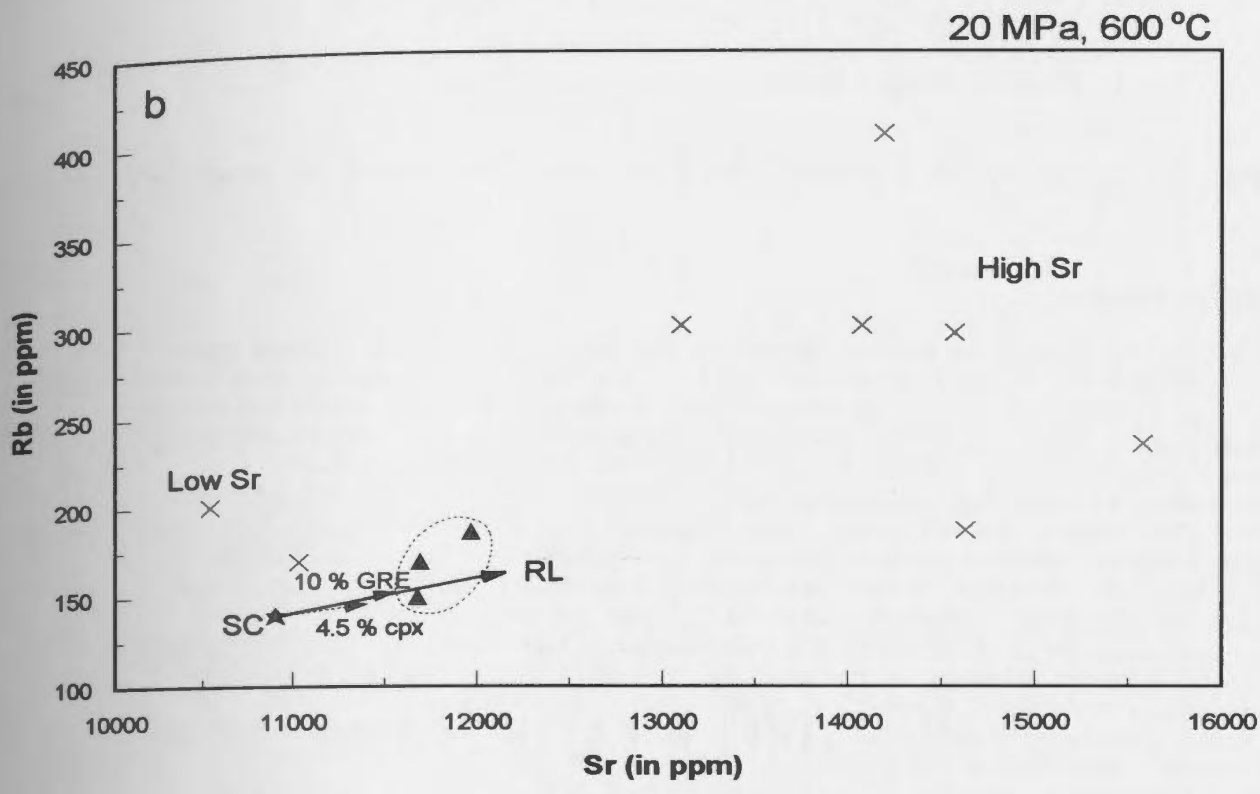
20 MPa, 600 °C
b
High Sr
Low Sr
10 % GRE
RL
SC
4.5 % cpx
Rb (in ppm)
Sr (in ppm)
450
400
350
300
250
200
150
100
10000
11000
12000
13000
14000
15000
16000

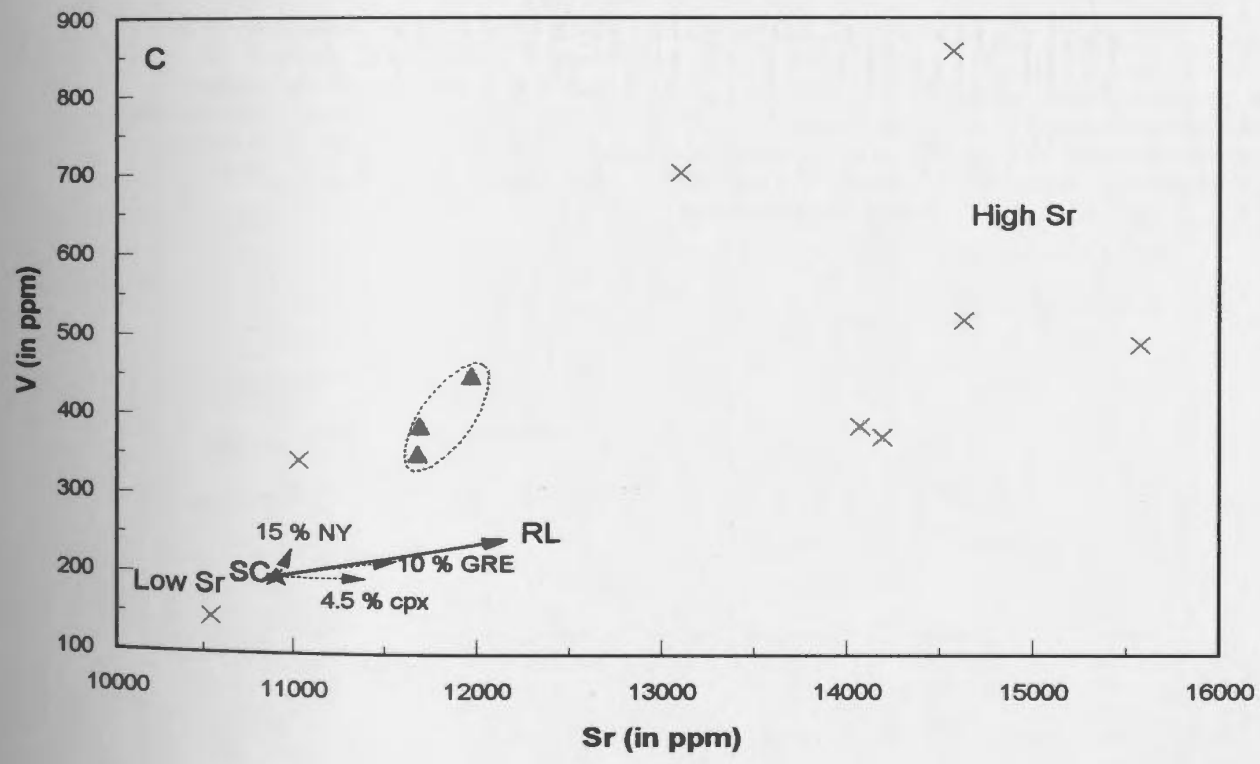
c
High Sr
15 % NY
RL
Low Sr
SC
10 % GRE
4.5 % cpx
V (in ppm)
Sr (in ppm)
900
800
700
600
500
400
300
200
100
10000
11000
12000
13000
14000
15000
16000

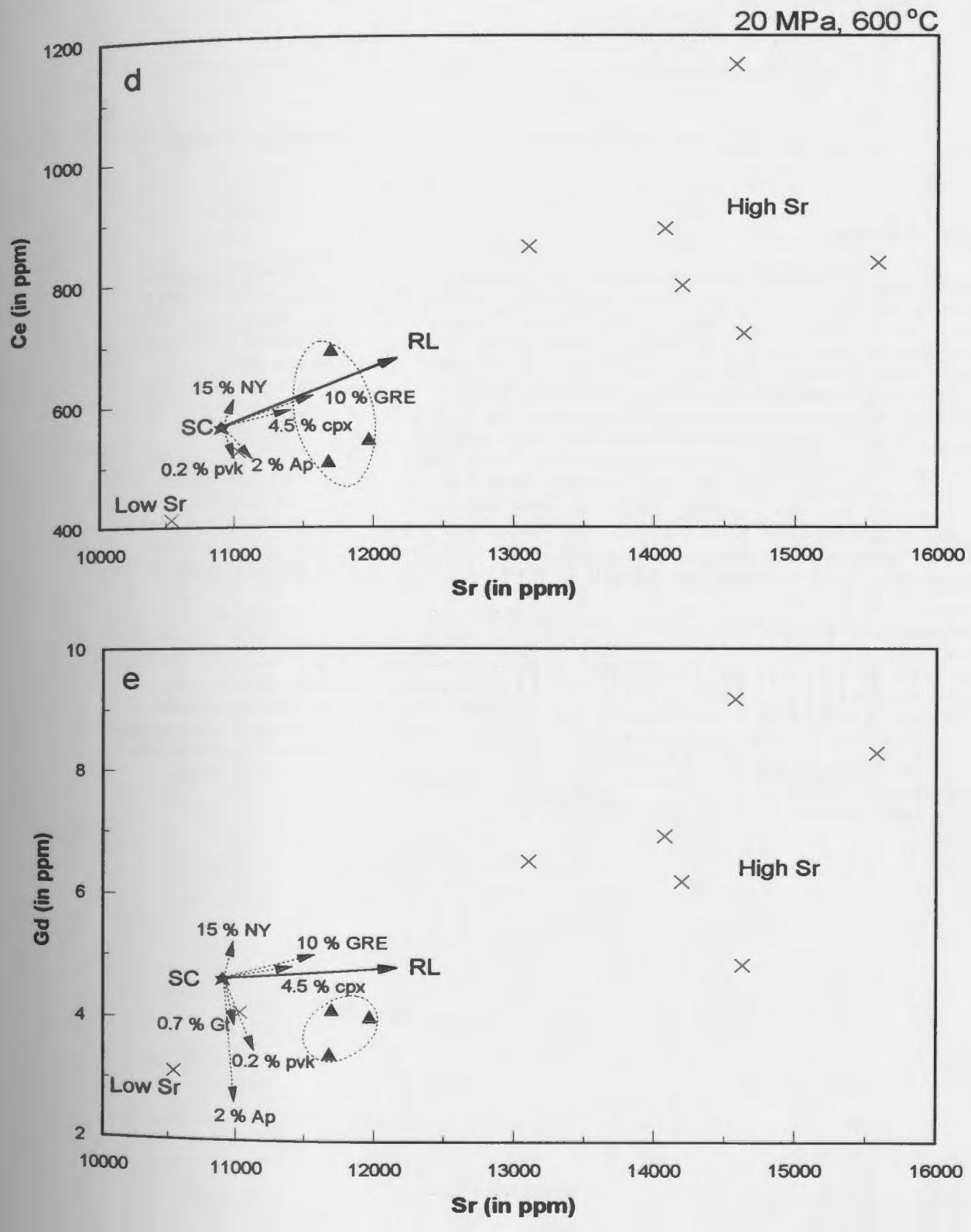
20 MPa, 600 °C
d
1200
1000
800
600
400
Ce (in ppm)
High Sr
RL
15 % NY
10 % GRE
SC
4.5 % cpx
0.2 % pvk
2 % Ap
Low Sr
10000
11000
12000
13000
14000
15000
16000
Sr (in ppm)
e
10
8
6
4
2
Gd (in ppm)
High Sr
15 % NY
10 % GRE
SC
RL
4.5 % cpx
0.7 % Gt
0.2 % pvk
Low Sr
2 % Ap
10000
11000
12000
13000
14000
15000
16000
Sr (in ppm)

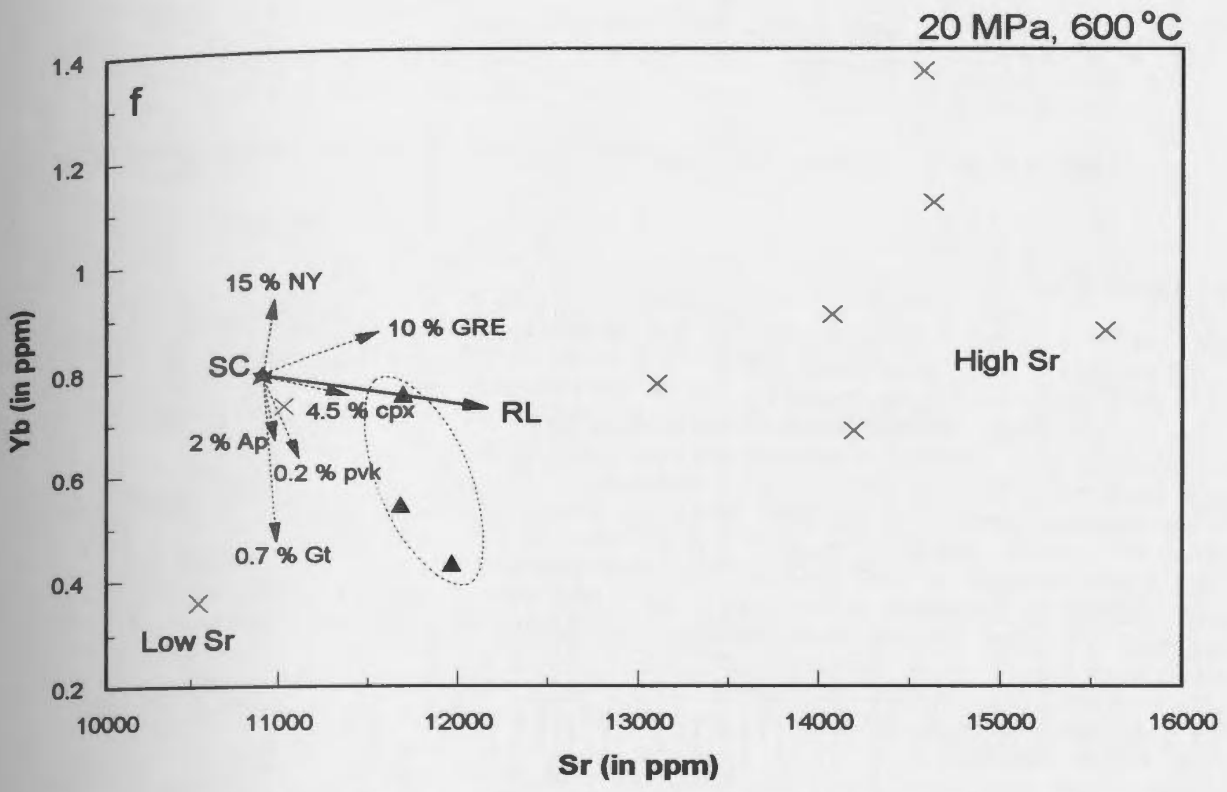
20 MPa, 600 °C
f
Yb (in ppm)
Sr (in ppm)
15 % NY
10 % GRE
SC
4.5 % cpx
RL
2 % Ap
0.2 % pvk
0.7 % Gt
High Sr
Low Sr

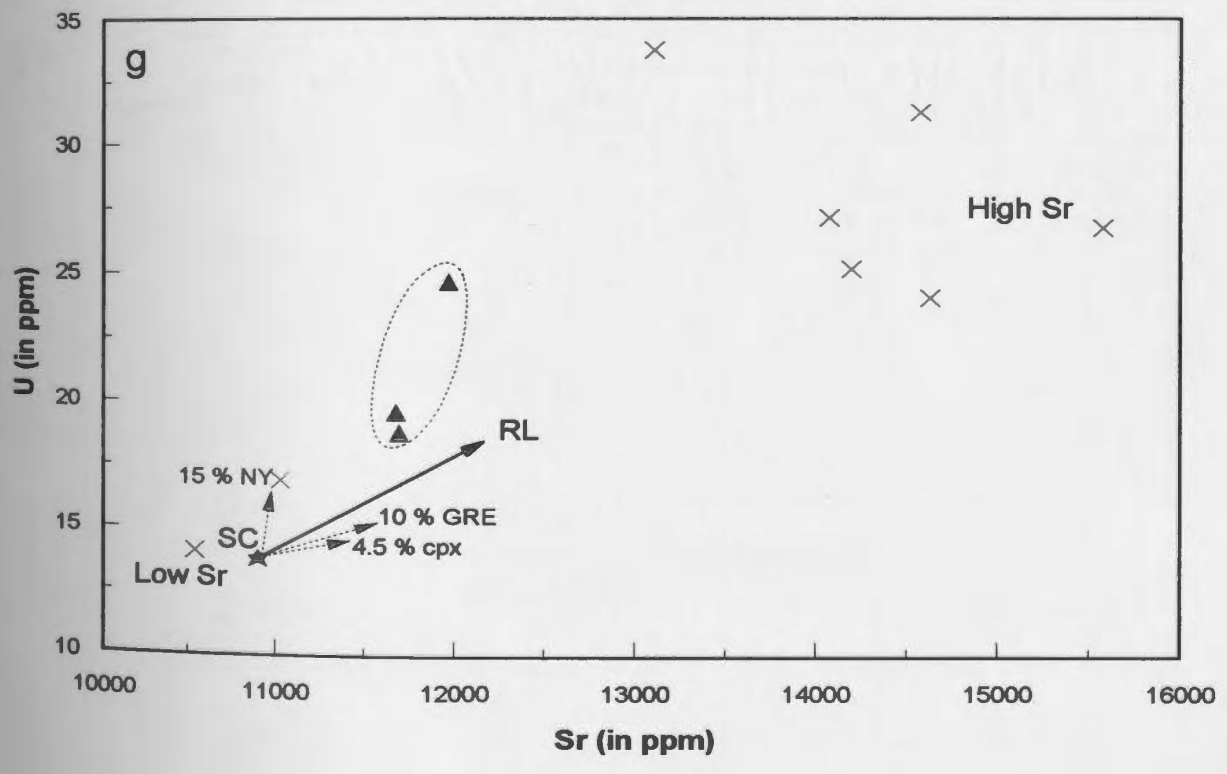
g
U (in ppm)
Sr (in ppm)
RL
15 % NY
10 % GRE
SC
4.5 % cpx
High Sr
Low Sr

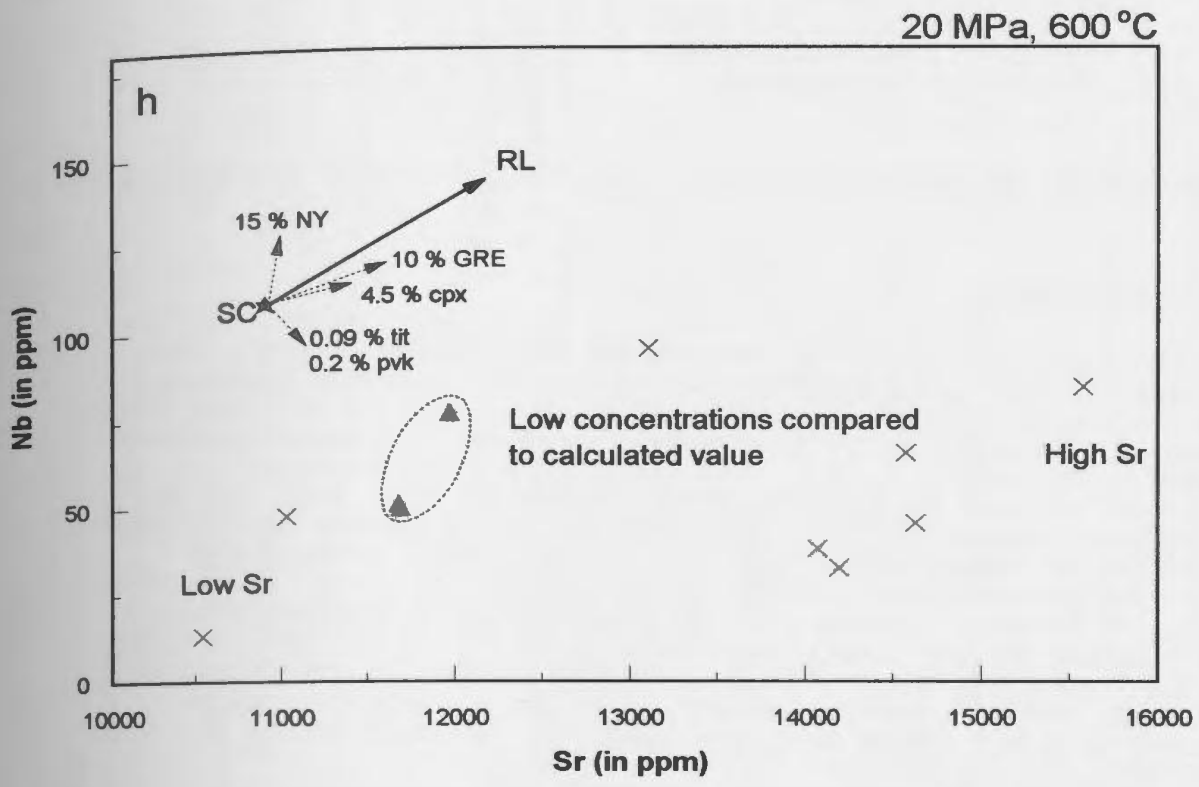
20 MPa, 600 °C
h
RL
15 % NY
10 % GRE
4.5 % cpx
SC
0.09 % tit
0.2 % pvk
Low concentrations compared
to calculated value
High Sr
Low Sr
Nb (in ppm)
Sr (in ppm)
150
100
50
0
10000
11000
12000
13000
14000
15000
16000

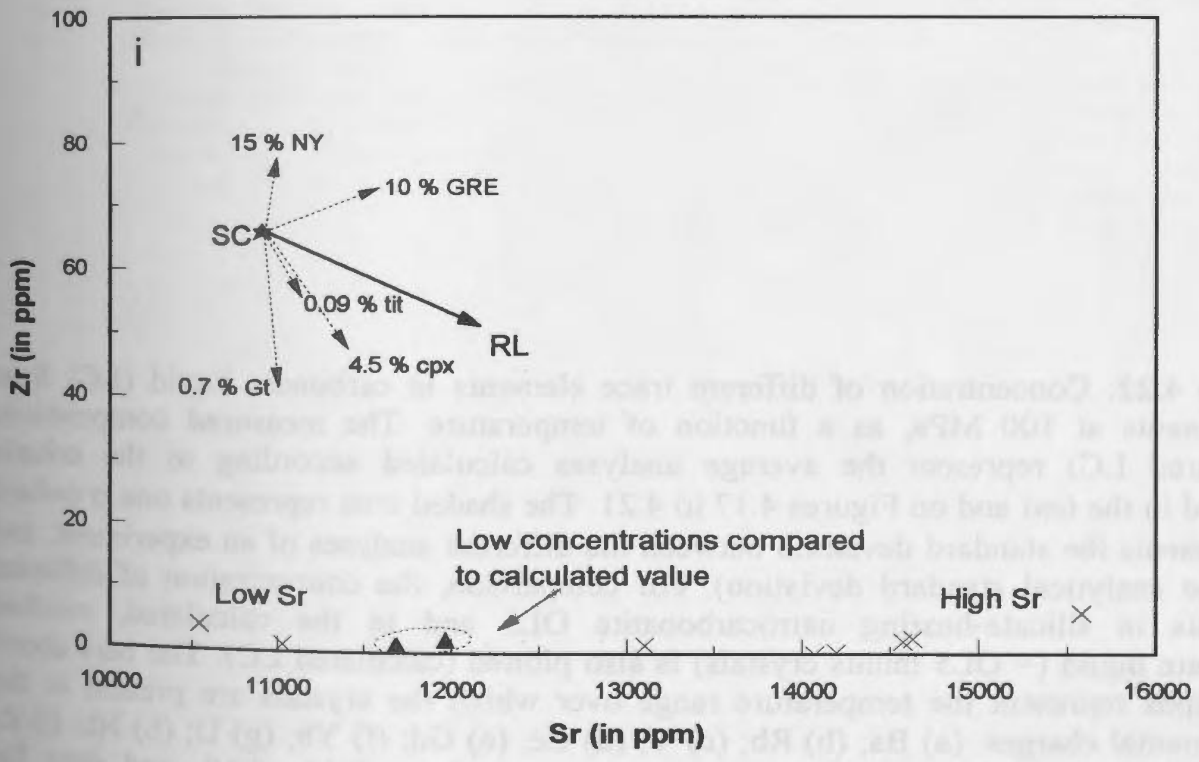
i
15 % NY
10 % GRE
SC
0.09 % tit
RL
4.5 % cpx
0.7 % Gt
Low concentrations compared
to calculated value
Low Sr
High Sr
Zr (in ppm)
Sr (in ppm)
100
80
60
40
20
0
10000
11000
12000
13000
14000
15000
16000

Figure 4.22: Concentration of different trace elements in carbonate liquid (LC) from experiments at 100 MPa, as a function of temperature. The measured compositions (measured LC) represent the average analyses calculated according to the criteria outlined in the text and on Figures 4.17 to 4.21. The shaded area represents one σ (where σ represents the standard deviation between the different analyses of an experiment, and also the analytical standard deviation). For comparison, the concentration of different elements in silicate-bearing natrocarbonatite OL5 and in the calculated, residual carbonate liquid (= OL5 minus crystals) is also plotted (calculated LC). The bars above the graphs represent the temperature range over which the crystals are present in the experimental charges. (a) Ba; (b) Rb; (c) V; (d) Ce; (e) Gd; (f) Yb; (g) U; (h) Nb; (i) Zr and (u) Hf. Data for measured concentrations are from Table 4.10, and data for calculated, residual liquid are in Appendix A4 (Tab. A4.4).

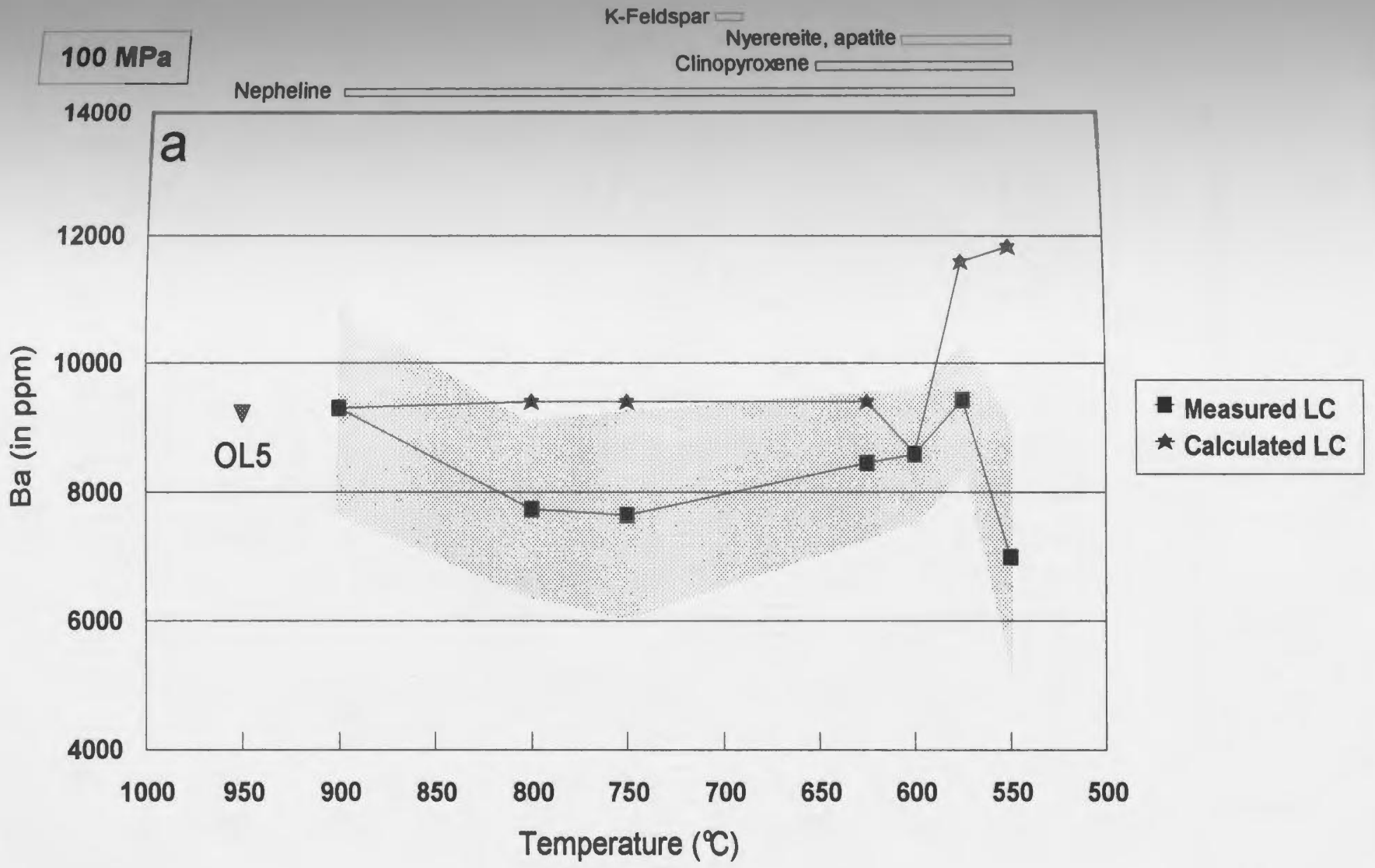
100 MPa
K-Feldspar
Nyerereite, apatite
Clinopyroxene
Nepheline
a
OL5
Ba (in ppm)
14000
12000
10000
8000
6000
4000
1000
950
900
850
800
750
700
650
600
550
500
Temperature (°C)
Measured LC
Calculated LC

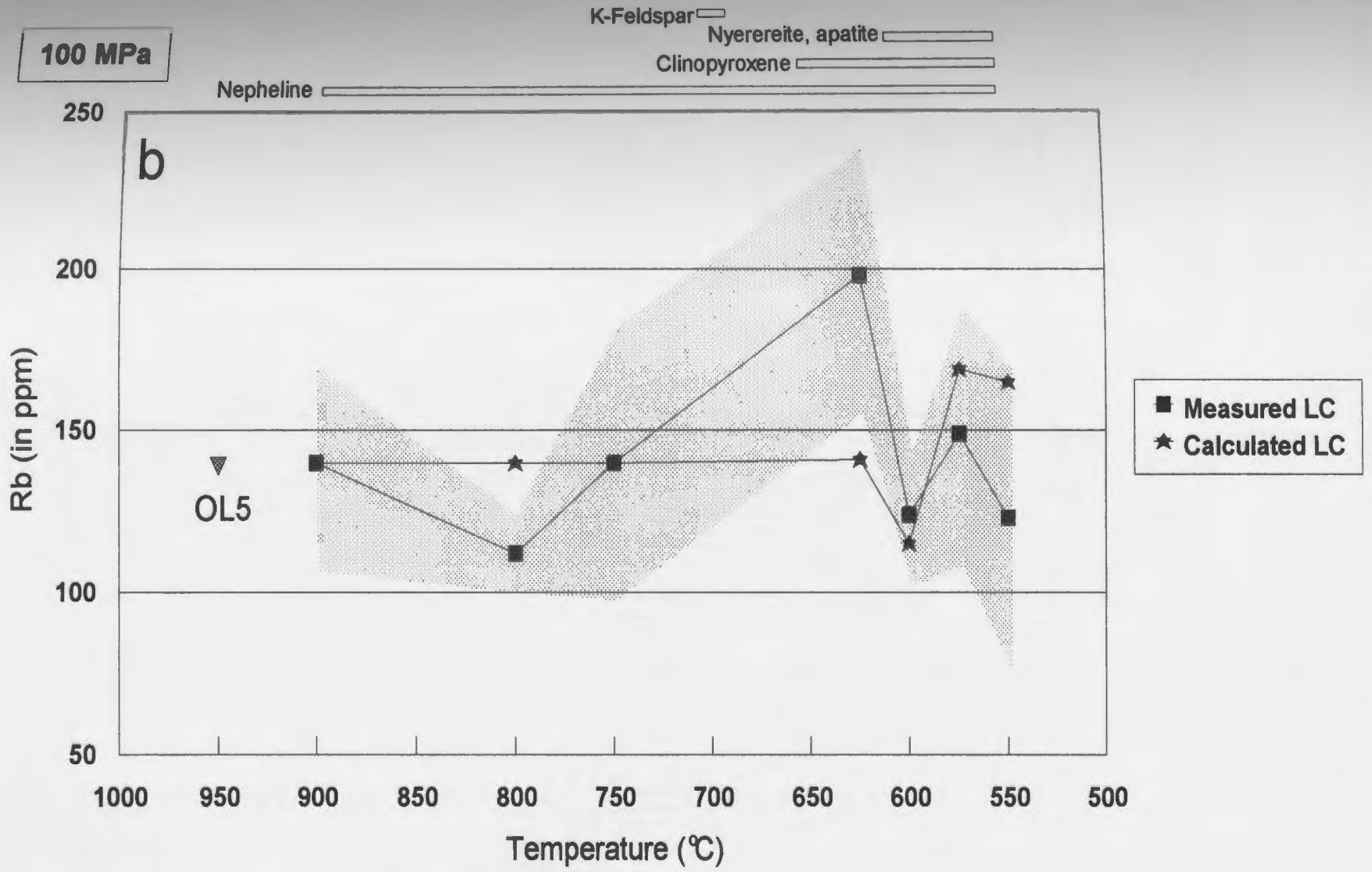
100 MPa
K-Feldspar
Nyerereite, apatite
Clinopyroxene
Nepheline
b
OL5
Rb (in ppm)
250
200
150
100
50
1000
950
900
850
800
750
700
650
600
550
500
Temperature (°C)
Measured LC
Calculated LC

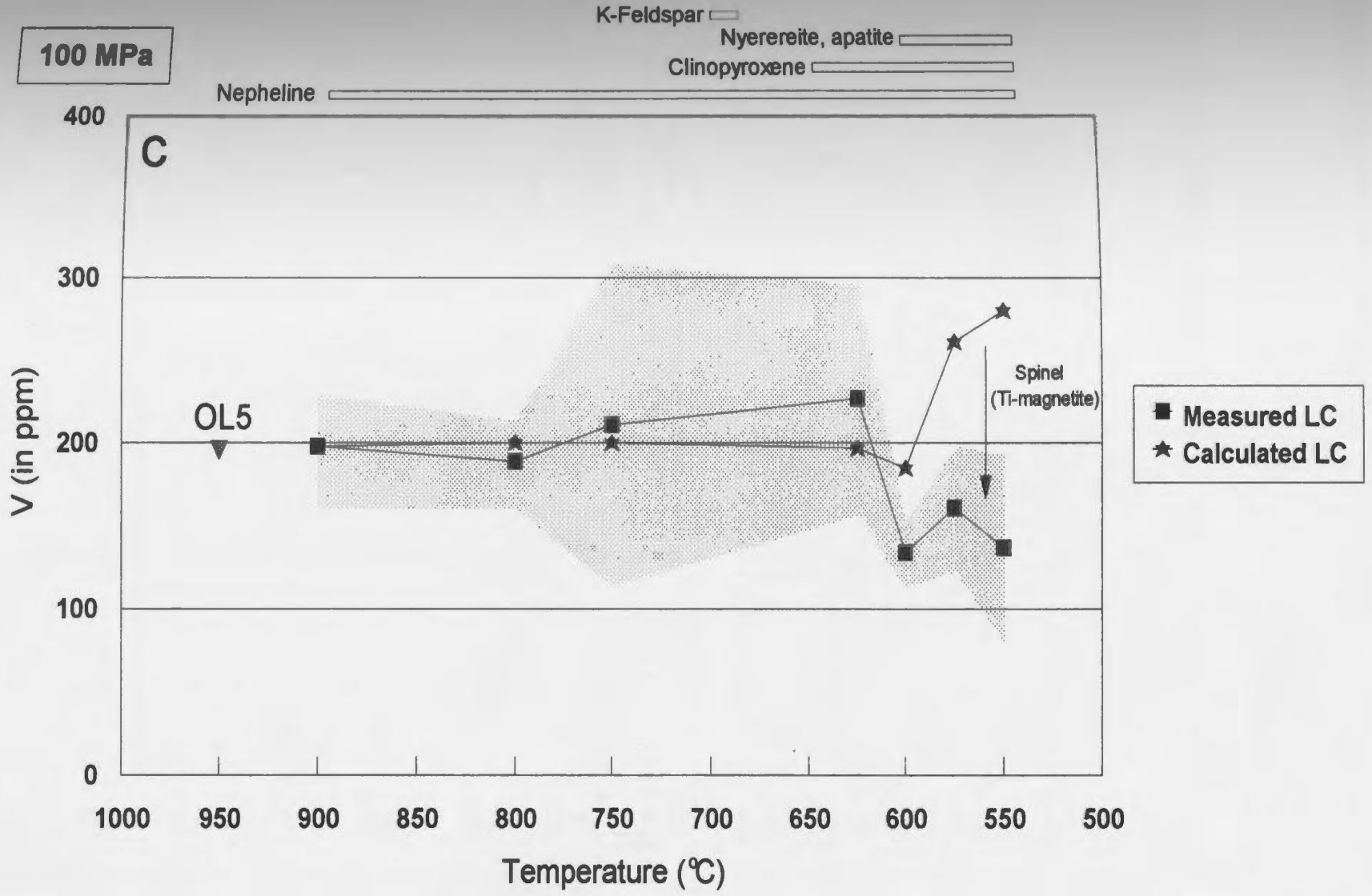
100 MPa
K-Feldspar
Nyerereite, apatite
Clinopyroxene
Nepheline
C
OL5
Spinel
(Ti-magnetite)
Measured LC
Calculated LC
V (in ppm)
400
300
200
100
0
1000
950
900
850
800
750
700
650
600
550
500
Temperature (°C)

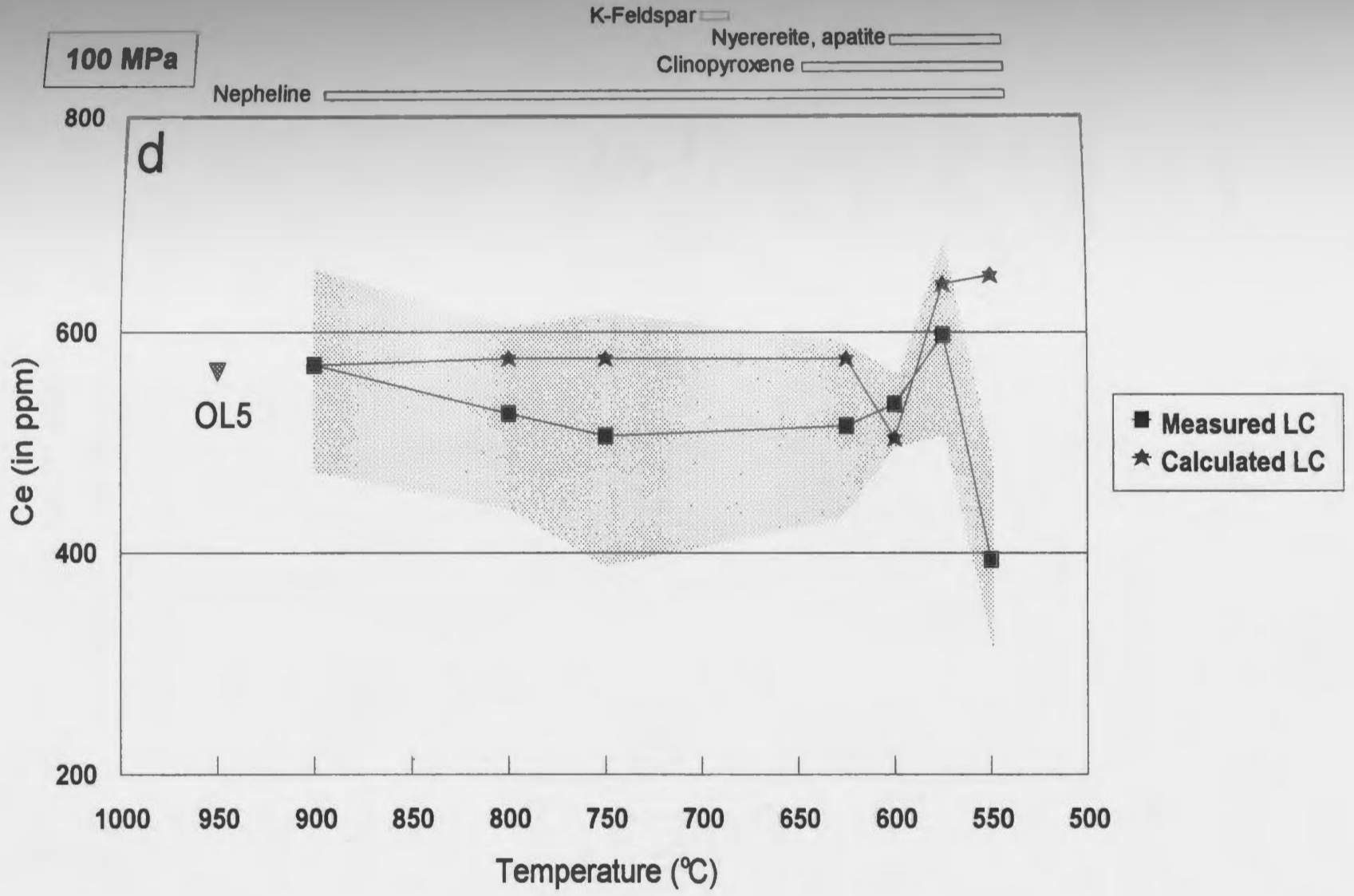
K-Feldspar
Nyerereite, apatite
Clinopyroxene
Nepheline
100 MPa
d
OL5
Ce (in ppm)
800
600
400
200
1000
950
900
850
800
750
700
650
600
550
500
Temperature (°C)
Measured LC
Calculated LC

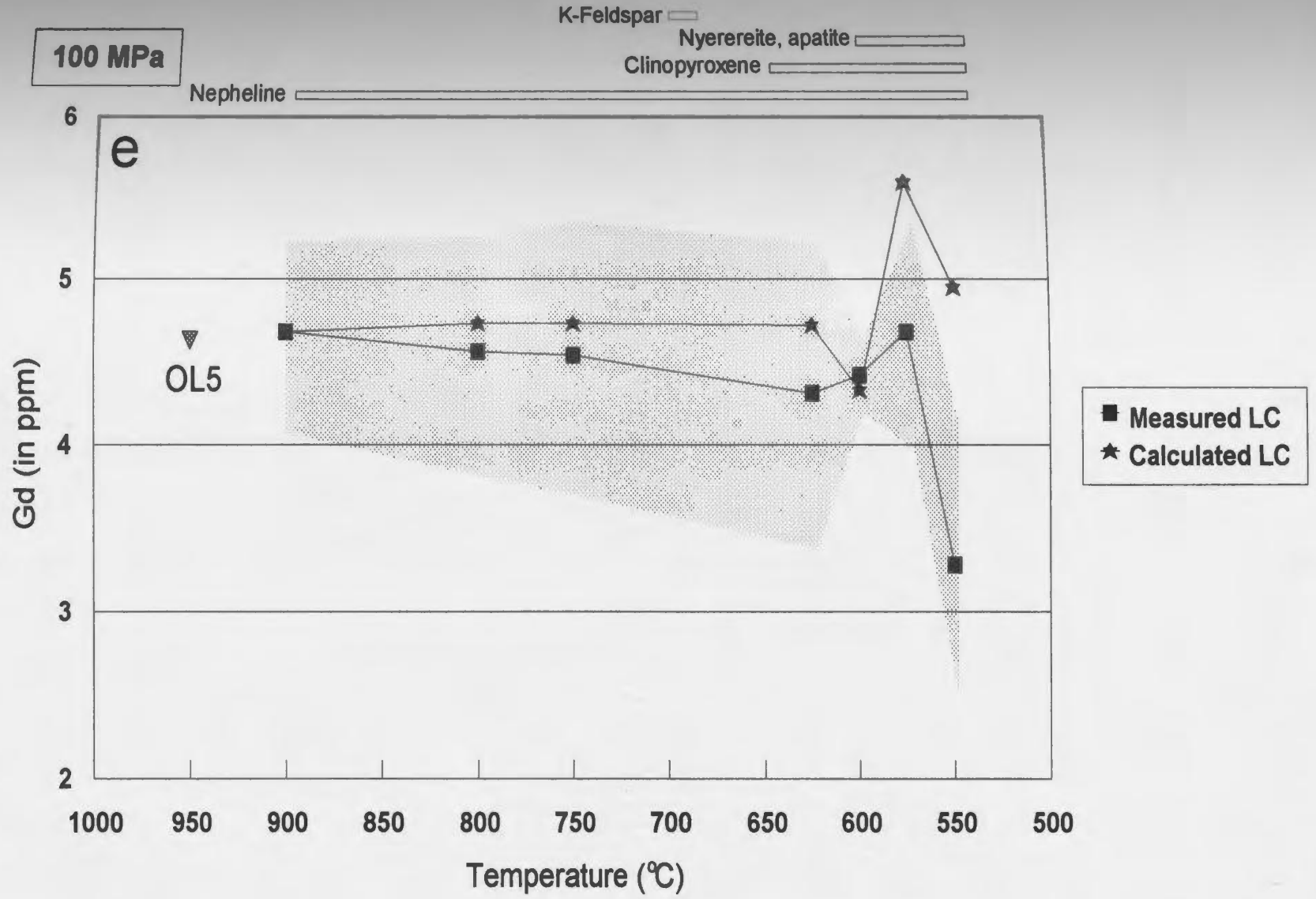
100 MPa
K-Feldspar
Nyerereite, apatite
Clinopyroxene
Nepheline
e
OL5
Gd (in ppm)
6
5
4
3
2
1000
950
900
850
800
750
700
650
600
550
500
Temperature (°C)
Measured LC
Calculated LC

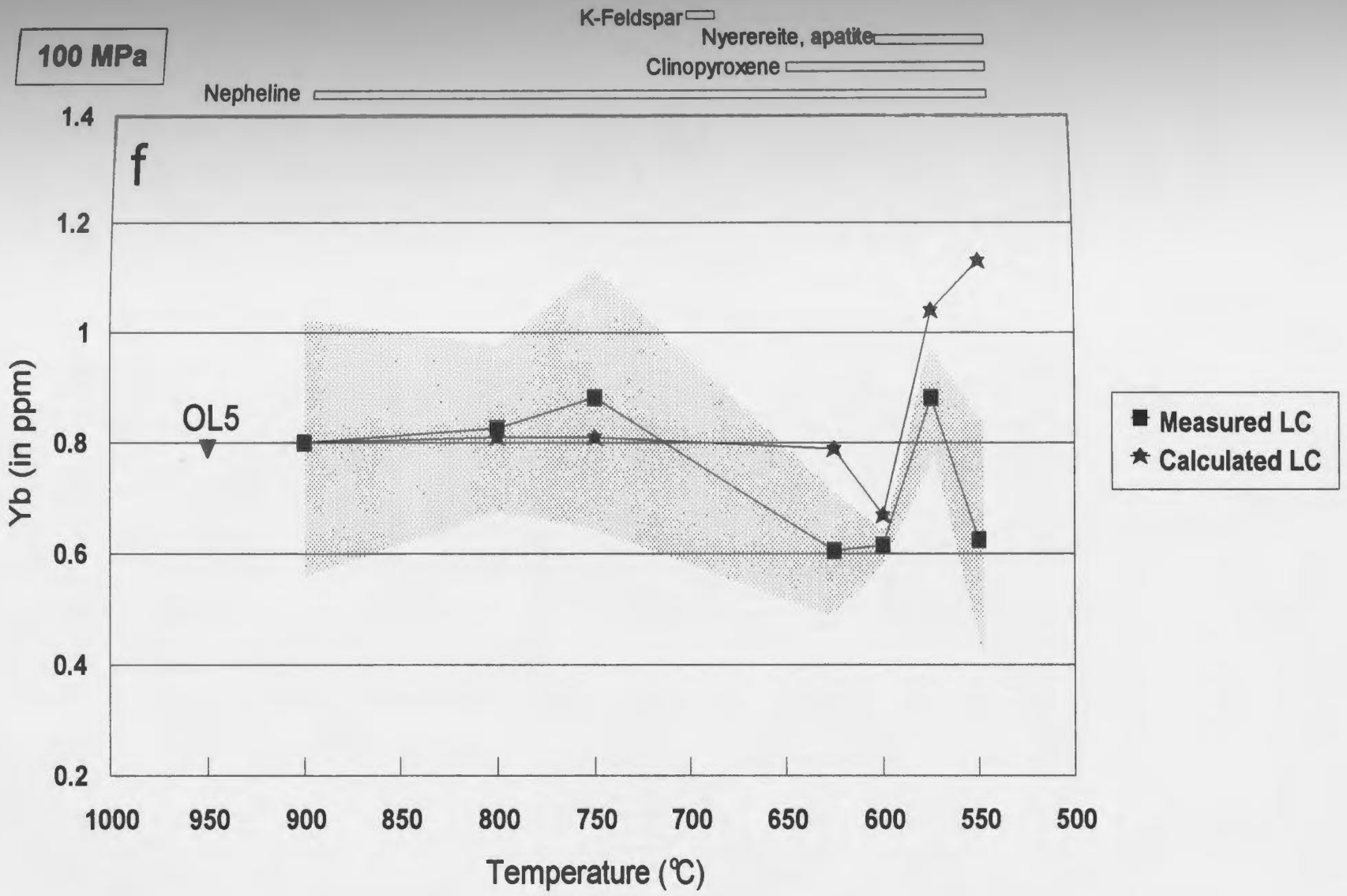
100 MPa
K-Feldspar
Nyerereite, apatite
Clinopyroxene
Nepheline
f
OL5
Yb (in ppm)
1.4
1.2
1
0.8
0.6
0.4
0.2
1000
950
900
850
800
750
700
650
600
550
500
Temperature (℃)
Measured LC
Calculated LC

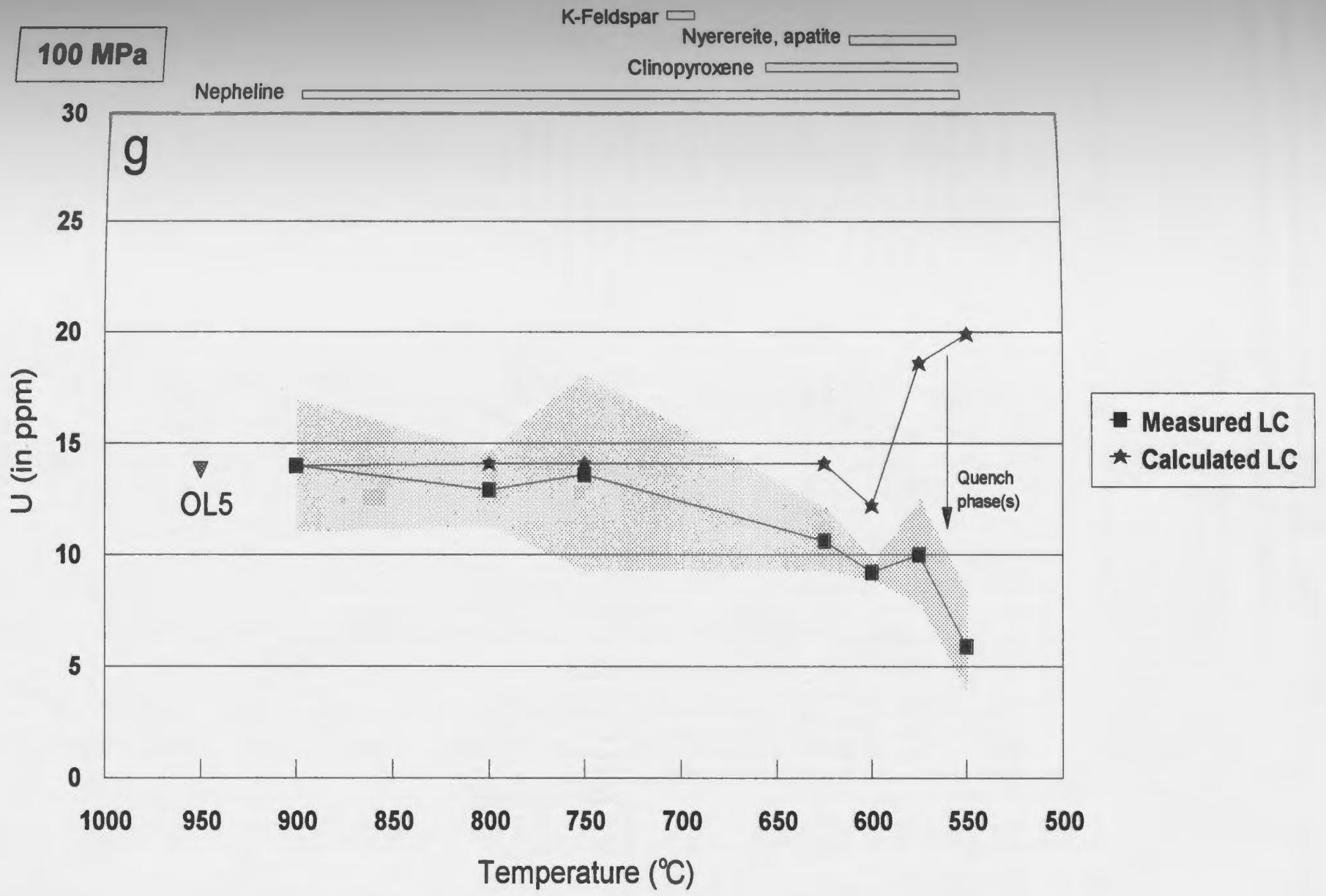
100 MPa
K-Feldspar
Nyerereite, apatite
Clinopyroxene
Nepheline
g
30
25
20
15
10
5
0
U (in ppm)
OL5
Quench phase(s)
Measured LC
Calculated LC
1000
950
900
850
800
750
700
650
600
550
500
Temperature (°C)

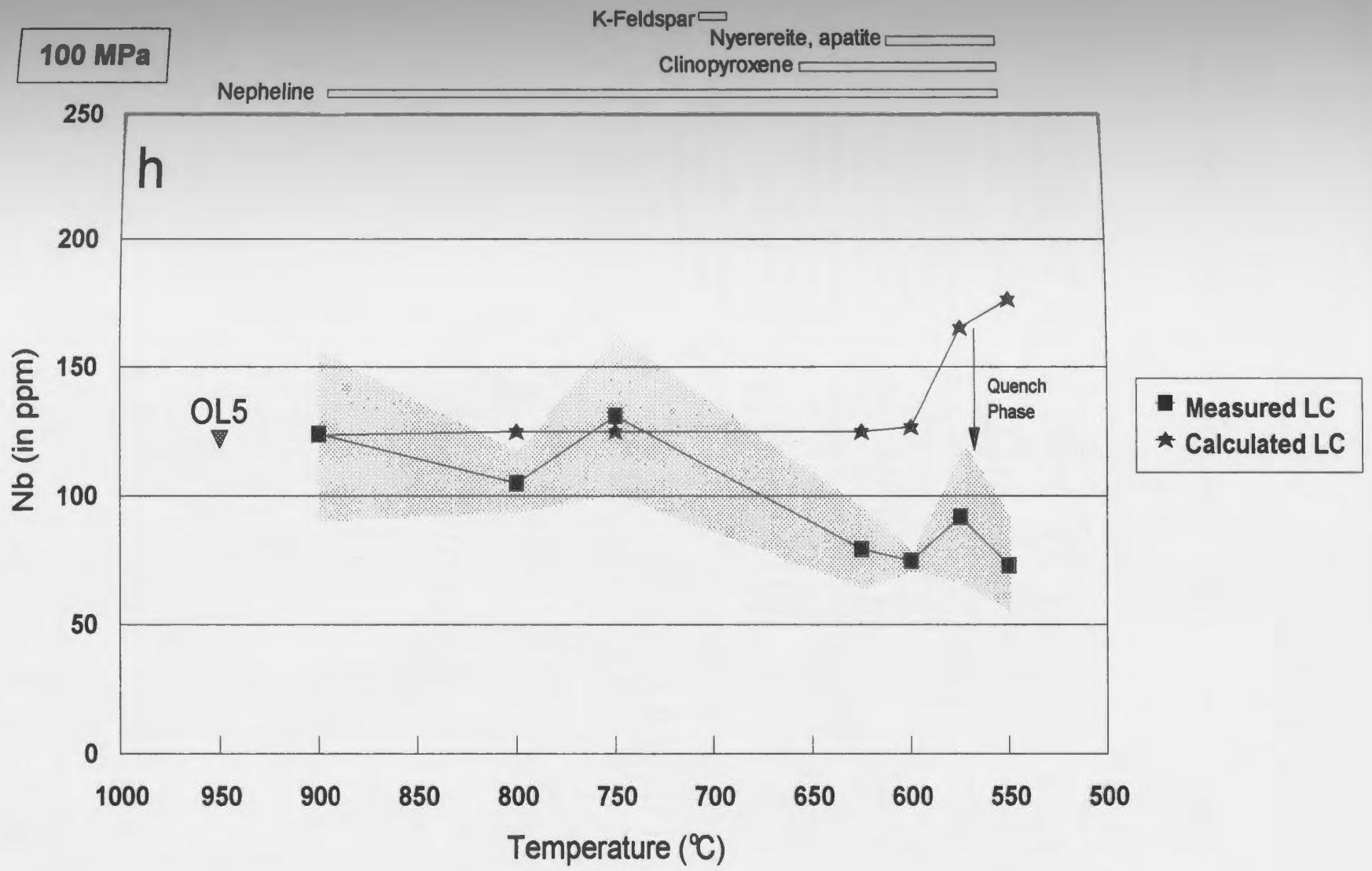
100 MPa
K-Feldspar
Nyerereite, apatite
Clinopyroxene
Nepheline
h
OL5
Quench
Phase
Measured LC
Calculated LC
Nb (in ppm)
250
200
150
100
50
0
1000
950
900
850
800
750
700
650
600
550
500
Temperature (°C)

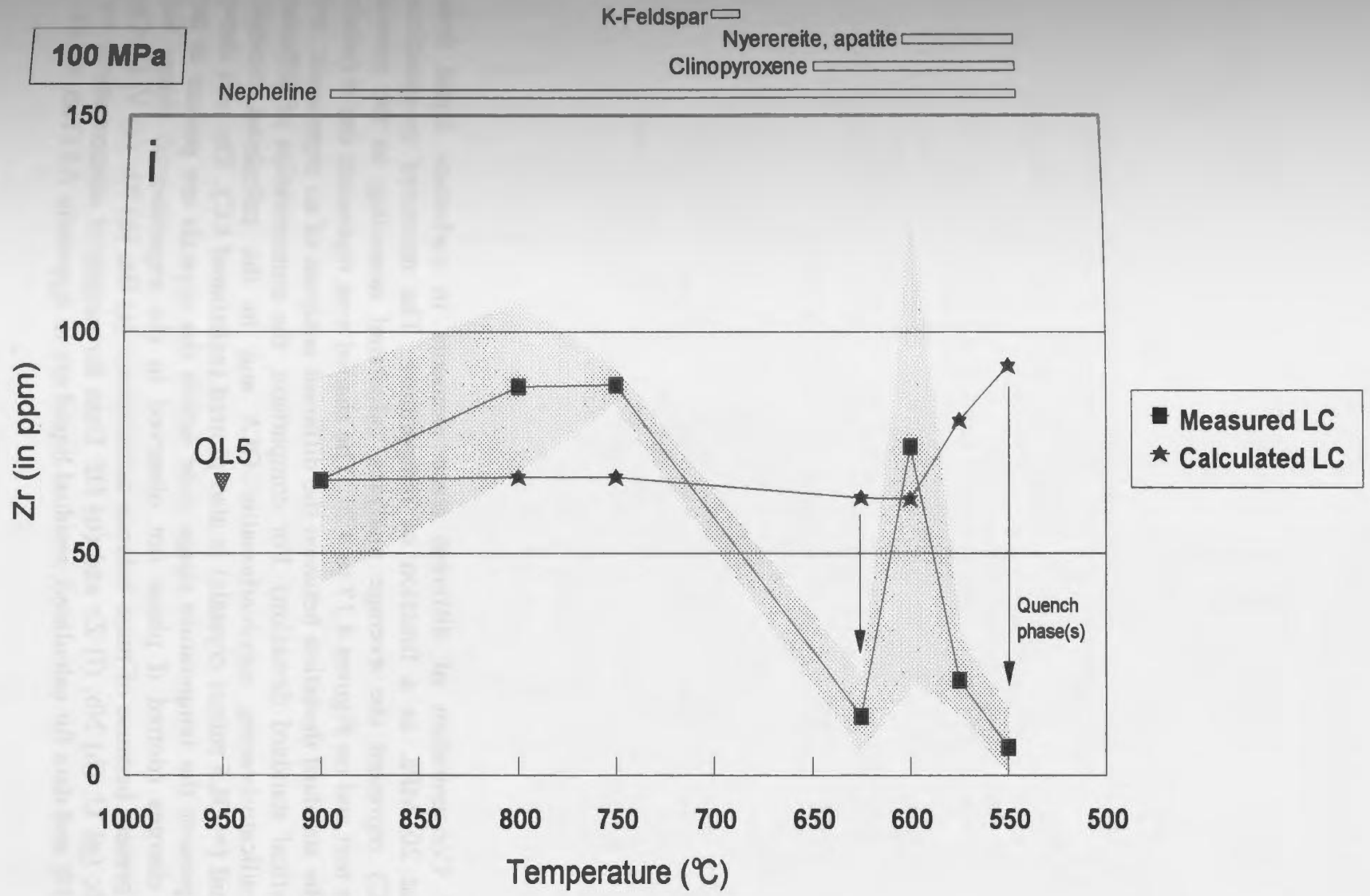
100 MPa
K-Feldspar
Nyerereite, apatite
Clinopyroxene
Nepheline
i
OL5
Zr (in ppm)
150
100
50
0
1000
950
900
850
800
750
700
650
600
550
500
Temperature (°C)
Quench phase(s)
Measured LC
Calculated LC

Figure 4.23: Concentration of different trace elements in carbonate liquid from experiments at 20 MPa, as a function of temperature. The measured compositions (measured LC) represent the average analyses calculated according to the criteria outlined in the text and on Figures 4.17 to 4.21. The shaded area represents one σ (where σ represents the standard deviation between the different analyses of an experiment, and also the analytical standard deviation). For comparison, the concentration of different elements in silicate-bearing natrocarbonatite OL5 and in the calculated, residual carbonate liquid (= OL5 minus crystals) is also plotted (calculated LC). The bars above the graphs represent the temperature range over which the crystals are present in the experimental charges (dotted if phase not observed in the experimental charge but thought to be present because of mass balance calculation). (a) Ba; (b) Rb; (c) V; (d) Ce; (e) Gd; (f) Yb; (g) U; (h) Nb; (i) Zr and (u) Hf. Data for measured concentrations are from Table 4.10, and data for calculated, residual liquid are in Appendix A4 (Tab. A4.4).

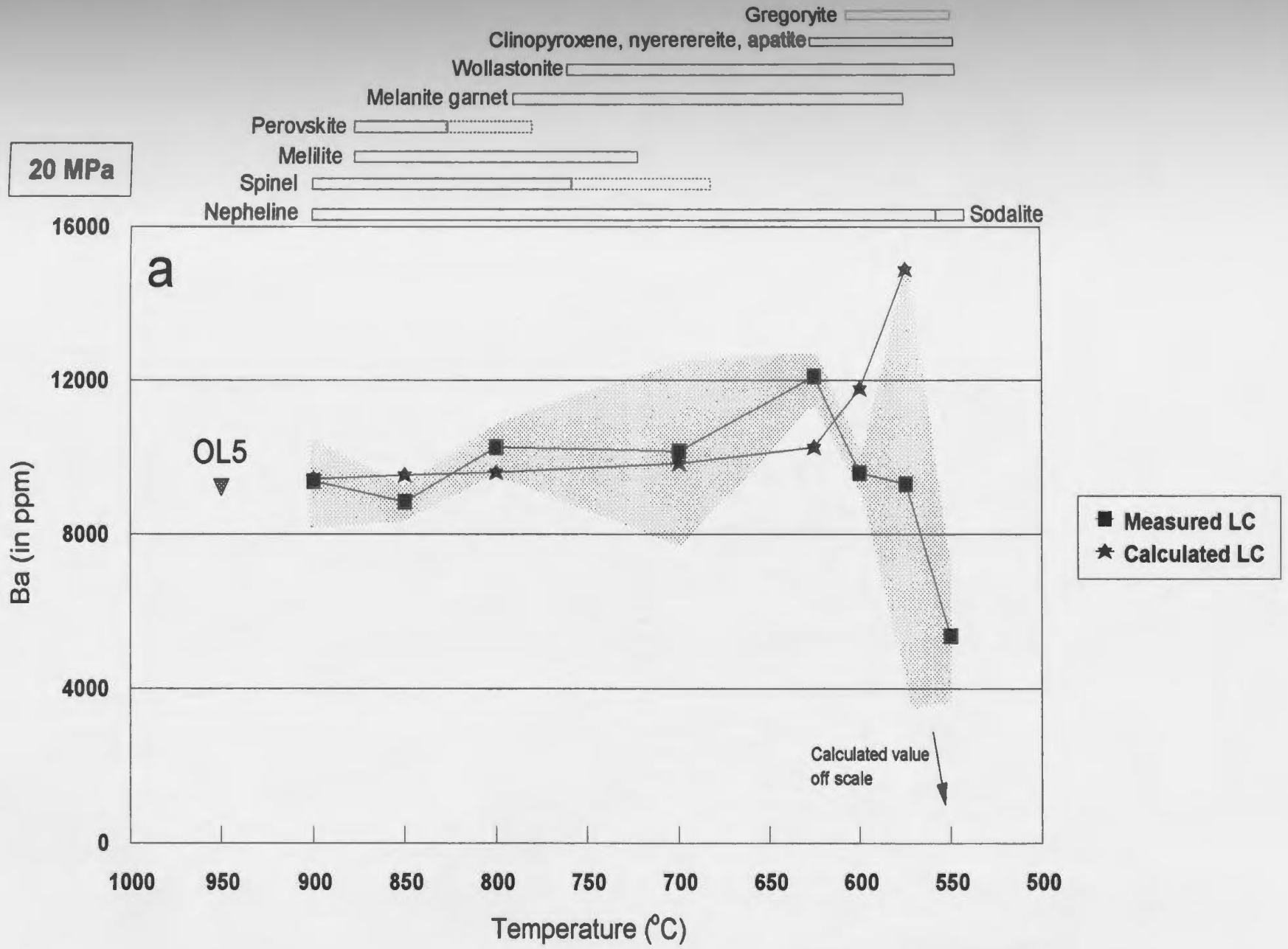
Gregoryite
Clinopyroxene, nyerereite, apatite
Wollastonite
Melanite garnet
Perovskite
Melilite
Spinel
Nepheline
Sodalite
20 MPa
a
OL5
16000
12000
8000
4000
0
Ba (in ppm)
Calculated value
off scale
Measured LC
Calculated LC
1000
950
900
850
800
750
700
650
600
550
500
Temperature (°C)

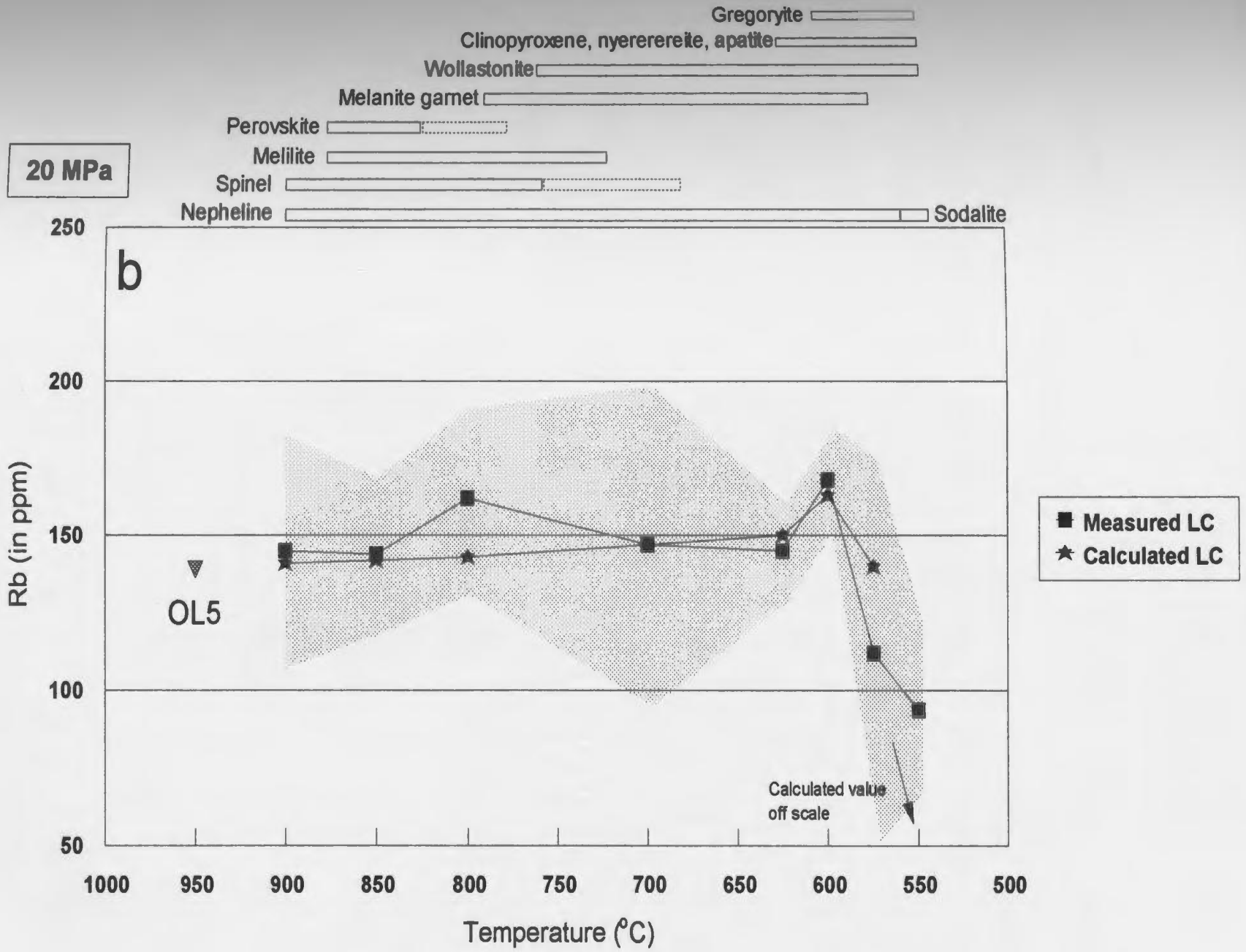
Gregoryite
Clinopyroxene, nyerereretie, apatite
Wollastonite
Melanite garnet
Perovskite
Melilite
Spinel
Nepheline
Sodalite
20 MPa
b
250
200
150
100
50
Rb (in ppm)
OL5
Calculated value
off scale
Measured LC
Calculated LC
1000
950
900
850
800
750
700
650
600
550
500
Temperature (°C)

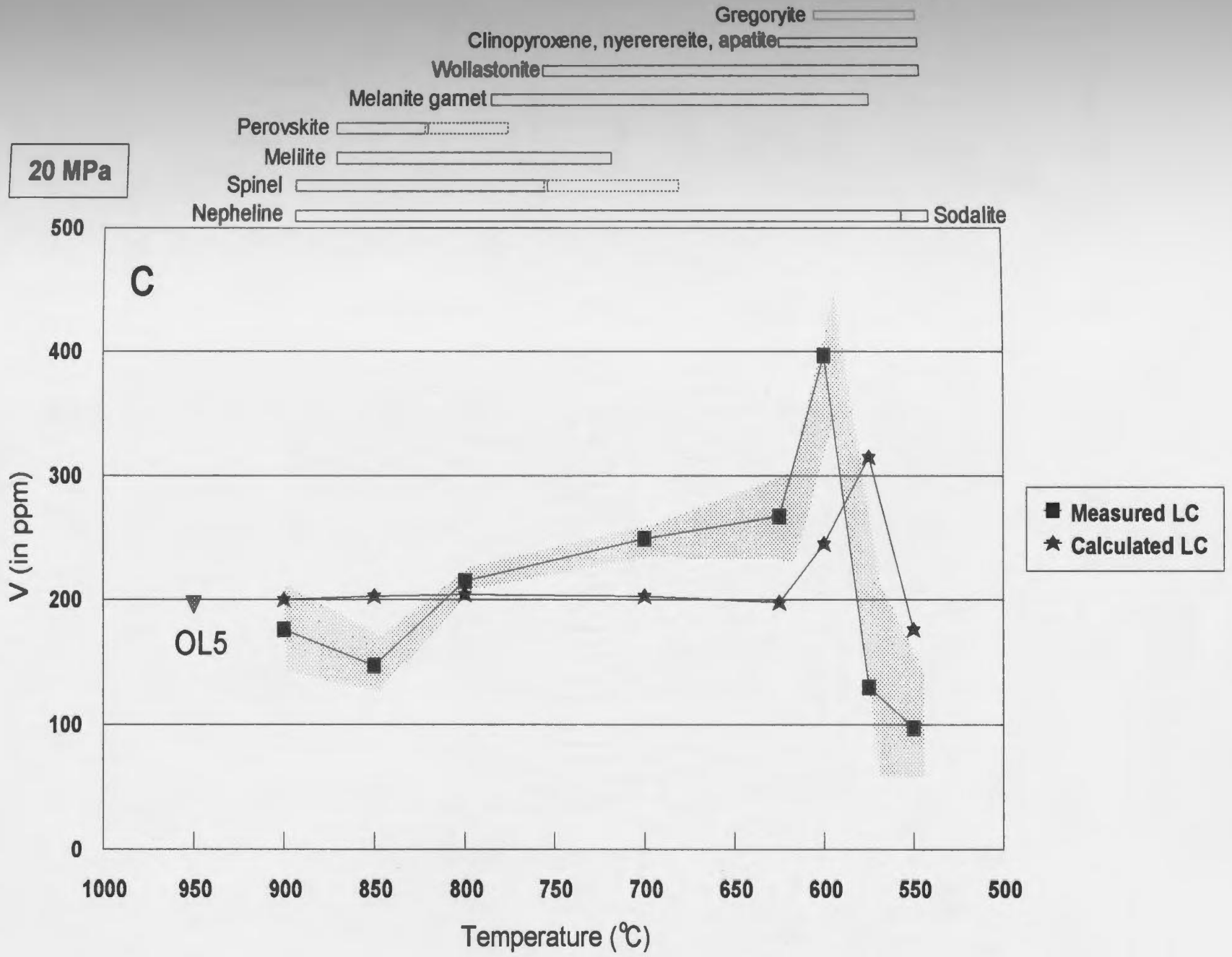
Gregoryite
Clinopyroxene, nyerereite, apatite
Wollastonite
Melanite garnet
Perovskite
Melilite
Spinel
Nepheline
Sodalite
20 MPa
C
OL5
V (in ppm)
500
400
300
200
100
0
1000
950
900
850
800
750
700
650
600
550
500
Temperature (℃)
Measured LC
Calculated LC

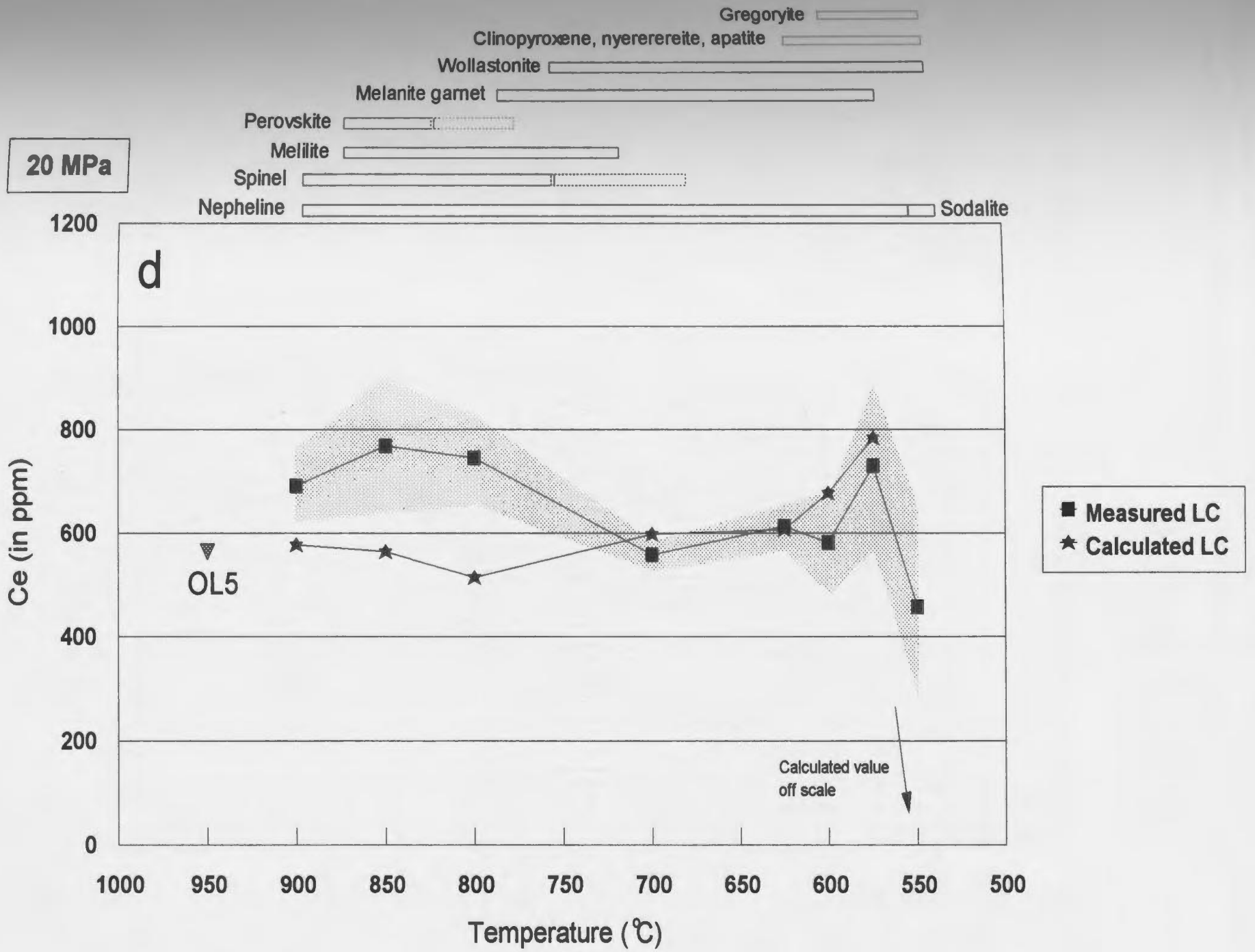
Gregoryite
Clinopyroxene, nyerereereite, apatite
Wollastonite
Melanite garnet
Perovskite
Melilite
Spinel
Nepheline
Sodalite
20 MPa
d
1200
1000
800
600
400
200
0
Ce (in ppm)
OL5
Calculated value
off scale
1000
950
900
850
800
750
700
650
600
550
500
Temperature (℃)
Measured LC
Calculated LC

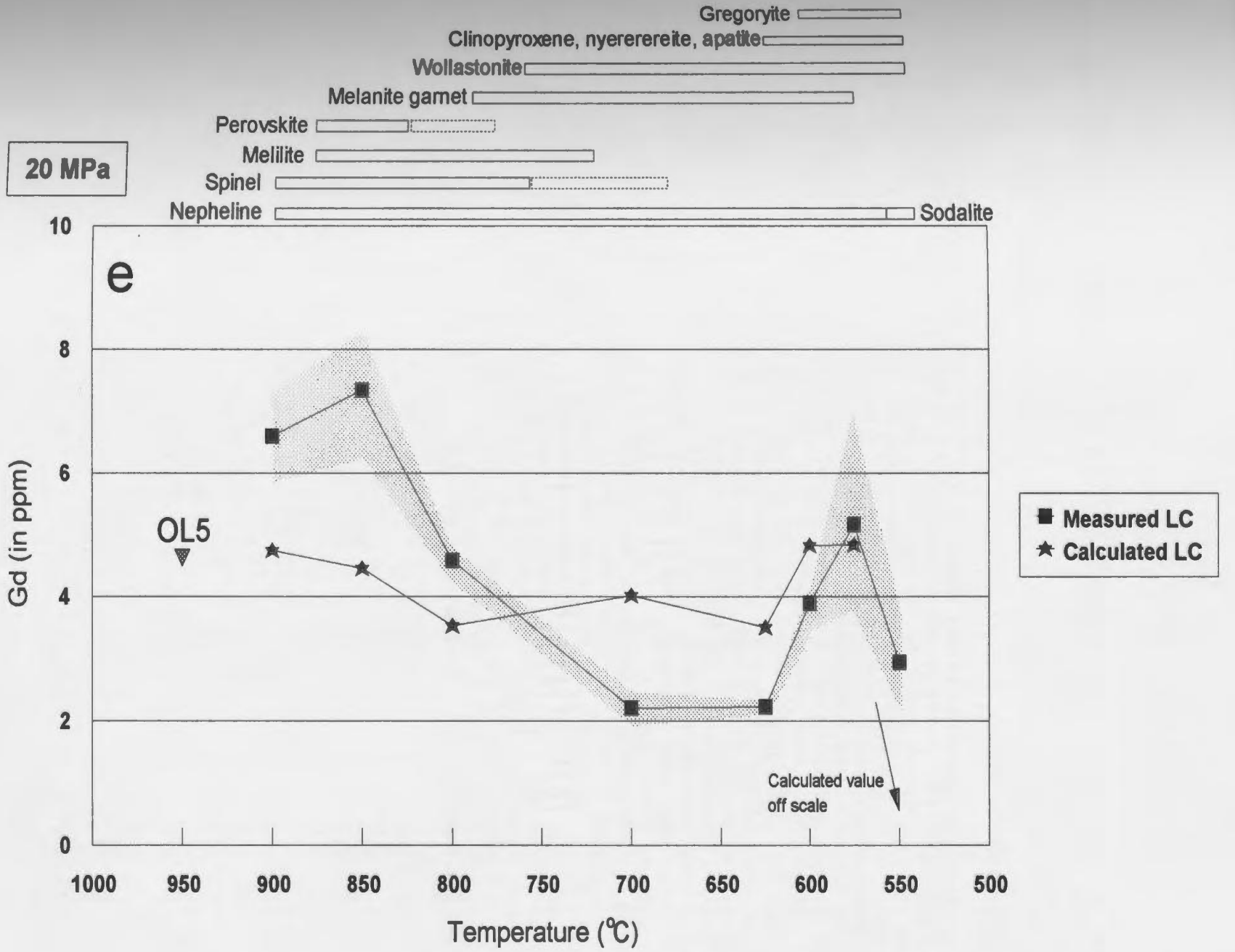
Gregoryite
Clinopyroxene, nyerereite, apatite
Wollastonite
Melanite garnet
Perovskite
Melilite
Spinel
Nepheline
Sodalite
20 MPa
e
OL5
Calculated value
off scale
Measured LC
Calculated LC
Gd (in ppm)
Temperature (℃)
10
8
6
4
2
0
1000
950
900
850
800
750
700
650
600
550
500

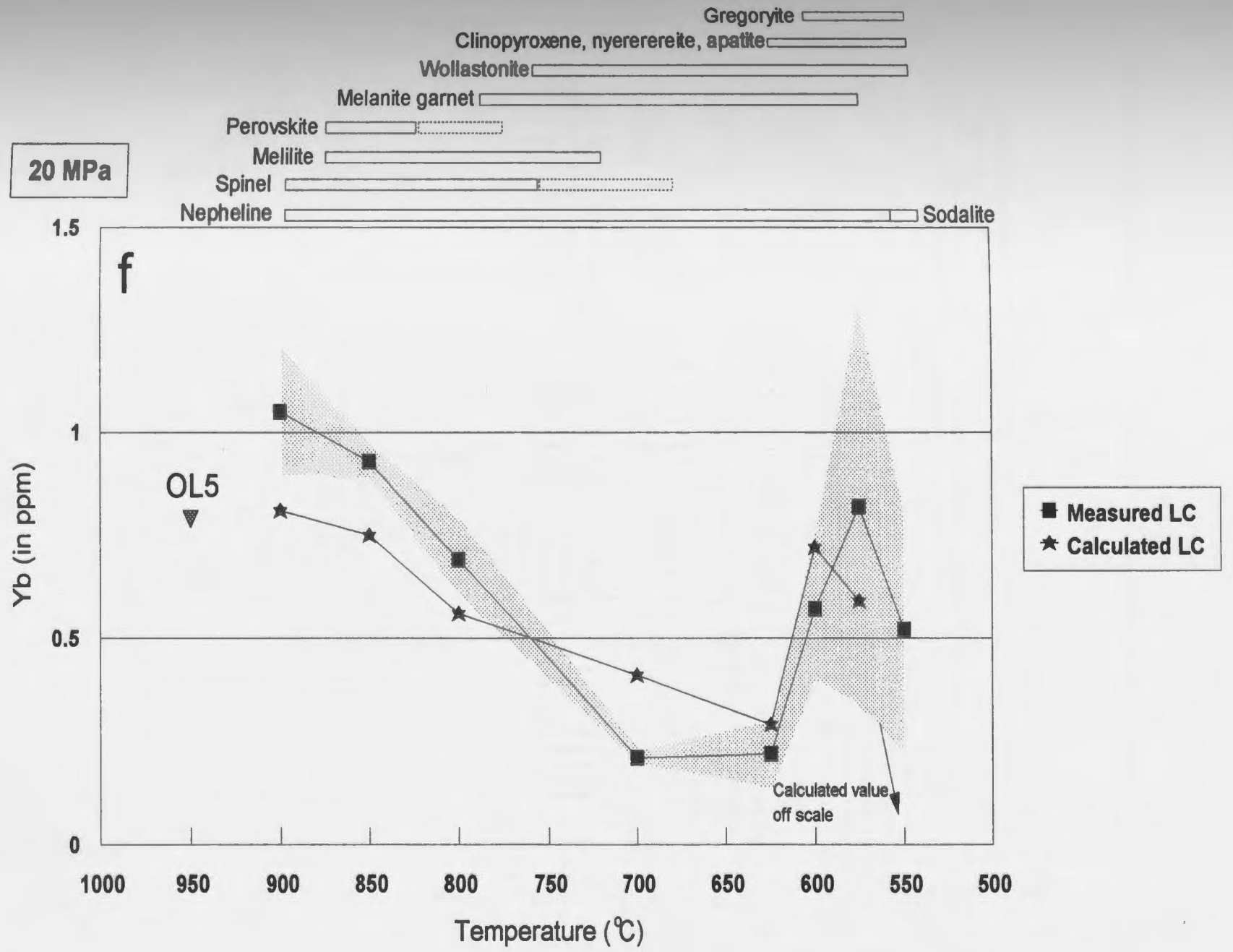
Gregoryite
Clinopyroxene, nyerereite, apatite
Wollastonite
Melanite garnet
Perovskite
Melilite
Spinel
Nepheline
Sodalite
20 MPa
f
OL5
Yb (in ppm)
1.5
1
0.5
0
Measured LC
Calculated LC
Calculated value
off scale
1000
950
900
850
800
750
700
650
600
550
500
Temperature (℃)

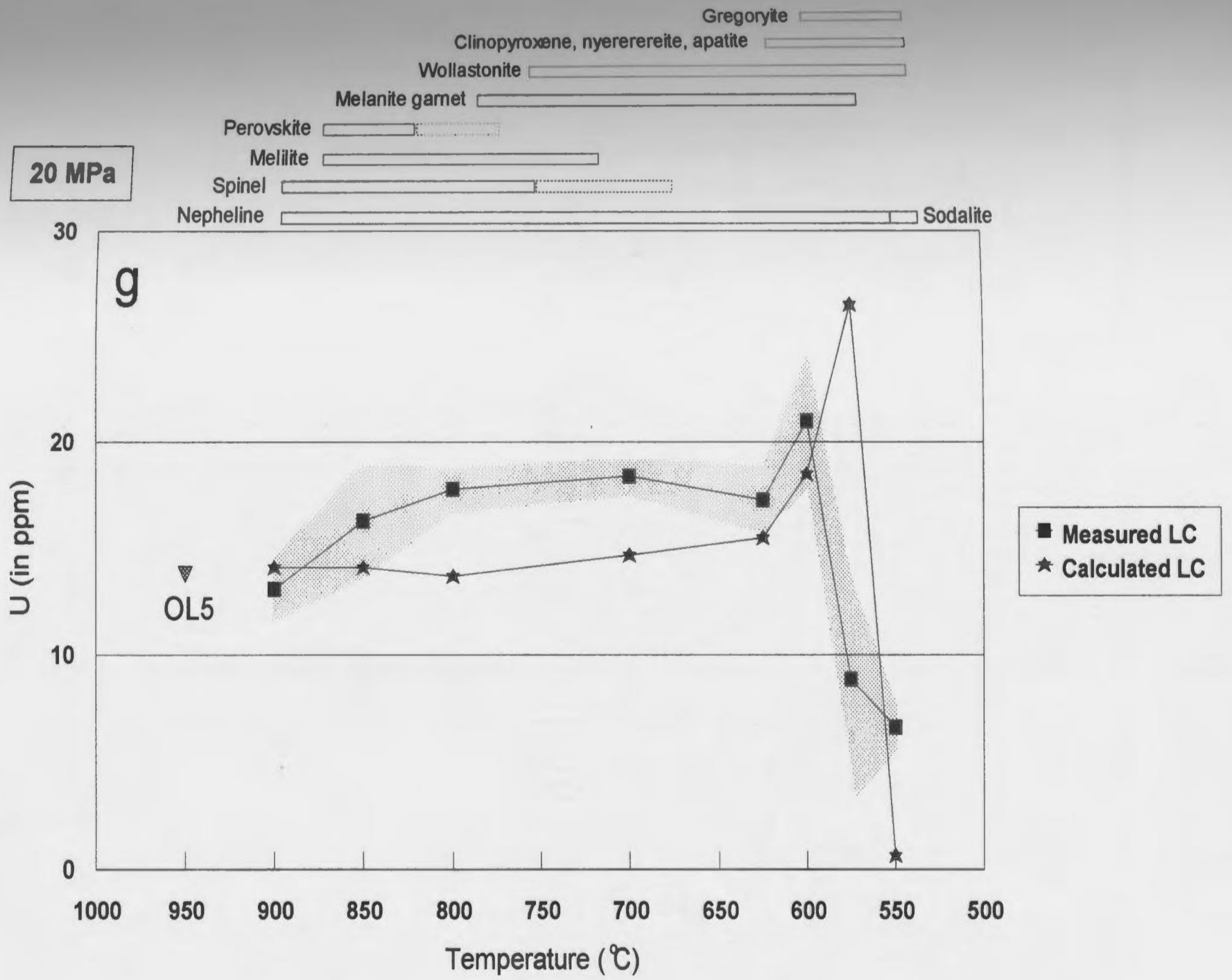
Gregoryite
Clinopyroxene, nyerereite, apatite
Wollastonite
Melanite garnet
Perovskite
Melilite
Spinel
Nepheline
Sodalite
20 MPa
g
OL5
U (in ppm)
Temperature (℃)
Measured LC
Calculated LC
30
20
10
0
1000
950
900
850
800
750
700
650
600
550
500

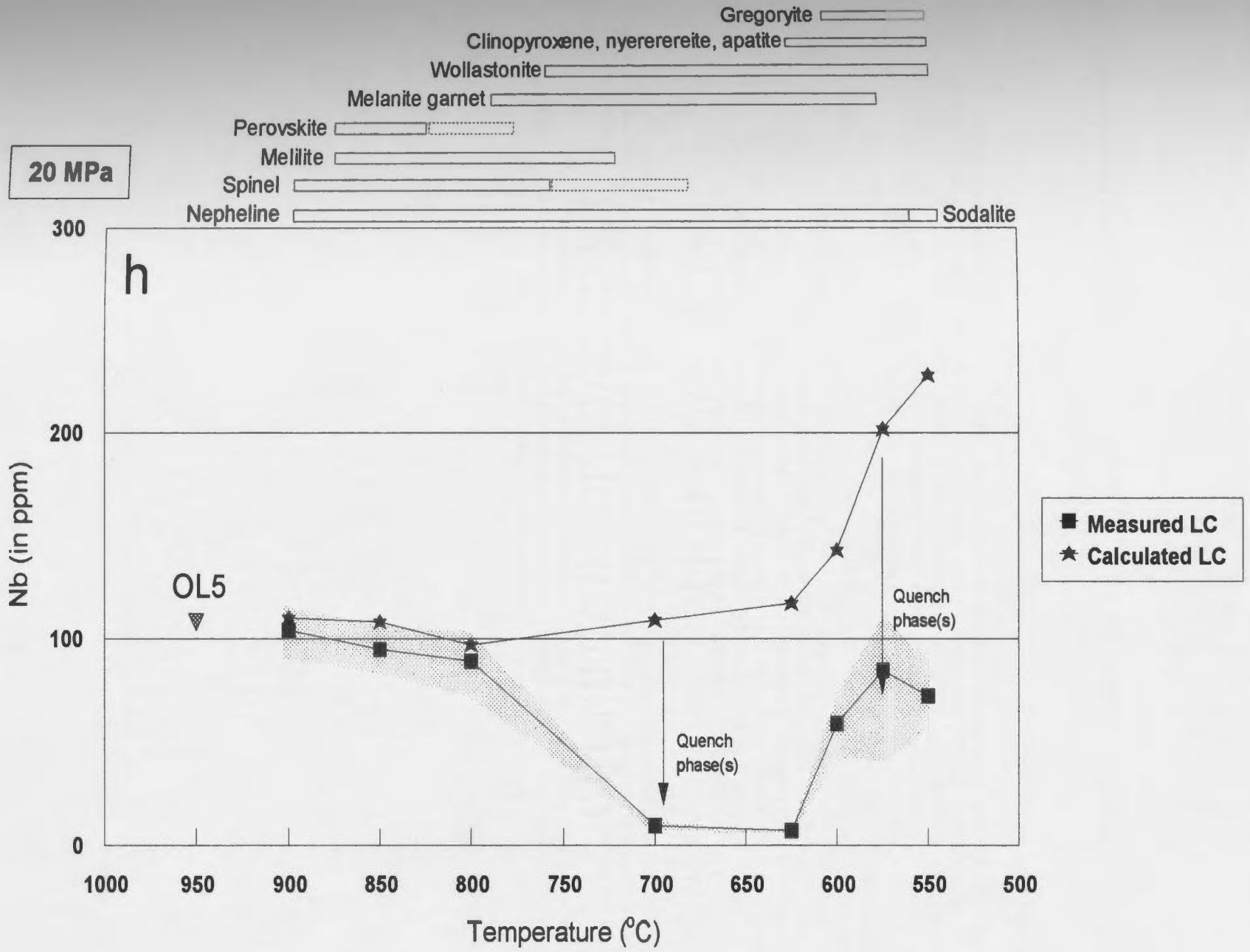
Gregoryite
Clinopyroxene, nyerereireite, apatite
Wollastonite
Melanite garnet
Perovskite
Melilite
Spinel
Nepheline
Sodalite
20 MPa
h
300
200
100
0
Nb (in ppm)
OL5
Quench phase(s)
Quench phase(s)
Measured LC
Calculated LC
1000
950
900
850
800
750
700
650
600
550
500
Temperature (°C)

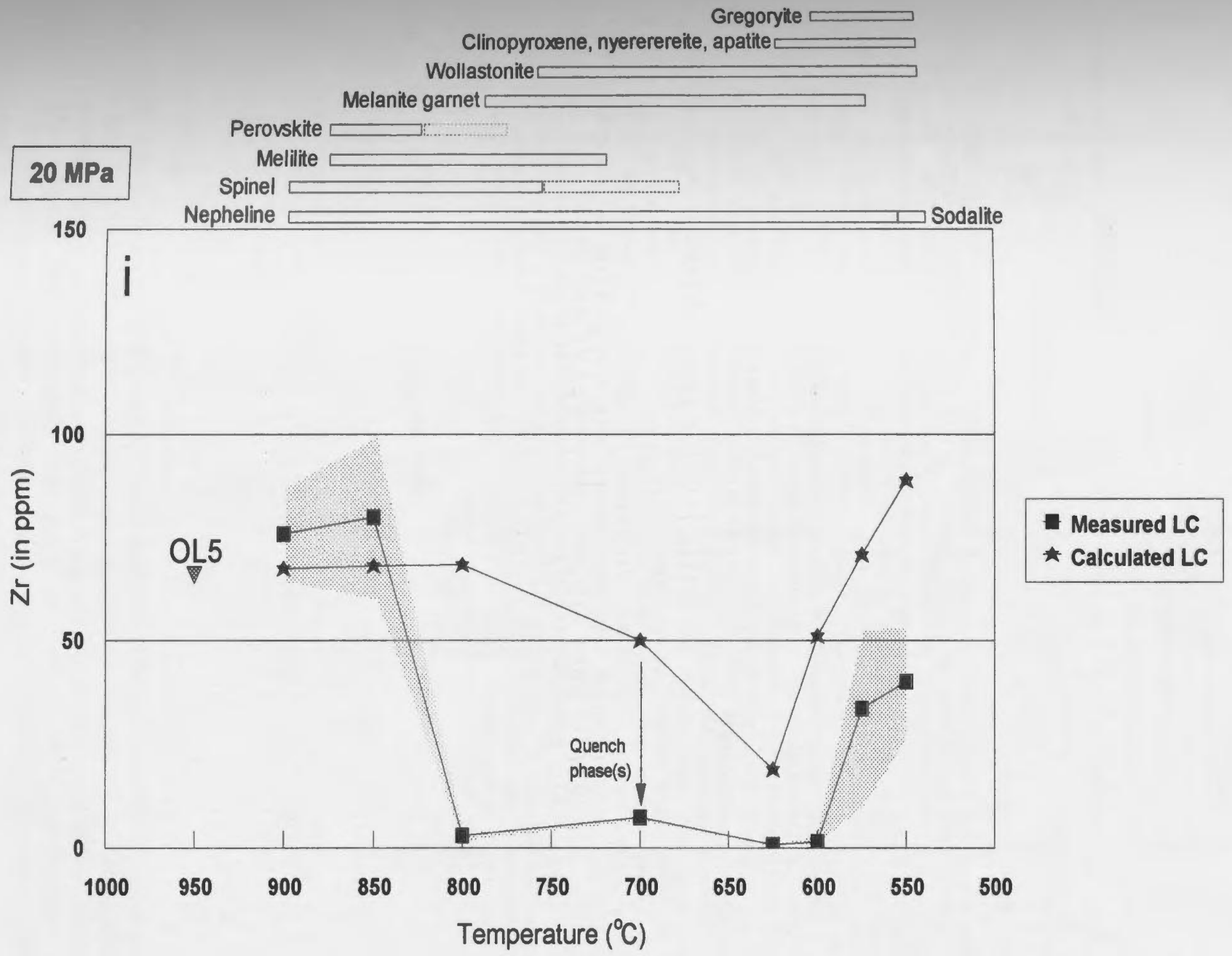
Gregoryite
Clinopyroxene, nyerereite, apatite
Wollastonite
Melanite garnet
Perovskite
Melilite
Spinel
Nepheline
Sodalite
20 MPa
i
OL5
Quench phase(s)
Measured LC
Calculated LC
Zr (in ppm)
Temperature (°C)
150
100
50
0
1000
950
900
850
800
750
700
650
600
550
500

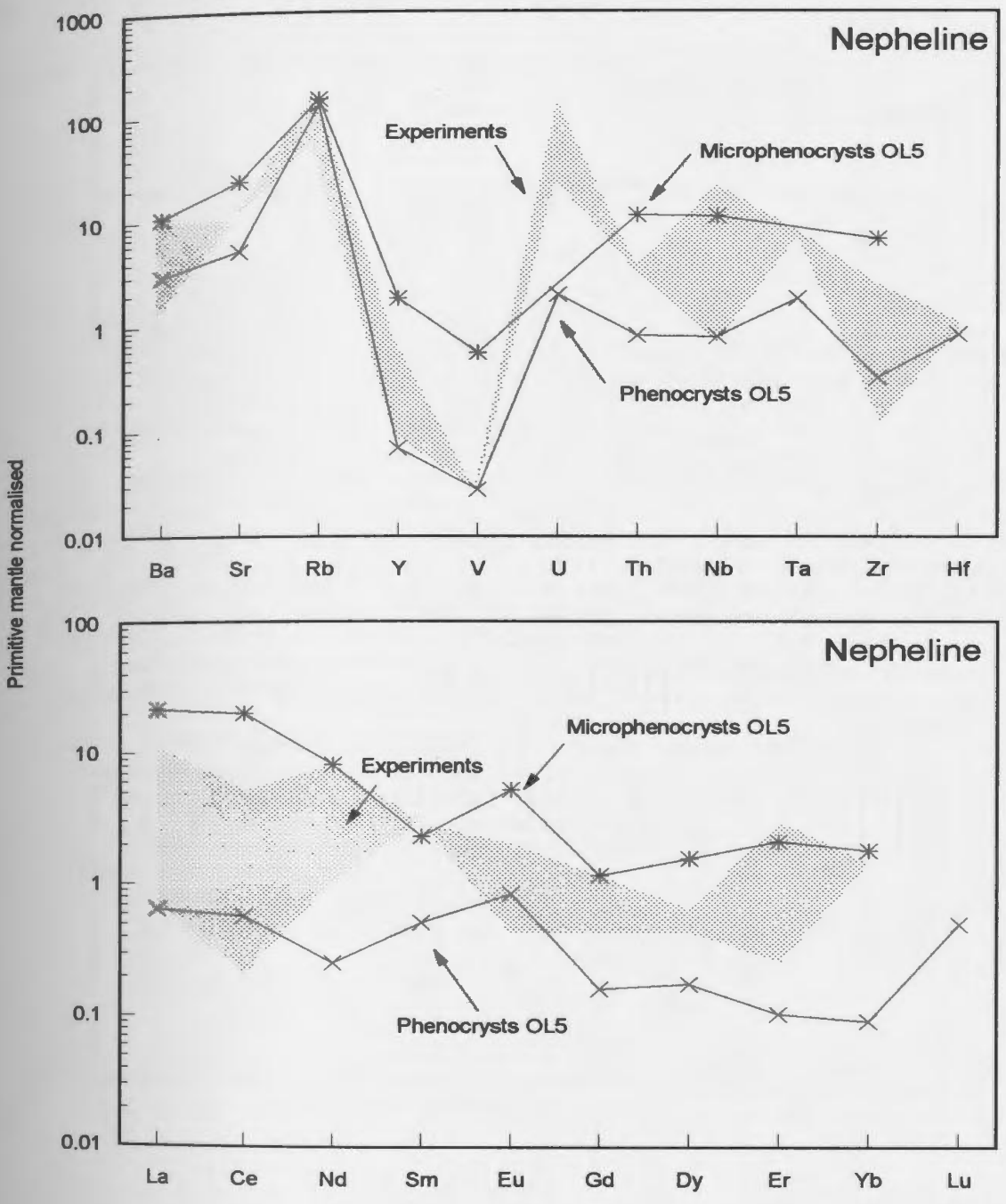

Figure 4.24: Trace element concentrations normalised to primitive mantle of nepheline phenocrysts and microphenocrysts in silicate-bearing natrocarbonatite OL5. Phenocrysts are set in the groundmass, and microphenocrysts are set in the groundmass of the silicate spheroids. The shaded area represents the range of normalised concentrations of nepheline in OL5-experiments. Data are from Table 4.1 and Table 4.9; primitive mantle normalising values are from McDonough and Sun (1995).

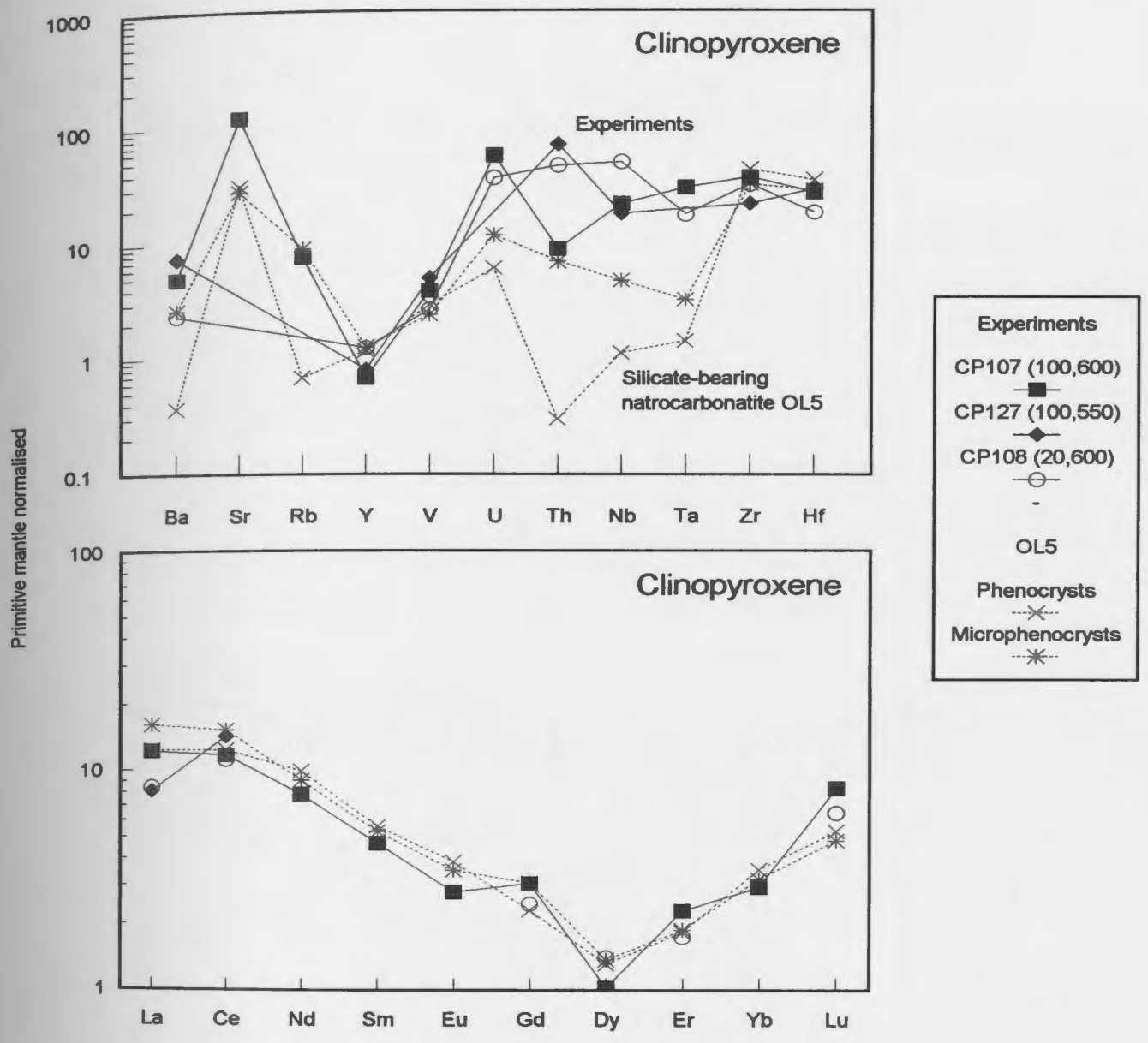

Figure 4.25: Trace element concentrations normalised to primitive mantle for clinopyroxene in OL5-experiments and in silicate-bearing natrocarbonatite OL5. In OL5, phenocrysts are set in the groundmass, and microphenocrysts are set in the groundmass of the silicate spheroids. For the experiments, pressure (in MPa) and temperature (in °C) are shown in brackets beside the experiment number (labelled as CPxx) in the legend. Data are from Table 4.2 and Table 4.9; primitive mantle normalising values are from McDonough and Sun (1995).

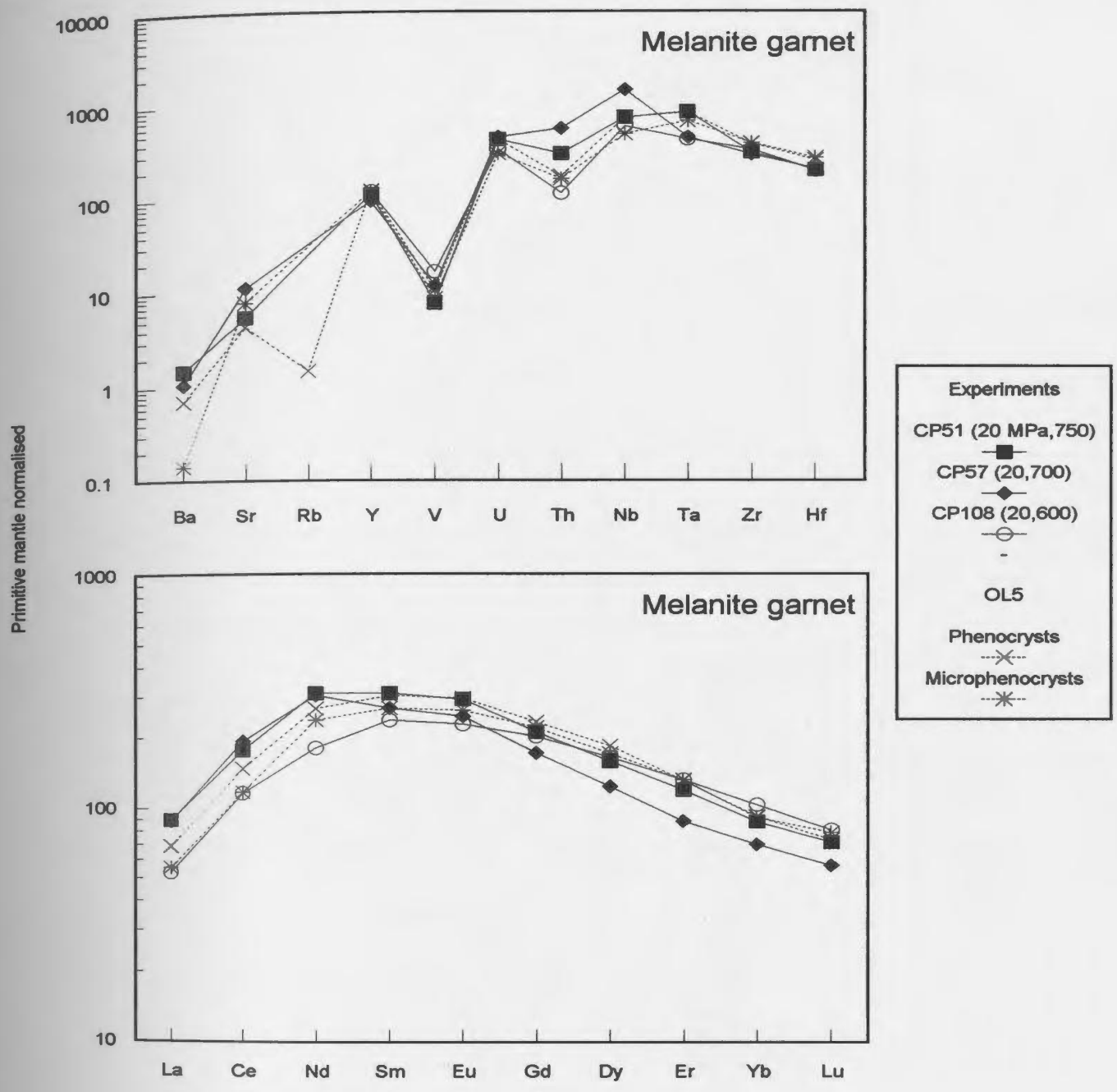

Figure 4.26: Trace element concentrations normalised to primitive mantle for melanite garnet in OL5-experiments and in silicate-bearing natrocarbonatite OL5. In OL5, phenocrysts are set in the groundmass, and microphenocrysts are in an inclusion in a clinopyroxene in a silicate spheroid. For the experiments, pressure (in MPa) and temperature (in °C) are shown in brackets beside the experiment number (labelled as CPxx) in the legend. Data are from Table 4.3 and Table 4.9; primitive mantle normalising values are from McDonough and Sun (1995).

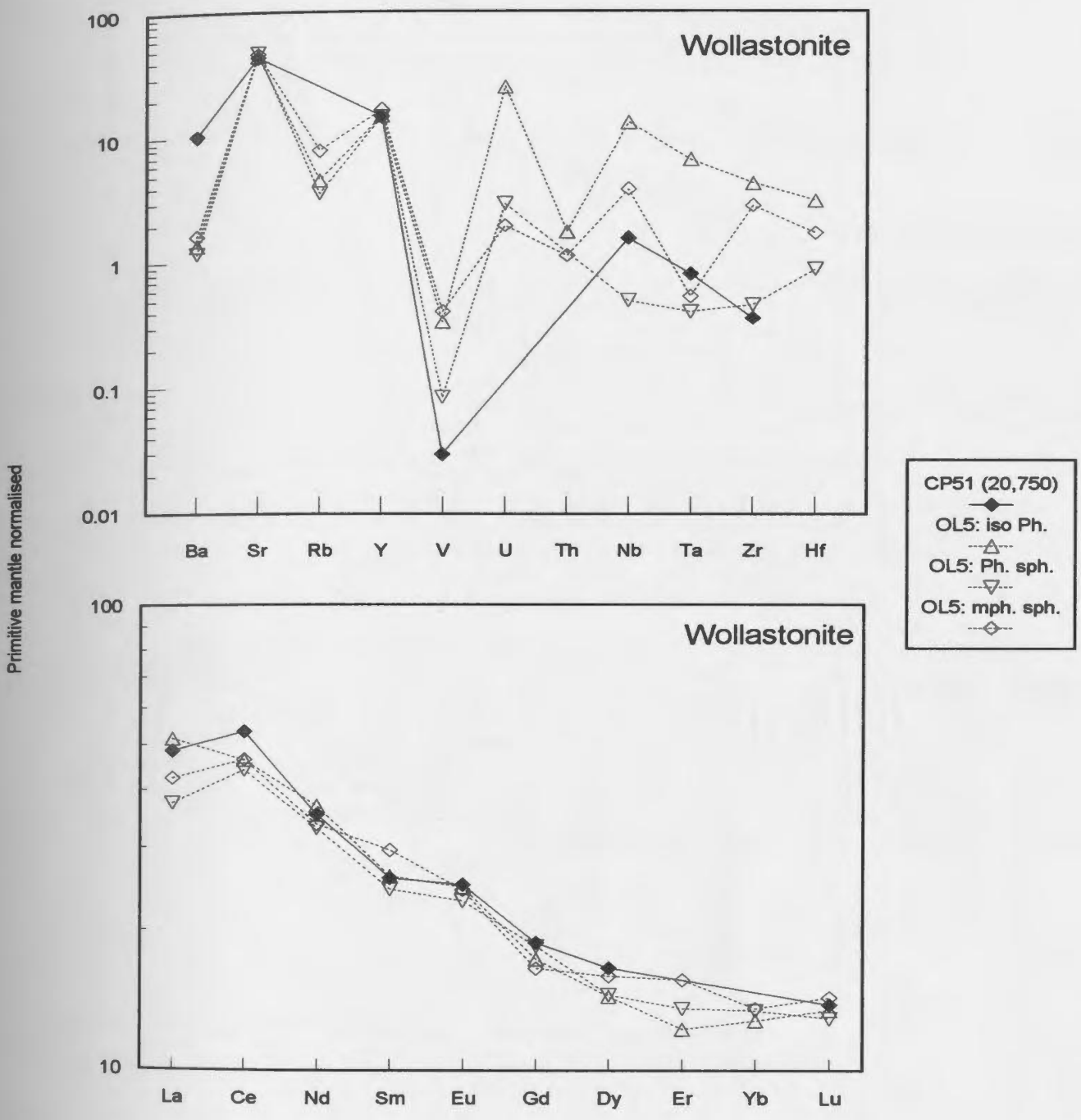

Figure 4.27: Trace element concentrations normalised to primitive mantle for wollastonite in experiment CP51 (20 MPa, 750 °C) and in silicate-bearing natrocarbonatite OL5. In OL5, isolated phenocrysts (iso Ph.), phenocrysts in spheroids (Ph. sph) and microphenocrysts in spheroids (mph. sph.) are plotted separately. Data are from Table 4.4 and Table 4.9; primitive mantle normalising values are from McDonough and Sun (1995).

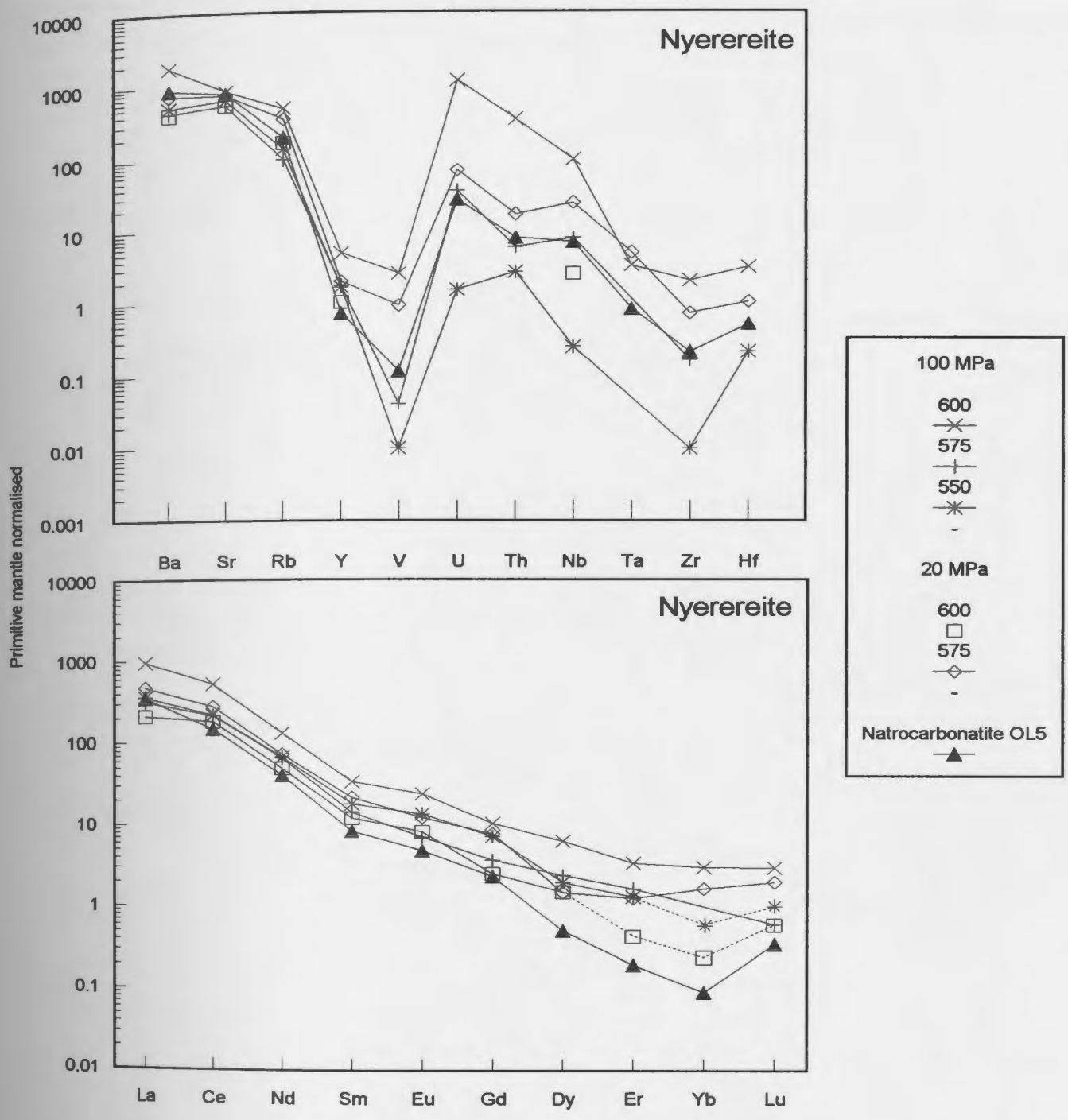

Figure 4.28: Trace element concentrations normalised to primitive mantle for nyerereite in [illegible]5-experiments and in silicate-bearing natrocarbonatite OL5. Temperature (in °C) is shown beside each symbol in the legend for both pressures (100 and 20 MPa). Data are from Table 4.6 and Table 4.9; primitive mantle normalising values are from McDonough and Sun (1995).

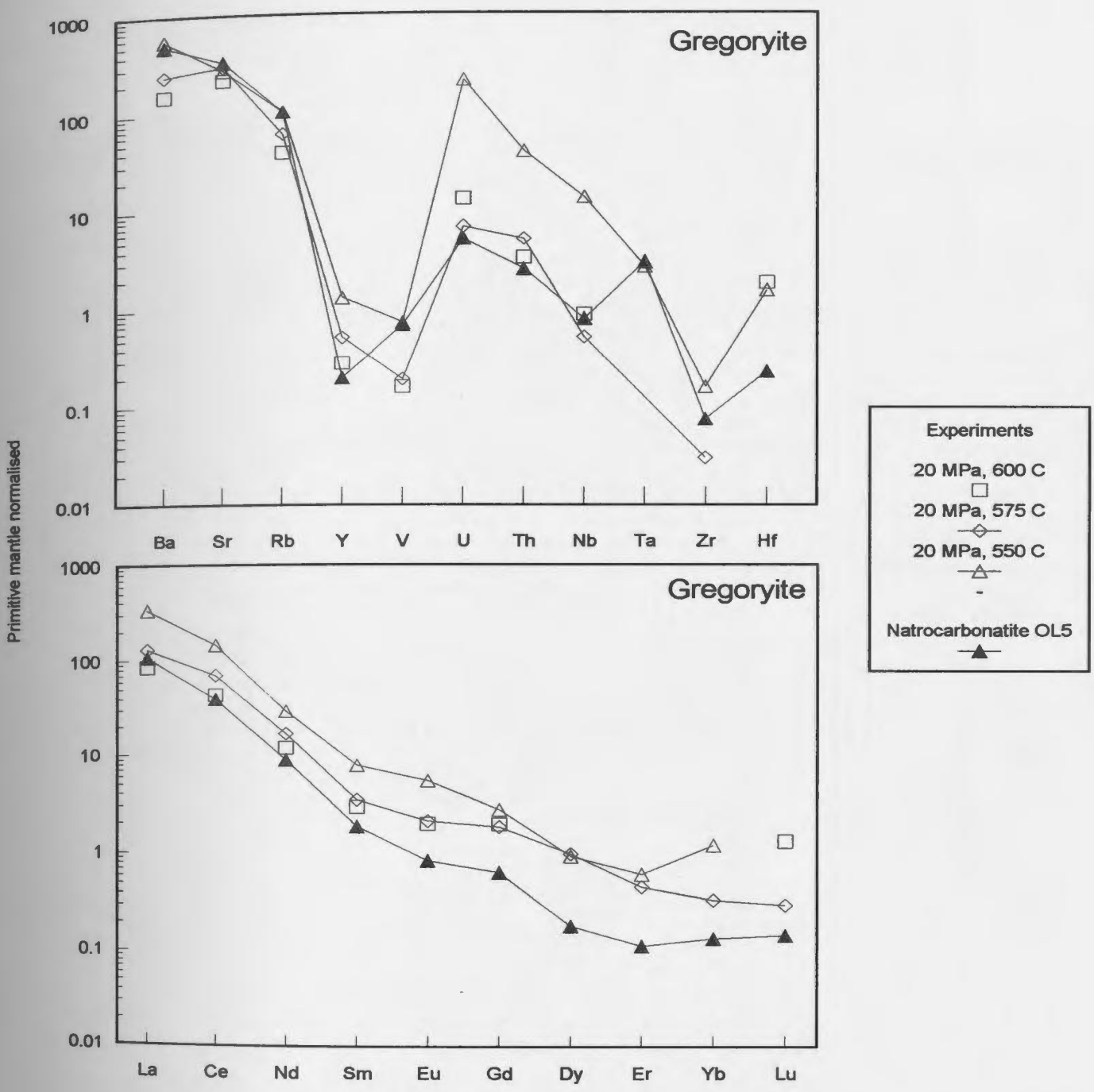

Figure 4.29: Trace element concentrations normalised to primitive mantle for gregoryite from the OL5-experiments and in silicate-bearing natrocarbonatite OL5. Pressure (in MPa) and temperature (in °C) are shown in brackets beside the experiment number (labelled as CPxx) in the legend. Data are from Table 4.7 and Table 4.9; primitive mantle normalising values are from McDonough and Sun (1995).

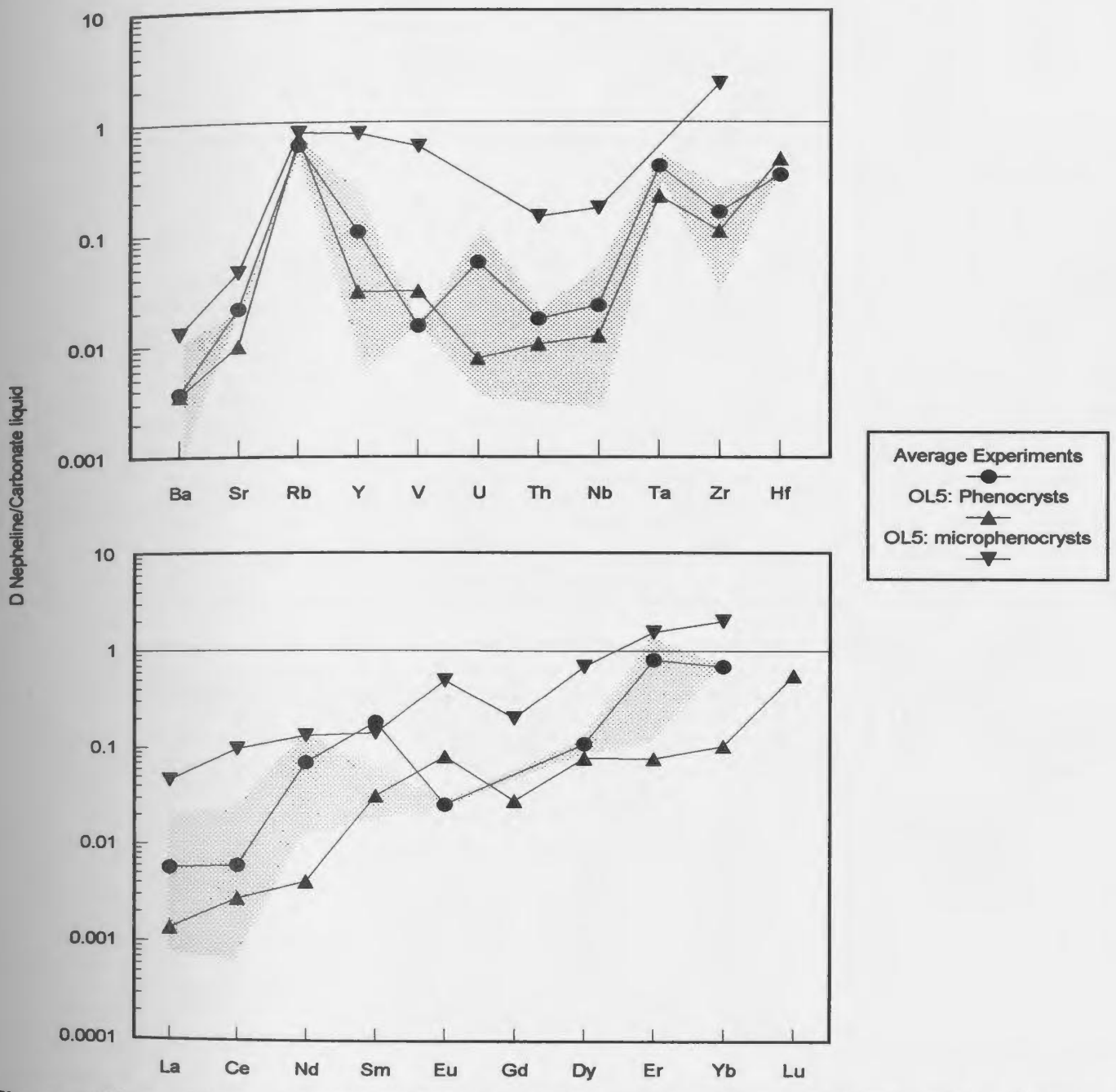

Figure 4.30: Partition coefficients (D) of trace elements between nepheline and carbonate liquid in OL5-experiments and in silicate-bearing natrocarbonatite OL5. The average of D-values are plotted for the experiments, and the shaded area represents the range of D-values for the experiments. For the experiments, D's are calculated between crystal and measured concentration of carbonate liquid, except for D_U and D_{Ta} in CP107, and D_{HFSE} in CP112 which are calculated against calculated concentration of carbonate liquid (see Tab. 4.11). For lava OL5, D's are calculated between nepheline and CEL (see Tab. 4.11). Data are from Table 4.12.

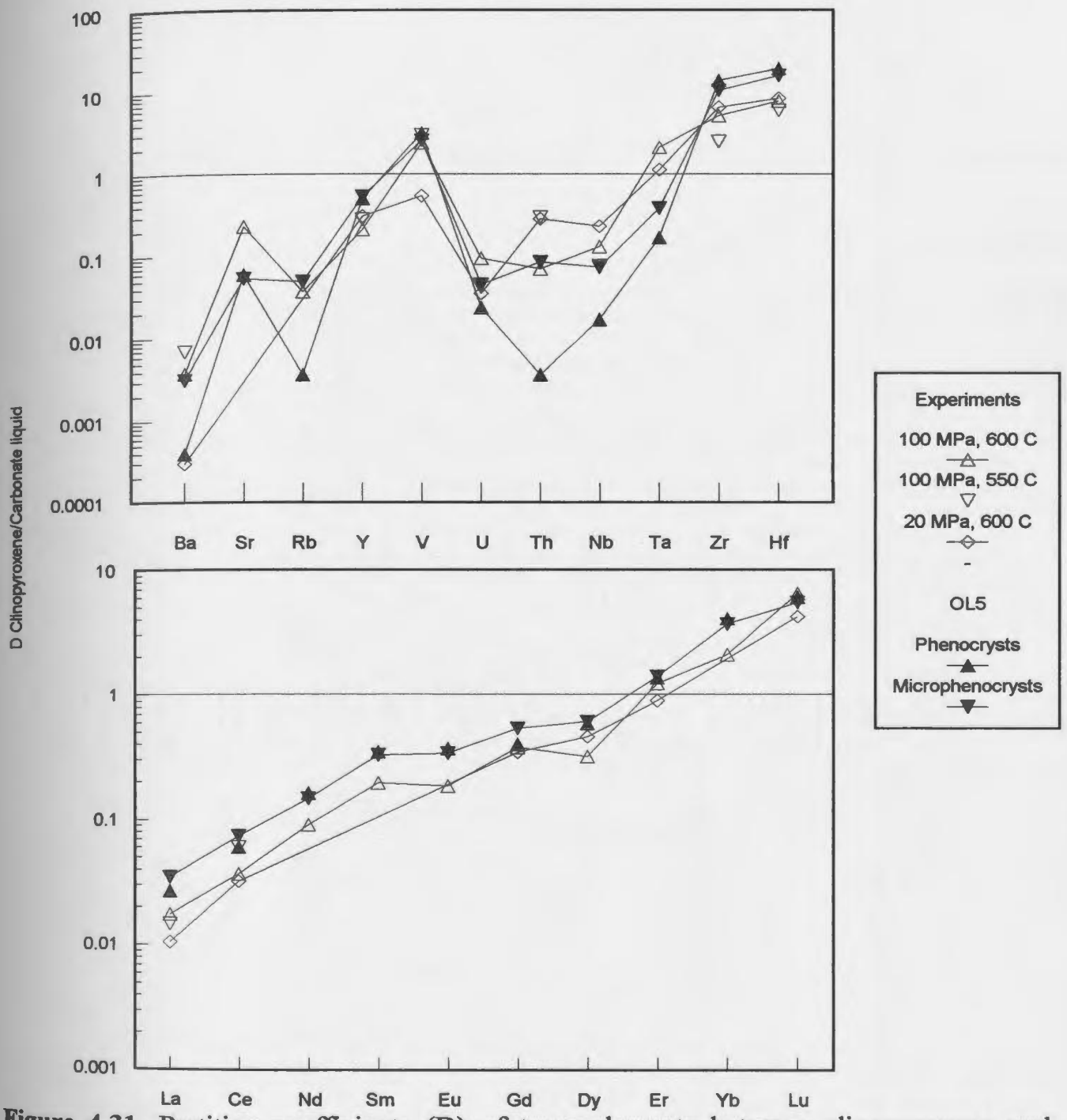

Figure 4.31: Partition coefficients (D) of trace elements between clinopyroxene and carbonate liquid in OL5-experiments and in silicate-bearing natrocarbonatite OL5. Pressure (in MPa) and temperature (in °C) are shown in brackets beside the symbol in the legend. For the experiments, D's are calculated between crystal and measured concentration of carbonate liquid, except for D_U, D_{Nb} and D_{Ta} in CP107, D_{Th}, D_{Nb}, D_{Zr} and D_{Hf} in CP127, and D_{HFSE} in CP108 which are calculated against calculated concentration of carbonate liquid (see Tab. 4.11). For lava OL5, D's are calculated between clinopyroxene and CEL (see Tab. 4.11). Data are from Table 4.12.

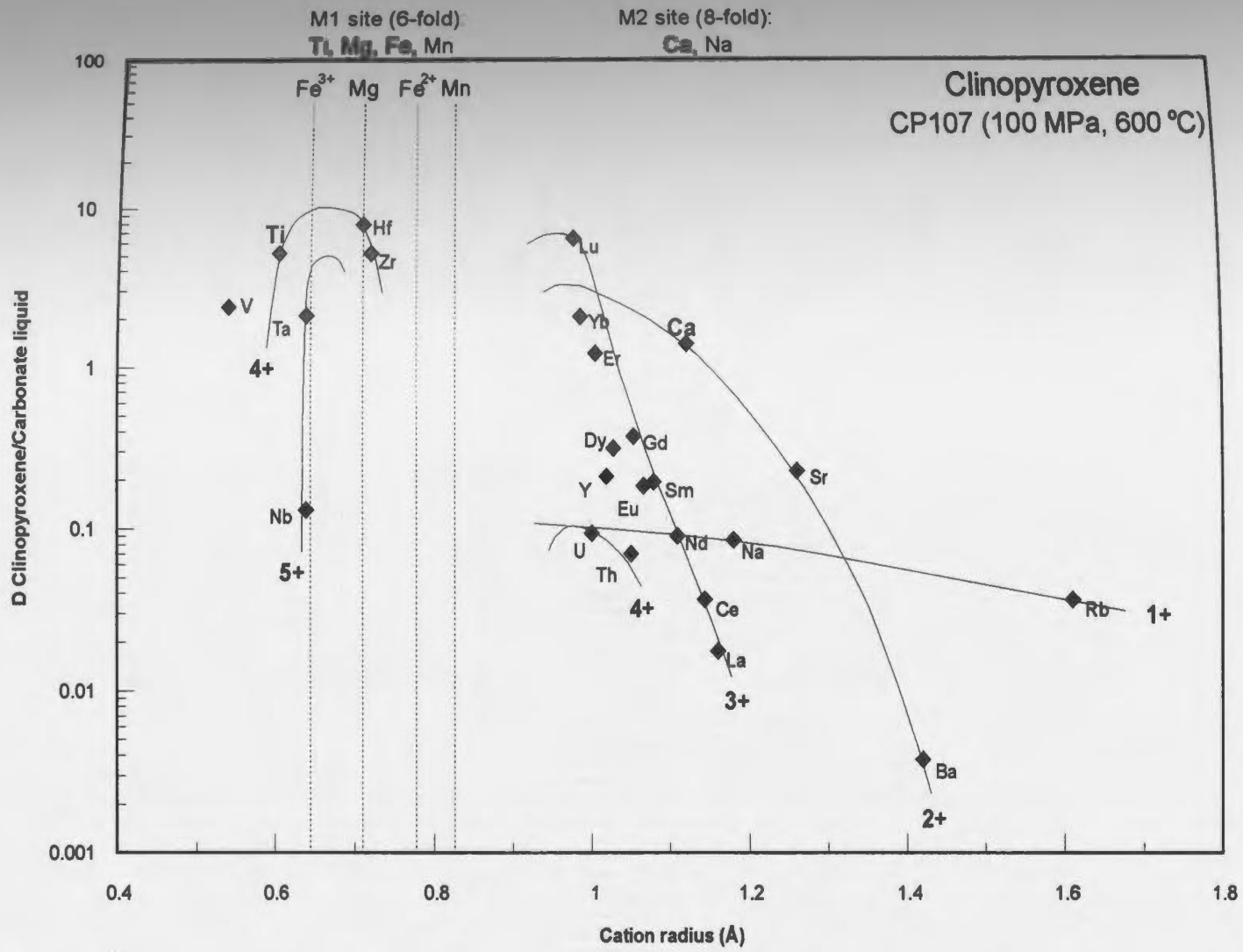

Figure 4.32: Variation of partition coefficients (D) between clinopyroxene and carbonate liquid as a function of ionic radius (in ångstroms) for experiment CP107 (100 MPa, 600 °C). Curves for 1+, 2+, 3+ and 4+ valencies are labelled. Also plotted are the ionic radii for Fe^{3+}, Mg^{2+}, Fe^{2+} and Mn^{2+} under 6-fold coordination. Data for D's are from Table 4.12 and data for ionic radii are from Shannon (1976).

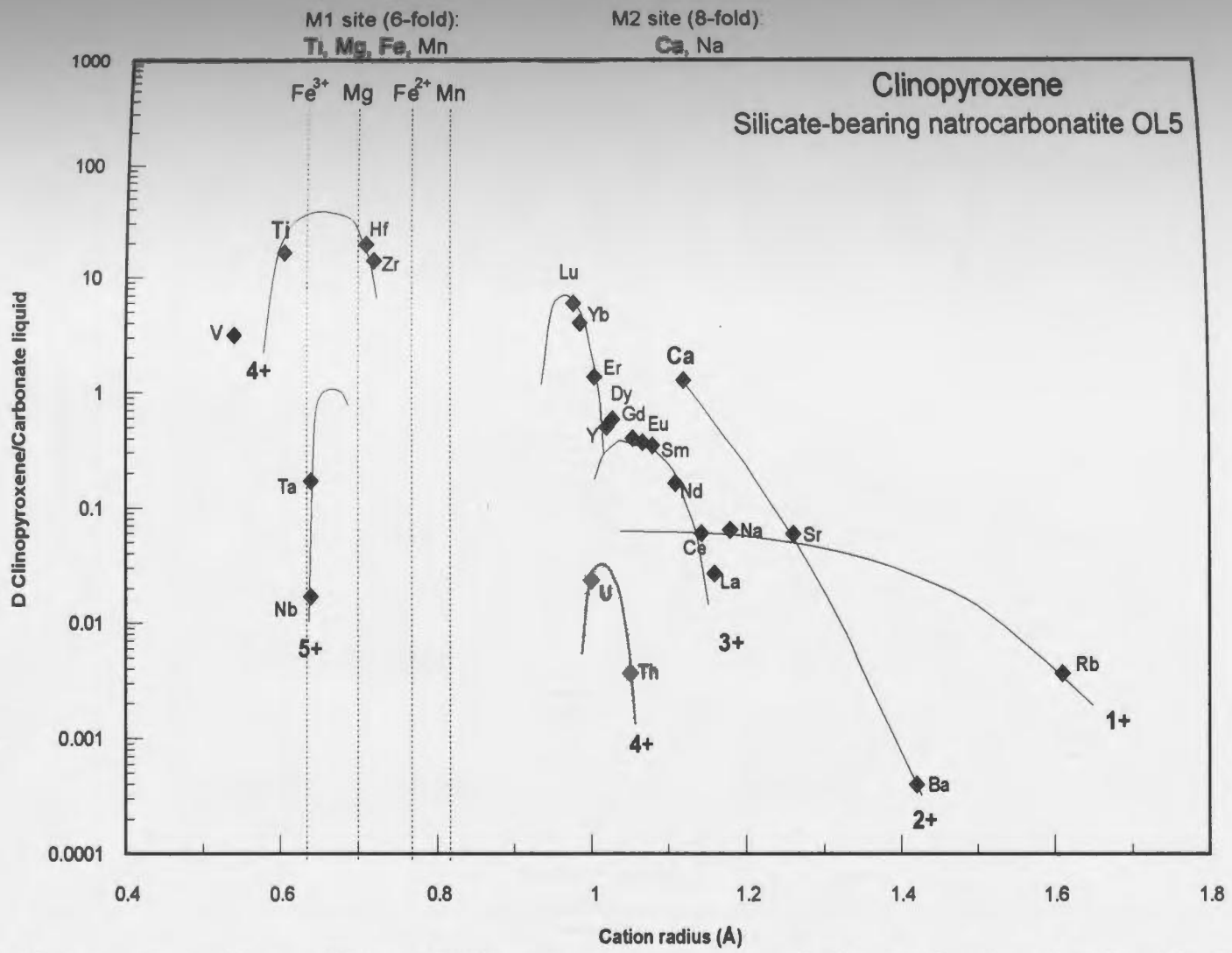

Figure 4.33: Variation of partition coefficients (D) between clinopyroxene and CEL as a function of ionic radius (in ångstroms) for silicate-bearing natrocarbonatite OL5. Curves for 1+, 2+, 3+ and 4+ valencies are labelled. Also plotted are the ionic radii for Fe^{3+}, Mg^{2+}, Fe^{2+} and Mn^{2+} under 6-fold coordination. Data for D's are from Table 4.12 and data for ionic radii are from Shannon (1976).

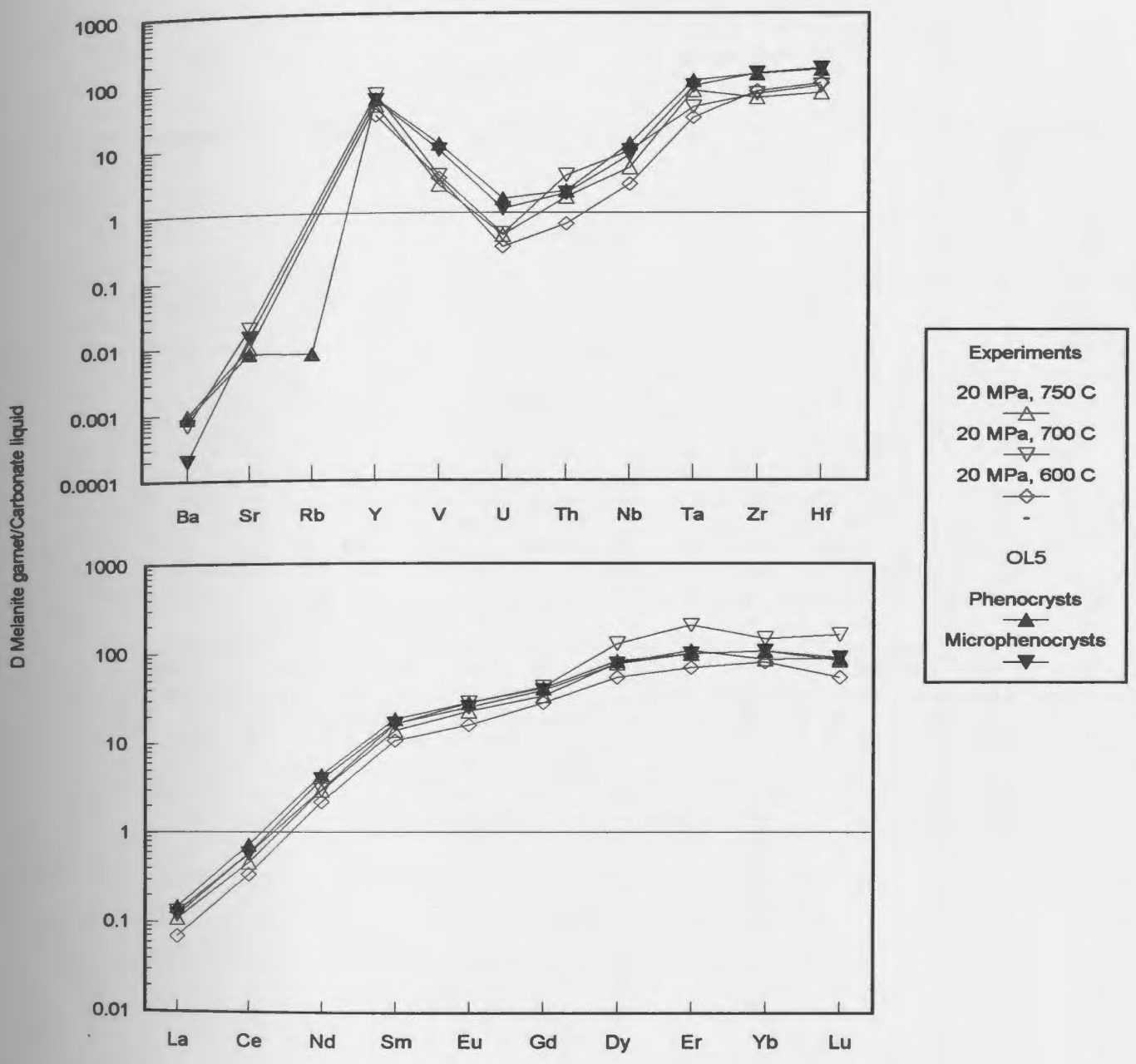

Figure 4.34: Partition coefficients (D) of trace elements between melanite garnet and carbonate liquid in OL5-experiments and in silicate-bearing natrocarbonatite OL5. Pressure (in MPa) and temperature (in °C) are shown in brackets in the legend beside the symbol. For the experiments, D's are calculated between crystal and measured concentrations of carbonate liquid, except for all trace elements in CP51, D_{HFSE} in CP57 and in CP108, which are calculated against calculated concentration of carbonate liquid (see Tab. 4.11). For lava OL5, D's are calculated between melanite garnet and CEL (see Tab. 4.11). Data are from Table 4.12.

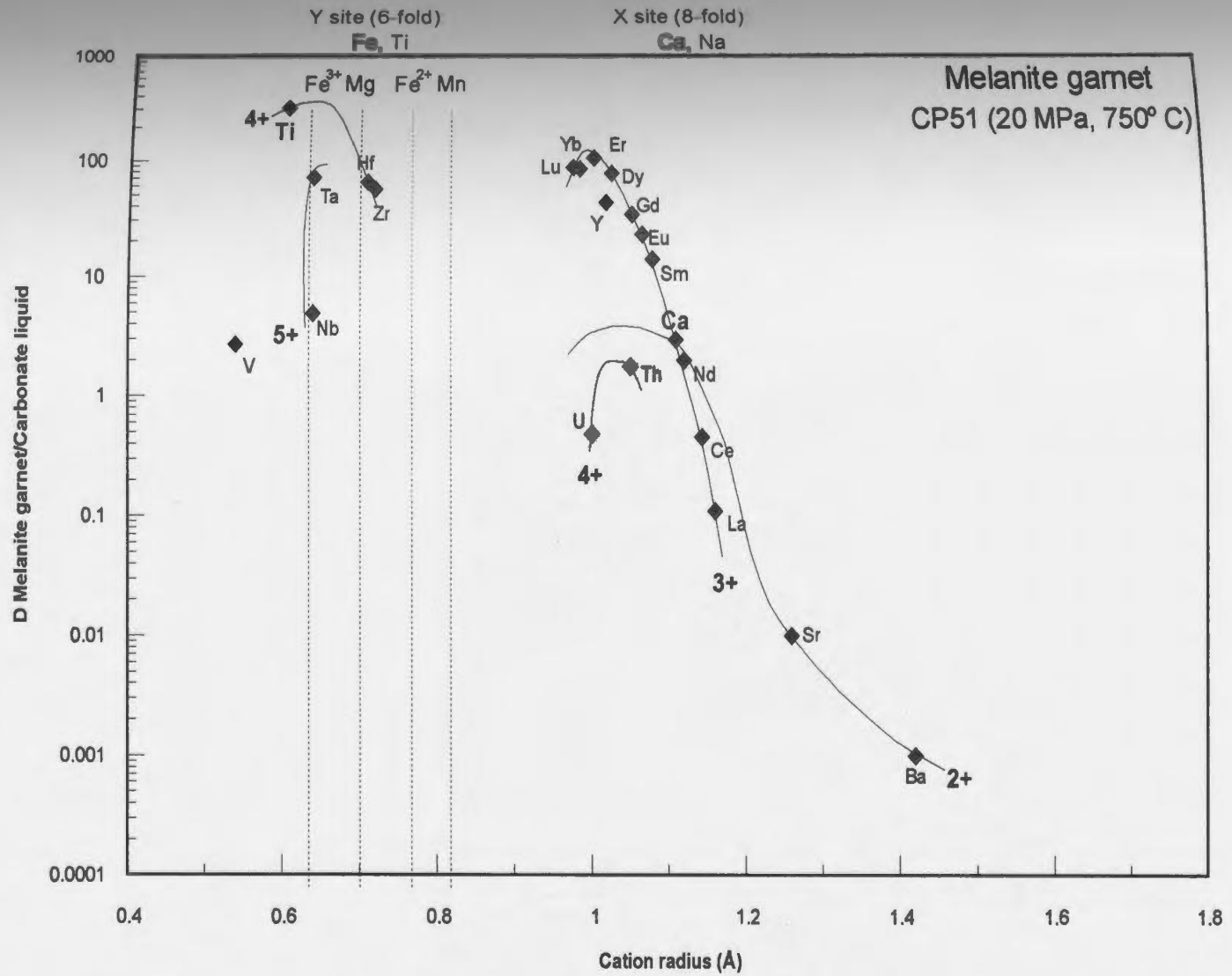

Figure 4.35: Variation of partition coefficients (D) between melanite garnet and carbonate liquid as a function of ionic radius (in ångstroms) for experiment CP51 (20 MPa, 750 °C). Curves for 2+, 3+ and 4+ valencies are labelled. Also plotted are the ionic radii for Fe^{3+}, Mg^{2+}, Fe^{2+} and Mn^{2+} under 6-fold coordination. Data for D's are from Table 4.12 and data for ionic radii are from Shannon (1976).

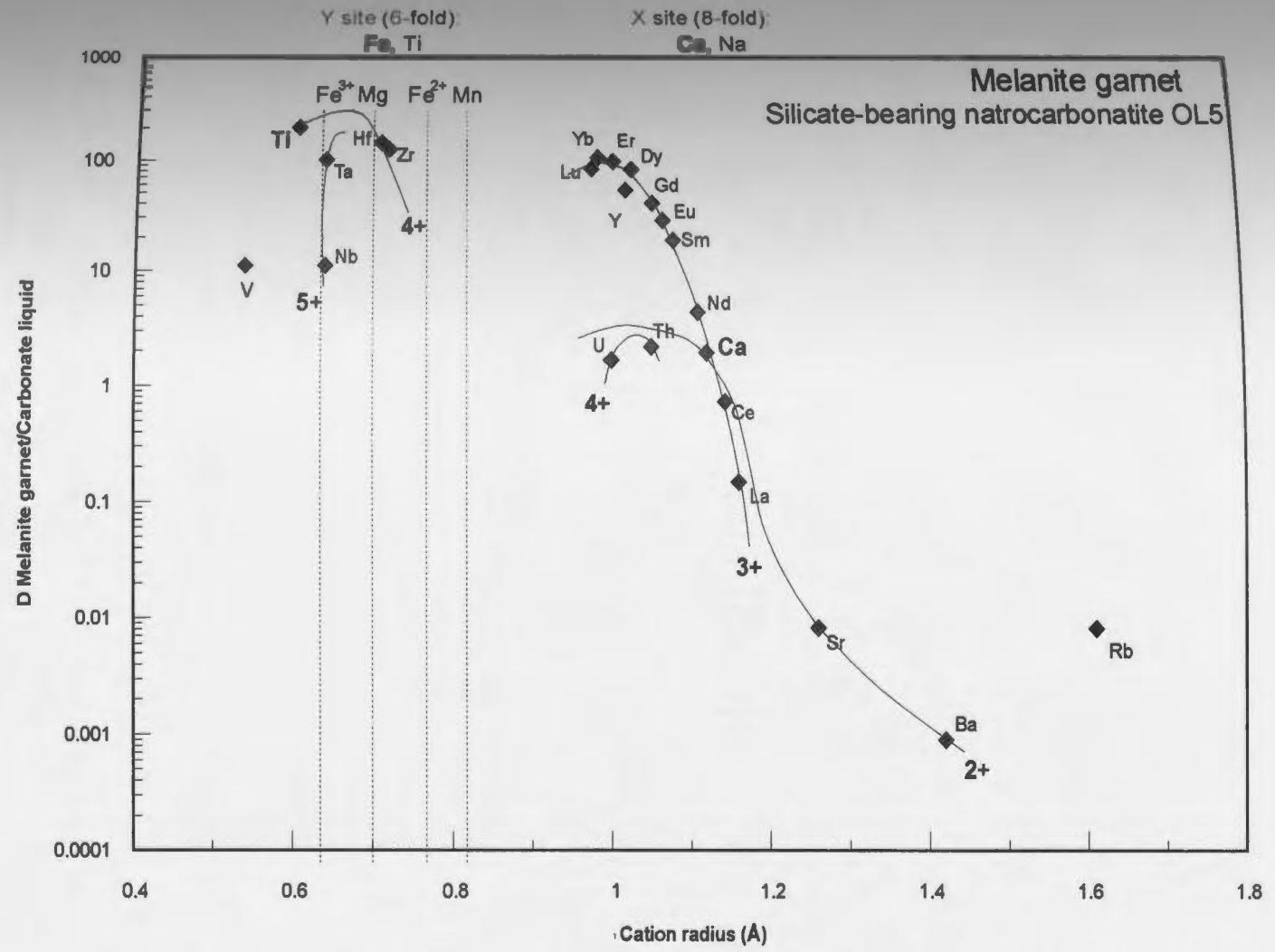

Figure 4.36: Variation of partition coefficients (D) between melanite garnet and CEL as a function of ionic radius (in ångstroms) for silicate-bearing natrocarbonatite OL5. Curves for 2+, 3+ and 4+ valencies are labelled. Also plotted are the ionic radii for Fe^{3+}, Mg^{2+}, Fe^{2+} and Mn^{2+} under 6-fold coordination. Data for D's are from Table 4.12 and data for ionic radii are from Shannon (1976).

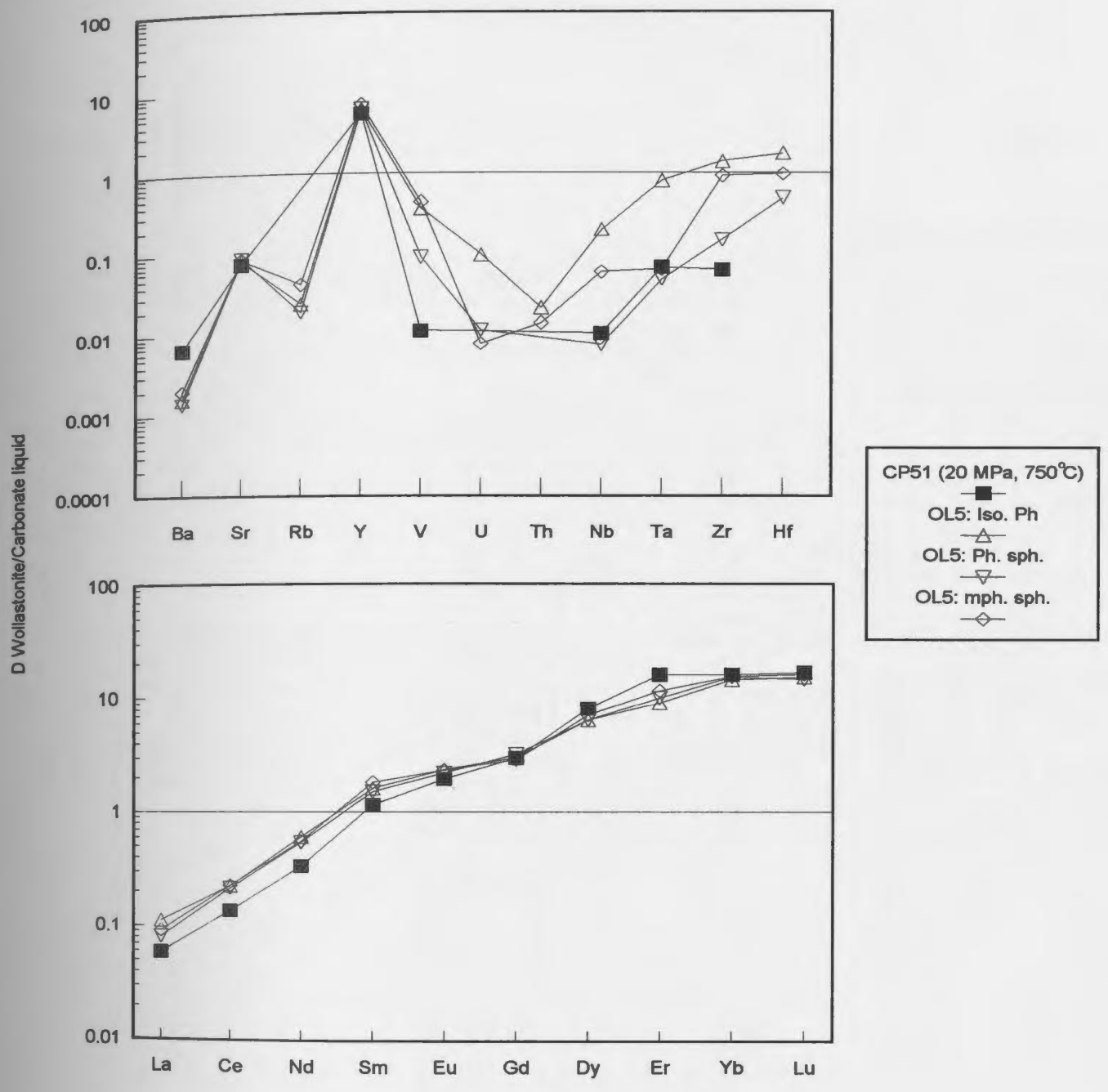

Figure 4.37: Partition coefficients (D) of trace elements between wollastonite and carbonate liquid in experiment CP51 (20 MPa, 750 °C) and in silicate-bearing natrocarbonatite OL5. For the experiment, D's for all trace elements are calculated between wollastonite and calculated concentration of carbonate liquid (see Tab. 4.11). For OL5, D's are calculated between wollastonite and CEL (see Tab. 4.11); isolated phenocrysts (iso Ph.), phenocrysts in spheroids (Ph. sph) and microphenocrysts in spheroids (mph. sph.) are plotted separately. Data are from Table 4.12.

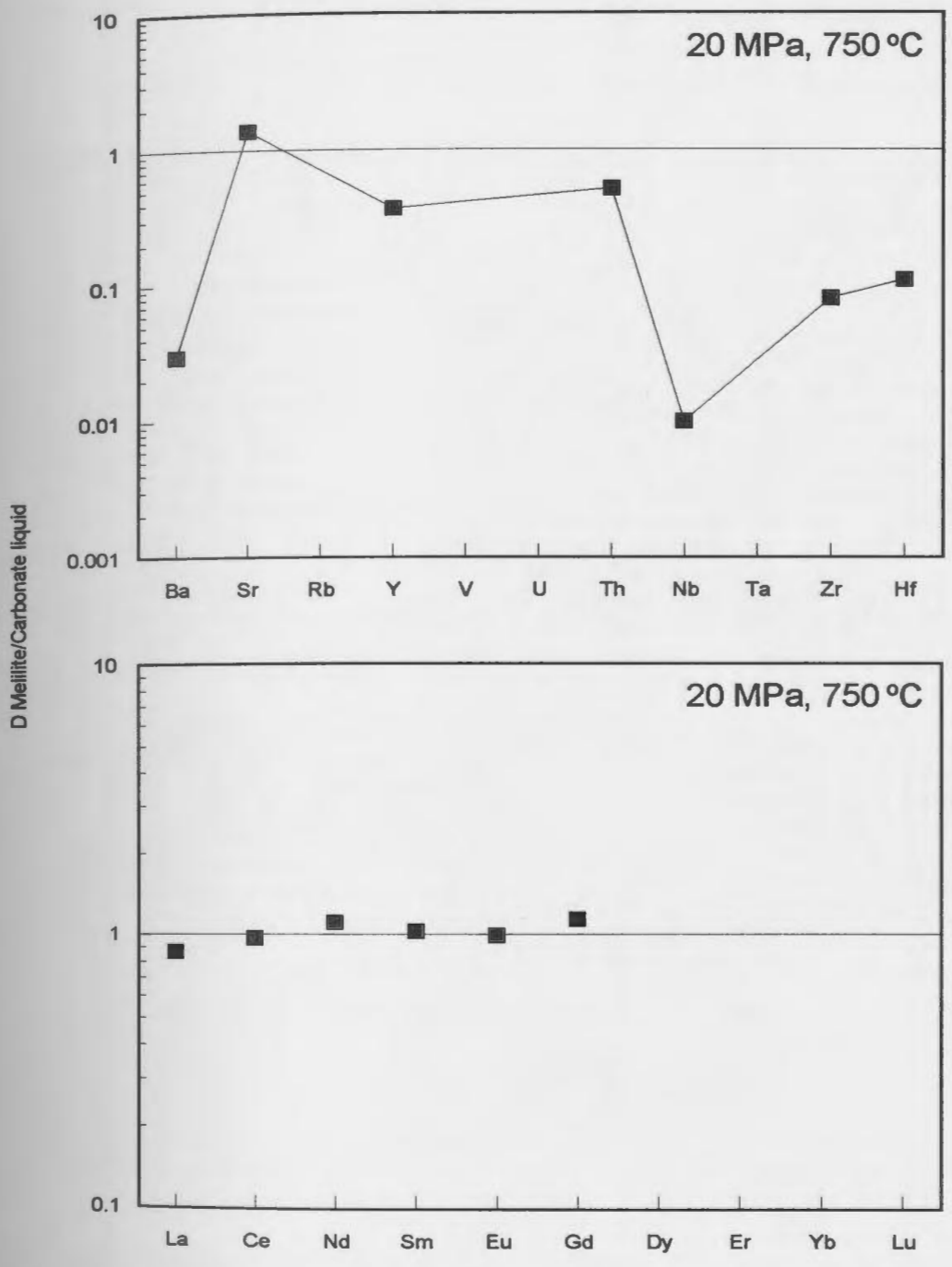

Figure 4.38: Partition coefficients (D) of trace elements between melilite and carbonate liquid from experiment CP51 (20 MPa, 750 °C). Partition coefficients for all trace elements are calculated between melilite and calculated concentration of carbonate liquid (see Tab. 4.11). Data are from Table 4.12.

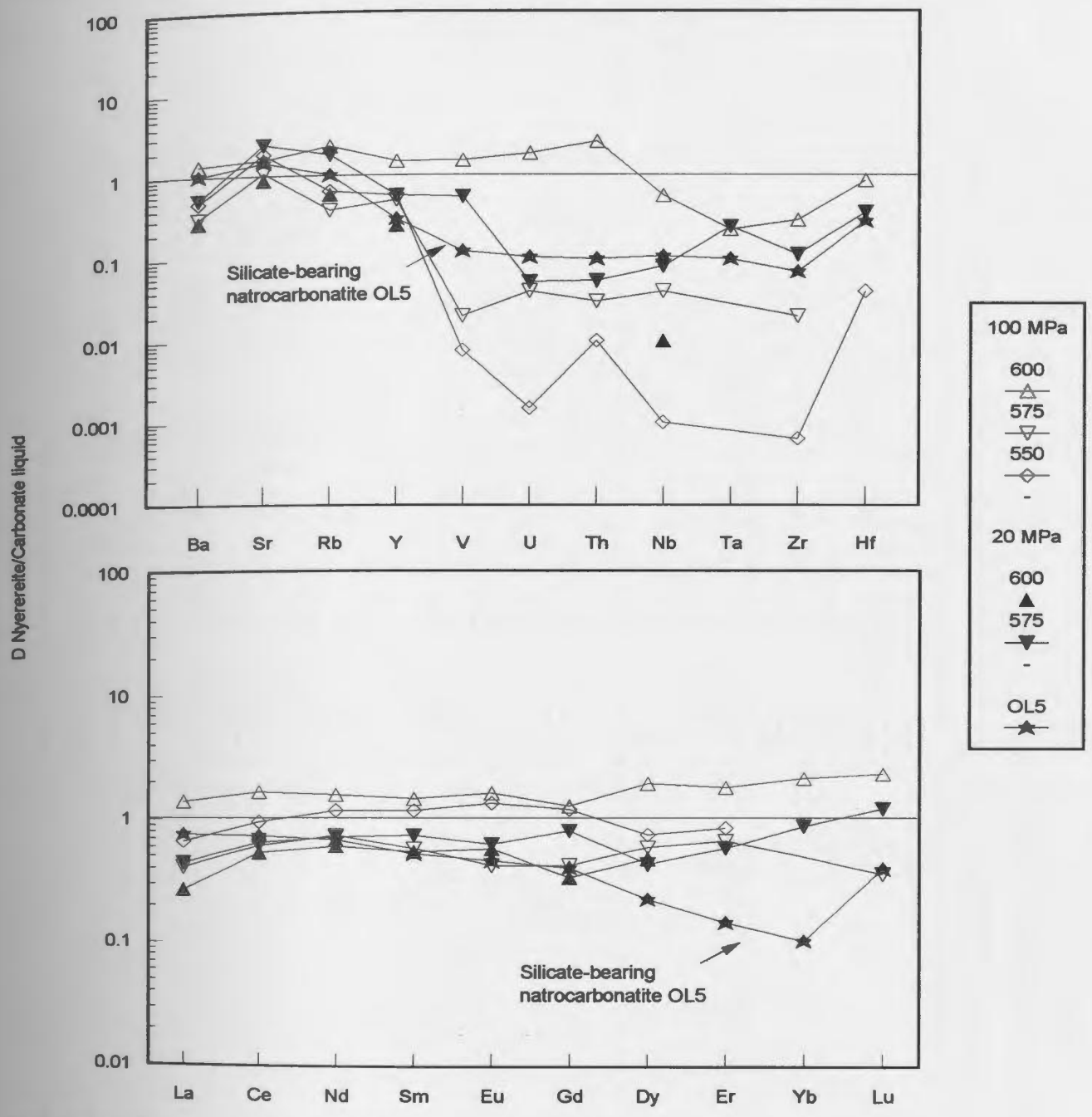

Figure 4.39: Partition coefficients (D) of trace elements between nyerereite and carbonate liquid in OL5-experiments and in silicate-bearing natrocarbonatite OL5. Open symbols represent experiments at 100 MPa, and filled symbols represent experiments at 20 MPa. Temperature (in °C) is shown beside the symbols in the legend. For the experiments, D's are calculated between the crystal and the measured concentration of carbonate liquid, except for D_U, D_{Nb} and D_{Ta} in CP107, D_U, D_{Th}, D_{Nb}, and D_{Zr} in CP128, D_U, D_{Th}, D_{Nb}, D_{Zr} and D_{Hf} in CP127, D_{Nb} in CP108, and D_{HFSE} in CP126, which are calculated against calculated concentration of carbonate liquid (see Tab. 4.11). For OL5, D's are calculated between nyerereite and CEL (see Tab. 4.11). Data are from Table 4.12.

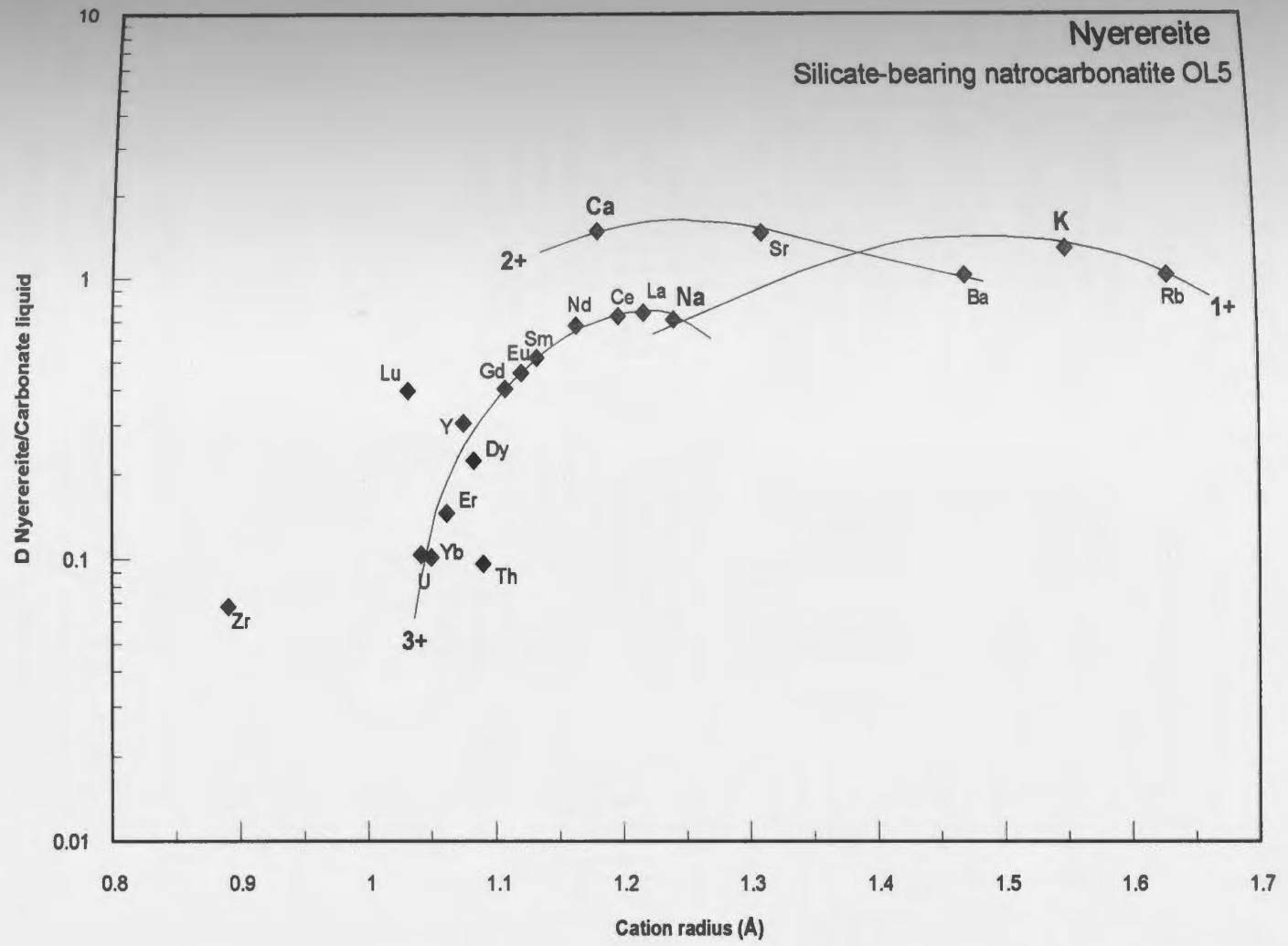

Figure 4.40: Variation of partition coefficients (D) between nyerereite and CEL as a function of ionic radius (in ångstroms) in silicate-bearing natrocarbonatite OL5. Curves for 1+, 2+, 3+ and 4+ valencies are labelled. Data are for D's are from Table 4.12 and data for ionic radii (using 9-fold coordination) are from Shannon (1976).

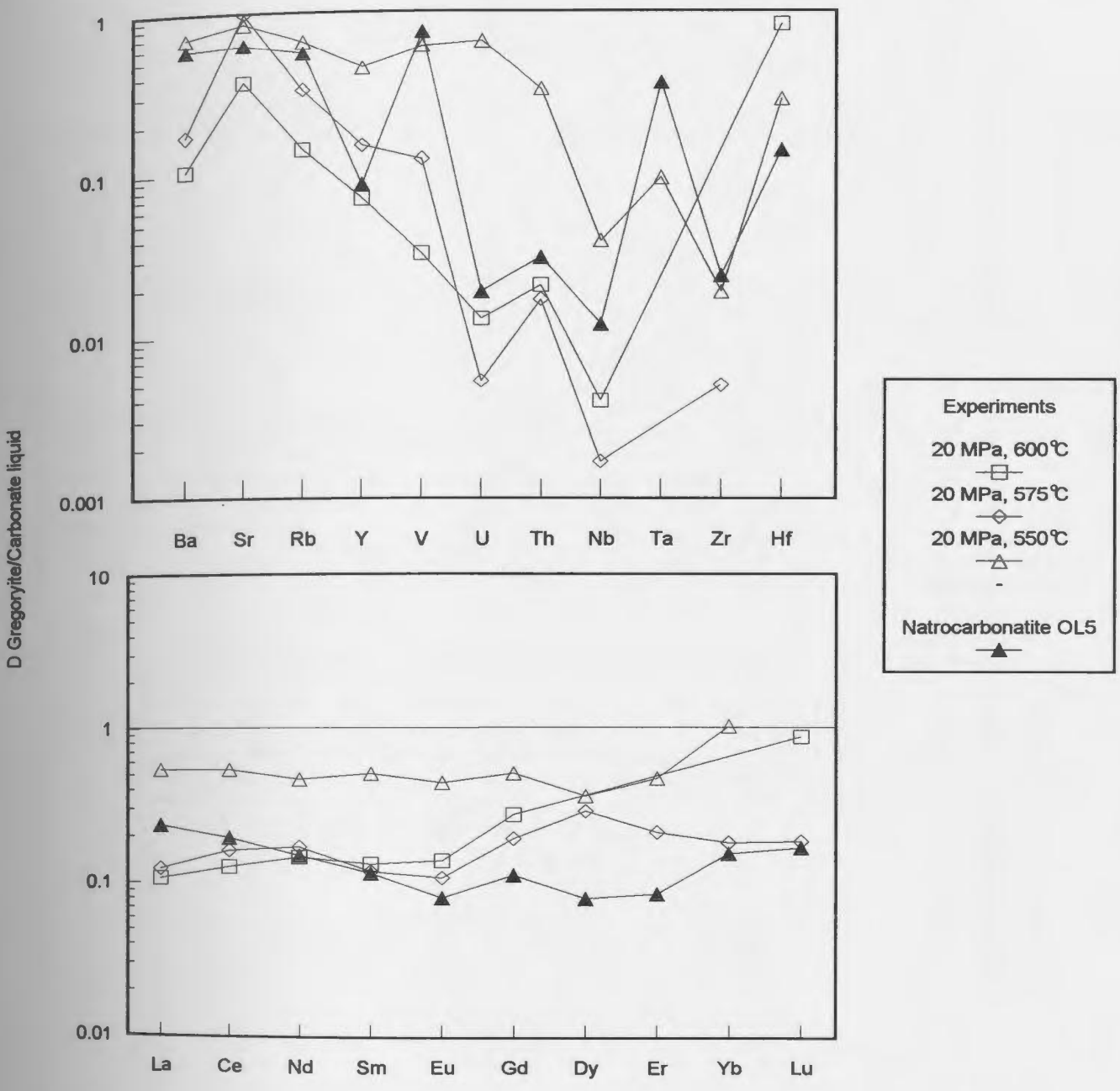

Figure 4.41: Partition coefficients (D) of trace elements between gregoryite and carbonate liquid in OL5-experiments and in silicate-bearing natrocarbonatite OL5. Pressure (in MPa) and temperature (in °C) are shown in brackets beside the symbol in the legend. For the experiments, D's are calculated between crystal and measured concentration of carbonate liquid, except for D_{HFSE}, which are calculated against calculated concentration of carbonate liquid (see Tab. 4.11). For OL5, D's are calculated between gregoryite and CEL (see Tab. 4.11). Data are from Table 4.12.

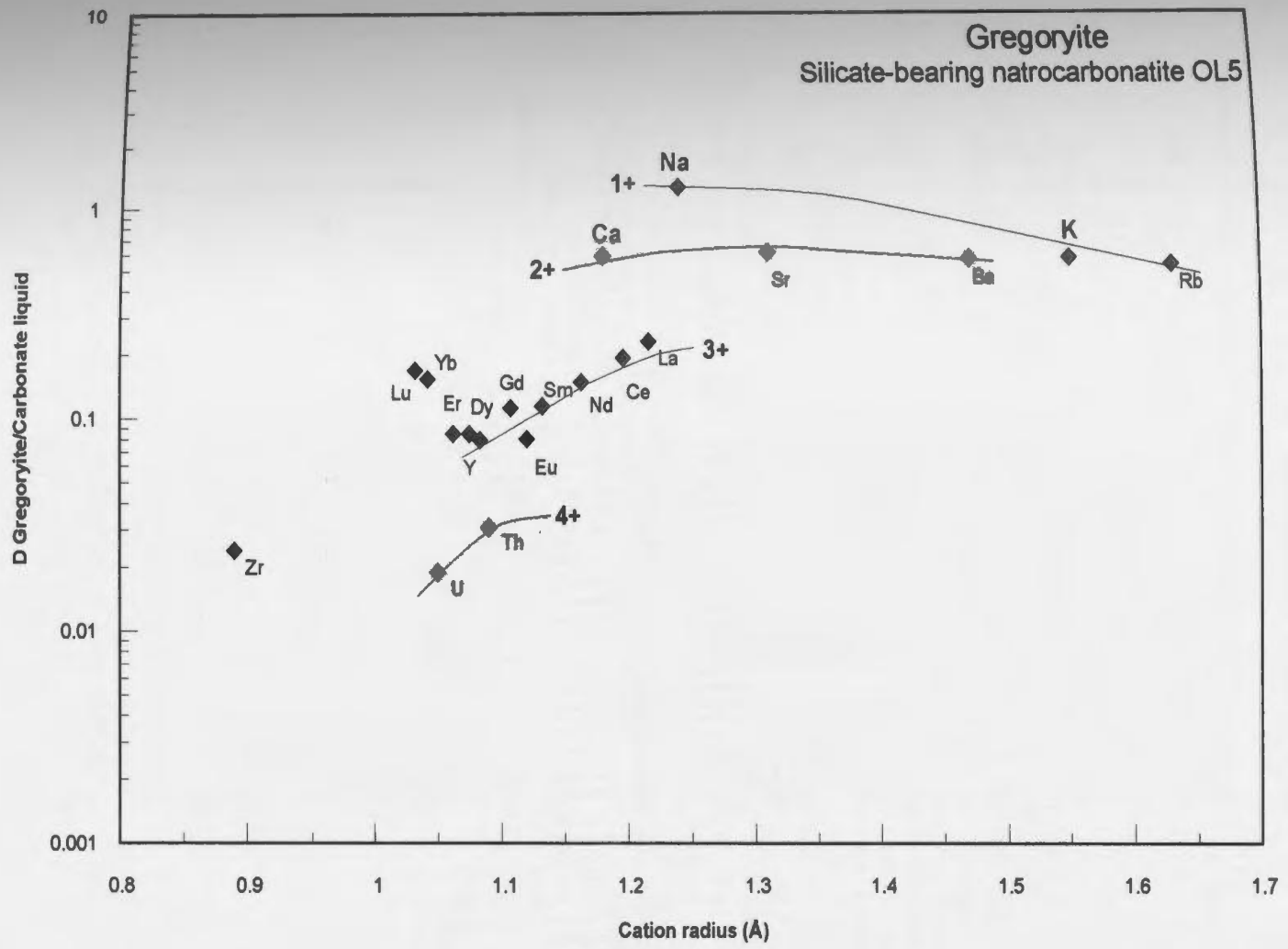

Figure 4.42: Variation of partition coefficients (D) between gregoryite and CEL as a function of ionic radius (in ångstroms) in silicate-bearing natrocarbonatite OL5. Curves for 1+, 2+, 3+ and 4+ valencies are labelled. Data for D's are from Table 4.12 and data for ionic radii (using 9-fold coordination) are from Shannon (1976).

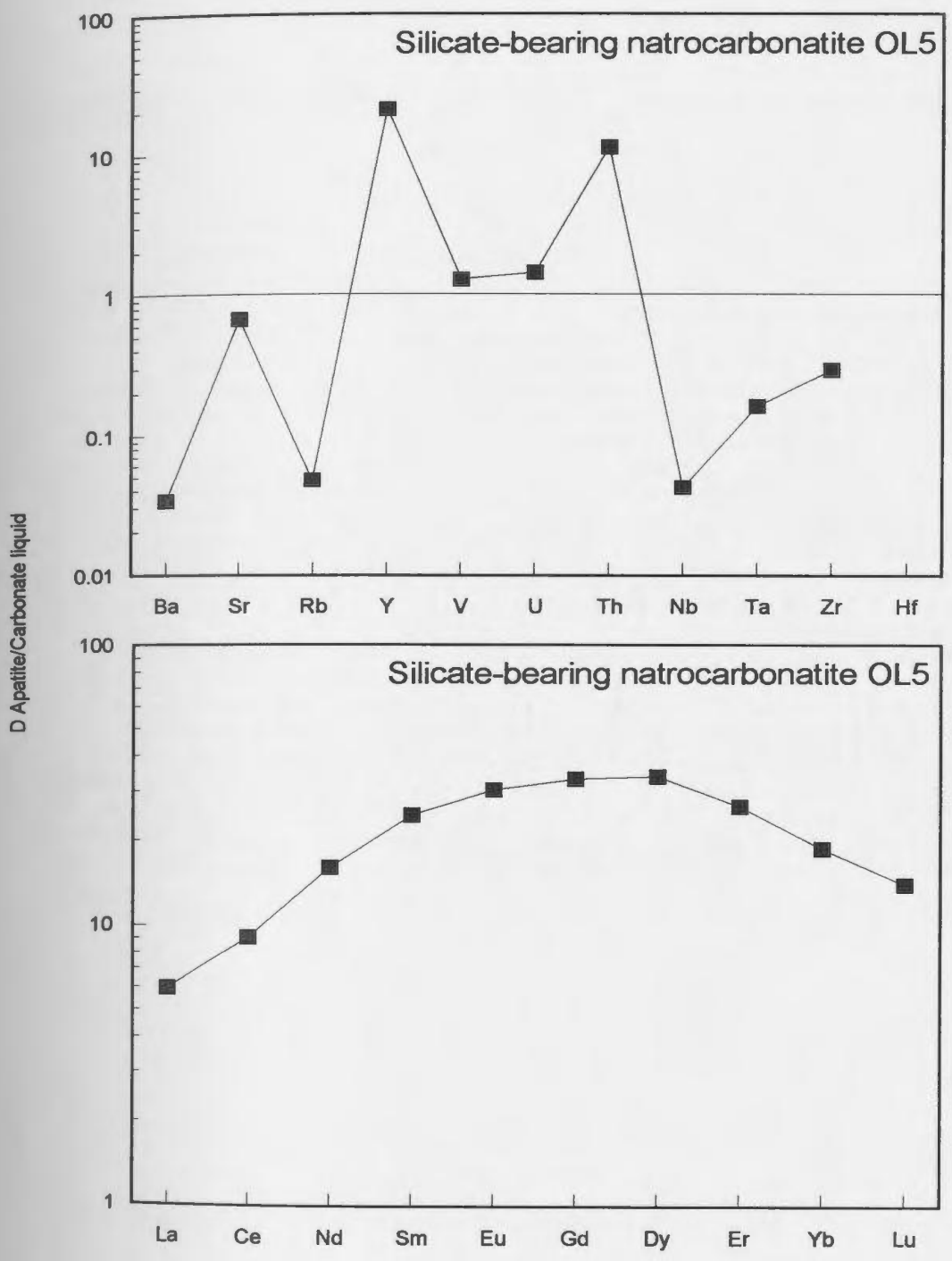

Figure 4.43: Partition coefficients (D) of trace elements between apatite and CEL in silicate-bearing natrocarbonatite OL5. Data are from Table 4.12.

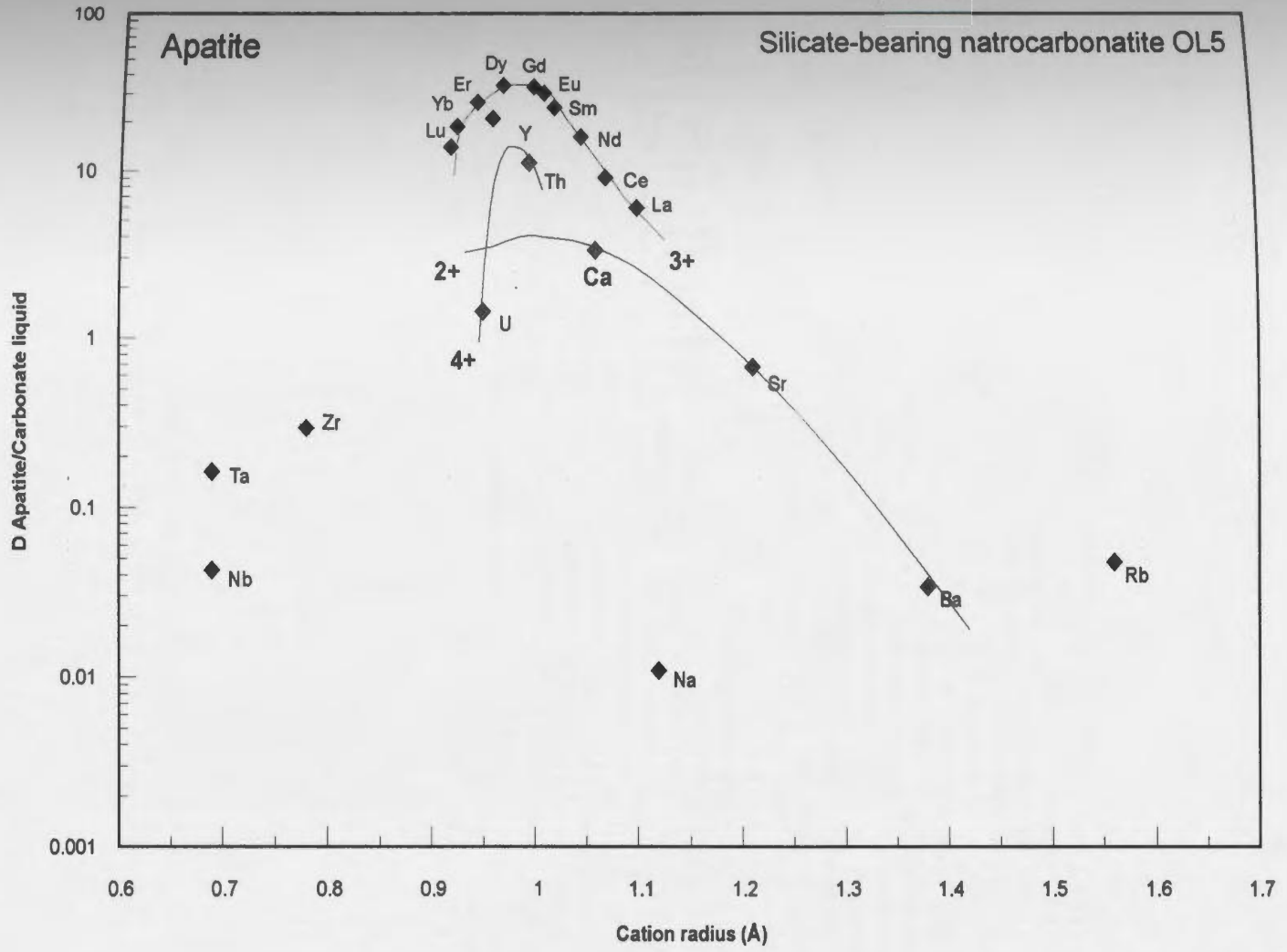

Figure 4.44: Variation of partition coefficients (D) between apatite and CEL as a function of ionic radius (in ångstroms) in silicate-bearing natrocarbonatite OL5. Curves for 2+, 3+ and 4+ valencies are labelled. Data for D's are from Table 4.12 and data for ionic radii (using 7-fold coordination) are from Shannon (1976).

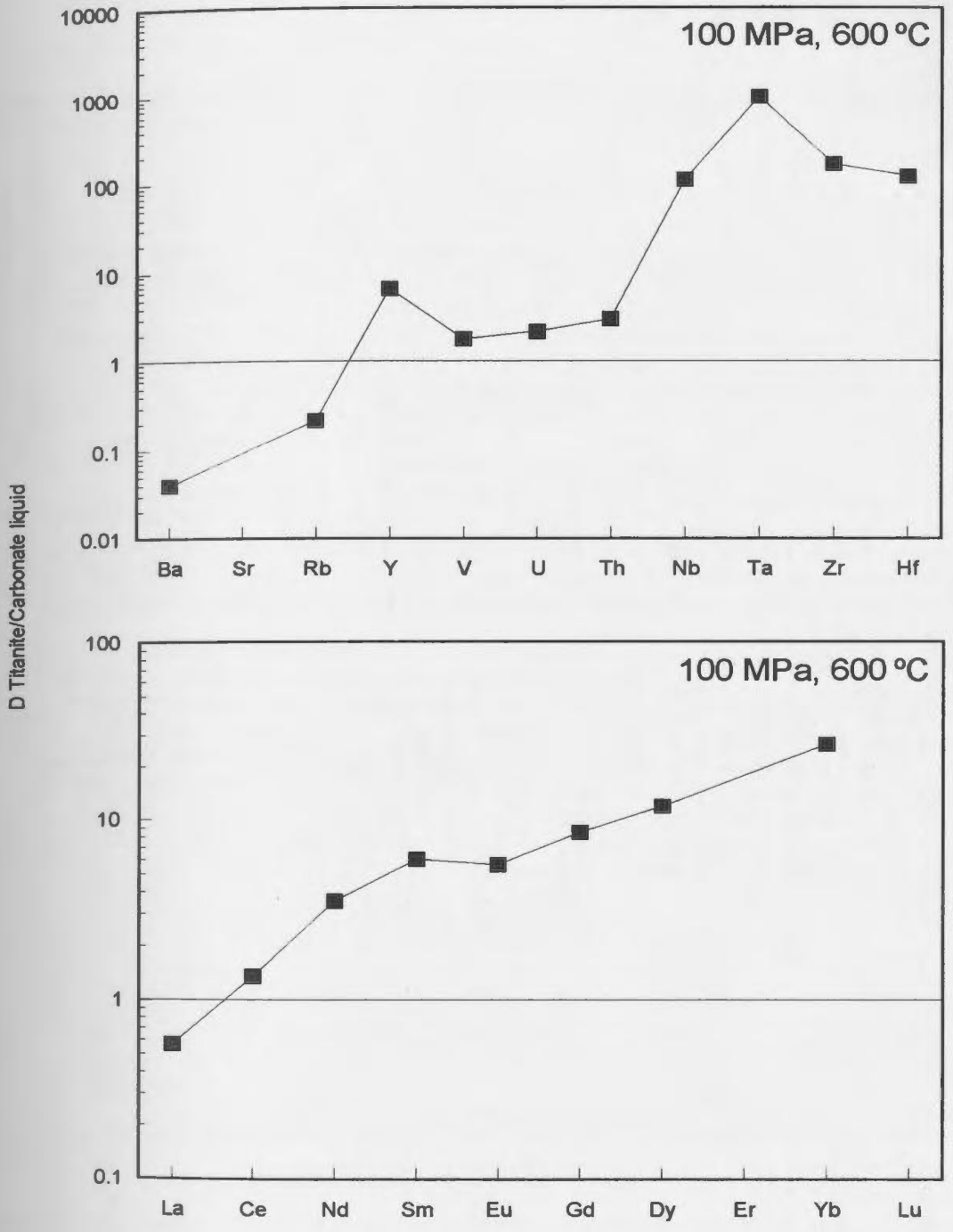

Figure 4.45: Partition coefficients (D) of trace elements between titanite and carbonate liquid from experiment CP107 (100 MPa, 600 °C). Data are from Table 4.12.

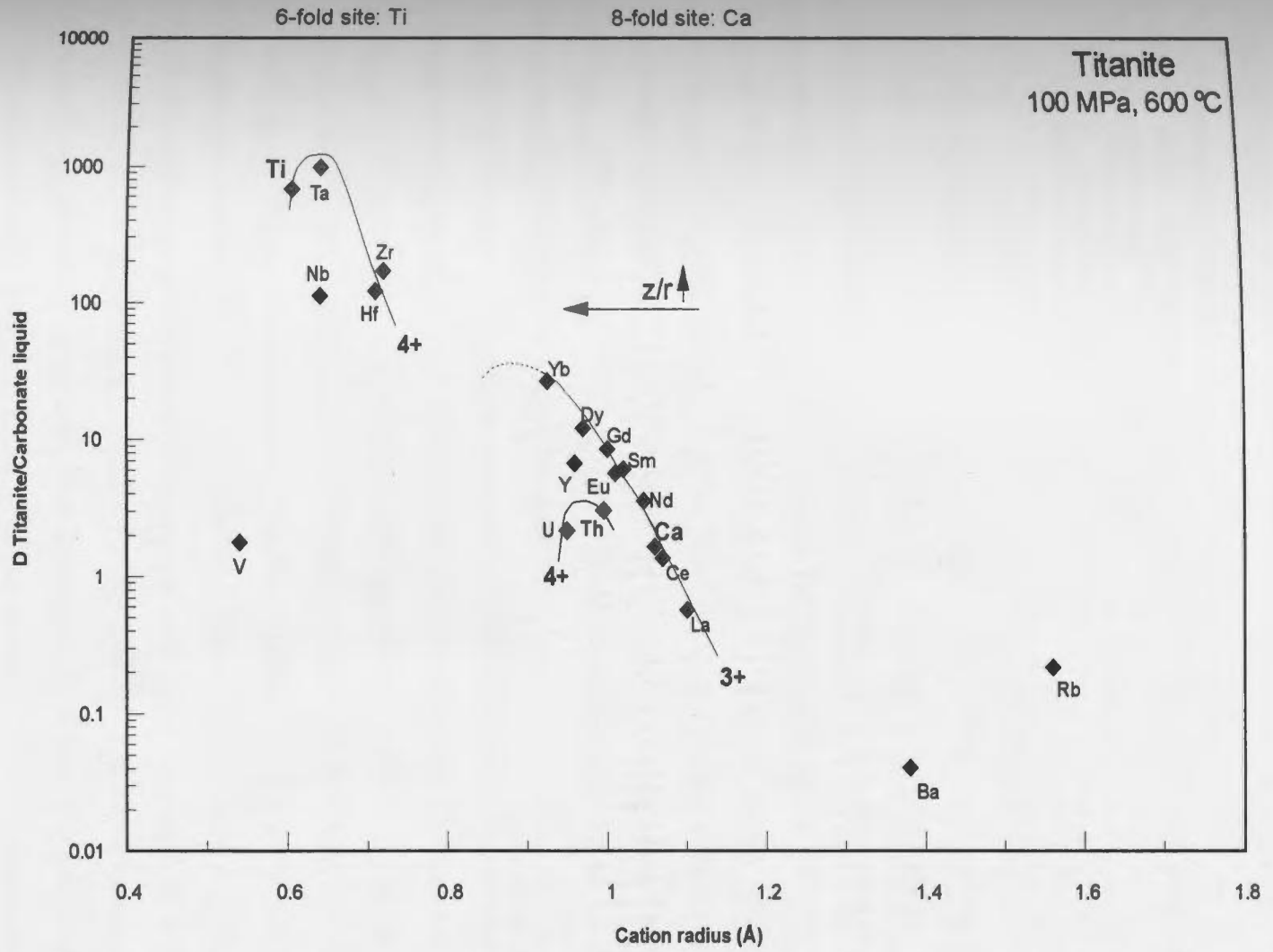

Figure 4.46: Variation of partition coefficients (D) between titanite and carbonate liquid as a function of ionic radius (in ångstroms) in experiment CP107 (100 MPa, 600 °C). Curves for 2+, 3+ and 4+ valencies are labelled. Data for D's are from Table 4.12 and data for ionic radii are from Shannon (1976).

CHAPTER 5 – CRYSTALLISATION OF SILICATE-BEARING NATROCARBONATITES AND FORMATION OF SILICATE-FREE NATROCARBONATITES – PART II: CONSTRAINTS FROM TRACE ELEMENT DATA.

"Carbonatites are known to contain the highest amounts of REE of any igneous rocks, but where these elements reside among the many different mineral species is less well understood." Hornig-Kjarsgaard (1998)

5.1 - Introduction

Major element data were used in Chapter 3 to demonstrate that at Oldoinyo Lengai, silicate-bearing natrocarbonatite OL5 is a possible parental magma. Major element data showed that after separating from a wollastonite nephelinite parent, OL5 records mostly bulk equilibrium crystallisation at 20 MPa, 615 °C. It was also shown that equilibrium crystallisation of OL5 at these P-T conditions could produce a residual liquid with the composition of silicate-free natrocarbonatite, although the nature of the crystallisation process could not be determined from the major element data. The purpose of this chapter is to use the trace element data presented in Chapter 4 to elaborate on the petrogenetic model that was introduced in Chapter 3, since trace elements are more sensitive than major elements to differentiation processes.

Differentiation of a magma involves both physical and chemical aspects. The degree of differentiation of a magma depends on the mechanism of chemical differentiation (surface or bulk equilibrium crystallisation) and the efficiency of the physical separation process (crystal settling or liquid movement). Two end member situations envisaging combination of these chemical and physical processes can be described: 1) bulk equilibrium crystallisation in which the whole crystal assemblage is always equilibrating with all the melt, and is never effectively isolated from the melt (*e.g.*, suspension due high convective velocities and/or small percentage of settling crystals); and 2) surface equilibrium crystallisation (Rayleigh fractionation) in which there is rapid and complete separation of crystals and melt, such that the crystals can not reequilibrate. In modern

petrology, it is usually envisaged that it is convective movement of the liquid away from the crystal faces which is responsible for crystal – liquid fractionation.

During bulk equilibrium crystallisation, crystals are homogeneous because they reequilibrate constantly with the liquid. Crystal zoning indicates that the crystals do not completely reequilibrate with the liquid, possibly because there is surface equilibrium crystallisation only. The zoning patterns might be complicated by kinetic effects (*e.g.* adsorption/desorption on crystal sites), or injection of new magma. Note that bulk equilibrium crystallisation is the chemical process that is prevalent in the experiments, although it was shown in Chapter 4 that disequilibrium might be introduced during quenching.

This Chapter is divided in two parts. First, trace element compositions of different phases in silicate-bearing lava OL5 will be examined and compared to their equivalents in OL5-experiments, especially at 20 MPa and 600-625 °C, in order to confirm that OL5 underwent mostly bulk equilibrium crystallisation at these P-T conditions.

Second, trace element compositions of different silicate-free natrocarbonatites will be compared to those of silicate-bearing natrocarbonatite OL5, of carbonate liquids from the OL5-experiments (products of bulk equilibrium crystallisation) and of calculated residual liquids from Rayleigh fractionation of OL5. The comparison of all of the trace element results will be the basis for inferring whether silicate-free natrocarbonatites can be produced by bulk or surface equilibrium crystallisation of silicate-bearing natrocarbonatite OL5.

In Chapter 3 it was suggested that convective fractionation is the process operating in the magma chamber. Convective fractionation is compatible with different crystallisation processes affecting the magma simultaneously in different parts of the magma chamber. For example, OL5 might undergo bulk equilibrium crystallisation in the main magma chamber, and Rayleigh fractionation on the walls of the magma chamber. Note that since many abbreviations will be used in this chapter, they are presented in Table 5.1 in order to facilitate the reading.

5.2 - Equilibrium crystallisation of lava OL5

In order to determine which phases control the trace element budget in silicate-bearing natrocarbonatite OL5, and to further understand its magmatic evolution, trace element compositions of individual phases in lava OL5 are compared to each other and to the whole rock. Moreover, a mass balance calculation using trace elements is undertaken in order to investigate whether phases that have not been analysed could have been involved in the crystallisation process. Furthermore, trace element compositions of crystals and liquid phases are compared between lava OL5 and experiments at 20 MPa, 600-625 °C, in order to confirm that lava OL5 mostly recorded bulk equilibrium crystallisation at these P-T conditions.

5.2.1: Trace element composition of whole rock and of different phases in lava OL5

5.2.1.1: Comparison between trace element composition of different phases in lava OL5

Trace element compositions of phases found in silicate-bearing natrocarbonatite OL5 were presented in Table 4.9. In Chapter 4, compositions were plotted separately for different phases and compared to those in the experiments. In this chapter, the compositions of all phases are presented on a single plot (Fig. 5.1). Trace element data from the literature for perovskite, titanite and melilite are also shown. These phases are known to be present in silicate-bearing natrocarbonatites (Dawson et al., 1996), including OL5, although no data on these phases were obtained in this study. In order not to overload the plots, trace element compositions of microphenocrysts have not been plotted. Data for the rare earth elements are discussed first.

Both whole rock and most primary minerals are strongly enriched in REE, with enrichment factors decreasing from La to Lu (Fig. 5.1a). The REE reside mainly in the Ca-bearing phases, *i.e.* perovskite, apatite, nyerereite, gregoryite and Ca-silicates. REE patterns are parallel to subparallel for groundmass, groundmass of spheroids, bulk rock and most crystal phases (in order of decreasing REE content: perovskite,

apatite, titanite, melilite, nyerereite, gregoryite, nepheline). Only melanite garnet, clinopyroxene and wollastonite have REE-patterns which are not parallel to the general trend exhibited by other phases.

REE patterns in silicate-bearing natrocarbonatites are controlled predominantly by carbonate phases (because of their high modal amounts and moderate REE abundances), and by perovskite, apatite and titanite (because of their high REE contents). The generally parallel to subparallel REE distribution of nyerereite, gregoryite, perovskite, apatite, titanite and the whole rock also suggests that if additional phases are involved, then they have either similar REE distribution patterns, or have such low REE concentrations that they do not influence the bulk-rock pattern.

In lava OL5, the phase that has a REE pattern differing most from the norm is melanite garnet, which has a convex pattern flattening out towards the HREE. Crystallisation of garnet with such a REE distribution would selectively increase La in relation to the other REE in the residual melt. Wollastonite has a flatter pattern than the whole rock, and clinopyroxene has a concave pattern upward (relatively flat); however, because these two minerals are in low modal amounts in lava OL5, and because their REE concentrations are not high compared to that of the whole rock, their fractionation will not significantly affect the trace element budget.

Comparison of REE in lava OL5 to other carbonatite-related rocks shows: 1) lower REE in nepheline than that of nepheline in urtite from Oka (Eby, 1975), and no positive Eu anomaly; 2) clinopyroxene has a similar REE composition to that in alnoite from Oka (Eby, 1975), but it does not have a positive Eu anomaly; 3) garnet has similar REE concentrations as in ijolite from Oka (Eby, 1975); 4) melilite has similar REE concentrations as melilite from Oka (Eby, 1975); 5) apatite is less enriched than in sövite from Oka (Eby, 1975), and it does not have a negative Eu anomaly; apatite has similar REE concentrations as in jacupirangite at Oldoinyo Lengai (Dawson et al., 1994b), and it contains more REE than in apatite sövite from Siilinjarvi, Finland (Hornig-Kjarsgaard, 1998).

Normalised abundance patterns for the remaining trace elements are illustrated in Figure 5.1b. Most notable is that the patterns for the individual phases are not parallel to that of the whole rock. The distribution of the elements can be summarised as follows: Ba, Sr and Rb are mainly concentrated in carbonate crystals and in groundmass; V in melanite garnet and in clinopyroxene; HFSE in titanite, perovskite, melanite garnet, and groundmass of spheroids; Zr and Hf are also significantly present in clinopyroxene; and U and Th are mainly concentrated by perovskite.

The fact that the trace element patterns for individual minerals are not parallel to that of the whole rock suggests that mineral fractionation could modify the patterns observed in rocks derived via fractionation. For example, crystallisation of perovskite is expected to modify the concentration of U and Th in the residual liquid, even if it crystallises in small amounts. Similarly, crystallisation of titanite, perovskite or melanite garnet is expected to modify the concentration of HFSE in the residual liquid, even for small degrees of crystallisation. Most phases plotted in Figure 5.1b typically have U/Th, Nb/Ta and Zr/Hf ratios that are fairly similar to that of the whole rock, except titanite and melanite garnet which have lower Nb/Ta than in the whole rock, and perovskite and apatite which have lower U/Th than in the whole rock. Therefore, elements that form normally coherent pairs are not expected to be decoupled from one another during crystallisation of OL5, except for Nb/Ta with crystallisation of titanite and melanite garnet, and U/Th with crystallisation of perovskite and apatite. The fractionation of any of the crystal phases whose trace element compositions are plotted in Figure 5.1 is not expected to change the Zr/Hf ratio of the residual liquid.

5.2.1.2: Mass balance calculations on lava OL5

Using trace element compositions measured on each phase by LAM-ICP-MS, and phase proportions determined in Chapter 3, a calculated bulk composition of OL5 can be compared to the measured whole-rock trace element composition of lava OL5. The measured trace element composition of natural rock OL5 is referred to as MNR,

whereas the calculated composition using phase proportions determined in Chapter 3 is referred to as CNR1 (Tab. 5.1). The results are plotted in Figure 5.2, and show that the calculated trace element concentrations (CNR1) are generally a little low compared to the measured whole rock (MNR), for V, LREE, U, Th and Nb.

Perovskite, titanite and apatite, even in low modal amounts, can significantly affect the trace element budget of silicate-bearing natrocarbonatite (without modifying the major element composition). Therefore, a second calculation was performed adding (in place of groundmass) 0.03 titanite, 0.2 perovskite, 0.2 apatite and 0.01 melilite (all in volume percent). Note that the amount of these phases that can be added is constrained by the whole rock composition. The proportions and source of other phases are as follows: 2 % nepheline (phenocrysts); 0.1 % nepheline (microphenocrysts spheroids); 3 % clinopyroxene (phenocrysts); 0.1 % clinopyroxene (microphenocrysts spheroids), 0.7 % melanite garnet (phenocrysts); 0.1 % melanite garnet (microphenocrysts spheroids); 0.025 % wollastonite (isolated phenocrysts); 0.025 % wollastonite (phenocrysts spheroids); 0.1 % wollastonite (microphenocrysts spheroids); 0.3 % apatite (isolated phenocrysts); 37 % nyerereite; 36.35 % gregoryite; 1.2 % groundmass spheroids and 18.76 % groundmass.

The results of this second calculation (CNR2) and comparison with the measured whole rock (MNR) are illustrated in Figure 5.3. The new calculated composition provides a slightly better fit for the MREE and some HFSE; however, several elements (Ba, V, LREE, U, Th and Nb) still have lower concentrations than does the natural rock. Possible explanations that might account for the differences include: 1) the analyses of the groundmass might not be representative due to heterogeneity of the groundmass in OL5. In particular, some quench phases rich in Ba, V, LREE, U, Th and Nb might be under-represented (see Church and Jones, 1995; Heinrich, 1966); 2) perovskite and titanite in OL5 might have a significantly different composition compared to those used for the calculations. For example, microprobe analysis of perovskite in experiment CP45 (see Tab. 3.7) yielded concentrations of La and Ce higher than those that were used in the calculations (from Dawson et al., 1994b); and

3) analytical uncertainty in the OL5 bulk composition. Trace element compositions determined for lava OL5 by solution ICP-MS (Simonetti et al., 1997; see Tab. 2.2) and by LAM-ICP-MS (this study; see Tab. 4.10) are in good agreement. However, because the lava is heterogeneous and may contain minor phases enriched in some trace elements, this might affect the solution ICP-MS data (if these minor phases were not digested because it was not a sinter run), and it might also affect the LAM-ICP-MS data if the minor phases are under-represented by the analyses. Overall, however, the calculated (by method 1 or 2) versus measured abundances are in good agreement.

5.2.2: Comparison with the experiments

Major element data obtained on lava OL5 showed that the cores of the phenocrysts have similar compositions as the crystals from OL5-experiments at 20 MPa, 600-625 °C. However, some phenocrysts have compositional variations at their rims, and the presence of these zoned crystals, along with the microphenocrysts, suggests that some portion of the phenocrysts in OL5 failed to achieve equilibrium with the liquid because of their high growth rate.

In the present section, trace element compositions of the cores of phenocrysts in lava OL5 are compared to those of crystals in OL5-experiments. Then, trace element compositions of carbonate liquids in lava OL5 and in OL5-experiments at 20 MPa, 600-625 °C are compared. As previously discussed in Chapters 3 and 4, obtaining the composition of the carbonate liquid in both natural rock and experimental run products is not straightforward, and, in fact, it will be shown that the trace element data can improve the estimations of the liquid compositions.

5.2.2.1: Crystal phases

Trace element compositions of different crystal phases in silicate-bearing natrocarbonatite OL5 have been compared to the corresponding phases in the experiments (see Chapter 4; Fig. 4.24 to Fig. 4.29). It is important to remember that in silicate-bearing natrocarbonatite OL5, isolated phenocrysts and phenocrysts in the

spheroids have been shown to have similar trace element compositions, except for wollastonite. This is consistent with the fact that these silicate crystals form at similar P-T conditions, whether they are isolated or in aggregates.

Some of the phases in the experimental run products of OL5 either did not demonstrate any P-T sensitivity in their composition or were characterised by compositional heterogeneity or trace element concentration levels near detection limits (see Chapter 4). These latter phases (nepheline, clinopyroxene, wollastonite) are not considered here. Those phases that are of use are melanite garnet, nyerereite and gregoryite.

Melanite garnet produced at 20 MPa and 750, 700 and 600 °C is broadly similar in composition to that in the erupted OL5 lava (see Fig. 4.26). While there is no systematic effect of temperature on trace element composition of melanite garnet in 20 MPa-experiments, it is worth noting that the melanite garnet from experiment CP108 (20 MPa, 600 °C) is the garnet having the most similarity to that in the natural rock, particularly with regard to Th concentration and the shape of the REE-pattern. Nyerereite in experiments at 20 MPa, 575-600 °C has very similar trace element concentrations as nyerereite in silicate-bearing natrocarbonatite OL5 (see Fig. 4.28). Although the composition of nyerereite at 100 MPa, 575 °C is similar to that in lava OL5 (see Fig. 4.28), the absence of gregoryite, melanite garnet and wollastonite at 100 MPa, 575 °C precludes these conditions as being responsible for the formation of nyerereite in lava OL5. Moreover, gregoryite in experiments at 20 MPa, 575-600 °C has relatively similar concentrations of LFSE, Y, Nb, Zr and LREE as gregoryite in silicate-bearing natrocarbonatite OL5, although it has higher MREE and HREE (see Fig. 4.29). The gregoryite at 550 °C has much higher trace element concentrations than in lava OL5, which is also consistent with a higher temperature for the conditions of formation of lava OL5, *i.e.* 20 MPa, 615 °C.

In summary, the trace element compositions of melanite garnet, nyerereite and gregoryite in experiments and in lava OL5 are most similar for P-T conditions of 20

MPa, 615 °C. This is consistent with arguments presented earlier based on phase assemblages (see also Fig. 3.3) and major element data.

5.2.2.2: Liquid phase

Comparison between the measured composition of the quenched carbonate liquid phase in experiments at 20 MPa, 625 and 600 °C (measured experimental liquid = MEL), and the calculated equivalent liquid in natural OL5 (CEL = groundmass + carbonate crystals + siliceous mesostasis; see Chap. 3) is shown in Figure 5.4. Two calculations have been performed to calculate the trace element composition of CEL in natural OL5 (see Tab. 5.1): the first one (CEL1) does not include perovskite and titanite, while the second one (CEL2) does - since it was demonstrated above that minor amounts of these two crystals are probably present in the groundmass. In the case of the experimental run products, the calculated composition (= bulk OL5 minus crystals) of carbonate liquid in a hypothetical experiment at 20 MPa, 615 °C (= HEL) has also been plotted, since the measured composition of carbonate liquid was shown to be affected by quenching (see section 4.2.3.2 in Chapter 4).

The groundmass of natural OL5 has higher concentrations of Zr and Hf (Fig. 5.4a) and REE (Fig. 5.4b) compared to the calculated values for the carbonate liquid in a hypothetical experiment at 20 MPa, 615 °C (HEL). The liquid composition of natural rock OL5 (CEL), on the other hand, has a trace element composition very similar to that of the calculated, experimental composition at 20 MPa, 615 °C (HEL). The fit of these two liquid compositions is better when some perovskite and titanite are included in the calculation of the natural rock composition, *i.e.* it is better for CEL2 than for CEL1. This similarity supports the contention that lava OL5 is the product of bulk equilibrium crystallisation of the exsolved magma at 20 MPa, 615 °C, and that small amounts of perovskite and titanite are present in its groundmass.

5.3 - Formation of silicate-free natrocarbonatites

In Chapter 3, it was suggested that silicate-free natrocarbonatites are likely to have been derived by fractionation of a silicate-bearing natrocarbonatites at $P \leq 20$ MPa and 590 °C $\leq T \leq$ 615 °C. In this section, trace elements are used to address whether the crystal fractionation process was accompanied by Rayleigh fractionation or bulk equilibrium crystallisation. Also, the possibility of additional processes involved in the petrogenesis of silicate-free natrocarbonatites, such as the role of fluids, is examined.

5.3.1: Description of the different types of silicate-free natrocarbonatites

The silicate-free natrocarbonatites at Oldoinyo Lengai are erupted as two varieties, porphyritic and aphyric. The porphyritic ones form the majority of the erupted lavas, the aphyric variety being volumetrically unimportant (Keller and Krafft, 1990). Porphyritic lavas contain as much as 61.9 volume % phenocrysts of carbonate crystals nyerereite and gregoryite and are gas-rich (vesicle = 13.9 volume %), whereas aphyric lavas are phenocryst-poor, gas-poor mobile lavas (Dawson et al., 1990). The relationship between these two varieties of silicate-free natrocarbonatite has been attributed to: (1) filter pressing of porphyritic natrocarbonatites during eruption yielding the aphyric variety (Gittins and Jago, 1998); and (2) gas separation in the chamber giving rise to a phenocryst-rich surface froth and a trapped liquid (Dawson et al., 1990).

Gittins and Jago (1998) used compositional trends between aphyric and porphyritic varieties to suggest that the porphyritic natrocarbonatites best approximate the parental magma composition. This is in agreement with Keller and Krafft (1990) who showed that porphyritic samples collected during the June 1988 eruption do not show much impact of crystal accumulation (or liquid subtraction). This hypothesis is at odds with that of Mitchell (1997), who argued that aphyric natrocarbonatites best resemble the original magma and that porphyritic ones are the product of mixing between the parental magma and nyerereite and gregoryite cumulates. However, these latter arguments are difficult to reconcile with a variety of observations, suggesting porphyritic natrocarbonatites are parental. However, there is variability among porphyritic natrocarbonatites from different

eruptions, and it is necessary to find which silicate-free porphyritic natrocarbonatites are the least evolved.

Many porphyritic silicate-free natrocarbonatites have been erupted and analysed this century (*e.g.*, Dawson, 1962b). More recently, porphyritic silicate-free natrocarbonatites have been erupted at Oldoinyo Lengai in June and November 1988 (Dawson et al., 1990; Krafft and Keller, 1989; Gittins and Jago, 1998), in June 1993 (Simonetti et al., 1997) and in 1963 (Peterson, 1990). Based on an evaluation of the data and petrogenetic evolution, as outlined by the various authors, it is clear that among the most recent erupted natrocarbonatites, the November 1988 lavas represent the less evolved silicate-free natrocarbonatite lavas. Note that these lavas were erupted at 585 ± 10 °C.

5.3.2: Trace element compositions of different silicate-free natrocarbonatites

Trace element concentrations normalised to primitive mantle of selected silicate-free natrocarbonatites from Oldoinyo Lengai are presented in Figure 5.5, as are data for silicate-bearing natrocarbonatite OL5. Data for three lavas from November 1988 have been plotted, and for the remaining eruptions, one representative analysis is shown. All lavas that have been plotted are porphyritic, except for lava OL2 erupted in 1993.

The compositional range between different lavas is small for Ba, Sr, Rb, V and LREE. However, there is more variability in the levels of Y, U, Th, Nb, Ta, Zr, Hf, MREE and HREE. The origin of the heterogeneity reflects, in part, differences in the way the samples were analysed. Sample BD4169 was analysed by solution ICP-MS (Dawson et al., 1995b) and by LAM-ICP-MS (this study). For this study, trace element compositions were determined for nyerereite, gregoryite and groundmass in lava BD4169 (see Tab. A4.3), and the trace element composition of the whole rock was calculated by using the proportions of the different phases (see Dawson et al., 1990). The data from LAM-ICP-MS are lower for many of the HFSE and HREE, probably because minor phases have not been analysed in the groundmass. However, the data obtained by LAM-ICP-MS are included because of the indirect evidence they provide on minor phases present and their similarity with the pattern exhibited by aphyric lava OL2.

Figure 5.5 shows that trace element composition of porphyritic, silicate-free natrocarbonatites from the November 1988 eruption are fairly similar to that of lava OL5. Among the elements analysed, only Nb has significantly lower concentration than in OL5 (one order of magnitude lower for lavas BD4152 and BD4169). Levels in lava OL2 (June 1993) are significantly lower for some elements (Y, V, MREE, HREE, Th, Nb and Hf). Lava OL102 erupted in June 1988 does not exhibit as many discrepancies compared to lava OL5 as OL2 does, apart from low Th, Nb, Hf and especially Ta, which is < 0.025 ppm in OL102. Note that Keller and Spettel (1995) had already pointed out the low contents of Nb, Zr and Y of these silicate-free natrocarbonatites compared to other carbonatites.

Dawson et al. (1995b) showed that for silicate-free natrocarbonatites extruded in November 1988, compositional variations arise mainly between phenocryst-rich and aphyric varieties, with the aphyric variety being richer in Ba, Rb and rare earth elements. Similarly, Keller and Spettel (1995) showed that for silicate-free natrocarbonatites erupted in June 1988, the concentration of Ba, Sr, Rb, Y, V, La, Ce, Nd, Sm, Eu, Lu, U, Th, Nb increases whereas the concentration of Hf decreases during crystallisation.

Gittins and Jago (1998) showed that aphyric lavas represent a later phase of magmatic evolution than do the porphyritic types, so that their compositions can indicate the direction of evolutionary trends. Compositional trends from porphyritic to aphyric natrocarbonatites both in June and in November 1988 show increasing concentration of Ba, Sr, Rb, Y, La, Ce, Nd, Sm, Eu, Lu with increasing degree of crystallisation (*i.e.* with crystallisation of nyerereite and gregoryite). According to Keller and Krafft (1990), the enrichment factor is about 1.5 – 1.7 for the most incompatible elements. The fact that the enrichment factor is the same for most trace elements is explained by gregoryite, nyerereite and liquid having subparallel trace element patterns.

The compositional trends between porphyritic and aphyric natrocarbonatites noted above are not observed between silicate-free natrocarbonatites from November 1988 and silicate-free natrocarbonatites from other eruptions. Most trace element abundances are lower in the most evolved varieties compared to the least evolved (November 1988)

variety of silicate-free natrocarbonatites, which is the opposite to what would be expected by crystallisation of nyerereite and gregoryite only.

In conclusion, the petrogenetic link between natrocarbonatites erupted in November 1988 (less evolved) and other silicate-free natrocarbonatites is not simply crystallisation of nyerereite and gregoryite. Major element trends in the eruptions in June 1988 and 1993, and low eruption temperatures in June 1988, suggest that more nyerereite and gregoryite crystallised in these eruptions than in November 1988. Furthermore, trace element trends suggest that fractionation of additional phases, other than nyerereite and gregoryite, is needed to explain the depletion of trace elements in lavas from eruptions in June 1988 and 1993 as compared to that in November 1988 (see Fig. 5.5).

5.3.3: Crystallisation processes based on trace element compositions of silicate-free natrocarbonatites and experiments

In Chapter 3 it was shown, using major elements, that silicate-free natrocarbonatites could be produced by bulk equilibrium crystallisation of silicate-bearing natrocarbonatites at 20 MPa, 600-625 °C, because it is at these conditions that the SiO_2 content of carbonate liquid is the lowest (0.43-0.76 wt. %) in the experiments. Also at 20 MPa, the SiO_2 content of carbonate liquid in the experiments increases at $T < 600$ °C, therefore silicate-free natrocarbonatites cannot form by bulk equilibrium crystallisation of silicate-bearing natrocarbonatites at $T < 600$ °C (and 20 MPa). It was also stated that removal of silicate crystals by Rayleigh fractionation would help to explain the silica-poor character of the silicate-free natrocarbonatites. In this chapter, trace element data are used to determine the process(es) which produce(s) silicate-free natrocarbonatite from silicate-bearing natrocarbonatite: bulk equilibrium crystallisation at 20 MPa, 600-625 °C, surface equilibrium crystallisation (Rayleigh fractionation), and/or a more complicated process.

Trace element concentrations of representative silicate-free natrocarbonatites from different eruptions (BD4156 for November 1988, OL102 for June 1988 and OL2 for June 1993) are plotted in Figure 5.6, normalised to primitive mantle. Measured compositions

of the carbonate liquid (MEL) have been plotted for the experiments at 20 MPa, 600-625 °C, as well as the calculated composition of a hypothetical experiment at 20 MPa, 615 °C (HEL), because it was previously shown that the trace element composition of carbonate liquid could be modified during the quenching of the experiments. In experimental run products, trace elements which show a significant discrepancy between measured and calculated values, *i.e.* between MEL and HEL (lower measured than calculated values), include the HFSE for both temperatures, and Th and HREE at 600 °C.

The calculated composition of the residual liquid from ~ 25 % Rayleigh fractionation of OL5 (RFL) over the arbitrary temperature interval of 615-590 °C is also plotted in Figure 5.6. The details of this calculation (*i.e.*, partition coefficients that were used, phases crystallising at different temperatures) are given in Appendix A5. The equation that has been used is: $C_L/C_O = F^{(D-1)}$, where C_L is the weight concentration of a trace element in the liquid, C_O is the weight concentration in the parental liquid, F is the fraction of melt remaining and D is the bulk distribution coefficient of the fractionating assemblage during crystal fractionation (Rollinson, 1993). For the calculation of the composition of the residual liquid of Rayleigh fractionation of OL5 (RFL) over the temperature interval 615 °C - 590 °C, a first increment was used, consisting of nepheline (2 %), clinopyroxene (3 %), melanite garnet (0.7 %), wollastonite (0.05 %), nyerereite (10 %), gregoryite (2.5 %) and apatite (0.3 %) in the proportions expected at 20 MPa-615 °C. The next steps are going down temperature by 3 °C, using the same D's. Crystal phases and proportions used for the calculation are the same as in experiment CP108 (20 MPa, 600 °C). However, 0.3 % spinel has been removed in the calculation to account for decreasing FeO, and 0.005 % titanite and perovskite have been removed for each temperature increment. The total amount of crystallisation over the temperature interval 615 °C - 590 °C is ~ 25 % (including 18.6 % for the first increment).

The residual carbonate liquid produced by 25 % Rayleigh fractionation (RFL) (using this calculation) contains 0.21 wt. % SiO_2, similar to SiO_2 in silicate-free natrocarbonatites. It has trace element concentrations very similar to that of liquid produced by bulk equilibrium crystallisation (HEL), because Ti-bearing phases (which

are the phases in which trace elements mostly partition) cannot precipitate in large amounts, since the amount of titanium is low in OL5 (= 0.1 wt. %). There is only 0.003 % TiO_2 present in the residual carbonate liquid of the present calculation, so titanite, perovskite and melanite garnet (+ Ti-magnetite) cannot be removed in larger amounts. However, there are some compositional differences between carbonate liquid produced by Rayleigh fractionation (RFL) compared to carbonate liquid produced by bulk equilibrium crystallisation (HEL): the former has HREE ~ 2 times lower and Ta, Zr and Hf, and Y, V slightly lower than in the latter (Fig. 5.6).

Trace element compositions of silicate-free natrocarbonatites from November 1988 compare very well to measured trace element compositions of carbonate liquid from the experiment at 20 MPa, 600 °C (MEL) for the elements which do not show discrepancy between measured and calculated values (Fig. 5.6). For the elements which do show a discrepancy (*i.e.* HREE at 600 °C), they are more similar to the calculated composition (HEL) of carbonate liquid than to the measured composition (MEL).

Silicate-free natrocarbonatite OL2 (June 1993) has similar concentrations of Ba, Sr, Rb and V to those in carbonate liquid from the OL5-experiments, but compared to the calculated composition in the experiment at 20 MPa, 615 °C (HEL) and to the modelled carbonate liquid composition produced by Rayleigh fractionation (RFL), it has lower U, Th, HFSE, LREE and MREE (Fig. 5.6). However, its trace element composition compares very well to that of the measured composition of carbonate liquid (MEL) at 20 MPa, 625-600 °C (except for U, LREE). Porphyritic silicate-free natrocarbonatite OL102 (June 1988) has REE concentrations more similar to the calculated composition of carbonate liquid produced by bulk equilibrium crystallisation of OL5 at 20 MPa, 615 °C (HEL) or to carbonate liquid produced by Rayleigh fractionation (RFL), but available data on U, Th and HFSE indicates that it is depleted in these elements, like OL2 (June 1993).

The trace element concentrations in BD4156 (November 1988) could be explained by either bulk equilibrium crystallisation or Rayleigh fractionation of OL5. In contrast, these processes cannot explain the low concentrations of U, Th and HFSE in OL2 (June

1993) and in OL102 (June 1988). Since fractionation of neither the Ti-rich phases, nor the carbonate crystals (as mentioned above) can explain the trace element depletion in silicate-free natrocarbonatites from June 1988 and 1993 compared to those from November 1988, another explanation needs to be found.

Thorium and HFSE concentrations of silicate-free natrocarbonatites OL2 (June 1993) and OL102 (June 1988) compare well with the measured composition of carbonate liquid in OL5-experiments at 20 MPa, 625-600 °C (MEL). In OL5-experiments, low concentrations in the carbonate liquid were attributed to the presence of quench phases or fluid phases in the experimental charge which are under-represented in the analyses (see Chapter 4). Similar low values in natural lavas could be attributed to similar processes. In the magmatic chamber, phases rich in U, Th, HFSE (and REE) could be fractionated out of the natrocarbonatite magma, hence their lower concentrations in silicate-free natrocarbonatites from June 1988 and 1993 compared to the November 1988 eruption. Crystals in the experiments that have been shown to contain large amounts of these trace elements (perovskite, titanite, melanite garnet, and maybe Ti-magnetite) also contain significant titanium, which is in low abundance in OL5 (= 0.1 wt. %). Mass balance requires that these phases not be fractionated in large amounts. The primary crystallisation of these crystals does not readily explain the depletion of U, Th, HFSE (and REE) in some silicate-free natrocarbonatites, suggesting they may also be fractionated by phases which do not contain significant titanium.

Wall and Mariano (1996) showed that rare earth minerals (*e.g.* bastnaesite, parisite, synchysite, monazite and ancylite) tend to form in the final stages of carbonatite emplacement, usually not as primary minerals from the carbonatite magma, but as precipitates from hydrothermal or carbothermal solutions. They also demonstrated that these minerals often occur as fracture or void fillings, or as disseminated, fine-grained, polycrystalline aggregates overprinting early-formed minerals. Moreover, Gittins (1989) showed that Cl, F and S (or sulphate) are probable constituents of carbonatite fluids at Oldoinyo Lengai. Complexing of U, Th, HFSE and REE with Cl (and F?) from the fluid phase emanating from the magma could produce the precipitation of minerals enriched in

these elements and deficient in TiO_2. Precipitation of these phases could explain the depletion of certain trace elements in silicate-free natrocarbonatites from June 1988 and 1993 compared to November 1988 eruption.

Numerous phases rich in U, Th, HFSE and REE and poor in titanium are found in alkalic rocks, as reported in Khomyakov (1995). These include lueshite ($NaNbO_3$), baddeyleite (ZrO_2), or tuliokite [$Na_6BaTh(CO_3)_6.6H_2O$)]. Klein and Hurlbut (1993) also report pyrochlore $(Ca,Na)_2(Nb,Ta)_2(O,OH,F)$ and fergusonite ($YNbO_4$) which are good candidates to deplete natrocarbonatite magma in trace elements without concomitant Ti depletion. Figure 5.6 shows that Zr/Hf in lava OL2 (June 1993) is low compared to its calculated value in the experiments. The decoupling of these geochemically similar elements can be explained by the precipitation of these exotic phases. Note that it was shown previously that the fractionation of crystal phases whose trace element compositions are plotted in Figure 5.1 cannot change the Zr/Hf ratio of the residual liquid.

5.3.4: Formation of natrocarbonatites - magma chamber processes

Experimental studies at appropriate P-T-X conditions (Kjarsgaard et al., 1995) illustrated that natrocarbonatite melts generated by liquid immiscibility from nephelinitic hosts can contain significant SiO_2 (1.26-5.15 wt. %; see also Fig. 3.1) in solution. This suggests that silicate-free natrocarbonatites (< 0.5 wt. % SiO_2) cannot be directly generated by immiscibility at relevant P-T-X, but must be differentiates from silicate-bearing natrocarbonatite parent magmas. Thus natrocarbonatite magma chamber processes require examination to test whether crystal fractionation-differentiation processes are of petrologic importance at Oldoinyo Lengai.

Carbonatitic magma has low density and viscosity. The density of (silicate-free) natrocarbonatite magma has been estimated to be ~ 2.0 x 10^3 kg/m^3 by Wolff (1994). Norton and Pinkerton (1997) measured the viscosity of natrocarbonatites from the 1988 eruption. These measurements showed that degassed, phenocryst-poor lavas have viscosities ranging from 1 to 5 Pa.s, *i.e.* considerably lower than in basaltic lavas;

whereas a highly vesicular lava with a high phenocryst content had a viscosity of 120 Pa.s. However, Dawson et al. (1994a) calculated that the poorly vesiculated and crystal-rich lavas from the Chaos Crags flow (June 1993) had an apparent viscosity of 3×10^7 to 7×10^8 Pa.s, *i.e.* the effect of high crystallinity in the flows is to increase the viscosity to values similar to those observed for rhyolites.

The physical properties of natrocarbonatites are relevant to their potential behaviour in magma chamber(s). Sparks et al. (1984) suggested that *in situ* nucleation on the wall of the magma chamber is the most probable site for crystallisation, and that when crystallisation occurs, the melt immediately adjacent to the growing crystals can convect away from its point of origin. Sparks et al. (1984) termed this process convective fractionation, and indicated that during crystallisation along the margins of a chamber, highly fractionated magmas can be generated without requiring large amounts of crystallisation because the removal and concentration of chemical components affects only a small fraction of the total magma. Sparks et al. (1984) suggested that, if the density of the differentiated liquid is low, these liquids can efficiently segregate to the top of the magma chamber. Convective fractionation processes are likely to be very efficient on low-density and low-viscosity natrocarbonatite melts.

The comparison of trace element compositions of liquids between experiments and natural lavas cannot be used to distinguish between different crystal fractionation processes (*i.e.*, bulk equilibrium crystallisation / Rayleigh fractionation) because, in this study, these two crystallisation processes produce residual liquids of fairly similar major and trace element compositions (Fig. 5.6). However, it is reasonable to argue that the production of silicate-free natrocarbonatites from silicate-bearing natrocarbonatites by *in situ* crystallisation is more likely characterised by Rayleigh fractionation than by bulk equilibrium crystallisation. Indeed, the residual silica-poor liquids produced by crystallisation of silicate phases from silicate-bearing natrocarbonatite magma has low density and viscosity and is therefore expected to separate easily from the crystals, by ascending toward the roof of the chamber.

In situ crystallisation is also in agreement with the precipitation of phases rich in U, Th, HFSE and REE from hydrothermal or carbothermal solutions in fracture or void fillings that has been invoked to explain the depletion of these elements in silicate-free natrocarbonatites from June 1988 and 1993 compared to silicate-bearing magma. Volatiles (CO_2, SO_3, F and Cl) present in the fluid phase accompanying the carbonatite magma can play an important role in crystal fractionation, by favouring cracks in the walls of the magma chamber, and also by complexing with some trace elements originally in the magma. Eggler (1987) showed that although all major and trace elements (except REE) have very low solubility in CO_2 fluids, the solubility of nearly all elements (present as chloride complexes) is fairly high in Cl-rich fluids. During *in situ* crystallisation, complexation of U, Th, HFSE and REE with Cl (and F?) from the fluid phase emanating from the magma could produce the precipitation of minerals in the cracks of the wall of the magma chamber.

5.4 - Petrogenetic model

A petrogenetic model for the formation of silicate-bearing and silicate-free natrocarbonatites, as constrained by experimental studies, is illustrated in Figure 5.7, and discussed in greater detail below. Previous experimental studies by Kjarsgaard et al. (1995) estimated exsolution of silicate-bearing natrocarbonatite at temperatures of 700 - 750 °C, at 100 MPa. Any exsolved silica-rich natrocarbonatite melt may carry nepheline, wollastonite, clinopyroxene, melilite and melanite garnet, which precipitated in equilibrium with two liquids (Kjarsgaard et al., 1995; see Chapter 3); hence, a variety of silicate crystals may be available early on in the cooling history. Any silica-rich natrocarbonatite parent magma which separates from its nephelinite parent will evolve independently. At 100 MPa, the natrocarbonatite melt would immediately precipitate nepheline on cooling (see Fig. 3.3). However, based on the new experimental data of this study, it is proposed that once the silicate-bearing natrocarbonatite has exsolved from its parent and separated, it evolves at 20 MPa pressure. During the temperature interval between exsolution (750 °C) and eruption (~ 615 °C) of silicate-bearing

natrocarbonatites, silicate (and oxide) minerals co-precipitate for the first 125 °C of cooling, being joined by carbonate crystals at temperatures ≤ 625 °C.

In a high level (~ 20 MPa) magma chamber, *in situ* crystallisation of silicate minerals on the walls of the magma chamber produces a silica-poor residual natrocarbonatite magma. Because of its low density, the silica-poor natrocarbonatite magma segregates to the top of the chamber, where nyerereite, gregoryite and apatite precipitate. Because the residual melt separates from the crystals that precipitate from it, it is Rayleigh fractionation, not bulk equilibrium crystallisation, that produces silicate-free natrocarbonatite from silicate-bearing natrocarbonatite magma. Due to the lower temperature on the walls compared to the center of the magma chamber, some crystals can fractionate *in situ* which are not necessarily found in lava OL5 (see Langmuir, 1989). The precipitation of U-, Th-, HFSE- and REE-bearing minerals from fluids emanating from the magma can explain their depletion in some silicate-free natrocarbonatites.

Here it is assumed that during *in situ* crystallisation, none of the residual liquid returns to the magma chamber. This has the consequence that the formation of silicate-free natrocarbonatites by *in situ* crystallisation does not modify the composition of silicate-bearing natrocarbonatites in the main chamber. Because of the highly effective manner in which convective fractionation works (Sparks et al., 1984), the silicate-bearing natrocarbonatite parent magma is dominant in the magma chamber where mainly silicate mineral phases precipitate. If convective velocities in the low pressure 20 MPa magma chamber are sufficiently high, the silicate crystals may be retained in the magma which undergoes bulk equilibrium crystallisation. However, shortly before and/or during eruption, rapid crystal growth (especially of carbonate crystals, see Chapter 3) prevents the crystals from re-equilibrating with the melt, and crystal zoning indicates that the late-stage history of silicate-bearing natrocarbonatites is characterised by surface equilibrium crystallisation only, and maybe local disequilibrium (at the surface of the crystals). Moreover, some crystals might be fractionated out, as the residual silicate-bearing natrocarbonatite moves up into the volcanic edifice. Pyle et al. (1995) have suggested that at Odoinyo Lengai there is a very shallow plumbing system, comprised of small (10 m

radius) chambers containing transient foam layers, which in turn are connected at depth to a larger chamber. Silica-poor natrocarbonatite magma segregated at the top of the 20 MPa magma chamber subsequently moves into these 10 m radius near surface magma chambers, where nyerereite, gregoryite and apatite continue to crystallise, before eruption.

5.5 - Conclusions

Comparison of the results obtained by petrological and experimental studies on silicate-bearing natrocarbonatite OL5 indicates that this sample is a suitable candidate for a natrocarbonatite parent magma. A critical feature of the experimental phase relationships for OL5 is that nepheline crystallises first, and a variety of silicate minerals co-precipitate over a protracted cooling interval. Crystallisation at 20 MPa is dominated by ferromagnesian silicates and nepheline down to 635 °C.

Silicate-free natrocarbonatite lavas are the typical product at Oldoinyo Lengai. Their predominance is thought to be due to their low density and viscosity. The preferred model for the origin of these lavas is that they are differentiates which form in a high level (20 MPa) magma chamber by the *in situ* crystallisation of silicate-bearing natrocarbonatites. The removal of the silicate component of the parent magma, by sidewall crystallisation, gives rise to a low-density, phenocryst-poor magma which rises along the wall to the top of the chamber. Between the high level chamber (20 MPa) and the surface these magmas may undergo further differentiation in very small diameter, near surface magma chambers, dominantly precipitating nyerereite and gregoryite.

Convective fractionation is an appropriate crystallisation process that explains how silicate-bearing natrocarbonatites may undergo different crystallisation processes within the magma chamber. For example, bulk equilibrium crystallisation within the main magma chamber produces the erupted silicate-bearing natrocarbonatites and, at the same time, Rayleigh fractionation on the walls of the magma chamber produces a residual silicate-free natrocarbonatite magma. The preservation of the original silicate-bearing natrocarbonatite magma in the main magma chamber after its separation from its parent

magma permits the study of liquid immiscibility between silicate and carbonate magmas in Chapters 6 and 7.

Table 5.1: List of abbreviations used for the different liquids in the OL5-experiments and in natural lava OL5.

Abbreviation	Significance
MNR	**M**easured composition of **N**atural **R**ock OL5 (= whole-rock, *cf.* Tab. 4.10)
CNR1	**C**alculated composition of **N**atural **R**ock OL5 (whole-rock) using phase proportions determined in Chapter 3
CNR2	Same as CNR1, but adding (in place of groundmass) 0.03 titanite, 0.2 perovskite, 0.5 apatite and 0.01 melilite (all in volume percent)
MEL	**M**easured composition of **L**iquid in the **E**xperiments (= at 20 MPa, 625 and 600 °C)
CEL	**C**alculated **E**quivalent **L**iquid in lava OL5 (= groundmass + carbonate crystals + siliceous mesostasis, *cf.* Tab. 3.11) - **CEL1** = does not include perovskite and titanite; **CEL2** = includes perovskite and titanite.
HEL	Composition of the carbonate **L**iquid in a **H**ypothetical **E**xperiment at 20 MPa, 615 °C (= bulk OL5 minus crystals)
RFL	**R**esidual **L**iquid of **R**ayleigh **F**ractionation of OL5

Figure 5.1: Trace element concentrations normalised to primitive mantle of different phases in silicate-bearing natrocarbonatite lava OL5. a: REE; b: other elements. Data from Table 4.9; primitive mantle normalising values are from McDonough and Sun (1995). Source of additional data include: trace element data for perovskite from Dawson et al. (1994b), and from Onuma et al. (1981) for U and Th, and extrapolated for Eu, Dy, Er, Yb and Lu. The perovskite data in Dawson et al. (1994b) are from a jacupirangite from Oldoinyo Lengai, and the data in Onuma et al. (1981) are from a melilite-nepheline basalt. Trace element data for titanite are from OL5-experiment CP107 (100 MPa, 600 °C) (see Tab. 4.8), except for Sr, Er and Lu which are taken from two-liquid experiments CP11 and CP64 (see Chapter 7). Trace element data for melilite are taken from OL5-experiment CP51 (20 MPa, 750 °C) (see Tab. 4.5).

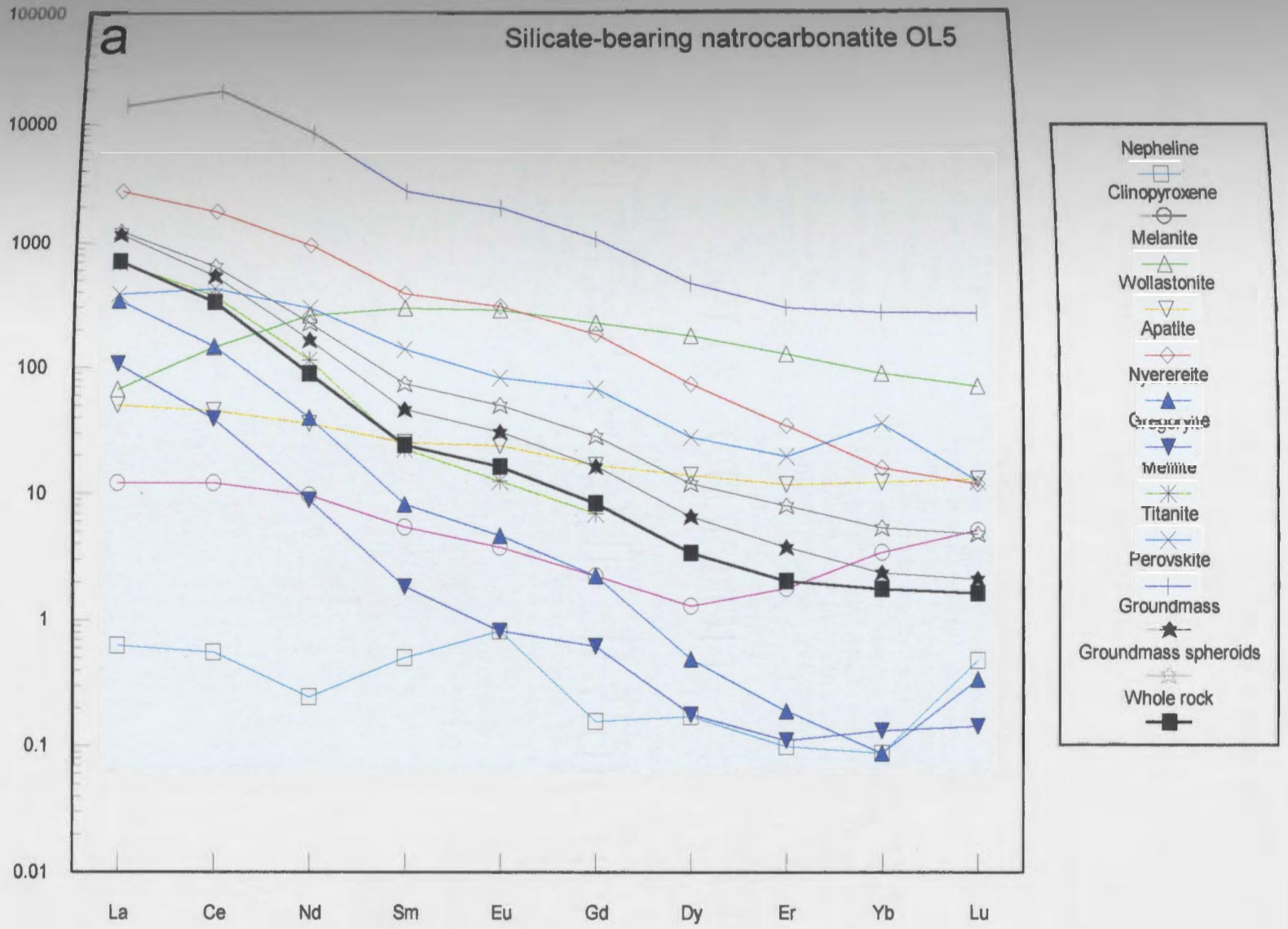
a
Silicate-bearing natrocarbonatite OL5
Primitive mantle normalized
100000
10000
1000
100
10
1
0.1
0.01
La
Ce
Nd
Sm
Eu
Gd
Dy
Er
Yb
Lu
Nepheline
Clinopyroxene
Melanite
Wollastonite
Apatite
Nyerereite
Gregoryite
Melilite
Titanite
Perovskite
Groundmass
Groundmass spheroids
Whole rock

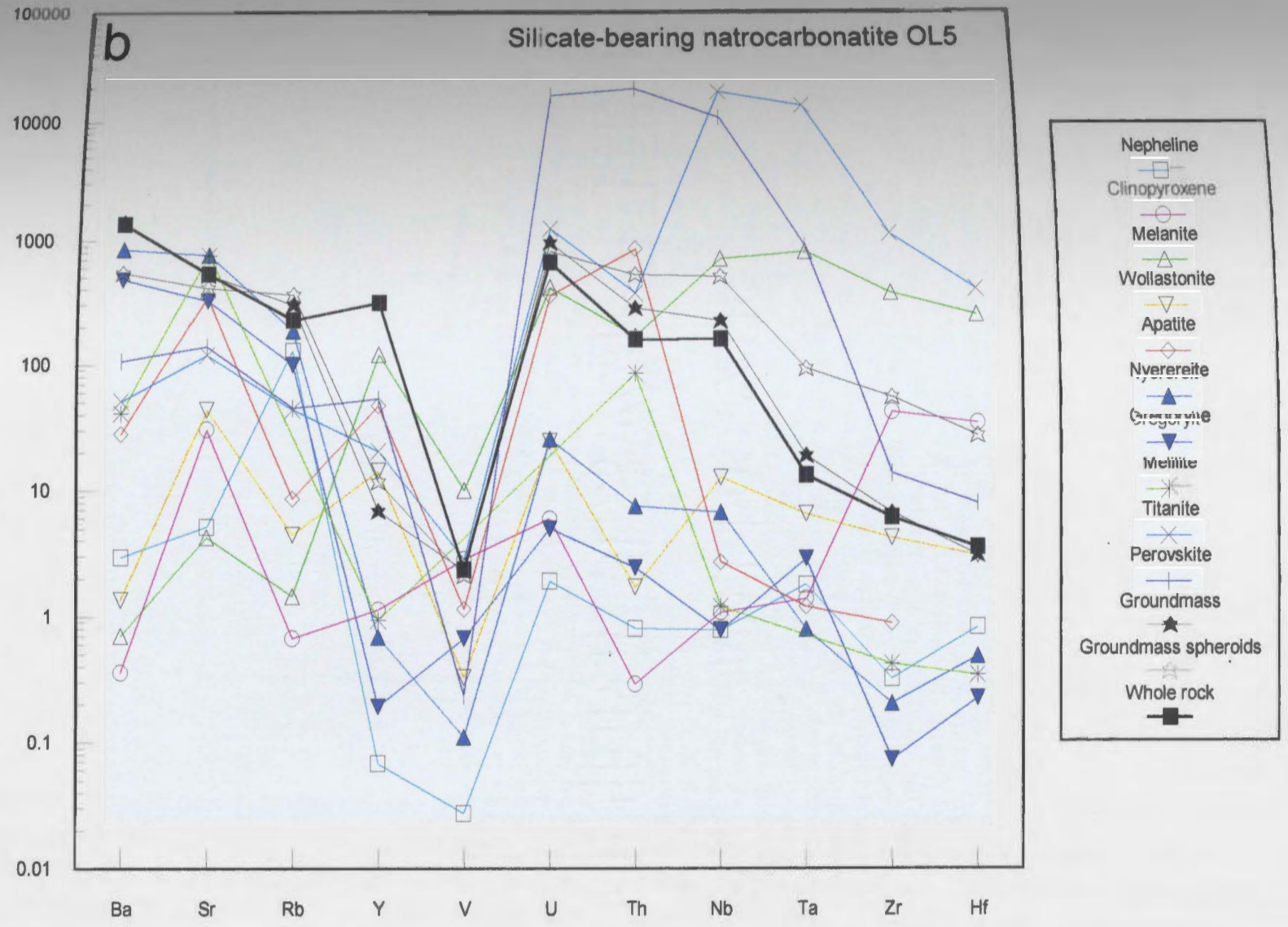
b
Silicate-bearing natrocarbonatite OL5
Primitive mantle normalized
100000
10000
1000
100
10
1
0.1
0.01
Ba
Sr
Rb
Y
V
U
Th
Nb
Ta
Zr
Hf
Nepheline
Clinopyroxene
Melanite
Wollastonite
Apatite
Nyerereite
Gregoryite
Melilite
Titanite
Perovskite
Groundmass
Groundmass spheroids
Whole rock

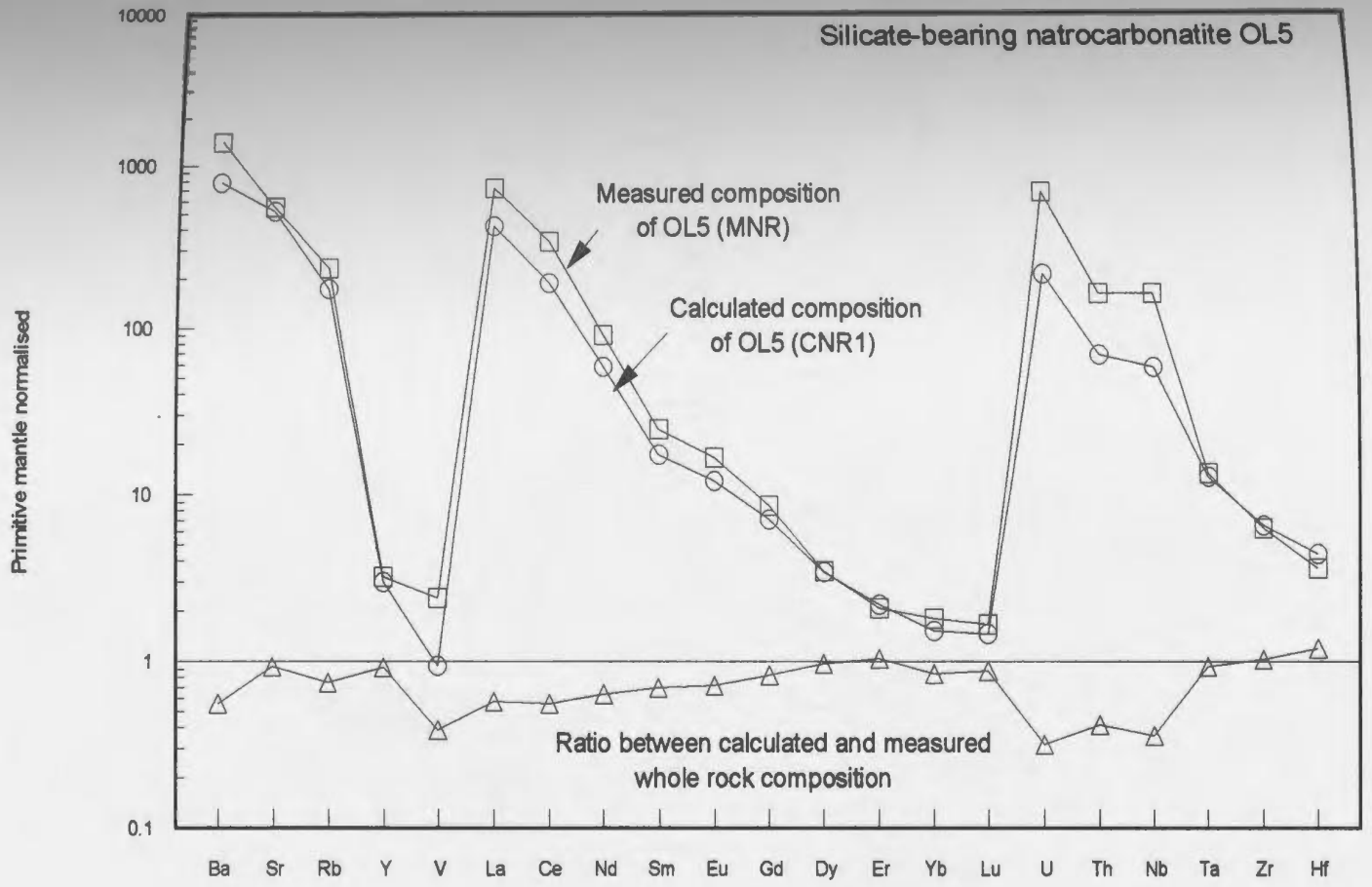

Figure 5.2: Comparison between calculated (CNR1) and measured (MNR) whole-rock trace element concentrations of silicate-bearing natrocarbonatite OL5, normalised to primitive mantle (*cf.* Tab. 5.1 for abbreviations). The ratio between calculated (CNR1) and measured (MNR) compositions of the whole rock is also plotted. The calculated composition CNR1 is based on phase proportions observed for OL5 (see Tab. 4.11) and the LAM-ICP-MS analyses. The measured whole-rock composition of OL5 is from Table 4.10; primitive mantle normalising values are from McDonough and Sun (1995). Details and results of the calculation are given in Table A5.1 in Appendix A5.

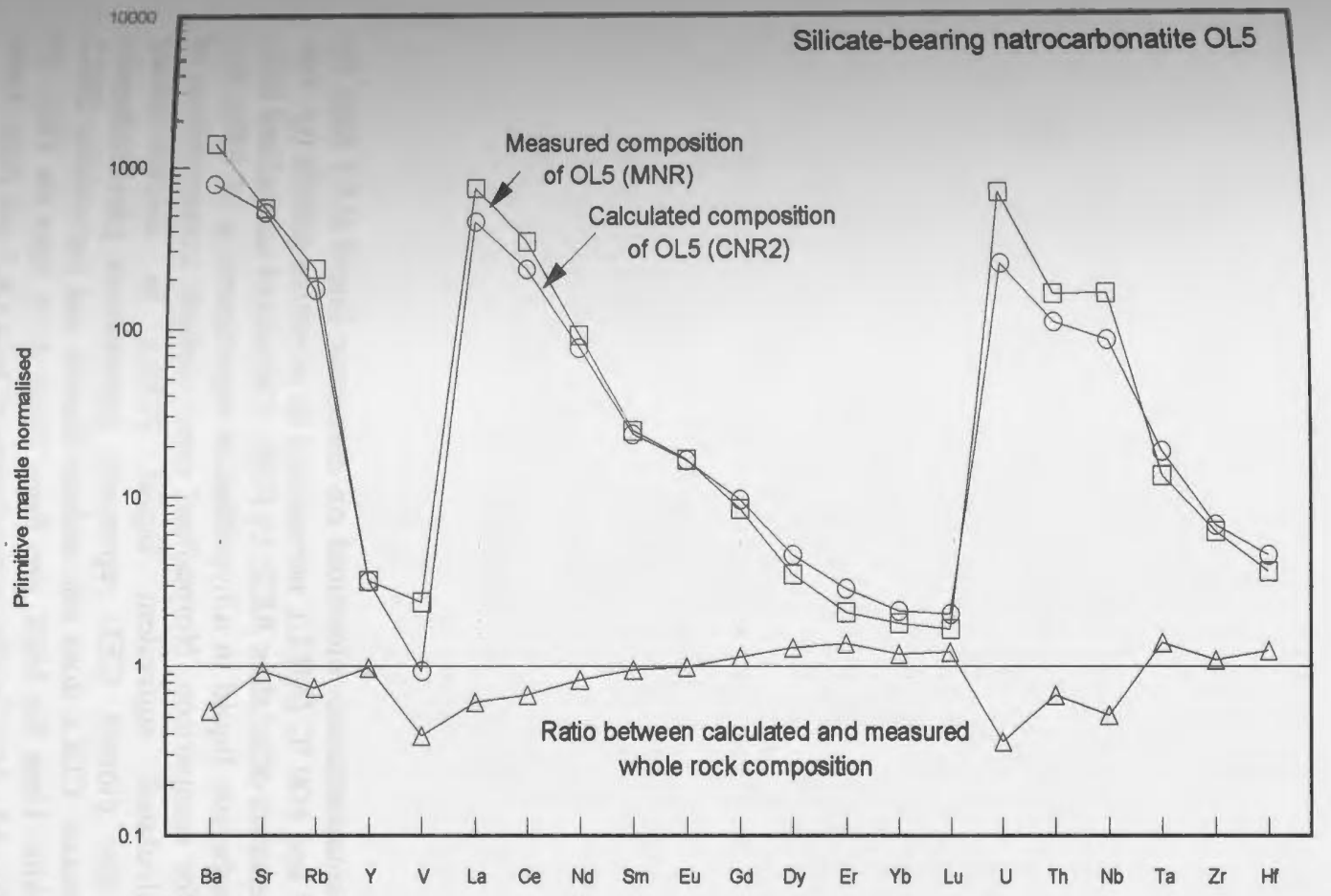

Figure 5.3: Comparison between calculated (CNR2) and measured (MNR) whole-rock trace element concentrations of silicate-bearing natrocarbonatite OL5, normalised to primitive mantle (see Tab. 5.1 for abbreviations). The ratio between calculated (CNR2) and measured (MNR) compositions of the whole rock is also plotted. The calculated composition CNR2 includes titanite, perovskite, melilite, and apatite in place of groundmass (see text). The measured whole-rock composition of OL5 is from Table 4.10; primitive mantle normalising values are from McDonough and Sun (1995). Details and results of the calculation are given in Table A5.1 in Appendix A5. Sources of additional data are described in caption of Figure 5.1.

Figure 5.4: Trace element concentrations measured on carbonate liquid (LC) from the experiments at 20 MPa, 625 and 600 °C (MEL), normalised to primitive mantle (*cf.* Tab. 5.1 for abbreviations). a) Elements other than REE; b) REE. Calculated normalised trace element concentrations of carbonate liquid in a hypothetical experiment at 20 MPa, 615 °C (HEL) are also plotted for comparison. Normalised trace element concentrations of groundmass, and of calculated equivalent liquid (CEL) in silicate-bearing natrocarbonatite OL5 are also plotted. CEL represents groundmass plus carbonate crystals plus siliceous mesostasis. CEL1 does not include titanite and perovskite; CEL2 includes titanite and perovskite. Data for MEL are from Table 4.10; data for HEL are from Table A4.4 in Appendix A4; data for the groundmass of lava OL5 are from Table 4.9, and data for CEL1 and CEL2 are from Table A5.1 in Appendix A5; primitive mantle normalising values are from McDonough and Sun (1995). (a) elements other than REE; (b) REE.

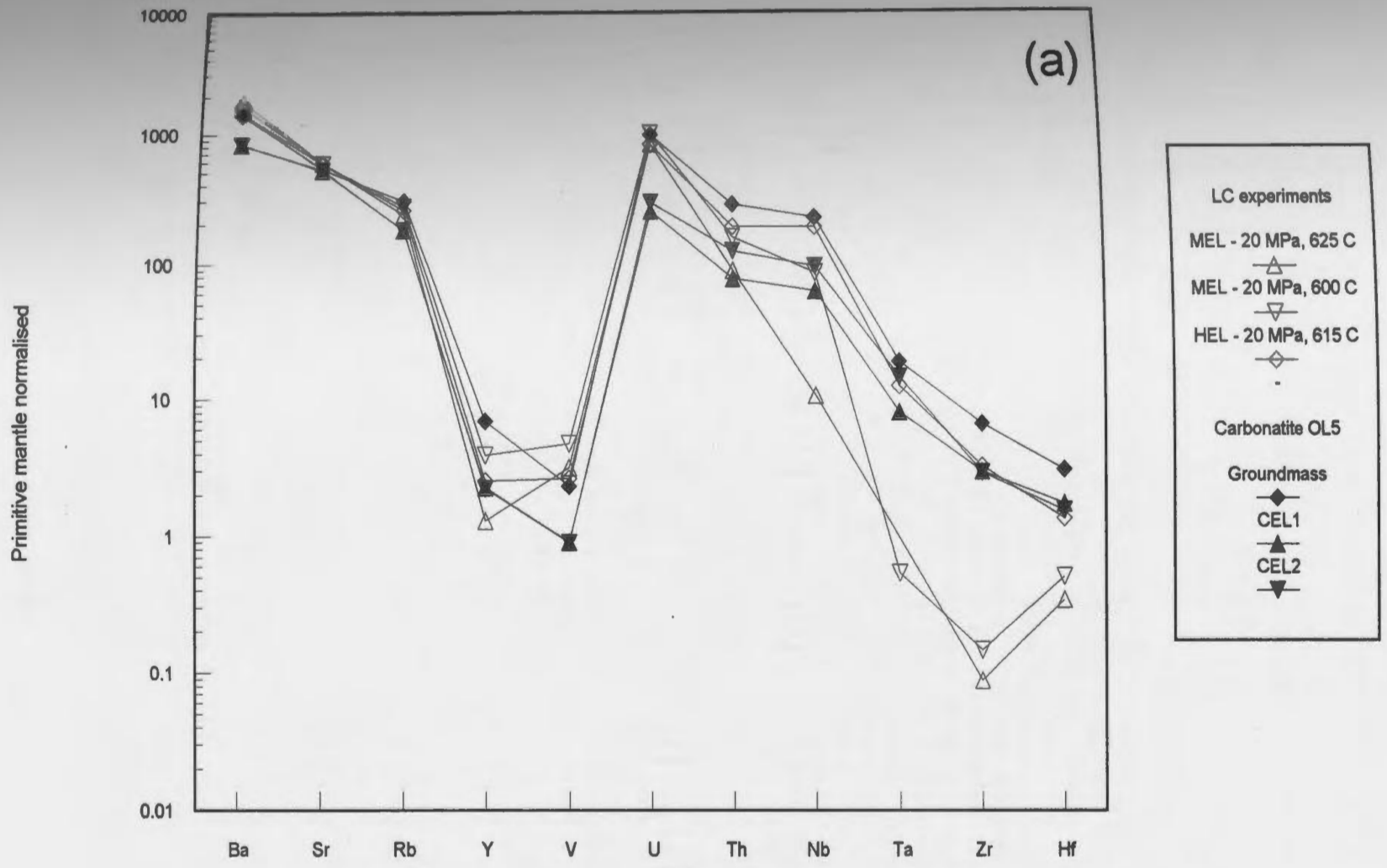
(a)
Primitive mantle normalised
10000
1000
100
10
1
0.1
0.01
Ba
Sr
Rb
Y
V
U
Th
Nb
Ta
Zr
Hf
LC experiments
MEL - 20 MPa, 625 C
MEL - 20 MPa, 600 C
HEL - 20 MPa, 615 C
Carbonatite OL5
Groundmass
CEL1
CEL2

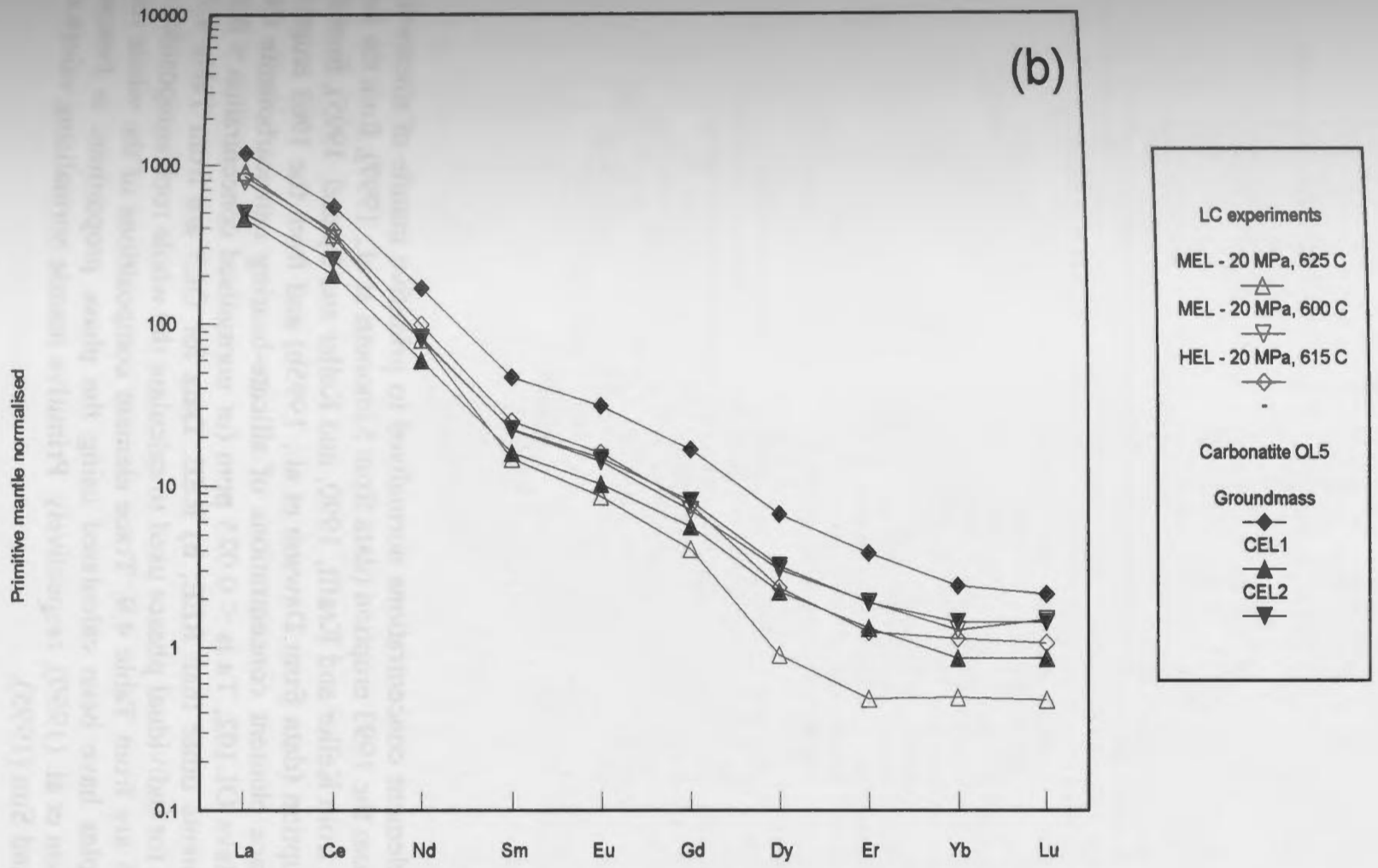
(b)
Primitive mantle normalised
10000
1000
100
10
1
0.1
La
Ce
Nd
Sm
Eu
Gd
Dy
Er
Yb
Lu
LC experiments
MEL - 20 MPa, 625 C
MEL - 20 MPa, 600 C
HEL - 20 MPa, 615 C
Carbonatite OL5
Groundmass
CEL1
CEL2

Figure 5.5: Trace element concentrations normalised to primitive mantle of silicate-free natrocarbonatites from the 1993 eruption (data from Simonetti et al., 1997), from the June 1988 eruption (data from Keller and Krafft, 1990, and Keller and Spettel, 1995), from the November 1988 eruption (data from Dawson et al., 1995b) and from the 1963 eruption. For comparison, trace element concentrations of silicate-bearing natrocarbonatite OL5 are also shown. In lava OL102, Ta is < 0.025 ppm (or normalised concentration < 0.68; see arrow). a) Elements other than REE; b) REE. Data for OL5 are from Table 4.10. LAM-ICP-MS data for individual phases used to calculate the whole rock composition of BD4169 and CML5 are from Table 4.9. Trace element compositions of the whole rock for these two samples have been calculated using the phase proportions in Peterson (1990) and in Dawson et al. (1990), respectively. Primitive mantle normalising values are from McDonough and Sun (1995).

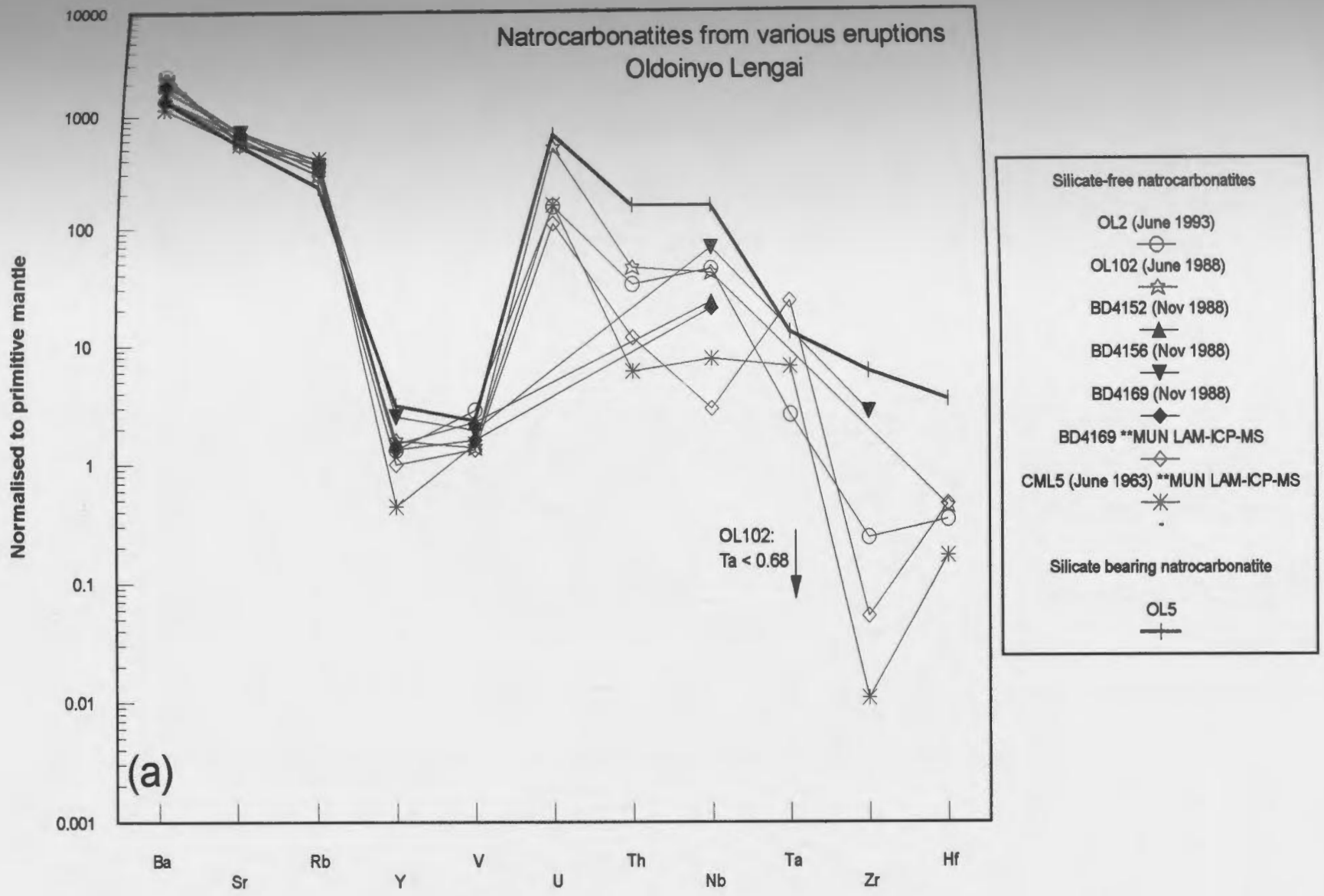
Natrocarbonatites from various eruptions
Oldoinyo Lengai
Normalised to primitive mantle
10000
1000
100
10
1
0.1
0.01
0.001
(a)
OL102:
Ta < 0.68
Ba
Sr
Rb
Y
V
U
Th
Nb
Ta
Zr
Hf
Silicate-free natrocarbonatites
OL2 (June 1993)
OL102 (June 1988)
BD4152 (Nov 1988)
BD4156 (Nov 1988)
BD4169 (Nov 1988)
BD4169 **MUN LAM-ICP-MS
CML5 (June 1963) **MUN LAM-ICP-MS
Silicate bearing natrocarbonatite
OL5

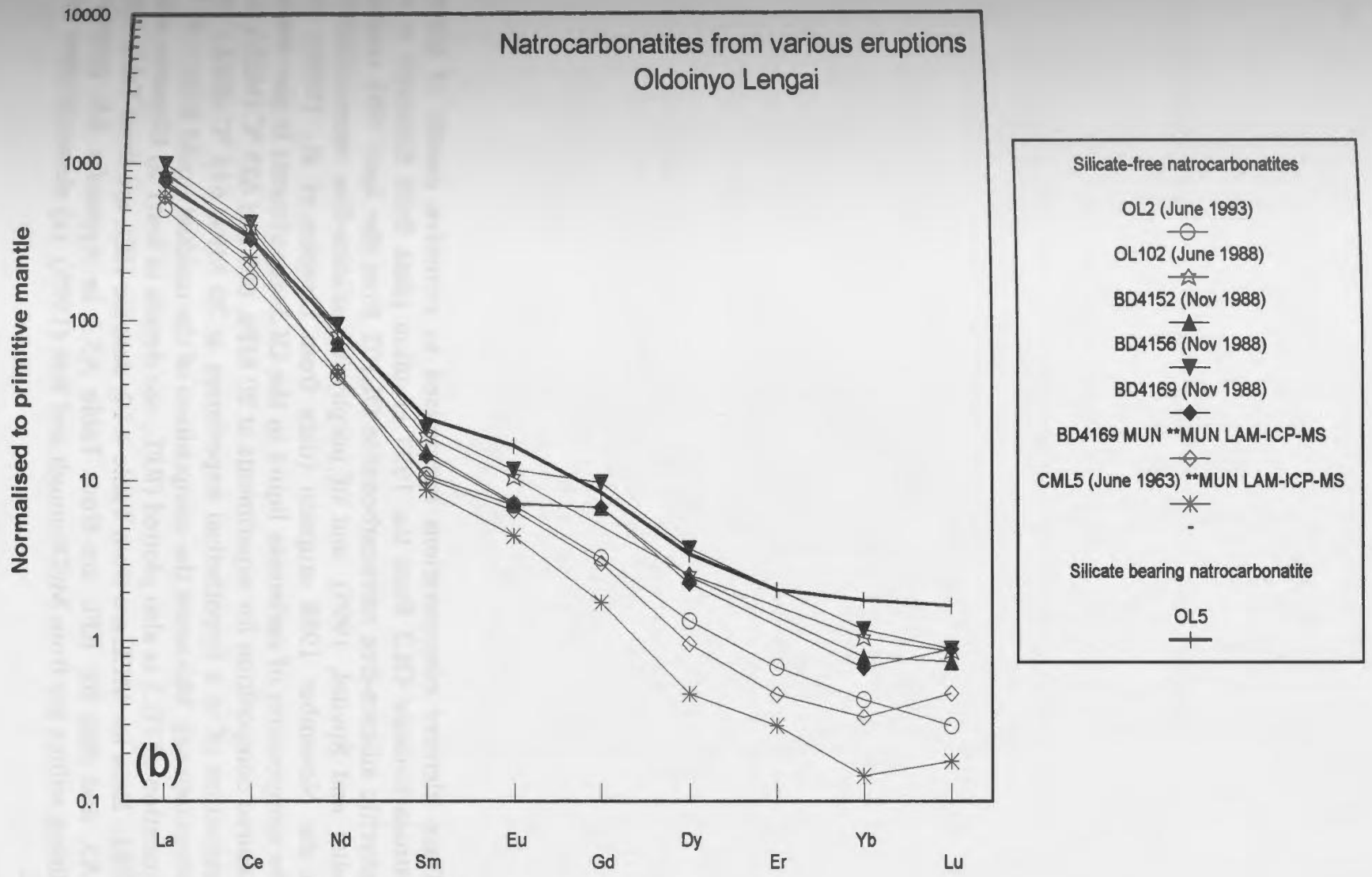
Natrocarbonatites from various eruptions
Oldoinyo Lengai
Normalised to primitive mantle
10000
1000
100
10
1
0.1
(b)
La
Ce
Nd
Sm
Eu
Gd
Dy
Er
Yb
Lu
Silicate-free natrocarbonatites
OL2 (June 1993)
OL102 (June 1988)
BD4152 (Nov 1988)
BD4156 (Nov 1988)
BD4169 (Nov 1988)
BD4169 MUN **MUN LAM-ICP-MS
CML5 (June 1963) **MUN LAM-ICP-MS
Silicate bearing natrocarbonatite
OL5

Figure 5.6: Trace element concentrations normalised to primitive mantle of aphyric silicate-free natrocarbonatite OL2 from the 1993 eruption (data from Simonetti et al., 1997), of porphyritic silicate-free natrocarbonatite OL102 from the June 1988 eruption (data from Keller and Spettel, 1995), and of porphyritic silicate-free natrocarbonatite BD4156 from the November 1988 eruption (data from Dawson et al., 1995b). For comparison, the composition of carbonate liquid in the OL5-experiments is also shown, including: Measured composition for experiments at 20 MPa, 600 and 625 °C (MEL), and calculated composition of in a hypothetical experiment at 20 MPa, 615 °C (HEL) (see Tab. 5.1 for abbreviations). Moreover the composition of the residual liquid from ~ 25 % Rayleigh fractionation of OL5 is also plotted (RFL; see details in text). a) Elements other than REE; b) REE. Data for MEL are from Table 4.10; data for HEL are from Table A5.1 in Appendix A5, and data for RFL are from Table A5.1 in Appendix A5; primitive mantle normalising values are from McDonough and Sun (1995). (a) elements other than REE; (b) REE.

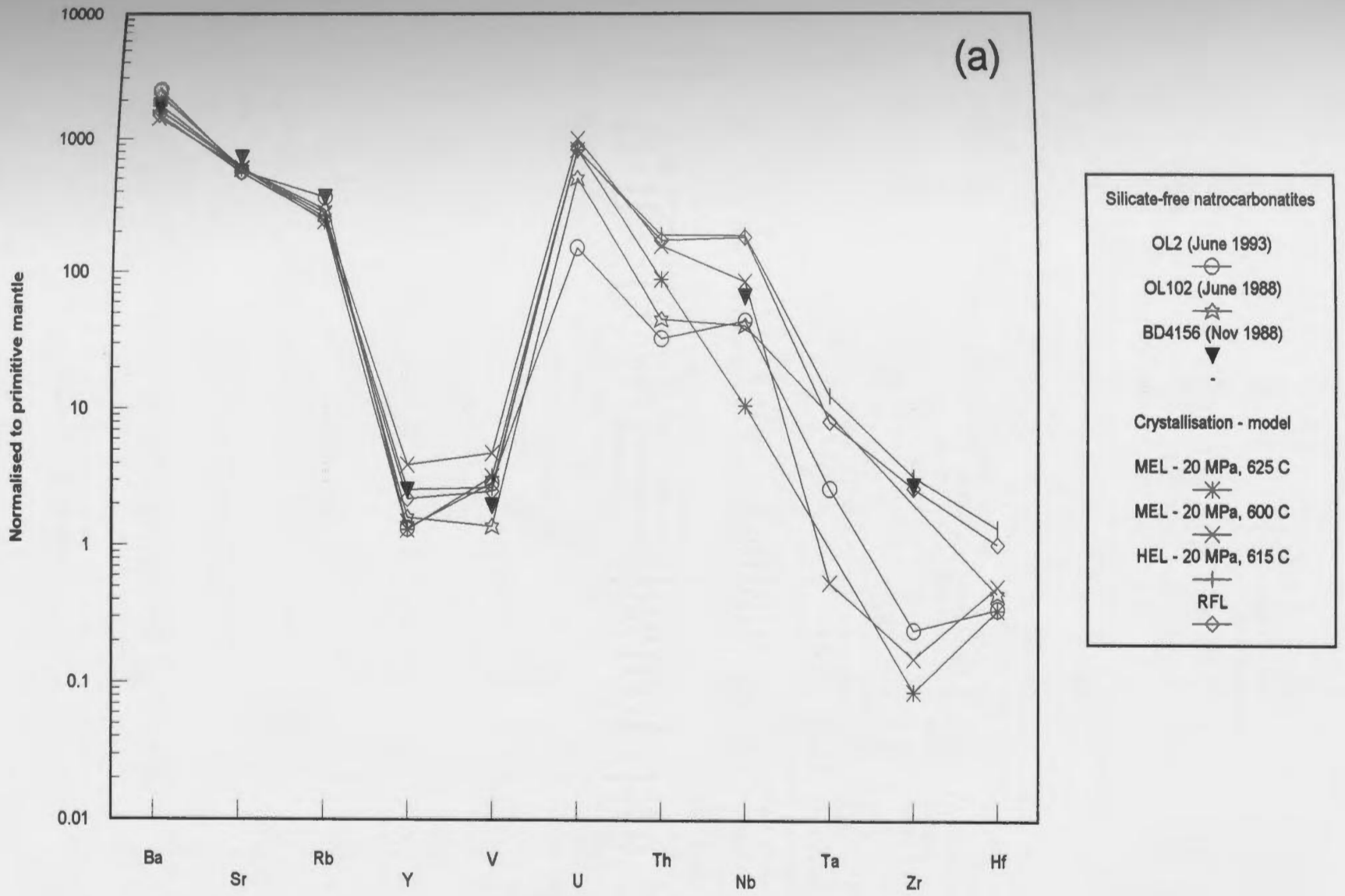
(a)
Normalised to primitive mantle
10000
1000
100
10
1
0.1
0.01
Ba
Sr
Rb
Y
V
U
Th
Nb
Ta
Zr
Hf
Silicate-free natrocarbonatites
OL2 (June 1993)
OL102 (June 1988)
BD4156 (Nov 1988)
Crystallisation - model
MEL - 20 MPa, 625 C
MEL - 20 MPa, 600 C
HEL - 20 MPa, 615 C
RFL

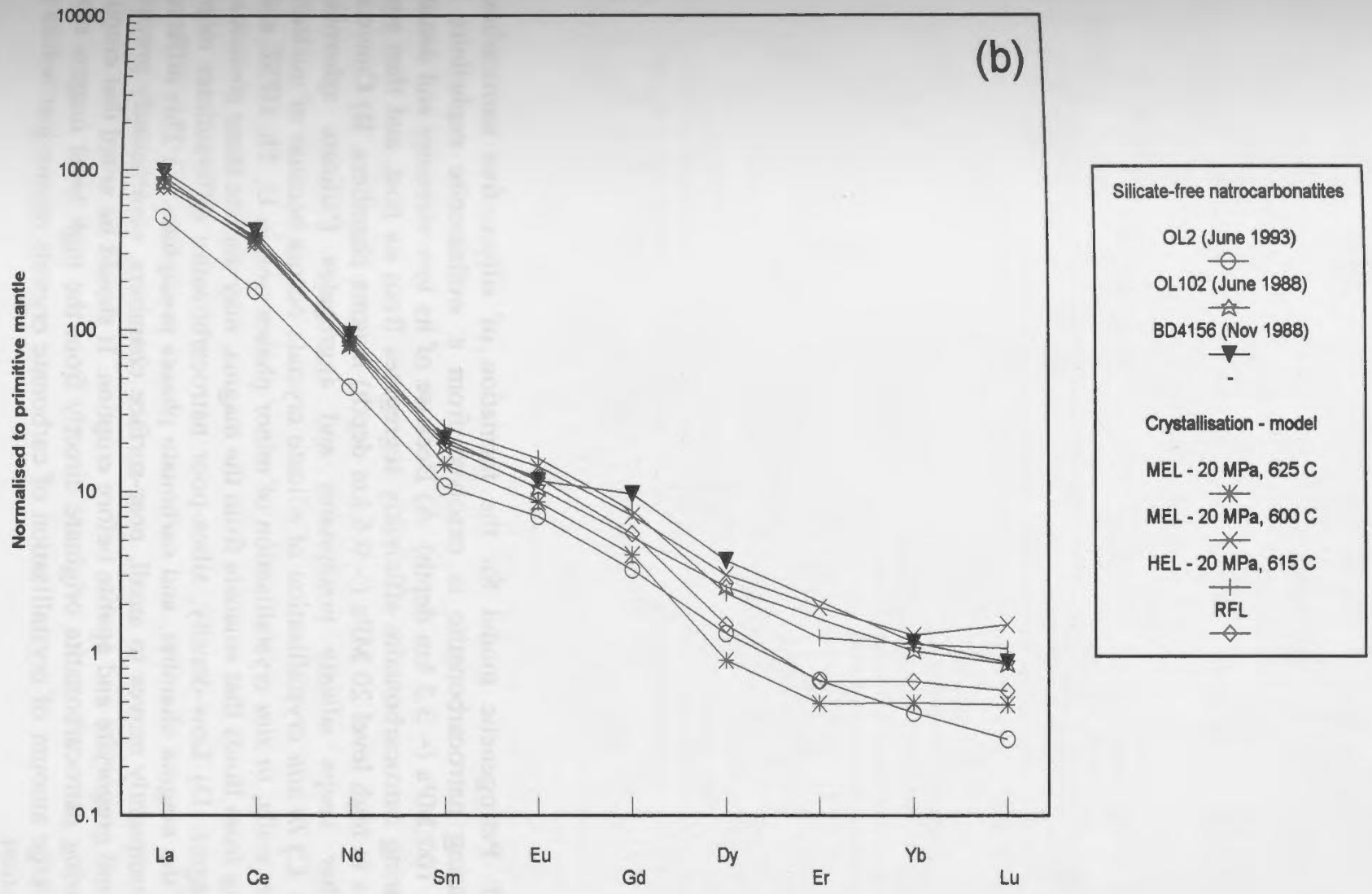
(b)
Normalised to primitive mantle
10000
1000
100
10
1
0.1
La
Ce
Nd
Sm
Eu
Gd
Dy
Er
Yb
Lu
Silicate-free natrocarbonatites
OL2 (June 1993)
OL102 (June 1988)
BD4156 (Nov 1988)
Crystallisation - model
MEL - 20 MPa, 625 C
MEL - 20 MPa, 600 C
HEL - 20 MPa, 615 C
RFL

Figure 5.7: Petrogenetic model for the formation of silicate-free natrocarbonatites. Silicate-bearing natrocarbonatite is exsolved from a wollastonite nephelinite parent magma at 100 MPa (~ 3.3 km depth). A) Because of its low viscosity and density, the silicate-bearing natrocarbonatite efficiently segregates from its host, and then separates and collects in high level 20 MPa (~ 0.6 km depth) magma chambers. B) Convection in this chamber keeps silicate precipitates and aggregates ('silicate spheroids') in suspension. C) *In situ* crystallisation of silicate crystals occurs because of nucleation on the chamber walls; *in situ* crystallisation of minor phases rich in U, Th, HFSE and REE precipitating from fluids that emanate from the magma, may deplete these elements in the residual magma. D) Low-density, silica-poor natrocarbonatite differentiates migrate to the roof of the magma chamber, and carbonate phases precipitate. E) This differentiated magma subsequently moves to small, near-surface chambers, continuously precipitating nyerereite and gregoryite and apatite before eruption. It should be noted that eruptions of silicate-bearing natrocarbonatite originate directly from the high level magma chamber, and that a large amount of crystallisation of carbonate crystals occurs just before and/or during eruption.

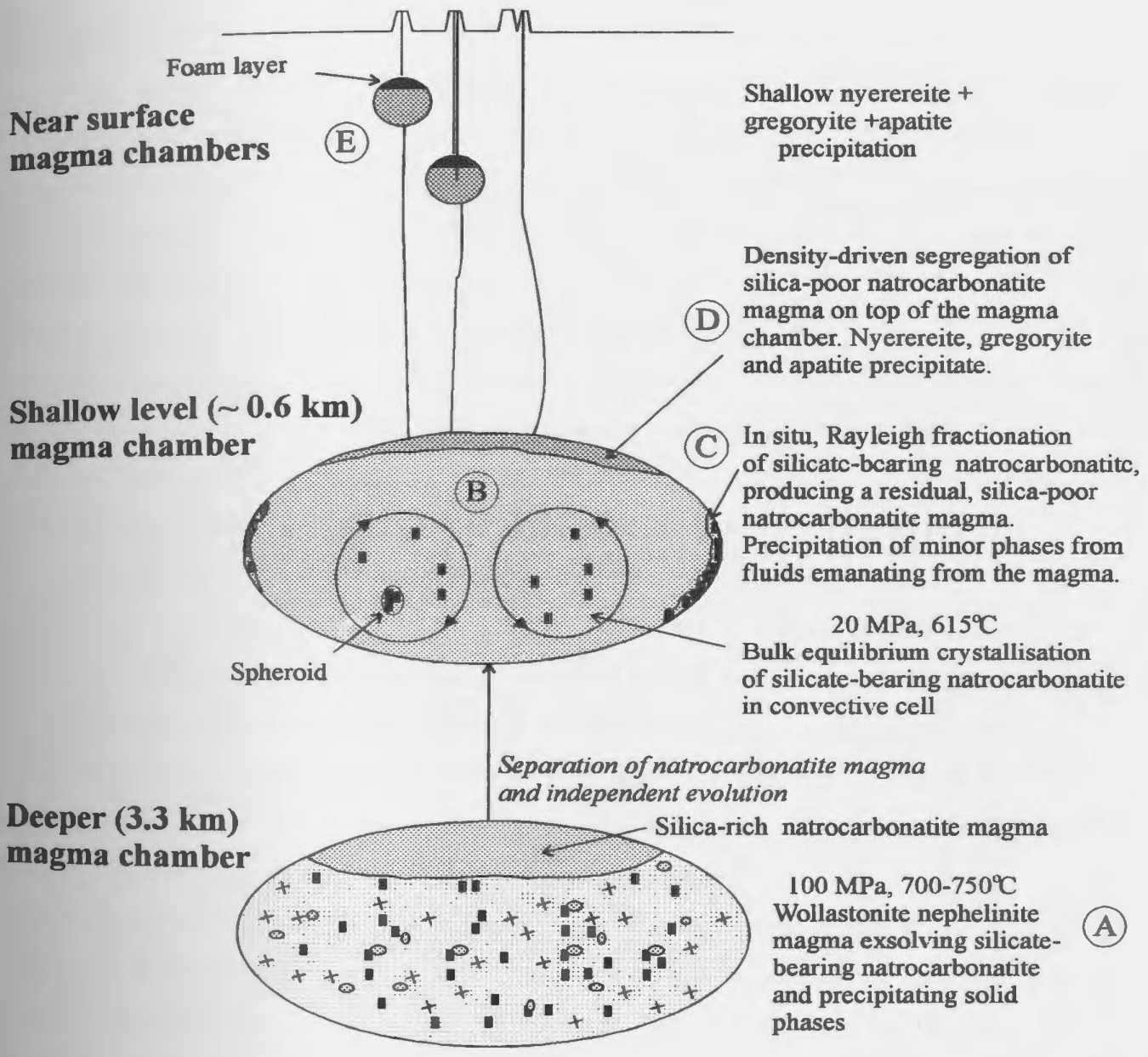
Foam layer
Near surface magma chambers
E
Shallow nyerereite + gregoryite +apatite precipitation
Density-driven segregation of silica-poor natrocarbonatite magma on top of the magma chamber. Nyerereite, gregoryite and apatite precipitate.
D
Shallow level (~ 0.6 km) magma chamber
C
In situ, Rayleigh fractionation of silicate-bearing natrocarbonatite, producing a residual, silica-poor natrocarbonatite magma. Precipitation of minor phases from fluids emanating from the magma.
B
20 MPa, 615°C
Bulk equilibrium crystallisation of silicate-bearing natrocarbonatite in convective cell
Spheroid
Separation of natrocarbonatite magma and independent evolution
Deeper (3.3 km) magma chamber
Silica-rich natrocarbonatite magma
100 MPa, 700-750°C
Wollastonite nephelinite magma exsolving silicate-bearing natrocarbonatite and precipitating solid phases
A

CHAPTER 6: ORIGIN OF SILICATE-BEARING NATROCARBONATITES BY LIQUID IMMISCIBILITY FROM WOLLASTONITE NEPHELINITE - PART I: CONSTRAINTS FROM MAJOR ELEMENT DATA.

6.1 - Introduction

At Oldoinyo Lengai, olivine-free nephelinite-phonolite tuffs and lavas comprise > 99 % of the volcano (Donaldson et al., 1987). The association of natrocarbonatites with nephelinites has lead many authors (*e.g.* Peterson and Kjarsgaard, 1995; Kjarsgaard et al., 1995) to consider these lavas to be related by liquid immiscibility. Kjarsgaard et al. (1995) estimated the P-T conditions of liquid immiscibility to be 100 MPa, 750 °C at Oldoinyo Lengai, and showed that the K_2O-rich (6.35-8.40 wt. %) nature of natrocarbonatite flows precluded the pressure of exsolution to be higher than 100 MPa. In support of this model, Pyle et al. (1991) showed that for the 1988 natrocarbonatite lava from the Oldoinyo Lengai volcano, ^{238}U-^{230}Th-^{226}Ra disequilibria are consistent with an origin by immiscibility of 4-22 wt. % natrocarbonatite from a nephelinite magma.

The aim of this chapter is to further examine the hypothesis that silicate-bearing natrocarbonatite and wollastonite nephelinite are related by liquid immiscibility, and to determine what the likely conditions of exsolution of natural lavas are. The immiscibility conditions are determined by comparing phase assemblages and compositions of the different phases in natural lavas, to those produced in experiments. Based on previous studies, these experiments were made at P-T-X conditions appropriate for Oldoinyo Lengai. Wollastonite nephelinite HOL14 and silicate-bearing natrocarbonatite OL5 are the natural lavas that were analysed and used for experimental mixes in this study. Wollastonite nephelinite HOL14 was erupted in 1966 (Peterson, 1990) and silicate-bearing natrocarbonatite OL5 in 1993 (Simonetti et al., 1997). The fact that they are not from the same eruption is not considered a problem, since the question is to know if OL5-like silicate-bearing natrocarbonatites can be genetically related to HOL14-like wollastonite nephelinites, not to know if silicate-bearing natrocarbonatite OL5 is genetically related to wollastonite nephelinite HOL14.

Although natrocarbonatites are possibly the product of 4-22 % liquid immiscibility from wollastonite nephelinite (Pyle et al., 1991), experiments were also prepared using higher proportions of carbonatite in the bulk composition, in order: 1) to examine the pseudobinary system at 20 and 100 MPa; and 2) to facilitate the analyses of carbonate liquid in experiments at 20, 40 and 100 MPa. Experiments using only natrocarbonatite lava OL5 as the starting composition (OL5-experiments, see Chapter 3) were made at 20 and 100 MPa, and 550 °C ≤ T ≤ 900 °C, whereas experiments containing silicate in the starting composition were made at 20, 40 and 100 MPa, and 700 °C ≤ T ≤ 900 °C. Most experiments are unbuffered-, sealed tube-experiments. In addition, two C/CH_4 buffered-, one open tube- and one 200 MPa-experiments were also made.

The data are presented separately for the three different pressures (20, 40 and 100 MPa), three different ranges of temperature (T ≤ 700 °C; 700 °C < T ≤ 800 °C; T > 800 °C) and for different bulk starting compositions, so that the effect of pressure, temperature and bulk composition on phase assemblages and compositions can be examined. Bulk composition is labelled as weight fraction of wollastonite nephelinite HOL14/silicate-bearing natrocarbonatite OL5. The major element compositions of different starting mixtures are given in Table 2.2. The terminology used to define the different experiments is: (a) HOL14-experiments for the experiments prepared using only wollastonite nephelinite HOL14 in the starting composition; (b) LS-experiments (= silicate liquid experiments) for the experiments which contain only silicate liquid (plus crystals) but which are not HOL14-experiments; (c) LC-experiments (= carbonate liquid experiments) for the experiments that contain only carbonate liquid (plus crystals) but which are not OL5-experiments; and (d) two-liquid experiments for the experiments containing conjugate carbonate and silicate liquids. Individual analyses used to calculate average compositions of crystals and liquids are presented in Appendix A6; in the present chapter, only average analyses are presented, and the number of analyses is indicated in the tables.

Figure 6.1 presents a SEM photograph of the two-liquid experimental charge CP8 prepared at 103 MPa, 700 °C, using a 90/10 bulk composition. One crystal of

clinopyroxene criss-crosses the boundary between silicate and carbonate liquids. Figure 6.1 illustrates that in two-liquid experiments, although silicate crystals are in equilibrium with both conjugate liquids, they are mainly present in the silicate liquid (see also Figs. 2.12 and 2.14). The observation that silicate crystals are scarce in the carbonate liquid, but that the carbonate liquid in two-liquid experiments is silica-rich, suggests that crystals in erupted silicate-bearing natrocarbonatite OL5 are formed mostly during crystal fractionation, after the separation of the immiscible liquids (see Fig. 3.1).

The observation that silicate liquid in two-liquid experiments contains silicate crystals indicates that at least some of the crystals in wollastonite nephelinite HOL14 could have formed at the time of liquid immiscibility. One question to be answered is: did most of the crystals in HOL14 form at the time of liquid immiscibility, or did the crystals form during subsequent crystallisation? Unlike carbonate magma which has 150 °C to cool down between liquid immiscibility (~ 750 °C) and eruption (~ 600 °C), the silicate magma may have a much narrower temperature interval over which to cool down. Kjarsgaard et al. (1995) cited calculated eruption temperatures for highly peralkaline silicate lavas at Oldoinyo Lengai from 500 to 775 °C. These estimates are based on the nepheline thermometers of Hamilton (1961) and Peterson (1989a). The occurrence of subhedral pyrite phenocrysts in HOL14 suggests eruption temperatures below 743 °C (Toulmin and Barton, 1964). If the eruption temperature of wollastonite nephelinite HOL14 is ~ 740 °C, then time for crystallisation after liquid immiscibility is limited, and most crystals would have formed at the time of exsolution, or earlier at higher temperature. Alternatively, if the eruption temperature of HOL14 is lower, then crystallisation after exsolution could be more important. These questions can be addressed by comparing phase assemblages and mineral compositions in the natural rock with those produced in the experiments.

6.2 - Previous studies

Field observations and most experimental studies on synthetic and natural carbonatites suggest that liquid immiscibility is the process involved in the genesis of natrocarbonatites at Oldoinyo Lengai. Peterson (1989a) documented the occurrence of a

subset of lavas which were highly peralkaline at Oldoinyo Lengai, *i.e.* combeite and wollastonite nephelinites. Keller and Krafft (1990) further noted that the peralkaline combeite-bearing nephelinite lava was closely related to the natrocarbonatite lava, both in time and space, and that Sr and Nd isotopes of natrocarbonatites and combeite-nephelinites were virtually indistinguishable; therefore, suggesting that both magmas types were comagmatic. Most experimental studies concerned with the origin of natrocarbonatite from Oldoinyo Lengai have focused on liquid immiscibility. However, based on experiments, Sweeney et al. (1995a) argued that the natrocarbonatites from Oldoinyo Lengai could be formed by direct partial melting from the mantle.

Experimental evidence for silicate/carbonate liquid immiscibility in synthetic, geologically relevant systems was first demonstrated by Koster van Groos and Wyllie (1963, 1966, 1968, 1973; see Chapter 1). Freestone and Hamilton (1980) produced pairs of immiscible liquids from mixtures of phonolite found at Oldoinyo Lengai and a synthetic analogue of the natrocarbonatite found at the same location. By comparing major element compositions of silicate and carbonate liquids in natural and in experimental samples, they found that natrocarbonatites could be formed by liquid immiscibility from phonolites at 3 kbar (300 MPa) and 1050 °C. However, their experiments could not produce the exact equivalent of the natural lavas. Kjarsgaard et al. (1995) studied the same system at lower pressure, temperature and carbonate content in the bulk composition. By comparing major element compositions of silicate and carbonate liquids in natural and in experimental samples, they found that natrocarbonatites could be formed by liquid immiscibility from wollastonite nephelinites at 100 MPa and 750 °C.

In conjunction with their early work, Freestone and Hamilton (1980) developed the so-called "Hamilton plots", which combine the main components [(SiO_2 + Al_2O_3 ± TiO_2)-(CaO ± FeO, MgO, MnO)-alkalis] into three groups, which are then projected from CO_2. As pointed out by Brooker (1995), comparing major element compositions of silicate and carbonate liquids in natural and in experimental samples on these plots leads to non-unique solutions. Brooker (1995) showed that the number of non-bridging oxygens per

tetrahedron (NBO/T) of the silicate melt (which describes how depolymerized the melt is) is a better parameter to determine P-T conditions of liquid immiscibility. He also showed that another advantage of this parameter is that it is also important in describing CO_2 saturation in the silicate liquid as well as the liquid immiscibility process.

Previous experimental studies designed to study liquid immiscibility between carbonatites and nephelinites/phonolites at crustal pressures showed that the size of the two liquid field increases with increasing pressure and decreasing temperature (Freestone and Hamilton, 1980; Hamilton et al., 1989), and with increasing alkali content (Brooker, 1995). Lee and Wyllie (1997b) studied the join $NaAlSiO_4$-$NaAlSi_3O_8$-$CaCO_3$ at 1 GPa, and showed that the miscibility gap does not extend to the Na_2O-free side of the tetrahedron.

6.3 - Results

6.3.1: Phase assemblages in the experiments

Back scattered electron images, obtained on a scanning electron microscope, coupled with electron microprobe data have been used to identify the different phases in the experimental charges, and to evaluate their proportions. Assemblages are presented on a separate phase diagram for each pressure (20, 40 and 100 MPa). The extent of the miscibility gap (area where two liquids are present in the experiments) was also studied as a function of P-T-X.

6.3.1.1: Experiments at 20, 40 and 100 MPa

Phase assemblages in experiments at 20 MPa and $700 \leq T \leq 900$ °C are given in Table 6.1, and plotted in Figure 6.2. Phase assemblages in the OL5-experiments have already been discussed in Chapter 3, and will not be discussed again in this chapter; however, results are plotted for the pseudobinary diagram in order to be complete. At 20 MPa, run products typically consist of one or two liquid(s) plus crystals (mainly nepheline, clinopyroxene, wollastonite, melanite garnet, melilite), and a co-existing vapour (fluid) phase. The composition of the fluid phase was not determined but is

thought to be rich in CO_2 and H_2O (see Kjargaard et al., 1995). Note the presence of nyerereite and gregoryite in the OL5-experiments at low temperature, and their absence from the other experiments. Minor crystal phases observed include combeite, perovskite, titanite, apatite, vishnevite, alkali feldspar and spinel. In two liquid assemblages, although silicate crystals are in equilibrium with both liquids, they are rarely found in the carbonate liquid (see Fig. 6.1). Nepheline is present in all the experiments at 20 MPa. The remaining major silicate crystals (melilite, wollastonite, clinopyroxene) and apatite are stable at higher temperature for experiments containing more nephelinite HOL14 in the bulk composition, as shown by the slope of crystal phase boundaries. This feature is not observed for melanite garnet at intermediate bulk composition. Melilite is present in most higher temperature experiments, whereas clinopyroxene is present at lower temperature (over the whole compositional range). Wollastonite is present over a wide T-X range (but not at high temperature/low HOL14 and low temperature). Apatite is mostly present in experiments containing high nephelinite content in the bulk composition (from ~ 700 to > 900 °C), and extends towards high OL5 fraction at low temperature (T ~ 650 °C). This suggests that with increasing carbonate content in the bulk composition, apatite becomes more soluble in the liquid at fixed P-T conditions.

At 40 MPa, only a few experimental charges were prepared (8 experiments in total). The experiments at 40 MPa were prepared mostly to facilitate comparison of two-liquid partitioning of major and trace elements with data from 20 and 100 MPa. Run data and a 40 MPa isobaric phase diagram are presented in Table 6.2 and Figure 6.3, respectively. Phases found in the 40 MPa experiments are similar to those in 20 MPa experiments. However, nyerereite, gregoryite, combeite, perovskite and feldspar are absent, and pyrrhotite is present. The absence of nyerereite and gregoryite is due to no experiments being run with a high carbonate fraction, whereas the absence of combeite is due to a pressure effect (combeite is present at 20 MPa, 700 °C, for a 50/50 bulk composition, but is absent at 40 MPa for similar T-X conditions). The presence of pyrrhotite is due to a pressure effect (pyrrhotite is absent at 20 MPa, 700

°C, for a 90/10 bulk composition, but is present at 40 MPa for similar T-X conditions). As in the 20 MPa-experiments, crystal phases are stable at higher temperature for experiments containing high nephelinite in the bulk composition.

Run data and the phase diagram for 100 MPa are presented in Table 6.3 and Figure 6.4, respectively. Phases found in the 100 MPa experiments are similar to those in the 20 MPa experiments. However, combeite, perovskite and gregoryite are absent, and pyrrhotite is present. It was shown in Chapter 3 that gregoryite is found at 20 MPa, but not at 100 MPa. Similarly, the absence of combeite and perovskite at 100 MPa is thought to be due to a pressure effect, because these two phases are present at 20 MPa for given T-X conditions and absent at 100 MPa at the same T-X conditions. The presence of pyrrhotite is also due to a pressure effect (pyrrhotite is absent at 20 MPa, 800 °C, for a 50/50 bulk composition, but is present at 100 MPa for similar T-X conditions). As in the 20 MPa-experiments, nepheline is present in all of the experiments (except in the HOL14-experiment at 900 °C). The remaining major silicate crystals are stable at higher temperature for experiments containing high nephelinite in the bulk composition.

In summary, for all pressures, the stability field of crystal phases generally shifts towards lower temperatures with increasing natrocarbonatite OL5 in the bulk composition. Moreover, at 100 MPa, crystal phases tend to precipitate at lower temperatures than at 20 MPa. The examination of the phase assemblages also shows that the miscibility gap widens with increasing pressure and that at 100 MPa, it widens with decreasing temperature; whereas, at 20 MPa it shrinks with decreasing temperature.

6.3.1.2: Other experiments

In this section, data are presented for one experiment at 200 MPa, one open-tube experiment and two C/CH_4 buffered experiments.

One sealed-tube experiment (CP109) was made by Dr. Bruce Kjarsgaard at 200 MPa, using an externally heated pressure vessel. This experiment was made at 750 °C, using a mixture containing 80 wt. % wollastonite nephelinite HOL14 and 20 wt.

% natrocarbonatite OL5. The phase assemblage of CP109 is given in Table 6.4. It contains silicate glass and quenched carbonate liquid, nepheline, clinopyroxene, melanite garnet and a vapour phase. Unfortunately, an attempt to prepare equivalent experiments at lower pressures for comparison was unsuccessful. However, a comparison has been made between phase assemblages in experiment CP109 and in experiments prepared at 100 and 40 MPa, 800 and 700 °C, using mixtures of 80 wt. % wollastonite nephelinite HOL14 and 20 wt. % natrocarbonatite OL5. The phase assemblages in the experiments at 100 and 40 MPa are similar to the phase assemblage in experiment CP109, except for wollastonite which is also present at 700 °C. Therefore, pressure decreasing from 200 to 40 MPa does not appear to affect the phase assemblages at these T-X conditions, although wollastonite may be present at 750 °C at 40 and 100 MPa.

One open-tube experiment (CP78) was prepared in order to assess the effect of partial pressure of carbon dioxide (P_{CO2}) on phase assemblages and compositions. This experiment was made at 100 MPa and 800 °C, using a mixture of 90 wt. % wollastonite nephelinite HOL14 and 10 wt. % natrocarbonatite OL5, and will be compared (in the discussion) to experiment CP5, the equivalent sealed-tube experiment.

Two C/CH_4 buffered experiments (CP31 and CP27) were made to assess the effect of oxygen fugacity on phase assemblages and compositions. Experiment CP31 is an C/CH_4 buffered experiment which was run at 100 MPa and 700 °C using a mixture of 90 wt. % wollastonite nephelinite HOL14 and 10 wt. % natrocarbonatite OL5. Its run products include silicate glass, quenched carbonate liquid, nepheline, clinopyroxene, wollastonite, pyrrhotite, apatite, titanite and a vapour phase (see Tab. 6.4). Experiment CP27 was run at 40 MPa and 800 °C, using 90 wt. % wollastonite nephelinite HOL14 and 10 wt. % natrocarbonatite OL5. Its run products are silicate liquid, nepheline, wollastonite, sodalite, apatite and a vapour phase (see Tab. 6.4). Kjarsgaard et al. (1995) suggested that the presence of sodalite and pyrite in the natural rocks (instead of vishnevite in the experiments) was due to lower f_{O2} in the

natural rocks. The comparison between buffered (CP27 and CP31) and unbuffered (CP2 and CP8) experiments shows that more reducing conditions favour the appearance of sodalite and pyrrhotite in place of vishnevite, although sodalite was found only in experiment CP27 and pyrrhotite in experiment CP31.

6.3.2: Major element data of crystals from experiments

Major element compositions of crystals for all experiments are presented in tables for each phase. The major element composition of crystals are plotted separately for HOL14-experiments and for the remaining experiments (*i.e.*, LS-, two liquid- and LC-experiments).

In this chapter, the proportion of the different end-members for nepheline crystals (kalsilite, $Na_2Fe_2Si_2O_8$, nepheline, anorthite, corundum and quartz) is calculated using the method of Peterson (1989a). The proportion of normative nepheline (Ne), quartz (Qz) and kalsilite (Ks) is used to plot the compositions of the nepheline crystals in Ne-Qz-Ks triangular diagrams.

For clinopyroxene, the ferrous/ferric ratios are calculated using the method of Droop (1987). For each clinopyroxene crystal, the structural formula based on 12 oxygens is reported, as well as the normalised proportion of Mg, (Fe^{2+} + Mn) and Na, which is used to plot the composition in diopside-hedenbergite-aegirine (Di-He-Ae) triangular diagrams. Mg #, calculated as $Mg/(Mg+Fe^{2+})x100$ (molecular proportions), is also reported.

For melanite garnet, Fe is arbitrarily recast as Fe^{3+} since recalculation and assignment of cations for Ti-Fe-garnet crystals by charge balance is problematic, since both Fe and Ti occur in two valence states (see Kjarsgaard et al., 1995). For garnet, the structural formula based on 12 oxygens is reported, as well as the normalised proportion of Fe^{3+}, Al and Ti, which is used to plot the composition on Fe^{3+}-Al-Ti triangular diagrams.

The method of Droop (1987) is also used to calculate the ferrous/ferric ratios for wollastonite, titanite and spinel. Note also that to compare the data from this study with

those from previous studies, the compositions reported in other studies have been recalculated following the same methodology used in this study.

6.3.2.1: Major element data for crystals from HOL14-experiments (starting composition = 100/0)

Major element compositions of nepheline in HOL14-experiments are reported in Table 6.5 and plotted in Figure 6.5. Nepheline crystals from the HOL14-experiments show a narrow compositional range ($Ne_{73.4-78.5}$; $Ks_{18.1-22.7}$; $Qz_{2.9-4.3}$). They contain significant amounts of Fe_2O_3 (from 1.9 to 3.2 wt. %). Nepheline crystals in HOL14-experiments analysed for this study have similar compositions as those reported by Kjarsgaard et al. (1995).

The composition of nepheline in HOL14-experiments is temperature dependent. At 20 MPa, over a 200 °C cooling interval (900 - 700 °C), there is an increase in K_2O content (from 5.8 to 7.0 wt. %), with concomitant decrease in Na_2O (from 16.8 to 15.9 wt. %) and CaO (from 0.34 to 0.20 wt. %, and below detection at T < 800 °C). This leads to decreasing nepheline and anorthite components and increasing kalsilite component. Both at 800 and 700 °C, Na_2O (and nepheline component) decreases and K_2O (and kalsilite component) increases with pressure decreasing from 100 to 20 MPa. P-T compositional trends exhibited by nepheline are illustrated in Figure 6.5, *i.e.*, decrease in Ne and increase in Ks components with decreasing pressure and temperature. Figure 6.5 illustrates that the Qz component tends to increase with decreasing temperature, and to decrease with decreasing pressure.

Major element compositions of clinopyroxene in HOL14-experiments are reported in Table 6.6 and plotted in Figure 6.6. Clinopyroxene crystals are mainly of the low-Al, low-Ti diopside-hedenbergite-aegirine variety. They exhibit a very wide range of compositions, from $Di_{64.4}He_{26.2}Ae_{9.5}$ to $Di_{39.4}He_{41.2}Ae_{19.4}$. Kjarsgaard et al. (1995) analysed clinopyroxene in HOL14-experiments at 106 MPa, 750 °C (BK424) and 108 MPa, 700 °C (BK436). Compared to clinopyroxene crystals from this study at 100 MPa, 800 and 700 °C ($Di_{41.7}He_{38.5}Ae_{19.7}$ and $Di_{60.5}He_{27.9}Ae_{11.6}$), that in experiment

BK424 (106 MPa, 750 °C) has a similar composition ($Di_{39.3}He_{35.6}Ae_{25.1}$), whereas, that in BK436 (106 MPa, 750 °C) ($Di_{26.1}He_{32.0}Ae_{41.9}$) is more aegirine rich/diopside poor (see Fig. 6.6). Clinopyroxene compositions in HOL14-experiments do not show any systematic compositional variation with temperature at 100 MPa and 20 MPa (Tab. 6.6; Tab. 6.6). They also do not show any effect of pressure at 900, 800 and 700 °C (Tab. 6.6; Tab. 6.6).

Major element compositions of melanite garnet (Ti-andradite) in HOL14-experiments are reported in Table 6.7 and plotted in Figure 6.7. Melanite garnet crystals in HOL14-experiments show a narrow compositional range from $Fe_{64.0}Al_{3.5}Ti_{32.5}$ to $Fe_{67.9}Al_{2.7}Ti_{29.3}$. Kjarsgaard et al. (1995) analysed melanite garnet in HOL14-experiments at 106 MPa, 750 °C and 108 MPa, 700 °C. Their respective compositions ($Fe_{58.9}Al_{4.5}Ti_{36.6}$ and $Fe_{62.4}Al_{3.7}Ti_{34.0}$) are more Ti-rich than the melanite garnet from this study at 100 MPa, 800 and 700 °C, which have compositions of $Fe_{64.8}Al_{3.7}Ti_{31.5}$ and $Fe_{66.2}Al_{3.6}Ti_{30.1}$. Figure 6.7 illustrates the absence of any systematic compositional variation with P-T of melanite garnet from HOL14-experiments, with pressure and temperature changes, as well as the discrepancy between data from this study and those of Kjarsgaard et al. (1995).

Major element compositions of wollastonite from HOL14-experiments are reported in Table 6.8, as well as the structural formulae calculated for 12 oxygens. They contain fairly high amounts of FeO (FeO_t varies from 1.0 to 1.5 wt. %) and MnO (0.3-0.6 wt. %), and have similar compositions as wollastonite reported by Kjarsgaard et al. (1995). At 900 °C, with pressure decreasing from 100 to 20 MPa, FeO_t increases from 1.0 to 1.5 wt. %, and Fe^{3+}/Fe^{2+} decreases from two thirds of total Fe to zero. At 20 MPa, with temperature decreasing from 900 to 750 °C, iron changes from totally ferrous to totally ferric at 750 °C (for similar FeO_t), and MnO increases from 0.3 to 0.6 wt. %.

Apatite was analysed in one HOL14-experiment (CP38: 100 MPa, 900 °C). Its major element composition is presented in Table 6.9, including SiO_2 (0.37 wt. %), FeO (0.43 wt. %), F (3.6 wt. %) and SrO (1.3 wt. %).

Titanite was analysed in one HOL14-experiment (CP54: 20 MPa, 700 °C). The major element composition is presented in Table 6.10, as well as its formula based on 4 Si cations. The calculation of the formula is approximative because rare earth elements, which enter the large, seven-fold site, have not been taken into account. Moreover, the number of oxygens is not known and has been assumed to be equal to 20. Titanite in experiment CP54 contains Al_2O_3 (0.50 wt. %), FeO (2.0 wt. %), and F (0.30 wt. %). The presence of these minor elements is compatible with the description of titanite by Deer et al. (1992).

Spinel was analysed in two HOL14-experiment at 800 °C (CP74 and CP60, respectively at 100 and 20 MPa). Major element compositions are presented in Table 6.11, as well as structural formulae based on 32 oxygens (see Deer et al., 1992). Spinel crystals from experiments at 100 and 20 MPa contain mostly iron (magnetite end-member), but also minor Al, Ti, Mg and Mn. The presence of these minor elements is compatible with the description of spinel by Deer et al. (1992). These spinel crystals also contain a significant amount of SiO_2, CaO and Na_2O, which suggests inclusions of glass in the spinel or some analytical artifact.

The major element composition of feldspar in HOL14-experiment CP46 (20 MPa, 750 °C) is reported in Table 6.12, as well as its structural formula based on 32 oxygens (see Deer et al., 1992). This alkali feldspar is sanidine containing 10.4 wt. % K_2O and 2.2 wt. % Na_2O. It also contains 1.2 wt. % BaO (= celsian end-member), 0.12 wt. % TiO_2 and 2.7 wt. % FeO_t. Kjarsgaard et al. (1995) analysed feldspar in a two-liquid experiment BK429 (108 MPa, 700 °C) and in an open tube-, HOL14-experiment BK426 (51 MPa, 700 °C) (see Tab. 6.12). Both crystals have compositions similar to the feldspar analysed in experiment CP46, although the feldspar from experiment BK429 contains higher K_2O.

6.3.2.2: Major element data of crystals in experiments on the join HOL14/OL5 at 20, 40 and 100 MPa

Major element analyses of crystals from the experiments prepared on the join HOL14/OL5 are presented together, in order of decreasing pressure, decreasing temperature and decreasing weight fraction of wollastonite nephelinite HOL14 in the starting composition.

Major element compositions of nepheline are reported in Table 6.5 and plotted in Figure 6.8. Nepheline crystals show a fairly narrow compositional range ($Ne_{73.6-78.8}$; $Ks_{18.8-23.7}$; $Qz_{0.5-5.3}$), and they contain significant amounts of Fe_2O_3 (from 1.4 to 2.9 wt. %). Nepheline crystals analysed for this study have similar compositions as those reported by Kjarsgaard et al. (1995) for similar P-T-X conditions. The data reported in Table 6.5 were evaluated to determine if there was compositional variations of nepheline as a function of pressure and temperature. At constant T-X conditions, Na_2O content decreases and K_2O content increases with pressure decreasing from 100 to 20 MPa. Moreover, at constant P-X conditions, Na_2O content decreases and K_2O increases systematically, with temperature decreasing from 900 to 700 °C. Figure 6.8 illustrates the increase in the kalsilite component and the decrease in the nepheline component with decreasing temperature and pressure. Further examination of major element compositions of nepheline in Table 6.5 shows that SiO_2, Al_2O_3, Fe_2O_3 and CaO do not show any systematic variation as a function of pressure or temperature.

Major element compositions of clinopyroxene are reported in Table 6.6 and plotted in Figure 6.9. Clinopyroxene crystals are mainly of the low-Al, low-Ti diopside-hedenbergite-aegirine variety. They exhibit a range of compositions, from $Di_{59.8}He_{27.6}Ae_{12.7}$ to $Di_{31.5}He_{32.9}Ae_{35.6}$. Clinopyroxene crystals analysed by Kjarsgaard et al. (1995) are more aegirine- and hedenbergite-rich/diopside-poor than the clinopyroxene crystals produced in this study at similar conditions (Tab. 6.6; Fig. 6.9). The compositions do not show any systematic variation with temperature at fixed P-X conditions, except for TiO_2 content (and Ti in *M*1 site) which increases and

MnO content (and Mn in the *M*1 site) which decreases with decreasing temperature, at 100 MPa and 40 MPa. There is no systematic compositional variation with pressure at fixed T-X conditions, except for CaO which decreases, and MnO which increases, with decreasing pressure at 700 °C and for various bulk compositions. Figure 6.9 illustrates the scatter of the data and the absence of a compositional trend as a function of pressure and temperature.

Major element compositions of melanite garnet are reported in Table 6.7 and plotted in Figure 6.10. They show a narrow compositional range similar to that found in melanite garnet crystals analysed by Kjarsgaard et al. (1995). Figure 6.10 illustrates the absence of any compositional trend as a function of pressure and temperature. It also illustrates the Al-poor character of melanite garnet analysed by Kjarsgaard et al. (1995) compared to melanite garnet analysed in the present study.

Major element compositions of wollastonite from LS-, two liquid- and LC-experiments are reported in Table 6.8. They contain a fairly high amount of FeO (FeO_t varies from 0.4 to 2.7 wt. %) and MnO (0.3 to 0.8 wt. %), in agreement with the previous study by Kjarsgaard et al. (1995). Wollastonite reported by Kjarsgaard et al. (1995) at 108 MPa, 700 °C has a fairly similar composition to the wollastonite from this study at 100 MPa, 700 °C. Compositions of wollastonite show no systematic variation as a function of pressure and temperature.

Major element compositions of apatite are reported in Table 6.9. La_2O_3 and Ce_2O_3 have been analysed by electron microprobe (WDS) in apatite from 20 MPa-experiments CP42 (850 °C) and CP64 (700 °C). They show respective concentrations of 0.14 and 0.32 wt % for La_2O_3 and below detection and 0.7 wt. % for Ce_2O_3. The limited set of data indicates that with pressure decreasing from 100 to 40 MPa, SiO_2, FeO, CaO, Na_2O, K_2O and Cl increase; whereas, MnO, P_2O_5, F and SrO decrease. Moreover, at 20 MPa, apatite crystals from 90/10-experiments show decreasing SiO_2, FeO and K_2O and increasing CaO, P_2O_5 and F with temperature decreasing from 900 to 850 °C.

Major element compositions of titanite analysed in three two-liquid experiments are presented in Table 6.10. The data set is very limited but shows that titanite from different experiments have similar compositions, and that the main variation is the ferric/ferrous iron ratio.

Spinel was analysed in one LC-experiment (CP81: 20 MPa, 775 °C, 10/90), and in one two-liquid experiment (CP50: 20 MPa, 750 °C, 50/50). Major element compositions are presented in Table 6.11. They contain mostly iron (magnetite end-member), and also minor Al, Ti, Mg, Mn and Ca, like spinel crystals from the HOL14-experiments.

The major element composition of feldspar in two-liquid experiment CP8 (100 MPa, 700 °C, 90/10) is reported in Table 6.12. It is an alkali feldspar (sanidine) containing 14.5 wt. % K_2O and 1.7 wt. % Na_2O, and also 1.7 wt. % BaO (= celsian end-member), 0.07 wt. % TiO_2 and 1.06 wt. % FeO_t. Feldspar analysed by Kjarsgaard et al. (1995) in a two-liquid experiment BK429 (108 MPa, 700 °C) has a very similar composition as feldspar from the two-liquid experiments CP8 (this study) except for higher FeO_t (= 2.8 wt. %).

Major element compositions of melilite are reported in Table 6.13 and plotted in Figure 6.11. With all iron recast as Fe^{2+}, the total number of cations range from 5.02 to 5.11 based on 7 oxygens. The ferrous/ferric ratios calculated using the method of Droop (1987) in order to give a total number of cations of 5 typically leads to 1/3 to 2/3 of the total iron being trivalent iron. Melilite crystals from the 20 MPa-experiments exhibit a range of compositions from $Na_{47.9}Mg_{26.1}Fe_{25.9}$ to $Na_{49.7}Mg_{16.9}Fe_{33.4}$. Pressure and temperature do not have any systematic effect on the major element composition of melilite from LS-, two liquid- and LC-experiments.

Major element compositions of combeite in two liquid- and LC-experiments are reported in Table 6.14. They contain significant amounts of FeO_t (0.5 to 1.2 wt. %), MnO (0.5 to 0.7 wt. %) and MgO (0.07 to 0.30 wt. %). At 20 MPa, for 40/60 and for 30/70 bulk compositions, FeO_t and MnO increase, whereas Na_2O decreases with temperature decreasing from 800 to 750 °C. Both at 20 MPa, 800 °C and 20 MPa, 750

°C, SiO_2, MnO, MgO, CaO increase, whereas, FeO decreases with increasing proportion of natrocarbonatite in the starting composition from 60 to 70 wt. %, although the compositional changes are very small. Note that experiments with 60 wt. % natrocarbonatite in the bulk composition are in the two-liquid field, and those with 70 wt. % natrocarbonatite in the bulk composition contain only carbonate liquid. By comparison, combeite analysed by Kjarsgaard et al. (1995) in open-tube experiments contain more FeO_t (~ 1.9 wt. %) and Na_2O (~ 22 wt. %), and less CaO (~ 25 wt. %).

The major element compositions of vishnevite in LS- and two-liquid-experiments are reported in Table 6.15. Vishnevite crystals contain between 0.8 to 2.8 wt. % Cl and between 3 to 6 wt. % SO_3. The relative abundance of these elements is consistent with data from Kjarsgaard et al. (1995) which indicate S >> Cl. H_2O was not analysed but can have concentrations > 10 wt. % (Deer et al., 1992), hence the low totals. Vishnevite in experiment CP8 (103 MPa, 700 °C, 90/10) can be compared to vishnevite in experiment BK429 (108 MPa, 700 °C) of Kjarsgaard et al. (1995), which contains more Fe_2O_3 (3.4 vs. 1.2 wt. %) and CaO (1.3 vs. 0.7 wt. %), and less Na_2O (17.2 vs. 20.9 wt. %) and K_2O (1.6 vs. 2.9 wt. %). With decreasing temperature, CaO and SO_3 decrease, whereas Fe_2O_3, Na_2O and K_2O increase. Experiments prepared at 900 °C using a 90/10 bulk composition show that with pressure decreasing from 100 to 20 MPa, there is little compositional variation.

6.3.2.3: Major element data of crystals from 200 MPa-experiment CP109

The major element composition of nepheline in experiment CP109 (750 °C) is reported in Table 6.5 and plotted in Figure 6.8. The composition of the nepheline from experiment CP109 is $Ne_{78.0}Ks_{18.0}Qz_{4.0}$, *i.e.*, it contains higher Ne and lower Ks than nepheline from two-liquid experiments at lower pressure, in agreement with the compositional trends exhibited by nepheline with increasing pressure. Moreover, it contains 3.1 wt. % Fe_2O_3, which is more than in nepheline from any other two-liquid experiments at lower pressure.

The major element composition of clinopyroxene in 200 MPa-experiment CP109 is reported in Table 6.6 and plotted in Figure 6.9. Its composition ($Di_{52.1}He_{31.5}Ae_{16.4}$) is within the compositional range of clinopyroxene in the two-liquid experiments at lower pressure (which do not show any systematic compositional variation as a function of pressure).

The major element composition of melanite garnet in 200 MPa-experiment CP109 is reported in Table 6.7 and plotted in Figure 6.10. Its composition ($Fe_{65.1}Al_{3.3}Ti_{31.6}$) is within the compositional range of melanite garnet crystals in the two-liquid experiments at lower pressure (which do not show any systematic compositional variation as a function of pressure).

6.3.2.4: Major element data of crystals from C/CH$_4$ buffered-experiments

Experiments CP31 (100 MPa, 700 °C, bulk composition 90/10) and CP27 (40 MPa, 800 °C, bulk composition 90/10) are the C/CH_4 buffered runs with equivalent bulk compositions to experiments CP8 and CP2. The major element compositions of nepheline in experiments CP31 and CP27 are reported in Table 6.5. The compositions of the nepheline from the C/CH_4 buffered experiments, plotted on a Ne-Qz-Ks ternary diagram (Fig. 6.8), plot close to those of the nepheline from unbuffered experiments run at the same conditions. The compositional changes with decreasing f_{O2} are indicated by an arrow on the plots, from CP8 to CP31 at 100 MPa, and from CP2 to CP27 at 40 MPa. Nepheline crystals in C/CH_4 buffered experiments contain less Fe_2O_3 and more K_2O than those produced in unbuffered runs.

The major element composition of clinopyroxene from experiment CP31 is reported in Table 6.6, as well as its structural formula and the proportions of Mg, (Fe^{2+} + Mn) and Na. Compared to clinopyroxene in the unbuffered experiment, clinopyroxene in CP31 has a significantly different composition (less TiO_2, Al_2O_3, MgO and CaO; more total iron, MnO and Na_2O). The composition of the clinopyroxene from CP31 ($Di_{40.3}He_{39.1}Ae_{19.6}$) is plotted on the ternary Di-He-Ae diagram (Fig. 6.9). It is more hedenbergite/aegirine-rich, and diopside-poor than the clinopyroxene from CP8 ($Di_{52.4}He_{31.8}Ae_{15.8}$). However, because of the scatter

observed in the composition of clinopyroxene from the unbuffered experiments, the compositional differences between clinopyroxene in buffered experiment CP31 and in its buffered equivalent CP8, may not be real.

Compositions of wollastonite from experiments CP31 and CP27 are reported in Table 6.8. These wollastonite crystals contain a fairly high amount of FeO_t (~ 1 wt. %) and MnO (~ 0.5 wt. %), similar to wollastonite crystals from the sealed-tube experiments. Wollastonite crystals from buffered experiments have lower Na_2O and K_2O than their equivalent in unbuffered experiments.

Data for apatite from experiments CP31 and CP27 are reported in Table 6.9. There is no apatite in the unbuffered experiments for comparison. These apatite crystals contain significant amounts of F (~ 2.5 wt. %) and SrO (~ 1.2 wt. %). They also contain SiO_2 (~ 0.7 wt. %) and Na_2O (~ 0.2 wt. %), like other apatite crystals described in LS-experiments (this chapter) and in OL5-experiments (Chapter 3).

The composition of sodalite in experiment CP27 is reported in Table 6.15. It contains 6 wt. % Cl and 1 wt. % SO_3, and a low amount of F (0.05 wt. %). Note that sodalite does not precipitate in equivalent unbuffered experiments. Compared to sodalite in combeite nephelinite HOL6 analysed by Peterson (1989a), it has less Fe_2O_3 (0.8 vs. 3.5 wt. %) and more K_2O (3.4 vs. 2.1 wt. %).

The major element composition of pyrrhotite from experiment CP31 is reported in Table 6.16, with FeO and SO_3 recalculated to Fe and S. Pyrrhotite is fairly pure. The minor element which is in the highest abundance is TiO_2 (= 0.12 wt. %).

6.3.2.5: Major element data of crystals from open-tube experiment CP78

The major element composition of nepheline in CP78 is reported in Table 6.5. Nepheline from experiment CP78 ($Ne_{73.1}Ks_{25.8}Qz_{1.1}$) is significantly enriched in kalsilite and depleted in nepheline components compared to nepheline from equivalent sealed-tube experiment CP5 ($Ne_{79.1}Ks_{20.3}Qz_{0.6}$), as illustrated in Figure 6.8. The kalsilite-rich character of nepheline in open- compared to sealed-tube experiments was also shown by Kjarsgaard et al. (1995).

Data for clinopyroxene in experiment CP78 are reported in Table 6.6 and plotted in Figure 6.9. It is more enriched in hedenbergite and depleted in diopside and aegirine components than clinopyroxene in equivalent sealed-tube experiment CP5 ($Di_{39.0}He_{40.7}Ae_{20.3}$ versus $Di_{52.7}He_{13.2}Ae_{34.1}$). However, note that clinopyroxene generally shows a very wide range of compositions, and that Kjarsgaard et al. (1995) reported clinopyroxene crystals in open-tube experiments richer in a diopside component compared to those in sealed-tube experiments.

Combeite in open-tube experiment CP78 is reported in Table 6.14. It contains a significant amount of FeO_t (1.6 wt. %), MnO (0.35 wt. %) and MgO (0.3 wt. %). There is no combeite in the equivalent sealed-tube experiment for comparison.

Major element composition of pyrrhotite in open-tube experiment CP78 is reported in Table 6.16. It contains 65.6 wt. % Fe and 34.4 wt. % S.

6.3.3: Major element composition of liquids from experiments

Major element data as determined by electron microprobe for silicate and carbonate liquids from the experiments are presented in Table 6.17, along with Mg #, peralkalinity (Na+K)/Al for silicate liquid, and distribution coefficients between silicate and carbonate liquids. Mg # represents $Mg/(Mg+Fe_{total})$ (molecular proportion), with all iron expressed as Fe^{2+} for both liquids. Composition of the liquids from HOL14- and two-liquid experiments are plotted in triangular diagrams $MO\text{-}M_2O\text{-}MO_2+M_2O_3$ (Hamilton plots), where MO represents CaO+MgO+FeO+MnO, M_2O represents Na_2O+K_2O and $MO_2+M_2O_3$ represents $SiO_2+TiO_2+Al_2O_3$. Note that in Table 6.17, data for all liquids measured are presented, but that compositions for liquids in LS- and LC-experiments will not be plotted because they are not used to determine the P-T-X conditions of formation of natural lavas from Oldoinyo Lengai.

6.3.3.1: Major element composition of silicate liquid in HOL14-experiments

The silicate liquids range from nephelinitic to phonolitic and are similar to those reported by Kjarsgaard et al. (1995). They are peralkaline, with molar (Na+K)/Al ranging from 1.1 to 1.9 and have low Mg # (0.05 to 0.17). These findings are

consistent with those from natural lavas at Oldoinyo Lengai. According to Peterson and Kjarsgaard (1995), there are only 5 lavas at Oldoinyo Lengai with Mg # > 0.25, and the most evolved silicate lavas at Oldoinyo Lengai, with molar (Na+K)/Al > 7 in the glass, are the most peralkaline known. Low analytical totals are due to the fact that CO_2 and H_2O have not been analysed. CO_2 and H_2O contents in natural nephelinites can be quite high, as shown by Dawson et al. (1985) who reported a CO_2 content of 2.4 wt. % and H_2O content of 2.3 wt. % in natural wollastonite nephelinite BD66.

At 100 MPa and 20 MPa, with temperature decreasing from 900 to 800 °C, SiO_2 and K_2O increase and CaO, Na_2O and Mg # decrease in silicate liquid from HOL14-experiments. With temperature decreasing from 900 to 800 °C, peralkalinity (Na+K)/Al decreases from 1.6 to 1.1 at 100 MPa, but stays constant (1.7-1.8) at 20 MPa. At 900 and 800 °C, with pressure decreasing from 100 to 20 MPa, Al_2O_3 content and Mg # decrease, whereas FeO, MnO, Na_2O, K_2O, F, Cl, and peralkalinity (Na+K)/Al increase.

The compositions of the silicate liquid in HOL14-experiments are plotted on a Hamilton triangular diagram (Fig. 6.12). The tendency for $SiO_2 + TiO_2 + Al_2O_3$ to increase with decreasing temperature is illustrated on the plot.

6.3.3.2: Major element composition of carbonate and silicate liquids in LS-, two liquid-, and LC-experiments

There is no systematic effect of decreasing temperature on major element compositions of silicate and carbonate liquids from LS- and two-liquid-experiments (Tab. 6.17). The effect of decreasing pressure on major element compositions of silicate and carbonate liquids is more significant, including a tendency for Al_2O_3 to decrease, and for FeO, MnO, P_2O_5, F, BaO and (Na+K)/Al to increase (some exceptions) in the silicate liquid, and for CaO to decrease, and for Na_2O, K_2O, Cl, SO_3 and BaO to increase in carbonate liquid.

Note that the measured CaO concentration of silicate liquid in experiment CP102 (100 MPa, 800 °C, 80/20) is thought to be significantly low, by comparison with the CaO concentration of silicate liquid in experiments prepared at the same P-T conditions, with different bulk compositions (CP5 and CP13; see Tab. 6.17). For later calculations, it is assumed that the concentration of CaO in the silicate liquid of experiment CP102 is equal to 4.7 wt. %, *i.e.* twice the measured value.

Composition of coexisting silicate and carbonate liquids in two-liquid experiments are plotted on a Hamilton diagram (Fig. 6.13), with different symbols for different pressures, and for three different ranges of temperature ($T > 800$ °C, 700 °C $< T \leq 800$ °C, $T < 700$ °C). With decreasing temperature, $SiO_2 + TiO_2 + Al_2O_3$ tends to increase, and $Na_2O + K_2O$ and $CaO + MgO + FeO + MnO$ tend to decrease in the silicate liquid, although the effect is not significant for some P-X conditions. The effect of decreasing temperature on carbonate liquid from two-liquid experiments is not consistent between different P-X conditions. When there is a compositional variation with decreasing temperature, it is due to a $CaO + MgO + FeO + MnO$ decrease/$Na_2O + K_2O$ increase, or even to a $SiO_2 + TiO_2 + Al_2O_3$ increase (see Fig. 6.13).

Figure 6.13 also illustrates the effect of decreasing pressure from 100 to 20 MPa, *i.e.*, $SiO_2 + TiO_2 + Al_2O_3$ decrease in the silicate liquid, and $CaO + MgO + FeO + MnO$ decrease and $Na_2O + K_2O$ increase in the carbonate liquid. The effect of pressure on liquid compositions is more significant and consistent than the effect of temperature.

Symbols on Figure 6.13 are the same for experiments prepared with different bulk compositions. The bulk compositions are not labelled beside the symbols in order not to overload the plot, and because upon examination of the possible effect of bulk composition on the composition of the liquids, there does not appear to be a consistent effect on the major element composition of carbonate and silicate liquid from the two-liquid experiments.

Compositions of silicate and carbonate liquids from two-liquid experiments at 100 MPa, for a 50/50 bulk composition are plotted on a Hamilton plot (Fig. 6.14) in order to illustrate the effect of temperature on liquid composition. Compositions of silicate and carbonate liquids from two-liquid experiments at 900 °C, for 50/50 bulk composition are plotted on a Hamilton plot (Fig. 6.15) in order to illustrate the effect of pressure on liquid composition.

Tie lines drawn on Figures 6.14 and 6.15 join coexisting silicate and carbonate liquids from the same experiments. At 100 MPa, with decreasing temperature, the composition of carbonate liquid evolves towards high Na_2O + K_2O/low CaO + MgO + FeO + MnO, and that of silicate liquid towards high SiO_2 + TiO_2 + Al_2O_3. The combination of the compositional variations on carbonate and silicate liquids produced by decreasing temperature leads to counter-clockwise rotation of the tie-lines, although it is not very pronounced (Fig. 6.14). Figure 6.15 illustrates that with decreasing pressure the composition of carbonate liquid evolves towards high Na_2O + K_2O/low CaO + MgO + FeO + MnO, and that of silicate liquid towards low SiO_2 + TiO_2 + Al_2O_3. This combination of compositional variations leads to counter-clockwise rotation of the tie-lines. In summary, pressure is the parameter that has a more enhanced and consistent effect on coexisting silicate and carbonate liquids compared to temperature.

Distribution coefficients between silicate and carbonate liquids are reported in Table 6.17. SiO_2, TiO_2, Al_2O_3, FeO and MnO partition preferentially into silicate liquid, whereas CaO, Na_2O, P_2O_5, F, Cl, SO_3, BaO and SrO partition into the carbonate liquid. K_2O partitions into the silicate liquid at 100 MPa and into the carbonate liquid at 20 MPa. The partitioning of MgO is variable. These observations are consistent with those made by Kjarsgaard et al. (1995).

The effects of decreasing temperature on distribution coefficients between silicate and carbonate liquid are: K_2O increases at 100 and 40 MPa (less clear at 20 MPa), Na_2O tends to decrease at all pressures, CaO decreases at all pressures, MnO decreases at 100 MPa, and MgO, F, Cl decrease at 100 and 40 MPa (see Fig. 6.16).

The effects of decreasing pressure on distribution coefficients between silicate and carbonate liquid are: SiO_2 tends to decrease at 900 °C; K_2O and Cl decrease; and FeO, MnO, MgO, CaO, P_2O_5 increase (see Fig. 6.17).

6.3.3.3: Major element composition of carbonate and silicate liquid in other experiments

Data for the 200 MPa-experiment CP109 are reported in Table 6.17. The silicate liquid has a phonolitic composition, is peralkaline (with a molar (Na+K)/Al value of 1.7) and a Mg # of 0.05. The carbonate liquid has a Mg # of 0.26. The compositions of the silicate and carbonate liquid have been plotted on a Hamilton plot (Fig. 6.13), along with those from two-liquid experiments at lower pressure. The silicate liquid has $SiO_2 + TiO_2 + Al_2O_3$ equal to 70.8, $Na_2O + K_2O$ to 19.5 and CaO + MgO + FeO + MnO to 9.7. Its high $SiO_2 + TiO_2 + Al_2O_3$ value compared to that in lower pressure experiments is in agreement with the compositional trends observed with increasing pressure for the composition of the silicate liquid.

The composition of silicate liquid from buffered experiments CP31 and CP27 is reported in Table 6.17. The silicate liquids are of nephelinitic composition and are peralkaline, with molar (Na+K)/Al of > 2.6 and Mg # ≤ 0.24. Although no carbonate liquid has been analysed in these two experiments, the compositions of the silicate liquids are plotted on a Hamilton plot along with silicate liquids in equivalent unbuffered experiments (Fig. 6.18). For CP31, $SiO_2 + TiO_2 + Al_2O_3$ is equal to 66.9, $Na_2O + K_2O$ is equal to 21.2 and CaO + MgO + FeO + MnO is equal to 11.9. Unfortunately, silicate liquid in CP8 could not be analysed for comparison. Compared to silicate liquid from unbuffered experiment CP2, silicate liquid from buffered experiment CP27 contains less FeO and K_2O, and more TiO_2, MgO, CaO and Na_2O. On the Hamilton plot, silicate liquid from experiment CP27 ($SiO_2 + TiO_2 + Al_2O_3$ = 62.3; $Na_2O + K_2O$ = 21.8; CaO + MgO + FeO + MnO = 16.0) plots very close to that in the equivalent unbuffered experiment CP2 (Fig. 6.18).

The major element composition of the silicate liquid from open tube-experiment CP78 is reported in Table 6.17, as well as its peralkalinity (5.03) and Mg

(0.15). This silicate liquid is characterised by higher peralkalinity than that of any silicate liquid in experiments at 100 MPa, and its total of 100 wt. % indicates the absence of CO_2 and H_2O in its composition. Compared to experiment CP5 (equivalent sealed-tube experiment), the silicate liquid in experiment CP78 has higher peralkalinity (5.03 versus 2.32), less CO_2 + H_2O (total of 100 versus 90.6 wt. %), and higher Mg # (0.15 versus 0.11). It also has higher concentrations of all of the oxides, except for lower Al_2O_3 (5.4 versus 10.6 wt. %). Its composition has been plotted on a Hamilton plot (Fig. 6.18) where it has a slightly lower SiO_2 + TiO_2 + Al_2O_3 (57.1 versus 63.7) and higher CaO + MgO + FeO + MnO (23.2 versus 16.7) than silicate liquid in equivalent sealed-tube experiment CP5. Silicate liquid from both experiments plot at similar Na_2O + K_2O values, which are equal to 19.7.

6.4 - Discussion

6.4.1: Structure of silicate and carbonate liquids

Before discussing the results of this study, a brief review of the structure of silicate and carbonate melts is presented. Previous studies (Hamilton et al., 1989; Brooker, 1995; Jones et al., 1995) outlined the importance of the structure of the silicate melt in controlling distribution of major elements (and partitioning of trace elements) between silicate and carbonate liquids.

6.4.1.1: Structure of silicate liquid

The structure of silicate melts has been summarised by Brooker (1995). The basic building block of silicate melts is the SiO_4 tetrahedron, in which four oxygens are equally spaced around the Si atom and held in position by relatively strong (covalent) bonds. If SiO_4 tetrahedra (charge = 4-) are isolated, as in olivine or carbonate melt, they need a charge balance of 4+, which can be provided by $2Ca^{2+}$ or $4Na^{+}$. The alkali and alkaline earth cations are too large to accommodate a tetrahedral oxygen arrangement and therefore sit in polyhedra of higher coordination, sharing the oxygens of several SiO_4 tetrahedra. If the concentration of SiO_2 is high, then

tetrahedra can link together by sharing oxygens between the tetrahedra. As the concentration of these bridging oxygens increases, the structure is said to polymerise. Polymerisation or interconnectivity of the melt network can also be considered as a function of the amount of metal cations present which break up or modify the network. As these cations coordinate the oxygens of SiO_4 tetrahedra, these oxygens are no longer available for bridging between tetrahedra and are referred to as non-bridging oxygens.

Si^{4+} and the elements that replace it in the tetrahedral site, such as Al^{3+}, are called network formers. Replacement of Si^{4+} by Al^{3+} is accompanied by charge balancing (*e.g.* by Na^{+}). The addition of further cations in excess of that required to charge balance, breaks up the polymerised structure by coordinating with some of the tetrahedral oxygens, and these cations are referred to as network modifiers. Some individual ions, usually with intermediate field strength, such as P^{5+}, Ti^{4+}, Al^{3+}, Fe^{3+} and Fe^{2+} cannot be classified simply as network-formers or network-modifiers (Wilding, 1998), and have a dual role (Brooker, 1995).

The term bridging oxygen per silicon, or more generally, bridging oxygen per tetrahedrally coordinated cation (where the tetrahedrally coordinated cation could also be the charge deficient tetrahedral components Al^{3+}, Fe^{3+}, Fe^{2+}, Ti^{4+} and P^{5+}) is a general term that describes the degree of polymerisation of the silicate melt. Kohn and Schofield (1994) showed that although this parameter cannot account for all of the subtleties of melt structure, it seems to be the best simple approximation.

6.4.1.2: Structure of carbonate liquid

Treiman (1989) presented an overview of the structure of carbonatite magmas. He showed that carbonatite magmas are ionic liquids, composed of individual ions bound without covalency, and that this accounts for their very low viscosity. Genge et al. (1995) reported additional information on carbonate melt structure by studying carbonate glasses in the system K_2CO_3-$MgCO_3$. Although this system is not relevant to natural lavas, it is suitable for a study of carbonate liquid structure because in this system, carbonate glasses can quench from melt. To paraphrase Genge et al. (1995),

carbonate glasses cannot form network structures *sensus stricto*. Rather the structure in the carbonate glass is a "flexible" framework made by the "bridging" of carbonate ions by strongly interacting metal cations. This flexible framework is supported by framework modifying cations and molecular groups. In their model, bridging species are those which link the framework structure together; whereas, non-bridging species are those not directly involved in the framework structure and exist due to charge-balancing requirements of framework modifying species. Elements described as framework formers are C and O (form carbonate groups), and Ca^{2+}, Mg^{2+} and Sr^{2+} that interact strongly with the carbonate group. Framework modifiers are those species which have only weak interaction with CO_3^{2-}, such as the alkalis, and molecular groups such as metal hydrate/hydroxyl complexes.

6.4.2: Effect of parameters on phases in experiments

6.4.2.1: Effect of different parameters on the miscibility gap

The miscibility gap is represented by the grey shaded regions on Figures 6.2, 6.3 and 6.4 (20, 40 and 100 MPa, respectively), and this gap widens with increasing pressure. At 20 and 100 MPa (and by analogy at 40 MPa), the miscibility gap shrinks with decreasing temperature on the carbonate liquid side (right limb), but its size increases with decreasing temperature on the silicate liquid side (left limb). At 20 MPa, the miscibility field is thought to close at 650 °C < T < 700 °C, by extrapolation of the limbs at T ≤ 700 °C. At 100 MPa, the miscibility gap slightly decreases in width with decreasing temperature, but it is still wide at T = 680 °C. The slopes of the limbs are very steep at 100 MPa because the temperatures at which these experiments were made are significantly lower than the high temperature consolute point, and significantly higher than the low temperature consolute point (*i.e.*, the solvus closes at high and at low temperature). At 20 MPa, the right limb is significantly shallower than at 100 MPa because the temperature is close to the low temperature consolute point. The results of this study are compatible with the observations of Freestone and Hamilton (1980) and Hamilton et al. (1989) that between 70 MPa and 760 MPa, and

900 and 1250 °C, the size of the miscibility gap increases with increasing pressure. The decreasing size of the miscibility gap with decreasing temperature at 20 MPa has not been previously observed, but occurs because of the lower temperatures used in this study, *i.e.* the closeness to the low temperature consolute point.

The study of Koster van Groos and Wyllie (1966) illustrated a radical decrease in the size of the two-liquid field at very low pressures (between 33 and 7 MPa) at 900 °C. However, the results of this study show that the left limb of the miscibility gap is only slightly affected by decreasing pressure between 100 and 20 MPa, and that at 20 MPa is still at fairly high SiO_2 + TiO_2 + Al_2O_3 values, therefore liquid immiscibility may still occur at 20 MPa.

Kjarsgaard et al. (1995) showed that understanding the liquid immiscibility process lies in comprehending the relationship between P_{total}, CO_2 saturation and the one liquid/two liquid field boundary (see Fig. 6.19, from Kjarsgaard et al., 1995). Koster van Groos and Wyllie (1966) illustrated that a stable two-liquid field depends on whether the vapour saturated liquidus surface intersects the two-liquid region. They suggested that variation in CO_2 saturation level of a liquid is controlled by a series of pressure dependent decarbonation reactions, with increase of CO_2 saturation level at higher pressure. Moreover, CO_2 solubility in silicate liquid has been shown to be pressure dependent, with solubility increasing at higher pressures (Brooker, 1995, 1998). With increasing pressure, CO_2 solubility increases and the vapour-saturated liquid moves up in CO_2 space. The net observed effect is that with higher pressure, the silicate/carbonate two liquid field increases in width. Brooker (1995) also showed that CO_2 solubility in silicate liquid increases with decreasing temperature. The opposite effect of temperature and pressure on CO_2 solubility in silicate liquid could account, at least partially, for the opposite effect of temperature and pressure on the size of the miscibility gap (on the left limb).

For the present study, CO_2 + H_2O saturation is thought to have been achieved in all the runs because an excess fluid phase was usually noticed (loss of weight and hissing when opening the capsule). The fact that volatile saturation is achieved does

not necessarily indicate that CO_2 saturation is achieved; however, CO_2 saturation is believed to have been achieved in the experiments of this study because of the low pressure at which they were prepared. This is important since CO_2 saturation is required to maximise the immiscibility gap for a given P, T and X (Brooker, 1995, 1998). Brooker (1995) showed that the CO_2 concentration at which silicate liquids reach saturation is an important parameter in producing liquid immiscibility, and that it appears to be an inverse function of the SiO_2+Al_2O_3 content of the melt, and a direct function of its NBO/T (non-bridging oxygens per tetrahedra) value. Because in the present study the probe shortfall represents CO_2 + H_2O, it was not possible to examine the trend of CO_2 as a function of SiO_2+Al_2O_3 and as a function of NBO/T.

Brooker (1995) described how the CO_2 saturation of the silicate melt and, therefore, the liquid immiscibility process, can be explained as a function of the polymerisation of the silicate melt. He showed that molecular CO_2 is not stable in silicate melt, and that carbonates are formed by attracting cations and non-bridging oxygens to form carbonate groups that are attached covalently to tetrahedra by bridging oxygens. He also showed that for most compositions, increasing the network modifying cations in the melt (as indicated by higher values of NBO/T) increases CO_2 solubility, up to some point where a carbonate melt unmixes. In order to expel the cations and carbonate to a separate phase, the carbonate bridging oxygen is replaced with an oxygen from another tetrahedron; the carbonate becomes ionic, the silicate network polymerises and the SiO_2+Al_2O_3 of the silicate melt is increased. Brooker (1995) showed that the structure of the silicate melt is more unstable with alkalis than with Ca, which explains why liquid immiscibility is favoured in alkali-rich systems. He summarised the immiscibility process by the following reaction path, where "f" stands for fluid phase and "m" for melt:

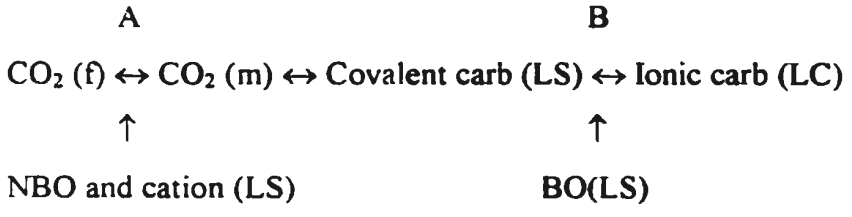

In conclusion, liquid immiscibility is controlled by CO_2 saturation of the silicate liquid. CO_2 solubility in the silicate liquid (therefore liquid immiscibility) is dependent on pressure, on temperature, and also on the degree of polymerisation of the silicate liquid (which itself is pressure and temperature dependent).

6.4.2.2: Effect of PCO_2

One open-tube experiment (CP78) was prepared in order to assess the effect of carbon dioxide partial pressure (P_{CO2}) on phase assemblages and compositions. This experiment at 100 MPa and 800 °C, prepared with a mixture of 90 wt. % wollastonite nephelinite HOL14 and 10 wt. % natrocarbonatite OL5, can be compared to experiment CP5, an equivalent sealed-tube experiment at the same P-T-X conditions. Experiment CP78 contains (minor) silicate glass, nepheline, clinopyroxene, combeite, pyrrhotite and vapour phase (see also Tab. 6.4), whereas experiment CP5 contains silicate glass, quenched carbonate liquid, nepheline, clinopyroxene, melanite garnet, wollastonite, pyrrhotite, apatite and vapour phase (see also Tab 6.3).

The partial pressure of CO_2 is zero or extremely low in open-tube (CP78) as compared to sealed-tube (CP5) experiments. The comparison of phase assemblages between the two experiments shows that carbonate liquid, melanite garnet, wollastonite and apatite are not stable at low P_{CO2}: whereas, combeite ($Na_2Ca_2Si_3O_9$) is stabilised. Lower P_{CO2} in open-tube experiment CP78 explains the absence of carbonate liquid. The lowering of P_{CO2} shrinks the miscibility gap, and carbonate liquid is not exsolved. Kjarsgaard et al. (1995) suggested two reactions to explain these differences:

$(4)NaAlSiO_{4(s)} + (2)(Na,K,Ca) - CO_{3(\text{sil melt complexes})} + (4)SiO_{2(\text{sil melt})}$

$\rightarrow (4)(Na,K)AlSiO_{4(s)} + Na_2Ca_2Si_3O_{9(s)} + CO_{2(f)}.$

$(2)NaAlSiO_{4(s)} + (Na,K,Ca) - CO_{3(\text{sil melt complexes})} + (2)SiO_{2(\text{sil melt})} + CaSiO_{3(s)}$

$\rightarrow (2)(Na,K)AlSiO_{4(s)} + Na_2Ca_2Si_3O_{9(s)} + CO_{2(f)}.$

According to Kjarsgaard et al. (1995), these potential reactions are consistent with decreased solubility of CO_2 in the melt, the appearance of combeite as a solid phase, the increased kalsilite component of nepheline and lower SiO_2 plus higher peralkalinity in the remaining silicate liquid. Most of these features are observed in the open-tube experiment CP78 of this study, *i.e.*, disappearance of wollastonite, increased kalsilite component of nepheline (Ks = 25.8 instead of 20.3), higher peralkalinity in the remaining silicate liquid (5.03 instead of 2.32), as well as decreased solubility of CO_2 in the melt indicated by the lower volatile content of silicate liquid in experiment CP5 (total = 100 vs. 89.6 wt. %). Lower SiO_2 content was not observed, as the SiO_2 content of the silicate liquid in CP78 (46.3 wt. %) is higher than in CP5 (43.1 wt. %). Kjarsgaard et al. (1995) also suggested that the peralkalinity of silicate liquid had to be > 4.28 for combeite to appear, and the peralkalinity of 5.0 of the silicate liquid in CP78 is consistent with this observation.

The phase assemblages in closed-tube experiments are more similar to natural lavas (*i.e.*, silicate-bearing natrocarbonatite OL5 and wollastonite nephelinite HOL14) than those in open-tube experiments. Open-tube experiment CP78 is not a good analogue to natural lavas, since low P_{CO2} prevents the formation of two conjugate liquids.

6.4.2.3: Effect of different parameters on combeite stability and composition

In the present study, combeite has been observed in two cases: in open-tube experiment CP78, and in sealed-tube experiments CP122, CP124, CP125, CP16 and CP65, at 20 MPa, at 700 °C ≤ T ≤ 800 °C and 50 wt. % ≤ X_{LC} ≤ 70 wt. %, where X_{LC} represents the weight fraction of silicate-bearing natrocarbonatite OL5 in the bulk starting composition. These latter experiments will be called sealed-tube, combeite-experiments, as opposed to experiments CP78 and experiments BK426, BK432, BK417 and BK423 (Kjarsgaard et al., 1995), which are open-tube, combeite-experiments. Kjarsgaard et al. (1995) previously suggested that: 1) wollastonite and combeite are not a stable phase assemblage, and that 2) two liquids + combeite is not a stable phase assemblage. This is not what is observed in sealed tube-, combeite-

experiments, where combeite is associated with wollastonite, carbonate liquid and, for experiments CP122 and CP124, with silicate liquid. The different run conditions (*i.e.*, different carbonate content in the bulk composition) can explain the difference. As quoted from Kjarsgaard et al. (1995), "It is suggested that combeite and natrocarbonatite are an incompatible phase assemblage, although one could argue that these two phases are compatible at P-T conditions not studied here. In this respect, note that Dawson et al. (1989) attributed the formation of combeite to the mixing of nephelinite and natrocarbonatite magma in the ash cloud during eruption."

In natural lavas, combeite occurs in two different environments: as euhedral crystals in combeite nephelinite (*e.g.* HOL10, see Table 6.14, data from Peterson, 1989a), and in coronas replacing wollastonite and clinopyroxene in silicate-bearing natrocarbonatites from the 1966 eruption, which have been interpreted as a product of mixing between natrocarbonatite and silicate magmas.

A comparison of the major element composition of combeite from the natural lavas with those from the experiments has been made to determine if the two types of combeite in the natural lavas are equivalent to the two types of combeite in the experiments (sealed tube- versus open tube-experiments). Data in Table 6.14 show that combeite from sealed tube-experiments contain less FeO (0.5 to 1.2 wt. %) compared to combeite in open tube-experiments CP78 (this study) and BK432 and BK417 (Kjarsgaard et al., 1995) (1.6 to 2.1 wt. %). Euhedral combeite from HOL10 has FeO (= 1.4 wt. %), CaO (= 25.2 wt. %) and Na_2O (= 21.5 wt. %) comparable to combeite in open tube-experiments, whereas combeite crystals in coronas in silicate-bearing natrocarbonatites from the 1966 eruption have lower FeO (= 0.3 and 0.4 wt. %), higher CaO (= 27.2 and 28.2 wt. %) and lower Na_2O (= 20.6 and 20.7 wt. %), more comparable to combeite in sealed tube-experiments.

In conclusion, combeite forms in two different environments: at low P_{CO2} in peralkaline nephelinite, and at 20 MPa, 700 °C $\leq$ T $\leq$ 800 °C and high carbonate fraction, like for example in the case of mixing (1966 natrocarbonatite lavas). When it forms in nephelinite at low P_{CO2}, it contains higher FeO and Na_2O, and lower CaO

than when it forms in replacement of wollastonite or clinopyroxene in natrocarbonatite mixing with silicate magma. The relatively low peralkalinity of the silicate liquid in CP122 and CP124 (2.14 and 2.18) shows that silicate liquid does not need to be extremely peralkaline in this case. Note also that Veksler et al. (1998b) found combeite in silicate liquid in two liquid experiment at 965 °C and they interpreted this crystal as being a liquidus phase. Note also that they observed combeite in the SiO_2-Al_2O_3-CaO-Na_2O-CO_2 system, but not in the system containing additional MgO, K_2O and P_2O_5 in the starting composition.

6.4.2.4: Effect of P, T and X on liquid compositions – Hamilton plots

Before using Hamilton plots to determine the P-T-X conditions of liquid immiscibility at Oldoinyo Lengai, the validity of using these plots for the bulk compositions of the present study will first be examined. Brooker (1998) showed that Hamilton plots are acceptable for the Freestone and Hamilton (1980) data, for which liquid compositions are dominated by SiO_2, Al_2O_3, CaO and alkalis, with low MgO and FeO, but that this representation is not entirely suitable for many "natural" compositions, where FeO_{tot} and MgO are present in significant quantities. Liquid compositions in the present study are poor in MgO and FeO, and as a result, the main components are well represented in Hamilton plots, where they are split into the three groups [(SiO_2 + Al_2O_3)-CaO-alkalis] and where the minor amounts of other components can be added to any corner with little effect.

Freestone and Hamilton (1980) showed that pressure and temperature have an opposite effect on liquid compositions. With increasing P_{CO2} and decreasing temperature, they observed an expansion of the miscibility gap and concomitantly, a rotation of the tie lines so that the carbonate liquids become richer in CaO.

The effect of pressure on liquid compositions, described in section 6.3.3.2, is the same as that observed by Freestone and Hamilton (1980), *i.e.* opening of the miscibility gap with increasing pressure (Fig. 6.15). However, in this study, the effect of temperature on liquid compositions is not opposite to that of pressure. For this study, counterclockwise rotation of the tie lines with decreasing temperature (Fig.

6.14) was observed at 100 MPa, and increasing $SiO_2 + TiO_2 + Al_2O_3$ of the carbonate liquid and consequent shrinking of the miscibility gap (see Fig. 6.13) were observed at 20 MPa. These effects of temperature were not observed by Freestone and Hamilton (1980) because they worked at different temperature conditions (*cf.* section 6.4.2.1), producing different solvus shapes. For this study, pressure effects on the major element composition of the liquids are more enhanced and consistent than the effects of temperature, likely as a consequence of the shape of the solvus itself.

6.4.2.5: Effect of NBO/T on major element distribution between silicate and carbonate liquids

Brooker (1995) showed that plotting distribution coefficients as a function of NBO/T ("partition plots") has several advantages: 1) unlike Hamilton diagrams which require an estimate of both pressure and temperature, partition plots have the advantage that the method is independent of P and T; 2) with liquid immiscibility, there are two constantly variable compositional parameters, *i.e.* the liquid compositions, and plotting D's against NBO/T of the silicate liquid allows one to fix one of these parameters; and 3) NBO/T is a function of the structure of the silicate melt and therefore gives an insight into the mechanisms of liquid immiscibility and the processes which describe the partitioning of the elements between the two liquids. Brooker (1995) showed that the success of this method is due to the fact that there are some dramatic changes in the silicate melt structure for relatively small changes in composition; whereas, the carbonate melts are probably much less complex with more subtle and continuous changes.

Figure 6.20 (from Brooker, 1995) demonstrates the different types of partitioning trends that can be found in the diagrams of this section. The inverted triangles could represent components such as SiO_2 or Al_2O_3 which strongly favour the silicate liquid. They have D's > 1 for all values of NBO/T, especially for low NBO/T values (*i.e.*, they are network formers in the silicate liquid). The normal triangles could be for CaO which strongly favours the carbonate liquid. They have D's < 1 for all values of NBO/T, especially for low NBO/T (*i.e.*, they are network modifiers in

the silicate liquid). The diamonds illustrate the possible trend for a component that plays a dual role, *e.g.* FeO. They may well cross the parity line, *i.e.* they may have D's <1 for some NBO/T values and >1 for others. All the elements have D's which tend towards 1 at NBO/T > 3, which is the consulate point at which the solvus closes and at which the composition of both liquids is similar.

Figure 6.21 shows distribution coefficients of major elements between silicate and carbonate liquids as a function of NBO/T (values given in Appendix A6). The curves are drawn in order to fit as many points as possible while preserving the shape of the partitioning trends presented in Figure 6.20. Note that the data for experiments CP122 and CP124 have not been plotted and are not discussed when examining partition trends, since the NBO/T values of the silicate liquid in these two experiments are low compared to the other experiments at 20 MPa (Tab. A6.4). The two experiments CP122 and CP124 are the only two-liquid experiments containing combeite. The silicate liquids of these two experiments contain significantly more SiO_2 than silicate liquid in the other 20 MPa-experiments, hence their lower NBO/T value. Although the reason for high SiO_2 in the silicate liquid from these two experiments is not understood, it is clear that experiments CP122 and CP124 are at odds with the other two-liquid experiments.

Figure 6.21 illustrates that the values of NBO/T of the silicate liquid appear to be dependent on pressure (P) and temperature (T). At fixed T-X conditions, NBO/T values decrease (polymerisation increases) with decreasing pressure, and at fixed P-X conditions, NBO/T of silicate melt decreases with decreasing temperature. Moreover, NBO/T values at 20 and 100 MPa do not overlap.

For SiO_2 and Al_2O_3 (Fig. 6.21 a and c), D values are always >1, and they increase with decreasing NBO/T, in agreement with the fact that both these elements are network formers in the silicate liquid. Brooker (1995) showed that SiO_2 and Al_2O_3 have higher values of $D_{LS/LC}$ at a given NBO/T for lower pressure. This observation was used to plot D values of these two elements on different curves at 20 and 100 MPa. CaO, Na_2O, P_2O_5, F, Cl, SO_3, BaO and SrO all plot at $D_{LS/LC}$ <1 for all NBO/T

values (Figs. 6.21 g, h, j, k, l, m, n and o, respectively), and D values decrease with decreasing NBO/T, in agreement with the study of Brooker (1995). This suggests that all these elements are network modifiers in the silicate liquid, although some (minor) Na_2O might satisfy a role as charge balancing cation for the tetrahedral Al first (see Brooker, 1995). TiO_2, FeO, MnO, MgO and K_2O all cross the parity line (D = 1), which suggests that they have a dual role (Figs. 6.21 b, d, e, f and i).

The dual role observed for K_2O (Fig. 6.21 i) is compatible with the findings of Brooker (1995), who showed that for Al-rich compositions, at low NBO/T, K_2O may be preferentially allocated to a charge balancing role. The comparison of partitioning trends exhibited by K_2O (Fig. 6.21 i) and Na_2O (Fig. 6.21 h) shows that at low NBO/T, D values are higher for K_2O (>1) than for Na_2O (<1), suggesting that K_2O has a more important role than Na_2O as charge balancing tetrahedral Al. The dual role of MgO (Fig. 6.21 f) is also compatible with the study of Brooker (1995), who showed that some Mg can behave like Ca (*i.e.* favours the carbonate liquid and is a network modifier in the silicate liquid), whereas some could behave as a network former, or take a charge balancing role in place of some Na (here mostly K). The partitioning trend for FeO (Fig. 6.21 d) indicates that Fe has a dual role (it would cross the parity line similarly to Mg, but at even lower NBO/T), which is compatible with Fe^{3+} and Fe^{2+} being known to occur as both network formers and modifiers in silicate melts (Waychunas et al., 1988; Mysen, 1988). TiO_2 appears to have a dual role (Fig. 6.21 b), because even though all D values that have been measured are > 1, the parity line would be crossed at very low NBO/T. Brooker (1995) noted that TiO_2 behaves like SiO_2 for most studies (network former), but it also showed a dual role for the Shombole data.

D values show some scatter for Na_2O, MnO, P_2O_5, F, Cl, SO_3, BaO and SrO. For Na_2O, the scatter is explained by volatilisation during the electron microprobe analyses. The scatter exhibited by the remaining elements is thought to be due to their low concentrations, *i.e.* their concentrations are close to limits of detection when determined by electron microprobe.

Note that Si, Al, Ti and P were assumed to be in a tetrahedral position for the calculation of NBO/T values. However, it was suggested above that Ti has a dual role and that P is a modifier. Because the assignment of these cations to tetrahedral or octahedral positions does not modify the value of NBO/T significantly, NBO/T was not recalculated.

In summary, the partitioning trends are in general agreement with those presented by Brooker (1995). Two-liquid partitioning for major elements is well described as a function of the degree of polymerisation of the silicate liquid. The role played by the different elements in the silicate liquid, as deduced from the partitioning trends, is in agreement with what is known from the literature on silicate melts. The lack of overlap between NBO/T values at 20 and 100 MPa will be of great importance when examining the data for natural pairs.

6.4.2.6: Summary of experiments

The study of phase assemblages in the wollastonite nephelinite - silicate-bearing natrocarbonatite system shows that a miscibility gap is present at 20, 40 and 100 MPa, and that silicate crystals are in equilibrium with both liquids in two-liquid assemblages over the temperature interval 700-900 °C. The miscibility gap is wider at higher pressure. Pressure has more effect than temperature on the shape of the immiscibility field, and therefore on liquid compositions. Hamilton plots show that with increasing pressure, $SiO_2 + TiO_2 + Al_2O_3$ increases in the silicate liquid, while $Na_2O + K_2O$ increases and $CaO + FeO + MgO + MnO$ decreases in the carbonate liquid. The effect of increasing temperature is less clear, but it is not the opposite as that of increasing pressure.

The problem with examining liquid compositions on Hamilton plots is that an infinite number of P-T-X combinations can produce liquids of similar composition. This can be overcome by studying distribution of major elements between immiscible liquids as a function of the polymerisation of the silicate liquids. Because NBO/T is pressure dependent, plotting D's as a function of NBO/T allows determination of pressure of exsolution more thoroughly (see below).

6.4.3: Origin of crystals in erupted wollastonite nephelinite HOL14

The aim of this section is to infer the origin of crystals in wollastonite nephelinite HOL14. Depending on when crystals formed in lava HOL14, *i.e.* during exsolution or during subsequent crystallisation, the equivalent of silicate liquid from the two-liquid experiments is represented in HOL14 by the groundmass or by the whole rock composition. One must determine what the equivalent of silicate liquid from the experiments is in the natural lava, in order to use adequate liquid pairs when comparing two-liquid partitioning between natural and experimental samples (*e.g.*, in section 6.4.4).

The origin of crystals in wollastonite nephelinite HOL14 will be determined by comparing: 1) crystal assemblages and compositions; and 2) crystal proportions, between erupted wollastonite nephelinite HOL14 and experiments. Note that the petrography of wollastonite nephelinite HOL14 has been described in detail in Chapter 2 and in Peterson (1989a), and a SEM picture was presented in Chapter 2 (see Fig. 2.9).

In order to compare the crystal assemblages in experiments and in natural lava HOL14, phase diagrams are presented in Figures 6.22, 6.23 and 6.24, where experiments containing major crystal phases similar to those in lava HOL14 (*i.e.* nepheline, wollastonite, clinopyroxene and melanite garnet), are indicated on the figure by a shaded area (pie slices highlighted). There is a wide P-T-X range for which major phases are similar to one another in experimental and natural samples, especially at 20 MPa (Fig. 6.22). However, if minor phases are taken into account, the number of experiments having similar crystal phases as those in natural lava HOL14 is more limited. When titanite and vishnevite (= equivalent of sodalite at higher fugacity of oxygen) are taken into account, the P-T-X conditions at which crystal assemblages are equivalent are: 1) at 100 MPa, ~ 700 °C, and 90/10; and 2) at 20 MPa, 700-750 °C, and 100/0. Note that no experiments are available for a 90/10 bulk composition at 750 °C, 40 and 100 MPa. However, at these conditions, crystal phases could be similar to those in natural lava HOL14.

It is difficult to use minor phases in order to constrain the P-T-X conditions of crystallisation of wollastonite nephelinite HOL14 because they are present in only small

amounts in the capsules and can be missed. It is likely that at 100 MPa and for a 90/10 bulk composition, the field for which the phase assemblage (including vishnevite and titanite) is the same as in wollastonite nephelinite HOL14 extends to 750 °C. Therefore, the comparison of phases assemblages between lava HOL14 and the experiments is compatible with liquid immiscibility occurring at 100 MPa and 750 °C, as suggested by Kjarsgaard et al. (1995). Note that there is no wollastonite in HOL14-experiments at 100 MPa. Therefore, if liquid immiscibility occurred at this pressure, wollastonite (at least) was present in lava HOL14 at the time of exsolution, and did not form during subsequent crystallisation.

In order to further constrain the P-T conditions of formation of crystals in wollastonite nephelinite HOL14, major element compositions of crystals in lava HOL14 are compared to those in HOL14- and two-liquid-experiments. Are major element compositions of crystal phases in lava HOL14 comparable to those in two-liquid experiments or to those in HOL14-experiments, *i.e.*, did they form mostly at the time of liquid immiscibility (same composition as in two-liquid experiments) or during subsequent crystallisation (same composition as in HOL14-experiments)? Note that compositions of crystals in wollastonite nephelinite HOL14 are compared to those in unbuffered experiments, *i.e.* at lower oxygen fugacity, but this is not considered to be a problem since no significant effect of f_{O2} was observed on the major element composition of crystals (see Fig. 6.8 for nepheline).

The composition of nepheline in lava HOL14 is reported in Table 6.5 and plotted in Figure 6.25. Rim/core analyses show that nepheline exhibits zoning with an iron-rich rim, but near-constant K_2O content. Kjarsgaard et al. (1995) also observed an Fe-rich rim for nepheline in HOL14, and Peterson (1989a) observed oscillatory zoning in nepheline crystals from nephelinites. Nepheline phenocrysts in HOL14 analysed by Kjarsgaard et al. (1995) and Peterson (1989a) have lower Fe_2O_3 and slightly higher Ks/lower Ne than nepheline reported in this study.

Figure 6.25 illustrates that nepheline compositions in wollastonite nephelinite HOL14 are in the range of compositions for nepheline in the HOL14-experiments,

although the Qz component is slightly lower, and they also overlap the range of compositions of the high pressure, high temperature-, two-liquid-experiments. Compositions of nepheline from wollastonite nephelinite HOL14 are similar to those in two-liquid experiments at 100 MPa, $700 < T \leq 800$ °C. This indicates that they may have crystallised at these P-T conditions.

Clinopyroxene analyses for lava HOL14 are reported in Table 6.6 and plotted in Figure 6.26. Analyses of cores have been performed on four different clinopyroxene phenocrysts, which exhibit a very narrow compositional range ($Di_{44.3-46.2}He_{31.4-33.8}Ae_{20.5-24.3}$) compared to the range exhibited by clinopyroxene crystals from the experiments. Two clinopyroxene crystals (cpx2 and cpx3) do not have significantly different compositions for rims and cores. However, thorough examination of major element compositions in Table 6.6 shows that compared to cores, rims of cpx2 and cpx3 have lower Fe_2O_3, MgO, Na_2O and Mg #, and higher FeO and CaO. One clinopyroxene (cpx1) shows a marked zoning, with the rim much more enriched in an aegirine component ($Di_{18.2}He_{11.9}Ae_{70.0}$) compared to the core ($Di_{46.2}He_{32.1}Ae_{21.6}$). An inclusion of clinopyroxene in nepheline is richer in the diopside component ($Di_{58.3}He_{23.9}Ae_{17.8}$) compared to clinopyroxene phenocrysts. Peterson (1989a) analysed clinopyroxene microphenocrysts in green and brown glasses. They both plot at high aegirine values compared to cores of clinopyroxene phenocrysts (see Fig. 6.6). In the green glass, which contains 16.0 wt. % Na_2O, the composition of the clinopyroxene is $Di_{22.4}He_{24.9}Ae_{52.6}$, and in the brown glass which contains 2.16 wt. % Na_2O, the composition of the clinopyroxene is $Di_{26.4}He_{30.4}Ae_{43.3}$, i.e., it also contains less Na. The mesocryst analysed by Peterson (1989a) has a composition ($Di_{40.5}He_{37.7}Ae_{21.7}$) fairly close to cores of phenocrysts.

Figure 6.25 illustrates that the compositional range exhibited by clinopyroxene phenocrysts in lava HOL14 is overlapped by the compositional ranges of clinopyroxene crystals from both HOL14- and two-liquid-experiments. Therefore, it is not possible to use these data to infer whether clinopyroxene in lava HOL14 formed during of after liquid immiscibility.

The composition of melanite garnet in erupted HOL14 is reported in Table 6.7 and plotted in Figure 6.27. Analyses of cores for two different garnet crystals show different compositions: $Fe_{60.1}Al_{3.1}Ti_{36.3}$ and $Fe_{65.2}Al_{4.3}Ti_{30.5}$. The rim of the first melanite garnet compared to its core has: lower TiO_2, MgO and CaO, and higher Al_2O_3 and Fe_2O_3. Three analyses of the rim of a melanite garnet crystal compared to its core showed that the rim is Fe-rich, Ti-poor compared to the core, although the zoning is not as strong as reported in Kjarsgaard et al. (1995). Also plotted in Figure 6.27 are compositions of melanite garnet in lava HOL14 from Kjarsgaard et al. (1995): one unzoned microphenocryst, and one zoned phenocryst (one core and one rim analyses plotted). The core of a phenocryst ($Fe_{58.6}Al_{3.0}Ti_{38.4}$) analysed by Kjarsgaard et al. (1995) plots fairly close to the core of a melanite garnet of this study. The rim of a phenocryst ($Fe_{64.5}Al_{3.9}Ti_{31.5}$) and microphenocryst ($Fe_{63.6}Al_{4.3}Ti_{32.1}$) analysed by Kjarsgaard et al. (1995) plots fairly close to the rim of melanite garnet of this study, *i.e.* at high Fe^{3+}/low Ti compared to core phenocryst.

Figure 6.27 illustrates that the two melanite garnet grains that have been analysed have different compositions for their cores. One of them is richer in Ti/poorer in Fe^{3+} and cannot have formed by crystallisation subsequent to liquid immiscibility because it has high Ti/low Fe^{3+} compared to melanite garnet from HOL14-experiments. It likely formed at the time of exsolution, although it is not possible to determine the precise P-T-X conditions because of scatter of the data. The second melanite garnet has lower Ti/higher Fe^{3+} and was formed at different P-T-X conditions. This second garnet could have formed during subsequent crystallisation because it has a composition similar to that of melanite garnet in HOL14-experiments.

Titanite data from wollastonite nephelinite HOL14 are presented in Table 6.10. Titanite in HOL14 contains FeO (1.76 wt. %) and Al_2O_3 (0.38 wt. %). No literature data for HOL14 are available for comparison, but titanite in HOL14 is similar to titanite in ijolite BD35 (Dawson et al., 1995c), except that half of the iron is trivalent in BD35. The comparison between compositions of titanite in wollastonite nephelinite HOL14 and in HOL14- and two-liquid-experiments (Tab. 6.10) cannot be used to determine whether

titanite in lava HOL14 crystallised during or after liquid immiscibility. However, note that the composition of titanite in HOL14-experiment at 100 MPa, 700 °C is very similar to that of titanite in lava HOL14.

The comparison between compositions of phenocrysts in lava HOL14 and of crystals in the experiments showed that most crystals analysed in lava HOL14 may have crystallised at ~ 100 MPa, 750 °C (suggested to be the P-T conditions of liquid immiscibility by Kjarsgaard et al., 1995). Crystals in lava HOL14 are not corroded (suggests absence of mixing), but most are zoned. Zoning may indicate that some crystallisation occurred after exsolution, and that crystals formed during exsolution (cores) did not re-equilibrate during subsequent crystallisation. Most nepheline, clinopyroxene, melanite garnet and wollastonite crystals exhibit zoning with Fe-rich rims, which could reflect the increasing concentration of this component in the residual liquid during crystallisation. In conclusion, crystal compositions are compatible with exsolution at 100 MPa, 750 °C, followed by crystallisation.

The comparison of the phase proportions between lava HOL14 and the experiments can also be used to constrain the origin of crystals in HOL14. Phase proportions in the experiments at 100 MPa, 750 °C, for a 90/10-bulk composition are fairly similar to those in erupted wollastonite nephelinite HOL14 (in Peterson, 1989a; Kjarsgaard et al., 1995), except for higher clinopyroxene in the experiments (~ 15 % versus 7.2 %). Erupted wollastonite nephelinite HOL14 is ~ 40 % crystallised, *i.e.*, it is slightly less crystallised than an experiment at 100 MPa, 750 °C, for a 90/10-bulk composition (~ 50 %). This confirms that if liquid immiscibility occurred at 100 MPa, 750 °C, subsequent crystallisation can only have been minor.

6.4.4: Are wollastonite nephelinite and silicate-bearing natrocarbonatite conjugate liquids?

In order to determine at which P-T-X conditions the silicate-bearing natrocarbonatite (represented by OL5) and wollastonite nephelinite (represented by HOL14) became immiscible, the compositions of OL5 and HOL14 are compared to those of silicate and

carbonate liquids from the experiments, in Hamilton plots and in partition plots. As Kjarsgaard et al. (1995) pointed out, "comprehension of the immiscibility problem requires examination of liquid composition, not rock compositions."

It was previously shown that for silicate-bearing natrocarbonatite OL5, the whole rock composition is the equivalent of carbonate liquid in the experiments because most crystals are formed during subsequent crystallisation. Note, however, that melilite from a silicate spheroid in silicate-bearing natrocarbonatite OL5 has a composition close to that of melilite in two-liquid experiments (see Fig. 6.11) suggesting that it could have formed at the time of exsolution. It is more difficult to determine what is the equivalent of the silicate liquid. Since crystallisation subsequent to liquid immiscibility is probably minor (see section 6.4.3), the groundmass of lava HOL14 appears to be a better equivalent of silicate liquid from the experiments than the whole rock.

The major element analysis of wollastonite nephelinite HOL14 (Peterson, 1989a) is reported in Table 6.17, together with an analysis of the groundmass. Compared to the whole rock, the groundmass has higher SiO_2 (50 vs. 46 wt. %), FeO (10 vs. 7.7 wt. %), F (0.8 vs. 0.2 wt. %), SO_3 (0.9 vs. 0.3 wt. %) and BaO (0.5 vs. 0.2 wt. %), and lower Al_2O_3 (14 vs. 16 wt. %) and CaO (2.7 vs. 5.9 wt. %). Examination of Table 6.17 shows that the groundmass has a high total (100 wt. %) compared to the silicate liquid from two-liquid experiments. This suggests that the groundmass of lava HOL14 is volatile-free, therefore that it lost some volatiles. These volatiles might have segregated into the zeolite-carbonate globules (see Peterson, 1989a). However, since Hamilton diagrams and partition plots (D's vs. NBO/T) are made on a volatile-free basis, the conclusions are not affected by volatile loss from the silicate liquid. This also suggests that the origin of zeolite-carbonate globules in wollastonite nephelinite HOL14 is not mixing, since mixing would also have increased the volatile content of the groundmass (especially CO_2).

The liquid compositions in the natural lavas and in the experiments were first compared on a Hamilton plot, in order to determine the P-T-X conditions of liquid immiscibility at Oldoinyo Lengai (Fig. 6.13). Although this plot can lead to a large number of solutions for the P-T-X conditions, it is worth examination. For silicate-

bearing natrocarbonatite OL5, only the composition of the whole rock is plotted as it is thought to represent the equivalent of liquid from the experiments, and for wollastonite nephelinite HOL14, both groundmass and whole rock compositions are plotted. Note that groundmass and whole rock compositions plot very close to one another. Note that the experiments are made at higher f_{O2} than for wollastonite nephelinite HOL14, but that oxygen fugacity does not affect the composition of silicate liquid on Hamilton plots where all iron is plotted as Fe^{2+} (see Fig. 6.18), though it probably affects the FeO/Fe_2O_3 ratio (not measured).

The comparison of liquid compositions in a Hamilton plot (Fig. 6.13) shows that the silicate liquid of experiment CP109 (200 MPa, 750 °C, 10/90) fits the composition of groundmass of wollastonite nephelinite HOL14 fairly well (although at higher SiO_2 + TiO_2 + Al_2O_3), but that the carbonate liquid plots at higher CaO + MgO + FeO + MnO/lower Na_2O + K_2O than the whole rock of silicate-bearing natrocarbonatite OL5. The discrepancy in carbonate liquid compositions indicates that liquid immiscibility cannot have taken place at 200 MPa. The carbonate liquids of experiments at 20 MPa plot close to whole rock compositions of silicate-bearing natrocarbonatite OL5, whereas the silicate liquids of experiments at 20 MPa plot at low SiO_2 + TiO_2 + Al_2O_3 compared to groundmass of wollastonite nephelinite HOL14. The discrepancy in silicate liquid compositions suggests that liquid immiscibility cannot have taken place at 20 MPa either.

On the other hand, compositions of silicate and carbonate liquids at 100 MPa and intermediate temperature (700 °C < T ≤ 800 °C) plot close to the groundmass composition of wollastonite nephelinite HOL14 and the whole rock composition of silicate-bearing natrocarbonatite OL5, respectively. CP103 (100 MPa, 800 °C, 10/90), CP102 (100 MPa, 800 °C, 80/20) and CP97 (100 MPa, 750 °C, 20/80) are all fairly good analogues, but since the effect of temperature and composition is not clear on the compositions of both liquids, it is not possible to narrow down the T-X conditions. In conclusion, the Hamilton plot (Fig. 6.13) indicates that 100 MPa is the most probable pressure of liquid immiscibility, but this plot cannot be used to determine the T-X conditions of liquid immiscibility precisely. However, the conditions previously

estimated by Kjarsgaard et al. (1995), *i.e.* 100 MPa, 750 °C, are compatible with the results of the present study.

It was previously shown that the Hamilton plots can give a large number of solutions when determining P-T-X conditions of liquid immiscibility. Moreover, Brooker (1995) showed that compositions which plot in a reasonable area on a Hamilton plot do not necessarily plot at reasonable values on a partition plot ($D_{LS/LC}$ versus NBO/T). Therefore, partition coefficients of major elements between wollastonite nephelinite HOL14 (groundmass) and silicate-bearing natrocarbonatite OL5 (whole rock) are plotted as a function of NBO/T of wollastonite nephelinite HOL14 (groundmass), along with the experimental data (Fig. 6.21). The NBO/T values for different samples are given in Appendix A6 (Tab. A6.4). $D_{HOL14/OL5}$ is plotted as a function of NBO/T in Figure 6.21, along with data for the experiments. Examination of $D_{LS/LC}$ as a function of NBO/T can constrain pressure of exsolution more thoroughly, since NBO/T is a function of pressure. Values of NBO/T of silicate liquid are lower at 100 MPa than at 20 MPa. The value of NBO/T of groundmass of erupted wollastonite nephelinite HOL14 is low (= 0.63), in the range of the values of NBO/T of silicate liquids from 100 MPa. Moreover, for the elements which plot on different curves for different pressures, *i.e.* SiO_2 and Al_2O_3, $D_{LS/LC}$ for the natural pair plot on the 100 MPa curve. These two observations confirm that it is at this pressure that the two magmas are exsolved. Liquid immiscibility cannot have occurred at 20 MPa or 40 MPa, because the NBO/T values are too high for the given D values. It cannot have occurred at 200 MPa either, as demonstrated by the lower value (0.411) of NBO/T of silicate liquid in experiment CP109 (80/20, 200 MPa, 750 °C). Most values for the natural pair are reasonable, since they fall on the curves determined from the experiments. In conclusion, the comparison between natural lavas and experiments demonstrates that liquid immiscibility occurred at approximately 100 MPa.

Below, the major element compositions of natural HOL14 (groundmass) and OL5 (whole rock) are compared to the composition of silicate and carbonate liquids in the experiments prepared at conditions close to those previously estimated for liquid immiscibility. The major element composition of the groundmass of HOL14 is similar to

the composition of silicate liquid in two-liquid experiments prepared at 100 MPa, 800 °C, using 90 and 80 % wollastonite nephelinite in the bulk composition, except for slightly higher Na_2O in the groundmass of HOL14 (13.6 vs. < 11.3 wt. %). This suggests that alkalis did not segregate from the groundmass of HOL14 into the globules, as volatiles did. More importantly, similar compositions of silicate liquid in natural and experimental samples are in agreement with the conditions of exsolution previously determined. On the other hand, silicate-bearing natrocarbonatite OL5 (whole rock) contains significantly more Na_2O, K_2O and Cl than the carbonate liquid in the experiments prepared at the most appropriate P-T-X conditions for comparison (*i.e.*, 100 MPa, 800 °C, 80/20 bulk composition – CP102; 100 MPa, 800 °C, 50/50 bulk composition – CP13; and 100 MPa, 700 °C, 70/30 bulk composition – CP67). Low Na_2O, K_2O and Cl measured for the carbonate liquid in the experiments could be partially explained by the fact that the data for carbonate liquid in two-liquid experiments are not corrected for volatilisation, and also because salts could partition into vesicles in the experimental charges. In summary, most of the major element data on carbonate and silicate liquids from natural and silicate pairs indicate that silicate-bearing natrocarbonatite is the product of liquid immiscibility from a carbonated wollastonite nephelinite at ~ 100 MPa, 750 °C.

6.5 - Conclusions

Comparison between phase assemblages and major element compositions of crystal and liquid phases in experiments and in natural lavas HOL14 and OL5 supports the hypothesis that silicate-bearing natrocarbonatites are exsolved from wollastonite nephelinite at conditions of 100 MPa and 750 °C. Liquid immiscibility produces silica-rich natrocarbonatite (well represented by silicate-bearing natrocarbonatite OL5) and wollastonite nephelinite, well represented by HOL14. The low temperatures of liquid immiscibility are compatible with both of the calculated (silicate = 500-775 °C) and measured (carbonate ~ 600 °C) eruption temperatures for lavas from Oldoinyo Lengai.

During cooling, the parental wollastonite nephelinite magma crystallises silicate phases. The CO_2 builds up until the silicate liquid reaches the miscibility gap. Liquid immiscibility is favoured by the alkali-rich nature of nephelinite at Oldoinyo Lengai.

Brooker (1995) showed that in most cases, silicate compositions only just enter the two liquid field and the carbonate fraction is very small, whereas silicate magmas unusually high in alkalis may subsequently yield higher proportions of carbonate liquid. The alkali-rich nature of wollastonite nephelinite at Oldoinyo Lengai accounts for why the immiscible fraction of natrocarbonatites at Oldoinyo Lengai may be as high as volume 10-20 % (Pyle et al., 1991).

Once the two liquids become immiscible, they separate within the magma chamber at ~ 3.3 km (100 MPa), although some minor incomplete segregation might occur. After the separation of the immiscible magmas, the natrocarbonatite magma undergoes significant crystallisation (see Chapter 3 and 5) over a 150 °C cooling interval, whereas the crystallisation of wollastonite nephelinite is thought to be less important, and most crystals form at the time of liquid immiscibility.

Table 6.1: Phase assemblages in experimental run products at 20 MPa, for different starting compositions shown as proportion of wollastonite nephelinite HOL14/silicate-bearing natrocarbonatite OL5 (in wt. %), at different temperature (T). Run times (in hours) are also shown.

	Bulk composition	T (C)	Time (h)	Phase assemblage
CP110	HOL14	900	4	LS+Ne+Cpx+Mela+Wo+F
CP23	HOL14(90)OL5(10)	900	6:45	LS+Ne+Wo+Melilite+Vish+Ap+F
CP91	HOL14(80)OL5(20)	900	4	LS+LC+Ne+Wo+Melilite+F
CP22	HOL14(50)OL5(50)	900	6:45	LS+LC+Ne+Melilite+F
CP120	HOL14(40)OL5(60)	900	4	LS+LC+Ne+Melilite+F
CP121	HOL14(30)OL5(70)	900	4	LS+LC+Ne+Melilite+F
CP111	HOL14(20)OL5(80)	900	4	LS+LC+Ne+Melilite+F
CP82	HOL14(10)OL5(90)	900	04:20	LC+Ne+Melilite+spinel+F
CP40	HOL14	850	46	LS+Ne+Cpx+Mela+Wo+F
CP41	HOL14(95)OL5(5)	850	46	LS+Ne+Cpx+Wo+Ap+F
CP42	HOL14(90)OL5(10)	850	46	LS+Ne+Wo+Ap+F
CP52	HOL14(80)OL5(20)	850	42:15	LS+LC+Ne+Wo+Melilite+F
CP43	HOL14(70)OL5(30)	850	46	LS+LC+Ne+Wo+Melilite+F
CP53	HOL14(50)OL5(50)	850	42:15	LS+LC+Ne+Wo+Melilite+F
CP130	HOL14(20)OL5(80)	850	28	LC+Ne+Mela+Wo+Melilite+F
CP131	HOL14(10)OL5(90)	850	28	LC+Ne+Melilite+F
CP60	HOL14	800	109:30	LS+Ne+Cpx+Mela+Wo+spinel+F
CP15	HOL14(90)OL5(10)	800	68	LS+Ne+Cpx+Mela+Wo+Vish+spinel+Ap+F
CP113	HOL14(80)OL5(20)	800	67	LS+LC+Ne+Mela+Wo+Melilite+F
CP14	HOL14(50)OL5(50)	800	68	LS+LC+Ne+Mela+Wo+Melilite+F
CP122	HOL14(40)OL5(60)	800	39	LS+LC+Ne+Mela+Wo+Melilite+Combeite+F
CP123	HOL14(30)OL5(70)	800	39	LC+Ne+Mela+Wo+Melilite+Combeite+F
CP114	HOL14(20)OL5(80)	800	67	LC+Ne+Mela+Wo+Melilite+F
CP81	HOL14(10)OL5(90)	775	65	LC+Ne+Mela+Melilite+Wo+spinel+F
CP46	HOL14	750	116:30	LS+Ne+Cpx+Mela+Wo+Fd+Vish+Titanite+F
CP47	HOL14(95)OL5(5)	750	116:30	LS+Ne+Cpx+Mela+Wo+F
CP48	HOL14(90)OL5(10)	750	116:30	LS+LC+Ne+Cpx+Mela+Wo+Vish+F
CP50	HOL14(50)OL5(50)	750	116:30	LS+LC+Ne+Cpx+Mela+Wo+spinel+F
CP124	HOL14(40)OL5(60)	750	95	LS+LC+Ne+Cpx+Mela+Wo+Combeite+F
CP125	HOL14(30)OL5(70)	750	95	LC+Ne+Cpx+Mela+Wo+Combeite+F
CP115	HOL14(20)OL5(80)	750	88	LC+Ne+Mela+Melilite+Wo+F
CP54	HOL14	700	164	LS+Ne+Cpx+Mela+Vish+Titanite+F
CP55	HOL14(95)OL5(5)	700	164	LS+Ne+Cpx+Mela+Wo+Pvk+F
CP17	HOL14(90)OL5(10)	700	166	LS+LC+Ne+Cpx+Mela+Wo+F
CP64	HOL14(80)OL5(20)	700	476	LS+LC+Ne+Cpx+Mela+Wo+Titanite+Ap+F
CP16	HOL14(50)OL5(50)	700	166	LC+Ne+Cpx+Mela+Wo+Combeite+F
CP65	HOL14(50)OL5(50)	700	476	LC+Ne+Cpx+Mela+Wo+Combeite+F

Note: abbreviations used are: LS: silicate liquid; LC: carbonate liquid; F: fluid phase; Ne: nepheline; Cpx: clinopyroxene; Mela: melanite garnet; Wo: wollastonite; Vish: vishnevite; Ap: apatite; Pvk: perovskite; Fd: alkali feldspar.

Table 6.2: Phase assemblages in experimental run products at 40 MPa, for different starting compositions shown as proportion of wollastonite nephelinite HOL14/silicate-bearing natrocarbonatite OL5 (in wt. %), at different temperatures (T). Run times (in hours) are also shown.

Sample	Bulk composition	T (C)	Time (h)	Phase assemblage
CP19	HOL14(90)OL5(10)	900	38	LS+LC+Ne+Wo+Melilite+Vish+Ap+F
CP18	HOL14(50)OL5(50)	900	38	LS+LC+Ne+F
CP2	HOL14(90)OL5(10)	800	68	LS+LC+Ne+Cpx+Mela+Wo+Vish+spinel+F
CP1	HOL14(50)OL5(50)	800	68	LS+LC+Ne+Mela+Wo+F
CP11	HOL14(90)OL5(10)	700	165	LS+LC+Ne+Cpx+Mela+Wo+Titanite+Py+F
CP68	HOL14(80)OL5(20)	700	479	LS+LC+Ne+Cpx+Mela+Wo+F
CP69	HOL14(70)OL5(30)	700	479	LS+LC+Ne+Cpx+Mela+Wo+Titanite+F
CP10	HOL14(50)OL5(50)	700	165	LC+Ne+Cpx+Mela+Wo+Titanite+F

Abbreviations used are: LS: silicate liquid; LC: carbonate liquid; F: fluid phase; Ne: nepheline; Cpx: clinopyroxene; Mela: melanite garnet; Wo: wollastonite; Vish: vishnevite; Ap: apatite; Py: pyrrhotite.

Table 6.3: Phase assemblages in experimental run products at pressure (P) ~ 100 MPa, for different starting compositions shown as proportion of wollastonite nephelinite HOL14/silicate-bearing natrocarbonatite OL5 (in wt. %), at different temperatures (T). Run times (in hours) are also shown.

Sample	Bulk composition	P (MPa)	T (C)	Time (h)	Phase assemblage
CP38	HOL14	100	900	6:15	LS+Cpx+Mela+Wo+Ap+F
CP21	HOL14(90)OL5(10)	100	900	4:15	LS+LC+Ne+Mela+Vish+Ap+F
CP92	HOL14(80)OL5(20)	100	900	4	LS+LC+Ne+Vish+F
CP20	HOL14(50)OL5(50)	100	900	4:15	LS+LC+Ne+F
CP93	HOL14(20)OL5(80)	100	900	4	LS+LC+Ne+F
CP89	HOL14(10)OL5(90)	100	900	4:30	LS+LC+Ne+F
CP74	HOL14	100	800	64	LS+Ne+Cpx+Mela+Melilite+Vish+spinel+F
CP5	HOL14(90)OL5(10)	100	800	68	LS+LC+Ne+Cpx+Mela+Wo+Py+Ap+F
CP102	HOL14(80)OL5(20)	100	800	382	LS+LC+Ne+Cpx+Mela+F
CP13	HOL14(50)OL5(50)	100	800	68	LS+LC+Ne+Py+F
CP103	HOL14(10)OL5(90)	100	800	382	LS+LC+Ne+F
CP97	HOL14(20)OL5(80)	100	750	382	LS+LC+Ne+Cpx+Mela+F
CP72	HOL14	100	700	190	LS+Ne+Cpx+Mela+Melilite+F
CP8	HOL14(90)OL5(10)	103	700	146	LS+LC+Ne+Cpx+Mela+Wo+Vish+Fd+Titanite+F
CP66	HOL14(80)OL5(20)	100	700	479	LS+LC+Ne+Cpx+Mela+Wo+F
CP67	HOL14(70)OL5(30)	100	700	479	LS+LC+Ne+Cpx+Mela+Fd+F
CP7	HOL14(50)OL5(50)	103	700	146	LS+LC+Ne+Cpx+Mela+Ap+F
CP117	HOL14(10)OL5(90)	100	700	87	LC+Ne+Cpx+Mela+F

Abbreviations used are: LS: silicate liquid; LC: carbonate liquid; F: fluid phase; Ne: nepheline; Cpx: clinopyroxene; Mela: melanite garnet; Wo: wollastonite; Ap: apatite; Vish: vishnevite; Py: pyrrhotite; Fd: alkali feldspar.

Table 6.4: Phase assemblages in open tube-, C/CH4 buffered- and 200 MPa-experimental run products, prepared at different starting compositions shown as proportion of wollastonite nephelinite HOL14/silicate-bearing natrocarbonatite OL5 (in wt. %), at different pressures (P) and temperatures (T). Run times (in hours) are also shown.

Sample	Bulk composition	P (MPa)	T (C)	Time (h)	Phase assemblage
Open-tube					
CP78	HOL14(90)OL5(10)	100	800	116	LS+Ne+Cpx+Combeite+Py+F
CH4/C buffer					
CP27	HOL14(90)OL5(10)	40	800	88	LS+Ne+Wo+Sodalite+Ap+F
CP31	HOL14(90)OL5(10)	100	700	410:30	LS+LC+Ne+Cpx+Wo+Py+Ap+Titanite+F
Sealed-tube					
CP109	HOL14(80)OL5(20)	200	750	200	LS+LC+Ne+Cpx+Mela+F

Abbreviations used are: LS: silicate liquid; LC: carbonate liquid; F: fluid phase; Ne: nepheline; Cpx: clinopyroxene; Mela: melanite garnet; Wo: wollastonite; Ap: apatite; Py: pyrrhotite.

Table 6.5: Major element microprobe analyses of nepheline from the experiments on the HOL14/OL5 join, and from natural erupted wollastonite nephelinite HOL14.

SAMPLE	CP74	CP72	CP110	CP40	CP80	CP46	CP54	CP109	CP21	CP92
Type	HOL14	HOL14	HOL14	HOL14	HOL14	HOL14	HOL14	2 liq	2 liq	2 liq
# of analyses	1	1	2	3	3	2	2	2	2	4
Composition	100/0	100/0	100/0	100/0	100/0	100/0	100/0	80/20	90/10	80/20
Pressure	100	100	20	20	20	20	20	200	100	100
Temperature	800	700	900	850	800	750	700	750	900	900
SiO2	42.90	43.41	43.04	43.13	42.66	42.92	42.93	43.62	43.03	42.91
Al2O3	32.35	30.66	31.82	32.24	32.27	32.40	31.39	30.57	31.25	31.54
Fe2O3	1.97	3.19	2.19	2.09	2.25	1.94	2.75	3.06	2.30	2.69
CaO	0.10	b.d.	0.34	0.28	0.20	b.d.	b.d.	0.10	0.21	0.23
Na2O	16.77	16.61	16.84	16.66	16.49	16.30	15.94	17.08	16.64	16.58
K2O	5.92	6.13	5.76	5.59	6.12	6.43	6.98	5.56	6.56	6.05
Ks	18.3	19.0	17.8	17.2	18.9	19.9	21.7	17.2	20.4	18.8
Nf	3.6	5.8	4.0	3.8	4.1	3.5	5.0	5.6	4.2	4.9
Ne	75.1	72.4	75.1	74.2	73.4	73.0	70.2	74.7	74.3	73.1
An	0.5	0.0	1.8	1.4	1.0	0.0	0.0	0.5	1.1	1.2
Cn	-0.6	-1.4	-1.5	-0.4	-0.4	-0.2	-0.7	-1.9	-2.3	-1.1
Qz	3.2	4.1	2.8	3.7	3.0	3.8	3.8	3.9	2.4	3.1

SAMPLE	CP20	CP93	CP89	CP5	CP78	CP102	CP13	CP103	CP97	CP8
Type	2 liq	2 liq	2 liq	2 liq	2 liq	2 liq	2 liq	2 liq	2 liq	2 liq
# of analyses	3	2	3	1	1	1	2	1	1	3
Composition	50/50	20/80	10/90	90/10	100/0	80/20	50/50	10/90	20/80	90/10
Pressure	100	100	100	100	100	100	100	100	100	103
Temperature	900	900	900	800	800 OT	800	800	800	750	700
SiO2	42.87	43.03	42.85	42.61	42.34	41.95	43.45	42.89	43.25	43.13
Al2O3	32.09	31.52	32.41	31.63	31.26	33.27	31.81	32.07	32.68	31.52
Fe2O3	1.53	2.84	1.78	1.85	2.29	1.54	1.62	2.21	1.55	1.96
CaO	0.17	b.d.	0.20	0.20	0.20	b.d.	0.48	0.10	b.d.	0.16
Na2O	17.12	16.81	16.85	17.26	15.88	16.75	16.44	16.48	16.54	16.66
K2O	6.21	5.80	5.91	6.46	8.04	6.50	6.20	6.25	5.98	6.57
Ks	19.2	18.0	18.2	20.1	25.1	20.1	19.1	19.3	18.4	20.3
Nf	2.8	5.2	3.2	3.4	4.2	2.8	3.0	4.0	2.8	3.6
Ne	77.7	73.9	75.8	78.1	71.2	76.0	74.1	73.4	74.5	74.9
An	0.9	0.0	1.0	1.0	1.0	0.0	2.5	0.5	0.0	0.8
Cn	-2.3	-0.7	-1.0	-3.2	-2.7	-0.4	-1.9	-0.6	-0.0	-2.2
Qz	1.7	3.7	2.7	0.6	1.1	1.4	3.2	3.3	4.3	2.6

Note: Pressure is in MPa, temperature in oC. Starting composition is shown as proportion of wollastonite nephelinite HOL14/silicate-bearing natrocarbonatite OL5 (in wt. %) for the present study, and as proportion of wollastonite nephelinite HOL14/synthetic natrocarbonatite (in wt. %) for the data of Kjarsgaard et al. (1995). Types of experiments are HOL14-experiments, silicate liquid (LS)-experiments, two-liquid (2 liq)-experiments and carbonate liquid (LC)-experiments.
Analyses for this study are recalculated to 100 wt. %. Normative abundance of end-members determined by the method of Peterson (1989a). Abbreviations used are: Ks: kalsilite; Nf: Na2Fe2Si2O8; Ne: nepheline; An: anorthite; Cn: corundum; Qz: quartz; b.d.: below detection; Ph: phenocryst; mph: microphenocryst; c: core; r: rim; OT: open tube; Buf.: buffered.
Sources for additional data are: P89a: Peterson (1989a) and KHP95: Kjarsgaard et al. (1995).

Table 6.5 (suite).

SAMPLE	CP31	CP66	CP67	CP117	CP19	CP18	CP2	CP27	CP1	CP11
Type	2 liq	2 liq	2 liq	LC	2 liq	2 liq	2 liq	2 liq	2 liq	2 liq
# of analyses	1	1	1	2	3	4	2	1	2	1
Composition	90/10	80/20	70/30	10/90	90/10	50/50	90/10	90/10	50/50	90/10
Pressure	100	100	100	100	40	40	40	40	40	40
Temperature	700 Buf.	700	700	700	900	900	800	800 Buf.	800	700
SiO2	42.80	42.57	42.42	42.47	43.52	43.29	43.09	42.97	44.12	42.66
Al2O3	32.11	31.63	32.16	32.57	31.07	31.12	31.07	31.82	30.18	31.98
Fe2O3	1.54	2.74	2.32	1.60	1.99	2.30	2.50	1.55	2.68	2.03
CaO	0.11	0.30	0.20	0.20	0.19	0.18	0.15	0.19	0.09	0.16
Na2O	16.51	16.36	16.53	16.48	16.55	16.53	16.27	16.28	16.63	16.25
K2O	6.94	6.41	6.37	6.68	6.69	6.58	6.93	7.20	6.30	6.92
Ks	21.5	19.9	19.8	20.7	20.7	20.4	21.6	22.3	19.5	21.5
Nf	2.8	5.1	4.3	2.9	3.6	4.2	4.6	2.8	4.9	3.7
Ne	75.0	72.0	73.6	74.7	74.3	73.7	72.2	74.0	73.3	72.9
An	0.6	1.5	1.0	1.0	1.0	0.9	0.8	1.0	0.5	0.8
Cn	-1.9	-1.0	-0.9	-1.2	-2.7	-2.2	-2.0	-2.3	-2.6	-1.3
Qz	2.1	2.5	2.2	1.9	3.0	3.0	2.9	2.2	4.4	2.4

SAMPLE	CP68	CP69	CP10	CP23	CP91	CP22	CP120	CP121	CP111	CP82
Type	2 liq	2 liq	2 liq	LS	2 liq	2 liq	2 liq	2 liq	2 liq	LC
# of analyses	1	1	3	1	1	3	1	2	2	2
Composition	80/20	70/30	50/50	90/10	80/20	50/50	40/60	30/70	20/80	10/90
Pressure	40	40	40	20	20	20	20	20	20	20
Temperature	700	700	700	900	900	900	900	900	900	900
SiO2	42.51	42.94	43.65	42.56	42.91	43.06	42.97	42.93	42.84	42.38
Al2O3	32.75	32.28	31.32	31.92	32.11	31.32	31.69	31.45	32.44	32.55
Fe2O3	1.75	1.97	1.67	2.34	2.09	1.84	2.29	2.28	1.49	1.81
CaO	b.d.	0.20	0.14	0.17	b.d.	0.28	b.d.	0.20	0.15	0.20
Na2O	15.98	15.79	16.35	16.13	15.95	16.36	16.48	16.60	16.52	16.50
K2O	7.00	6.81	6.88	6.88	6.94	7.14	6.57	6.54	6.57	6.57
Ks	21.7	21.1	21.3	21.4	21.5	22.2	20.4	20.3	20.3	20.4
Nf	3.2	3.6	3.0	4.3	3.8	3.4	4.2	4.2	2.7	3.3
Ne	72.0	70.6	73.8	71.8	71.3	73.8	73.4	74.1	74.9	74.4
An	0.0	1.0	0.7	0.9	0.0	1.5	0.0	1.0	0.8	1.0
Cn	0.0	-0.2	-2.4	-1.0	-0.3	-2.8	-1.2	-2.0	-1.2	-1.0
Qz	3.2	3.9	3.5	2.6	3.8	2.0	3.2	2.4	2.6	1.9

Table 6.5 (suite).

SAMPLE	CP41	CP42	CP52	CP43	CP53	CP130	CP131	CP15	CP113	CP14
Type	LS	LS	2 liq	2 liq	2 liq	LC	LC	LS	2 liq	2 liq
# of analyses	3	3	2	2	1	1	1	1	1	1
Composition	95/5	90/10	80/20	70/30	50/50	20/80	10/90	90/10	80/20	50/50
Pressure	20	20	20	20	20	20	20	20	20	20
Temperature	850	850	850	850	850	850	850	800	800	800
SiO2	43.23	43.61	43.11	42.60	43.23	43.06	42.65	42.86	42.78	42.89
Al2O3	32.31	31.19	31.91	32.72	31.16	32.27	32.41	32.08	31.84	31.18
Fe2O3	1.91	2.79	2.40	1.50	2.85	1.35	1.73	1.50	2.41	2.08
CaO	0.15	0.14	0.19	0.19	0.19	b.d.	b.d.	0.09	b.d.	0.05
Na2O	16.44	16.16	15.80	16.18	15.87	16.66	16.56	16.35	16.26	16.44
K2O	5.96	6.12	6.60	6.81	6.70	6.66	6.65	7.13	6.70	7.36
Ks	18.4	18.9	20.4	21.1	20.8	20.6	20.6	22.1	20.8	22.9
Nf	3.5	5.1	4.4	2.7	5.2	2.5	3.2	2.7	4.4	3.8
Ne	73.5	70.8	69.8	73.3	69.6	75.8	74.7	74.3	72.2	74.0
An	0.8	0.7	1.0	1.0	1.0	0.0	0.0	0.5	0.0	0.3
Cn	-0.3	-0.5	-0.0	-0.7	-0.8	-1.6	-1.0	-1.9	-0.7	-2.8
Qz	4.1	5.1	4.4	2.6	4.2	2.7	2.5	2.3	3.3	1.9

SAMPLE	CP122	CP123	CP114	CP81	CP48	CP124	CP125	CP115	CP55	CP17
Type	2 liq	LC	LC	LC	2 liq	2 liq	LC	LC	LS	2 liq
# of analyses	1	2	2	3	1	1	2	1	1	1
Composition	40/60	30/70	20/80	10/90	90/10	40/60	30/70	20/80	95/5	90/10
Pressure	20	20	20	20	20	20	20	20	20	20
Temperature	800	800	800	775	750	750	750	750	700	700
SiO2	42.87	42.65	42.13	42.98	43.30	42.59	42.47	42.43	42.59	42.85
Al2O3	32.05	31.97	31.93	31.99	32.16	32.21	32.18	32.26	32.37	31.76
Fe2O3	2.00	2.00	2.04	1.84	1.79	1.71	1.84	1.85	1.78	1.41
CaO	b.d.	b.d.	0.43	0.20	b.d.	b.d.	b.d.	0.20	0.20	0.32
Na2O	16.08	16.34	16.41	16.28	16.49	16.23	16.34	16.33	15.84	16.17
K2O	7.00	7.04	7.06	6.72	6.26	7.27	7.16	6.94	7.22	7.49
Ks	21.7	21.9	22.0	20.8	19.3	22.6	22.3	21.5	22.4	23.3
Nf	3.7	3.7	3.8	3.4	3.3	3.1	3.4	3.4	3.3	2.6
Ne	72.1	73.4	73.9	73.2	74.0	73.4	73.7	73.6	71.4	73.8
An	0.0	0.0	2.2	1.0	0.0	0.0	0.0	1.0	1.0	1.7
Cn	-0.8	-1.4	-2.4	-1.3	-0.6	-1.4	-1.4	-1.4	-0.8	-2.8
Qz	3.4	2.4	0.5	2.9	4.0	2.3	2.0	1.8	2.7	1.6

Table 6.5 (suite).

SAMPLE	CP64	CP16	CP65	BK424	BK430	BK436	BK437	HOL14	HOL14	HOL14
Type	2 liq	LC	LC	HOL14	2 liq	HOL14	2 liq			
# of analyses	1	3	2	KPH95	KPH95	KPH95	KPH95	1	3	KPH95
Composition	80/20	50/50	50/50	100/0	90/10	100/0	90/10	Ph-c.	Ph-r.	Ph-c.
Pressure	20	20	20	106	106	108	108			
Temperature	700	700	700	750	750	700	700			
SiO2	42.43	43.02	42.48	42.43	41.57	42.66	42.86	43.86	43.71	42.67
Al2O3	32.29	31.30	31.70	32.75	33.20	32.39	32.96	30.82	29.86	33.30
Fe2O3	1.86	1.79	2.40	2.35	2.12	2.11	1.75	1.98	2.88	1.26
CaO	0.20	0.24	0.20	0.17	0.13	0.15	0.05	b.d	b.d.	0.23
Na2O	16.05	16.24	15.92	16.52	17.02	16.60	17.03	17.39	17.41	16.59
K2O	7.19	7.40	7.30	6.24	6.54	6.70	6.23	6.13	6.16	6.51
Ks	22.3	23.0	22.7	19.2	20.2	20.7	19.1	18.9	19.1	20.0
Nf	3.4	3.3	4.4	4.3	3.9	3.8	3.2	3.6	5.3	2.3
Ne	72.3	73.4	70.9	73.1	76.1	74.0	76.2	78.0	76.9	75.2
An	1.0	1.3	1.0	0.9	0.7	0.8	0.3	0.0	0.0	1.2
Cn	-1.1	-2.9	-1.3	0.0	-0.8	-1.2	-0.8	-3.4	-3.9	-0.7
Qz	2.1	1.9	2.3	2.5	-0.1	1.9	2.2	2.8	2.6	2.1

SAMPLE	HOL14	HOL14	HOL14
Type			
# of analyses	KHP95	P89a	P89a
Composition	Ph-r.	Ph.	mph.
Pressure			
Temperature			
SiO2	42.58	42.55	42.68
Al2O3	32.75	32.52	32.24
Fe2O3	1.64	1.45	2.18
CaO	0.23	0.06	0.13
Na2O	16.48	16.37	16.66
K2O	6.59	6.61	6.50
Ks	20.3	20.5	20.1
Nf	3.0	2.7	4.0
Ne	74.3	74.6	74.2
An	1.2	0.3	0.7
Cn	-0.9	-0.8	-1.1
Qz	2.1	2.7	2.2

Table 6.6: Major element microprobe analyses of clinopyroxene from the experiments on the HOL14/OL5 join, and from natural erupted wollastonite nephelinite HOL14.

SAMPLE	CP38	CP74	CP72	CP110	CP40	CP60	CP46	CP54	CP109	CP5	CP78	CP102	CP97	CP8	CP31	CP66	CP67
Type	HOL14	HOL14	HOL14	HOL14	HOL14	HOL14	HOL14	HOL14	2 liq	2 liq	2 liq	2 liq	2 liq	2 liq	2 liq	2 liq	2 liq
# of analyses	1	2	2	2	1	1	2	1	6	1	1	1	2	3	3	2	2
Composition	100/0	100/0	100/0	100/0	100/0	100/0	100/0	100/0	80/20	90/10	90/10	80/20	20/80	90/10	90/10	80/20	70/30
Pressure	100	100	100	20	20	20	20	20	200	100	100	100	100	103	100	100	100
Temperature	900	800	700	900	850	800	750	700	750	800	800 OT	800	750	700	700 Buf.	700	700
SiO2	51.08	50.57	51.49	50.77	49.68	51.40	51.34	50.49	50.71	49.49	50.31	51.95	51.66	50.15	50.55	51.08	51.14
TiO2	0.45	0.49	0.71	0.78	1.01	0.59	0.49	0.50	0.67	0.45	0.52	0.45	0.52	0.82	0.51	0.61	0.55
Al2O3	0.70	0.99	0.98	1.62	1.94	0.79	0.92	0.79	1.27	0.81	0.99	0.59	0.54	1.58	1.08	1.07	0.78
Fe2O3	6.96	7.35	4.45	4.61	6.71	4.70	5.86	8.87	6.46	14.84	7.54	7.03	5.23	6.58	7.11	5.84	6.82
FeO	7.29	11.14	8.03	7.45	11.69	7.32	10.76	8.71	8.96	2.77	11.31	10.40	7.95	8.92	11.06	9.00	7.35
MnO	0.60	0.49	0.49	0.39	0.58	0.49	0.63	0.49	0.47	0.60	0.70	0.49	0.44	0.33	0.65	0.49	0.49
MgO	9.33	7.08	10.37	10.82	6.57	10.77	7.87	7.41	8.74	7.56	6.46	7.42	10.21	8.56	6.94	9.07	9.57
CaO	21.58	19.30	21.96	22.33	19.33	22.64	19.72	19.96	20.61	19.71	19.59	18.50	21.80	21.07	19.55	20.83	21.25
Na2O	2.01	2.57	1.52	1.22	2.49	1.28	2.40	2.77	2.12	3.77	2.59	3.17	1.66	1.98	2.54	2.00	2.05
	Structural formula for O =12.																
Si	3.89	3.91	3.90	3.84	3.84	3.89	3.94	3.89	3.88	3.79	3.90	3.98	3.92	3.84	3.90	3.90	3.89
Al	0.06	0.09	0.09	0.14	0.16	0.07	0.06	0.07	0.11	0.07	0.09	0.02	0.05	0.14	0.10	0.10	0.07
Al	0.00	0.00	0.00	0.00	0.02	0.00	0.02	0.00	0.00	0.00	0.00	0.03	0.00	0.00	0.00	0.00	0.00
Fe3+	0.40	0.43	0.25	0.26	0.39	0.27	0.34	0.51	0.37	0.86	0.44	0.41	0.30	0.38	0.41	0.34	0.39
Ti	0.03	0.03	0.04	0.05	0.06	0.03	0.03	0.03	0.04	0.03	0.03	0.03	0.03	0.05	0.03	0.04	0.03
Mg	1.06	0.82	1.17	1.22	0.76	1.22	0.90	0.85	1.00	0.86	0.75	0.85	1.16	0.98	0.80	1.03	1.09
Fe2+	0.46	0.72	0.51	0.47	0.76	0.46	0.69	0.56	0.57	0.18	0.73	0.67	0.50	0.57	0.71	0.57	0.47
Mn	0.04	0.03	0.03	0.03	0.04	0.03	0.04	0.03	0.03	0.04	0.05	0.03	0.03	0.02	0.04	0.03	0.03
Ca	1.76	1.60	1.78	1.81	1.60	1.84	1.62	1.65	1.69	1.62	1.63	1.52	1.77	1.73	1.62	1.70	1.73
Na	0.30	0.39	0.22	0.18	0.37	0.19	0.36	0.41	0.31	0.56	0.39	0.47	0.24	0.29	0.38	0.30	0.30
Mg	57.0	41.7	60.5	64.4	39.4	64.0	45.3	45.8	52.1	52.7	39.0	42.0	59.8	52.4	40.3	53.4	57.5
(Fe2+)+Mn	27.1	38.5	27.9	26.2	41.2	26.1	36.8	32.0	31.5	13.2	40.7	34.6	27.6	31.8	39.1	31.3	26.4
Na	15.9	19.7	11.6	9.5	19.4	9.9	18.0	22.2	16.4	34.1	20.3	23.3	12.7	15.8	19.6	15.3	16.0
Mg#	69.5	53.1	69.7	72.1	50.0	72.4	56.6	60.3	63.5	83.0	50.5	56.0	69.6	63.1	52.8	64.3	69.9

Note: Pressure is in MPa, temperature in oC, and starting composition is shown as proportion of wollastonite nephelinite HOL14/silicate-bearing natrocarbonatite OL5 (in wt. %).
Types of experiments are HOL14-experiments, silicate liquid (LS)-experiments, two-liquid (2 liq)-experiments and carbonate liquid (LC)-experiments.
For this study, totals are recalculated to 100 wt. %. Mg # = Mg/(Mg+Fe2+)*100.
Numbers of ions on the basis of 12 oxygens. FeO and Fe2O3 determined by stoichiometry utilizing the method of Droop (1987). Mg, (Fe2+)+Mn and Na are normalized molar proportions.
Abbreviations used are: OT: open tube; Buf.: buffered; b.d.: below detection; Ph: phenocryst; mph: microphenocryst; c: core; r: rim; Meso: mesocryst; gg: green glass; bg: brown glass.
Sources for additional data are: P89a: Peterson (1989a) and KHP95: Kjarsgaard et al. (1995).

Table 6.6 (suite).

SAMPLE	CP7	CP2	CP11	CP68	CP69	CP10	CP41	CP15	CP48	CP50	CP124	CP125	CP55	CP17	CP64	CP16	CP65
Type	2 liq	2 liq	2 liq	2 liq	2 liq	2 liq	LS	LS	2 liq	2 liq	2 liq	LC	LS	2 liq	2 liq	LC	LC
# of analyses	3	1	3	1	1	4	1	2	1	2	1	2	2	1	1	2	2
Composition	50/50	90/10	90/10	80/20	70/30	50/50	95/5	90/10	90/10	50/50	40/60	30/70	95/5	90/10	80/20	50/50	50/50
Pressure	103	40	40	40	40	40	20	20	20	20	20	20	20	20	20	20	20
Temperature	700	800	700	700	700	700	850	800	750	750	750	750	700	700	700	700	700
SiO2	50.72	51.07	50.91	51.40	50.64	50.76	50.42	51.75	51.30	51.26	51.29	51.40	50.63	49.73	49.46	50.67	50.62
TiO2	0.60	0.54	0.60	0.54	0.60	0.67	0.56	0.58	0.43	0.59	0.51	0.53	0.58	0.83	1.04	0.49	0.44
Al2O3	1.12	0.96	1.07	0.69	1.19	0.91	1.32	0.97	0.49	0.88	1.12	0.75	0.84	1.59	1.56	0.92	0.89
Fe2O3	6.89	6.43	7.29	4.98	11.71	8.25	7.41	4.09	8.91	6.21	4.88	6.59	7.26	7.15	8.13	7.93	7.97
FeO	7.51	7.75	7.31	9.11	9.15	6.01	8.93	9.09	11.08	11.40	10.23	7.40	10.14	10.47	12.01	8.06	9.54
MnO	0.44	0.50	0.48	0.59	0.59	0.43	0.66	0.51	0.77	0.64	0.57	0.50	0.45	0.53	0.59	0.48	0.54
MgO	9.60	9.55	9.34	9.45	5.24	9.61	8.70	10.11	6.08	7.23	8.72	9.83	7.49	7.31	5.56	8.60	7.51
CaO	21.19	21.24	20.76	21.56	16.32	21.04	19.77	21.27	17.30	19.13	20.79	20.91	20.18	20.17	18.73	20.50	19.92
Na2O	1.94	1.95	2.23	1.67	4.55	2.32	2.24	1.62	3.64	2.67	1.90	2.10	2.43	2.23	2.93	2.35	2.57
	Structural formula for O =12.																
Si	3.86	3.89	3.87	3.92	3.91	3.86	3.86	3.93	3.97	3.95	3.92	3.90	3.90	3.84	3.85	3.88	3.90
Al	0.10	0.09	0.10	0.08	0.09	0.08	0.12	0.07	0.03	0.06	0.08	0.07	0.08	0.15	0.14	0.08	0.08
Al	0.00	0.00	0.00	0.00	0.02	0.00	0.00	0.01	0.01	0.02	0.02	0.00	0.00	0.00	0.00	0.00	0.00
Fe3+	0.40	0.37	0.42	0.29	0.68	0.47	0.43	0.23	0.52	0.36	0.28	0.38	0.42	0.42	0.48	0.46	0.46
Ti	0.03	0.03	0.03	0.03	0.04	0.04	0.03	0.03	0.03	0.03	0.03	0.03	0.03	0.05	0.06	0.03	0.03
Mg	1.09	1.08	1.06	1.07	0.60	1.09	0.99	1.14	0.70	0.83	0.99	1.11	0.86	0.84	0.65	0.98	0.86
Fe2+	0.48	0.49	0.47	0.58	0.59	0.38	0.57	0.58	0.72	0.73	0.65	0.47	0.65	0.68	0.78	0.52	0.61
Mn	0.03	0.03	0.03	0.04	0.04	0.03	0.04	0.03	0.05	0.04	0.04	0.03	0.03	0.04	0.04	0.03	0.04
Ca	1.73	1.73	1.69	1.76	1.35	1.71	1.62	1.73	1.43	1.58	1.70	1.70	1.67	1.67	1.56	1.68	1.64
Na	0.29	0.29	0.33	0.25	0.68	0.34	0.33	0.24	0.55	0.40	0.28	0.31	0.36	0.33	0.44	0.35	0.38
Mg	57.9	57.1	56.2	55.4	31.5	59.1	51.2	57.4	34.8	41.4	50.6	57.9	45.2	44.6	33.8	52.3	45.5
(Fe2+)+Mn	26.9	27.7	26.3	31.9	32.9	22.3	31.7	30.6	38.1	38.7	35.1	26.1	35.8	37.7	43.0	29.1	34.3
Na	15.2	15.2	17.5	12.8	35.6	18.6	17.1	12.0	27.1	19.9	14.3	16.0	19.1	17.7	23.2	18.6	20.2
Mg#	69.5	68.7	69.5	64.9	50.5	74.0	63.5	66.5	49.5	53.1	60.3	70.3	56.6	55.4	45.2	65.5	58.4

Table 6.6 (suite).

SAMPLE	BK424	BK430	BK436	BK437	HOL14	HOL14	HOL14	HOL14	HOL14	HOL14	HOL14	HOL14	HOL14	HOL14	HOL14
Type	HOL14	2 liq	HOL14	2 liq									Meso, gg	mph, gg	mph, bg
# of analyses	KHP95	KHP95	KHP95	KHP95	3	3	2	1	4	3	4	1	P89a	P89a	P89a
Composition	100/0	90/10	100/0	90/10	cpx1-c.	cpx2-c.	cpx3-c.	cpx4-c.	cpx1-r.	cpx2-r.	cpx3-r.	incl. in ne.			
Pressure	106	108	106	108											
Temperature	750	700	750	700											
SiO2	50.35	51.56	50.99	51.04	50.68	50.59	50.33	49.91	49.75	50.37	49.95	48.33	50.46	50.68	51.73
TiO2	0.65	0.46	0.71	0.61	0.44	0.46	0.38	0.73	1.21	0.43	0.65	1.90	0.62	1.86	0.38
Al2O3	0.90	0.42	1.00	0.52	0.55	0.65	0.89	1.05	0.48	0.61	1.08	2.05	1.32	0.61	0.36
Fe2O3	7.97	12.31	13.11	16.25	8.79	9.54	9.56	8.63	23.12	9.32	8.91	8.95	8.74	16.39	14.46
FeO	10.11	10.75	9.83	8.67	8.82	8.47	8.65	9.29	2.79	9.42	9.87	6.07	10.61	7.38	9.01
MnO	0.45	0.83	0.49	0.66	0.57	0.59	0.69	0.42	0.42	0.74	0.59	0.51	0.57	0.37	0.43
MgO	6.35	4.11	4.34	2.90	7.59	7.20	7.34	7.38	2.76	6.76	6.63	9.03	6.74	3.91	4.60
CaO	19.31	13.68	15.28	12.10	19.83	19.47	19.28	20.04	11.27	19.46	19.49	21.04	19.36	11.56	13.75
Na2O	3.12	5.73	5.35	7.10	2.73	3.03	2.89	2.54	8.19	2.90	2.81	2.13	2.78	7.08	5.81
	Structural formula for O =12.														
Si	3.91	4.00	3.91	3.96	3.90	3.89	3.88	3.85	3.85	3.89	3.86	3.70	3.86	3.92	3.98
Al	0.08	0.00	0.09	0.04	0.05	0.06	0.08	0.10	0.04	0.06	0.10	0.19	0.12	0.06	0.02
Al	0.00	0.04	0.00	0.00	0.00	0.00	0.00	0.00	0.00	0.00	0.00	0.00	0.00	0.00	0.01
Fe3+	0.49	0.77	0.81	1.04	0.51	0.55	0.55	0.50	1.35	0.54	0.52	0.52	0.50	0.95	0.84
Ti	0.04	0.03	0.04	0.04	0.03	0.03	0.02	0.04	0.07	0.03	0.04	0.11	0.04	0.11	0.02
Mg	0.74	0.48	0.50	0.34	0.87	0.83	0.84	0.85	0.32	0.78	0.77	1.03	0.77	0.45	0.53
Fe2+	0.64	0.65	0.58	0.47	0.57	0.55	0.56	0.60	0.18	0.61	0.64	0.39	0.68	0.48	0.58
Mn	0.03	0.04	0.03	0.04	0.04	0.04	0.05	0.03	0.03	0.05	0.04	0.03	0.04	0.02	0.03
Ca	1.61	1.14	1.25	1.01	1.64	1.61	1.59	1.66	0.94	1.61	1.62	1.73	1.59	0.96	1.13
Na	0.47	0.86	0.80	1.07	0.41	0.45	0.43	0.38	1.23	0.44	0.42	0.32	0.41	1.06	0.87
Mg	39.3	23.4	28.1	17.5	46.2	44.3	44.9	45.7	18.2	41.7	41.0	58.3	40.5	22.4	26.4
(Fe2+)+Mn	35.6	34.1	32.0	27.0	32.1	31.4	32.1	33.8	11.9	35.1	36.4	23.9	37.7	24.9	30.4
Na	25.1	42.5	41.9	55.6	21.6	24.3	23.0	20.5	70.0	23.2	22.6	17.8	21.7	52.6	43.3
Mg#	52.8	40.5	44.0	37.4	60.5	60.2	60.2	58.6	63.8	56.2	54.5	72.6	53.1	48.6	47.6

Table 6.7: Major element microprobe analyses of melanite garnet from the experiments on the HOL14/OL5 join, and from natural erupted wollastonite nephelinite HOL14.

SAMPLE	CP74	CP72	CP110	CP40	CP60	CP46	CP54	CP109	CP21	CP102	CP97	CP8	CP66	CP67	CP7	CP117
# of analyses	1	2	2	3	2	3	2	2	2	2	2	2	2	2	3	4
Type	HOL14	HOL14	HOL14	HOL14	HOL14	HOL14	HOL14	2 liq	2 liq	2 liq	2 liq	2 liq	2 liq	2 liq	2 liq	LC
Composition	100/0	100/0	100/0	100/0	100/0	100/0	100/0	80/20	90/10	80/20	20/80	90/10	80/20	70/30	50/50	10/90
Pressure	100	100	20	20	20	20	20	200	100	100	100	103	100	100	103	100
Temperature	800	700	900	850	800	750	700	750	900	800	750	700	700	700	700	700
SiO2	30.84	31.55	30.86	30.69	30.08	30.48	29.86	30.44	29.58	28.59	29.32	30.46	29.81	30.17	29.21	30.10
TiO2	11.80	10.96	10.80	11.67	11.57	11.76	12.24	11.80	13.89	14.29	13.37	12.40	12.23	12.18	12.66	12.71
Al2O3	0.89	0.84	0.64	0.98	0.84	0.99	0.84	0.79	0.99	0.69	0.84	0.83	1.03	0.69	0.98	0.86
Fe2O3t	24.24	24.09	25.00	24.04	24.24	24.06	24.14	24.30	22.37	23.61	23.62	23.46	24.02	23.83	23.60	23.40
MnO	0.30	0.35	0.40	0.32	0.34	0.30	0.39	0.40	0.47	0.49	0.30	0.34	0.29	0.39	0.35	0.30
MgO	0.40	0.35	0.50	0.59	0.59	0.63	0.59	0.50	0.70	0.79	0.69	0.55	0.54	0.49	0.60	0.58
CaO	31.14	31.16	31.31	31.15	31.75	31.17	31.49	31.33	31.68	30.85	31.36	31.20	31.43	31.75	31.85	31.50
Na2O	0.40	0.69	0.50	0.42	0.49	0.46	0.44	0.45	0.24	0.69	0.50	0.66	0.54	0.49	0.68	0.54
K2O	b.d.	b.d.	b.d.	0.13	0.10	0.14	b.d.	b.d.	0.08	b.d.	b.d.	0.09	0.10	b.d.	0.08	b.d.
	Structural formula for O = 12.															
Si	2.59	2.65	2.60	2.58	2.54	2.56	2.52	2.56	2.49	2.42	2.47	2.56	2.51	2.54	2.47	2.53
Al	0.09	0.08	0.08	0.10	0.08	0.10	0.08	0.08	0.10	0.07	0.08	0.08	0.10	0.07	0.10	0.08
Ti	0.32	0.27	0.34	0.33	0.38	0.34	0.40	0.36	0.41	0.51	0.44	0.36	0.38	0.39	0.43	0.38
Fe3+	1.53	1.52	1.58	1.52	1.54	1.52	1.53	1.54	1.42	1.50	1.50	1.48	1.52	1.51	1.50	1.48
Ti	0.42	0.42	0.35	0.41	0.36	0.40	0.38	0.39	0.46	0.40	0.41	0.43	0.39	0.38	0.37	0.42
Mg	0.05	0.04	0.06	0.07	0.07	0.08	0.07	0.06	0.09	0.10	0.09	0.07	0.07	0.06	0.08	0.07
Mn	0.02	0.02	0.03	0.02	0.02	0.02	0.03	0.03	0.03	0.04	0.02	0.02	0.02	0.03	0.02	0.02
Ca	2.80	2.80	2.83	2.80	2.87	2.81	2.85	2.83	2.85	2.80	2.83	2.81	2.84	2.87	2.89	2.84
Na	0.06	0.11	0.08	0.07	0.06	0.07	0.07	0.07	0.04	0.11	0.08	0.11	0.09	0.08	0.11	0.09
K	0.00	0.00	0.00	0.01	0.01	0.02	0.00	0.00	0.01	0.00	0.00	0.01	0.01	0.00	0.01	0.00
Fe3+	64.8	66.2	67.9	64.6	65.3	64.4	64.0	65.1	59.2	60.6	61.7	63.1	63.4	64.3	62.4	62.5
Al	3.7	3.6	2.7	4.1	3.5	4.2	3.5	3.3	4.1	2.8	3.4	3.5	4.3	2.9	4.1	3.6
Ti	31.5	30.1	29.3	31.3	31.2	31.5	32.5	31.6	36.7	36.7	34.9	33.4	32.3	32.8	33.5	33.9

Note: Pressure is in MPa, temperature in oC, and starting composition is shown as proportion of wollastonite nephelinite HOL14/silicate-bearing natrocarbonatite OL5 (in wt. %).
Types of experiments are HOL14-experiments, silicate liquid (LS)-experiments, two-liquid (2 liq)-experiments and carbonate liquid (LC)-experiments.
For this study, totals are recalculated to 100 wt. %. Numbers of ions on the basis of 12 oxygens. Fe3+, Al and Ti are normalized molar proportions. Abbreviations used are:
b.d.: below detection; Ph: phenocryst; mph: microphenocryst; c: core; r: rim. Sources for additional data: KHP95: Kjarsgaard et al. (1995).

Table 6.7 (suite)

SAMPLE	CP2	CP1	CP11	CP68	CP69	CP10	CP130	CP15	CP113	CP14	CP122	CP123	CP114	CP81	CP48	CP50
# of analyses	2	1	1	1	2	2	1	2	2	2	1	4	1	1	2	1
Type	2 liq	2 liq	2 liq	2 liq	2 liq	2 liq	LC	LS	2 liq	2 liq	2 liq	2 liq	LC	LC	2 liq	2 liq
Composition	90/10	50/50	90/10	80/20	70/30	50/50	20/80	90/10	80/20	50/50	40/60	30/70	20/80	10/90	90/10	50/50
Pressure	40	40	40	40	40	40	20	20	20	20	20	20	20	20	20	20
Temperature	800	800	700	700	700	700	850	800	800	800	800	800	800	775	750	750
SiO2	28.77	30.65	29.42	30.50	30.10	30.84	29.11	30.29	30.77	29.25	29.37	30.05	28.91	31.23	32.44	29.67
TiO2	13.28	11.87	13.39	11.49	12.14	11.44	14.53	12.39	10.84	13.93	13.43	12.02	13.56	11.48	11.09	13.04
Al2O3	0.89	0.85	0.67	0.79	0.89	0.91	1.23	0.68	0.80	1.04	0.76	0.77	1.09	0.41	0.77	1.08
Fe2O3t	23.27	23.96	23.20	24.65	24.02	23.78	22.43	23.84	24.69	22.07	24.05	24.38	22.88	21.83	23.73	23.86
MnO	0.39	0.50	0.36	0.40	0.30	0.21	0.00	0.42	0.30	0.31	b.d.	0.39	0.40	0.52	0.34	0.29
MgO	0.57	0.37	0.55	0.50	0.59	0.51	0.77	0.51	0.50	0.68	0.73	0.61	0.89	0.83	0.49	0.49
CaO	32.24	31.16	31.94	31.68	31.48	31.89	31.32	31.44	31.56	31.71	31.66	31.24	31.88	32.16	30.52	31.08
Na2O	0.59	0.47	0.33	b.d.	0.39	0.37	0.60	0.39	0.55	0.92	b.d.	0.54	0.40	1.24	0.53	0.48
K2O	b.d.	0.16	0.15	b.d.	0.10	0.05	b.d.	0.03	b.d.	0.09	b.d.	b.d.	b.d.	0.31	0.09	b.d.
	Structural formula for O = 12.															
Si	2.44	2.58	2.48	2.57	2.54	2.59	2.45	2.55	2.59	2.46	2.47	2.53	2.44	2.63	2.70	2.50
Al	0.09	0.08	0.07	0.08	0.09	0.09	0.12	0.07	0.08	0.10	0.08	0.08	0.11	0.04	0.08	0.11
Ti	0.47	0.34	0.45	0.35	0.38	0.32	0.43	0.38	0.33	0.43	0.45	0.39	0.45	0.33	0.22	0.40
Fe3+	1.48	1.52	1.47	1.56	1.52	1.50	1.42	1.51	1.57	1.40	1.52	1.55	1.45	1.38	1.49	1.51
Ti	0.37	0.41	0.40	0.37	0.39	0.40	0.48	0.40	0.36	0.45	0.40	0.37	0.41	0.39	0.47	0.43
Mg	0.07	0.05	0.07	0.06	0.07	0.06	0.10	0.06	0.06	0.09	0.09	0.08	0.11	0.10	0.06	0.06
Mn	0.03	0.04	0.03	0.03	0.02	0.01	0.00	0.03	0.02	0.02	0.00	0.03	0.03	0.04	0.02	0.02
Ca	2.93	2.81	2.89	2.86	2.84	2.87	2.82	2.84	2.85	2.86	2.86	2.82	2.88	2.90	2.72	2.80
Na	0.10	0.08	0.05	0.00	0.06	0.06	0.10	0.06	0.09	0.15	0.00	0.09	0.06	0.20	0.09	0.08
K	0.00	0.02	0.02	0.00	0.01	0.01	0.00	0.00	0.00	0.01	0.00	0.00	0.00	0.03	0.01	0.00
Fe3+	61.3	64.5	61.7	66.0	64.0	64.9	57.7	63.9	67.2	58.7	62.2	64.9	60.0	64.3	65.9	61.8
Al	3.7	3.6	2.8	3.3	3.7	3.9	5.0	2.9	3.4	4.3	3.1	3.2	4.5	1.9	3.4	4.4
Ti	35.0	31.9	35.6	30.7	32.3	31.2	37.4	33.2	29.5	37.0	34.7	32.0	35.5	33.8	30.8	33.8

Table 6.7 (suite).

SAMPLE	CP124	CP125	CP115	CP55	CP17	CP64	CP16	CP65	BK424	BK430	BK436	BK437
# of analyses	1	2	1	2	2	1	1	2	HOL14	2 liq	HOL14	2 liq
Type	2 liq	LC	LC	LS	2 liq	2 liq	LC	LC	KPH95	KPH95	KPH95	KPH95
Composition	40/60	30/70	20/80	95/5	90/10	80/20	50/50	50/50	100/0	90/10	100/0	90/10
Pressure	20	20	20	20	20	20	20	20	106	106	108	108
Temperature	750	750	750	700	700	700	700	700	750	750	700	700
SiO2	29.25	29.33	29.01	29.93	30.15	30.74	29.12	29.72	28.27	30.04	28.73	30.10
TiO2	14.38	13.51	14.57	11.86	12.42	10.64	14.03	12.85	13.48	11.07	12.68	11.47
Al2O3	0.61	0.86	1.20	0.83	0.83	1.08	0.61	0.98	1.05	0.09	0.87	0.37
Fe2O3t	23.12	23.36	22.67	24.42	23.41	24.42	22.67	23.54	21.68	23.66	23.27	23.52
MnO	b.d.	0.41	0.37	0.34	0.45	0.39	0.31	0.20	0.32	0.34	0.41	0.38
MgO	0.69	0.59	0.75	0.59	0.53	0.49	0.76	0.44	0.48	0.42	0.44	0.31
CaO	31.21	31.29	31.43	31.35	31.57	31.83	31.96	31.73	31.12	32.22	30.83	32.02
Na2O	0.73	0.63	b.d.	0.49	0.60	0.39	0.50	0.44	0.64	0.62	0.32	1.05
K2O	b.d.	b.d.	b.d.	0.20	0.05	b.d.	0.04	0.10	0.14	0.16	0.14	0.19
	Structural formula for O = 12.											
Si	2.46	2.47	2.44	2.53	2.54	2.59	2.46	2.50	2.46	2.58	2.48	2.56
Al	0.06	0.09	0.12	0.06	0.08	0.11	0.06	0.10	0.11	0.01	0.09	0.04
Ti	0.48	0.44	0.44	0.39	0.38	0.30	0.48	0.40	0.44	0.41	0.43	0.40
Fe3+	1.47	1.48	1.43	1.55	1.48	1.55	1.44	1.49	0.11	0.01	0.09	0.04
Ti	0.44	0.42	0.48	0.36	0.41	0.37	0.41	0.42	0.44	0.30	0.40	0.34
Mg	0.09	0.07	0.09	0.07	0.07	0.06	0.10	0.06	0.06	0.05	0.06	0.04
Mn	0.00	0.03	0.03	0.02	0.03	0.03	0.02	0.01	0.02	0.02	0.03	0.03
Ca	2.82	2.83	2.83	2.84	2.85	2.87	2.89	2.86	2.90	2.96	2.86	2.92
Na	0.12	0.10	0.00	0.08	0.10	0.06	0.08	0.07	0.11	0.10	0.05	0.17
K	0.00	0.00	0.00	0.02	0.01	0.00	0.00	0.01	0.02	0.02	0.02	0.02
Fe3+	60.1	61.1	57.9	65.0	63.1	66.4	60.2	62.1	58.9	67.9	62.4	66.1
Al	2.5	3.5	4.8	3.5	3.5	4.6	2.5	4.1	4.5	0.4	3.7	1.6
Ti	37.4	35.3	37.2	31.6	33.4	28.9	37.3	33.9	36.6	31.7	34.0	32.2

Table 6.7 (suite)

SAMPLE	HOL14	HOL14	HOL14	HOL14	HOL14	HOL14
# of analyses	2	3	1	mph	Ph-c.	Ph-r.
Type				KHP95	KHP95	KHP95
Composition	gt1,core	gt1,rim	gt2			
Pressure						
Temperature						
SiO2	29.28	30.36	30.77	29.54	29.02	30.37
TiO2	13.73	11.51	11.48	12.06	14.57	11.71
Al2O3	0.76	0.93	1.04	1.02	0.73	0.93
Fe2O3t	22.90	24.21	24.58	23.86	22.21	23.95
MnO	0.40	0.39	0.49	0.36	0.31	0.30
MgO	0.63	0.57	0.61	0.52	0.75	0.38
CaO	31.71	31.48	30.40	31.61	31.72	31.29
Na2O	0.59	0.54	0.63	0.42	0.43	0.57
K2O	b.d.	b.d.	b.d.	0.00	0.02	0.10
	Structural formula for O = 12.					
Si	2.47	2.56	2.56	2.51	2.45	2.57
Al	0.08	0.09	0.10	0.10	0.07	0.09
Ti	0.45	0.35	0.34	0.39	0.48	0.34
Fe3+	1.45	1.53	1.54	0.10	0.07	0.09
Ti	0.42	0.38	0.37	0.38	0.45	0.40
Mg	0.08	0.07	0.08	0.07	0.09	0.05
Mn	0.03	0.03	0.03	0.03	0.02	0.02
Ca	2.87	2.84	2.84	2.88	2.87	2.83
Na	0.10	0.09	0.10	0.07	0.07	0.09
K	0.00	0.00	0.00	0.00	0.00	0.01
Fe3+	60.6	65.1	65.2	63.6	58.6	64.5
Al	3.1	3.9	4.3	4.3	3.0	3.9
Ti	36.3	30.9	30.5	32.1	38.4	31.5

Table 6.8: Major element microprobe analyses of wollastonite from the experiments on the HOL14/OL5 join, and from natural erupted wollastonite nephelinite HOL14.

SAMPLE	CP38	CP110	CP46	CP5	CP8	CP31	CP19	CP2	CP27	CP1	CP11	CP68	CP10	CP23	CP91	CP42	CP43
Type	HOL14	HOL14	HOL14	2 liq	2 liq	2 liq	2 liq	2 liq	2 liq	2 liq	2 liq	2 liq	2 liq	LS	2 liq	LS	2 liq
# of analyses	1	1	1	1	2	1	2	2	1	1	2	1	2	2	1	2	2
Composition	100/0	100/0	100/0	90/10	90/10	90/10	90/10	90/10	90/10	50/50	90/10	80/20	50/50	90/10	80/20	90/10	70/30
Pressure	100	20	20	100	103	100	40	40	40	40	40	40	40	20	20	20	20
Temperature	900	900	750	800	700	700	900	800	800	800	700	700	700	900	900	850	850
Others						Buf.			Buf.								
SiO2	51.35	51.59	50.57	51.39	51.38	52.39	50.37	52.72	51.18	50.78	51.20	51.13	50.67	51.38	51.64	51.79	52.14
Al2O3	b.d.	b.d.	0.20	0.24	0.05	b.d.	0.56	1.29	0.18	0.02	0.02	b.d.	0.10	0.43	b.d.	1.45	0.19
Fe2O3	0.72	0.00	1.67	0.41	0.95	0.00	1.17	0.00	1.19	0.77	1.30	1.18	1.65	1.30	0.00	1.51	0.00
FeO	0.38	1.49	0.00	1.39	0.11	0.83	0.00	1.61	0.32	0.00	0.00	0.13	0.00	0.00	1.29	0.20	0.68
MnO	0.31	0.30	0.60	0.60	0.73	0.45	0.49	0.37	0.55	0.47	0.35	0.30	0.76	0.33	0.50	b.d.	0.48
MgO	b.d.	0.20	b.d.	0.16	0.07	0.06	0.19	0.15	0.07	0.19	0.11	0.30	0.09	0.17	b.d.	0.21	b.d.
CaO	47.14	46.42	46.86	45.39	46.04	46.06	46.36	41.78	45.63	47.16	46.27	46.97	45.85	45.44	46.58	43.30	45.94
Na2O	b.d.	b.d.	b.d.	0.04	0.18	0.01	0.25	1.05	0.14	0.19	0.32	b.d.	0.28	0.26	b.d.	0.73	b.d.
K2O	0.10	b.d.	0.10	0.24	0.11	0.05	0.36	0.60	0.24	0.08	0.17	b.d.	0.29	0.41	b.d.	0.83	b.d.
SrO	b.d.	b.d.	b.d.	0.14	0.35	0.16	0.24	0.45	0.50	0.34	0.24	b.d.	0.31	0.29	b.d.	b.d.	0.58
	Structural formula for O = 12.																
Si	3.98	4.00	3.94	3.99	3.99	4.04	3.92	4.06	3.98	3.95	3.98	3.97	3.95	3.98	4.01	3.99	4.03
Al	0.00	0.00	0.02	0.02	0.01	0.00	0.05	0.12	0.02	0.00	0.00	0.00	0.01	0.04	0.00	0.13	0.02
Fe3+	0.04	0.00	0.10	0.02	0.06	0.00	0.07	0.00	0.07	0.05	0.08	0.07	0.10	0.08	0.00	0.09	0.00
Mg	0.00	0.02	0.00	0.02	0.01	0.01	0.02	0.02	0.01	0.02	0.01	0.03	0.01	0.02	0.00	0.02	0.00
Fe2+	0.02	0.10	0.00	0.09	0.01	0.05	0.00	0.10	0.02	0.00	0.00	0.01	0.00	0.00	0.08	0.01	0.04
Mn	0.02	0.02	0.04	0.04	0.05	0.03	0.03	0.02	0.04	0.03	0.02	0.02	0.05	0.02	0.03	0.00	0.03
Ca	3.92	3.86	3.91	3.78	3.83	3.81	3.87	3.44	3.80	3.93	3.85	3.90	3.83	3.77	3.87	3.57	3.81
Na	0.00	0.00	0.00	0.01	0.03	0.00	0.04	0.16	0.02	0.03	0.05	0.00	0.04	0.04	0.00	0.11	0.00
K	0.01	0.00	0.01	0.02	0.01	0.00	0.04	0.06	0.02	0.01	0.02	0.00	0.03	0.04	0.00	0.08	0.00
Sr	0.00	0.00	0.00	0.01	0.02	0.01	0.01	0.02	0.02	0.02	0.01	0.00	0.01	0.01	0.00	0.00	0.03

Note: Pressure is in MPa, temperature in oC, and starting composition is shown as proportion of wollastonite nephelinite HOL14/silicate-bearing natrocarbonatite OL5 (in wt. %). Types of experiments are HOL14-experiments, silicate liquid (LS)-experiments, two-liquid (2 liq)-experiments and carbonate liquid (LC)-experiments. For this study, totals are recalculated to 100 wt. %. FeO and Fe2O3 determined by stoichiometry utilizing the method of Droop (1987). Abbreviations used are: b.d.: below detection; Ph: phenocryst; mph: microphenocryst; c: core; r: rim; Buf.: buffered. Sources for additional data are: P89a: Peterson (1989a) and KHP95: Kjarsgaard et al. (1995).

Table 6.8 (suite).

SAMPLE	CP53	CP130	CP15	CP113	CP14	CP81	CP48	CP124	CP125	CP17	CP64	BK436	BK437	HOL14	HOL14	HOL14
Type	2 liq	LC	LS	2 liq	2 liq	LC	2 liq	2 liq	LC	2 liq	2 liq	HOL14	2 liq			
# of analyses	1	3	1	1	2	1	1	1	2		1	KPH95	KPH95	KHP95	KHP95	P89a
Composition	50/50	20/80	90/10	80/20	50/50	10/90	90/10	40/60	30/70	90/10	80/20	100/0	90/10	Ph	mph.	Ph.
Pressure	20	20	20	20	20	20	20	20	20	20	20	108	108			
Temperature	850	850	800	800	800	775	750	750	750	700	700	700	700			
Others																
SiO2	51.70	51.45	51.08	52.00	51.39	51.94	51.37	51.51	51.38	51.53	51.68	50.88	49.61	51.06	50.94	50.77
Al2O3	b.d.	b.d.	0.29	b.d.	0.03	0.20	b.d.	b.d.	b.d.	1.48	b.d.	0.03	0.21	0.03	0.04	0.03
Fe2O3	0.88	0.55	1.56	0.00	1.08	0.00	0.82	0.48	1.17	2.91	0.00	0.95	0.00	0.00	0.03	0.45
FeO	0.19	0.00	0.00	0.93	0.00	0.40	0.33	0.16	0.00	0.04	0.49	0.00	1.22	0.98	1.30	0.55
MnO	0.78	0.53	0.48	b.d.	0.32	0.50	0.29	0.59	0.73	0.73	0.30	0.38	0.33	0.04	0.42	0.00
MgO	b.d.	b.d.	0.20	b.d.	0.10	b.d.	b.d.	0.20	b.d.	0.09	b.d.	0.00	0.00	0.06	0.06	0.14
CaO	45.96	46.87	45.43	47.08	46.41	46.97	46.99	46.97	46.10	40.27	47.53	45.87	47.18	47.21	46.52	46.61
Na2O	0.29	0.40	0.29	b.d.	0.31	b.d.	b.d.	b.d.	0.44	1.09	b.d.	0.05	0.30	0.08	0.07	0.05
K2O	0.19	0.20	0.39	b.d.	0.18	b.d.	0.19	0.10	0.18	1.15	b.d.	0.09	0.20	0.03	0.13	0.02
SrO	b.d.	b.d.	0.29	b.d.	0.18	b.d.	b.d.	b.d.	b.d.	0.71	b.d.			0.00	0.00	
	Structural formula for O = 12.															
Si	4.01	3.99	3.97	4.02	3.99	4.01	3.99	3.99	3.99	3.99	4.00	4.01	3.91	3.98	3.97	3.99
Al	0.00	0.00	0.03	0.00	0.00	0.02	0.00	0.00	0.00	0.13	0.00	0.00	0.02	0.00	0.00	0.00
Fe3+	0.05	0.03	0.09	0.00	0.06	0.00	0.05	0.03	0.07	0.17	0.00	0.00	0.07	0.06	0.08	0.03
Mg	0.00	0.00	0.02	0.00	0.01	0.00	0.00	0.02	0.00	0.01	0.00	0.00	0.00	0.01	0.01	0.02
Fe2+	0.01	0.00	0.00	0.06	0.00	0.03	0.02	0.01	0.00	0.00	0.03	0.06	0.00	0.00	0.00	0.03
Mn	0.05	0.03	0.03	0.00	0.02	0.03	0.02	0.04	0.05	0.05	0.02	0.03	0.02	0.00	0.03	0.00
Ca	3.82	3.90	3.78	3.90	3.86	3.89	3.91	3.90	3.83	3.34	3.94	3.88	3.99	3.94	3.89	3.92
Na	0.04	0.06	0.04	0.00	0.05	0.00	0.00	0.00	0.07	0.16	0.00	0.01	0.05	0.01	0.01	0.01
K	0.02	0.02	0.04	0.00	0.02	0.00	0.02	0.01	0.02	0.11	0.00	0.01	0.02	0.00	0.01	0.00
Sr	0.00	0.00	0.01	0.00	0.01	0.00	0.00	0.00	0.00	0.03	0.00	0.00	0.00	0.00	0.00	0.00

Table 6.9. Major element microprobe analyses of apatite from the experiments on the HOL14/OL5 join, and from natural ijolite BD7.

Sample	CP38	CP21	CP31	CP7	CP19	CP27	CP23	CP42	CP64	CP64	BD7
Type	HOL14	2 liq	2 liq	2 liq	2 liq	2 liq	LS	LS	2 liq	2 liq	Ijolite
# of analyses	3	1	1	1	1	1	1	1	1	2	DSS95
Composition	100/0	90/10	90/10	50/50	90/10	90/10	90/10	90/10	80/20	80/20	
Pressure	100	100	100	103	40	40	20	20	20	20	
Temperature	900	900	700	700	900	800	900	850	700	700	
Others			Buffered			Buffered					
SiO2	0.37	0.49	0.55	0.69	0.72	0.88	2.49	0.3	0.5	0.60	0.8
FeO	0.43	0.19	0.10	0.21	0.50	0.19	0.52	0.4	b.d	b.d.	
MnO	b.d.	0.12	0.08	0.01	0.04	0.02	0.07	b.d	b.d	b.d.	
MgO	b.d.	b.d.	b.d.	b.d.	b.d.	b.d.	b.d.	b.d	b.d	b.d.	
CaO	54.07	53.96	55.02	53.13	54.90	54.05	50.99	53.9	54.9	55.10	54.1
Na2O	b.d.	0.06	0.18	0.45	0.17	0.23	0.59	b.d	b.d	b.d.	0.09
K2O	0.10	0.18	0.01	0.08	0.22	0.25	0.25	0.2	.0<	b.d.	
P2O5	40.93	39.50	39.04	38.87	38.48	38.60	38.39	40.2	40.8	40.50	40.1
F	3.63	3.43	2.21	2.02	2.11	2.78	3.14	4.3	2.8	2.80	1.38
Cl	b.d.	0.04	0.03	0.02	0.05	b.d.	0.01	b.d	b.d	b.d.	0.03
BaO	b.d.	b.d.	b.d.	0.04	b.d.	b.d.	b.d.	2	2	b.d.	
SrO	1.27	1.74	0.91	1.62	0.99	1.63	3.69	b.d	b.d	1.70	
La2O3								0.14	0.32		0.08
Ce2O3								b.d	0.7		0.14
Total	100.80	99.71	98.13	97.14	98.18	98.63	100.14	101.30	101.00	100.70	96.72
Total-O=F,Cl	99.27	98.26	97.19	96.28	97.28	97.46	98.82	99.49	99.82	99.52	96.13

Note: Pressure is in MPa, temperature in oC, and starting composition is shown as proportion of wollastonite nephelinite HOL14/silicate-bearing natrocarbonatite OL5 (in wt. %). Types of experiments are HOL14-experiments, silicate liquid (LS)-experiments and two-liquid (2 liq)-experiments. Abbreviations used are: b.d.: below detection. Sources for additional data: DSS95: Dawson et al. (1995c).

Table 6.10: Major element microprobe analyses of titanite from the experiments on the HOL14/OL5 join, from natural wollastonite nephelinite HOL14 and from ijolite BD7.

SAMPLE	CP54	CP11	CP10	CP64	HOL14	BD35
Type	HOL14	2 liq	2 liq	2 liq		Ijolite
# of analyses	1	1	1	1	6	DSS95
Composition	100/0	90/10	50/50	80/20		
Pressure	20	40	40	20		
Temperature	700C	700C	700C	700C		
SiO2	30.60	30.53	30.98	30.50	30.03	29.7
TiO2	37.70	38.31	39.30	37.70	37.16	36.6
Al2O3	0.50	0.53	0.22	0.30	0.38	0.41
Fe2O3	0.00	1.94	0.07	0.00	0.00	0.84
FeO	2.00	0.00	1.61	1.80	1.76	0.88
MnO	b.d.	0.25	b.d.	b.d.	b.d.	
MgO	b.d.	b.d.	b.d.	b.d.	b.d.	
CaO	28.30	27.66	28.08	28.40	27.97	28.0
Na2O	b.d.	0.33	0.31	b.d.	b.d.	0.11
K2O	b.d.	0.14	0.05	b.d.	b.d.	
F	0.30	0.22	0.34	b.d.		
Total	99.40	99.91	100.97	98.70	97.30	96.54
Total -O=F	99.27	99.82	100.82	98.70	97.30	96.54
	Structural formula for Si = 4.					
Si	4.00	4.00	4.00	4.00	4.00	4.00
Al	0.08	0.08	0.03	0.05	0.06	0.07
Fe3+	0.00	0.19	0.01	0.00	0.00	0.09
Ti	3.71	3.78	3.82	3.72	3.72	3.71
Mg	0.00	0.00	0.00	0.00	0.00	0.00
Fe2+	0.22	0.00	0.17	0.20	0.20	0.10
Mn	0.00	0.03	0.00	0.00	0.00	0.00
Na	0.00	0.08	0.08	0.00	0.00	0.03
Ca	3.96	3.88	3.88	3.99	3.99	4.04
K	0.00	0.02	0.01	0.00	0.00	0.00
F	0.12	0.09	0.14	0.00	0.00	0.00

Note: Pressure is in MPa, temperature in oC, and starting composition is shown as proportion of wollastonite nephelinite HOL14/silicate-bearing natrocarbonatite OL5 (in wt. %).
Types of experiments are HOL14-experiments and two-liquid (2 liq)-experiments.
FeO and Fe2O3 determined by stoichiometry utilizing the method of Droop (1987).
Abbreviations used are: b.d.: below detection.
Sources for additional data: DSS95: Dawson et al. (1995c).

Table 6.11: Major element microprobe analyses of spinel from the experiments on the HOL14/OL5 join.

SAMPLE	CP74	CP60	CP81	CP50
Type	HOL14	HOL14	LC	2 liq
# of analyses	1	1	4	2
Composition	100/0	100/0	10/90	50/50
Pressure	100	20	20	20
Temperature	800	800	775	750
SiO2	2.30	7.80	0.63	2.01
TiO2	0.56	1.26	3.47	1.94
Al2O3	1.10	3.60	0.25	0.39
Fe2O3	64.21	57.34	62.95	63.04
FeO	30.32	25.40	28.96	29.48
MnO	0.70	0.60	2.40	0.92
MgO	0.50	0.40	0.75	0.49
CaO	0.60	1.30	0.35	0.47
Na2O	0.60	3.60	0.53	0.87
TOTAL	100.89	101.30	100.29	99.61
	Structural formula for O = 32.			
Si	0.68	2.16	0.19	0.61
Al	0.39	1.17	0.09	0.14
Fe3+	14.35	11.92	14.27	14.28
Ti	0.13	0.26	0.79	0.44
Mg	0.22	0.17	0.34	0.22
Fe2+	7.53	5.87	7.30	7.42
Mn	0.18	0.14	0.61	0.24
Ca	0.19	0.39	0.11	0.15
Na	0.35	1.93	0.31	0.51

Note: Pressure is in MPa, temperature in oC, and starting composition is shown as proportion of wollastonite nephelinite HOL14/silicate-bearing natrocarbonatite OL5 (in wt. %).
Types of experiments are HOL14-experiments, two-liquid (2 liq)-experiments and carbonate liquid (LC)-experiments. Numbers of ions on the basis of 32 oxygens. FeO and Fe2O3 determined by stoichiometry utilizing the method of Droop (1987).

Table 6.12: Major element microprobe analyses of feldspar from the experiments on the HOL14/OL5 join.

SAMPLE	CP46	CP8	BK426	BK429
Type	HOL14	2 liq	HOL14	2 liq
# of analyses	1	2	KHP95	KHP95
Composition	100/0	90/10	100/0	95/5
Pressure	20	103	51	108
Temperature	750	700	700	700
Other			Open tube	
SiO2	62.1	63.88	62.94	61.14
TiO2	0.12	0.08		
Al2O3	17.7	17.87	16.46	18.6
FeOt	2.7	1.06	4.93	2.82
MnO	b.d.	0.07		
MgO	b.d.	0.03		
CaO	0.4	0.11	0.26	0.77
Na2O	2.2	1.66	3.53	2.18
K2O	10.4	14.49	11.18	13.06
BaO	1.2	1.67		
SrO	b.d.	0.02		
Total	96.82	100.91	99.30	98.57
	Structural formula for O = 32.			
Si	11.86	11.88	11.85	11.59
Ti	0.02	0.01		
Al	3.98	3.92	3.65	4.16
Fe	0.43	0.16	0.78	0.45
Mn		0.01		
Mg		0.01		
Ca	0.08	0.02	0.05	0.16
Na	0.81	0.60	1.29	0.80
K	2.53	3.44	2.69	3.16
Ba		0.12		
Sr	0.09	0.00		

Note: Pressure is in MPa, temperature in oC, and starting composition is shown as proportion of wollastonite nephelinite HOL14/silicate-bearing natrocarbonatite OL5 (in wt. %).
Types of experiments are HOL14-experiments and two-liquid (2 liq)-experiments.
Numbers of ions on the basis of 32 oxygens.
Abbreviations used are: b.d.: below detection.
Sources for additional data: KHP95: Kjarsgaard et al. (1995).

Table 6.13: Major element microprobe analyses of melilite from the experiments on the HOL14/OL5 join.

SAMPLE	CP19	CP23	CP91	CP22	CP121	CP111	CP82	CP52	CP43	CP53	CP130	CP131	CP113	CP14	CP122	CP123	CP114	CP81	CP115
Type	2 liq	LS	2 liq	2 liq	2 liq	2 liq	LC	2 liq	2 liq	2 liq	LC	LC	2 liq	2 liq	2 liq	LC	LC	LC	LC
# of analyses	1	2	2	5	1	1	2	2	4	2	2	2	2	7	4	4	1	1	1
Composition	90/10	90/10	80/20	50/50	30/70	20/80	10/90	80/20	70/30	50/50	20/80	10/90	80/20	50/50	40/60	30/70	20/80	10/90	20/80
Pressure (MPa)	40	20	20	20	20	20	20	20	20	20	20	20	20	20	20	20	20	20	20
Temperature	900	900	900	900	900	900	900	850	850	850	850	850	800	800	800	800	800	775	775
SiO2	43.06	43.38	44.15	42.93	43.40	42.94	42.89	44.46	43.54	44.37	43.19	42.99	43.01	42.61	43.09	42.99	43.08	43.70	42.76
Al2O3	7.64	6.85	7.73	7.29	6.86	7.21	7.68	7.38	7.56	6.68	5.99	7.48	6.40	6.45	6.01	6.27	6.67	6.90	6.28
FeOt	7.94	8.72	7.94	7.73	8.51	8.51	7.64	8.75	7.86	8.98	10.58	7.44	9.33	9.27	9.68	9.47	8.66	7.40	8.62
MnO	0.40	0.27	0.30	0.40	0.49	0.80	0.74	0.40	0.35	0.45	0.90	0.86	0.20	0.46	0.49	0.50	0.70	0.80	0.57
MgO	3.67	4.01	4.12	3.93	3.85	3.40	3.52	3.92	4.02	4.08	3.00	3.73	3.92	3.62	3.51	3.63	3.68	4.20	4.13
CaO	30.06	29.72	29.68	29.41	29.23	28.93	28.90	29.06	28.40	29.32	27.06	28.49	27.73	28.66	27.25	27.57	28.26	28.60	28.62
Na2O	5.65	5.42	5.98	5.83	5.59	5.81	5.75	5.84	5.60	5.87	6.79	6.26	6.05	6.11	6.57	6.36	5.97	5.90	5.49
K2O	b.d.	0.15	0.10	0.23	b.d.	0.30	0.20	0.19	0.12	0.24	0.30	0.22	0.15	0.22	0.24	0.23	0.10	b.d.	0.20
SrO	1.59	1.48	n.d.	2.26	2.05	2.10	2.68	n.d.	2.53	n.d.	2.20	2.53	3.22	2.60	3.15	2.98	2.89	2.50	3.34
	Structural formula for O = 7.																		
Si	2.00	2.02	2.02	2.00	2.02	2.01	2.00	2.04	2.02	2.05	2.04	2.01	2.02	2.01	2.04	2.03	2.02	2.03	2.02
Al	0.42	0.38	0.42	0.40	0.38	0.40	0.42	0.40	0.41	0.36	0.33	0.41	0.36	0.36	0.34	0.35	0.37	0.38	0.35
Mg	0.25	0.28	0.28	0.27	0.27	0.24	0.25	0.27	0.28	0.28	0.21	0.26	0.28	0.25	0.25	0.26	0.26	0.29	0.29
Fe2+	0.31	0.34	0.30	0.30	0.33	0.33	0.30	0.34	0.31	0.35	0.42	0.29	0.37	0.37	0.38	0.37	0.34	0.29	0.34
Mn	0.02	0.01	0.01	0.02	0.02	0.03	0.03	0.02	0.01	0.02	0.04	0.03	0.01	0.02	0.02	0.02	0.03	0.03	0.02
Na	0.51	0.49	0.53	0.53	0.50	0.53	0.52	0.52	0.50	0.53	0.62	0.57	0.55	0.56	0.60	0.58	0.54	0.53	0.50
Ca	1.50	1.48	1.46	1.47	1.46	1.45	1.45	1.43	1.41	1.45	1.37	1.43	1.40	1.45	1.38	1.39	1.42	1.42	1.45
K	0.00	0.01	0.01	0.01	0.00	0.02	0.01	0.01	0.01	0.01	0.02	0.01	0.01	0.01	0.01	0.01	0.01	0.00	0.01
Sr	0.04	0.04	0.00	0.06	0.06	0.06	0.07	0.00	0.07	0.00	0.06	0.07	0.09	0.07	0.09	0.08	0.08	0.07	0.09
Na	47.5	44.2	47.6	47.8	45.7	48.0	48.9	46.2	46.3	45.6	49.7	50.8	46.2	47.4	48.9	48.1	47.6	47.9	44.3
Fe2+	28.8	30.7	27.2	27.4	30.0	30.3	28.0	29.9	28.1	30.1	33.4	26.0	30.7	31.0	31.1	30.9	29.8	25.9	30.0
Mg	23.7	25.1	25.2	24.8	24.2	21.6	23.0	23.9	25.6	24.4	16.9	23.2	23.0	21.6	20.0	21.1	22.6	26.2	25.6

Note: Pressure is in MPa, temperature in oC, and starting composition is shown as proportion of wollastonite nephelinite HOL14/silicate-bearing natrocarbonatite OL5 (in wt. %). Types of experiments are silicate liquid (LS)-experiments, two-liquid (2 liq)-experiments and carbonate liquid (LC)-experiments.
Numbers of ions on the basis of 7 oxygens. Abbreviations used are: b.d.: below detection.

Table 6.14: Major element microprobe analyses of combeite from the experiments on the HOL14/OL5 join, and from natural lavas from Oldoinyo Lengai.

SAMPLE	CP78	CP122	CP123	CP124	CP125	CP16	CP65	BK432	BK417	HOL10	"8"	"9"
Type	LS	2 liq	LC	2 liq	LC	LC	LC	LS	LS	Comb. Ne.	Sil. natr.	Sil. natr.
# of analyses	2	9	5	3	2	3	6			P89a	DSS92	DSS92
Composition	90/10	40/60	30/70	40/60	30/70	50/50	50/50	HOL14-10	HOL6	Ph. gg		
Pressure	100	20	20	20	20	20	20	51	51			
Temperature	800	800	800	750	750	700	700	700	700			
Others	Open tube							Open tube	Open tube			
SiO2	51.20	51.56	51.72	51.39	51.45	50.07	51.40	50.27	50.54	50.89	50.02	50.50
FeO	1.55	0.62	0.51	0.82	0.75	1.17	1.03	1.64	2.13	1.39	0.26	0.40
MnO	0.35	0.54	0.56	0.64	0.65	0.61	0.72			0.52	0.28	0.32
MgO	0.30	0.28	0.30	0.20	0.30	0.07	0.20			0.26	0.07	0.24
CaO	27.85	29.24	29.67	28.37	28.75	27.43	27.83	24.39	25.46	25.15	28.16	27.15
Na2O	18.80	18.86	18.94	19.20	18.95	19.18	19.82	22.79	21.47	21.50	20.56	20.66
K2O	0.15	0.15	0.14	0.10	b.d.	0.17	b.d.	0.13	0.17	0.03	0.19	0.23
SrO						0.35						
TOTAL	100.20	101.25	101.84	100.72	100.85	99.05	101.00	99.22	99.77	99.74	99.54	99.50

Note: Pressure is in MPa, temperature in oC, and starting composition is shown as proportion of wollastonite nephelinite HOL14/silicate-bearing natrocarbonatite OL5 (in wt. %).
Types of experiments are silicate liquid (LS)-experiments, two-liquid (2 liq)-experiments and carbonate liquid (LC)-experiments.
Abbreviations used are: b.d.: below detection; Comb. Ne.: combeite nephelinite; Sil. natr.: silicate-bearing natrocarbonatite; Ph.: phenocryst; gg: green glass.
Sources for additional data are: P89a: Peterson (1989a) and DSS92: Dawson et al. (1992).

Table 6.15: Major element microprobe analyses of vishnevite and sodalite from the experiments on the HOL14/OL5 join, and from natural lavas from Oldoinyo Lengai.

	Vishnevite													Sodalite	
SAMPLE	CP21	CP92	CP8	CP19	CP2	CP23	CP15	BK424	BK430	BK429	DD78 #1	DD78 #2	DDKBW	CP27	HOL6
Type	2 liq	2 liq	2 liq	2 liq	2 liq	LS	LS	HOL14	2 liq	2 liq	Pyroxenite	Pyroxenite	Pyroclast	2 liq	Comb. Ne.
# of analyses	1	4	1	3	2	1	1	KHP95	KHP95	KHP95	DD78	DD78	DDKBW87	2	P89a
Composition	90/10	80/20	90/10	90/10	90/10	90/10	90/10	100/0	90/10	95/5	hopper	vermicular		90/10	mph. gg
Pressure	100	100	103	40	40	20	20	106	106	108				40	
Temperature	900	900	700	900	800	900	800	750	750	700				800	
Others														Buffered	
SiO2	38.48	36.35	40.97	38.44	40.39	40.58	39.73	39.65	38.82	37.16	35.56	34.86	35.59	38.64	38.84
Al2O3	28.77	29.25	27.12	29.18	29.44	29.57	29.3	30.61	30.39	27.76	29.94	27.94	29.86	30.5	28.64
Fe2O3	1.09	1.33	3.37	2.01	2.23	2.22	2.36	3.69	1.56	1.24	1.01	2.20	0.27	0.76	3.46
CaO	3.46	2.83	1.33	2.45	1.34	2.26	1.44	2.03	1.32	0.74	1.7	1.76	4.57	0.13	0.15
Na2O	11.83	18.28	17.21	10.48	10.6	11.04	12.13	17.18	19.37	20.87	21.03	21.55	15.79	21.58	24.14
K2O	2.4	2.43	2.94	2.41	2.57	2.67	3.09	1.54	1.92	1.58	1.24	1.16	2.59	3.41	2.07
F	b.d.	b.d.	b.d.	0.01	b.d.	b.d.	b.d.							0.05	
Cl	1.78	1.58	0.75	2.23	2.57	2.77	2.82				1.8	0.99	1	6.32	6.35
SO3	5.46	5.15	3.05	5.77	4.67	5.81	4.33				5.19	6.93	6.97	0.96	
BaO	0.04	b.d.	0.25	0.21	0.29	0.33	0.21							b.d.	
SrO	0.23	b.d.	0.26	0.14	0.13	0.15	0.13							0.17	
Total	93.54	97.20	97.25	93.33	94.23	97.40	95.54	94.70	93.38	89.35	97.47	97.39	96.64	102.52	103.65
Total-O=F,Cl	93.14	96.85	97.08	92.82	93.65	96.78	94.90	94.70	93.38	89.35	97.06	97.17	96.41	101.07	102.21

Note: Pressure is in MPa, temperature in oC, and starting composition is shown as proportion of wollastonite nephelinite HOL14/silicate-bearing natrocarbonatite OL5 (in wt. %). Types of experiments are silicate liquid (LS)-experiments and two-liquid (2 liq)-experiments.
Abbreviations used are: b.d.: below detection; Comb. Ne.: combeite nephelinite; mph.: microphenocryst; gg: green glass.
Sources for additional data are: P89a: Peterson (1989a); DD78: Donaldson and Dawson (1978); DDKBW87: Donaldson et al. (1987)

Table 6.16: Major element microprobe analyses of pyrrhotite from the experiments on the HOL14/OL5 join.

Sample	CP31	CP78
Type	2 liq	2 liq
# of analyses	1	1
Composition	90/10	90/10
Pressure	100	100
Temperature	700	800
Other	Buffered	Open tube
SiO2	0.08	
TiO2	0.12	
Al2O3	0.03	
Fe**	62.29	65.62
MnO	0.06	
MgO	b.d.	
CaO	0.11	
Na2O	b.d.	
K2O	0.09	
P2O5	b.d.	
F	b.d.	
Cl	b.d.	
S**	37.22	34.38
BaO	b.d.	
SrO	b.d.	

Note: Pressure is in MPa, temperature in oC, and starting composition is shown as proportion of wollastonite nephelinite HOL14/silicate-bearing natrocarbonatite OL5 (in wt. %).
Abbreviations used are: b.d.: below detection.
**FeO was recalculated as Fe and SO3 as S.

Table 6.17: Major element microprobe analyses of silicate and carbonate liquids from experiments on the HOL14/OL5 join, and from natural erupted wollastonite nephelinite HOL14 and silicate-bearing natrocarbonatite OL5. Distribution coefficients between silicate and carbonate liquids are also given (partitioning LS/LC).

SAMPLE	CP38	CP74	CP110	CP40	CP80	CP54	CP109	CP21	CP92	CP20	CP93	CP89	CP5	CP78	CP102
Type	HOL14	HOL14	HOL14	HOL14	HOL14	HOL14	2 liq	2 liq	2 liq	2 liq	2 liq	2 liq	2 liq	2 liq	2 liq
Composition	100/0	100/0	100/0	100/0	100/0	100/0	80/20	90/10	80/20	50/50	20/80	10/90	90/10	90/10	80/20
Pressure	100	100	20	20	20	20	200	100	100	100	100	100	100	100	100
Temperature	900	800	900	850	800	700	750	900	900	900	900	900	800	800	800
Other														open tube	
Silicate liquid															
# an	5	4	5	4	4	2	5	6	10	5	7	5	6	4	5
SiO2	46.77	51.88	49.04	49.98	51.45	n.d.	49.46	43.62	42.73	41.69	41.67	50.56	43.08	46.25	50.98
TiO2	1.04	0.37	0.94	1.04	0.88	0.42	0.49	1.09	1.00	1.00	0.72	0.76	1.32	2.03	0.41
Al2O3	15.30	15.80	15.20	13.30	13.30	14.60	14.90	12.20	12.78	11.77	13.08	12.82	10.84	5.35	13.66
FeO	7.61	6.85	8.38	10.10	9.43	5.75	6.78	6.31	8.49	7.84	7.07	5.94	9.17	12.45	7.63
MnO	0.27	0.30	0.28	0.47	0.33	b.d.	0.33	0.30	0.42	0.45	0.43	0.50	0.34	0.60	0.38
MgO	0.86	0.30	0.50	0.45	0.25	0.25	0.20	0.93	0.81	0.75	0.50	0.55	0.62	1.20	0.60
CaO	5.90	1.68	4.42	4.40	2.53	4.80	1.80	7.45	7.36	6.29	5.61	3.90	4.31	7.53	2.37
Na2O	11.16	5.63	11.86	10.23	10.33	8.95	10.62	11.99	13.05	13.69	13.31	6.05	11.27	12.30	7.68
K2O	5.12	7.05	5.90	5.98	7.10	5.25	7.28	5.87	5.61	5.44	6.29	7.16	5.73	6.16	7.31
P2O5	0.23	1.00	0.40	0.40	0.40	0.70	b.d.	0.34	0.33	0.22	0.38	0.51	0.22	0.78	0.46
F	0.17	0.45	0.42	0.40	0.60	0.60	0.40	0.36	0.78	0.33	0.69	0.52	0.41	1.53	0.46
Cl	0.31	0.29	0.35	0.45	0.31	0.38	0.28	0.42	0.41	0.41	0.40	0.38	0.60	0.83	0.31
SO3	0.52	0.20	0.48	0.63	0.60	b.d.	b.d.	0.21	0.25	0.22	0.23	b.d.	1.10	1.33	b.d.
BaO	0.18	b.d	0.40	0.40	0.50	b.d.	b.d.	0.20	0.50	0.55	0.50	b.d.	0.36	0.93	b.d.
SrO	0.30	0.93	b.d.	0.80	b.d.	0.60	0.70	0.54	b.d.	0.44	0.83	0.90	0.44	1.10	1.05
Total	95.74	92.72	98.57	98.01	98.02	n.d.	93.04	93.81	94.52	91.09	91.69	90.54	89.61	100.36	93.29
(Na+K)/Al	1.56	1.07	1.70	1.75	1.86	1.40	1.70	2.14	2.16	2.41	2.20	1.38	2.32	5.03	1.50
Mg/(Mg+Fe)	0.17	0.07	0.10	0.07	0.05	0.07	0.05	0.17	0.15	0.15	0.11	0.14	0.11	0.15	0.12
Carbonate liquid															
# an							7		4	6	16	14			7
SiO2							1.49		0.38	1.20	3.27	5.44			2.20
TiO2							0.06		0.08	0.12	0.16	0.17			0.07
Al2O3							0.20		b.d.	0.08	0.46	0.61			0.20
FeO							1.34		0.73	1.12	1.41	1.89			1.32
MnO							0.32		0.30	0.21	0.29	0.33			0.30
MgO							0.27		0.55	0.24	0.38	0.44			0.71
CaO							19.44		25.53	22.31	16.91	15.24			15.77
Na2O							21.97		20.23	21.86	24.87	23.32			22.70
K2O							3.64		3.83	4.27	5.48	4.76			3.73
P2O5							1.39		2.10	1.43	1.20	1.21			1.71
F							2.53		0.83	0.93	2.02	2.14			2.37
Cl							0.38		0.50	0.37	0.77	0.58			0.38
SO3							3.54		3.53	2.13	2.52	2.21			4.32
BaO							0.83		0.60	1.13	0.89	0.85			0.87
SrO							2.10		1.55	1.43	1.44	1.46			1.93
Total							59.50		60.71	58.83	62.07	60.66			58.58
Mg/(Mg+Fe)							0.26		0.57	0.27	0.32	0.29			0.49
Partitioning LS/LC															
SiO2							33.3		114	34.6	12.7	9.29			23.2
TiO2							7.98		13.3	8.49	4.57	4.39			5.94
Al2O3							74.5		n.d	143	28.5	21.1			68.3
FeO							5.05		11.7	6.99	5.01	3.15			5.80
MnO							1.04		1.40	2.20	1.48	1.51			1.26
MgO							0.75		1.47	3.19	1.32	1.24			0.84
CaO							0.08		0.29	0.28	0.33	0.26			0.15
Na2O							0.48		0.65	0.63	0.54	0.26			0.34
K2O							2.00		1.47	1.27	1.15	1.50			1.96
P2O5							n.d.		0.16	0.15	0.32	0.42			0.27
F							0.16		0.94	0.36	0.34	0.24			0.20
Cl							0.74		0.82	1.12	0.52	0.65			0.81
SO3							n.d.		0.07	0.10	0.09	n.d.			n.d.
BaO							n.d.		0.83	0.48	0.56	n.d.			n.d.
SrO							0.33		n.d.	0.31	0.58	0.61			0.54

Note: Pressure is in MPa, temperature in oC, and starting composition is shown as proportion of wollastonite nephelinite HOL14/silicate-bearing natrocarbonatite OL5 (in wt. %). Types of experiments are HOL14-experiments, silicate liquid (LS)-experiments, two-liquid (2 liq)-experiments and carbonate liquid (LC)-experiments.
Abbreviations used are: b.d., below detection.
Sources for additional data are: P89a: Peterson (1989a) and ** Belanger (for OL5 WR).

Table 6 17 (suite)

SAMPLE	CP13	CP103	CP97	CP31	CP67	CP7	CP117	CP19	CP18	CP2	CP27	CP1	CP11	CP10	CP23
Type	2 liq	2 liq	2 liq	2 liq	2 liq	2 liq	LC	2 liq	2 liq	2 liq	2 liq	2 liq	2 liq	2 liq	LS
Composition	50/50	10/90	20/80	90/10	70/30	50/50	10/90	90/10	50/50	90/10	90/10	50/50	90/10	50/50	90/10
Pressure	100	100	100	100	100	103	100	40	40	40	40	40	40	40	20
Temperature	800	800	750	700	700	700	700	900	900	800	800	800	700	700	900
Other				buffered							buffered				
Silicate liquid															
# an	8	4	4	5				4	6	2	4	5	1		6
SiO2	43 85	44 88	49 93	46.27				44.23	36.32	47 04	47 30	42.91	50.64		46.07
TiO2	1 10	0.75	0.74	0.75				1.35	1.13	0 82	1 76	0 92	1 21		1 39
Al2O3	10.49	11.66	12.83	9.66				10.16	6.85	9 21	9.14	6.29	8.91		10.23
FeO	7 61	8.39	7 35	6.72				10.23	8.64	10.27	8.03	10.89	9.62		10.34
MnO	0 46	0 44	0 40	0 34				0.49	0.57	0.51	0.49	0 73	0 49		0.43
MgO	0 77	0 43	0.35	0.23				0.96	1.02	0 73	1 42	1 24	0 26		0.95
CaO	5 39	2.92	2 18	2.79				6.70	11 77	2.92	4 97	6.46	2.14		6.81
Na2O	13 01	11 56	10.03	10 40				12.46	14.72	11 87	14.11	10.87	5 68		11 45
K2O	5 81	8 85	7 30	7 54				5 98	4.85	7 11	6 22	6 35	8.27		6 26
P2O5	0 21	b d	0 30	0 18				0.43	0.49	0 19	0.45	0.33	0.15		0.48
F	0 37	0 53	0 40	0 40				0.32	0.70	0.45	0.50	0 47	0.51		0 48
Cl	0 45	0 28	0 26	0 34				0.44	0.55	0.48	0 66	0 43	0 46		0 38
SO3	0 74	b d	b d	0 42				0 30	0.39	0 19	0 64	0 23	0 65		0 26
BaO	0 36	b d	b d	0.27				0.43	0 69	0.71	0 62	0.47	0.53		0.67
SrO	0 34	b d	b d	0.52				0.28	0.93	0 38	0.52	0 50	0.40		0.40
Total	90 97	90 68	92.07	86 82				94.75	89.41	92.64	96.82	89 10	89 92		96 60
(Na+K)/Al	2.64	2.45	1 90	2.82				2.66	4.43	2.95	3 28	3.94	2.05		2.50
Mg/(Mg+Fe)	0 15	0.08	0.08	0.06				0.14	0.17	0 11	0.24	0 17	0 05		0 14
Carbonate liquid															
# an	6	19	18		9	5	11		5			5		5	
SiO2	3 53	3 23	2 21		1 33	2 09	6 00		2.33			1 50		1 53	
TiO2	0 23	0 16	0 13		0 12	0 08	0 12		0 14			0 08		0 03	
Al2O3	0 25	0 25	0 20		0 25	0 14	2.14		0.17			0 15		0 24	
FeO	1 77	1 56	1 38		0 74	0 94	1 61		1 03			0 93		0 78	
MnO	0 33	0 38	0 32		0.32	0 20	0.33		0.16			0 17		0 25	
MgO	0 52	0 48	0 35		0 20	0 13	0 36		0.28			0 42		0 04	
CaO	19 39	13 64	18 11		19 89	20 52	13 65		20.94			15.03		13 18	
Na2O	23 37	24.94	24 23		24 93	24 81	23 97		23.34			27 85		30.92	
K2O	3 70	5 04	5 21		4.56	5 01	4.53		5.14			5 17		3 86	
P2O5	1 18	1 18	1 21		1.08	0.80	1 10		1.18			1 17		1 40	
F	1 16	2.52	2.32		1 21	0 59	0.90		0.66			1 54		0 91	
Cl	0 60	1 21	0 74		0.44	1 33	0 78		0.81			2.02		0 87	
SO3	1 06	2 80	2 16		2.95	1 45	2.31		2.18			3.26		1 96	
BaO	1 01	1 01	0 92		0.75	0 71	0 63		0.99			1.38		1 17	
SrO	1 44	1 45	1 61		2.04	1.64	1.17		1.43			1 69		1 60	
Total	59 51	59.83	61 08		60.81	60.44	59.59		60 76			62.36		58 73	
Mg/(Mg+Fe)	0 34	0 36	0 31		0.33	0 20	0.28		0.33			0.45		0 08	
Partitioning LS/LC															
SiO2	12.4	13 9	22.6						15.6			28.6			
TiO2	4 80	4 80	5 91						8.18			11 5			
Al2O3	42.5	46 6	64 2						40.1			43.4			
FeO	4 31	5 37	5 31						8.37			11 7			
MnO	1 40	1 18	1 25						3.63			4 21			
MgO	1 50	0 90	1 01						3.62			2.92			
CaO	0.28	0.21	0 12						0.56			0.43			
Na2O	0 56	0.46	0.41						0.63			0.39			
K2O	1 57	1 75	1.40						0.94			1 23			
P2O5	0 18	n.d.	0.25						0.42			0.29			
F	0 32	0.21	0.17						1.07			0.30			
Cl	0.76	0.23	0.35						0.67			0.21			
SO3	0 70	n.d.	n.d.						0.18			0.07			
BaO	0.36	n.d.	n.d.						0.69			0.34			
SrO	0 23	n.d.	n.d.						0.65			0.30			

Table 6 17 (suite)

SAMPLE	CP91	CP22	CP120	CP121	CP111	CP82	CP41	CP42	CP52	CP43	CP53	CP130	CP131	CP15	CP113
Type	2 liq	2 liq	2 liq	2 liq	2 liq	LC	LS	LS	2 liq	2 liq	2 liq	LC	LC	LS	2 liq
Composition	80/20	50/50	40/60	30/70	20/80	10/90	95/5	90/10	80/20	70/30	50/50	20/80	10/90	90/10	80/20
Pressure	20	20	20	20	20	20	20	20	20	20	20	20	20	20	20
Temperature	900	900	900	900	900	900	850	850	850	850	850	850	850	800	800
Other															
Silicate liquid															
# an.	9	5	9	10	4		5	5	4	8	5			3	3
SiO2	42.26	35.60	34.51	36.54	38.09		47.36	45.70	42.53	37.83	37.15			46.19	43.70
TiO2	1.33	1.22	1.35	1.42	1.86		1.54	1.52	1.71	1.33	1.61			1.13	1.42
Al2O3	7.84	5.44	4.70	5.01	3.89		10.48	8.65	8.15	5.08	4.62			8.54	5.93
FeO	10.17	8.89	10.37	9.82	11.35		11.90	11.04	12.15	10.35	10.96			11.78	12.17
MnO	0.47	0.67	0.91	0.72	1.15		0.48	0.48	0.55	0.56	0.78			0.56	0.53
MgO	0.97	0.94	1.06	1.05	0.87		0.84	1.10	1.13	1.04	0.78			1.10	1.33
CaO	9.27	13.27	14.92	11.99	9.83		5.18	7.38	7.80	10.88	10.94			5.01	6.17
Na2O	14.39	16.17	15.30	14.71	12.74		11.54	12.18	10.33	17.01	14.53			13.64	13.40
K2O	5.43	4.47	4.36	5.03	6.31		5.68	5.58	5.60	5.34	5.28			6.41	5.77
P2O5	0.69	0.53	0.54	0.52	0.55		0.38	0.60	0.88	0.86	0.60			0.34	0.70
F	0.94	0.78	1.19	1.18	1.47		0.68	0.78	1.20	1.17	1.20			0.62	1.13
Cl	0.54	0.41	0.38	0.41	0.40		0.67	0.75	0.62	0.56	0.42			0.49	0.59
SO3	0.41	0.27	0.28	0.29	b.d.		0.90	0.92	0.40	1.08	0.20			0.23	0.60
BaO	0.50	0.79	0.80	0.69	0.70		b.d.	0.65	0.67	0.63	0.62			0.49	0.63
SrO	0.87	0.73	0.95	0.73	0.99		0.80	0.73	0.77	0.99	0.90			0.36	b.d.
Total	96.07	90.20	91.61	90.11	90.18		98.43	98.07	92.46	94.71	90.57			96.89	94.07
(Na+K)/Al	3.77	5.78	6.36	5.92	7.14		2.40	3.01	3.75	6.65	6.41			3.44	4.77
Mg/(Mg+Fe)	0.14	0.16	0.15	0.16	0.12		0.11	0.15	0.14	0.15	0.11			0.14	0.16
Carbonate liquid															
# an	3	5	22	19	10	6				2	8	17	9		
SiO2	2.47	3.05	5.24	4.75	3.85	4.45				2.30	1.98	4.95	4.40		
TiO2	0.10	0.17	0.18	0.19	0.19	0.13				0.09	0.12	0.11	0.13		
Al2O3	0.23	0.14	0.35	0.29	0.20	1.50				b.d.	0.19	1.90	2.38		
FeO	0.67	0.80	1.51	1.29	1.34	1.15				1.02	0.91	1.16	1.46		
MnO	b.d	0.10	0.29	0.25	0.23	0.30				b.d.	0.19	0.31	0.35		
MgO	0.30	0.26	0.39	0.38	0.30	0.30				0.30	0.33	0.32	0.50		
CaO	16.33	16.15	14.45	14.40	15.07	15.07				15.44	11.67	13.28	14.25		
Na2O	28.63	25.43	25.43	26.11	28.64	21.40				20.43	27.44	21.51	20.46		
K2O	5.63	6.74	5.85	6.82	6.97	6.53				7.77	6.71	9.81	6.78		
P2O5	1.43	1.10	1.23	1.42	1.32	1.23				1.88	1.68	1.01	1.20		
F	2.87	1.77	2.10	2.27	3.18	2.00				2.77	3.11	2.49	1.91		
Cl	2.50	1.06	1.80	2.42	2.12	1.74				4.07	1.09	1.59	2.13		
SO3	5.80	2.44	2.88	3.54	2.92	2.12				3.00	5.27	2.56	2.29		
BaO	0.90	1.16	0.97	0.90	1.04	0.92				1.12	1.03	1.15	0.96		
SrO	1.57	1.33	1.29	1.25	1.46	1.33				1.70	1.20	1.24	1.23		
Total	69.24	61.70	63.98	66.28	68.83	60.16				61.88	62.90	63.40	60.43		
Mg/(Mg+Fe)	0.45	0.36	0.31	0.34	0.29	0.32				0.34	0.39	0.33	0.38		
Partitioning LS/LC															
SiO2	17.1	11.7	6.59	7.69	9.89					16.4	18.7				
TiO2	12.9	7.03	7.36	7.50	9.69					14.8	14.0				
Al2O3	33.6	38.3	13.3	17.1	19.5					n.d.	24.3				
FeO	15.3	11.1	6.85	7.62	8.47					10.1	12.0				
MnO	n.d	6.93	3.10	2.88	4.92					n.d.	4.11				
MgO	3.22	3.65	2.71	2.79	2.89					3.46	2.34				
CaO	0.57	0.82	1.03	0.83	0.65					0.70	0.94				
Na2O	0.50	0.64	0.60	0.56	0.44					0.83	0.53				
K2O	0.96	0.66	0.74	0.74	0.90					0.69	0.79				
P2O5	0.48	0.48	0.44	0.37	0.42					0.46	0.36				
F	0.33	0.44	0.57	0.52	0.46					0.42	0.39				
Cl	0.21	0.38	0.21	0.17	0.19					0.14	0.39				
SO3	0.07	0.11	0.10	0.08	n.d.					0.36	0.04				
BaO	0.56	0.68	0.83	0.77	0.67					0.57	0.60				
SrO	0.55	0.55	0.74	0.58	0.68					0.58	0.75				

Table 6.17 (suite).

SAMPLE	CP14	CP122	CP123	CP114	CP81	CP47	CP48	CP50	CP124	CP125	CP115	CP55	CP16
Type	2 liq	2 liq	LC	LC	LC	LS	2 liq	2 liq	2 liq	LC	LC	LS	LS
Composition	50/50	40/60	30/70	20/80	10/90	95/5	90/10	50/50	40/60	30/70	20/80	95/5	50/50
Pressure	20	20	20	20	20	20	20	20	20	20	20	20	20
Temperature	800	800	800	800	775	750	750	750	750	750	750	700	700
Other													
Silicate liquid													
# an	4	4				1	2		1			1	
SiO2	38.70	49.84				49.20	43.05		48.17			37 6	
TiO2	1.41	0.46				1 31	1.38		0.92			0.71	
Al2O3	4 66	6.19				9.10	6.20		5.40			13.5	
FeO	11 29	12.86				12.00	12.35		12.76			5.7	
MnO	0.95	1.43				0.50	0.60		1.17			b.d.	
MgO	0.90	1 58				0.30	0.55		1 41			0.4	
CaO	8 65	5 44				3.20	4.25		4.61			5.2	
Na2O	15 50	4 10				2.80	4.90		3.71			10.8	
K2O	5 44	4 99				5.60	6.05		5.24			5.1	
P2O5	0 50	0.55				0.30	0.30		b.d.			0.5	
F	0 76	1 38				0.60	1 15		1 11			0.7	
Cl	0 47	0 40				0 56	0 57		0 39			0 26	
SO3	0 26	b d				0 20	0.55		b d			1.4	
BaO	0 56	0 82				3<	0.70		0 77			b d	
SrO	0 66	1 06				0 90	0.70		b d			b.d	
Total	90 89	90 88				86 57	83.29		85.66			61 67	
(Na+K)/Al	6 74	1 96				1 17	2.36		2.18			1 73	
Mg/(Mg+Fe)	0 12	0 18				0.04	0.07		0 16			0 11	
Carbonate liquid													
# an	5	7	9	6	17			4	4	14	6		4
SiO2	1 83	5 40	6.24	7 85	2.31			1 25	7 20	4.42	6 92		4.64
TiO2	0 11	0.12	0.27	0 16	0.07			0.05	0 14	0 12	0 10		0.09
Al2O3	0.09	2.73	3.34	2.37	3.42			0.19	1.97	2.06	2.06		0.46
FeO	0 66	1 40	1.39	1.87	0.67			0.84	1.25	0 94	1 42		1.01
MnO	0 20	0 27	0.23	0.30	0.35			0.22	0.28	0.33	0.33		0 33
MgO	0 24	0.44	0.39	0.40	0.39			0.46	0.40	0.37	0 40		0 11
CaO	14 80	9 87	10 20	15.17	13.89			10 31	11.35	11 14	12.01		13.36
Na2O	25 77	22.30	22.78	24 82	23 36			27 51	17 30	21 64	27 07		25.93
K2O	7 95	7 73	6 23	5 07	5 59			6 45	8.75	9 45	5.98		6.46
P2O5	1 14	1 11	1 15	1 32	1 26			1 81	0.93	1 11	1 04		1 43
F	1 66	2 30	1 98	2 35	2.43			4.49	2 20	2 68	2.06		1 77
Cl	1 99	2.63	1 14	0 72	1 00			2 88	0.96	2.03	1 52		0.92
SO3	2.54	2.37	2.16	2 23	2 82			4 06	2.65	1 81	2.19		2.44
BaO	1 36	1 17	0.97	1 03	1.04			1 35	1.03	1.18	0.98		1.51
SrO	1 29	1 27	1 13	1 55	1.52			1.77	1.35	1.60	1 32		1.74
Total	61 83	61.11	59.57	67.19	60.14			63.62	57 75	60.86	65.40		62.21
Mg/(Mg+Fe)	0 33	0 36	0 33	0 28	0.51			0.49	0.36	0 41	0.33		0 17
Partitioning LS/LC													
SiO2	21 1	9 23							8.69				
TiO2	13.3	3 81							6.57				
Al2O3	54 8	2.27							2.75				
FeO	13.2	9 19							10.2				
MnO	4 76	5 27							4 25				
MgO	3 73	3 57							3.53				
CaO	0 60	0 55							0.41				
Na2O	0 60	0 18							0.21				
K2O	0 68	0 65							0.60				
P2O5	0 44	0 49							n.d.				
F	0 45	0 60							0.50				
Cl	0 23	0.15							0.41				
SO3	0 10	n.d.							n.d.				
BaO	0.41	0.53							0.75				
SrO	0.51	0.83							n.d.				

Table 6 17 (suite)

SAMPLE	HOL14	HOL14	HOL14	HOL14
Type	WR	gmass	glass	glass
Composition			green	brown
Pressure	P89a		P89a	P89a
Temperature				
Other				
Silicate liquid				
# an				
SiO2	45.7	49.86	49.97	49.71
TiO2	0.97	1.12	1.32	2.16
Al2O3	15.9	13.58	8.00	2.99
FeO	7.69	10.07	10.97	13.6
MnO	0.3	0.41	0.42	0.41
MgO	0.78	0.37	0.43	1.02
CaO	5.94	2.68	3.20	1.69
Na2O	11.4	13.56	15.98	2.16
K2O	4.99	6.13	6.27	2.59
P2O5	0.28	n.d.	0.31	0.13
F	0.22	0.78	0.57	0.21
Cl	0.29	0.31		
SO3	0.31	0.94		
BaO	0.18	0.50		
SrO	0.25			
Total	95.20	100.31	97.44	78.67
(Na+K)/Al	1.52	2.13	4.13	2.13
Mg/(Mg+Fe)	0.15	0.06	0.07	0.12
Carbonate liquid	OL5**	OL5	OL5	
# an	WR	gmass	gmass sph	
SiO2	3.20	4.08	30.50	
TiO2	0.10	0.18	0.40	
Al2O3	0.90	0.36	5.93	
FeO	1.30	3.23	5.23	
MnO	0.35	0.93	0.50	
MgO	0.40	0.50	0.45	
CaO	15.40	17.01	24.20	
Na2O	28.30	31.70	15.45	
K2O	6.13	8.13	3.58	
P2O5	1.07	0.72	0.60	
F	1.64	3.82	2.08	
Cl	2.54	11.72	0.79	
SO3	2.55	3.54	2.30	
BaO	0.90	1.03	b.d.	
SrO	1.30	1.01	0.60	
Total	66.08	87.96	92.61	
Mg/(Mg+Fe)				
	HOL14/OL5			
Partitioning LS/LC	gm/WR			
SiO2	15.6			
TiO2	11.2			
Al2O3	15.1			
FeO	7.77			
MnO	1.17			
MgO	0.93			
CaO	0.17			
Na2O	0.48			
K2O	1.00			
P2O5	n.d.			
F	0.48			
Cl	0.12			
SO3	0.37			
BaO	0.55			
SrO	n.d.			

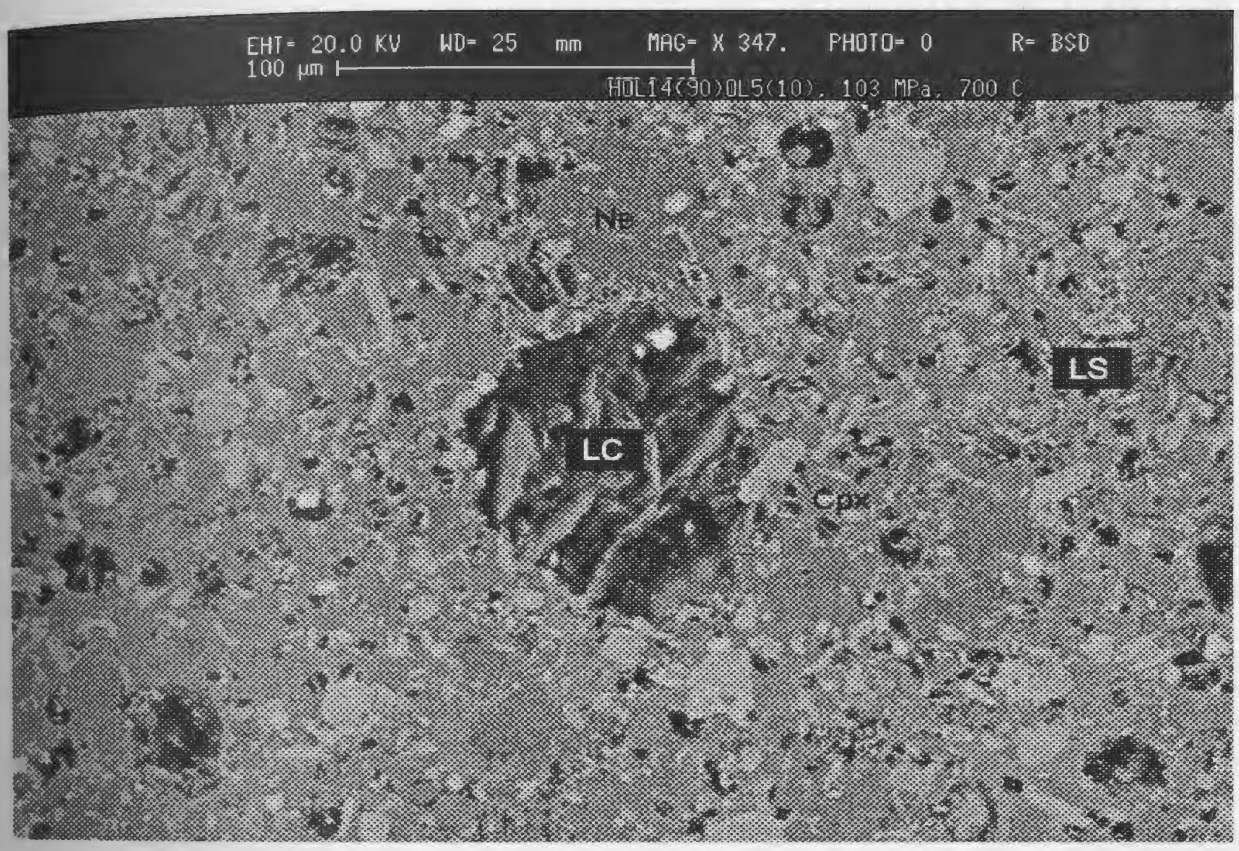

Figure 6.1: SEM photograph of two-liquid experiment CP8 showing that silicate crystals are present in the silicate liquid (grey matrix) but are scarce in the carbonate liquid. Note that a clinopyroxene crystal criss crosses the boundary between silicate glass and quenched carbonate liquid. Abbreviations used: LC: carbonate liquid; LS: silicate liquid; Ne nepheline; Cpx: clinopyroxene.

Figure 6.2: Isobaric phase diagram at 20 MPa. The shaded area represents the miscibility gap. The presence of the main silicate crystal phases is indicated by the pie slices, whereas the presence of minor crystal phases is indicated beside the pie symbol. The presence of silicate liquid, two liquids or carbonate liquid is indicated by the symbols s, 2 and c, respectively, labelled in the pie slice for liquid.
Other abbreviations used are: Ne: nepheline; Cpx: clinopyroxene; Mela: melanite garnet; Wo: wollastonite; Meli: melilite; Vish: vishnevite; Ap: apatite; Pvk: perovskite; Fd: feldspar; NY: nyerereite; GRE: gregoryite. HOL14: wollastonite nephelinite HOL14; OL5: silicate-bearing natrocarbonatite OL5.

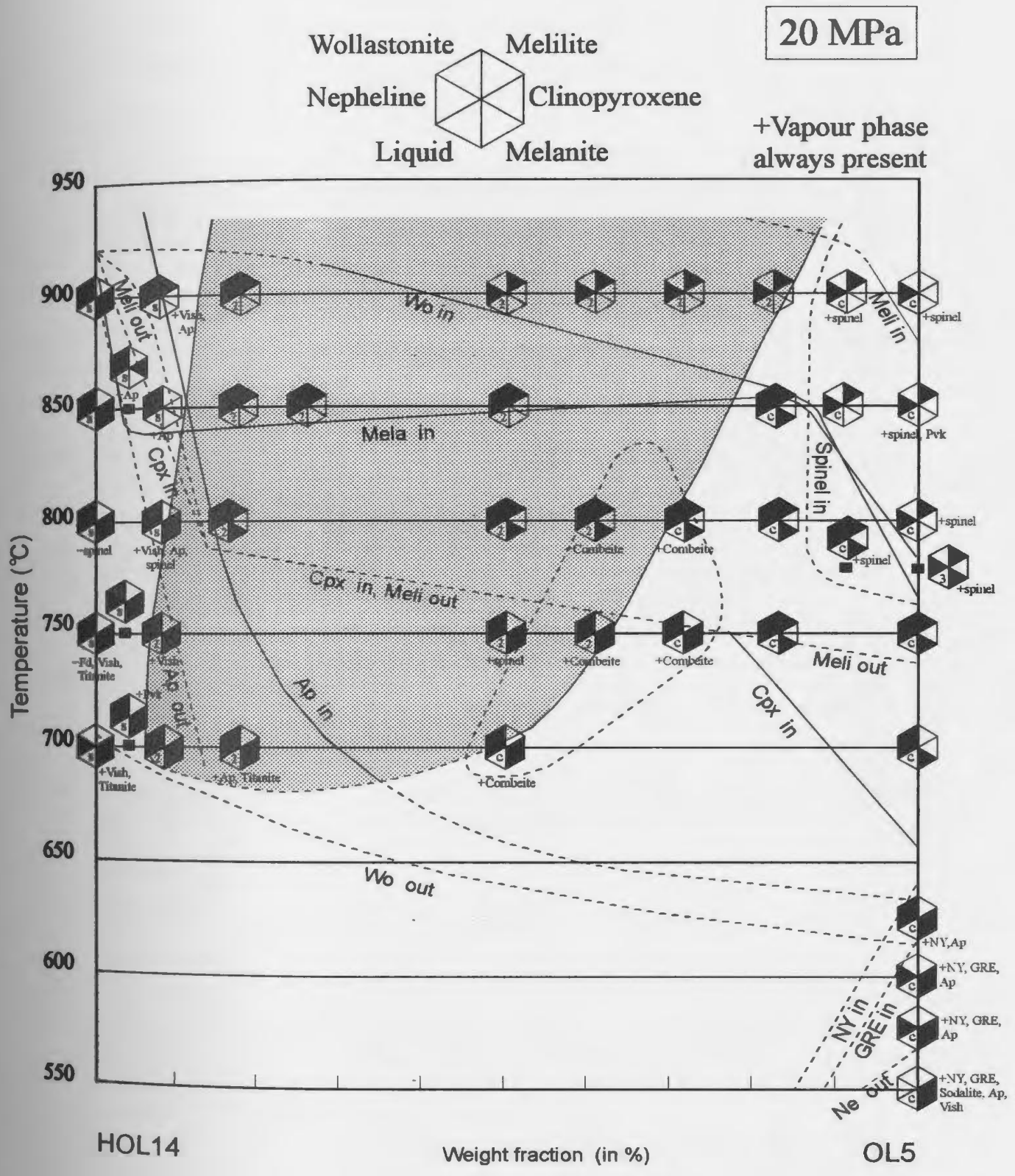
20 MPa
Wollastonite
Melilite
Nepheline
Clinopyroxene
Liquid
Melanite
+Vapour phase always present
950
900
850
800
750
700
650
600
550
Temperature (°C)
Meli out
Wo in
Mela in
Cpx in
Spinel in
Meli in
Cpx in, Meli out
Ap in
Ap out
Cpx in
Meli out
Wo out
NY in
GRE in
Ne out
+spinel
+spinel, Pvk
+Combeite
+Vish, Ap
+Vish, Ap, spinel
+Fd, Vish, Titanite
+Vish, Titanite
+Ap, Titanite
+NY,Ap
+NY, GRE, Ap
+NY, GRE, Ap
+NY, GRE, Sodalite, Ap, Vish
HOL14
Weight fraction (in %)
OL5

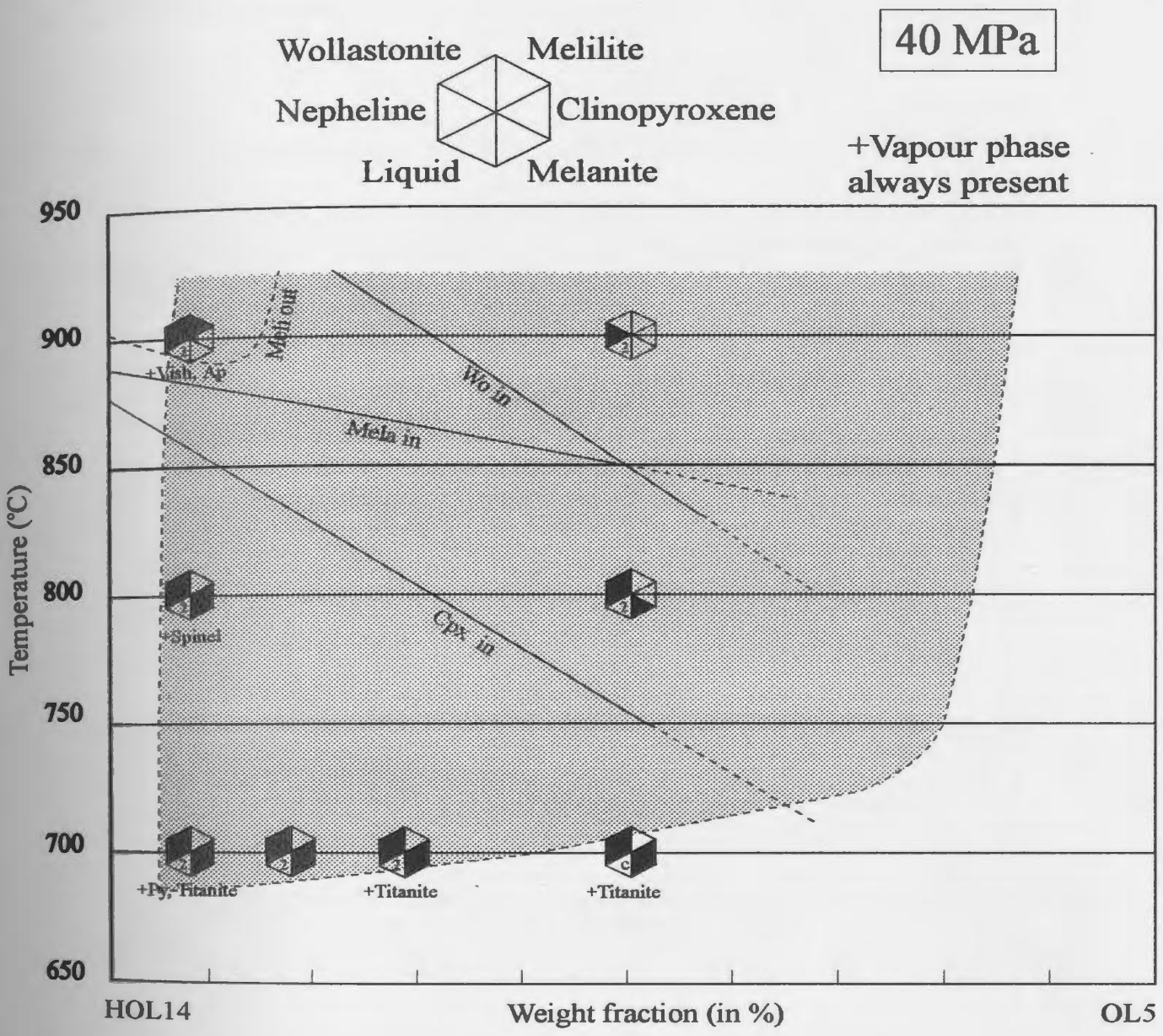

Figure 6.3: Isobaric phase diagram at 40 MPa. The shaded area represents the miscibility gap. The presence of the main silicate crystal phases is indicated by the pie slices, whereas the presence of minor crystal phases is indicated beside the pie. The presence of silicate liquid, two liquids or carbonate liquid is indicated by the symbols s, 2 and c, respectively, labelled in the pie slice for liquid.
Other abbreviations used are: Cpx: clinopyroxene; Mela: melanite garnet; Wo: wollastonite; Meli: melilite; Vish: vishnevite; Ap: apatite; Py: pyrrhotite. HOL14: wollastonite nephelinite HOL14; OL5: silicate-bearing natrocarbonatite OL5.

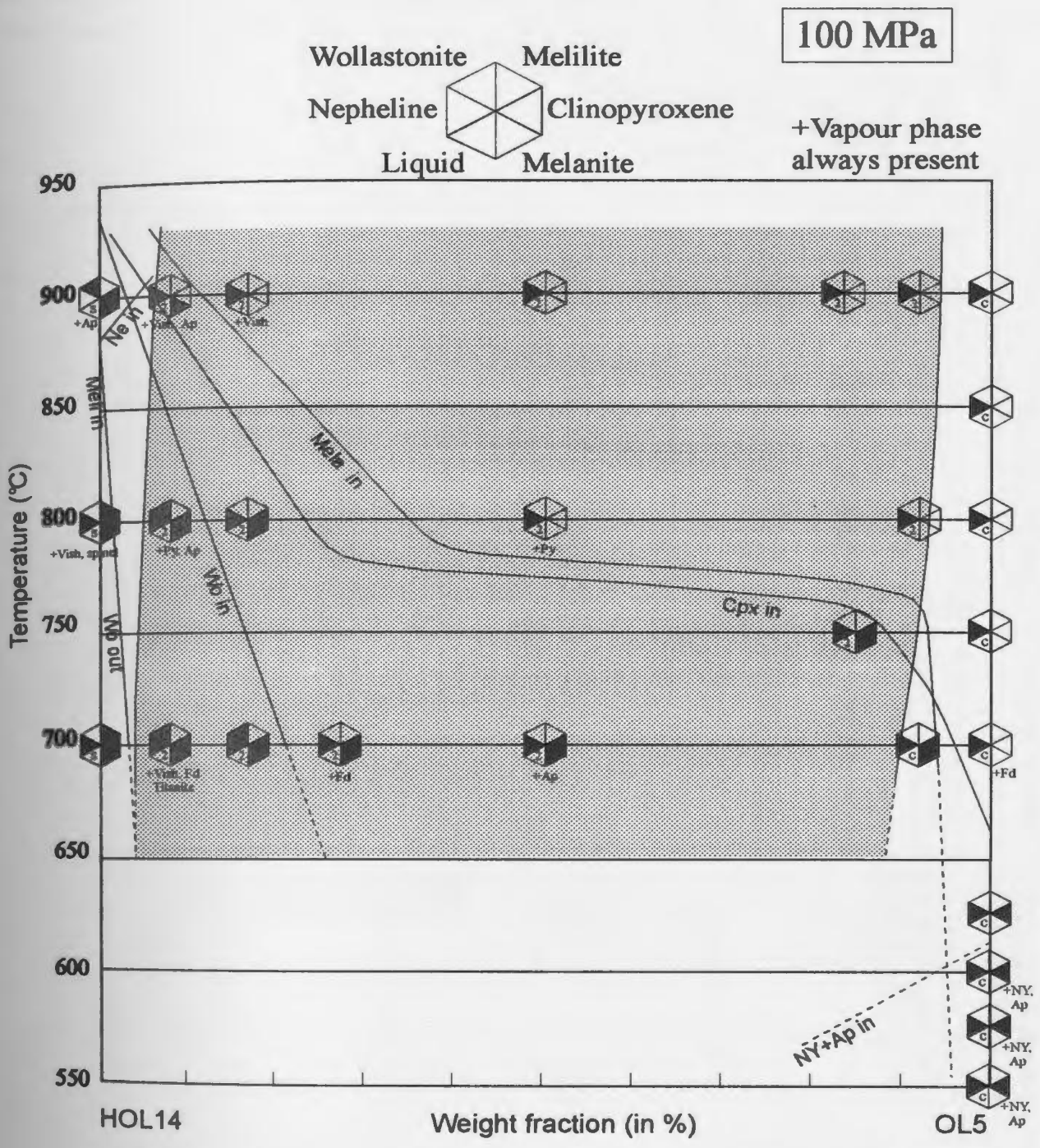

Figure 6.4: Isobaric phase diagram at 100 MPa. The shaded area represents the miscibility gap. The presence of the main silicate crystal phases is indicated by the pie slices, whereas the presence of minor crystal phases is indicated beside the pie. The presence of silicate liquid, two liquids or carbonate liquid is indicated by the symbols s, 2 and c, respectively, labelled in the pie slice for liquid.
Other abbreviations used are: Ne: nepheline; Cpx: clinopyroxene; Mela: melanite garnet; Wo: wollastonite; Meli: melilite; Vish: vishnevite; Ap: apatite; Py: pyrrhotite; Fd: feldspar; NY: nyerereite; GRE: gregoryite. HOL14: wollastonite nephelinite HOL14; OL5: silicate-bearing natrocarbonatite OL5.

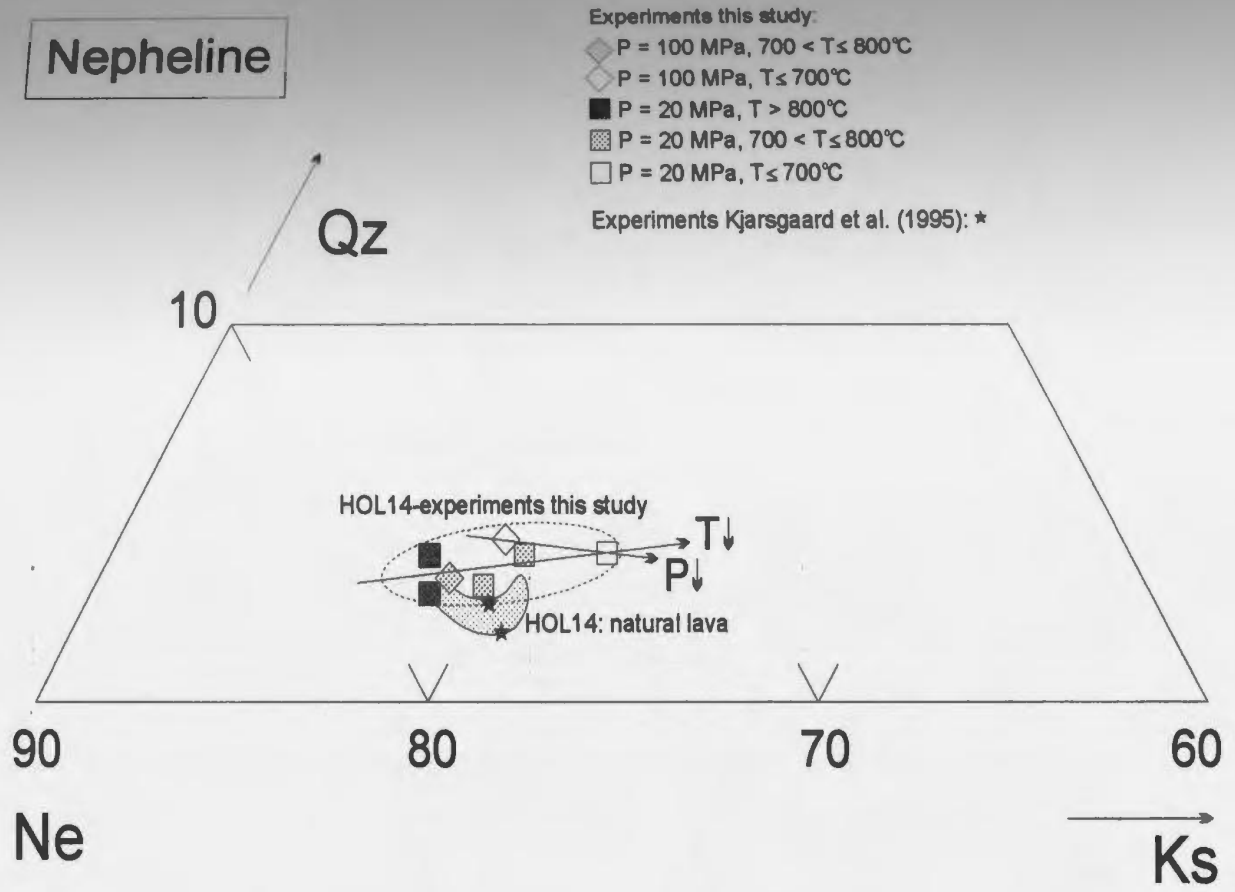

Figure 6.5: Plot of nepheline microprobe analyses from HOL14-experiments and natural wollastonite nephelinite lava (HOL14) onto part of the nepheline (Ne) – kalsilite (Ks) – quartz (Qz) triangular plot (mol. %). Squares represent nephelines from 20 MPa experiments, and diamonds represent 100 MPa experiments. Open symbols represent experiments at T ≤ 700 °C, half-filled symbols experiments at 700 °C < T ≤ 800 °C, and filled symbols experiments at T > 800 °C. Stars (★) represent the compositions of nepheline from Kjarsgaard et al. (1995), in HOL14-experiments at 106 MPa, 750 °C and at 108 MPa, 700 °C. The shaded area represents the compositional range exhibited by nephelines from erupted wollastonite nephelinite HOL14. Data are from Table 6.5.

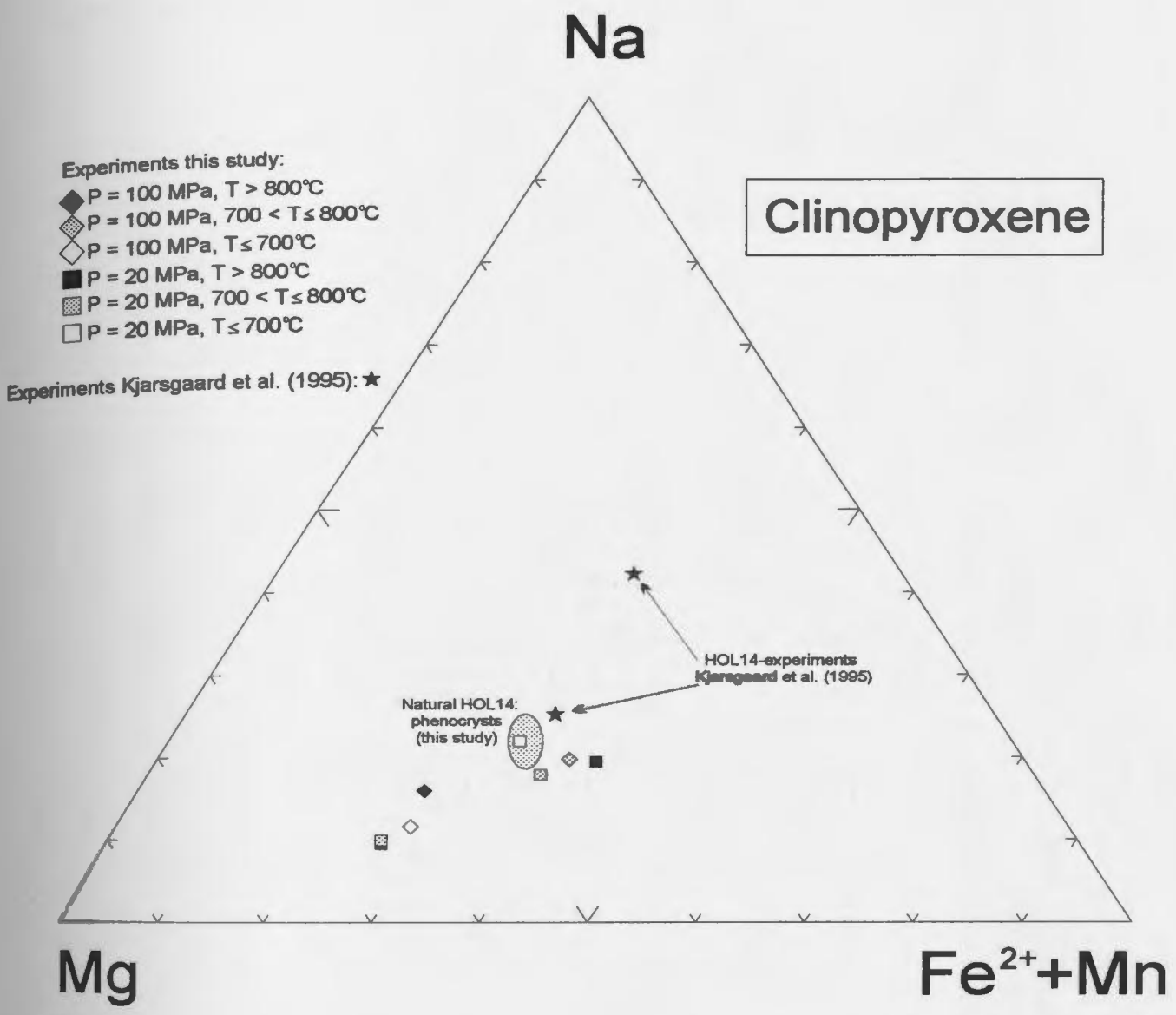

Figure 6.6: Plot of clinopyroxene microprobe analyses from HOL14-experiments and natural wollastonite nephelinite HOL14 onto the Mg (diopside) - Na (aegirine) - Fe^{2+}+Mn (hedenbergite) triangular plot (atomic %). Squares represent clinopyroxene crystals from 20 MPa experiments, and diamonds from 100 MPa experiments. Open symbols represent experiments at T ≤ 700 °C, half-filled symbols experiments at 700 °C < T ≤ 800 °C, and filled symbols experiments at T > 800 °C. Stars (★) represent the composition of clinopyroxene from Kjarsgaard et al. (1995), in HOL14-experiments at 106 MPa, 750 °C and at 108 MPa, 700 °C. The shaded area represents the compositional range exhibited by clinopyroxene phenocrysts from erupted wollastonite nephelinite HOL14. Data are from Table 6.6.

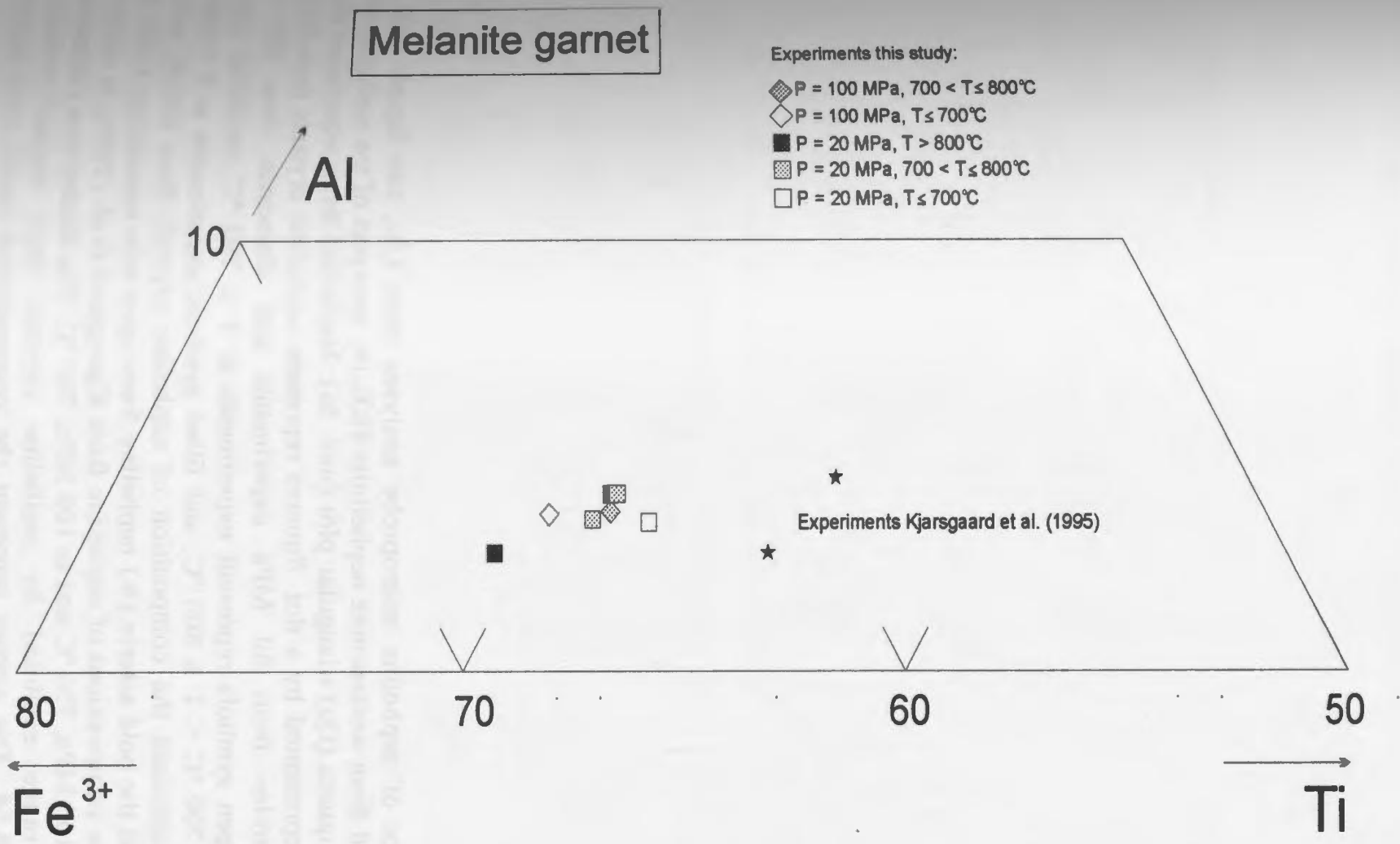

Figure 6.7: Plot of melanite garnet microprobe analyses from HOL14-experiments and natural wollastonite nephelinite HOL14 onto part of the Al - Fe^{3+} - Ti ternary (atomic %) diagram. Squares represent melanite garnet crystals from 20 MPa experiments, and diamonds from 100 MPa experiments. Open symbols represent experiments at T ≤ 700 °C, half-filled symbols experiments at 700 °C < T ≤ 800 °C, and filled symbols experiments at T > 800 °C. Stars (★) represent the composition of melanite garnet from Kjarsgaard et al. (1995), in HOL14-experiments at 106 MPa, 750 °C and at 108 MPa, 700 °C. Data are from Table 6.7.

Figure 6.8: Plot of nepheline microprobe analyses from LS-, two liquid-, and LC-experiments, and from wollastonite nephelinite HOL14, onto part of the nepheline (Ne) – kalsilite (Ks) – quartz (Qz) triangular plot (mol. %). Nepheline from experiment CP109 (200 MPa) is represented by a dot. Squares represent nepheline crystals from 20 MPa experiments, circles from 40 MPa experiments and diamonds from 100 MPa experiments. Open symbols represent experiments at $T \leq 700$ °C, half-filled symbols experiments at 700 °C $< T \leq 800$ °C, and filled symbols experiments at $T > 800$ °C. Asterixes (+) represent the composition of nepheline crystals from C/CH_4 buffered experiments, and the bold asterix (✳) nepheline from open tube experiment CP78. Stars (★) represent the compositions of nepheline from Kjarsgaard et al. (1995), in two liquid-experiments at 106 MPa, 750 °C and at 108 MPa, 700 °C. The shaded area represents the compositional range exhibited by nepheline crystals from erupted wollastonite nephelinite HOL14. The arrows represent the compositional trends with decreasing pressure (P), temperature (T), f_{O2} and P_{CO2}. Data are from Table 6.5.

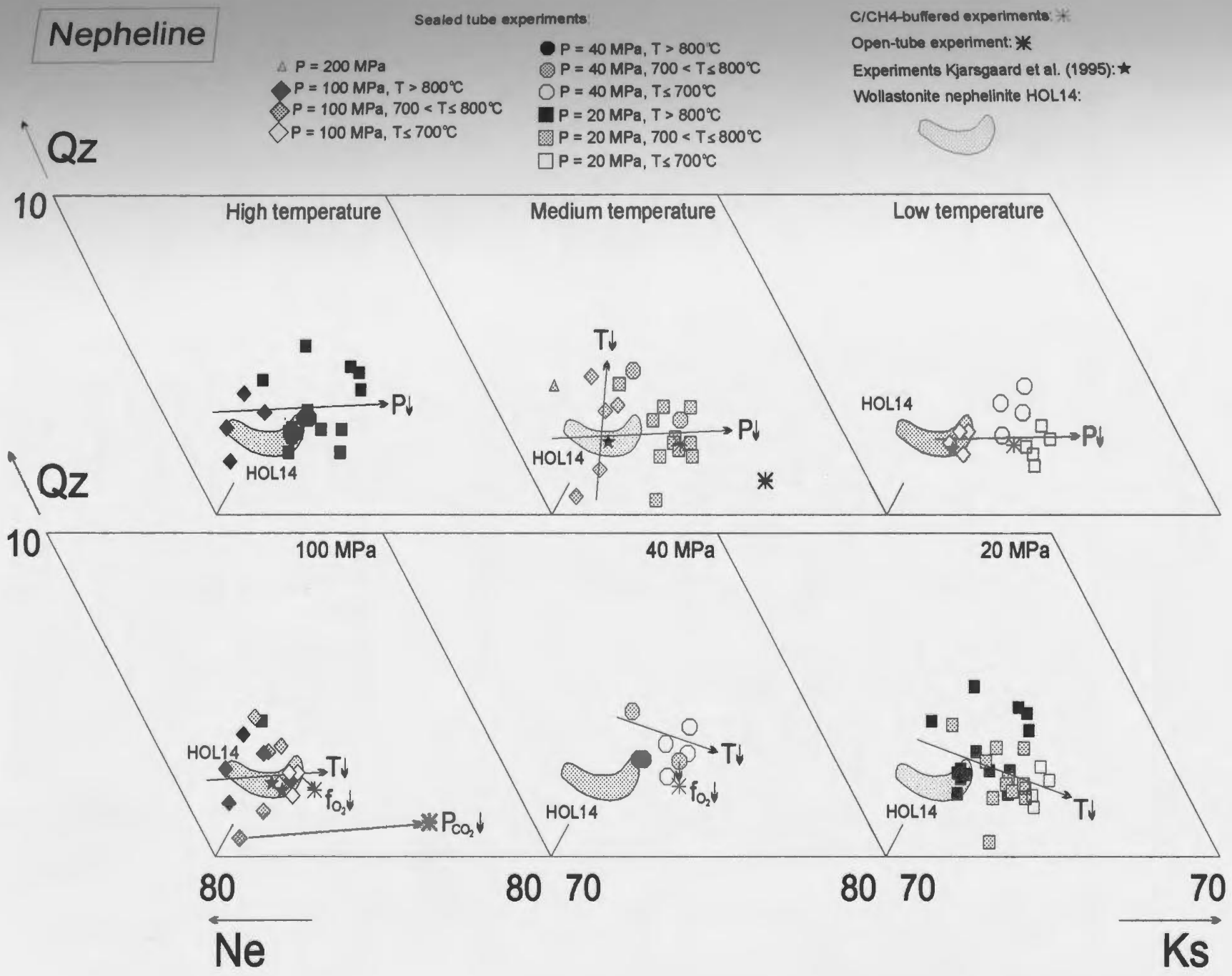
Nepheline
Sealed tube experiments:
P = 200 MPa
P = 100 MPa, T > 800°C
P = 100 MPa, 700 < T≤ 800°C
P = 100 MPa, T≤ 700°C
P = 40 MPa, T > 800°C
P = 40 MPa, 700 < T≤ 800°C
P = 40 MPa, T≤ 700°C
P = 20 MPa, T > 800°C
P = 20 MPa, 700 < T≤ 800°C
P = 20 MPa, T≤ 700°C
C/CH4-buffered experiments:
Open-tube experiment:
Experiments Kjarsgaard et al. (1995):
Wollastonite nephelinite HOL14:
Qz
10
High temperature
Medium temperature
Low temperature
P↓
T↓
HOL14
Qz
10
100 MPa
40 MPa
20 MPa
T↓
f_{O_2}↓
P_{CO_2}↓
HOL14
80
80 70
80 70
70
Ne
Ks

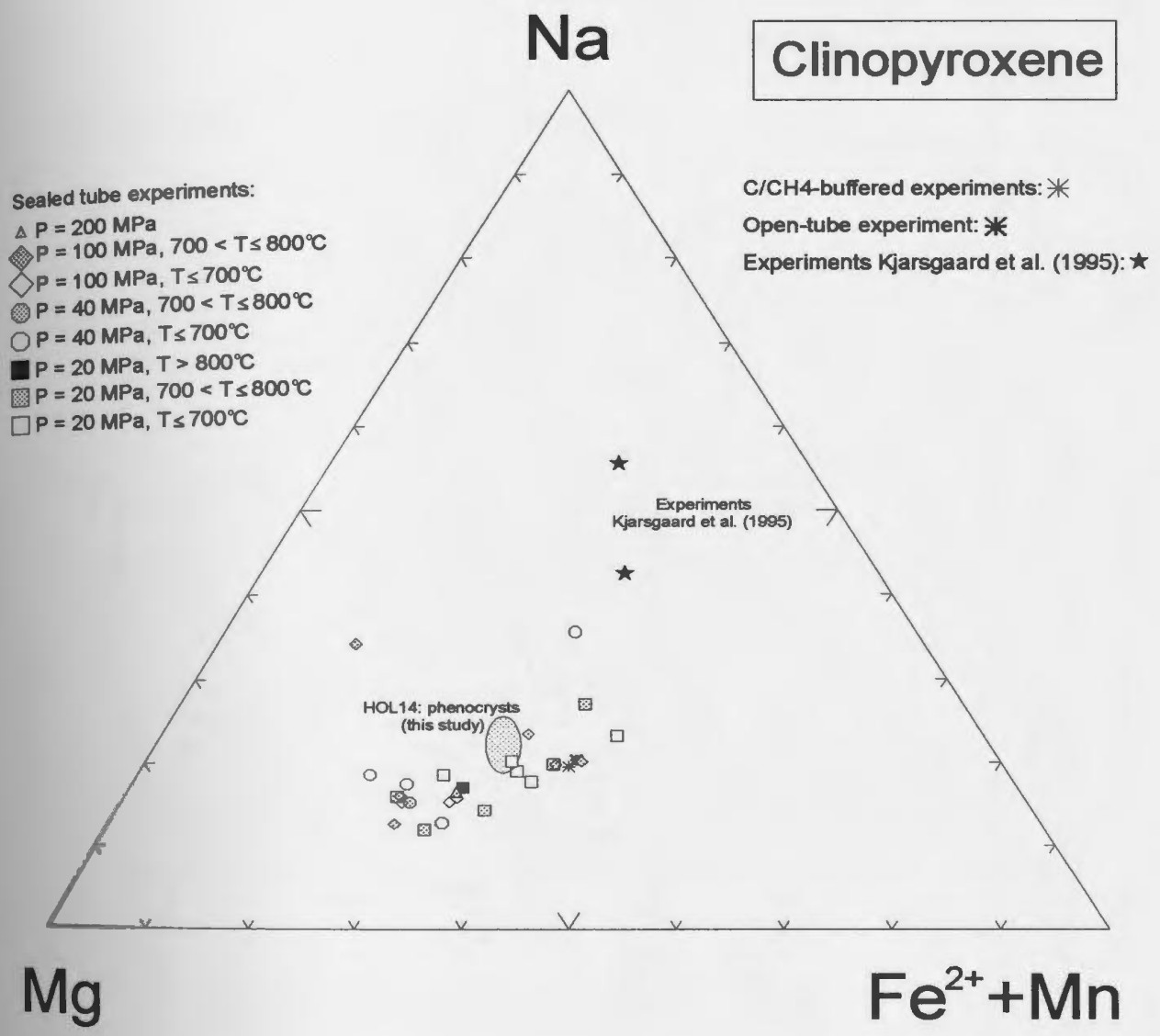

Figure 6.9: Plot of clinopyroxene microprobe analyses from LS-, two liquid-, and LC-experiments, and from wollastonite nephelinite HOL14, onto the Mg (diopside) - Na (aegirine) - Fe^{2+}+Mn (hedenbergite) triangular plot (atomic %). Clinopyroxene from experiment CP109 (200 MPa) is represented by a dot. Squares represent clinopyroxene crystals from 20 MPa experiments, circles from 40 MPa experiments and diamonds from 100 MPa experiments. Open symbols represent experiments at T ≤ 700 °C, half-filled symbols experiments at 700 °C < T ≤ 800 °C, and filled symbols experiments at T > 800 °C. Asterixes (✳) represent the composition of clinopyroxene crystals from C/CH_4 buffered experiments, and the bold asterix (✳) clinopyroxene from open tube experiment CP78. Stars (★) represent the composition of clinopyroxene from Kjarsgaard et al. (1995), in two liquid-experiments at 106 MPa, 750 °C and at 108 MPa, 700 °C. The shaded area represents the compositional range exhibited by clinopyroxene phenocrysts from erupted wollastonite nephelinite HOL14. Data are from Table 6.6.

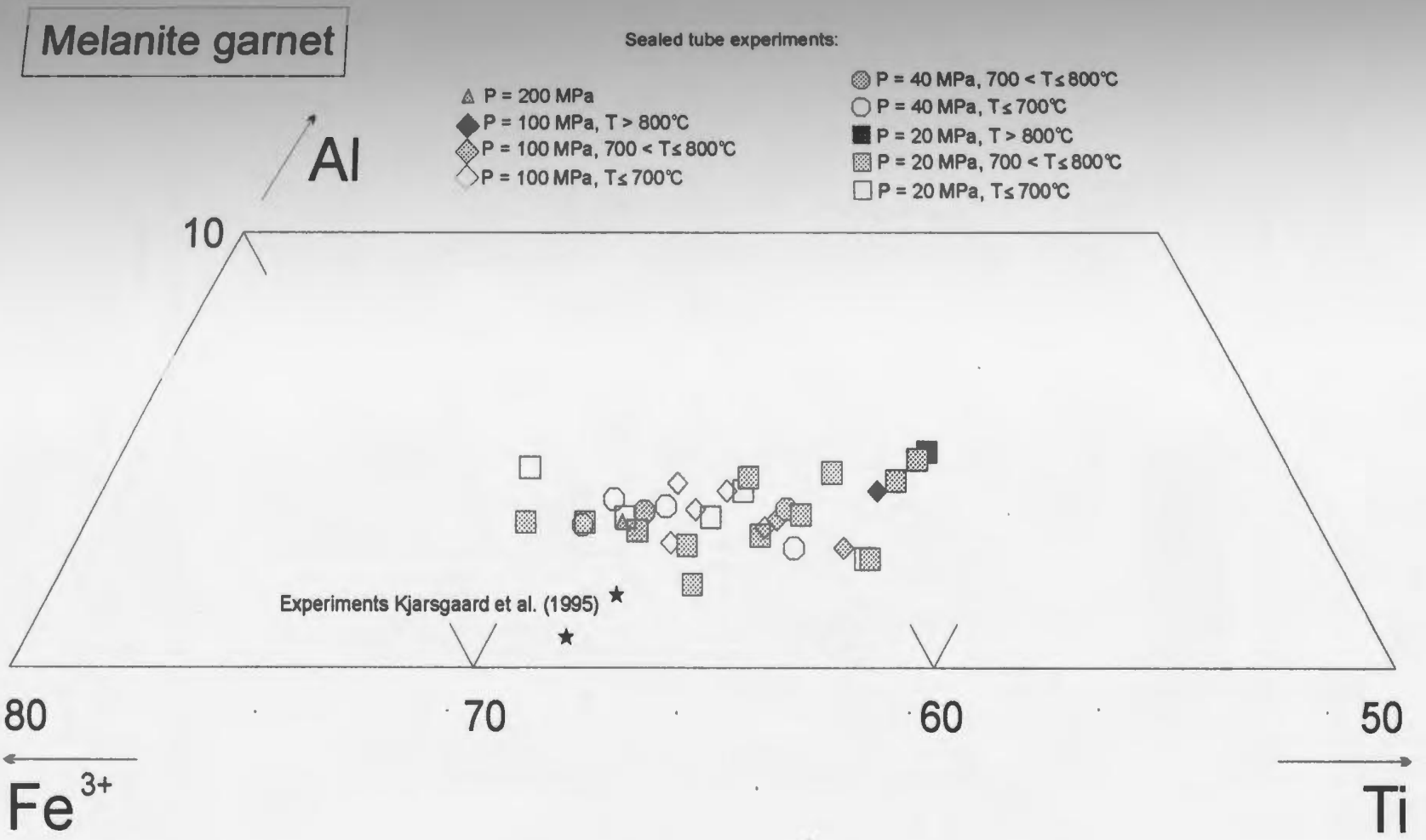

Figure 6.10: Plot of melanite garnet microprobe analyses from LS-, two liquid-, and LC-experiments, and from wollastonite nephelinite HOL14, onto part of the Al - Fe^{3+} - Ti ternary (atomic %). Melanite garnet from experiment CP109 (200 MPa) is represented by a dot. Squares represent melanite garnet crystals from 20 MPa experiments, circles from 40 MPa experiments and diamonds from 100 MPa experiments. Open symbols represent experiments at T ≤ 700 °C, half-filled symbols experiments at 700 °C < T ≤ 800 °C, and filled symbols experiments at T > 800 °C. Stars (★) represent the composition of melanite garnet from Kjarsgaard et al. (1995), in two liquid-experiments at 106 MPa, 750 °C and at 108 MPa, 700 °C. Data are from Table 6.7.

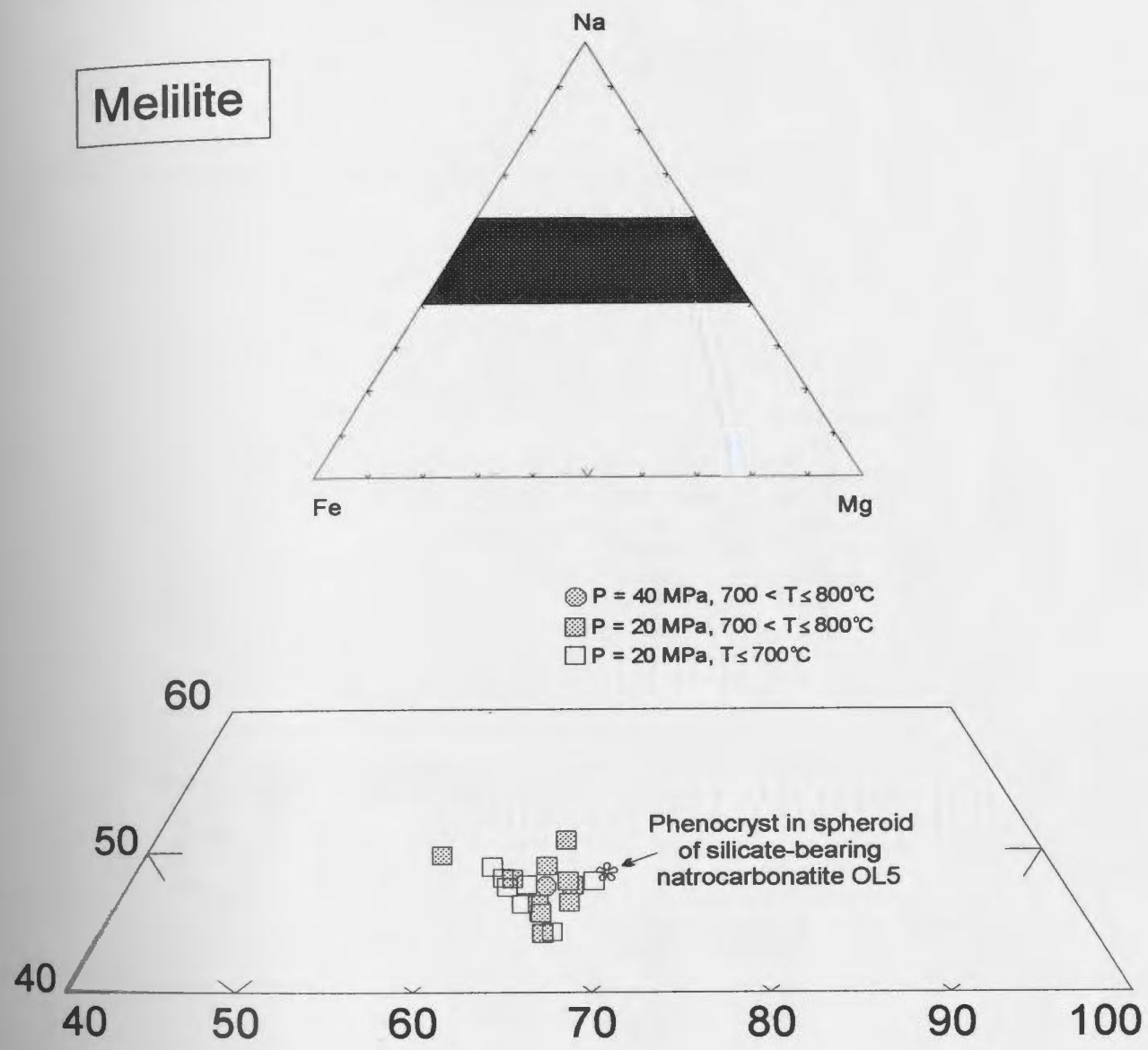

Figure 6.11: Plot of melilite microprobe analyses from two-liquid experiments and from silicate-bearing natrocarbonatite OL5 in terms of ternary Fe (Fe-åkermanite), Mg (åkermanite) and Na (soda melilite) end members. Squares represent melilites from 20 MPa experiments, and circles from 40 MPa experiments. Open symbols represent experiments at T ≤ 700 °C, and half-filled symbols are experiments at 700 °C < T ≤ 800 °C. White "flower": phenocryst in spheroids in silicate-bearing natrocarbonatite OL5. Data are from Table 6.13 and 3.5.

Figure 6.12: Hamilton triangular diagram representing the compositions of silicate liquid from HOL14-experiments. Squares represent silicate liquid from 20 MPa experiments, and diamonds from 100 MPa experiments. Half-filled symbols represent experiments at 700 °C < T ≤ 800 °C, and filled symbols are experiments at T > 800 °C. The area of interest is enlarged. Data are from Table 6.17.

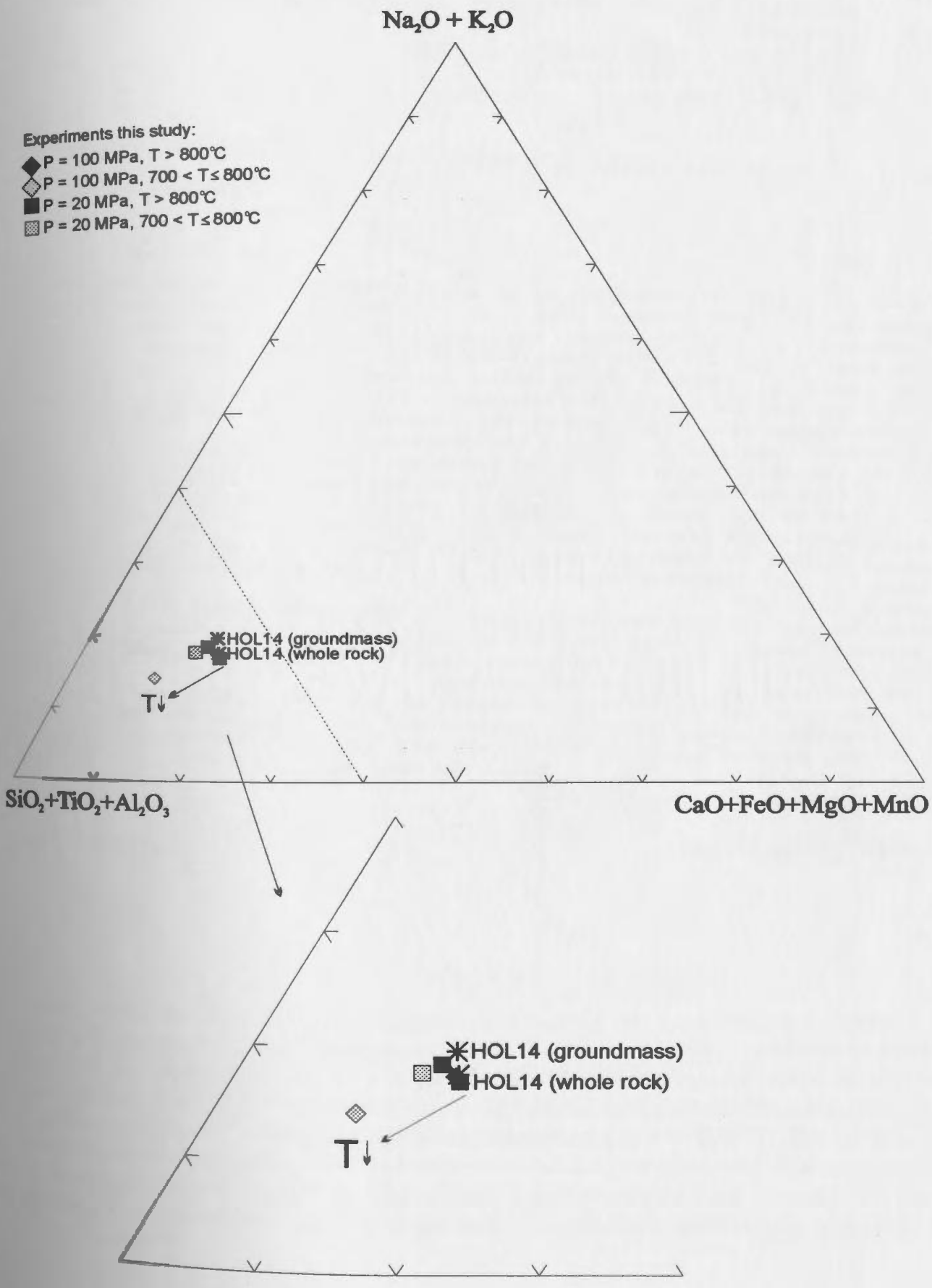
$Na_2O + K_2O$
Experiments this study:
P = 100 MPa, T > 800°C
P = 100 MPa, 700 < T≤ 800°C
P = 20 MPa, T > 800°C
P = 20 MPa, 700 < T≤ 800°C
HOL14 (groundmass)
HOL14 (whole rock)
T↓
$SiO_2+TiO_2+Al_2O_3$
$CaO+FeO+MgO+MnO$
HOL14 (groundmass)
HOL14 (whole rock)
T↓

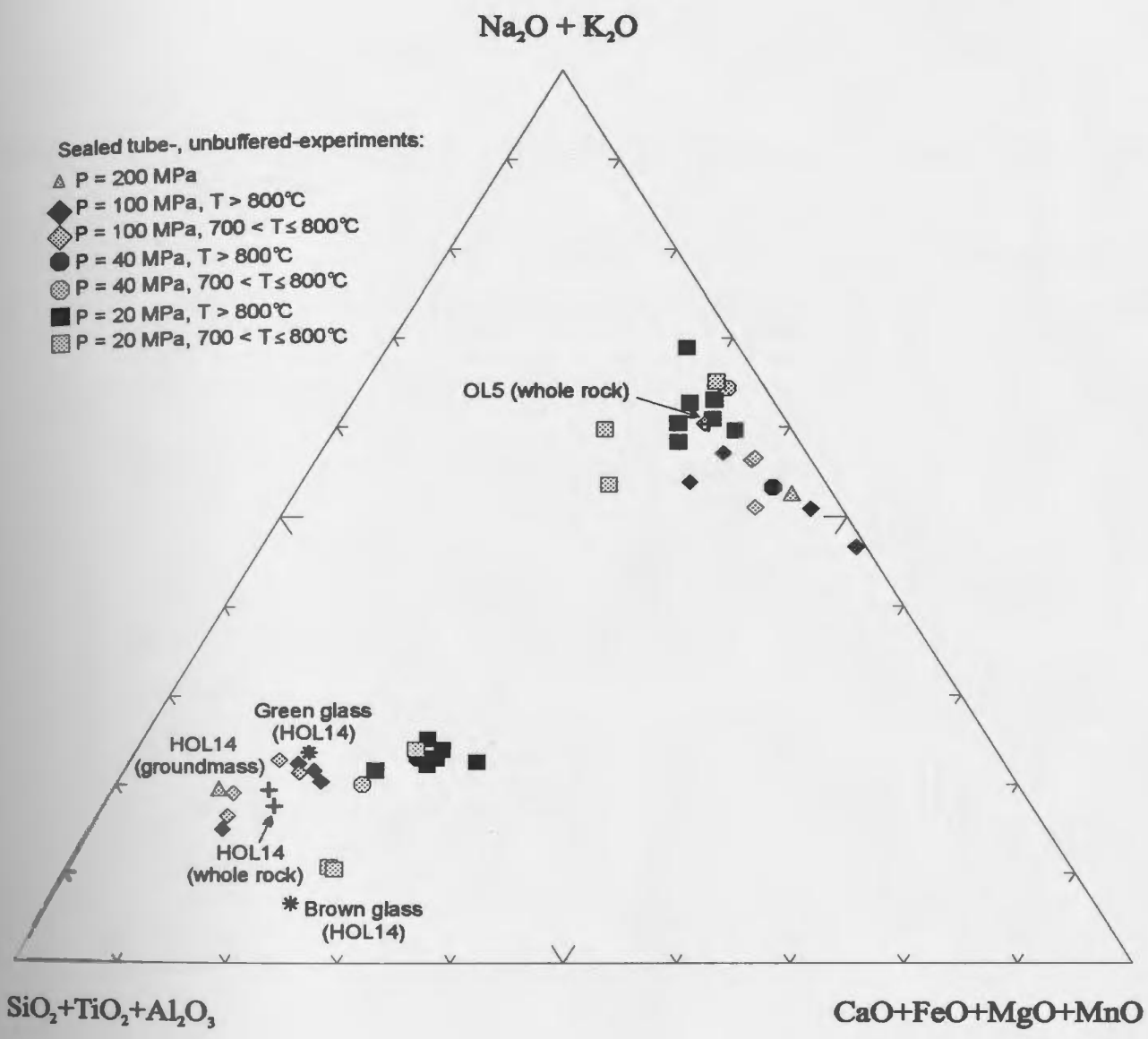

Figure 6.13: Hamilton triangular diagram representing the compositions of silicate and carbonate liquids from two liquid-experiments. Squares represent liquids from 20 MPa experiments, circles from 40 MPa experiments, diamonds from 100 MPa experiments and triangles from 200 MPa experiments. Half-filled symbols represent experiments at 700 °C < T ≤ 800 °C, and filled symbols are experiments at T > 800 °C. The composition of wollastonite nephelinite HOL14 (whole rock and groundmass) and of silicate-bearing natrocarbonatite OL5 are indicated by crosses (+). The composition of green and brown glasses from wollastonite nephelinite HOL14 are indicated by asterixes (*). Data are from Table 6.17.

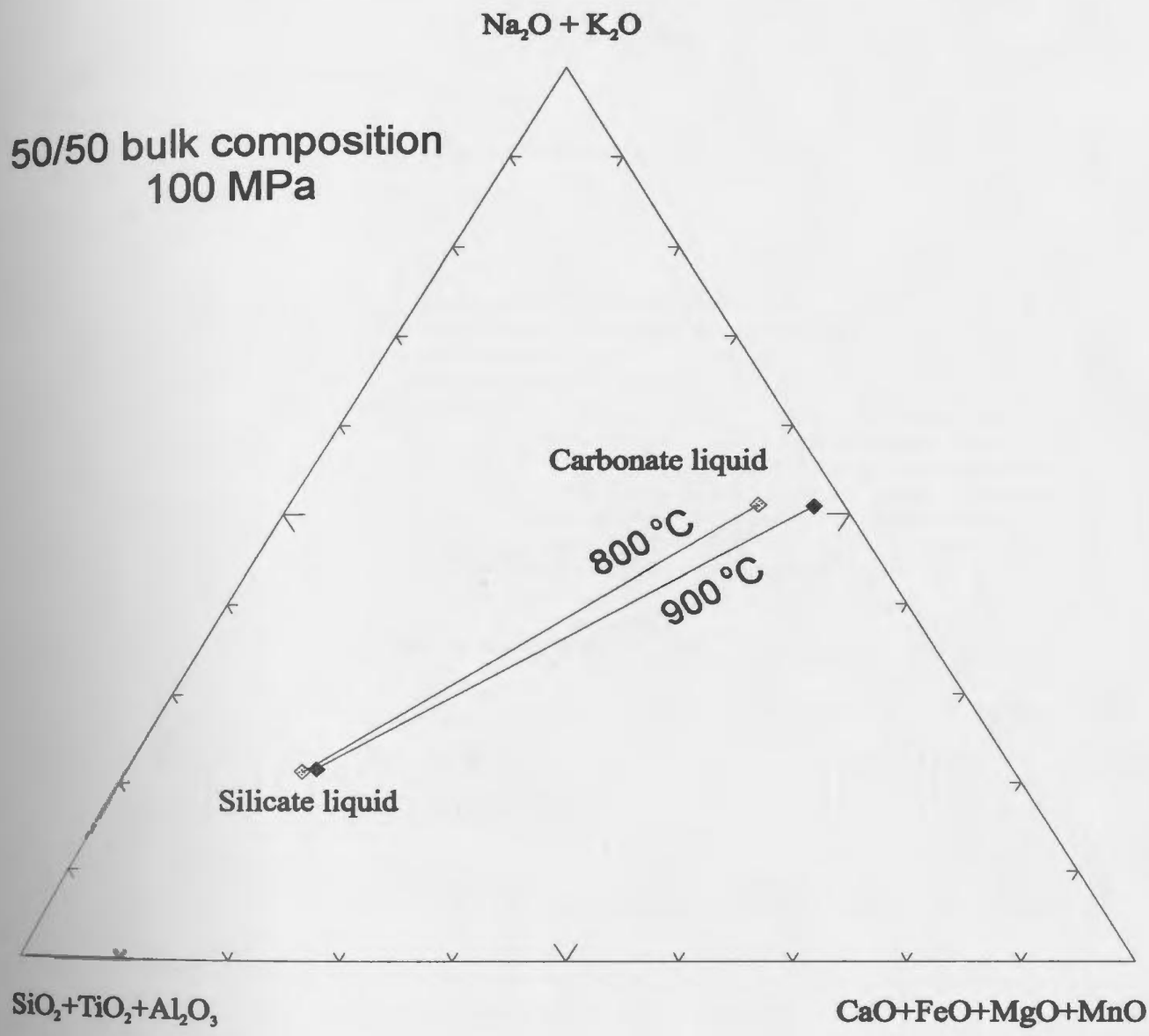

Figure 6.14: Hamilton triangular diagram representing the compositions of silicate and carbonate liquids from two-liquid experiments at 100 MPa. Tie-lines join the symbols representing compositions of silicate and carbonate liquids from the same experiments. With decreasing temperature, composition of carbonate liquid evolves towards high M_2O/low MO, and that of silicate liquid towards high $MO_2+M_2O_3$, the combination of the compositional variations on carbonate and silicate liquids produced by decreasing temperature leads to counter-clockwise rotation of the tie-lines, although it is not very significant. Half-filled symbols experiments at 700 °C < T ≤ 800 °C, and filled symbols experiments at T > 800 °C. Data are from Table 6.17.

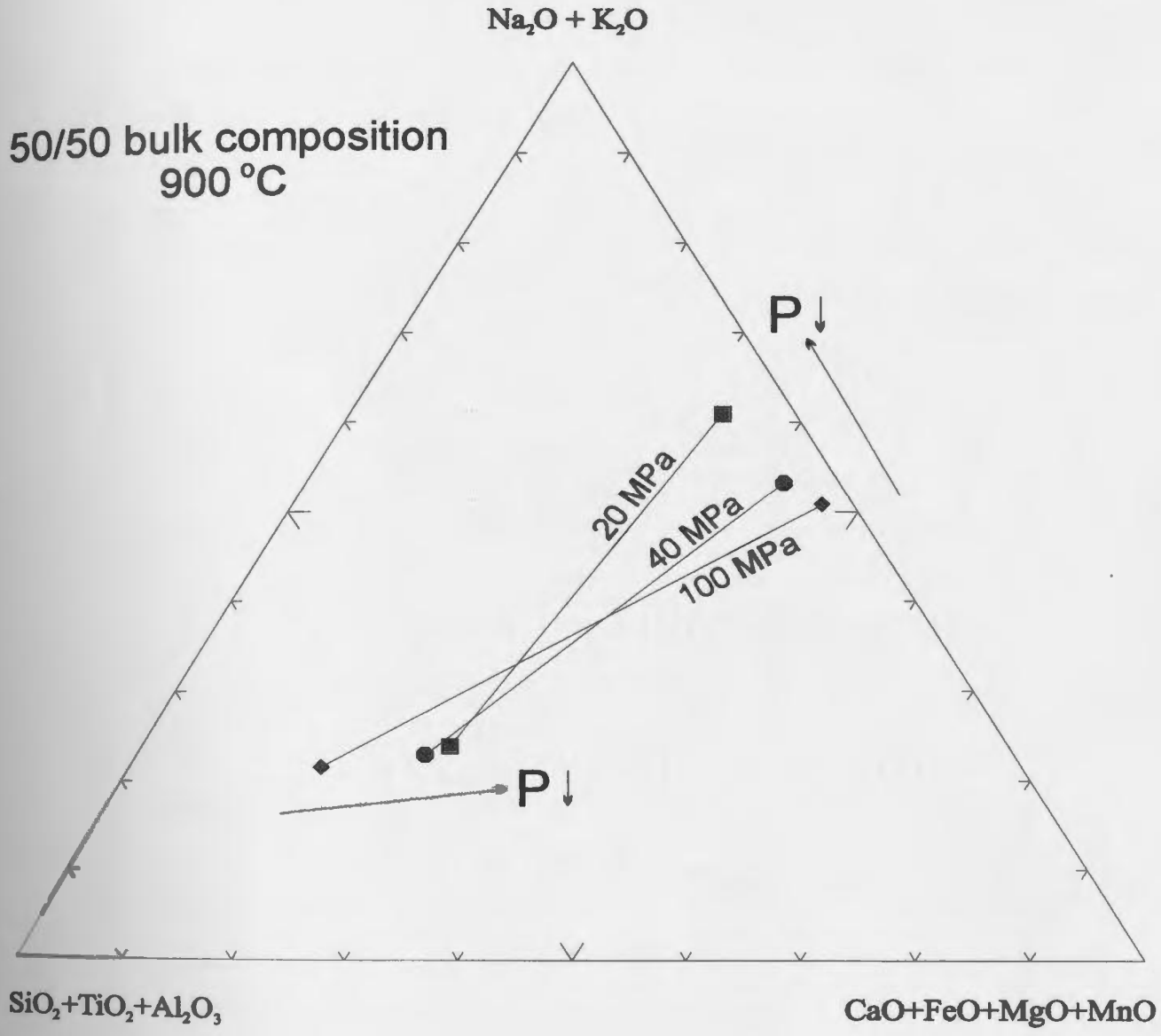

Figure 6.15: Hamilton triangular diagram representing the compositions of silicate and carbonate liquids from two-liquid experiments at 900 °C. Tie-lines join the symbols representing compositions of silicate and carbonate liquids from the same experiments. With decreasing pressure (P; arrows), the composition of carbonate liquid evolves towards high M_2O/low MO, and that of silicate liquid towards low $MO_2+M_2O_3$, and the combination of the compositional variations on carbonate and silicate liquids produced by decreasing pressure also leads to counter-clockwise rotation of the tie-lines. Squares represent liquids from 20 MPa experiments, circles from 40 MPa experiments, diamonds from 100 MPa experiments and triangles from 200 MPa experiments. Data are from Table 6.17.

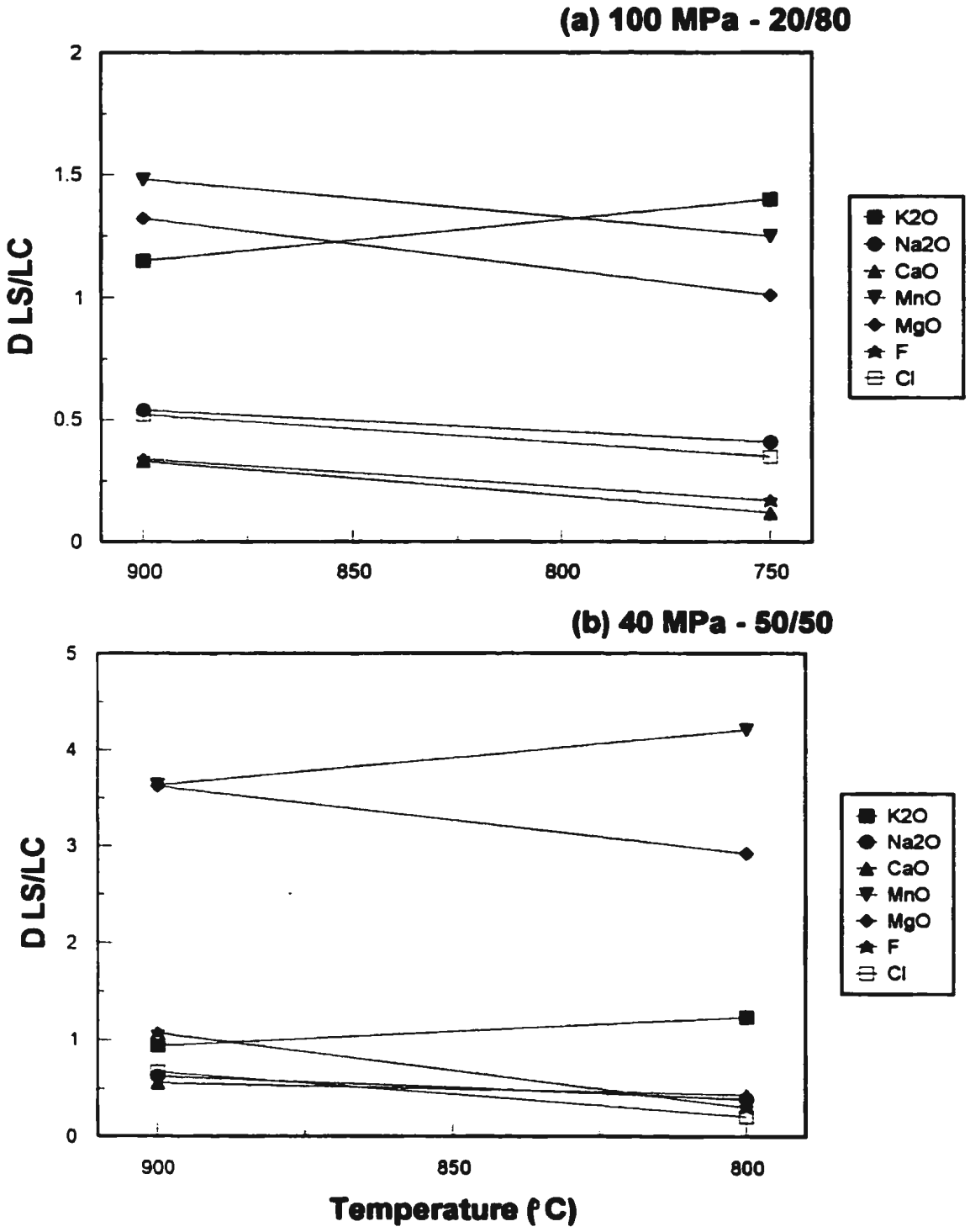

Figure 6.16: Effect of temperature on the distribution coefficients of selected major elements between silicate and carbonate liquids from the experiments. Data are from Table 6.17.

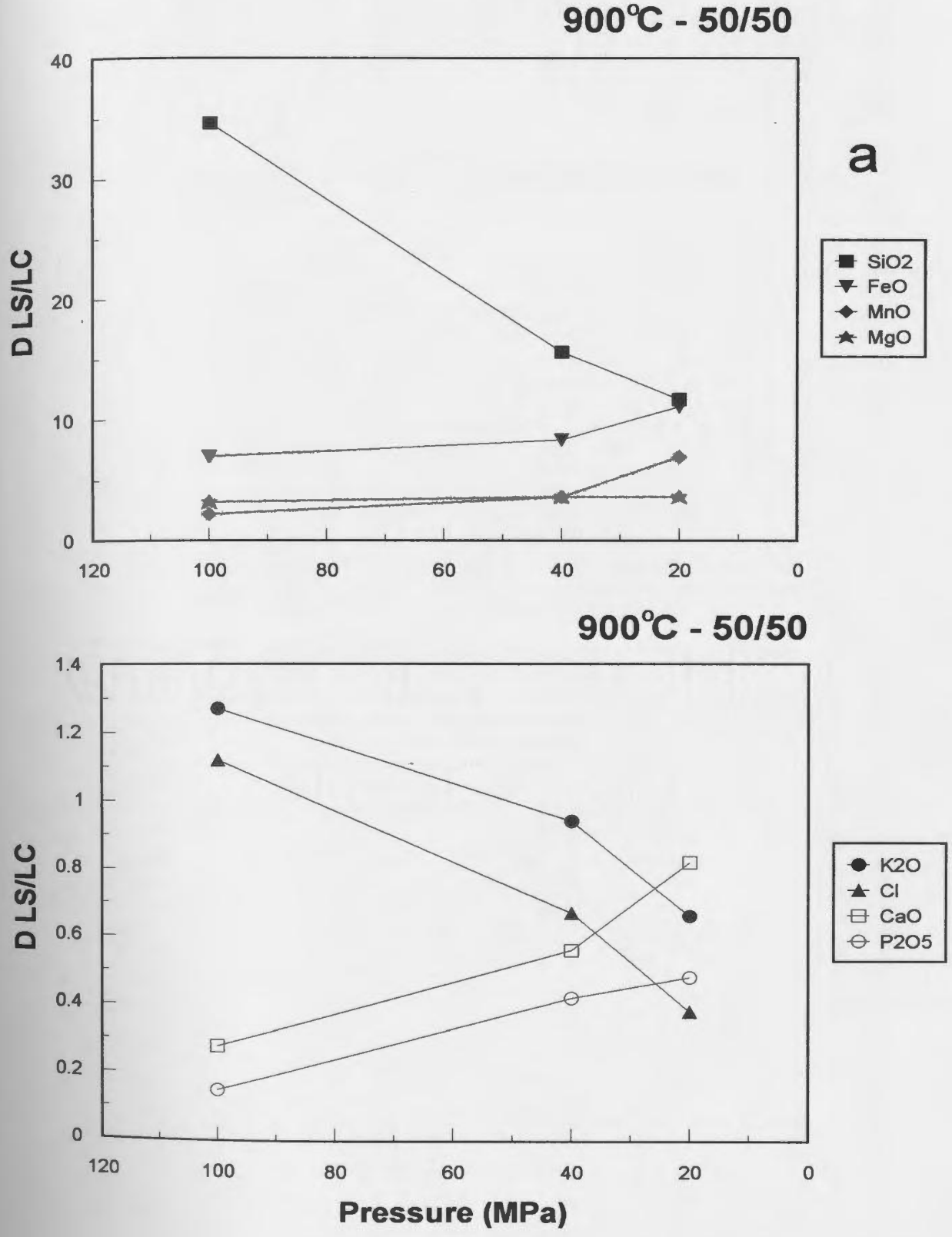

Figure 6.17: Effect of pressure on the distribution coefficients of selected major elements between silicate and carbonate liquids from the experiments. a) 900 °C, 50/50 bulk composition; b) 800 °C, 50/50 bulk composition. Data are from Table 6.17.

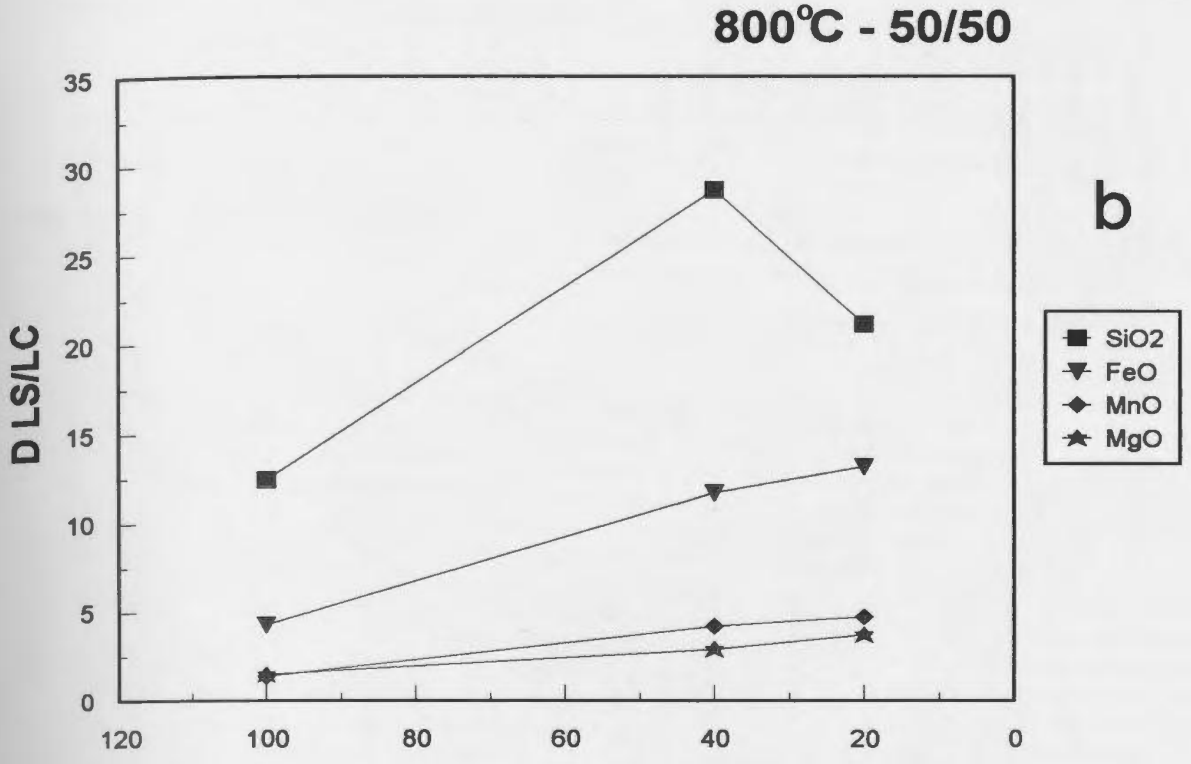
800°C - 50/50
b
D LS/LC
35
30
25
20
15
10
5
0
120
100
80
60
40
20
0
SiO2
FeO
MnO
MgO

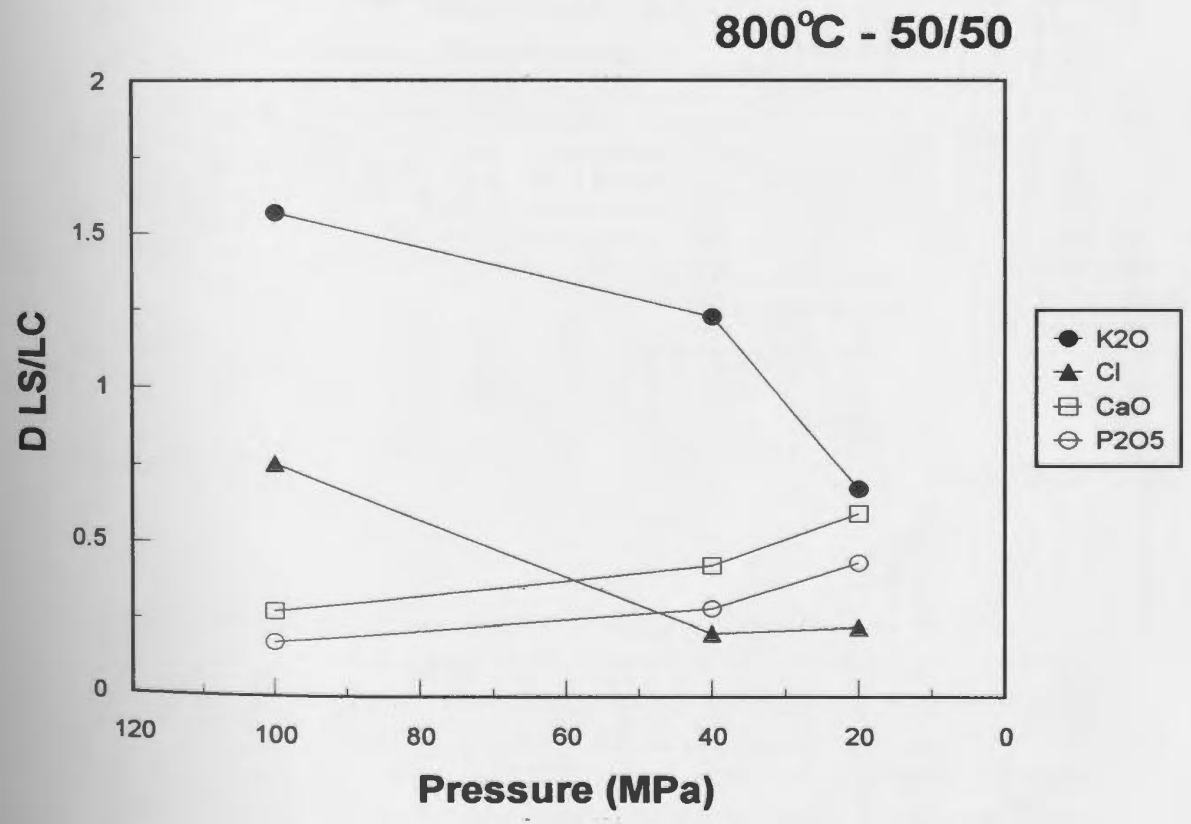
800°C - 50/50
D LS/LC
2
1.5
1
0.5
0
120
100
80
60
40
20
0
Pressure (MPa)
K2O
Cl
CaO
P2O5

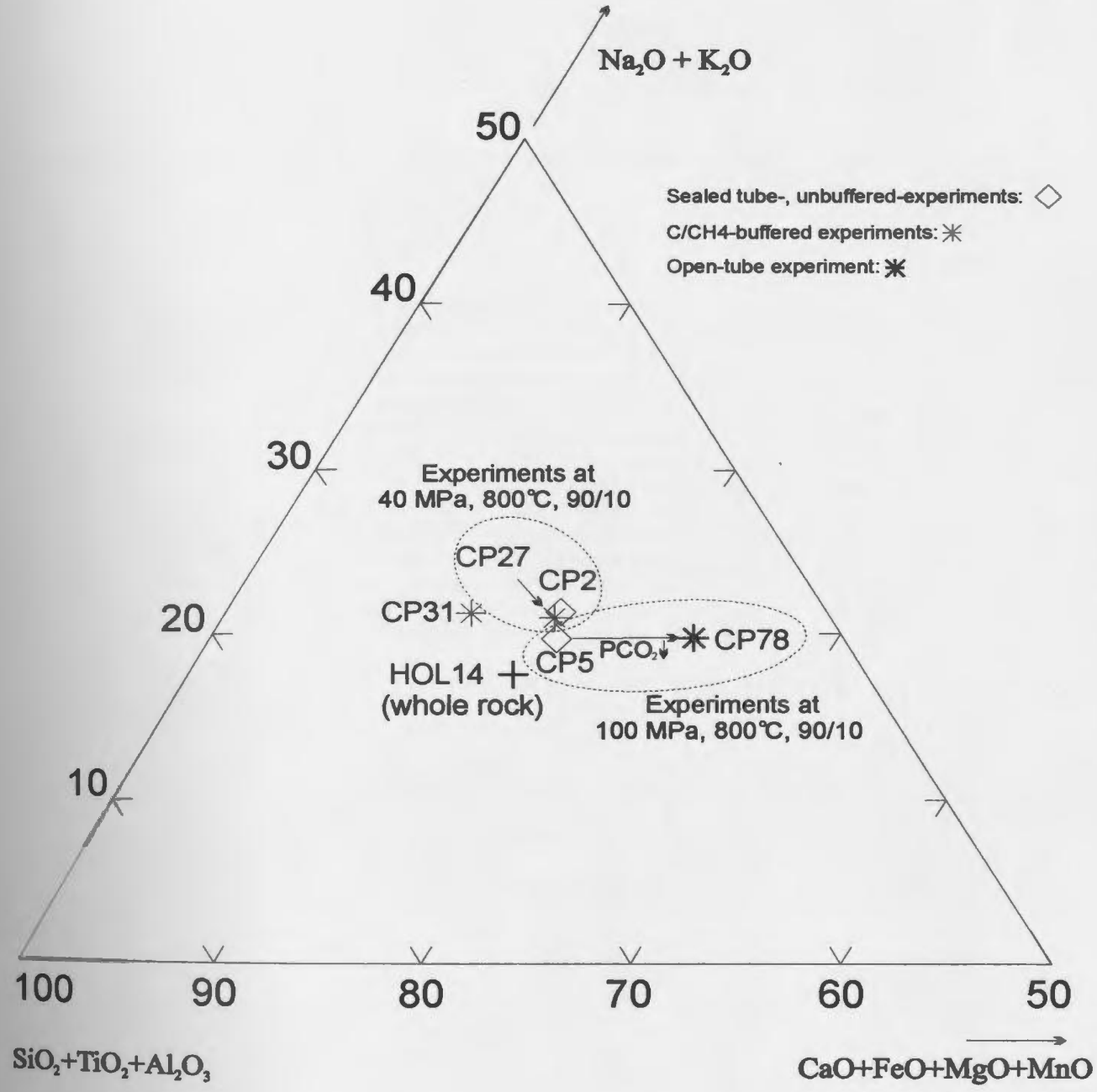

Figure 6.18: Hamilton triangular diagram representing the compositions of silicate liquid from C/CH_4 buffered-experiments CP27 and CP31 (symbol ✳), and from open tube-experiment CP78 (symbol ✳). For comparison with C/CH_4 buffered-experiment CP27, equivalent unbuffered-experiment CP2 is also plotted (open diamond). For comparison with open tube buffered-experiment CP78, equivalent sealed tube-experiment CP5 is also plotted (open diamond), and the compositional trend with decreasing P_{CO2} is represented by an arrow. Composition of wollastonite nephelinite HOL14 is plotted (symbol +). Data are from Table 6.17.

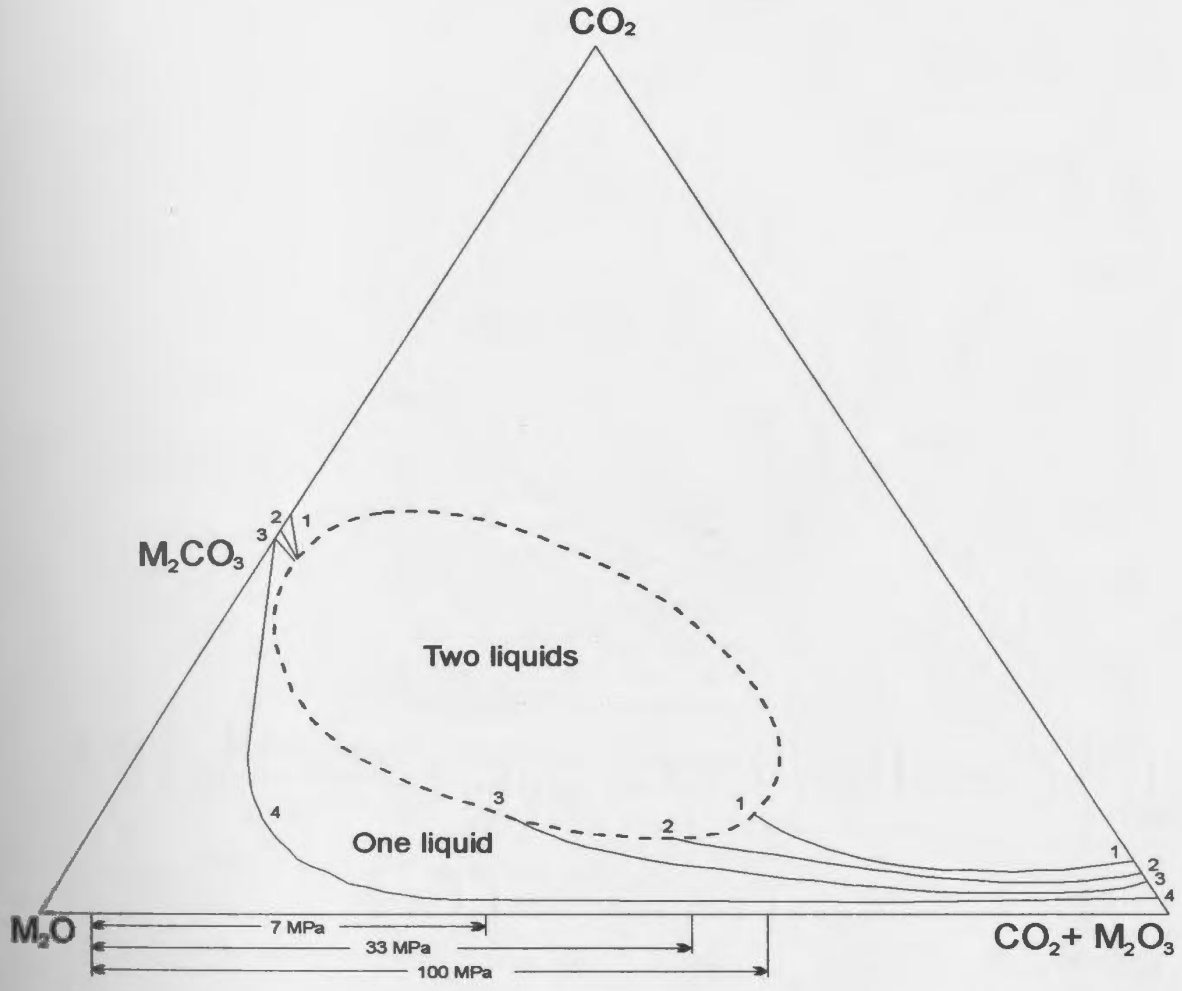

Figure 6.19: Schematic diagram illustrating the intersection of the CO_2-saturated liquid (*heavy solid lines* labelled *1 to 4*) and the two-liquid field (*dashed lines*). With increasing pressure, CO_2 solubility increases and the vapour-saturated liquidus moves "up" in CO_2 space, as shown by the *heavy lines* labelled *4* (lowest pressure) to *1* (highest pressure). Note that line *4* does not intersect the two liquid field (1 atm) and that lines *3*, *2* and *1* (7, 33 and 100 MPa, respectively) intersect larger volumes of the two liquid field. This increased width of the two-liquid field is shown below the triangle (for 7, 33 and 100 MPa, respectively), as a projection from CO_2 through the intersection of the vapour-saturated liquidus for *1* to *3* (omitted for clarity). $M_2O = Na_2O + K_2O$; $MO_2 = SiO_2 + TiO_2$; $M_2O_3 = Al_2O_3 + Fe_2O_3$. From Kjarsgaard et al. (1995).

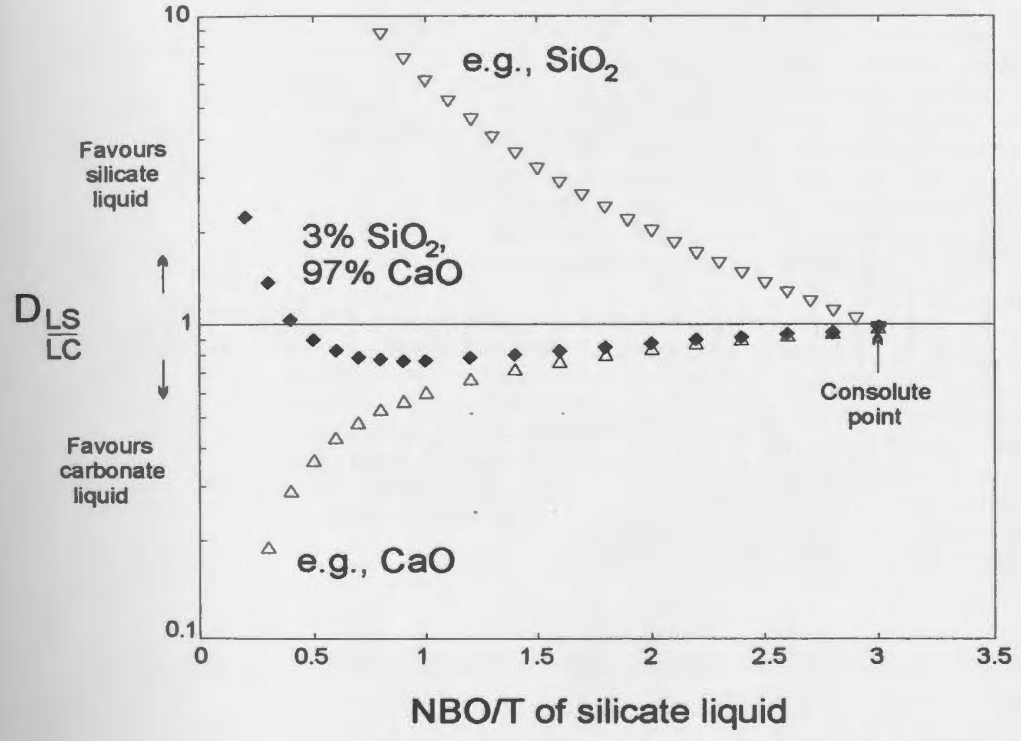

Figure 6.20: Typical partitioning trends, where distribution coefficients are plotted as a function of NBO/T (non-bridging oxygens per tetrahedra) of the silicate liquid. Inverted triangles based on SiO_2 trends, and normal triangles based on CaO trends in later figures. Diamonds are generated by combining 3 % of the SiO_2 trend with 97 % of the CaO. Note inverted triangles continue off scale. The consulate point represents the point at which the solvus closes and at which the composition of both liquids is similar. From Brooker (1995).

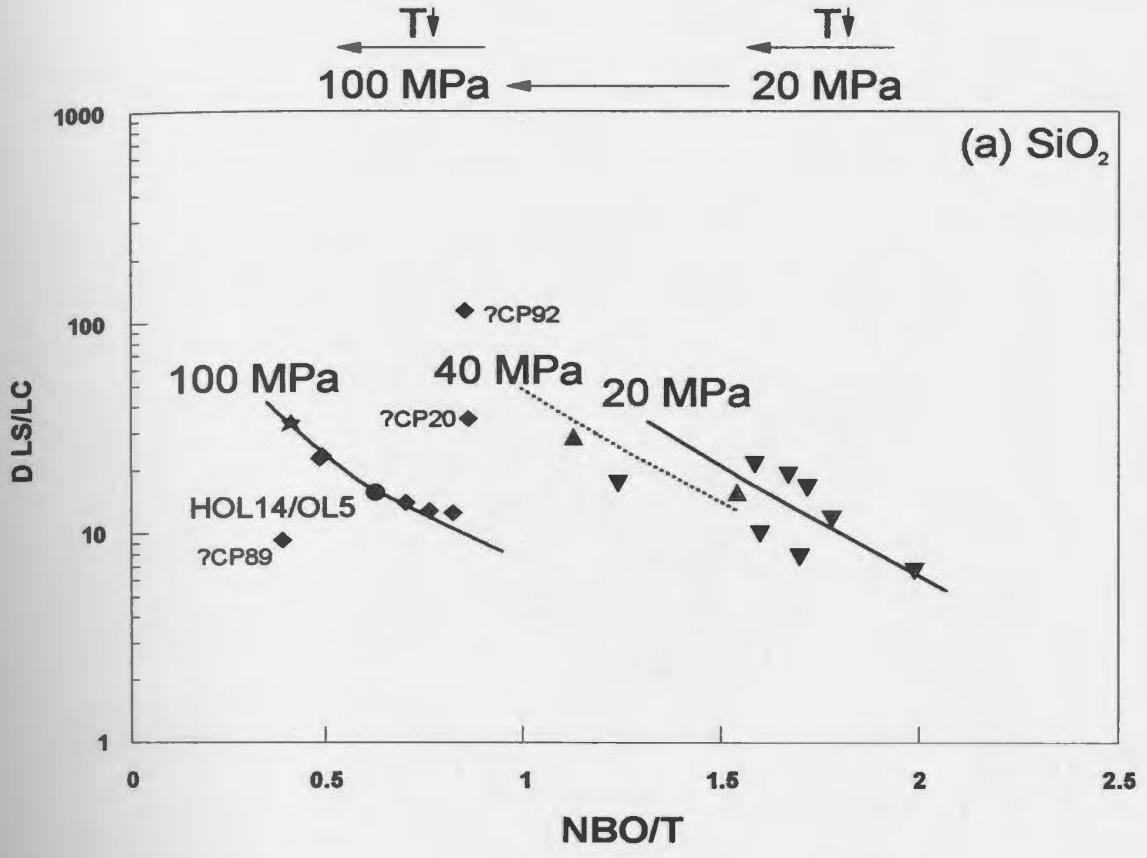

Figure 6.21: Distribution coefficients between silicate and carbonate liquids ($D_{LS/LC}$) as a function of NBO/T (non-bridging oxygens per tetrahedra) of the silicate liquid for (a) SiO_2, (b) TiO_2, (c) Al_2O_3, (d) FeO, (e) MnO, (f) MgO, (g) CaO, (h) Na_2O, (i) K_2O, (j) P_2O_5, (k) F, (l) Cl, (m) SO_3, (n) BaO, (o) SrO. Inverted triangles represent data for 20 MPa experiments, normal triangles for 40 MPa experiments, diamonds for 100 MPa experiments, the star for 200 MPa-experiment CP109 and the dot for the natural pair (groundmass HOL14/whole rock OL5). The arrows above the graphs represent the evolution of NBO/T values with increasing pressure from 20 to 100 MPa, and for each pressure, the evolution of NBO/T values with decreasing temperature (T). For the elements TiO_2, FeO, MnO and MgO that have a dual role, the arrows on the graphs indicate that with decreasing NBO/T, their role as network modifiers (Mod.) increases relatively to their role as network formers (Form.) (deduced from Fig. 6.20). The opposite trend is observed for K_2O. Data for $D_{LS/LC}$ are from Table 6.17 and data for NBO/T are from Table A6.4 in Appendix A4.

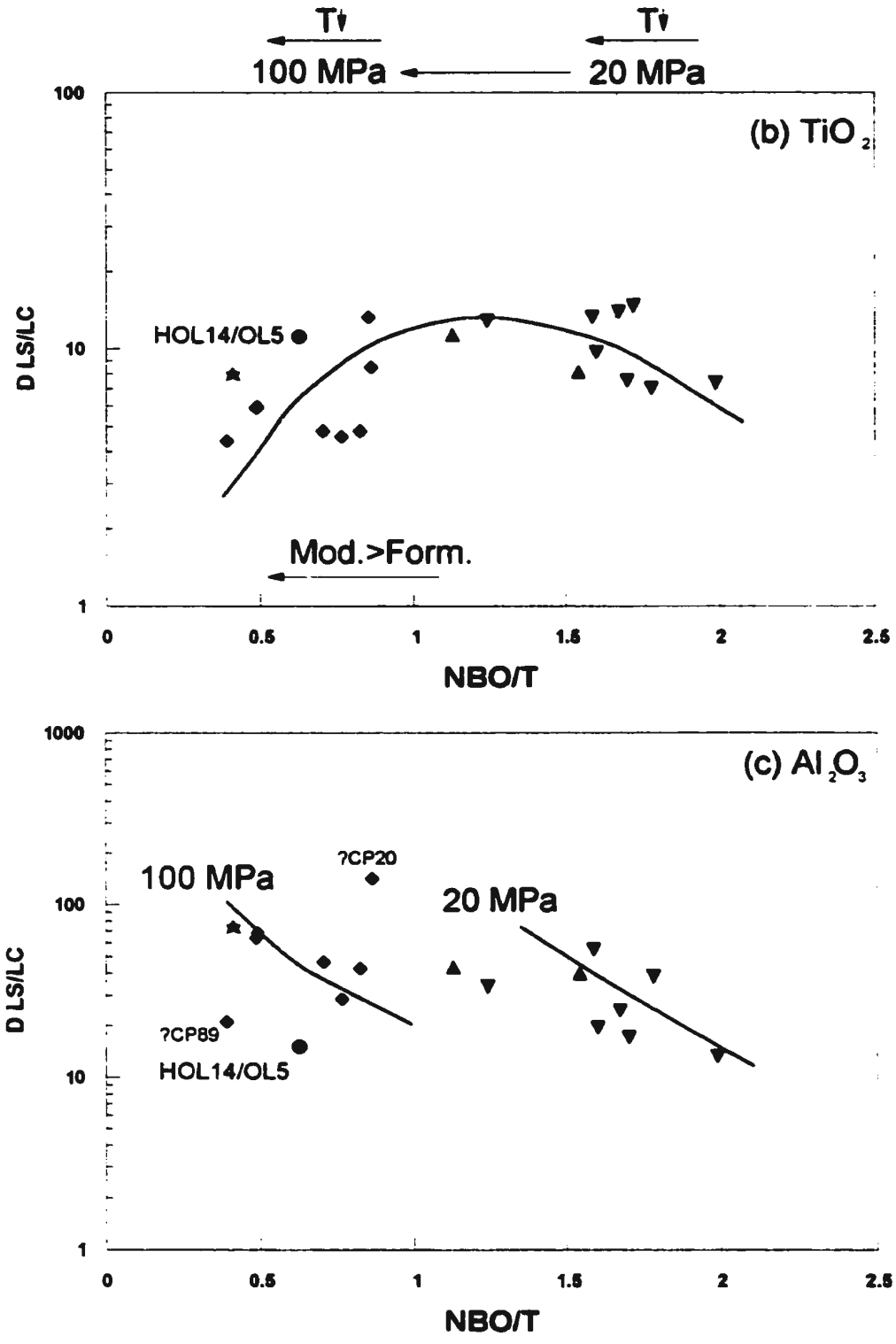
T↓
T↓
100 MPa
20 MPa
(b) TiO2
D LS/LC
HOL14/OL5
Mod.>Form.
NBO/T
(c) Al2O3
100 MPa
20 MPa
?CP20
?CP89
HOL14/OL5

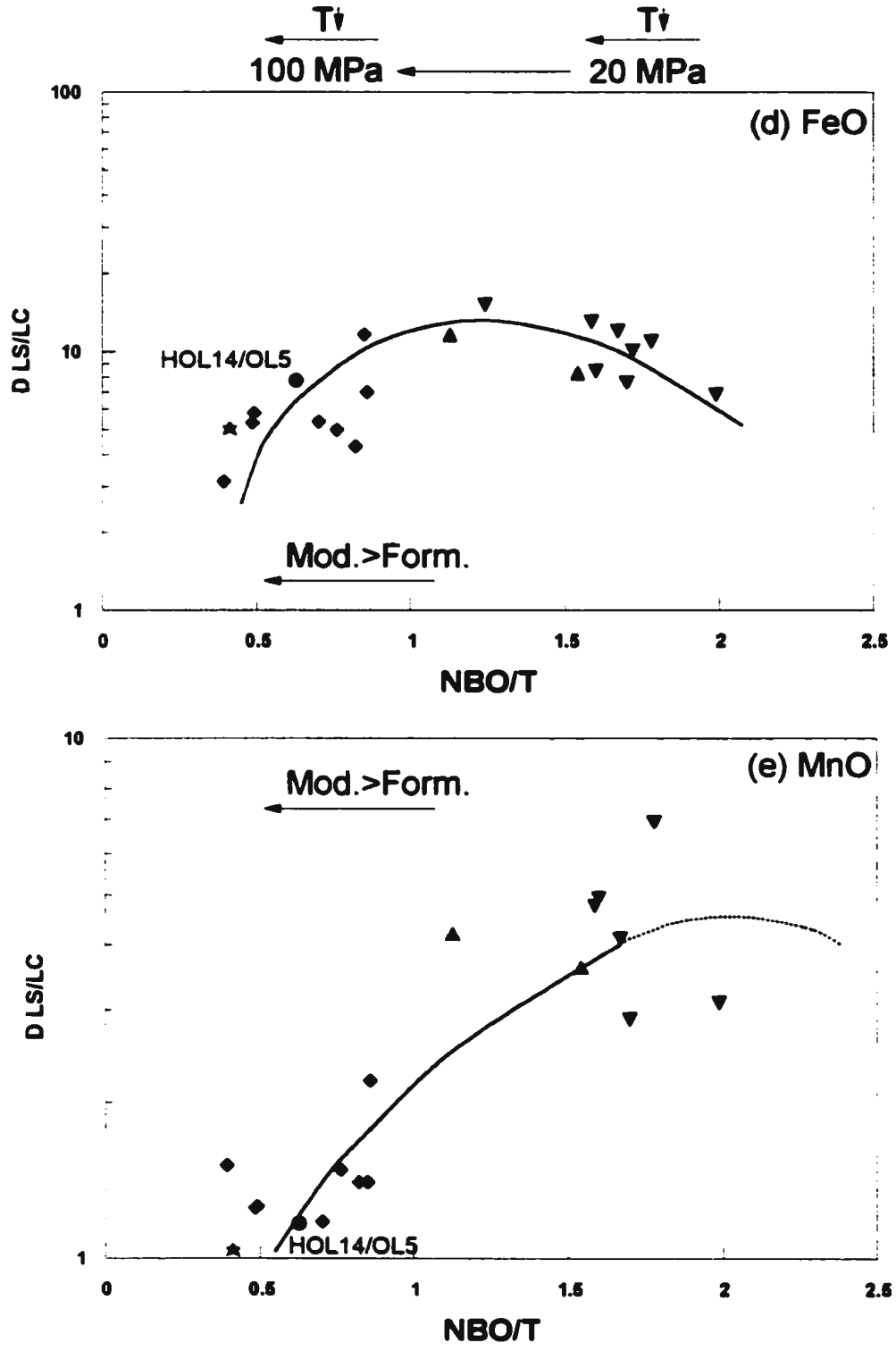
T↓
T↓
100 MPa
20 MPa
(d) FeO
100
10
1
D LS/LC
HOL14/OL5
Mod.>Form.
0
0.5
1
1.5
2
2.5
NBO/T
(e) MnO
Mod.>Form.
10
1
D LS/LC
HOL14/OL5
0
0.5
1
1.5
2
2.5
NBO/T

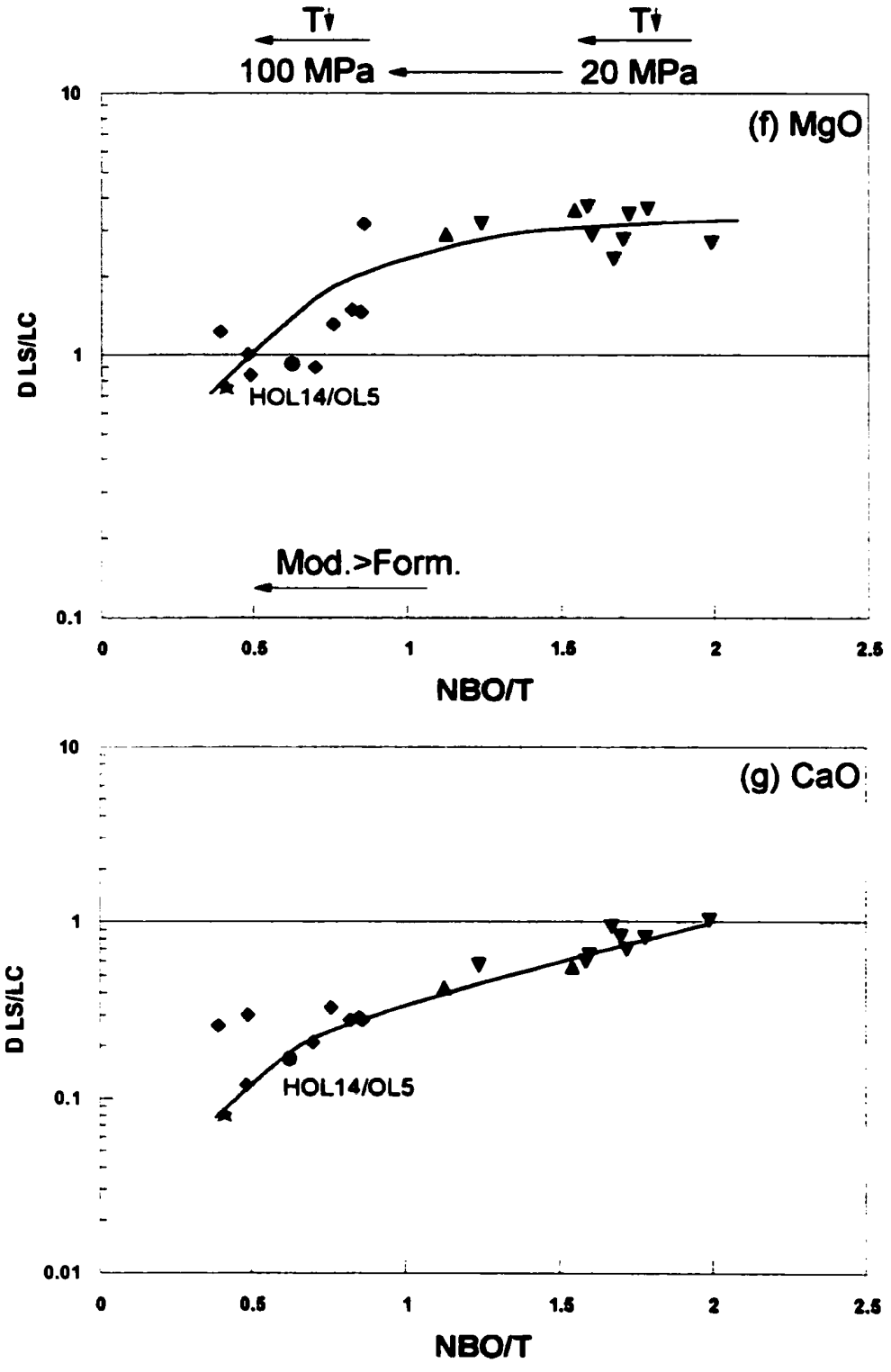
T↓
T↓
100 MPa
20 MPa
(f) MgO
D LS/LC
10
1
0.1
HOL14/OL5
Mod.>Form.
0
0.5
1
1.5
2
2.5
NBO/T
(g) CaO
D LS/LC
10
1
0.1
0.01
HOL14/OL5
0
0.5
1
1.5
2
2.5
NBO/T

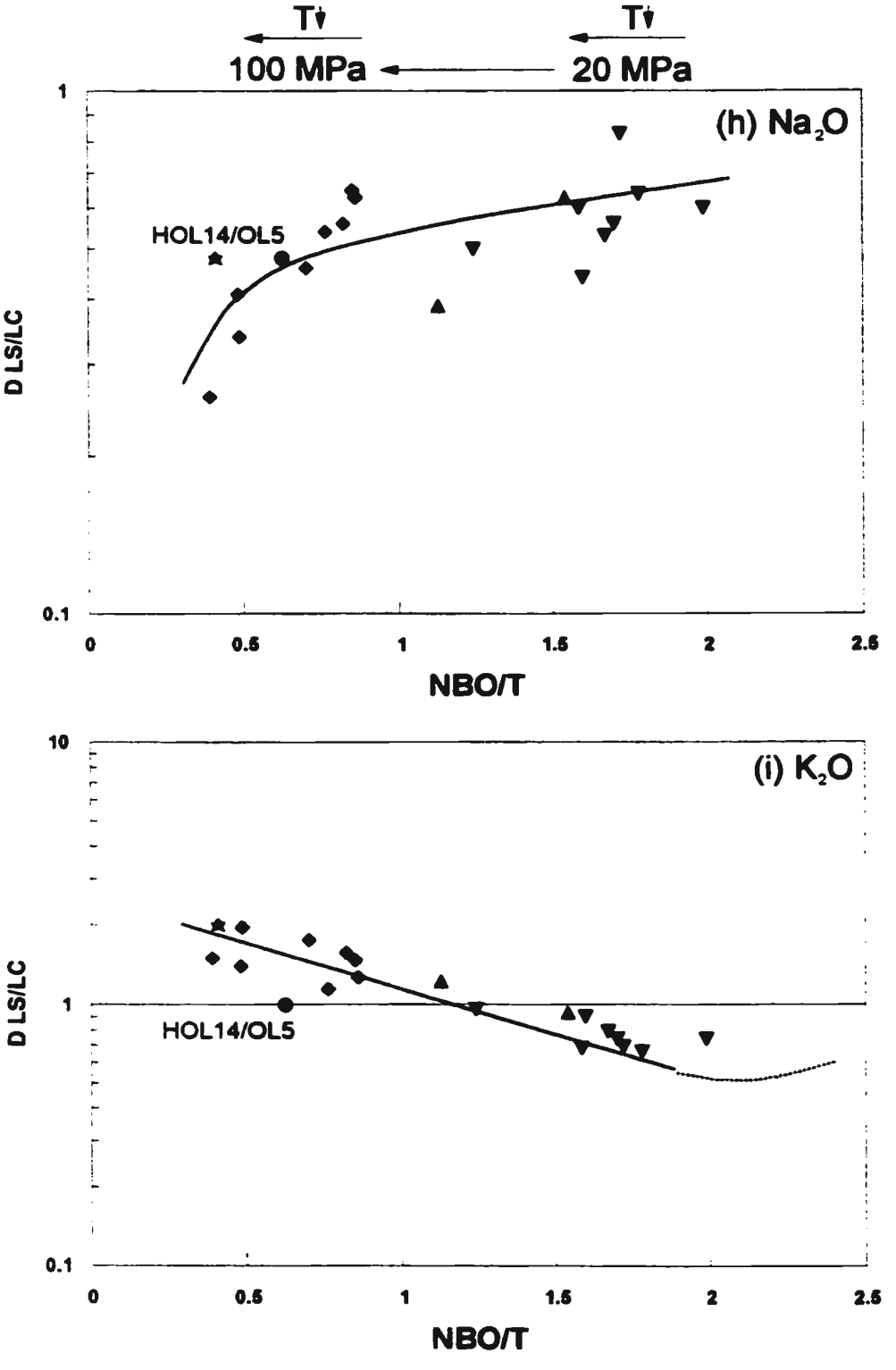
T↓
T↓
100 MPa
20 MPa
(h) Na_2O
HOL14/OL5
D LS/LC
NBO/T
(i) K_2O
HOL14/OL5
D LS/LC
NBO/T

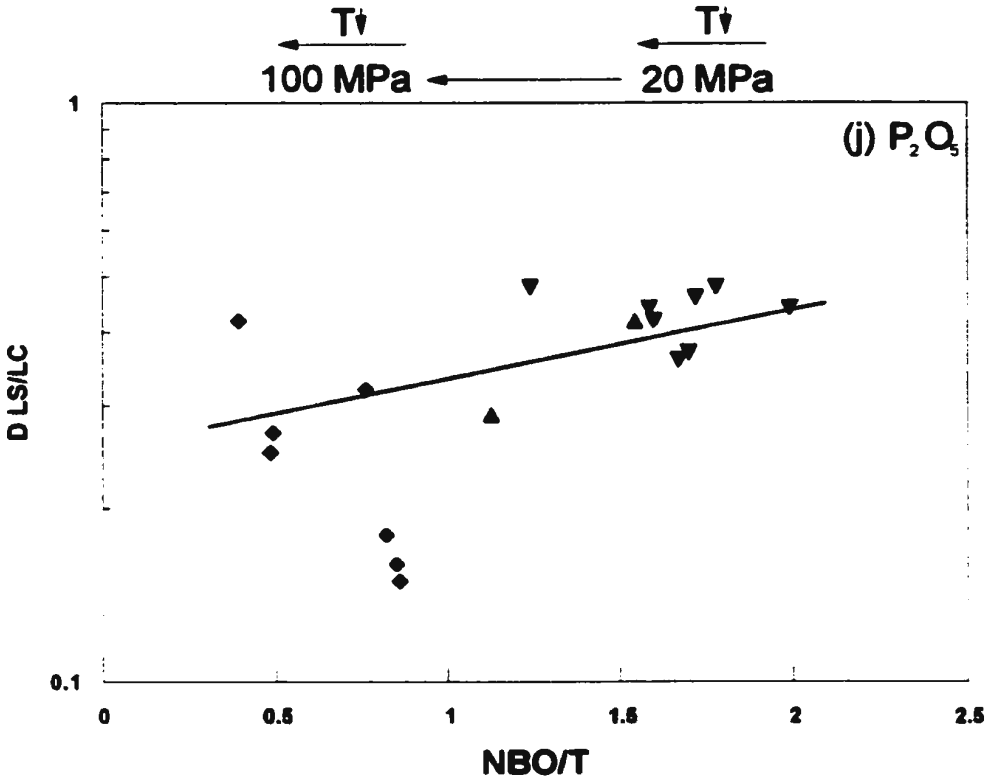
T↓
T↓
100 MPa
20 MPa
(j) P_2O_5
D LS/LC
1
0.1
0
0.5
1
1.5
2
2.5
NBO/T

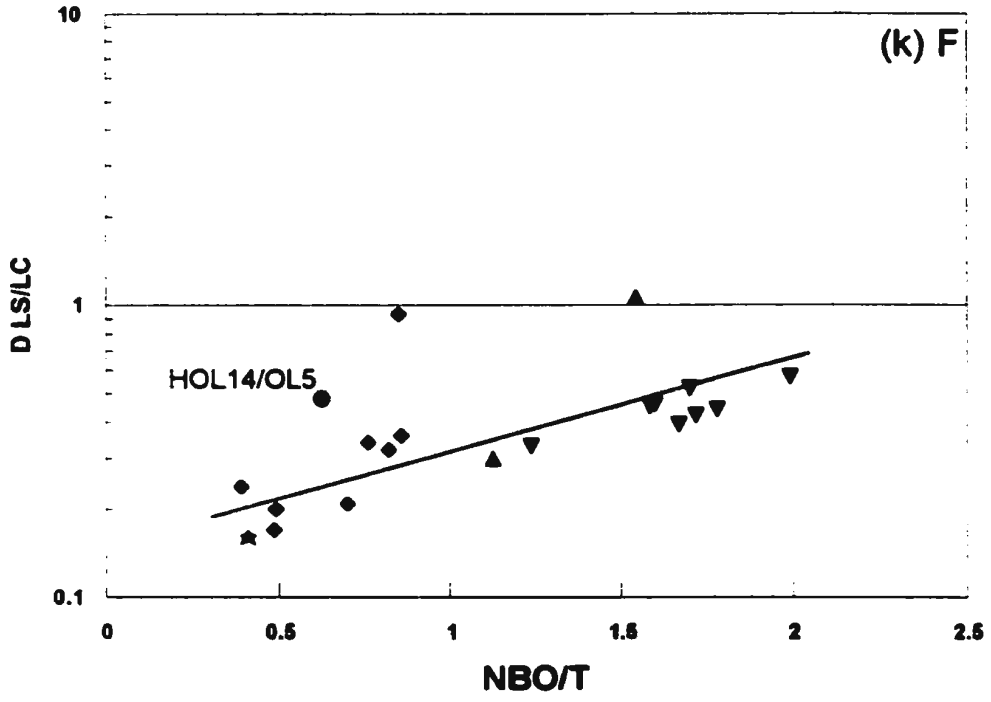
(k) F
D LS/LC
10
1
0.1
HOL14/OL5
0
0.5
1
1.5
2
2.5
NBO/T

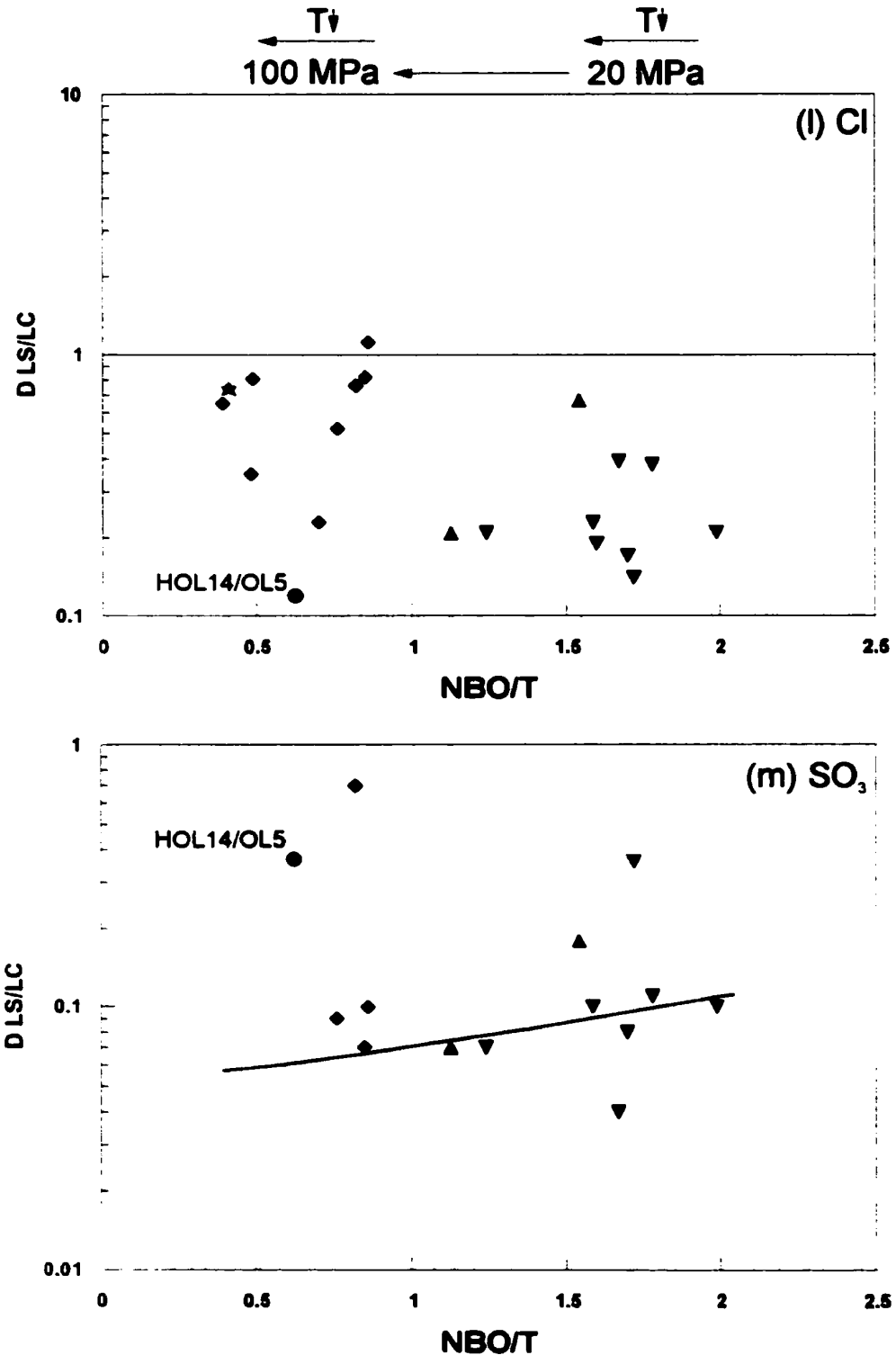
T↓
T↓
100 MPa
20 MPa
(l) Cl
D LS/LC
10
1
0.1
HOL14/OL5
0
0.5
1
1.5
2
2.5
NBO/T
(m) SO3
D LS/LC
1
0.1
0.01
HOL14/OL5
0
0.5
1
1.5
2
2.5
NBO/T

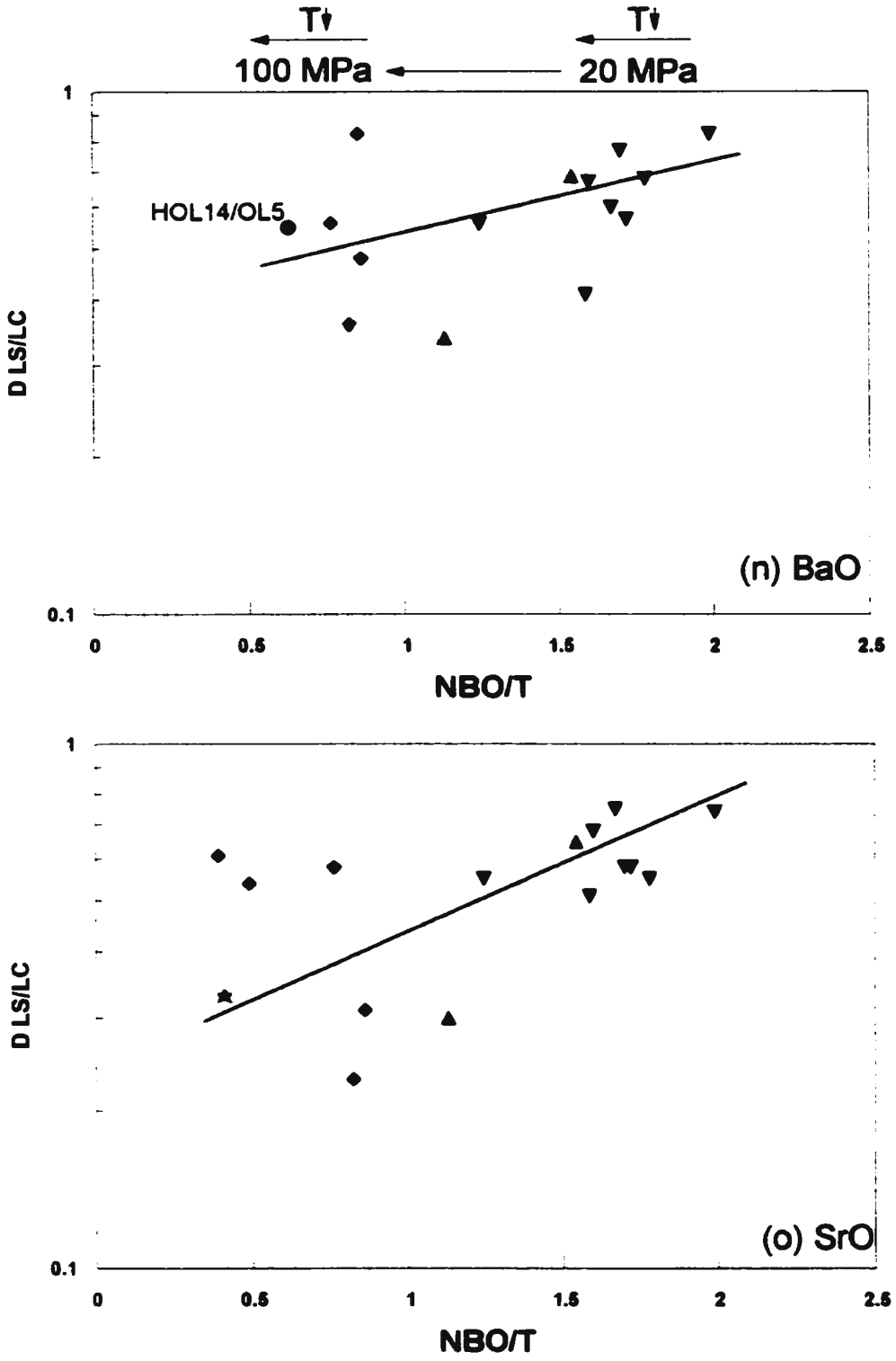
T↓
T↓
100 MPa
20 MPa
1
HOL14/OL5
D LS/LC
(n) BaO
0.1
0
0.5
1
1.5
2
2.5
NBO/T
1
D LS/LC
(o) SrO
0.1
0
0.5
1
1.5
2
2.5
NBO/T

Figure 6.22: Isobaric phase diagram at 20 MPa. The presence of the main silicate crystal phases is indicated by the pie slices, whereas the presence of minor crystal phases is indicated beside the pie. The presence of silicate liquid, two liquids or carbonate liquid is indicated by the symbols s, 2 and c, respectively, labelled in the pie slice for liquid. The experiments containing major crystal phases similar to those in lava HOL14 (*i.e.* nepheline, wollastonite, clinopyroxene and melanite garnet) are indicated by a shaded area (pie slices highlighted). The miscibility gap is represented by the dashed line. Other abbreviations used are: Ne: nepheline; Cpx: clinopyroxene; Mela: melanite garnet; Wo: wollastonite; Meli: melilite; Vish: vishnevite; Ap: apatite; Pvk: perovskite; Fd: feldspar; NY: nyerereite; GRE: gregoryite.

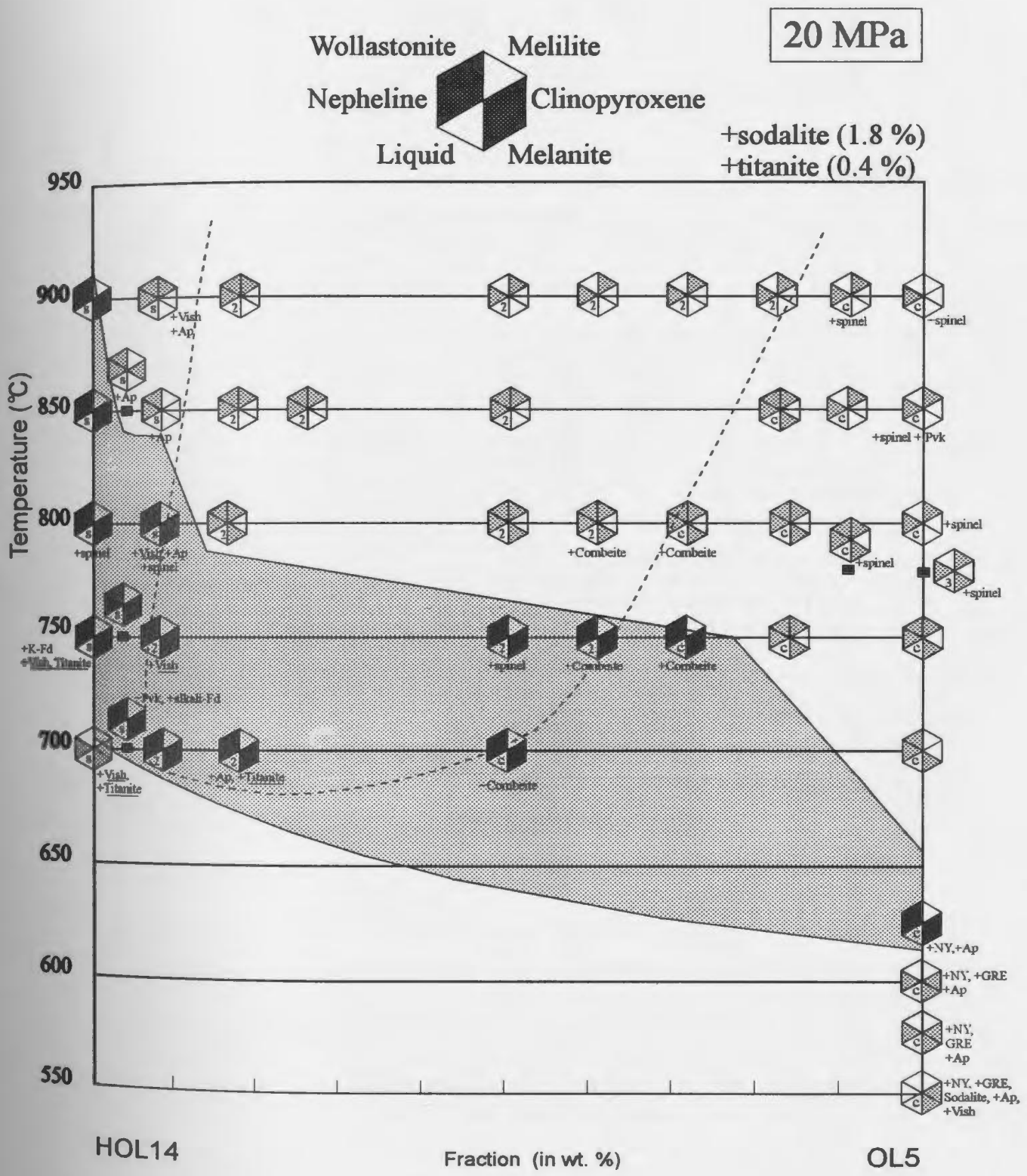
20 MPa
Wollastonite
Melilite
Nepheline
Clinopyroxene
Liquid
Melanite
+sodalite (1.8 %)
+titanite (0.4 %)
Temperature (°C)
950
900
850
800
750
700
650
600
550
+Vish
+Ap
+spinel
+Ap
+spinel + Pvk
+Combeite
+Combeite
+spinel
+spinel
+spinel
+K-Fd
+Vish, Titanite
+Vish
+spinel
+Combeite
+Combeite
+Vish,
+Titanite
+Ap, +Titanite
~Combeite
+NY,+Ap
+NY, +GRE
+Ap
+NY,
GRE
+Ap
+NY, +GRE,
Sodalite, +Ap,
+Vish
HOL14
Fraction (in wt. %)
OL5

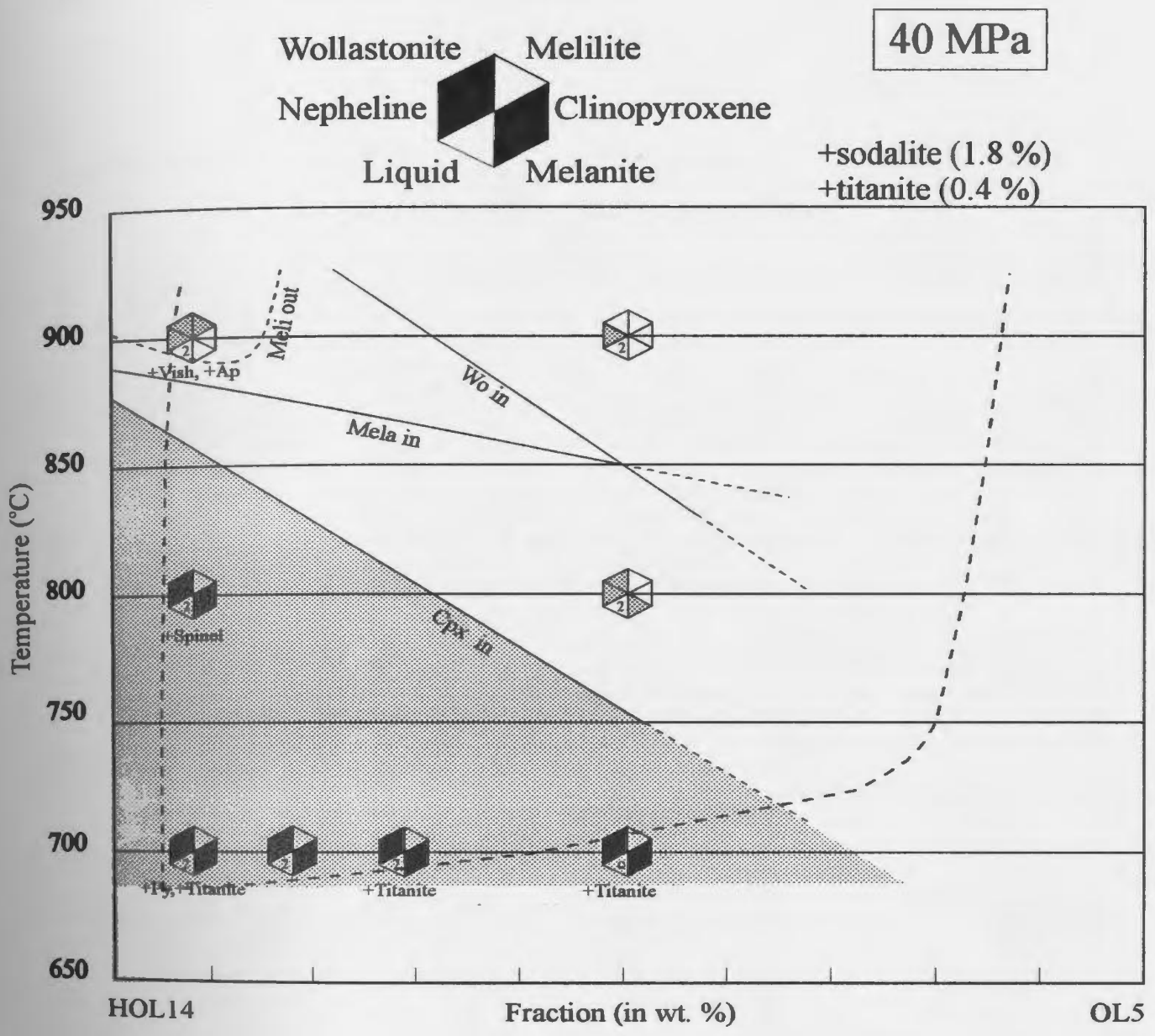

Figure 6.23: Isobaric phase diagram at 40 MPa. The presence of the main silicate crystal phases is indicated by the pie slices, whereas the presence of minor crystal phases is indicated beside the pie. The presence of silicate liquid, two liquids or carbonate liquid is indicated by the symbols s, 2 and c, respectively, labelled in the pie slice for liquid. The experiments containing major crystal phases similar to those in lava HOL14 (*i.e.* nepheline, wollastonite, clinopyroxene and melanite garnet) are indicated by a shaded area (pie slices highlighted). The miscibility gap is represented by the dashed line. Other abbreviations used are: Cpx: clinopyroxene; Mela: melanite garnet; Wo: wollastonite; Meli: melilite; Vish: vishnevite; Ap: apatite; Py: pyrrhotite.

Figure 6.24: Isobaric phase diagram at 100 MPa. The presence of the main silicate crystal phases is indicated by the pie slices, whereas the presence of minor crystal phases is indicated beside the pie. The presence of silicate liquid, two liquids or carbonate liquid is indicated by the symbols s, 2 and c, respectively, labelled in the pie slice for liquid. The experiments containing major crystal phases similar to those in lava HOL14 (*i.e.* nepheline, wollastonite, clinopyroxene and melanite garnet) are indicated by a shaded area (pie slices highlighted). The miscibility gap is represented by the dashed line.
Other abbreviations used are: Ne: nepheline; Cpx: clinopyroxene; Mela: melanite garnet; Wo: wollastonite; Meli: melilite; Vish: vishnevite; Ap: apatite; Py: pyrrhotite; Fd: feldspar; NY: nyerereite; GRE: gregoryite.

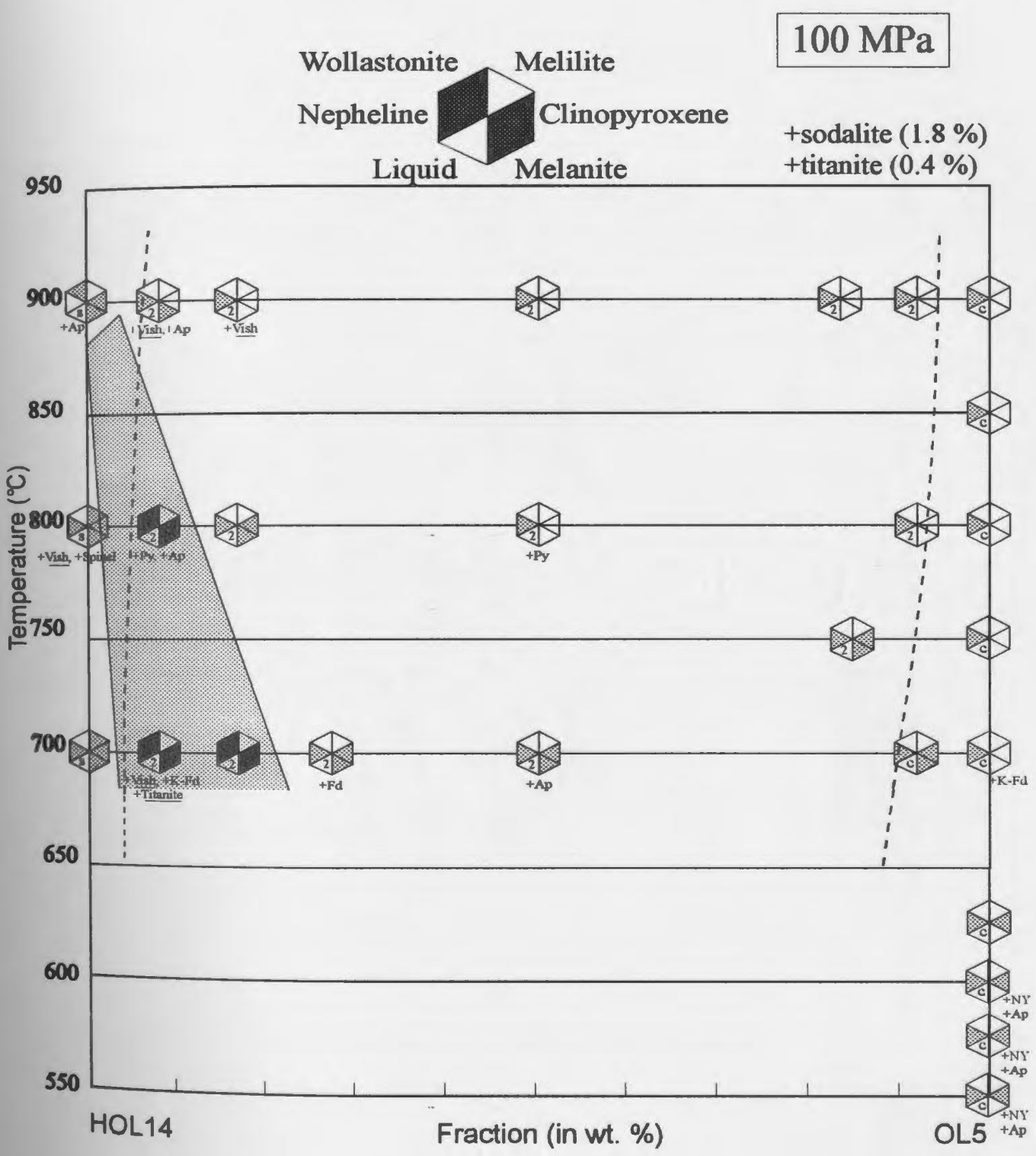
100 MPa
Wollastonite
Melilite
Nepheline
Clinopyroxene
Liquid
Melanite
+sodalite (1.8 %)
+titanite (0.4 %)
950
900
850
800
750
700
650
600
550
Temperature (°C)
+Ap
+Vish, +Ap
+Vish
+Vish, +Spinel
+Py, +Ap
+Py
+Vish, +K-Fd
+Titanite
+Fd
+Ap
+K-Fd
+NY
+Ap
+NY
+Ap
+NY
+Ap
HOL14
Fraction (in wt. %)
OL5

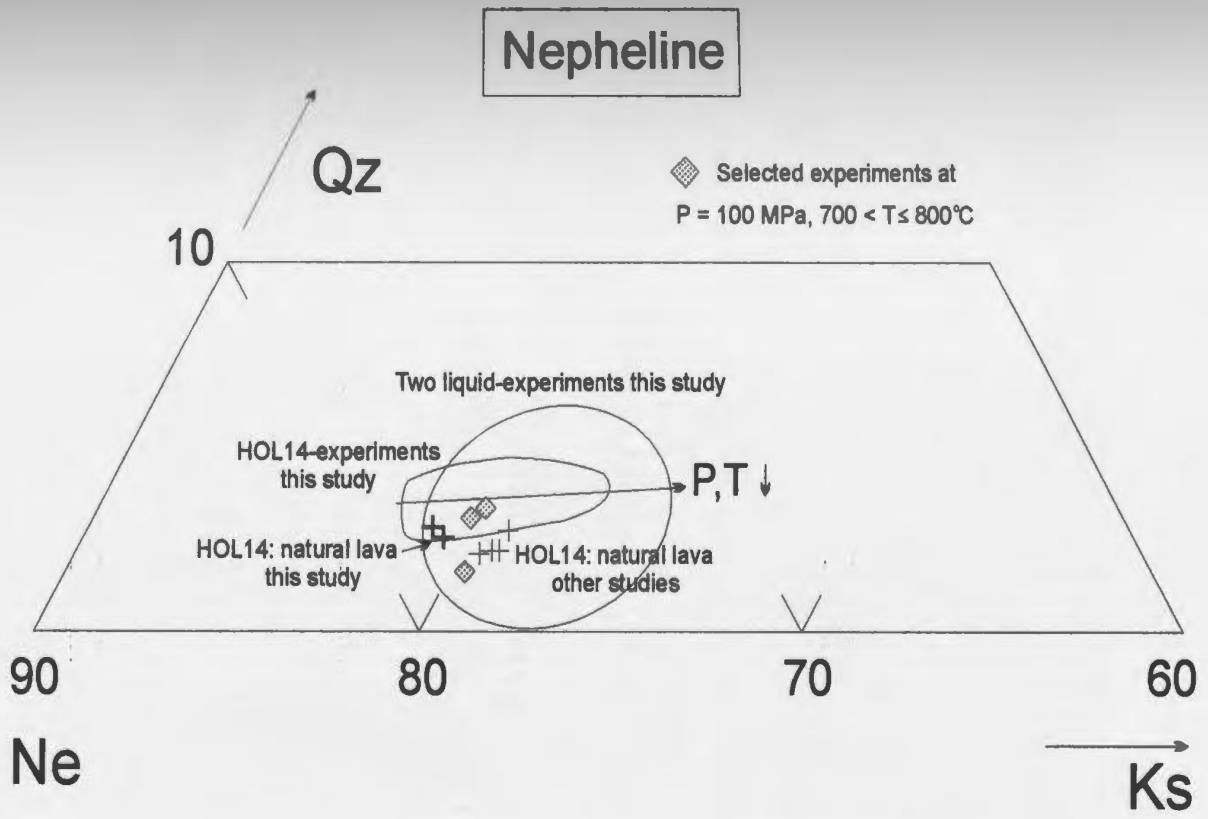

Figure 6.25: Plot of nepheline microprobe analyses from erupted wollastonite nephelinite HOL14 onto part of the nepheline (Ne) – kalsilite (Ks) – quartz (Qz) triangular plot (mol. %) (this study: +; other studies: +). The indicated areas represent nephelines from HOL14- and two-liquid experiments. The arrow represents the general compositional trend exhibited by nepheline from two-liquid experiments with decreasing pressure (P) and temperature (T). Moreover, nepheline compositions from selected experiments at P = 100 MPa and 700 °C < T ≤ 800 °C are plotted. Data are from Table 6.5, and additional data are from Peterson (1989a) and Kjarsgaard et al. (1995).

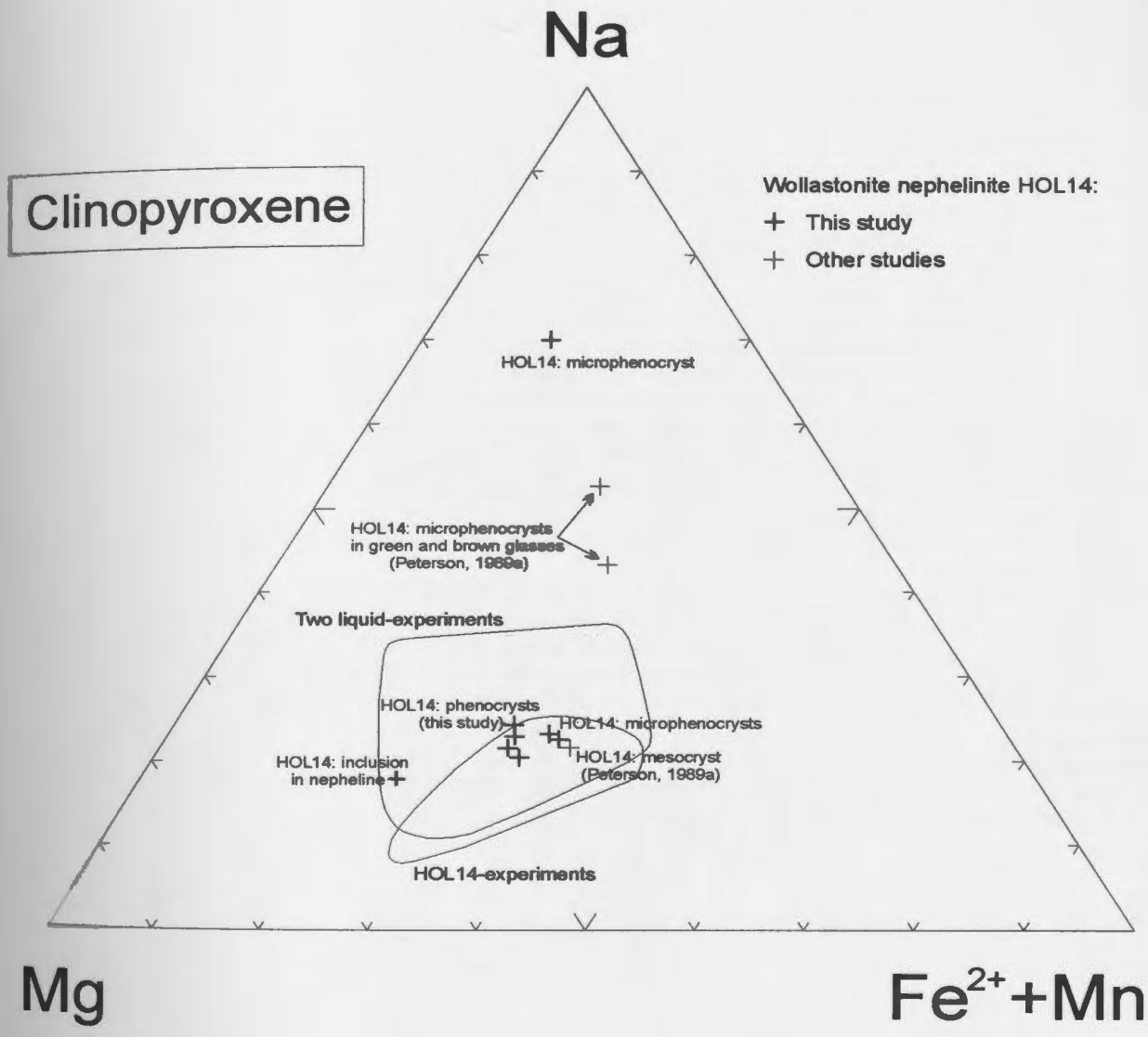

Figure 6.26: Plot of clinopyroxene microprobe analyses from erupted wollastonite nephelinite HOL14 onto the Mg (diopside) - Na (aegirine) - Fe^{2+}+Mn (hedenbergite) triangular plot (atomic %). The indicated areas represents clinopyroxene crystals from HOL14- and two liquid-experiments. Data for this study (+) are from Table 6.6; additional data (+) are from Peterson (1989a).

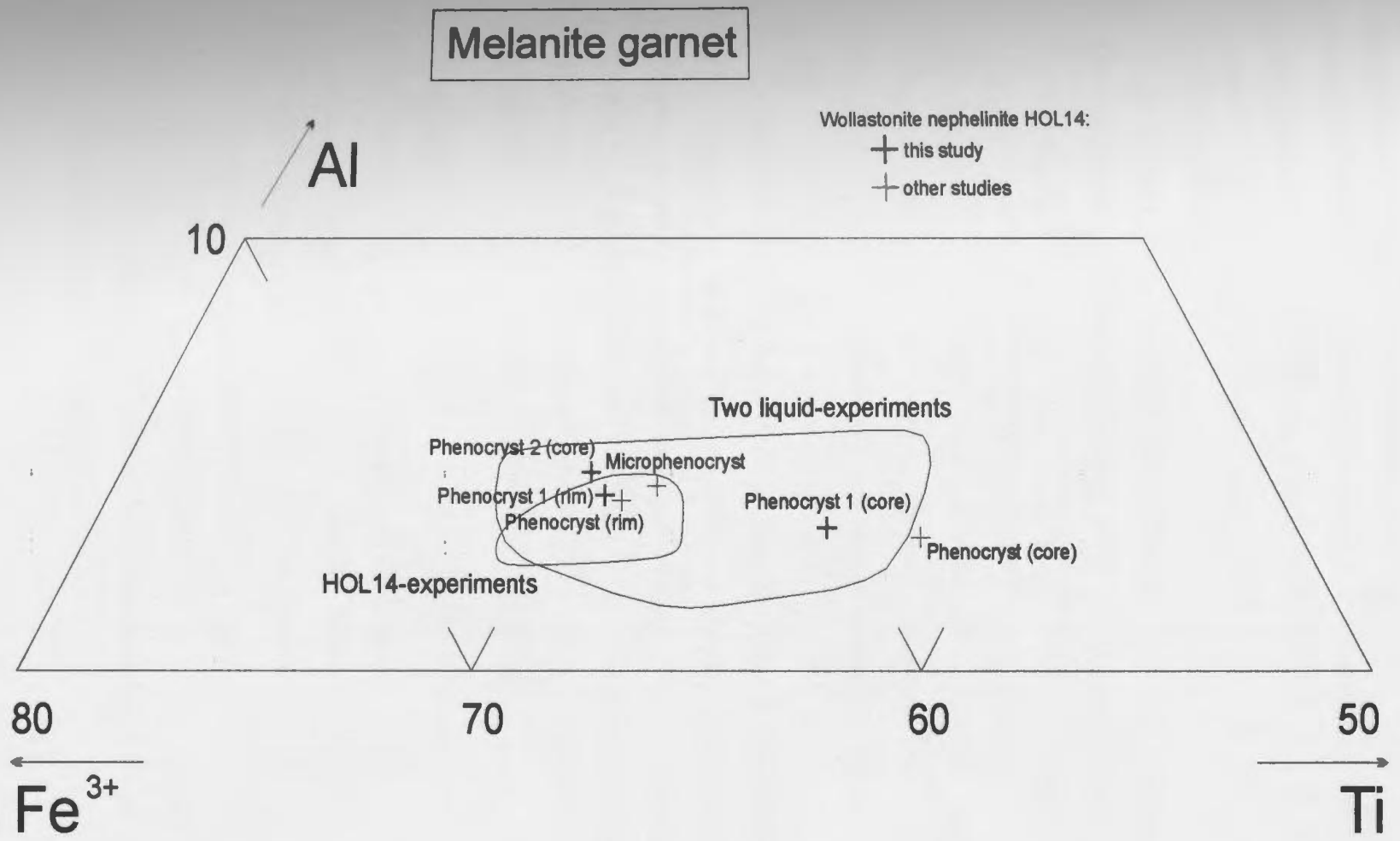

Figure 6.27: Plot of melanite garnet microprobe analyses from erupted wollastonite nephelinite HOL14 onto part of the Al - Fe^{3+} - Ti ternary (atomic %). The indicated areas represent melanite garnets from HOL14- and two-liquid experiments. Data for this study (+) are from Table 6.7; additional data (+) are from Kjarsgaard et al. (1995).

CHAPTER 7: ORIGIN OF SILICATE-BEARING NATROCARBONATITES BY LIQUID IMMISCIBILITY FROM WOLLASTONITE NEPHELINITE - PART II: CONSTRAINTS FROM TRACE ELEMENT DATA

7.1 - Introduction

This chapter presents all the trace element data that have been collected on liquid and crystal phases from the experiments on the HOL14/OL5 join. The aim of this chapter is to provide a complete trace element data set for natural and experimental samples, and also to give insight on processes controlling trace element partitioning between immiscible liquids, *i.e.* by examining the effect of structure of the silicate liquid on trace element partitioning. A comparison between the data on two-liquid trace element partition coefficients from this study and previous studies is also presented.

After the complete data set is presented, the data for natural lavas are compared to the data from the experiments at the P-T-X conditions close to those previously suggested to be the conditions of liquid immiscibility a Oldoinyo Lengai, in order to confirm the conditions of liquid immiscibility determined from major element data (in Chapter 6). As in Chapter 4, the terminology of Beattie et al. (1993) will be used wherein "D's" refer to partition coefficients between silicate and carbonate liquid pairs, and "K_D's" refers to exchange coefficients, *i.e.* ratio of partition coefficients.

7.2 - Results

The average of several analyses for each phase are presented in tables with the number of individual analyses used indicated. The data for individual analyses and the composition of different starting mixtures are presented in Appendix A7. The method of arriving at the final concentrations used is iterative, and follows the procedure outlined in Chapter 4. Note that for clarity of the diagrams, error bars are not plotted, but they can be fairly significant. Analytical precision (equivalent to error bars) is reported at the 1 σ (1 standard deviation) level in Appendix A7.

7.2.1: Trace element partitioning between immiscible liquids from the experiments

Trace element compositions of silicate and carbonate liquids are presented in Table 7.1. In order to select the best average analyses for the liquid compositions, individual trace element patterns for silicate and carbonate liquids were examined from various experiments. Entire analyses that were significantly different from others were removed, as well as individual elements that did not produce a smooth pattern (for REE). Trace element concentrations of silicate liquid in experiment CP102 (100 MPa, 800 °C, 80/20) have been recalculated to account for the fact the CaO concentration determined by EMP was determined to be low (see Chapter 6).

Trace element partition coefficients between silicate and carbonate liquids ($D_{LS/LC}$) are reported in Table 7.1. Under most P-T-X conditions, trace elements partition preferentially into the silicate liquid ($D_{LS/LC}$ >1), except for Ba and Sr that always partition into the carbonate liquid. For all P-T-X conditions, HREE partition into the silicate liquid more strongly than LREE. $D_{LS/LC}$ is < 1 only for 100 MPa experiments, and only for some elements (V, Sr, Ba, LREE). This is consistent with the findings of Veksler et al. (1998b).

To illustrate the relative effect of pressure and temperature, D's are plotted in Figures 7.1 and 7.2, respectively. The effect of pressure on partitioning between silicate and carbonate liquids can be examined at 900 °C, for a 50/50 bulk composition, between experiments CP20, CP18 and CP22 prepared at 100, 40 and 20 MPa, respectively (Fig. 7.1). Figure 7.1 illustrates that with pressure decreasing from 100 to 20 MPa, $D_{LS/LC}$ decreases for most trace elements, except Rb (V and Hf unchanged). There is no significant or discernible change between 100 and 40 MPa. Although there is a tendency for D's to decrease with increasing pressure at 900 °C for the 80/20 mix, it is unclear at 20 MPa because of poor data quality (not illustrated).

The effect of temperature on partitioning between silicate and carbonate liquids can be examined at 100 MPa, 50/50 and 20/80 bulk compositions (between experiments CP20 and CP13, and CP93 and CP97, respectively). Figure 7.2a illustrates the effect of temperature on partitioning between silicate and carbonate liquids at 100 MPa, for a

80/20 bulk composition. With temperature decreasing from 900 to 800 °C, $D_{LS/LC}$ decreases for most trace elements (not Rb, Y, V, U, Th and Nb for which compositions do not vary). $D_{LS/LC}$ decreases more for LREE than for HREE, which leads to a steepening of the slope of the REE-D-pattern. For experiments prepared at 100 MPa, for a 50/50 bulk composition, no effect of temperature is observed, as illustrated in Figure 7.2b.

In summary, Ba, Sr, Rb and V tend to partition into carbonate liquid at all conditions, whereas HFSE, Th and U tend to partition into silicate liquid at all conditions. REE tend to partition into silicate liquid at 20 and 40 MPa, and into carbonate liquid at 100 MPa. HREE partition into the silicate liquid more than LREE do. The data of this study agree with those of Veksler et al. (1998b), who showed that there was a decoupling of Zr and Hf (high D values) from the other HFSE and REE. The general tendency for trace element partition coefficients between silicate and carbonate liquids is to decrease with increasing pressure and decreasing temperature.

7.2.2: Trace element compositions of crystals from the experiments and from wollastonite nephelinite HOL14

7.2.2.1: Nepheline

Trace element analyses of nepheline from the experiments are reported in Table 7.2, and concentrations normalised to primitive mantle are plotted in Figure 7.3. The concentrations of most elements are close to detection limit, and it is difficult to obtain data on small nepheline crystals because of the spray from underlying silicate or carbonate liquid (see explanation in Chapter 4). Data from different experiments are plotted separately in Figure 7.3. For some of the trace elements which have been analysed, the range between highest and lowest value is one order of magnitude or higher, and cannot be explained by pressure or temperature effect, but rather by scatter due to analytical problems (see Chapter 4). The lowest values probably represent more accurate analyses because they are less affected by contamination; however, these values are closer to detection limit, and are therefore not precise.

Rubidium is abundant and has the most consistent concentrations among nepheline crystals from different experiments. If nepheline from experiment CP16 is excluded (Rb = 118 ppm), Rb concentrations are in the range of 52-86 ppm. Cerium, niobium and zirconium also have fairly consistent concentrations among nepheline crystals from different experiments. Cerium has concentrations varying from 0.8 to 1.5 ppm, Nb has concentrations varying from 1.3 to 1.7 ppm, whereas Zr has concentrations varying from 1.7 to 6.7 ppm. Lanthanum shows a wider compositional range (from 0.43 to 3.7 ppm). The remaining trace elements have concentrations that are below detection limits in nepheline for most experiments. Lutetium and hafnium were analysed in nepheline from experiment CP7 only, and have concentrations of 0.12 and 0.65 ppm, respectively.

Trace element analyses of nepheline from the wollastonite nephelinite lava HOL14 are also reported in Table 7.2, and concentrations normalised to primitive mantle are plotted in Figure 7.3. Many of the trace elements are at or below detection limits in nepheline, hence the scatter exhibited by the REE-pattern. Individual analyses performed on nepheline yield consistent values for Ba, Sr, Rb, La, Ce, and Zr (see Tab. A7.5 in Appendix A7). Average concentrations are 22 ppm for Ba, 144 ppm for Sr, 110 ppm for Rb, 0.48 ppm for La, 0.29 ppm for Ce, and 0.74 ppm for Zr.

7.2.2.2: Clinopyroxene

Trace elements analyses of clinopyroxene from the experiments are reported in Table 7.3. Concentrations normalised to primitive mantle are plotted in Figure 7.4.

For experiments, despite the fact that most elements are close to detection limit and that analytical uncertainties are high (see Tab. A7.3 in Appendix A7), data have been plotted separately for the different experiments. Trace elements show significant scatter between different experiments, for the same reasons as these observed for nepheline. Yttrium, La, Ce and Zr are the elements for which most data are available, and among these elements, Zr is the element showing the most consistent concentrations (225 - 593 ppm). The consistency exhibited by Zr concentrations is due to their high values. The compositional ranges exhibited by the other elements

are: 2.0 - 14 ppm for Y, 1.9 – 14.0 ppm for La, and 8.1 - 25 ppm for Ce. Fewer data are available for the remaining elements. Despite the scatter and the scarcity of the data, Figure 7.4 exhibits that the REE-patterns are overall concave up, with La_{pm} ~ 10, Er_{pm} ~ 2 and Lu_{pm} ~ 8. No effect of pressure or temperature on the trace element compositions of clinopyroxene can be deduced from these data.

Trace element analyses of clinopyroxene from lava HOL14 are also reported in Table 7.3, and concentrations normalised to primitive mantle are plotted in Figure 7.4. The REE-pattern is fairly smooth and concave up, with La_{pm} ~ 6, Dy_{pm} ~ 1.4 and Lu_{pm} ~ 3.2. Strontium, Zr, Hf have the highest normalised concentrations (> 28).

7.2.2.3: Melanite garnet

Trace element analyses of melanite garnet from the experiments are reported in Table 7.4. Trace element data for garnet are more accurate compared to the data for nepheline and clinopyroxene, because of the higher concentration levels. The compositional range between highest and lowest values is less than an order of magnitude for all elements except Ba (2.3 - 84 ppm).

Since analyses were made on a considerable number of melanite garnet crystals, data are presented for selected experiments only. Data are presented in Figures 7.5 and 7.6 in order to show the effect of bulk composition and pressure on melanite garnet. Patterns for REE are convex up, with normalised concentrations of Sm (114-325) higher than those of La (19-90) and Lu (33-98). The middle REE, U, Th and HFSE have the highest normalised concentrations (>100). Niobium and zirconium have very high concentrations, in the range of 142 - 947 ppm and 2024 - 4474 ppm, respectively. Figure 7.5 illustrates that at 40 MPa and 700 °C, concentrations of most trace elements increase in melanite garnet with increasing carbonate content in the starting composition. The same effect is observed for melanite garnet in experiments at 100 MPa, 700 °C, and 20 MPa and 700 °C (not illustrated). Figure 7.6 illustrates that at 800 °C, for a 90/10 bulk composition, concentrations of most trace elements increase in melanite garnet with decreasing pressure. The same effect is observed for

melanite garnet in experiments at 700 °C, for various bulk compositions (not illustrated). Trends illustrated in Figures 7.5 and 7.6 are probably related to changing the trace element concentrations in the silicate liquid, *i.e.* $D_{Garnet/LS}$ are probably the same for different experiments, although it is not possible to confirm this since LAM-ICP-MS analyses of silicate liquid at these low temperatures are not possible. No effect of temperature was observed (not illustrated).

Trace element analyses of melanite garnet from lava HOL14 are also reported in Table 7.4, and normalised concentrations are plotted in Figures 7.5 and 7.6. The REE-pattern is convex up, with $La_{pm} \sim 44$, $Eu_{pm} \sim 190$ and $Lu_{pm} \sim 77$. High field strength elements, U and Y have high normalised concentrations, between ~ 110 and ~ 420.

7.2.2.4: Wollastonite

Analyses of trace elements in wollastonite from five different experiments are reported in Table 7.5, and illustrated in Figure 7.7. The compositional range exhibited by several wollastonite crystals is generally narrow, *i.e.* less than a factor of 3 between the highest and lowest values: 54-122 ppm for Y, 41-124 ppm for La, 84-189 ppm for Ce, and 34-79 for Zr. For the remaining elements, data are available only for LC-experiment CP16. Despite the scatter exhibited by the trace element concentrations determined for wollastonite from this experiment, Figure 7.7 illustrates the relatively shallow slope of the REE-pattern, with $La_{pm}/Er_{pm} = 3.8$ for CP16 (20 MPa, 700 °C, 50/50), and $La_{pm}/Yb_{pm} \sim 19$ for CP31 (100 MPa, 700 °C, 90/10, C/CH_4-buffered).

Data for wollastonite from lava HOL14, normalised to primitive mantle, are also plotted in Figure 7.7. This mineral exhibits a smooth REE-pattern which flattens towards HREE, with $La_{pm} \sim 27$ and $HREE_{pm} \sim 11$. Strontium is present in high concentration (1564 ppm).

7.2.2.5: Melilite

Trace element analyses of melilite crystals from LS- and two-liquid experiments are reported in Table 7.6 and plotted in Figure 7.8. The compositional range exhibited by

melilite crystals from the experiments is lower than one order of magnitude between highest and lowest values for all of the elements. The REE-pattern is steep, with La_{pm}/Er_{pm} ~ 100. Strontium has very high concentrations, ranging from 11498 to 20289 ppm (= 1.36 to 2.40 wt. % SrO). These concentrations are in agreement with those obtained by EMP (1.48 to 2.60 wt. % SrO; see Tab. 6.13).

The compositional range can be explained as a function of variations in pressure, temperature and bulk composition, as illustrated in Figure 7.8. Comparison between melilite crystals in experiments CP23 and CP15 (both at 20 MPa and 90/10 bulk composition, at 900 and 800 °C, respectively) and between melilite crystals in experiments CP22 and CP14 (both at 20 MPa and 50/50 bulk composition, at 900 and 800 °C, respectively) shows an increase in trace element concentrations with decreasing temperature. Moreover, comparison between melilite crystals in experiments CP19 and CP23 (both at 900 °C, 90/10 bulk composition, at 40 and 20 MPa respectively) shows an increase in V, La, Ce and Sm, and a decrease in Rb and U with decreasing pressure, although it is not very significant and data are only available on these two experiments to quantify the effect of pressure. As for melanite garnet, these trends are probably related to changing the composition of the silicate liquid, *i.e.* $D_{Melilite/LS}$ are probably the same for different experiments.

7.2.2.6: Titanite, apatite and combeite

Trace elements analyses of titanite, apatite and combeite are reported in Table 7.7. The results for titanite are plotted in Figure 7.9. Titanite crystals from experiments CP11 (40 MPa, 700 °C, 90/10) and CP64 (20 MPa, 700 °C, 80/20) have high concentrations of HFSE: normalised values of Nb and Ta are > 2000; Nb has concentrations of 2409 and 4765 ppm in experiments CP11 and CP64, respectively; and Zr has concentrations of 2757 and 5256 ppm. REE-patterns are steep, with La_{pm}/Lu_{pm} ~ 35. It is not possible using the current set of experiments to investigate the effect of P-T-X on trace element compositions of titanite. Note that Ba, Sr and U have very different concentrations between the two different experiments, but the

limited amount of data makes this difficult to interpret. Trace element concentrations for titanite in lava HOL14 are also plotted in Figure 7.9. The REE-pattern is smooth and steep (La_{pm} = 416, Lu_{pm}= 10.6). Normalised concentrations of Nb and Ta are very high (3946 and 2816, respectively). Niobium and Zr have the highest concentrations (2596 and 4454 ppm, respectively). Strontium is also present in a high amount (1087 ppm).

Values obtained for apatite from experiment CP31 (100 MPa, 700 °C, 90/10, C/CH_4 buffer) are plotted in Figure 7.10. Apatite has a very steep normalised REE-pattern (La_{pm}/Lu_{pm} ~ 1000), with high concentrations of LREE (La > 1700 ppm). Barium, Sr, U and Th also have high normalised values (> 300). The concentration of Ba is 4063 ppm, and the concentration of Sr is 13712 ppm.

Results for combeite are shown in Figure 7.11. Combeite crystals are from experiments CP16 and CP65, both prepared at 20 MPa, 700 °C, for a 50/50 bulk composition. They have similar concentrations in experiment CP16 and its duplicate CP65, which indicates that equilibrium was achieved in these experiments. They have a fairly shallow REE-pattern (La_{pm}/Lu_{pm} ~ 5). Strontium and Zr have high concentrations (3433-3635 ppm for Sr, and 2275-2972 ppm for Zr).

7.2.2.7: Summary

In summary, most trace elements are present in low concentrations in nepheline, clinopyroxene and wollastonite, whereas they are in high abundance in melanite garnet, titanite, apatite, melilite and combeite. Melanite garnet and titanite are characterised by high concentrations of MREE and HFSE (especially Zr for melanite garnet, and Nb and Zr for titanite). Apatite, melilite and combeite are characterised by high concentrations of LREE, Ba and Sr. Moreover, combeite contains significant amount of U, Nb and Zr compared to the majority of other minerals.

7.3 - Controls on silicate/carbonate liquid partitioning

The effects of pressure and temperature on silicate/carbonate liquid partitioning were investigated briefly in section 7.2.1. Pressure and temperature affect the shape of the

solvus, *i.e.* the composition of both liquids. Therefore, it is better to examine the trace element partitioning between the two liquids as a function of the structure of the silicate melt, in order to reduce the number of parameters, and because it gives more insight into the mechanisms of trace element partitioning.

Hamilton et al. (1989) and Brooker (1995) showed that the enrichment of many trace elements into the carbonate liquid is favoured by increasing pressure and/or lowering temperature, and that because both of these processes result in an increase in the polymerisation of the immiscible silicate liquid, it is more suitable to study two-liquid trace element partitioning as a function of the structure of the silicate melt, *i.e.*, the parameter NBO/T. Brooker (1995) also suggested that formation of (carbonato-) complexes within the carbonate liquid could have significant control on trace element partitioning, therefore trace element partitioning between immiscible liquids will also be studied as a function of the carbonate liquid.

The structure of the silicate melt has been shown to have a major role on the distribution of major elements between silicate and carbonate liquids (see Brooker, 1995; Chapter 6), as well as on partitioning of trace elements between silicate and carbonate liquids (Hamilton et al., 1989; Jones et al., 1995). The influence of the structure of the silicate liquid on trace element partitioning will be examined by utilising two different methods: 1) by plotting partition coefficients as a function of NBO/T of the silicate liquid, which can give information on what role trace elements have in the silicate liquid, *i.e.*, formers, modifiers, or dual role; and 2) by plotting partition coefficients between silicate and carbonate liquid as a function of the ionic radius of trace elements on "Onuma diagrams", which can also give insight on sites the trace elements occupy in the silicate liquid. The possible role of complexes in the carbonate melt, and also in the silicate liquid, on trace element partitioning complicates the interpretation of the data, and this will also be examined.

7.3.1: Effect of polymerisation of the silicate liquid on $D_{LS/LC}$

7.3.1.1: Barium, Sr and V

The variations in $D_{LS/LC}$ are shown as a function of the degree of polymerisation of the silicate liquid (NBO/T; Fig. 7.12). Barium, Sr and V have D <1 for all NBO/T values (Figs. 7.12a, b and c). This partitioning behaviour indicates that Ba, Sr and V behave similarly to CaO (see Fig. 6.21g), and are probably network modifiers.

7.3.1.2: Rubidium

Figure 7.12d shows that the partition trend for Rb crosses the parity line at a NBO/T value of ~ 0.7, and that D values are > 1 at lower NBO/T values. This trend is similar to that of K_2O (Fig. 6.21 i), and suggests that Rb behaves similarly to K_2O, *i.e.* it has a dual role as a network former and modifier, and is preferentially allocated to a charge balancing role at low NBO/T values.

7.3.1.3: REE and yttrium

Yttrium and REE have D >1 for high values of NBO/T, and <1 for low values of NBO/T (Fig. 7.12e to Fig. 7.12o). The curves would tend to unity at NBO/T ~ 3. The behaviour of REE indicates that they have a dual role as network modifiers and network formers (assuming that D values are only a function of the structure of the silicate melt). Figure 7.13 illustrates that D's are higher for HREE than for LREE and that the NBO/T value for which the partition curves cross the parity line is higher for LREE than for HREE. These trends are similar to those previously presented by Brooker (1995).

Brooker (1995) showed that the general trend of increasing REE affinity for the more depolymerised silicate melts is consistent with the conclusions of Ellison and Hess (1989), who suggest that REE have coordination polyhedra of NBO's and these are favoured by a depolymerised distribution of Q species (where Q species describe the number of bridging oxygens per tetrahedra). Ellison and Hess (1989) investigated the partitioning behaviour of REE between immiscible silicate liquids, and suggested that a silicate melt will not distinguish between LREE and HREE. Vicenzi et al.

(1994) also did not observe any effect of composition of silicate melt on relative partitioning of REE. The findings of Ellison and Hess (1989) and Vicenzi et al. (1994) indicate that the difference of two-liquid partitioning behaviour between LREE and HREE cannot be explained by differences in the solution mechanisms in the silicate liquid for different REE as a function of the silicate melt structure (NBO/T). Therefore, Brooker (1995) suggested that the difference in the partitioning behaviour of different REE could be controlled by carbonato-REE complexes in the carbonate melt. In this case, the lower values of $D_{LS/LC}$ for LREE than for HREE indicates that carbonato-complexes in the carbonate melt would form preferentially with LREE than for HREE. These ideas are discussed further below.

In order to further investigate the partitioning mechanisms of REE between immiscible silicate and carbonate melts, exchange coefficients $K_D^{Lu/La}$ (*i.e.* D_{Lu}/D_{La}) have been plotted as a function of NBO/T of the silicate liquid (Fig. 7.14). Values of $K_D^{Lu/La}$ are given in Table A7.4 in Appendix A7. Figure 7.14 illustrates that $K_D^{Lu/La}$ between silicate and carbonate liquids increases with decreasing NBO/T (increasing polymerisation) of the silicate melt. This trend can be interpreted in two different ways: 1) it is real, *i.e.* $K_D^{Lu/La}$ depend directly on the degree of polymerisation of the silicate melt (NBO/T); or 2) it is apparent, i.e. $K_D^{Lu/La}$ depend on carbonato-complexes in the carbonate melt. In this latter case, the formation of complexes in the carbonate melt could be dependent on pressure and temperature. Since these parameters also affect polymerisation of the silicate melt, $K_D^{Lu/La}$ plotted as a function of NBO/T of the silicate melt would show an apparent trend.

If the trend exhibited by $K_D^{Lu/La}$ as a function of NBO/T of the silicate melt is real (case 1), it means that the silicate liquid does distinguish between LREE and HREE. This is in disagreement with Ellison and Hess (1989). The study by Ellison and Hess (1989) was made on silicate melts much richer in SiO_2 (up to 80 wt. % SiO_2) and perhaps more importantly, no CO_2, F or Cl was present in their system. In the present study, the presence of CO_2 and halogens in silicate liquid is expected to affect the solution mechanisms of REE significantly, since carbonato- and halogen-complexes

can also form in silicate liquids. Indeed, Mysen (1988) and Brooker (1995) suggested that CO_2 interacts with metal cations in silicate melts to form carbonate complexes. Ponader and Brown (1989b) showed that REE form complexes with fluorine in silicate melts, whereas no evidence for REE-Cl complexes was found for the compositions they studied. The presence of volatiles in the silicate liquid could have two consequences: 1) CO_2 and F could depolymerise the silicate melt (see Brooker, 1995; see also Figure 6.21k which shows a positive correlation between $D_{LS/LC}$ (F) and NBO/T); and 2) carbonato- (and fluoro-) complexes could form in the silicate melt; note that the formation of carbonato-complexes is facilitated by increasing NBO/T of the silicate melt, since these complexes are linked to non-bridging oxygens (Brooker, 1995). Values of $K_D^{Lu/La} > 1$ indicate that complexes could form preferentially with HREE than with LREE in the silicate melt. Moreover, the negative correlation between $K_D^{Lu/La}$ and NBO/T may indicate that the preference of complexes to form with HREE compared to LREE could be lower at high NBO/T (*i.e.*, increasing CO_2) than at low NBO/T.

In conclusion, data for REE partitioning between immiscible liquids are consistent with those of Hamilton et al. (1989), and trends for individual REE agree with the conclusion of Ellison and Hess (1989) that there is increasing REE affinity for the more depolymerised silicate melts. However, a differential partitioning of LREE and HREE is observed as a function of NBO/T of the silicate melt. This might indicate that the presence of volatiles in the system allows the silicate melt to distinguish between different REE. Volatiles could depolymerise the melt, and also favour formation of carbonato- and fluoro-complexes, with preferential complexing with HREE compared to LREE, especially when the silicate melt is more polymerised (low NBO/T).

On the other hand, if the findings of Ellison and Hess (1989) that silicate melt does not distinguish between LREE and HREE are applicable to the volatile-rich system of this study, then the decoupling of REE as a function of NBO/T of the silicate melt is apparent, and is better explained by formation of carbonato- and halogen-complexes

of REE in the carbonate melt, with preferential complexing with LREE compared to HREE, especially at high pressure and low temperature (apparently at high NBO/T of the silicate melt). It is likely that there are carbonato- and halogen-complexes of REE in both liquids, therefore both liquids effect REE-partitioning.

7.3.1.4: U, Th and HFSE

High field strength elements and Th have D values >1 for all NBO/T values (Fig. 12 q to u). Values fall on a convex curve which would cross the parity line at lower NBO/T. Uranium exhibits a similar trend but has D values <1 for low NBO/T values of the silicate melt (Fig. 12 p). Partitioning trends indicate that all of these elements have a dual role in the silicate melt, as network formers and modifiers (assuming that D values are only a function of the structure of the silicate melt). Exchange coefficients between silicate and carbonate liquids for elements that usually form coherent pairs (U-Th, Nb-Ta, and Zr-Hf) are reported in Table A7.4 in Appendix A7. Figure 7.15 illustrates the variations of exchange coefficients for U-Th, Nb-Ta and Zr-Hf pairs as a function of NBO/T of the silicate melt. Figure 7.15a shows that Th partitions into the silicate liquid more than U does, and that $K_D^{U/Th}$ does not depend on the degree of polymerisation of the silicate melt. Figure 7.15b shows that Ta partitions into silicate liquid more than Nb does, and that $K_D^{Nb/Ta}$ increases with increasing NBO/T of the silicate melt. Figure 7.15c shows that there is no decoupling of Zr and Hf between silicate and carbonate liquids.

The difference in trends of $K_D^{Nb/Ta}$ and $K_D^{U/Th}$ as a function of NBO/T indicates that the decoupling mechanisms must be different between these two element pairs. Formation of complexes could be important in the carbonate liquid, as indicated by Cooper et al. (1998), who showed that because carbonate melts have a high dielectric constant, they are likely to form stable complexes with many incompatible elements. Knudsen (1989) also showed that elements like Nb, Ta, U and Th are likely to be soluble in carbonate magmas as complexes with ligands like PO_4^{3-}, F^- and CO_3^{2-}. The formation of halogen-complexes with these elements seems to be more controversial in silicate melts. Farges (1991) and Ponader and Brown (1989b) reviewed numerous

studies that explained positive correlations between U, Th and HFSE and halogens as a result of formation of metal/halogen complexes in silicate melts. However, Farges et al. (1991) showed no clear evidence of F or Cl complexes with Zr in silicate melts, Farges et al. (1992) showed no clear evidence of F or Cl complexes with U, and Farges (1991) showed no clear evidence of F or Cl complexes around Th in halogen-containing glasses. To the author's knowledge, all studies on the structure of silicate melts are made on CO_2-free systems and nothing is known about carbonato-complexes of U, Th and HFSE in silicate melts. However, it is probable that these occur.

The absence of correlation between $K_D^{U/Th}$ and NBO/T of the silicate melt (Fig. 7.15a) indicates that it is not the structure of the silicate melt that controls the decoupling between U and Th. On the other hand, the positive correlation between $K_D^{Nb/Ta}$ and NBO/T of the silicate melt (Fig. 7.15b) indicates that the structure of the silicate melt may control the decoupling between Nb and Ta. Figures 7.12 r and s illustrate that Nb and Ta have dual roles as network modifiers and formers, and that for low NBO/T values, they are mostly network modifiers, whereas higher values of NBO/T enhances their presence as network formers. Pentahedral sites (TiO_5) are known in silicate liquids (see Fig. 52 in Brown et al., 1995). Niobium and Ta in tetrahedral and pentahedral sites (network formers) form covalent bonds with the bridging oxygens; whereas Nb and Ta in large polyhedral sites (network modifiers) are at greater distances from the bridging and non-bridging oxygens and, therefore, are more likely to form ionic bonds with oxygens, although they also form covalent bonds with bridging and non-bridging oxygens. According to Dickinson (1986), the value of the ionisation potential of a cation is a direct measure of its ability to hold electrons (*i.e.*, to form covalent bonds rather than ionic bonds, by sharing its electrons). Tantalum has higher ionisation potential than Nb, and is expected to interact more strongly with bridging and non-bridging oxygens. Increasing polymerisation (decreasing NBO/T) is expected to increase the formation of covalent bonds with bridging oxygens and the formation of covalent bonds relatively to ionic

bonds with non-bridging oxygens. This could partly explain why partitioning of Ta relative to Nb in the silicate melt is enhanced at low NBO/T values.

The size of the sites where elements partition into and their coordination number increase with increasing NBO/T value. In highly polymerised melts, Nb and Ta might be present as Nb^{5+} and Ta^{5+} that form covalent bonds with bridging and non-bridging oxygens (stronger for Ta). Conversely, at high NBO/T, the polyhedra have a larger size, and Nb and Ta might also be present as free cations Nb^{5+} and Ta^{5+} that form ionic bonds with non-bridging oxygens, and possibly as complexes with halogens and CO_3^{2-}. It is likely that these bonds would not differentiate between Nb and Ta as much as the covalent bonds. The different bonds formed by Nb and Ta for different degrees of polymerisation of the silicate melt could explain the positive correlation between $K_D^{Nb/Ta}$ and NBO/T of the silicate melt. This trend could also be partly explained by the formation of carbonato- and halogen-complexes with Nb and Ta in the carbonate liquid.

In summary, many parameters may affect the relative partitioning of Nb and Ta between silicate and carbonate liquids, *i.e.* the structure of the silicate liquid, and perhaps pressure and temperature, which also could affect the formation of carbonato- and fluoro-complexes in both liquids. The net effect is an increase of $K_D^{Nb/Ta}$ with decreasing polymerisation of the silicate melt.

7.3.1.5: Summary

Trace elements usually partition into carbonate liquid when the silicate melt becomes more polymerised. D's for all of the trace elements, Lu/La and Nb/Ta vary as a function of the structure of the silicate melt, and also as a function of the composition of the carbonate melt. It remains problematic to determine the relative role of both liquids. CO_2 and F have a major role on trace element partitioning because they depolymerise the silicate melt, and the presence of NBO's facilitates the partitioning of trace elements into the silicate melt, especially those trace elements forming complexes with CO_3^{2-} and F (and Cl). Jones et al. (1995) showed that the Soret effect of the carbonate liquid on trace element partitioning was small, but most of their

experiments were made on halogen-free systems. This study, on the other hand, shows that the major element composition of the carbonate liquid might has some control on two-liquid trace element partitioning in halogen-bearing systems. NBO/T is a function of pressure and temperature (NBO/T generally decreases with increasing pressure and decreasing temperature) and some trends might be apparent, *i.e.* not depend on the structure of the silicate melt only, but also on the formation of complexes in the carbonate liquid depending on these three parameters.

7.3.2: Effect of ionic field strength on $D_{LS/LC}$

Another way to study the possible effect of the structure of the silicate melt on trace element partitioning is to examine trace element partition coefficients as a function of ionic radius, *i.e.* by applying "Onuma diagrams" to liquid-liquid partitioning. Onuma diagrams for crystal-liquid systems give insight into the structure of a crystal. By analogy, information on the structure of the silicate liquid and on processes effecting trace element fractionation might be obtained from the study of "Onuma diagrams", if silicate liquid has the main control on trace element partitioning and the control of the carbonate liquid is small, as suggested by Jones et al. (1995). For purposes of discussion, first it will be assumed that silicate liquid has the main control on trace element partitioning. Since it has been shown above that D's can also vary as a function of the carbonate liquid, this also will be further discussed in this section.

Before plotting D's as a function of ionic radius, the ionic radii of different elements must be determined. The radii of the different elements are taken from Shannon (1976). Values of ionic radii in Shannon (1976) are mostly for oxides and fluorides and may be inappropriate for liquids. Moreover, determination of the coordination number and of the valency of the elements plotted is not straightforward. First of all, if partitioning of trace elements depends on the structure of both silicate and carbonate liquids, then they do not necessarily have the same coordination number in both liquids. For plotting purposes, the assumption is made that the partitioning is dependent on the structure of the silicate liquid. Even then, it is difficult to assign a coordination number for different elements in silicate liquids because the structure of silicate liquids is more random than for crystals

(see Figure 52, Brown et al., 1995). The coordination number of different elements may vary as a function of the element considered, and as a function of the composition and polymerisation degree of the silicate liquid (Ponader and Brown, 1989a). For the present study, it was assumed that only Si and Al have a four-fold position. For simplicity, a six-fold coordination was used for all trace elements, and for Ti, Fe^{2+}, Mg and P. Many elements have a dual role, and choosing a coordination number of 6 averages the "errors" due to some of the cations present in tetrahedra, and some in polyhedra with a higher coordination number than 6.

The valency of heterovalent elements can vary as a function of oxygen fugacity and of composition of the liquid. Usually the valency of REE is 3+, but Eu^{2+} and Ce^{4+} also exist. For the purpose of this study, all REE (and Y) were assumed to have a 3+ valency. Barium and Sr are divalent, and Rb monovalent. Niobium, Ta and V were assumed to be pentavalent, but note that Nb and Ta are heterovalent, and can also be present as 3+ and 4+. Zirconium, Hf, U and Th were assumed to be tetravalent, although U is heterovalent (4+ and 6+).

The Onuma plot for results from experiment CP13 (NBO/T = 0.82, *i.e.* fairly polymerised) is presented in Figure 7.16. Three near-parallel curves can be drawn for the 3+, 4+ and 5+ valencies, respectively. All REE and Y plot on the 3+ curve. Titanium, Hf, Zr and Th plot on the 4+ curve, but not U. Niobium, Ta and V plot on the 5+ curve. The fact that partition coefficients plotted as a function of the ionic radius for different elements fall on parallel curves depending on their valency, and that these curves peak at an approximately similar radius value (~ 0.7 Å), agrees with the results of Jones et al. (1995) who showed that D's are a function of the ionic field strength (z/r) for different elements, *i.e.*, of their radius and valency. Do the curves reflect the effect of the structure of silicate melts on trace element partitioning, or not? If yes, does a radius of 0.7 Å correspond to the average size of the sites in the silicate melt where the trace elements partition (by analogy with crystals), or not?

First, it is assumed that partitioning is dependent on the structure of the silicate melt. From Ellison and Hess (1989), Mahood and Hildreth (1983), and Flynn and Burnham

(1978) it can be proposed that the high degree of polymerisation of high-silica liquids constrains the size of the octahedral "sites" for network-modifying cations in the liquid to a maximum size of 0.95 Å, which lies within the range of octahedral radii of trivalent REE (Shannon, 1976). Therefore, in the present study for which the silicate liquid is more depolymerised, the size of the polyhedral sites would be expected to be ≥ 0.95 Å. If cations in the silicate liquid were not present as complexes, then the curves on the Onuma diagram (Fig. 7.16) would indicate that these cations are present in 0.70 Å octahedral sites. This result is unlikely because 0.7 Å is an extremely low value compared to the 0.95 Å value considered to be the size of the polyhedral sites in the polymerised silicate liquid. Although some of the discrepancy could be explained by the fact that Shannon's cationic radii data were used to plot Figure 7.16, and his data are not meant for liquids, the results suggest that the radius of 0.7 Å probably does not correspond to the actual size of the site where cations go into the silicate liquid. If a radius of 0.7 Å does not correspond to the average size of the sites where trace elements partition into, what does this value represent? As shown before, it is likely that cations are not isolated cations, but form halogen- and carbonato-complexes in the silicate liquid. If cations are present together with halogens and CO_3^{2-} as complexes, the size of the complexes could be > 0.70 Å (and probably > 0.95 Å), and the Onuma curves apparent peak at 0.7 Å reflects only the cations that are represented, not the actual size of the sites. This explanation would be consistent with the previous section, *i.e.*, the slope of the Onuma curve shows that HREE form complexes preferentially to LREE within the silicate liquid (D's higher). It would also suggest that Th and HFSE do form halogen- and/or carbonato-complexes in the silicate liquid.

A second possibility to explain the Onuma curves may be related to the formation of carbonato-complexes within the carbonate liquid. Genge et al. (1995) showed that there are two possibilities for cations to enter the carbonatite melt. By analogy with the structure of silicate melts, there can be bridging or non-bridging cations. Bridging cations are expected to be smaller than non-bridging cations or complexes (see their Fig. 11). Sr and Ba could partition into the small site (= bridging cations), and larger cations (*e.g.*,

Rb) and complexes partition into the larger site (= non-bridging cations). There is difficulty with interpreting the data from this study because if it is the structure of the carbonate liquid that controls partitioning, then the ionic radii used on the Onuma diagram are inadequate because cations are present between carbon anions, not oxygen anions, and because the coordination numbers used are inadequate. Although the absolute values for the cationic radii used might be inadequate, the relative partitioning behaviour of different trace elements might indicate that trace elements would enter the carbonate liquid preferentially in this order: LREE > HREE > HFSE.

Additional information about decoupling of trace elements from usually coherent pairs is given by the examination of the "Onuma diagram" presented in Figure 7.16. Decoupling processes have been shown to be different for different element pairs. Examination of Figure 7.16 shows that Th plots on the 4+ curve, but U does not. Farges and Brown (1996) showed that Th is present as Th^{4+} and U^{6+} is present as uranyl complexes in silicate melts. However, Farges et al. (1992) showed that uranium can occur as U^{4+} in peralkaline melts. The data of the present study suggest that uranium may be present as U^{6+} in the silicate melt, and that the difference between Th occurring as Th^{4+} and U as U^{6+} (in uranyl complexes) might explain their decoupling as seen on Figure 7.15a. Decoupling between U and Th would be due to their different valencies. If Nb and Ta have the same valency (5+), therefore decoupling between these two elements is not due to difference in valency, but rather to the formation of complexes, preferentially with Ta in the silicate melt (or Nb in the carbonate melt?), especially at low NBO/T of the silicate liquid (or high pressure and/or low temperature and/or high fraction of carbonate in bulk composition). However, it is also possible that some niobium is present as Nb^{3+} (see Wolff, 1984) and that this can account for some of the decoupling between Nb and Ta. The absence of decoupling for Zr and Hf (both 4+) might indicate that relative complexing of these two elements is not affected by P-T-X-NBO/T.

In conclusion, the structure of the silicate liquid and/or the composition of the carbonate liquid control the trace element partitioning, and partitioning dependent on the size and valency of the cations. Cations are likely to form complexes with CO_3^{2-}, F and

Cl in both the carbonate and silicate liquids. If the structure of the silicate liquid exerts the main control, then the peak of the Onuma curves reflects the sites where cations partition into, which are polyhedra defined by non-bridging oxygens. The cations that have a radius of 0.7 Å have high D's because the halogen- and carbonato-complexes they form have the most suitable size compared to the size of the sites available in the melt structure (preferentially HFSE > HREE > LREE). If the carbonate liquid exerts the main control, the trace elements incorporate preferentially in order: LREE > HREE > HFSE. Decoupling of U and Th is due to their different valency; whereas decoupling between Nb and Ta is more complicated, and involves formation of complexes, preferentially with Ta in the silicate melt (or Nb in the carbonate melt?), especially at low NBO/T of the silicate liquid (or high pressure and/or low temperature), although it might also be partly due to some niobium being trivalent.

7.3.3: Comparison with previous studies

The conditions at which previous studies (Wendlandt and Harrison, 1979; Hamilton et al., 1989; Jones et al., 1995) have been performed are often inappropriate for a comparison with natural rocks from Oldoinyo Lengai, *i.e.* synthetic material, using too high a pressure, temperature and carbonate fraction in the bulk composition. Lack of *in situ* analytical tools and/or other analytical complications further limit the data from many of these studies. On the other hand, the study by Veksler et al. (1998b) was very appropriate for a comparison with natural rocks from Oldoinyo Lengai. They worked on a spiked, synthetic sodium-rich mixture, appropriate for comparison with natural lavas from Oldoinyo Lengai, at 965-1015 °C and 0.42-0.92 kbar (42-92 MPa). The set of elements used by Veksler et al. (1998b) is much more complete (REE and HFSE), and the method of separation of the two liquids by rotating autoclave and centrifuge is very efficient. They showed that at these P-T-X conditions, most of the REE partition preferentially into the silicate liquid, but that La, Sr and Ba strongly partition into the carbonate liquid. They also showed that Nb/Ta are strongly fractionated by two-liquid partitioning.

Two-liquid trace element partitioning data from previous studies have been summarised in Veksler et al. (1998b). Data from previous studies whose experimental conditions match as closely as possible the conditions used in this study and from experiment CP20 (100 MPa, 900 °C, 50/50 bulk composition) are presented in Table 7.8 and plotted in Figure 7.17. However, comparison of the data obtained in this study with that from previous studies is difficult because many experimental parameters vary and the conditions used for the other studies can be fairly dissimilar to those used in the present study. Data from experiment CP20 agree fairly well with those of Veksler et al. (1998b) and those from other studies, although there is a paucity of data for the comparison. Usually D's calculated for experiment CP20 are lower than those determined for other studies because of the lower pressure for this study.

Veksler et al. (1998b) summarised a comparison between their data and those of others. It is interesting to compare data from this study to data from Veksler et al. (1998b) because both were completed using the same LAM-ICP-MS instrument. Veksler et al. (1998b) present the $D_{LS/LC}$ for Ba, Sr, Y, selected REE and HFSE for an experiment at 85 MPa and 1015 °C. Their $D_{LS/LC}$ values are higher than those from experiment CP20, in agreement with the fact that they worked at higher temperature. Both studies show similar ratios for Nb/Ta, which have been attributed by Veksler et al. (1998b) to decoupling produced by liquid immiscibility. Data for experiment CP20 fit those from a phonolitic system (phonolite-natrocarbonatite) better than a nephelinitic system (nephelinite-Ca-carbonatite) as studied by Hamilton et al. (1989).

7.4 – Comparison with natural lavas

In Chapter 6, conditions of liquid immiscibility at Oldoinyo Lengai were determined by comparison of phase assemblages and major element data between experiments and natural lavas (wollastonite nephelinite HOL14 and silicate-bearing natrocarbonatite OL5). Liquid immiscibility was suggested to occur at ~ 100 MPa, 750 °C. The aim of this section is to further constrain the P-T-X conditions of liquid immiscibility by comparing trace element data between natural and experimental samples.

The comparison between natural and experimental samples includes: 1) partition coefficients between silicate and carbonate liquids (especially vs. NBO/T); 2) trace element composition of carbonate liquid, *i.e.* natrocarbonatite lava OL5 (whole rock) and carbonate liquid in the experiments at the appropriate P-T-X conditions; 3) trace element composition of silicate liquid, *i.e.* wollastonite nephelinite HOL14 (groundmass) and silicate liquid in the experiments at the appropriate P-T-X conditions; 4) trace element compositions of crystal phases in lava HOL14 and in the experiments at appropriate P-T-X conditions. For all phases, data are not available for experiments at 100 MPa, 750 °C and 90/10 to 80/20 bulk compositions, and data at P-T-X conditions close to those are used.

7.4.1: Partition coefficients between silicate and carbonate liquids – Comparison between experimental and natural samples

In this section, partition coefficients between silicate and carbonate liquids in the experiments are compared to their natural equivalent, *i.e.* D's between wollastonite nephelinite HOL14 (groundmass) and silicate-bearing natrocarbonatite (OL5). First, D's are examined as a function of NBO/T of the silicate liquid, since partition plots are the most useful plots for determining conditions of liquid immiscibility. Then, the D-patterns for different P-T-X conditions are compared between natural and experimental samples, in order to ascertain that they are in agreement with the P-T conditions of exsolution previously determined.

In Figure 7.12, $D_{HOL14/OL5}$ (= $D_{LS/LC}$ for the natural liquid pair) for different trace elements have been plotted as a function of NBO/T of the groundmass of lava HOL14, along with values for the experiments. D's for the natural liquid pair were calculated using groundmass for wollastonite nephelinite HOL14 (represents LS), and whole rock for silicate-bearing natrocarbonatite OL5 (represents LC). Figure 7.12 shows that $D_{LS/LC}$ for the natural liquid pair plot at similar NBO/T values to those of the 100 MPa experiments, and D's for different trace elements generally plot on the partitioning curves defined by the experiments. Only V, Dy, Er and Yb show a discrepancy between calculated D's ($D_{HOL14/OL5}$) and expected D's (value on the curve interpolated from the

experiments). The good agreement between $D_{HOL14/OL5}$ and D's for the experiments at 100 MPa confirms that liquid immiscibility between wollastonite nephelinite HOL14 and silicate-bearing natrocarbonatite OL5 occurred at ~ 100 MPa.

Patterns of $D_{HOL14/OL5}$ (= $D_{LS/LC}$ for the natural liquid pair) are presented in Figure 7.18, together with D-patterns for the experiments. Figure 7.18 shows that for the natural groundmass/whole rock pair, Ba, Sr and LREE partition slightly into silicate-bearing natrocarbonatite OL5 ($0.2 < D < 1$), Rb, MREE, V, U and Th partition similarly between silicate and natural "liquids" ($D \sim 1$), and Y, HREE and HFSE partition into wollastonite nephelinite HOL14 ($2 < D < 20$). For the experiments at 20 MPa, all of the REE partition into silicate liquid, whereas at 100 MPa, LREE partition into carbonate liquid and HREE into silicate liquid for most experiments. The range of REE-D-values for the natural pair is not overlapped by the D values measured on the experiments at 20 MPa, but it is overlapped by the D values measured on the experiments at 100 MPa. For the remaining elements, the range of D-patterns for the experiments at both pressures overlaps that of the natural rock. Experiments at 100 MPa are the only ones showing LREE enrichment in carbonate liquid, which confirms that liquid immiscibility probably occurred at 100 MPa, not at 20 or 40 MPa. Data for the 20 and 40 MPa experiments are not used in the further discussion.

In order to determine the T-X conditions of liquid immiscibility, trace element partition coefficients for the natural pair are compared to those of 100 MPa-experiments at different temperatures and bulk compositions (Fig. 7.19). Experiments CP20 (50/50, 900 °C), CP93 (20/80, 900 °C), CP13 (50/50, 800 °C) and CP103 (10/90, 800 °C) have REE-D-patterns centred on the pattern for the natural pair, but the patterns for the experiments are much shallower. Experiment CP97 (20/80, 750 °C) has lower REE-D-values and a shallow REE-D-pattern, whereas experiment CP92 (80/20, 900 °C) has higher REE-D-values and a shallow REE-D-pattern compared to the natural pair.

Among all the experiments, only the experiment CP102 (80/20, 800 °C) has a REE-D-pattern whose slope is similar to that shown by the natural pair. It is also the experiment that was prepared at the conditions the closest to those previously established

to be the conditions of liquid immiscibility at Oldoinyo Lengai, *i.e.* ~ 100 MPa, 750 °C. The similarity between the REE-D-pattern of the natural pair and that of experiment CP102 confirms the P-T conditions previously suggested for liquid immiscibility at Oldoinyo Lengai. Moreover, the carbonate content is also reasonable, since Pyle et al. (1991) showed that the natrocarbonatites could be the product of 4-22 wt. % liquid immiscibility from a nephelinite magma. Because none of the other experiments shown on Figure 7.19 hass a REE-D-pattern which matches the REE-D-pattern of the natural pair, none of the other P-T-X conditions are acceptable for liquid immiscibility at Oldoinyo Lengai.

In conclusion, the data are compatible with silicate-bearing natrocarbonatite being the product of 10-20 % immiscibility from wollastonite nephelinite at 100 MPa, 750 °C. For the experiment CP102, discrepancies between D's measured on natural and experimental samples for some elements (*i.e.* V, U, Th, Ta, Zr and Hf) will be examined in the next section, when comparing the absolute concentrations between liquids in natural and experimental samples.

7.4.2: Trace element concentrations of liquid and crystal phases: comparison between natural and experimental samples

7.4.2.1: Trace element concentrations of liquids in experiments and in natural lavas

Whole rock trace element concentrations of erupted silicate-bearing natrocarbonatite OL5 are compared to those of carbonate liquid from selected experiments at 100 MPa and 800 °C (Fig. 7.20). The composition of silicate-bearing natrocarbonatite OL5 is within the compositional range exhibited by carbonate liquids from the experiments. Especially, it is in good agreement with the carbonate liquid from experiment CP102 (100 MPa, 800 °C, 80/20) for most trace elements, in agreement with the fact that lava OL5 exsolved at approximately these conditions. Yttrium, U, Th, Ta, Zr and Hf show low values in the carbonate liquid of the experiment CP102 compared to other experiments and to lava OL5 (whole rock). These low values are probably due to

fractionation of some phases in the carbonate liquid during the quenching of the experiments, as has been shown to occur in OL5-experiments (see Chapter 4).

Trace element concentrations of the groundmass of erupted wollastonite nephelinite HOL14 are compared to those of silicate liquid from selected experiments at 100 MPa in Figure 7.21. The comparison is very good for the experiment CP102 prepared at 800 °C with 80 wt. % nephelinite HOL14 in the bulk composition, except for MREE and HREE concentrations slightly lower in the silicate liquid of experiment CP102. The good agreement between the composition of silicate liquid in experiment CP102 and in the groundmass of lava HOL14 confirms the conditions of liquid immiscibility previously established.

7.4.2.2: Trace element concentrations of crystal phases in experiments and in natural lavas

Trace element concentrations of melanite garnet from erupted wollastonite nephelinite HOL14 are compared to those from selected experiments at ~ 100 MPa, 700 and 900 °C (Fig. 7.22). The comparison is very good for most elements, but MREE and HREE are slightly more enriched in the melanite garnet from erupted wollastonite nephelinite HOL14 compared to the experiments. Although no data are available for garnet in an experiment at 100 MPa, 750 °C and 80/20-bulk composition, the data presented in Figure 7.22 suggest that at theses conditions, melanite garnet would be similar to that in wollastonite nephelinite HOL14.

For the remaining crystal phases, the data presented in Chapter 7 are not used for comparison with similar phases in lava HOL14, since the data are either scarce, scattered, or at inappropriate conditions for comparison, therefore they do not show compositional trends with pressure and temperature that can be used to further constrain the conditions of their crystallisation in the natural lava HOL14. Note, however, that trace element data on crystal phases from experimental and natural samples are generally in the same range.

7.5 - Conclusion

Under most conditions, most trace elements partition into the silicate liquid. Trace element partition coefficients between silicate and carbonate liquids have also been shown to decrease with increasing pressure and decreasing temperature, in agreement with previous studies.

The mechanisms explaining the trace element partitioning between immiscible liquids are complex, and are best described as a function of the NBO/T value of the silicate liquid. Unlike crystals in which the structure is well defined and in which trace elements substitute for major elements on specific sites, trace elements might form carbonato- and halogen- complexes within silicate and carbonate liquids. Trace element partitioning appears to be dependent on the radius and valency of the different elements, although in detail, it is usually difficult to determine what parameter has the main control on partitioning, *i.e.* solution mechanisms in the silicate or in the carbonate liquid.

Partition coefficients are well described as a function of the structure of the silicate melt and/or the composition of the carbonate melt. Different parameters participate in determining which structures form (especially the oxygen framework in silicate liquid and the carbon framework in carbonate liquid), but, once a structure is formed, it is the valency and effective size of the various cations competing for a structural position which appears to be the dominant factor in partitioning of trace elements.

The conditions of liquid immiscibility determined from phase assemblages and major element data (Chapter 6) are confirmed by trace element data. The comparison of trace element partition coefficients as a function of NBO/T of the silicate melt between natural and experimental samples confirms that silicate-bearing natrocarbonatites from Oldoinyo Lengai can be produced by liquid immiscibility at ~ 100 MPa. The trace element compositions of the natural lavas HOL14 and OL5 (and the trace element partition coefficients) are also compatible with silicate-bearing natrocarbonatites being produced by liquid immiscibility at ~ 750 °C from 10-20 % wollastonite nephelinite. In conclusion, major and trace element data suggest that silicate-bearing natrocarbonatites exsolved at ~ 100 MPa, 750 °C, from 10-20 % wollastonite nephelinite.

The results of this study have implications for the petrogenesis of carbonatites in general. For most conditions, trace elements are enriched in the silicate liquid rather than in the carbonatitic liquid, as previously shown by Veksler et al. (1998b), Wendlandt and Harrison (1979) and Jones et al. (1995). Therefore, liquid immiscibility alone cannot explain the high concentrations in trace elements observed on natural carbonatites. Another result of importance is that liquid immiscibility decouples elements from usually coherent pairs (Nb-Ta and U-Th). Trace element decoupling could therefore be used to monitor the liquid immiscibility process.

Table 7.1. Trace element LAM-ICP-MS analyses of silicate and carbonate liquids from the experiments on the HOL14/OL5 join, and from wollastonite nephelinite HOL14 and silicate-bearing natrocarbonatite OL5.

SAMPLE	CP21	CP92	CP20	CP93	CP5	CP102	CP13	CP103	CP97	CP31	CP7	CP19	CP18	CP2	CP27	CP1
Type	2 liq	2 liq	2 liq	2 liq	2 liq	2 liq	2 liq	2 liq	2 liq	2 liq	2 liq	2 liq	2 liq	2 liq	LS	2 liq
Composition	90/10	80/20	50/50	20/80	90/10	80/20	50/50	10/90	20/80	90/10	50/50	90/10	50/50	90/10	90/10	50/50
Pressure	100	100	100	100	100	100	100	100	100	100	103	40	40	40	40	40
Temperature	900	900	900	900	800	800	800	800	750	700	700	900	900	800	800	800
Other										buffered					buffered	
Silicate liquid																
# an.	5	5	7	8	3	5	5	8	5	2		5	7	3	3	
Ba	2492	2684	2865	2951	2316	1813	2503	1678	1037	1823		2887	4834	2449	4101	
Sr	3187	3414	3416	3442	2891	2152	2956	1703	1056	1492		3384	6680	3232	5134	
Rb	119	102	132	122	101	138	130	220	146	86.8		110	110	105	143	
Y	35.2	33.9	30.4	23.6	29.7	20.4	34.4	19.7	16.3	24.6		35.2	44.2	21.2	48.3	
V	156	133	107	61.2	172	111	97.1	50.4	43.9	64.2		192	144	144	305	
La	135	188	240	283	116	139	223	171	98.1	65.1		154	429	156	207	
Ce	177	233	327	382	165	186	320	235	143	121		206	547	161	282	
Nd	51.0	58.2	76.6	86.4	44.3	43.2	76.4	53.5	36.2	25.2		51.2	123	44.5	72.6	
Sm	8.46	8.60	9.04	9.28	8.98	5.04	10.2	7.00	4.47	4.49		10.4	17.0	6.95	16.0	
Eu	2.75	2.75	2.87	2.50	2.44	1.74	2.70	1.77	1.25	1.23		3.60	4.26	1.69	4.90	
Gd	7.08	5.99	5.98	5.31	5.88	3.91	6.20	4.60	2.81	4.56		8.10	9.03	4.29	10.6	
Dy	6.36	5.26	5.12	3.77	5.35	2.88	5.34	4.16	2.31	5.25		6.31	4.85	3.07	7.51	
Er	3.58	2.67	2.92	1.62	2.78	1.35	3.10	2.14	1.42	2.51		3.48	2.76	1.51	4.90	
Yb	3.25	2.74	2.46	1.97	2.69	1.73	3.01	2.04	1.43	2.99		2.56	2.60	1.57	n.d.	
Lu	0.49	0.41	0.37	0.27	0.36	0.26	0.30	0.33	0.22	0.42		0.46	0.59	0.27	0.61	
U	7.61	8.22	11.6	14.0	7.61	9.00	13.1	17.4	13.3	8.70		8.35	13.3	5.73	16.2	
Th	9.66	9.86	16.7	31.4	9.06	10.6	19.0	42.8	26.6	8.22		10.1	16.9	7.03	16.2	
Nb	203	192	191	143	218	174	198	180	176	142		220	217	183	336	
Ta	2.28	2.04	2.33	1.93	2.38	1.50	2.46	3.20	2.21	1.50		2.02	2.30	1.42	3.23	
Zr	912	769	887	1152	892	750	1118	1663	1037	674		1009	998	862	1570	
Hf	16.5	11.6	14.5	17.4	12.7	9.80	16.0	27.4	13.9	11.1		16.7	15.3	14.1	24.4	
Carbonate liquid																
# an.		7	9	12		9	7	8	10		7		6			6
Ba		4215	11369	12083		9748	7561	7547	13295		9881		9442			15088
Sr		10390	13744	12215		12783	11230	8884	14052		14381		12788			14433
Rb		66.4	136	230		154	103	176	232		129		156			89.7
Y		12.9	27.7	31.3		7.10	28.4	17.2	28.0		38.0		13.6			15.4
V		143	398	389		481	273	288	458		288		513			370
La		155	476	687		389	420	407	694		539		273			525
Ce		206	541	760		417	469	473	770		643		315			563
Nd		49.1	114	159		69.8	107	99.0	167		156		56.5			98.1
Sm		5.65	12.3	15.2		5.20	11.8	9.46	15.4		17.1		6.04			8.01
Eu		1.83	3.38	3.91		1.24	3.13	2.28	3.83		4.04		1.32			1.94
Gd		3.72	7.63	8.11		1.96	6.02	4.74	7.73		9.86		2.68			3.61
Dy		2.34	5.32	4.97		1.28	5.06	2.61	4.72		7.36		2.28			1.96
Er		0.91	2.56	2.41		0.52	2.18	1.30	2.12		3.35		1.36			0.91
Yb		0.77	2.00	2.26		0.56	1.61	1.16	1.86		3.59		1.34			0.74
Lu		0.09	0.27	0.28		0.10	0.22	0.15	0.27		0.43		0.20			0.11
U		1.52	10.2	18.5		4.73	8.45	13.9	20.3		17.5		6.34			7.93
Th		0.69	4.42	14.8		2.04	5.19	11.4	13.9		12.1		1.47			3.24
Nb		16.7	160	220		72.6	148	150	232		192		92.8			72.0
Ta		0.20	0.75	1.04		0.10	0.75	0.64	0.54		0.42		0.29			0.25
Zr		3.00	48.1	140		12.2	79.3	75.0	41.0		63.1		22.8			6.11
Hf		0.09	0.61	1.58		0.33	1.06	0.74	0.46		1.22		0.61			n.d.
Partitioning	LS/LC															
Ba		0.64	0.25	0.24		0.19	0.33	0.22	0.08				0.51			
Sr		0.33	0.25	0.28		0.17	0.26	0.19	0.08				0.52			
Rb		1.54	0.97	0.53		0.90	1.26	1.25	0.64				0.71			
Y		2.62	1.10	0.75		2.87	1.21	1.14	0.58				3.25			
V		0.93	0.27	0.16		0.23	0.36	0.18	0.10				0.28			
La		1.21	0.50	0.41		0.36	0.53	0.42	0.14				1.57			
Ce		1.14	0.60	0.50		0.44	0.65	0.50	0.19				1.73			
Nd		1.19	0.67	0.54		0.62	0.73	0.54	0.22				2.18			
Sm		1.52	0.74	0.61		0.97	0.87	0.74	0.29				2.81			
Eu		1.50	0.85	0.64		1.41	0.86	0.77	0.32				3.22			
Gd		1.61	0.78	0.66		1.99	1.03	0.97	0.36				3.14			
Dy		2.25	0.98	0.76		2.25	1.05	1.46	0.49				2.13			
Er		2.95	1.14	0.75		2.56	1.42	1.65	0.67				2.03			
Yb		3.57	1.23	0.87		3.14	1.57	1.76	0.73				1.95			
Lu		4.77	1.36	0.97		2.50	1.38	2.21	0.81				2.92			
U		5.39	1.14	0.75		1.90	1.55	1.25	0.65				2.09			
Th		14.3	3.79	2.13		5.21	3.65	3.75	1.92				11.5			
Nb		11.5	1.20	0.65		2.40	1.34	1.20	0.76				2.34			
Ta		10.2	3.09	1.86		14.3	3.27	5.02	4.08				7.86			
Zr		256	18.4	8.21		61.3	14.1	22.2	25.3				43.8			
Hf		131	23.9	11.0		29.3	16.9	37.0	30.4				25.1			

Note: Pressure is in MPa, temperature in oC, and starting composition is shown as proportion of wollastonite nephelinite HOL14/silicate-bearing natrocarbonatite OL5 (in wt. %). Types of experiments are: silicate liquid (LS)-experiments, two-liquid (2 liq)-experiments and carbonate liquid (LC)-experiments.
Abbreviations used are: n.d.: not determined; WR: whole rock; gmass: groundmass; D: partition coefficient.
Analysis of whole rock HOL14 was performed by solution-ICP-MS at MUN, and trace element composition of whole rock OL5 was determined by LAM-ICP-MS (see Chapter 4).

Table 7 1 (suite).

SAMPLE	CP23	CP91	CP22	CP120	CP121	CP43	CP53	CP14	CP50	CP65		
Type	LS	2 liq	2 liq	2 liq	2 liq	2 liq	2 liq	2 liq	2 liq	LC		
Composition	90/10	80/20	50/50	40/60	30/70	70/30	50/50	50/50	50/50	50/50		
Pressure	20	20	20	20	20	20	20	20	20	20		
Temperature	900	900	900	900	900	850	850	800	750	700		
Other												
Silicate liquid											HOL14	HOL14
# an.	5	2	6	5	5	5					WR	gmass
Ba	3283	3387	5777	5445	4534	5365					1653	2402
Sr	3587	4261	6764	6692	5300	6224					2127	2530
Rb	121	117	129	112	153	97.0					102	105
Y	39.6	38.0	47.1	70.5	63.6	47.1					37.6	28.8
V	218	184	155	125	137	201					160	193
La	161	204	503	863	591	328					89.4	118
Ce	219	244	643	1054	720	419					121	159
Nd	62.5	65.8	139	244	174	99.9					36.4	42.7
Sm	9 07	9.23	15.7	24.9	20.9	13.1					6.59	6.71
Eu	2.72	2.87	4.53	7 50	5.68	4.07					2.13	2.35
Gd	7 20	7.02	10.6	15.1	12.5	9.32					6.31	5.30
Dy	6.78	6.00	8.25	9.98	9.08	7.75					5.74	4.94
Er	4 12	3.34	4.29	4.65	4.35	4.02					3.26	2.75
Yb	4.25	3.50	3.95	4.55	4.59	3.74					3.09	2.48
Lu	0 49	0.40	0.59	0.70	0.83	0.54					0.44	0.29
U	9.12	8.56	16.3	26.5	25.4	12.4					6.92	6.82
Th	11.2	10.3	21.2	32.8	24.1	15.9					8.30	11.4
Nb	249	215	247	317	412	243					260	236
Ta	3 13	2.29	2.58	3.26	3.75	2.70					2.93	2.04
Zr	1060	962	1042	933	810	1126					929	831
Hf	17 0	13.5	15 3	12.9	11 8	17 7					15.2	12.4
Carbonate liquid											OL5	OL5
# an			6	9	9	3	3	7	2	1	WR	gmass
Ba		11762	10907	8951	7991	12441	9259	11111	8960	7749	9213	9566
Sr		10675	9693	8374	7663	12526	7791	11065	11728	9721	10905	10708
Rb		102	228	201	254	189	200	116	122	138	139	185
Y		8.60	15 9	24.5	27.3	8.34	14.1	16.3	8.19	9 56	13.8	30.3
V		240	642	319	427	754	403	376	320	190	198	194
La		125	295	470	397	127	276	372	341	383	468	783
Ce		118	378	538	469	140	323	408	383	449	564	920
Nd		20.0	68.5	112	97.1	28.0	58.7	78.6	62.8	78.9	114	211
Sm		3.18	6.46	11.2	10.5	2.92	5.90	9.08	4.67	6.40	10.0	19.2
Eu		1 01	2.06	3.06	2.89	0.98	1 71	1.99	1.20	1 53	2.56	4.83
Gd		1.54	3.65	6.06	5.87	1.66	3.32	4.22	2.09	2.81	4.63	9.19
Dy		2.26	2.91	4.41	3.82	1.14	2.17	2.53	1.06	1.86	2.34	4.56
Er		b d.	1 23	1.92	1.82	0.59	0.93	1.32	0.55	0.83	0.91	1.70
Yb		0.53	1.11	1.81	1.77	b.d.	0.57	1.32	0.49	0.63	0.79	1.07
Lu		0.09	0.14	0.24	0.23	0.05	0.09	0.17	0.11	0.07	0.11	0.15
U		2.10	6.86	11 3	11.2	2.64	4.42	6.96	5.13	14.6	13.8	20.3
Th		1.00	1.88	6.15	5.53	1.03	1.17	3.28	2.14	11.9	12.9	23.2
Nb		6.18	113	162	217	48.9	74.9	120	41.3	246	108	153
Ta		0 13	0.43	1.02	1.05	0 24	0 23	0.52	0.09	1.05	0.50	0.72
Zr		2.00	45 4	136	157	6.13	15.4	50.7	26.8	123	65.9	77.7
Hf		n.d.	0 73	1.66	1.94	0 20	0.34	0.75	0.79	2.23	1.02	0.89
Partitioning LS/LC											HOL14/OL5 WR/WR	HOL14/OL5 gm/WR
Ba		0.29	0 53	0.61	0.57	0.43					0.18	0.26
Sr		0.40	0 70	0.80	0.69	0.50					0.20	0.23
Rb		1.15	0.56	0.56	0.60	0.51					0.73	0 75
Y		4.42	2.96	2.87	2.33	5.65					2.73	2.09
V		0.77	0.24	0.39	0.32	0.27					0.82	0.99
La		1 63	1.71	1.84	1.49	2.58					0.19	0.25
Ce		2.06	1.70	1.96	1.53	2.99					0.21	0.28
Nd		3.29	2.03	2.18	1.79	3.57					0.32	0.38
Sm		2.91	2.43	2.23	2.00	4.49					0.66	0.67
Eu		2.83	2.20	2.44	1.97	4.15					0.83	0.92
Gd		4.56	2.89	2.48	2.13	5.61					1.36	1.14
Dy		2.66	2.84	2.26	2.38	6.80					2.45	2.11
Er		n.d.	3 50	2.42	2.39	6.82					3.57	3.02
Yb		6.65	3.55	2.83	2.60	n.d.					3.92	3 14
Lu		4.47	4 32	2.96	3.61	10.8					3.89	2.57
U		4.07	2.37	2.35	2.27	4.68					0.50	0.64
Th		10 4	11 3	5 34	4.36	15 5					0.64	0.68
Nb		26 3	2 19	1.96	1 90	4.97					2.60	2.19
Ta		17 8	5.97	3.20	3.57	11.1					5.86	4.07
Zr		480	23.0	6.88	5.16	184					14.1	12.8
Hf		n.d.	21.0	7.77	6.08	90.6					14.8	12.1

Table 7.2: Trace element LAM-ICP-MS analyses of nepheline in the experiments and in erupted wollastonite nephelinite HOL14 (in ppm).

Sample	P	T	X	# an.	La	Ce	Nd	Sm	Eu	Gd	Dy	Er	Yb	Lu
Experiments														
CP20	100	900	50/50	3	b.d.								b.d.	
CP5	100	800	90/10	3		0.77							b.d.	
CP13	100	800	50/50	3	b.d.	b.d.	b.d.	b.d.	b.d.	b.d.	b.d.	b.d.	b.d.	b.d.
CP8	103	700	90/10	1	b.d.	b.d.							b.d.	
CP31**	100	700	90/10	4	b.d.								b.d.	
CP7	103	700	50/50	8	1.21	1.48							b.d.	0.12
CP19	40	900	90/10	3	b.d.								b.d.	
CP18	40	900	50/50	3	0.71	1.47							b.d.	
CP2	40	800	90/10	1	b.d.	b.d.								
CP27**	40	800	90/10	1	b.d.	b.d.							b.d.	
CP1	40	800	50/50	3									b.d.	
CP10	40	700	50/50	7	b.d.	b.d.							b.d.	
CP22	20	900	50/50	1	0.43	1.39								
CP15	20	800	90/10	1	b.d.	b.d.	b.d.	b.d.	b.d.	b.d.	b.d.	b.d.	b.d.	b.d.
CP14	20	800	50/50	1	3.72								b.d.	
CP17	20	700	90/10	1	b.d.	b.d.							b.d.	
CP16	20	700	50/50	6									b.d.	
HOL14				5	0.48	0.29	0.51	b.d.	0.05	b.d.	0.11	b.d.	0.13	b.d.

Sample	Ba	Sr	Rb	Y	V	U	Th	Nb	Ta	Zr	Hf
Experiments											
CP20	b.d.	b.d.	68.6					b.d.			
CP5			54.5							b.d.	
CP13	b.d.	b.d.	67.9	b.d.	b.d.	b.d.	b.d.	b.d.	b.d.	b.d.	b.d.
CP8			71.0					b.d.		b.d.	
CP31**			61.2							b.d.	
CP7			81.8					1.26		3.94	0.65
CP19			52.1								
CP18			62.1					1.69		2.87	
CP2			55.6					b.d.		3.80	
CP27**			85.6					b.d.		1.71	
CP1			75.7					1.65		6.67	
CP10			67.3					b.d.		b.d.	
CP22			66.1					1.31		3.11	
CP15	b.d.	b.d.	63.7	b.d.	b.d.	b.d.	b.d.	b.d.	b.d.	b.d.	b.d.
CP14			67.4					b.d.		b.d.	
CP17			71.2					b.d.		b.d.	
CP16	b.d.		118								
HOL14	21.5	144	110	0.72	14.4	b.d.	b.d.	0.57	b.d.	0.74	b.d.

Note: # an.: number of analyses; b.d.: below detection.
Pressure (P) is in MPa, temperature (T) is in oC, and starting composition is shown as proportion of wollastonite nephelinite HOL14/silicate-bearing natrocarbonatite OL5 (in wt. %).
**CP31 and CP27 are C/CH4-buffered experiments. Other experiments are unbuffered.

Table 7.3: Trace element LAM-ICP-MS analyses of clinopyroxene in the experiments and in erupted wollastonite nephelinite HOL14 (in ppm).

Sample	P	T	X	# an.	La	Ce	Nd	Sm	Eu	Gd	Dy	Er	Yb	Lu
Experiments														
CP5	100	800	90/10	1	7.15	18.3							b.d.	
CP8	103	700	90/10	4	7.77	25.2							b.d.	
CP31**	100	700	90/10	6	7.32	16.9							5.43	
CP7	103	700	50/50	6	6.06	15.0	11.6		0.54	1.50	2.23	0.78	1.60	0.57
CP2	40	800	90/10	2	6.65	13.1							1.08	
CP11	40	700	90/10	3	1.92	8.06							b.d.	
CP10	40	700	50/50	2	13.7	24.9							b.d.	
CP15	20	800	90/10	2	3.77	12.0							b.d.	
CP17	20	700	90/10	2									b.d.	
CP16	20	700	50/50	9	7.17	19.4	21.4	6.27		3.55			1.57	
HOL14				4	3.96	11.0	5.12	1.27	0.40	1.07	0.93	0.61	0.99	0.22

Sample	Ba	Sr	Rb	Y	V	U	Th	Nb	Ta	Zr	Hf
Experiments											
CP5				b.d.						363	
CP8				14.3						483	
CP31**				7.40						593	
CP7	9.21	557		3.24	210	0.32		4.51		225	6.35
CP2				1.95						289	
CP11				4.77						408	
CP10				10.3						504	
CP15				6.01						319	
CP17				7.65						387	
CP16				6.04	145			4.54		292	7.78
HOL14	4.71	558	b.d.	1.51	223	0.10	0.05	2.54	0.10	436	11.8

Note: # an.: number of analyses; b.d.: below detection.
Pressure (P) is in MPa, temperature (T) is in oC, and starting composition is shown as proportion of wollastonite nephelinite HOL14/silicate-bearing natrocarbonatite OL5 (in wt. %).
**CP31 is a C/CH4-buffered experiment. Other experiments are unbuffered.

Table 7.4: Trace element LAM-ICP-MS analyses of melanite garnet in the experiments and in erupted wollastonite nephelinite HOL14 (in ppm).

Sample	P	T	X	# an.	La	Ce	Nd	Sm	Eu	Gd	Dy	Er	Yb	Lu
Experiments														
CP21	100	900	90/10	1	23.1	113	132		28.3	81.7	107			4.05
CP8	103	700	90/10	4	28.5	119	151	51.9	23.6	68.7	76.1	38.6	28.3	3.65
CP66	100	700	80/20	1	20.5	94.0	140	46.8	23.3	64.5			24.9	3.26
CP67	100	700	70/30	1	22.1	108	138	58.2	24.4	71.7	74.8	38.8	33.0	4.14
CP7	103	700	50/50	5	32.3	217	300	110	43.9	121	105	61.0	38.2	6.64
CP2	40	800	90/10	8	18.4	107	132	58.5	26.0	86.6	99.8	55.6	46.0	4.63
CP11	40	700	90/10	3	18.5	88.0	121	51.9	22.5	75.1	88.5	58.4	38.8	5.43
CP68	40	700	80/20	1	39.7	134	167	71.1	30.0	82.0	94.2	54.6	40.5	5.20
CP69	40	700	70/30	1		203	276	96.4	31.7	92.1	105	50.1	42.9	3.12
CP10	40	700	50/50	2	58.4	255	338	132	37.9	130	133	57.5	36.1	4.89
CP40	20	850	100/0	1	35.9	123	126		28.5	81.3	85.7	37.5	40.7	4.62
CP15	20	800	90/10	3	40.6	158	194	79.5	29.4	106	117	52.6	40.8	5.70
CP14	20	800	50/50	4	35.3	181	250	74.6	29.2	92.4	104	51.8	37.4	4.21
CP54	20	700	100/0	1	12.1	74.1	114		19.9	49.9	53.4	26.4		2.63
CP17	20	700	90/10	6	31.5	154	179	77.9	30.0	90.9	100	49.4	44.5	4.88
CP16	20	700	50/50	5	48.4	180	277	106	36.2	130	113	57.3	48.0	6.07
CP65	20	700	50/50	1	50.3	249	335	110	37.0	99.9	92.5	35.0	29.1	3.89
HOL14				2	28.5	127	167	70.1	29.1	89.6	105	56.8	41.7	5.19

Sample	Ba	Sr	Rb	Y	V	U	Th	Nb	Ta	Zr	Hf
Experiments											
CP21	b.d.	b.d.	b.d.	568	1124	7.18	3.15	200	3.14	4220	
CP8		b.d.	b.d.	352	1100	7.33	5.77	468	6.79	2792	56.0
CP66	24.8	b.d.	b.d.	421	831	5.71	5.54	947	13.0	2934	68.1
CP67	15.8	b.d.	b.d.	379	1294	4.64	3.33	389	12.0	3902	77.0
CP7	16.8	b.d.	b.d.	548	1177	8.21	10.4	458	16.5	3539	50.5
CP2	8.19	b.d.	9.28	482	1347	4.38	2.77	215	7.17	3448	75.8
CP11	84.4	458	b.d.	404	1501	4.75	1.70	172	4.95	3055	71.9
CP68		561	15.3	462	944	5.68	5.80	352	19.0	4066	91.8
CP69		2051	b.d.	494	1182	9.19	8.77	795	21.9	3201	84.9
CP10		584	12.0	577	1096	10.8	10.9	494	26.9	4474	73.2
CP40		517	b.d.	409	1115	5.88	6.49	186	6.98	3008	88.0
CP15		b.d.	17.2	472	1282	7.88	9.20	208	8.65	3377	69.1
CP14	73.6		40.2	480	1136	8.23	26.2	575	22.1	4328	85.9
CP54	2.26	b.d.	b.d.	274	1332	4.01	2.65	142	3.67	2889	67.6
CP17	53.3	1042	28.7	433	995	6.19	9.18	227	5.59	3674	77.9
CP16	38.6		26.9	513	1269	13.4	21.1	338	11.9	3683	56.7
CP65	44.8	b.d.	b.d.	397	862	7.42	12.4	488	20.9	3766	75.0
HOL14	1.23	89.1		489	1538	5.22	4.29	276	12.5	3773	83.8

Note: # an.: number of analyses; b.d.: below detection.
Pressure (P) is in MPa, temperature (T) is in oC, and starting composition is shown as proportion of wollastonite nephelinite HOL14/silicate-bearing natrocarbonatite OL5 (in wt. %).

Table 7.5: Trace element LAM-ICP-MS analyses of wollastonite in the experiments and in erupted wollastonite nephelinite HOL14 (in ppm).

Sample	P	T	X	# an.	La	Ce	Nd	Sm	Eu	Gd	Dy	Er	Yb	Lu
Experiments														
CP31**	100	700	90/10	1	124	161							7.05	
CP1	40	800	50/50	1	74.6	189							5.32	
CP11	40	700	90/10	1	76.4	126							16.2	
CP14	20	800	50/50	1	40.5	122							b.d.	
CP16	20	700	50/50	4	45.7	83.6	41.5	7.20	5.13	9.10	5.81	8.06	b.d.	
HOL14				2	17.7	49.8	24.8	5.57	2.24	6.58	7.35	5.08	4.85	0.73

Sample	Ba	Sr	Rb	Y	V	U	Th	Nb	Ta	Zr	Hf
Experiments											
CP31**				89.4							
CP1				85.3						47.2	
CP11				122						79.1	
CP14				53.8						b.d.	
CP16	147			58.8				11.7		34.0	
HOL14	72.6	1564	4.68	35.0	3.12	0.25	0.06	1.31	0.02	6.57	2.38

Note: # an.: number of analyses; b.d.: below detection.
Pressure (P) is in MPa, temperature (T) is in oC, and starting composition is shown as proportion of wollastonite nephelinite HOL14/silicate-bearing natrocarbonatite OL5 (in wt. %).
**CP31 is a C/CH4-buffered experiment. Other experiments are unbuffered.

Table 7.6: Trace element LAM-ICP-MS analyses of melilite in the experiments (in ppm).

Experiment	P	T	X	# an.	La	Ce	Nd	Sm	Eu	Gd	Dy	Er	Yb	Lu
CP19	40	900	90/10	3	73.5	127	36.4	4.36	1.31	b.d.	b.d.	b.d.	b.d.	b.d.
CP23	20	900	90/10	7	105	150	39.4	6.22	1.24	1.49	1.37	b.d.	b.d.	b.d.
CP22	20	900	50/50	6	239	339	74.0	5.11	2.23	2.83	b.d.	b.d.	b.d.	b.d.
CP15	20	800	90/10	1	304	383							b.d.	
CP14	20	800	50/50	22	449	636	128	10.8	3.11	5.82	2.31	1.56	b.d.	1.96

Experiment	Ba	Sr	Rb	Y	V	U	Th	Nb	Ta	Zr	Hf
CP19	272	11776	7.56	6.57	14.6	0.86	b.d.	8.73	b.d.		6.01
CP23	261	11498	6.15	5.94	17.8	0.59	0.88	7.70	b.d.	14.3	b.d.
CP22	615	16546	11.9	5.49	25.0	0.95	2.90	6.54	0.69	15.3	b.d.
CP15											
CP14	641	20289	33.8	8.22	16.6	4.63	3.66	8.88	1.06	9.02	3.48

Note: # an.: number of analyses; b.d.: below detection.
Pressure (P) is in MPa, temperature (T) is in oC, and starting composition is shown as proportion of wollastonite nephelinite HOL14/silicate-bearing natrocarbonatite OL5 (in wt. %).

Table 7.7: Trace element LAM-ICP-MS analyses of titanite, apatite and combeite in the experiments and in erupted wollastonite nephelinite HOL14 (in ppm).

Sample	P	T	X	# an.	La	Ce	Nd	Sm	Eu	Gd	Dy	Er	Yb	Lu
Titanite Experiments														
CP11	40	700	90/10	1	312	694	342	58.9	21.1	57.2	34.3	8.92	3.98	b.d.
CP64	20	700	800/20	1	294	691	426	99.6	26.9	65.2	43.6	13.3	5.64	0.87
HOL14				6	270	587	300	64.2	22.1	51.0	37.0	12.5	6.18	0.71
Apatite														
CP31**	100	700	90/10	1	1754	4585	1024	95.8	28.3	56.2	21.8	8.70	3.27	0.29
Combeite														
CP16	20	700	50/50	10	193	507	231	52.2	17.8	46.0	38.7	21.5	23.3	3.86
CP65	20	700	50/50	2	217	723	263	56.4	18.8	45.4	35.9	25.6	19.1	4.33

Sample	Ba	Sr	Rb	Y	V	U	Th	Nb	Ta	Zr	Hf
Titanite Experiments											
CP11	809	2446	82.8	100	640	24.3	7.29	2409	71.3	2757	64.0
CP64	45.2	972	b.d.	177	721	4.25	4.79	4765	106	5256	129
HOL14	116	1087	3.49	141	532	4.24	3.32	2596	104	4454	123
Apatite											
CP31**	4063	13712	16.6	125	93.6	5.63	44.1	8.33	b.d.	19.1	0.94
Combeite											
CP16	58.4	3635	18.4	302	37.4	13.4	44.2	4.71		2972	39.5
CP65	38.7	3433	7.04	235	9.17	27.3	59.0	11.9	0.44	2275	24.0

Note: # an.: number of analyses; b.d.: below detection.
Pressure (P) is in MPa, temperature (T) is in oC, and starting composition is shown as proportion of wollastonite nephelinite HOL14/silicate-bearing natrocarbonatite OL5 (in wt. %).
**CP31 is a C/CH4-buffered experiment. Other experiments are unbuffered.

Table 7.8: Partition coefficients (D) between silicate (LS) and carbonate (LC) liquids. Comparison between the data from this study and data from previous studies.

Reference	CP20, this study	VPJDD98	W&H79	HB&E89	HB&E89	JWPMB95
P,T:	100 MPa, 900 °C	84-94 MPa, 965-1015 °C	500 MPa, 1200 °C	100 MPa, 1150 °C (Ne)	100 MPa, 1150 °C (Ph)	1 GPa, 1100 °C
Ba	0.25	0.19		4.48	0.56	0.48
Sr	0.25	0.24				
Rb	0.97					
Y	1.10	2.63				
V	0.27					
La	0.50	0.75		3.18	1.64	
Ce	0.60		0.38	2.84	1.78	0.91
Nd	0.67	1.09				
Sm	0.74	1.54	0.27	4.56	2.28	
Eu	0.85			3.78	2.18	
Gd	0.78			3.73	2.30	
Dy	0.96					
Er	1.14	3.03				
Yb	1.23			4.48	4.08	
Lu	1.36			4.80	4.67	
U	1.14					3.23
Th	3.79					5.00
Nb	1.20	1.99				2.78
Ta	3.09	10.1		2.61	3.67	
Zr	18.4	62.5		2.83	0.85	
Hf	23.9	108		116	408	

Abbreviations used are: VPJDD98: Veksler et al. (1998); W&H79: Wendlandt and Harrison (1979); HB&E89: Hamilton et al. (1989); JWPMB95: Jones et al. (1995).

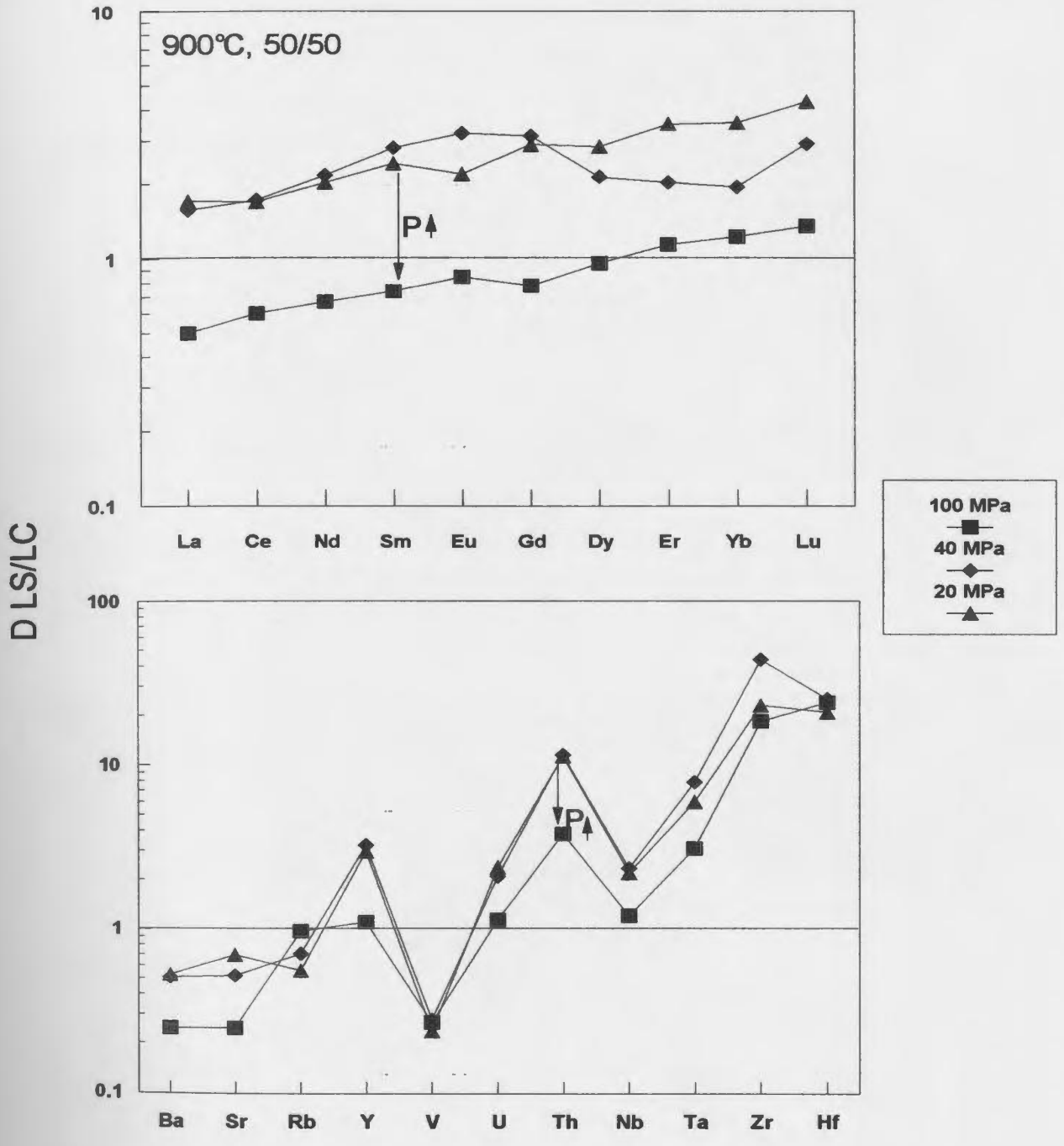

Figure 7.1: Trace element partition coefficients (D) between silicate liquid (LS) and carbonate liquid (LC) as a function of pressure (shown in the legend) for experiments prepared at 900 °C using a 50/50-bulk composition. The direction toward which $D_{LS/LC}$ evolve with increasing pressure (P) is indicated. Data are from Table 7.1.

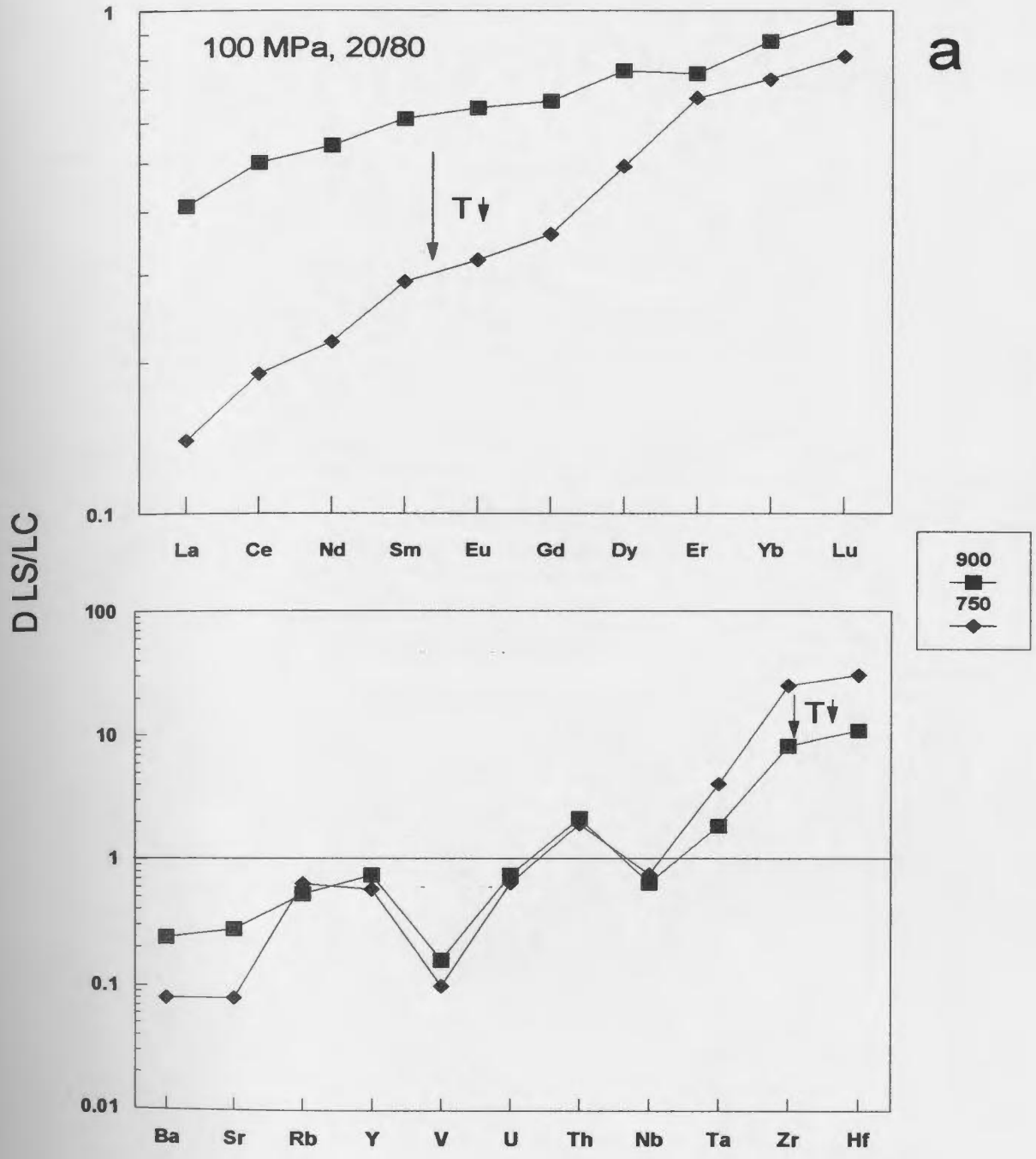

Figure 7.2: Trace element partition coefficients (D) between silicate liquid (LS) and carbonate liquid (LC) from the experiments as a function of temperature (shown in °C in the legend). a) 100 MPa and 80/20-bulk composition; b) 100 MPa and 50/50-bulk composition. The direction toward which $D_{LS/LC}$ evolve with increasing temperature (T) is indicated. Data are from Table 7.1.

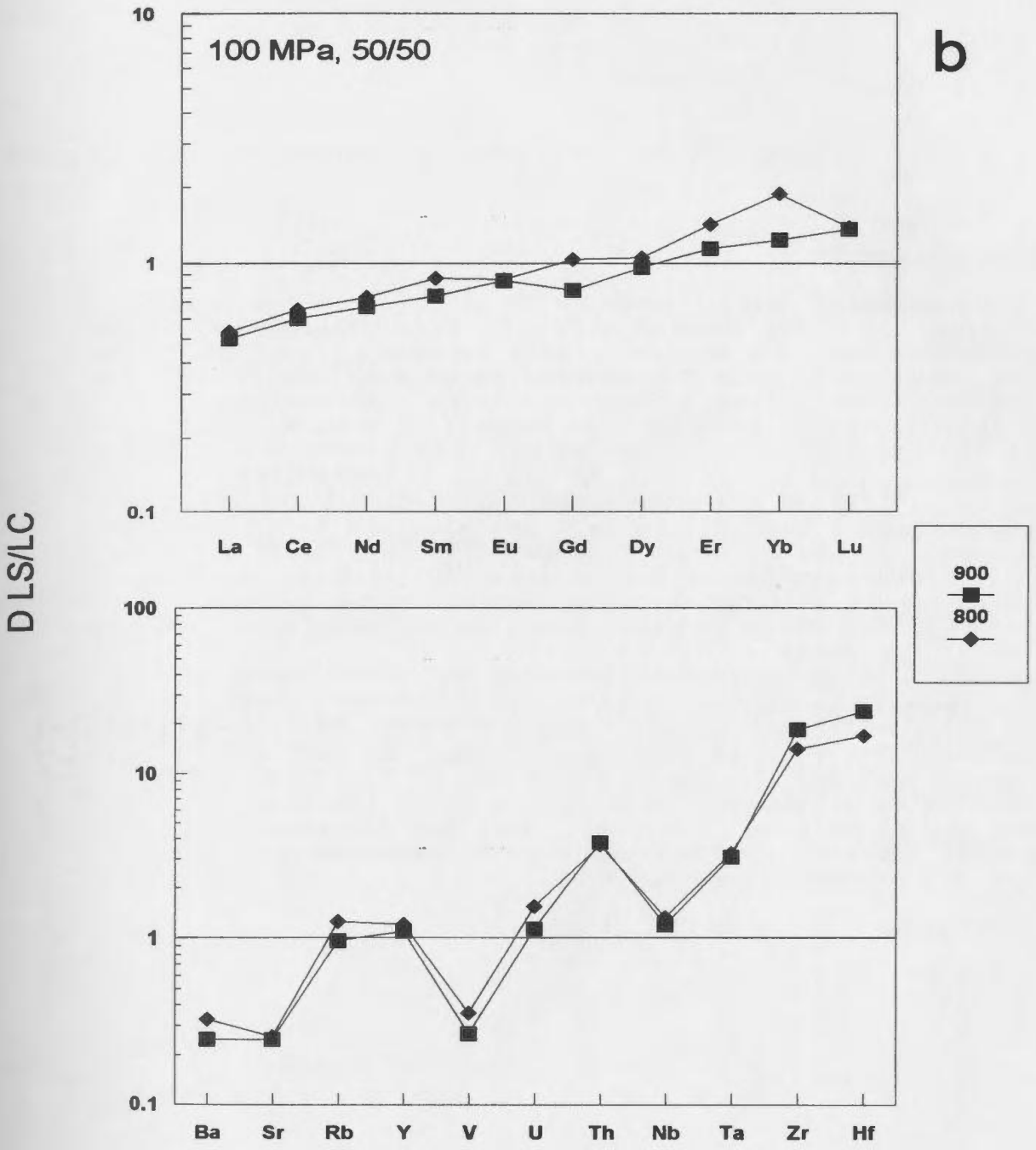
100 MPa, 50/50
b
D LS/LC
10
1
0.1
La
Ce
Nd
Sm
Eu
Gd
Dy
Er
Yb
Lu
900
800
100
10
1
0.1
Ba
Sr
Rb
Y
V
U
Th
Nb
Ta
Zr
Hf

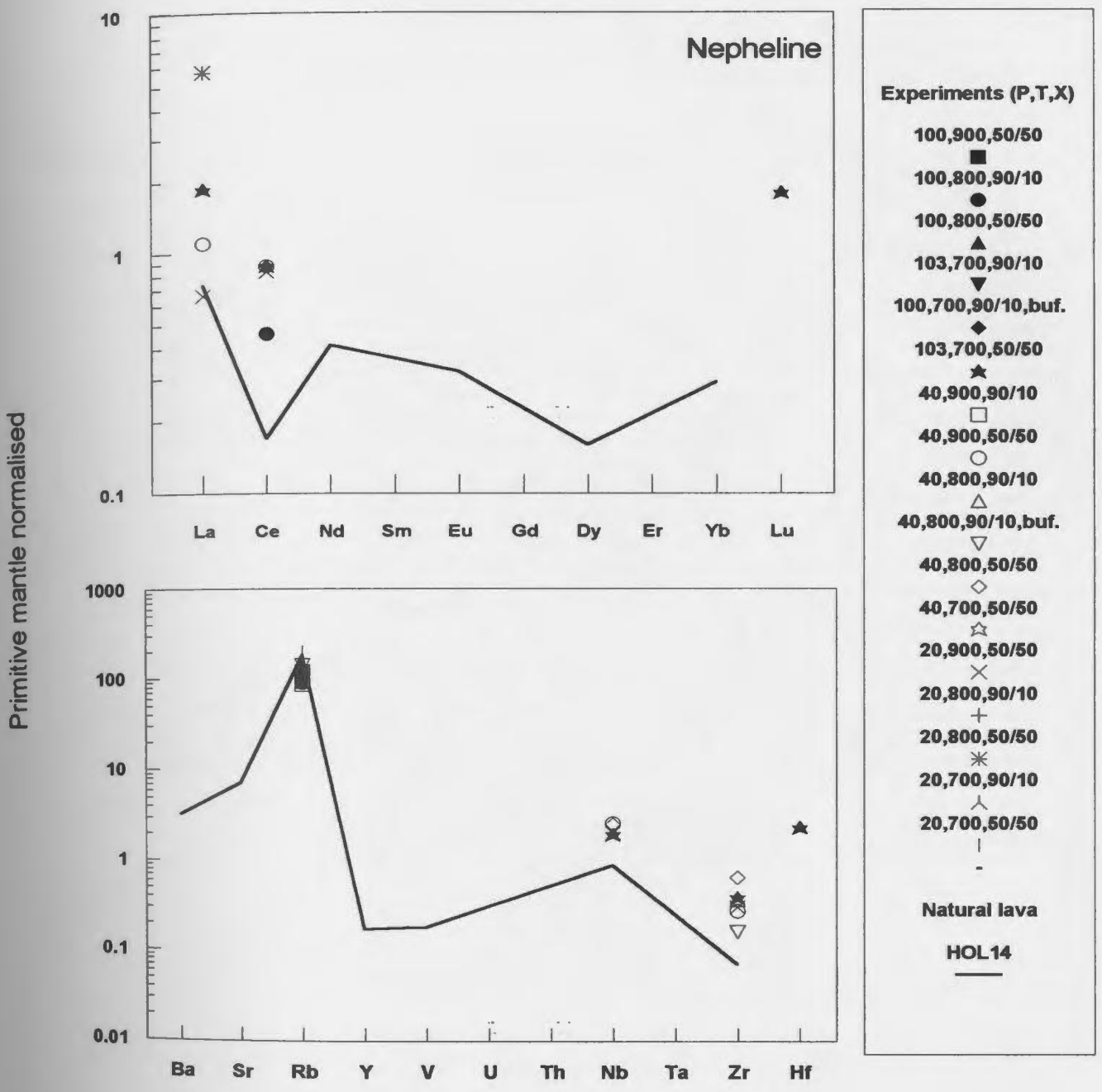

Figure 7.3: Trace element concentrations normalised to primitive mantle of nepheline from experiments and from erupted wollastonite nephelinite lava HOL14. For the experiments, pressure (in MPa), temperature (in °C) and bulk composition (shown as weight fraction of wollastonite nephelinite HOL14 / weight fraction of silicate-bearing carbonatite OL5) are shown in the legend above the symbols. Data are from Table 7.2. Note that the small crystal sizes and low concentrations for most elements resulted in no data being available for many of the elements. Primitive mantle normalising values are from McDonough and Sun (1995).

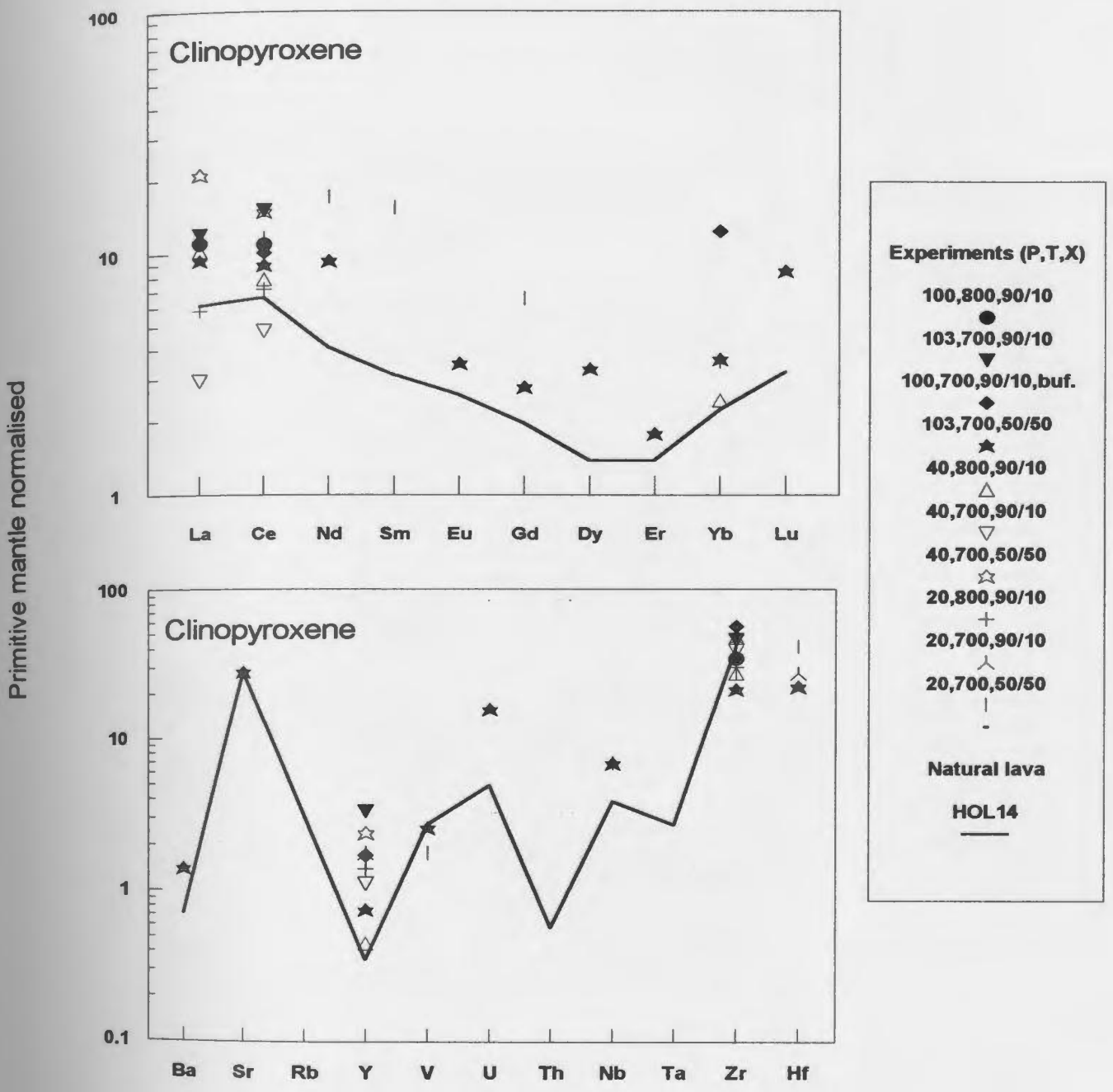

Figure 7.4: Trace element concentrations normalised to primitive mantle of clinopyroxene from experiments and from erupted wollastonite nephelinite lava HOL14. For the experiments, pressure (in MPa), temperature (in °C) and bulk composition (shown as weight fraction of wollastonite nephelinite HOL14 / weight fraction of silicate-bearing [redacted]ocarbonatite OL5) are shown in the legend above the symbols. Data are from Table 7.3; primitive mantle normalising values are from McDonough and Sun (1995).

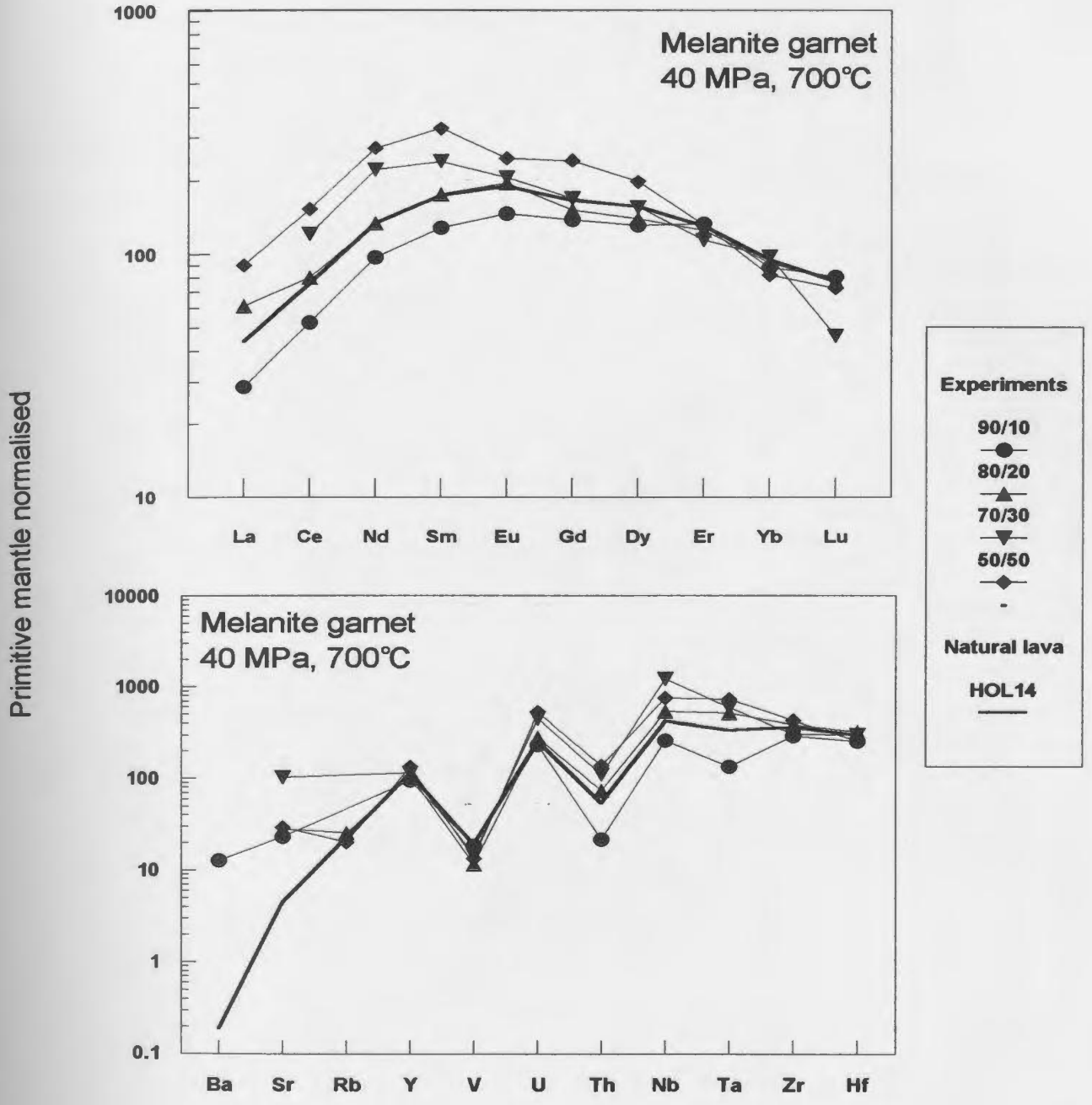

Figure 7.5: Trace element concentrations normalised to primitive mantle of melanite garnet from experiments at 40 MPa, 700 °C, and from erupted wollastonite nephelinite lava HOL14. For the experiments, bulk composition (shown as weight fraction of wollastonite nephelinite HOL14 / weight fraction of silicate-bearing natrocarbonatite OL5) is shown in the legend above the symbols. Data are from Table 7.4; primitive mantle normalising values are from McDonough and Sun (1995).

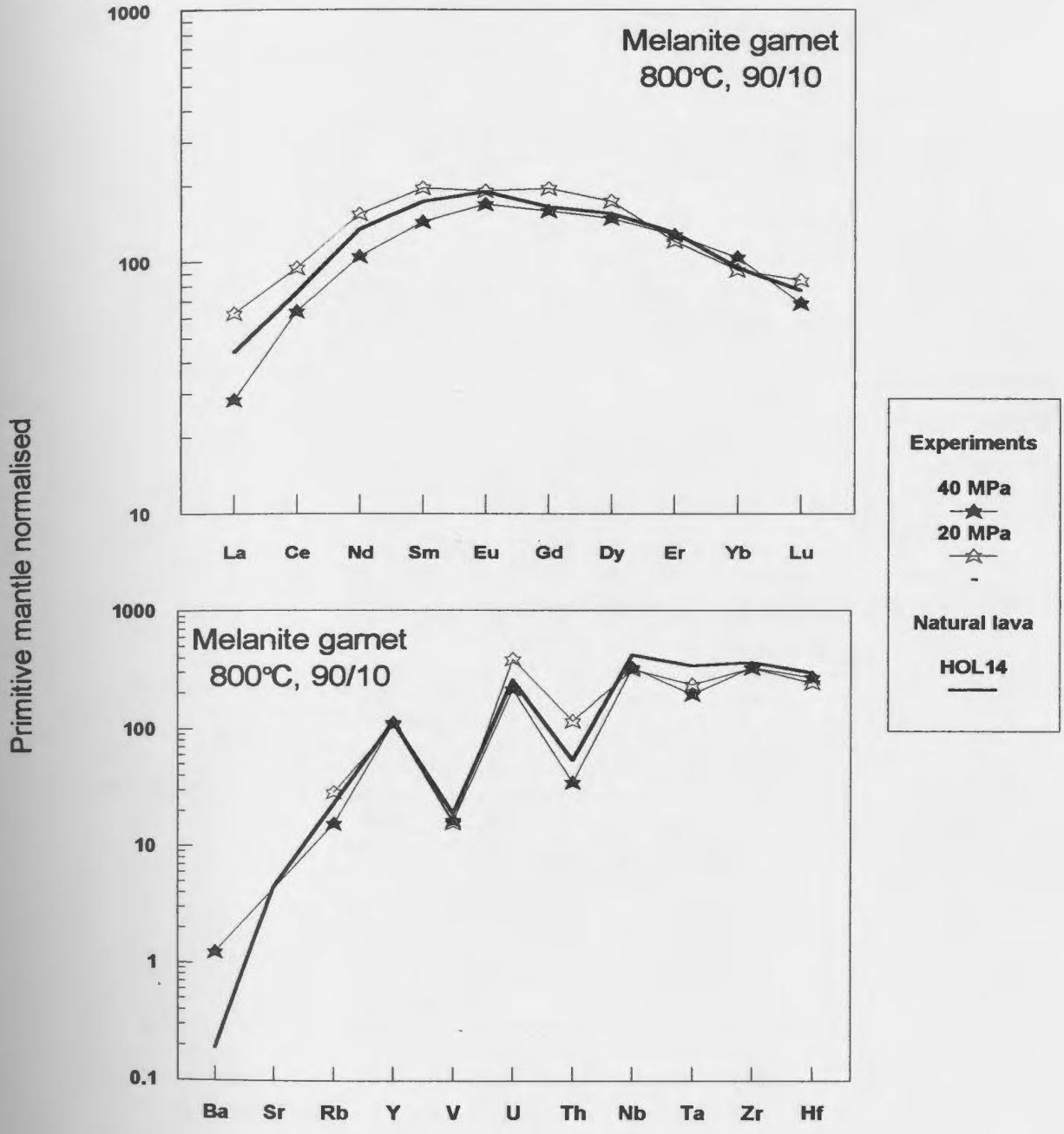

Figure 7.6: Trace element concentrations normalised to primitive mantle of melanite garnet from experiments at 800 °C, prepared using starting mixtures of 90 wt. % wollastonite nephelinite HOL14 and 10 wt. % silicate-bearing natrocarbonatite OL5, and from natural wollastonite nephelinite lava HOL14. For the experiments, pressure is shown in the legend above the symbols. Data are from Table 7.4; primitive mantle normalising values are from McDonough and Sun (1995).

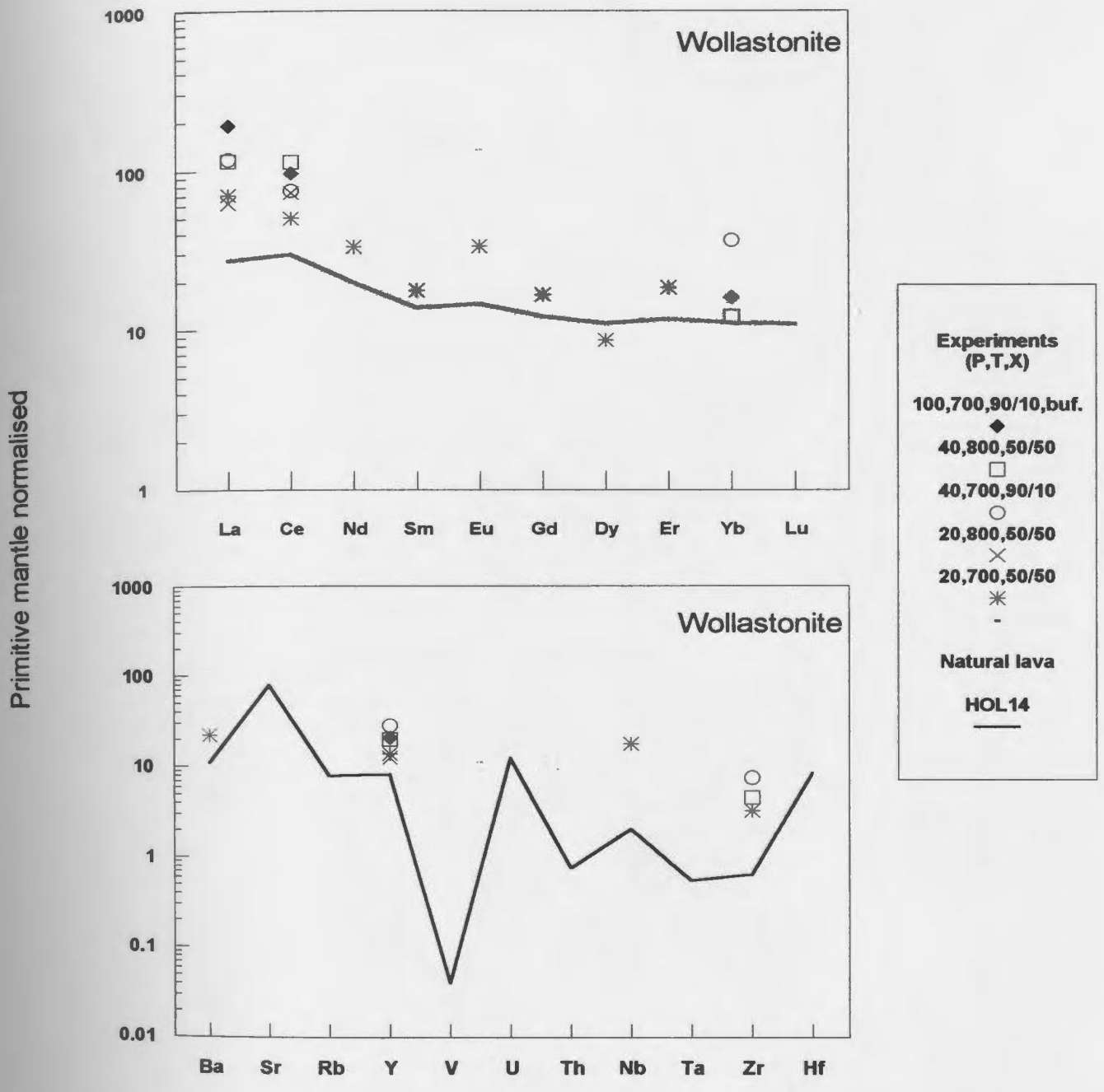

Figure 7.7: Trace element concentrations normalised to primitive mantle of wollastonite from experiments and from erupted wollastonite nephelinite lava HOL14. For the experiments, pressure (in MPa), temperature (in °C) and bulk composition (shown as weight fraction of wollastonite nephelinite HOL14 / weight fraction of silicate-bearing natrocarbonatite OL5) are shown in the legend above the symbols. Data are from Table 7.5; primitive mantle normalising values are from McDonough and Sun (1995).

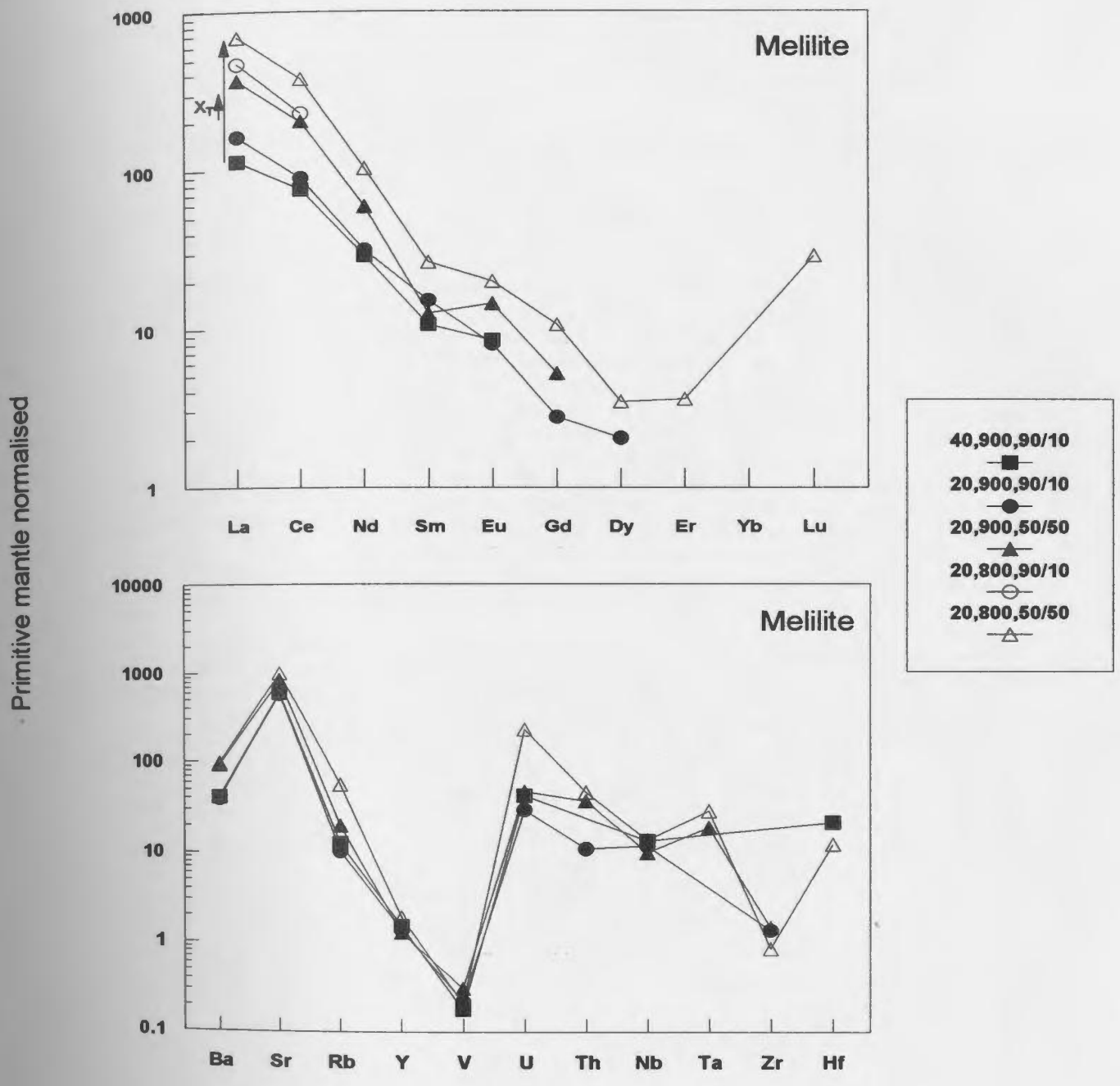

Figure 7.8: Trace element concentrations normalised to primitive mantle of melilite from experiments. Pressure (in MPa), temperature (in °C) and bulk composition (shown as weight fraction of wollastonite nephelinite HOL14 / weight fraction of silicate-bearing carbonatite OL5) are shown in the legend above the symbols. The arrow represents the compositional trend with increasing temperature. Data are from Table 7.6; primitive mantle normalising values are from McDonough and Sun (1995).

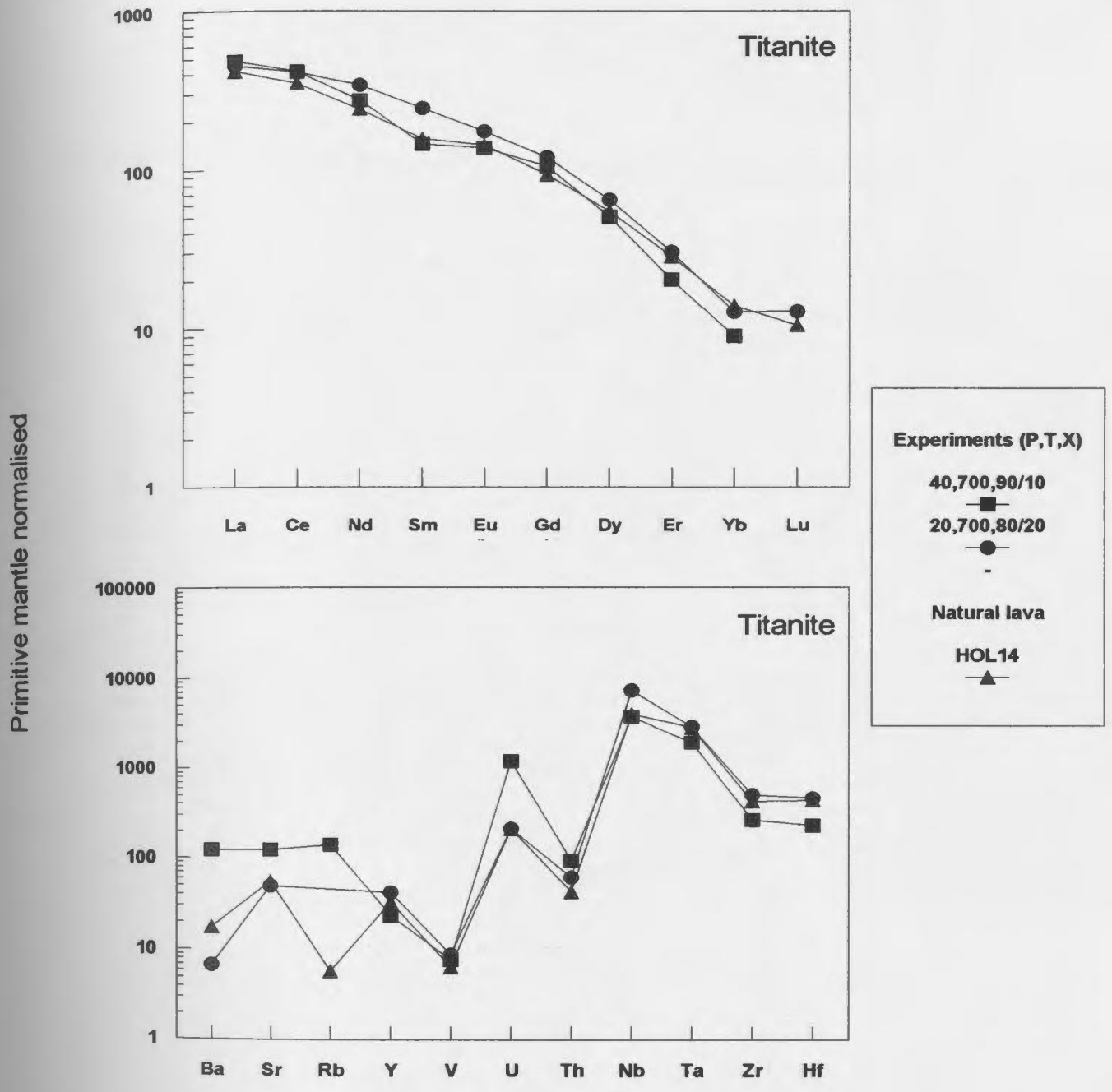

Figure 7.9: Trace element concentrations normalised to primitive mantle of titanite from experiments and from erupted wollastonite nephelinite lava HOL14. For the experiments, pressure (in MPa), temperature (in °C) and bulk composition (shown as weight fraction of wollastonite nephelinite HOL14 / weight fraction of silicate-bearing natrocarbonatite OL5) are shown in the legend above the symbols. Data are from Table 7.7; primitive mantle normalising values are from McDonough and Sun (1995).

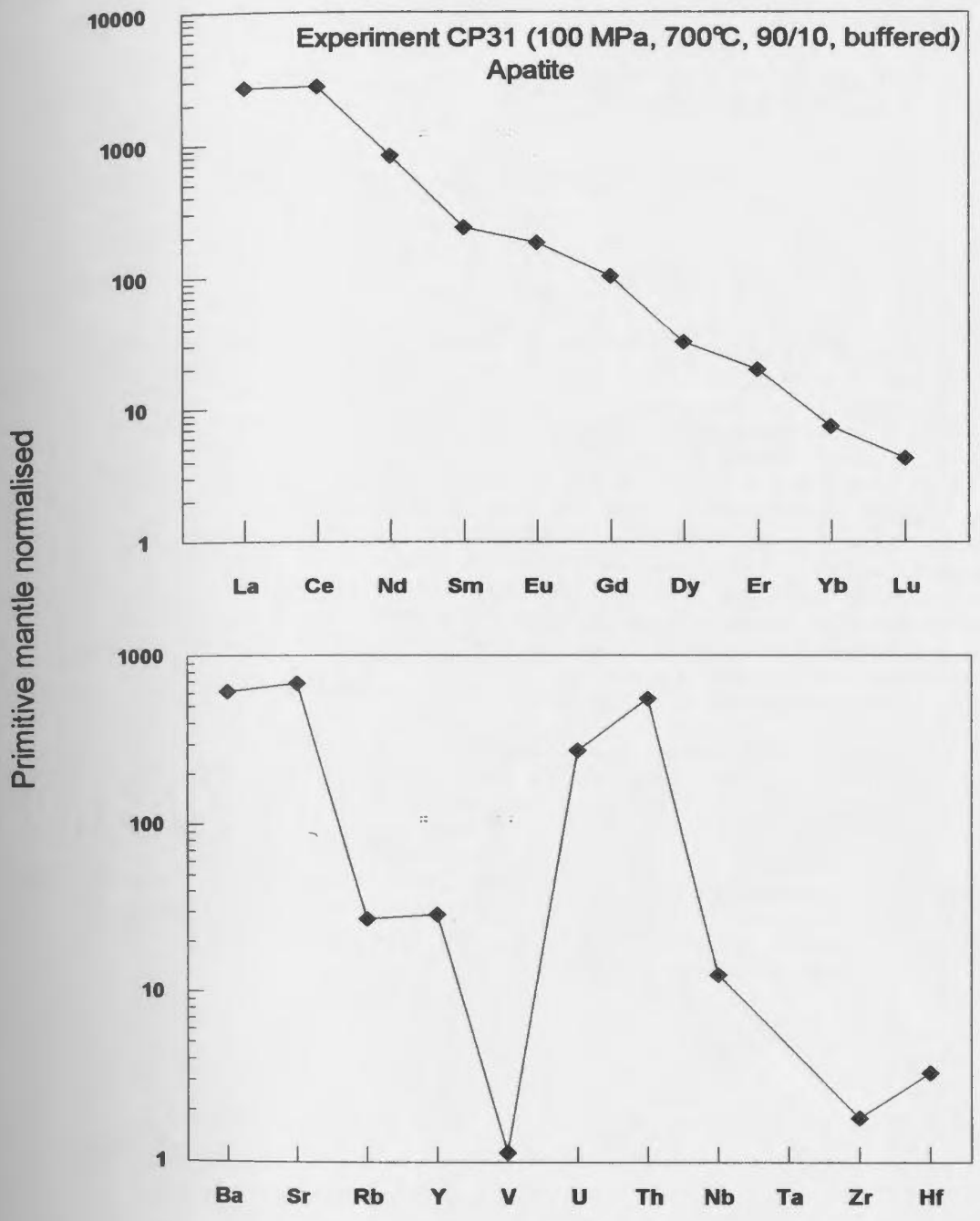

Figure 7.10: Trace element concentrations normalised to primitive mantle of apatite from experiment CP31 (100 MPa, 700 °C, 90/10, C/CH_4-buffered). Data are from Table 7.7; primitive mantle normalising values are from McDonough and Sun (1995).

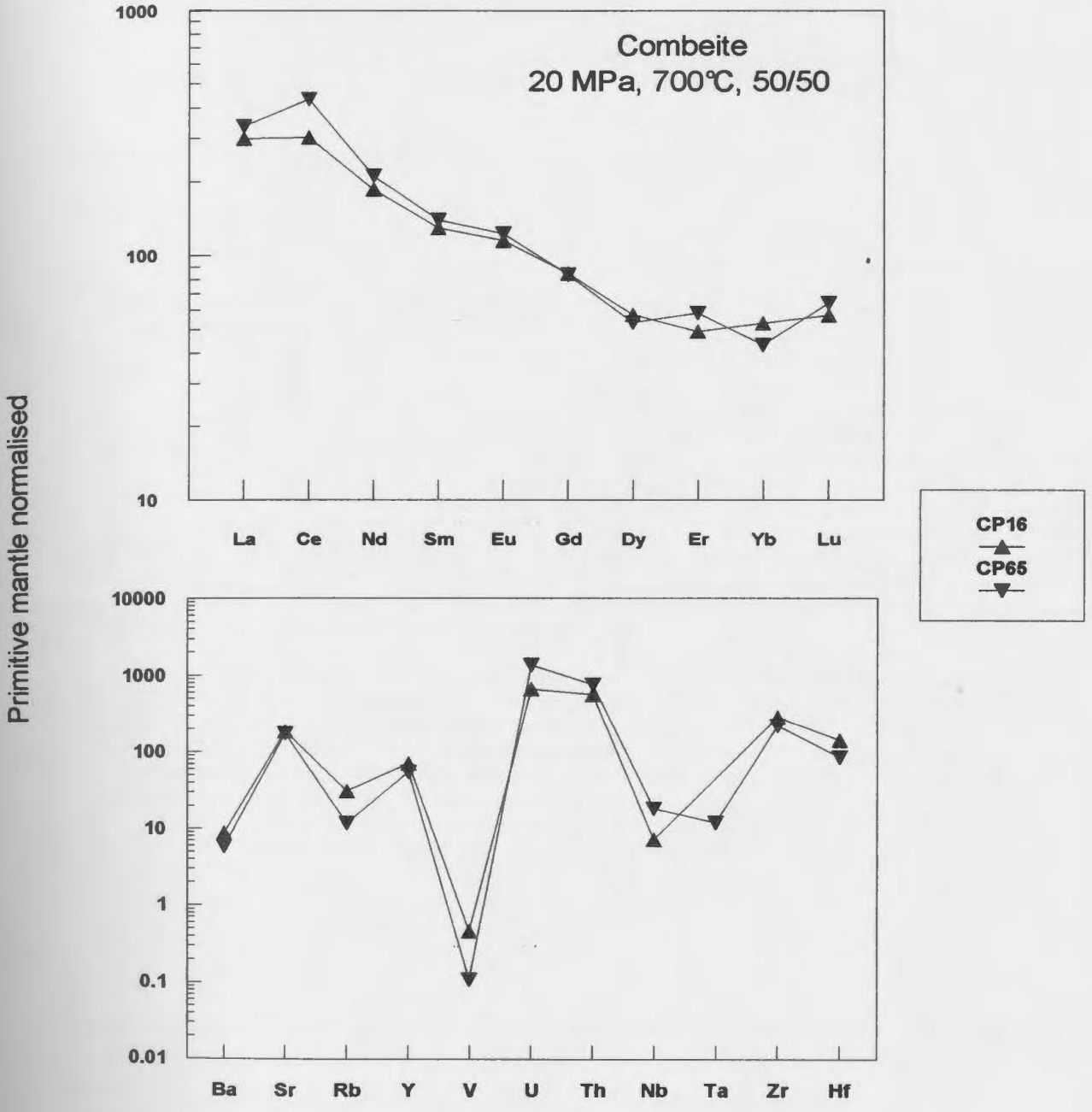

Figure 7.11: Trace element concentrations normalised to primitive mantle of combeite from experiments CP16 and CP65 (20 MPa, 700 °C, 50/50). Data are from Table 7.7; primitive mantle normalising values are from McDonough and Sun (1995).

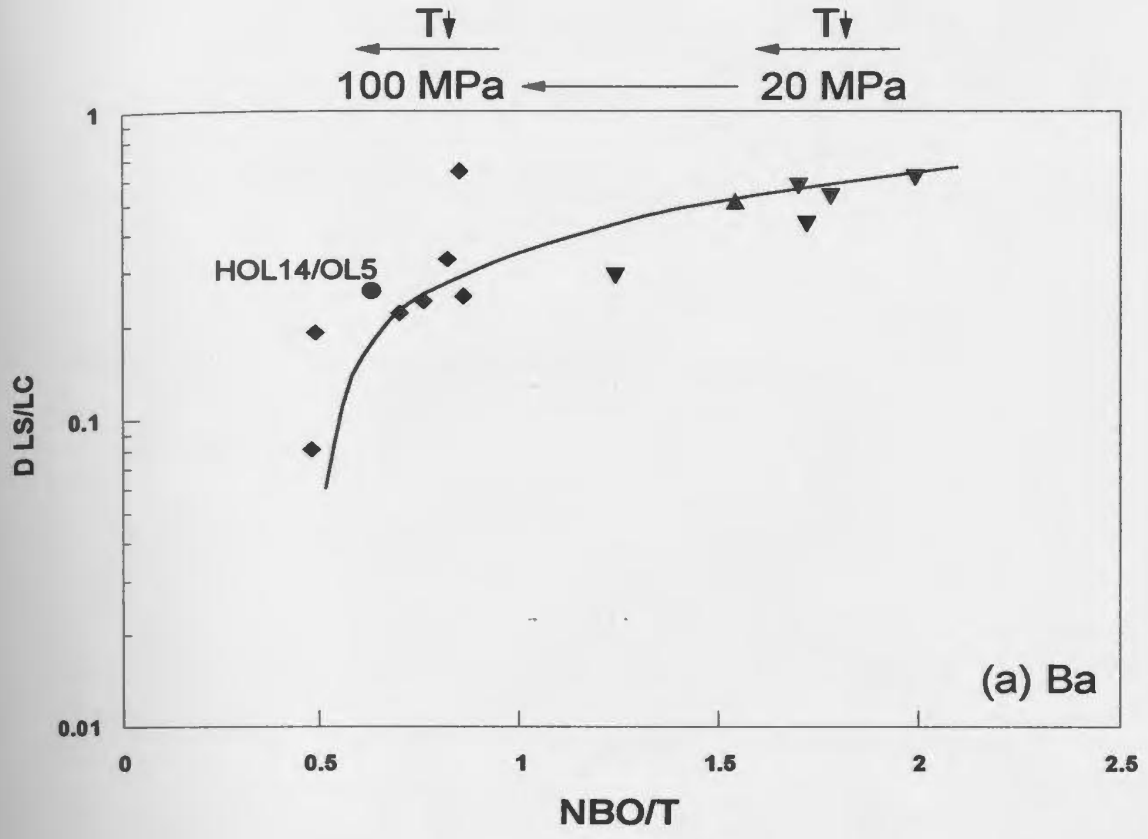

Figure 7.12: Trace element partition coefficients between silicate and carbonate liquids ($D_{LS/LC}$) as a function of NBO/T (non-bridging oxygens per tetrahedra) of the silicate liquid for (a) Ba; (b) Sr; (c) V; (d) Rb; (e) Y; (f) La; (g) Ce; (h) Nd; (i) Sm; (j) Eu; (k) Gd; (l) Dy; (m) Er; (n) Yb; (o) Lu; (p) U; (q) Th; (r) Nb; (s) Ta; (t) Zr; and (u) Hf. Inverted triangles represent data for 20 MPa experiments, normal triangles for 40 MPa experiments, diamonds for 100 MPa experiments and the dot for the natural pair (groundmass HOL14/whole rock OL5). The arrows above the graphs represent the evolution of NBO/T values with increasing pressure from 20 to 100 MPa, and for each pressure, the evolution of NBO/T values with decreasing temperature (T). For the elements Y, U, Th, REE and HFSE that have a dual role, the arrows on the graphs indicate that with decreasing NBO/T, their role as network modifiers (Mod.) increases relatively to their role as network formers (Form.). The opposite trend is observed for Rb. Data for D values are from Table 7.1 and data for NBO/T values are from Table A6.4 in Appendix A6.

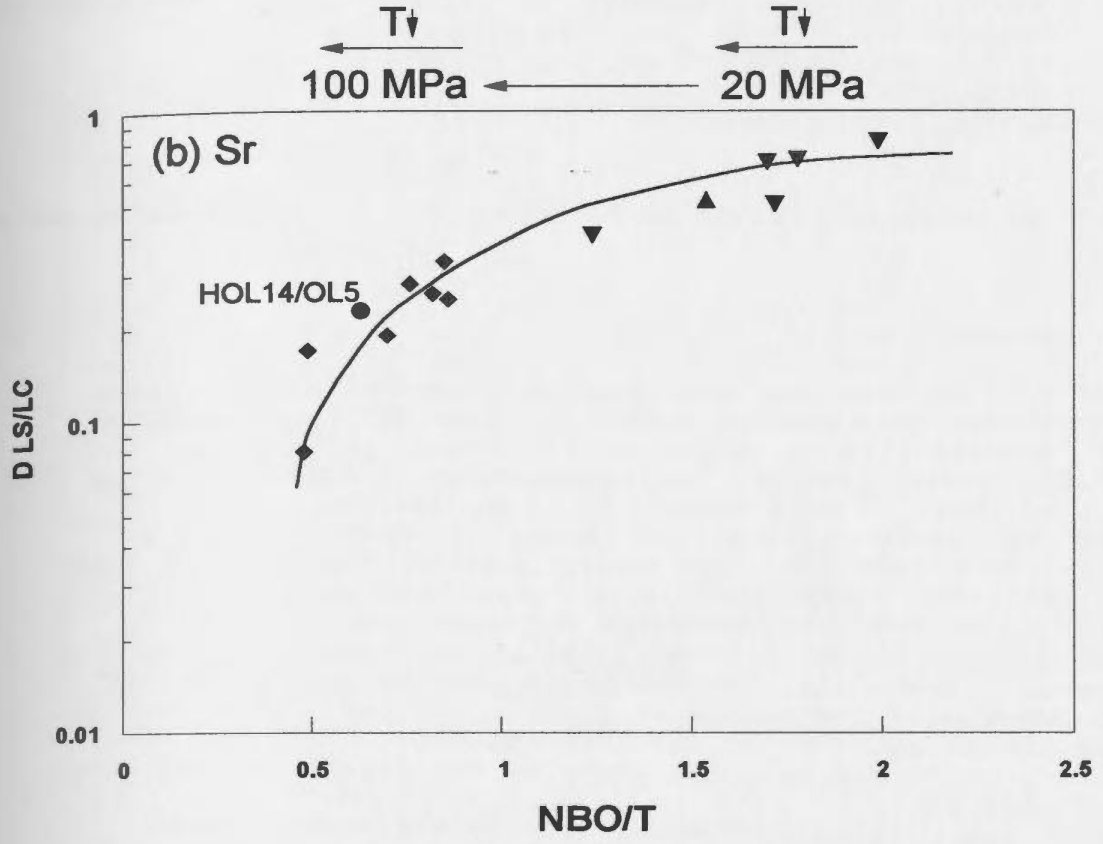
T↓
T↓
100 MPa
20 MPa
(b) Sr
HOL14/OL5
D LS/LC
1
0.1
0.01
0
0.5
1
1.5
2
2.5
NBO/T

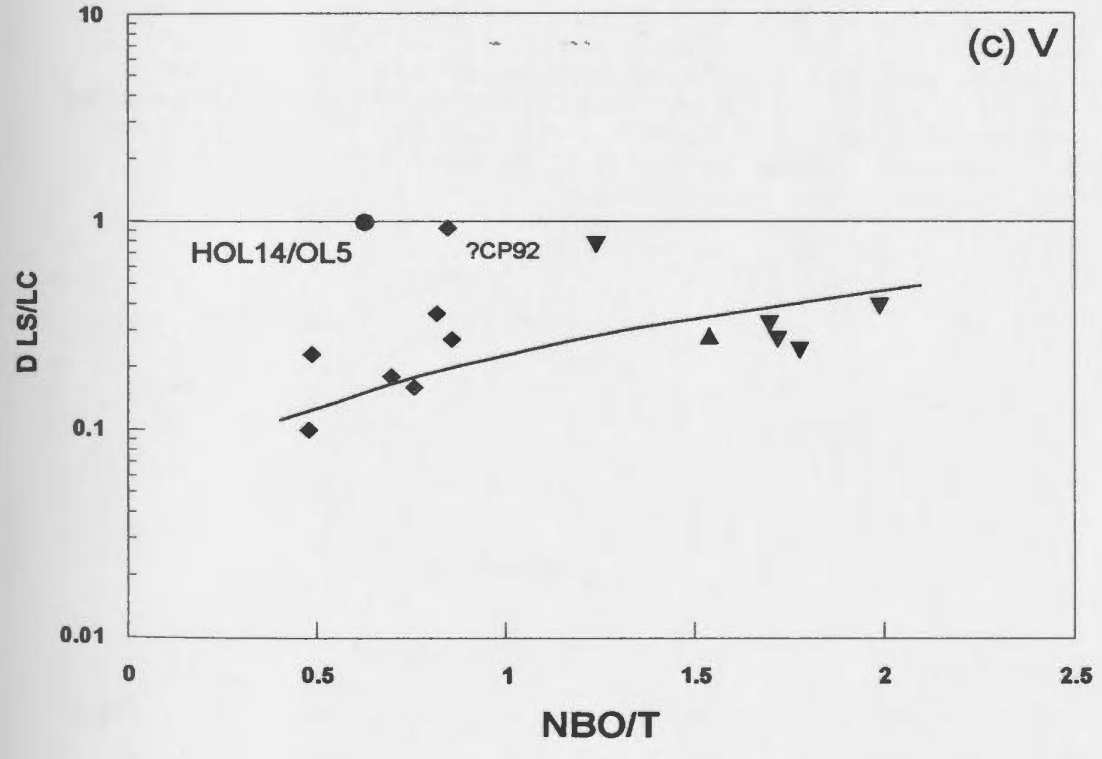
(c) V
HOL14/OL5
?CP92
D LS/LC
10
1
0.1
0.01
0
0.5
1
1.5
2
2.5
NBO/T

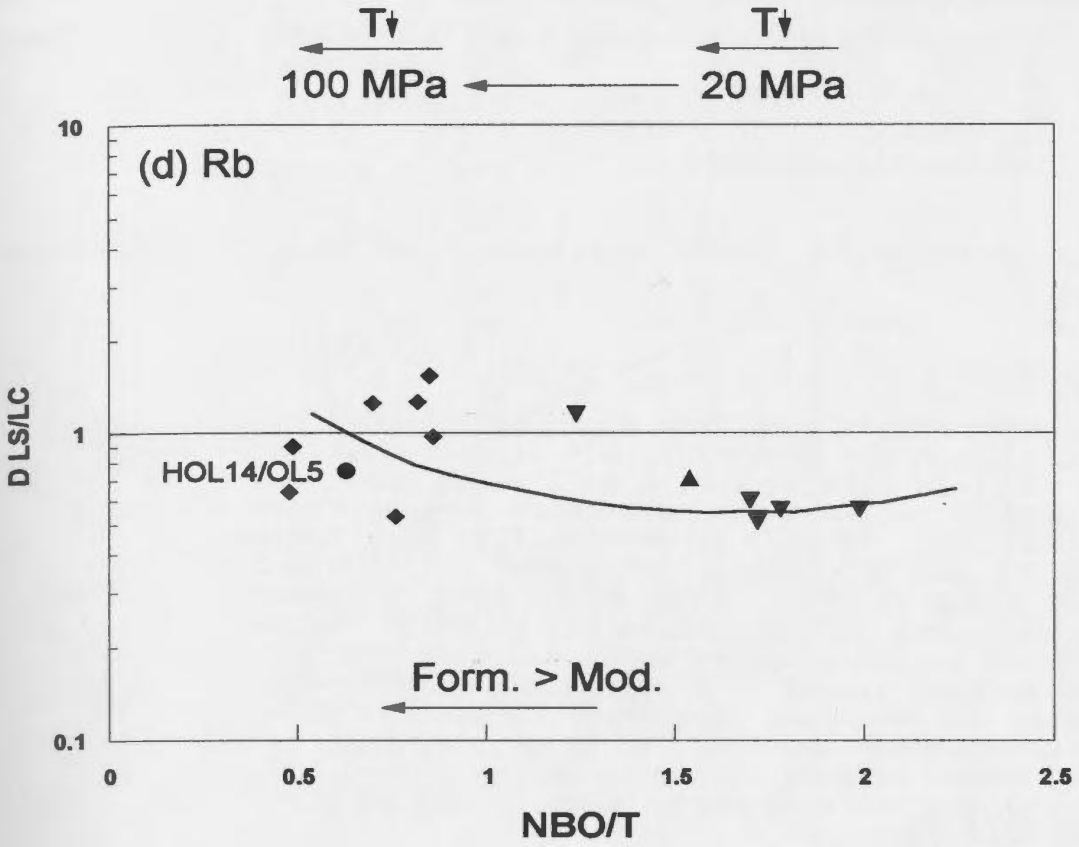
T↓
T↓
100 MPa
20 MPa
(d) Rb
10
1
0.1
D LS/LC
HOL14/OL5
Form. > Mod.
0
0.5
1
1.5
2
2.5
NBO/T

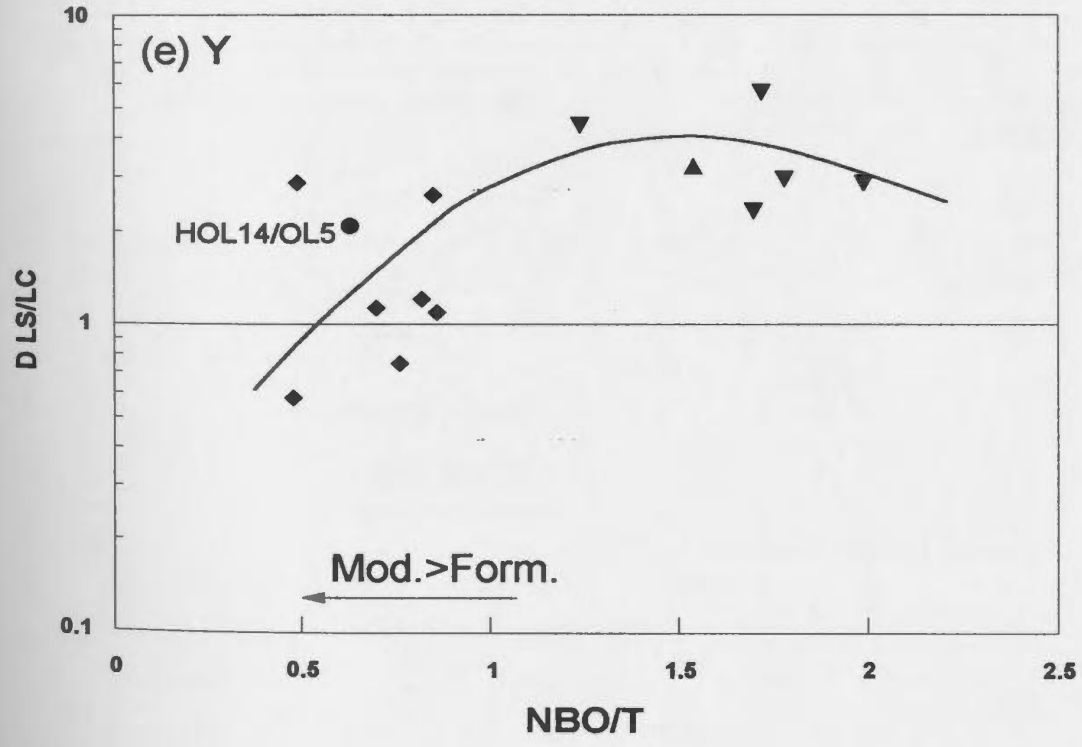
(e) Y
10
1
0.1
D LS/LC
HOL14/OL5
Mod.>Form.
0
0.5
1
1.5
2
2.5
NBO/T

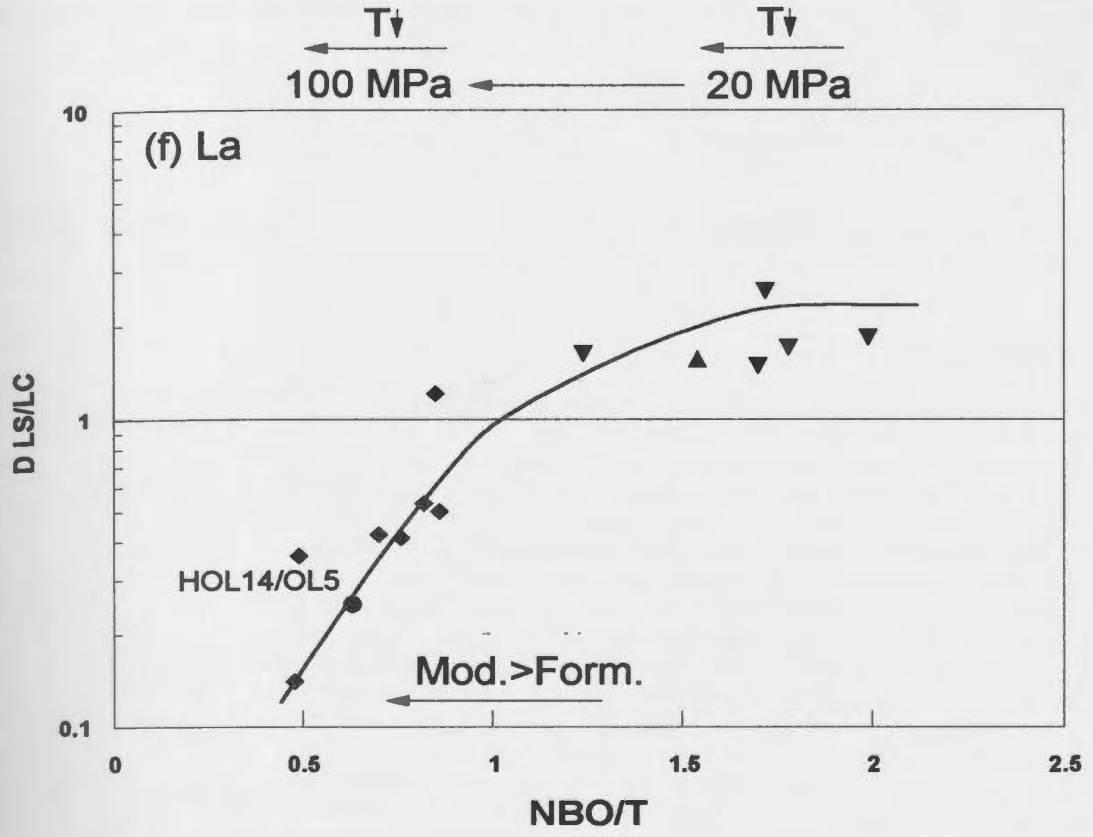
T↓
T↓
100 MPa
20 MPa
(f) La
10
1
0.1
D LS/LC
HOL14/OL5
Mod.>Form.
0
0.5
1
1.5
2
2.5
NBO/T

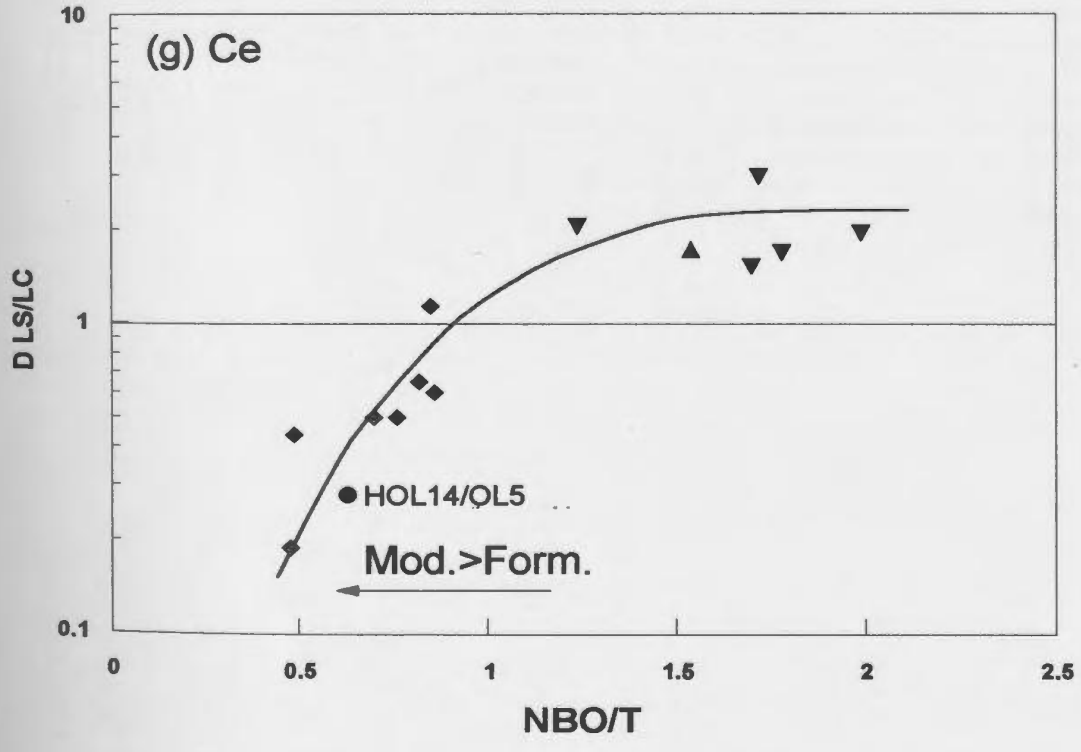
(g) Ce
10
1
0.1
D LS/LC
HOL14/OL5
Mod.>Form.
0
0.5
1
1.5
2
2.5
NBO/T

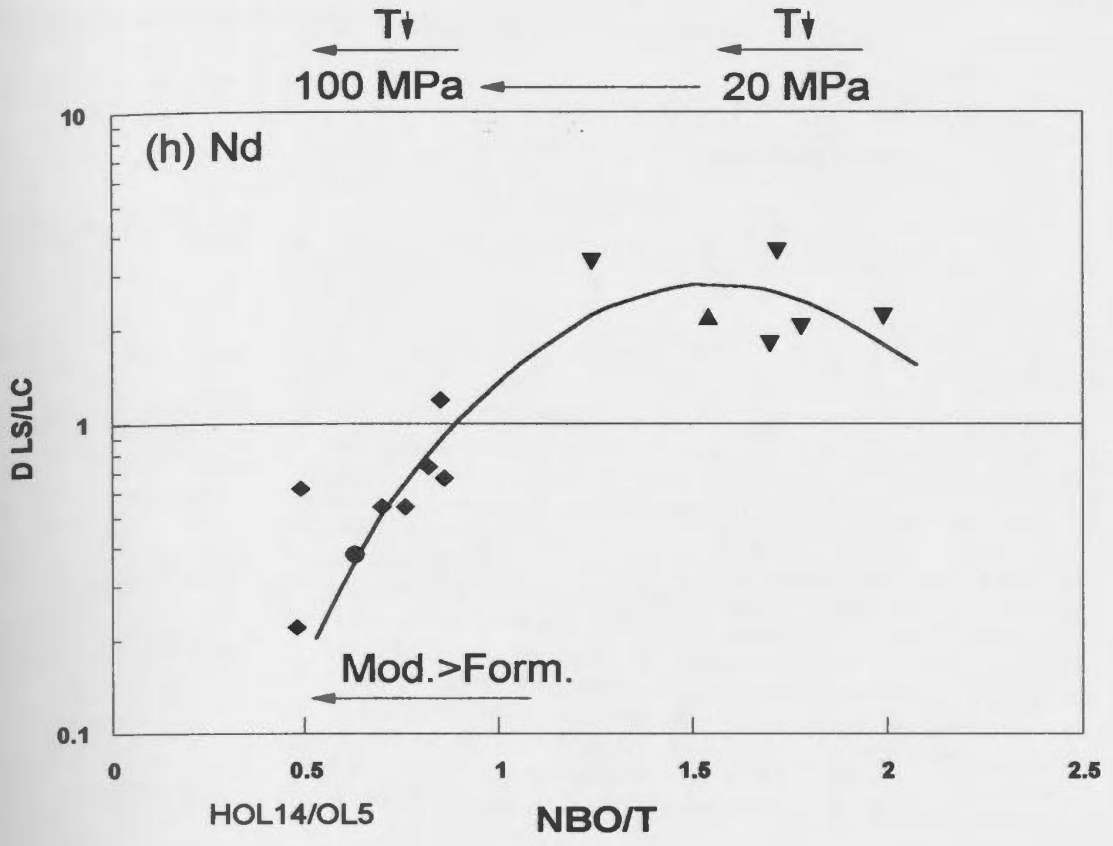
T↓
T↓
100 MPa
20 MPa
(h) Nd
10
1
0.1
D LS/LC
Mod.>Form.
0
0.5
1
1.5
2
2.5
HOL14/OL5
NBO/T

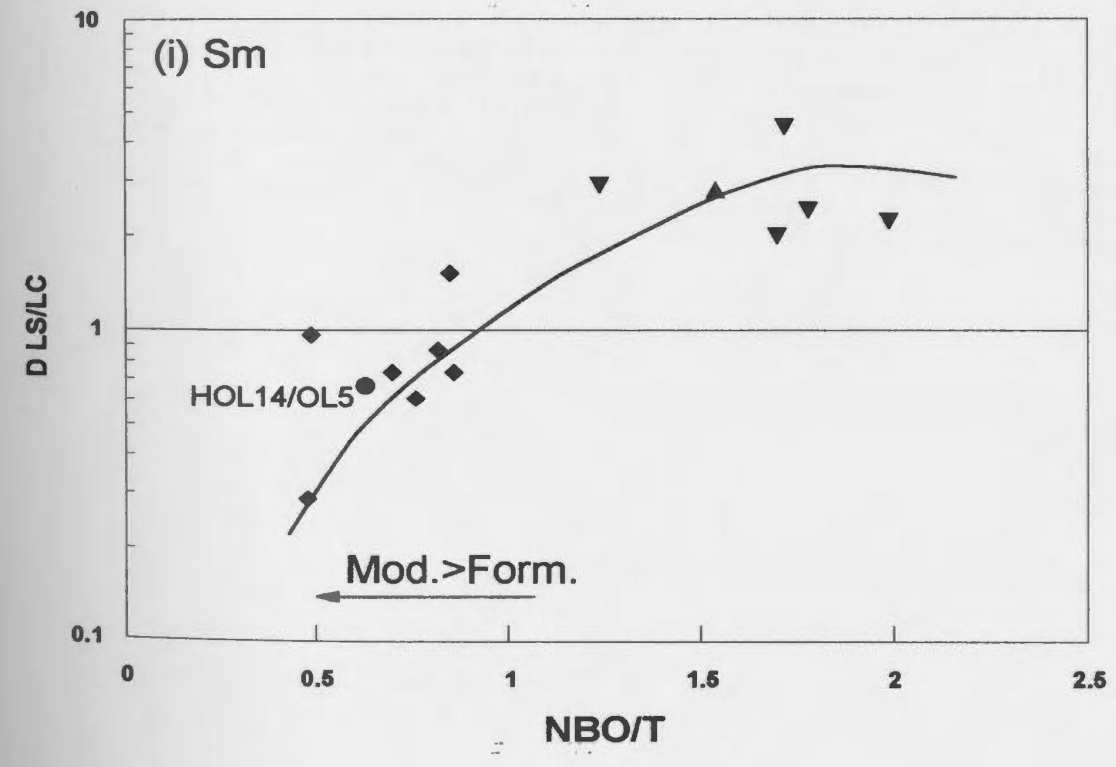
(i) Sm
10
1
0.1
D LS/LC
HOL14/OL5
Mod.>Form.
0
0.5
1
1.5
2
2.5
NBO/T

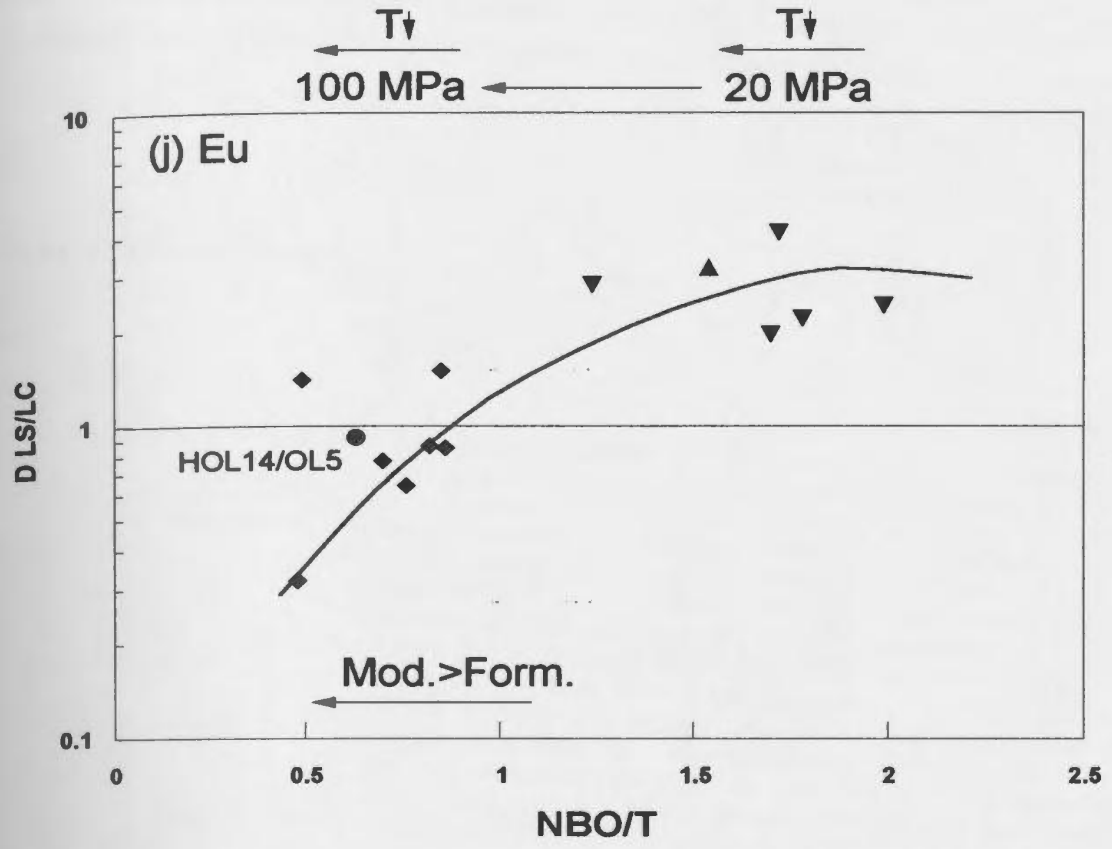
T↓
T↓
100 MPa
20 MPa
(j) Eu
10
1
0.1
D LS/LC
HOL14/OL5
Mod.>Form.
0
0.5
1
1.5
2
2.5
NBO/T

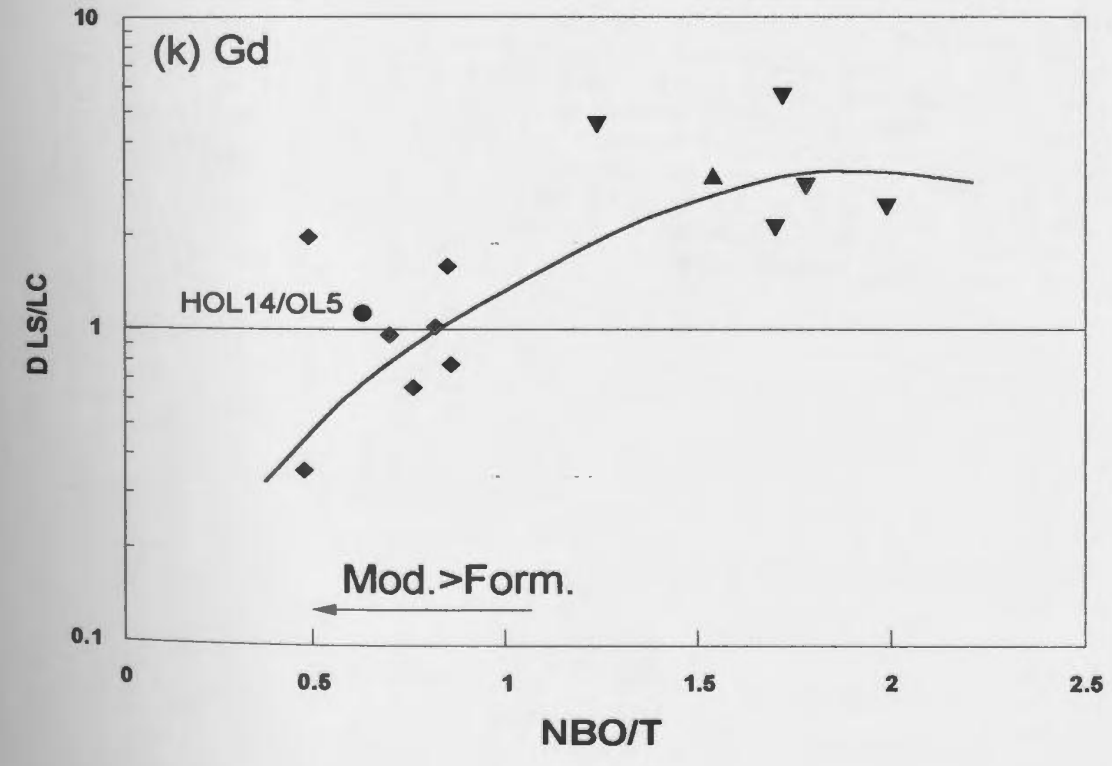
(k) Gd
10
1
0.1
D LS/LC
HOL14/OL5
Mod.>Form.
0
0.5
1
1.5
2
2.5
NBO/T

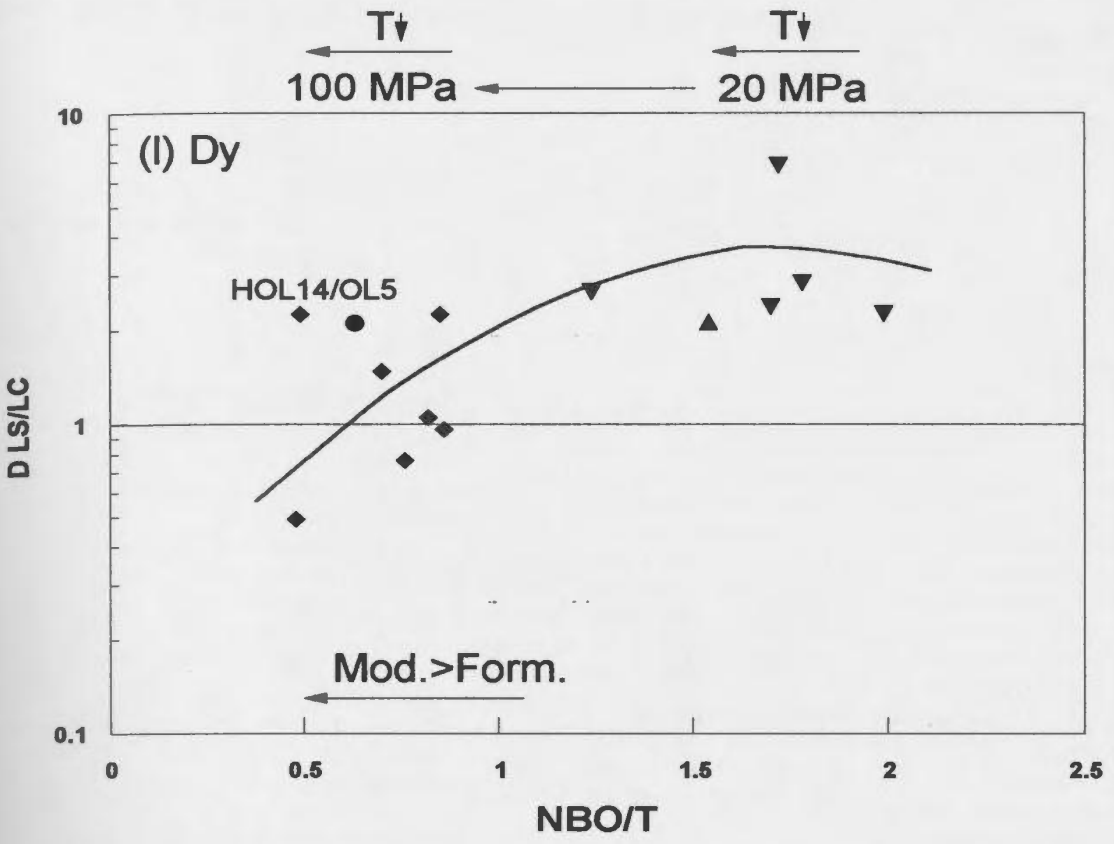
T↓
T↓
100 MPa
20 MPa
(l) Dy
HOL14/OL5
Mod.>Form.
D LS/LC
NBO/T
10
1
0.1
0
0.5
1
1.5
2
2.5

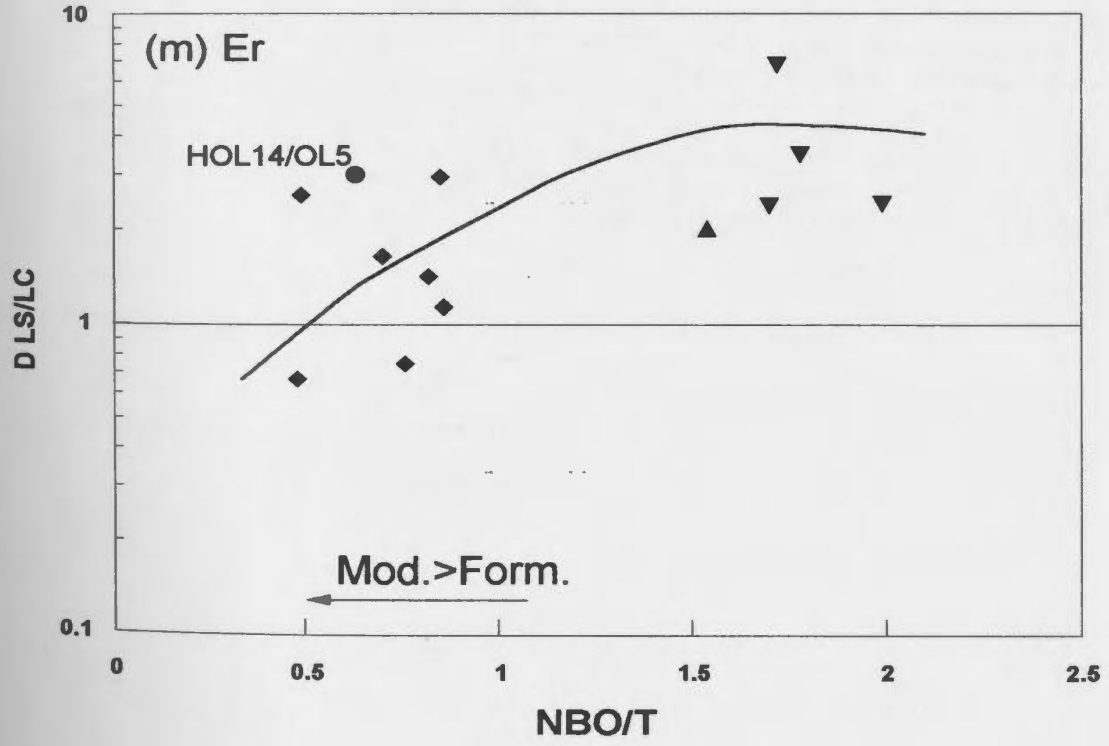
(m) Er
HOL14/OL5
Mod.>Form.
D LS/LC
NBO/T
10
1
0.1
0
0.5
1
1.5
2
2.5

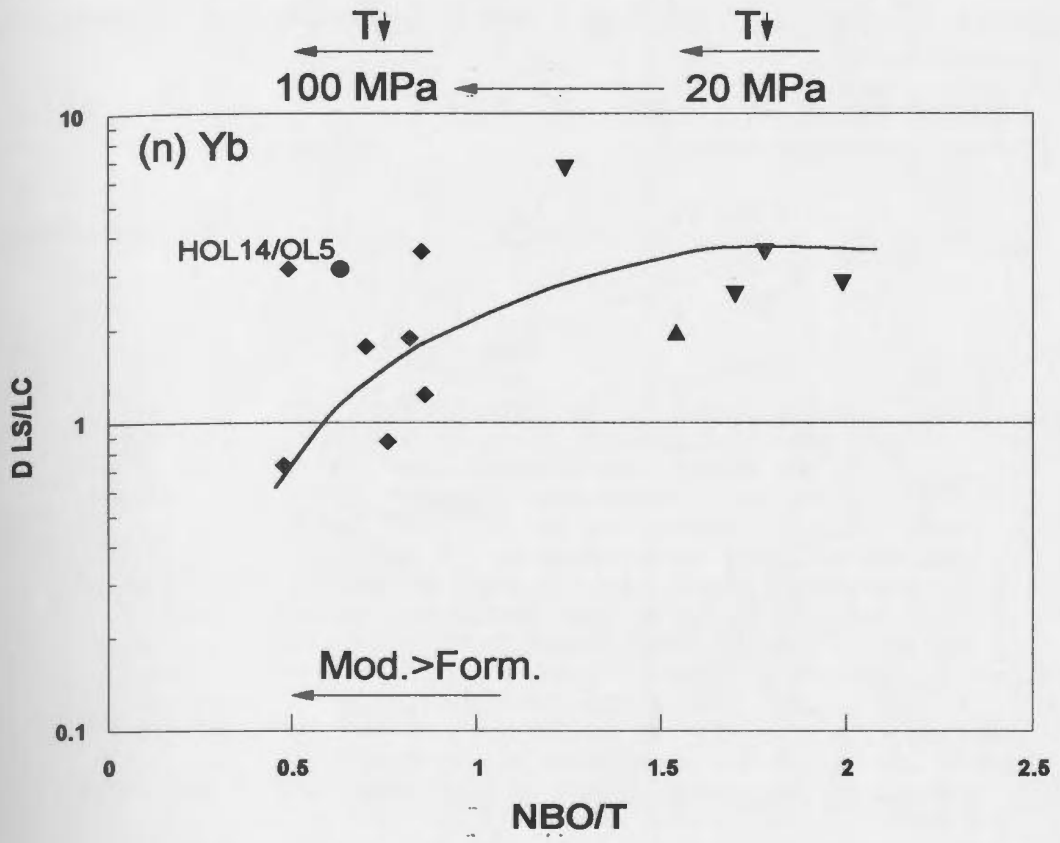
T↓
T↓
100 MPa
20 MPa
(n) Yb
HOL14/OL5
D LS/LC
10
1
0.1
Mod.>Form.
0
0.5
1
1.5
2
2.5
NBO/T

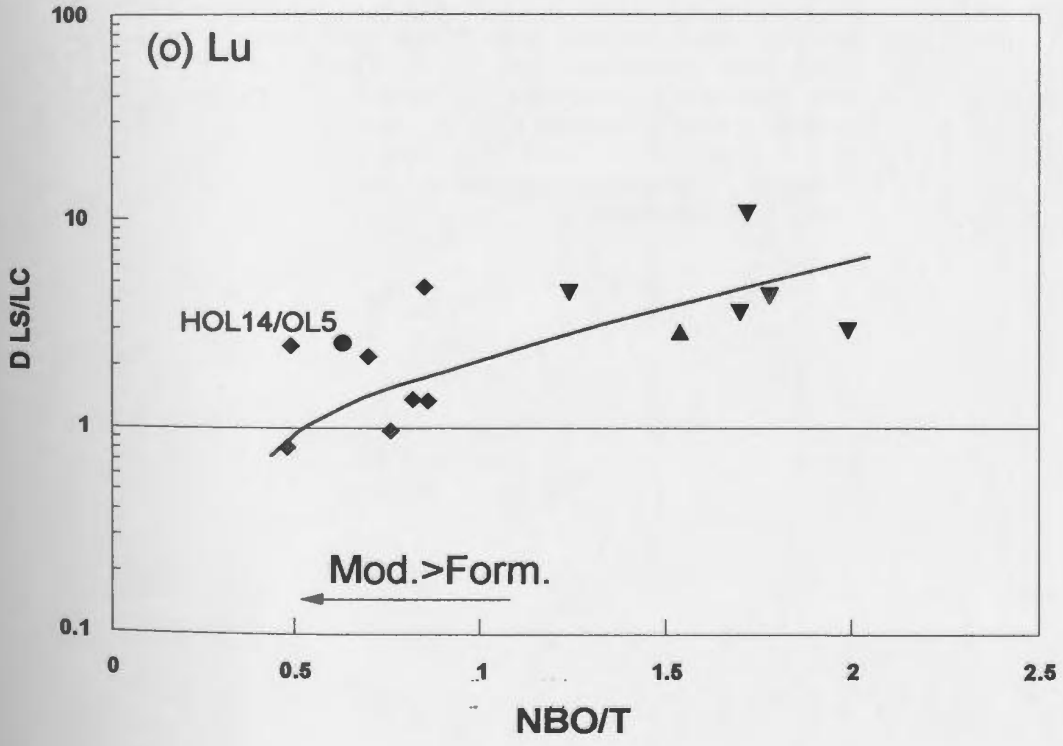
(o) Lu
HOL14/OL5
D LS/LC
100
10
1
0.1
Mod.>Form.
0
0.5
1
1.5
2
2.5
NBO/T

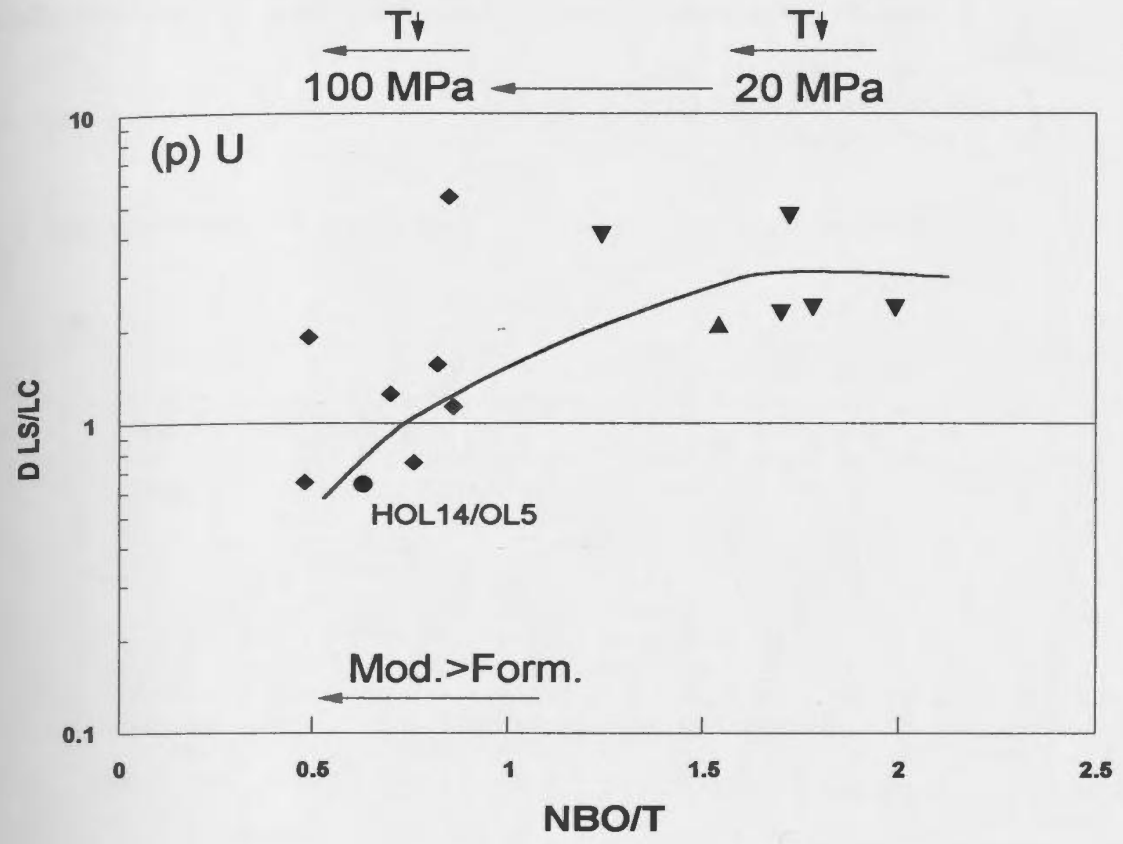
T↓
T↓
100 MPa
20 MPa
(p) U
10
1
0.1
D LS/LC
HOL14/OL5
Mod.>Form.
0
0.5
1
1.5
2
2.5
NBO/T

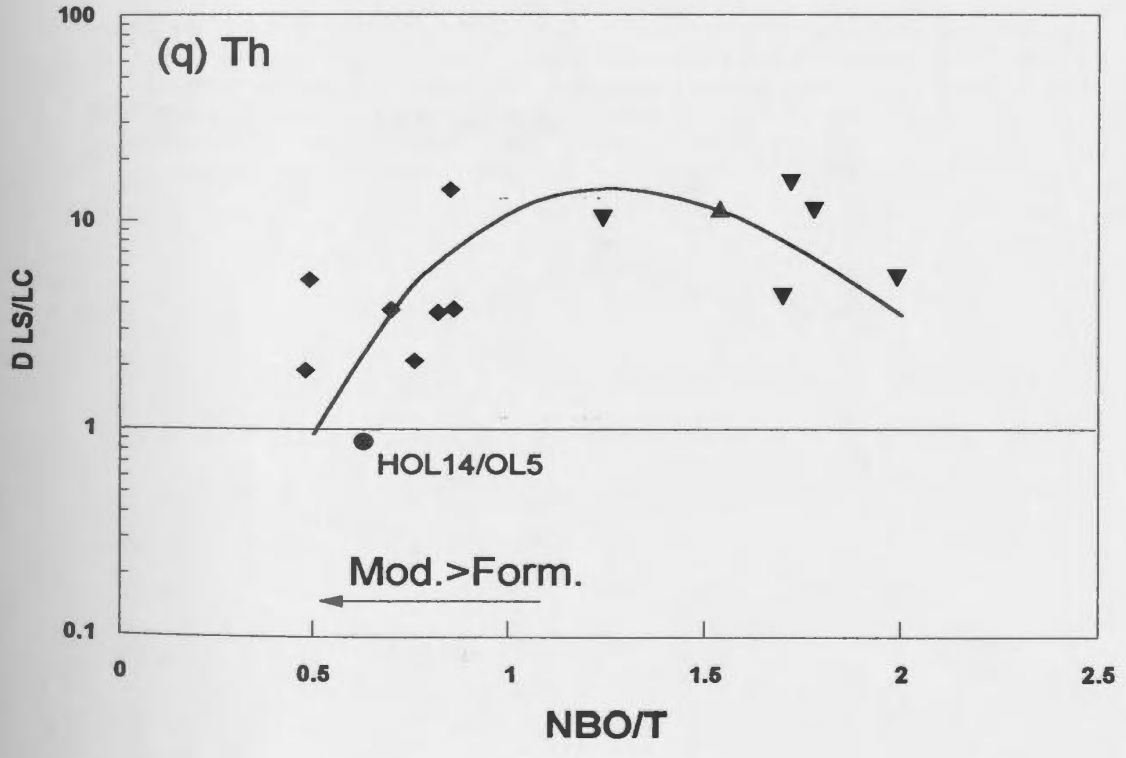
(q) Th
100
10
1
0.1
D LS/LC
HOL14/OL5
Mod.>Form.
0
0.5
1
1.5
2
2.5
NBO/T

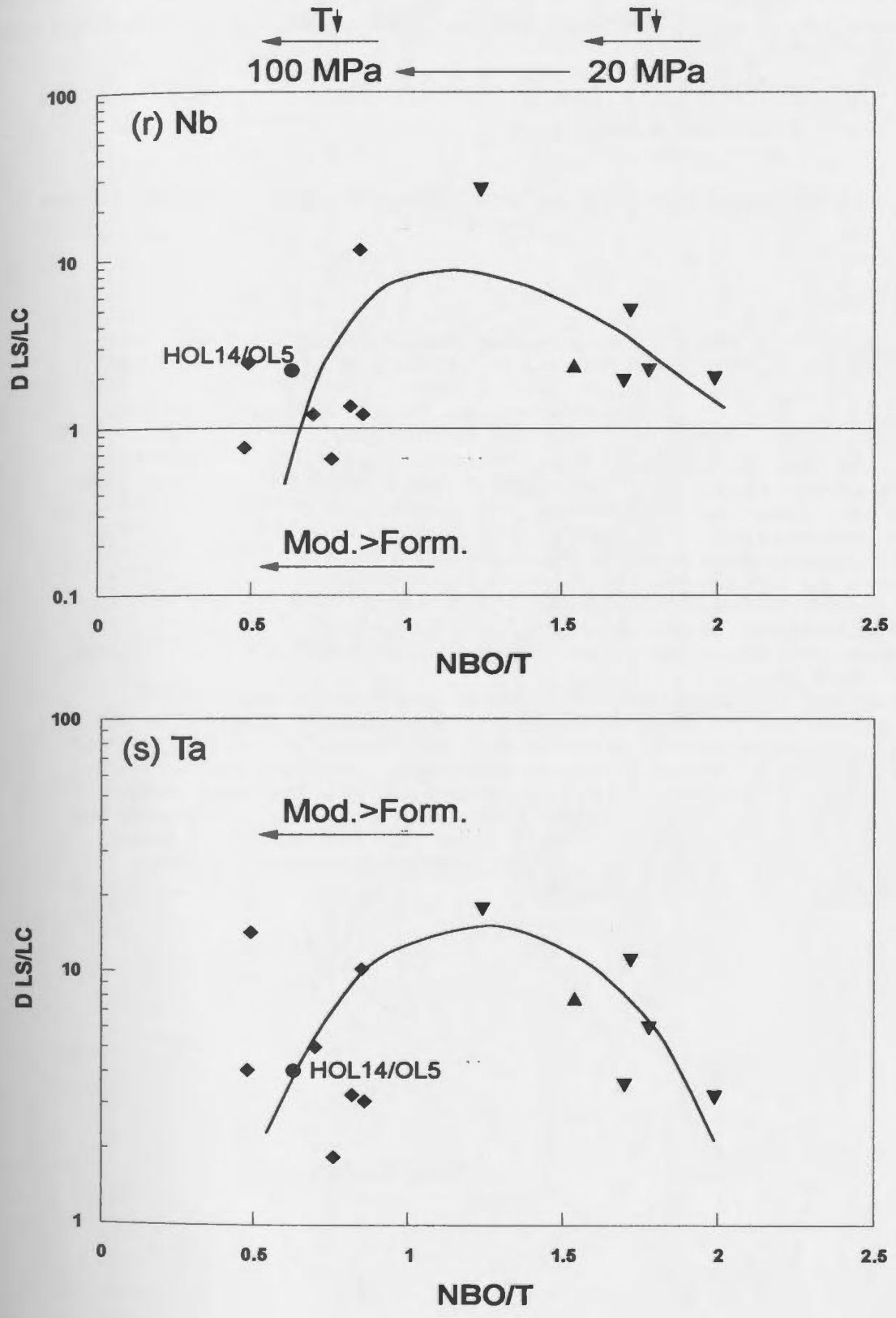
T↓
T↓
100 MPa
20 MPa
(r) Nb
100
10
1
0.1
D LS/LC
HOL14/OL5
Mod.>Form.
0
0.5
1
1.5
2
2.5
NBO/T
(s) Ta
Mod.>Form.
100
10
1
D LS/LC
HOL14/OL5
0
0.5
1
1.5
2
2.5
NBO/T

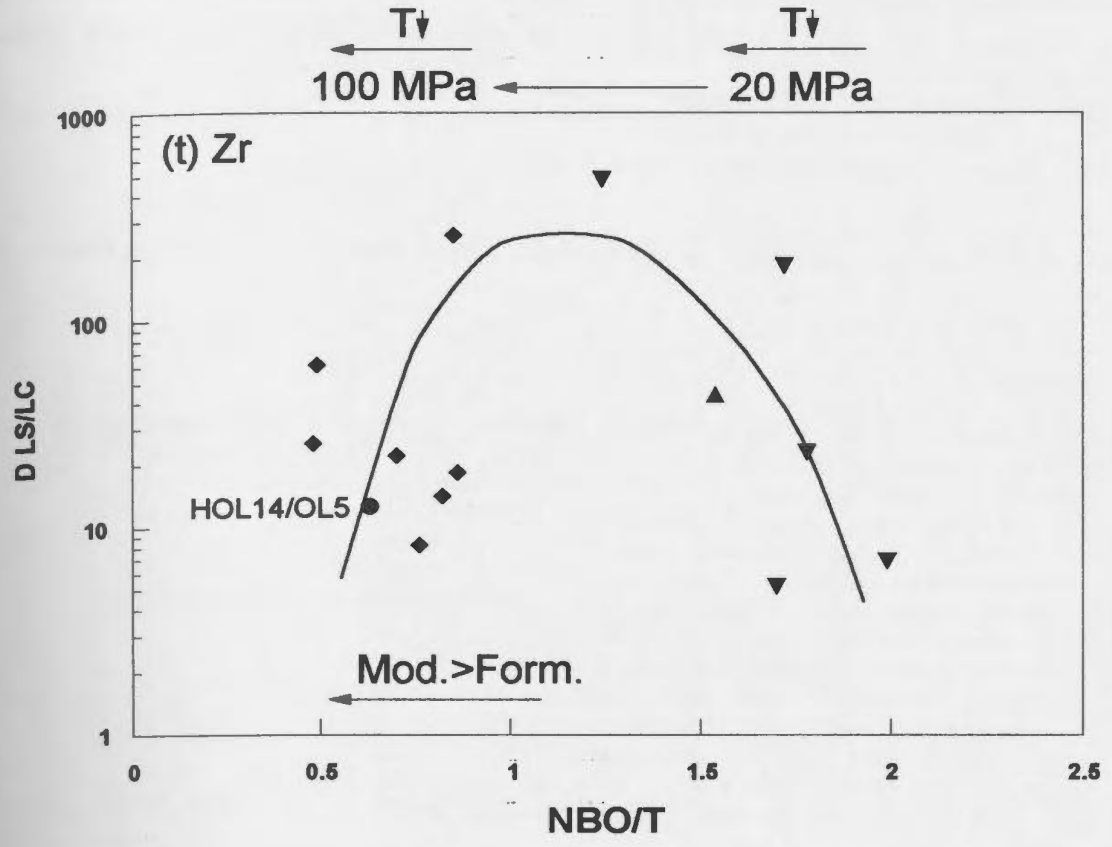
T↓
T↓
100 MPa
20 MPa
(t) Zr
1000
100
10
1
D LS/LC
HOL14/OL5
Mod.>Form.
0
0.5
1
1.5
2
2.5
NBO/T

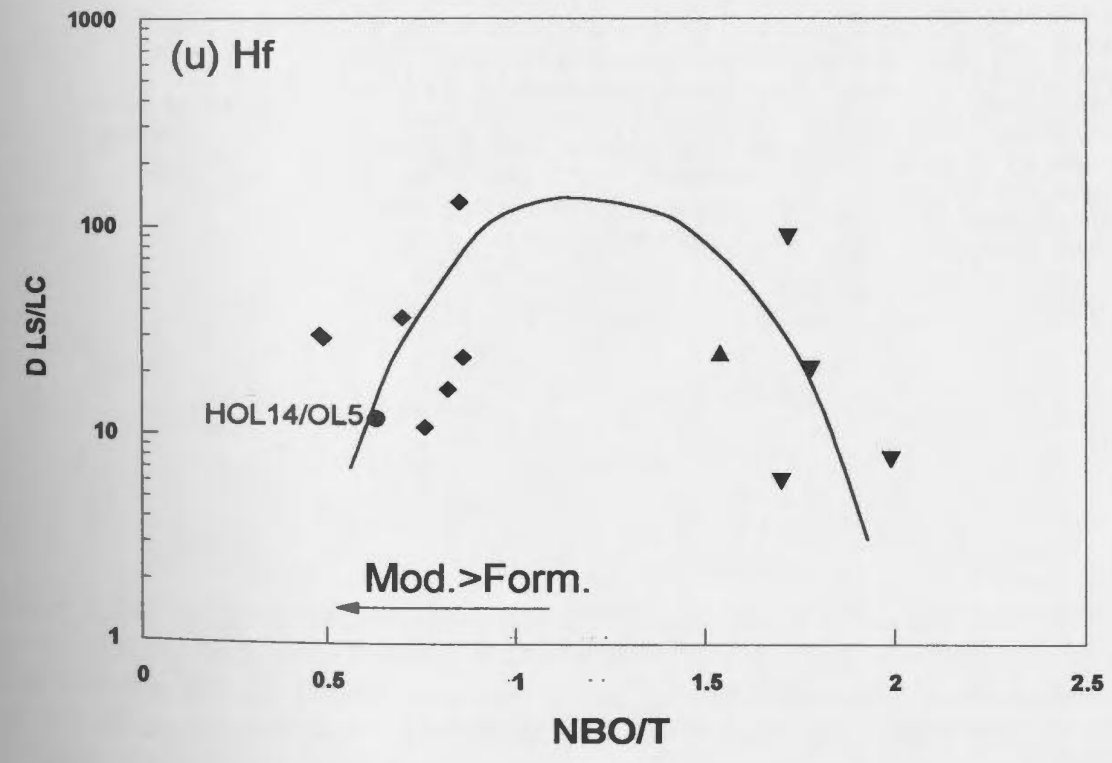
(u) Hf
1000
100
10
1
D LS/LC
HOL14/OL5
Mod.>Form.
0
0.5
1
1.5
2
2.5
NBO/T

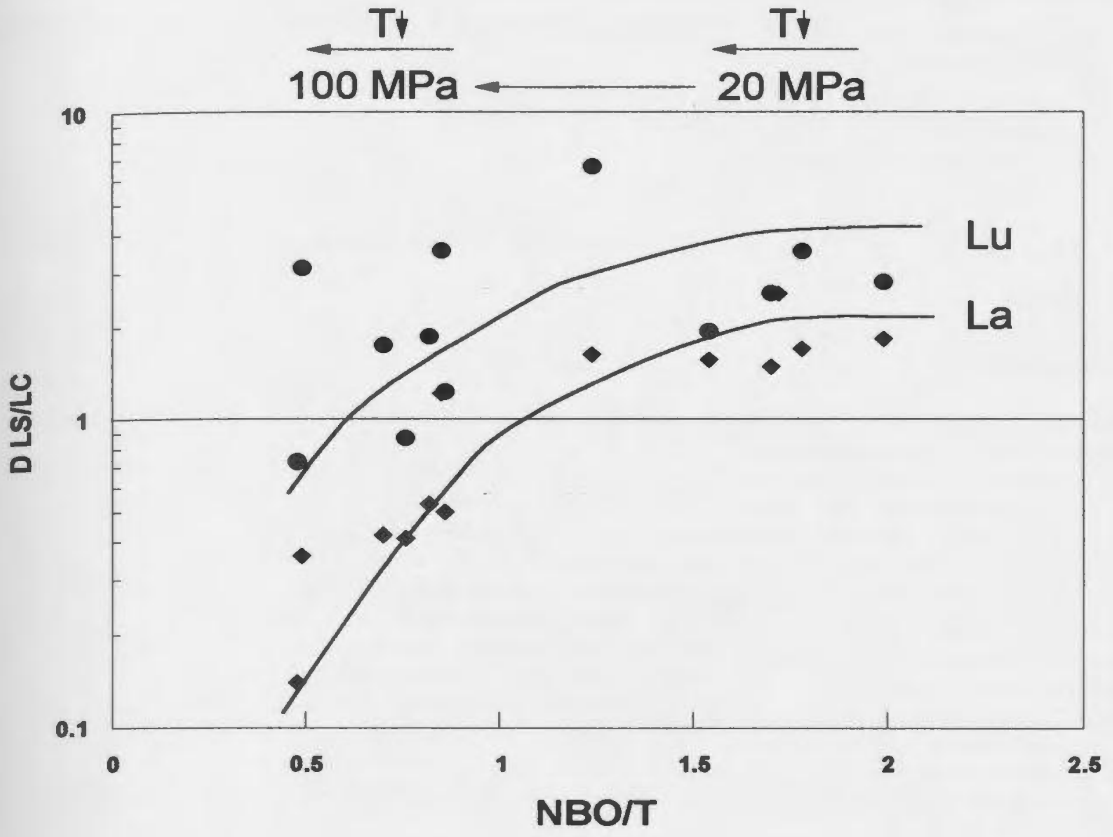

Figure 7.13: Trace element partition coefficients (D) for La and Lu between silicate liquid (LS) and carbonate liquid (LC) from the experiments, as a function of the NBO/T of the silicate liquid. The arrows above the graphs represent the evolution of NBO/T values with increasing pressure from 20 to 100 MPa, and for each pressure, the evolution of NBO/T values with decreasing temperature (T). Data for D values are from Table 7.1 and data for NBO/T values are from Table A6.4 in Appendix A6.

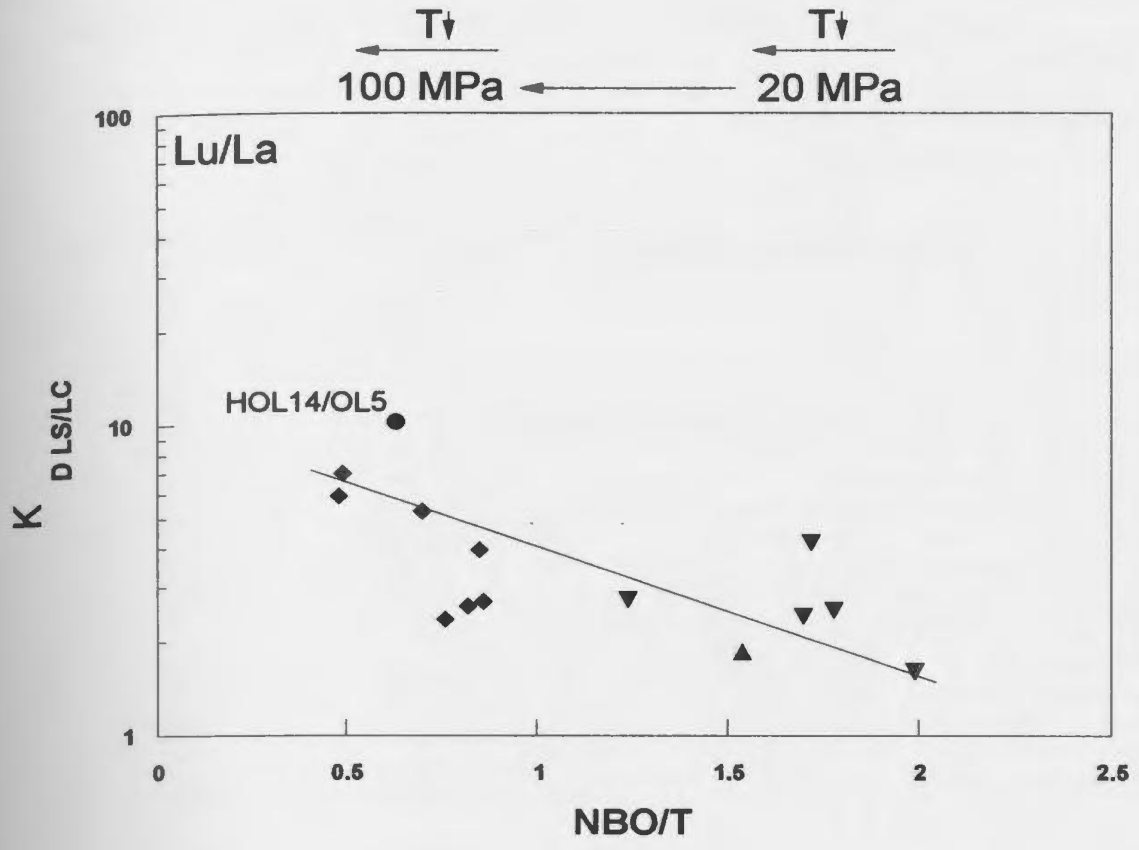

Figure 7.14: Exchange coefficients ($K_{D\ Lu/La}$) between silicate liquid (LS) and carbonate liquid (LC) from the experiments and from the natural pair, as a function of the NBO/T of the silicate liquid. Inverted triangles represent data for 20 MPa experiments, normal triangles for 40 MPa experiments, diamonds for 100 MPa experiments and the dot for the natural pair (groundmass HOL14/whole rock OL5). The arrows above the graphs represent the evolution of NBO/T values with increasing pressure from 20 to 100 MPa, and for each pressure, the evolution of NBO/T values with decreasing temperature (T). Data for K_D values are from Table A7.4 in Appendix A7 and data for NBO/T values are from Table A6.4 in Appendix A6.

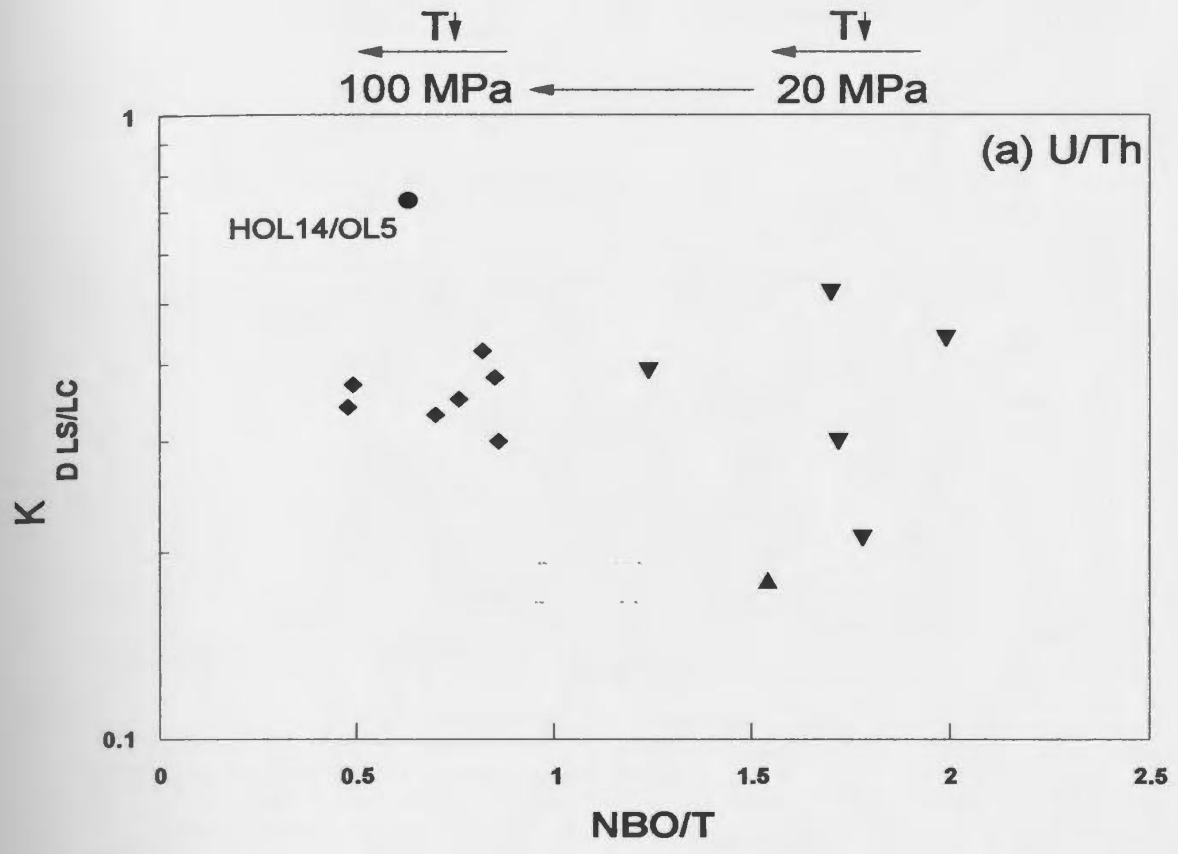

Figure 7.15: Exchange coefficients (K_D) for element pairs between silicate liquid (LS) and carbonate liquid (LC) from the experiments and for the natural pair as a function of NBO/T of the silicate liquid. (a) U/Th, (b) Nb/Ta and (c) Zr/Hf. Inverted triangles represent data for 20 MPa experiments, normal triangles for 40 MPa experiments, diamonds for 100 MPa experiments and the dot for the natural pair (groundmass HOL14/whole rock OL5). The arrows above the graphs represent the evolution of NBO/T values with increasing pressure from 20 to 100 MPa, and for each pressure, the evolution of NBO/T values with decreasing temperature (T). Data for K_D values are from Table A7.4 in Appendix A7 and data for NBO/T values are from Table A6.4 in Appendix A6.

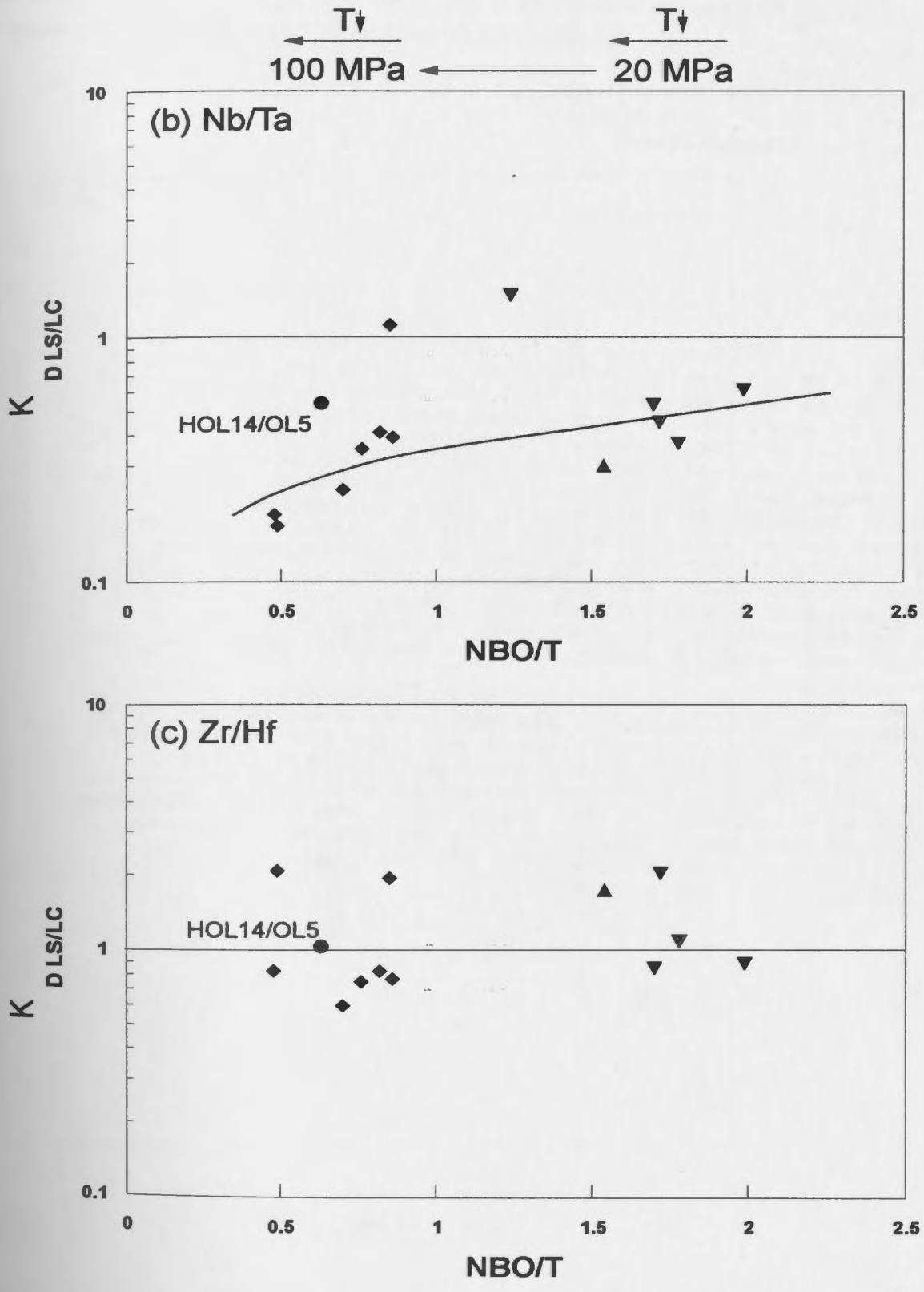
T↓
T↓
100 MPa
20 MPa
(b) Nb/Ta
HOL14/OL5
K D LS/LC
NBO/T
(c) Zr/Hf
HOL14/OL5
K D LS/LC
NBO/T
10
1
0.1
0
0.5
1
1.5
2
2.5

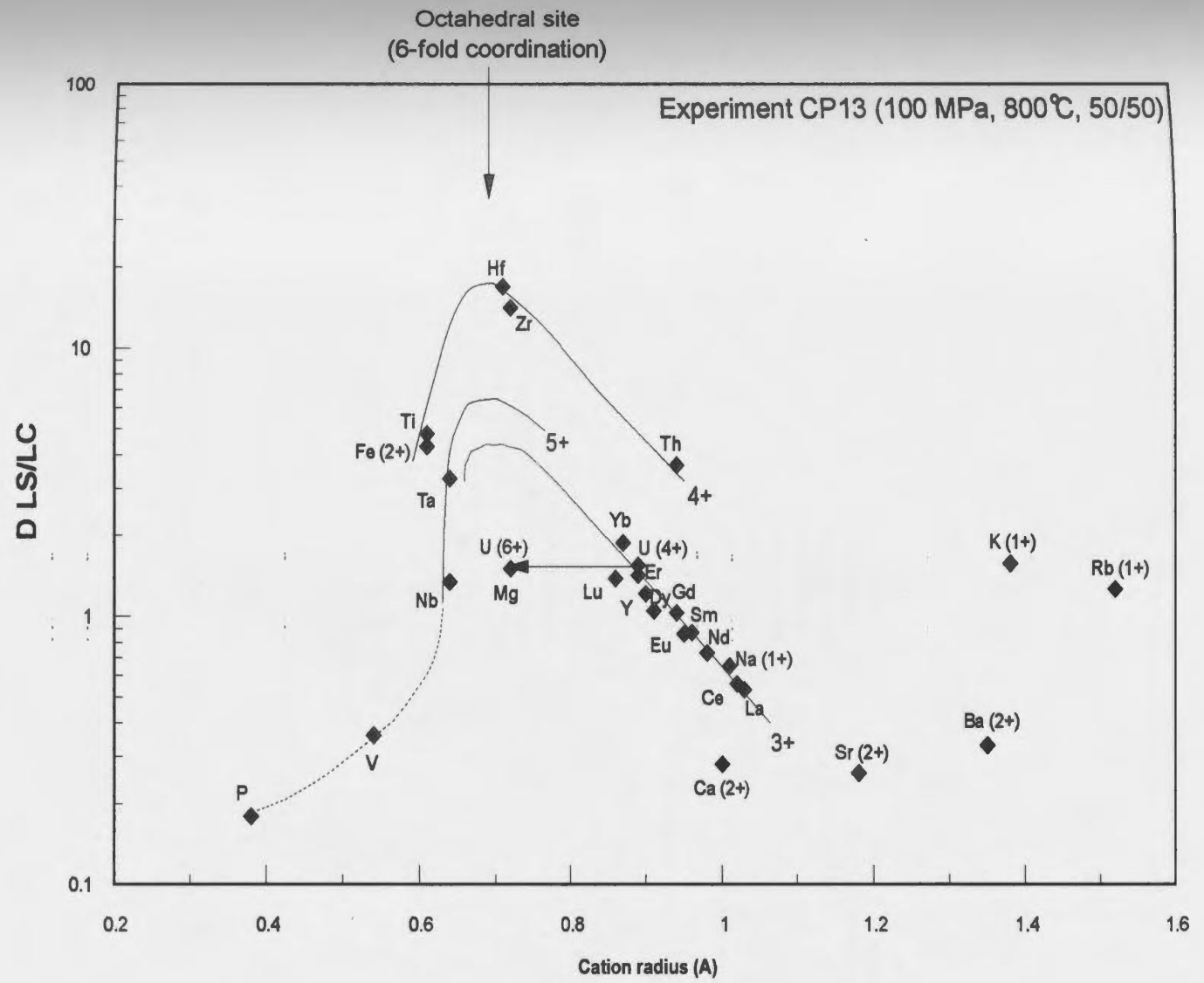

Figure 7.16: Trace element partition coefficients (D) between silicate liquid (LS) and carbonate liquid (LC) as a function of ionic radius (in Å) for the experiment CP13 (100 MPa, 800 °C, 50/50). Curves for 3+, 4+ and 5+ valencies are labelled. Cation radii are from Shannon (1976). Data for D values are from Table 7.1.

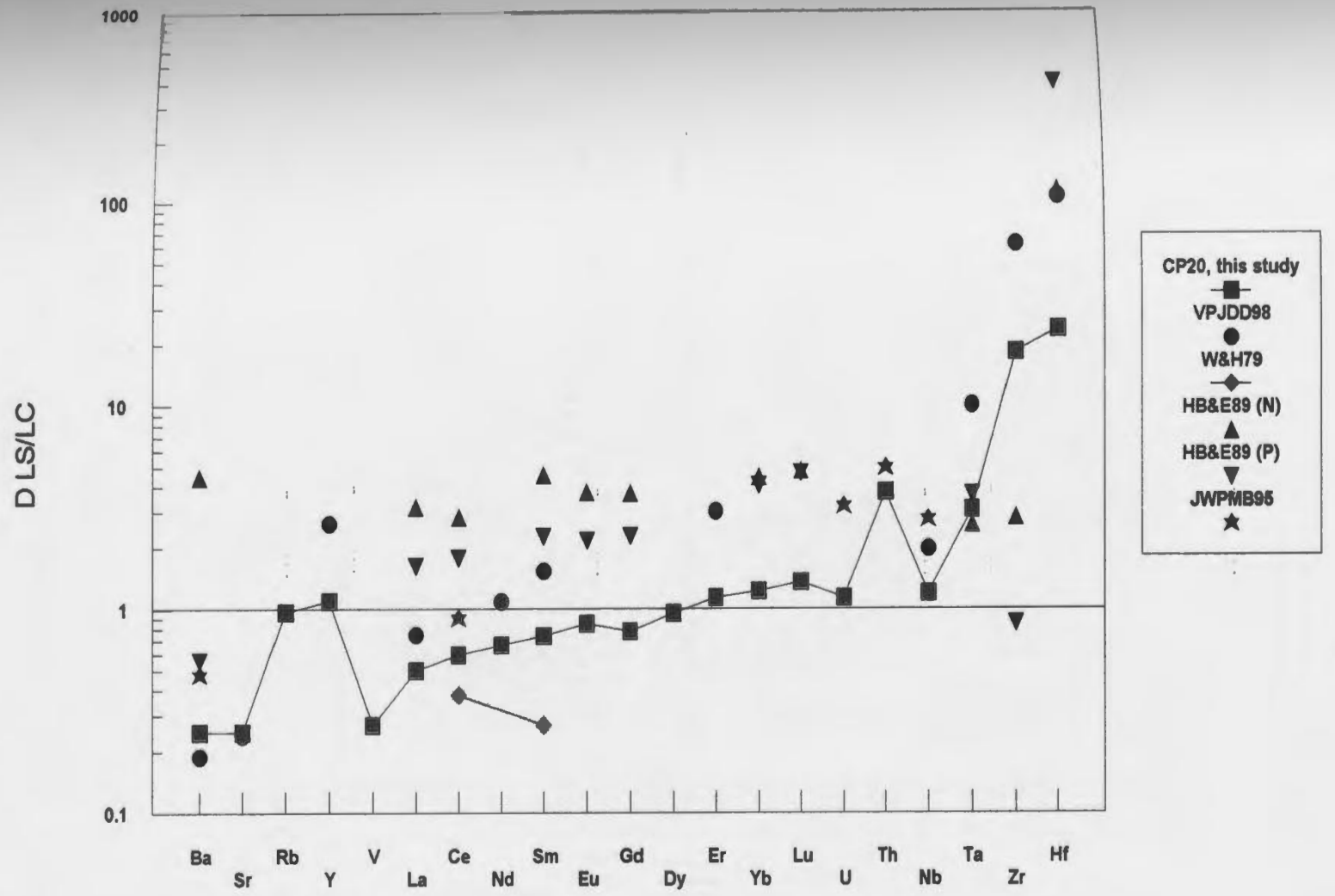

Figure 7.17: Plot of trace element partition coefficients (D) between silicate liquid (LS) and carbonate liquid (LC). Comparison between data for the experiment CP20 (100 MPa, 900 °C, 50/50) and data from other studies. Abbreviations used are: VPJDD98: Veksler et al. (1998b); W&H79: Wendlandt and Harrison (1979); HB&E89: Hamilton et al. (1989); N: nephelinite system; P: phonolite system; and JWPMB95: Jones et al. (1995). See Table 7.8 for the experimental conditions used for the different studies.

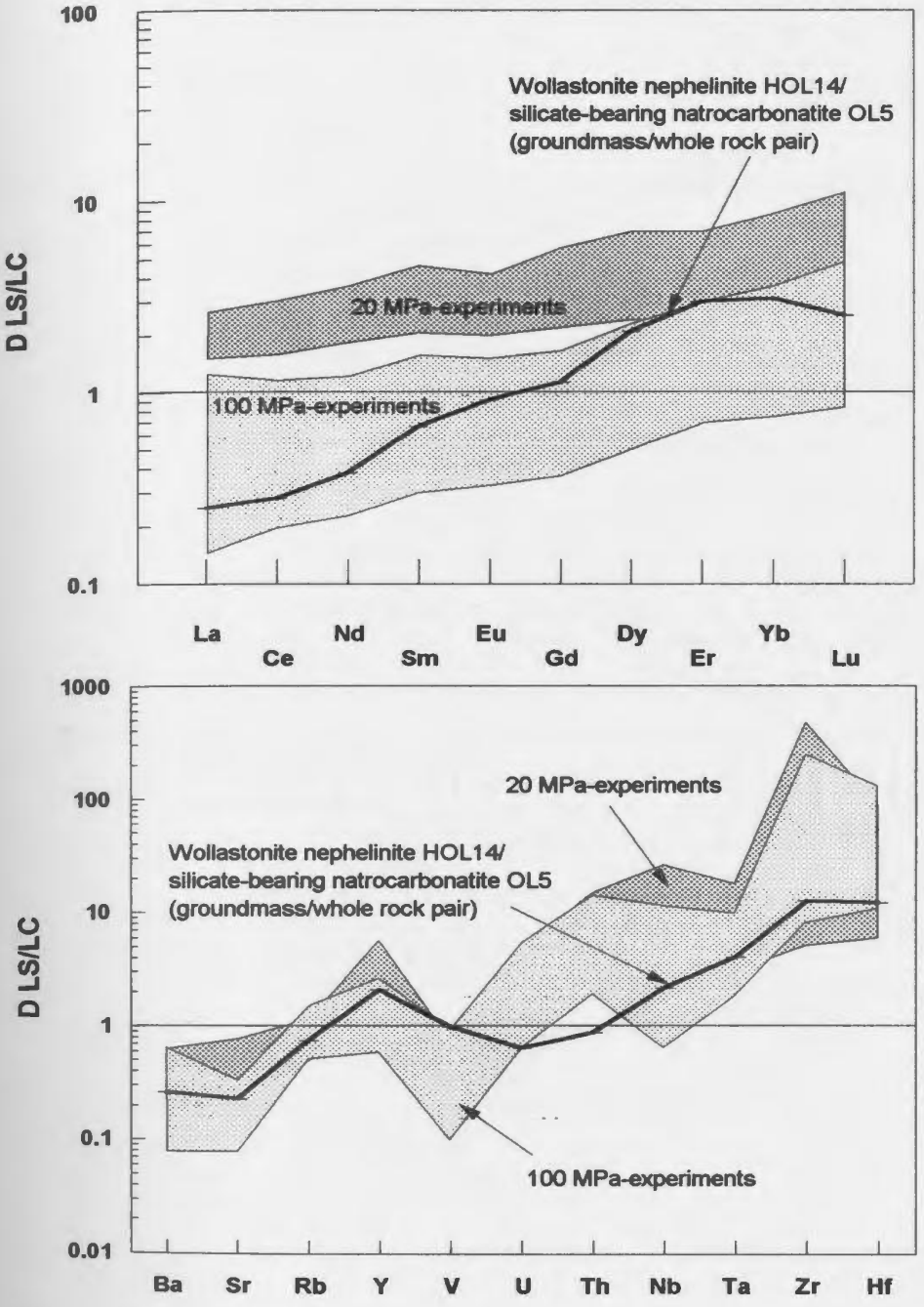

Figure 7.18: Trace element partition coefficients (D) between silicate liquid (LS) and carbonate liquid (LC). Comparison between data for the natural pair wollastonite nephelinite HOL14 (groundmass)/silicate-bearing natrocarbonatite OL5 (whole rock), and experiments at 100 and 20 MPa. For the experiments, the range of D values is shown for each pressure. Data are from Table 7.1.

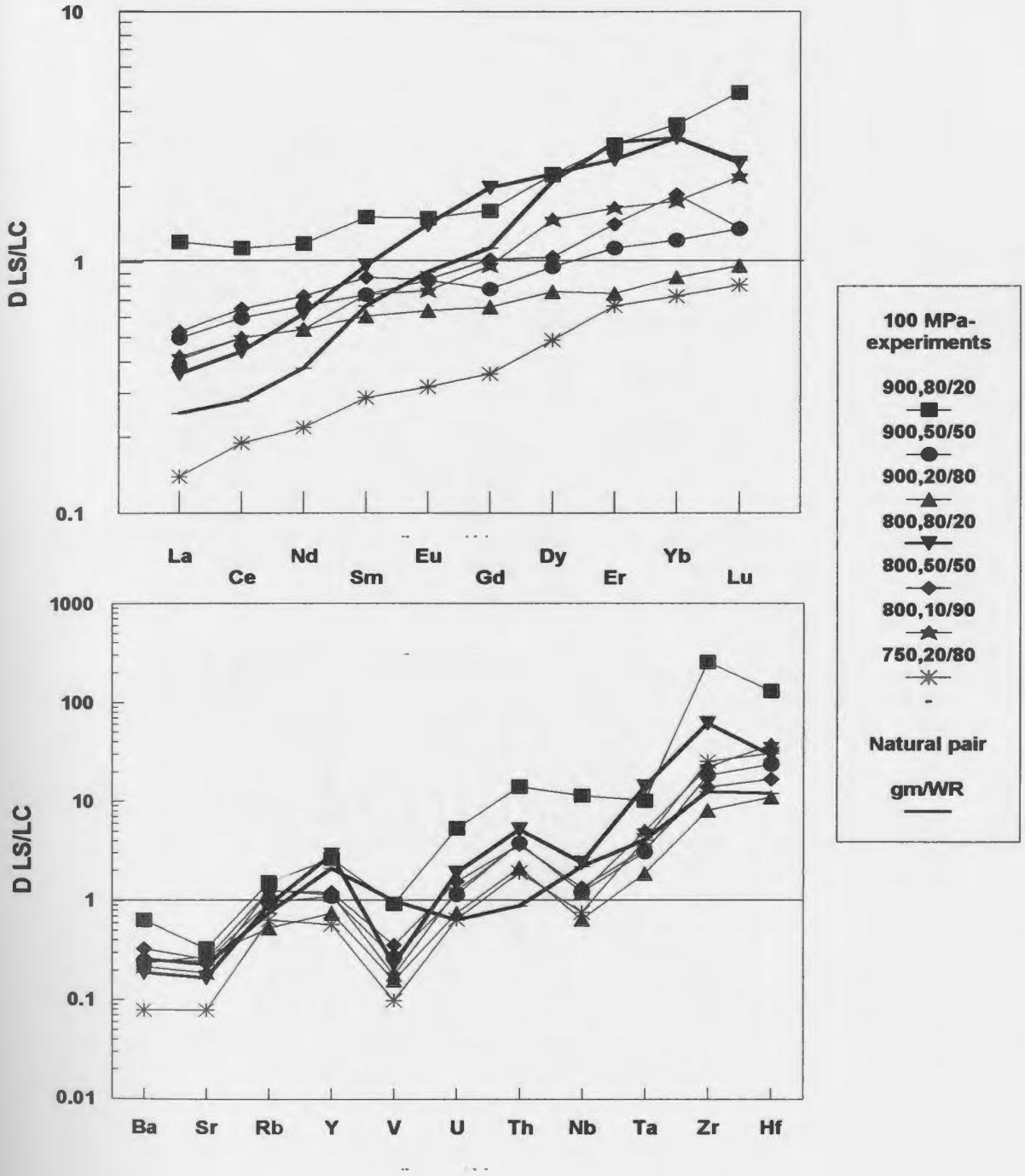

Figure 7.19: Trace element partition coefficients (D) between silicate liquid (LS) and carbonate liquid (LC). Comparison between data for the natural pair wollastonite nephelinite HOL14 (groundmass = gm)/silicate-bearing natrocarbonatite OL5 (whole rock = WR), and from experiments at 100 MPa. For the experiments, temperature (in °C) and bulk composition (shown as weight fraction of wollastonite nephelinite HOL14/silicate-bearing natrocarbonatite OL5) are shown in the legend. Data are from Table 7.1.

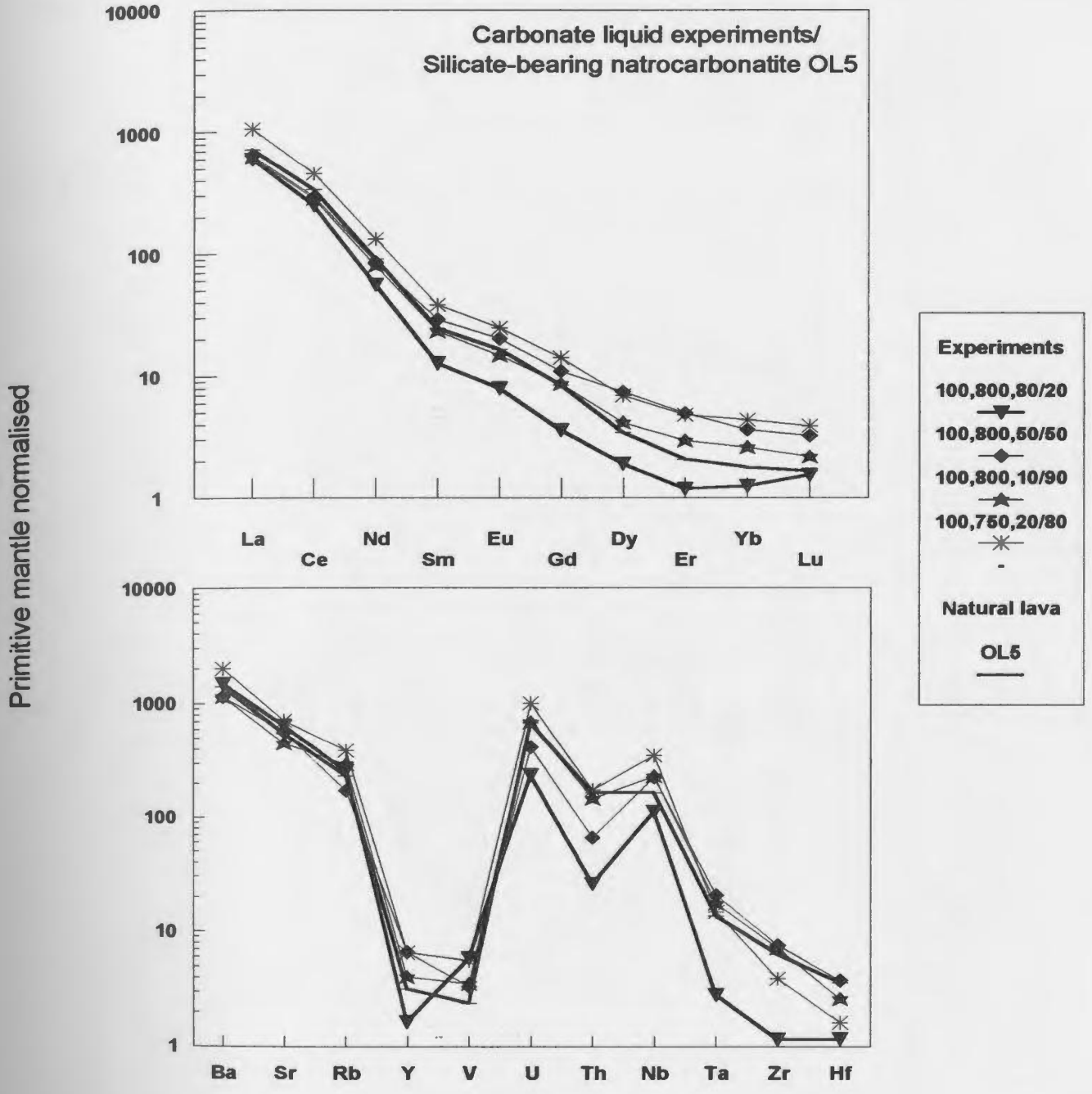

Figure 7.20: Trace element concentrations normalised to primitive mantle of carbonate liquid from selected experiments at 100 MPa and 800 °C, for various bulk compositions shown as weight fraction of wollastonite nephelinite HOL14/weight fraction of silicate-bearing natrocarbonatite OL5, and for whole rock of erupted silicate-bearing natrocarbonatite OL5. For the experiments, P-T-X conditions are indicated in the legend. Data are from Table 7.1; primitive mantle normalising values are from McDonough and Sun (1995).

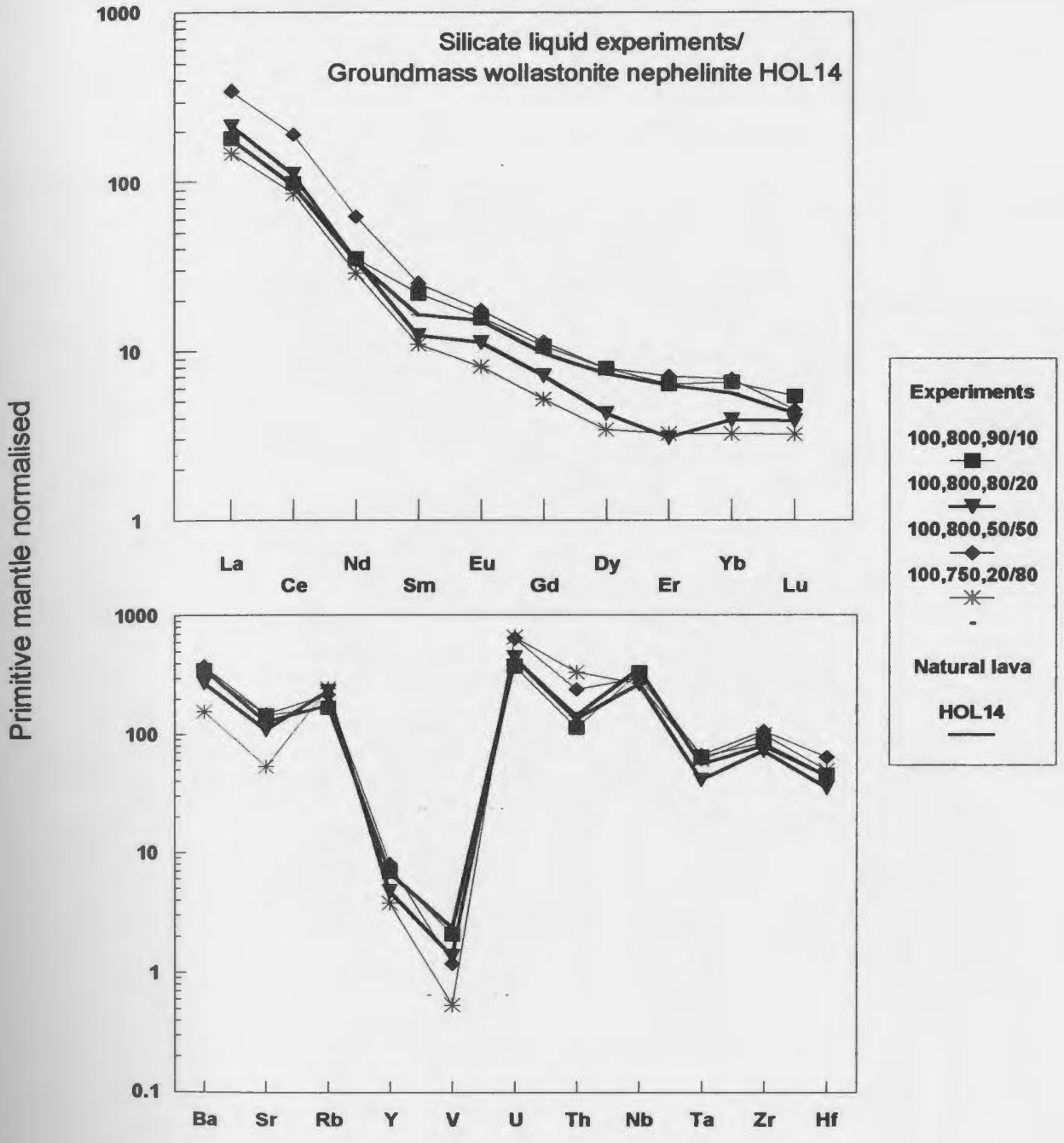

Figure 7.21: Trace element concentrations normalised to primitive mantle of silicate liquid from selected experiments at 100 MPa and 800 °C, for various bulk compositions shown as weight fraction of wollastonite nephelinite HOL14/weight fraction of silicate-bearing natrocarbonatite OL5, and for groundmass of erupted wollastonite nephelinite HOL14. For the experiments, P-T-X conditions are indicated in the legend. Data are from Table 7.1; primitive mantle normalising values are from McDonough and Sun (1995).

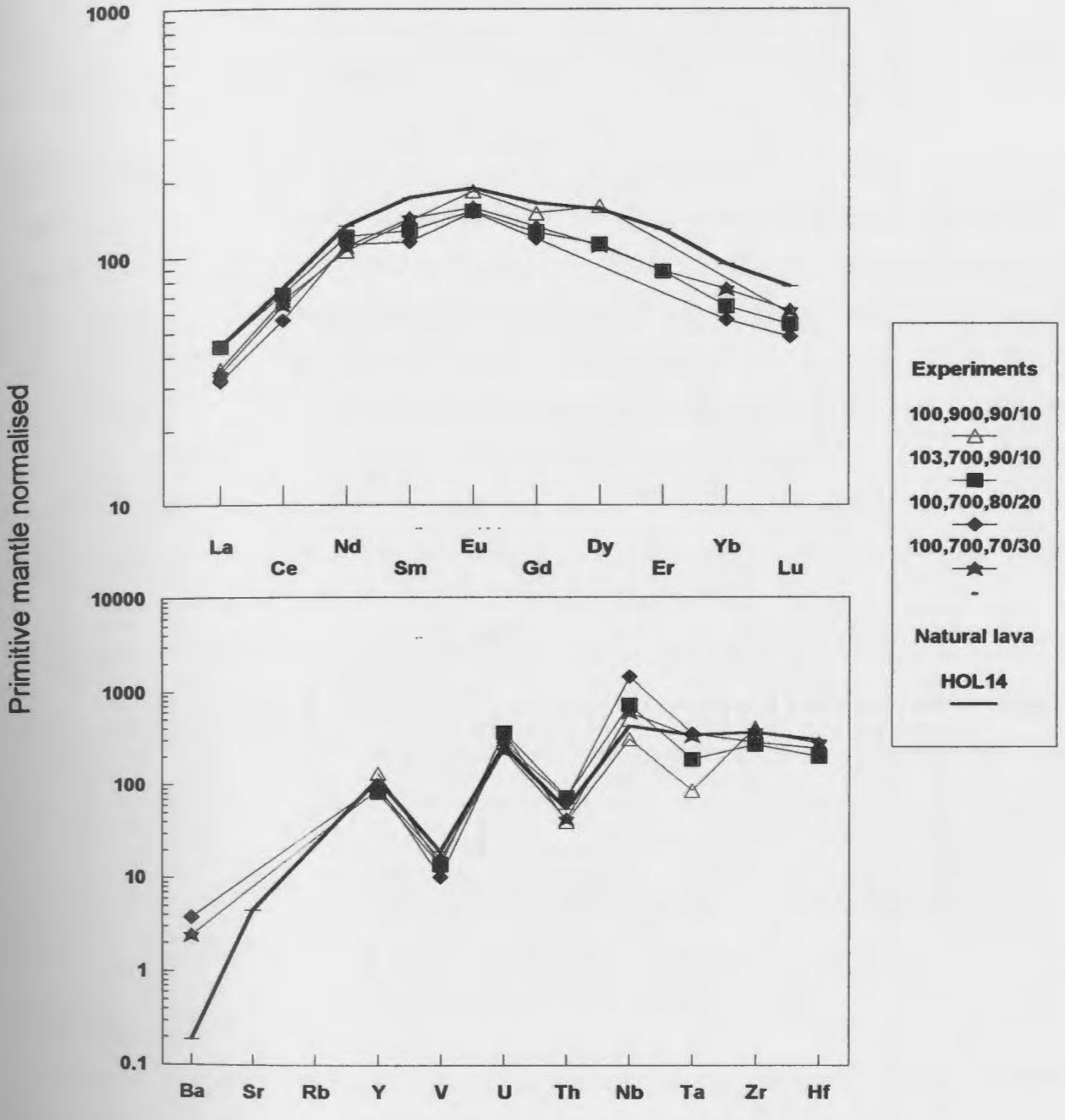

Figure 7.22: Trace element concentrations normalised to primitive mantle of melanite garnet from selected experiments at ~ 100 MPa, 700 °C, for various bulk compositions shown as weight fraction of wollastonite nephelinite HOL14/weight fraction of silicate-bearing natrocarbonatite OL5, and from erupted wollastonite nephelinite HOL14. For the experiments, P-T-X conditions are indicated in the legend. Data are from Table 7.4; primitive mantle normalising values are from McDonough and Sun (1995).

CHAPTER 8: ROLE OF VOLATILES - COMPARISON BETWEEN NATRO- AND CALCIO-CARBONATITES

8.1 – Introduction

Carbonatites contain large amounts of volatiles and incompatible elements and are an integral part of understanding the geochemical evolution of the mantle. They serve as a guide to studying the heterogeneity of the metasomatised lithosphere since that is their ultimate source, and also because carbonatite magmas are efficient metasomatic agents that can add further heterogeneities during their ascent. The importance of volatiles at different steps of the formation of natrocarbonatites from Oldoinyo Lengai (at crustal conditions) has been highlighted in this thesis. In this Chapter, the effect of volatiles is examined, in detail, throughout the whole history of carbonatites, including at mantle conditions.

Although natrocarbonatites from Oldoinyo Lengai have unique compositions amongst carbonatites, which are mainly represented by calciocarbonatites, many authors have attempted to see if there is a genetic link between these two types of rocks. The findings of previous studies and of this study concerning the possibility of a genetic link between natro- and calcio-carbonatites are also reviewed in this Chapter, in order to examine the relevance of natrocarbonatites to the study of carbonatites in general. Suggestions for further work are also given.

8.2 – Role of volatiles

"One curious feature in their [halogens] distribution is the strong correlation with elements that are generally considered "immobile" under crustal conditions (but incompatible under mantle conditions!) such as Zr (Bailey and Macdonald, 1975). These are volatile elements that may have a key function in alkaline magmatism."
Bailey and Hampton (1990)

Alkaline magmatism is distinguished from calc-alkaline by higher CO_2+SO_2 contents, with relatively smaller proportions of H_2O, and by high Cl and F (Bailey and

Hampton, 1990). The less soluble species, such as CO_2, (and S?) are normally lost in a fugitive fluid phase (Bailey and Macdonald, 1987), whereas halogens can have different volatility at different conditions (Bailey and Hampton, 1990). The present section examines the role of volatile elements in the genesis and evolution of carbonatites, especially natrocarbonatites from Oldoinyo Lengai. Summarised here is the role of volatiles during the different steps of evolution of carbonated (silicate or carbonate) magma:

1) The formation of carbonated, silicate or carbonatitic magma in the mantle is triggered by a plume that carries heat and volatiles. The role of the volatiles is to lower the solidus of the peridotite and to provide some of the main constituents (*e.g.*, carbon) of the alkaline magmas. The ultimate source of the magma is the lithosphere, which is most likely metasomatised, with Nb, REE, Ti, U and Zr embodied in titanates (Jones, 1989). Note that carbonatite metasomatism has been demonstrated in the northern Tanzanian mantle by Rudnick et al. (1993), suggesting that the mantle below Oldoinyo Lengai is metasomatised.

One characteristic of carbonatites and associated silicate rocks, beside their enrichment in alkalis and volatile components, is their enrichment in many trace elements. CO_2 is not a likely agent for transporting minor-element suite to the melting site, but F and Cl are (Gittins, 1989). Carbon, however, can form complexes with trace elements once it is in silicate or carbonatitic magma, as CO_3^{2-}. Therefore, complexing of trace elements with halogens and CO_3^{2-} can explain their high concentrations in both carbonate and silicate melts.

2) Volumes of rising magma are usually small because they are the products of a small degree of partial melting of the mantle. The magma is very reactive with the surrounding mantle and must ascent very fast in order not to undergo thermal and/or chemical death. The presence of volatiles lowers the density and viscosity of the magma, and facilitates its ascent (Lange, 1994). Volatiles also partition into the fluid phase that may be associated with the magma (see Cooper et al., 1998). The presence of an immiscible fluid phase together with the magma can facilitate its ascent. This occurs because the presence of a low-viscosity fluid phase at a total pressure roughly equal to $P_{lithosphere}$ ahead of the magma greatly reduces the overall strength of the surroundings, and also because migrating melts may be thermally and chemically active (Spera, 1980).

3) In the case of a carbonated-nephelinite or -melilitite magma exsolving carbonatite magmas, volatiles are important in controlling when liquid immiscibility occurs, and how major and trace elements are distributed between conjugate silicate and carbonate melts because of the formation of carbonato- and halogen-complexes (see Chapters 6 and 7).

4) In the case of natrocarbonatites from Oldoinyo Lengai, volatiles may play an important role during *in situ* crystallisation, by complexing with some trace elements and depleting the residual magma in these elements (see Chapter 7);

5) Finally, volatiles may also play an important role during and after eruption. Natrocarbonatite lavas from Oldoinyo Lengai have the lowest eruption temperatures recorded for any lava, and the presence of F and Cl (which lowers the liquidus of the magma) is mainly responsible for allowing the magmas to be maintained in the liquid state at these low temperatures.

Volatiles also play an important role in determining if the eruption is explosive or not. At Oldoinyo Lengai, CO_2 in lavas might be released in more or less large volumes during eruption. Release of important volumes of CO_2 leads to explosive eruption (*e.g.*, June 1966). However, degassing of CO_2 from Oldoinyo Lengai volcano is usually quiescent (Koepenick et al., 1996), but can nevertheless have significant consequences. Indeed, degassing during the ascent of silicate-bearing natrocarbonatite OL5 was suggested to be responsible for the extensive crystallisation of nyerereite and gregoryite as a result of undercooling (Chapter 3).

Finally, volatiles play an important role during fenitisation (see details in next section). Fenitisation is usually described as loss of alkalis and volatiles with water, before, during or after emplacement. Aureoles of fenites are found in numerous carbonatite complexes. At Oldoinyo Lengai, however, fenites are found as xenoliths in erupted lavas (Kramm and Sindern, 1998), and fenitisation is not sufficient to produce residual alkali-poor carbonatites. This may be due to gases at Oldoinyo Lengai being the most H_2O-poor (and CO_2-rich) reported for any volcano (Koepenick et al., 1996).

8.3 – Link between calcio- and natro-carbonatites

The majority of carbonatites are CaO-rich and contain less than 2 wt. % Na_2O, and thus, natrocarbonatites from Oldoinyo Lengai (~ 30 wt. % Na_2O) are unique. However, many workers (*e.g.* LeBas, 1981; Dawson et al., 1987) consider the alkali-poor composition of carbonatite rocks found in the field as unrepresentative of the magma

from which these rocks originate. They focus on incorporating alkali-rich compositions into genetic models to cover the vast majority of (calcio)carbonatites.

One of the reasons for wanting to integrate atypical natrocarbonatites from Oldoinyo Lengai into a larger frame, is that Oldoinyo Lengai is the only active, and therefore the most studied, carbonatite volcano. Oldoinyo Lengai exemplifies that Na_2CO_3 is highly soluble in meteoric water or other solvents. The alkali-rich carbonatite at Oldoinyo Lengai is erupted as a black lava which turns white in eight days, and in some instances is dissolved away in a matter of weeks by meteoric water. High solubility of Na_2CO_3 has two consequences: 1) it shows that lava must be collected fresh (preferentially still hot, see Church and Jones, 1995), and this is only possible at Oldoinyo Lengai; and 2) it indicates that natrocarbonatites are prone to losing alkalis during and shortly after emplacement. Because many calciocarbonatite complexes are surrounded by an aureole of fenitisation, many authors argued that they were previously natrocarbonatites from which alkali fluids escaped (*e.g.*, von Eckermann, 1948; von Knorring, 1962; Dawson, 1964; Cooper et al., 1975; Gittins et al., 1975; LeBas, 1977). Arguments for or against this hypothesis are presented below, along with other hypotheses linking natrocarbonatites and calciocarbonatites.

8.3.1: Are natrocarbonatites parental to calciocarbonatites?

There are different ways that have been proposed to explain how natrocarbonatites could be the parent of calciocarbonatites: 1) alkalis could be lost by fenitisation during or shortly after the emplacement of the natrocarbonatite (*i.e.*, loss of fluids by fenitisation could produce "solid calciocarbonatites"); 2) alkalis could be lost by fenitisation during cooling of the superheated natrocarbonatite magma; and 3) with crystallisation of Na- and K-rich carbonate crystals, natrocarbonatite magma could fractionate into a calcio-carbonatite. These three hypotheses are reviewed below, and it is shown that none of them is acceptable.

8.3.1.1: Formation of "solid calciocarbonatites"

Some authors have identified former nyerereite phenocrysts, pseudomorphed by calcite, in the tuffaceous deposits of extinct carbonatite volcanoes (Turner, 1988;

Deans and Roberts, 1984; Hay, 1983), and interpreted this to indicate the original magma was a natrocarbonatite. This hypothesis has been criticised, mainly because primary phenocrysts of calcite are also recognised in all of these deposits, whereas, pseudomorphs of gregoryite have never been found in calciocarbonatites. According to Cooper et al. (1975), natrocarbonatites *sensus stricto* contain nyerereite and gregoryite, but no calcite (see Fig. 8.1; from Cooper et al., 1975). Additional evidence against an origin of "solid calciocarbonatites" from natrocarbonatite is the fact that the replacement of nyerereite by calcite would represent an unrealistically large volume reduction (Deans and Roberts, 1984; Twyman and Gittins, 1987), and that some carbonatites lack a fenite aureole (*e.g.* Guli; see Kogarko et al., 1991) and must have been poor in alkalis.

Evidence against the formation of calciocarbonatites from natrocarbonatites are found at Oldoinyo Lengai. The products of alteration of natrocarbonatites are nahcolite ($NaHCO_3$), sylvite (KCl) and trona [$Na_3H(CO_3)_3.2H_2O$] (Keller and Krafft, 1990), not calcite, therefore the alteration of natrocarbonatites does not produce calcitic carbonatites. Moreover, one xenolith of calciocarbonatite (BD83) found at Oldoinyo Lengai has been interpreted as being of magmatic origin (Gittins and Harmer, 1997), not of secondary origin, *i.e.*, not as an altered natrocarbonatite having undergone alkali leaching.

8.3.1.2: Fenitisation during cooling

LeBas (1981) suggested that the parental natrocarbonatite liquid has 500°C of superheat and loses alkalis progressively as the magma cools to its liquidus temperature of 400-600 °C, by which stage it has become a calcitic-dolomitic liquid, and this liquid then differentiates to produce the commoner types of carbonatite rocks. This hypothesis was criticised by Twyman and Gittins (1987) who showed that the liquid cannot lose alkalis during cooling and then fractionate crystals once saturation is achieved, because in order for saturation to be achieved, crystallisation must first occur. More importantly, results from Kjarsgaard et al. (1995) and from this study (Chapter 6) refute the idea that a superheat of 500 °C exists.

Lee and Wyllie (1997b) added further arguments against changing immiscible natrocarbonatite liquids to $CaCO_3$-rich liquids by removing alkalis via vapour loss. They showed that adjustments to vapour loss would be made not by change in liquid composition but by precipitation of calcite and silicate minerals.

8.3.1.3: Fractionation of natrocarbonatites

Since there are many arguments against derivation of calciocarbonatites via fenitisation, some authors (*e.g.* LeBas, 1987) proposed that they could be derived by crystal fractionation from (silicate-free) natrocarbonatites. However, Peterson and Kjarsgaard (1995) showed that it was not possible to derive other carbonatite melts, such as sövite magmas with calcite phenocrysts, from natrocarbonatite, since natrocarbonatite has a much lower crystallisation temperatures than other carbonatites (Cooper et al., 1975). This study shows that silicate-free natrocarbonatites are themselves a product of extensive fractionation of silicate-bearing natrocarbonatite (Chapter 3).

8.3.2: Are calciocarbonatites parent to natrocarbonatites?

In order to link calcio- and natro-carbonatites genetically, it has also been proposed that natrocarbonatites could be the product of fractionation from calciocarbonatites (*e.g.*, Twyman and Gittins, 1987). According to Jago and Gittins (1991), addition of about 8 wt. % fluorine lowers the minimum melting and liquidus temperatures to a similar extent as does the addition of very large amounts of water. This has the effect of breaking the "thermal barrier" imposed by the nyerereite composition in the system Na_2CO_3-K_2CO_3-$CaCO_3$, thereby allowing a low-alkali sodic carbonatite magma to differentiate into a highly sodic carbonatite magma of the Oldoinyo Lengai type. However, Peterson and Kjarsgaard (1995) rejected this hypothesis because: (1) the required bulk compositions and crystallisation sequences do not resemble natural examples; (2) it does not resolve the relationship between natrocarbonatite and contemporaneous silicate magmas; and (3) less alkaline carbonate magmas have not recently been erupted at Oldoinyo Lengai, although they appear at many other centres where natrocarbonatite is not found.

The only recent sample of calciocarbonatite at Oldoinyo Lengai is the xenolith mentioned in section 8.3.1.1. Even if this calciocarbonatite is of magmatic origin, as suggested by Gittins and Harmer (1997), it does not imply that calciocarbonatites and natrocarbonatites are genetically related at Oldoinyo Lengai, because they can evolve from different magmas and/or along different differentiation paths. Calciocarbonatites are not thought to be directly related to natrocarbonatites, and their origin must be considered separately.

8.3.3: Are calcio- and natro-carbonatites formed by liquid immiscibility from different nephelinite parents, or not?

At Oldoinyo Lengai, the carbonatite and many of the silicate lavas have unusually high $Na_2O + K_2O$ (35 % and 18 % respectively), whereas, at Shombole (Kenya), the nephelinites are less alkaline (averaging 12 % $Na_2O + K_2O$) and the carbonatites they are associated with are calcic. The Shombole trend is the most common lineage observed in nephelinite-carbonatite centres. Based on experiments in subsystems of the join Di-Ak-Ne-Lc-Qz, Peterson (1989b) suggested that two fractionation trends in sodic alkaline ultramafic liquids could be predicted and that the products might correspond to the contrasting suites of peralkaline nephelinites from Shombole and Oldoinyo Lengai. The Shombole trend has olivine nephelinite as its parental magma, and its differentiation products are mildly peralkaline [(Na+K)/Al ~ 1.15] nephelinites, whereas the "Oldoinyo Lengai" trend has melilite or olivine-melilite nephelinite as its parental magma, and produces extremely peralkaline [(Na+K)/Al ~ 1.4-2.3] wollastonite- and combeite-bearing nephelinites. Peterson and Kjarsgaard (1995) suggested that the two types of carbonatites, *i.e.*, calciocarbonatites at Shombole and natrocarbonatites at Oldoinyo Lengai, were exsolved from nephelinites of low and high peralkalinity, respectively.

However, recent experimental work demonstrated that sövites cannot form directly by liquid immiscibility from nephelinite magmas (Lee and Wyllie, 1998), and that sövites are better interpreted as cumulates from an immiscible carbonate liquid conjugate to low peralkalinity wollastonite nephelinite (Kjarsgaard, 1998). The residual alkali-rich melts after calcite fractionation may be responsible for fenitisation (Lee and Wyllie, 1997b).

8.4 – Conclusion

A general petrogenetic model developed from the results of this study is now summarised. At Oldoinyo Lengai, silicate-bearing natrocarbonatites are likely to be the product of ~ 10-20 % liquid immiscibility from wollastonite nephelinite at ~ 100 MPa, 750 °C. The silicate-bearing natrocarbonatite efficiently segregates from its host, and then separates and collects in high level 20 MPa magma chamber(s), where silicate phases crystallise extensively. In the shallow (~ 0.6 km depth) magma chamber, the silicate-bearing natrocarbonatite magma undergoes convective fractionation. Rapid convection in the chamber keeps precipitating silicate phases and aggregates ('silicate spheroids') in suspension. *In situ* sidewall crystallisation of silicate crystals occurs by nucleation of these phases on the chamber walls. In addition, *in situ* formation of minor phases rich in U, Th, HFSE and REE, transported in halogen-rich fluids exsolving from the magma, may deplete these elements in the residual magma. The removal of the silicate component of the parent magma, by sidewall crystallisation gives rise to a low-density magma that rises along the wall to the top of the chamber, where this low-density, silica-poor natrocarbonatite differentiates and carbonate phases precipitate. This differentiated magma subsequently moves to the small near surface chambers, where nyerereite, gregoryite and apatite can crystallise before eruption.

Because highly peralkaline nephelinites similar to the parental magmas of natrocarbonatites from Oldoinyo Lengai are rarely found in alkaline ultramafic centres, natrocarbonatite is believed to have little general relevance for the evolution of such complexes. Natrocarbonatite is a variety of carbonatite associated solely with the Lengai trend and is not a viable parental magma for other carbonatites.

In conclusion, the general case is that calcium-rich carbonatites (but not sövites) are produced by liquid immiscibility from a moderately peralkaline nephelinite. Fractionation of calcite produces a cumulate sövite, and a residual liquid that may be alkali-rich, but not a natrocarbonatite *sensus stricto*. The residual, alkali-rich liquid may lose alkalis via fenitisation, but does not evolve to an alkali-poor liquid, since loss of alkalis is compensated for by crystallisation of calcite and silicate crystals. The alkali-rich

carbonatite at Oldoinyo Lengai, which is a natrocarbonatite *sensus stricto*, is only produced by liquid immiscibility from peralkaline wollastonite nephelinite. Fenitisation at Oldoinyo Lengai could (partly?) be due to loss of fluids during *in situ* crystallisation. However, fenitisation does not greatly affect the magmatic compositions or processes since the residual liquid is a silicate-free natrocarbonatites, not a sövite. Note that for all carbonatites, fenitisation affects only small volumes of very fractionated magma.

Phase equilibria and geochemical parameters have been used to arrive to the conclusions of this study. In retrospect it is clear that the results could have been improved and some suggestions are proposed as a guide for future studies: 1) preparation of the experimental samples using a centrifuge autoclave in order to better separate liquid and crystal phases; 2) more rapid quench in order to decrease the heterogeneity of carbonate liquid; 3) impregnation of experimental charges with resin in order to better preserve the original phase assemblages during polishing; 4) successive polish sections of individual experimental charges in order to have a better estimate of their phase proportions; 5) preparation of more samples at the P-T-X conditions of interest; and 6) minimisation of the surface contamination during LAM-ICP-MS analyses by using a jet of Ar gas on ablated sample.

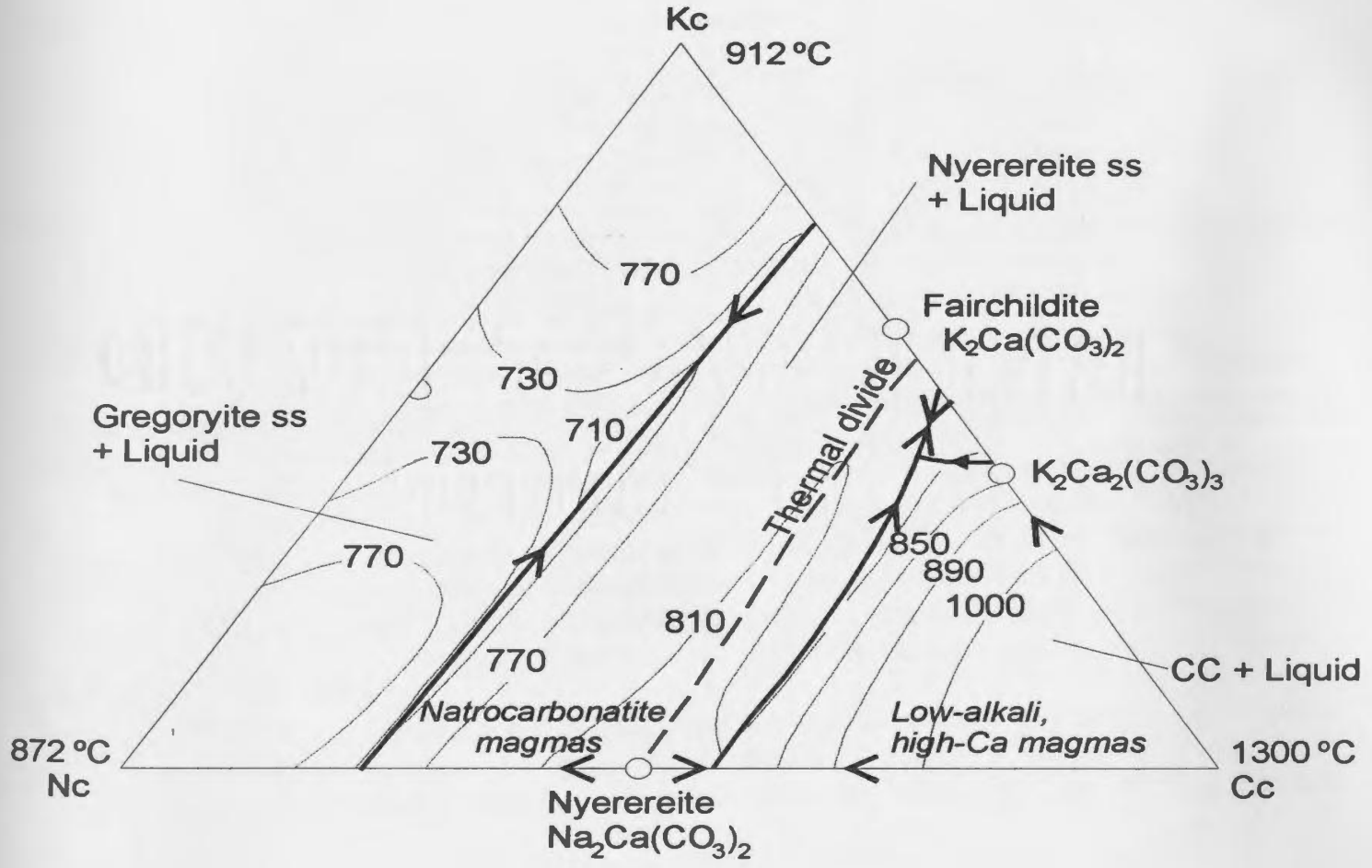

Figure 8.1: Isobaric ternary phase diagram for K_2CO_3-Na_2CO_3-$CaCO_3$ at 100 MPa after Cooper et al. (1975).

REFERENCES

Abraham, F.F., 1974. Homogeneous nucleation theory: the pretransition theory of vapor condensation. *Advances in Theoretical Chemistry, Supplement I, Academic Press, New York.* 263 p.

Bailey, D.K, 1989. Carbonate melt from the mantle in the volcanoes of south-east Zambia. *Nature* **388:** 415-418.

Bailey, D.K., 1993. Carbonate magmas. *Journal of the Geological Society of London* **150:** 637-651.

Bailey, D.K. & Hampton, C.M., 1990. Volatiles in alkaline magmatism. *Lithos* **26:** 157-165.

Bailey, D.K. & Macdonald, R., 1975. Fluorine and chlorine in peralkaline liquids and the need for magma generation in an open system. *Mineralogical Magazine* **40:** 405-414.

Bailey, D.K. & Macdonald, R., 1987. Dry peralkaline felsic liquids and carbon dioxide flux through the Kenya rift zone. In: Mysen, B.O. (ed.). Magmatic Processes: Physicochemical Principles. *Geochemistry Society Special Publication, 1,* pp. 91-105.

Barker, D.S., 1989. Field relations of carbonatites. In: K. Bell (ed.). Carbonatites. Genesis and evolution. *Unwin Hyman, London,* pp. 278-300.

Barker, D.S. & Nixon, P.H., 1989. High-Ca, low-alkali carbonatite volcanism at Fort Portal, Uganda. *Contributions to Mineralogy and Petrology* **103:** 166-177.

Beattie, P., Drake, M., Jones, J., Leeman, W., Longhi, J., McKay, G., Nielsen, R., Palme, H., Shaw, D., Takahashi, E. & Watson, B., 1993. Terminology for trace-element partitioning. *Geochimica et Cosmochimica Acta* **57:** 1605-1606.

Beckett, J.R., Spivack, A.J., Hutcheon, I.D., Wasserburg, G.J. & Stolper, E.M, 1990. Crystal chemical effects on the partitioning of trace elements between mineral and melt: an experimental study of melilite with applications to refractory inclusions from carbonaceous chondrites. *Geochimica et Cosmochimica Acta* **54:** 1755-1774.

Bell, K. & Blenkinsop, J., 1989. Neodymium and strontium isotope geochemistry of carbonatites. In: K. Bell (ed.). Carbonatites. Genesis and evolution. *Unwin Hyman, London,* pp. 278-300.

Bell, K. & Dawson, J.B., 1995. Nd and Sr isotope systematics of the active carbonatite volcano, Oldoinyo Lengai. In: Bell, K. & Keller, J. (eds). Carbonatite volcanism: Oldoinyo Lengai and the petrogenesis of natrocarbonatites. *Springer-Verlag, Berlin,* pp. 100-112.

Bell, K. & Keller, J. (eds) 1995. *Carbonatite volcanism: Oldoinyo Lengai and the petrogenesis of natrocarbonatites. IAVCEI Proceedings in Volcanology 4.* Berlin: Springer-Verlag.

Bell, K., Kjarsgaard, B.A. & Simonetti, A., 1998. Introduction. In: Bell, K., Kjarsgaard, B.A. & Simonetti, A. (eds). Carbonatites – Into the twenty first century. *Journal of Petrology* **39:** 1839-1845.

Bell, K. & Simonetti, A., 1996. Carbonatite magmatism and plume activity: implications for the Nd, Pb and Sr isotope systematics of Oldoinyo Lengai. *Journal of Petrology* **37:** 1321-1339.

Blundy, J.D. & Wood, B.J., 1994. Prediction of crystal-melt partition coefficients from elastic moduli. *Nature* **372:** 452-454.

Bouch, J.E., Hole, M.J. & Trewin, H., 1997. Rare earth and high field strength element partitioning behaviour in diagenetically precipitated titanites. *Neues Jahrbuch Mineral Abhandlungen* **172:** 3-21.

Brenan, J.M. & Watson, E.B., 1991. Partitioning of trace elements between carbonate melt and clinopyroxene and olivine at mantle P-T conditions. *Geochimica et Cosmochimica Acta* **55:** 2203-2214.

Brooker, R.A., 1995. Carbonatite genesis; the role of liquid immiscibility to 25 kbar. *Ph.D. thesis, University of Manchester, England.*

Brooker, R.A., 1998. The effect of CO_2 saturation on immiscibility between silicate and carbonate liquids: an experimental study. In: Bell, K., Kjarsgaard, B.A. & Simonetti, A. (eds). Carbonatites – Into the twenty first century. *Journal of Petrology* **39:** 1905-1915.

Brooker, R.A. and Hamilton, D.L., 1990. Three liquid immiscibility and the origin of carbonatites. *Nature* **346:** 459-462.

Brown, G.E.Jr., Farges, F. & Calas, G., 1995. X-ray scattering and X-ray spectroscopy studies of silicate melts. In: Stebbins, J.F., McMillan, P.F. & Dingwell, D.B. (eds). Structure, dynamics and properties of silicate melts. *Reviews in Mineralogy No.32*, pp. 319-410.

Brueckner, H.K. & Rex, D.C., 1980. K-A and Rb-Sr geochronology and Sr isotopic study of the Alnö alkaline complex, northeastern Sweden. *Lithos* **13:** 111-119.

Buckley, H.A. & Woolley, A.R., 1990. Carbonates of the magnesite-siderite series from four carbonatite complexes. *Mineralogical Magasine* **54:** 413-418.

Cesbron, F.P., 1989. Mineralogy of the rare-earth elements. In: Möller, P., Cerný, P. & Saupé, F. (ed.). Lanthanides, tantalum and niobium. *Special Publication No.7 of the Society for Geology Applied to Mineral Deposits. Springer-Verlag. Berlin*, pp. 3-26.

Chakhmouradian, A.R. & Mitchell, R.H., 1997. Compositional variation of the perovskite-group minerals from the carbonatite complexes of the Kola Peninsula, Russia. *Canadian Mineralogist* **35:** 1293-1310.

Chakhmouradian, A.R. & Mitchell, R.H., 1998. Compositional variation of the perovskite-group minerals from the Khibina Complex, Kola Peninsula, Russia. *Canadian Mineralogist* **36:** 953-969.

Cherniak, D.J., 1998. REE diffusion in calcite. *Earth and Planetary Science Letters* **160:** 273-287.

Church, A.A. & Jones, A.P., 1995. Silicate-carbonate immiscibility at Oldoinyo Lengai. *Journal of Petrology* **36:** 869-889.

Cooper, A.F., Gittins, G. & Tuttle, O.F., 1975. The system Na_2CO_3-K_2CO_3-$CaCO_3$ at 1 kilobar and its significance in carbonatite petrogenesis. *American Journal of Science* **275:** 534-560.

Cooper, A., Wood, B.J. & Ragnarsdottir, 1998. The properties of carbonated fluids in the systems Na_2CO_3-H_2O and K_2CO_3-H_2O at 1000 °C. *Mineralogical Magazine* **62A:** 347-348.

Dalton, J.A., 1993. Carbonate stability at high pressures and temperatures: implications for the origin of carbonatite magmas and the storage of carbon within the earth. *Ph.D. thesis. University of Bristol, England.*

Dalton, J.A. & Presnall, D.C., 1998. The continuum of primary carbonatitic-kimberlitic melt compositions in equilibrium with lherzolite: data from the system CaO-MgO-Al_2O_3-SiO_2-CO_2 at 6 GPa. In: Bell, K., Kjarsgaard, B.A. & Simonetti, A. (eds). Carbonatites – Into the twenty first century. *Journal of Petrology* **39:** 1953-1964.

Dalton, J.A. & Wood, B.J., 1993a. The composition of primary carbonate melts and their evolution through wallrock reaction in the mantle. *Earth and Planetary Science Letters* **119:** 511-525.

Dalton, J.A. & Wood, B.J., 1993b. The stability of Fe and Mg between olivine and carbonate and the stability of carbonate under mantle conditions. *Contributions to Mineralogy and Petrology* **114:** 501-509.

Dawson, J.B., 1962a. The geology of Oldoinyo Lengai. *Bulletin Volcanologique* **24:** 349-387.

Dawson, J.B., 1962b. Sodium carbonate lavas from Oldoinyo Lengai, Tanganyika. *Nature* **195:** 1075-1076.

Dawson, J.B., 1964. Reactivity of the cations in carbonate magma. *Geological Association of Canadian Proceedings* **15:** 103-113.

Dawson, J.B., 1966. Oldoinyo Lengai – An active volcano with sodium carbonatite flows. In: Tuttle, O.F. and Gittins, J., (eds). Carbonatites. *Wiley, London*, pp. 155-168.

Dawson, J.B., 1989. Sodium carbonatites extrusions from Oldoinyo Lengai, Tanzania: implications for carbonatite genesis. In: Bell, K. (Ed.). Carbonatites. Genesis and evolution. *Unwin Hyman, London*, pp. 255-277.

Dawson, J.B., 1998. Peralkalinite-natrocarbonatite relationships at Oldoinyo Lengai, Tanzania. In: Bell, K., Kjarsgaard, B.A. & Simonetti, A. (eds). Carbonatites – Into the twenty first century. *Journal of Petrology* **39:** 2077-2094.

Dawson, J.B., Garcon, M.S. & Roberts, B., 1987. Altered former alkalic carbonatite lava from Oldoinyo Lengai, Tanzania: Inferences for calcitic carbonatite lavas. *Geology* **15:** 765-768.

Dawson, J.B., Keller, J. & Nyamweru, C, 1995a. Historic and recent eruptive activity of Oldoinyo Lengai. In: Bell, K. & Keller, J. (eds). Carbonatite volcanism: Oldoinyo Lengai and the petrogenesis of natrocarbonatites. *Springer-Verlag, Berlin*, pp. 4-22.

Dawson, J.B., Pinkerton, H., Norton, G.E. & Pyle, D.M., 1990. Physicochemical properties of lakali carbonatite lavas: Data from the 1988 eruption of Oldoinyo Lengai, Tanzania. *Geology* **18:** 260-263.

Dawson, J.B., Pinkerton, H., Norton, G.E., Pyle, D.M., Browning, P., Jackson, D & Fallick, A.E., 1995b. Petrology and geochemistry of Oldoinyo Lengai lavas extruded in November 1988: magma source, ascent and crystallization. In: Bell, K. & Keller,

J. (eds). Carbonatite volcanism: Oldoinyo Lengai and the petrogenesis of natrocarbonatites. *Springer-Verlag, Berlin*, pp. 47-69.

Dawson, J.B., Pinkerton, H., Pyle, D.M. & Nyamweru, C, 1994a. June 1993 eruption of Oldoinyo Lengai, Tanzania: exceptionally viscous and large carbonatite lava flows and evidence for coexisting silicate and carbonate magmas. *Geology* **22:** 799-802.

Dawson, J.B., Pyle, D.M. & Pinkerton, H., 1996. Evolution of natrocarbonatite from a wollastonite nephelinite parent: evidence from the June, 1993 eruption of Oldoinyo Lengai, Tanzania. *The Journal of Geology* **104:** 41-54.

Dawson, J.B., Smith, J.V. & Jones, A.P., 1985. A comparative study of bulk rock and mineral chemistry of olivine melilitites and associated rocks from East and South Africa. *Neues Jahrbuch Mineral Abhandlungen* **152:** 143-175.

Dawson, J.B., Smith, J.V. & Steele, I.M., 1989. Combeite $(Na_{2.3}Ca_{1.74}others_{0.12})Si_3O_9$ from Oldoinyo Lengai, Tanzania. *Journal of Geology* **97:** 365-372.

Dawson, J.B., Smith, J.V. & Steele, I.M., 1992. 1966 ash eruption of the carbonatite volcano Oldoinyo Lengai: mineralogy of lapilli and mixing of silicate and carbonate magmas. *Mineralogical Magazine* **56:** 1-16.

Dawson, J.B., Smith, J.V. & Steele, I.M., 1994b. Trace-element distribution between coexisting perovskite, apatite and titanite from Oldoinyo Lengai, Tanzania. In: Foley, S.F. & van der Laan, S.R. (eds). Trace-element partitioning with application to magmatic processes. *Chemical Geology* **117:** 285-290.

Dawson, J.B., Smith, J.V. & Steele, I.M., 1995c. Petrology and mineral chemistry of plutonic igneous xenoliths from the carbonatite volcano, Oldoinyo Lengai, Tanzania. *Journal of Petrology* **36:** 797-826.

Deans, T. & Roberts, R., 1984. Carbonatite tuffs and lava clasts of the Tideret foothills, werstern Kenya: a study of calcified natrocarbonatites. *Journal of the Geological Society of London* **141:** 563-580.

Debenedetti, P.G., 1996. Metastable liquids: concepts and principles. *Princeton University Press, Princeton.* 412 p.

Deer, W.A., Howie, R.A. & Zussman, J., 1992. An introduction to the rock-forming minerals – Second edition. *Wiley and Sons, New York.* 696 p.

Dickinson, J.E. Jr., 1986. Liquidus phase equilibria and melt structure. In: Scarfe, C.M. (ed). Short course in silicate melts. *Mineralogical Association of Canada* **12:** 154-179.

Donaldson, C.H. & Dawson, B, 1978. Skeletal crystallization and residual glass compositions in a cellular alkalic pyroxenite nodule from Oldoinyo Lengai. *Contributions to Mineralogy and Petrology* **67:** 139-149.

Donaldson, C.H., Dawson, J.B., Kanaris-Sotiriou, R., Batchelor, R.A. & Walsh, N.J., 1987. The silicate lavas of Oldoinyo Lengai, Tanzania. *Neues Jahrbuch Mineralogie Abhandlungen* **156**: 247-279.

Dowty, E., 1980. Crystal growth and nucleation theory and the numerical simulation of igneous crystallization. In: Hargraves, R.B. (ed.). Physics of Magmatic Processes. *Princeton University Press, Princeton,* p. 419-485.

Droop, G.T.R., 1987. A general equation for estimating Fe3+ concentrations in ferromagnesian silicates and oxides from microprobe analyses, using stoichiometric criteria. *Mineralogical magazine* **51:** 431-435.

Eby, G.N., 1975. Abundance and distribution of the rare earth elements and yttrium in rocks and minerals of the Oka carbonatite complex, Quebec. *Geochimica et Cosmochimica Acta* **39:** 597-620.

Eckermann, H. von, 1948. The alkaline district of Alnö island. *Sverig. Geol. Underok. Series Ca*, No. 36.

Eckermann, H. von, 1961. The petrogenesis of the Alnö alkaline rocks. *Bulletin of the Geological Institutions of University of Uppsala, New Series* **40:** 25-46.

Eckermann, H. von, 1966. Progress of research on the Alnö carbonatite. In: Tuttle, O.F. and Gittins, J., (eds). Carbonatites. *Wiley, London*, pp. 3-31.

Eggler, D.H., 1975. Carbonatite generation by a reaction in the system CaO-MgO-SiO_2-CO_2 at 30 kbar pressure. *Physics and Chemistry of the Earth* **9:** 869-891.

Eggler, D.H., 1978. The effect of CO_2 upon partial melting of peridotite in the system Na_2O-CaO-Al_2O_3-MgO-SiO_2-CO_2 at 35 kb, with an analysis of melting in a peridotite-H_2O-CO_2 system. *American Journal of Science* **278:** 305-343.

Eggler, D.H., 1987. Solubility of major and trace elements in mantle metasomatic fluids: experimental constraints. In: Menzies, M.A. & Hawkesworth, C.J. (eds). Mantle metasomatism. *Academic Press, New York*, pp. 21-41.

Ellison, A.J.G. & Hess, P.C., 1989. Solution properties of rare earth elements in silicate melts: inferences from immiscible liquids. *Geochimica et Cosmochimica Acta* **53:** 1965-1974.

Falloon, T.J. and Green, D.H., 1990. Solidus of carbonated fertile peridotite under fluid-saturated conditions. *Geology* **18:** 195-199.

Farges, F., 1991. Structural environment aroun Th^{4+} in silicate glasses: implications for the geochemistry of incompatible Me^{4+} elements. *Geochimica et Cosmochimica Acta* **55:** 3303-3319.

Farges, F. & Brown Jr., G.E., 1996. Coordination of high field strength elements (Ti, Zr, Mo, Th and U) in silicate melts. *Terra Nova Abstract supplement* **1:** 18.

Farges, F., Ponader, C.W. & Gordon, E.B.Jr., 1991. Structural environments of incompatible elements in silicate glass/melt systems: I. Zirconium at trace levels. *Geochimica et Cosmochimica Acta* **55:** 1563-1574.

Farges, F., Ponader, C.W., Calas, G. & Gordon, E.B.Jr., 1992. Structural environments in silicate glass/melt systems: II. U^{IV}, U^{V}, and U^{VI}. *Geochimica et Cosmochimica Acta* **56:** 4205-4220.

Ferguson, J. & Currie, K.L., 1971. Evidence for liquid immiscibility in alkaline ultrabasic dykes at Callander Bay, Ontario. *Journal of Petrology* **12**: 561-586.

Flynn, R.T. & Burnham, C.W., 1978. An experimental determination of rare earth partition coefficients between a chloride containing vapor phase and silicate melts. *Geochimica et Cosmochimica Acta* **42:** 685-701.

Freestone, I.C. and Hamilton, D.L., 1980. The role of liquid immiscibility in the genesis of carbonatites: an experimental study. *Contributions to Mineralogy and Petrology* **73:** 105-117.

Fryer, B.J., Jackson, S. & Longerich, H., 1995. The design, operation and role of the laser ablation microprobe coupled with an inductively coupled plasma mass spectrometer (LAM-ICP-MS) in the earth sciences. *Canadian Mineralogist* **33:** 303-312.

Gaetani, G.A. & Grove, T.L., 1995. Partitioning of rare earth elements between clinopyroxene and silicate melt: crystal-chemical controls. *Geochimica et Cosmochimica Acta* **59:** 1951-1962.

Genge, M.J., Jones, A.P. & Price, G.D., 1995. An infrared and Raman study of carbonate glasses: Implications for the structure of carbonatite magmas. *Geochimica et Cosmochimica Acta* **59:** 927-937.

Gerlach, D.C., Cliff, R.A., Davies, G.R., Norry, M. & Hodgson, N., 1988. Magma sources of the Cape Verdes archipelago: isotopic and trace element constraints. *Geochimica et Cosmochimica Acta* **52:** 2979-2992.

Gittins, J., 1989. The origin and evolution of carbonatite magmas. In: Bell, K. (eds). Carbonatites: Genesis and evolution. *Unwin Hyman, London*, pp. 580-600.

Gittins, J., Allen, C.R. & Cooper, A.F., 1975. Phlogopitization of pyroxenite: its bearing on the composition of carbonatite magmas. *Geological Magazine* **112:** 503-507.

Gittins, J. & Harmer, R.E., 1997. Dawson's Oldoinyo Lengai calciocarbonatite: a magmatic sovite or an extremely altered natrocarbonatite? *Mineralogical Magazine* **61:** 351-355.

Gittins, J. & Jago, B.C., 1998. Differentiation of natrocarbonatite magma at Oldoinyo Lengai volcano, Tanzania. *Mineralogical Magazine* **62:** 759-768.

Gittins, J. & McKie, D., 1980. Alkalic carbonatite magmas: Oldoinyo Lengai and its wider applicability. *Lithos* **13:** 213.

Green, T.H., 1994. Experimental studies of trace-element partitioning applicable to igneous petrogenesis – Sedona 16 years later. In: Foley, S.F. & van der Laan, S.R. (eds). Trace-element partitioning with application to magmatic processes. *Chemical Geology* **117:** 1-36.

Green, T.H. & Adam, J. & Sie, S.H., 1992. Trace element partitioning between silicate minerals and carbonatite at 25 kbar and application to mantle metasomatism. *Mineralogy and Petrology* **46:** 179-184.

Green, T.H. & Pearson, N.J., 1986. Rare earth element partitioning between sphene and coexisting silicate liquid at high pressure and temperature. *Chemical Geology* **55:** 105-119.

Green, D.H. & Wallace, M.E., 1988. Mantle metasomatism by ephemeral carbonatite melts. *Nature* **336:** 459-462.

Hamilton, D.L., 1961. Nephelines as crystallization temperature indicators. *Journal of Geology* **69:** 321-329.

Hamilton, D.L., Bedson, P. & Esson, J., 1989. The behaviour of trace elements in the evolution of carbonatites. In: K. Bell (ed.). Carbonatites. Genesis and evolution. *Unwin Hyman, London*, pp. 405-427.

Hamilton, D.L., Freestone, I.C., Dawson, J.B. & Donaldson, C.H., 1979. Origin of carbonatites by liquid immiscibility. *Nature* **279:** 52-54.

Hamilton, D.L. & Kjarsgaard, B.A., 1993. The immiscibility of silicate and carbonate liquids. *South African Journal of Geology* **96 (3):** 139-142.

Hansen, K., 1980. Lamprophyres and carbonatitic lamprophyres related to rifting in the Labrador Sea. *Lithos* **13:** 145-152.

Harmer, R.E. & Gittins, J., 1997. The origin of dolomitic carbonatites: field and experimental constraints. *Journal of African Earth Sciences* **25:** 5-28.

Harmer, R.E. & Gittins, J., 1998. The case of primary, mantle-derived carbonatite magma. In: Bell, K., Kjarsgaard, B.A. & Simonetti, A. (eds). Carbonatites – Into the twenty first century. *Journal of Petrology* **39:** 1895-1903.

Hart, S.R. & Davis, K.E., 1978. Nickel partitioning between olivine and silicate melt. *Earth and Planetary Science Letters* **40:** 203-219.

Hauri, E.H., Wagner, T.P. & Grove, T.L., 1994. Experimental and natural partitioning of Th, U, Pb and other trace elements between garnet, clinopyroxene and basaltic melts. In: Foley, S.F. & van der Laan, S.R. (eds). Trace-element partitioning with application to magmatic processes. *Chemical Geology* **117:** 149-166.

Hay, R.L., 1983. Natrocarbonatite tephra of Kerimasi volcano, Tanzania. *Geology* **11:** 599-602.

Heinrich, E.W., 1966. The geology of carbonatites. *Rand McNally, New York*. 608 p.

Hogarth, D.D., 1989. Pyrochlore, apatite and amphibole: distinctive minerals in carbonatite. In: K. Bell (ed.). Carbonatites. Genesis and evolution. *Unwin Hyman, London*, pp. 105-148.

Holloway, J.R. & Wood, B.J., 1988. Simulating the Earth: experimental geochemistry. Unwin Hyman, London. 196 p.

Holmes, A., 1952. The potash ankermanite-mela leucite lavas of Nabugando and Mbuya craters, South-West Uganda. *Transcripts of the Geological Society of Edinburgh* **15:** 187-213.

Hornig-Kjarsgaard, I., 1998. Rare earth elements in sövitic carbonatites and their mineral phases. In: Bell, K., Kjarsgaard, B.A. & Simonetti, A. (eds). Carbonatites – Into the twenty first century. *Journal of Petrology* **39:** 2105-2121.

Huang, W.L. & Wyllie, P.J., 1976. Melting relationships in the systems CaO-CO_2 and MgO-CO_2 to 33 kilobars. *Geochimica et Cosmochimica Acta* **40:** 129-132.

Ivanikov, V.V., Rukhlov, A.S. & Bell, K., 1998. Magmatic evolution of the melilite-carbonatite-nephelinite dyke series of the Turiy Peninsula (Kandalaksha Bay, White Sea, Russia). In: Bell, K., Kjarsgaard, B.A. & Simonetti, A. (eds). Carbonatites – Into the twenty first century. *Journal of Petrology* **39:** 2043-2059.

Jackson, S.E., Longerich, H.P., Dunning, G.R. & Fryer, B.J., 1992. The application of laser-ablation microprobe-inductively coupled plasma-mass spectrometer (LAM-ICP-MS) to *in situ* trace-element determinations in minerals. *Canadian Mineralogist* **30:** 1049-1064.

Jago, B.C. & Gittins, J., 1991. The role of fluorine in carbonatite magma evolution. *Nature* **349:** 56-58.

Janz, G.J., Allen, C.B., Bansal, N.P., Murphy, R.M. & Tompkins, R.P.T., 1979. *Physical properties data compilations relevant to energy storage. II. Molten salts: data on single and multicomponent systems; National Data Reference Data Service NSRDS-NBS.*.

Jenner, G.A., Foley, S., Jackson, S.E., Green, T., Fryer, B.J. & Longerich, H., 1993. Determination of partition coefficients for trace elements in high pressure-temperature experimental run products by laser ablation microprobe - inductively coupled plasma mass spectrometry (LAM-ICP-MS). *Geochimica Cosmochimica Acta* **58**: 5099-5103.

Jensen, B.B., 1973. Patterns of trace element partitioning. *Geochimica Cosmochimica Acta* **37**: 2227-2242.

Jones, A.P., 1989. Upper-mantle enrichment by kimberlitic or carbonatitic magmatism. In: Bell, K. (eds). Carbonatites: Genesis and evolution. *Unwin Hyman, London*, pp. 448-463.

Jones, J.H., Walker, D., Picket, D.A., Murrel, M.T. & Beate, P., 1995. Experimental investigations of the partitioning of Nb, Mo, Ba, Ce, Pb, Ra, Th, Pa and U between immiscible carbonate and silicate liquids. *Geochimica and Cosmochimica Acta* **51:** 769-782.

Kay, I.M., Young, R.A. & Posner, A.S., 1964. Crystal structure of hydroxyapatite. *Nature* **204:** 1050-1052.

Keller, J. & Hoefs, J., 1995. Stable isotope characteristics of recent natrocarbonatites from Oldoinyo Lengai, June 1988. In: Bell, K. & Keller, J. (eds). Carbonatite volcanism: Oldoinyo Lengai and the petrogenesis of natrocarbonatites. *Springer-Verlag, Berlin*, pp. 113-123.

Keller, J. & Krafft, M., 1990. Effusive natrocarbonatite activity of Oldoinyo Lengai, June 1988. *Bulletin volcanologique* **52:** 629-645.

Keller, J. & Spettel, B., 1995. The trace element composition and petrogenesis of natrocarbonatites. In: Bell, K. & Keller, J. (eds) . Carbonatite volcanism: Oldoinyo Lengai and the petrogenesis of natrocarbonatites. *Springer-Verlag, Berlin*, pp. 70-86.

Khomyakov, A.P., 1995. Mineralogy of hyperagpaitic alkaline rocks. *Clarendon Press, Oxford.* 223 p.

King, B.C., 1949. The Napak area of southern Karamoja, Uganda. Geological Survey of Uganda, Memoir V.

King, B.C., 1965. Petrogenesis of the alkaline igneous rock suites of the volcanic and intrusive centers of eastern Uganda. *Journal of Petrology* **6:** 67-100.

King, B.C. and Sutherland, D.S., 1966. The carbonatite complexes of eastern Uganda. In: Tuttle, O.F. and Gittins, J., (eds). Carbonatites. *Wiley, London*, pp. 73-126.

Kirpatrick, R.J., Robinson, G.R. & Hayes, J.F., 1976. Kinetics of crystal growth from silicate melts: anorthite and diopside. *Journal of Geophysical Research* **81:** 5715-5720.

Kjarsgaard, B.A., 1990. Nephelinite-carbonatite genesis: Experiments on liquid immiscibility in alkali silicate-carbonate systems. *Ph.D. thesis. University of Manchester, Manchester.*

Kjarsgaard, B.A., 1998. Phase relations of a carbonated high-CaO nephelinite at 0.2 and 0.5 GPa. In: Bell, K., Kjarsgaard, B.A. & Simonetti, A. (eds). Carbonatites – Into the twenty first century. *Journal of Petrology* **39:** 2061-2075.

Kjarsgaard, B.A. and Hamilton, D.L., 1988. Liquid immiscibility and the origin of alkali-poor carbonatites. *Mineralogical Magazine* **52:** 43-55.

Kjarsgaard, B.A. & Hamilton, D.L., 1989. The genesis of carbonatites by liquid immiscibility. In: K. Bell (ed.). Carbonatites. Genesis and evolution. *Unwin Hyman, London*, pp. 388-404.

Kjarsgaard, B.A., Hamilton, D.L. & Peterson, T.D., 1995. Peralkaline nepheline/carbonatite liquid immiscibility: comparison of phase compositions in experiments and natural lavas from Oldoinyo Lengai. In: Bell, K. & Keller, J. (eds). Carbonatite volcanism: Oldoinyo Lengai and the petrogenesis of natrocarbonatites. *Springer-Verlag, Berlin*, pp. 163-190.

Kjarsgaard, B.A. & Peterson, T.D., 1991. Nephelinite-carbonatite liquid immiscibility at Shombole volcano, East Africa: Petrogenetic and experimental evidence. *Mineralogical Magazine* **43:** 293-314.

Klein, C. & Hurlbut, C.S., 1993. Manual of Mineralogy (21st ed). *Wiley and Sons, New York*. 693 p.

Klemme, S., van der Laan, S.R., Foley, S.F. & Günther, D., 1995. Experimentally determined trace and minor element partitioning between clinopyroxene and carbonatite melt under upper mantle conditions. *Earth and Planetary Science Letters* **133:** 439-448.

Knorring, O. von, 1962. Geochemical characteristics of carbonatites. *Nature* **194:** 860-861.

Knudsen, C., 1989. Pyrochlore group minerals from the Qaqarssuk carbonatite complex. In: Möller, P., Cerný, P. & Saupé, F. (ed.). Lanthanides, tantalum and niobium. *Special Publication No.7 of the Society for Geology Applied to Mineral Deposits. Springer-Verlag. Berlin*, pp. 80-99.

Koberski, U. & Keller, J., 1995. Catholuminescence observations of natrocarbonatites and related peralkaline nephelinites at Oldoinyo Lengai. In: Bell, K. & Keller, J. (eds). Carbonatite volcanism: Oldoinyo Lengai and the petrogenesis of natrocarbonatites. *Springer-Verlag, Berlin*, pp. 87-99.

Koepenick, K.W., Brantley, S.L., Thompson, J.M., Rowe, G.L., Nyblade, A.A. & Moshy, C., 1996. Volatile emissions from the crater and flank of Oldoinyo Lengai, Tanzania. *Journal of Geophysical Research* **101:** 13819-13830.

Kogarko, L.N., Plant, D.A., Henderson, C.M.B. & Kjarsgaard, B.A., 1991. Na-rich carbonate inclusions in perovskite and calzirtite from the Guli intrusive Ca-carbonatite, polar Siberia. *Contributions to Mineralogy and Petrology* **109:** 124-129.

Kohn, S.C. & Schofield, P.F., 1994. The importance of melt composition in controlling trace-element behaviour: an experimental study of Mn and Zn partitioning between forsterite and silicate melts. In: Foley, S.F. & van der Laan, S.R. (eds). Trace-element partitioning with application to magmatic processes. *Chemical Geology* **117:** 73-87.

Korobeinikov, A.N., Mitrofanov, F.P., Gehör, S., Laakoji, K., Pavlov, V.P. & Mamontov, V.P., 1998. Geology and copper sulphide mineralization of the Salmagorskii Ring igneous complex, Kola peninsula, NW Russia. In: Bell, K., Kjarsgaard, B.A. & Simonetti, A. (eds). Carbonatites – Into the twenty first century. *Journal of Petrology* **39:** 2033-2041.

Koster Van Groos, A.F., 1975. The effect of high CO_2 pressure on alkalic rocks and its bearing on the formation of alkalic ultrabasic rocks and the associated carbonatites. *American Journal of Science* **275:** 163-185.

Koster Van Groos, A.F. & Wyllie, P.J., 1963. Experimental data bearing on the role of liquid immiscibility in the genesis of carbonatites. *Nature* **199:** 801-802.

Koster Van Groos, A.F. & Wyllie, P.J., 1966. Liquid immiscibility in the system Na_2O-Al_2O_3-SiO_2-CO_2 at pressures to 1 kilobar. *American Journal of Science* **264:** 234-255.

Koster Van Groos, A.F. & Wyllie, P.J., 1968. Liquid immiscibility in the join $NaAlSi_3O_8$- Na_2CO_3-H_2O and its bearing on the genesis of carbonatites. *American Journal of Science* **266:** 932-967.

Koster Van Groos, A.F. & Wyllie, P.J., 1973. Liquid immiscibility in the join $NaAlSi_3O_8$- $CaAl_2Si_2O_8$-Na_2CO_3-H_2O. *American Journal of Science* **273:** 465-487.

Krafft, M. and Keller, J., 1989. Temperature measurements in carbonatite lava lakes and flows from Oldoinyo Lengai, Tanzania. *Science* **245:** 168-170.

Kramm, U., 1994. Isotope evidence for ijolite formation by fenitization: Sr-Nd data of ijolites from the type locality Iivaara, Finland. *Contributions to Mineralogy and Petrology* **115:** 279-286.

Kramm, U. & Sindern, S., 1998. Nd and Sr isotope fenites from Oldoinyo Lengai, Tanzania, and the genetic relationships between nephelinites, phonolites and carbonatites. In: Bell, K., Kjarsgaard, B.A. & Simonetti, A. (eds). Carbonatites – Into the twenty first century. *Journal of Petrology* **39:** 1997-2004.

Kwon, S.T., Tilton, G.R. and Grünenfelder, 1989. Lead isotope relationships on carbonatites and alkalic complexes: an overview. In: K. Bell (ed.). Carbonatites. Genesis and evolution. *Unwin Hyman, London*, pp. 360-387.

Lahaye, Y., Lambert, D. & Walters, S., 1997. Ultraviolet laer sampling and high resolution inductively coupled plasma-mass spectrometry of NIST and BCR-2G glass reference materials. *Geostandards Newsletter* **21**: 205-214.

Lange, R.A., 1994. The effect of H_2O, CO_2 and F on the density and viscosity of silicate melts. In: Carroll, M.R. & Holloway, J.R. (eds). Volatiles in magmas. *Reviews in Mineralogy No. 30* , pp. 331-369.

Langmuir, C.H., 1989. Geochemical consequences of *in situ* crystallization. *Nature* **340:** 199-205.

LaTourrette, T.Z. & Burnett, D.S., 1992. Experimental determination of U and Th partitioning between clinopyroxene and natural and synthetic basaltic liquid. *Earth and Planetary Science Letters* **100:** 227-244.

LeBas, M.J., 1977. Carbonatite-nephelinite volcanism. *Wiley, London.* 347 p.

LeBas, M.J., 1981. Carbonatite magmas. *Mineralogical Magazine* **44:** 133-140.

LeBas, M.J., 1987. Nephelinites and carbonatites. In: Fitton, J.G. and Upton. B.G.J. (eds). Alkaline igneous rocks. *Geological Society Special Publication No 30., Blackwell, London*, pp. 53-85.

LeBas, M.J., 1989. Diversification of carbonatites. In: Bell, K. (eds). Carbonatites: Genesis and evolution. *Unwin Hyman, London*, pp. 428-447.

Lee, W. & Wyllie, P.J., 1994. Experimental data bearing on liquid immiscibility, crystal fractionation, and the origin of calciocarbonatites and natrocarbonatites. *International Geological Review* **36:** 797-819.

Lee, W. & Wyllie, P.J., 1996. Liquid immiscibility in the join $NaAlSi_3O_8$-$CaCO_3$ to 2.5 GPa and the origin of calciocarbonatite magmas. *Journal of Petrology* **37:** 1125-1152.

Lee, W. & Wyllie, P.J., 1997a. Liquid immiscibility between nephelinite and carbonatite from 1.0 to 2.5 GPa compared with mantle melt compositions. *Contributions to Mineralogy and Petrology* **127:** 1-16.

Lee, W. & Wyllie, P.J., 1997b. Liquid immiscibility in the join $NaAlSiO_4$-$NaAlSi_3O_8$-$CaCO_3$ at 1.0 GPa: implications for crustal carbonatites. *Journal of Petrology* **38:** 1113-1135.

Lee, W. & Wyllie, P.J., 1998. Petrogenesis of carbonatite magmas from mantle to crust, constrained by the system CaO-(MgO + FeO*)-(Na_2O + K_2O)-(SiO_2 + Al_2O_3 + TiO_2)-CO_2. *Journal of Petrology* **39:** 495-517.

Lee, W., Wyllie, P.J. & Rossman, G.R., 1994. CO_2-rich glass, round calcite crystals and no liquid immiscibility in the system CaO-SiO_2-CO_2 at 2.5 GPa. *American Mineralogist* **79:** 1135-1144.

Leeman, W.P & Lindstrom, D.J., 1978. Partitioning of Ni^{2+} between basaltic and synthetic melts and olivines – an experimental study. *Geochimica et Cosmochimica Acta* **42:** 801-816.

Lesher, C.E., 1986. Effect of silicate liquid composition on mineral-liquid element partitioning from Soret diffusion studies. *Journal of Geophysical Research* **91:** 6123-6141.

Lofgren, G., 1980. Experimental studies on the dynamic crystallization of silicate melts. In: Hargraves, R.B. (ed.). Physics of Magmatic Processes. *Princeton University Press, Princeton*, p. 487-551.

Longerich, H.P., Jackson, S.E. & Günther, D., 1996. Laser ablation inductively coupled plasma mass spectrometric transient signal data acquisition and analyte concentration calculation. *Journal of Analytical Atomic Spectrometry* **11:** 899-904.

Lundstrom, C.C., Shaw, H.F., Ryerson, F.J., Williams, Q & Gill, J., 1998. Crystal chemical control of clinopyroxene-melt partitioning in the Di-Ab-An system: implications for elemental fractionations in the depleted mantle. *Geochimica et Cosmochimica Acta* **62:** 2849-2862.

Macdonald, R., Kjarsgaard, B.A., Skilling, I.P., Davies, G.R., Hamilton, D.H. and Black, S., 1993. Liquid immiscibility between trachyte and carbonate in ash flow tuffs from Kenya. *Contributions to Mineralogy and Petrology* **114:** 276-287.

Mahood, G. & Hildreth, W., 1983. Large partition coefficients for trace elements in high-silica rhyolites. *Geochimica et Cosmochimica Acta* **47:** 11-30.

McDonough, W.F. & Sun, S.-s., 1995. The composition of the Earth. *Chemical Geology* **120:** 223-253.

McKie, D. & Frankis, E.J., 1977. Nyerereite: a new volcanic carbonate mineral from Oldoinyo Lengai, Tanzania. *Zeitschrift für Kristallographie* **145:** 73-95.

Milton, C., 1968. The "natro-carbonatite lava" of Oldoinyo Lengai, Tanzania. *Geological Society of America Program with Abstract*, 202.

Mitchell, R.H., 1997. Carbonate-carbonate immiscibility, neighborite and potassium iron sulphide from Oldoinyo Lengai natrocarbonatite. *Mineralogical Magazine* **61:** 779-789.

Moore, K.R. & Wood, B.J., 1998. The transition from carbonate to silicate melts in the $CaO-MgO-SiO_2-CO_2$ system. In: Bell, K., Kjarsgaard, B.A. & Simonetti, A. (eds). Carbonatites – Into the twenty first century. *Journal of Petrology* **39:** 1943-1951.

Morogan, V., 1994. Ijolite versus carbonatite as sources of fenitization. *Terra Nova* **6:** 166-176.

Morogan, V. & Martin, R.F., 1985. Mineralogy and partial melting of fenitized crustal xenoliths in the Oldoinyo Lengai carbonatite volcano, Tanzania. *American Mineralogist* **70:** 1114-1126.

Mysen, 1988. Structure and properties of silicate melts. *Developments in Geochemistry 4, Elsevier, Amsterdam.* 354 p.

Mysen, B.O. & Virgo, D., 1980. Trace element partitioning and melt structure: an experimental study at one atomsphere. *Geochimica et Cosmochimica Acta* **44:** 1917-1930.

Nickel, E.H. & McAdam, R.C., 1963. Niobian perovskite from Oka, Quebec; a new classification for minerals of the perovskite group. *Canadian Mineralogist* **7:** 683-697.

Nielsen, R.L, Forsythe, L.M., Gallahan, W.E. & Fisk, M.R., 1994. Major- and trace-element magnetite-melt equilibria. In: Foley, S.F. & van der Laan, S.R. (eds). Trace-element partitioning with application to magmatic processes. *Chemical Geology* **117:** 167-191.

Norton, G. & Pinkerton, H., 1997. Rheological properties of natrocarbonatite lavas from Oldoinyo Lengai, Tanzania. *European Journal of Mineralogy* **9:** 351-364.

Odezynskij. M., 1990. Phase relations of carbonates and silicates in a model Martian mantle at 25 kilobars. *MSc thesis. Arizona State University, U.S.A.*

Onuma, N., Higushi, H., Watika, H. & Nagasawa, H., 1968. Trace element partition between two pyroxenes and the host lava. *Earth and Planetary Science Letters* **5:** 47-51.

Onuma, N., Ninomiya, S. & Nagasawa, H., 1981. Mineral/groundmass partition coefficients for nepheline, melilite, clinopyroxene and perovskite in melilite-nephelinite basalt, Nyiragongo, Zaire. *Geochemical Journal* **15:** 221-228.

Pearce, N., Perkins, W., Westgate, J., Gorton, M., Jackson, S., Neal, C. & Chenery, S., 1997. A compilation of new and published major and trace element data for NIST SRM 610 and NIST SRM 612 glass reference materials. *Geostandards Newsletter* **21**: 115-144.

Peterson, T.D., 1989a. Peralkaline nephelinites. I. Comparative petrology of Shombole and Oldoinyo L'engai, East Africa. *Contributions to Mineralogy and Petrology* **101:** 458-478.

Peterson, T.D., 1989b. Peralkaline nephelinites. II. Low pressure fractionation and the hypersodic lavas of Oldoinyo Lengai. *Contributions to Mineralogy and Petrology* **102:** 336-346.

Peterson, T.D., 1990. Petrology and genesis of natrocarbonatite. *Contributions to Mineralogy and Petrology* **105:** 143-155.

Peterson, T.D. & Kjarsgaard, B.A., 1995. What are the parental magmas at Oldoinyo Lengai? In: Bell, K. & Keller, J. (eds). Carbonatite volcanism: Oldoinyo Lengai and the petrogenesis of natrocarbonatites. *Springer-Verlag, Berlin*, p. 149-162.

Peterson, T.D & Marsh, B.D., 1986. Sodium metasomatism and mineral stabilities in alkaline ultramafic rocks: implications for the origin of the sodic lavas at Oldoinyo Lengai. *Eos* **67:** 389-390.

Pinkerton, H., Norton, G.E., Dawson, J.B. & Pyle, D.M., 1995. Field observations and measurements of the physical properties of Oldoinyo Lengai alkali carbonatite lavas, November 1988. In: Bell, K. & Keller, J. (eds). Carbonatite volcanism: Oldoinyo Lengai and the petrogenesis of natrocarbonatites. *Springer-Verlag, Berlin*, pp. 23-36.

Ponader, C.W. & Brown, G.E. Jr., 1989a. Rare earth elements in silicate glass/melt systems: I. Effects of composition on the coordination environments of La, Gd, and Yb. *Geochimica et Cosmochimica Acta* **53:** 2893-2903.

Ponader, C.W. & Brown, G.E. Jr., 1989b. Rare earth elements in silicate glass/melt systems: II. Interactions of La, Gd, and Yb with halogens. *Geochimica et Cosmochimica Acta* **53:** 2905-2914.

Purton, J.A., Allan, N.L. & Blundy, J.D., 1997. Calculated solution energies of heterovalent cations in forsterite and diopside: implications for trace element partitioning. *Geochimica et Cosmochimica Acta* **61:** 3927-3936.

Pyle, D.M., 1995. Decay series evidence for transfer and storage times of natrocarbonatite magma. In: Bell, K. & Keller, J. (eds). Carbonatite volcanism: Oldoinyo Lengai and the petrogenesis of natrocarbonatites. *Springer-Verlag, Berlin*, pp. 124-136.

Pyle, D.M., Dawson, J.B. and Ivanovich, M., 1991. Short-lived decay series disequilibria in the natrocarbonatite lavas of Oldoinyo Lengai, Tanzania: constraints on the timing of magma genesis. *Earth and Planetary Science Letters* **105:** 378-396.

Pyle, D.M., Pinkerton, H., Norton, G.E. & Dawson, J.B., 1995. The dynamics of degassing at Oldoinyo Lengai. In: Bell, K. & Keller, J. (eds) . Carbonatite volcanism: Oldoinyo Lengai and the petrogenesis of natrocarbonatites. *Springer-Verlag, Berlin*, pp. 37-46.

Rankin. A.H., & Le Bas, M.J., 1974. Liquid immiscibility between silicate and carbonate melts in naturally occurring ijolite magma. *Nature* **250:** 206-209.

Reed, S.J.B., 1996. Electron microprobe analysis and scanning electron microscopy in geology. *Cambridge University Press, Cambridge.* 201 p.

Rollinson, H.R., 1993. Using geochemical data: Evaluation, Presentation, Interpretation. *John Wiley & Sons, Inc., New York*, 352 p.

Romanchev, B.P., & Sokolov, S.V., 1979. Liquation in the production and geochemistry of the rocks in carbonatite complexes. *Geochemistry International* **16:** 125-135.

Rudnick, R.L., McDonough, W.F. & Chappell, B.W., 1993. Carbonatite metasomatism in the northern Tanzanian mantle: petrographic and geochemical characteristics. *Earth and planetary Science Letters* **114:** 463-475.

Russel, J.K., Groat, L.A. & Halleran, A.A.D., 1994. LREE-rich niobian titanite from Mount Bison, British Columbia: chemistry and exchange reactions. *Canadian Mineralogist* **32:** 575-587.

Ryerson, F.J. & Hess, P.C., 1978. Implications of liquid-liquid distribution coefficients to mineral-liquid partitioning. *Geochimica et Cosmochimica Acta* **42:** 921-932.

Schock, H.H., 1979. Distribution of rare-earth and other trace elements in magnetites. *Chemical Geology* **26:** 119-133.

Secher, K. & Larsen, M., 1980. Geology and mineralogy of the Sarfartôq carbonatite complex, southern West Greendland. *Lithos* **13:** 199-212.

Shannon, R.D., 1976. Revised effective ionic radii and systematic studies of interatomic distances in halides and chalcogenides. *Acta Crystallographica* **A32:** 751-767.

Sheidman, V.A., 1999. Nonuniversality of nucleation kinetics following a finite rate quench. *Journal of Geophysical Research* **E59:** 4441-4444.

Shimizu, N., 1981. Trace element incorporation into growing augite phenocrysts. *Nature* **289:** 575-577.

Simonetti, A., Bell, K. & Shrady, C., 1997. Trace and rare-earth-element geochemistry of the June 1993 natrocarbonatite lavas, Oldoinyo Lengai (Tanzania): implications for the origin of carbonatite magmas. *Journal of volcanology and geothermal research* **75:** 89-106.

Simonetti, A., Goldstein, S.L., Schmidberger, S.S. & Viladkar, S.G., 1998. Geochemical and Nd, Pb, and Sr isotope data from Deccan alkaline complexes – inferences for mantle sources and plume – lithosphere interaction. In: Bell, K., Kjarsgaard, B.A. & Simonetti, A. (eds). Carbonatites – Into the twenty first century. *Journal of Petrology* **39:** 1847-1864.

Sparks, R.S.J., Huppert, H.E. & Turner, F.R.S., 1984. The fluid dynamics of evolving magma chambers. *Philosophical Transactions of the Royal Society of London* **A310:** 511-534.

Spedding, P.L. & Mills, R., 1965. Trace-ion diffusion in molten alkali carbonates. *Journal of Electrochemistry Society* **112:** 594.

Spera, F.J., 1980. Aspects of magma transport. In: Hargraves, R.B. (ed.). Physics of Magmatic Processes. *Princeton University Press, Princeton*, p. 265-323.

Sweeney, R.J., Falloon, T.J. & Green, D.H., 1995a. Experimental constraints on the possible mantle origin of natrocarbonatite. In: Bell, K. & Keller, J. (eds). Carbonatite volcanism: Oldoinyo Lengai and the petrogenesis of natrocarbonatites. *Springer-Verlag, Berlin*, pp. 191-207.

Sweeney, R.J., Green, D.H. & Sie, S.H., 1992. Trace and minor element partitioning between garnet and amphibole and carbonatitic melt. *Earth and Planetary Science Letters* **113:** 1-14.

Sweeney, R.J., Prozesky, V. & Przybylowicz, W., 1995b. Selected trace and minor element partitioning between peridotite minerals and carbonatite melts at 18-46 kb pressure. *Geochimica et Cosmochimica Acta* **59:** 3671-3683.

Takahashi, E., 1978. Partitioning of Ni^{2+}, Co^{2+}, Fe^{2+}, Mn^{2+}, and Mg^{2+} between olivine and silicate melts: composition depedence of partition coefficients. *Geochimica et Cosmochimica Acta* **42:** 1829-1844.

Taylor, H.P.Jr., Frechen, J. & Degens, E.T., 1967. Oxygen and carbon isotope studies of carbonatites from the Laacher See district, West Germany and Alnö district, Sweden. *Geochimica and Geochimica Acta* **31:** 407-430.

Thibault, Y., Edgar, A.D. and Lloyd, F.E., 1992. Experimental investigations of melts produced from a carbonated phlogopite lherzolite: Implications for metasomatism in the continental lithospheric mantle. *American Mineralogist* **77:** 784-794.

Tilton, G.R. & Bell, K., 1994. Sr-Nd-Pb isotope relationships in Late Archaen carbonatites and alkaline complexes: applications to the geochemical evolution of the Archean mantle. *Geochimica et Cosmochimica Acta* **58:** 3145-3154.

Toulmin, P. III & Barton, P.B. Jr., 1964. A thermodynamic study of pyrite and pyrrhotite. *Geochimica et Cosmochimica Acta* **28:** 641-671.

Treiman, A.H., 1989. Carbonatite magma: properties and processes. In: Bell, K. (Ed.). Carbonatites. Genesis and evolution. *Unwin Hyman, London*, pp. 89-104.

Turner, D.C., 1988. Volcanic carbonatites of the Kaluwe complex, Zambia. *Journal of the Geological Society of London* **145:** 95-106.

Twyman, J.D. & Gittins, J., 1987. Alkalic carbonatite magmas: parental or derivative? In: Fitton, J.G. and Upton, B.G.J. (eds). Alkaline Igneous Rocks. *Geological Society Special Publication No. 30., Blackwell, London*, pp. 85-94.

Van Orman, J.A., Grove, T.L. & Shimizu, N., 1998. Uranium and thorium diffusion in diopside. *Earth and Planetary Science Letters* **160:** 505-519.

Veena, K., Pandey, B.K., Krishnamurthy, P. & Gupta, J.N., 1998. Pb, Sr and Nd isotopic systematics of the carbonatites of Sung Valley, Meghalaya, Northeast India: implications for contemporary plume-related mantle source characteristics. In: Bell, K., Kjarsgaard, B.A. & Simonetti, A. (eds). Carbonatites – Into the twenty first century. *Journal of Petrology* **39:** 1875-1884.

Veksler, I.V., Nielsen, T.F.D. & Sokolov, S.V., 1998a. Mineralogy of crystallized melt inclusions from Gardiner and Kovdor ultramafic alkaline complexes: implications for carbonatite genesis. In: Bell, K., Kjarsgaard, B.A. & Simonetti, A. (eds). Carbonatites – Into the twenty first century. *Journal of Petrology* **39:** 2015-2031.

Veksler I.V., Petibon C.M., Jenner G.A., Dorfman A.M. & Dingwell, D.B., 1998b. Partitioning of trace elements between immiscible silicate and carbonate liquids: an experimental study in the rotating centrifuge autoclave. *Journal of Petrology* **39:** 2095-2104.

Verwoerd, W.J., 1978. Liquid immiscibility and the carbonatite-ijolite relationship: preliminary data on the join $NaFe^{3+}Si_2O_6$-$CaCO_3$ and related compositions. *Carnegie Institution of Washington Yearbook* **77:** 767-774.

Vicenzi, E., Green, T. & Sie, S., 1994. Effect of oxygen fugacity on trace-element partitioning between immiscible silicate melts at atmospheric pressure: a proton and electron microscope study. In: Foley, S.F. & van der Laan, S.R. (eds). Trace-element partitioning with application to magmatic processes. *Chemical Geology* **117:** 355-360.

Viladkar, S.G. & Wimmenauer, W., 1986. Mineralogy and geochemistry of the Newania carbonatite-fenite complex, Rajasthan, India. *Neues Jahrbuch Mineral Abhandlungen* **156:** 1-21.

Walker, D., Beattie, P. & Jones, J.H., 1992. Partitioning of U-Th-Pb and other incompatibles between augite and carbonate liquid at 1200 °C and 55 kbar. *Eos* **72:** 574 (abstract).

Wall, F. & Mariano, A.N., 1996. Rare earth minerals in carbonatites: a discussion centred on the Kangankunde carbonatite, Malawi. In: Jones et al. (Ed.). Rare earth minerals: chemistry, origin and ore deposits. *Chapman & Hall, London*, pp. 193-225.

Wallace, M.E. and Green, D.H., 1988. An experimental determination of primary carbonatite magma composition. *Nature* **335:** 343-346.

Watkinson, D.H. and Wyllie, P.J., 1971. Experimental study of the join $NaAlSiO_4$-$CaCO_3$-H_2O and the genesis of alkalic rock-carbonatite complexes. *Journal of Petrology* **12:** 357-378.

Watson, E.B., 1977. Partitioning of manganese between forsterite and silicate liquid. *Geochimica et Cosmochimica Acta* **41:** 1363-1374.

Watson, E.B. & Green, T.H , 1981. Apatite/liquid partition coefficients for the rare earth elements and strontium. *Earth and Planetary Science Letters* **56:** 405-421.

Waychunas, G.A., Brown Jr, G.E., Ponader, C.W. & Jackson, W.E., 1988. Evidence from X-ray absorption for network-forming Fe^{2+} in molten alkali silicates. *Nature* **332:** 251-253.

Wendlandt, R.F. & Harrison, W.J., 1979. Rare earth partitioning between immiscible carbonatite and silicate liquids and CO_2 vapor: results and implications for the formation of light rare earth-enriched rocks. *Contributions to Mineralogy and Petrology* **69:** 409-419.

Wilding, M.C., 1998. High pressure melts receive attention at workshop. *Eos* **79:** 264.

Wolff, J.A., 1994. Physical properties of carbonatite magmas inferred from molten salt data, and application to extraction patterns from carbonatite-silicate magma chambers. *Geological Magazine* **131:** 145-153.

Wolff, J.A., 1984. Variation in Nb/Ta during differentiation of phonolitic magma, Tenerife, Canary Islands. *Geochimica et Cosmochimica Acta* **48:** 1345-1348.

Wood, B.J. & Fraser, D.G., 1976. Elementary thermodynamics for Geologists. *Oxford University Press, Oxford*, 303 p.

Woolley, A.R., 1989. The spatial and temporal distribution of carbonatites. In: Bell, K. (Ed.). Carbonatites. Genesis and evolution. *Unwin Hyman, London*, pp. 15-37.

Woolley, A.R., & Kempe, D.R.C., 1989. Carbonatites: nomenclature, average chemical compositions, and element distribution. In: Bell, K. (Ed.). Carbonatites. Genesis and evolution. *Unwin Hyman, London*, pp. 1-14.

Woolley, A.R., Williams, C.T., Wall, F., Garcia, D. & Moute, J., 1995. The Bingo carbonatite-ijolite-nepheline syenite complex, Zaire; geology, petrography, mineralogy and petrochemistry. *Journal of African Earth Sciences* **21:** 329-348.

Wyllie, P. J., 1984. Constraints imposed by experimental petrology on possible and impossible magma sources and products. *Philosophical Transactions of the Royal Society of London* **A310:** 439-456.

Wyllie, P.J., 1987. Transfer of subcratonic carbon into kimberlites and rare earth carbonatite. In: Mysen, B.O. (ed.). Magmatic Processes: Physicochemical Principles. *Geochemical Society Special Publication 1*. pp. 107-119.

Wyllie, P.J., 1989. Origin of carbonatites: Evidence from phase equilibrium studies. In: Bell, K. (Ed.). Carbonatites. Genesis and evolution. *Unwin Hyman, London*, pp. 500-545.

Wyllie, P.J. & Lee, W.-J., 1998. Model system controls on conditions of formation of magnesiocarbonatite and calciocarbonatite magmas from the mantle. In: Bell, K., Kjarsgaard, B.A. & Simonetti, A. (eds). Carbonatites – Into the twenty first century. *Journal of Petrology* **39:** 1885-1893.

Yaxley, G.M., Crawford, A.J. & Green, D.H., 1991. Evidence for carbonatite metasomatism in spinel peridotite xenoliths from Western Victoria, Australia. *Earth and Planetary Science Letters* **107:** 305-317.

APPENDICES

The appendices are divided according to the Chapters, *i.e.*, APPENDIX A.xxx refers to Chapter xxx (*e.g.*, APPENDIX A2 refers to Chapter 2).

For all crystal and liquid phases, the average compositions are calculated using "pureavg" and the standard deviation are calculated using "purestds", in order not to take into account the analyses which are below detection or not determined.

APPENDIX A2

Table A2.1: List of all experimental charges showing the bulk composition as proportion of wollastonite nephelinite HOL14 /silicate-bearing natrocarbonatite OL5 (in wt. %), the pressure (P), the temperature (T) and the run time (in hours) at which samples were performed. Moreover, open-tube and C/CH4 buffered experiments are indicated.

Sample	Bulk composition	P (MPa)	T (C)	Time (h)	Other
CP1	HOL14(50)OL5(50)	40	800	68	
CP2	HOL14(90)OL5(10)	40	800	68	
CP5	HOL14(90)OL5(10)	100	800	68	
CP7	HOL14(50)OL5(50)	103	700	146	
CP8	HOL14(90)OL5(10)	103	700	146	
CP10	HOL14(50)OL5(50)	40	700	165	
CP11	HOL14(90)OL5(10)	40	700	165	
CP13	HOL14(50)OL5(50)	100	800	68	
CP14	HOL14(50)OL5(50)	20	800	68	
CP15	HOL14(90)OL5(10)	20	800	68	
CP16	HOL14(50)OL5(50)	20	700	166	
CP17	HOL14(90)OL5(10)	20	700	166	
CP18	HOL14(50)OL5(50)	40	900	38	
CP19	HOL14(90)OL5(10)	40	900	38	
CP20	HOL14(50)OL5(50)	100	900	4:15	
CP21	HOL14(90)OL5(10)	100	900	4:15	
CP22	HOL14(50)OL5(50)	20	900	6:45	
CP23	HOL14(90)OL5(10)	20	900	6:45	
CP27	HOL14(90)OL5(10)	40	800	88	CH4/C buffer
CP31	HOL14(90)OL5(10)	100	700	410:30	CH4/C buffer
CP38	HOL14	100	900	6:15	
CP40	HOL14	20	850	46	
CP41	HOL14(95)OL5(5)	20	850	46	
CP42	HOL14(90)OL5(10)	20	850	46	
CP43	HOL14(70)OL5(30)	20	850	46	
CP45	OL5	20	850	46	
CP46	HOL14	20	750	116:30	
CP47	HOL14(95)OL5(5)	20	750	116:30	
CP48	HOL14(90)OL5(10)	20	750	116:30	
CP50	HOL14(50)OL5(50)	20	750	116:30	
CP51	OL5	20	750	116	
CP52	HOL14(80)OL5(20)	20	850	42:15	
CP53	HOL14(50)OL5(50)	20	850	42:15	
CP54	HOL14	20	700	164	
CP55	HOL14(95)OL5(5)	20	700	164	
CP57	OL5	20	700	164	
CP60	HOL14	20	800	109:30	
CP61	OL5	20	800	109	
CP64	HOL14(80)OL5(20)	20	700	476	
CP65	HOL14(50)OL5(50)	20	700	476	
CP66	HOL14(80)OL5(20)	100	700	479	

Table A2.1 (suite).

CP67	HOL14(70)OL5(30)	100	700	479	
CP68	HOL14(80)OL5(20)	40	700	479	
CP69	HOL14(70)OL5(30)	40	700	479	
CP72	HOL14	100	700	190	
CP74	HOL14	100	800	64	
CP78	HOL14(90)OL5(10)	100	800	116	Open-tube
CP79	OL5	100	800	116	
CP80	OL5	20	775	65	
CP81	HOL14(10)OL5(90)	20	775	65	
CP82	HOL14(10)OL5(90)	20	900	04:20	
CP88	OL5	100	900	4:30	
CP89	HOL14(10)OL5(90)	100	900	4:30	
CP90	OL5	20	900	4	
CP91	HOL14(80)OL5(20)	20	900	4	
CP92	HOL14(80)OL5(20)	100	900	4	
CP93	HOL14(20)OL5(80)	100	900	4	
CP96	OL5	100	750	382	
CP97	HOL14(20)OL5(80)	100	750	382	
CP98	OL5	100	700	161	
CP102	HOL14(80)OL5(20)	100	800	382	
CP103	HOL14(10)OL5(90)	100	800	382	
CP106	OL5	100	850	20	
CP107	OL5	100	600	114	
CP108	OL5	20	600	114	
CP109	HOL14(80)OL5(20)	200	750	200	
CP110	HOL14	20	900	4	
CP111	HOL14(20)OL5(80)	20	900	4	
CP112	OL5	20	550	88	
CP113	HOL14(80)OL5(20)	20	800	67	
CP114	HOL14(20)OL5(80)	20	800	67	
CP115	HOL14(20)OL5(80)	20	750	88	
CP117	HOL14(10)OL5(90)	100	700	87	
CP118	OL5	100	625	87	
CP120	HOL14(40)OL5(60)	20	900	4	
CP121	HOL14(30)OL5(70)	20	900	4	
CP122	HOL14(40)OL5(60)	20	800	39	
CP123	HOL14(30)OL5(70)	20	800	39	
CP124	HOL14(40)OL5(60)	20	750	95	
CP125	HOL14(30)OL5(70)	20	750	95	
CP126	OL5	20	575	114	
CP127	OL5	100	550	114	
CP128	OL5	100	575	255	
CP129	OL5	20	625	236	
CP130	HOL14(20)OL5(80)	20	850	28	
CP131	HOL14(10)OL5(90)	20	850	28	

Table A2.2: Individual major element electron microprobe analyses of groundmass (GMASS), nyerereite (NY) and gregoryite (GRE) in silicate-free natrocarbonatite CML5 (in wt. %).

Sample	SiO2	TiO2	Al2O3	FeO	MnO	MgO	CaO	Na2O	K2O	P2O5	F	Cl	SO3	BaO	SrO	Total
Groundmass																
GMASS, 1	0.4	.03<	-.1<	.1<	0.7	1.2	11.3	27.3	6.2	0.7	3.2	2.2	2.8	3.5	2.0	61.5
GMASS, 2	0.3	0.04	.0<	.1<	.1<	0.3	12.6	27.4	7.9	0.5	2.8	5.2	2.6	1.4	1.6	62.6
GMASS, 3	0.3	-.00<	.0<	.1<	.1<	.1<	13.8	29.6	5.3	0.7	2.2	1.8	2.9	.3<	1.3	57.9
GMASS, 4	0.4	.03<	-.0<	*0.7	0.6	0.6	12.3	26.3	8.9	0.3	2.2	5.1	3.3	2.8	1.6	64.4
GMASS, 5	0.3	.02<	.1<	.1<	.1<	.2<	11.7	28.4	6.8	0.6	1.3	3.5	2.7	1.0	1.3	57.6
GMASS, 6	0.2	.01<	-.0<	-.0<	.1<	0.7	11.5	28.0	5.9	0.7	2.2	2.2	2.6	2.3	1.7	58.0
GMASS, 7	0.3	0.06	-.0<	.0<	0.3	0.6	11.2	27.8	8.1	0.6	1.6	3.9	2.8	2.9	1.9	62.1
GMASS, 8	0.3	.02<	-.0<	.2<	0.3	1.0	10.8	26.6	9.3	0.7	2.1	4.8	2.4	3.3	2.1	63.7
GMASS, 9	0.4	.03<	.1<	.1<	.1<	.2<	11.0	29.2	8.9	0.7	1.9	6.0	2.9	0.5	1.0	62.5
GMASS, 10	0.2	.03<	.0<	-.0<	.2<	0.4	11.1	28.0	7.6	0.5	1.1	3.3	2.5	1.2	1.3	57.2
GMASS, 11	0.3	.00<	0<	.1<	.2<	0.5	11.7	27.5	6.9	0.6	1.9	3.0	2.7	1.6	1.5	58.2
Nyerereite																
NY1				.1<	.1<	.1<	32.1	15.4	10.0	0.5	0.2	0.2	0.9	0.9	3.0	63.2
NY2				-.0<	-.0<	.0<	31.9	14.8	9.8	0.5	.1<	0.2	1.1	0.7	3.0	62.0
NY3				.0<	.2<	.1<	32.2	15.7	9.9	0.6	0.1	0.2	1.1	0.8	3.1	63.7
NY4				.1<	.1<	.2<	31.2	14.9	9.8	0.4	.1<	0.2	1.1	1.7	3.4	62.7
NY5				.1<	.2<	.1<	32.7	13.9	9.2	0.6	0.2	0.2	1.3	0.8	3.0	61.9
NY6				-.0<	*0.3	-.1<	32.7	13.8	10.1	0.5	.1<	0.2	1.1	0.8	3.2	62.4
NY7				.0<	.1<	.1<	32.7	13.8	9.9	0.4	0.2	0.2	1.2	0.9	3.0	62.1
NY8				-.1<	.1<	.1<	33.0	14.0	9.8	0.5	.1<	0.2	1.1	0.8	3.0	62.2
NY9				*0.3	-.0<	.0<	32.7	14.1	9.5	0.3	0.2	0.2	1.1	0.8	2.8	61.7
NY10				-.0<	.1<	.0<	32.7	14.2	9.6	0.6	0.2	0.2	1.1	0.9	3.1	62.6
NY11				-.0<	.2<	-.0<	32.4	14.4	9.6	0.6	-.0<	0.2	1.0	1.0	3.0	62.2
NY12				-.0<	.1<	.2<	32.6	14.0	9.6	0.5	.1<	0.2	1.2	0.7	2.9	61.7
NY13				.1<	.0<	.1<	32.4	14.2	9.6	0.7	0.2	0.2	1.1	1.1	3.0	62.5
NY14				.1<	.1<	-.1<	32.5	13.9	9.4	0.4	0.3	0.2	1.1	0.6	3.0	61.4
NY15				.1<	.1<	-.0<	32.6	14.0	9.6	0.5	0.2	0.1	1.1	1.0	3.2	62.3
NY16				.1<	.0<	.1<	32.8	14.1	9.7	0.5	0.2	0.2	1.0	0.7	3.2	62.4
Gregoryite																
GRE1				.0<	.1<	.1<	10.5	29.9	5.0	2.2	0.2	0.5	5.2	0.6	0.8	54.9
GRE2				-.1<	.2<	.1<	8.4	35.3	4.8	2.7	0.3	0.6	6.1	.3<	0.6	58.8
GRE3				.1<	.0<	.1<	12.5	33.8	5.7	2.5	0.2	0.4	5.2	0.6	1.2	62.1
GRE4				-.0<	.1<	.1<	7.3	38.2	3.9	3.1	0.1	1.0	4.5	.2<	0.7	58.9
GRE5				.0<	.1<	.2<	9.5	38.8	4.9	2.9	0.1	0.6	4.8	0.4	0.9	62.9
GRE6				-.0<	.1<	-.0<	8.8	39.5	4.5	3.2	.1<	0.6	4.8	0.4	0.8	62.6
GRE7				.0<	.1<	*0.3	10.5	38.4	4.8	3.0	0.2	0.5	4.6	0.4	0.9	63.3
GRE8				.0<	.1<	*0.2	12.0	33.2	4.8	3.1	0.1	0.5	4.1	1.0	1.5	60.3
GRE9				.1<	.1<	.2<	11.1	38.1	5.9	2.5	0.4	0.6	5.1	0.4	1.1	65.2
GRE10				.1<	*0.2	.1<	12.1	36.5	5.1	2.6	0.3	0.4	4.5	0.5	1.0	63.0
GRE11				.1<	-.0<	.1<	9.1	39.5	4.7	2.6	.1<	0.5	4.8	0.4	0.8	62.4
GRE12				.1<	-.0<	.0<	10.9	35.9	5.4	2.5	0.1	0.5	4.6	0.3	0.8	61.0
GRE13				.1<	.2<	.2<	8.5	40.3	4.5	2.6	0.2	0.5	4.9	.3<	0.6	62.1
GRE14				-.1<	.1<	.2<	10.2	38.5	5.4	2.8	0.2	0.5	4.8	0.6	1.0	64.0
GRE15				.0<	-.1<	.1<	8.3	38.6	5.0	2.8	0.2	0.8	5.2	.2<	0.7	61.6

Asterixes (*) indicate the analyses that were rejected.

Propagation of error

Generalities (from Henry Longerich)

The most realistic case is for indeterminate or random error.
For R = f (A, B, C)

$$dR = \frac{\partial R}{\partial A}\, dA + \frac{\partial R}{\partial B}\, dB + \frac{\partial R}{\partial C}\, dC$$

If the variations are small such that they do not effect the partials, then approximately:

$$\Delta_R = \frac{\partial R}{\partial A}\, \Delta_A + \frac{\partial R}{\partial B}\, \Delta_B + \frac{\partial R}{\partial C}\, \Delta_C$$

squaring both sides:

$$\Delta_R^2 = \left(\frac{\partial R}{\partial A}\, \Delta_A \right)^2 + \left(\frac{\partial R}{\partial B}\, \Delta_B \right)^2 + \left(\frac{\partial R}{\partial C}\, \Delta_C \right)^2 +$$

$$2 \left(\frac{\partial R}{\partial A}\, \frac{\partial R}{\partial B}\, \Delta_A\, \Delta_B \right) + 2 \left(\frac{\partial R}{\partial A}\, \frac{\partial R}{\partial C}\, \Delta_A\, \Delta_C \right) + 2 \left(\frac{\partial R}{\partial B}\, \frac{\partial R}{\partial C}\, \Delta_B\, \Delta_C \right)$$

If measurements are repeated N times, then:

$$(\Delta_X^2)_{Average} = \sigma_X^2$$

and if the variables are uncorrelated then the average is zero:

$$(\Delta_A \Delta_B)_{Average} = 0$$

and then it follows that:

$$\sigma_R^2 = \left(\frac{\partial R}{\partial A} \sigma_A \right)^2 + \left(\frac{\partial R}{\partial B} \sigma_B \right)^2 + \left(\frac{\partial R}{\partial C} \sigma_C \right)^2$$

If the operators are addition and/or subtraction *e. g.*:
R = A + B - C
all the partials are equal to 1, and it follows that:

$$\sigma_R^2 = \sigma_A^2 + \sigma_B^2 + \sigma_C^2$$

If the operators are multiplication and/or division *e. g.*:

$$R = \frac{A\ B}{C}$$

$$\sigma_R^2 = \left(\frac{B}{C} \right)^2 \sigma_A^2 + \left(\frac{A}{C} \right)^2 \sigma_B^2 + \left(- \frac{A\ B}{C^2} \right)^2 \sigma_C^2$$

$$\left(\frac{\sigma_R}{R} \right)^2 = \left(\frac{\frac{B}{C}}{\frac{A\ B}{C}} \right)^2 \sigma_A^2 + \left(\frac{\frac{A}{C}}{\frac{A\ B}{C}} \right)^2 \sigma_B^2 + \left(\frac{-\frac{A\ B}{C^2}}{\frac{A\ B}{C}} \right)^2 \sigma_C^2$$

$$\left(\frac{\sigma_R}{R} \right)^2 = \left(\frac{\sigma_A}{A} \right)^2 + \left(\frac{\sigma_B}{B} \right)^2 + \left(\frac{\sigma_C}{C} \right)^2$$

Application to the data from the thesis

Sources of uncertainty:

A – Electron microprobe analyses

A1: Electron microprobe analyses of crystals: for homogeneous crystals, the uncertainty is analytical, and can be measured on reference standards. To determine the analytical precision, a run of 20 analyses of periclase, corundum, wollastonite and hematite was performed, indicating relative standard deviations of 0.4 % to 0.7 % for Mg, Al, Si, Ca and Fe. In the calculations, I assume that the RSD for CaO is 0.5 %. For heterogeneous crystals, RSD_{CaO} calculated as 1 σ/concentration (with 1σ = 1 standard deviation of the mean) would be higher than 0.5 %.

A2: Electron microprobe analyses of carbonate liquid: most of the uncertainty is due to the heterogeneity of the carbonate liquid (quenched texture). It is not analytical and measurable on standards, it depends on the heterogeneity of each sample and on how many analyses are performed. I measure 1 standard deviation of the mean (σ) on different analyses (and then RSD = 1 σ/concentration). This uncertainty also includes part of the analytical uncertainty, but because carbonate liquid is so heterogeneous, the analytical uncertainty is small compared to the uncertainty due to the texture of the sample. For CaO in carbonate liquid, standard deviation of the mean (1 σ) is usually ~ 1-2 %, concentration ~ 15 wt. % and RSD for CaO is usually ~ 10-15 %. The RSD on CaO is not as high as some other elements because its absolute concentration is high and because nyerereite and gregoryite, which are the main quenched crystals, contain a large amount of CaO.

B – LAM-ICP-MS analyses

B1: LAM-ICP-MS analyses of crystals: There are three main sources of uncertainty: 1) part of the uncertainty comes from the fact that there is an uncertainty in the CaO concentration that is used as internal standard (obtained by electron microprobe analysis); 2) another source of uncertainty is analytical, and can be measured on reference standards. The precision has been measured for trace elements on reference standards BCR-2 and NIST 612, and the RSD was found to be ~ 3-10 % for most elements; 3) another source of uncertainty comes from the surface spray from previous analyses, *e.g.* carbonate or silicate liquid might spray on the surface of crystals. This is not a random error, it is systematic (unidirectional), and therefore it should not be taken into account when doing the propagation of error calculation. Moreover, heterogeneity of the crystals would increase RSD_i calculated as 1 σ/concentration (with 1σ = 1 standard deviation of the mean).

B2: LAM-ICP-MS analyses of carbonate liquid: Like for electron microprobe analyses, most of the uncertainty is due to the heterogeneity of the sample. It is not analytical and

measurable on standards, it depends on the heterogeneity of each sample and on how many analyses are performed. I measure 1 standard deviation of the mean (σ) on different analyses (and then RSD = 1 σ/concentration). This uncertainty also includes part of the analytical uncertainty (measurable on standards), but because carbonate liquid is so heterogeneous, the analytical uncertainty is small compared to the uncertainty due to the texture of the sample. I calculate 1 σ and RSD for each trace element for each sample. For most trace elements, the RSD is very high, much higher than the RSD for CaO which was found to be ~ 10-15 %. A second source of uncertainty comes from the fact that there is uncertainty on the CaO concentration that is used for the internal standard.

Comment 1: Silicate liquid: When several analyses of silicate liquid are performed, 1 standard deviation of the mean (σ) can be measured between different analyses. If this uncertainty is higher than the analytical uncertainty (measured on crystals) because the glass is not perfectly homogeneous, it should be used. However, if the silicate liquid is homogeneous, then 1 standard deviation of the mean (σ) measured between different analyses is low, and the analytical uncertainty (measured on crystals) should be used.

Comment 2: The propagation of error calculation that I plan to undertake takes into account the uncertainty due to analytical precision and heterogeneity of liquid (and crystal) phases. It does not take care of systematic errors that are unidirectional and that include:

1) uncertainty in the accuracy of concentrations of major and trace elements in probe and LAM-ICP-MS calibrations standards. Accuracy is "measured" on reference standards, but discrepancies (or similarities) compared to literature values could be due to calibration or reference standards. Because accuracy of standards should be within 2 %, and because calibration standards affect all analyses the same way, this is not a problem;

2) volatilisation associated with probe analyses – systematic, affects only a few elements, excluding CaO;

3) bias compared to Belanger (ICP-ES) – systematic, affects only a few elements, excluding CaO;

4) systematic error due to on the surface of crystals – depends on each analysis, *i.e.* contaminating material, amount of contaminating material, time analysis. In fact, part of this error is taken into account when RSD is calculated as 1 σ/concentration (with 1σ = 1 standard deviation of the mean).

Moreover, there is also an uncertainty on concentration Primitive Mantle (PM) that we do not take into account. And what we call "standard deviation" is only an estimate of the standard deviation, because we do not have an infinity of samples.

How do we calculate RSD's/plot error bars?

A: On trace element concentration plots (normalised to PM)

A1 – Trace element crystals

Example: homogeneous clinopyroxene containing 20 wt. % CaO analysed by electron microprobe first → RSD = 0.5 %.

Then LAM-ICP-MS analysis → $C_{Ba,cpx} = R_{Ba,cpx}/S$ (S is the sensitivity)

→ $C_{Ba,\,cpx} = R_{Ba,\,cpx} * (C_{Ba,NIST610} * R_{Ca,NIST610} * C_{Ca,\,cpx}) / (R_{Ba,NIST610} * R_{Ca,\,cpx} * C_{Ca,NIST610})$

Most of the uncertainty comes from combined $R_{Ba,NIST610}$, $R_{Ca,NIST610}$, $R_{Ba,samp}$ and $R_{Ca,samp}$. I measured 1 σ (standard deviation of the mean) for the different trace elements on numerous analyses of BCR-2 and NIST 612, using NIST 610 as the external standard. For example, RSD is around 6 % for Ba and 3 % for Ce. This uncertainty is an estimate of the uncertainty from combined $R_{Ba,NIST610}$, $R_{Ca,NIST610}$, $R_{Ba,samp}$ and $R_{Ca,samp}$. I will call the RSD due to the combination of these 4 count rates $RSD_{R,Ba}$ when Ba is the element considered. The uncertainty on $C_{Ca,samp}$ is 0.5 % (from probe). The uncertainties on $C_{Ba,NIST610}$ and $C_{Ca,NIST610}$ are systematic and is not taken into account in calculation (but concentrations should be accurate within 2 %).

→ $(RSD\ C_{Ba,cpx})^2 = (RSD_{R,Ba})^2 + (RSD_{Ca,cpx})^2$.

→ If $RSD_{R,Ba}$ = 6 % and $RSD_{Ca,cpx}$ = 0.5 %, then RSD $C_{Ba,cpx}$ = 6.02 %, in other words RSD $C_{Ba,cpx}$ = 6 % and uncertainty due to probe does not weigh much.

A2 – Trace element carbonate liquid

Example: carbonate liquid sample CP107.

First step = probe analysis. Most of the uncertainty is due to the heterogeneity of the sample → measure 1 standard deviation of the mean (σ) between different analyses (and then RSD = 1 σ/concentration). This uncertainty also includes minor analytical uncertainty. For CaO in carbonate liquid of experiment CP107, standard deviation (1 σ) is 2.2 % and RSD is 15 %.

Second step = LAM-ICP-MS analysis → $C_{Ba,samp} = R_{Ba,samp}/S$

→ $C_{Ba,samp} = R_{Ba,samp} * (C_{Ba,NIST610} * R_{Ca,NIST610} * C_{Ca,samp}) / (R_{Ba,NIST610} * R_{Ca,samp} * C_{Ca,NIST610})$

Most of the uncertainty comes from combined $R_{Ba,NIST610}$, $R_{Ca,NIST610}$, $R_{Ba,samp}$ and $R_{Ca,samp}$. The uncertainty due to this term is approximated by 1 standard deviation of the mean (σ) between different analyses (measured for each trace element), since the carbonate liquid is extremely heterogeneous. The high value of 1 σ is mostly due to the heterogeneity of the sample (*i.e.*, dominated by $R_{Ba,samp}$), but it also includes part of the minor analytical uncertainty (see A1 – Trace element crystals). When 1 σ so measured happens to be less than 1 σ measured on different analyses of BCR-2 and NIST 612, I should have to use this latter value. Like for crystals, I will call the RSD due to the combination of these 4 count rates $RSD_{R,Ba}$ when Ba is the element considered. The uncertainty on $C_{Ca,samp}$ is usually 10-15 % (from probe), 15 % for LC in CP107. The uncertainties on $C_{Ba,NIST610}$ and $C_{Ca,NIST610}$ are systematic and is not taken into account in calculation (but concentrations should be accurate within 2 %).

→ $(RSD\ C_{Ba,LC})^2 = (RSD_{R,Ba})^2 + (RSD_{Ca,LC})^2$.

→ If RSD_{Ba} = 12 % and $RSD_{Ca,LC}$ = 15 %, then RSD $C_{Ba,LC}$ = 20 %.

A3 – Trace element silicate liquid: depending on the homogeneity of the silicate liquid, the calculation should be carried out according to case A1 (same as crystals) or case A2 (same as carbonate liquid).

B: Distribution coefficients

B1 – $D_{crystal/LC}$ (major elements on a few Onuma diagrams)

$D_{crystal/LC} = C_{crystal}/C_{LC}$.

If we take the example of $D_{crystal/LC}$ for Ca in experiment CP107:
The RSD should be dominated by the term due to the heterogeneity of the carbonate liquid. I measured 1 standard deviation of the mean (σ) on different analyses (and then RSD = σ/concentration). This uncertainty also includes minor analytical uncertainty. For CaO in carbonate liquid of experiment CP107, standard deviation (1 σ) is 2.2 % and RSD is 15 %.

B2 – $D_{LS/LC}$ (major elements - partitioning trends)
$D_{LS/LC} = C_{LS}/C_{LC}$.
If silicate liquid fairly homogeneous, the calculation is the same as calculation for $D_{crystal/LC}$.
If silicate liquid heterogeneous, then, like for carbonate liquid, we calculate 1 standard deviation of the mean (σ) between different analyses (and then RSD = σ/concentration). This uncertainty also includes minor analytical uncertainty, and then:
$(RSD\ D_{LS/LC})^2 = (RSD\ C_{LS})^2 + (RSD\ C_{LC})^2$

C: Partition coefficients

C1 – $D_{crystal/liquid}$ (trace elements, D-patterns, Onuma diagrams)
$D_{crystal/LC} = C_{crystal}/C_{LC}$.
If we take the example of $D_{crystal/LC}$ for Ba in experiment CP107:

$$D^{Ba}_{crystal/LC} = [R_{Ba,xal}*(\underline{C_{Ba,NIST610}}* R_{Ca,NIST610}* C_{Ca,xal})/(R_{Ba,NIST610}* R_{Ca,xal}* \underline{C_{Ca,NIST610}})]/ [R_{Ba,LC}*(\underline{C_{Ba,NIST610}}* R_{Ca,NIST610}* C_{Ca,LC})/(R_{Ba,NIST610}* R_{Ca,LC}* \underline{C_{Ca,NIST610}})]$$

From what was said before, we expect most of the contribution to the uncertainty for crystals to be due to combined R terms (+ minor term due to uncertainty in internal standard CaO) → $(RSD\ C_{Ba,cpx})^2 = (RSD_{R,Ba,1})^2 + (RSD_{Ca,cpx})^2$. Also, from what was said before, we expect most of the contribution to the uncertainty for carbonate liquid to be due to combined R terms and to uncertainty in internal standard CaO → $(RSD\ C_{Ba,LC})^2 = (RSD_{R,Ba,2})^2 + (RSD_{Ca,LC})^2$.
As a result, $(RSD\ D^{Ba}_{crystal/LC})^2 = (RSD_{R,Ba,1})^2 + (RSD_{Ca,cpx})^2 + (RSD_{R,Ba,2})^2 + (RSD_{Ca,LC})^2$.
→ If $RSD_{R,Ba,1}$ = 6 %, $RSD_{Ca,cpx}$ = 0.5 %, $RSD_{R,Ba,2}$ = 12 % and $RSD_{Ca,LC}$ = 15 %, then $RSD\ D^{Ba}_{crystal/LC}$ = 21% (dominated by LC).

C2 – $D_{LS/LC}$ (D-patterns, partitioning trends)
$(RSD\ D^{Ba}_{LS/LC})^2 = (RSD_{R,Ba,1})^2 + (RSD_{Ca,LS})^2 + (RSD_{R,Ba,2})^2 + (RSD_{Ca,LC})^2$.
If silicate liquid homogeneous, the calculation is the same as for $D_{crystal/LC}$, *i.e.* $RSD_{R,Ba,1}$ calculated as 1 σ for different trace elements on numerous analyses of BCR-2 and NIST 612 (using NIST 610 as the external standard).
If silicate liquid heterogeneous, then $RSD_{R,Ba,1}$ calculated in a similar way as $RSD_{R,Ba,2}$, *i.e.* 1 standard deviation of the mean (σ) between different analyses (measured for each trace element).

Other comments:
1) The error bars will be plotted as ± 1 σ.

2) For some phases in some samples, there is only one analysis available, and if the phase is not homogeneous, we have to assume a value for standard deviation and RSD, by interpolating the RSD's compared to the RSD's of other elements in the same phase (and taking into account the concentration of the elements because elements in lower abundance usually have higher RSD's).

Example of calculation

Here I present the most complicated case of propagation of error, in order to illustrate as many points as possible that have been spoken about in the text above. This is the case of calculating 1 σ for $D_{cpx/CEL}$ (clinopyroxene/calculated equivalent liquid) in silicate-bearing natrocarbonatite OL5.
This case is slightly more complicated than for $D_{cpx/carbonate\ liquid}$ in experiments because for an element i in CEL that is contained in different phases I (with I = 1 to n) → $conc_i$ CEL = sum (X_ICEL * $conc_i$ I), and standard deviation (X_ICEL * $conc_i$ I) = X_ICEL * standard deviation ($conc_i$ I).

Details of the calculation are given in Table A2.3 and error bars for $D_{cpx/CEL}$ in silicate-bearing natrocarbonatite OL5 are presented in Figure A2.1. Comments concerning this calculation are given below:
Probe clinopyroxene: RSD_{Ca} calculated as 1 σ/concentration (with 1σ = 1 standard deviation of the mean) is higher than 0.5 % because the clinopyroxene crystal is not perfectly homogeneous.
Probe phases in CEL: for nyerereite and garnet, RSD_{Ca} calculated as 1 σ/concentration (with 1σ = 1 standard deviation of the mean) happened to be lower than 0.5 %, so I recalculated STDS for a RSD value of 0.5 %. Only one analysis of each gregoryite phenocrysts and wollastonite microphenocrysts was performed. Because these two crystals are expected to be heterogeneous, I chose a RSD value of 5 % instead of 0.5 % (value for homogeneous phases). For CEL, I obtained $STDS_{CaO}$ = 0.91 % and RSD_{CaO} = $STDS_{CaO}$ / $conc_{CaO}$ = 5.52 %.

LAM-ICP-MS clinopyroxene: RSD_i calculated as 1 σ/concentration (with 1σ = 1 standard deviation of the mean) are fairly high because the clinopyroxene crystal is not perfectly homogeneous.

LAM-ICP-MS phases in CEL: some RSD values were missing, so I assumed a value for these based on the abundance of the elements and the RSD's of the other elements. These values are underlined in the table.

Note that once the standard and relative standard deviations of the CEL are determined, the calculation is similar to that for carbonate liquid from the experiments.

Tab A2 3 Calculation of propagation of error on 1 standard deviation on the mean for trace element partition coefficients between clinopyroxene and calculated equivalent liquid (CEL) in silicate-bearing natrocarbonatite OL5

Major elements	nb analyses	STDS	RSD			
cpx	8	1.5	7 10%			
CEL				norm prop	prop	RSD was
gmass	8	3 78	22 30%	0 232988	0 19	
NY	3	0 117021	0 50%	0 331085	0 27	0 47%
GRE	1	0 49	5 00%	0 415083	0 3385	
gmass sph	4	1 05	4 30%	0 014715	0 012	
ne mph	2	1 77	5 40%	0 001226	0 001	
cpx mph	8	0 91	4 50%	0 001226	0 001	
gt mph	2	0 150091	0 50%	0 001226	0 001	0 27%
wo mph	1	2 36	5 00%	0 001226	0 001	
gre mph	2	1 47	3 20%	0 001226	0 001	
					0 8155	
		s d CEL	RSD CEL			
		0 91	5 52%			

Trace elements		MgO	Al2O3	SiO2	CaO	CaO	TiO2	Ba	Sr	Rb	Y	V	U	Th	Nb	Ta	Zr	Hf
cpx	16	3 45	0 58	4 33	0 53	1 15	0 19	2 49	242 45	0 23	1 16	104 02	0 13	0 01	0 38	0 03	108 81	2 91
RSD		61 10%	45 24%	9 55%	2 56%	5 48%	30 82%	101 93%	39 63%	55 19%	23 20%	43 46%	108 29%	47 35%	48 48%	57 41%	23 78%	28 95%
CEL																		
gmass	10	0 15	0 28	0 14	n d	1 15	0 06	4221 88	1525 45	74 83	10 12	88 78	4 08	8 04	53 80	0 35	25 34	0 35
		10 07%	27 20%	3 06%	n d	8 83%	43 42%	44 13%	14 25%	40 58%	33 40%	51 48%	28 82%	34 69%	35 08%	48 07%	35 25%	39 54%
NY	5	0 02	0 01	n d	0 00	1 39	n d	1568 14	2744 75	15 80	1 26	2 84	0 35	0 51	3 10	0 02	1 48	0 08
		24 88%	70 71%	n d	0 00%	5 82%	n d	28 97%	17 58%	13 71%	41 77%	31 75%	84 88%	82 25%	88 40%	88 00%	88 33%	43 45%
GRE	4	0 03	n d	n d	0 00	0 49	n d	878 39	223 84	7 87	0 50	11 21	0 09	0 20	0 27	0 03	0 44	0 05
		27 85%	n d	n d	0 00%	4 47%	n d	28 97%	3 37%	12 88%	58 11%	19 78%	88 40%	100 37%	82 41%	25 71%	95 73%	75 88%
gmass sph	16	0 23	2 22	7 37	0 00	2 25	0 19	3225 88	5338 78	117 48	18 00	62 88	5 08	18 85	131 18	1 40	205 15	2 73
		58 28%	44 27%	32 62%	0 00%	9 80%	30 18%	87 88%	83 82%	52 54%	38 75%	35 35%	29 78%	45 30%	37 83%	38 40%	34 27%	34 20%
ne mph	14	0 09	0 07	5 17	n d	0 11	0 01	7 87	17 07	18 45	0 18	0 48	0 02	0 04	0 38	0 05	3 12	0 23
used ph		88 88%	0 23%	13 83%	n d	26 08%	50 85%	38 38%	18 27%	23 32%	84 38%	21 08%	81 24%	98 14%	72 42%	88 87%	80 18%	85 35%
cpx mph	8	2 83	0 44	5 10	0 00	1 07	0 15	14 88	181 58	0 58	2 08	40 26	0 14	0 11	2 88	0 07	103 74	3 53
		58 08%	27 52%	10 38%	0 00%	5 33%	30 70%	84 80%	32 04%	10 86%	36 72%	20 53%	97 88%	19 58%	84 30%	98 85%	30 18%	43 11%
gt mph	15	1 14	0 20	4 72	0 07	1 17	0 80	2 88	24 54	0 44	65 91	119 11	1 86	3 43	110 88	7 48	584 82	11 25
used Ph		91 23%	19 00%	15 75%	0 22%	3 83%	8 49%	80 85%	28 23%	49 13%	12 34%	14 05%	21 29%	24 77%	22 82%	23 88%	14 28%	15 18%
wo mph	3	n d	n d	n d	0 00	3 83	0 02	1 09	32 27	4 04	8 20	10 02	0 02	0 06	0 80	0 01	22 82	0 28
		n d	n d	n d	0 00%	8 54%	18 45%	10 00%	3 51%	85 45%	8 66%	30 00%	50 00%	50 00%	31 27%	50 00%	78 58%	57 72%
gre mph	4	0 03	n d	n d	0 00	0 49	n d	878 39	223 84	7 87	0 50	11 21	0 09	0 20	0 27	0 03	0 44	0 05
used Ph		27 85%	n d	n d	0 00%	4 47%	n d	28 97%	3 37%	12 88%	58 11%	19 78%	88 40%	100 37%	82 41%	25 71%	95 73%	75 88%
standard deviation CEL		0 04	0 07	0 11	0 00	0 57	0 01	1182 88	883 33	18 80	2 42	23 75	1 42	1 80	12 88	0 09	8 88	0 10
conc CEL								5563 81	10549 01	110 19	8 81	75 62	5 22	8 34	42 85	0 31	32 28	0 51
RSD CEL								21 30%	8 32%	18 88%	24 43%	31 41%	27 31%	30 02%	28 58%	28 15%	20 75%	19 21%
RSD's																		
RSD cpx probe		7 10%	7 10%	7 10%	7 10%	7 10%	7 10%	7 10%	7 10%	7.10%	7 10%	7 10%	7 10%	7.10%	7 10%	7 10%	7 10%	7.10%
RSD cpx ICP		61 10%	45 24%	9 55%	2 56%	5 48%	30 82%	101 93%	39 63%	55 19%	23 20%	43 46%	108 29%	47 35%	48 48%	57 41%	23 78%	28 95%
RSD CEL probe		5 52%	5 52%	5 52%	5 52%	5 52%	5 52%	5 52%	5 52%	5 52%	5 52%	5 52%	5 52%	5 52%	5 52%	5 52%	5 52%	5 52%
RSD CEL ICP								21 30%	8 32%	18 88%	24 43%	31 41%	27 31%	30 02%	28 58%	28 15%	20 75%	19 21%
RSD Dcpx/CEL								105%	41%	58%	35%	54%	112%	57%	58%	65%	33%	36%
D cpx/CEL								0 0004	0 0585	0 0037	0 5055	3 1645	0 0237	0 0037	0 0171	0 171	14 1884	19 8886
1 sigma Dcpx/CEL								0 000418	0 034242	0 002161	0 176263	1 720405	0 026553	0 002101	0 009978	0 110413	4 848717	7 137322
D-1sigma								-1 8E-05	0 035258	0 001539	0 329237	1 444085	-0 00285	0 001588	0 007122	0 060587	9 519883	12 75128
D+1sigma								0 000818	0 083742	0 005881	0 681783	4 884805	0 050253	0 005801	0 027078	0 281413	18 81812	27 02942

Abbreviations used are s d standard deviation, CEL calculated equivalent liquid, gmass groundmass, NY nyererite, GRE gregoryite, gt garnet, cpx clinopyroxene, wo wollastonite, mph microphenocryst, sph spheroid, conc concentration, norm normalised, prop proportion Note underlined data are data that have been modified or interpolated

Tab A2 3 (suite)

Trace elements	La	Ce	Nd	Sm	Eu	Gd	Dy	Er	Yb	Lu
cps	1 36	3 78	3 80	0 84	0 14	0 60	0 34	0 40	0 42	0 13
RSD	16 85%	18 18%	30 63%	37 00%	23 28%	48 20%	38 01%	49 86%	27 34%	36 57%
CEL										
gmass	307 71	325 31	64 04	6 19	1 53	3 02	1 61	0 63	0 44	0 08
	39 32%	35 35%	30 36%	32 17%	31 61%	32 89%	35 27%	37 19%	40 82%	40 22%
NY	32 18	49 10	5 63	0 54	0 08	0 36	0 05	0 01	0 01	0 01
	14 18%	19 44%	10 95%	15 82%	10 86%	28 45%	15 37%	8 32%	15 00%	24 85%
GRE	14 03	13 02	1 84	0 20	0 07	0 13	0 07	0 03	0 02	0 01
	18 86%	18 31%	16 88%	25 60%	53 85%	36 05%	58 86%	58 57%	25 00%	60 00%
gmass sph	248 02	325 62	64 74	8 66	2 83	5 64	2 88	1 53	1 02	0 13
	29 98%	26 46%	29 40%	31 52%	33 34%	35 67%	34 73%	42 29%	41 75%	37 83%
ns mph	0 19	0 58	0 18	0 12	0 11	0 08	0 08	0 03	0 03	0 03
used ph	46 64%	60 88%	51 88%	58 51%	85 66%	64 80%	68 32%	64 02%	66 14%	66 44%
cps mph	4 36	11 19	4 23	0 85	0 20	1 17	0 34	0 27	0 32	0 11
	41 88%	43 77%	37 51%	30 19%	37 28%	68 82%	36 78%	33 48%	22 84%	35 23%
gt mph	6 44	36 74	47 78	14 08	4 78	12 75	18 14	8 74	7 27	0 80
used Ph	14 44%	15 86%	14 30%	11 36%	10 50%	10 02%	14 53%	18 82%	17 71%	18 25%
wo mph	2 70	5 12	4 81	1 48	0 29	2 18	2 87	1 03	1 48	0 33
	8 84%	8 57%	11 42%	12 37%	7 77%	24 29%	26 70%	15 00%	24 83%	34 44%
gre mph	14 03	13 02	1 84	0 20	0 07	0 13	0 07	0 03	0 00	0 00
used Ph	18 86%	18 31%	16 88%	25 60%	53 85%	36 05%	58 86%	58 57%	20 00%	60 00%
standard deviation CEL	72 80	77 85	15 11	1 48	0 36	0 72	0 38	0 15	0 10	0 01
conc CEL	288 15	342 78	75 80	6 53	1 58	3 08	1 51	0 58	0 36	0 08
RSD CEL	24 34%	22 71%	19 88%	22 58%	22 58%	23 28%	25 18%	25 70%	28 88%	24 13%
RSD's										
RSD cps probe	7 10%	7 10%	7 10%	7 10%	7 10%	7 10%	7 10%	7 10%	7 10%	7 10%
RSD cps ICP	16 85%	18 18%	30 63%	37 00%	23 28%	48 20%	38 01%	49 86%	27 34%	36 57%
RSD CEL probe	5 52%	5 52%	5 52%	5 52%	5 52%	5 52%	5 52%	5 52%	5 52%	5 52%
RSD CEL ICP	24 34%	22 71%	19 88%	22 58%	22 58%	23 28%	25 18%	25 70%	28 88%	24 13%
RSD Dcps/CEL	31%	30%	38%	44%	34%	54%	48%	57%	38%	45%
D cps/CEL	0 0288	0 0807	0 184	0 3483	0 3715	0 4024	0 5803	1 3885	4 0434	6 0542
1 sigma Dcps/CEL	0 008321	0 018682	0 081772	0 153834	0 125039	0 218409	0 274388	0 778136	1 582915	2 707865
D-1sigma	0 019578	0 042218	0 102228	0 184466	0 246461	0 183691	0 315832	0 580364	2 450585	3 346535
D+1sigma	0 035221	0 079182	0 229772	0 502134	0 496539	0 620809	0 884608	2 148836	5 636215	8 781865

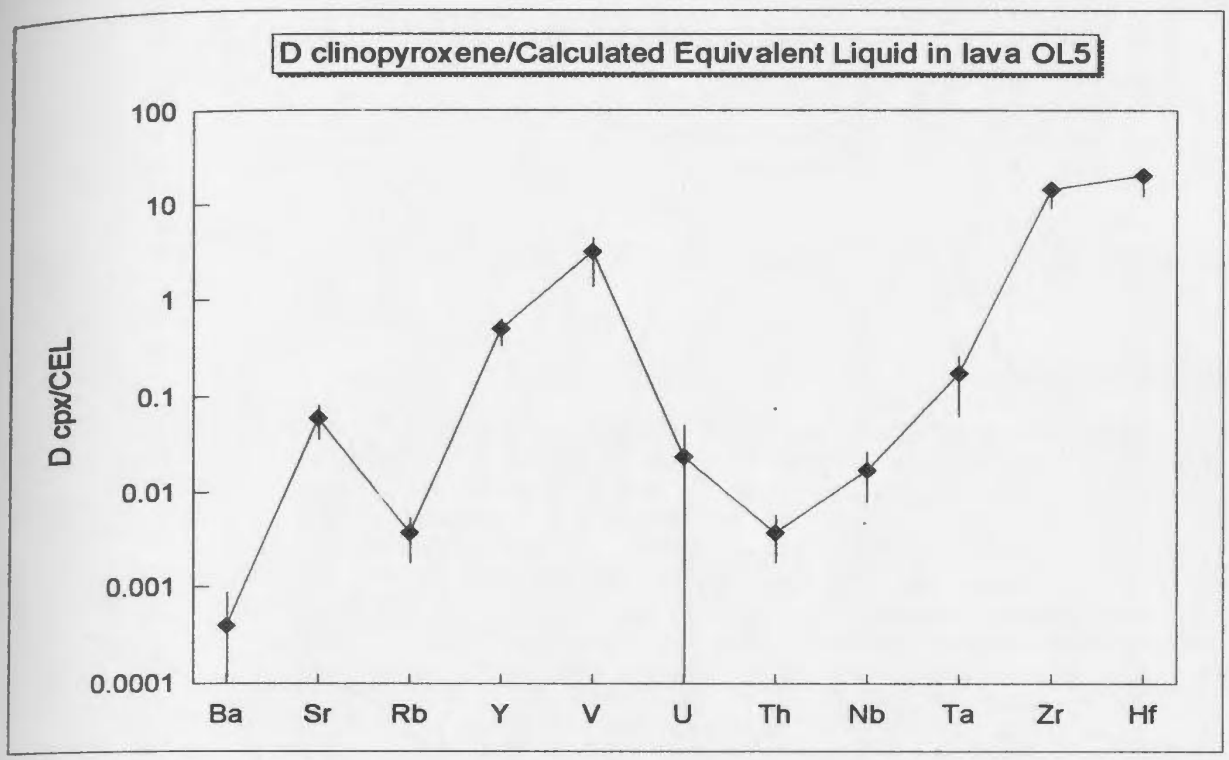

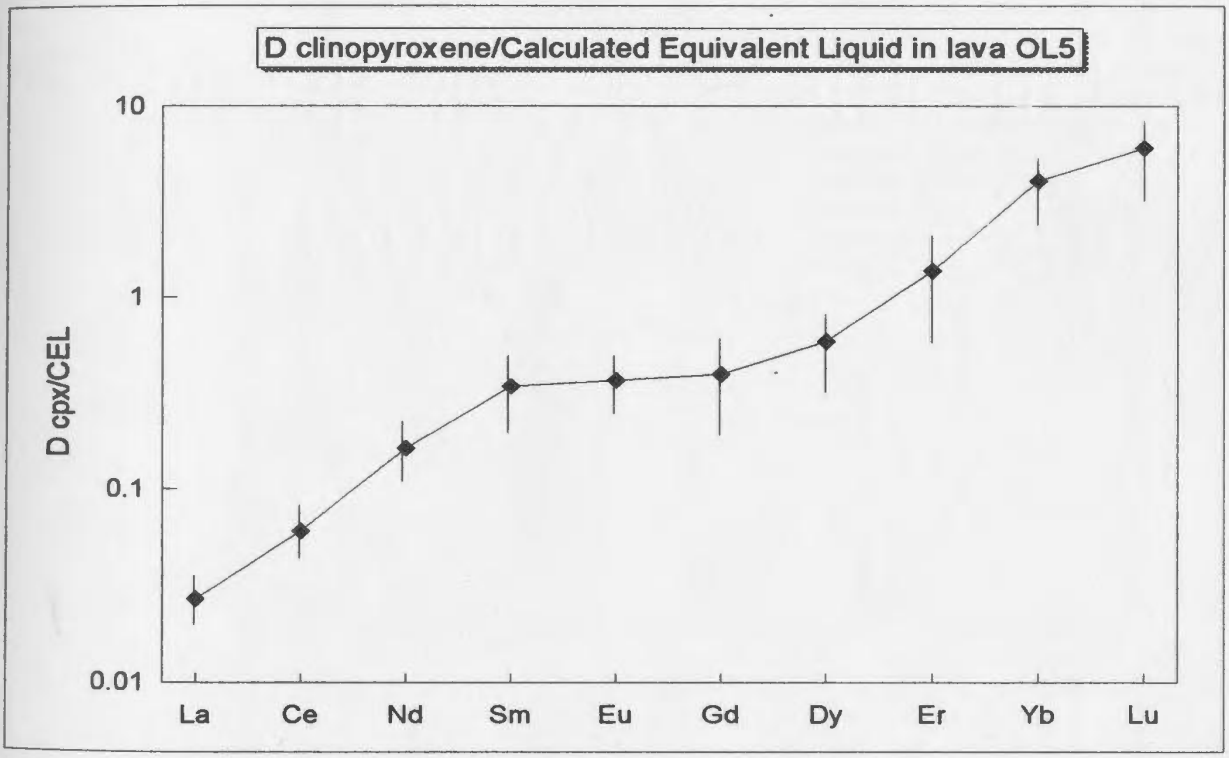

Figure A2.1: Trace element partition coefficients between clinopyroxene and Calculated Equivaelnt Liquid in silicate-bearing natrocarbonatite OL5.

APPENDIX A3

Table A3.1: Microprobe analyses of crystal phases in OL5-experiments - individual and average analyses (in wt. %).

SAMPLE	SiO2	TiO2	Al2O3	FeO	MnO	MgO	CaO	Na2O	K2O	P2O5	F	Cl	SO3	BaO	SrO	TOTAL
CP45																
Nepheline	43.7		32.7	1.3			0.2	16.7	6.2							100.7
Nepheline	43.4		32.7	1.5			.1<	16.8	6.3							100.6
Average	43.54		32.68	1.36			0.19	16.72	6.26							100.65
Melilite	*40.7*		*2.3*	*11.8*	*1.3*	*3.8*	*30.8*	*3.2*	*0.2*						*3.7*	*97.80*
Melilite	43.7		7.7	8.3	0.6	4.5	31.0	5.0	0.2						2.6	101.80
Melilite	43.7		7.2	6.7	0.6	4.8	30.3	5.1	b.d.						2.6	101.04
Average without first	43.69		7.45	6.50	0.69	4.67	30.66	5.08	0.20						2.61	101.53
CP51																
Melanite	30.8	11.17	0.8	22.9	0.4	0.6	31.0	0.5	0<							98.04
Melanite	29.7	13.50	0.4	21.4	0.3	0.5	30.6	0.7	.1<							97.16
Average	30.22	12.33	0.58	22.14	0.34	0.54	30.87	0.58	b.d.							97.60
Nepheline	43.8		31.5	2.3			0.4	15.9	6.4							100.31
Nepheline	44.2		32.5	1.1			0.3	16.0	6.3							100.31
Average	43.98		32.00	1.70			0.33	15.95	6.35							100.31
CP57																
Melanite	30.3	10.60	0.7	22.5	0.3	0.5	32.3	0.4	0<							97.60
Melanite	27.9	15.00	0.8	20.8	0.3	0.7	32.2	0.3	- 0<							98.00
Average	29.10	12.80	0.75	21.65	0.30	0.60	32.25	0.35	b.d.							97.80
Nepheline	42.2		31.8	1.9			1<	16.2	6.9							99.00
CP61																
Melilite	42.2		6.5	6.9	0.9	4.2	30.0	5.4	0.3						2.3	98.70
Melilite	42.8		6.7	7.0	0.9	4.4	30.3	5.6	0.2						2.4	100.30
Average	42.50		6.60	6.95	0.90	4.30	30.15	5.50	0.25						2.35	99.50
CP79																
Nepheline	43.3		33.2	1.1			0.2	17.2	6.5							101.50
Nepheline	43.4		32.4	1.8			1<	17.3	6.2							101.10
Nepheline	43.8		33.4	1.5			1<	17.2	6.2							102.10
Average	43.50		33.00	1.47			0.20	17.23	6.30							101.57
CP80																
Melilite	43.8		7.6	6.7	0.9	4.1	29.4	5.7	1<						2.5	100.70
Melilite	44.2		8.1	5.7	0.8	4.4	29.4	6.4	1<						2.2	101.20
Melilite	43.7		6.3	7.3	1.0	4.8	30.7	5.4	0.1						2.3	101.60
Average	43.90		7.33	6.57	0.90	4.43	29.83	5.83	0.10						2.33	101.22
Ti-Magnetite	0.3	3.32	0.3	86.3	2.8	0.7	0.3	0.4								94.42
Ti-Magnetite	0.4	4.00	.1<	86.2	3.0	0.6	0.2	0.5								95.10
Ti-Magnetite	0.6	5.00	0.3	84.4	2.8	0.6	0.3	3<								94.00
Ti-Magnetite	0.5	5.10	0.3	83.9	3.3	0.8	0.2	0.5								94.60
Ti-Magnetite	0.3	2.79	0.3	88.0	2.7	0.9	0.2	0.4								95.59
Average	0.42	4.04	0.30	85.76	2.92	0.76	0.24	0.45								94.89
Nepheline	43.1		33.4	1.2			0.2	17.0	7.1							102.00
Nepheline	42.8		33.0	1.2			0.3	16.7	7.0							101.00
Average	42.95		33.20	1.20			0.25	16.85	7.05							101.50
Melanite	29.1	10.10	0.7	24.1	0.3	0.5	31.3	2<	0.2							96.30
CP88																
Nepheline	43.7		32.8	1.6			1<	17.3	5.9							101.37
CP90																
Nepheline	43.5		30.8	2.6			0.5	16.4	6.0							99.80
CP96																
Nepheline	42.5		33.5	1.1			1<	17.1	6.8							100.98
Nepheline	43.3		32.4	2.3			1<	17.1	6.6							101.70
Average	42.90		32.92	1.71			b.d.	17.12	6.70							101.34
CP98																
K-Feldspar	64.7		18.1	0.7			- 1<	1.6	15.0							100.10
Nepheline	42.5		33.1	1.2			0.2	16.6	6.9							100.50
Nepheline	42.8		32.5	2.1			0.2	16.6	6.7							100.90
Nepheline	43.6		32.6	1.4			0.2	16.5	6.3							100.60
Average	42.97		32.73	1.57			0.20	16.57	6.63							100.67

SAMPLE	SiO2	TiO2	Al2O3	FeO	MnO	MgO	CaO	Na2O	K2O	P2O5	F	Cl	SO3	BaO	SrO	TOTAL
CP108																
Nepheline	43.2		33.3	1.9			.1<	17.6	6.3							102.30
Nepheline	43.7		33.2	1.1			0.5	17.3	6.1							101.90
Average	43.45		33.25	1.50			0.50	17.45	6.20							102.10
CP107																
Nepheline	43.1		32.9	1.2			1<	16.4	7.0							100.65
Nepheline	43.2		32.9	1.4			.1<	16.8	6.9							101.20
Average	43.15		32.91	1.32			b.d.	16.62	6.94							100.93
Clinopyroxene	*52.6*	*0.83*	*0.5*	*20.6*	*1.2*	*4.9*	*11.9*	*7.4*								*99.82*
Clinopyroxene	*53.0*	*0.98*	*0.9*	*18.5*	*0.6*	*6.4*	*15.2*	*5.5*								*100.86*
Clinopyroxene	52.3	0.42	0.5	16.2	0.5	8.1	19.8	3.1								100.92
Clinopyroxene	52.4	0.43	0.5	14.7	0.5	9.1	20.2	2.6								100.43
Clinopyroxene	51.1	0.57	0.6	13.2	0.3	9.5	21.3	1.6								98.57
Average last 3	51.93	0.47	0.60	14.70	0.43	8.90	20.43	2.50								99.97
Quench nyererente				2<	1<	0<	33.5	16.2	5.6	0.8	-.01<	.02<	1.1	1<	2.1	59.30
Quench nyererente				0.3	1<	0<	33.9	16.5	5.7	0.9	0<	.04<	1.3	0.4	2.1	61.10
Average				0.30	b.d.	b.d.	33.70	16.35	5.65	0.85	b.d.	b.d.	1.20	0.40	2.10	60.55
Nyererente				0<	1<	0<	33.3	17.0	5.8	0.8	0<	0.07	1.3	3<	2.0	60.27
Nyererente				1<	0<	0<	33.3	16.9	5.7	0.7	0<	.04<	1.3	3<	2.0	59.90
Nyererente				2<	1<	0<	34.5	15.7	5.7	1.1	0<	0.08	1.2	3<	2.3	60.58
Nyererente				1<	1<	1<	34.2	16.9	5.8	0.9	1<	.01<	1.1	0.5	2.2	61.60
Nyererente				1<	0<	0<	34.7	15.9	5.6	1.0	1<	.05<	1.0	0.4	2.2	60.80
Nyererente				0<	.2<	1<	34.1	16.9	6.0	0.9	1<	.01<	1.3	0.5	2.2	61.90
Nyererente				2<	0.2	-.0<	34.6	15.7	5.7	1.2	1<	0.09	1.2	0.7	2.3	61.89
Average				b.d.	0.20	b.d.	34.13	16.43	5.76	0.94	b.d.	0.08	1.20	0.53	2.17	61.44
Apatite	0.9						54.0	0.3		42.1	3.0				3<	100.30
CP108																
Melanite	30.8	11.75	1.2	22.0	0.4	0.7	31.8	.3<	1<							98.59
Melanite	29.7	13.30	1.2	21.1	0.4	0.6	31.6	0.7	0<							98.60
Melanite	29.8	14.10	0.6	21.5	0.6	0.6	31.3	0.7	0<							99.00
Average	30.02	13.05	0.99	21.54	0.48	0.63	31.56	0.70	b.d.							98.97
Clinopyroxene	50.3	1.17	2.0	15.2	0.4	8.7	21.1	1.7								100.57
Clinopyroxene	52.5	0.40	0.6	15.5	0.5	8.7	20.9	2.1								101.20
Clinopyroxene	52.0	0.49	0.8	15.1	0.5	8.7	20.0	2.8								100.39
Average	51.60	0.69	1.13	15.27	0.47	8.70	20.67	2.20								100.72
Gregoryite				1<	0.2	2<	11.7	38.2	4.3	3.5	0.4	0.40	4.3	2<	0.8	63.80
Gregoryite				1<	.2<	1<	12.0	37.1	4.1	3.5	0.2	0.21	4.2	2<	1.0	62.31
Gregoryite				2<	0<	1<	12.8	35.3	4.2	3.7	0.2	0.21	4.2	2<	0.9	61.51
Average				b.d.	0.20	b.d.	12.17	36.87	4.20	3.57	0.27	0.27	4.23	b.d.	0.90	62.54
Quench nyererente				0<	0.2	0<	32.7	17	7.2	0.8	0<	0.08	1.3	0.5	2.5	62.28
Nyererente				-.0<	2<	-.1<	32.9	16.9	7.1	0.9	.04<	0.09	1.1	0.5	2.3	61.79
Nyererente				-.0<	1<	-.0<	32.5	16.4	7.3	0.7	1<	0.10	1.4	0.6	2.3	61.30
Nyererente				0.2	2<	2<	33.2	16.4	7.2	0.7	0<	0.08	0.9	0.5	2.4	61.58
Nyererente				1<	1<	2<	33.5	16.6	7.4	0.7	1<	0.07	1.0	0.5	2.5	62.27
Nyererente				-.0<	2<	0<	33.3	16.1	7.4	0.9	-.0<	0.07	1.2	0.4	2.6	61.97
Nyererente				1<	2<	1<	33.2	16.3	7.2	0.7	0<	.05<	1.2	2<	2.3	60.90
Average				0.20	b.d.	b.d.	33.10	16.45	7.27	0.77	b.d.	0.08	1.13	0.50	2.40	61.90
CP112																
Clinopyroxene	*52.0*	*0.30*	*0.8*	*21.8*	*0.6*	*4.9*	*18.2*	*3.5*								*102.10*
Clinopyroxene	51.6	0.52	0.8	13.8	0.4	9.6	22.1	1.3								99.98
Clinopyroxene	52.1	0.47	0.8	14.9	0.5	8.9	21.5	2.0								101.19
Clinopyroxene	51.3	0.64	1.1	15.3	0.6	8.7	21.3	2.0								100.95
Average without first	51.67	0.54	0.90	14.65	0.51	9.06	21.62	1.76								100.71
Melanite	31.08	11.68	0.60	22.97	2<	0.40	31.81	0.71	1<							99.25
Apatite	0.69						53.34	3<		42.39	4.01				0.71	101.14
Sodalite	*37.2*		*24.5*	*5.6*			*5.7*	*19.6*	*2.1*			*4.78*	*0.8*			*100.3*
Sodalite	37.9		29.8	1.6			1<	22.4	2.5			6.41	2<			100.6
Sodalite	38.4		29.6	1.4			1<	22.9	2.6			6.25	0.7			101.8
Average last 2	38.15		29.69	1.50			b.d.	22.66	2.55			6.33	0.70			101.22
Nyererente				1<	0.2	1<	32.1	16.7	7.8	0.5	-.1<	0.09	1.0	0.5	2.7	61.59
Nyererente				0<	.1<	-.1<	32.3	16.1	8.1	0.5	0<	.05<	1.2	0.5	2.6	61.30
Average				b.d.	0.20	b.d.	32.20	16.40	7.95	0.50	b.d.	0.09	1.10	0.50	2.65	61.59

SAMPLE	SiO2	TiO2	Al2O3	FeO	MnO	MgO	CaO	Na2O	K2O	P2O5	F	Cl	SO3	BaO	SrO	TOTAL
Gregoryite				.1<	1<	.2<	12.0	34.2	4.4	2.7	0.8	0.29	5.6	0.4	1.0	61.39
CP118																
Quench nyerereite				.3<	2<	.2<	33.5	18.7	5.7	0.9	2<	1<	1 2	.5<	2.1	62.03
Quench nyerereite				0.4	2<	.2<	27.8	19.1	5.1	0.8	2<	.1<	1 1	0.6	2.3	57.38
Quench nyerereite				.0<	1<	.1<	34.2	16.0	5.9	0.8	- 0<	0.07	1 4	0.6	2.3	61.27
Average				0.37	b.d.	b.d.	31.83	17.94	5.56	0.85	b.d.	0.07	1.20	0.69	2.24	60.75
Nepheline	43 09		32.54	2 14			0.25	16.7	8.87							101.59
Na-clinopyroxene	*52.16*	*2.16*	*1 33*	*21 88*	*0 5*	*3.65*	*7.81*	*9.44*								*98.93*
Clinopyroxene	50.97	0.61	1.44	17.49	0.52	7.69	20.57	2.32								101.60
CP126																
Na-clinopyroxene	*50.2*	*1.15*	*0.7*	*17.8*	*1 7*	*4.9*	*13.7*	*7.4*								*97 46*
Na-clinopyroxene	*49.9*	*0.65*	*0.3*	*20.6*	*2.4*	*3.7*	*13.3*	*6.7*								*97.53*
Na-clinopyroxene	*50.1*	*0.87*	*0.5*	*19.2*	*1.7*	*4.9*	*13.6*	*6.9*								*97 77*
Na-clinopyroxene	*49.3*	*0.95*	*0.5*	*20.8*	*3.0*	*3.2*	*15.2*	*6.0*								*98.95*
Average	*49.88*	*0.91*	*0.50*	*19.59*	*2.22*	*4 18*	*13.93*	*6.73*								*97.93*
Melanite	32.5	7 60	1.1	23.4	0.4	0.3	31.8	0.3	0<							97 40
Melanite	30.7	11 00	0.7	22.4	0.4	0.5	31.6	0.3	.0<							97 60
Average	31 60	9.30	0 90	22.90	0 40	0.40	31.70	0.30	b.d.							97 50
Nepheline	43.23		33.17	1 43			b.d.	16.6	7 54							101 97
Nyerereite				- 0<	- 0<	0<	33.2	14.6	7.7	0.7	1<	0.15	1.2	0.6	2.5	60.65
Nyerereite				3<	2<	2<	33.3	14.8	7 3	0.8	2<	0.12	1 2	5<	2.7	60.13
Nyerereite				- 1<	1<	2<	33.0	14 0	7 8	0.7	0 2	04<	1.2	0.5	2.6	60.00
Average				b d	b.d.	b.d.	33.16	14 45	7 61	0 72	0 20	0.14	1.19	0.55	2.61	60 63
CP127																
Na-clinopyroxene	*50 9*	*3 30*	*1 4*	*25 1*	*0 4*	*1.3*	*2.6*	*11 6*								*96.60*
Na-clinopyroxene	*51 4*	*1 04*	*1 0*	*15 3*	*0 5*	*8.3*	*15 8*	*4 5*								*97 84*
Clinopyroxene	53.46	0.13	.2<	11.64	1.83	10.34	20.05	3.3								100.75
Nepheline	42 9		33 0	1 4			1<	16 3	7 1							100 64
Nepheline	43.0		32 8	1 5			1<	17 0	7 0							101 32
Average	42.96		32.90	1 40			b.d.	16.66	7 06							100.98
Nyerereite				1<	0.2	2<	34.1	15.6	5.7	0 5	- 0<	05<	1 2	0.5	2.5	60 50
Nyerereite				1<	1<	1<	33.6	15 9	5.7	0 6	0<	04<	1 2	0 6	2.4	60 20
Nyerereite				1<	0.2	0<	33.6	15.6	5.8	0.5	05<	02<	1 1	0 6	2.4	60.20
Average				b d.	0 20	b d.	33 90	15.63	5.73	0 53	b.d.	b.d	1 17	0.57	2.43	60 36
CP128																
Nepheline	43 23		32.85	1 29			0 22	16.61	8.74							100.94
Clinopyroxene	*50 9*	*0 49*	*0 5*	*17 7*	*0 5*	*7 1*	*19 5*	*3 0*								*99.71*
Clinopyroxene	*51 4*	*0 47*	*0 6*	*15 9*	*0 4*	*8 4*	*20 3*	*2 3*								*99.77*
Clinopyroxene	*50 9*	*1 66*	*0 9*	*21 2*	*0 4*	*4 6*	*11 6*	*7 3*								*98.56*
Clinopyroxene	*53 1*	*1 14*	*0 7*	*15 6*	*0 3*	*8.6*	*17.7*	*4 6*								*101.74*
Average first 2	*51 17*	*0 48*	*0 56*	*16 82*	*0 46*	*7 74*	*19 90*	*2 63*								*99.74*
Nyerereite				1<	2<	0<	34 0	15.7	5.5	0 7	1<	06<	1 4	3<	2.2	59 50
Nyerereite				2<	1<	2<	34.4	15.7	5.6	0.7	0<	03<	1 2	0 5	2.3	60.40
Nyerereite				1<	0.3	1<	34 0	15.5	5.6	0.7	0.1	- 01<	1 1	0.6	2.4	60.30
Nyerereite				2<	1<	1<	33.3	15.3	5.7	0.5	0.2	0 10	1 1	0.5	2.3	59.00
Average				b d	0.30	b.d.	33.93	15.55	5 60	0.65	0.15	0.10	1 20	0.53	2.30	59.80
CP129																
Melanite	*33 9*	*5 06*	*0.6*	*24 5*	*0 4*	*0.5*	*32.3*	*0.5*	*b.d.*							*97.80*
Melanite	32.0	8.70	0.6	23.8	.3<	0.6	32.0	0.5	.1<							98.16
Clinopyroxene	52.6	0 20	0 57	15 28	0 43	8 86	19.6	2.96								100.50
Wollastonite	50 1			3<	0.64		46.14	0 87								97.95
Nyerereite				.3<	3<	2<	33.9	16 9	7 1	0.9	2<	0.12	1.1	0.7	2.3	62.83
Nyerereite				3<	2<	2<	33 6	16.9	7 3	1 0	2<	0 10	1 1	5<	2.4	62.62
Average				b.d	b.d.	b.d.	33.63	16.68	7 20	0.91	b.d.	0.11	1 10	0.65	2.36	63.04
Nepheline	43 69		31 49	2 33			1<	16.32	6.95							100.78
Apatite	0 39						53.73	3<		43.26	3.61				1.07	102.06

Table A3.1 (suite).

**CP45	SiO2	TiO2	FeO	CaO	Na2O	La2O3	Ce2O3	SrO	Total
Perovskite	3.3	39.80	5.0	28.5	1.5	4.5	8.1	1.9	93.9
Perovskite	1.3	40.10	5.2	27.9	1.4	4.7	8.6	2.1	92.1
Perovskite	1.6	39.50	5.8	27.5	1.8	4.8	8.0	2.0	91.2
Average	2.07	39.80	5.33	27.97	1.57	4.67	8.23	2.00	92.40

Note: The data are raw data, i.e., all iron is reported as FeO, the data for the carbonate crystals are not corrected, and the totals are not recalculated to 100 wt. %.
Italics indicate whole analyses rejected, asterixes (*) indicate individual elemental analysis rejected, and bold font indicates that only one analysis was taken into account. b.d.: below detection.

Table A3.2: Microprobe analyses of crystal phases and of groundmass in lava OL5 - individual and average analyses (in wt. %).

Sample	SiO2	TiO2	Al2O3	FeO	MnO	MgO	CaO	Na2O	K2O	P2O5	F	Cl	SO3	BaO	SrO	Total
Correction factors																
Nyerereite	1	1	1	1	1	1	0.78	1.63	0.82	0.69	1.35	1.32	1.00	0.69	0.73	
Gregoryite	1	1	1	1	1	1	0.87	1.15	0.83	0.73	1.96	0.99	0.87	0.56	0.88	
Groundmass	1	1	1	1	1	1	1	1.16	1.10	1	0.69	2.35	1	1	0.88	
OL5																
Groundmass																
GMASS, 1	*10.0	0.3	*2.1	*7.2	1.3	0.4	20.4	23.0	5.2	0.9	5.8	3.2	2.7	- 1<	1.1	83.57
GMASS, 2	4.3	0.2	0.5	4.3	0.9	0.4	13.2	24.3	9.9	0.9	4.1	7.3	4.1	.3<	1.0	75.37
GMASS, 3	1.6	0.1	0.3	1.5	0.6	0.4	10.5	32.2	11.4	0.6	4.0	7.8	3.7	1.2	1.2	77.27
GMASS, 4	*8.7	0.1	*1.1	4.8	0.8	2<	21.0	27.8	3.9	0.6	6.8	2.5	2.7	.3<	1.2	82.00
GMASS, 5	5.5	0.2	0.3	*5.9	0.8	0.6	14.5	28.7	11.3	0.8	4.8	7.7	4.3	0.4	1.1	86.87
GMASS, 6	*6.5	0.2	*1.2	3.9	0.5	0.2	17.5	27.9	8.1	0.8	5.5	5.6	2.4	3<	0.9	81.25
GMASS, 7	4.2	0.1	0.4	1.4	0.3	2<	15.6	31.2	4.9	0.8	4.9	3.3	3.3	0.4	1.2	72.04
GMASS, 8	4.8	0.1	0.3	3.5	1.2	.1<	21.2	29.7	3.4	0.6	8.2	2.1	5.0	.2<	1.4	81.46
GMASS, 9	*8.7	0.3	*1.1	*8.2	2.0	1.0	19.2	21.6	8.3	0.5	6.1	5.4	3.7	2.1	1.2	89.24
Average	4.08	0.18	0.36	3.23	0.93	0.50	17.01	27.38	7.38	0.72	5.58	4.99	3.54	1.03	1.14	81.01
Corrected	4.08	0.18	0.36	3.23	0.93	0.50	17.01	31.71	8.13	0.72	3.83	11.72	3.54	1.03	1.01	
Crystals																
Gregoryite																
GRE1				2<	1<	0<	11.3	35.9	4.3	4.8	0.1	0.6	3.3	0.7	1.0	62.12
Corrected				b.d.	b.d.	b.d.	9.85	41.35	3.57	3.52	0.20	0.62	2.88	0.39	0.88	63.26
Nyerereite																
NY1				- 1<	2<	1<	32.6	14.0	9.3	0.7	- 03<	0.2	0.9	0.7	2.8	61.23
NY2				0<	2<	1<	32.9	13.5	9.6	0.8	0.3	0.2	0.9	0.9	3.1	62.16
NY3				0<	0<	1<	32.7	14.5	9.5	0.6	1<	0.2	1.0	0.8	3.2	62.47
Average				b.d.	b.d.	b.d.	32.73	14.00	9.47	0.70	0.30	0.19	0.93	0.80	3.03	62.15
Corrected				b.d.	b.d.	b.d.	24.56	22.85	7.73	0.49	0.41	0.25	0.94	0.55	2.22	59.99
Clinopyroxene																
CPX4	*51.0*	*0.5*	*0.8*	*21.0*	*0.5*	*5.3*	*17.7*	*3.7*								*100.48*
CPX1	*51.6*	*0.5*	*0.7*	*19.0*	*0.6*	*6.1*	*18.3*	*3.4*								*100.15*
CPX2	51.5	0.5	0.8	18.9	0.5	6.2	18.7	3.3								100.52
CPX3	50.4	1.2	2.2	12.0	0.4	10.4	22.5	1.2								100.22
CPX5	52.2	0.5	0.8	18.2	0.5	8.1	20.1	2.8								101.30
CPX6	51.5	1.1	1.9	15.2	0.5	8.5	21.4	2.1								102.19
CPX7	50.4	1.3	2.1	11.9	0.3	10.3	22.5	1.2								100.13
CPX8	51.4	1.2	2.3	13.0	0.4	10.4	21.8	1.7								101.95
Average without first 2	51.23	0.97	1.68	14.53	0.43	8.98	21.17	2.05								101.05
Wollastonite																
Wo1	51.5			1.1	0.4	1<	46.3	2<								99.3
Wo2	51.9			0.5	0.8	1<	46.9	1<								100.1
Wo3	52.1			1.1	0.3	0.2	46.8	0<								100.5
Wo4	52.4			1.1	0.3	0.3	46.8	1<								100.9
Wo5	52.1			0.9	0.4	0.2	47.5	1<								101.1
Wo6	52.2			0.9	0.4	0.2	46.8	.1<								100.5
Wo7	51.4			0.9	0.5	0.3	47.5	0.3								100.9
Wo8	*46.7*			*2.7*	*0.8*	*0.5*	*43.5*	*1.3*								*95.5*
Average without last	51.94			0.93	0.44	0.24	46.94	0.30								100.8
Nepheline																
Ne3	44.2		33.6	1.4			1<	17.3	6.4							102.90
Ne4	42.9		33.1	2.2			1<	16.9	7.0							102.05
Ne5	42.9		33.3	1.8			0.2	16.9	7.0							102.05
Ne6	44.5		33.4	1.3			0.5	16.8	6.5							103.00
Ne8	43.1		33.3	1.1			0.4	16.2	6.6							100.76
Ne9	42.9		33.6	1.2			0.2	17.3	6.8							101.95
Ne10	44.1		32.5	1.9			1<	17.2	6.7							102.38
Ne11	43.0		32.5	1.5			1<	17.0	6.2							100.24
Ne12	43.7		33.3	1.6			1<	17.6	6.6							102.76
Ne13	42.9		33.2	1.8			0.1	17.2	7.0							102.23
Average	43.42		33.16	1.58			0.28	17.04	6.68							102.03
Melanite garnet																
Gt1	30.4	12.4	0.6	22.1	0.3	0.5	31.3	0.6								98.29
Gt2	31.1	11.3	0.8	22.7	0.3	0.7	31.9	0.5								99.30
Gt3	29.2	13.1	0.7	21.3	0.4	0.6	31.0	0.7								96.96
Gt4	29.2	13.9	0.8	21.0	0.4	0.7	31.7	2<								97.63
Average	29.98	12.68	0.73	21.78	0.35	0.63	31.48	0.60								98.04
Pyrrhotite																
Py1	0.7	00<	- 2<	57.8	2.9	- 0<	0.2	3.8	11.3	- 2<	0<	0<	85.6	1<	- 2<	162.22

Sample	SiO2	TiO2	Al2O3	FeO	MnO	MgO	CaO	Na2O	K2O	P2O5	F	Cl	SO3	BaO	SrO	Total
Apatite																
Ap	1.0						54.2	0.3		42.3	2.6					100.4
Ap1, rim	0.7						54.3	0.4		42.4	n.a.					97.8
Ap2, rim	0.9						54.6	0.3		42.0	n.a.					97.8
Ap3, rim	1 1						54.0	3<		41.2	n.a.					96.3
Ap4, rim	0.8						54.7	2<		42.1	n a.					97 6
Ap5, core	0.7						54.7	.0<		42.9	n.a.					98.3
Ap6, core	0.6						54.6	0.3		41.9	n.a.					97 4
Ap7, core	0.9						54.4	0.5		41 6	n.a.					97.4
Ap8, core	1.1						54.4	0.3		41.8	n.a.					97.6
Average	0.87						54.43	0.36		42.02	2.60					100.27
(Si,Al)(Ca,Na,Fe)F	36.3	0 6	12.5	4 4	.2<	0.8	28.1	8.5	3.6	1<	5.7	0.1	- 0<	2<	0.7	101.25
Groundmass spheroids																
Gmass spheroid 1	32.0	0.4	6.3	5.0	0.5	0.6	22.9	15.4	4.0	0 5	1.0	0.9	1 7		0.6	91 81
Gmass spheroid 2	30.3	0.6	5.4	5.2	0.5	0.3	23.8	17 2	2.4	0.5	2.3	0.3	0.9		0.6	90.34
Gmass spheroid 3	28.6	0.3	6.3	3.7	0.4	0.4	25.1	15.2	4.5	0.4	3.0	1.4	0.8		3<	90.09
Gmass spheroid 4	31.1	0.3	5.7	7.0	0.6	0.5	25.0	14 0	3.4	1.0	2.0	0.5	5.8		3<	96.90
Gmass spheroid 5	*35.3*	*1.2*	*10.9*	*7.3*	*0.8*	*0.6*	*18.2*	*10.6*	*7.8*	*1<*	*1.4*	*3.2*	*1.9*		*- 1<*	99.18
Gmass spheroid 6	*6.6*	*0 2*	*2.2*	*8.8*	*2.5*	*0.3*	*16.6*	*28.2*	*4.5*	*1 0*	*6.0*	*2.4*	*6.0*		*1.2*	86.51
Average first 4	30 50	0.40	5 93	5 23	0.50	0.45	24.20	15.45	3.58	0.60	2.08	0.79	2.30		0.60	92.59
Phenocrysts in spheroids																
Clinopyroxene																
CPX2	*52.4*	*0.9*	*1.6*	*10 7*	*0.3*	*11 7*	*23.4*	*1 3*								*102.30*
CPX1	52.3	0 7	0 8	16.3	0 5	8 2	20.0	2 7								101.50
CPX3	51 6	0 4	0 9	17 9	0.8	7 1	20.2	2 5								101 40
CPX4	52 2	0.7	1.0	14 6	0 4	9.4	21.3	2 0								101 60
CPX5	52.0	0.6	1.4	13.8	0.6	9.5	21.8	1 8								101 46
CPX6	51 9	0.5	0 4	13 7	0.6	9.6	21 5	1 8								99.99
CPX7	52.1	0.6	1 1	13.4	0.4	9 8	21.9	2 0								101.33
CPX8	51 8	0 7	1 0	13.0	0.4	10.0	21.8	1.7								100.41
Average without first	51 99	0 60	0.94	14.67	0.53	9.09	21.21	2.07								101 10
Melanite garnet																
Gt1	*31 2*	*9 8*	*0 4*	*23 4*	*0.4*	*0.4*	*31.4*	*0.6*		*1<*						*97 60*
Gt2	30 2	12.8	0 9	21 8	0.4	0 6	31 7	0.8		0 3						99.43
Gt3	30 5	11 3	0 9	22.0	2<	0.4	31 8	0 4		0 5						97.82
Gt4	30 8	11 4	1 0	22.2	0.3	0.7	31.7	0 4		0.4						98.88
Average without first	30 50	11 83	0 93	22.00	0 35	0.57	31.73	0.53		0.40						98.71
Wollastonite																
Wo1	51 9			0 9	0.4	1<	46.9									100 1
Wo2	52.3			0.9	0.4	0.2	47 1									100.9
Wo3	52.6			1.0	0.4	0 3	47 3									101.6
Wo4	51 8			1.0	0 3	0.2	46.9									100.2
Average	52 15			0.95	0.38	0 23	47.05									100.76
Nepheline																
Ne1	42.8		32.7	2.3			0.2	16.8	7 0							101.8
Ne2	42.6		33.2	1.1			0<	17 3	6 5							100.7
Ne3	44.2		32.8	1.5			0.8	17 0	5 9							102.2
Ne4	43 7		33.3	1.1			0.3	16.9	6.7							102.0
Average	43.33		33.00	1.50			0.43	17.00	6 53							101 78
Melilite																
Meli1	43 4	1<	/ 9	7 2	2<	4 3	30.7	5.7	1<							99.21
Microphenocrysts in spheroids																
Nepheline																
Ne2 core	44 0		31.6	2.2			1<	16.5	7 0							101.28
Ne4 core	44 5		34.1	1 3			0.3	16 3	6 8							103.34
Average core	44 25		32.85	1.75			0.30	16.40	6.90							102.31
Ne5 rim	46 0	1<	32.6	2.4	- 0<	1<	0.2	15 3	7 0	- 1<			- 04<			103.43
Clinopyroxene																
CPX1 core	*46.7*	*3.1*	*5 0*	*12.8*	*0.4*	*9.5*	*22.2*	*1.7*								*101 4*
CPX11 core	*52.6*	*0.80*	*1.6*	*10.1*	*0.5*	*12.2*	*23.4*	*1 6*								*102.8*
CPX2 core	52 0	0.60	0.8	20.1	0.8	6.3	18.3	3.9								102.8
CPX3 core	53.0	0.40	0.6	14.9	0.5	9.3	20.8	2.5								102.0
CPX4 core	53.7	0.50	0.6	14.6	0.5	9.7	20.5	2.6								102.7
CPX5 core	52.7	0.60	0 7	16.8	0.6	8.1	20.8	2.6								102.9
CPX6 core	53.2	0 20	0 4	14.2	0.4	9.7	21.2	2.2								101.5
CPX7 core	50.4	1 30	2.2	16.2	0.5	8.2	20 8	2.4								102.0
CPX8 core	51.9	0.40	0 9	18.5	0.7	7 0	19.8	3 0								102.2
CPX9 core	51.7	0 50	0 8	17 1	0.7	7.8	20.0	3.2								101.8
CPX10 core	52.8	0.50	0 7	18.2	0.5	7.7	19.4	3.3								103.1
Average without first 2	52.38	0 56	0 86	16.73	0.58	8.20	20.18	2.86								102.33

Sample	SiO2	TiO2	Al2O3	FeO	MnO	MgO	CaO	Na2O	K2O	P2O5	F	Cl	SO3	BaO	SrO	Total
CPX1 nm	51.2	0.90	1 7	17.0	0.5	7.9	20.5	2.4								102.1
CPX2 nm	53.2	0.60	1.0	13.2	0.4	10.7	22.2	2.1								103.4
CPX3 nm	53.3	0.60	0.8	14.6	0.4	9.7	20.7	2.6								102.7
CPX4 nm	53.0	0.40	0.8	15.6	0.4	9.3	20.5	2.6								102.6
CPX5 nm	53.2	0.50	0.8	14.5	0.4	9.6	20.9	2.5								102.4
CPX6 nm	52.7	0.50	0.9	19.5	0.7	6.3	18.6	3.7								102.9
CPX7 nm	50 7	0.90	2.1	11.8	0.4	10.8	22.2	2.0								100.9
Average nm	52.47	0.63	1.16	15.17	0.46	9.19	20.80	2.56								102.43
Melanite garnet																
Gt1	31.2	10.5	0.7	22.3	0.5	0.3	31.6	0.7								97 8
Gt2	30.5	9.0	0.6	23.0	2<	0.6	31.5	1.6								96.8
Average	30.85	9.75	0.65	22.65	0.50	0.45	31.55	1.15								97.55
Gregoryite																
GRE1		0.1		0.3	.1<	0.3	7.4	40.9	3.0	3.2	05<	0 7	4.1	0.7	1.0	62.23
GRE2		0.1		0.5	1<	0.5	7.8	39.1	3.3	3.4	0.2	1.0	4.1	0.6	0 9	62.10
Average		0 08		0.40	b.d.	0.40	7.60	40.00	3.15	3.30	0.20	0.81	4.10	0.65	0.95	62.16
Corrected		0 08		0.40	b.d.	0.40	6.63	46.07	2.61	2.42	0.40	0.79	3.58	0.36	0.83	64.58
Wollastonite																
Wo nm	53.3			0.8	0.4	0.3	47.1	0.3								102.42
Wo core	52.3			0.9	0.4	0.3	47.2	0.4								101.42
Average	52.80			0 85	0.40	0.30	47.15	0.35								101 92

Note the correction factors that are applied to carbonate phases are indicated at the beginning of the table, and the corrected values for the carbonate phases are also indicated. Correction factors for nyerereite and gregoryite are from Table 2.3, and correction factors for the groundmass are given in Table A3.5.
Italics indicate whole analyses rejected and asterixes (*) indicate individual elemental analysis rejected.
Abbrevations used are: b.d.: below detection; gmass: groundmass; GRE: gregoryite; NY: nyerereite; CPX: clinopyroxene; Wo: wollastonite; Ne: nepheline; Gt: garnet; Py: pyrrhotite; Ap: apatite; Melt: melilite.

Table A3.3: Uncorrected major element microprobe analyses of carbonate liquid (LC) from OL5-experiments (in wt. %) - individual and average analyses, standard deviation (STDS) and relative standard deviation (RSD).

Sample	SiO2	TiO2	Al2O3	FeO	MnO	MgO	CaO	Na2O	K2O	P2O5	F	Cl	SO3	BaO	SrO	Total
CP45																
LC45,1	*0.8*	*03<*	*0.2*	*0.3*	*0.2*	*0.6*	*13.4*	*25.1*	*4.9*	*1.6*	*2.3*	*1.74*	*3.5*	*1.5*	*1.4*	*57.4*
LC45,3	*1.0*	*03<*	*0.3*	*0.3*	*1<*	*2<*	*15.4*	*25.3*	*5.0*	*1.8*	*3.1*	*0.91*	*3.4*	*1.4*	*1.7*	*59.6*
LC45,5	*1.5*	*0.09*	*-0<*	*0.8*	*.1<*	*-0<*	*18.9*	*26.9*	*5.5*	*1.7*	*.1<*	*0.21*	*2.1*	*0.5*	*1.4*	*59.5*
LC45,6	*1.4*	*0.06*	*1<*	*1.0*	*0.3*	*2<*	*14.7*	*24.9*	*4.0*	*1.6*	*6.1*	*0.37*	*2.8*	*0.9*	*1.3*	*59.3*
LC45,9	*1.6*	*0.10*	*1<*	*0.8*	*0.4*	*1<*	*18.2*	*21.4*	*6.6*	*1.2*	*1.6*	*1.74*	*2.1*	*0.9*	*1.7*	*58.2*
LC45,2	1.7	0.06	1<	0.9	0.2	0.4	15.8	27.2	4.2	*1.8	1.5	0.71	3.2	0.8	1.6	59.9
LC45,4	2.2	0.05	1<	0.7	.2<	0.3	15.8	26.8	4.1	*1.9	2.2	*0.24	3.1	1.2	1.6	60
LC45,7	2.4	0.09	1<	1.3	0.4	*0.2	13.5	*19.9	7.5	1.2	*5.2	*4.07	2.6	*1.5	1.3	61.2
LC45,8	2.1	0.07	0.2	1.2	0.3	0.3	15.4	22.3	5.4	1.2	2.2	1.47	*3.4	*1.7	1.5	58.6
LC45,10	2.2	*0.12	.1<	1.2	0.4	0.4	14.4	22.7	4.5	1.4	3.8	1.00	3.2	*1.5	1.7	58.4
LC45,11	1.9	03<	0.2	1.2	0.4	0.5	19.0	21.9	6.2	0.8	3.7	1.39	1.8	0.9	1.8	61.4
LC45,12	1.9	0.06	0<	*1.4	0.4	0.4	17.3	23.4	4.8	1.1	3.0	0.49	2.4	1.0	1.5	59.1
Average last 7	2.01	0.07	0.19	1.05	0.34	0.38	15.89	24.04	5.25	1.13	2.74	1.01	2.74	0.99	1.50	59.33
STDS	0.23	0.02	0.00	0.23	0.08	0.07	1.83	2.34	1.25	0.22	0.92	0.42	0.52	0.18	0.12	
RSD	11%	23%	0%	22%	25%	19%	12%	10%	24%	19%	34%	42%	19%	18%	8%	
CP51																
LC51,1	*0.7*	*-01<*	*0<*	*0.3*	*1<*	*2<*	*15.0*	*22.0*	*5.4*	*1.5*	*0.8*	*1.40*	*3.1*	*0.7*	*1.4*	*52.1*
LC51,2	*0.2*	*-01<*	*-0<*	*1<*	*0.2*	*1<*	*9.9*	*31.9*	*9.8*	*1.2*	*8.8*	*7.09*	*3.1*	*0.8*	*0.9*	*73.80*
LC51,3	*1.7*	*00<*	*1<*	*0.4*	*0.3*	*1<*	*8.4*	*31.2*	*10.9*	*0.7*	*9.9*	*10.69*	*3.5*	*1.3*	*0.9*	*79.8*
LC51,4	*0.7*	*0.06*	*-1<*	*1.1*	*0.7*	*0.9*	*11.8*	*21.8*	*12.7*	*0.4*	*11.7*	*8.23*	*2.0*	*1.0*	*1.0*	*73.9*
LC51,5	1.9	-00<	0<	1.3	0.8	0.5	*8.4	*33.7	3.8	*1.9	1.2	1.39	*4.6	1.1	*1.1	61.4
LC51,6	0.3	-01<	0<	0.3	2<	1<	19.2	22.4	5.0	1.1	1.1	*0.20	1.9	0.6	1.6	53.6
LC51,7	0.4	03<	1<	2<	0.3	0.2	14.5	29.5	4.3	*1.9	1.8	0.43	3.3	0.9	1.6	59
LC51,8	0.4	-04<	0<	2<	1<	-0<	21.2	*21.3	7.0	0.6	2.9	0.69	1.9	*2.3	*2.6	60.9
LC51,9	2.6	-01<	0<	0.3	0.3	1<	12.2	28.7	3.6	*1.9	1.6	0.74	3.5	1.1	1.4	58.2
LC51,10	0.6	-03<	1<	0.3	0.3	0.4	16.1	*20.4	5.9	1.2	1.5	1.14	3.1	1.1	1.4	53.3
LC51,11	2.8	*0.07	*1.8	0.9	0.3	0.3	12.1	25.3	4.4	1.0	*8.9	0.63	2.2	1.2	1.4	63.4
LC51,12	0.3	0.04	-1<	0.5	0.2	1<	12.0	25.5	*10.2	1.3	4.9	*5.39	3.1	0.6	*1.0	64.8
LC51,13	1.4	*0.06	1<	1.7	0.5	0.5	14.5	23.4	5.6	1.2	3.4	1.84	3.7	0.8	1.5	60.2
LC51,14	0.6	02<	0<	0.3	2<	1<	17.0	22.6	8.1	*0.9	4.2	*2.93	2.1	1.2	1.7	61.6
Average last 10	1.13	0.04	n.d.	0.68	0.37	0.38	15.43	25.34	5.35	1.06	2.50	0.96	2.74	0.97	1.47	58.42
STDS	0.99	n.d.	n.d.	0.53	0.20	0.13	3.26	2.86	1.49	0.25	1.38	0.50	0.68	0.25	0.12	
RSD	88%	n.d.	n.d.	78%	53%	33%	21%	11%	28%	24%	55%	51%	25%	25%	8%	
CP57																
LC57,1	*2.2*	*0.09*	*0.3*	*1.4*	*1<*	*1<*	*13.4*	*22.6*	*4.3*	*1.1*	*0.4*	*1.40*	*1.4*	*.3<*	*1.2*	*49.9*
LC57,2	*0.5*	*-05<*	*0<*	*0.3*	*0.3*	*0.3*	*7.4*	*21.3*	*4.3*	*0.7*	*2.3*	*5.30*	*1.8*	*0.7*	*1.0*	*46.3*
LC57,3	*1.3*	*-04<*	*-0<*	*1.1*	*0.7*	*0.7*	*9.8*	*30.8*	*8.9*	*0.5*	*6.5*	*5.00*	*3.9*	*1.1*	*1.3*	*71.4*
LC57,4	*0.8*	*-11<*	*-0<*	*0.6*	*0.7*	*1.1*	*10.0*	*31.3*	*6.9*	*0.8*	*11.5*	*5.60*	*3.3*	*1.4*	*1.3*	*75.1*
LC57,7	*3.2*	*-05<*	*2.4*	*0.3*	*0.2*	*0.4*	*13.3*	*25.9*	*7.0*	*1.8*	*5.0*	*1.25*	*2.1*	*0.7*	*1.3*	*64.8*
LC57,14	*2.6*	*02<*	*0.5*	*1.8*	*0.3*	*0.4*	*14.8*	*25.5*	*5.7*	*0.8*	*3.2*	*2.12*	*2.2*	*0.6*	*1.2*	*61.6*
LC57,5	0.8	-07<	-1<	0.7	0.5	*0.7	11.4	26.9	4.5	*0.4	*6.1	*2.31	2.1	0.9	1.3	58.7
LC57,6	0.2	-04<	-0<	-0<	2<	0<	10.6	22.2	*13.2	*0.7	1.5	1.36	*8.2	0.9	*1.1	60
LC57,8	2<	-03<	-0<	-0<	0.2	0.3	15.8	26.0	6.3	1.4	1.0	1.32	2.0	*0.4	1.3	56
LC57,9	0.4	-04<	0<	2<	0.2	1<	15.6	27.9	6.5	0.9	3.3	1.94	*1.7	0.9	1.6	61
LC57,10	0.2	-06<	0<	-0<	1<	1<	18.1	27.2	6.6	0.9	4.6	0.90	*1.3	0.6	1.7	62.3
LC57,11	0.2	-06<	1<	1<	2<	2<	16.1	28.7	6.3	1.3	2.1	*3.80	2.8	1.2	1.5	64.00
LC57,12	0.6	-07<	-0<	0.5	0.3	2<	16.4	24.8	*7.9	0.6	3.1	*2.90	2.0	0.6	1.5	61.5
LC57,13	0.6	-04<	0<	0.3	0.5	0.5	14.2	*31.1	5.5	1.4	3.8	*3.10	2.6	1.2	1.5	66.1
Average last 7	0.43	b.d.	b.d.	0.50	0.34	0.40	14.78	26.24	5.98	1.12	2.77	1.38	2.30	0.90	1.49	58.62
STDS	0.24	n.d.	n.d.	0.20	0.15	0.14	2.57	2.18	0.84	0.26	1.29	0.43	0.37	0.24	0.15	
RSD	57%	n.d.	n.d.	40%	45%	35%	17%	8%	14%	25%	47%	31%	16%	27%	10%	
CP61																
LC61,1	*1.1*	*-11<*	*0<*	*0.7*	*0.4*	*0.7*	*10.7*	*33.7*	*7.9*	*0.6*	*13.5*	*4.60*	*2.5*	*1.3*	*1.2*	*79*
LC61,2	*1.2*	*-07<*	*-1<*	*0.8*	*0.4*	*0.6*	*13.1*	*31.2*	*8.8*	*0.8*	*10.0*	*5.30*	*2.3*	*1.3*	*1.4*	*77.1*
LC61,3	*1.4*	*-05<*	*1<*	*0.6*	*0.6*	*0.3*	*5.1*	*18.9*	*2.8*	*0.8*	*1.3*	*10.20*	*1.5*	*1.1*	*0.9*	*45.4*
LC61,4	*1.6*	*00<*	*1<*	*1.1*	*0.7*	*0.3*	*8.3*	*26.4*	*4.0*	*1.2*	*1.0*	*0.87*	*2.8*	*0.6*	*1.1*	*49.9*
LC61,8	*0.4*	*-03<*	*-1<*	*0.3*	*.0<*	*.2<*	*16.6*	*29.6*	*5.5*	*1.1*	*1.8*	*0.86*	*2.8*	*0.7*	*1.7*	*61.50*
LC61,9	*0.3*	*-01<*	*-0<*	*2<*	*1<*	*0<*	*20.7*	*25.4*	*6.7*	*1.2*	*0.4*	*0.42*	*2.2*	*0.4*	*1.7*	*59.5*
LC61,10	*0.4*	*-02<*	*0<*	*1<*	*0<*	*0<*	*19.2*	*26.5*	*6.7*	*1.7*	*0.5*	*0.51*	*2.3*	*0.5*	*1.7*	*60.1*
LC61,5	1.2	-08<	1<	0.4	0.4	0.3	*9.1	33.0	*3.0	0.8	*6.7	1.26	2.9	*1.6	1.3	62
LC61,6	1.3	-02<	1<	0.5	0.4	0.2	13.0	31.7	4.8	1.5	4.1	1.02	*3.7	0.8	1.3	64.5
LC61,7	0.8	-02<	1<	0.4	2<	.1<	14.9	27.8	6.5	1.5	1.5	2.40	3.1	0.8	1.4	61.1
LC61,11	0.8	-01<	1<	0.4	2<	0<	20.0	25.1	6.3	1.3	0.7	0.44	2.0	0.5	1.6	59
LC61,12	2.0	-05<	1<	0.9	0.5	0.4	*10.4	*36.6	6.0	0.8	*10.5	*2.60	3.3	1.4	1.2	76.7
LC61,13	0.9	-06<	1<	0.4	0.2	1<	14.6	27.3	5.6	1.2	2.6	1.67	2.7	0.7	1.5	59.6
LC61,14	1.9	-07<	1<	0.7	0.6	*0.6	*8.6	31.4	4.4	0.8	*9.1	*4.20	*3.6	1.2	1.2	68.40
LC61,15	0.9	-05<	0<	0.5	0.2	0.3	16.8	25.3	6.9	1.0	3.3	1.42	3.1	1.3	1.6	62.5
LC61,16	2.3	-07<	1<	1.0	0.6	0.5	*9.9	31.8	*7.7	0.7	*7.4	*5.20	3.1	1.1	*1.1	72.3
LC61,17	2.3	-03<	0<	1.8	*1.1	0.5	14.4	29.9	*1.4	*0.3	4.5	0.21	*4.8	1.0	1.7	64
Average last 10	1.44	b.d.	b.d.	0.70	0.41	0.37	15.62	29.26	5.81	1.07	2.78	1.23	2.89	0.98	1.42	63.97
STDS	0.62	n.d.	n.d.	0.44	0.17	0.12	2.47	2.97	0.91	0.32	1.48	0.77	0.43	0.30	0.19	
RSD	43%	n.d.	n.d.	64%	40%	33%	16%	10%	16%	30%	53%	62%	15%	31%	13%	

Sample	SiO2	TiO2	Al2O3	FeO	MnO	MgO	CaO	Na2O	K2O	P2O5	F	Cl	SO3	BaO	SrO	Total
CP79																
LC79,2	2.4	0.09	0.2	1.2	0.3	0.3	16.7	25.2	5.5	1.2	2.6	1.14	2.4	0.8	1.8	61.95
LC79,6	2.2	*0.07	.1<	1.1	0.3	0.3	15.4	23.5	*4.9	1.2	2.2	*0.58	3.2	0.9	1.6	57.48
LC79,8	2.4	0.12	0.3	1.0	0.3	0.3	*17.8	23.9	*4.9	*1.3	2.7	*0.70	2.2	0.9	1.8	60.85
LC79,1	*1.5*	*0.07*	*0<*	*0.9*	*0.2*	*0.3*	*17.1*	*24.3*	*4.8*	*1.3*	*2.8*	*0.79*	*3.5*	*0.8*	*1.5*	*59.85*
LC79,3	*0.8*	*.03<*	*1<*	*0.4*	*.1<*	*.1<*	*20.7*	*21.9*	*4.9*	*1.2*	*1.4*	*0.20*	*1.8*	*1.1*	*1.8*	*56.22*
LC79,4	*1.8*	*0.09*	*0.2*	*0.9*	*0.2*	*0.3*	*17.2*	*23.2*	*4.3*	*1.2*	*1.2*	*0.33*	*2.1*	*0.6*	*1.5*	*55.12*
LC79,5	*1.6*	*0.09*	*0.2*	*0.7*	*0.3*	*2<*	*17.3*	*25.2*	*5.1*	*1.3*	*5.7*	*0.67*	*2.1*	*1.1*	*1.7*	*62.98*
LC79,7	*1.2*	*0.05*	*.1<*	*0.8*	*0.2*	*.2<*	*19.4*	*23.1*	*5.0*	*0.9*	*2.4*	*0.34*	*2.1*	*0.8*	*1.8*	*58.15*
LC79,9	*1.6*	*0.10*	*0.2*	*0.7*	*.2<*	*0.4*	*11.2*	*17.9*	*3.1*	*1.1*	*2.0*	*0.44*	*2.5*	*0.8*	*1.1*	*43.13*
LC79,10	*2.4*	*0.09*	*0.2*	*1.1*	*0.3*	*0.3*	*11.2*	*20.0*	*3.5*	*1.1*	*1.6*	*0.64*	*2.6*	*0.7*	*1.3*	*47.01*
LC79,11	*1.7*	*0.05*	*0.3*	*0.5*	*0.3*	*0.3*	*11.2*	*23.9*	*3.7*	*1.3*	*6.2*	*0.70*	*2.6*	*0.8*	*1.2*	*54.74*
LC79,12	*13.6*	*0.08*	*10.6*	*1.1*	*1<*	*.0<*	*11.7*	*19.7*	*5.4*	*0.7*	*1.9*	*0.36*	*1.9*	*0.9*	*1.1*	*68.96*
Average first 3	2.33	0.11	0.25	1.10	0.30	0.30	16.05	24.20	5.50	1.20	2.50	1.14	2.60	0.87	1.73	60.18
STDS	0.12	0.02	0.07	0.10	0.00	0.00	0.92	0.89	n.d.	0.00	0.26	n.d.	0.53	0.06	0.12	
RSD	5%	20%	28%	9%	0%	0%	6%	4%	n.d.	0%	11%	n.d.	20%	7%	7%	
CP80																
CP80,1	1.2	.01<	-.0<	0.5	0.4	0.4	15.7	26.3	5.2	*1.4	3.7	*0.53	3.1	1.0	1.7	61.30
CP80,2	1.6	.03<	*0.3	0.5	0.3	0.3	13.9	25.7	*4.9	1.2	2.7	*0.51	*3.3	1.1	1.3	57.68
CP80,3	1.4	.01<	.1<	0.4	0.2	0.3	16.2	*27.5	*4.9	*1.5	3.3	*0.54	3.0	1.2	1.5	61.91
CP80,4	0.9	0.04	0<	0.4	0.2	0.2	16.5	24.2	5.4	1.1	3.2	*0.42	3.1	1.0	1.6	58.30
CP80,5	1.1	.02<	0<	0.4	0.3	.2<	*18.1	24.0	5.6	1.2	2.1	*0.38	2.2	1.0	1.6	57.79
CP80,6	1.1	0.04	1<	0.4	0.3	0.4	*12.0	26.2	*4.3	1.0	*5.4	*0.40	2.9	1.0	1.2	58.60
CP80,7	0.9	0.04	1<	0.4	0.3	0.4	*18.5	26.7	5.5	1.2	2.5	*0.53	2.3	1.1	1.6	62.03
CP80,8	1.1	.02<	1<	0.3	.1<	0.2	16.7	26.1	5.1	*1.5	3.2	*0.56	2.6	0.9	*1.8	59.98
CP80,9	1.4	.03<	0<	0.8	0.4	0.3	14.3	26.7	5.2	*1.5	2.9	*0.72	*3.3	1.2	1.5	60.17
CP80,10	1.0	-.00<	.1<	0.4	0.3	0.3	14.4	27.3	*4.6	*1.4	3.6	*0.59	*3.3	1.1	1.5	59.73
CP80,11	1.0	-.00<	1<	0.5	0.3	0.3	*19.0	25.1	5.7	1.3	1.7	*0.70	2.6	1.2	*1.8	61.07
CP80,12	1.0	0.04	-.0<	0.4	0.3	0.3	*19.3	25.7	5.7	1.3	1.9	*0.62	2.4	0.9	*1.8	61.65
CP80,13	1.0	-.02<	1<	0.5	0.2	0.3	14.0	*28.0	5.3	1.3	*4.0	1.21	*3.2	1.0	1.5	61.45
CP80,14	1.1	0.04	0<	0.5	0.2	0.3	15.4	27.2	*4.8	*1.7	2.3	*0.35	3.1	1.0	1.7	59.67
CP80,15	1.3	.03<	-.0<	0.4	0.3	0.3	15.9	24.7	*5.0	1.2	2.4	*0.46	2.6	0.8	1.5	58.82
CP80,16	1.2	0.03	1<	0.5	0.3	0.4	17.0	24.7	5.4	1.1	2.1	*0.50	2.9	1.2	1.6	58.91
CP80,17	1.3	.01<	0.2	0.5	0.4	0.4	15.3	24.9	*4.7	1.2	3.8	*0.37	2.6	0.7	1.4	57.86
CP80,18	1.0	.01<	0<	0.4	0.2	1<	*18.5	*22.5	5.8	1.1	1.7	*0.59	2.7	1.1	*1.9	57.41
CP80,19	1.3	.03<	1<	0.7	0.4	0.3	17.6	25.8	5.3	1.3	3.2	*0.57	*3.4	*1.4	1.6	62.98
CP80,20	1.1	0.05	0<	0.4	0.3	0.4	17.2	24.9	6.5	1.3	3.3	0.94	2.8	1.2	*1.8	61.98
CP80,21	1.1	.03<	-.0<	0.6	0.3	0.4	16.8	25.5	5.3	1.2	3.5	*0.53	*3.4	1.1	1.7	61.38
CP80,22	1.1	0.05	0<	0.5	0.3	0.2	17.5	25.5	5.1	*1.5	2.1	*0.34	2.7	1.0	*1.8	59.80
CP80,23	1.3	0.04	1<	0.6	0.4	0.3	17.0	25.2	*5	*1.4	3.0	*0.46	2.9	1.0	1.7	60.10
CP80,24	1.2	.00<	0<	0.4	0.4	0.4	16.3	*27.7	5.4	*1.4	*5.3	*0.52	2.6	1.1	1.7	64.58
Average	1.15	0.04	0.20	0.46	0.30	0.32	15.98	25.62	5.47	1.20	2.77	1.08	2.73	1.04	1.55	59.93
STDS	0.17	0.01	n.d.	0.11	0.07	0.07	1.20	0.93	0.35	0.09	0.68	0.19	0.27	0.13	0.14	
RSD	15%	15%	n.d.	23%	23%	21%	8%	4%	6%	8%	24%	18%	10%	13%	9%	
CP88																
LC88,1	3.3	0.10	0.3	1.4	0.4	0.4	14.4	24.8	4.8	0.9	2.5	1.44	2.4	1.0	1.5	59.66
LC88,3	2.6	0.11	0.2	1.4	0.4	*0.2	15.8	*21.9	4.2	1.2	2.2	0.52	2.1	*1.2	1.6	55.60
LC88,5	1.8	0.05	0.3	0.9	0.3	0.3	15.8	22.5	4.4	0.9	*3.5	*0.37	2.1	1.1	1.6	55.97
LC88,6	3.7	0.09	0.7	1.4	0.4	0.4	15.5	23.3	4.1	1.1	2.2	*0.30	2.6	0.7	1.4	58.01
LC88,7	3.4	0.12	0.5	1.4	0.4	0.5	15.8	*21.3	4.7	1.0	2.3	0.61	*1.9	0.8	1.5	56.22
LC88,2	*1.2*	*0.08*	*1<*	*1.0*	*0.4*	*0.2*	*17.2*	*23.2*	*4.0*	*1.2*	*1.7*	*0.33*	*2.2*	*0.8*	*1.4*	*54.98*
LC88,4	*7.1*	*0.07*	*4.8*	*1.2*	*0.3*	*1<*	*12.3*	*22.2*	*4.1*	*1.0*	*2.6*	*0.31*	*2.2*	*0.6*	*1.4*	*60.31*
LC88,8	*17.5*	*0.10*	*13.3*	*1.3*	*0.2*	*1<*	*10.2*	*21.6*	*5.3*	*0.9*	*1.0*	*0.45*	*1.5*	*0.5*	*0.9*	*74.95*
LC88,9	*3.5*	*0.13*	*1.3*	*1.1*	*0.4*	*0.3*	*11.4*	*16.1*	*4.1*	*0.8*	*1.4*	*0.51*	*2.1*	*0.8*	*1.2*	*45.15*
LC88,10	*1.9*	*0.05*	*0.5*	*0.8*	*0.3*	*1<*	*16.6*	*19.7*	*4.2*	*1.1*	*1.5*	*0.36*	*1.7*	*0.8*	*1.5*	*51.14*
LC88,11	*2.7*	*0.06*	*1.9*	*0.8*	*0.2*	*0.2*	*11.9*	*15.2*	*3.5*	*0.7*	*1.5*	*0.38*	*1.7*	*0.8*	*1.2*	*42.68*
LC88,12	*2.7*	*0.10*	*1.4*	*0.9*	*0.3*	*0.4*	*14.0*	*20.3*	*4.0*	*1.1*	*2.1*	*0.33*	*2.3*	*1.0*	*1.9*	*52.69*
LC88,13	*0.8*	*0.03*	*0.2*	*0.4*	*0<*	*0.3*	*14.6*	*15.9*	*3.4*	*0.7*	*1.4*	*0.35*	*1.5*	*0.9*	*1.5*	*42.10*
LC88,14	*2.0*	*0.08*	*0.3*	*0.8*	*0.2*	*.1<*	*13.4*	*16.2*	*3.7*	*0.8*	*2.0*	*0.61*	*1.9*	*0.9*	*1.2*	*44.01*
LC88,15	*2.8*	*0.09*	*1.2*	*0.7*	*0.3*	*0.2*	*13.6*	*21.7*	*3.9*	*1.3*	*1.9*	*0.39*	*2.5*	*0.7*	*1.5*	*52.83*
LC88,16	*1.5*	*0.07*	*0.2*	*0.6*	*0.2*	*0.3*	*11.4*	*13.7*	*3.2*	*0.7*	*1.8*	*0.39*	*1.8*	*1.0*	*1.4*	*38.42*
LC88,17	*0.7*	*0.04*	*0<*	*0.3*	*0.3*	*2<*	*14.1*	*17.4*	*3.5*	*1.0*	*2.6*	*0.32*	*1.8*	*1.1*	*1.6*	*44.85*
LC88,18	*1.2*	*0.07*	*1<*	*0.7*	*0.3*	*0.4*	*14.2*	*18.5*	*4.3*	*0.7*	*2.3*	*0.63*	*2.2*	*1.2*	*1.4*	*48.09*
LC88,19	*1.2*	*0.04*	*0.3*	*0.5*	*0.2*	*0.2*	*15.6*	*16.8*	*3.9*	*0.7*	*1.4*	*0.32*	*1.5*	*0.9*	*1.5*	*45.11*
LC88,20	*1.0*	*0.08*	*0.2*	*0.4*	*1<*	*2<*	*16.9*	*23.0*	*4.2*	*1.2*	*1.4*	*0.36*	*2.2*	*0.8*	*1.7*	*53.39*
LC88,21	*2.1*	*0.09*	*0.4*	*1.1*	*0.4*	*0.4*	*14.5*	*20.7*	*4.4*	*1.0*	*2.1*	*0.67*	*2.2*	*1.0*	*1.5*	*52.58*
LC88,22	*1.6*	*0.06*	*0.4*	*0.7*	*2<*	*0.3*	*12.3*	*20.1*	*3.3*	*0.7*	*3.9*	*0.58*	*1.4*	*0.7*	*1.3*	*47.39*
LC88,23	*2.0*	*0.05*	*0.4*	*0.4*	*1<*	*0.3*	*8.4*	*17.6*	*2.6*	*0.8*	*1.9*	*0.53*	*1.5*	*0.4*	*0.9*	*37.81*
LC88,24	*2.7*	*0.08*	*0.6*	*1.1*	*0.2*	*0.3*	*11.1*	*16.6*	*3.1*	*0.9*	*0.9*	*0.34*	*1.9*	*0.7*	*0.9*	*41.44*
LC88,25	*1.6*	*0.07*	*0.4*	*0.7*	*0.2*	*.2<*	*13.4*	*16.2*	*3.2*	*0.8*	*0.7*	*0.30*	*1.5*	*0.4*	*1.1*	*40.53*
LC88,26	*2.0*	*0.08*	*0.5*	*0.7*	*2<*	*0.2*	*14.5*	*18.2*	*3.4*	*1.0*	*0.7*	*0.27*	*1.6*	*0.8*	*1.2*	*45.14*
LC88,27	*1.7*	*0.06*	*0.2*	*0.8*	*1<*	*0.2*	*14.6*	*18.3*	*3.4*	*1.1*	*0.8*	*0.26*	*2.0*	*0.7*	*1.3*	*45.36*
Average first 5	2.96	0.09	0.40	1.30	0.38	0.40	15.46	23.53	4.44	1.02	2.30	0.86	2.30	0.90	1.52	57.86
STDS	0.76	0.03	0.20	0.22	0.04	0.08	0.61	1.17	0.30	0.13	0.14	0.51	0.24	0.18	0.08	
RSD	26%	29%	50%	17%	12%	20%	4%	5%	7%	13%	6%	59%	11%	20%	6%	

Sample	SrO2	TiO2	Al2O3	FeO	MnO	MgO	CaO	Na2O	K2O	P2O5	F	Cl	SO3	BaO	SrO	Total
CP90																
LC90,1	*2.0*	*0.11*	*0.2*	*0.6*	*.1<*	*0.2*	*17.1*	*19.1*	*7.4*	*1.1*	*1.6*	*0.85*	*2.0*	*0.7*	*1.4*	*54.44*
LC90,2	*2.2*	*0.09*	*0.3*	*0.7*	*0.2*	*.2<*	*15.6*	*19.0*	*5.5*	*1.0*	*2.5*	*0.89*	*2.5*	*1.0*	*1.4*	*52.81*
LC90,3	*2.0*	*0.06*	*0.3*	*0.6*	*0.2*	*0.4*	*14.1*	*19.6*	*2.8*	*0.7*	*2.3*	*0.65*	*1.4*	*1.0*	*1.5*	*47.64*
LC90,4	*2.8*	*0.11*	*0.2*	*0.8*	*0.5*	*0.6*	*18.2*	*26.8*	*7.0*	*1.1*	*5.6*	*1.68*	*2.5*	*1.1*	*1.7*	*70.72*
LC90,5	*2.8*	*0.10*	*0.3*	*0.8*	*0.3*	*0.4*	*14.7*	*28.9*	*6.0*	*1.0*	*7.5*	*2.19*	*2.9*	*1.5*	*1.5*	*71.02*
LC90,8	*3.0*	*0.14*	*0.2*	*0.8*	*0.4*	*0.5*	*16.3*	*20.0*	*6.7*	*2.1*	*2.6*	*1.04*	*2.3*	*0.9*	*1.8*	*58.96*
LC90,12	*3.2*	*0.13*	*0.2*	*1.1*	*0.4*	*0.6*	*16.8*	*25.4*	*5.7*	*2.1*	*4.9*	*1.67*	*3.3*	*1.7*	*1.9*	*69.11*
LC90,6	2.3	0.11	1<	0.8	0.3	0.4	15.1	24.2	*8.3	1.0	*5.9	1.20	*5.3	0.9	1.4	67.23
LC90,7	2.4	0.09	0.2	0.8	0.3	0.4	17.6	*21.1	6.6	1.0	3.1	0.83	2.2	0.8	1.6	59.06
LC90,9	2.4	0.10	0.3	0.8	.2<	.2<	16.8	*19.9	6.4	0.8	2.7	0.76	*3.9	0.6	1.4	56.82
LC90,10	2.1	0.09	0.3	0.6	0.3	0.3	14.4	*21.1	4.4	0.8	*3.4	0.76	*3.4	0.6	1.3	53.87
LC90,11	2.8	0.08	0.2	0.8	1<	0.4	16.9	26.2	6.4	1.6	*3.5	1.53	2.9	1.2	1.5	66.07
LC90,13	2.6	0.11	1<	0.8	0.4	*0.2	15.8	26.6	*7.4	1.2	2.1	*3.6	2.4	1.1	1.7	66.14
LC90,14	2.7	0.09	0.2	0.7	0.4	0.4	17.7	25.2	6.6	1.3	*3.6	1.63	2.3	1.0	*1.9	65.62
LC90,15	2.5	0.09	1<	0.8	0.3	0.5	*19.0	24.8	*7.2	0.7	*6.3	*2.04	1.9	*1.8	*2.0	69.81
LC90,16	2.6	0.12	0.2	0.9	*0.2	0.4	16.4	26.9	*7.0	1.5	2.8	*1.88	3.2	1.3	1.7	67.08
LC90,17	2.6	0.11	0.3	0.7	0.3	0.4	15.4	25.9	*7.3	1.3	*4.7	*1.88	3.1	1.2	1.7	66.91
LC90,18	2.6	0.11	0.2	*1.4	0.4	0.4	17.6	23.3	*7.9	1.2	3.0	1.26	3.0	0.7	1.6	64.67
LC90,19	2.3	0.10	0.2	0.8	0.3	0.3	16.7	25.0	*7.2	1.4	2.3	1.75	2.9	0.7	1.6	63.61
LC90,20	2.4	*0.14	0.2	0.8	0.3	0.4	*18.5	24.3	8.3	1.0	2.9	1.27	2.3	1.2	1.7	63.69
Average last 13	2.48	0.10	0.23	0.78	0.33	0.39	16.40	25.24	6.12	1.14	2.70	1.22	2.62	0.94	1.56	62.25
STDS	0.19	0.01	0.05	0.08	0.05	0.05	1.10	1.15	0.85	0.28	0.37	0.37	0.45	0.26	0.14	
RSD	8%	12%	21%	10%	15%	14%	7%	5%	14%	25%	14%	31%	17%	27%	9%	
CP96																
LC96,1	2.5	*0.07	*0.8	1.3	0.3	2<	15.7	22.0	4.8	0.9	2.8	0.49	2.0	1.2	1.4	56.35
LC96,2	2.1	0.09	0.2	*0.9	*0.2	0.4	15.7	22.4	6.7	1.2	1.7	0.39	4.3	1.2	1.5	58.90
LC96,4	2.8	0.11	0.2	1.2	0.3	*0.3	*18.8	*19.3	*4.5	0.8	2.6	0.17	1.6	1.1	*2.1	55.76
LC96,5	1.7	*0.07	1<	*0.9	0.3	*0.3	17.1	22.0	4.7	1.1	2.6	0.40	2.3	*1.7	*1.9	57.19
LC96,6	1.7	*0.07	1<	*0.7	0.3	*0.2	*20.0	21.6	5.2	1.4	*1.1	0.27	1.7	0.8	*1.8	56.87
LC96,7	2.7	0.10	0.3	1.2	0.4	0.4	13.6	21.4	*4.3	*0.8	*6.2	0.60	3.4	1.2	1.4	57.79
LC96,3	*6.3*	*0.04*	*4.2*	*0.6*	*-0<*	*2<*	*18.5*	*18.6*	*4.5*	*0.9*	*0.7*	*0.17*	*1.2*	*0.6*	*1.3*	*57.73*
LC96,8	*2.4*	*0.12*	*0.2*	*1.1*	*0.2*	*0.5*	*15.9*	*15.9*	*5.1*	*1.1*	*4.4*	*0.55*	*2.6*	*1.2*	*1.6*	*52.77*
LC96,9	*1.0*	*.02<*	*0.2*	*0.2*	*1<*	*1<*	*18.0*	*17.6*	*3.8*	*0.9*	*0.8*	*0.28*	*1.6*	*0.4*	*1.2*	*45.86*
LC96,10	*1.6*	*0.06*	*0.3*	*0.6*	*0.2*	*0.4*	*13.9*	*15.7*	*3.8*	*1.1*	*1.3*	*0.55*	*1.5*	*0.7*	*1.3*	*43.00*
LC96,11	*1.9*	*0.05*	*0.2*	*0.8*	*0.3*	*0.3*	*14.0*	*15.7*	*3.7*	*1.3*	*2.0*	*0.61*	*2.7*	*0.9*	*1.6*	*46.03*
LC96,12	*1.9*	*0.06*	*0.8*	*0.8*	*0.2*	*0.3*	*13.9*	*14.9*	*3.8*	*0.9*	*1.7*	*0.58*	*1.6*	*0.9*	*1.2*	*43.56*
LC96,13	*1.7*	*0.11*	*0.2*	*1.1*	*0.4*	*0.3*	*10.9*	*22.9*	*4.0*	*1.3*	*1.4*	*0.47*	*2.4*	*1.2*	*1.3*	*49.71*
LC96,14	*1.5*	*0.07*	*1<*	*0.8*	*0.2*	*0.3*	*14.6*	*20.1*	*4.8*	*1.3*	*1.8*	*0.45*	*1.7*	*0.7*	*1.5*	*49.60*
LC96,15	*1.4*	*0.09*	*0<*	*0.9*	*0.3*	*0.3*	*13.5*	*19.3*	*4.5*	*0.9*	*2.8*	*0.30*	*2.1*	*1.6*	*1.9*	*49.81*
LC96,16	*3.1*	*0.09*	*0.2*	*1.0*	*0.4*	*0.4*	*16.7*	*21.1*	*4.2*	*1.1*	*1.4*	*0.23*	*1.7*	*1.0*	*1.6*	*54.44*
LC96,17	*1.2*	*.02<*	*1<*	*0.3*	*1<*	*0<*	*21.5*	*19.2*	*4.3*	*1.1*	*0.3*	*0.18*	*1.3*	*0.4*	*1.6*	*51.29*
LC96,18	*2.5*	*0.11*	*0.2*	*1.3*	*0.3*	*0.6*	*9.7*	*20.0*	*3.6*	*1.4*	*2.5*	*0.35*	*3.4*	*1.0*	*1.1*	*48.21*
Average first 6	2.25	0.10	0.23	1.23	0.32	0.40	15.53	21.88	5.35	1.08	2.43	0.39	2.55	1.10	1.43	56.27
STDS	0.49	0.01	0.06	0.06	0.04	0.00	1.44	0.39	0.93	0.24	0.49	0.15	1.07	0.17	0.06	
RSD	22%	10%	25%	5%	14%	0%	9%	2%	17%	22%	20%	40%	42%	16%	4%	
CP98																
LC98,4	1.9	0.09	0.2	1.4	0.4	0.4	14.7	26.3	*4.3	*1.5	2.1	*0.50	2.3	0.8	1.6	58.34
LC98,6	1.8	0.09	0<	1.2	*0.5	*0.3	15.4	25.8	4.8	1.3	*4.1	0.71	3.0	1.0	1.4	61.26
LC98,9	2.0	0.14	0<	1.5	*0.5	0.4	16.6	26.1	4.9	1.0	3.5	*0.48	2.3	*1.4	*1.9	62.60
LC98,10	2.1	0.09	*0.9	1.1	2<	*0.3	*19.7	23.2	6.2	1.2	3.7	1.41	*1.9	0.9	1.7	64.34
LC98,1	*1.6*	*0.12*	*1<*	*1.1*	*0.2*	*0.2*	*13.4*	*26.1*	*4.4*	*1.0*	*3.3*	*0.80*	*2.6*	*1.1*	*1.5*	*57.51*
LC98,2	*3.6*	*0.10*	*0.8*	*1.2*	*0.3*	*0.4*	*14.8*	*23.6*	*5.0*	*1.2*	*1.8*	*0.67*	*2.2*	*1.1*	*1.4*	*58.26*
LC98,3	*1.2*	*0.07*	*1<*	*0.8*	*0.4*	*0.2*	*16.5*	*23.5*	*5.6*	*1.3*	*2.0*	*1.47*	*2.2*	*1.2*	*1.7*	*58.17*
LC98,5	*1.3*	*0.06*	*1<*	*1.2*	*0.4*	*0.4*	*15.6*	*23.2*	*5.1*	*1.1*	*1.7*	*0.77*	*2.5*	*1.0*	*1.6*	*56.04*
LC98,7	*1.5*	*0.10*	*0.2*	*1.2*	*0.3*	*0.4*	*15.4*	*27.8*	*3.9*	*1.8*	*1.9*	*0.59*	*2.4*	*0.9*	*1.7*	*60.04*
LC98,8	*1.4*	*0.13*	*0<*	*1.1*	*0.3*	*0.3*	*19.4*	*24.5*	*5.8*	*1.1*	*3.4*	*1.22*	*2.2*	*1.0*	*2.0*	*63.92*
LC98,11	*9.1*	*0.06*	*6.9*	*1.3*	*0.3*	*2<*	*13.8*	*24.2*	*4.7*	*0.9*	*1.3*	*0.30*	*1.7*	*0.7*	*1.5*	*66.79*
LC98,12	*0.5*	*.02<*	*-0<*	*0.5*	*1<*	*.1<*	*19.9*	*25.0*	*4.6*	*1.3*	*1.5*	*0.37*	*2.0*	*1.4*	*2.0*	*58.93*
LC98,13	*12.8*	*0.06*	*3.7*	*0.8*	*0.4*	*2<*	*12.8*	*20.0*	*6.8*	*1.0*	*1.8*	*0.71*	*2.3*	*0.8*	*1.2*	*65.08*
LC98,14	*13.1*	*0.08*	*4.0*	*1.0*	*0.3*	*2<*	*12.9*	*20.3*	*6.7*	*0.9*	*2.4*	*0.49*	*2.0*	*1.2*	*1.1*	*66.59*
LC98,15	*10.1*	*0.11*	*2.9*	*1.0*	*0.3*	*2<*	*13.3*	*21.4*	*6.2*	*1.0*	*3.6*	*0.66*	*2.3*	*0.9*	*1.4*	*65.36*
LC98,16	*17.4*	*0.06*	*5.0*	*1.2*	*0.3*	*0.2*	*11.1*	*16.5*	*7.7*	*1.0*	*2.1*	*1.24*	*1.7*	*1.2*	*1.1*	*67.66*
LC98,17	*24.7*	*.02<*	*7.2*	*1.0*	*0.2*	*0.3*	*10.1*	*14.1*	*8.3*	*0.9*	*1.2*	*0.42*	*1.3*	*0.6*	*1.0*	*71.34*
LC98,18	*22.1*	*0.04*	*6.4*	*1.1*	*0.3*	*0.2*	*11.4*	*16.6*	*7.6*	*0.9*	*1.2*	*0.37*	*1.4*	*0.7*	*1.2*	*71.36*
Average first 4	1.95	0.10	0.20	1.30	0.40	0.40	15.57	25.35	5.30	1.17	3.10	1.08	2.53	0.90	1.57	60.90
STDS	0.13	0.03	n.d.	0.18	n.d.	0.00	0.96	1.45	0.78	0.15	0.87	0.49	0.40	0.10	0.15	
RSD	7%	24%	n.d.	14%	n.d.	0%	6%	6%	15%	13%	28%	47%	16%	11%	10%	

Sample	SiO2	TiO2	Al2O3	FeO	MnO	MgO	CaO	Na2O	K2O	P2O5	F	Cl	SO3	BaO	SrO	Total
CP106																
LC106,1	*3.1*	*0.12*	*0.5*	*1.2*	*0.4*	*0.5*	*14.4*	*25.1*	*7.0*	*1.2*	*3.2*	*2.30*	*2.7*	*1.3*	*1.3*	*64.33*
LC106,2	*1.4*	*0.07*	*0<*	*0.8*	*0.4*	*0.3*	*16.6*	*24.7*	*7.7*	*1.1*	*2.7*	*3.00*	*2.1*	*0.9*	*1.4*	*63.12*
LC106,3	*1.7*	*0.06*	*0.3*	*0.7*	*0.4*	*.2<*	*20.6*	*23.0*	*5.6*	*1.3*	*2.4*	*0.55*	*2.1*	*0.7*	*1.8*	*61.16*
LC106,11	*7.5*	*0.08*	*4.9*	*1.3*	*0.2*	*0.3*	*14.2*	*21.5*	*6.0*	*0.9*	*1.4*	*0.99*	*2.0*	*0.7*	*1.4*	*63.60*
LC106,14	*3.2*	*0.12*	*0.5*	*1.2*	*0.3*	*0.4*	*17.0*	*22.2*	*6.0*	*1.2*	*1.1*	*1.35*	*1.8*	*0.8*	*1.5*	*58.71*
LC106,19	*1.9*	*0.11*	*1<*	*1.2*	*0.5*	*0.4*	*14.5*	*24.5*	*7.1*	*1.3*	*1.6*	*3.00*	*2.6*	*0.8*	*1.3*	*60.98*
LC106,4	2.4	0.11	0.3	1.0	0.4	0.4	15.9	24.5	5.8	1.3	2.6	0.82	2.9	0.9	1.5	60.87
LC106,5	2.8	0.09	0.3	1.3	0.3	0.4	16.4	25.2	6.3	1.3	2.5	*1.85	2.2	0.9	1.5	63.48
LC106,6	2.3	0.08	0.3	1.1	0.3	0.3	*19.0	23.4	5.7	1.3	1.5	0.68	*1.9	1.0	*1.8	60.63
LC106,7	2.9	*0.16	0.3	1.4	*0.5	0.5	*8.9	26.2	*7.0	*1.4	2.2	*3.20	2.9	1.0	*1.1	59.64
LC106,8	2.9	0.13	0.3	1.5	0.4	0.4	15.7	24.7	4.9	*1.4	2.1	0.91	*2.1	1.1	1.6	60.03
LC106,9	2.7	0.11	0.3	1.4	.1<	0.3	15.8	22.9	5.6	1.1	1.7	1.22	*2.1	1.1	1.4	57.55
LC106,10	2.7	*0.14	0.4	1.4	0.3	0.4	15.6	22.5	5.6	1.2	1.4	0.90	*2.0	0.9	1.5	56.83
LC106,12	3.0	0.13	0.2	*1.7	0.4	0.5	14.5	*21.8	6.2	1.3	2.1	1.67	2.4	1.0	1.6	58.63
LC106,13	2.4	0.09	0.3	1.2	0.3	0.3	14.5	25.6	5.5	1.2	*4.7	1.13	2.9	0.8	1.6	62.55
LC106,15	2.8	0.09	0.3	1.2	0.4	0.4	15.0	24.0	4.9	1.3	2.2	1.42	2.4	*1.4	1.4	59.17
LC106,16	2.5	*0.14	0.2	1.3	0.3	0.5	17.0	24.3	5.3	1.3	2.8	1.21	2.2	1.1	*1.8	62.12
LC106,17	2.3	0.09	*0.1	1.2	0.3	0.4	14.9	26.5	4.9	1.1	3.2	*2.50	2.4	*1.2	1.5	62.75
LC106,18	2.7	0.12	0.4	1.1	0.4	0.3	17.5	22.9	*6.9	1.2	1.5	1.45	2.6	0.7	1.6	61.28
LC106,20	3.0	0.10	0.3	1.5	0.3	0.4	16.4	*22.0	*7.9	1.3	2.3	*2.70	2.3	1.0	1.6	63.15
LC106,21	2.9	0.11	0.2	1.4	0.5	0.3	13.8	27.1	5.5	1.3	*1.3	1.35	2.3	*1.2	1.5	60.79
Average last 15	2.69	0.10	0.29	1.29	0.35	0.39	15.62	24.60	5.52	1.25	2.16	1.16	2.50	0.96	1.53	60.39
STDS	0.25	0.02	0.06	0.16	0.07	0.07	1.06	1.47	0.47	0.08	0.54	0.31	0.26	0.12	0.08	
RSD	9%	16%	21%	12%	19%	19%	7%	6%	8%	6%	25%	26%	11%	13%	5%	
CP107																
LC107,1	*3.6*	*0.14*	*0.5*	*1.8*	*2<*	*0.4*	*11.4*	*20.8*	*4.9*	*1.3*	*1.4*	*1.04*	*2.7*	*0.9*	*1.2*	*52.27*
LC107,2	*10.8*	*0.07*	*6.3*	*1.3*	*2<*	*1<*	*10.3*	*22.1*	*5.2*	*2.0*	*1.0*	*1.10*	*2.1*	*0.6*	*1.2*	*64.06*
LC107,8	*7.6*	*0.07*	*4.4*	*1.3*	*0.4*	*2<*	*14.4*	*22.4*	*7.1*	*1.1*	*2.2*	*2.70*	*2.0*	*0.9*	*1.3*	*67.87*
LC107,10	*7.1*	*0.10*	*3.0*	*1.1*	*0.3*	*2<*	*10.7*	*23.7*	*4.8*	*1.2*	*2.2*	*1.32*	*1.8*	*0.8*	*1.0*	*58.95*
LC107,17	*6.0*	*0.07*	*2.6*	*1.3*	*0.5*	*2<*	*8.9*	*24.2*	*7.0*	*2.5*	*1.3*	*2.60*	*3.7*	*1.0*	*1.0*	*62.66*
LC107,3	3.9	0.09	0.8	1.1	0.3	0.3	*21.2	*22.9	4.9	0.9	*0.4	0.40	*1.4	3<	*2.0	60.69
LC107,4	1.5	03<	0.3	*0.8	*0.2	0<	18.3	24.1	5.3	1.0	*0.8	1.13	2.2	1.0	1.8	58.33
LC107,5	4.0	0.07	1.9	0.9	*0.2	*0.2	11.8	25.2	5.6	1.4	*1.0	1.77	2.4	0.8	1.2	58.51
LC107,6	2.5	0.06	0.6	1.2	0.4	0.3	13.5	23.8	5.2	*1.8	1.9	1.57	2.5	1.2	1.5	58.13
LC107,7	3.1	0.12	1.1	1.0	0.5	0.3	13.0	25.0	5.9	1.3	2.5	2.40	2.8	1.1	1.3	61.26
LC107,9	2.7	0.10	0.7	1.0	0.3	2<	15.2	*22.5	*8.7	1.3	1.6	*4.30	2.0	1.1	1.5	62.88
LC107,11	2.4	0.04	0.6	*0.8	0.3	2<	16.3	25.5	5.1	0.9	1.6	0.81	2.2	1.3	1.6	59.28
LC107,12	0.7	0.04	0.3	*0.8	0.3	*0.2	15.8	24.8	4.4	*4.7	2.7	1.38	2.5	0.9	1.4	60.95
LC107,13	5.6	02<	*2.7	1.1	0.3	0.4	11.6	25.4	5.5	1.3	1.4	1.52	2.3	1.1	1.5	61.50
LC107,14	1.4	02<	0.9	*0.3	1<	1<	*21.8	*22.6	4.8	0.7	*0.9	0.29	*1.3	0.8	1.9	57.98
LC107,15	0.3	01<	-0<	*0.3	2<	2<	*20.1	25.0	4.5	1.1	3.6	0.63	*1.6	*0.6	1.7	59.50
LC107,16	4.2	0.19	1.0	2.2	0.4	*0.2	14.4	26.8	4.8	*2.1	4.3	1.43	2.3	0.8	1.3	66.18
Average last 11	2.69	0.09	0.82	1.21	0.35	0.33	14.43	25.04	5.09	1.10	2.45	1.21	2.36	1.01	1.52	59.70
STDS	1.57	0.05	0.46	0.45	0.08	0.05	2.20	0.81	0.47	0.24	1.05	0.64	0.23	0.18	0.22	
RSD	58%	56%	57%	37%	22%	15%	15%	3%	9%	22%	43%	52%	10%	18%	14%	
CP108																
LC108,2	0.5	02<	-0<	*0.4	0.4	2<	15.4	*28.5	6.8	1.0	4.1	*2.40	2.8	1.1	1.6	65.12
LC108,3	0.7	-00<	1<	0.7	0.3	0<	15.0	*28.8	5.4	1.3	2.8	1.32	2.6	0.7	1.6	61.06
LC108,4	1.3	01<	0.2	0.8	0.5	*0.3	11.4	*30.1	4.4	1.3	2.7	1.18	3.4	1.5	1.4	60.72
LC108,6	0.5	01<	0<	0.7	*0.2	0.2	14.1	*29.4	8.2	0.7	*4.8	1.85	2.9	1.2	1.6	64.45
LC108,10	1.3	02<	-0<	0.8	0.5	*0.3	15.4	26.6	7.0	0.8	4.1	*2.60	2.4	1.0	1.7	64.65
LC108,11	0.7	02<	1<	0.7	0.4	2<	15.1	26.2	*7.7	0.7	2.6	*2.70	3.0	1.1	1.6	62.51
LC108,14	0.5	02<	-0<	*0.6	0.5	*0.5	10.9	*30.6	7.0	0.6	*7.5	*4.40	2.8	*1.7	1.5	68.92
LC108,18	0.6	03<	0<	0.7	*0.7	1<	10.3	*31.4	7.1	1.0	*4.4	*4.30	3.4	1.3	1.3	66.23
LC108,1	*0.4*	*01<*	*1<*	*0.3*	*0.5*	*.2<*	*13.0*	*29.4*	*6.6*	*1.2*	*4.5*	*2.70*	*3.2*	*1.1*	*1.5*	*64.35*
LC018,5	*0.2*	*02<*	*-0<*	*0.3*	*0.2*	*1<*	*17.4*	*27.5*	*5.5*	*1.2*	*1.9*	*1.45*	*2.4*	*0.7*	*1.5*	*60.30*
LC108,7	*0.3*	*02<*	*1<*	*2<*	*0.3*	*1<*	*10.1*	*32.4*	*5.3*	*1.2*	*3.5*	*2.02*	*3.9*	*0.7*	*1.2*	*60.71*
LC108,8	*0.3*	*01<*	*0<*	*0.5*	*0.5*	*2<*	*10.2*	*29.0*	*9.2*	*0.5*	*7.6*	*5.30*	*3.4*	*1.7*	*1.6*	*69.66*
LC108,9	*0.3*	*01<*	*-0<*	*2<*	*0.4*	*0.3*	*14.8*	*28.6*	*5.9*	*0.8*	*5.4*	*1.33*	*3.3*	*1.2*	*1.5*	*63.86*
LC108,12	*0.2*	*-01<*	*1<*	*0.3*	*0.4*	*2<*	*13.2*	*30.0*	*6.1*	*0.8*	*4.6*	*2.18*	*3.2*	*1.0*	*1.5*	*63.58*
LC108,13	*0.3*	*0.03*	*-1<*	*0.4*	*0.5*	*0.2*	*13.0*	*29.7*	*5.6*	*1.0*	*3.5*	*1.70*	*3.3*	*1.6*	*1.7*	*62.59*
LC108,15	*0.3*	*00<*	*-1<*	*0.4*	*0.3*	*0.3*	*13.3*	*27.2*	*7.7*	*0.7*	*5.4*	*3.40*	*3.0*	*1.2*	*1.6*	*64.79*
LC108,16	*0.3*	*02<*	*0<*	*0.4*	*0.3*	*1<*	*13.4*	*26.6*	*8.8*	*0.6*	*6.7*	*4.40*	*3.1*	*1.9*	*1.8*	*68.24*
LC108,17	*0.3*	*02<*	*-1<*	*0.3*	*0.4*	*1<*	*12.0*	*27.9*	*9.7*	*0.7*	*3.8*	*5.70*	*2.9*	*1.1*	*1.4*	*66.14*
LC108,19	*1.0*	*02<*	*0.2*	*0.7*	*0.7*	*0.5*	*8.2*	*32.1*	*9.4*	*1.0*	*7.6*	*6.00*	*3.7*	*1.2*	*1.0*	*73.34*
LC108,20	*0.3*	*03<*	*-1<*	*0.6*	*0.5*	*0.4*	*8.3*	*30.9*	*10.7*	*0.6*	*10.0*	*7.10*	*3.6*	*1.5*	*1.2*	*75.47*
Average first 8	0.76	b.d.	0.20	0.73	0.43	0.20	13.45	26.40	6.27	0.93	3.28	1.45	2.91	1.13	1.54	59.66
STDS	0.34	n.d.	n.d.	0.05	0.08	n.d.	2.20	0.28	1.02	0.27	0.77	0.35	0.35	0.25	0.13	
RSD	45%	n.d.	n.d.	7%	19%	n.d.	16%	1%	16%	29%	24%	24%	12%	22%	8%	
CP112																
LC112,1	*9.9*	*0.11*	*2.1*	*3.4*	*0.6*	*0.6*	*4.8*	*29.3*	*2.4*	*0.9*	*1.9*	*0.62*	*2.4*	*1.2*	*0.7*	*60.98*
LC112,2	*5.0*	*0.58*	*1.2*	*2.6*	*0.3*	*1.0*	*12.7*	*14.4*	*10.9*	*1.8*	*10.7*	*3.20*	*11.3*	*2.0*	*0.9*	*78.75*
LC112,3	*0.7*	*01<*	*0<*	*0.8*	*0.4*	*0.4*	*10.8*	*22.3*	*9.6*	*0.6*	*10.5*	*5.30*	*3.5*	*2.0*	*1.4*	*68.29*
LC112,5	*0.9*	*02<*	*0<*	*0.8*	*0.5*	*1<*	*8.7*	*26.5*	*8.8*	*1.1*	*5.8*	*3.80*	*4.5*	*2.0*	*1.4*	*64.90*
LC112,5 (only one kept	1.6	0.05	0.4	1.1	0.5	0.4	10.5	21.3	5.9	1.2	3.5	2.15	3.6	1.5	1.4	55.14

Sample	SiO2	TiO2	Al2O3	FeO	MnO	MgO	CaO	Na2O	K2O	P2O5	F	Cl	SO3	BaO	SrO	Total
CP118																
LC118,1	*1.5*	*0.07*	*0.3*	*0.8*	*0.2*	*0.2*	*12.5*	*15.6*	*4.0*	*0.6*	*0.4*	*1.23*	*1.9*	*0.6*	*1.1*	*40.93*
LC118,2	*0.6*	*01<*	*0.2*	*0.7*	*0.2*	*0.3*	*10.2*	*23.9*	*2.6*	*0.7*	*3.9*	*0.59*	*1.9*	*0.5*	*0.9*	*47.36*
LC118,3	*2.0*	*0.03*	*0.4*	*1.0*	*2<*	*.2<*	*13.7*	*23.0*	*3.7*	*0.9*	*3.6*	*0.35*	*2.1*	*1.0*	*1.4*	*53.15*
LC118,14	*5.5*	*0.09*	*1.0*	*1.5*	*0.3*	*0.4*	*15.8*	*24.9*	*4.9*	*1.3*	*1.4*	*0.63*	*2.6*	*1.0*	*1.4*	*62.61*
LC118,4	0.4	*0.04	0<	1.0	0.3	0.3	16.6	23.6	6.9	0.5	*5.4	*3.00	2.2	0.9	1.6	62.82
LC118,5	0.3	.02<	-.0<	*0.8	0.3	0.4	15.5	26.1	4.8	0.6	1.9	1.02	2.6	*1.2	1.4	57.09
LC118,6	1.0	0.11	.1<	*1.6	0.3	0.4	*11.7	*28.4	*3.4	0.6	3.2	*0.37	3.2	0.9	1.2	56.51
LC118,7	0.6	*0.05	1<	1.1	*0.2	*0.5	14.5	*27.4	*3.5	0.7	*4.9	0.55	2.5	0.9	1.3	58.71
LC118,8	1.4	*0.05	0.3	1.0	0.3	0.3	16.0	26.2	4.6	0.9	1.6	0.97	2.4	1.0	1.6	58.69
LC118,9	4.1	0.15	*1.3	1.0	0.3	0.3	*18.3	24.4	5.8	1.1	1.5	1.33	*1.7	0.9	1.8	63.90
LC118,10	1.4	0.08	0.3	1.0	0.4	*0.5	15.5	26.6	5.9	1.1	1.7	1.70	2.6	*1.1	1.5	61.37
LC118,11	4.0	0.06	*1.4	1.2	0.3	0.4	16.3	25.6	5.0	1.7	1.7	0.60	2.3	1.0	1.8	63.48
LC118,12	3.7	0.08	0.9	1.0	0.3	.2<	16.2	23.5	*9.2	1.6	1.6	*4.20	*1.7	1.0	1.4	66.36
LC118,13	3.3	0.07	0.8	1.0	0.4	0.4	15.3	*27.4	4.8	1.8	2.8	0.63	2.5	0.7	1.5	63.20
LC118,15	3.7	0.08	1.1	*0.8	0.4	0.3	15.8	26.2	5.9	1.3	*4.8	1.54	2.3	*1.1	1.8	67.10
LC118,16	2.0	0.07	0.4	*0.6	.1<	0.3	*18.5	23.2	4.7	1.3	1.7	0.50	2.2	1.0	1.6	58.38
Average last 12	2.16	0.09	0.63	1.04	0.33	0.34	15.74	25.07	5.40	1.10	1.94	0.98	2.50	0.92	1.54	59.79
STDS	1.50	0.03	0.34	0.07	0.05	0.05	0.63	1.37	0.78	0.45	0.57	0.45	0.31	0.10	0.20	
RSD	69%	36%	54%	7%	15%	15%	4%	5%	14%	41%	29%	46%	12%	11%	13%	
CP126																
LC126,1	*0.4*	*-00<*	*0.3*	*0.3*	*0.3*	*0.2*	*5.4*	*19.7*	*4.3*	*0.3*	*8.0*	*2.33*	*3.1*	*2.0*	*0.9*	*47.60*
LC126,2	*0.5*	*0.04*	*1<*	*0.5*	*0.4*	*0.3*	*6.4*	*18.9*	*8.2*	*2<*	*6.0*	*5.50*	*2.9*	*1.5*	*1.0*	*52.16*
LC126,6	*0.2*	*01<*	*-1<*	*0.3*	*0.4*	*0.2*	*6.9*	*19.2*	*10.9*	*0.4*	*5.2*	*8.00*	*2.7*	*1.6*	*0.9*	*56.96*
LC126,3	0.9	*0.04	0.4	0.4	0.6	0.2	8.1	21.3	*8.1	0.4	6.2	*4.90	3.3	*1.3	1.0	55.12
LC126,4	0.6	03<	0<	0.5	0.7	0.2	7.6	24.4	6.2	0.4	*8.5	3.20	2.9	2.1	1.1	58.31
LC126,5	0.6	02<	-.0<	0.6	0.5	0.6	7.5	27.1	7.3	0.4	*11.6	4.20	3.5	2.1	1.2	67.25
LC126,7	3.2	*0.05	1<	1.4	0.5	*0.6	7.4	22.7	*8.9	0.5	3.9	*5.9	2.5	1.2	0.9	59.73
Average last 4	1.33	n.d.	0.40	0.73	0.58	0.33	7.15	23.88	6.75	0.43	5.05	3.70	3.05	1.80	1.05	58.21
STDS	1.26	n.d.	n.d.	0.46	0.10	0.23	0.70	2.50	0.78	0.05	1.63	0.71	0.44	0.52	0.13	
RSD	95%	n.d.	n.d.	63%	17%	69%	10%	10%	12%	12%	32%	19%	15%	29%	12%	
CP127																
LC127,1	2.9	0.05	0.7	0.9	0.4	0.5	7.9	21.4	*10.3	*2.6	*10.0	*5.70	*1.8	1.0	*0.8	67.04
LC127,2	4.5	0.05	1.2	1.2	*0.5	*0.4	11.2	20.3	5.5	*2.7	5.0	1.29	2.1	1.1	1.3	58.38
LC127,3	5.7	0.26	0.9	2.5	0.4	0.6	8.3	18.2	8.1	1.1	6.3	*5.00	*1.9	1.0	*0.8	61.16
LC127,4	5.6	0.06	2.2	1.1	*0.5	0.3	9.3	21.7	4.1	*2.5	*16.5	0.75	*1.3	1.4	1.2	68.50
LC127,5	3.6	0.04	1.2	1.1	*0.5	0.5	4.5	18.8	7.5	1.7	*8.1	3.30	3.2	0.9	*0.7	55.49
LC127,6	*4.1*	*0.04*	*1.1*	*1.4*	*0.6*	*0.4*	*10.5*	*18.8*	*4.2*	*1.6*	*6.0*	*0.69*	*1.8*	*0.9*	*1.1*	*53.32*
LC127,7	*2.5*	*0.04*	*0.6*	*1.2*	*0.5*	*0.3*	*10.7*	*19.4*	*5.3*	*1.0*	*2.2*	*1.55*	*2.4*	*1.0*	*1.1*	*49.74*
LC127,8	*2.7*	*0.05*	*0.6*	*1.2*	*0.4*	*0.2*	*12.3*	*18.4*	*4.6*	*2.3*	*1.6*	*1.10*	*1.6*	*1.1*	*1.3*	*49.51*
LC127,9	*4.0*	*0.06*	*1.2*	*0.8*	*0.5*	*0.3*	*12.2*	*19.0*	*6.0*	*1.4*	*1.7*	*0.61*	*3.1*	*1.0*	*1.3*	*53.10*
LC127,10	*4.0*	*0.04*	*1.2*	*1.0*	*0.3*	*0.4*	*6.3*	*19.2*	*5.2*	*2.0*	*4.6*	*1.80*	*2.0*	*0.8*	*0.7*	*49.61*
LC127,11	*5.4*	*0.08*	*1.3*	*1.3*	*0.4*	*0.2*	*8.0*	*13.7*	*4.0*	*1.6*	*3.4*	*0.84*	*2.0*	*1.0*	*1.0*	*44.06*
LC127,12	*1<*	*0.03*	*-1<*	*0.3*	*0<*	*-0<*	*0<*	*31.6*	*8.0*	*0.3*	*0.1*	*3.60*	*4.9*	*-1<*	*2<*	*49.08*
LC127,13	*1.1*	*0.06*	*0.4*	*1.0*	*0.4*	*0.3*	*8.0*	*17.7*	*4.0*	*1.6*	*2.9*	*0.82*	*2.6*	*1.0*	*1.1*	*43.02*
LC127,14	*4.8*	*0.08*	*1.7*	*1.2*	*0.7*	*0.4*	*7.7*	*16.8*	*3.8*	*2.2*	*2.4*	*0.91*	*1.4*	*1.2*	*1.0*	*46.34*
LC127,15	*3.6*	*0.07*	*1.1*	*1.2*	*0.5*	*0.6*	*6.7*	*13.1*	*4.2*	*2.3*	*2.3*	*0.82*	*2.5*	*0.6*	*0.8*	*40.58*
LC127,16	*4.3*	*0.20*	*2.8*	*1.9*	*0.4*	*0.7*	*5.8*	*12.0*	*3.6*	*1.3*	*1.6*	*1.13*	*1.6*	*0.6*	*0.6*	*36.77*
LC127,17	*4.7*	*0.06*	*1.7*	*1.3*	*0.5*	*0.2*	*9.9*	*18.1*	*4.5*	*2.6*	*1.1*	*1.02*	*2.2*	*1.2*	*1.2*	*50.23*
LC127,18	*10.4*	*0.07*	*2.8*	*1.1*	*0.4*	*2<*	*4.0*	*21.5*	*5.4*	*0.8*	*10.5*	*0.92*	*2.4*	*0.7*	*0.5*	*61.26*
Average first 5	4.46	0.09	1.24	1.36	0.40	0.48	8.24	20.08	6.30	1.40	5.65	1.78	2.65	1.08	1.25	56.48
STDS	1.23	0.09	0.56	0.65	0.00	0.13	2.45	1.55	1.84	0.42	0.92	1.34	0.78	0.19	0.07	
RSD	27%	102%	47%	48%	0%	26%	30%	8%	29%	30%	16%	75%	29%	18%	6%	
CP128																
LC128,1	*7.9*	*0.16*	*1.7*	*2.0*	*0.6*	*0.5*	*9.3*	*19.7*	*4.4*	*1.5*	*2.5*	*0.78*	*1.6*	*1.1*	*1.0*	*54.75*
LC128,2	*2.7*	*0.11*	*0.7*	*1.2*	*0.3*	*2<*	*13.5*	*17.7*	*4.0*	*1.8*	*2.0*	*0.57*	*2.0*	*1.0*	*1.5*	*48.97*
LC128,3	*3.7*	*0.08*	*1.0*	*1.3*	*0.4*	*0.3*	*10.2*	*16.9*	*5.2*	*1.8*	*1.6*	*2.00*	*2.0*	*1.0*	*0.9*	*48.27*
LC128,4	*3.6*	*0.11*	*1.0*	*1.3*	*0.6*	*0.6*	*10.1*	*17.6*	*5.9*	*1.6*	*2.1*	*2.31*	*2.1*	*1.1*	*1.2*	*51.25*
LC128,5	*4.3*	*0.04*	*1.3*	*0.7*	*0.2*	*0.3*	*7.0*	*15.7*	*5.3*	*1.2*	*2.0*	*1.92*	*2.3*	*0.6*	*1.0*	*43.84*
LC128,6	*6.1*	*0.07*	*3.1*	*1.1*	*0.2*	*0.4*	*13.2*	*21.9*	*6.0*	*2.5*	*1.8*	*2.30*	*2.0*	*0.7*	*1.3*	*62.59*
LC128,12	*5.3*	*0.05*	*1.7*	*0.8*	*0.3*	*0.4*	*11.7*	*17.2*	*7.0*	*2.1*	*10.3*	*3.00*	*1.4*	*0.9*	*1.1*	*63.22*
LC128,13	*6.6*	*0.42*	*1.8*	*1.4*	*0.4*	*0.6*	*11.0*	*18.2*	*5.7*	*1.5*	*9.7*	*1.42*	*2.4*	*1.5*	*1.2*	*63.80*
LC128,17	*8.0*	*0.05*	*3.0*	*1.1*	*0.4*	*0.3*	*9.8*	*24.9*	*7.1*	*1.0*	*3.5*	*3.30*	*2.8*	*1.1*	*1.0*	*65.38*
LC128,8	*4.8*	*0.08*	*1.3*	*1.1*	*0.5*	*0.4*	*9.6*	*23.4*	*5.2*	*2.0*	*2.8*	*6.10*	*2.1*	*1.1*	*0.8*	*61.23*
LC128,7	4.1	0.18	0.9	1.7	0.4	0.4	12.5	*19.4	*4.4	1.6	*5.7	1.28	*1.40	1.1	1.4	56.35
LC128,9	4.1	0.07	1.2	1.5	*0.6	0.4	10.8	21.4	5.5	1.1	2.4	1.80	2.3	1.1	1.3	55.39
LC128,10	4.0	0.06	1.1	1.1	0.4	0.6	10.9	*16.9	*8.1	1.6	2.6	*4.00	2.2	1.0	1.0	57.76
LC128,11	4.6	0.05	1.2	1.1	0.3	0.4	13.8	*19.1	6.6	*2.6	1.9	1.75	2.6	1.2	1.2	58.68
LC128,14	3.3	0.08	0.8	1.3	0.3	0.4	12.5	21.6	5.6	1.5	4.4	1.54	2.5	0.9	1.2	58.04
LC128,15	4.3	0.05	1.2	1.5	0.5	0.5	*5.9	25.0	*3.4	1.6	*5.8	1.23	2.0	1.5	*0.9	55.42
LC128,16	1.8	0.06	1<	*0.9	0.4	0.4	11.4	27.0	6.9	0.7	3.4	*2.90	3.1	1.4	1.3	61.64
LC128,18	1.5	0.05	*0.2	*0.6	0.2	0.3	10.6	22.9	5.1	1.3	2.6	1.34	2.8	*0.5	1.0	50.94
LC128,19	2.6	03<	1.4	*0.6	0.3	0.2	13.1	24.3	6.9	1.4	3.2	*2.70	2.3	0.8	1.3	61.22
Average last 9	3.37	0.08	1.11	1.37	0.35	0.40	11.95	23.70	6.10	1.35	2.96	1.49	2.50	1.13	1.21	59.06
STDS	1.14	0.04	0.20	0.24	0.09	0.11	1.19	2.16	0.79	0.32	0.81	0.25	0.37	0.24	0.15	
RSD	34%	58%	18%	18%	26%	26%	10%	9%	13%	23%	27%	16%	15%	21%	12%	

Sample	SiO2	TiO2	Al2O3	FeO	MnO	MgO	CaO	Na2O	K2O	P2O5	F	Cl	SO3	BaO	SrO	Total
CP129																
LC129,1	0.6	-.01<	1<	0.6	0.5	*0.5	*6.8	*35.9	7.3	1.1	5.0	*4.80	4.5	1.5	0.9	70.01
LC129,2	0.9	.01<	0<	*0.4	0.4	*0.5	15.9	25.9	*8.9	*0.7	*7.2	0.50	4.6	1.5	2.0	69.44
LC129,3	0.4	-.00<	0<	.2<	0.4	*0.3	17.0	27.2	7.2	1.2	3.2	2.09	2.2	0.9	1.8	63.76
LC129,4	0.3	-.01<	-.0<	0<	0.2	.2<	17.3	28.7	6.1	0.6	3.9	2.30	2.2	1.0	1.9	64.64
LC129,5	0.6	.03<	-.0<	0.5	0.6	*0.4	11.4	*30.8	4.7	1.0	3.5	*2.50	2.7	1.1	1.3	61.03
LC129,6	0.3	-.00<	1<	2<	0.2	1<	17.6	27.6	5.6	1.0	2.0	1.07	2.4	0.8	1.7	60.30
LC129,7	0.3	.02<	-.1<	-.0<	0.3	.0<	*19.3	25.6	6.4	*0.7	1.4	0.62	2.3	0.9	1.9	59.84
LC129,8	0.9	-.01<	0<	*0.4	0.5	*0.6	10.6	*30.7	*7.6	1.0	*7.8	0.71	4.5	*1.6	1.5	68.38
LC129,9	0.4	.02<	-.0<	1<	.1<	1<	*21.8	24.0	6.7	*0.6	*6.9	0.72	*1.8	1.5	*2.4	66.94
LC129,10	0.4	.02<	-.0<	2<	0.2	1<	16.4	26.2	5.6	1.0	1.6	0.90	2.3	0.6	1.7	59.03
LC129,11	0.2	-.01<	-.0<	*0.4	0.3	*0.3	9.2	28.4	3.7	1.0	2.4	0.37	*5.5	0.7	1.1	53.53
LC129,12	0.5	.02<	1<	*0.3	0.4	1<	16.9	21.9	*10.5	*0.7	3.0	1.04	3.2	1.1	1.7	61.43
LC129,13	0.7	.03<	-.1<	*0.4	0.4	*0.3	15.7	25.2	*8.5	1.0	4.0	*4.9	2.1	0.9	1.6	65.62
LC129,14	0.6	.00<	-.1<	*0.4	0.4	*0.4	13.2	28.1	*7.6	0.9	2.7	*4.80	3.1	1.1	1.6	64.66
LC129,15	0.4	.02<	-.0<	.2<	0.3	*0.3	18.8	25.8	7.3	1.1	*5.8	*3.60	*1.4	1.3	1.9	67.99
LC129,16	0.2	.01<	0<	.1<	.2<	0.2	16.0	27.6	6.7	0.9	2.2	2.13	2.4	1.1	1.7	61.27
LC129,17	0.3	.02<	-.0<	2<	0.3	.2<	15.9	*29.3	5.9	1.2	2.7	1.85	2.6	0.7	1.6	62.39
LC129,18	0.3	-.02<	0<	.1<	0.2	.2<	17.9	25.6	6.7	1.0	1.7	1.02	2.4	1.1	2.0	59.83
LC129,19	0.2	.01<	-.1<	1<	.2<	.2<	16.1	27.1	6.4	1.1	1.2	1.39	2.1	0.6	1.8	59.93
LC129,20	0.2	.01<	0<	1<	0.3	*0.3	16.1	29.0	5.6	1.0	2.6	1.39	2.5	0.9	1.8	61.68
LC129,21	0.3	.03<	1<	1<	0.4	*0.7	13.0	26.4	6.2	0.9	4.7	1.62	2.5	0.9	1.6	59.27
LC129,22	0.3	.01<	-.0<	2<	0.3	*0.3	10.8	29.1	5.9	0.8	3.5	*2.70	3.0	0.8	1.4	58.93
LC129,23	0.3	.01<	0<	1<	0.2	0.2	*19.5	26.2	6.5	1.0	0.5	0.94	2.1	0.7	1.6	59.72
LC129,24	0.6	.01<	0<	*0.3	0.4	*0.3	13.5	28.5	*8.2	*0.6	*6.4	*5.40	3.1	1.5	1.6	70.33
LC129,25	0.5	.02<	-.2<	*0.3	0.4	1<	14.6	26.7	6.1	1.1	1.4	2.07	3.3	0.9	1.5	58.85
Average	0.43	b.d.	b.d.	0.55	0.35	0.20	15.04	26.80	6.14	1.01	2.66	1.26	2.82	1.00	1.63	59.89
STDS	0.20	n.d.	n.d.	0.07	0.11	0.00	2.75	1.79	0.88	0.11	1.20	0.62	0.79	0.29	0.26	
RSD	47%	n.d.	n.d.	13%	32%	0%	18%	7%	14%	11%	45%	49%	28%	28%	16%	

Note: Italics indicate whole analyses rejected and asterixes (*) indicate individual elemental analysis rejected.
b.d.: below detection

Example of calculation of the composition of the residual liquid, for two experiments (CP96 and CP126)

Table A3.4a gives the details of the calculation of the residual liquid in the experiment CP96, that contains 2 vol. % nepheline. The first row represent the measured (corrected) composition of the carbonate liquid in the experiment CP96 (LC96). The second and third rows represent the bulk composition (OL5) and the composition of the nepheline in the experiment CP96 (Ne 96), respectively. The fourth row represents the composition of the crystals removed (here 2 % nepheline), and the first row represents the composition of the residual liquid (= OL5 minus crystals). This composition is renormalised to 100 wt. % in the last row, by multiplying each value by 100/(100-2.03).

Table A3.4b gives the details of the calculation of the residual liquid in the experiment CP126, that contains numerous crystals, including nyerereite and gregoryite. The calculation is similar to that for the residual liquid in experiment CP96, except that the normalisation takes into account the CO_2 of the carbonate crystals. The total weight of crystals removed is equal to 33.18 wt. % when the CO_2 form the carbonate crystals is not taken into account, and to 49.68 wt. % when this CO_2 is taken into account, assuming that the CO_2 content of nyerereite is 40 wt. % and that of gregoryite is 30 wt. %. The composition is renormalised to 100 wt. % in the last row, by multiplying each value by 100/(100-49.68).

Table A3.4a: Calculation of the composition of the residual liquid in the experiment CP96.

Corrected	SiO2	TiO2	Al2O3	FeO	MnO	MgO	CaO	Na2O	K2O	P2O5	F	Cl	SO3	BaO	SrO	Total
LC96	2.25	0.10	0.23	1.23	0.32	0.40	15.53	25.34	5.90	1.08	1.66	0.91	2.55	1.10	1.27	59.87
OL5 (Belanger)	3.2	0.1	0.9	1.30	0.35	0.4	15.4	28.3	6.13	1.07	1.64	2.54	2.55	0.904	1.301	66.08
Ne 96	42.90		32.92	1.71			b.d.	17.12	6.70							101.34
crystals removed	0.66	0.00	0.66	0.03	0.00	0.00	0.00	0.34	0.13	0.00	0.00	0.00	0.00	0.00	0.00	2.03
OL5 - crystals	2.34	0.10	0.24	1.26	0.35	0.40	15.40	27.96	6.00	1.07	1.64	2.54	2.55	0.90	1.30	64.05
OL5 - crystals (normalised)	2.39	0.10	0.25	1.29	0.36	0.41	15.72	28.54	6.12	1.09	1.67	2.59	2.60	0.92	1.33	65.38

Nepheline from experiment CP96 (Ne 96) was used for the calculation of the composition of the residual liquid.

Table A3.4b: Calculation of the composition of the residual liquid in the experiment CP126.

Corrected	SiO2	TiO2	Al2O3	FeO	MnO	MgO	CaO	Na2O	K2O	P2O5	F	Cl	SO3	BaO	SrO	Total	
LC126	1.33	n.d.	0.20	0.73	0.58	0.33	7.15	27.65	7.44	0.43	3.46	8.70	3.05	1.80	0.93	63.76	
OL5 (Belanger)	3.2	0.1	0.9	1.30	0.35	0.4	15.4	28.3	6.13	1.07	1.64	2.54	2.55	0.904	1.301	66.08	
Ne 126	43.23		33.17	1.43			b.d.	16.6	7.54							102	
cpx 108	51.60	0.69	1.13	15.27	0.47	8.70	20.67	2.20								100.7	
mela 126	31.60	9.30	0.90	22.90	0.40	0.40	31.70	0.30	b.d.							97.5	
Wo 129	50.1				0.94		46.14									97.18	
NY126				b.d.	b.d.	b.d.	24.89	23.58	6.21	0.5	0.27	0.18	1.19	0.38	1.91	59.11	
Ap 31	0.9						54			42.1	3				.3<	100	
GRE 108				b.d.	0.2	b.d.	10.61	42.46	3.48	2.62	0.53	0.27	3.7	b.d.	0.79	64.66	
crystals removed	2.54	0.06	0.70	0.58	0.05	0.26	9.97	13.84	2.54	0.67	0.17	0.09	0.91	0.11	0.69	33.18	**49.68
OL5 - crystals	0.66	0.04	0.20	0.72	0.30	0.14	5.43	14.46	3.59	0.40	1.47	2.45	1.64	0.79	0.61	32.90	
OL5 - crystals (normalised)	1.31	0.08	0.40	1.43	0.60	0.27	10.80	28.73	7.14	0.80	2.92	4.86	3.26	1.57	1.21	65.38	

** 49.48 wt. % is the total weight of the crystals that have been removed, including CO2 from nyerereite and gregoryite. CO2 is assumed to be equal to 40 wt. % in nyerereite, and 30 wt. % in gregoryite. The total of 33.18 wt. % does not include the CO2 from the carbonate crystals.
Crystals used for the calculation are from experiment CP126 when available, and from the experiments at the closest conditions otherwise.
Abbreviations used are: Ne: nepheline; Cpx: clinopyroxene; Mela: melanite garnet; Wo: wollastonite; NY: nyerereite; Ap: apatite; GRE: gregoryite.
The number beside the crystals indicates the experiment number.

Ratio between measured composition of the carbonate liquid and the calculated composition of the residual liquid (= OL5 minus crystals), for each experiment and for the average of the experiments. Calculation of a correction factor applied to carbonate liquid from OL5-experiments

For the calculation of the average value of the ratio between measured composition of the carbonate liquid and the calculated composition of the residual liquid, some outliers have not been taken into account, and are indicated by an asterix (*). Most elements have not been corrected, as indicated by a correction factor equal to 1.00. Note the very good agreement between measured and calculated CaO contents of the carbonate liquid. This is important since CaO is usually used as the internal standard for the LAM-ICP-MS data. The elements for which a correction factor is applied are: Na_2O, K_2O, F, Cl and SrO.

Table A3.5: Ratio between measured composition of the carbonate liquid and the calculated composition of the residual liquid (= OL5 minus crystals), for each experiment and for the average of the experiments. Calculation of a correction factor applied to carbonate liquid from OL5-experiments.

Experiment	P (MPa)	T (C)	SiO2	TiO2	Al2O3	FeO	MnO	MgO	CaO	Na2O	K2O	P2O5	F	Cl	SO3	BaO	SrO
CP88	100	900	1.06	0.93	*0.69	1.01	1.07	0.99	0.99	0.83	*0.72	0.94	1.39	0.33	0.89	0.99	1.16
CP106	100	850	1.04	1.03	0.72	0.99	1.00	0.95	1.00	0.86	0.90	*1.15	1.30	0.45	0.97	1.04	1.15
CP79	100	800	0.98	1.03	1.02	0.85	*0.84	*0.73	1.02	0.85	0.90	1.10	1.49	0.44	1.00	0.94	*1.31
CP96	100	750	0.94	0.98	0.95	0.96	0.90	0.98	0.99	*0.77	0.87	0.99	1.45	*0.15	0.98	*1.19	1.08
CP98	100	700	0.89	1.00	1.02	1.01	1.12	0.98	0.99	0.89	0.87	1.07	*1.85	0.41	0.97	0.97	1.18
CP118	100	625	0.94	0.89	1.11	0.92	0.94	1.04	1.02	0.87	0.87	1.01	1.16	0.38	0.96	1.00	1.16
CP107	100	600	1.05	0.82	0.97	0.98	0.94	1.05	1.03	0.86	*0.79	0.96	1.28	0.41	*0.84	1.01	1.17
CP128	100	575	1.08	*0.59	1.03	0.93	0.95	1.10	1.00	0.79	0.90	1.04	1.36	0.44	*0.81	0.99	1.01
CP127	100	550	1.08	*0.64	1.07	*0.76	0.98	0.92	*0.74	*0.68	0.93	1.02	*2.39	0.49	*0.84	0.95	1.13
CP90	20	900	1.04	1.16	0.79	0.84	0.95	0.96	1.04	0.88	0.99	1.04	1.61	0.47	1.00	1.02	1.17
CP45	20	850	0.93	1.00	0.88	1.15	0.98	0.99	1.01	0.84	0.85	1.02	1.62	0.39	1.04	1.06	1.13
CP61	20	800	0.83	n.d.	n.d.	0.89	*1.20	1.01	1.00	*1.01	0.93	0.96	1.63	0.46	1.08	1.04	1.07
CP80	20	775	1.00	*1.33	*2.25	0.80	0.92	1.08	1.04	0.87	0.86	1.06	1.60	0.40	1.01	1.09	1.18
CP51	20	750	0.87	*2.09	n.d.	0.95	1.10	0.96	1.00	0.86	0.85	0.94	1.45	0.37	1.02	1.02	1.08
CP57	20	700	0.86	n.d.	n.d.	0.68	1.04	0.95	1.00	0.88	0.94	0.98	1.58	0.51	*0.84	0.93	1.07
CP129	20	625	1.00	n.d.	n.d.	0.88	0.91	*1.37	1.02	0.89	0.95	0.98	1.44	0.44	1.00	1.01	1.19
CP108	20	600	0.83	n.d.	*0.65	0.80	0.99	1.09	0.98	0.90	0.95	0.94	1.51	0.43	0.99	0.98	1.15
CP126	20	575	1.01	n.d.	1.01	*0.50	0.95	*1.21	*0.68	0.83	0.94	0.53	*1.73	*0.76	0.94	*1.14	*0.86
CP112	20	550	*0.69	*0.33	0.76	*0.37	*0.50	*0.78	*2.96	0.90	*0.65	*1.43	*0.70	*0.23	1.08	*0.53	*1.68
Average			0.97	0.98	0.94	0.91	0.98	1.00	1.01	0.86	0.91	0.97	1.46	0.43	1.00	1.00	1.13
Correction factor			1.00	1.00	1.00	1.00	1.00	1.00	1.00	0.86	0.91	1.00	1.46	0.43	1.00	1.00	1.13

Asterixes (*) indicate the values that are not taken into account in the calculation of the average. n.d.: not determined.

APPENDIX A4

Table A4 1. Trace (and major) element LAM-ICP-MS analyses of crystals in OL5-experiments - Individual and average analyses, standard deviation (STDS) and relative standard deviation (RSD)

Sample	MgO wt %	Al2O3 wt %	SiO2 wt %	CaO wt %	CaO wt %	TiO2 wt %	Ba ppm	Sr ppm	Rb ppm	Y ppm	V ppm	La ppm	Ce ppm	Nd ppm	Sm ppm	Eu ppm	Gd ppm	Dy ppm	Er ppm	Yb ppm	Lu ppm	U ppm	Th ppm	Nb ppm	Ta ppm	Zr ppm	Hf ppm
CP45																											
Ne1	*<1 84*	*33 0*	*40 0*	*<19 0*	*<2 42*	*<0 08*	*146*	*<1187*	*107*	*3 38*	*<41 0*	*16 7*	*35 9*	*5 33*	*<3 93*	*0 27*	*0 89*	*<1 61*	*<1 13*	*0 00*	*<0 73*	*1 72*	*3 47*	*25 9*	*<0 76*	*56 7*	*0 32*
Ne2	*<2 74*	*33 0*	*32 6*	*<21 7*	*<3 37*	*<0 11*	*36 4*	*<1592*	*89 5*	*<2 57*	*<31 2*	*10 7*	*13 8*	*bd*	*bd*	*bd*	*0 62*	*bd*	*<2 87*	*<5 31*	*<0 49*	*bd*	*<2 33*	*<0 59*	*<0 57*	*<7 98*	*bd*
Ne3	<0 02	33 0	35 8	<0 53	0 22	bd	21 8	165	112	<0 33	2 19	*1 55	*0 30	<1 24	bd	0 10	<0 46	<0 61	bd	0 65	bd	0 48	bd	0 35	bd	<0 50	0 31
Ne4	0 05	33 0	38 6	<1 03	0 40	0 01	*382	273	100	bd	<2 81	*3 06	*5 76	*0 49	<2 55	0 08	<1 98	<0 31	bd	b.d.	bd	<0 12	<0 12	0 57	<1 52	<0 43	<0 44
Ne5	<4 71	33 0	<54 8	<46 1	<6 12	<0 27	<32 0	<3220	94 7	<5 17	<44 4	0 51	*3 27	<14 8	<1 38	bd	<0 82	<5 53	b.d	<4 87	bd	bd	bd	bd	b.d.	<7 21	bd
Ne6	<3 20	33 0	<39 5	<27 7	<5 08	<0 13	*75 4	<2468	91 1	<2 37	<28 0	0 77	<2 45	*1 97	bd	bd	bd	bd	<1.36	bd	bd	bd	bd	bd	<1 08	*4 58	b.d
Ne7	<3 16	33 0	35 8	<23 1	<3 80	<0 09	18 2	<1457	82 5	<4 18	<40 2	0 71	bd	<8 38	<0 78	<0 94	bd	bd	<0 50	<6 22	<0 89	bd	<1.34	<0 93	<0 83	<4 06	bd
Ne8	<8 57	33 0	<66 5	<54 6	<8 31	<0 19	29 3	<3609	105	<8 19	<113	<1 91	*0 91	*6 84	bd	bd	<2 27	bd	bd	bd	<0 53	bd	bd	<2 25	<0 29	bd	bd
Average last 6	0 05	33 0	36 7	bd	0 31	0 01	23 1	219	97 6	bd	2 19	0 66	nd	nd	bd	0 09	bd	bd	bd	0 65	bd	0 48	b.d	0 46	bd	n.d.	0.31
STDS	n d	0 00	1 61		0 13	n d	5 67	76 4	10 4		n d	0 14				0 01				n.d.		n d		0.16			n.d
RSD	n d	0%	4%		41%	n d	25%	35%	11%		n d	21%				16%				n d		n d		34%			n d
Quenched NY	0 83	0 22	3 02	24 5	26 2	0 10	14159	17064	185	27 8	216	688	810	165	16 0	3 95	7 37	4 02	1 65	1 36	0 14	15 6	9 26	99 6	0 20	94 1	1 13
CP51																											
Mel1	3 26	7 50	35 3	27 3	26 3	<0 02	278	15482	<10 03	4 14	<6 29	462	638	147	9 38	1 98	3 90	<0 87	<2 15	<0 91	<0 28	<0 28	7 01	0 81	<0 16	4 54	0 10
Mela1	0 57	0 70	26 2	30 9	31 1	11 0	9 84	89 3	<2 50	492	565	57 9	298	389	124	45 0	120	110	54 8	40 1	5 03	8 75	24 1	488	31 2	*5193	*100
Mela2	0 58	1 19	29 4	30 9	28 2	8 14	*40 7	129	<5 77	472	691	*227	*708	*544	128	45 4	110	104	50 9	37 5	4 65	*15 5	*54 3	*822	*26 2	3304	57 7
Average	0 58	0 95	27 8	30 9	29 7	9 55	9 84	109	bd	482	628	57 9	298	389	126	45 2	115	107	52 9	38 8	4 84	8 75	24 1	488	31 2	3304	57 7
STDS	0 01	0 35	2 23	0 00	2 06	1 99	n d	28 3		13 6	89 1	n d	n d	n d	3 09	0 24	7 10	3 89	2 76	1 82	0 27	n d.	n d.	n d	n d.	n d.	n d.
RSD	1%	37%	8%	0%	7%	21%	n d	26%		3%	14%	n d	n d	n d	2%	1%	6%	4%	5%	5%	6%	n d	n d	n d	n d	n d.	n.d.
Wo1	**<0.08**	**<0.04**	**47.9**	**44.5**	**42.6**	**0.83**	**68.3**	**865**	**<5.96**	**62.7**	**2.62**	**31.5**	**89.6**	**44.2**	**10.5**	**3.85**	**10.2**	**11.2**	***7.96**	***7.30**	**0.93**	**<0.28**	**<0.23**	**1.03**	**0.83**	**3.77**	**<0.46**
Wo2	*0 09*	*<0 04*	*40 8*	*44 5*	*45 0*	*0 03*	**674*	*1465*	*6 12*	*55 7*	*6 41*	*62 4*	*127*	*57 0*	*10 8*	*3 88*	*10 2*	*11 0*	*5 52*	*5 63*	*0 81*	*1 09*	*0 53*	*3 87*	*<0 20*	*4 18*	*0 06*
CP57																											
Mela1	*<2 44*	*<1 35*	*<45 9*	*<48 0*	*26 8*	*7 74*	*394*	*5038*	*<59 5*	*156*	*752*	*131*	*950*	*536*	*113*	*22 8*	*62 5*	*48 7*	*11 8*	*5 24*	*<0 85*	*86 7*	*52 0*	*2489*	*15 9*	*1981*	*47 9*
Mela2	<0 54	1 08	35 4	32 3	30 0	10 1	12 3	<129	<10 0	526	805	75 5	436	432	132	44 8	115	119	48 7	39 6	4 65	*27 4	*121	*1774	20 4	4038	73 4
Mela3	0 45	0 89	38 5	32 3	33 2	10 7	*368	360	<6 36	400	1026	60 0	300	309	92 3	34 7	95 2	83 7	37 9	26 6	3 59	7 46	16 7	*343	18 1	3464	62 9
Mela4	0 64	0 91	33 3	32 3	30 6	9 85	<1 54	86 6	<4 21	461	571	57 7	351	389	122	43 5	113	101	46 7	33 4	3 26	11 5	45 0	1132	*38 6	4374	72 6
Mela5	<3 24	<1 98	<73 3	<60 8	26 6	5 03	11 9	<1034	<83 9	368	1168	51 4	300	357	102	35 9	89 0	54 5	30 9	32 3	4 92	8 25	67 8	1237	10 7	1703	*27 7
Mela6	0 64	0 80	29 5	32 3	29 1	8 71	1 96	<99 7	<7 35	405	631	68 3	367	356	110	38 4	89 1	79 2	38 1	23 8	3 29	13 2	52 5	973	19 2	3435	61 8
Mela7	<0 62	0 56	30 6	32 3	36 9	9 87	2 19	<894	<4 15	351	1571	31 2	198	261	82 4	35 8	76 2	77 1	40 7	29 5	4 72	5 72	14 8	504	18 0	2632	52 2
Mela8	0 95	0 62	27 2	32 3	36 3	7 08	*39 9	<1183	<6 43	331	818	*318	*1010	561	121	34 4	81 5	72 5	28 3	31 1	2 33	*30 2	72 5	921	*32 4	2460	34 8
Average last 7	0 67	0 83	32 4	32 3	31 8	8 78	7 09	223	bd	406	941	57 3	325	380	109	38 2	94 2	83 8	38 7	30 9	3 82	9 23	44 9	953	16 9	3158	59 6
STDS	0 21	0 20	4 16	0 00	3 83	2 04	5 79	194		68 0	347	15 3	80 2	96 6	17 7	4 25	14 9	20 7	7 51	5 08	0 96	3 06	24 7	281	3 82	940	14 4
RSD	31%	24%	13%	0%	12%	23%	82%	87%		17%	37%	27%	25%	25%	16%	11%	16%	25%	19%	16%	25%	33%	55%	29%	23%	30%	24%
Ne1	<1 10	32 2	21 7	<15 8	<2.03	<0 02	<16 1	<1229	108	<0 86	<20 0	<0 28	*0 28	*0 37	<5 92	<0 75	bd	<4 50	<2 06	bd	bd	bd	bd	bd	bd	bd	<3 95
Ne2	<2 40	32 2	<28 1	<29 2	<3 05	<0 20	<30 0	<2197	130	<3 62	<76 8	bd	bd	*2 9	<11 7	<2.44	bd	<3.40	<4.41	bd	<0 19	<3 79	<4 08	<2 71	<0 73	bd	bd
Ne3	<3 59	32 2	<46 6	<35 4	<4 99	bd	<35 0	<3212	181	<7 69	<102	<2.04	bd	bd	<14 1	bd	<9 45	bd	bd	b.d.	bd	<2 63	<3.10	<4.13	<0 81	<1.48	<4.28
Ne4	<1 42	32 2	<32 3	<21 5	<3 00	<0 09	8 31	<2013	58 1	<2 79	<55.6	bd.	*0 17	*2 43	<5 14	<0 86	bd	<2.44	bd	*1.25	bd	bd	<4.19	<3 21	bd.	<11.2	bd.
Ne5	<4 15	32 2	<79 0	<51.0	<8 33	<0 33	*1496	<5164	100	bd	<168	*10 7	*13 8	bd	bd	<5 22	<6 85	bd	bd	bd	*1.26	*2 96	<5.06	<10 6	<3 10	bd	<4 98
Average	bd	32 2	21 7	bd	bd	bd	8 31	bd	115	bd	bd	nd	nd	nd	bd	bd	bd	bd	bd	nd	nd	nd	bd	bd	bd	bd	bd
STDS		0 00	n d				n d		44 8																		
RSD		0%	n d				n d		39%																		

Sample	MgO	Al2O3	SiO2	CaO	CaO	TiO2	Ba	Sr	Rb	Y	V	La	Ce	Nd	Sm	Eu	Gd	Dy	Er	Yb	Lu	U	Th	Nb	Ta	Zr	Hf
CP79																											
Ne1	<0 09	33 0	36 7	<4 61	<0 37	0 02	15 6	<330	103	bd	<2 99	<0 39	<0 35	*0 19	bd	bd	bd	<1 36	0 09	bd	bd	0 04	0 04	0 15	bd	<1 40	<0 43
Ne2	<0 06	33 0	45 0	<4 66	<0 36	0 01	10 9	<412	118	<0 83	<3 64	bd	0 34	<1 40	bd	bd	<1 71	bd	<0 65	bd	<1 05	<2 13	0 04	bd	bd	<1 46	<0 91
Ne3	0 05	33 0	54 6	<3 79	<0 24	0 01	7 78	<239	79 2	0 07	<0 78	<0 12	*0 02	<2 48	<1 68	bd	<0 17	<0 85	<1 70	*0 17	<0 20	bd	0 04	<0 34	bd	<0 10	bd
Ne4	<0 34	33 0	20 7	<17 6	<1 18	<0 03	<25 3	<1126	103	<0 39	<14 2	*0 30	<2 08	<11 7	bd	<3 86	<7 64	bd	<6 27	<9 20	bd	<3 41	bd	<1 81	<0 28	<4 63	bd
Ne5	<0 15	33 0	50 4	<10 2	<0 52	bd	<22 9	<608	131	<0 67	<4 58	<0 45	0 38	bd	<4 14	<2 34	<0 92	bd	0 15	bd	*0 23	<0 70	bd	0 37	<0 55	3 30	<0 74
Average	0 05	33 0	41 5	bd	bd	0 01	11 4	bd	107	0 07	bd	nd	0 36	nd	bd	bd	bd	bd	0 12	nd	nd	0 04	0 04	0 26	bd	3 30	bd
STDS	nd	0 00	13 4			0 01	3 94		19 4	nd			0 03						0 04			nd	0 00	0 16		nd	
RSD	nd	0%	32%			43%	34%		18%	nd			8%						35%			n.d	0%	60%		nd	
CP88																											
Ne	<0 33	32 9	28 4	<3 63	<1 32	<0 01	33 5	<238	74 9	<0 59	<8 60	<0 45	0 60	<2 35	<1 31	0 07	<1 44	<0 84	<0 92	<1 43	<0 35	<0 48	<0 69	<0 77	bd	<0 69	<3 40
CP90																											
Ne1	*<0 37*	*30 7*	*42 0*	*<20 9*	*<1 40*	*<0 02*	**414*	*<1542*	*80 7*	*<2 81*	*<14 3*	*6 54*	*10 0*	*bd*	*<6 37*	*bd*	*<5 57*	*bd*	*bd*	*bd*	*bd*	*<1 14*	*b.d.*	*<2 61*	*<2.56*	*<7.37*	*b.d.*
Ne2	*<0 21*	*30 7*	*46 9*	*<19 3*	*<1 35*	*<0 01*	*93 4*	*<1145*	*49 1*	*<1 41*	*<7 31*	*4 65*	*6 61*	*<10 3*	*bd*	*bd*	*<3 34*	*bd*	*<2 85*	*bd*	*bd.*	*bd.*	*bd*	*1.43*	*<0.25*	*<4.63*	*bd*
Ne3	*<0 12*	*30 7*	*36 2*	*<9 03*	*<0 60*	*<0 01*	*<15 3*	*<594*	*62 2*	*<1 94*	*<4 27*	*bd*	*0 14*	*bd*	*<4 58*	*bd*	*<4 12*	*1 36*	*bd*	*bd*	*bd*	*<0 70*	*<0 26*	*<1.08*	*bd*	*bd*	*bd*
Ne4	**<0.21**	**30.7**	**31.2**	**<12.3**	**<1.07**	**<0.02**	**26.7**	**<1121**	**70.3**	**<2.31**	**<9.79**	**0.49**	**0.76**	**b.d.**	**<10.2**	**b.d.**	**b.d.**	**0.29**	**b.d.**	**b.d.**	**b.d.**	**b.d.**	**b.d.**	**<1.39**	**b.d.**	**<2.07**	**<9.33**
CP96																											
Ne1	**<9.15**	**32.9**	**43.3**	**<10.5**	**<0.70**	**<0.02**	**<1.37**	**<569**	**68.5**	**<1.44**	**<3.62**	**0.54**	**<0.79**	**b.d.**	**b.d.**	**<1.92**	**<3.92**	**b.d.**	**b.d.**	**b.d.**	**b.d.**	**<0.95**	**b.d.**	**<0.44**	**<0.97**	**<1.97**	**<3.00**
Ne2	*<0 15*	*32 9*	*39 8*	*<7 93*	*<0 77*	*0 01*	*682*	*<677*	*74 8*	*<0 85*	*<7 77*	*<1 06*	*0 82*	*2 85*	*bd*	*bd*	*bd*	*bd*	*bd*	*<3.97*	*<1 05*	*<2 23*	*bd*	*bd*	*bd.*	*<1.39*	*bd*
CP106																											
Ne1	<0 65	33 3	53 1	<15 1	<1 58	<0 05	6 76	<1111	113	1 14	<34 3	0 12	<0 57	<7 94	bd	bd	bd	0 45	b.d	bd.	<0 86	<1.11	<0 20	<1 68	bd	<3 41	<3 15
Ne2	<0 88	33 3	81 5	<14 2	<1 68	<0 04	24 4	<1254	114	0 50	<22 2	0 68	0 39	bd	<4 82	<0 90	<0 74	<2.15	bd	<1.67	<0 51	<1.43	<1.75	bd.	bd.	<2 62	<1.62
Ne3	<0 93	33 3	22 7	<23 3	<2 28	0 02	18 5	<1358	83 5	<1 18	<29 8	0 24	bd	<2 31	bd	bd	<0 40	bd	<1.71	<3 01	<0 88	b.d.	b.d.	<0.44	bd.	<1.59	b.d
Ne4	<2 72	33 3	45 2	<44 5	<3 22	0 03	27 6	<2308	*193	<8 68	<54 0	*7 10	*2 47	<7 14	<8 05	<0 80	bd	bd	<5 29	<6.20	bd	<2.67	b.d.	<3 63	<1.49	bd	bd
Ne5	<0 71	33.3	31.1	<12 2	<1 18	<0 05	22 1	<854	87.5	<2 15	<18 1	1 15	1.03	bd	bd	0 32	bd	bd	<0 30	<0.42	<0.15	0 78	bd.	<1.07	bd	1.40	<6.06
Average	bd	33 3	46 7	bd	bd	0 03	19 9	bd	99 6	0 82	bd	0 55	0 71	bd	bd	0 32	bd	0 45	b.d	bd	bd	0 78	b.d	bd.	bd.	1.40	bd.
STDS		0 00	22 8			0 01	8 04		16 4	0 45		0.47	0 45			nd		nd				nd				n.d	
RSD		0%	49%			28%	41%		16%	55%		86%	64%			nd		nd				nd				n.d	
CP107																											
NY1	0 52	<0 01	<1 93	25 6	29 5	0 02	16150	17497	319	21 9	183 2	724	992	258	22 4	3 60	8.21	4 33	1 19	0 72	0 48	14 8	25 4	19 6	<0 06	1 08	1 03
NY2	1.03	0.74	2 41	25.6	31 1	0 08	12539	16860	438	40 1	345 1	992	1116	214	19 4	4 73	9 12	4 66	1 88	1 34	0 14	15 0	16.9	69.5	0 21	17.4	0.46
NY3	0.43	0 94	<9 06	25 6	24 0	0 18	25108	12223	*2013	21 6	*837	413	1648	139	22 6	8 71	2.32	2 57	*8 36	<1 78	<0 90	67.3	49.7	104	b.d	14 6	<2.45
NY4	1.28	0 27	*13 5	25 8	18 0	0 25	13894	15491	*2324	22 8	*1366	508	554	112	12 7	1 23	4 58	6.31	<2 46	<2.87	<0 86	60 1	34 1	58 4	b.d.	*130	b.d.
NY5	0 37	0 38	<10.6	25 6	29 6	0 30	13256	15132	*1207	17 5	*1040	911	1304	264	11 8	4 55	8 27	6 07	<1.91	1 60	<1.23	29 9	58.7	*348	<0.64	25.1	b.d
NY6	<0 08	<0 07	<4 43	25 6	15 4	<0 01	2553	8445	65 9	6 08	<7 55	163	286	55 8	7 30	0 78	0 91	<1 38	<0 38	bd	<0 10	*0 45	*0.21	<0 43	bd.	bd	bd
NY7	0 20	0 49	<3 43	25 6	17 9	0 04	8766	17825	312	32 6	203	787	786	155	13 1	3 23	5 64	1 97	1 45	1 06	<0 22	4.21	10 9	30 7	b.d	8 42	<0 77
NY8	0 79	1 94	<3 97	25 6	23 1	0 07	16774	18879	651	32 0	350	1255	1400	247	17 4	5 89	8 99	5 52	1 37	1.83	0 17	18.6	30 2	85 1	<0 11	31 0	1 15
NY9	<0 18	<0 11	<7.47	25 6	35 3	0 04	7606	17011	212	12 5	37 3	405	514	141	8 25	2 88	5 70	2 51	<3 19	<0 94	<0 25	4 40	1 10	47.2	bd	3 60	bd
NY10	<0 20	<0 15	<10 4	25 8	26 2	<0 02	3502	22584	181	6 29	<9 02	234	475	79 9	7 92	2 56	1 99	<3 02	<2 36	bd	0 03	1 54	<1.37	1.55	bd	<2 88	b.d
NY11	0 25	0 39	<5 30	25 8	28 4	0 12	9594	19403	134	14 9	136	499	681	168	11.0	2 98	6 42	3 91	<1 34	<2 48	0 16	11 3	7.71	150	0 03	68 4	<1.60
Average	0 61	0.74	2 41	25 6	25 3	0 12	11795	16486	287	20 7	206	626	887	167	14 0	3 74	5 65	4 21	1 47	1.31	0.20	22 7	26.1	62 9	0.12	21.2	0.88
STDS	0 39	0 58	nd	0 00	6 27	0 10	6433	3746	189	10 9	123	337	437	71 3	5 63	2 21	2 92	1 60	0 29	0.44	0 17	23 2	19 3	45 8	0 13	21.8	0.37
RSD	64%	79%	nd	0%	25%	82%	55%	23%	66%	52%	60%	54%	49%	43%	40%	59%	52%	38%	20%	33%	86%	102%	74%	73%	106%	102%	42%
Ne1	<0 16	32 9	46 1	<17 1	<0 86	<0 02	<24 8	<1057	66 1	<1 16	<13 1	1 39	bd	0 62	<6 61	bd	<3 27	bd	bd	bd	bd	bd.	bd	<1 07	<0 92	<2 70	bd
Ne2	<0 23	32 9	39 2	<19 7	<0 92	<0 02	<18 8	<1233	86 8	<1 32	<17 7	<0 80	bd	<5 79	<6 58	bd	bd	<2 29	b.d	bd	bd	bd.	<2 52	<1.84	0.30	<6 55	<1.64
Ne3	<0 31	32 9	45 5	<19 5	<1 02	<0 01	27 0	<1135	105	<2 39	<12 1	1 39	3 21	bd	<5 20	<1 39	bd	<3 26	bd	<1 71	<0.16	0 62	bd	<0 86	<0 47	bd	bd.
Ne4	<0 45	32 9	56 7	<20 3	<1.11	<0 04	*174	<1766	112	0 15	<18 9	2 31	3 23	<18 8	bd	bd	bd	0 29	bd	<10 4	bd	bd	bd	<2.49	bd	<5 85	<6.42
Ne5	<0 26	32 9	31 7	<11 7	<0 71	<0 02	48 9	<1161	114	0 40	<9 30	<1 92	<1 38	2 54	bd	<1 26	bd	bd	<1 18	bd	bd	bd	bd	<1.42	<0 75	<1.03	<5 84

Sample	MgO	Al2O3	SiO2	CaO	CaO	TiO2	Ba	Sr	Rb	Y	V	La	Ce	Nd	Sm	Eu	Gd	Dy	Er	Yb	Lu	U	Th	Nb	Ta	Zr	Hf
Ne6	<0 37	32 9	21 4	<14 2	<0 93	<0 02	31 4	<1544	83 4	0 66	<29 8	bd	<1 15	0 70	<7 23	<0 62	bd	bd	<3 64	<2 03	bd	bd	<2 71	<1 25	<0 37	<4 19	<3 09
Ne7	<0 65	32 9	42 1	<40 6	<3 01	<0 04	46 1	<2620	166	<7 01	<35 9	1 13	0 36	<9 92	bd	bd	<2 95	<3 87	1 32	<5 97	<2 03	<3 39	bd	<2 21	<0 53	<4 51	bd
Ne8	<0 47	32 9	47 0	<29 2	<2 32	<0 09	<43 7	<2733	93 1	<6 94	<37 3	0 58	bd	<10 2	bd	bd	bd	bd	bd	bd	<1 28	<1 55	<4 02	<3 46	bd	bd	bd
Ne9	<0 54	32 9	69 3	<35 5	<3 03	<0 11	<29 9	<3234	120	<4 02	<19 0	<3 08	<1 61	<33 9	<6 81	<3 57	bd	bd	<5 85	bd	<0 91	bd	0 26	bd	<0 58	<6 13	bd
Average	bd	32 9	44 3	bd	bd	bd	38 3	bd	105	0 40	bd	1 36	2 27	1 29	bd	bd	bd	0 29	1 32	bd	bd	0 62	0 26	bd	0 30	bd	bd
STDS		0 00	13 7				10 8		28 1	0 26		0 63	1 65	1 09				nd	nd			nd	nd		nd		
RSD		0%	31%				28%		27%	63%		46%	73%	84%				nd	nd			nd	nd		nd		
Cpx1	*5 45*	*1 84*	*21 8*	*16 2*	*20 4*	*0 39*	*6682*	*8987*	*79 6*	*14 8*	*215*	*318*	*441*	*108*	*10 6*	*3 96*	*4 27*	*2 29*	*1.39*	*<2 93*	*0 39*	*10 0*	*7 02*	*44 2*	*0 20*	*379*	*7.69*
Cpx2	*<0 26*	*0 39*	*19 7*	*36 5*	*20 4*	*1 46*	*231*	*<1517*	*<9 87*	*619*	*422*	*486*	*1804*	*1136*	*194*	*64 1*	*127*	*119*	*42 3*	*35 2*	*5 02*	*86 3*	*367*	*1201*	*2 30*	*230*	*<4 11*
Cpx3	*13 0*	*3 63*	*146*	*<71 9*	*20 4*	*3 93*	*578*	*<7228*	*<53 5*	*<19 2*	*2711*	*40 3*	*87 3*	*36 2*	*<21 1*	*bd*	*<13 5*	*bd*	*<28 8*	*<20 8*	*bd*	*bd*	*7 56*	*64 5*	*2 74*	*26272*	*158*
Cpx4	9 08	1 02	76 1	21 6	20 4	0 34	22 3	<613	<5 39	2 70	*1113	5 08	12 7	11 0	*0 28	<1 30	<1 47	0 53	<2 03	1 80	<0 63	bd	bd	2 64	<0 16	660	12 6
Cpx5	4 40	0 51	43 6	12 4	20 4	0 37	10 1	<750	<5 26	<1 72	272	8 28	11 5	21 1	<4 19	bd	0 98	bd	bd	0 26	<0 47	0 69	bd	17 3	bd.	302	6 68
Cpx6	9 83	1 60	46 2	<20 3	20 4	0 54	36 0	<1360	<11 2	4 08	333	4 82	14 7	bd	1 89	*2 24	1 99	0 49	bd	bd	bd	bd	<2 31	10 9	<0.17	331	10 1
Cpx7	6 15	0 32	36 1	<33 0	20 4	0 35	<48 5	<3017	<16 2	3 32	186	<3 30	13 6	<22 4	bd	<4 45	<15 0	<9 29	bd	<25 1	bd	bd	bd	<6 72	<3.05	341	<14 7
Cpx8	11 1	*3 58	44.0	32 8	20 4	*1 35	<44 2	<1516	<11 1	*10 2	277	14 4	37 5	19 7	<3 22	<0 86	2 02	1 07	bd	*7 58	<1 65	<2.00	0 51	7 47	<1 54	637	10 0
Cpx9	5 92	1 04	49 8	<34 5	20 4	0 48	*140	2416	<19 6	3 89	398	15 2	25 6	4 41	<1 16	*2 48	*5 21	bd	<5 61	<4 93	1 04	<3 59	<2 70	25 6	1.13	*2306	*72 9
Cpx10	2 63	0 39	19 6	16 8	20 4	0 25	28 9	<880	4 58	2 64	270	2 63	29 3	5 03	bd	0 58	bd	bd	1 00	0 90	<0 54	0 54	<0 71	21.2	bd	213	2 08
Cpx11	9 70	1.13	48 3	36 0	20 4	0 55	67 9	<2045	<13 4	2 44	283	10 5	25 1	3 08	<7 37	<2 76	bd	<5 69	bd	<10 1	<1 16	2 24	bd	19 0	<0 89	264	<3 76
Cpx12	3.16	0 82	48 5	<41 0	20 4	0 31	<53 7	<3378	<28 5	2 95	593	4 35	16 5	bd	<9 09	bd	bd.	b.d.	<7.04	<13 7	bd	bd	<4 10	24 6	bd.	358	6.18
Cpx13	3 24	0 85	44 8	<21 3	20 4	0 39	<34 2	<1614	<12 7	1 22	263	6 20	11 2	4 08	<6 92	0 28	bd	<3 03	<4 05	2.19	0 08	<3 89	0 92	2 92	bd.	*1103	*41.6
Average last 10	6 52	0 85	45.7	23 9	20 4	0 40	33 0	2416	4 58	2 91	319	7 94	19 8	9 76	1 89	0 43	1.66	0.70	1 00	1 29	0.56	1 16	0 72	14 6	1.13	388	7 93
STDS	3 18	0 41	13 9	10 2	0 00	0 10	21 7	nd	nd	0 90	117	4 51	9 04	7.70	nd	0 21	0 59	0 32	nd.	0.87	0 68	0 94	0 29	8 90	nd.	167	3 72
RSD	49%	48%	30%	42%	0%	26%	66%	nd	nd	31%	37%	57%	46%	79%	nd	49%	36%	46%	nd	68%	121%	81%	41%	61%	nd.	43%	47%
Titanite	<0 44	0 68	<28 0	33 8	28 0	36 8	346	<2871	26 8	90 9	240	256	729	380	58 1	13 0	37 6	26 2	<5 29	16 4	<0 35	26 4	30 8	12389	530	12549	120
CP108																											
NY1	*0 96*	*<0 37*	*<14 5*	*24 8*	*35 5*	*0 07*	*25985*	*28121*	*242*	*32 7*	*522*	*945*	*1423*	*271*	*26 5*	*8 66*	*10 0*	*5 63*	*0 38*	*<5.22*	*0 38*	*44 9*	*25 2*	*88 6*	*0 11*	*39 3*	*0 52*
NY2	*0 37*	*0 14*	*<6 19*	*24 8*	*26 0*	*1 21*	*7568*	*11423*	*98 8*	*86 5*	*231*	*440*	*640*	*200*	*25 4*	*8 99*	*21 5*	*16 3*	*7.99*	*6 07*	*0 67*	*18 5*	*24.6*	*856*	*5 17*	*619*	*7.87*
NY3	<1 62	<0 99	<47 0	<38 0	16 1	<0 12	1650	3290	89 0	<5 79	<93 2	65 1	399	46 0	<15 3	bd	bd	bd	<10 4	bd	bd	bd	bd.	1 41	bd.	<16.5	bd
NY4	<0 77	<0 36	<16 2	24 8	20 5	<0 02	3881	18446	87 0	6 18	<37 1	211	300	90 6	8 35	1 69	0 98	1 35	bd.	<5 63	<0 21	bd.	<1.35	<0 58	bd	<10 1	*0 62
NY5	<0 38	<0 14	<6 06	24 8	27 0	<0 01	2557	10378	123	2 38	<10 1	136	223	50 8	1 48	0 85	1.70	0 65	bd.	<1 55	bd	bd	<0 62	1.85	<0 31	*0.76	bd
Average last 3	bd	bd	bd	24 8	21.2	b,d	2696	10705	99 8	4.28	bd	137	308	62 5	4 92	1 27	1 34	1 00	bd,	bd	bd	bd	bd	1.63	bd	n.d	n.d.
STDS				0 00	5 46		1122	7583	20 4	2 69		73 1	88 6	24 5	4 86	0 59	0 51	0 49						0 31			
RSD				0%	26%		42%	71%	20%	63%		53%	29%	39%	99%	47%	38%	49%						19%			
GRE1	*0 20*	*0 08*	*<3 77*	*9 63*	*7 52*	*<0 01*	*6277*	*8055*	*<65 0*	*<8 98*	*91 5*	*349*	*432*	*83 2*	*6 97*	*0 93*	*2 63*	*2.85*	*1.08*	*0 55*	*0 11*	*7 62*	*8 12*	*<15 7*	*<0 09*	*4 60*	*<0.65*
GRE2	<0 27	<0 14	<6 83	18 1	9 63	<0 02	860	5782	25 7	0.50	19 8	58 6	76 3	15 4	<4 04	0 28	1 12	b.d	<1 29	bd	bd	<0 38	0 12	0 26	bd	b.d	<2.22
GRE3	<0 36	<0 18	<9 19	11 2	9 63	<0 01	1314	3990	21 5	1 88	<9 92	74 4	84 7	18 6	1 84	0 58	0 88	<0 39	<0 80	<1 81	0 06	0 39	0 46	<0 39	<0 12	<1 83	<2 98
GRE4	<0 13	<0 08	<4 71	25 6	9 63	0 04	889	3687	29 3	1 21	9 42	47 9	74 6	13 4	<1 36	0 21	<0 73	<0 59	<0 67	bd	bd	0.19	<0 52	0 91	<0 03	*12.6	0 52
GRE5	<0 37	<0 16	<10 2	10 6	9 63	<0 02	1351	5636	29 9	<1 52	14 4	67 5	93 9	21 1	0 56	0 42	1 23	bd	bd	bd	0 05	0 22	0 39	<1 01	bd	<2.40	b.d
GRE6	<0 33	<0 14	<7 01	<6 44	9 63	<0 01	690	2677	12 5	<1 07	8 32	30 4	44 0	7 92	<0 97	0 05	bd	bd	bd	bd	0 16	bd	0 09	<0 54	<0 20	<1.83	b.d
Average last 5	bd	bd	bd	16 4	9 63	0 04	1021	4354	23 8	1 20	13 0	55 8	74 7	15 3	1 20	0 31	1 08	bd	b.d	bd	0 09	0 27	0 27	0 59	bd	bd	0 52
STDS				7 02	nd	nd	295	1330	7.14	0 69	5 25	17 3	18 8	5 05	0 91	0 20	0 18				0 06	0 11	0 19	0 46			nd
RSD				43%	nd	nd	29%	31%	30%	58%	40%	31%	25%	33%	75%	66%	17%				68%	40%	71%	79%			nd
Ne1	*<0 51*	*33 0*	*29 2*	*<20 2*	*<1 73*	*<0 04*	*823*	*<1395*	*42 9*	*6 99*	*<16 6*	*138*	*172*	*15 5*	*<5 33*	*0 45*	*bd*	*bd*	*bd*	*bd*	*0 34*	*0 72*	*4 05*	*2 20*	*<0 35*	*<5.30*	*<6.56*
Ne2	*<0 92*	*33 0*	*35 6*	*<18 9*	*<1 65*	*0 08*	*140*	*<1065*	*104*	*<3 39*	*<26 2*	*5 18*	*14 8*	*3 88*	*bd*	*<1 70*	*bd*	*bd*	*<0 98*	*bd*	*<0 63*	*<0 69*	*0 71*	*<1.78*	*0 06*	*b.d.*	*<6 04*
Ne3	*<2 88*	*33 0*	*<57 0*	*<64 5*	*<6 34*	*<0 16*	*719*	*<4494*	*115*	*<8 55*	*<79 7*	*93 1*	*68 2*	*<23 4*	*<10 7*	*bd*	*<17 6*	*bd*	*bd*	*bd*	*bd*	*bd.*	*bd.*	*<7.88*	*bd*	*bd*	*bd.*
Ne4	*<6 96*	*33 2*	*<152*	*<140*	*20 7*	*1 19*	*2219*	*10253*	*98 9*	*<12 0*	*737*	*244*	*398*	*<90 6*	*<50 0*	*bd*	*bd*	*2.13*	*<11.2*	*bd*	*<0 96*	*<3 69*	*46 0*	*547*	*2.31*	*1722*	*35 5*
Ne5	<0 78	33 0	23 4	<17 5	<1 92	<0 06	10 1	<1321	87 7	<1 51	<23 2	bd	*0 27	bd	bd	<1 95	<0 46	<3 11	bd	bd	bd	0 78	bd	<1 32	bd	<5.87	<1.37
Ne6	<0 53	33 0	28 7	<12 1	<1 25	<0 08	6 01	<852	48 8	<1 73	<22 7	*0 71	bd	bd	bd	bd	bd	bd	<1 58	bd	<0 09	<1.39	0 30	<0 91	bd	<2 25	bd.
Average last 2	bd	33 0	26 0	bd	bd	bd	8 08	bd	68 3	bd	bd	nd	nd	bd	bd	bd	bd	bd	bd	bd	bd	0 78	0 30	bd	bd	bd	bd.

Sample	MgO	Al2O3	SiO2	CaO	CaO	TiO2	Ba	Sr	Rb	Y	V	La	Ce	Nd	Sm	Eu	Gd	Dy	Er	Yb	Lu	U	Th	Nb	Ta	Zr	Hf
STDS		0 00	3 74				2 92		27 5													nd	nd				
RSD		0%	14%				36%		40%													nd	nd				
Mela1	1 60	1 67	28 6	31 6	41 1	11 7	*55 4	<1023	<6 13	634	1311	39 8	217	256	119	46 2	123	134	69 5	53 5	6 50	7 17	6 76	409	14 5	4309	59 3
Mela2	1 03	0 85	39 6	31 6	41 4	13 4	<4 26	<821	<3 20	424	1291	40 4	209	243	88 9	30 8	93 6	95 7	43 6	29 7	3 29	7 39	9 42	483	20 6	3490	52 7
Mela3	0 87	1 33	42 9	31 6	42 0	12 2	<14 1	<892	<6 61	502	1426	22 3	159	182	82 7	29 2	115	105	61 6	54 6	6 66	5 89	11 0	279	13 1	2809	60 4
Average	1 17	1 28	37 0	31 6	41 5	12 4	nd	bd	bd	520	1343	34 2	195	227	97 0	35 4	111	112	58 2	45 9	5 48	6 82	9 06	390	16 1	3536	57 5
STDS	0 38	0 41	7 49	0 00	0 43	0 85				106	72 9	10 3	31 7	39 6	19 6	9 35	15 1	20 1	13 3	14 1	1 90	0 81	2 14	103	4 00	751	4 18
RSD	33%	32%	20%	0%	1%	7%				20%	5%	30%	16%	17%	20%	26%	14%	18%	23%	31%	35%	12%	24%	26%	25%	21%	7%
Cpx1	*4 16*	*1 50*	*91 5*	*<53 6*	*20 7*	*1 85*	*931*	*<3787*	*<15 6*	*20 4*	*1284*	*140*	*140*	*<42 8*	*<9 37*	*3 41*	*<1 17*	*<6 83*	*9 71*	*15 8*	*<3 64*	*4 73*	**45 6*	*1076*	**5 56*	*1180*	*<8 88*
Cpx2	*8 40*	*0 78*	*51 1*	*<30 5*	*20 7*	*0 38*	*5885*	*7367*	*47 9*	*15 3*	*316*	**473*	**534*	**116*	*<6 96*	*2 35*	*3 77*	*<4 17*	*1 63*	*<4 35*	*<0 20*	**13 2*	*8 88*	*86 7*	*b d*	*980*	*14 5*
Cpx3	*7 95*	*1 28*	*55 3*	*<43 0*	*20 7*	*0 61*	**360*	*<2902*	*<19 5*	**18 7*	**716*	**36 1*	**65 4*	*<17 9*	*<13 7*	*1 76*	*<4 24*	*<5 77*	*4 11*	*5 65*	*0 89*	*2 71*	*8 93*	**914*	*<0 56*	*471*	*<11 1*
Cpx4	*14 0*	*2 79*	*65 0*	*<43 4*	*20 7*	*0 51*	**373*	*<3556*	*<15 3*	*2 91*	*129*	**28 6*	*24 5*	*b d*	**11 2*	*2 36*	*b d*	**8 15*	*3 02*	*5 30*	*b d*	*b d*	*b d*	*26 8*	*1 79*	*477*	**18 6*
Cpx5	6 73	1 94	66 0	22 4	20 7	0 48	3 35	<1392	<9 53	4 78	193	6 62	19 6	*4 90	<2 24	<0 67	0 86	0 83	<3 49	*0 26	0 48	<1 39	b d	*2 49	<0 97	324	1 51
Cpx6	5 75	1 07	43 6	14 7	20 7	0 49	*28 1	<963	<7 68	5 80	278	4 72	16 0	<7 05	<3 08	<0 92	1 82	0 92	<2 40	*2 01	0 37	b d	b d	*1 42	b d	312	4 15
Cpx7	8 19	0 73	24 7	<21 0	20 7	0 44	<22 1	<1325	<12 3	3 80	179	3 21	*6 93	*11 0	<7 04	b d	<2 97	1 11	<7 13	<1 55	0 45	0 74	3 73	33 1	0 66	424	7 78
Cpx8	4 83	1 71	40 6	15 0	20 7	0 55	<11 9	<1026	<8 67	6 72	219	7 35	20 7	*6 60	*5 30	*0 91	*4 12	<2 23	0 76	b d	<0 11	b d	<2 09	<1 67	<0 60	299	7 74
Average last 4	6 38	1 36	43 7	17 3	20 7	0 49	3 35	b d	b d	5 28	217	5 48	18 8	n d	n d	n d	1 34	0 95	0 76	n d	0 43	0 74	3 73	33 1	0 66	340	5 30
STDS	1 44	0 56	17 0	4 35	0 00	0 05	n d			1 26	43 6	1 87	2 46	b d	n d	n d	0 68	0 14	n d	n d	0 06	n d	n d	n d	n d	57 2	3 04
RSD	23%	41%	39%	25%	0%	9%	n d			24%	20%	34%	13%	b d	n d	n d	51%	15%	n d	n d	13%	n d	n d	n d	n d	17%	57%
CP112																											
NY1	*<0 78*	*0 26*	*<6 98*	*24 2*	*20 0*	*<0 03*	*9168*	*14757*	*140*	*11 4*	*66 1*	*363*	*562*	*104*	*7 18*	*1 58*	*4 17*	*2 72*	*<0 99*	*<0 46*	*<0 34*	*13 3*	*4 93*	*7 59*	*<0 04*	*0 53*	*b d.*
NY2	<0 83	<0 29	<8 27	24 2	23 4	0 10	16598	16518	362	24 5	340	852	1088	217	18 1	5 19	6 23	5 17	0 75	2 05	<0 24	17 1	23 9	160	0 33	47 6	<1 77
NY3	2 21	<0 53	<17 5	24 2	39 8	b d	34970	35861	507	*62 9	214	1425	1825	335	14 5	7 91	10 7	5 74	2 28	*0 60	0 58	38 4	44 7	54 8	b d.	22 3	<1 92
Average last 2	2 21	b d	b d	24 2	31 6	0 10	25784	26189	434	24 5	277	1138	1457	276	16 3	6 55	6 47	5 46	1 52	2 05	0 58	27 8	34 3	107	0 33	34 9	b d
STDS	n d			0 00	11 6	n d	12991	13878	102	n d	89 3	405	521	83 6	2 54	1 92	3 16	0 40	1 08	n d	n d	15 1	14 7	74 3	n d.	17 9	
RSD	n d			0%	37%	n d	50%	52%	24%	n d	32%	36%	36%	30%	16%	29%	37%	7%	71%	n d	n d	54%	43%	69%	n d.	51%	
GRE1	0 32	<0 07	<2 54	8 28	9 81	<0 01	3250	5823	69 7	3 75	35 4	167	176	34 7	3 45	0 69	1 40	<0 47	0 25	b d	<0 04	3 68	2 04	5 84	b d	0 66	b d
GRE2	<0 37	<0 10	<4 17	<3 94	9 81	0 01	4839	5129	56 3	4 88	54 1	265	310	36 5	2 47	1 04	0 73	0 65	0 29	<0 47	<0 11	5 52	3 74	12 0	0 05	2 67	<0 09
GRE3	<0 27	<0 09	<2 63	10 8	9 81	0 06	3137	5497	58 5	8 29	89 1	233	255	41 8	3 81	0 84	2 41	0 62	<0 11	0 54	<0 08	3 71	3 70	*27 8	0 15	*18 1	0 44
Average	0 32	.b d	b d	9 55	9 81	0 04	3742	5483	61 5	5 64	59 5	221	247	37 7	3,24	0 86	1 51	0 64	0 27	0 54	b d	4 30	3 16	8 92	0 10	1 67	0 44
STDS	n d			1 80	0 00	0 04	952	347	7 21	2 36	27 2	49 9	67 1	3 67	0 69	0 18	0 85	0 02	0 03	n d		1 05	0 97	4 35	0 07	1 42	n d
RSD	n d			19%	0%	101%	25%	6%	12%	42%	46%	23%	27%	10%	21%	20%	56%	3%	10%	n d		24%	31%	49%	71%	85%	n.d.
Ne1	<4 91	33 0	<33 9	<27 0	<3 98	<0 13	67 9	<1872	*14 8	<1 10	<44 3	7 23	9 10	10 4	1 18	b d	b d	<1 62	0 38	<8 89	b d	1 04	<0 33	14 0	0 27	24 7	<5 71
Mela1	*<3 24*	*<1 71*	*<65 2*	*<42 2*	*31 8*	*15 5*	**193*	*<3104*	*138*	*361*	*2272*	*99 7*	*422*	*329*	*85 0*	*25 5*	*71 5*	*96 6*	*45 5*	**12 0*	*3 71*	*23 1*	*32 9*	*347*	*28 7*	*2495*	**17 0*
CP118																											
Ne1	*<4 36*	*32 5*	*<40 5*	*<38 7*	*<5 37*	*<0 07*	**995*	*2850*	*126*	*<3 67*	*<83 6*	**126*	**108*	**14 5*	*0 42*	*b d*	**1 76*	*b d*	*b d.*	*b d*	*<1 46*	*0 89*	*<1 60*	*4 32*	*b d*	*13 6*	*b d*
Ne2	<2 22	32 5	33 7	<14 3	<2 38	<0 13	7 79	<1293	56 6	<3 39	<14 0	bd	<0 80	bd	<7 32	bd	<1 48	<3 49	bd.	bd.	<0 60	bd	<1 28	<1 19	<0 19	bd.	<3 16
Ne3	<8 11	32 5	<68 7	<64 4	<8 37	<0 24	<59 9	<3386	115	3 14	<80 0	bd	3 34	bd	<14 1	<2 14	<5 45	bd	bd.	bd	bd	<5 37	bd	bd.	<0 84	<14 9	bd
Ne4	<4 55	32 5	45 3	<36 5	<4 48	<0 17	56 5	<2125	78 9	<6 71	<80 9	5 90	5 20	bd	<5 20	bd	bd	bd	bd.	bd	bd	bd.	<3 28	bd.	bd	<6 38	bd.
Ne5	<6 13	32 5	<57 8	<53 5	<7 99	<0 19	*194	<2945	129	<1 58	<77 2	3 23	6 26	<13 3	<10 7	bd	<4 48	bd	<6 87	bd	bd	bd	<2 09	<5 83	bd	<9 16	<9 05
Ne6	<21 69	32 5	<225	<155	<21 6	<1 00	<380	11404	<80 5	<12 5	<483	<2 36	bd	bd	<17 6	bd	bd	bd	<18 9	bd	bd	bd	<10 3	<4 57	b d.	<5 99	<25 4
Ne7	<7 68	32 5	<89 1	<87 1	<10 9	bd	<62 1	<5950	60 9	<2 87	<127	bd	bd	<24 2	<23 3	bd	bd	bd	bd	bd	bd	bd	bd	bd	<12 0	b d	<2 77	bd
Average last 6	bd	32 5	39 5	bd	bd	bd	32 1	bd	88 2	3 14	bd	4 57	4 93	nd	nd	bd	nd	bd	bd	bd	bd	bd	bd	bd	bd	bd	bd
STDS		0 00	8 24				34 4		32 6	nd		1 89	1 48														
RSD		0%	21%				107%		37%	nd		41%	30%														

Sample	MgO	Al2O3	SiO2	CaO	CaO	TiO2	Ba	Sr	Rb	Y	V	La	Ce	Nd	Sm	Eu	Gd	Dy	Er	Yb	Lu	U	Th	Nb	Ta	Zr	Hf
CP126																											
NY1	*0 44*	*0 05*	*3 23*	*24 9*	*17 4*	*0 08*	*11911*	*16777*	*583*	*32 8*	*259*	*895*	*1068*	*199*	*11 1*	*4 01*	*6 29*	*1 42*	*1 17*	*<0 49*	*0 09*	*16 9*	*17 9*	**91 6*	**0 37*	**63 8*	**1 65*
NY2	*0 11*	*<0 01*	*<1 31*	*24 9*	*25 4*	*b d*	*14581*	*17916*	*339*	*31 2*	*141*	*949*	*1084*	*226*	*13 9*	*4 39*	**11 9*	*4 80*	*1 87*	*0 71*	*0 20*	*17 5*	*17 2*	*16 0*	*0 02*	*0 86*	*0 33*
NY3	0 08	0 22	<1 84	24 9	30 3	0 02	5866	15148	172	9 42	50 9	364	606	91 2	10 4	2 10	5 09	0 43	<0 68	b d	<0 03	1 78	2 19	22 8	b d.	11.22	<1.45
NY4	<0 05	0 06	<5 97	24 9	46 6	<0 01	4457	18758	137	5 06	12 8	311	472	109	12 9	2 57	4 68	b d	0 55	b d	<0 63	1 78	<0 15	3 81	b d	5 95	b d
NY5	0 02	<0 01	<1 78	24 9	22 8	<0 00	2442	10657	104	5 91	7 75	184	279	64 4	6 72	1 07	2 56	0 76	0 14	b d	<0 14	0 49	0 41	0 72	b d	0 64	0 29
NY6	0 23	0 02	<1 64	24 9	26 5	0 04	6930	14153	408	13 2	221	374	528	106	5 49	1 81	4 44	1 77	0 92	0 72	0 13	**26 0*	**22 6*	35 6	0 18	12 0	<1 08
Average last 4	0 11	0 10	b d	24 9	31 5	0 03	4924	14679	205	8 40	73 1	308	471	92 6	8 90	1 89	4 19	0 99	0 54	0 72	0 13	1 35	1 30	15 7	0 18	7 45	0 29
STDS	0 11	0 11		0 00	10 5	0 01	1940	3332	138	3 71	100	87 6	139	20 3	3 42	0 63	1 12	0 70	0 39	n d	n d	0 74	1.26	16 5	n d	5.27	n.d.
RSD	98%	106%		0%	33%	47%	39%	23%	67%	44%	137%	28%	30%	22%	38%	33%	27%	71%	73%	n d	n d	55%	97%	105%	n d	71%	n d.
GRE1	0 02	<0 01	<0 90	9 64	10 9	<0 00	1767	6363	40 3	3 04	18 9	114	156	*40 1	*4 09	0 44	1 29	0 38	0 15	b d	0 02	0 26	0 35	0 89	b d	<0 17	b d.
GRE2	<0 06	<0 03	<2 70	8 39	10 9	<0 00	1417	7956	29 3	3 09	12 7	104	128	13 6	b d	<0 56	<1 39	<1 63	b d	<1 87	<0 56	b d	0 54	0 36	b d	<0 90	b d
GRE3	<0 04	<0 03	<2 72	17 1	10 9	<0 00	1978	6400	29 7	2 80	16 0	74 1	121	13 9	1 11	<0 57	1 33	1 23	<0 41	<2 05	b d	0 17	b d	0 20	<0 33	0 37	b d
GRE4	0 03	<0 00	<0 62	11 0	10 9	<0.00	1503	4696	46 8	1 96	*60 5	82 8	110	23 8	1 53	0 41	0 85	0 52	0 08	0 19	0 02	*0 64	*1.44	*2 85	<0 02	<0 24	b d.
GRE5	0 03	<0 01	<1 08	9 95	10 9	<0 00	1208	4950	29 7	1 63	11 9	69 8	90 3	19 1	1 14	0 32	0 59	0 43	0 16	0 15	<0 06	0 02	<0 25	0 03	<0 02	<0 52	<0 10
GRE6	0 06	<0 02	<1 83	10 3	10 9	<0 00	1406	5203	39 8	1 53	19 1	66 2	108	24 5	b d	0 14	b d	b d	*1.06	b d	b d	0 10	0 47	0 33	b d	<0 97	b d
GRE7	0 03	<0 01	<1 05	10 8	10 9	<0 00	1917	6390	43 0	1 23	17 2	89 1	120	35 9	1 89	<0 22	0 96	0 77	0 42	0 11	<0 17	b d	0 26	0.25	b d.	0 26	<0 95
Average	0 03	b d	b d	11 0	10 9	b d	1599	5994	36 9	2 18	16 0	85 7	119	21 8	1 42	0 33	1 00	0 67	0 20	0.15	0 02	0 14	0.41	0 34	b d	0 32	b.d.
STDS	0 02			2 80	0 00		290	1133	7 26	0 78	3 06	17 9	20 3	8 32	0 37	0 14	0 31	0 35	0.15	0 04	n d	0 10	0.12	0 29		0 08	
RSD	45%			25%	0%		18%	19%	20%	36%	19%	21%	17%	38%	26%	41%	31%	52%	74%	27%	n d	74%	31%	85%		25%	
CP127																											
NY1	*1 02*	*1 08*	*<3 15*	*25 4*	*27 7*	*0 17*	*21893*	*20884*	*733*	*62 3*	*332*	*1699*	*2356*	*270*	*31 1*	*9 76*	*8 36*	*8 02*	*2 83*	*3 49*	*0 38*	*16 5*	*53 5*	*198*	*0 47*	*11 1*	*<1 16*
NY2	*0 19*	*0 57*	*5 09*	*25 4*	*26 6*	*0 09*	*17518*	*22718*	*459*	*26 7*	*376*	*962*	*1209*	*246*	*18 1*	*5 60*	*8 09*	*4 44*	*1 05*	*1 23*	*0 25*	*17 9*	*48 0*	*166*	*0 07*	*3 54*	*0 40*
NY3	0 02	<0 00	<0 70	25 4	26 8	<0 00	3297	11707	85 8	6 71	0 98	200	331	74 7	6 53	2 32	3 17	1 09	0 56	*0.07	*0 01	b d.	0 27	<0.07	<0 01	<0 14	<0 59
NY4	0 01	<0 01	<0 97	25 4	25 6	<0 00	2840	11883	81 4	5 38	1 28	223	337	78 8	7 05	1 98	4 32	0 98	0 46	<0 21	b d	0 05	0 18	0 16	<0 05	0 06	b.d.
NY5	0 04	<0 01	<1 31	25 4	29 6	<0 00	4034	14623	74 6	8 66	0 90	278	452	104	8 53	2 03	4 31	1 86	0 67	b.d.	<0 06	0 01	0 17	<0.10	b d	b.d.	0 06
Average last 3	0 02	b d	b d	25 4	27 3	b d	3391	12738	80 6	6 92	1 05	234	373	85 8	7 37	2 11	3 93	1 31	0 56	n d	n d	0 03	0 21	0.16	b d	0 06	0 06
STDS	0 02			0 00	2 06		602	1635	5 67	1 65	0 20	39 8	67 8	15 8	1 04	0 18	0 66	0 48	0 11	n d	n d	0 03	0 06	n d		n d	n.d.
RSD	65%			0%	8%		18%	13%	7%	24%	19%	17%	18%	18%	14%	9%	17%	37%	19%	n d	n d	94%	27%	n.d.		n d.	n.d.
Cpx1	10 0	1 06	51 3	26 9	20 1	0 45	49 2	<962	<8 31	3 40	411	5 28	23 9	*3 45	b d	b d	b d	*2 50	<8 53	<5 31	b d	<3 46	5 58	12 0	b d	233	8.49
CP128																											
NY1	*0 50*	*1 12*	*6 32*	*24 8*	*23 7*	*0 19*	*23303*	*24896*	*321*	*31 8*	*366*	*1058*	*1596*	*266*	*24 0*	*5 40*	*11 5*	*5 30*	*2 03*	*1 77*	*0 33*	*28 0*	*39 2*	*198*	*0 53*	*65 2*	*1 05*
NY2	*1 44*	*1 66*	*7 83*	*24 8*	*22 2*	*0 25*	*33798*	*27152*	*421*	*38 9*	*629*	*1434*	*1871*	*372*	*38 5*	*8 04*	*13 2*	*8 47*	*3 47*	*1 91*	*0 55*	*33 2*	*57 5*	*367*	*0 73*	*66 3*	*<1 45*
NY3	*0 38*	*0 21*	*<2 06*	*24 8*	*27 3*	*0 07*	*7616*	*12227*	**109*	*15 8*	**141*	*407*	*532*	*108*	*12 3*	*2 54*	*3 39*	*3 07*	*1 47*	*0 83*	*0 14*	**8 09*	**9 84*	**79 3*	*<0 22*	*8 52*	*b d.*
NY4	0 05	<0 01	<1 62	24 8	28 4	<0 00	2745	11488	62 8	7 34	1 22	199	343	79 5	5 01	1 42	2 03	1 80	0 71	*0 08	0 04	b d	0 20	<0 04	<0 13	<0 36	b d.
NY5	0 03	<0 01	<1 32	24 8	19 8	b d	3014	9798	52 7	7 27	4 99	213	389	86 3	6 59	0 75	1 93	1 38	<0 54	*0 14	b d	0 71	0 72	5 10	<0 20	1 64	<1 24
Average last 2	0 04	n d	b d	24 8	24 1	n d	2880	10643	57 7	7 31	3 11	206	366	82 9	5 80	1 09	1 98	1 59	0 71	n d	0 04	0 71	0 46	5 10	b d	1 64	b d.
STDS	0 01	n d		0 00	6 10	n d	190	1195	7 09	0 05	2 67	10 3	32 5	4 82	1 12	0 47	0 07	0 30	n d		n d	n d	0 37	n d		n d	
RSD	35%	n d		0%	25%	n d	7%	11%	12%	1%	86%	5%	9%	6%	19%	44%	4%	19%	n d		n d	n d	80%	n d		n d	

Note: italics indicate whole analyses rejected, asterixes (*) indicate individual elemental analysis rejected, and bold font indicates that only one analysis was taken into account.
Abbreviations used are: b d., below detection, n d. not determined, Ne: nepheline, NY: nyerereite, meli: melilite, Mela: melanite garnet, Wo: wollastonite, Cpx: clinopyroxene, GRE: gregoryite

Table A4 2 Trace (and major) element LAM-ICP-MS analyses of carbonate liquid (LC) in OL5-experiments - individual and average analyses, standard deviation (STDS) and relative standard deviation (RSD)

Sample	MgO wt %	Al2O3 wt %	SiO2 wt %	CaO wt %	CaO wt %	TiO2 wt %	Ba ppm	Sr ppm	Rb ppm	Y ppm	V ppm	La ppm	Ce ppm	Nd ppm	Sm ppm	Eu ppm	Gd ppm	Dy ppm	Er ppm	Yb ppm	Lu ppm	U ppm	Th ppm	Nb ppm	Ta ppm	Zr ppm	Hf ppm
LC45																											
LC45,1	*0 96*	*0 33*	*4 68*	*16 0*	*17 6*	*0 18*	*11280*	*11285*	*185*	*44 8*	*318*	*1005*	*1233*	*243*	*22 2*	*5 95*	*12*	*6 84*	*3 18*	*1 99*	*0 30*	*27 4*	*16 6*	*161*	*0 33*	*149*	*1 42*
LC45,2	*0 99*	*0 23*	*3 79*	*16 0*	*17 2*	*0 14*	*13435*	*11445*	*287*	*37 0*	*330*	*893*	*1111*	*209*	*19 7*	*5 28*	*10 3*	*5 65*	*2 27*	*1 81*	*0 26*	*23 3*	*12 6*	*128*	*0 35*	*114*	*1 51*
LC45,3	0 62	0 25	3 31	18 0	16 9	0 13	9233	10392	168	27 7	147	636	818	158	15 2	3 86	7 82	4 33	1 69	*1 45	0 17	17 3	11 1	104	0 27	*121	*1 48
LC45,4	0 72	0 20	2 91	16 0	16 7	0 11	9061	10330	150	29 3	172	693	876	169	18 6	4 07	8 14	4 63	1 76	*1 72	0 16	18 5	10 4	99 8	0 25	94 4	1 02
LC45,4	0 58	0 15	2 48	16 0	16 7	0 09	8383	10303	116	21 3	124	515	627	126	11 8	3 09	6 19	3 44	1 48	0 94	0 13	13 3	7 19	83 0	0 17	66 4	0 62
Average last 3	0 64	0 20	2 90	16 0	16 76	0 11	8893	10342	145	26 1	148	615	774	151	14 51	3 67	7 38	4 13	1 64	0 94	0 15	16 4	9 57	95 5	0 23	80 4	0 92
STDS	0 07	0 05	0 42	0 00	0 12	0 02	450	45 6	26 4	4 21	23 9	90 8	130	22 1	2 48	0 52	1 05	0 62	0 15	n d	0 02	2 73	2 09	11 0	0 05	19 8	0 14
RSD	11%	25%	14%	0%	1%	18%	5%	0%	18%	16%	16%	15%	17%	15%	17%	14%	14%	15%	9%	n d	14%	17%	22%	12%	23%	25%	15%
LC51																											
LC51,1	1.70	1 07	5 93	14 7	15 8	0 12	12867	11191	218	24 6	303	808	1030	186	16 6	4 05	7 25	3 73	1 50	1 02	0 13	31.0	18 8	194	0 54	*74 2	*1 14
LC51,2	0 79	0 03	1 70	14 7	15 7	0 01	12949	11817	179	15 8	313	750	886	159	11 1	2 84	4 65	1 83	0 73	0 66	0 12	21.0	16 9	84.9	0 03	0 83	<0.06
LC51,3	1 17	0 05	2 49	14 7	14 0	0 02	13716	10552	177	24 9	459	1358	1630	297	23 6	5 39	9 93	3 16	1 22	0 86	0 17	31.2	33 7	122	0 06	1.43	<0.12
Average	1.22	0 38	3 37	14 7	15 2	0 05	13177	11187	191	21 8	358	972	1182	214	17 1	4 09	7 28	2 91	1 15	0 85	0 14	27.7	22 5	133	0 21	1 13	n d.
STDS	0 46	0 59	2 25	0 00	1 00	0 06	468	633	23 2	5 14	87.1	335	395	73 1	6 26	1 28	2 64	0 98	0 39	0 18	0 03	5.83	9 70	55 3	0 29	0 42	n d
RSD	37%	155%	67%	0%	7%	122%	4%	6%	12%	24%	24%	35%	33%	34%	37%	31%	36%	34%	34%	21%	19%	21%	43%	41%	136%	38%	n d.
LC57																											
LC57,1	0 98	0 03	0 93	14 6	15 8	b d	*2039	*1434	121	7 55	251	*1062	*1059	152	7 37	1 44	2 44	0 65	0 22	0 20	0 01	18 2	*8 36	6 83	0 02	*0 61	0 17
LC57,2	1 30	0 05	1 73	14 6	15 5	0 01	11725	12178	206	6 12	*362	*890	*949	142	7 09	1 51	2 23	0 55	0 19	0 22	0 03	*25.1	11 9	10 9	<0 03	*0 98	0 10
LC57,3	0 75	0 03	1 07	14 6	14 6	0 01	8393	10233	106	5 38	242	454	552	81 7	5 12	1 02	1 90	0 73	0 15	<0 19	0 03	*11.2	*5 66	10 9	0 03	7 35	0 10
Average	1 01	0 04	1 24	14 6	15 3	0 01	10059	11206	145	6 35	246	454	552	125	6 53	1 32	2 19	0 64	0 19	0 21	0 02	18 2	11 9	9 54	0 03	7 35	0 12
STDS	0 28	0 01	0 43	0 00	0 65	0 00	2356	1375	53 2	1 10	67	n d	n d	38 1	1 23	0 27	0 27	0 09	0 04	0 01	0 01	n d.	n d.	2 35	0 01	n d	0 04
RSD	27%	31%	34%	0%	4%	0%	23%	12%	37%	17%	3%	n d	n d	30%	19%	20%	12%	14%	19%	7%	49%	n d.	n d.	25%	28%	n d	33%
LC61																											
LC61,1	0 50	0 06	1 68	14 5	14 9	0 04	9780	10441	130	*19 5	194	*781	*969	*177	*14 5	*3 45	*6 50	*2 73	*1 10	*0 88	*0.12	17.2	*16 2	94.1	0 20	2 62	0.10
LC61,2	0 62	0 08	1.73	14 5	15 4	0 04	9933	9930	170	*20 2	204	*754	*927	*172	*14 2	*3 23	*6 06	*2 62	*1 02	0 72	0 08	15 8	14 4	94 7	0 19	2 87	0.29
LC61,3	0 37	0 04	1 12	14 5	15 1	0 03	8815	10280	*114	15 7	*131	615	751	139	11 2	2 58	4 45	1 99	0 73	0 55	0 08	*12 2	*9 90	64 8	0 13	2 03	0 06
LC61,4	0 39	0 06	1 48	14 5	15 0	0 03	*7648	*9566	*114	13 9	*139	505	632	114	9 95	2 25	4 05	1 90	0 74	0 66	0 08	*11.6	13.7	76 4	0 18	3 70	0 08
Average	0 47	0 06	1 50	14 5	15.1	0 04	9509	10217	150	14 8	199	560	692	126	10 6	2 42	4 25	1 95	0 74	0 64	0 08	16 5	14 0	82 5	0 18	2 86	0 13
STDS	0 12	0 02	0 28	0 00	0 20	0 01	606	262	28 7	1 29	7 19	77 4	84	17 7	0 86	0 23	0 28	0 06	0 01	0 09	0 00	0 98	0 50	14 5	0 03	0 68	0 11
RSD	25%	27%	18%	0%	1%	16%	6%	3%	19%	9%	4%	14%	12%	14%	8%	10%	7%	3%	1%	13%	0%	6%	4%	18%	18%	24%	86%
LC79																											
LC79,1	0 63	0 21	3 04	17 7	17 4	0 14	8235	10696	138	14 6	221	466	540	115	10 1	2 49	4 69	2 54	0 97	0 64	0 11	14 5	16.0	104	0 50	72 2	1.14
LC79,2	0 55	0 30	3 20	17 7	17 7	0 14	7292	11018	110	16 4	170	444	520	108	9 80	2 50	4 46	2 73	1 05	0 89	0 11	13 0	14.1	111	0 60	117	1 84
LC79,3	0 58	0 28	3 34	17 7	17.0	0 14	6325	9663	105	13 1	171	378	442	96 2	9 19	2 16	4 05	2 10	0 64	0 71	0 09	11 8	11.6	99 4	0 62	115	1.78
LC79,4	0 72	0 23	3 36	17 7	18.1	0 18	10603	12455	130	21.0	234	585	664	142	12 4	3 07	6 15	3 30	1 35	1 10	0 13	16 4	16.3	133	0 58	77.7	1.28
LC79,5	0 74	0 27	3 69	17 7	17 6	0 18	9199	10981	135	16 7	231	615	652	125	10 3	2 79	5 05	2 49	1 10	0 81	0 08	13 4	11.2	120	0 62	82 4	1.29
LC79,6	0 83	0 31	4 06	17 7	17 6	0 17	9504	11231	124	19 8	223	569	663	140	12 5	3 11	5 77	3 07	1 29	1 12	0 11	16 6	16 6	129	0 66	115	1.91
LC79,7	*1 05*	*0 44*	*5 28*	*17 7*	*18 0*	*0 26*	*10840*	*12568*	*207*	*28 4*	*327*	*723*	*814*	*171*	*15 6*	*3 93*	*7 52*	*4 18*	*1 80*	*1 78*	*0 21*	*23 8*	*25 4*	*200*	*1 11*	*177*	*2 58*
LC79,8	*1 22*	*0 27*	*5 21*	*17 7*	*17 2*	*0 26*	*9794*	*11421*	*207*	*25 1*	*378*	*842*	*727*	*150*	*14 5*	*3 65*	*7 06*	*4 26*	*1 80*	*1 42*	*0 22*	*26 5*	*27.7*	*194*	*0 76*	*63 4*	*0 86*
LC79,9	*0 94*	*0 46*	*5 19*	*17 7*	*17 4*	*0 22*	*8591*	*10611*	*134*	*20 3*	*267*	*487*	*591*	*123*	*11 0*	*2 91*	*5 69*	*3 21*	*1 36*	*1 20*	*0 16*	*19 0*	*20 0*	*155*	*0 84*	*156*	*2 24*
LC79,10	*1 01*	*0 25*	*5 02*	*17 7*	*17 6*	*0 21*	*15406*	*12869*	*220*	*31 2*	*288*	*842*	*916*	*188*	*16 3*	*4 31*	*8 53*	*4 66*	*1 67*	*1 51*	*0 20*	*20 7*	*22 4*	*154*	*0 69*	*115*	*1 97*
Average first 6	0 68	0 27	3 45	17 7	17 6	0 18	8526	11007	124	16 9	208	510	580	121	10 7	2 69	5 03	2 71	1 10	0 91	0 11	14 3	14 3	116	0 60	96.6	1.54
STDS	0 11	0 04	0 37	0 00	0 36	0 02	1560	900	13 6	3 00	29 7	93 5	93 1	18 1	1 38	0 37	0 80	0 43	0 19	0 16	0 02	1 93	2 42	13 5	0 05	21 2	0 34
RSD	16%	15%	11%	0%	2%	13%	18%	8%	11%	18%	14%	18%	16%	15%	13%	14%	16%	16%	18%	18%	17%	14%	17%	12%	9%	22%	22%

Sample	MgO	Al2O3	SiO2	CaO	CaO	TiO2	Ba	Sr	Rb	Y	V	La	Ce	Nd	Sm	Eu	Gd	Dy	Er	Yb	Lu	U	Th	Nb	Ta	Zr	Hf
LC88																											
LC88,1	*0 69*	*0 76*	*5 24*	*15 3*	*16 2*	*0.24*	*10680*	*11795*	*217*	*20 8*	*348*	*612*	*697*	*140*	*12 6*	*3 08*	*5 78*	*2 90*	*1 35*	*0 98*	*0 13*	*23 0*	*19 3*	*207*	*0 99*	*110*	*1.51*
LC88,2	*0 73*	*0 49*	*5 07*	*15 3*	*15 9*	*0.24*	*11341*	*12313*	*243*	*17 7*	*336*	*611*	*725*	*150*	*12 5*	*3 27*	*6 46*	*3 30*	*1 36*	*1 05*	*0 15*	*24.0*	*20 6*	*194*	*0 80*	*110*	*1 61*
LC88,3	*0 64*	*0 44*	*4 56*	*15 3*	*15 3*	*0.20*	*8108*	*10534*	*152*	*14 7*	*307*	*495*	*560*	*114*	*9 86*	*2 58*	*4 63*	*2 43*	*1 04*	*0 88*	*0 12*	*17 3*	*13 9*	*166*	*0 83*	*127*	*1.72*
LC88,4	*0 46*	*0 35*	*4 44*	*15 3*	*15 7*	*0.20*	*8524*	*10559*	*146*	*16 9*	*183*	*478*	*554*	*119*	*11 1*	*2 61*	*5 06*	*2 78*	*1 07*	*0 93*	*0 12*	*18 0*	*13 2*	*165*	*0 83*	*70 3*	*0 94*
LC88,5	0 56	0 30	2 94	15 3	15 1	0.14	10916	11528	142	14 8	210	517	641	124	10 8	2 78	4 95	2 45	0 98	1 01	0 12	15 8	14 9	118	0 57	66.5	1 04
LC88,6	0 57	0 50	3 44	15 3	15 7	0.15	10724	11875	140	16 6	219	562	663	134	11 7	3 17	5 53	2 92	1 12	0 95	0 13	17 4	15 3	138	0 69	87 8	1.30
LC88,7	0 35	0 37	2 22	15 3	15 3	0.09	8748	10644	99 2	11 6	137	438	522	110	9 70	2 33	4 33	2 13	0 74	0 62	0 08	10 2	10 1	76 5	0 37	53.5	0.78
LC88,8	0 59	0 59	3 63	15 3	15 5	0.14	9615	10432	180	16 7	209	494	594	116	10 1	2 72	4 74	2 47	1 10	1 03	0 13	15 7	15 3	125	0 61	98 0	1 63
LC88,9	0 47	0 36	2 24	15 3	14 7	0.11	8405	10860	164	13 3	219	449	540	104	9 09	2 20	4 27	2 11	0 80	0 58	0 14	12 9	12 5	89 5	0 36	48.1	0 70
LC88,10	0 55	0 25	2 23	15 3	15 2	0.13	6704	9897	101	9 39	176	340	414	91 5	8 49	2 09	3 89	1 93	0 71	0 53	0 07	10 6	9 30	98 1	0 39	42 2	0 67
Average last 8	0 52	0 40	2 78	15 3	15 2	0.13	9185	10873	138	13 7	195	467	563	113	9 98	2 55	4 62	2 34	0 91	0 79	0 11	13 8	12 9	107	0 50	65 7	1.02
STDS	0 09	0 13	0 85	0 00	0 36	0.02	1581	726	32 6	2 90	32 7	76 9	91 2	15 0	1 16	0 41	0 58	0 36	0 18	0 23	0 03	2 97	2.71	23 3	0 14	22 9	0.38
RSD	18%	32%	23%	0%	2%	18%	17%	7%	24%	21%	17%	16%	16%	13%	12%	16%	13%	15%	20%	30%	26%	22%	21%	22%	29%	35%	38%
LC90																											
LC90,1	*0 94*	*0 32*	*3 95*	*16 7*	*17 6*	*0.17*	*15973*	*13354*	*215*	*32 7*	*359*	*1070*	*1134*	*241*	*20 8*	*5 15*	*10 6*	*5 51*	*2 22*	*1 61*	*0 20*	*21 2*	*22 9*	*171*	*0 77*	*131*	*2.23*
LC90,2	*0 68*	*0 32*	*3 74*	*16 7*	*15 3*	*0.15*	*12002*	*11326*	*137*	*27 2*	*212*	*845*	*911*	*200*	*17 9*	*4 41*	*8.59*	*4 66*	*1 79*	*1 37*	*0 20*	*18 1*	*20 5*	*141*	*0 66*	*116*	*1.67*
LC90,3	*0 62*	*0 37*	*3 25*	*16 7*	*16 6*	*0.18*	*6411*	*9388*	*111*	*26 2*	*111*	*675*	*874*	*174*	*15 0*	*4 42*	*7 77*	*4 68*	*1 85*	*1.34*	*0 13*	*17.1*	*25 2*	*144*	*1 06*	*150*	*1.82*
LC90,4	0 49	0 22	2 69	16 7	15 6	0.11	7791	*9841	107	17 3	156	545	616	132	12 1	2 94	5.95	3 04	1 17	0 84	0 09	11.7	11 6	67.0	0 36	60.2	0.79
LC90,5	0 58	0 27	2 84	16 7	17 3	0.14	10165	12290	213	24 3	182	733	819	179	15 7	4 09	7 70	4.03	1 60	1 11	0 17	16 3	17 4	125	0 63	92 5	1.54
LC90,6	0 46	0 24	2 88	16 7	16 4	0.11	8780	11754	132	21 6	154	650	709	159	14 2	3.46	7.19	3 76	1 23	1 21	0 15	13 8	16 2	108	0 51	84.9	1.15
LC90,7	0 51	0 24	2 44	16 7	16 3	0.11	9120	11614	144	20 9	153	613	668	147	13 8	3 23	6 76	3 25	1 36	1 22	0 13	13.0	15 0	101	0 55	82 9	1.30
LC90,8	0 55	0 20	2 56	16 7	16 6	0.12	9242	11517	120	21 1	165	660	703	156	13 6	3 57	6 36	3 54	1 22	1 08	0 11	13 4	13 8	105	0 48	73.3	1.18
LC90,9	0 61	0 25	3 01	16 7	16 5	0.13	10573	11981	171	23 3	198	720	776	168	14 6	3 86	7 41	3 67	1 43	1.18	0 14	13 6	14 5	119	0 51	82 9	1.33
LC90,10	0 65	0 20	2 59	16 7	15 6	0.11	11339	10919	*230	19 4	252	807	647	139	11 8	3 17	5 77	2 98	1.11	0 89	0 11	11 6	11 3	98 9	0 41	65.1	1.08
Average last 7	0 55	0 23	2 72	16 7	16 4	0.12	9573	11679	148	21 1	180	647	705	154	13 7	3 47	6 74	3 47	1 30	1 08	0 13	13 4	14 3	108	0 50	77.4	1.19
STDS	0 07	0 03	0 20	0 00	0 55	0.01	1196	464	38 6	2 34	35 8	65 7	71 6	16 4	1 40	0 40	0 74	0 39	0 17	0 15	0 03	1 58	2 21	12 9	0 08	11.6	0.24
RSD	12%	11%	7%	0%	3%	10%	12%	4%	26%	11%	20%	10%	10%	11%	10%	12%	11%	11%	13%	14%	21%	12%	15%	12%	17%	15%	20%
LC96																											
LC96,1	*1.09*	*0 41*	*8 85*	*17 1*	*16 9*	*0.42*	*21725*	*15734*	*388*	*40 0*	*594*	*1294*	*1406*	*261*	*23 3*	*6.19*	*12 3*	*6 42*	*2 59*	*1.53*	*0 24*	*30 9*	*39 7*	*349*	*1.18*	*159*	*2.39*
LC96,2	*0.85*	*0 23*	*5 36*	*17 1*	*17.8*	*0.29*	*14785*	*14767*	*263*	*22 5*	*435*	*681*	*778*	*175*	*16 7*	*3 99*	*7.86*	*4.48*	*1.68*	*1.32*	*0 22*	*31 7*	*26 5*	*222*	*0 67*	*90 2*	*1.36*
LC96,3	0 30	0 24	3 33	17 1	16 9	0.12	7053	9962	103	11 6	149	407	475	101	9 08	2 22	4 20	1 88	0 72	0 77	0 08	11.0	10 2	98 6	0 52	92.4	1.28
LC96,4	0 44	0 26	4 15	17 1	17 6	0.19	9557	12062	146	13 1	272	435	535	120	11 8	2 66	5 05	2 42	1 01	0 97	0 11	19 6	14 9	156	0 70	100	1.44
LC96,5	0 23	0 16	2 21	17 1	17 6	0.08	5754	9845	99	12 1	107	386	442	97 3	6 85	2 02	4 20	1.78	0 75	0 63	0 09	7 32	8.34	*67.1	*0.36	*64.3	*0.91
LC96,6	0 69	0 32	4 39	17.1	16 7	0.21	11474	11960	186	24 1	359	739	789	181	13 7	3 36	6 60	3 18	1 39	1 32	0 13	20.2	20 8	174	0 65	*124	*1 96
LC96,7	0 29	0 25	3 57	17 1	18 2	0.16	7092	11180	164	11 4	177	372	440	105	9 58	2 31	4 06	2 19	0 84	0 81	0 09	12 0	10 8	134	0 55	102	1 29
LC96,8	0 27	0 15	3 24	17 1	17.6	0.13	7707	11972	113	12 1	150	380	464	110	9 96	2 59	4 44	2 76	1 21	0 79	0 10	15 3	11.9	121	0 52	*45.2	*0 37
LC96,9	0 68	0 33	4 03	17 1	17.3	0.14	8575	11083	223	22 1	233	643	668	130	11 1	3 00	5 67	2 93	1.62	1.24	0 11	13 6	16 0	124	0 63	*149	*2.03
LC96,10	0 98	0 23	5 09	17 1	17 6	0.23	9972	12388	200	17 9	407	558	638	135	12 7	3 12	5 69	3 26	1 28	1 22	0 11	20 7	16 2	197	0 77	92 3	1.36
Average last 8	0 49	0 24	3 75	17 1	17 5	0.16	8398	11306	154	15 6	232	490	556	120	10 8	2 66	4 99	2 55	1 10	0 97	0 10	15 0	13 6	144	0 62	96 6	1.34
STDS	0 27	0 06	0 87	0 00	0 51	0.05	1863	972	48 9	5 12	107	140	128	21 4	1.77	0 47	0 92	0 57	0 33	0 26	0 02	4 88	4 07	33 9	0 10	4.97	0 07
RSD	56%	27%	23%	0%	3%	32%	22%	9%	30%	33%	46%	29%	23%	18%	16%	18%	19%	22%	30%	27%	15%	33%	30%	24%	15%	5%	6%
LC107																											
LC107,1	0 51	0 80	4 02	15 1	15 4	0.13	9801	10714	146	13 9	155	496	586	113	10 5	2 47	4 59	2 27	0 83	0 68	0 09	9 45	9.82	81 3	0 18	117	1.56
LC107,2	0 28	0 84	2 41	15 1	16 0	0.08	8210	11185	114	14 7	125	447	537	110	9 63	2 37	4 67	2 29	0 87	0 63	0 09	9 87	11.4	75 5	0 16	38.0	0 53
LC107,3	*0 60*	*1 70*	*5 26*	*15 1*	*15 0*	*0.16*	*7879*	*10424*	*137*	*15 0*	*240*	*381*	*435*	*101*	*9 03*	*2 36*	*4 26*	*2 33*	*1 12*	*0 97*	*0 10*	*10 7*	*13 0*	*81 1*	*0 10*	*245*	*2.94*
LC107,4	*0 71*	*0 48*	*4 33*	*15 1*	*14 7*	*0.21*	*11383*	*11857*	*152*	*27 6*	*174*	*572*	*655*	*128*	*12 5*	*3 12*	*6.38*	*3 66*	*1 46*	*1 29*	*0 17*	*15.4*	*20 3*	*185*	*0 55*	*117*	*1.63*
LC107,5	*0 27*	*0 26*	*1 33*	*15 1*	*15 5*	*0.06*	*7424*	*10364*	*77 6*	*15 4*	*81 4*	*390*	*450*	*96 5*	*8 50*	*2 16*	*4 16*	*2 20*	*0 84*	*0 63*	*0 10*	*8 22*	*8 96*	*55 6*	*0 07*	*32 5*	*0 46*
Average first 2	0 40	0 82	3 22	15 1	15 7	0.11	9006	10949	130	14 3	140	471	561	112	10 0	2 42	4.63	2 28	0 85	0 65	0 09	9 66	10 6	78 4	0 17	77.7	1.05
STDS	0 16	0 03	1 14	0 00	0 44	0.04	1126	333	22 6	0 59	21 4	34 3	34 6	1 96	0 58	0 07	0 06	0 01	0 03	0 02	0 00	0 30	1.12	4 08	0 01	56.2	0 73
RSD	41%	3%	35%	0%	3%	34%	12%	3%	17%	4%	15%	7%	6%	2%	6%	3%	1%	1%	3%	3%	0%	3%	11%	5%	8%	72%	70%
LC108																											
LC108,1	*<0 54*	*<0 12*	*<2.35*	*13 2*	*11 4*	*b d*	*7177*	*10843*	*166*	*13 1*	*338*	*445*	*516*	*94 2*	*7.06*	*1 86*	*4.03*	*1 84*	*0 67*	*0.72*	*0 08*	*16 7*	*13 0*	*46 4*	*b d*	*1 16*	*0.25*
LC108,2	*<0 60*	*<0 16*	*<2 42*	*13 2*	*19 1*	*<0 05*	*11195*	*15310*	*230*	*24 0*	*482*	*683*	*816*	*145*	*11 4*	*2 96*	*8 16*	*3 12*	*1 52*	*0 86*	*0 12*	*26 3*	*22 2*	*82 4*	*0 05*	*6.44*	*0 45*
LC108,3	*1 51*	*<0 27*	*<4.61*	*13 2*	*14 8*	*b d*	*10559*	*14379*	*183*	*17 2*	*512*	*540*	*705*	*122*	*10 7*	*3 30*	*4 80*	*2 73*	*0 65*	*1.09*	*b d*	*23 7*	*16 5*	*44 1*	*0 05*	*2.45*	*0.33*
LC108,4	*<1 02*	*<0 14*	*<2 85*	*13 2*	*14 5*	*<0 03*	*13378*	*13951*	*398*	*23 7*	*368*	*714*	*779*	*156*	*13 2*	*3 27*	*6 11*	*3 02*	*0 91*	*0 67*	*0 09*	*24 8*	*18 7*	*31 5*	*<0 01*	*0.38*	*0.32*

Sample	MgO	Al2O3	SiO2	CaO	CaO	TiO2	Ba	Sr	Rb	Y	V	La	Ce	Nd	Sm	Eu	Gd	Dy	Er	Yb	Lu	U	Th	Nb	Ta	Zr	Hf
LC108,5	*<0 27*	*<0 08*	*<1 28*	*13 2*	*15 6*	*<0 01*	*6808*	*10361*	*197*	*10 7*	*143*	*346*	*406*	*89 8*	*7 88*	*1 79*	*3 08*	*1 30*	*0 54*	*0 35*	*0 07*	*13 8*	*9 84*	*°12 9*	*0 04*	*°3 99*	*°2 34*
LC108,6	*<0 87*	*<0 16*	*<2 87*	*13 2*	*15 0*	*0 02*	*17259*	*14325*	*290*	*30 0*	*843*	*1113*	*1135*	*215*	*18 2*	*4 17*	*9 03*	*3 99*	*1 54*	*1 34*	*0 20*	*30 7*	*25 1*	*63 9*	*<0 04*	*2 08*	*0 20*
LC108,7	*<0 83*	*<0 15*	*<2 77*	*13 2*	*15 4*	*<0 03*	*14034*	*13831*	*293*	*26 1*	*381*	*817*	*871*	*158*	*12 4*	*4 17*	*6 83*	*2 92*	*1 73*	*0 88*	*0 11*	*26 7*	*26 4*	*37 1*	*0 02*	*0 06*	*0 10*
LC108,8	*0 78*	*<0 17*	*<2 68*	*13 2*	*12 1*	*0 01*	*14223*	*12879*	*294*	*26 3*	*693*	*777*	*841*	*160*	*12 0*	*3 33*	*6 43*	*3 14*	*1 51*	*0 76*	*0 20*	*33 3*	*21 1*	*93 2*	*0 01*	*1 43*	*0 25*
LC108,9	<1 02	<0 24	<3 92	13 2	12 8	<0 03	9485	11493	166	22 9	381	615	679	118	10 4	2 43	4 09	1 89	1 01	0 74	0 10	18 5	12 2	48 8	<0 07	1 28	0 13
LC108,10	<1 19	<0 17	<3 51	13 2	13 1	<0 06	9423	11479	146	14 4	347	445	500	94 8	7 55	1 79	3 39	2 11	0 80	0 53	<0 06	19 3	11 6	49 9	0 03	1 21	0 21
LC108,11	<0 55	<0 15	<2 49	13 2	13 9	<0 02	9402	11763	182	12 8	444	457	536	93 9	8 67	2 31	3 98	2 08	0 68	0 42	0 10	24 2	14 6	75 3	0 01	2 28	0 09
Average	b d	b d	b d	13 2	13 3	b d	9437	11579	165	16 7	391	506	572	102	8 88	2 18	3 82	2 03	0 83	0 56	0 10	20 7	12 8	58 0	0 02	1 59	0 14
STDS	n d	n d	n d	0 00	0 58	n d	42 9	160	18 0	5 42	48 9	94 9	94 8	13 9	1 45	0 34	0 38	0 12	0 17	0 16	0 00	3 12	1 56	15 0	0 01	0 60	0 06
RSD	n d	n d	n d	0%	4%	n d	0%	1%	11%	32%	13%	19%	17%	14%	16%	16%	10%	6%	20%	29%	0%	15%	12%	26%	71%	38%	43%
LC112																											
LC112,1	*0 40*	*0 17*	*2 84*	*9 27*	*9 80*	*0 09*	*5233*	*6484*	*75 3*	*13 8*	*87 6*	*408*	*454*	*82 1*	*7 76*	*1 96*	*3 71*	*2 00*	*0 67*	*0 82*	*0 14*	*7 70*	*12 9*	*108*	*0 38*	*74 7*	*0 99*
LC112,2	*0 26*	*1 07*	*2 11*	*9 27*	*9 32*	*0 02*	*8436*	*8051*	*104*	*14 4*	*70 1*	*456*	*466*	*86 2*	*7 19*	*1 79*	*3 30*	*1 61*	*0 58*	*0 48*	*0 08*	*8 84*	*11 9*	*41 7*	*0 12*	*13 3*	*0 39*
LC112,3	*<0 55*	*<0 12*	*<2 01*	*9 27*	*9 19*	*<0 03*	*3419*	*6704*	*73 9*	*4 46*	*30 5*	*181*	*215*	*41 8*	*2 88*	*0 63*	*1 90*	*0 51*	*0 29*	*0 13*	*0 02*	*3 51*	*3 62*	*12 5*	*0 04*	*3 00*	*0 10*
LC112,4	*0 75*	*0 16*	*<2 19*	*9 27*	*11 3*	*<0 04*	*6160*	*8350*	*117*	*12 5*	*112*	*383*	*467*	*92 3*	*8 62*	*2 15*	*3 54*	*1 77*	*1 01*	*0 37*	*<0 04*	*10 9*	*8 97*	*49 5*	*0 05*	*11 5*	*0 25*
LC112,5	0 96	0 19	<3 38	9 27	14 0	0 07	°1179	°1060	°200	17 2	106	710	752	124	°10 9	2 72	°8 55	2 89	°1 13	1 01	0 09	°14 0	°16 8	72 0	0 19	50 6	0 52
LC112,6	0 85	0 17	1 51	9 27	9 51	0 05	7839	6891	122	17 7	163	556	569	93 8	7 80	2 16	3 66	1 91	0 62	0 43	0 09	7 80	12 8	93 8	0 26	27 8	0 61
LC112,7	0 77	<0 09	<1 72	9 27	8 84	0 05	4739	5785	85 9	8 00	87 5	254	308	52 9	4 39	1 14	1 65	0 81	0 41	0 30	0 08	5 69	6 70	61 4	0 20	42 3	0 65
LC112,8	0 15	0 76	1 65	9 27	9 07	0 05	3798	5516	52 5	8 10	43 2	207	278	61 9	6 19	1 46	3 00	1 24	0 56	0 42	0 07	6 54	9 93	62 8	0 25	47 5	0 56
LC112,9	0 42	0 26	2 32	9 27	8 37	0 07	4381	5378	86 6	8 64	88 2	292	386	66 0	5 60	1 64	2 92	1 69	0 45	0 39	<0 03	6 41	9 84	84 6	0 27	48 1	0 66
LC112,10	0 31	<0 17	<2 79	9 27	11 1	0 05	5445	7747	111	14 4	83 3	373	388	75 0	7 06	2 17	3 18	1 72	0 74	<0 40	<0 09	5 92	8 28	49 4	0 11	19 4	0 50
Average	0 58	0 35	1 83	9 27	10 1	0 06	5240	6263	92	12 3	95 3	399	447	78 9	6 21	1 88	2 88	1 71	0 56	0 51	0 08	6 47	9 50	70 7	0 21	39 3	0 58
STDS	0 33	0 28	0 43	0 00	2 09	0 01	1570	1021	27 0	4 63	39 3	196	181	26 1	1 32	0 57	0 74	0 70	0 13	0 28	0 01	0 82	2 25	16 3	0 06	12 7	0 07
RSD	57%	81%	24%	0%	21%	16%	30%	16%	29%	37%	41%	49%	40%	33%	21%	31%	26%	41%	24%	56%	12%	13%	24%	23%	28%	32%	12%
LC118																											
LC118,1	0 27	0 47	2 05	15 9	17 5	0 09	8173	11348	151	11 2	158	403	521	101	9 04	2 16	3 90	1 61	0 57	0 51	0 07	10 3	9 80	83 8	0 10	16 4	0 17
LC118,2	0 40	0 19	1 17	15 9	16 7	0 08	8599	11460	255	12 6	207	464	554	111	9 58	2 39	4 25	2 28	0 85	0 61	0 09	12 0	8 54	74 7	0 04	9 38	0 14
LC116,3	0 38	0 01	0 35	15 9	16 2	0 07	9712	10870	182	°24 9	272	°844	°682	128	12 1	2 80	5 69	°3 38	°1 48	°1 30	°0 19	12 4	17 8	69 0	0 01	5 40	0 36
LC118,4	0 28	0 07	0 93	15 9	15 5	0 06	6679	10368	229	7 79	329	314	404	76 3	7 53	1 77	3 18	1 42	0 56	0 55	0 06	9 46	8 87	66 1	0 02	27 9	0 62
LC118,5	0 69	<0 02	<0 87	15 9	15 6	0 09	9386	11380	180	13 5	177	512	595	112	9 44	2 85	4 67	2 33	1 08	0 77	0 09	9 31	14 1	105	0 02	7 76	0 10
LC118,6	*0 56*	*0 15*	*1 63*	*15 9*	*16 5*	*0 16*	*9592*	*11902*	*135*	*13 4*	*159*	*469*	*544*	*114*	*9 40*	*2 35*	*4 46*	*2 36*	*0 95*	*0 75*	*0 10*	*12 0*	*12 8*	*168*	*0 21*	*28 8*	*0 27*
LC118,7	*1 44*	*0 32*	*5 50*	*15 9*	*12 8*	*0 19*	*10765*	*12540*	*446*	*11 5*	*445*	*512*	*819*	*118*	*9 92*	*2 58*	*4 07*	*2 11*	*1 05*	*0 55*	*0 05*	*16 9*	*17 1*	*228*	*0 13*	*26 0*	*<0 10*
LC118,8	*0 80*	*0 83*	*4 84*	*15 9*	*15 1*	*0 17*	*7432*	*9340*	*198*	*10 1*	*244*	*388*	*507*	*88 7*	*7 74*	*2 09*	*3 49*	*1 97*	*0 75*	*0 59*	*0 08*	*9 08*	*8 87*	*184*	*0 09*	*19 9*	*<0 51*
LC118,9	*0 29*	*0 42*	*2 46*	*15 9*	*16 0*	*0 21*	*8100*	*10494*	*119*	*13 0*	*162*	*409*	*476*	*103*	*9 36*	*2 28*	*4 36*	*2 07*	*0 97*	*0 77*	*0 09*	*12 1*	*10 0*	*226*	*0 14*	*27 5*	*0 24*
LC118,10	*0 70*	*0 10*	*<2 94*	*15 9*	*17 3*	*0 29*	*17623*	*15952*	*384*	*21 7*	*530*	*835*	*921*	*186*	*17 2*	*4 25*	*7 72*	*4 47*	*1 63*	*1 83*	*0 32*	*29 4*	*32 4*	*331*	*<0 11*	*26 4*	*0 32*
Average first 5	0 40	0 19	1 13	15 9	16 3	0 08	8510	11085	199	11 3	229	424	518	105	9 53	2 39	4 34	1 96	0 77	0 61	0 08	10 7	11 8	79 6	0 04	13 4	0 28
STDS	0 17	0 20	0 71	0 00	0 81	0 01	1192	463	41 9	2 51	70 6	85 4	82 2	19 0	1 64	0 45	0 93	0 43	0 25	0 11	0 02	1 41	4 01	15 5	0 04	9 11	0 22
RSD	42%	110%	63%	0%	5%	10%	14%	4%	21%	22%	31%	20%	16%	18%	17%	19%	21%	22%	33%	19%	19%	13%	34%	19%	96%	68%	78%
LC126																											
LC126,1	0 29	0 07	0 90	7 1	7 31	0 13	10974	6113	129	21 1	256	567	605	108	10 6	2 87	6 18	4 14	1 87	1 56	0 21	13 9	15 6	57 0	0 19	39 0	1 05
LC126,2	0 28	0 04	2 70	7 1	6 84	0 09	5394	5017	79 5	9 80	103	°278	°334	°65 1	°5 71	°1 44	2 89	1 56	0 61	0 64	0 08	6 98	9 08	133	0 51	62 3	0 89
LC126,3	0 22	0 22	2 19	7 1	7 18	0 05	5476	5130	86 9	9 26	73 9	°324	°397	°71 2	°6 03	°1 51	°2 75	1 43	0 51	0 56	0 06	4 59	8 48	77 6	0 20	27 4	0 41
LC126,4	0 26	0 03	0 81	7 1	7 42	0 02	17286	8437	213	23 2	144	810	844	146	13 2	3 12	6 30	3 12	1 18	0 88	0 12	12 7	17 8	100	0 04	0 61	0 13
LC126,5	0 21	0 03	2 29	7 1	7 01	0 04	7062	5119	49 6	9 16	69 3	°353	°365	°81 7	°5 36	°1 37	°2 42	1 20	0 48	0 44	0 06	5 88	8 45	53 4	0 12	37 8	0 65
LC126,6	*0 18*	*0 01*	*<0 52*	*7 1*	*6 87*	*b d*	*9233*	*6639*	*102*	*15 5*	*52 2*	*505*	*506*	*87 2*	*7 82*	*1 73*	*3 61*	*1 87*	*0 71*	*0 43*	*0 08*	*6 28*	*11 8*	*36 7*	*0 02*	*0 56*	*<0 06*
LC126,7	*0 15*	*0 02*	*<0 43*	*7 1*	*7 58*	*0 01*	*11127*	*6538*	*105*	*13 7*	*57 5*	*568*	*583*	*99 7*	*8 03*	*1 97*	*3 83*	*1 85*	*0 80*	*0 56*	*0 06*	*6 68*	*11 5*	*35 3*	*<0 01*	*0 46*	*0 19*
LC126,8	*0 19*	*0 01*	*<0 31*	*7 1*	*7 46*	*0 01*	*13534*	*6556*	*166*	*17 6*	*158*	*659*	*647*	*101*	*8 69*	*2 14*	*4 26*	*2 17*	*0 97*	*0 66*	*0 09*	*9 72*	*17 7*	*56 1*	*0 01*	*0 13*	*0 12*
LC126,9	*0 08*	*0 01*	*0 43*	*7 1*	*7 58*	*0 01*	*6566*	*5159*	*86 0*	*6 22*	*80 6*	*248*	*332*	*59 2*	*5 27*	*1 24*	*2 21*	*0 95*	*0 37*	*0 22*	*0 03*	*11 6*	*4 62*	*23 3*	*0 04*	*2 61*	*0 06*
Average first 5	0 25	0 08	1 74	7 10	7.15	0 07	9238	5963	112	14 5	129	689	725	127	11 88	3 00	5 12	2 29	0 93	0 82	0 11	8 82	11 9	84 2	0 21	33 4	0 63
STDS	0 04	0 08	0 92	0 00	0 23	0 04	5036	1453	63 5	7 00	77 0	172	169	26 4	1 82	0 18	1 94	1 28	0 60	0 45	0 06	4 22	4 48	33 0	0 18	22 4	0 37
RSD	14%	104%	53%	0%	3%	67%	55%	24%	57%	48%	60%	25%	23%	21%	15%	6%	38%	56%	64%	55%	60%	48%	38%	39%	84%	67%	59%
LC127																											
LC127,1	*0 08*	*0 09*	*0 38*	*8 24*	*8 30*	*0 02*	*3262*	*5710*	*39 7*	*7 05*	*31 2*	*159*	*195*	*42 0*	*4 02*	*0 94*	*1 78*	*0 92*	*0 36*	*0 30*	*0 04*	*1 86*	*3 45*	*24 6*	*0 03*	*2 55*	*0 06*
LC127,2	*0 22*	*0 28*	*1 30*	*8 24*	*8 40*	*0 02*	*4443*	*6213*	*71 3*	*7 71*	*56 0*	*225*	*295*	*52 1*	*4 25*	*1 23*	*2 13*	*0 98*	*0 40*	*0 32*	*0 05*	*2 53*	*4 85*	*38 7*	*0 05*	*2 43*	*0 09*
LC127,3	0 15	0 09	<0 85	8 24	8 37	0 04	5497	6661	188	9 52	196	303	329	61 4	5 24	1 16	2 74	1 24	0 49	0 53	0 05	8 52	8 38	74 6	0 06	1 51	<0 10
LC127,4	<0 28	0 13	<4 22	8 24	7 43	0 03	9185	7579	183	14 2	200	363	432	75 5	7 53	1 88	4 07	2 27	0 75	0 91	0 17	7 45	17 5	100	<0 07	1 75	<0.55

Sample	MgO	Al2O3	SiO2	CaO	CaO	TiO2	Ba	Sr	Rb	Y	V	La	Ce	Nd	Sm	Eu	Gd	Dy	Er	Yb	Lu	U	Th	Nb	Ta	Zr	Hf
LC127,5	<0 18	0 19	<2 41	8 24	9 67	0.03	6810	7287	58 0	15 4	77 5	369	432	81 6	7 26	1 99	3 49	2 01	0 96	0 93	0 14	4 56	12 2	50 6	0 03	1 54	<0 32
LC127,6	<0 42	0 30	<4 88	8 24	7 13	0.08	8818	6064	107	12 5	242	481	496	90 1	8 36	<3 03	4 59	2 11	0 62	<0 74	<3 05	5 88	20 7	*210	<0 09	3 50	<0 66
LC127,7	<0 81	<0 32	<12 87	8 24	*33 7	0.05	3517	4720	192	7 92	*365	322	278	52 5	2 53	0 63	<1 46	<0 82	0 29	<3.23	0 02	<7 11	5 24	71 8	0 02	<4 53	1.65
LC127,8	0 36	0 42	1 90	8 24	8 95	0.04	6648	7738	190	9 92	174	327	408	66 0	5 75	1 51	2 50	1 44	0 53	0 5	0 07	8 50	9 98	84 6	0 06	2 02	0 28
LC127,9	0 31	0 31	1 71	8 24	8 36	0.06	9358	7129	120	16 1	149	511	557	103	8 92	2 24	4 61	2 64	1 05	0 89	0 12	8 05	16 9	98 1	0 14	15 8	0 33
LC127,10	0 39	0 26	1 04	8 24	8 65	0.03	9166	6972	134	12 2	114	415	457	81 1	7 07	1 81	3 52	1 94	0 84	0 70	0 10	6 51	15 9	76 9	0 05	1 83	0 12
LC127,11	0 24	0 19	1 06	8 24	8 08	0.06	3307	5212	50 4	6 85	52 8	193	235	47 3	4 20	1 06	1 89	0 91	0 40	0 26	0 04	1 85	3 88	38 1	0 15	29 2	0 53
LC127,12	0 25	0 49	1 38	8 24	8 95	0.03	7268	7569	92 2	11 6	151	380	437	81 0	7 13	1 70	3 33	1 77	0 69	0 51	0 07	7 55	10 4	62 1	0 04	2 73	0 11
LC127,13	0 30	0 16	0 62	8 24	8 54	0.03	7146	7869	102	11 6	80 0	301	326	65 7	5 67	1 46	2 75	1 51	0 63	0 50	0 07	4 89	9 28	61 3	0 04	2 26	0 10
LC127,14	0 26	0 46	1 96	8 24	7 71	0.06	5966	6110	104	14 0	97 3	323	361	63 0	5 46	1 52	2 65	1 39	0 51	0 50	0 06	2 25	8 99	82 3	0 08	10 5	2 15
LC127,15	0 29	0 23	0 89	8 24	8 26	0.03	8209	8102	97 0	14 4	111	353	379	76 1	6 74	1 75	3 27	1 79	0 78	0 64	0 09	4 54	11 6	74 3	0 04	2 94	0 18
Average	0 28	0 27	1 32	8 24	8 34	0.04	6992	6847	123	12 0	137	357	394	72 6	6 30	1 56	3 28	1 75	0 66	0 62	0 08	5 88	11 6	72 9	0 06	6 30	0 61
STDS	0 07	0 13	0 50	0 00	0 70	0.02	2024	1047	47 8	2 85	57 9	81 4	88 7	15 4	1 74	0 44	0 84	0 48	0 22	0 21	0 04	2 30	4 93	18 1	0 04	8 44	0 76
RSD	25%	49%	38%	0%	8%	38%	29%	15%	39%	24%	42%	23%	23%	21%	28%	28%	26%	27%	33%	34%	52%	39%	42%	25%	67%	134%	125%
LC128																											
LC128,1	*0 24*	*0 09*	*0 38*	*11 1*	*11.4*	*0.03*	*6137*	*8193*	*68 8*	*10 5*	*76 8*	*339*	*390*	*82 8*	*7 72*	*1 77*	*3 36*	*1 74*	*0 71*	*0.59*	*0.07*	*5.23*	*7 33*	*32 3*	*0 12*	*13 8*	*0.25*
LC128,2	*0 36*	*0 39*	*1 51*	*11 1*	*11 1*	*0.05*	*8294*	*8485*	*116*	*10 8*	*118*	*409*	*480*	*94 2*	*8 16*	*2 08*	*3 92*	*1 93*	*0 75*	*0 59*	*0 09*	*8 60*	*10 6*	*58 2*	*0 11*	*11 3*	*0 19*
LC128,3	0 45	0 38	1 45	11 1	11 2	0.07	9506	8952	128	16 8	131	512	590	111	10 2	2 58	4 93	2 75	1 10	0 88	0 12	7 79	14 2	106	0 09	11 8	0 16
LC128,4	0 32	0 52	2 16	11 1	11 8	0.08	8096	8283	150	11 1	158	408	492	98 4	8 44	2 26	3 96	2 13	0 87	0 80	0 09	10 1	10 6	61.4	0.11	36 7	0 68
LC128,5	0 28	0 38	1 56	11 1	11.4	0.07	8825	8698	119	14 5	112	476	557	111	10 1	2 52	4 92	2 66	1 06	0 82	0 12	8 09	12 2	75 9	0 07	21 1	0 25
LC128,6	0 51	0 79	4 66	11 1	10 4	0.09	7367	7160	148	9 48	178	411	516	93 1	8 21	2 24	3 59	*1 64	*0 48	*0 49	0 10	8.44	9 37	82 2	0.11	18 8	0 21
LC128,7	0 30	0 60	2 10	11 1	11 4	0.07	9637	9351	113	12 0	166	447	520	100	9 06	2 18	4 39	2 25	0.72	0.74	0 09	12.4	11 2	71 7	0 14	15 6	0 29
LC128,8	0 27	1 47	4 42	11 1	12 4	0.06	8220	10090	170	14 0	163	632	720	119	10 4	3 07	4 95	2 82	1 01	0 71	*0 07	8.99	9 03	50 6	0.10	12 3	0 21
LC128,9	0 39	0 57	3 55	11 1	12 2	0.09	10157	10542	197	17 2	190	*631	*839	*144	*13 5	*3 38	*5 82	3 08	1 33	0.99	0 10	12.2	12 8	115	0 19	17.8	0 43
LC128,10	0 23	0 78	3 91	11 1	10 8	0.07	7989	7821	74 7	11 0	80 5	395	476	92 8	8 06	1 96	3 58	1 89	0 82	0 77	0 10	6 08	13 5	116	0 34	25.2	0 43
Average	0 34	0 69	2 98	11 1	11 4	0.08	8724	8862	137	13 3	149	469	553	104	9 20	2 40	4 33	2 51	0 99	0 82	0 10	9.27	11 6	84 8	0 14	19 9	0 33
STDS	0 10	0 35	1 30	0 00	0 71	0.01	967	1129	37 3	2 83	34 3	83 1	82 8	10 1	1 00	0 36	0 62	0 43	0 20	0 09	0 01	2.20	1 89	24 8	0 09	8.11	0.17
RSD	28%	51%	44%	0%	6%	14%	11%	13%	27%	21%	23%	18%	15%	10%	11%	15%	14%	17%	21%	12%	12%	24%	16%	29%	61%	41%	52%
LC129																											
LC129,1	*1 17*	*0.02*	*0 98*	*15 3*	*16 0*	*0 01*	*19202*	*14094*	*213*	*11 4*	*406*	*1056*	*1054*	*164*	*10 9*	*2 18*	*3 74*	*1 31*	*0 40*	*0 33*	*0 05*	*33 3*	*13 8*	*11 7*	*0 01*	*1 40*	*0.17*
LC129,2	*0 63*	*0.02*	*<1.46*	*15 3*	*15 8*	*0 01*	*15098*	*13029*	*259*	*9 98*	*324*	*924*	*933*	*150*	*9 86*	*2 12*	*3 36*	*1 21*	*0 30*	*0 33*	*0 05*	*26.2*	*11.5*	*10 3*	*<0.02*	*1.17*	*<0.16*
LC129,3	*0 31*	*0 01*	*<0 74*	*15 3*	*15 8*	*0 01*	*10781*	*11406*	*355*	*4 40*	*203*	*551*	*573*	*98 5*	*5 77*	*1 34*	*1 94*	*0 47*	*0 16*	*0.16*	*0.02*	*14 6*	*4.38*	*6 94*	*0 02*	*0.83*	*0 08*
LC129,4	*0 41*	*0 02*	*<0 81*	*15 3*	*15 7*	*b d*	*9037*	*11170*	*132*	*4 30*	*211*	*468*	*517*	*92 0*	*5 78*	*1 20*	*2 05*	*0 57*	*0 18*	*<0.14*	*0 03*	*16.1*	*6 06*	*5 40*	*<0 03*	*0 58*	*0 07*
LC129,5	*0 25*	*<0 04*	*<2.31*	*15 3*	*14 4*	*<0 00*	*11234*	*11062*	*142*	*3 90*	*147*	*428*	*450*	*74 5*	*3 74*	*4 80*	*0 99*	*0 57*	*0 18*	*b d*	*0.02*	*5 81*	*4 54*	*3 69*	*<0 06*	*1.01*	*<0 28*
LC129,6	*0 40*	*<0 02*	*<1.19*	*15 3*	*15 8*	*b d*	*8862*	*10447*	*112*	*4 83*	*158*	*522*	*566*	*95 1*	*6 66*	*1 12*	*2 04*	*0 58*	*0 18*	*0 14*	*0 03*	*12 0*	*6 32*	*5 06*	*0.01*	*0 58*	*<0 18*
LC129,7	*0 24*	*<0 01*	*<1 22*	*15 3*	*16 4*	*b d*	*7820*	*10827*	*100*	*4 43*	*125*	*453*	*462*	*78 7*	*4 83*	*0 91*	*1 59*	*0 46*	*0 11*	*<0 13*	*0 02*	*10 3*	*3 80*	*4 84*	*0.01*	*0 57*	*<0.15*
LC129,8	0 61	0.01	0 93	15 3	15 8	b d	13121	12105	133	5 67	252	668	666	106	6 61	1 41	2 23	0 66	0 24	0 14	0 02	18 1	7.30	7 60	<0 01	0 94	0 10
LC129,9	0 50	<0 02	<0 95	15 3	15 2	0 01	11814	12257	145	5 76	251	605	634	108	8 46	1 43	2 37	0 65	0 20	0 31	0 03	19 0	7 43	7 68	<0.02	0 93	0 10
LC129,10	0 43	<0 02	<1 13	15 3	16 5	b d	12094	12076	166	5 92	313	527	573	94 9	5 38	1 26	2 21	0 57	<0 20	0 22	0 05	15 9	7 71	6 83	<0.02	0 96	<0 09
Average last 3	0 51	0 01	0 93	15 3	15 9	0 01	12343	12146	148	5 78	272	600	624	103	6 15	1 37	2 27	0 63	0 22	0 22	0 03	17 7	7 46	7 37	b d.	0 94	0 10
STDS	0 09	n d	n d	0 00	0 66	n d	688	98	16 4	0 13	35 5	71	48	6 9	0 67	0 09	0 09	0 05	0 03	0 09	0 02	1.61	0.21	0 47	n d.	0 02	0 00
RSD	18%	n d	n d	0%	4%	n d	6%	1%	11%	2%	13%	12%	8%	7%	11%	7%	4%	8%	13%	38%	46%	9%	3%	6%	n d.	2%	0%

Note that the compositions were calculated using CaO that was calculated before filtering of the major element data. After filtering, the CaO content of the carbonate liquid might be different than what is indicated in this table, and the trace element data have been recalculated according to the corrected CaO value. Values underlines are these used for selection of the data using variation diagrams. Italics indicate whole analyses rejected and asterixes (*) indicate individual elemental analysis rejected

Table A4 3 LAM-ICP-MS analyses of crystal phases and of groundmass in silicate-bearing natrocarbonatite OL5 and in silicate-free natrocarbonatites CML5, CML9 and BD4169 - individual and average analyses, standard deviation (STDS) and relative standard deviation (RSD)

Sample	MgO wt %	Al2O3 wt %	SiO2 wt %	CaO wt %	CaO wt %	TiO2 wt %	Ba ppm	Sr ppm	Rb ppm	Y ppm	V ppm	La ppm	Ce ppm	Nd ppm	Sm ppm	Eu ppm	Gd ppm	Dy ppm	Er ppm	Yb ppm	Lu ppm	U ppm	Th ppm	Nb ppm	Ta ppm	Zr ppm	Hf ppm
OL5																											
Nepheline, Ph																											
Ne1 rim	*<0 79*	*33 0*	*32 1*	*<3 75*	*<0 64*	*<0 03*	*11 4*	*103*	*77 5*	*<0 42*	*<10 2*	*0 75*	*3 11*	*0 62*	*0 23*	*<0 07*	*0 27*	*0 23*	*<0 26*	*<0 56*	*<0 01*	*<0 63*	*0 03*	*0 57*	*b d*	*1 31*	*<0 08*
Ne2 rim	*<1 87*	*33 0*	*<50 8*	*<7 72*	*<1 57*	*0 07*	*245*	*336*	*105*	*2 82*	*<32 9*	*19 2*	*51 9*	*16 9*	*<0 14*	*<0 44*	*0 92*	*1 52*	*<0 13*	*b d*	*0 05*	*<0 49*	*<1 61*	*19 1*	*0 82*	*20 0*	*0 35*
Ne3 rim	*<0 89*	*33 0*	*50 4*	*<2 86*	*1 67*	*0 07*	*227*	*474*	*101*	*4 36*	*23 3*	*41 4*	*81 0*	*17 1*	*5 18*	*0 84*	*1 68*	*1 67*	*0 23*	*0 29*	*<0 06*	*1 55*	*3 15*	*31 4*	*0 25*	*24 6*	*0 70*
Ne4 int	*<0 28*	*33 0*	*33 4*	*<0 91*	*0 26*	*0 01*	*40 4*	*106*	*76 5*	*0 40*	*<2 94*	*1 51*	*3 03*	*1 11*	*<0 66*	*<0 08*	*<0 10*	*0 10*	*0 08*	*0 02*	*b d*	*<0 10*	*0 19*	*3 28*	*0 03*	*4 06*	*0 09*
Ne5 int	*<0 18*	*33 0*	*41 6*	*0 80*	*0 88*	*0 02*	*225*	*334*	*117*	*0 46*	*7 91*	*8 60*	*10 2*	*1 76*	*0 14*	*<0 07*	*0 10*	*<0 04*	*<0 08*	*<0 09*	*<0 06*	*0 14*	*0 10*	*2 56*	*<0 04*	*12 9*	*0 24*
Ne6 int	*<0 25*	*33 0*	*45 2*	*<0 95*	*0 75*	*0 10*	*192*	*333*	*110*	*3 68*	*14 2*	*20 0*	*33 2*	*9 34*	*1 41*	*0 34*	*1 00*	*0 97*	*0 30*	*0 26*	*0 05*	*1 86*	*3 46*	*37 7*	*0 44*	*94 2*	*1 50*
Ne7 int	*<0 66*	*33 0*	*45 1*	*<2 73*	*<0 66*	*0 04*	*41 5*	*131*	*118*	*0 65*	*<8 25*	*4 69*	*13 7*	*1 55*	*0 55*	*<0 21*	*0 18*	*0 08*	*0 16*	*b d*	*<0 03*	*0 39*	*0 39*	*6 43*	*<0 13*	*5 74*	*<0 61*
Ne8 core	*<0 43*	*33 0*	*63 9*	*<5 89*	*3 08*	*0 10*	*1534*	*632*	*107*	*<0 61*	*49 5*	*22 6*	*19 6*	*4 58*	*2 08*	*<0 21*	*<0 39*	*0 29*	*0 39*	*b d*	*b d*	*<0 59*	*0 23*	*0 57*	*<0 05*	*34 3*	*1 05*
Ne9 core	0 05	32 9	37 9	<0 63	0 28	0 02	11 3	76 5	67 6	0 15	1 71	0 53	1 44	0 28	<0 11	<0 06	<0 08	<0 10	0 08	<0 21	<0 02	<0 06	0 09	1 02	<0 02	6 90	0 02
Ne10 core	0 06	32 9	33 7	<0 61	0 24	0 01	24 9	107	82 2	*2 23	2 19	*3 23	1 67	0 32	0 37	b d	<0 24	<0 10	*0 2	<0 23	b d	0 05	0 10	0 92	0 07	1 64	<0 16
Ne11 core	0 24	32 9	33 8	0 97	*1 30	*0 06	19 6	142	45 7	*2 09	*25 8	0 52	*10 9	*3 03	*1 05	0 25	*0 48	0 23	0 07	<0 18	0 07	0 07	0 13	1 10	0 13	*20 7	0 62
Ne12 core	<0 05	32 9	31 6	<0 74	<0 36	0 01	21 6	94 0	48 4	0 14	2 04	0 37	0 55	b d	b c	b d	<0 12	<0 12	<0 13	b d	b d	<0 05	0 05	0 56	b d.	4 94	b d
Ne13 core	<0 11	32 9	39 4	<1 69	<0 48	0 01	14 1	<153	71 0	0 63	<5 66	0 28	0 47	<1 25	<0 34	<0 09	<0 36	<0 23	0 02	0 03	b d	b.d.	0 03	0 62	b d	<1 98	b d.
Ne14 core	<0 82	32 9	26 6	<18 8	<4 54	<0 24	23 7	<1553	<63 3	<9 95	<63 0	0 58	<0 65	b d	<4 67	b d	<2 49	<17 5	b d	<2 22	<0 38	<0 35	b.d.	b.d.	b d.	<19 3	*2 8
Ne15 core	<0 06	32 9	42 4	<1 53	0 42	0 02	35 8	118	98 5	0 57	2 22	*1 93	*3 24	<1 06	0 29	<0 09	0 12	0 18	<0 21	<0 28	<0 15	<0 10	*0 26	*2 63	0 04	3 66	<0 28
Ne16 core	0 22	32 9	41 3	<0 96	0 56	0 03	17 9	104	102	0 25	3 18	0 72	1 27	0 40	<0 16	<0 04	<0 21	<0 10	0 01	0 06	0 01	<0 07	0 02	0 75	0 03	*13 0	0 31
Ne17 core	0 09	32 9	46 2	<1 20	0 35	*0 08	12 9	82 8	90 4	<0 32	2 09	0 68	2 00	*0 91	0 19	0 11	<0 15	0 15	0 06	<0 21	<0 04	<0 07	<0 20	*5 68	*0 43	*22 3	0 42
Ne18 core	<0 25	33 0	32 9	<0 99	0 36	0 01	34 8	103	65 4	0 18	<1 70	*0 06	0 29	<0 32	0 06	<0 07	0 03	0 07	b d	<0 25	<0 03	<0 12	*0 22	0 18	<0 02	0 99	<0 27
Ne19 core	<0 18	33 0	38 5	<0 65	0 43	0 03	18 9	114	86 1	0 18	2 70	0 27	0 71	0 22	<0 10	<0 03	0 05	0 06	<0 06	0 05	0 02	<0 02	0 09	0 27	<0 02	8 60	0 24
Ne20 core	<0 40	33 0	34 7	<1 63	<0 34	<0 01	12 9	98 9	81 0	0 30	<5 47	0 19	0 24	0 58	0 13	<0 08	b d	0 02	<0 11	<0 58	b.d.	<0 02	0 03	0 06	<0 05	0 41	<0 48
Ne21 core	<0 29	33 0	40 7	<1 20	<0 24	<0 01	15 0	102	91 3	<0 19	<1 97	0 22	1 00	<0 34	<0 26	0 03	0 15	<0 06	0 03	0 01	b.d.	0 02	0 05	0 24	b.d.	0 50	0 03
Ne22 core	<0 24	33 0	40 4	<0 90	<0 21	<0 01	16 2	117	99 2	<0 09	<2 54	0 23	0 84	0 10	<0 16	<0 03	<0 08	<0 09	<0 13	0 03	b d	0 02	<0 06	0 09	<0 02	<0 19	0 04
Average last 14	0 13	32 90	37 14	0 97	0 38	0 02	20 0	105	79 1	0 30	2 30	0 42	0 95	0 32	0 21	0 13	0 09	0 12	0 05	0 04	0 03	0 04	0 07	0 53	0 07	3 46	0 24
STDS	0 09	0 07	5 17	n d	0 11	0 01	7 67	17 1	18 4	0 19	0 49	0 19	0 58	0 16	0 12	0 11	0 06	0 08	0 03	0 03	0 03	0 02	0 04	0 38	0 05	3 12	0 23
RSD	69%	0%	14%	n d	28%	51%	38%	16%	23%	64%	21%	47%	61%	52%	60%	86%	65%	68%	64%	66%	96%	61%	58%	72%	67%	90%	95%
Nepheline, mph-c sph	<2 01	32 5	51 1	11 3	10 4	0 13	71 8	481	89 8	7 88	45 9	14 0	33 7	10 1	0 93	0 80	0 63	1 04	0 91	0 78	<0 13	<0 29	0 90	7 30	<0 21	71 9	<1 10
Clinopyroxene, Ph																											
Cpx1 rim	*1 09*	*1 36*	*44 5*	*21 5*	*21 6*	*0 50*	*<0 84*	*412*	*<0 71*	*5 28*	*205*	*6 75*	*21 9*	*11 5*	*2 52*	*0 72*	*1 39*	*0 96*	*0 54*	*0 64*	*0 15*	*0 03*	*b d*	*0 68*	*0 09*	*316*	*7 95*
Cpx2 rim	*0 94*	*1 31*	*49 6*	*21 5*	*22 4*	*0 48*	*<0 61*	*437*	*<1 01*	*4 40*	*165*	*5 95*	*20 1*	*10 6*	*1 93*	*0 57*	*1 34*	*0 77*	*0 53*	*0 79*	*0 25*	*b d*	*0 03*	*0 70*	*0 04*	*282*	*6 66*
Cpx3 rim	*0 91*	*<0 70*	*52 7*	*21 5*	*22 4*	*0 41*	*2 70*	*1198*	*<1 03*	*3 10*	*238*	*8 49*	*23 5*	*11 3*	*1 47*	*0 38*	*0 89*	*0 48*	*0 26*	*0 87*	*0 23*	*0 08*	*b d*	*0 49*	*<0 04*	*366*	*8 52*
Cpx4 rim	*0 51*	*1 80*	*53 6*	*21 5*	*25 4*	*0 79*	*<2 06*	*614*	*<2 72*	*3 69*	*294*	*6 97*	*23 2*	*5 96*	*1 47*	*0 65*	*1 12*	*0 60*	*<0 45*	*0 54*	*0 30*	*b d*	*<0 06*	*1 13*	*0 01*	*330*	*7 14*
Cpx5 rim	*0 50*	*1 00*	*49 5*	*21 5*	*22 5*	*0 65*	*29 1*	*600*	*1 18*	*4 08*	*230*	*12 6*	*36 3*	*11 8*	*1 79*	*0 61*	*1 41*	*0 92*	*0 35*	*1 23*	*0 25*	*1 07*	*0 65*	*4 41*	*<0 06*	*270*	*5 73*
Cpx6 rim	*<1 93*	*<1 58*	*43 1*	*21 5*	*19 0*	*0 76*	*4 66*	*386*	*<2 04*	*22 4*	*146*	*7 76*	*24 9*	*22 8*	*5 86*	*2 64*	*5 27*	*4 58*	*2 28*	*3 02*	*0 49*	*0 45*	*0 61*	*18 4*	*1 40*	*410*	*7 60*
Cpx7 rim	*2 74*	*<1 70*	*39 9*	*21 5*	*23 3*	*1 25*	*108*	*553*	*5 80*	*21 5*	*323*	*13 2*	*69 0*	*41 5*	*7 61*	*5 74*	*7 14*	*7 23*	*4 37*	*2 65*	*0 76*	*4 33*	*0 52*	*40 2*	*2 46*	*357*	*7 74*
Cpx8 core	*3 02*	*<1 39*	*43 6*	*21 5*	*19 9*	*0 42*	*98 1*	*516*	*6 66*	*4 59*	*147*	*11 2*	*28 6*	*10 3*	*1 35*	*0 71*	*1 57*	*0 75*	*0 53*	*0 50*	*0 35*	*0 19*	*0 24*	*3 62*	*0 13*	*259*	*5 40*
Cpx9 core	*8 68*	*0 77*	*42 1*	*20 4*	*18 0*	*0 49*	*<3 22*	*737*	*<12 4*	*<6 75*	*163*	*4 54*	*9 14*	*4 37*	*<2 94*	*0 50*	*b d*	*b d*	*b d*	*<0 62*	*<0 15*	*<0 14*	*<0 14*	*<1 95*	*b d*	*226*	*3 56*
Cpx10 core	*7 38*	*1 91*	*61 7*	*20 4*	*20 8*	*0 61*	*°23 4*	*<618*	*<19 6*	*4 99*	*°730*	*4 87*	*11 8*	*5 79*	*3 17*	*<0 50*	*<0 70*	*1 22*	*<0 65*	*2 41*	*°1 05*	*<0 14*	*0 07*	*1 77*	*b d*	*332*	*5 08*
Cpx11 core	*3 89*	*0 98*	*57 2*	*20 4*	*18 9*	*0 58*	*°9 91*	*565*	*<2 65*	*3 14*	*°697*	*7 11*	*14 4*	*6 44*	*1 17*	*0 17*	*0 59*	*0 40*	*0 18*	*1 83*	*0 45*	*0 05*	*0 13*	*°31 9*	*0 62*	*558*	*8 68*
Cpx12 core	*<3 15*	*<2 90*	*50 9*	*21 5*	*23 8*	*1 59*	*<5 71*	*389*	*<4 06*	*5 91*	*303*	*12 7*	*46 9*	*52 6*	*16 6*	*5 22*	*8 84*	*13 5*	*5 10*	*6 26*	*0 83*	*1 96*	*2 25*	*56 6*	*2 55*	*683*	*14 4*
Cpx13 core	*2 81*	*<1 41*	*44 3*	*21 5*	*19 8*	*1 33*	*24 3*	*559*	*2 30*	*33 9*	*336*	*14 9*	*56 0*	*37 4*	*10 5*	*4 07*	*7 72*	*5 48*	*4 45*	*2 35*	*0 41*	*1 17*	*1 16*	*43 5*	*2 47*	*529*	*11 5*
Cpx14 core	*2 48*	*<1 54*	*36 4*	*21 5*	*20 2*	*1 59*	*38 6*	*434*	*1 94*	*29 4*	*388*	*9 90*	*55 4*	*40 4*	*12 1*	*4 40*	*8 44*	*6 21*	*3 82*	*2 59*	*0 34*	*2 69*	*0 56*	*48 6*	*2 48*	*405*	*6 14*
Cpx15 core	*4 83*	*2 65*	*28 0*	*21 5*	*19 4*	*0 90*	*156*	*679*	*22 4*	*20 7*	*120*	*47 2*	*85 9*	*32 1*	*8 03*	*1 58*	*5 53*	*3 83*	*1 72*	*2 93*	*0 38*	*0 62*	*<0 39*	*4 17*	*0 18*	*1116*	*45 7*
Cpx16 core	*5 21*	*2 17*	*39 3*	*20 4*	*19 1*	*0 93*	*15 4*	*328*	*2 42*	*14 0*	*90 5*	*13 5*	*32 5*	*20 0*	*6 37*	*2 01*	*3 24*	*2 47*	*0 85*	*1 85*	*0 58*	*<0 47*	*0 39*	*3 93*	*0 50*	*969*	*23 7*
Cpx17 core	8 09	1 11	44 6	20 4	21 2	0 63	0 87	538	<0 57	5 57	188	8 69	19 4	11 7	2 78	0 50	0 74	0 85	<0 25	1 04	0 17	<20 5	<0 13	1 46	*0 61	509	8 68
Cpx18 core	8 53	1 85	40 0	20 4	20 3	0 66	0 26	318	*1 3	6 41	102	6 77	16 5	12 1	2 77	0 77	2 09	1 32	0 80	1 29	0 29	0 01	0 02	0 79	0 08	388	9 50
Cpx19 core	8 95	0 59	50 2	20 4	20 8	0 39	0 20	1109	<0 03	3 10	193	8 73	21 8	10 7	1 54	0 48	0 83	0 48	0 35	0 98	0 24	<0 17	0 02	0 37	0 01	389	9 62
Cpx20 core	6 52	1 17	44 6	20 4	19 7	0 57	*21 7	545	0 73	4 24	332	7 67	16 6	9 17	1 50	0 47	0 92	0 64	0 47	1 50	0 33	0 08	0 01	0 93	0 05	486	9 42

Sample	MgO	Al2O3	SiO2	CaO	CaO	TiO2	Ba	Sr	Rb	Y	V	La	Ce	Nd	Sm	Eu	Gd	Dy	Er	Yb	Lu	U	Th	Nb	Ta	Zr	Hf
Cpx21 core	7 97	1 02	41 1	20 4	20 1	0 79	5 52	416	0 18	*14 8	129	11 5	28 5	19 6	*4 68	*1 38	*3 5	*2 74	1 50	2 57	0 54	0 20	*0 53	*17 5	*0 90	722	16 7
Cpx22 core	6 42	1 10	38 8	20 4	19 3	0 90	6 86	470	0 56	*14 0	283	8 66	28 9	18 7	3 93	*1 56	2 88	*2 76	1 17	1 71	0 34	*0 6	*0 35	*18 4	*0 74	444	8 57
Cpx23 core	7 66	2 55	47 5	20 4	21 4	0 63	*541	1069	*13 1	5 82	299	*32 7	*46 5	17 4	<1 06	0 67	1 08	1 38	1 53	1 75	0 31	0 32	<0 38	*5 37	<0 21	346	7 34
Cpx24 core	10 4	2 53	49 6	20 4	<25 0	1 06	b d	<620	<22 2	*18 3	164	10 4	24 2	18 2	3 78	0 74	*3 58	1 36	1 20	*3 64	0 63	<0 73	<0 24	<2 39	0 11	*1242	*32 7
Cpx25 core	7 44	0 60	48 8	20 4	20 0	0 38	0 50	985	<0 44	3 40	191	7 16	18 8	9 83	1 60	0 43	0 82	0 60	0 51	1 21	0 29	b d	<0 03	0 35	0 02	485	13 1
Cpx26 core	6 22	0 88	52 0	20 4	20 1	0 45	3 24	661	0 30	4 96	312	7 12	18 5	9 76	1 80	0 49	1 03	0 82	0 65	1 92	0 51	b d	b d	0 55	0 03	592	15 0
Cpx27 core	7 45	1 42	48 3	20 4	20 3	0 57	0 67	466	0 28	4 33	258	7 25	19 1	11 0	1 83	0 47	1 09	0 69	0 57	1.26	0 30	<0 02	0 03	1 25	0 08	344	6 87
Cpx28 core	1 22	1 36	45 1	21 5	23 3	0 49	<1 28	391	<1 23	7 35	155	7 23	20 1	12 7	3 13	0 90	1 67	1 10	1 08	1 54	0 46	<0 19	0 04	0 93	<0 10	431	9 27
Cpx29 core	1 24	0 99	39 1	21 5	21 7	0 46	<1 00	585	<1 05	4 89	211	7 13	19 4	10 4	1 96	0 62	1 06	0 67	0 41	1 23	0 17	<0 06	<0 18	0 36	0 06	343	6 89
Cpx30 core	1 18	1 31	45 1	21 5	22 5	0 53	4 88	603	<1 11	4 70	170	7 08	21 8	10 2	1 83	0 65	1 30	1 33	0 42	2 10	0 31	0 01	<0 02	0 45	<0 83	338	7 72
Cpx31 core	0 48	<0 90	41 1	21 5	22 1	0 66	<1 45	668	<1 45	4 80	323	7 42	17 8	8 32	1 54	0 56	0 72	0 47	0 53	1.50	0 35	<0 26	<0 03	0 55	0 04	496	10.7
Cpx32 core	0 46	1 09	51 1	21 5	22 1	0 87	1 42	591	<1 37	5 65	521	8 00	21 3	8 93	1 90	0 55	1 22	0 75	0 82	1 69	0 47	<0 31	<0 10	0 81	0 05	551	11 6
Average last 16	5 64	1 30	45 3	20 7	21 0	0 63	2 44	628	0 41	5 02	239	8 06	20 8	12 4	2 28	0 59	1 25	0 89	0 80	1 55	0 36	0 12	0 02	0 73	0 05	458	10 1
STDS	3 45	0 59	4 33	0 53	1 15	0 19	2 49	242	0 23	1 16	104	1 36	3 79	3 80	0 84	0 14	0 60	0 34	0 40	0 42	0 13	0 13	0 01	0 36	0 03	109	2 91
RSD	61%	45%	10%	3%	5%	31%	102%	39%	55%	23%	43%	17%	18%	31%	37%	23%	48%	38%	50%	27%	37%	108%	47%	49%	57%	24%	29%
Clinopyroxene, mph sph																											
Cpx1 core	*<4 97*	*<4 37*	*61 7*	*20 7*	*23 8*	*0 47*	*212*	*1069*	*13 6*	*9 18*	*350*	*69 5*	*123*	*20 7*	*5 13*	*0 63*	*2 01*	*0 74*	*<1 83*	*<4.19*	*0 29*	*1 83*	*4 42*	*35 3*	*<0 70*	*263*	*5.13*
Cpx2 core	*2 37*	*2 24*	*42 5*	*20 7*	*20 3*	*0 63*	*7 03*	*711*	*<2 74*	*3 37*	*580*	*8 54*	*18 3*	*5 57*	*0 50*	*0 17*	*0 61*	*1 01*	*0 17*	*0 70*	*0 32*	*b d.*	*0 16*	*4 37*	*<0 43*	*634*	*15 3*
Cpx3 core	*<35 4*	*<18 7*	*<276*	*<56 0*	*25 2*	*1 06*	*107*	*<609*	*<34 2*	*<6 73*	*477*	*19 0*	*28 3*	*17 7*	*<4 39*	*2 01*	*7 00*	*<4 34*	*<9 73*	*b d.*	*1 95*	*<6 80*	*1.74*	*9 86*	*b d*	*564*	*34 2*
Cpx4 core	<3 11	<3 72	<75 3	20 7	20 2	0 39	25 6	473	<4 51	4 66	195	10 0	21 0	10 9	<0 31	0 62	0 91	1 29	1.22	1.18	0 31	0 11	*0 05	6 95	0 09	217	6 52
Cpx5 core	9 76	2 08	<30 4	20 7	20 4	0 78	7 46	334	<2 77	9 90	*59 0	9 10	22 6	20 8	3 03	*2 12	3 61	*2 23	0 61	1 06	0 49	<0 61	b d.	1 56	0 24	554	16 1
Cpx6 core	3 13	1 02	42 3	20 7	19 8	0 45	*276	812	5 00	3 63	*640	16 6	37 8	9 47	1.16	0 29	0 98	0 52	0.74	1 28	0 29	0 41	0.67	5 96	0 08	384	7.12
Cpx7 core	4 34	<1 12	53 1	20 7	20 8	0 55	9 85	561	<1 79	4 46	168	10 7	43 2	12 7	1 96	0 66	1.08	1 01	<0 56	1 59	0 14	0.15	0 49	1 31	0 06	332	7.17
Cpx8 core	4 11	1 59	47 0	20 7	20 6	0 54	*0 52	398	<1 38	5 80	177	5 46	15 1	8 77	2 33	0 62	3 07	0 88	0 70	1 54	0 37	b d	<0 12	0 56	<0 05	318	7 96
Cpx9 core	3 07	1.75	45 9	20 7	18 9	0 40	*74 6	477	5 84	6 51	*434	17 4	33 8	10 7	2 61	0 46	1.36	1 30	*0 23	1.13	0 35	0 38	*1.26	*15 6	*0 43	411	9.76
Cpx10 core	<4 66	<3 97	50 4	20 7	21 9	0 29	4 88	824	<5 40	4 01	174	6 29	12 9	10 4	<1 53	0 40	<0 99	0 56	<1.49	2 05	<0 60	0 27	0 46	*10 4	<0 26	288	6.29
Cpx11 core	2 79	<1.63	56 2	20 7	18 6	0 44	39 8	635	<1 81	3 96	266	8 20	18 5	6 54	1 81	<0 31	0 69	<0 68	<0 85	1.43	<0.22	0 11	<0 35	2 57	0.13	265	4.54
Average last 8	4 53	1 61	49 1	20 7	20 1	0 48	17 5	567	5 42	5 37	196	10 5	25 6	11.3	2 15	*0 54*	1 67	0 93	0 82	1 41	0 33	0 24	0 55	3 15	0 12	344	8 18
STDS	2 63	0 44	5 10	0 00	1 07	0 15	14 9	182	*0 59*	2 08	40 3	4 39	11 2	4 23	0 65	0 20	1 17	0 34	0 27	0 32	0 11	0 14	0 11	2 66	0 07	104	3 53
RSD	58%	28%	10%	0%	5%	31%	85%	32%	11%	39%	21%	42%	44%	38%	30%	37%	70%	37%	33%	23%	35%	57%	20%	84%	60%	30%	43%
Garnet, Ph																											
Gt1 rim	*0 63*	*0 99*	*24 2*	*31 5*	*28 6*	*9 82*	*25 0*	*96 6*	*<0 87*	*587*	*676*	*40 4*	*215*	*280*	*109*	*43 8*	*125*	*134*	*65 6*	*43 9*	*5 53*	*7 54*	*12 8*	*571*	*35 1*	*4457*	*80 3*
Gt2 rim	*0 43*	*0 68*	*23 5*	*31 5*	*31 0*	*9 30*	*9 12*	*99 0*	*1 09*	*499*	*922*	*43 0*	*242*	*304*	*107*	*42 8*	*112*	*112*	*54 5*	*35 7*	*4 83*	*8 07*	*11 5*	*448*	*27 3*	*3885*	*67 3*
Gt3 rim	*<0 43*	*0 67*	*26 6*	*31 5*	*27 9*	*9 30*	*8 26*	*90 0*	*0 80*	*441*	*938*	*43 5*	*245*	*310*	*108*	*40 2*	*106*	*95 7*	*45 5*	*33 6*	*4 28*	*8 91*	*10 5*	*409*	*23 4*	*3768*	*65 0*
Gt4 rim	*<0 68*	*0 88*	*35 9*	*31 5*	*33 8*	*10 2*	*22 2*	*143*	*2 11*	*426*	*1152*	*55 3*	*298*	*356*	*123*	*44 7*	*113*	*108*	*50 9*	*35 8*	*4 12*	*10 2*	*11 1*	*382*	*23 5*	*3622*	*74 7*
Gt5 rim	*<3 08*	*<2 10*	*45 4*	*31 7*	*33 9*	*11 7*	*<3 11*	*<80 2*	*<3 85*	*675*	*987*	*41 0*	*231*	*326*	*123*	*45 3*	*136*	*141*	*70 2*	*48 6*	*5 19*	*6 51*	*11 7*	*358*	*22 0*	*4796*	*85 5*
Gt6 rim	*<2 36*	*<2 13*	*<26 7*	*31 7*	*31 0*	*10 9*	*<2 06*	*<59 8*	*<2 89*	*611*	*914*	*42 6*	*251*	*361*	*135*	*50 9*	*136*	*138*	*67 1*	*47 6*	*6 11*	*8 77*	*14 3*	*383*	*26 4*	*4618*	*84 0*
Gt7 rim	*<3 05*	*<3 19*	*<39 0*	*31 7*	*30 9*	*9 42*	*11 9*	*<100*	*<3 91*	*537*	*936*	*31 3*	*181*	*237*	*96 2*	*36 2*	*107*	*126*	*46 9*	*39 6*	*4 52*	*6 08*	*9 80*	*250*	*16 9*	*3548*	*72 5*
Gt8 rim	*<3 64*	*<3 02*	*<38 1*	*31 7*	*32 7*	*11 2*	*21 4*	*<91 6*	*<3 76*	*500*	*1277*	*35 5*	*203*	*269*	*109*	*39 9*	*105*	*114*	*50 5*	*38 1*	*4 73*	*8 25*	*8 63*	*468*	*25 8*	*3137*	*56 5*
Gt9 core	*0 49*	*0 89*	*33 7*	*31 7*	*35 4*	*11 5*	*<5 49*	*<539*	*<16 6*	*385*	*1147*	*30 6*	*187*	*305*	*86 0*	*32 4*	*71 2*	*73 5*	*41 7*	*23 5*	*4 77*	*6 53*	*6 68*	*322*	*19 6*	*3224*	*59 4*
Gt10 core	1 93	1 01	37.6	31 7	30 0	9 52	*16 4	130	1 09	509	955	39 8	227	331	114	41 1	121	104	48 7	39 0	4 75	6 86	10 6	305	19 3	4634	76 1
Gt11 core	0 99	1 00	32.3	31 7	31 8	10 2	*18 5	104	*2 47	486	820	48 5	268	369	126	45 5	122	112	48 9	38 5	4 44	8 80	17.0	490	34 5	4485	76 1
Gt12 core	4 01	1 02	35 4	31 7	29 6	9 44	3 99	*204	0 39	513	699	38 4	210	299	107	42 2	116	109	51 3	35 2	4 36	7 15	14.7	469	29 9	4089	65 9
Gt13 core	0 57	0 93	25 0	31 7	30 8	12 0	1.76	68 6	*0 08	492	896	41 4	216	322	112	40 0	111	102	45 4	34 0	4 00	6 98	12.0	670	35 0	3748	55.0
Gt14 core	0 54	1 12	28 2	31 7	31 2	10 2	6 84	85 6	<0 66	624	707	52 8	290	421	153	56 9	158	153	72 9	52 5	6 51	9 55	*22.7	468	35 8	4973	97.5
Gt15 core	1 40	1.58	28 2	31 7	30 8	11 6	11 2	94 9	1 21	701	792	33 6	172	260	108	44 1	136	151	73 0	56 2	6 21	6 55	9 62	358	19 0	4427	76 0
Gt16 core	0 44	1 11	21 1	31 7	*24 4	10 6	6 15	<335	<8 68	542	742	38 2	203	266	119	44 4	130	148	70 7	48 2	5 50	5 33	9 06	344	19 0	3197	70 8
Gt17 core	0 88	1.09	27 3	31 5	28 6	9 76	3 45	126	<0 70	563	799	46 3	236	300	114	45.7	131	133	64 7	47 3	5 55	9.91	12 3	474	32.4	4103	81.3
Gt18 core	<0 39	0 99	30 4	31 5	28 5	9 95	1 24	84 2	<0 58	577	816	42 1	252	312	123	46 4	130	144	69 8	46 2	5 86	10 6	12 3	466	32 1	4148	76 2
Gt19 core	0 51	0 80	27 9	31 5	30 8	9 23	<1 06	102	<0 73	430	984	43 8	254	308	113	39 7	107	100	48 4	34 0	3 93	8 13	11 7	407	24 7	3600	67 8
Gt20 core	<2 01	<1 53	32 1	31 7	31 9	11 1	*47 7	92 4	<1 99	572	790	59 5	320	416	150	53 8	145	135	56 4	39 4	5 58	10 7	20 2	450	33 4	5305	96.2
Gt21 core	<1 75	<1 23	29 2	31 7	29 0	10 3	4 45	63 4	<1 53	495	780	47 6	267	358	131	46 8	128	121	54 6	38 2	4 07	8 81	17.7	487	33 2	4049	73 9
Gt22 core	<1 91	<2 19	37 4	31.7	32 0	11 3	3 07	66 1	<2 06	508	1154	42 2	244	321	122	43 2	118	119	52 3	34 3	3 89	10 1	12 2	573	33 9	3464	66.4
Gt23 core	<1 42	<1 45	26 3	31 7	31 2	11 3	5 11	49 7	<1 46	504	885	48 1	290	371	134	49 7	128	122	56 0	39.7	5 50	12 0	16.9	634	42 4	3743	70.6

Sample	MgO	Al2O3	SiO2	CaO	CaO	TiO2	Ba	Sr	Rb	Y	V	La	Ce	Nd	Sm	Eu	Gd	Dy	Er	Yb	Lu	U	Th	Nb	Ta	Zr	Hf
Gt24 core	<1 50	<1 36	33 5	31 7	30 1	11 7	<2 23	63 6	<1 91	493	896	46 9	289	359	133	45 4	128	118	53 1	33 3	4 10	9 91	17 4	661	41 5	3545	63 4
Average last 15	1 25	1 07	30 0	31 6	30 5	10 6	4 73	86 9	0 89	534	848	44 6	249	334	124	45 6	127	125	57 9	41 1	4 95	8 75	13 8	484	31 1	4101	74.2
STDS	1 14	0 20	4 72	0 07	1 17	0 90	2 88	24 5	0 44	65 9	119	6 44	39 7	47 8	14 1	4 79	12 7	18 1	9 74	7 27	0 90	1 86	3 43	111	7 46	585	11 3
RSD	91%	19%	16%	0%	4%	8%	61%	28%	49%	12%	14%	14%	16%	14%	11%	10%	10%	15%	17%	18%	18%	21%	25%	23%	24%	14%	15%
Gt included in cpx sph	1 95	1 30	30 9	31 7	31 3	8 56	0 95	156	b d	517	693	35 8	198	297	109	40 5	121	116	58 2	40 6	5 32	8 14	12 9	325	25 4	4159	77 9
Isolated wollastonite																											
Wo1 core	0 50	0 18	46 9	46 9	47 4	0 19	*53 5	952	2 88	65 7	24 2	47 0	96 2	54 8	11 9	3 92	10 5	10 2	5 16	5 75	0 89	*0 88	*0 82	10 5	0 32	60 5	0 98
Wo2 core	1 01	0 12	52 2	46 9	46 0	0 19	13 1	917	1 00	76 5	30 8	25 4	68 4	39 2	10 4	4 03	10 5	12 2	6 93	7 01	1 02	0 18	0 26	5 25	0 19	52 1	0 79
Wo3 core	0 18	<0 08	58 2	46 9	46 7	0 03	5 10	868	<7 18	38 4	<7 32	26 4	72 6	43 2	10 8	3 39	7 01	6 85	3 11	3 24	0 41	b d	0 02	<1 28	b d	<6 95	b d
Wo4 core	<0 55	<2 36	<47 4	46 9	46 0	<0 08	*801	844	4 38	71 9	<21 7	34 9	73 6	47 4	9 10	3 86	9 59	9 64	6 24	6 52	1 31	0 84	<0 66	9 87	0 23	23 0	<0 87
Average	0 56	0 15	52 4	46 9	46 5	0 14	9 11	895	2 75	63 1	27 5	33 4	77 7	46 2	10 6	3 80	9 42	9 71	5 36	5 63	0 91	0 51	0 14	8 55	0 25	45 2	0 89
STDS	0 42	0 04	5 65	0 00	0 67	0 09	5 67	46 6	1 69	17 1	4 68	10 0	12 5	6 66	1 17	0 28	1 67	2 19	1 67	1 68	0 38	0 47	0 17	2 87	0 07	19 7	0 13
RSD	74%	28%	11%	0%	1%	68%	62%	5%	62%	27%	17%	30%	16%	14%	11%	7%	18%	23%	31%	30%	41%	92%	121%	34%	27%	43%	15%
Wollastonite, Ph sph																											
Wo1 core	0 19	<0 05	55 7	47 1	46 5	<0 03	2 58	1209	<8 34	44 8	<5 56	23 8	61 0	37 3	8 93	2 55	8 13	6 58	4 80	4 01	0 75	b d	<0 07	<2 35	b d	<2 70	b d
Wo2 core	0 36	0 08	56 7	47 1	46 3	0 05	13 1	770	<4 75	76 8	<7 64	28 6	78 5	49 0	10 9	4 50	11 8	11 6	7 05	7 75	1 18	0 07	- 0 09	*2 39	0 02	8 89	0 25
Wo3 core	<1 72	<0 92	42 7	47 1	48 5	0 05	*223	1121	2 18	65 2	7 83	*51 3	101	48 0	9 97	3 83	11 8	11 6	5 88	6 55	0 79	0 10	<0 29	0 49	<0 06	*12 8	<0 08
Wo4 core	<1 25	<0 64	52 5	47 1	49 8	0 04	5 06	882	<0 97	61 1	<4 46	22 7	65 5	35 6	10 9	3 13	9 31	9 76	5 75	5 09	0 77	<0 11	b d	0 18	<0 05	1 49	<0 29
Wo5 core	<1 04	<0 48	50 8	47 1	46 3	0 04	10 7	794	<0 82	64 4	5 99	21 7	64 0	36 5	8 98	3 77	9 27	9 42	6 18	6 18	0 86	0 01	<0 16	0 31	0 01	4 20	<0 28
Average	0 28	0 06	51 7	47 1	47.5	0 05	7 86	955	2 16	62 5	6 91	24 2	74 0	41 3	9 93	3 56	10 1	9 79	5 93	5 92	0 87	0 06	b d	0 33	0 02	4 86	0 25
STDS	n d	n d	5 57	0 00	1 59	0 01	4 87	198	n d	11 5	1 30	3 09	16 5	6 62	0 97	0 74	1 65	2 06	0 81	1 43	0 18	0 05	n d	0 16	0 01	3 74	n.d.
RSD	n d	n d	11%	0%	3%	13%	62%	21%	n d	18%	19%	13%	22%	16%	10%	21%	16%	21%	14%	24%	20%	76%	n d	48%	47%	77%	n d
Wollastonite, mph sph																											
Wo1 core	*<7 11*	*<3 37*	*70 9*	*47 2*	*33 4*	*0 94*	*1485*	*4258*	*106*	*9 90*	*891*	*193*	*256*	*72 6*	*6 83*	*0 45*	*2 54*	*b d*	*3 38*	*3 51*	*0 90*	*0 70*	*2 40*	*27 2*	*0 76*	*873*	*14 8*
Wo2 core	*<3 98*	*6 46*	*51 7*	*47 2*	*45 4*	*0 70*	*1517*	*5529*	*91 1*	*122*	*283*	*1405*	*1753*	*534*	*53 4*	*13 3*	*26 9*	*19 7*	*6 13*	*12 0*	*0 62*	*24 0*	*101*	*658*	*2 65*	*1168*	*19 9*
Wo3 core	<1 40	<1.23	55 9	47 2	46 7	0 10	10 9	889	1 87	78 7	26 3	29 4	81 5	43 8	11 5	4 07	9 45	14 0	6 85	7 04	1 20	0 04	0 09	1 99	0 02	24 3	0 69
Wo4 core	<7 02	<5 98	<89 1	47 2	40 5	<0 12	<7 14	917	<11 0	68 6	<27 2	25 5	74 3	36 7	13 7	3 68	6 62	8 71	*11 8	4 93	<0 81	<1 07	<1 03	3 12	<0 97	10 4	0 29
Wo5 core	<8 23	<4 39	<65 3	47 2	47 5	0 13	*169	953	7 58	67 5	40 5	*88 5	*148	45 8	10 8	3 50	10 9	9 49	*10 5	<4 91	0 73	*0 85	<2 63	*10 9	b d	55 2	*1 46
Average last 3	b d	b d	55 9	47 2	44 9	0 12	10 9	920	4 73	71 6	33 4	27 4	77 9	42 1	12 0	3 75	9 00	10 7	6 85	5 99	0 97	0 04	0 09	2 56	0 02	29 9	0 49
STDS	n d	n d	n d	0 00	3 83	0 02	n d	32 3	4 04	8 20	10 0	2 70	5 12	4 81	1 48	0 29	2 19	2 87	n d	1 49	0 33	n d	n d	0 80	n d	22 9	0 28
RSD	n d	n d	n d	0%	9%	18%	n d	4%	85%	9%	30%	10%	7%	11%	12%	8%	24%	27%	n d	25%	34%	n d	n d	31%	n d	77%	58%
Apatite																											
Ap1 core	<2 14	<2 39	<62 7	54 4	39 8	<0 07	343	6131	7 54	183	67 2	1395	2357	983	138	47 9	84 7	45 3	15 8	7 16	0 97	6 58	50 4	1 9	0 07	7 16	b d
Ap2 core	<2 31	<2 68	<52 4	54 4	60 7	<0 08	134	6956	4 98	292	141	1747	3191	1239	199	59 6	134	70 8	21 4	10 4	1 06	12 0	75 7	2 11	<0 13	8 78	<1 15
Ap3 core	<2 20	<2 05	<39 3	61 7	54 4	<0 07	209	5863	3 31	247	86 5	1552	2816	1294	166	53 3	123	61 4	17 3	8 16	0 67	5 76	67.2	1 47	<0 22	10 5	<0 17
Ap4 core	<0 13	<0 05	<2 32	54 4	55 6	<0 03	73 5	9452	<6 33	113	91 8	2481	4152	1383	145	33 1	70 6	26 9	7 51	3 16	0 61	5 55	91 4	<1 35	0 02	11 6	b d
Average	b d	b d	b d	56 2	52 6	b d	190	7100	5 28	209	96 6	1789	3129	1225	162	48 5	103	51.1	15 5	7.23	0.83	7 49	71.2	1 83	0 05	9 51	b.d.
STDS	n d	n d	n d	3 63	8 97	n d	116	1635	2 13	77 7	31 4	471	762	172	27 5	11 3	30 3	19 3	5 85	3 04	0.23	3 07	17 1	0 33	0.03	1 98	n.d
RSD	n d	n d	n d	6%	17%	n d	61%	23%	40%	37%	32%	26%	24%	14%	17%	23%	29%	38%	38%	42%	27%	41%	24%	18%	76%	21%	n.d
Nyerereite																											
NY1 core	<0 08	<0 03	<1.31	24 7	*30 2	<0 02	8291	19543	140	3 08	8 44	268	337	60 4	2 84	0 77	1 81	0 36	0 09	b d	b d	0 21	0 24	<1 04	<0.05	<2 06	*0.33
NY2 core	<0 04	<0 01	<0 48	24 7	25 1	b d	5739	15619	109	1 60	6 91	245	251	48 5	3 04	0 59	1 10	0 30	0 08	<0 08	0 02	0 24	0 33	1 26	b d	0 71	0 11
NY3 core	<0 07	<0 03	<0 97	24 7	25 4	b d	5752	18750	96 9	2 51	8 15	232	234	46 8	4 23	0 77	0 91	0 29	<0 10	0 04	<0.03	0 42	0 54	2 51	<0.05	1 11	0 21
NY4 core	0 07	0 01	<0 33	24 7	22 7	b d	4898	12718	113	2 91	13 6	191	217	46 2	3 60	0 76	1 04	0 40	<0 12	*0 82	0 02	0 97	1 35	7 14	0 03	3 18	0 10
NY5 core	0 10	0 03	<1.12	24 7	25 8	0 01	4167	13373	118	5 04	*30 8	199	224	53 1	3 35	0 77	1 39	*1 00	<0 41	<0 17	0 03	0 82	*1.96	7 23	<0.07	3 72	<0 23
Average	0 09	0 02	b d	24.7	24 8	0 01	5769	15601	115	3 02	9 26	227	253	51 4	3 41	0 73	1 25	0 34	0 09	0 04	0 02	0 53	0 62	4 54	0 03	2 18	0 14
STDS	0 02	0 01	n d	0 00	1.39	n d	1556	2745	15 8	1 26	2 94	32 2	49 1	5 83	0 54	0 08	0 36	0 05	0 01	n d	0 01	0 35	0 51	3 10	n d	1 49	0 08
RSD	25%	71%	n d	0%	6%	n d	27%	18%	14%	42%	32%	14%	19%	11%	16%	11%	28%	15%	8%	n d	25%	65%	82%	68%	n d	68%	43%

Sample	MgO	Al2O3	SiO2	CaO	CaO	TiO2	Ba	Sr	Rb	Y	V	La	Ce	Nd	Sm	Eu	Gd	Dy	Er	Yb	Lu	U	Th	Nb	Ta	Zr	Hf
Gregoryite																											
GRE1 core	0 07	<0 02	<0 55	10 7	11 1	<0 01	2365	6568	51 2	0 49	50 2	63 3	56 8	10 2	0 69	0 10	0 20	0 04	0 03	<0 07	<0 02	0 05	0 11	0 36	<0 01	<0 74	0 01
GRE2 core	0 13	<0 01	<0 47	10 7	10 2	b d	4364	6848	59 7	1 06	44 5	79 4	79 6	13 4	0 98	<0 71	0 49	0 16	<0 05	<0 06	0 01	0 21	0 43	0 84	0 09	1.12	0.12
GRE3 core	0 10	<0 02	<0 56	10 7	11 3	<0 00	2531	6353	65 4	1 46	68 8	85 2	77 7	12 8	0 85	0 21	0 40	0 17	<0 07	0 06	0 01	*0 55	*0 91	*3 67	*1 33	0 95	0 04
GRE4 core	0 08	<0 01	<0 50	10 7	11 1	<0 00	3815	6781	69 6	0 39	63 0	54 9	55 6	9 42	0 53	0 08	0 30	b d	0 07	<0 24	b d	0 05	0 06	0 37	0 13	0 29	0 09
Average	0 10	b d	b d	10 7	10 9	b d	3269	6638	61 5	0 85	56 6	70 7	67 4	11 4	0 76	0 13	0 35	0 12	0 05	0 06	0 01	0 10	0 20	0 52	0 11	0 79	0 07
STDS	0 03	n d	n d	0 00	0 49	n d	976	224	7 97	0 50	11 2	14 0	13 0	1 94	0 20	0 07	0 13	0 07	0 03	n d	0 00	0 09	0 20	0 27	0 03	0 44	0 05
RSD	28%	n d	n d	0%	4%	n d	30%	3%	13%	59%	20%	20%	19%	17%	26%	54%	36%	59%	57%	n d	0%	89%	100%	52%	26%	56%	76%
Groundmass																											
gmass1	1 58	0 69	4 53	17 0	16 8	0 16	15970	10415	120	32 7	372	907	1078	209	20 3	5 23	8 72	5 01	2 16	1 05	0 16	19 8	22 6	161	1 31	86 8	1.43
gmass2	1 37	1 21	4 73	17 0	17 3	0 25	*28044	12581	275	45 8	*456	1448	1562	325	29 3	7 29	13 3	7 23	2 81	1 86	0 25	25 8	34 4	250	1 11	*130	*2.39
gmass3	<1 16	0 97	<5 47	17 0	18 2	0 14	10565	10577	182	35 5	258	909	1133	251	23 2	5 90	11 4	5 78	1 95	1 28	0 20	26 6	28 1	187	0 73	94 9	0 96
gmass4	<1 26	<0 56	<4 75	17 0	14 9	0 09	4389	8516	108	15 8	101	401	485	113	10 0	2 55	4 28	2 28	1 13	0 58	0 06	11 2	12 3	86 8	0 94	43 2	0 40
gmass5	<1 43	<0 82	<5 26	17 0	16 6	0 13	7424	9977	95 3	27 7	136	649	775	199	18 9	4 59	8 75	3 82	1 31	0 79	0 12	20 8	21 1	151	0 78	85.3	1.02
gmass6	<2 08	<0 94	<6 66	17 0	14 4	0 15	7294	9325	154	31 1	161	599	745	189	17 1	4 84	8 78	4 78	1 47	0 88	0 13	21 9	23 5	159	0 72	82.1	1.07
gmass7	<1 32	<0 72	<5 09	17.0	16 8	0 13	9764	9620	175	44 3	161	953	1137	285	26 7	6 40	13 3	6 24	2 45	1 64	0.18	29 6	34 3	194	0 60	98.2	1.15
gmass8	<1 66	<0 79	<6 29	17 0	16 5	0 05	11026	12753	286	24 9	224	699	819	180	15 3	4 32	8 42	3 53	1 37	0 79	0 16	16 1	17 2	95.8	0.18	37.4	0.54
gmass9	<1 12	<0 70	<3 77	17.0	17 1	0 06	4276	10456	156	15 9	49 8	408	508	136	11 2	2 46	4 94	2 37	0 76	0 58	0 06	11 8	11 5	78 1	0.21	36.3	0.44
gmass10	<2 16	<1.36	<8 45	17 0	17 2	0 16	15386	12865	296	29 5	283	853	962	220	20 4	4 94	10 1	4 57	1 60	1.27	0.14	19 8	26.7	166	0.63	83 0	1.03
gmass11	*<1 73*	*<1 11*	*<7.06*	*17.0*	*18 0*	*0 28*	*6680*	*9245*	*388*	*57 4*	*220*	*1227*	*1526*	*371*	*36 5*	*8 69*	*17.1*	*8 48*	*3 18*	*1 90*	*0 24*	**39 3*	*49 6*	**309*	**2 85*	*158*	**2 45*
gmass12	*<5 38*	*<2 59*	*<20.1*	*17.0*	*23 1*	*<0 06*	*8971*	*10961*	*203*	*11 6*	*146*	*453*	*452*	*105*	*10 1*	*2 23*	*3 78*	*2 44*	*0 99*	*0 35*	*0 06*	*20 7*	*4.93*	*46.4*	*0.97*	*44.3*	*0 72*
Average first 10	1 48	0 98	4.63	17 0	16 6	0 13	9566	10708	185	30 3	194	783	920	211	19 2	4 83	9 19	4 56	1.70	1 07	0.15	20 3	23 2	153	0 72	71.9	0 89
STDS	0 15	0 26	0 14	n d	1 15	0 06	4222	1525	74 9	10 1	99 8	308	325	64 0	6 19	1 53	3 02	1.61	0 63	0 44	0 06	6 08	8 04	53 6	0 35	25 3	0 35
RSD	10%	27%	3%	n.d	7%	43%	44%	14%	41%	33%	51%	39%	35%	30%	32%	32%	33%	35%	37%	41%	40%	30%	35%	35%	49%	35%	40%
Groundmass spherolds																											
gmass sph 1	*8 92*	*2 59*	*75 1*	*24 2*	*25 5*	*0 75*	*365*	*993*	*28*	*12 2*	*528*	*46 6*	*77 3*	*23 4*	*4 03*	*0 98*	*3 05*	*1 64*	*0 89*	*1 44*	*0 45*	*2 04*	*4 20*	*64.7*	*0.61*	*667*	*11.7*
gmass sph 2	*<7 29*	*8 94*	*<59.7*	*24 2*	*26 7*	*0 93*	*8623*	*12201*	*355*	*189*	*267*	**1568*	*2621*	*862*	**102*	**25 2*	**59 3*	**21 9*	*12 4*	*7 29*	*<0 97*	*102*	*163*	**1322*	*3 85*	*673*	*8 81*
gmass sph 3	<0 13	1 33	<9 80	24 2	22 3	0 20	9879	15193	159	19 9	187	714	829	189	16 8	3 77	8 07	3 25	1 24	0.70	0.10	9 09	19 8	117	1.01	192	3 24
gmass sph 4	0 20	2.20	<18 7	24 2	27 1	0 56	*15048	17898	472	32 2	313	750	984	237	21 0	5 86	10 7	5 27	2 13	1 22	0.10	19 3	22 8	237	2.48	376	3 73
gmass sph 5	0 21	5 51	25 1	24 2	23 1	0 75	5171	7813	202	65 1	226	950	1361	377	40 8	9 55	19 9	10 9	5 60	3 43	0 37	18 2	87.2	547	3.19	680	9.82
gmass sph 6	<0 13	3 01	20 4	24 2	26 2	0 68	6377	14231	177	54 0	163	972	1331	347	33 5	8 49	17 9	8 42	2 98	2.52	0 38	21.5	54 0	378	3.31	586	8.74
gmass sph 7	<0 48	6 43	24 2	24 2	24 9	0 60	5941	9023	184	62 5	194	745	1103	307	35 6	9 25	18 8	10 7	3 73	3 72	0.45	22 8	56 2	441	3 80	669	7.95
gmass sph 8	0 51	6 31	31.7	24 2	24 5	0 81	1982	6400	142	49 3	161	910	1181	269	28 3	7 36	14 7	7 96	3 36	2 87	0 41	22 3	48 0	368	5 24	941	11.7
gmass sph 9	0 67	2 95	13 1	24 2	23 7	0 46	*13117	14769	179	49 6	305	870	1121	297	31 4	7 66	14 8	7 78	3 19	2 56	0 33	17.4	55 6	356	2 49	433	5 50
gmass sph 10	<0 51	4 98	18 4	24 2	24 1	0 51	1317	4859	357	30 7	143	1090	1215	232	21 4	5 36	9 68	4 92	2 18	1 28	0.23	9.09	20.5	216	2 58	404	5.57
gmass sph 11	<1 61	9 79	16 9	24 2	24 5	0 81	1927	4545	437	71 2	162	1490	2016	494	46 6	13 6	24 1	10 8	4 71	1 95	0 45	20 7	44 3	444	4.76	681	7.66
gmass sph 12	<2 04	5 71	39 2	24 2	23 6	0 75	609	2490	194	19 4	212	589	686	149	13 6	3 86	4 90	3 37	1.40	1 14	0 19	6 19	11 5	159	2 27	607	8.93
gmass sph 13	<1.17	6 29	18 8	24 2	19 1	0 54	403	2747	100	54 1	83 7	503	670	201	23 0	6 55	12 2	7 63	4 80	2 95	0 39	12 7	32 6	280	4 29	648	11.6
gmass sph 14	<1.72	6 50	22 4	24 2	25 3	0 76	490	2732	114	70 7	97 6	916	1209	325	41 2	10 0	23 3	11 5	5 33	3 59	0 40	18 0	56.1	473	5.01	823	8.92
gmass sph 15	<1 30	6 49	18 4	24 2	24 1	0 81	855	3193	376	84 0	127	884	1190	355	41 7	10 9	21 9	11 8	8 65	3 40	0 40	19 2	55 1	518	5 92	670	12 0
gmass sph 16	<1 23	6 81	<29 0	24 2	18 8	0 90	1625	3249	176	69 3	153	550	916	285	34 2	9 57	20 3	11 3	4 19	3 77	0 51	20 6	48 0	450	5 12	762	8 91
gmass sph 17	<0 85	2 79	<12 5	24 2	21 4	0 53	6834	11802	126	54 2	163	781	1093	321	34 9	8 26	17.7	9 82	3 52	2 15	0 28	19 5	56 3	359	3 48	550	8.53
gmass sph 18	<0 98	3 26	<19 5	24 2	23 1	0 37	7939	12900	182	40 8	157	525	763	228	26 2	6 03	13 9	7.35	2 88	1.71	<0 19	16 9	26 0	203	1 89	354	4.94
Average last 16	0 40	5 02	22 6	24 2	23 5	0 63	3666	8365	224	51 7	178	827	1104	288	30 6	7 88	15 8	8 29	3 62	2 44	0 33	17.1	43 4	347	3 55	599	7 98
STDS	0 23	2 22	7 37	0 00	2 25	0 19	3226	5339	117	19 0	62 9	248	326	84 7	9 66	2 63	5 64	2 88	1 53	1 02	0.13	5 09	19 7	131	1 40	205	2.73
RSD	58%	44%	33%	0%	10%	30%	88%	64%	53%	37%	35%	30%	29%	29%	32%	33%	36%	35%	42%	42%	38%	30%	45%	38%	39%	34%	34%
BD4169																											
Nyerereite																											
NY1 core	<0 04	<0 02	<0 85	24 3	25 4	<0 00	5029	16167	123	2 49	6 50	301	319	57 2	3 49	0 80	1 43	0 34	<0 08	<0 11	<0 02	0 14	0 03	<0 14	<0 04	<0 12	0 02
NY2 core	<0 06	<0 03	<1 23	24 3	25 3	b d	5940	18552	118	3 51	8 70	311	377	63 0	5 01	0 84	1 02	0 53	<0 18	<0 19	<0 02	0 51	0 40	1 29	b d	<0 15	0 13
NY3 core	0 10	<0 07	<2 69	24 3	25 7	0 01	4921	17026	181	1 88	*94 6	145	167	30 0	1 70	0 76	<0 63	<0 65	<0 24	b d	<0 08	<0 05	b d	0 62	2 16	1 14	b d
Average	0 10	b d	b d	24 3	25 5	0 01	5297	17248	140	2 63	7 60	253	294	50 1	3 40	0 80	1 23	0 44	b d	b d	b d	0 33	0 22	0 96	2 16	1 14	0 08
STDS	n d	n d	n d	0 00	0 21	n d	559	1208	35 0	0 82	1 56	93 1	97.3	17 6	1 66	0 04	0 29	0 13	n d	n d	n d	0 26	0 26	0 47	n d	n d	0 08

Sample	MgO	Al2O3	SiO2	CaO	CaO	TiO2	Ba	Sr	Rb	Y	V	La	Ce	Nd	Sm	Eu	Gd	Dy	Er	Yb	Lu	U	Th	Nb	Ta	Zr	Hf
RSD	nd	nd	nd	0%	1%	nd	11%	7%	25%	31%	20%	37%	33%	35%	49%	5%	24%	31%	nd	nd	nd	81%	122%	50%	nd	nd	104%
Gregoryite																											
GRE1 core	0 05	<0 01	<0 30	9 10	9 60	<0 00	1816	6058	60 9	0 94	42 1	77 3	84 8	16 5	0 97	0 23	0 39	0 18	0 02	0 03	0 02	0 26	0 16	0 37	0 07	<0.17	0.06
GRE2 core	0 05	<0 01	<0 27	9 10	9 20	b d	1898	6133	56 1	0 67	36 8	70 9	77 1	13 6	0 89	0 18	0 32	0 13	0 04	0 01	0 01	0 05	0 02	<0 04	0 02	<0.04	0 01
GRE3 core	0 06	<0 01	<0 32	9 10	9 50	<0 00	1341	5500	48 3	1 01	29 8	70 0	81 5	15 7	1 14	0 26	0 52	0 13	0 03	<0 11	0 01	0 08	0 35	0.16	<0 02	<0.05	0 04
GRE4 core	0 06	<0 01	<0 40	9 10	9 98	<0 00	2265	6009	113	0 69	50 3	65 5	85 9	13 5	1 06	0 17	0 41	<0 11	0 03	b d	<0 05	0 19	0 07	0 24	0 03	0 06	0 04
Average	0 06	b d	b d	9 10	9 57	b d	1830	5925	69 5	0 83	39 7	70 9	82 3	14 8	1 02	0 21	0 41	0 15	0 03	0 02	0 01	0 15	0 15	0 26	0 04	0 06	0 04
STDS	0 01	n d	n d	0 00	0 32	n d	380	288	29 2	0 17	8 64	4 86	3 95	1 52	0 11	0 04	0 08	0 03	0 01	0 01	0 01	0.10	0 15	0 11	0 03	n d	0 02
RSD	10%	n d	n d	0%	3%	n d	21%	5%	42%	21%	22%	7%	5%	10%	11%	20%	20%	20%	27%	71%	43%	67%	97%	41%	66%	n d.	55%
Groundmass																											
gmass 1	1 08	0 07	<1 05	16 0	18 1	0 07	22284	16605	377	14 8	388	1167	989	168	12 2	2 42	4 93	2 40	0 90	0 88	0 11	*46 5	7 58	*221	0.33	*3.24	0 38
gmass 2	1 83	<0 04	<2 22	16 0	20 8	0 01	36798	20848	453	*24 6	*909	1347	1120	180	13 3	3 51	5 57	2 05	1 09	0 33	0 16	12 0	0 93	6 68	0.65	0 40	0 48
gmass 3	0 67	<0 02	<0 74	16 0	11 1	b d	13956	12280	157	7 56	261	516	489	68 6	5 16	1 14	2 17	0 84	0 48	<0 09	0 05	4 24	0 40	4 43	0 39	0 58	0 27
gmass 4	0 58	<0 02	<0 89	16 0	14 4	b d	17484	13093	321	7 62	286	665	585	76 1	5 37	1 29	2 04	0 88	0 36	0 29	0 07	3 36	0 21	*0 17	0 36	<0.37	0.22
gmass 5	1 21	<0 02	<1 00	16 0	18 0	0 02	24886	15172	521	15 1	426	1235	1176	165	11 1	3 01	4 30	1 57	0 59	<0 23	0 09	10 5	5 62	*34 3	0 53	0 45	<2.92
Average	1 07	0 07	b d	16 0	16 5	0 03	23081	15600	366	11 3	340	986	872	132	9 41	2 27	3 80	1 55	0 68	0 50	0 10	7 51	2 85	5 56	0 45	0 48	0.34
STDS	0 50	n d	n d	0 00	3 76	0 03	8755	3393	139	4 25	79 4	371	315	54 4	3 87	1 04	1 61	0 69	0 30	0 33	0 04	4 3	3 42	1 6	0 13	0 09	0 12
RSD	46%	n d	n d	0%	23%	96%	38%	22%	38%	38%	23%	38%	36%	41%	41%	46%	42%	45%	44%	66%	44%	58%	116%	29%	30%	19%	34%
CML5																											
Nyererente																											
NY1 core	0 08	0.00	<0 22	24 4	26 1	<0 00	5336	17486	146	1 42	9 29	307	442	66 8	3.98	0 88	0 94	0 16	<0.29	<0.26	<0 08	1 50	<0 09	2.32	<0 04	<0.24	<0.25
NY2 core	0 04	0.02	<0 26	24 4	22 0	b d	6456	15264	113	1.73	7 59	296	387	52 9	4 73	0 88	0 99	<0.18	0 20	<0 40	<0.10	*3.64	0 25	*7.56	0.70	<0.57	<0.26
NY3 core	0 11	0 03	<0 57	24 4	25 0	<0 00	7022	17554	121	0 84	12 7	283	375	61 1	3.88	0 49	0 72	0.34	b.d	b d	b d.	1.85	<0.12	5.13	0.48	<0.44	b d
NY4 core	<0.08	<0 03	<1 18	24 4	24 2	<0 01	6438	17178	98 9	1.72	7 71	263	361	60 9	3.10	0 46	<1 07	<0 73	b d	b d	<0 33	0.46	<0.30	0.95	<0.26	<1.59	<1.80
NY5 core	0 05	<0 00	<0 21	24 4	20 2	<0 00	5455	16368	121	<3 90	7 34	255	375	57 6	3 03	0 61	0 58	0 27	<0 13	<0 18	<0 04	0.95	0 19	1.72	<0.04	<0.21	<0.17
Average	0 07	0 02	b d	24 4	23 5	b d	6141	16770	120	1 43	8 93	281	388	59 9	3 74	0 66	0 81	0 26	0 20	b d	b d	1 19	0 22	2 53	0 59	b.d.	b d
STDS	0 03	0 02	n d	0 00	2 37	n d	722	965	17 1	0 42	2 24	21 9	31 5	5 11	0 70	0 21	0 19	0 09	n.d.	n d	n.d.	0.61	0 04	1 82	0 16	n d	n d
RSD	45%	92%	n d	0%	10%	n d	12%	6%	14%	29%	25%	8%	8%	9%	19%	31%	24%	35%	n d	n d	n d.	51%	19%	72%	26%	n.d.	n d
Gregoryite																											
GRE1 core	*0 93*	*0.03*	*0.20*	*8 68*	*8 81*	*b d*	*13099*	*7260*	*341*	*1 63*	*263*	*378*	*304*	*33 3*	*1 78*	*0 23*	*0 45*	*0 15*	*0 05*	*b d*	*<0 02*	*1 73*	*0.09*	*0 53*	*0.67*	*0.21*	*b d*
GRE2 core	0 16	b d	<0 07	8 68	8 93	b d	2388	5691	52 1	0 62	8 99	110	119	18 1	1 10	0 18	0 35	0 14	<0 08	0 03	b d	*3.52	*0 20	*3.75	0.18	<0.10	<0 06
GRE3 core	0 08	b d	0 05	8 68	8 83	b d	1933	5467	55 3	0 51	49 9	83 6	92 9	13 7	0 83	0 12	0 21	0 08	<0 04	0 02	<0 01	1.03	0 11	1.21	0.18	0.05	<0.07
GRE4 core	0 07	b d	<0 09	8 68	8 28	b d	1622	5012	53 5	0 33	48 4	64 9	68 7	8 74	0 60	0 10	0.15	<0 06	<0 07	<0.14	b d	0 64	0.01	0 60	0 10	<0.18	<0 13
GRE5 core	0 08	b d	<0 04	8 68	8 76	b d	2572	5559	88 8	0 40	30 1	82 0	88 8	12 8	0 78	0 13	0 25	0 04	0 04	<0 05	b d	0 26	0.02	0.65	0 05	<0.09	b d.
GRE6 core	0 08	0.01	0 03	8 88	8 62	b d	2914	5488	65 0	0 37	41 4	74 5	86 0	12 0	0 74	0 12	0 22	<0 04	0 05	<0.03	0.01	0 38	0 09	0 39	0 08	<0.05	<0.03
Average last 5	0 09	0.01	0 04	8 68	8 64	b d	2286	5443	62 9	0 45	51 9	83 1	89 5	13 1	0 81	0 13	0 24	0 09	0 05	0 03	0 01	0 58	0 08	0 71	0 12	0 05	b.d.
STDS	0 04	n d	0 01	0 00	0 24	n d	513	256	15 3	0 12	22 6	17 0	20 9	3 38	0 18	0 03	0 07	0 05	0 01	0 01	n d	0 34	0 05	0 35	0 06	n d.	n d
RSD	44%	n d	35%	0%	3%	n d	22%	5%	24%	26%	44%	20%	23%	26%	23%	23%	31%	58%	16%	28%	n d	59%	67%	49%	50%	n.d.	n d
Groundmass																											
gmass 1	0 66	0 01	0 23	12 7	12 6	b d	8198	9793	474	2 01	191	324	370	44 2	2 93	0 68	0 67	0 31	0 08	0 06	b d.	6 37	0 59	8 13	0 39	0 06	0 05
gmass 2	0 38	b d	0 12	12 7	12 9	b d	8274	10632	318	1 58	120	361	368	50 6	3 09	0 61	0 81	0 25	0 04	0 08	0 01	4 38	0 62	9 89	0 24	0 09	*0.02
gmass 3	0 87	0 03	0 30	12 7	11 0	0 01	9910	9804	365	2 23	214	396	439	53 2	3 52	0 78	1 11	0 39	0 16	0 07	0 01	*10 1	0 79	*14 2	*0 87	0 33	0 08
gmass 4	0 78	0 02	0 61	12 7	12 5	0 01	13308	12238	356	3 52	203	646	662	97 5	5 64	1 03	1 70	0 39	0 07	<0 12	0 03	*15 0	*2 37	*33 8	0 21	*0 86	<0 08
gmass 5	0 35	b.d	0 05	12 7	12 3	0 01	8788	10536	288	3 85	173	655	683	98 8	5 52	1 08	1 79	0 45	0 21	<0 04	0 01	3.70	*1 62	6 88	0 12	0 07	<0.09
gmass 6	0 35	b d	<0 04	12 7	13 6	b d	8408	11248	297	1 76	124	378	402	60 6	3 13	0 59	0 95	0 24	<0 06	<0 08	<0 01	1 90	0 69	2 63	0 10	<0 09	<0.10
gmass 7	0 59	0 01	0 13	12 7	12 5	b d	*21068	13282	270	*6 55	218	820	738	97 9	5 83	1 21	*2 26	0 73	0 26	0 16	0 02	7 09	0.75	8 88	0 13	0 28	0.10
Average	0 57	0 02	0 24	12 7	12 5	0 01	9481	11047	338	2 49	178	512	523	71 6	4 27	0 85	1 17	0 39	0 13	0 09	0 02	4 69	0 69	7 28	0 20	0 17	0 08
STDS	0 21	0 01	0 20	0 00	0 80	0 00	1978	1325	69 2	0 96	40 8	193	163	24 7	1 39	0 25	0 47	0 17	0 09	0 05	0 01	2 09	0 08	2 82	0 11	0 13	0 03
RSD	38%	55%	84%	0%	6%	0%	21%	12%	20%	38%	23%	38%	31%	34%	32%	29%	40%	42%	68%	49%	56%	45%	12%	39%	55%	77%	33%

Sample	MgO	Al2O3	SiO2	CaO	CaO	TiO2	Ba	Sr	Rb	Y	V	La	Ce	Nd	Sm	Eu	Gd	Dy	Er	Yb	Lu	U	Th	Nb	Ta	Zr	Hf
CML9																											
Nyerereite																											
NY1 core	0 19	0 01	0 16	24 4	20 0	b d	5940	12573	189	0 83	9 50	192	446	50 7	3 16	0 53	0 71	0 19	<0 07	0 05	<0 04	*3 13	0 11	1 96	0 16	0 19	<0 08
NY2 core	0 12	0 02	0 65	24 4	22 3	b d	5622	15790	132	1 15	11 2	292	383	50 9	2 68	0 50	0 81	0 19	<0 09	<0 09	<0 02	0 19	<0 06	0 23	0 05	0 18	<0 12
NY3 core	*0 54	0 03	0 39	24 4	17 7	0 01	5325	12989	199	0 52	6 80	215	397	45 4	1 99	0 59	1 21	0 16	b d	<0 26	<0 03	0 53	0 13	2 34	*0 36	0 52	<0 17
NY4 core	0 07	0 01	<0 14	24 4	25 4	b d	5948	13857	213	0 82	7 82	251	334	48 0	2 67	0 57	0 86	b d	0 07	<0 18	<0 03	0 43	<0 07	0 64	0 11	<0 29	<0 36
NY5 core	0 05	0 03	<0 11	24 4	23 2	<0 00	5937	17207	143	1 29	7 68	306	383	62 9	2 57	0 71	1 34	<0 12	<0 10	<0 19	0 01	0 29	0 13	0 70	0 04	<0 35	0 11
NY6 core	0 07	b d	<0 09	24 4	21 3	b d	5936	15823	143	1 45	8 57	284	353	59 1	2 79	0 62	0 83	0 25	b d	b d	b d	*5 78	0 15	1 85	0 03	<0 18	0 12
Average	0 10	0 02	0 40	24 4	21 8	0 01	5785	14706	170	1 01	8 60	257	382	52 8	2 64	0 59	0 96	0 20	0 07	0 05	0 01	0 36	0 13	1 29	0 08	0 30	0 12
STDS	0 06	0 01	0 25	0 00	2 67	n d	259	1839	34 5	0 35	1 57	45 6	38 6	6 74	0 38	0 07	0 25	0 04	n d	n d	n d	0 15	0 02	0 87	0 08	0 19	0 01
RSD	57%	50%	81%	0%	12%	n d	4%	13%	20%	34%	18%	18%	10%	13%	14%	13%	26%	19%	n d	n d	n d	42%	13%	67%	71%	65%	6%
Gregoryite																											
GRE1 core	*0 18*	*0 05*	*0 26*	*8 68*	*8 26*	*0 01*	*2231*	*5584*	*66 3*	*0 81*	*53 3*	*201*	*261*	*26 2*	*1 69*	*0 32*	*0 48*	*0 05*	*<0 04*	*<0 04*	*b d*	**1 73*	**0 49*	*3 41*	*0 38*	*0 44*	*0 04*
GRE2 core	0 31	0 02	0 37	8 68	8 81	b d	2353	5369	72 3	0 46	49 5	82 4	90 7	10 1	0 50	0 15	0 21	0 09	<0 05	<0 05	<0 01	0 64	0 08	1 45	0 47	0 70	<0 06
GRE3 core	0 21	0 01	0 11	8 68	7 96	b d	1808	5244	89 4	0 75	37 4	95 3	98 2	13 2	0 84	0 14	0 39	0 15	<0 06	0 03	0 02	*2 80	*0 46	4 62	0 23	0 35	<0 06
GRE4 core	0 11	0 00	0 05	8 68	9 08	0 01	1960	6031	77 7	0 28	31 6	60 7	71 9	8 40	0 54	0 10	0 15	0 04	<0 04	<0 08	<0 02	0 09	0 04	0 24	0 18	0 10	<0 07
GRE5 core	0 11	0 01	0 11	8 68	8 79	b d	2255	5958	83 4	0 44	31 4	66 8	84 1	10 4	0 74	0 10	0 20	0 10	<0 05	<0 05	b d	0 32	0 03	0 87	0 06	0 18	b d
GRE6 core	0 14	0 08	0 21	8 68	8 71	b d	1516	5155	51 5	0 29	29 7	55 9	70 9	9 68	0 59	0 12	0 20	<0 06	b d	<0 06	<0 02	0 11	0 05	0 10	0 05	0 09	<0 06
Average last 5	0 18	0 03	0 19	8 68	8 60	0 01	2021	5557	70 1	0 51	38 8	93 6	113	13 0	0 82	0 16	0 27	0 09	b d	0 03	0 02	0 29	0 05	1 78	0 23	0 31	0 04
STDS	0 08	0 02	0 12	0 00	0 41	0 00	320	369	11 0	0 23	10 2	54 4	73 2	6 64	0 45	0 08	0 13	0 04	n d	n d	n d.	0 26	0 02	1 84	0 17	0 24	n d
RSD	43%	97%	64%	0%	5%	0%	16%	7%	16%	45%	26%	58%	65%	51%	55%	54%	48%	51%	n d	n d	n d	88%	43%	103%	76%	76%	n d
Groundmass																											
gmass 1	1 49	0 06	0 47	12 7	11 4	0 01	18908	11941	345	3 57	264	670	632	77 0	3 57	0 84	1 07	0 34	0 13	<0 06	0 02	4 24	0 43	8 55	0 22	1 03	<0 09
gmass 2	0 55	*0 20	0 47	12 7	13 6	0 01	7030	10528	108	2 22	93 2	318	289	49 5	3 86	0 17	1 13	<0 29	<0 32	<0 62	<0 08	2 55	0 30	3 70	0 60	<0 87	b d
gmass 3	0 56	0 04	0 19	12 7	12 1	0 01	8320	10194	163	1 96	160	305	317	37 9	2 57	0 44	0 87	0 16	<0 11	<0 12	0 01	3 50	0 37	6 95	0 79	0 39	<0 06
gmass 4	2 52	0 06	0 38	12 7	10 8	0 01	21871	11902	266	4 99	521	716	795	72 1	4 90	1 45	1 61	0 68	0 29	0 35	0 03	5 04	0 27	4 14	0 38	0 50	0 16
gmass 5	0 60	0 04	0 28	12 7	10 9	0 01	6542	8987	155	1 39	99 0	219	232	30 6	1 44	0 46	0 48	0 17	*0 04	*0 03	0 01	1 95	0 13	2 32	0 44	0 52	0 04
gmass 6	1 52	0 10	0 59	12 7	11 5	0 02	17312	12524	212	4 17	293	734	738	90 7	5 28	1 21	1 79	0 57	0 13	0 18	0 03	5 65	*1 84	14 6	1 68	0 87	0 19
gmass 7	0 98	0 03	0 26	12 7	12 8	0 01	11158	10870	240	2 97	170	415	485	59 9	3 60	0 92	1 23	0 36	0 15	<0 15	<0 01	8 92	0 93	12 3	0 81	0 61	0 09
Average	1 17	0 08	0 38	12 7	11 8	0 01	13020	10964	213	3 04	229	482	498	59 7	3 60	0 78	1 17	0 41	0 15	0 19	0 02	4 55	0 61	7 22	0 70	0 65	0 10
STDS	0 73	0 03	0 14	0 00	1 00	0 00	6256	1228	79 5	1 29	150	218	228	21 7	1 31	0 46	0 44	0 27	0 08	0 12	0 01	2 33	0 28	4 60	0 48	0 25	0 07
RSD	62%	31%	37%	0%	8%	38%	48%	11%	37%	42%	65%	45%	46%	36%	36%	58%	38%	67%	51%	63%	50%	51%	45%	64%	69%	38%	68%

Note: italics indicate whole analyses rejected and asterixes (*) indicate individual elemental analysis rejected

Abbreviations used are b d below detection, n.d : not determined, Ne nepheline, NY nyererite, Ap apatite, Gt garnet, Wo wollastonite, Cpx clinopyroxene, GRE gregoryite, gmass groundmass,

Ph : phenocryst, mph microphenocryst, sph : spheroid, c: core, int interior

Table A4 4 Trace element compositions of residual carbonate liquid from OL5-experiments, calculated by removing the appropriate amount of crystals (see Table 3 9) from the starting composition (OL5, Tab 4 10)

Sample	P	T	Ba	Sr	Rb	Y	V	La	Ce	Nd	Sm	Eu	Gd	Dy	Er	Yb	Lu	U	Th	Nb	Ta	Zr	Hf
CP88	100	900	9307	11017	140	13 9	198	473	570	115	10 1	2 58	4 68	2 37	0 92	0 80	0 113	14 0	13 1	109	0 505	66.5	1 034
CP79	100	800	9404	11131	140	14 1	200	478	576	116	10 2	2 61	4 73	2 39	0 93	0 81	0 114	14 1	13 2	110	0 510	67 2	1 044
CP96	100	750	9403	11131	140	14.1	200	478	576	116	10 2	2 61	4 73	2 39	0 93	0 81	0 114	14 1	13 2	110	0 510	67.2	1 044
CP118	100	625	9404	11125	141	14 0	197	478	576	116	10 2	2 60	4 72	2 38	0 92	0 79	0 111	14 1	13 2	110	0 510	62 6	0 941
CP107	100	600	8603	9838	115	12 3	185	433	504	103	9 13	2 31	4 33	2 01	0 80	0 67	0 091	12 2	10 8	111	0 535	62.3	0 845
CP128	100	575	11592	11238	169	16 1	281	568	644	126	11 6	3 09	5 59	2 62	0 98	1 04	0 132	18 6	17 5	145	0 681	80 0	1 190
CP127	100	550	11824	10214	165	16 8	280	573	652	126	11 2	2 76	4 94	2 79	1 06	1 13	0 159	19 9	18 6	155	0.721	92.4	1 392
CP90	20	900	9437	11170	141	14 1	200	479	578	116	10 2	2 62	4 74	2 40	0 93	0 81	0 115	14 1	13 3	110	0 512	67.5	1.048
CP45	20	850	9540	11213	142	14 1	203	477	564	111	9 73	2 48	4 46	2 26	0 87	0.75	0 106	14 1	12 5	108	0.500	68 1	1 058
CP61	20	800	9608	11211	143	13 8	204	464	514	95	8 00	2 00	3 53	1 76	0 67	0 56	0 077	13 7	10 1	96 9	0.449	68 4	1.062
CP51	20	750	9690	11382	144	11 3	203	489	588	116	9 70	2 40	4 14	1 78	0 60	0 55	0 083	14 5	13 4	111	0.361	51 9	0 772
CP57	20	700	9846	11628	147	10 1	203	499	598	118	9 66	2 36	4 02	1 61	0 47	0 41	0 065	14 7	13 5	109	0 425	50 0	0 711
CP129	20	625	10264	11679	150	8 50	198	515	607	118	9 30	2 23	3 50	1·11	0 28	0 29	0 049	15 5	14 3	117	0 381	18 9	0.164
CP108	20	600	11783	12166	163	13 7	245	591	677	133	11 1	2 75	4 83	2 10	0 82	0 72	0 097	18 5	17 1	143	0 584	51 1	0 624
CP126	20	575	14896	11054	140	16 0	315	709	784	154	12 3	3 25	4 84	2 62	0 83	0 59	0 069	26 5	24 3	202	0 755	70 9	0 801
CP112	20	550	-13556	-9393	-300	-7 92	176	-443	-694	-112	2 42	-4 11	-2 26	-4 10	-0 71	-2 18	-0 757	0 6	-15 0	228	1.060	88 9	1 549

P is in MPa, T in oC

Table A4.5a: Clinopyroxene-carbonate melt partition coefficients from previous studies at mantle conditions.

Study	BW91	GAS92	WBJ92	WPMB9	KLFG95	SPP95
T (C)	1150	1000	1200	1200	1100	1150
P (GPa)	1.5	2.5	5.5	5.5	2	4.6
Ba	0.0005	0.006	0.0006	0.0004	0.07	
Sr	0.043	0.03			0.08	0.26
Rb		0.004				
Y		0.22			0.3	0.27
V					2.93	
La		0.02			0.07	
Ce	0.16		0.03	0.023	0.09	0.22
Nd					0.11	
Sm		0.08			0.13	
Eu					0.22	
Gd	0.5				0.26	
Dy					0.29	
Er					0.4	
Yb	0.3					
Lu						0.33
U			0.0048	0.0034		
Th			0.0093	0.0068		
Nb		0.01	0.0059	0.0046	0.1	0.22
Ta		0.03			0.15	0.22
Zr		0.29			0.48	0.29
Hf					0.16	

Abbreviations used are: BW91: Brenan and Watson (1991); GAS92: Green et al. (1992); WBJ92: Watson et al. (1992); JWPMB95: Jones et al. (1995); KLFG95: Klemme et al. (1995); SPP95: Sweeney et al. (1995); T: temperature; P: pressure.

Table A4.5b: Garnet-carbonate melt partition coefficients from previous studies at mantle conditions.

Study	GAS92	SGS92	SPP95	SPP95
T (C)	1000	1000	1150	1100
P (GPa)	2.5	2.7	4.6	3.4
Ba	0.003			
Sr	0.003	0.0017	0.008	0.062
Rb		<0.004		
Y	1.4	3.06	1.53	1.91
V				
La				
Ce		0.017		0.11
Nd				
Sm				
Eu				
Gd				
Dy				
Er				
Yb				
Lu	11.6	>30	5.2	5.4
U				
Th				
Nb	0.03	0.012	0.014	0.086
Ta		0.095	0.051	0.14
Zr	0.54	3.98	0.83	1.42
Hf				

Abbreviations used are: GAS92: Green et al. (1992); SGS92: Sweeney et al. (1992); SPP95: Sweeney et al. (1995); T: temperature; P: pressure.

APPENDIX A5

Table A5.1: Trace element composition of calculated equivalent liquid (CEL1 and CEL2), of calculated natural rock (CNR1 and CNR2), of liquid in a hypothetical experiment at 20 MPa, 615 C (HEL), and of residual liquid from Rayleigh fractionation of lava OL5 (RFL).

LC	Ba	Sr	Rb	Y	V	La	Ce	Nd	Sm	Eu	Gd	Dy	Er	Yb	Lu	U	Th	Nb	Ta	Zr	Hf
CEL1	5554	10549	110	9.91	75.6	299	343	75.6	6.53	1.59	3.09	1.51	0.58	0.38	0.06	5.22	6.34	42.8	0.31	32.3	0.51
CEL2	5558	10581	110	9.76	74.4	322	422	101	9.15	2.31	4.44	2.16	0.84	0.64	0.10	6.08	10.3	65.3	0.56	31.6	0.45
CNR1	5166	10365	104	13.0	77.4	274	318	73.5	7.12	1.86	3.90	2.33	0.97	0.68	0.10	4.40	5.55	38.6	0.46	69.1	1.25
CNR2	5165	10362	104	13.8	77.3	295	388	96.8	9.66	2.58	5.31	3.08	1.27	0.95	0.14	5.09	8.85	57.1	0.70	73.0	1.29
HEL	10855	11848	156	11.3	332.0	552	597	103.0	7.54	1.78	3.06	1.34	0.53	0.40	0.07	19.20	10.20	130.0	0.48	35.0	0.39
RFL	10137	11138	150	9.61	209	512	593	109	8.23	1.88	3.01	1.02	0.29	0.30	0.04	17.4	14.3	126	0.31	28.8	0.30

See table 5.1 for details of the abbreviations.

Calculation of residual liquid from Rayleigh fractionation of lava OL5

Table A5.2a presents the partition coefficients that were used for the calculation of the composition of the residual liquid from Rayleigh fractionation of lava OL5. Table A5.2b presents the details of the calculation of this composition.

The partition coefficients were calculated as follow: $D_{\text{Nepheline/carbonate liquid}}$ was calculated by averaging partition coefficients from the experiments (extrapolated for Gd and Lu); $D_{\text{Garnet/carbonate liquid}}$ was calculated by averaging partition coefficients from the experiments (extrapolated for Rb); for clinopyroxene, wollastonite, nyerereite and gregoryite, $D_{\text{Crystal/carbonate liquid}}$ were calculated by ratioing concentration of phenocrysts and CEL1 in silicate-bearing OL5; $D_{\text{titanite/carbonate liquid}}$ was calculated on a crystal-liquid pair from experiment CP107 (100 MPa, 600 °C) (extrapolated for Sr, Er and Lu); composition of perovskite in jacupirangite from Oldoinyo Lengai (Dawson et al., 1994) was used for most trace elements, U and Th from perovskite in melilite nepheline basalt are from Onuma et al. (1981). $D_{\text{perovskite/carbonate liquid}}$ were arbitrarily calculated by ratioing these concentrations against OL5 whole rock (extrapolated for Rb, V, Eu, HREE, D_{Ta} is assumed to be equal to D_{Nb}, and D_{Hf} to D_{Zr}); for spinel (Ti-magnetite), no trace element data for Ti-magnetite are available for this study. Partition coeffients have been determined between magnetite and silicate liquid only (Nielsen et al., 1994), which show that partitioning of HFSE and V into the magnetite is a function of D_{Ti} between magnetite and silicate liquid. D values for HFSE between magnetite and silicate melt can be as high as 2, and could be higher between magnetite and carbonate liquid. REE have also been shown to be able to partition into the magnetite (Schock, 1979). However, in Chapter 4 it was showen that spinel did not affect the trace element budget significantly, and therefore, D's have been arbitrarily assumed to be equal to 0.1 for all elements (see Green, 1994; D's between spinel and silicate liquid are ~ 0.1), and because spinel is in small amount, it does not affect trace element composition significantly. Note that in some cases, D's have been calculated and compared to expected, not measured, compositions of the carbonate liquid from the experiments because of quench problems (for details see Chapter 4). Note also that if the natural rock groundmass composition is different than what has been measured because some accessory phases are under-represented, then it can affect partition coefficients which have been calculated between crystals and CEL1.

The equation that has been used is for Rayleigh fractionation: $C_L/C_O = F^{(D-1)}$, where C_L is the weight concentration of a trace element in the liquid, C_O is the weight concentration in the parental liquid, F is the fraction of melt remaining and D is the bulk distribution coefficient of the fractionating assemblage during crystal fractionation (Rollinson, 1993).

Table A5.2a: Partition coefficients between different crystal phases and carbonate liquid, used for the calculation of the composition of the residual liquid from Rayleigh fractionation of silicate-bearing natrocarbonatite lava OL5.

Crystal phase	Ba	Sr	Rb	Y	V	La	Ce	Nd	Sm	Eu	Gd	Dy	Er	Yb	Lu	U	Th	Nb	Ta	Zr	Hf
Nepheline	0.0037	0.021	0.63	0.10	0.015	0.0058	0.0061	0.071	0.19	0.026	0.066	0.11	0.81	0.70	0.70	0.056	0.017	0.023	0.41	0.16	0.34
Clinopyroxene	0.0004	0.060	0.0037	0.51	3.17	0.027	0.061	0.16	0.35	0.37	0.40	0.59	1.37	4.05	6.06	0.024	0.0037	0.017	0.17	14.2	19.9
Melanite garnet	0.0008	0.015	0.0010	45.6	3.29	0.10	0.46	2.71	13.8	22.5	35.0	87.0	127	104	101	0.44	2.07	5.47	46.2	62.7	80.3
Wollastonite	0.0016	0.085	0.025	6.37	0.36	0.11	0.23	0.61	1.62	2.38	3.04	6.45	9.18	14.7	15.4	0.098	0.022	0.20	0.80	1.40	1.75
Nyerereite	1.04	1.48	1.05	0.30	0.12	0.76	0.74	0.68	0.52	0.46	0.40	0.22	0.15	0.10	0.40	0.10	0.097	0.11	0.098	0.068	0.28
Gregoryite	0.59	0.63	0.56	0.086	0.75	0.24	0.20	0.15	0.12	0.082	0.11	0.080	0.086	0.16	0.17	0.019	0.032	0.012	0.36	0.025	0.14
Apatite	0.034	0.67	0.048	21.1	1.28	5.98	9.13	16.2	24.8	30.4	33.3	33.9	26.5	18.8	14.1	1.44	11.2	0.043	0.16	0.29	2.38
Titanite	0.040	0.040	0.22	6.67	1.79	0.57	1.36	3.57	6.07	5.65	8.52	12.0	19.0	26.7	30.0	2.16	3.04	112	991	169	121
Perovskite	0.078	0.26	0.20	17.2	0.10	20.2	57.8	93.5	112	122	131	140	150	160	170	26.1	124	69.4	69.4	2.25	2.25

Table A5.2b Details of the calculation of the composition of the residual liquid from Rayleigh fractionation of silicate-bearing natrocarbonatite lava OL5

		Ba	Sr	Rb	Y	V	La	Ce	Nd	Sm	Eu	Gd	Dy	Er	Yb	Lu	U	Th	Nb	Ta	Zr	Hf
OL5		9213	10905	139	13.8	196	468	564	114	100	2.56	4.63	2.34	0.91	0.79	0.11	13.6	12.9	108	0.50	85.9	1.02
615 C																						
Nepheline	2.00%	0.0037	0.021	0.63	0.10	0.015	0.0058	0.0081	0.071	0.19	0.026	0.066	0.11	0.81	0.70	0.70	0.056	0.017	0.023	0.41	0.16	0.34
Clinopyroxene	3.00%	0.0004	0.059	0.0037	0.51	3.17	0.027	0.061	0.16	0.35	0.37	0.40	0.59	1.37	4.05	6.06	0.024	0.0037	0.017	0.17	14.2	19.9
Melanite garnet	0.70%	0.0008	0.015	0.0010	45.6	3.29	0.10	0.46	2.71	13.8	22.5	35.0	87.0	127	104	101	0.44	2.07	5.47	46.2	62.7	80.3
Wollastonite	0.05%	0.0016	0.085	0.025	6.37	0.36	0.11	0.23	0.61	1.62	2.38	3.04	6.45	9.18	14.7	15.4	0.098	0.022	0.20	0.80	1.40	1.75
Nyerereite	10.00%	1.04	1.48	1.05	0.30	0.12	0.76	0.74	0.68	0.52	0.48	0.40	0.22	0.15	0.10	0.40	0.10	0.097	0.11	0.098	0.068	0.28
Gregoryite	2.50%	0.59	0.63	0.56	0.086	0.75	0.24	0.20	0.15	0.12	0.082	0.11	0.080	0.086	0.16	0.17	0.019	0.032	0.012	0.36	0.024	0.14
Apatite	0.30%	0.034	0.67	0.048	21.1	1.28	5.98	9.13	16.2	24.8	30.4	33.3	33.9	26.5	18.8	14.1	1.44	11.2	0.043	0.16	0.29	2.38
Spinel	0.00%	0.10	0.10	0.10	0.10	0.10	0.10	0.10	0.10	0.10	0.10	0.10	0.10	0.10	0.10	0.10	0.10	0.10	0.10	0.10	0.10	0.10
Perovskite	0.00%	0.078	0.26	0.20	17.2	0.10	20.2	57.6	93.5	112	122	131	140	150	160	170	26.1	124	69.4	69.4	2.25	2.25
Titanite	0.00%	0.040	0.040	0.22	6.67	1.79	0.57	1.36	3.57	6.07	5.65	8.52	12.0	19.0	26.7	30.0	2.16	3.04	112	891	189	121
D total		0.84	0.91	0.71	2.35	0.83	0.55	0.60	0.79	1.30	1.67	2.17	4.09	5.66	5.07	5.39	0.11	0.32	0.27	1.62	4.73	6.50
Residual liquid		9918	11118	147	10.4	203	514	612	119	941	2.23	3.64	1.24	0.35	0.34	0.05	16.6	14.9	125	0.41	30.7	0.33
612 C																						
Nepheline	0.06%	0.0037	0.021	0.63	0.10	0.015	0.0058	0.0081	0.071	0.19	0.026	0.066	0.11	0.81	0.70	0.70	0.056	0.017	0.023	0.41	0.16	0.34
Clinopyroxene	0.06%	0.0004	0.059	0.0037	0.51	3.17	0.027	0.061	0.16	0.35	0.37	0.40	0.59	1.37	4.05	6.06	0.024	0.0037	0.017	0.17	14.2	19.9
Melanite garnet	0.02%	0.0008	0.015	0.0010	45.6	3.29	0.10	0.46	2.71	13.8	22.5	35.0	87.0	127	104	101	0.44	2.07	5.47	46.2	62.7	80.3
Wollastonite	0.00%	0.0016	0.085	0.025	6.37	0.36	0.11	0.23	0.61	1.62	2.38	3.04	6.45	9.18	14.7	15.4	0.098	0.022	0.20	0.80	1.40	1.75
Nyerereite	0.50%	1.04	1.48	1.05	0.30	0.12	0.76	0.74	0.68	0.52	0.48	0.40	0.22	0.15	0.10	0.40	0.10	0.097	0.11	0.098	0.068	0.28
Gregoryite	0.20%	0.59	0.63	0.56	0.086	0.75	0.24	0.20	0.15	0.12	0.082	0.11	0.080	0.086	0.16	0.17	0.019	0.032	0.012	0.36	0.024	0.14
Apatite	0.06%	0.034	0.67	0.048	21.1	1.28	5.98	9.13	16.2	24.8	30.4	33.3	33.9	26.5	18.8	14.1	1.44	11.2	0.043	0.16	0.29	2.38
Spinel	0.30%	0.10	0.10	0.10	0.10	0.10	0.10	0.10	0.10	0.10	0.10	0.10	0.10	0.10	0.10	0.10	0.10	0.10	0.10	0.10	0.10	0.10
Perovskite	0.005%	0.078	0.26	0.20	17.2	0.10	20.2	57.6	93.5	112	122	131	140	150	160	170	26.1	124	69.4	69.4	2.25	2.25
Titanite	0.005%	0.040	0.040	0.22	6.67	1.79	0.57	1.36	3.57	6.07	5.65	8.52	12.0	19.0	26.7	30.0	2.16	3.04	112	891	189	121
D total		0.55	0.78	0.58	2.40	0.50	0.65	1.20	1.83	2.80	3.11	3.53	4.40	4.89	4.00	3.82	0.29	1.35	0.90	5.22	2.49	3.11
Residual liquid		9974	11149	148	10.3	204	515	611	118	923	2.17	3.53	1.19	0.33	0.33	0.04	16.7	14.8	125	0.39	30.1	0.32
609 C																						
Nepheline	0.06%	0.0037	0.021	0.63	0.10	0.015	0.0058	0.0081	0.071	0.19	0.026	0.066	0.11	0.81	0.70	0.70	0.056	0.017	0.023	0.41	0.16	0.34
Clinopyroxene	0.06%	0.0004	0.059	0.0037	0.51	3.17	0.027	0.061	0.16	0.35	0.37	0.40	0.59	1.37	4.05	6.06	0.024	0.0037	0.017	0.17	14.2	19.9
Melanite garnet	0.00%	0.0008	0.015	0.0010	45.6	3.29	0.10	0.46	2.71	13.8	22.5	35.0	87.0	127	104	101	0.44	2.07	5.47	46.2	62.7	80.3
Wollastonite	0.00%	0.0016	0.085	0.025	6.37	0.36	0.11	0.23	0.61	1.62	2.38	3.04	6.45	9.18	14.7	15.4	0.098	0.022	0.20	0.80	1.40	1.75
Nyerereite	0.50%	1.04	1.48	1.05	0.30	0.12	0.76	0.74	0.68	0.52	0.48	0.40	0.22	0.15	0.10	0.40	0.10	0.097	0.11	0.098	0.068	0.28
Gregoryite	0.20%	0.59	0.63	0.56	0.086	0.75	0.24	0.20	0.15	0.12	0.082	0.11	0.080	0.086	0.16	0.17	0.019	0.032	0.012	0.36	0.024	0.14
Apatite	0.06%	0.034	0.67	0.048	21.1	1.28	5.98	9.13	16.2	24.8	30.4	33.3	33.9	26.5	18.8	14.1	1.44	11.2	0.043	0.16	0.29	2.38
Perovskite	0.005%	0.078	0.26	0.20	17.2	0.10	20.2	57.6	93.5	112	122	131	140	150	160	170	26.1	124	69.4	69.4	2.25	2.25
Titanite	0.005%	0.040	0.040	0.22	6.67	1.79	0.57	1.36	3.57	6.07	5.65	8.52	12.0	19.0	26.7	30.0	2.16	3.04	112	891	189	121
D total		0.70	1.02	0.75	2.21	0.56	1.11	1.58	2.38	3.18	3.67	3.97	4.01	3.50	3.09	3.04	0.35	1.74	1.08	8.01	1.86	2.40
Residual liquid		10001	11147	148	10.1	205	514	608	116	904	2.12	3.43	1.16	0.33	0.32	0.04	16.8	14.7	125	0.38	29.8	0.32
608 C																						
Nepheline	0.06%	0.0037	0.021	0.63	0.10	0.015	0.0058	0.0081	0.071	0.19	0.026	0.066	0.11	0.81	0.70	0.70	0.056	0.017	0.023	0.41	0.16	0.34
Clinopyroxene	0.06%	0.0004	0.059	0.0037	0.51	3.17	0.027	0.061	0.16	0.35	0.37	0.40	0.59	1.37	4.05	6.06	0.024	0.0037	0.017	0.17	14.2	19.9
Melanite garnet	0.00%	0.0008	0.015	0.0010	45.6	3.29	0.10	0.46	2.71	13.8	22.5	35.0	87.0	127	104	101	0.44	2.07	5.47	46.2	62.7	80.3
Wollastonite	0.00%	0.0016	0.085	0.025	6.37	0.36	0.11	0.23	0.61	1.62	2.38	3.04	6.45	9.18	14.7	15.4	0.098	0.022	0.20	0.80	1.40	1.75
Nyerereite	0.50%	1.04	1.48	1.05	0.30	0.12	0.76	0.74	0.68	0.52	0.48	0.40	0.22	0.15	0.10	0.40	0.10	0.097	0.11	0.098	0.068	0.28
Gregoryite	0.20%	0.59	0.63	0.56	0.086	0.75	0.24	0.20	0.15	0.12	0.082	0.11	0.080	0.086	0.16	0.17	0.019	0.032	0.012	0.36	0.024	0.14
Apatite	0.06%	0.034	0.67	0.048	21.1	1.28	5.98	9.13	16.2	24.8	30.4	33.3	33.9	26.5	18.8	14.1	1.44	11.2	0.043	0.16	0.29	2.38
Perovskite	0.005%	0.078	0.26	0.20	17.2	0.10	20.2	57.6	93.5	112	122	131	140	150	160	170	26.1	124	69.4	69.4	2.25	2.25
Titanite	0.005%	0.040	0.040	0.22	6.67	1.79	0.57	1.36	3.57	6.07	5.65	8.52	12.0	19.0	26.7	30.0	2.16	3.04	112	891	189	121
D total		0.70	1.02	0.75	2.21	0.56	1.11	1.58	2.38	3.18	3.67	3.97	4.01	3.50	3.09	3.04	0.35	1.74	1.08	8.01	1.86	2.40
Residual liquid		10026	11145	149	10.0	206	514	605	115	897	2.07	3.34	1.13	0.32	0.32	0.04	16.9	14.6	125	0.38	29.6	0.31

		Ba	Sr	Rb	Y	V	La	Ce	Nd	Sm	Eu	Gd	Dy	Er	Yb	Lu	U	Th	Nb	Ta	Zr	Hf
603 C																						
Nepheline	0.06%	0.0037	0.021	0.63	0.10	0.015	0.0058	0.0061	0.071	0.19	0.026	0.066	0.11	0.81	0.70	0.70	0.056	0.017	0.023	0.41	0.16	0.34
Clinopyroxene	0.06%	0.0004	0.059	0.0037	0.51	3.17	0.027	0.061	0.16	0.35	0.37	0.40	0.59	1.37	4.05	6.06	0.024	0.0037	0.017	0.17	14.2	19.9
Melanite garnet	0.00%	0.0008	0.015	0.0010	45.6	3.29	0.10	0.46	2.71	13.8	22.5	35.0	87.0	127	104	101	0.44	2.07	5.47	46.2	62.7	80.3
Wollastonite	0.00%	0.0016	0.085	0.025	6.37	0.36	0.11	0.23	0.61	1.62	2.38	3.04	6.45	9.18	14.7	15.4	0.098	0.022	0.20	0.80	1.40	1.75
Nyererenite	0.50%	1.04	1.48	1.05	0.30	0.12	0.76	0.74	0.68	0.52	0.46	0.40	0.22	0.15	0.10	0.40	0.10	0.097	0.11	0.098	0.068	0.28
Gregoryite	0.20%	0.59	0.63	0.56	0.086	0.75	0.24	0.20	0.15	0.12	0.082	0.11	0.080	0.086	0.16	0.17	0.019	0.032	0.012	0.36	0.024	0.14
Apatite	0.08%	0.034	0.67	0.048	21.1	1.28	5.98	9.13	16.2	24.8	30.4	33.3	33.9	26.5	18.8	14.1	1.44	11.2	0.043	0.16	0.29	2.38
Perovskite	0.005%	0.078	0.26	0.20	17.2	0.10	20.2	57.8	93.5	112	122	131	140	150	160	170	26.1	124	69.4	69.4	2.25	2.25
Titanite	0.005%	0.040	0.040	0.22	6.67	1.79	0.57	1.36	3.57	6.07	5.65	8.52	12.0	19.0	26.7	30.0	2.16	3.04	112	991	169	121
D total		0.70	1.02	0.75	2.21	0.56	1.11	1.58	2.38	3.18	3.67	3.97	4.01	3.50	3.09	3.04	0.35	1.74	1.06	6.01	1.96	2.40
Residual liquid		10055	11144	149	9.92	207	513	601	113	8.69	2.02	3.25	1.10	0.31	0.31	0.04	17.0	14.5	125	0.34	29.3	0.31
600 C																						
Nepheline	0.06%	0.0037	0.021	0.63	0.10	0.015	0.0058	0.0061	0.071	0.19	0.026	0.066	0.11	0.81	0.70	0.70	0.056	0.017	0.023	0.41	0.16	0.34
Clinopyroxene	0.06%	0.0004	0.059	0.0037	0.51	3.17	0.027	0.061	0.16	0.35	0.37	0.40	0.59	1.37	4.05	6.06	0.024	0.0037	0.017	0.17	14.2	19.9
Melanite garnet	0.00%	0.0008	0.015	0.0010	45.6	3.29	0.10	0.46	2.71	13.8	22.5	35.0	87.0	127	104	101	0.44	2.07	5.47	46.2	62.7	80.3
Wollastonite	0.00%	0.0016	0.085	0.025	6.37	0.36	0.11	0.23	0.61	1.62	2.38	3.04	6.45	9.18	14.7	15.4	0.098	0.022	0.20	0.80	1.40	1.75
Nyererenite	0.50%	1.04	1.48	1.05	0.30	0.12	0.76	0.74	0.68	0.52	0.46	0.40	0.22	0.15	0.10	0.40	0.10	0.097	0.11	0.098	0.068	0.28
Gregoryite	0.20%	0.59	0.63	0.56	0.086	0.75	0.24	0.20	0.15	0.12	0.082	0.11	0.080	0.086	0.16	0.17	0.019	0.032	0.012	0.36	0.024	0.14
Apatite	0.08%	0.034	0.67	0.048	21.1	1.28	5.98	9.13	16.2	24.8	30.4	33.3	33.9	26.5	18.8	14.1	1.44	11.2	0.043	0.16	0.29	2.38
Perovskite	0.005%	0.078	0.26	0.20	17.2	0.10	20.2	57.8	93.5	112	122	131	140	150	160	170	26.1	124	69.4	69.4	2.25	2.25
Titanite	0.005%	0.040	0.040	0.22	6.67	1.79	0.57	1.36	3.57	6.07	5.65	8.52	12.0	19.0	26.7	30.0	2.16	3.04	112	991	169	121
D total		0.70	1.02	0.75	2.21	0.56	1.11	1.58	2.38	3.18	3.67	3.97	4.01	3.50	3.09	3.04	0.35	1.74	1.06	6.01	1.96	2.40
Residual liquid		10083	11142	150	9.82	207	513	598	112	8.52	1.97	3.17	1.07	0.31	0.31	0.04	17.1	14.4	125	0.33	29.1	0.31
597 C																						
Nepheline	0.06%	0.0037	0.021	0.63	0.10	0.015	0.0058	0.0061	0.071	0.19	0.026	0.066	0.11	0.81	0.70	0.70	0.056	0.017	0.023	0.41	0.16	0.34
Clinopyroxene	0.06%	0.0004	0.059	0.0037	0.51	3.17	0.027	0.061	0.16	0.35	0.37	0.40	0.59	1.37	4.05	6.06	0.024	0.0037	0.017	0.17	14.2	19.9
Melanite garnet	0.00%	0.0008	0.015	0.0010	45.6	3.29	0.10	0.46	2.71	13.8	22.5	35.0	87.0	127	104	101	0.44	2.07	5.47	46.2	62.7	80.3
Wollastonite	0.00%	0.0016	0.085	0.025	6.37	0.36	0.11	0.23	0.61	1.62	2.38	3.04	6.45	9.18	14.7	15.4	0.098	0.022	0.20	0.80	1.40	1.75
Nyererenite	0.50%	1.04	1.48	1.05	0.30	0.12	0.78	0.74	0.68	0.52	0.46	0.40	0.22	0.15	0.10	0.40	0.10	0.097	0.11	0.098	0.068	0.28
Gregoryite	0.20%	0.59	0.63	0.56	0.086	0.75	0.24	0.20	0.15	0.12	0.082	0.11	0.080	0.086	0.16	0.17	0.019	0.032	0.012	0.36	0.024	0.14
Apatite	0.08%	0.034	0.67	0.048	21.1	1.28	5.98	9.13	16.2	24.8	30.4	33.3	33.9	26.5	18.8	14.1	1.44	11.2	0.043	0.16	0.29	2.38
Perovskite	0.005%	0.078	0.26	0.20	17.2	0.10	20.2	57.8	93.5	112	122	131	140	150	160	170	26.1	124	69.4	69.4	2.25	2.25
Titanite	0.005%	0.040	0.040	0.22	6.67	1.79	0.57	1.38	3.57	6.07	5.65	8.52	12.0	19.0	26.7	30.0	2.16	3.04	112	991	169	121
D total		0.70	1.02	0.75	2.21	0.56	1.11	1.58	2.38	3.18	3.67	3.97	4.01	3.50	3.09	3.04	0.35	1.74	1.06	6.01	1.96	2.40
Residual liquid		10110	11140	150	9.71	208	512	595	110	8.35	1.92	3.08	1.04	0.30	0.30	0.04	17.2	14.3	125	0.31	28.8	0.30
594 C																						
Nepheline	0.06%	0.0037	0.021	0.63	0.10	0.015	0.0058	0.0061	0.071	0.19	0.026	0.066	0.11	0.81	0.70	0.70	0.056	0.017	0.023	0.41	0.16	0.34
Clinopyroxene	0.06%	0.0004	0.059	0.0037	0.51	3.17	0.027	0.061	0.16	0.35	0.37	0.40	0.59	1.37	4.05	6.06	0.024	0.0037	0.017	0.17	14.2	19.9
Melanite garnet	0.00%	0.0008	0.015	0.0010	45.6	3.29	0.10	0.46	2.71	13.8	22.5	35.0	87.0	127	104	101	0.44	2.07	5.47	46.2	62.7	80.3
Wollastonite	0.00%	0.0016	0.085	0.025	6.37	0.36	0.11	0.23	0.61	1.62	2.38	3.04	6.45	9.18	14.7	15.4	0.098	0.022	0.20	0.80	1.40	1.75
Nyererenite	0.50%	1.04	1.48	1.05	0.30	0.12	0.76	0.74	0.68	0.52	0.46	0.40	0.22	0.15	0.10	0.40	0.10	0.097	0.11	0.098	0.068	0.28
Gregoryite	0.20%	0.59	0.63	0.56	0.086	0.75	0.24	0.20	0.15	0.12	0.082	0.11	0.080	0.086	0.16	0.17	0.019	0.032	0.012	0.36	0.024	0.14
Apatite	0.08%	0.034	0.67	0.048	21.1	1.28	5.98	9.13	16.2	24.8	30.4	33.3	33.9	26.5	18.8	14.1	1.44	11.2	0.043	0.16	0.29	2.38
Perovskite	0.001%	0.078	0.26	0.20	17.2	0.10	20.2	57.8	93.5	112	122	131	140	150	160	170	26.1	124	69.4	69.4	2.25	2.25
Titanite	0.001%	0.040	0.040	0.22	6.67	1.79	0.57	1.36	3.57	6.07	5.65	8.52	12.0	19.0	26.7	30.0	2.16	3.04	112	991	169	121
D total		0.71	1.02	0.75	2.12	0.56	1.03	1.33	1.97	2.68	3.14	3.39	3.37	2.79	2.29	2.18	0.22	1.20	0.27	1.36	1.21	1.88
Residual liquid		10137	11138	150	9.61	209	512	593	109	8.23	1.88	3.01	1.02	0.29	0.30	0.04	17.4	14.3	126	0.31	28.8	0.30

APPENDIX A6

Table A6.1: Major element microprobe analyses of carbonate liquid (LC) from experiments on the join HOL14/OL5 (in wt. %) - individual and average analyses, standard deviation (STDS) and relative standard deviation (RSD).

Sample	SiO2	TiO2	Al2O3	FeO	MnO	MgO	CaO	Na2O	K2O	P2O5	F	Cl	SO3	BaO	SrO	Total
CP1																
LC1,1	1.6	0.07	0.1	0.8	0.1	0.4	14.6	28.0	4.3	1.2	1.1	0.89	4.0	1.6	1.9	60.83
LC1,2	1.4	0.13	0.3	0.5	0.2	0.2	13.7	28.9	3.9	1.2	1.2	1.09	3.1	1.6	1.6	59.00
LC1,3	1.5	0.05	0.1	1.0	0.2	0.5	15.5	28.1	5.4	1.4	1.6	2.31	2.9	1.5	1.3	63.27
LC1,4	1.5	0.08	0.1	1.0	0.3	0.4	15.9	27.3	5.6	0.9	2.0	2.96	3.4	1.3	1.9	64.40
LC1,5	1.5	0.07	b.d.	1.3	0.1	0.6	15.5	26.9	6.8	1.2	1.7	2.84	2.9	0.9	1.7	64.17
Average	1.50	0.08	0.15	0.93	0.17	0.42	15.03	27.85	5.17	1.17	1.54	2.02	3.26	1.38	1.69	62.36
STDS	0.09	0.03	0.09	0.28	0.08	0.15	0.89	0.77	1.15	0.17	0.35	0.97	0.48	0.29	0.24	2.34
RSD	6%	38%	60%	31%	47%	36%	6%	3%	22%	15%	22%	48%	15%	21%	14%	4%
CP7																
LC7,1	*0.2*	*0.10*	*b.d.*	*1.7*	*0.3*	*0.0*	*16.1*	*15.3*	*5.6*	*1.3*	*0.1*	*0.69*	*1.8*	*1.4*	*1.1*	*45.56*
LC7,2	*0.6*	*0.09*	*0.0*	*0.1*	*0.1*	*0.0*	*12.5*	*24.3*	*2.5*	*0.8*	*1.2*	*0.48*	*2.9*	*0.8*	*1.2*	*47.44*
LC7,3	*2.1*	*0.15*	*0.1*	*1.9*	*0.3*	*0.1*	*13.7*	*22.2*	*4.8*	*0.7*	*0.8*	*1.63*	*1.9*	*1.1*	*0.9*	*52.23*
LC7,4	0.8	0.05	0.1	0.2	0.3	b.d.	20.1	23.2	5.2	0.8	0.9	1.73	1.3	0.8	2.1	57.52
LC7,5	2.9	0.04	0.2	1.2	0.2	0.1	18.7	26.3	5.1	0.9	0.5	1.58	1.6	0.8	1.6	61.62
LC7,6	3.5	0.06	0.1	2.2	0.4	0.2	19.4	27.0	4.5	0.8	0.1	0.67	1.5	0.3	1.5	62.26
LC7,7	0.6	0.07	0.1	0.5	0.1	b.d.	22.9	23.0	4.8	0.8	1.1	0.49	1.5	1.0	1.5	58.46
LC7,8	2.6	0.17	0.3	0.6	0.1	0.1	21.4	24.7	5.4	0.7	0.3	2.20	1.4	0.6	1.4	62.10
Average last 5	2.09	0.08	0.14	0.94	0.20	0.13	20.52	24.81	5.01	0.80	0.59	1.33	1.45	0.71	1.64	60.44
STDS	1.32	0.05	0.11	0.77	0.12	0.09	1.65	1.80	0.36	0.05	0.41	0.73	0.11	0.28	0.26	2.23
RSD	63%	67%	80%	83%	59%	67%	8%	7%	7%	7%	69%	55%	7%	39%	16%	4%
CP10																
CP10,1	*0.6*	*0.04*	*0.2*	*0.4*	*0.2*	*b.d.*	*10.9*	*30.9*	*2.7*	*0.6*	*0.1*	*0.39*	*0.7*	*0.3*	*0.9*	*48.96*
CP10,2	*1.8*	*0.03*	*0.3*	*0.7*	*0.3*	*0.0*	*15.1*	*22.7*	*4.0*	*1.8*	*0.1*	*0.62*	*1.8*	*0.8*	*1.7*	*51.69*
CP10,3	*0.8*	*0.04*	*0.1*	*0.6*	*0.4*	*b.d.*	*13.0*	*23.7*	*3.5*	*1.9*	*0.1*	*0.71*	*1.5*	*0.5*	*1.3*	*48.05*
CP10,4	*0.9*	*0.08*	*0.1*	*0.4*	*0.3*	*0.2*	*12.6*	*23.2*	*4.0*	*1.2*	*0.3*	*0.71*	*1.3*	*0.0*	*1.6*	*47.05*
CP10,5	*0.4*	*0.04*	*0.1*	*0.3*	*0.2*	*0.1*	*12.0*	*21.8*	*2.9*	*0.8*	*0.2*	*0.21*	*1.3*	*1.3*	*1.5*	*43.13*
CP10,6	*0.4*	*0.09*	*0.1*	*0.6*	*0.3*	*0.0*	*12.9*	*24.6*	*3.2*	*1.6*	*0.0*	*0.90*	*2.1*	*0.5*	*1.6*	*48.95*
CP10,12	*8.1*	*0.29*	*2.3*	*2.4*	*0.5*	*0.4*	*11.7*	*23.9*	*4.1*	*1.4*	*0.3*	*0.82*	*1.4*	*1.3*	*0.9*	*59.54*
CP10,7	0.3	0.03	0.1	0.5	0.2	0.0	14.9	29.3	4.5	1.1	0.4	0.61	1.8	1.5	1.9	57.13
CP10,8	3.0	"0.25	0.8	1.7	0.2	0.1	14.3	28.2	3.8	2.1	0.8	1.25	2.1	0.8	1.9	61.26
CP10,9	2.8	0.02	0.2	0.7	0.4	0.1	13.8	30.9	3.6	1.7	0.3	0.98	1.7	0.7	1.4	59.30
CP10,10	0.9	0.02	0.1	0.5	0.3	0.0	15.2	28.8	4.0	1.0	2.3	0.52	1 9	2.2	1.6	59.27
CP10,11	0.6	0.05	0.1	0.4	0.1	0.0	7.7	37.4	3.5	1.1	0.8	1.00	2.3	0.7	1.2	56.91
Average last 5	1.53	0.03	0.24	0.78	0.25	0.04	13.18	30.92	3.86	1.40	0.91	0.87	1.96	1.17	1.60	58.73
STDS	1.30	0.01	0.29	0.55	0.13	0.02	3.12	3.77	0.40	0.50	0.79	0.30	0.27	0.69	0.30	1.79
RSD	85%	47%	120%	70%	51%	57%	24%	12%	10%	36%	87%	35%	14%	59%	18%	3%
CP13																
CP13,6	*8.1*	*0.52*	*0.6*	*3.3*	*0.4*	*0.9*	*17.2*	*21.9*	*4.2*	*1.3*	*1.1*	*0.48*	*1.1*	*0.7*	*1.1*	*62.92*
CP13,1	3.7	0.27	0.3	1.8	0.3	0.6	19.5	24.0	3.6	1.6	1.1	0.65	1.0	1.0	1.7	61.11
CP13,2	3.1	0.16	0.3	1.8	0.5	0.6	19.8	21.4	5.8	1.0	1.6	0.94	1.1	1.1	1.6	60.62
CP13,3	2.5	0.30	0.3	2.4	0.4	0.7	19.5	23.2	2.9	1.5	1.8	0.67	1.0	1.0	1.6	59.72
CP13,4	5.8	0.17	0.2	1.5	0.5	0.4	19.5	22.6	2.6	0.9	1.2	0.39	1.1	1.0	1.5	59.26
CP13,5	1.2	0.17	0.1	1.1	0.2	0.3	19.1	26.5	3.0	1.1	0.8	0.49	1.0	0.8	1.1	57.04
CP13,7	4.8	0.30	0.4	2.0	0.1	0.5	19.0	22.6	4.4	0.9	0.4	0.44	1.2	1.0	1.1	59.32
Average last 6	3.53	0.23	0.25	1.77	0.33	0.52	19.39	23.37	3.70	1.18	1.16	0.60	1.06	1.01	1.44	59.51
STDS	1.61	0.07	0.09	0.42	0.14	0.13	0.32	1.76	1.19	0.29	0.50	0.20	0.10	0.10	0.27	1.42
RSD	46%	30%	37%	24%	42%	25%	2%	8%	32%	25%	43%	34%	9%	10%	18%	2%
CP14																
LC14,1	1.9	0.11	0.1	0.9	0.3	0.2	14.9	25.6	8.6	1.0	1.5	1.46	2.2	1.4	0.9	60.99
LC14,2	1.2	0.11	b.d.	0.9	0.1	0.3	15.7	26.0	8.1	1.1	1.7	2.09	2.4	1.8	1.4	62.93
LC14,3	1.8	0.10	0.1	0.8	0.2	0.3	14.8	24.8	8.7	1.0	2.1	2.68	2.4	1.2	1.8	62.67
LC14,4	1.5	0.06	0.1	0.7	0.2	0.2	12.9	26.5	7.2	1.3	1.5	2.11	2.6	1.7	1.2	59.76
LC14,5	2.7	0.15	0.1	1.0	0.3	0.2	15.6	25.9	7.2	1.3	1.5	1.62	3.0	0.8	1.2	62.72
Average	1.83	0.11	0.09	0.86	0.20	0.24	14.80	25.77	7.95	1.14	1.66	1.99	2.54	1.36	1.29	61.83
STDS	0.56	0.03	0.04	0.10	0.09	0.04	1.14	0.65	0.72	0.16	0.24	0.48	0.29	0.39	0.31	1.39
RSD	31%	30%	48%	12%	43%	17%	8%	3%	9%	14%	14%	24%	12%	29%	24%	2%
CP16																
LC16,1	4.2	0.07	0.2	0.9	0.3	0.1	12.4	28.9	4.2	1.5	0.5	0.57	3.1	1.0	1.5	59.47
LC16,2	2.9	0.10	0.2	1.0	0.1	0.1	13.1	24.7	6.7	2.3	1.3	0.99	2.0	2.0	1.8	59.30
LC16,3	1.3	0.05	0.1	0.7	0.5	0.1	13.5	26.4	7.9	0.7	2.0	0.91	2.6	1.7	2.2	60.68
LC16,4	6.7	0.12	0.3	1.1	0.4	0.1	14.4	26.9	7.1	1.2	3.9	1.16	2.7	1.6	1.8	69.21
LC16,5	*8.1*	*0.10*	*1.6*	*1.4*	*0.3*	*0.1*	*13.5*	*22.9*	*6.4*	*1.4*	*1.2*	*0.95*	*1.8*	*1.2*	*1.4*	*62.41*
Average first 4	4.64	0.09	0.46	1.01	0.33	0.11	13.36	25.93	6.46	1.43	1.77	0.92	2.44	1.51	1.74	62.21
STDS	2.28	0.03	0.10	0.14	0.17	0.03	0.83	1.73	1.57	0.67	1.42	0.25	0.44	0.43	0.26	4.74
RSD	49%	35%	23%	14%	51%	30%	6%	7%	24%	47%	80%	27%	18%	28%	15%	8%

Sample	SiO2	TiO2	Al2O3	FeO	MnO	MgO	CaO	Na2O	K2O	P2O5	F	Cl	SO3	BaO	SrO	Total
CP18																
LC18,1	2.6	0.20	0.1	1.2	0.2	0.3	20.3	23.4	5.3	1.1	*2.6	0.79	2.5	1.0	1.4	62.89
LC18,2	3.5	0.14	0.3	1.4	0.2	0.3	21.5	21.6	5.2	1.1	0.9	0.51	1.8	0.9	1.5	60.57
LC18,3	3.0	0.09	0.3	1.2	0.1	0.4	22.2	22.2	4.4	1.3	0.4	0.21	1.5	1.2	1.7	60.02
LC18,4	0.6	b.d.	0.1	0.2	0.1	b.d.	23.3	22.8	5.6	1.0	0.8	1.06	1.5	1.2	1.6	59.72
LC18,5	2.0	0.12	0.1	1.2	0.2	0.2	17.5	26.8	5.2	1.4	0.5	1.48	3.6	0.7	0.9	62.06
Average	2.33	0.14	0.17	1.03	0.16	0.28	20.94	23.34	5.14	1.18	0.66	0.81	2.18	0.99	1.43	60.76
STDS	1.13	0.05	0.09	0.45	0.07	0.05	2.21	2.04	0.46	0.17	0.22	0.49	0.91	0.19	0.32	1.37
RSD	48%	34%	51%	44%	43%	18%	11%	9%	9%	15%	34%	61%	42%	19%	23%	2%
CP20																
LC20,1	*0.7*	*0.12*	*0.1*	*1.0*	*0.3*	*0.7*	*20.9*	*19.2*	*3.2*	*1.8*	*2.1*	*0.18*	*2.0*	*1.2*	*1.5*	*54.83*
LC20,2	0.2	0.06	b.d.	0.3	0.2	0.1	21.9	19.7	5.4	1.2	1.9	0.38	1.9	1.3	1.3	56.03
LC20,3	2.3	*0.30	0.1	1.5	0.3	0.3	20.4	22.1	4.2	1.5	0.5	0.63	2.3	1.2	1.2	58.87
LC20,4	1.4	0.13	0.1	1.5	0.2	0.2	20.9	23.5	4.1	1.9	0.2	0.55	2.5	b.d.	0.9	58.11
LC20,5	*5.7	0.18	*0.8	1.6	0.1	0.5	22.3	19.6	3.0	1.5	2.0	0.20	2.0	1.6	1.7	62.75
LC20,6	1.0	0.11	0.1	1.0	0.3	0.1	23.7	22.2	4.4	1.3	0.2	0.32	2.2	0.7	1.7	59.31
LC20,7	1.1	0.11	0.1	0.8	0.1	0.3	24.7	24.0	4.6	1.2	0.8	0.11	1.9	0.8	1.7	62.20
Average last 6	1.20	0.12	0.08	1.12	0.21	0.24	22.31	21.86	4.27	1.43	0.93	0.37	2.13	1.13	1.43	58.83
STDS	0.75	0.04	0.02	0.52	0.08	0.14	1.64	1.85	0.78	0.26	0.80	0.20	0.24	0.38	0.32	2.54
RSD	62%	37%	27%	46%	37%	60%	7%	8%	18%	18%	86%	55%	11%	34%	23%	4%
CP22																
LC22,1	2.9	0.17	0.1	0.9	b.d.	0.2	14.8	26.8	6.6	1.1	1.2	0.76	2.5	0.7	1.4	60.22
LC22,2	3.2	0.19	0.1	0.9	0.1	0.3	16.6	24.8	7.4	0.9	3.1	0.96	2.9	1.5	1.4	64.41
LC22,3	1.8	0.12	0.1	0.5	b.d.	0.2	15.4	25.2	6.4	1.7	0.8	0.97	2.4	1.0	1.5	58.14
LC22,4	4.3	0.20	0.2	0.9	0.1	0.3	17.7	24.9	5.9	1.2	1.2	1.32	1.8	1.0	1.1	62.08
LC22,5	3.1	0.19	0.2	0.9	0.1	0.3	16.3	*18.4	7.3	0.7	2.5	1.29	2.6	1.5	1.2	56.44
Average	3.05	0.17	0.14	0.80	0.10	0.26	16.15	25.43	6.74	1.10	1.77	1.06	2 44	1.16	1.33	61.70
STDS	0.90	0.03	0.01	0.18	0.04	0.05	1.12	0.94	0.61	0.39	0.99	0.24	0.43	0.35	0.16	3.15
RSD	29%	18%	9%	22%	39%	21%	7%	4%	9%	35%	56%	23%	18%	30%	12%	5%
CP43																
LC43,1	3.3	0.11	b.d.	1.6	b.d.	0.3	16.6	21.5	6.8	2.2	2.7	3.50	3.5	0.5	1.5	63.93
LC43,2	1.3	0.07	b.d.	0.5	b.d.	b.d.	14.3	19.4	8.8	1.6	2.8	4.64	2.5	1.7	1.9	59.49
LC43,3	*1.9*	*0.06*	*b.d.*	*0.5*	*b.d.*	*0.3*	*12.3*	*16.3*	*4.1*	*1.8*	*3.7*	*1.90*	*1.9*	*0.9*	*1.6*	*47.13*
LC43,4	*8.1*	*0.29*	*0.7*	*2.9*	*b.d.*	*0.4*	*16.2*	*8.1*	*2.5*	*0.6*	*4.9*	*0.74*	*3.4*	*1.4*	*1.8*	*51.94*
LC43,5	*2.0*	*0.09*	*0.3*	*0.7*	*b.d.*	*0.2*	*11.8*	*7.3*	*8.9*	*1.8*	*2.8*	*3.22*	*3.8*	*1.0*	*1.4*	*45.19*
LC43,6	*1.9*	*0.06*	*0.2*	*0.5*	*b.d.*	*0.2*	*12.4*	*12.4*	*4.6*	*1.7*	*2.9*	*6.24*	*1.9*	*0.8*	*1.6*	*47.39*
Average first 2	2.30	0.09	b.d.	1.02	b.d.	0.30	15.44	20.43	7.77	1.88	2.77	4.07	3.00	1.12	1.70	61.88
STDS	1.46	0.03	n.d.	0.75	n.d.	n.d.	1.60	1.50	1.39	0.42	0.07	0.81	0.64	0.86	0.34	3.14
RSD	63%	31%	n.d.	73%	n.d.	n.d.	10%	7%	18%	22%	3%	20%	21%	77%	20%	5%
CP50																
LC50,1	*0.4*	*b.d.*	*b.d.*	*0.4*	*b.d.*	*0.4*	*8.4*	*16.2*	*14.3*	*0.5*	*2.0*	*9.55*	*2.8*	*2.5*	*1.7*	*59.17*
LC50,2	*3.5*	*b.d.*	*0.3*	*0.8*	*0.2*	*0.2*	*9.2*	*26.2*	*3.1*	*2.5*	*0.3*	*0.41*	*2.8*	*b.d.*	*1.4*	*50.89*
LC50,3	1.7	0.04	b.d.	1.1	0.3	0.6	11.1	27.3	6.1	2.1	2.8	1.95	4 2	1.4	2.0	62.61
LC50,4	1.1	b.d.	b.d.	0.6	0.2	0.3	11.4	22.8	6.6	1.2	3.6	2.84	3.8	1.5	1.8	57.61
LC50,5	0.5	b.d.	b.d.	b.d.	b.d.	b.d.	11.1	28.2	6.9	1.8	6.1	3.22	4.2	1.3	1.9	65.24
LC50,6	1.8	0.05	0.2	0.9	0.2	0.5	7.6	31.7	6.2	2.2	5.4	3.50	4.2	1.1	1.4	66.85
Average last 4	1.25	0.05	0.19	0.84	0.22	0.46	10.31	27.51	6.45	1.81	4.49	2.88	4.06	1.35	1.77	63.62
STDS	0.59	0.01	n.d.	0.25	0.08	0.15	1.80	3.65	0.35	0.44	1.54	0.67	0.20	0.17	0.30	4.04
RSD	47%	16%	n.d.	29%	26%	32%	17%	13%	5%	25%	34%	23%	5%	13%	17%	6%
CP53																
LC53,1	2.0	0.14	b.d.	0.8	b.d.	b.d.	13.0	26.3	5.9	1.6	2.9	0.96	5.8	1.1	1.3	61.72
LC53,2	3.1	0.17	0.2	1.4	0.2	0.2	11.9	29.7	5.3	2.4	4.0	1.20	5.3	1.2	1.4	67.47
LC53,3	1.9	0.11	b.d.	0.9	b.d.	b.d.	15.4	20.2	5.7	1.6	2.7	0.95	3.0	1.0	1.6	55.01
LC53,4	1.6	0.10	b.d.	0.8	b.d.	0.3	10.4	27.4	9.9	1.3	5.2	*4.45	5.8	1.1	1.2	69.29
LC53,5	2.4	0.11	b.d.	1.0	b.d.	b.d.	13.4	27.8	6.0	1.9	3.2	0.68	6.1	1.4	1.4	65.30
LC53,6	1.4	0.08	b.d.	0.6	b.d.	b.d.	9.4	27.6	9.8	1.7	1.8	*6.24	4.7	0.7	0.9	64.72
LC53,7	1.9	0.11	b.d.	0.9	b.d.	0.4	11.9	28.8	5.1	1.9	4.1	0.50	5.5	1.0	1.3	63.21
LC53,8	1.8	0.10	b.d.	1.1	b.d.	0.4	8.1	31.7	5.9	1.2	1.1	2.27	6.1	0.6	0.8	61.05
Average	1.98	0.12	0.19	0.91	0.19	0.33	11.67	27.44	6.71	1.68	3.11	1.09	5.27	1.03	1.20	62.90
STDS	0.54	0.03	n.d.	0.23	n.d.	0.10	2.35	3.35	1.96	0.37	1.31	0.63	1.05	0.26	0.26	4.40
RSD	27%	24%	n.d.	26%	n.d.	29%	20%	12%	29%	22%	42%	57%	20%	26%	22%	7%
CP67																
LC67,1	0.3	-.04<	-.1<	.2<	.0<	-.0<	25.5	22.5	4.1	1.1	0.9	0.10	1.6	0.9	2.4	59.42
LC67,2	0.8	-.07<	.1<	0.2	0.4	.0<	19.5	25.3	4.3	0.9	2.2	0.30	3.1	1.3	2.5	60.72
LC67,3	1.5	.01<	.1<	0.7	0.2	0.2	16.7	23.3	5.2	0.8	*6.5	0.53	4.6	0.6	2.0	63.03
LC67,4	0.7	-.02<	.1<	.1<	.1<	-.1<	23.8	23.9	4.1	1.0	1.0	0.51	2.2	0.6	2.1	59.85
LC67,5	3.4	0.09	.1<	1.3	0.3	.2<	15.3	29.2	3.5	1.4	0.4	0.36	3.5	0.5	1.3	60.62
LC67,6	2.5	.02<	0.2	0.8	.2<	.1<	22.6	22.3	4.3	1.0	0.9	0.13	2.2	.3<	2.2	59.04
LC67,7	1.2	-.01<	.1<	0.7	0.3	.2<	15.5	29.9	3.6	1.5	0.8	*2.80	4.3	0.6	1.8	62.87
LC67,8	*5.6	0.15	0.3	*2.2	0.4	.1<	15.9	26.0	6.3	1.2	1.8	0.54	*6.2	0.6	1.8	68.95

Sample	SiO2	TiO2	Al2O3	FeO	MnO	MgO	CaO	Na2O	K2O	P2O5	F	Cl	SO3	BaO	SrO	Total
LC67,9	0.2	-.08<	.1<	.2<	.1<	-.1<	24.2	22.0	5.6	0.8	1.7	1.08	2.1	0.9	2.3	61.01
Average	1.33	0.12	0.25	0.74	0.32	0.20	19.89	24.93	4.56	1.08	1.21	0.44	2.95	0.75	2.04	60.81
STDS	1.12	0.04	0.07	0.39	0.08	n.d.	4.17	2.94	0.94	0.25	0.61	0.31	1.10	0.27	0.37	3.04
RSD	84%	35%	28%	53%	26%	n.d.	21%	12%	21%	23%	51%	70%	37%	36%	18%	5%
CP81																
LC81,1	3.0	0.05	.1<	0.7	0.5	0.4	15.9	20.8	5.8	1.2	2.5	1.02	2.7	0.9	1.5	57.08
LC81,2	1.2	0.14	.1<	*3.5	0.4	0.6	12.9	18.3	7.4	0.9	3.9	1.11	2.7	1.2	1.5	55.82
LC81,3	1.6	.02<	.0<	0.5	.1<	.2<	14.6	20.8	7.2	1.0	2.9	1.59	2.2	1.3	1.6	55.13
LC81,4	4.4	0.10	.1<	1.4	0.5	0.5	14.8	19.2	7.4	1.1	2.5	*2.31	2.2	1.2	1.3	58.86
LC81,5	1.7	.00<	-.0<	0.6	0.3	0.3	14.5	24.7	6.4	1.3	1.9	1.89	2.5	1.2	1.5	58.88
LC81,6	1.0	0.04	-.1<	0.4	0.3	.2<	12.3	26.3	5.4	1.4	1.5	0.84	3.3	0.7	1.4	54.97
LC81,7	*6.0	*0.27	4.1	1.3	0.3	.2<	12.3	22.6	4.8	1.2	1.0	0.72	3.0	1.1	1.3	59.93
LC81,8	*7.0	0.05	5.4	1.0	0.4	0.3	11.6	23.3	4.7	1.3	1.4	*0.38	2.9	1.2	1.3	62.14
LC81,9	5.3	0.04	4.0	0.8	0.3	0.4	11.6	24.6	4.6	1.3	2.3	0.54	2.5	0.7	1.5	60.43
LC81,10	3.6	0.03	1.6	0.8	0.2	0.5	13.4	23.5	4.4	1.4	3.5	0.54	2.6	1.0	1.6	58.68
LC81,11	3.1	.02<	2.2	0.4	.2<	0.3	13.7	23.6	5.4	1.3	2.6	0.81	2.6	0.9	1.8	58.68
LC81,12	*7.3	0.13	3.2	*3.0	0.5	0.4	13.1	23.7	4.2	1.4	2.1	0.62	2.9	0.8	1.1	64.28
LC81,13	0.6	-.03<	.1<	0.3	0.2	0.4	14.9	25.5	5.2	1.2	3.2	0.74	3.2	1.2	1.7	58.19
LC81,14	1.0	0.05	.1<	0.4	0.4	.1<	15.9	25.0	5.5	1.3	3.1	0.72	3.1	1.1	1.9	59.33
LC81,15	3.9	.01<	-.0<	0.4	0.2	.1<	16.8	23.7	5.0	1.3	2.2	0.94	2.9	1.1	1.6	59.97
LC81,16	1.1	.02<	.0<	0.6	0.4	0.2	13.5	26.1	6.1	1.6	2.3	1.75	3.5	1.1	1.7	59.84
LC81,17	0.9	-.00<	-.0<	0.5	0.3	0.4	14.4	25.4	5.6	1.2	2.4	1.23	3.2	1.2	1.6	58.27
LC81,18	*0.9*	*0.04*	*.0<*	*0.4*	*.2<*	*0.2*	*13.6*	*21.9*	*4.4*	*1.2*	*1.5*	*0.30*	*2.5*	*1.2*	*1.5*	*49.80*
LC81,19	*1.2*	*0.03*	*.1<*	*1.0*	*0.4*	*0.4*	*12.7*	*22.3*	*5.6*	*1.3*	*1.9*	*1.07*	*2.3*	*0.9*	*1.5*	*52.66*
LC81,20	*0.6*	*0.07*	*.1<*	*0.3*	*0.3*	*.1<*	*14.3*	*23.4*	*5.1*	*1.3*	*2.3*	*0.79*	*3.3*	*1.2*	*1.7*	*54.66*
LC81,21	*1.2*	*.01<*	*.0<*	*0.6*	*0.2*	*0.3*	*13.4*	*22.3*	*6.2*	*1.1*	*2.4*	*1.12*	*2.7*	*1.2*	*1.5*	*54.17*
LC81,22	*15.4*	*0.20*	*8.2*	*1.4*	*0.2*	*0.2*	*13.3*	*18.8*	*4.4*	*1.0*	*1.9*	*0.41*	*1.6*	*0.3*	*1.2*	*68.67*
Average first 17	2.31	0.07	3.42	0.67	0.35	0.39	13.89	23.36	5.59	1.26	2.43	1.00	2.82	1.04	1.52	60.14
STDS	1.53	0.04	1.38	0.33	0.11	0.11	1.52	2.34	1.01	0.16	0.75	0.43	0.37	0.21	0.20	2.35
RSD	66%	60%	40%	50%	31%	26%	11%	10%	18%	13%	31%	43%	13%	20%	13%	4%
CP82																
LC82,1	6.7	0.13	2.9	1.5	0.4	0.3	14.8	21.9	4.6	1.3	1.8	0.67	2.1	0.9	1.3	61.31
LC82,2	5.4	*0.31	2.2	1.5	.1<	.2<	13.2	21.8	5.7	0.4	1.6	2.60	1.2	0.8	1.0	57.80
LC82,3	3.0	0.13	0.5	0.9	0.3	0.3	16.7	21.4	9.8	1.0	3.7	2.90	3.3	1.2	1.5	66.54
LC82,4	3.8	0.13	0.8	1.0	0.3	.2<	16.0	19.7	8.5	1.0	3.6	1.15	2.1	1.4	1.6	61.04
LC82,5	5.3	0.12	1.1	1.0	0.2	.1<	14.0	21.2	4.5	1.5	0.7	1.32	1.6	0.5	1.3	54.22
LC82,6	2.5	0.12	.1<	1.0	.2<	.1<	15.7	22.4	6.1	2.2	0.4	1.78	2.4	0.7	1.3	56.61
LC82,7	*0.7*	*.03<*	*.0<*	*0.3*	*.0<*	*.1<*	*4.4*	*12.2*	*1.8*	*0.7*	*0.3*	*1.84*	*0.8*	*0.3*	*0.3*	*23.66*
LC82,8	*1.4*	*0.11*	*-.0<*	*0.4*	*.1<*	*.0<*	*7.0*	*20.0*	*4.0*	*1.1*	*0.4*	*2.47*	*1.3*	*0.4*	*0.6*	*39.10*
LC82,9	*8.9*	*0.28*	*3.7*	*2.1*	*0.3*	*0.4*	*13.1*	*23.3*	*4.8*	*1.4*	*2.0*	*0.75*	*3.4*	*0.6*	*1.2*	*66.35*
Average first 6	4.45	0.13	1.50	1.15	0.30	0.30	15.07	21.40	6.53	1.23	2.00	1.74	2.12	0.92	1.33	60.16
STDS	1.61	0.01	1.01	0.27	0.08	0.00	1.31	0.93	2.16	0.60	1.40	0.87	0.72	0.33	0.21	4.34
RSD	36%	4%	67%	24%	27%	0%	9%	4%	33%	49%	70%	50%	34%	36%	15%	7%
CP89																
LC80,1	*23.7*	*0.17*	*15.2*	*1.8*	*.2<*	*.2<*	*7.3*	*19.1*	*5.8*	*0.5*	*1.2*	*0.49*	*1.3*	*0.7*	*0.9*	*78.04*
LC89,2	*24.7*	*0.18*	*15.4*	*2.1*	*0.3*	*0.3*	*6.5*	*18.9*	*5.4*	*0.7*	*0.9*	*0.28*	*1.5*	*0.5*	*0.6*	*78.31*
LC89,3	*10.2*	*0.13*	*6.1*	*1.6*	*0.4*	*0.2*	*14.2*	*21.8*	*5.2*	*0.9*	*1.4*	*0.79*	*1.5*	*0.7*	*1.6*	*66.70*
LC89,4	*16.1*	*0.11*	*10.3*	*2.1*	*0.3*	*0.3*	*12.2*	*21.3*	*5.3*	*1.0*	*1.1*	*0.56*	*1.3*	*0.3*	*1.3*	*73.66*
LC89,5	*23.5*	*0.23*	*13.4*	*2.8*	*0.3*	*0.3*	*8.3*	*18.3*	*6.1*	*0.9*	*0.9*	*0.32*	*1.3*	*.3<*	*0.9*	*77.34*
LC89,6	6.8	0.23	0.6	2.5	0.3	0.6	13.4	26.2	5.2	1.4	2.4	*1.55	2.2	0.6	1.4	65.26
LC89,7	5.2	0.17	0.6	1.8	0.4	0.4	16.8	23.2	5.4	1.2	2.3	1.16	2.1	1.0	1.8	63.21
LC89,8	6.8	0.22	1.0	2.2	0.3	0.5	13.3	24.8	*7.6	1.1	2.6	*2.90	2.9	1.0	1.4	68.69
LC89,9	3.5	0.14	0.4	1.1	0.3	0.4	13.5	24.7	4.5	1.2	2.1	0.88	2.3	0.6	1.4	56.97
LC89,10	8.6	0.17	*2.9	1.7	0.3	0.3	14.4	20.4	5.1	0.8	2.4	0.59	1.6	0.9	1.3	61.58
LC89,11	4.0	0.15	0.3	1.9	.2<	0.4	14.9	25.8	4.7	1.0	1.4	0.47	2.6	0.7	1.4	59.77
LC89,12	2.7	0.10	0.3	1.3	0.2	0.3	18.3	23.6	5.1	1.4	1.8	0.92	2.1	0.8	1.6	60.67
LC89,13	3.7	0.13	0.4	1.5	0.3	0.4	16.4	21.1	4.7	1.3	2.4	0.36	2.6	0.8	1.5	57.52
LC89,14	5.5	0.18	0.7	2.0	0.4	0.5	15.2	23.6	4.5	1.5	2.7	0.52	2.3	1.0	1.5	62.09
LC89,15	6.1	0.22	0.8	2.4	0.5	0.7	15.5	22.8	4.8	1.2	1.9	0.52	2.5	0.8	1.3	61.95
LC89,16	6.3	0.22	0.8	2.1	0.4	0.4	15.0	23.7	4.5	1.3	1.7	0.42	2.0	0.9	1.7	61.36
LC89,17	4.3	0.09	0.5	1.5	.2<	.2<	16.0	22.8	4.1	1.1	2.1	0.41	2.2	0.8	1.5	57.36
LC89,18	6.9	0.23	0.9	2.6	0.3	0.5	15.9	21.3	4.9	1.2	1.9	0.37	1.8	0.9	1.5	61.28
LC89,19	5.8	0.18	0.8	1.8	0.3	0.3	14.8	22.5	4.4	1.2	2.2	0.34	1.8	1.1	1.4	58.84
Average last 14	5.44	0.17	0.61	1.89	0.33	0.44	15.24	23.32	4.76	1.21	2.14	0.58	2.21	0.85	1.46	60.66
STDS	1.64	0.05	0.23	0.45	0.08	0.12	1.40	1.70	0.37	0.18	0.37	0.26	0.36	0.15	0.12	3.19
RSD	30%	27%	37%	24%	23%	27%	9%	7%	8%	15%	17%	45%	16%	18%	8%	5%
CP91																
LC91,1	1.6	0.08	0.2	0.6	.1<	0.3	17.6	24.2	5.0	1.0	2.8	*0.24	5.2	1.0	1.7	61.36
LC91,3	3.0	0.10	0.2	0.6	-.1<	.0<	15.7	30.4	5.6	1.7	2.7	2.20	5.5	0.8	1.5	69.95
LC91,6	2.8	0.13	0.3	0.8	.1<	.1<	15.7	31.3	6.3	1.6	3.1	2.80	6.1	0.9	1.5	73.33
LC91,2	*3.0*	*.04<*	*-.0<*	*0.5*	*-.0<*	*-.0<*	*10.5*	*28.1*	*9.4*	*1.4*	*1.7*	*7.20*	*4.0*	*0.4*	*5.0*	*71.21*
LC91,4	*0.9*	*.03<*	*-.0<*	*0.5*	*.1<*	*0.4*	*23.5*	*7.5*	*7.1*	*1.5*	*1.9*	*0.50*	*11.1*	*0.8*	*1.9*	*57.57*

Sample	SiO2	TiO2	Al2O3	FeO	MnO	MgO	CaO	Na2O	K2O	P2O5	F	Cl	SO3	BaO	SrO	Total
LC91,5	*5.0*	*0.16*	*1.1*	*1.0*	*.1<*	*0.3*	*12.3*	*13.2*	*3.2*	*0.4*	*3.5*	*0.31*	*4.3*	*0.8*	*1.2*	*46.83*
LC91,7	*1.5*	*0.04*	*1.3*	*0.4*	*.0<*	*.1<*	*7.8*	*8.9*	*3.7*	*0.2*	*0.6*	*0.33*	*4.7*	*.2<*	*0.7*	*30.13*
LC91,8	*1.1*	*0.06*	*0.2*	*0.4*	*-.0<*	*0.4*	*6.4*	*10.7*	*2.3*	*1.5*	*1.9*	*0.53*	*4.1*	*0.4*	*1.1*	*31.05*
LC91,9	*1.4*	*.02<*	*0.5*	*0.4*	*.1<*	*.1<*	*5.8*	*16.3*	*4.4*	*0.4*	*1.1*	*0.36*	*7.8*	*0.4*	*0.7*	*39.70*
Average first 3	2.47	0.10	0.23	0.67	b.d.	0.30	16.33	28.63	5.63	1.43	2.87	2.50	5.60	0.90	1.57	69.24
STDS	0.76	0.03	0.06	0.12	n.d.	n.d.	1.10	3.87	0.65	0.38	0.21	0.42	0.46	0.10	0.12	6.17
RSD	31%	24%	25%	17%	n.d.	n.d.	7%	14%	12%	26%	7%	17%	8%	11%	7%	9%
CP92																
LC92,1	0.3	.03<	.0<	0.8	0.3	0.8	24.5	19.3	4.2	2.2	1.2	0.59	4.2	1.0	1.5	60.76
LC92,2	0.5	.03<	.0<	0.5	.1<	.1<	27.0	20.7	3.9	2.2	.1<	0.34	3.2	.3<	1.4	59.62
LC92,3	0.3	0.07	.0<	0 9	.2<	0.3	25.6	20.4	3.5	2.0	0.8	0.32	3.5	0.4	1.7	59.71
LC92,4	0.4	0.08	-.0<	0.7	.1<	.1<	25.0	20.5	3.7	2.0	0.5	0.74	3.2	0.4	1.6	58.92
LC92,5	*0.2*	*0.04*	*.0<*	*1.9*	*.2<*	*0.7*	*32.3*	*11.1*	*0.7*	*2.3*	*1.4*	*0.57*	*2.3*	*0.5*	*1.4*	*55.53*
LC92,6	*0.3*	*0.04*	*.0<*	*2.0*	*0.4*	*0.3*	*37.1*	*7.5*	*0.8*	*2.3*	*0.3*	*0.66*	*2.4*	*0.6*	*1.6*	*56.38*
LC92,7	*0.2*	*0.08*	*-.0<*	*0.4*	*.1<*	*.2<*	*8.1*	*25.7*	*1.2*	*0.8*	*0.5*	*0.22*	*1.1*	*0.5*	*1.0*	*39.86*
LC92,8	*.1<*	*0.03*	*.1<*	*.1<*	*-.0<*	*.1<*	*1.1*	*27.1*	*0.2*	*.1<*	*-.01<*	*.01<*	*0.3*	*-.1<*	*.1<*	*28.69*
LC92,9	*0.1*	*0.04*	*.0<*	*.1<*	*.1<*	*.2<*	*1.4*	*27.8*	*0.4*	*.1<*	*.06<*	*.05<*	*0.2*	*.2<*	*0.3*	*30.35*
LC92,10	*.1<*	*-.00<*	*.1<*	*.0<*	*-.0<*	*.1<*	*0.1*	*26.5*	*0.3*	*-.0<*	*-.01<*	*0.28*	*0.4*	*-.1<*	*.0<*	*27.54*
LC92,11	*0.7*	*0.08*	*.0<*	*1.1*	*0.2*	*0.6*	*19.7*	*20.7*	*0.7*	*1.5*	*1.2*	*0.41*	*1.9*	*0.7*	*1.4*	*50.96*
LC92,12	*0.4*	*.01<*	*-.0<*	*1.0*	*.2<*	*0.4*	*26.8*	*16.6*	*0.8*	*2.2*	*0.2*	*0.65*	*2.0*	*0.4*	*1.6*	*53.18*
LC92,13	*0.3*	*0.05*	*.1<*	*0.8*	*0.3*	*.2<*	*17.4*	*21.9*	*0.6*	*1.2*	*0.8*	*0.43*	*1.5*	*0.4*	*1.0*	*46.63*
LC92,14	*0.2*	*0.09*	*.0<*	*2.0*	*0.2*	*0.3*	*3.3*	*28.1*	*0.4*	*0.4*	*1.3*	*0.07*	*0.6*	*.1<*	*0.2*	*37.17*
Average first 4	0.38	0.08	b.d.	0.73	0.30	0.55	25.53	20.23	3.83	2.10	0.83	0.50	3.53	0.60	1.55	60.71
STDS	0.10	0.01	n.d.	0.17	n.d.	0.35	1.08	0.63	0.30	0.12	0.35	0.20	0.47	0.35	0.13	0.76
RSD	26%	9%	n.d.	24%	n.d.	64%	4%	3%	8%	5%	42%	41%	13%	58%	8%	1%
CP93																
LC93,1	2.3	0.14	.1<	1.3	.2<	0.3	17.8	24.6	5.8	1.4	2.1	1.47	2.6	1.0	1.5	62.38
LC93,2	2.2	0.14	.1<	1.4	0.3	0.5	13.5	29.4	4.9	1.2	*4.4	0.46	3 4	*1.6	1.3	64.82
LC93,3	2.7	0.15	0.3	1.4	0.3	0.5	18.1	26.9	5.5	1.2	1.4	0.60	2.7	0.6	1.4	63.74
LC93,4	3.9	0.17	0.3	1.5	0.3	0.4	14.5	27.8	5.6	1.2	3.3	0.80	2.5	1.0	1.6	64.87
LC93,5	4.4	0.20	0.3	1.4	0.2	0.3	19.4	21.0	7.0	1.5	1.8	0.86	3.2	0.9	1.6	64.01
LC93,6	3.9	0.20	0.4	1.7	.1<	0.4	16.5	22.1	5.3	1.2	1.9	0.51	1.7	0.7	1.6	60.07
LC93,7	4.9	0.17	0.6	1.9	0.3	0.4	16.9	22.3	6.1	*2.0	1.7	0.93	2.1	0.6	1.7	62.50
LC93,8	3.3	0.16	0.3	1.1	.0<	0.2	22.0	21.6	5.5	1.1	1.2	0.40	1.7	1.0	1.7	61.23
LC93,9	1.7	0.11	.0<	0.9	.2<	0.3	12.9	27.9	3.9	1.2	2.2	*1.95	3.3	1.0	1.1	58.46
LC93,10	4.0	0.22	0.3	1.9	0.3	0.5	*10.0	28.3	5.5	1.3	2.1	0.62	2.8	1.0	1.3	60.20
LC93,11	1.5	0.13	.1<	1.5	0.2	0.3	*7.7	26.4	5.9	1.0	2.0	0.78	*6.5	0.8	0.9	55.51
LC93,12	2.7	0.09	0.9	0.8	.2<	.2<	20.1	22.3	5.4	1.2	1.8	0.41	2.2	1.2	1.9	61.01
LC93,13	3.3	0.13	0.4	1.0	0.3	0.4	17.1	25.6	4.7	0.9	2.5	1.41	2.4	0.9	1.4	62.48
LC93,14	3.5	0.12	0.4	1.1	0.2	.2<	15.7	25.8	5.7	1.1	3.1	1.03	2.6	1.1	1.5	63.00
LC83,15	*5.5	0.23	0.7	1.9	0.5	0.5	14.8	24.3	5.5	1.2	1.4	0.53	2.8	0.9	1.3	62.19
LC93,16	4.8	0.16	0.6	1.8	0.3	0.3	15.5	21.6	5.3	1.3	1.8	0.78	1.8	0.7	1.2	57.84
LC93,17	*7.2*	*0.28*	*1.2*	*2.3*	*0.3*	*0.5*	*17.6*	*24.1*	*6.1*	*1.4*	*3.6*	*1.09*	*2.0*	*0.8*	*1.5*	*70.00*
Average first 16	3.27	0.16	0.46	1.41	0.29	0.38	16.91	24.87	5.48	1.20	2.02	0.77	2.52	0.89	1.44	62.07
STDS	1.07	0.04	0.20	0.36	0.08	0.10	2.61	2.78	0.66	0.15	0.58	0.33	0.55	0.18	0.25	2.60
RSD	33%	25%	43%	26%	29%	26%	15%	11%	12%	12%	29%	43%	22%	20%	18%	4%
CP97																
LC97,1	*3.2*	*0.14*	*0.2*	*1.7*	*0.5*	*0.6*	*5.1*	*30.0*	*2.7*	*0.7*	*2.9*	*0.87*	*2.3*	*0.6*	*0.7*	*52.29*
LC97,2	*3.8*	*0.15*	*0.3*	*2.0*	*0.3*	*0.4*	*16.3*	*27.4*	*4.9*	*1.6*	*6.1*	*0.87*	*1.9*	*1.2*	*1.7*	*68.82*
LC97,5	**4.6*	**0.21*	*0.2*	**2.6*	*0.5*	**0.8*	*14.0*	*24.9*	**7.1*	*0.6*	*3.7*	**5.40*	*1.5*	**1.6*	*1.8*	*69.51*
LC97,3	1.8	0.07	.1<	1.1	.1<	0.3	22.2	23.3	5.2	1.3	1.1	0.26	1.7	0.5	1.7	60.50
LC97,4	2.2	0.12	.1<	1.1	0.3	0.3	17.5	26.4	5.5	1.2	2.3	1.64	2.3	0.8	1.7	63.37
LC97,6	1.9	0.08	0.2	0.9	0.3	.0<	22.0	23.3	5.1	1.2	1.3	0.46	1.6	0.9	1.7	60.87
LC97,7	2.6	0.13	.1<	1.6	0.3	0.6	15.6	27.7	4.6	*1.7	2.9	0.68	2.5	0.7	1.5	63.13
LC97,8	2.0	0.12	0.2	1.1	.2<	.2<	19.2	25.1	5.9	1.3	4.0	*2.30	2.8	1.1	1.7	66.76
LC97,9	1.8	0.11	.1<	1.0	0.3	0.3	16.9	26.7	5.8	0.9	3.2	0.64	*3.6	1.0	1.5	63.81
LC97,10	2.6	0.13	0.2	1.0	0.3	.2<	22.0	20.8	5.8	1.2	1.6	0.43	1.4	0.7	1.7	60.09
LC97,11	2.6	0.14	0.2	1.3	0.2	0.4	18.8	23.7	5.7	0.9	3.0	1.33	2.1	1.0	1.7	63.05
LC97,12	2.7	0.14	.1<	1.5	0.4	0.4	14.2	28.8	4.6	1.4	3.7	0.35	*3.3	1.2	1.5	64.24
LC97,13	1.8	0.10	.0<	0.9	0.3	0.3	20.6	24.8	5.1	1.2	1.3	0.41	1.5	0.7	1.8	60.83
LC97,14	2.2	0.13	.1<	1.3	0.3	0.4	20.7	23.4	*7.1	0.7	2.6	1.18	2.5	*1.5	1.8	65.77
LC97,15	3.1	0.18	0.2	1.7	0.2	0.4	14.6	26.4	4.6	1.3	*7.6	0.67	2.5	1.0	1.5	65.79
LC97,16	1.3	0.07	.1<	1.4	0.3	0.2	16.7	24.5	3.7	1.4	1.1	0.26	1 9	1.2	1.5	55.38
LC97,17	2.4	0.14	.1<	1.5	0.4	0.4	17.9	22.9	4.7	1.4	2.4	0.50	2.2	0.9	1.7	59.49
LC97,18	2.1	0.16	0.2	2.2	0.3	0.3	16.3	23.2	5.6	1.4	1.9	1.53	2.1	1.1	1.3	59.77
LC97,19	*3.7	*0.22	0.2	2.1	0.4	0.3	16.5	21.2	5.7	1.2	3.2	0.77	2.6	0.7	1.5	60.28
LC97,20	2.3	0.14	.1<	1.5	0.4	0.3	17.3	21.8	5.3	1.2	2.1	0.56	2.5	1.0	1.7	58.26
LC97,21	2.2	0.17	.1<	1.7	0.4	0.3	16.9	22.1	5.7	1.4	1.8	0.85	2.3	1.1	1.4	58.36
Average last 18	2.21	0.13	0.20	1.38	0.32	0.35	18.11	24.23	5.21	1.21	2.32	0.74	2.16	0.92	1.61	61.08
STDS	0.43	0.03	0.00	0.38	0.07	0.09	2.51	2.26	0.60	0.20	0.91	0.43	0.43	0.20	0.14	3.02
RSD	20%	25%	0%	28%	21%	26%	14%	9%	12%	17%	39%	59%	20%	22%	9%	5%

Sample	SiO2	TiO2	Al2O3	FeO	MnO	MgO	CaO	Na2O	K2O	P2O5	F	Cl	SO3	BaO	SrO	Total
CP102																
LC102,1	2.0	0.08	.0<	0.9	.2<	0.3	20.8	22.2	4.5	2.3	*0.5	0.32	4.2	0.6	2.3	60.86
LC102,2	1.7	0.05	.1<	0.8	0.2	0.5	17.9	21.9	4.5	2.1	1.4	0.19	5.0	0.4	1.9	58.54
LC102,3	2.7	0.08	.1<	1.6	0.5	0.5	12.4	25.7	3.2	1.4	2.9	0.54	*7.9	1.1	1.6	62.11
LC102,4	1.5	0.08	0.2	1.3	0.3	1.2	15.7	23.5	3.9	1.6	2.7	0.29	4.6	1.3	2.0	60.17
LC102,5	1.6	0.07	.0<	1.4	0.2	0.5	17.5	20.3	4.3	1.8	1.8	0.41	3.5	0.9	2.2	56.56
LC102,6	2.9	*0.11	0.2	*2.2	0.3	1.1	14.6	19.1	3.6	1.8	2.7	0.41	3.9	1.3	2.1	56.24
LC102,7	3.0	0.05	*0.6	1.9	0.3	0.9	11.5	26.2	2.1	1.0	2.7	0.51	4.7	0.5	1.4	57.43
LC102,8	*2.1*	*0.11*	*.0<*	*1.6*	*0.5*	*1.4*	*4.9*	*19.9*	*6.1*	*1.5*	*5.8*	*0.60*	*7.5*	*1.5*	*1.2*	*54.68*
LC102,9	*2.2*	*0.08*	*0.2*	*1.0*	*0.3*	*0.9*	*10.0*	*18.0*	*3.7*	*1.5*	*2.0*	*0.72*	*4.4*	*1.6*	*1.5*	*48.02*
LC102,10	*0.8*	*.01<*	*-.0<*	*1.1*	*0.3*	*0.3*	*14.5*	*22.6*	*3.7*	*1.6*	*1.2*	*0.40*	*5.1*	*0.9*	*1.9*	*54.32*
Average first 7	2.20	0.07	0.20	1.32	0.30	0.71	15.77	22.70	3.73	1.71	2.37	0.38	4.32	0.87	1.93	58.58
STDS	0.65	0.01	0.00	0.42	0.11	0.35	3.26	2.63	0.87	0.43	0.61	0.12	0.56	0.38	0.33	2.26
RSD	29%	22%	0%	32%	37%	49%	21%	12%	23%	25%	26%	32%	13%	43%	17%	4%
CP103																
LC103,1	3.4	0.12	0.2	1.6	0.4	0.5	11.3	24.0	4.6	1.3	2.6	0.98	2.3	1.0	1.4	55.75
LC103,2	2.7	0.12	0.2	1.2	0.3	0.5	14.0	26.0	5.0	1.2	3.1	1.99	2.8	1.0	1.4	61.62
LC103,3	3.4	0.15	0.2	1.4	0.4	0.4	14.7	25.5	5.0	1.2	2.8	1.07	3.0	0.9	1.4	61.49
LC103,4	*5.0	0.17	0.4	1.9	0.4	0.5	13.2	24.0	5.0	0.9	1.9	0.55	2.9	*1.4	1.4	59.43
LC103,5	3.4	0.14	0.3	1.6	0.3	0.5	12.5	25.6	4.3	1.3	2.0	0.97	3.8	1.1	1.4	58.99
LC103,6	2.8	0.12	0.2	1.3	0.3	0.4	12.8	26.8	4.8	1.2	2.8	1.16	2.7	1.0	1.3	59.75
LC103,7	3.3	0.13	.1<	1.2	0.3	0.4	15.7	24.3	*6.7	1.0	3.4	2.04	3.0	1.2	1.7	64.43
LC103,8	3.8	0.19	0.3	1.9	0.3	0.5	15.6	23.8	5.4	1.0	2.4	0.78	2.7	0.8	1.7	61.31
LC103,9	3.3	0.15	0.2	1.4	0.3	0.4	13.1	27.8	5.5	1.4	1.9	0.72	3.4	1.1	1.3	62.17
LC103,10	4.1	0.15	0.3	1.7	0.4	0.6	12.9	26.3	5.0	1.4	3.5	1.44	3.4	0.8	1.4	63.39
LC103,11	3.6	0.18	0.2	1.9	0.4	0.6	11.0	26.7	4.3	1.0	2.0	0.80	2.5	1.2	1.4	57.68
LC103,12	3.0	0.15	0.2	1.2	0.4	0.3	12.2	26.8	6.0	1.2	3.5	1.94	2.7	1.2	1.6	62.37
LC103,13	*4.4	0.17	0.3	2.0	0.4	0.5	10.9	28.6	5.1	0.9	2.6	1.26	2.5	1.2	1.2	62.13
LC103,14	2.8	0.15	0.2	1.9	0.4	0.3	12.5	24.6	*7.1	*1.8	*4.1	1.22	*5.1	1.1	1.3	64.61
LC103,15	3.8	0.20	0.3	*2.3	0.5	0.7	*4.3	28.7	*7.8	*1.9	2.5	1.75	3.8	0.5	*0.7	59.80
LC103,16	2.9	0.16	*2.1	1.3	.1<	.1<	20.1	21.2	5.3	1.1	1.7	0.83	2.3	1.2	*2.0	62.20
LC103,17	2.6	*0.08	0.3	1.0	.1<	.2<	*22.3	21.0	5.1	1.1	1.7	0.48	1.7	0.6	1.7	59.53
LC103,18	3.4	0.20	0.2	1.9	0.5	0.7	12.8	20.6	5.4	1.4	2.4	1.39	2.4	1.1	1.4	55.90
LC103,19	2.6	0.16	.1<	1.7	0.4	0.4	16.5	21.5	4.9	1.4	2.6	1.65	2.5	1.1	1.6	58.85
LC103,20	*2.6*	*0.12*	*.1<*	*1.2*	*0.4*	*0.4*	*11.8*	*21.1*	*4.8*	*1.7*	*3.4*	*1.76*	*2.0*	*1.2*	*1.4*	*54.06*
LC103,21	*15.7*	*0.24*	*7.6*	*2.7*	*0.3*	*0.3*	*9.1*	*21.9*	*6.9*	*1.1*	*1.7*	*0.91*	*1.3*	*0.7*	*1.2*	*71.74*
LC103,22	*26.4*	*0.46*	*9.6*	*5.2*	*0.5*	*0.5*	*3.8*	*21.2*	*6.9*	*0.9*	*1.7*	*0.61*	*1.9*	*0.6*	*1.0*	*81.12*
LC103,23	*15.1*	*0.23*	*6.9*	*2.5*	*0.2*	*0.3*	*13.9*	*19.1*	*6.7*	*0.7*	*1.9*	*0.89*	*1.5*	*0.9*	*1.3*	*72.09*
LC103,24	*40.3*	*0.36*	*19.3*	*5.0*	*0.2*	*0.2*	*3.4*	*14.2*	*7.1*	*.2<*	*1.7*	*0.24*	*0.2*	*.1<*	*0.9*	*93.35*
Average first 19	3.23	0.16	0.25	1.56	0.38	0.48	13.64	24.94	5.04	1.18	2.52	1.21	2.80	1.01	1.45	59.83
STDS	0.45	0.03	0.06	0.32	0.07	0.12	2.32	2.51	0.44	0.18	0.59	0.49	0.54	0.21	0.15	2.53
RSD	14%	16%	25%	20%	18%	25%	17%	10%	9%	15%	23%	40%	19%	21%	11%	4%
CP109																
CP109,1	*0.5*	*.03<*	*.1<*	*0.5*	*0.3*	*-.0<*	*19.1*	*20.9*	*3.0*	*1.4*	*0.8*	*0.47*	*3.3*	*0.7*	*1.9*	*52.85*
CP109,2	*2.1*	*0.12*	*0.2*	*2.0*	*0.4*	*0.3*	*16.0*	*17.0*	*2.9*	*1.1*	*1.5*	*0.34*	*2.8*	*1.0*	*1.5*	*49.35*
CP109,3	*0.6*	*0.05*	*.1<*	*0.7*	*.2<*	*.1<*	*10.3*	*18.9*	*2.8*	*1.1*	*2.3*	*0.63*	*4.3*	*0.9*	*1.3*	*43.81*
CP109,4	*1.6*	*0.07*	*0.2*	*1.6*	*0.4*	*0.2*	*14.9*	*18.1*	*2.7*	*1.1*	*1.2*	*0.32*	*3.5*	*0.9*	*1.6*	*48.40*
CP109,5	*0.7*	*0.03*	*.1<*	*0.7*	*0.3*	*.1<*	*6.1*	*14.1*	*1.9*	*0.8*	*2.0*	*0.58*	*3.9*	*0.9*	*0.9*	*32.87*
CP109,6	1.2	0.06	.1<	0.9	0.3	.1<	22.3	22.5	3.7	1.5	1.2	0.21	3.4	0.6	2.1	60.10
CP109,7	2.0	0.09	0.2	1.8	0.4	0.2	17.6	22.0	4.2	1.1	1.9	*1.95	3.2	0.9	2.0	59.51
CP109,8	1.9	0.08	.1<	1.7	0.4	.2<	17.6	22.0	3.4	1.5	3.0	0.67	4.0	*1.5	2.2	60.04
CP109,9	1.1	0.06	.1<	1.1	.2<	.1<	21.9	21.4	3.6	1.5	1.6	0.20	3.0	0.7	2.2	58.36
CP109,10	1.6	0.05	0.2	1.4	0.4	0.3	18.1	22.8	4.0	1.3	4.1	*0.94	4.4	1.1	2.1	62.79
CP109,11	1.4	0.04	0.2	1.2	0.2	0.3	19.3	20.8	3.4	1.3	4.1	0.56	3.2	1.0	2.0	58.87
CP109,12	1.2	0.05	.1<	1.3	0.2	.1<	19.3	22.3	3.2	1.5	1.8	0.26	3.6	0.7	2.1	57.63
Average last 7	1.49	0.06	0.20	1.34	0.32	0.27	19.44	21.97	3.64	1.39	2.53	0.38	3.54	0.83	2.10	59.50
STDS	0.36	0.02	0.00	0.32	0.10	0.06	1.95	0.68	0.36	0.16	1.21	0.22	0.50	0.20	0.08	1.66
RSD	24%	29%	0%	24%	31%	22%	10%	3%	10%	11%	48%	58%	14%	24%	4%	3%
CP111																
LC111,1	4.6	0.25	0.2	1.6	.1<	0.3	15.7	26.8	7.7	1.2	3.3	1.75	3.1	1.0	1.7	69.15
LC111,2	3.1	0.17	.1<	1.4	0.2	0.3	14.7	29.1	6.5	1.3	3.6	1.89	2.9	1.0	1.5	67.65
LC111,3	3.1	0.19	.1<	1.0	0.3	.1<	14.8	30.0	7.1	1.3	4.5	2.40	3.1	1.2	1.5	70.46
LC111,4	3.6	0.16	0.2	1.3	0.2	0.3	14.8	29.3	6.7	1.4	2.5	2.80	2.8	0.8	1.4	68.59
LC111,5	4.2	0.19	0.2	1.5	0.2	.1<	15.1	28.7	7.0	1.2	3.2	2.40	2.8	0.9	1.3	68.80
LC111,6	4.4	0.24	0.2	1.5	0.2	0.3	14.9	28.6	7.2	1.3	*2.0	*3.20	2.8	1.1	1.3	69.41
LC111,7	4.0	0.17	0.2	1.4	.2<	0.3	15.5	27.3	7.5	1.3	2.5	1.85	3.0	0.9	1.5	67.34
LC111,8	3.9	0.18	0.2	1.3	.2<	0.3	14.9	27.5	6.8	1.4	2.3	1.58	3.1	1.3	1.6	66.28
LC111,9	4.3	0.20	*0.3	1.5	*0.4	0.3	15.0	30.0	6.8	1.4	3.2	2.20	2.8	1.1	1.4	70.96
LC111,10	3.3	0.17	.1<	0.9	0.3	.2<	15.3	29.1	6.4	1.4	3.5	2.20	2.8	1.1	1.4	67.93
Average	3.85	0.19	0.20	1.34	0.23	0.30	15.07	28.64	6.97	1.32	3.18	2.12	2.92	1.04	1.46	68.83
STDS	0.55	0.03	0.00	0.23	0.05	0.00	0.33	1.11	0.42	0.08	0.68	0.39	0.14	0.15	0.13	1.43
RSD	14%	16%	0%	17%	22%	0%	2%	4%	6%	6%	22%	18%	5%	14%	9%	2%

Sample	SiO2	TiO2	Al2O3	FeO	MnO	MgO	CaO	Na2O	K2O	P2O5	F	Cl	SO3	BaO	SrO	Total
CP114																
LC114,1	10.2	0.15	1.8	1.4	0.3	0.2	16.3	24.2	3.9	*1.9	2.8	0.66	2.3	0.7	1.4	68.23
LC114,2	*10.8	0.19	2.8	2.4	.2<	0.6	15.2	24.2	4.6	1.3	2.3	0.65	2.3	1.0	1.6	69.82
LC114,3	6.8	0.24	2.2	1.9	0.3	0.3	14.0	26.3	5.6	1.5	2.2	0.89	2.5	1.2	1.4	67.31
LC114,4	*11.8	0.10	2.6	1.9	0.2	0.5	16.9	23.0	5.9	1.1	2.9	0.80	2.0	1.3	1.6	72.42
LC114,5	4.6	0.07	0.8	1.0	0.3	0.3	14.0	26.7	5.0	1.3	2.2	0.58	2.4	1.2	1.7	62.07
LC114,6	9.8	0.19	4.0	2.6	0.4	0.5	14.6	24.5	5.4	1.4	1.7	0.71	1.9	0.8	1.6	70.05
LC114,7	*14.6*	*0.57*	*7.4*	*4.3*	*.2<*	*.1<*	*11.9*	*22.4*	*5.8*	*1.1*	*2.2*	*0.75*	*2.0*	*0.9*	*1.0*	*74.91*
LC114,8	*12.3*	*0.17*	*2.3*	*2.5*	*0.4*	*0.7*	*17.0*	*23.7*	*4.9*	*1.4*	*3.9*	*1.17*	*2.4*	*0.9*	*1.9*	*75.52*
LC114,9	*14.6*	*0.29*	*5.6*	*3.0*	*0.3*	*0.9*	*14.8*	*21.0*	*5.2*	*1.0*	*3.1*	*0.67*	*1.9*	*0.8*	*1.8*	*75.10*
Average first 6	7.85	0.16	2.37	1.87	0.30	0.40	15.17	24.82	5.07	1.32	2.35	0.72	2.23	1.03	1.55	67.19
STDS	2.65	0.06	1.07	0.60	0.07	0.15	1.21	1.41	0.73	0.15	0.44	0.11	0.23	0.24	0.12	3.53
RSD	34%	40%	45%	32%	24%	39%	8%	6%	14%	11%	19%	16%	10%	23%	8%	5%
CP115																
LC115,1	*12.4*	*0.35*	*2.4*	*2.3*	*0.3*	*0.6*	*15.0*	*24.0*	*5.0*	*1.2*	*1.8*	*1.50*	*2.1*	*1.0*	*1.2*	*71.10*
LC115,2	*10.7*	*0.28*	*2.4*	*2.8*	*0.4*	*0.8*	*13.7*	*22.7*	*5.8*	*0.8*	*2.0*	*1.65*	*2.3*	*0.8*	*1.4*	*68.62*
LC115,3	*13.4*	*0.35*	*2.4*	*2.3*	*b.d.*	*0.6*	*15.0*	*24.0*	*5.0*	*1.2*	*1.8*	*1.50*	*2.1*	*1.0*	*1.2*	*70.79*
LC115,4	*10.7*	*0.28*	*2.4*	*2.8*	*0.4*	*0.8*	*13.7*	*22.7*	*5.8*	*0.8*	*2.0*	*1.65*	*2.3*	*0.8*	*1.4*	*68.62*
LC115,5	6.5	0.09	1.0	1.2	0.3	0.2	12.9	26.7	5.7	1.0	2.1	1.22	2.4	1.1	1.2	63.71
LC115,6	8.5	0.11	2.9	1.6	0.4	0.6	11.5	26.9	6.3	0.9	1.9	1.92	2.1	0.8	1.3	67.68
LC115,7	5.8	0.10	2.3	1.5	0.2	0.2	11.6	27.6	6.0	1.2	2.2	1.43	2.1	1.0	1.4	64.59
LC115,8	6.5	0.09	1.0	1.2	0.3	b.d.	12.9	26.7	5.7	1.0	2.1	1.22	2.4	1.1	1.2	63.48
LC115,9	8.5	0.11	2.9	1.6	0.4	0.6	11.5	26.9	6.3	0.9	1.9	1.92	2.1	0.8	1.3	67.68
LC115,10	5.8	0.10	2.3	1.5	b.d.	b.d.	11.6	27.6	6.0	1.2	2.2	1.43	2.1	1.0	1.4	64.14
Average first 6	6.92	0.10	2.06	1.42	0.33	0.40	12.01	27.07	5.98	1.04	2.06	1.52	2.19	0.98	1.32	65.40
STDS	1.25	0.01	0.87	0.19	0.08	0.23	0.69	0.42	0.26	0.13	0.12	0.32	0.17	0.14	0.09	1.95
RSD	18%	10%	42%	14%	26%	57%	6%	2%	4%	13%	6%	21%	8%	14%	7%	3%
CP117																
LC117,1	*0.6	0.08	.1<	0.9	0.4	0.4	15.2	27.1	3.5	1.5	1.4	0.33	2.8	0.6	1.5	56.41
LC117,2	3.3	0.09	1.5	1.3	0.4	0.3	15.4	25.6	3.7	1.1	*1.7	0.53	2.5	0.5	1.1	59.07
LC117,3	3.5	0.09	1.3	1.2	0.3	.1<	15.3	24.5	4.3	1.1	1.2	0.90	1.9	0.8	1.4	57.76
LC117,4	4.0	0.09	2.7	1.1	.2<	.1<	15.2	24.0	5.8	1.1	0.4	*1.93	2.0	0.7	1.4	60.32
LC117,5	8.7	0.16	3.5	1.9	0.3	0.3	13.6	23.5	5.2	1.1	1.1	1.24	2.2	0.5	1.2	64.66
LC117,6	3.9	0.14	1.6	1.3	0.3	0.2	13.8	24.8	5.0	1.2	0.6	1.19	2.3	0.6	1.3	58.30
LC117,7	4.8	0.15	1.8	1.5	0.3	0.5	11.9	24.0	4.2	1.0	0.3	1.13	2.1	0.7	1.1	55.46
LC117,8	8.0	0.11	*4.4	1.6	0.3	0.2	13.1	24.1	4.5	0.9	1.0	0.47	2.5	0.8	1.1	63.09
LC117,9	6.3	0.14	1.5	2.5	0.4	0.4	13.1	22.6	3.8	1.1	0.7	0.44	2.7	0.4	0.9	56.95
LC117,10	9.0	0.15	*5.0	2.2	0.3	0.4	11.4	23.1	4.0	0.9	1.4	0.76	2.1	0.4	1.0	62.05
LC117,11	8.5	0.15	3.2	2.2	0.3	0.5	12.1	20.4	5.8	*0.4	*1.9	*2.20	*1.6	0.9	0.9	61.11
LC117,12	*10.0*	*0.16*	*2.2*	*3.0*	*0.5*	*0.5*	*12.1*	*21.3*	*4.2*	*1.2*	*1.0*	*0.53*	*2.7*	*0.8*	*1.1*	*61.27*
LC117,13	*4.6*	*0.15*	*1.7*	*1.6*	*0.3*	*0.4*	*11.9*	*19.8*	*3.3*	*1.0*	*0.9*	*0.27*	*2.3*	*0.5*	*1.1*	*49.83*
LC117,14	*6.6*	*0.11*	*4.6*	*1.3*	*0.2*	*0.2*	*8.1*	*19.1*	*4.7*	*0.8*	*1.4*	*1.76*	*1.9*	*0.7*	*0.8*	*52.32*
Average first 11	6.00	0.12	2.14	1.61	0.33	0.36	13.65	23.97	4.53	1.10	0.90	0.78	2.31	0.63	1.17	59.59
STDS	2.36	0.03	0.86	0.52	0.05	0.11	1.47	1.70	0.81	0.17	0.42	0.35	0.30	0.17	0.21	2.94
RSD	39%	25%	40%	32%	15%	32%	11%	7%	18%	15%	46%	45%	13%	27%	18%	5%
CP120																
LC120,1	4.0	0.21	0.2	1.4	0.3	0.4	15.6	28.6	6.7	1.4	2.1	2.30	3.2	0.8	1.5	68.62
LC120,2	5.1	0.18	0.4	1.3	.2<	0.4	15.8	26.3	6.5	1.3	2.7	1.95	3.0	1.0	1.5	67.47
LC120,3	5.3	0.20	0.3	1.4	.2<	0.3	14.8	29.1	6.6	1.6	2.5	2.50	3.2	0.7	1.3	69.85
LC120,4	5.4	0.20	0.4	1.7	0.2	0.3	17.4	25.8	6.0	1.3	2.2	0.96	2.6	0.9	1.6	67.02
LC120,5	5.7	0.23	0.5	1.5	0.3	0.5	17.9	22.9	8.4	1.2	2.1	2.60	2.5	1.0	1.8	69.19
LC120,6	5.3	0.23	0.4	1.7	0.2	0.4	15.2	25.8	5.9	1.5	1.6	1.82	3.0	0.6	1.3	64.94
LC120,7	4.5	0.17	0.3	1.4	0.3	0.3	16.8	23.2	5.8	1.4	2.2	1.16	2.8	1.1	1.7	63.00
LC120,8	3.8	0.14	0.2	0.9	0.3	0.4	*7.5	31.4	8.4	1.0	*6.7	*5.60	3.6	1.1	1.0	71.86
LC120,9	5.3	0.18	0.4	1.6	0.3	0.5	13.4	28.9	5.7	1.6	2.2	1.73	3.8	0.9	1.1	67.59
LC120,10	6.1	0.24	0.4	1.9	.1<	0.3	11.9	28.5	4.0	1.2	*5.1	0.74	*4.0	1.2	1.1	66.54
LC120,11	5.3	0.20	0.3	1.8	.1<	0.4	13.9	25.6	7.2	0.9	2.2	*3.20	3.2	1.2	1.2	66.47
LC120,12	6.4	0.27	0.3	2.0	0.3	0.4	13.3	26.5	8.2	1.3	2.8	*3.20	3.2	0.9	1.3	70.43
LC120,13	5.7	0.23	0.4	1.9	0.3	0.5	15.7	25.8	8.0	1.2	1.9	2.60	3.1	0.7	1.3	69.29
LC120,14	4.6	0.20	0.4	1.2	0.2	0.3	15.8	26.1	6.5	1.4	1.7	1.69	2.9	1.0	1.1	65.11
LC120,15	1.7	0.07	0.4	0.7	0.4	0.4	15.4	24.6	5.0	1.1	1.5	1.61	2.4	1.3	1.4	58.15
LC120,16	6.5	0.39	*2.2	1.6	*0.5	0.3	13.3	24.5	4.0	1.3	1.5	*0.49	2.6	1.1	1.3	61.46
LC120,17	7.4	*1.57	*1.3	*3.9	0.3	0.4	14.3	23.5	4.4	0.9	2.7	1.22	2.8	1.1	0.9	66.82
LC120,18	3.9	0.08	*1.3	1.2	0.4	0.4	12.1	23.3	5.1	1.1	2.9	1.85	2.5	1.1	1.3	58.50
LC120,19	5.3	0.10	*1.2	1.3	0.3	0.5	14.4	25.2	3.7	1.3	1.8	*0.31	2.9	1.1	1.2	60.57
LC120,20	7.5	0.11	*2.4	1.8	0.4	0.4	13.7	24.4	3.7	1.1	2.8	*0.25	2.6	1.1	1.6	63.96
LC120,21	*9.5	0.10	*3.0	2.2	0.3	*0.7	12.0	19.4	5.6	0.9	1.1	2.30	2.0	0.7	1.0	60.70
LC120,22	*9.5	0.12	*4.8	1.3	0.2	.1<	10.8	20.1	3.4	1.1	1.4	*0.20	2.3	0.7	0.9	56.94
LC120,23	*10.9*	*0.14*	*2.5*	*2.5*	*0.3*	*0.4*	*14.3*	*23.5*	*4.4*	*1.2*	*2.1*	*0.26*	*2.4*	*0.8*	*1.3*	*66.99*
LC120,24	*3.0*	*0.10*	*1.1*	*1.1*	*0.3*	*0.3*	*12.9*	*18.2*	*4.0*	*1.0*	*0.9*	*0.94*	*2.2*	*0.9*	*1.1*	*47.93*
Average first 22	5.24	0.18	0.35	1.51	0.29	0.39	14.45	25.43	5.85	1.23	2.10	1.80	2.88	0.97	1.29	63.98
STDS	1.31	0.07	0.08	0.37	0.07	0.07	1.87	2.85	1.58	0.21	0.53	0.59	0.43	0.20	0.25	4.27
RSD	25%	41%	24%	24%	22%	18%	13%	11%	27%	17%	25%	33%	15%	20%	19%	7%

Sample	SiO2	TiO2	Al2O3	FeO	MnO	MgO	CaO	Na2O	K2O	P2O5	F	Cl	SO3	BaO	SrO	Total
CP121																
LC121,1	5.8	0.21	0.4	1.4	.1<	0.5	13.1	21.5	8.2	*0.8	2.8	2.60	3.3	1.0	1.2	62.76
LC121,2	4.4	0.22	0.2	1.1	.1<	0.2	17.2	21.8	9.3	1.4	1.1	1.35	*2.5	0.8	1.2	62.91
LC121,3	3.4	0.12	0.2	1.0	.1<	0.3	14.6	24.6	6.6	1.2	1.9	3.00	3.5	1.0	1.1	62.58
LC121,4	4.3	0.19	0.2	1.2	0.3	0.4	16.1	24.6	8.1	1.3	1.5	1.89	2.8	0.9	1.2	64.98
LC121,5	5.5	0.23	0.4	1.4	0.3	.2<	16.5	27.6	6.7	1.5	1.9	*0.82	3.4	0.5	1.3	67.82
LC121,6	5.0	0.22	0.2	1.5	.2<	0.5	11.1	*31.8	7.8	1.3	4.5	3.80	4.0	1.0	*1.0	73.75
LC121,7	5.4	0.21	0.3	1.4	0.3	0.5	12.9	28.3	9.2	1.0	*5.4	3.00	4.0	1.1	1.4	74.25
LC121,8	5.8	0.22	0.3	1.7	0.3	0.4	15.0	26.3	8.1	1.4	2.1	2.30	3.5	1.1	1.5	69.85
LC121,9	4.5	0.18	0.3	1.4	0.2	0.4	13.8	28.3	7.7	1.6	3.0	2.50	4.1	1.0	1.1	70.03
LC121,10	6.1	*0.29	0.4	1.6	0.2	0.4	14.1	26.1	7.9	1.6	2.5	2.60	3.2	1.1	1.3	69.50
LC121,11	5.7	*0.29	0.3	1.6	0.2	0.3	15.4	26.4	6.4	1.8	1.5	1.84	3.4	1.0	1.2	67.31
LC121,12	5.1	0.21	0.4	1.6	.2<	0.3	14.4	27.0	5.8	1.7	1.1	1.28	3.2	0.6	1.2	64.01
LC121,13	5.6	0.23	0.3	1.4	.1<	*0.6	10.2	26.2	5.3	*0.7	3.2	*6.90	3.4	*1.9	1.2	67.02
LC121,14	3.6	0.15	0.2	0.8	0.2	0.5	*9.3	25.8	5.0	*0.6	*7.6	*4.80	3.5	*1.7	1.1	64.77
LC121,15	4.8	0.18	0.3	1.1	.1<	0.4	12.9	25.7	6.1	1.0	*6.6	3.80	*2.7	0.8	1.2	67.69
LC121,16	3.0	0.18	-.0<	0.7	.1<	0.3	15.5	28.4	5.0	1.7	3.3	*0.27	4.1	0.8	1.4	64.57
LC121,17	5.5	0.18	0.3	1.7	0.3	0.5	13.8	26.8	5.6	1.2	2.3	1.49	*4.5	1.0	1.2	66.27
LC121,18	3.4	0.13	.1<	1.0	.2<	0.3	15.3	27.3	5.4	1.6	2.3	*0.63	3.8	0.7	1.4	63.25
LC121,19	3.4	0.15	.1<	0.9	0.2	0.2	17.3	27.3	5.4	*2.1	1.3	*0.23	3.4	*0.4	*1.6	63.86
LC121,20	*7.4*	*0.48*	*0.2*	*3.2*	*0.6*	*0.8*	*14.3*	*17.1*	*5.8*	*0.9*	*2.6*	*0.35*	*2.6*	*1.7*	*1.3*	*59.31*
Average first 19	4.75	0.19	0.29	1.29	0.25	0.38	14.40	26.11	6.82	1.42	2.27	2.42	3.54	0.90	1.25	66.28
STDS	0.99	0.03	0.08	0.31	0.05	0.10	1.92	1.97	1.42	0.25	0.93	0.84	0.37	0.18	0.12	3.52
RSD	21%	18%	26%	24%	21%	27%	13%	8%	21%	18%	41%	35%	10%	20%	9%	5%
CP122																
LC122,1	*13.3*	*0.43*	*5.9*	*2.7*	*0.2*	*0.7*	*10.4*	*20.9*	*6.7*	*0.8*	*3.6*	*2.40*	*2.6*	*0.7*	*1.1*	*72.54*
LC122,2	*3.3*	*0.03*	*0.9*	*1.2*	*.1<*	*0.6*	*10.3*	*17.3*	*7.2*	*1.2*	*2.6*	*1.24*	*2.6*	*1.2*	*1.6*	*51.24*
LC122,3	*1.3*	*0.04*	*.1<*	*0.8*	*.1<*	*0.5*	*8.5*	*18.5*	*4.9*	*0.7*	*2.4*	*0.52*	*2.2*	*1.3*	*1.3*	*42.80*
LC122,4	*1.8*	*.02<*	*0.7*	*0.7*	*.1<*	*0.3*	*10.0*	*22.7*	*6.6*	*1.3*	*2.3*	*3.10*	*2.9*	*1.0*	*1.3*	*54.72*
LC122,5	*22.0*	*0.33*	*12.4*	*3.5*	*.2<*	*0.5*	*8.3*	*17.3*	*7.0*	*0.5*	*1.3*	*1.01*	*1.7*	*1.1*	*0.9*	*78.01*
LC122,6	*21.5*	*0.53*	*9.9*	*4.4*	*0.3*	*0.8*	*8.8*	*20.2*	*5.9*	*0.7*	*1.7*	*1.15*	*1.7*	*0.7*	*.3<*	*78.26*
LC122,7	*20.7*	*0.38*	*10.8*	*4.0*	*0.3*	*0.5*	*7.0*	*20.4*	*6.7*	*0.7*	*1.9*	*0.92*	*1.6*	*0.7*	*.2<*	*76.69*
LC122,8	*31.9*	*0.35*	*9.7*	*3.5*	*0.4*	*0.3*	*13.0*	*18.1*	*5.1*	*0.4*	*1.2*	*1.14*	*1.2*	*0.6*	*-.0<*	*86.87*
LC122,9	*10.8*	*0.11*	*6.3*	*1.6*	*.1<*	*0.4*	*8.3*	*25.3*	*5.0*	*1.1*	*2.9*	*2.20*	*2.5*	*0.9*	*1.1*	*68.46*
LC122,10	*13.2*	*0.34*	*6.9*	*2.8*	*0.3*	*0.5*	*8.9*	*23.2*	*7.4*	*1.4*	*1.9*	*0.94*	*1.9*	*0.8*	*0.9*	*71.28*
LC122,11	*14.6*	*0.31*	*6.0*	*3.4*	*0.3*	*0.9*	*10.4*	*20.3*	*7.5*	*1.0*	*3.1*	*2.20*	*2.4*	*1.0*	*1.1*	*74.55*
LC122,12	*12.6*	*0.39*	*6.4*	*3.4*	*0.4*	*0.4*	*8.6*	*20.3*	*6.8*	*0.8*	*1.4*	*2.50*	*1.9*	*1.2*	*0.7*	*67.81*
LC122,13	6.3	0.10	3.4	1.3	0.3	0.5	10.0	22.1	7.9	0.8	*3.8	2.90	2.7	1.2	1.2	64.28
LC122,14	6.6	0.17	2.6	1.6	0.3	0.6	10.7	20.4	6.9	1.0	2.4	1.52	2.4	1.2	1.5	59.93
LC122,15	*9.3	0.12	*4.2	1.8	0.3	0.3	10.6	17.9	10.2	0.9	2.1	3.50	1.5	1.1	1.1	65.09
LC122,16	5.1	0.10	2.2	1.1	0.2	0.5	8.2	21.6	7.2	1.0	2.1	3.40	2.7	1.1	1.1	57.80
LC122,17	*1.3	.03<	.1<	*0.6	0.3	0.4	9.0	24.6	8.3	0.8	*3.9	*8.40	2.4	1.4	1.5	60.83
LC122,18	3.6	*0.25	*1.0	1.3	0.2	0.5	9.8	24.8	6.9	1.6	2.6	*4.10	*3.8	0.9	1.2	62.53
LC122,19	5.4	0.11	2.7	1.3	0.3	0.3	10.8	24.7	6.7	1.7	*4.5	1.82	2.5	1.3	1.3	65.39
Average last 7	5.40	0.12	2.73	1.40	0.27	0.44	9.87	22.30	7.73	1.11	2.30	2.63	2.37	1.17	1.27	61.11
STDS	1.18	0.03	0.50	0.25	0.05	0.11	0.97	2.61	1.24	0.38	0.24	0.91	0.45	0.16	0.17	2.87
RSD	22%	24%	18%	18%	18%	26%	10%	12%	16%	34%	11%	35%	19%	14%	13%	5%
CP123																
LC123,1	*9.8*	*0.28*	*5.5*	*1.9*	*0.2*	*0.2*	*8.4*	*14.7*	*5.5*	*0.6*	*1.8*	*0.38*	*1.3*	*0.9*	*0.6*	*52.04*
LC123,2	*13.2*	*0.15*	*4.8*	*2.0*	*.1<*	*1.0*	*9.8*	*13.2*	*4.0*	*0.7*	*1.9*	*0.36*	*1.2*	*0.5*	*0.8*	*53.64*
LC123,3	*9.8*	*0.10*	*5.0*	*1.5*	*.2<*	*0.5*	*8.6*	*15.8*	*5.2*	*0.6*	*2.6*	*0.59*	*1.6*	*0.8*	*0.9*	*53.41*
LC123,4	*2.6*	*0.20*	*0.7*	*1.0*	*.2<*	*0.2*	*10.4*	*21.0*	*6.5*	*1.1*	*2.1*	*1.76*	*2.3*	*1.1*	*1.3*	*52.36*
LC123,5	*13.3*	*0.20*	*8.4*	*2.0*	*.1<*	*0.4*	*7.9*	*15.7*	*5.8*	*0.9*	*1.8*	*0.77*	*0.8*	*0.7*	*0.6*	*59.44*
LC123,6	*11.1*	*0.28*	*6.8*	*2.1*	*0.3*	*0.4*	*7.6*	*16.0*	*5.2*	*0.8*	*1.7*	*0.89*	*1.2*	*0.7*	*0.8*	*55.90*
LC123,7	*17.9*	*0.37*	*6.9*	*2.1*	*0.2*	*0.3*	*14.4*	*19.6*	*6.2*	*0.8*	*1.9*	*1.91*	*1.5*	*0.5*	*.3<*	*74.54*
LC123,8	*16.9*	*0.38*	*10.4*	*3.4*	*.1<*	*0.3*	*9.4*	*20.0*	*7.8*	*1.2*	*2.0*	*0.86*	*1.5*	*0.8*	*0.6*	*75.55*
LC123,9	9.4	0.15	5.1	2.4	.1<	0.4	8.9	21.5	4.5	1.0	1.8	*0.21	2.6	0.6	1.0	59.64
LC123,10	8.8	0.10	6.2	1.1	.2<	0.4	7.9	19.1	6.1	1.0	2.6	0.60	1.8	0.9	1.0	57.60
LC123,11	4.9	0.49	2.1	1.7	0.2	0.4	10.5	20.4	6.3	1.3	2.3	1.12	2.0	1.0	1.4	56.21
LC123,12	8.2	0.26	4.2	2.0	0.2	0.7	8.9	18.0	5.9	0.4	*3.2	1.79	1.3	1.1	0.9	57.02
LC123,13	4.6	0.16	2.0	1.2	0.2	0.2	11.1	24.0	7.8	1.4	1.8	1.01	2.1	1.2	1.2	60.11
LC123,14	9.1	0.44	1.9	1.9	0.3	0.3	13.1	25.1	5.8	1.4	1.9	1.37	2.3	1.0	1.0	66.86
LC123,15	5.7	.01<	.0<	0.3	0.2	.2<	*17.4	23.9	7.3	1.4	1.8	0.76	*3.3	1.1	*1.7	64.87
LC123,16	2.2	.01<	.1<	.2<	0.3	0.3	10.3	28.6	6.1	*2.5	1.6	1.32	2.7	0.8	1.3	58.06
LC123,17	3.3	.02<	1.9	0.5	.2<	.2<	10.9	24.4	*10.5	1.3	1.9	*2.11	2.5	1.0	1.2	61.52
Average last 9	6.24	0.27	3.34	1.39	0.23	0.39	10.20	22.78	6.23	1.15	1.96	1.14	2.16	0.97	1.13	59.57
STDS	2.70	0.16	1.80	0.74	0.05	0.16	1.62	3.32	1.00	0.35	0.32	0.40	0.47	0.18	0.18	3.63
RSD	43%	61%	54%	53%	22%	41%	16%	15%	16%	30%	17%	35%	22%	19%	16%	6%
CP124																
LC124,2	6.2	0.12	*0.6	0.6	0.3	.1<	12.0	17.6	9.4	*2.1	2.6	1.09	3.1	1.0	1.3	57.77
LC124,3	9.2	0.07	1.7	1.0	0.3	0.3	11.5	17.0	8.0	0.7	1.8	0.76	2.8	1.0	1.3	57.51
LC124,6	*10.6	0.21	2.6	1.7	0.3	0.5	11.0	15.4	9.7	1.1	2.0	1.24	2.4	0.9	1.1	60.70

Sample	SiO2	TiO2	Al2O3	FeO	MnO	MgO	CaO	Na2O	K2O	P2O5	F	Cl	SO3	BaO	SrO	Total
LC124,7	6.2	0.16	1.6	1.7	0.2	0.4	10.9	19.2	7.9	1.0	2.4	0.76	2.3	1.2	1.7	57.73
LC124,1	4.9	0.04	.1<	0.6	.1<	.2<	10.8	19.4	7.7	0.9	1.8	1.02	2.1	0.9	1.6	51.79
LC124,4	1.5	0.06	0.2	1.7	0.2	.1<	10.7	20.5	7.9	1.1	1.6	0.68	2.3	1.4	2.0	51.84
LC124,5	2.0	0.11	0.3	1.1	.2<	.2<	11.1	20.2	8.0	1.3	1.5	0.68	2.5	1.3	1.9	52.00
LC124,8	16.3	0.55	5.4	5.2	0.3	0.4	10.9	19.7	5.4	1.2	2.2	0.42	1.8	0.6	0.7	71.15
LC124,9	19.5	0.55	6.8	5.1	0.3	0.5	11.7	17.4	6.9	1.2	1.9	1.01	1.2	0.7	0.8	75.50
LC124,10	14.9	0.29	6.2	3.0	0.3	0.2	9.9	17.5	7.3	1.9	1.5	0.75	1.2	1.1	0.8	66.80
LC124,11	16.0	0.35	3.5	2.9	0.2	0.6	13.6	11.0	7.6	0.5	1.7	0.71	2.0	0.9	1.2	62.92
LC124,12	15.4	0.25	2.9	2.4	.2<	0.4	13.4	12.8	7.1	1.0	2.0	1.47	1.6	0.7	0.9	62.39
LC124,13	12.6	0.20	2.2	2.6	0.2	0.5	12.3	16.0	7.7	1.4	2.8	1.46	3.6	0.9	1.0	65.43
LC124,14	14.3	0.36	4.1	4.0	0.3	0.9	10.5	20.7	6.2	1.5	1.8	0.32	4.0	0.7	0.9	70.50
LC124,15	13.4	0.17	3.7	2.2	0.2	0.4	11.9	16.8	7.6	1.6	2.3	1.34	1.6	0.8	0.9	65.05
LC124,16	20.7	0.43	4.4	4.5	0.5	0.9	13.0	12.2	6.6	0.4	1.5	0.81	1.7	0.6	.4<	68.22
LC124,17	23.1	0.46	8.1	5.6	0.3	1.2	9.6	13.1	7.0	1.1	1.4	0.97	1.1	0.4	0.5	73.86
Average first 4	7.20	0.14	1.97	1.25	0.28	0.40	11.35	17.30	8.75	0.93	2.20	0.96	2.65	1.03	1.35	57.75
STDS	1.73	0.06	0.55	0.54	0.05	0.10	0.51	1.57	0.93	0.21	0.37	0.24	0.37	0.13	0.25	1.52
RSD	24%	42%	28%	44%	18%	25%	4%	9%	11%	22%	17%	25%	14%	12%	19%	3%
CP125																
LC125,1	10.3	0.25	5.4	2.5	0.3	0.3	9.2	19.3	9.5	0.7	1.3	1.25	1.9	0.7	0.9	63.85
LC125,2	11.3	0.24	3.8	2.3	0.3	0.5	12.6	21.9	5.8	1.2	2.2	0.37	2.4	1.2	1.2	67.37
LC125,3	10.0	0.25	5.5	2.6	0.3	0.3	10.2	19.9	9.1	1.0	2.1	1.86	1.5	0.8	1.1	66.65
LC125,4	10.0	0.25	4.8	2.5	0.3	0.6	10.6	15.6	8.0	1.1	3.2	1.94	1.2	0.9	0.9	61.86
LC125,5	7.7	0.10	2.1	1.7	0.3	0.3	*14.0	18.0	8.9	0.9	2.8	1.66	1.7	1.5	1.6	63.06
LC125,6	6.9	0.15	2.8	1.3	0.4	0.2	10.9	19.9	8.7	1.3	2.4	2.50	1.5	0.9	1.5	61.33
LC125,7	8.5	0.20	3.0	*2.7	0.5	*0.9	11.9	18.3	9.0	1.3	*3.8	1.77	1.4	1.4	1.6	66.17
LC125,8	6.6	0.08	*3.9	1.7	0.3	0.5	10.1	22.8	8.7	1.5	3.7	1.67	1.7	1.4	1.5	65.92
LC125,9	0.6	0.05	*0.2	0.3	.2<	0.5	12.6	19.1	*16.0	0.7	3.4	*4.40	*3.0	*2.1	2.0	64.93
LC125,10	0.3	.00<	-.0<	*0.2	0.3	0.2	*9.2	26.2	8.4	*2.3	3.5	2.33	2.2	1.0	1.5	57.62
LC125,11	*0.2	.01<	-.0<	0.3	0.3	.1<	11.3	22.7	11.8	*2.4	3.1	3.20	2.1	1.6	1.8	60.94
LC125,12	3.1	.03<	0.4	0.3	0.3	.2<	11.2	22.4	11.3	1.4	1.9	*4.10	2.1	1.1	1.5	61.20
LC125,13	2.2	.03<	.0<	0.3	0.2	.2<	10.8	25.5	8.4	1.3	*1.7	1.34	1.8	0.8	1.4	55.78
LC125,14	3.8	0.13	2.0	1.4	0.4	0.5	10.4	21.9	11.1	0.7	2.5	*5.20	1.8	1.2	1.6	64.61
LC125,15	4.4	0.17	1.8	1.0	.1<	.2<	10.9	22.2	9.6	1.1	2.5	2.60	2.1	1.3	1.4	61.18
LC125,16	*9.5	0.07	2.3	1.5	0.4	0.5	12.5	19.0	8.9	1.0	2.4	2.17	1.3	0.9	*1.0	63.32
LC125,17	8.5	*0.37	*4.7	*2.3	0.2	0.3	10.6	20.3	9.5	0.8	2.0	*0.91	1.6	1.0	*0.9	64.06
LC125,18	0.4	.01<	-.0<	0.5	0.3	0.3	10.5	24.7	8.6	1.3	2.0	1.04	2.2	1.2	1.6	55.06
Average first 14	4.42	0.12	2.06	0.94	0.33	0.37	11.14	21.64	9.45	1.11	2.68	2.03	1.81	1.18	1.60	60.86
STDS	3.16	0.05	0.85	0.60	0.09	0.13	0.81	2.65	1.17	0.28	0.62	0.65	0.31	0.25	0.18	3.55
RSD	72%	44%	41%	64%	27%	36%	7%	12%	12%	25%	23%	32%	17%	21%	11%	6%
CP130																
LC130,1	6.1	.02<	3.3	0.9	.2<	.1<	9.1	18.7	6.6	0.7	1.4	1.10	2.1	0.6	0.8	51.46
LC130,2	11.7	0.24	3.2	2.9	0.4	0.5	16.6	16.8	11.2	0.7	1.8	1.39	1.6	1.3	1.2	71.64
LC130,3	10.1	0.17	2.7	2.3	0.5	0.5	15.8	16.8	10.5	0.6	2.0	1.30	1.8	0.9	1.4	67.47
LC130,4	2.1	0.04	.0<	0.4	0.3	.1<	13.4	23.3	8.7	0.9	2.5	1.82	2.4	1.2	1.4	58.51
LC130,5	3.0	0.04	0.4	0.7	0.3	.1<	13.0	23.3	7.7	1.2	3.5	1.07	2.8	0.8	1.2	58.81
LC130,6	8.0	0.28	3.4	2.1	0.4	0.2	13.8	22.7	9.0	1.2	1.7	1.16	2.2	0.8	1.1	68.25
LC130,7	7.2	0.11	1.8	2.0	0.3	0.5	12.7	23.4	7.4	1.0	3.0	1.00	2.2	0.8	1.2	64.74
LC130,8	2.9	0.05	.1<	0.8	0.3	0.2	12.1	24.4	7.5	0.5	4.3	1.54	1.8	2.4	1.6	60.24
LC130,9	1.7	0.04	-.1<	0.5	0.2	.1<	11.6	24.0	12.5	1.8	1.6	1.82	2.7	1.0	1.2	60.72
LC130,10	1.5	.02<	.0<	0.4	.2<	.1<	12.2	23.5	10.5	0.7	1.4	2.40	2.6	1.1	1.1	57.36
LC130,11	6.6	0.18	0.4	1.3	0.4	0.2	17.1	18.9	10.4	1.3	2.4	1.27	2.2	1.0	1.2	64.89
LC130,12	5.1	0.09	0.9	1.2	0.5	0.5	13.5	19.5	9.7	0.6	3.8	0.93	3.0	1.7	1.4	62.42
LC130,13	2.6	0.04	0.3	0.6	0.3	.1<	11.7	20.6	10.8	1.0	2.3	1.87	2.7	1.1	0.9	56.85
LC130,14	8.0	0.06	4.1	1.2	0.2	0.3	10.0	20.1	6.2	0.7	2.7	0.63	2.1	0.8	1.0	57.88
LC130,15	8.7	0.05	3.4	1.5	.1<	0.3	13.0	20.0	8.2	1.2	1.7	1.05	1.9	0.9	1.0	63.13
LC130,16	7.9	0.14	2.2	1.8	0.3	0.4	14.4	23.8	8.5	1.2	1.8	1.56	1.9	1.3	1.6	68.85
LC130,17	8.2	0.19	3.3	2.0	0.2	0.3	14.1	14.8	14.0	0.3	2.1	1.72	2.8	0.9	1.0	65.95
LC130,18	2.7	.00<	0.3	0.7	0.3	.1<	15.8	18.6	13.7	1.0	3.2	1.62	3.4	1.5	1.7	64.42
LC130,19	6.3	0.27	2.3	2.0	0.4	.2<	14.5	20.5	11.3	1.1	2.3	1.33	2.6	1.2	1.2	67.30
LC130,20	1.7	.03<	.1<	0.6	.1<	.1<	12.8	24.3	10.6	1.4	2.0	4.20	4.3	1.0	1.3	64.20
Average first 17	4.95	0.11	1.90	1.16	0.31	0.32	13.28	21.51	9.81	1.01	2.49	1.59	2.56	1.15	1.24	63.40
STDS	2.75	0.09	1.42	0.63	0.09	0.12	1.66	2.66	2.23	0.37	0.83	0.80	0.62	0.41	0.23	3.90
RSD	56%	76%	75%	54%	28%	37%	12%	12%	23%	36%	33%	51%	24%	36%	19%	6%
CP131																
LC131,1	1.5	0.10	*0.4	1.5	0.5	0.7	*7.5	*26.2	5.4	1.4	1.8	2.80	3.2	0.9	1.1	54.90
LC131,2	1.2	.02<	.0<	.2<	.1<	.1<	13.1	24.3	9.0	*1.7	2.3	2.40	*3.4	1.2	1.3	59.91
LC131,3	4.7	0.13	1.1	1.0	0.3	.2<	14.5	22.0	7.5	1.5	2.4	*3.70	2.5	1.2	1.4	64.07
LC131,4	6.0	*0.27	2.7	1.4	0.3	.1<	14.6	19.0	9.1	1.1	*3.5	1.96	2.8	*1.5	1.1	65.47
LC131,5	*9.5	0.17	*4.2	1.5	0.4	0.5	14.3	19.6	4.9	1.4	1.2	*0.53	1.8	0.9	1.1	61.88
LC131,6	7.7	0.19	3.4	1.5	0.3	0.3	14.4	19.1	4.1	1.5	1.5	*0.44	1.8	0.7	1.1	58.03
LC131,7	*9.7	0.13	2.5	1.9	0.3	0.6	15.2	18.7	6.6	0.8	1.5	1.35	2.4	1.0	1.2	63.81
LC131,8	3.2	.01<	*0.4	*0.6	0.4	0.4	14.3	21.2	7.5	0.9	*3.6	2.18	1.8	0.7	1.5	58.68
LC131,9	6.5	0.07	2.2	1.4	0.3	.2<	13.6	19.8	6.9	1.0	2.7	2.06	2.0	1.1	1.3	60.79

Sample	SiO2	TiO2	Al2O3	FeO	MnO	MgO	CaO	Na2O	K2O	P2O5	F	Cl	SO3	BaO	SrO	Total
LC131,10	*11.2*	*0.08*	*2.3*	*1.8*	*0.3*	*0.8*	*13.6*	*18.2*	*2.9*	*0.6*	*0.6*	*0.49*	*1.2*	*0.3*	*0.8*	*55.07*
LC131,11	*18.6*	*0.24*	*8.0*	*3.1*	*0.2*	*0.6*	*14.4*	*17.3*	*5.8*	*1.3*	*1.6*	*1.52*	*1.8*	*0.6*	*0.9*	*75.99*
Average first 9	4.40	0.13	2.38	1.46	0.35	0.50	14.25	20.46	6.78	1.20	1.91	2.13	2.29	0.96	1.23	60.43
STDS	2.52	0.04	0.84	0.26	0.08	0.16	0.64	1.92	1.73	0.28	0.56	0.48	0.53	0.20	0.15	3.36
RSD	57%	33%	35%	18%	22%	32%	4%	9%	26%	24%	29%	23%	23%	21%	12%	6%

Note: whole analyses not taken into account in average are in italics, and analyses of individual elements that are rejected from the calculation of the average are indicated by an asterix (*). b.d.: below detection.

Table A6.2: Major element microprobe analyses of silicate liquid (LS) from experiments on the join HOL14/OL5 (in wt. %) - individual and average analyses, standard deviation (STDS) and relative standard deviation (RSD).

Sample	SiO2	TiO2	Al2O3	FeO	MnO	MgO	CaO	Na2O	K2O	P2O5	F	Cl	SO3	BaO	SrO	Total
CP1																
LS1,1	44.3	0.90	6.3	10.6	0.7	1.3	7.6	9.8	6.2	0.3	0.2	0.38	0.2	0.4	0.3	89.60
LS1,2	41.5	0.91	6.1	10.9	0.7	1.2	6.2	13.4	6.1	0.5	0.5	0.54	0.3	1.3	0.6	90.45
LS1,3	42.5	0.93	6.3	10.5	0.6	1.2	5.5	12.6	6.4	0.4	0.5	0.32	0.2	0.2	0.3	88.43
LS1,4	44.3	0.91	6.2	11.0	0.8	1.3	6.9	8.9	6.5	0.3	0.5	0.40	0.1	0.3	0.5	88.93
LS1,5	42.0	0.93	6.6	11.5	0.8	1.3	6.2	9.8	6.6	0.2	0.5	0.52	0.3	0.1	0.7	88.07
Average	42.91	0.92	6.29	10.89	0.73	1.24	6.46	10.87	6.35	0.33	0.47	0.43	0.23	0.47	0.50	89.10
STDS	1.33	0.01	0.22	0.38	0.09	0.04	0.81	1.96	0.22	0.09	0.13	0.09	0.06	0.46	0.17	0.95
RSD	3%	1%	3%	4%	12%	3%	12%	18%	4%	27%	28%	22%	26%	98%	34%	1%
CP2																
LS2,1	46.7	0.82	9.4	10.2	0.5	0.7	2.8	11.2	7.1	0.3	0.3	0.46	0.2	0.7	0.1	91.45
LS2,2	47.4	0.82	9.0	10.4	0.6	0.7	3.1	12.5	7.1	0.1	0.6	0.49	0.2	0.7	0.6	94.23
LS2,3	*46.6*	*1.38*	*11.0*	*10.8*	*0.4*	*0.7*	*5.4*	*13.4*	*5.8*	*0.3*	*0.3*	*0.53*	*0.4*	*0.9*	*0.6*	*98.38*
LS2,4	*50.8*	*0.90*	*9.7*	*10.9*	*0.6*	*0.8*	*3.2*	*3.5*	*7.3*	*0.2*	*0.7*	*0.39*	*0.2*	*0.2*	*0.4*	*89.73*
LS2,5	*51.2*	*0.87*	*9.6*	*11.1*	*0.5*	*0.8*	*3.7*	*2.9*	*7.2*	*0.4*	*0.7*	*0.36*	*0.1*	*0.8*	*0.6*	*90.52*
LS2,6	*49.4*	*1.10*	*9.7*	*10.2*	*0.2*	*0.8*	*3.3*	*6.6*	*7.4*	*0.3*	*0.4*	*0.46*	*0.1*	*0.2*	*0.1*	*90.15*
Average first 2	47.04	0.82	9.21	10.27	0.51	0.73	2.92	11.87	7.11	0.19	0.45	0.48	0.19	0.71	0.38	92.84
STDS	0.52	0.00	0.27	0.12	0.07	0.00	0.21	0.91	0.03	0.11	0.19	0.02	0.00	0.03	0.36	1.97
RSD	1%	0%	3%	1%	14%	0%	7%	8%	0%	57%	43%	4%	0%	4%	96%	2%
CP5																
LS5,1	43.3	1.27	*13.1	8.1	0.2	0.4	2.6	11.4	6.3	0.2	0.6	0.44	2.0	b.d.	0.3	90.20
LS5,2	42.8	1.24	10.9	8.1	0.4	0.6	*6.9	10.6	5.3	*1.2	0.3	0.47	1.1	0.2	0.6	90.68
LS5,3	42.4	1.37	10.0	9.9	0.3	0.6	4.3	12.6	5.6	0.3	0.6	0.69	1.0	0.3	0.3	90.27
LS5,4	43.9	1.30	10.8	9.2	0.3	0.7	4.7	12.2	5.6	0.2	0.4	0.63	0.6	0.5	0.7	91.79
LS5,5	43.1	1.32	10.9	9.9	0.4	0.7	4.1	10.4	6.1	0.3	0.4	0.61	1.0	0.2	0.5	89.78
LS5,6	43.0	1.43	10.6	9.9	0.4	0.7	5.8	10.4	5.4	0.3	0.2	0.75	0.9	0.6	0.2	90.60
Average	43.08	1.32	10.64	9.17	0.34	0.62	4.31	11.27	5.73	0.22	0.41	0.60	1.10	0.36	0.44	89.61
STDS	0.49	0.07	0.37	0.90	0.09	0.11	1.15	0.97	0.39	0.07	0.15	0.12	0.47	0.17	0.19	0.69
RSD	1%	5%	4%	10%	27%	18%	27%	9%	7%	29%	36%	20%	43%	47%	43%	1%
CP11																
LS11.1	50.64	1.21	8.91	9.62	0.49	0.26	2.14	5.68	8.27	0.15	0.51	0.46	0.65	0.53	0.40	89.92
CP13																
LS13,1	43.3	1.03	10.5	7.6	0.6	0.8	5.6	12.9	5.7	0.1	0.3	0.46	0.8	0.2	0.3	90.31
LS13,2	43.3	1.11	10.1	7.9	0.4	0.7	5.4	13.3	6.1	0.2	0.4	0.51	0.7	0.5	0.2	90.91
LS13,3	43.2	1.13	10.4	7.9	0.4	0.8	5.4	12.4	5.6	0.2	0.4	0.42	0.7	b.d.	0.2	89.22
LS13,4	45.1	1.20	10.6	7.4	0.5	0.8	5.0	12.3	5.7	0.2	0.3	0.46	0.9	0.6	0.3	91.33
LS13,5	44.6	1.10	10.7	7.2	0.5	0.8	5.4	12.8	5.7	0.2	0.4	0.41	0.7	0.4	0.3	91.08
LS13,6	44.0	1.01	10.6	7.8	0.5	0.8	5.4	12.4	5.7	0.3	0.5	0.51	0.8	0.4	0.5	91.25
LS13,7	44.2	1.01	10.5	7.7	0.4	0.7	5.5	14.2	5.9	0.2	0.5	0.41	0.6	0.4	0.1	92.28
LS13,8	43.0	1.17	10.4	7.5	0.5	0.8	5.4	13.8	6.2	0.3	0.2	0.45	0.7	0.0	0.6	90.99
Average	43.85	1.10	10.49	7.61	0.46	0.77	5.39	13.01	5.81	0.21	0.37	0.45	0.74	0.36	0.34	90.97
STDS	0.76	0.07	0.18	0.23	0.05	0.04	0.19	0.69	0.20	0.06	0.09	0.04	0.08	0.18	0.17	0.88
RSD	2%	7%	2%	3%	10%	6%	4%	5%	3%	27%	24%	9%	11%	50%	50%	1%
CP14																
LS14.1	*43.5*	*0.13*	*7.1*	*8.2*	*0.4*	*3.3*	*27.5*	*6.5*	*0.6*	*0.1*	*b.d.*	*0.06*	*0.1*	*0.3*	*2.7*	*100.42*
LS14.2	*52.5*	*0.12*	*0.7*	*1.3*	*0.6*	*0.1*	*45.4*	*0.8*	*0.4*	*0.2*	*b.d.*	*0.02*	*b.d.*	*0.0*	*0.4*	*102.64*
LS14.3	*40.7*	*1.66*	*5.1*	*12.2*	*1.0*	*0.9*	*8.0*	*10.0*	*6.2*	*0.3*	*0.7*	*0.62*	*0.1*	*0.8*	*1.1*	*89.31*
LS14,4	37.7	1.36	4.8	11.1	0.9	0.8	9.5	16.0	5.4	0.5	0.6	0.44	0.4	0.9	0.6	90.84
LS14,5	38.9	1.49	4.6	11.5	1.2	1.0	8.2	14.1	5.6	0.5	0.8	0.49	0.3	0.6	0.6	89.81
LS14,6	39.1	1.32	4.5	10.7	0.9	0.8	*11.2	15.5	5.2	0.4	0.7	0.49	0.2	0.2	0.9	92.11
LS14,7	39.1	1.47	4.7	11.9	0.9	0.9	8.9	16.5	5.6	0.6	0.9	0.44	0.2	0.5	0.6	93.09
Average last 4	38.70	1.41	4.66	11.29	0.95	0.90	8.85	15.50	5.44	0.50	0.76	0.47	0.26	0.56	0.66	90.89
STDS	0.66	0.08	0.15	0.50	0.15	0.09	0.61	1.04	0.19	0.06	0.11	0.03	0.09	0.26	0.16	1.44
RSD	2%	6%	3%	4%	15%	11%	7%	7%	3%	13%	15%	6%	36%	47%	24%	2%
CP15																
LS15,1	46.8	1.17	8.6	12.0	0.6	1.1	5.1	13.9	6.4	0.3	0.5	0.53	0.3	0.7	b.d.	97.93
LS15,2	45.3	1.10	8.5	11.9	0.6	1.1	5.0	13.8	6.2	0.3	0.7	0.45	0.2	0.3	0.7	96.16
LS15,3	46.5	1.13	8.5	11.5	0.5	1.1	5.0	13.2	6.6	0.4	0.7	0.48	0.2	0.5	0.1	96.21
LS15.4	*42.4*	*1.30*	*8.1*	*11.4*	*0.5*	*0.9*	*5.2*	*12.2*	*6.0*	*0.4*	*0.6*	*0.55*	*0.4*	*0.2*	*0.6*	*90.83*
LS15,5	*47.7*	*1.28*	*7.8*	*12.7*	*0.6*	*1.1*	*4.2*	*11.4*	*6.6*	*0.3*	*0.6*	*0.48*	*0.3*	*0.2*	*0.4*	*95.79*
Average first 3	46.19	1.13	8.54	11.78	0.56	1.10	5.01	13.64	6.41	0.34	0.62	0.49	0.23	0.49	0.36	96.89
STDS	0.81	0.04	0.08	0.28	0.10	0.01	0.05	0.38	0.20	0.08	0.11	0.04	0.03	0.20	0.41	1.01
RSD	2%	3%	1%	2%	17%	1%	1%	3%	3%	24%	17%	8%	14%	41%	114%	1%

Sample	SiO2	TiO2	Al2O3	FeO	MnO	MgO	CaO	Na2O	K2O	P2O5	F	Cl	SO3	BaO	SrO	Total
CP18																
LS18,1	37.2	1.18	6.6	9.0	0.5	1.1	11.4	14.9	4.8	0.5	0.7	0.66	0.5	0.3	1.0	90.21
LS18,2	36.5	1.12	6.8	8.6	0.5	1.0	11.9	15.2	4.5	0.5	0.7	0.53	0.3	1.2	1.0	90.17
LS18,3	36.1	1.13	6.4	8.7	0.5	1.0	12.2	15.2	4.6	0.6	0.7	0.39	0.5	0.6	1.1	89.79
LS18,4	36.2	1.07	6.7	8.7	0.7	1.0	11.9	14.9	5.0	0.4	0.8	0.51	0.2	0.6	0.8	89.37
LS18,5	34.9	1.11	6.6	8.5	0.7	1.0	11.6	15.3	5.1	0.5	0.8	0.59	0.5	0.6	0.8	88.49
LS18,6	37.0	1.14	6.8	8.3	0.6	1.0	11.7	12.8	5.1	0.5	0.7	0.60	0.4	0.9	0.9	88.43
Average	36.32	1.13	6.65	8.64	0.57	1.02	11.77	14.72	4.85	0.49	0.70	0.55	0.39	0.69	0.93	89.41
STDS	0.81	0.04	0.12	0.16	0.12	0.05	0.32	0.18	0.24	0.09	0.04	0.10	0.13	0.34	0.14	0.71
RSD	2%	4%	2%	2%	21%	5%	3%	1%	5%	18%	6%	18%	34%	49%	15%	1%
CP19																
LS19,1	43.8	1.48	9.4	10.8	0.4	1.0	6.9	12.3	5.7	0.5	0.5	0.41	0.3	0.6	0.4	94.37
LS19,2	44.4	1.30	10.3	10.1	0.6	1.0	7.4	12.6	5.9	0.4	0.3	0.44	0.3	0.2	0.6	95.83
LS19,3	44.7	1.34	10.4	10.0	0.5	1.0	6.1	12.1	6.1	0.4	0.3	0.44	0.2	0.4	0.1	93.87
LS19,4	44.0	1.28	10.6	10.0	0.5	0.9	6.4	12.9	6.3	0.4	0.3	0.48	0.4	0.5	0.1	94.93
LS19,5	*46.2*	*1.35*	*10.5*	*9.8*	*0.5*	*1.0*	*6.2*	*9.1*	*6.0*	*0.5*	*0.4*	*0.44*	*0.3*	*0.7*	*0.3*	*93.19*
Average first 4	44.23	1.35	10.16	10.23	0.49	0.96	6.70	12.46	5.98	0.43	0.32	0.44	0.30	0.43	0.26	94.75
STDS	0.38	0.09	0.54	0.40	0.11	0.06	0.55	0.36	0.24	0.07	0.09	0.03	0.06	0.14	0.26	0.84
RSD	1%	7%	5%	4%	22%	6%	8%	3%	4%	15%	27%	6%	20%	32%	99%	1%
CP20																
LS20,1	41.9	0.97	11.7	7.6	0.4	0.7	6.7	13.7	5.4	0.3	0.4	0.41	0.2	b.d.	0.5	90.71
LS20,2	41.8	0.99	11.8	7.9	0.5	0.8	6.3	14.6	5.3	0.2	0.3	0.46	0.3	0.6	0.6	92.34
LS20,3	41.3	0.99	11.6	7.5	0.4	0.7	5.9	14.0	5.7	0.4	0.5	0.37	0.1	0.3	0.4	89.99
LS20,4	42.1	1.00	11.9	8.1	0.4	0.7	6.2	13.7	5.5	0.2	0.2	0.37	0.3	0.7	0.4	91.65
LS20,5	41.4	1.06	11.9	8.1	0.5	0.8	6.4	12.5	5.4	0.1	0.4	0.44	0.3	0.7	0.3	90.22
Average	41.69	1.00	11.77	7.84	0.45	0.75	6.29	13.69	5.44	0.22	0.33	0.41	0.22	0.55	0.44	91.09
STDS	0.35	0.03	0.10	0.26	0.07	0.07	0.28	0.75	0.14	0.09	0.09	0.04	0.11	0.19	0.15	0.99
RSD	1%	3%	1%	3%	16%	9%	5%	5%	3%	41%	28%	10%	50%	34%	34%	1%
CP21																
LS21,1	42.9	1.11	12.6	7.9	0.2	1.0	7.6	12.7	5.3	0.3	0.5	*0.60	0.2	b.d.	0.5	93.30
LS21,2	44.2	1.09	12.6	8.4	0.2	0.9	7.0	11.4	6.3	0.5	0.3	0.34	0.1	0.2	0.6	93.96
LS21,3	44.1	1.14	12.3	8.0	0.4	1.0	7.5	11.9	6.0	0.3	0.4	0.47	0.3	0.1	0.6	94.54
LS21,4	44.5	1.08	12.1	8.4	0.4	0.9	7.2	11.8	6.0	0.4	0.2	0.37	0.1	0.2	0.4	94.16
LS21,5	42.9	*1.20	11.7	8.4	0.3	0.9	7.7	11.7	5.8	0.4	0.4	0.44	0.4	*0.5	0.6	93.20
LS21,6	43.1	1.04	11.8	8.8	0.3	0.9	7.7	12.5	5.7	0.2	0.4	0.46	0.2	0.2	0.6	94.05
Average	43.62	1.09	12.20	8.31	0.30	0.93	7.45	11.99	5.87	0.34	0.36	0.42	0.21	0.20	0.54	93.81
STDS	0.72	0.04	0.37	0.32	0.09	0.04	0.30	0.51	0.34	0.11	0.09	0.06	0.11	0.08	0.10	0.52
RSD	2%	3%	3%	4%	32%	5%	4%	4%	6%	34%	24%	14%	51%	40%	19%	1%
CP22																
LS22,1	35.7	1.12	5.3	8.9	0.7	0.9	12.5	16.3	4.6	0.6	0.8	0.43	0.2	1.2	0.7	89.96
LS22,2	35.5	1.33	5.4	9.3	0.8	1.0	12.7	16.3	4.5	0.5	0.6	0.40	0.3	0.5	0.6	89.59
LS22,3	35.8	1.25	5.4	8.9	0.7	0.9	13.8	16.1	4.3	0.6	0.9	0.40	0.3	0.8	0.8	91.09
LS22,4	*33.9	1.18	5.5	8.8	0.7	0.9	13.5	16.0	4.5	0.6	0.9	0.36	0.4	1.0	0.7	88.90
LS22,5	35.4	1.24	5.6	8.6	0.6	1.0	13.7	16.2	4.3	0.4	0.7	0.44	0.2	0.5	0.9	89.77
Average	35.60	1.22	5.44	8.89	0.67	0.94	13.27	16.17	4.47	0.53	0.78	0.41	0.27	0.79	0.73	90.20
STDS	0.21	0.08	0.13	0.24	0.07	0.04	0.60	0.16	0.13	0.08	0.12	0.03	0.07	0.31	0.13	0.79
RSD	1%	6%	2%	3%	11%	5%	5%	1%	3%	15%	16%	8%	27%	38%	17%	1%
CP23																
LS23,1	*48.2*	*1.51*	*10.8*	*11.4*	*0.6*	*1.1*	*6.2*	*4.6*	*6.6*	*0.6*	*0.4*	*0.43*	*0.2*	*0.2*	*0.2*	*93.03*
LS23,2	44.9	1.28	9.9	10.3	0.4	1.0	7.3	12.5	5.7	0.5	0.5	0.44	0.4	b.d.	0.7	95.81
LS23,3	44.4	1.37	9.9	10.2	0.3	0.9	7.3	12.4	6.0	0.4	0.5	0.43	0.4	0.6	0.5	95.46
LS23,4	46.3	1.43	10.7	10.5	0.4	1.0	6.3	10.3	6.4	0.5	0.5	0.39	0.2	0.7	0.2	95.77
LS23,5	47.3	1.44	10.3	10.3	0.5	0.9	7.1	10.2	6.6	0.4	0.4	0.31	0.2	0.7	0.3	96.89
LS23,6	46.8	*1.67	10.0	10.6	0.5	0.9	6.4	11.5	6.4	0.5	0.5	0.33	0.2	0.9	0.4	97.59
LS23,7	46.7	1.43	10.6	10.4	0.5	0.9	6.5	11.7	6.6	0.6	0.5	0.38	0.2	0.5	0.3	97.67
Average last 6	46.07	1.39	10.23	10.34	0.43	0.95	6.81	11.45	6.26	0.48	0.48	0.38	0.26	0.67	0.40	96.60
STDS	1.15	0.07	0.35	0.15	0.08	0.05	0.47	1.00	0.36	0.09	0.07	0.05	0.08	0.15	0.17	0.98
RSD	2%	5%	3%	1%	18%	6%	7%	9%	6%	19%	14%	14%	30%	22%	42%	1%
CP27																
LS27,1	*48.9*	*2.04*	*9.2*	*8.3*	*0.5*	*1.5*	*4.8*	*10.9*	*6.4*	*0.5*	*0.5*	*0.77*	*0.7*	*0.7*	*1.1*	*96.50*
LS27,2	46.7	1.70	8.9	8.5	0.3	1.4	4.7	15.0	6.2	0.4	0.5	0.68	0.7	0.5	0.4	96.59
LS27,3	47.5	1.87	9.5	7.7	0.5	1.5	4.9	13.7	6.3	0.6	0.5	0.64	0.6	0.8	0.6	97.16
LS27,4	47.2	1.67	9.1	7.9	0.5	1.4	5.4	15.0	6.2	0.4	0.5	0.64	0.6	0.5	0.5	97.47
LS27,5	47.7	1.79	9.1	8.1	0.6	1.4	4.9	12.8	6.3	0.5	0.4	0.67	0.6	0.7	0.6	96.06
Average last 4	47.30	1.76	9.14	8.03	0.49	1.42	4.97	14.11	6.22	0.45	0.50	0.66	0.64	0.62	0.52	96.82
STDS	0.44	0.09	0.25	0.34	0.10	0.03	0.29	1.08	0.06	0.11	0.04	0.02	0.04	0.16	0.06	0.62
RSD	1%	5%	3%	4%	21%	2%	6%	8%	1%	25%	8%	3%	6%	25%	11%	1%
CP31																
LS31,1	45.3	0.79	9.4	7.0	0.4	0.2	3.2	9.6	8.0	0.3	0.5	0.39	0.6	0.4	0.6	86.63
LS31,2	45.0	0.76	9.4	7.2	0.4	0.2	3.0	10.4	7.0	0.1	0.5	0.44	0.8	0.2	0.5	85.89
LS31,3	47.4	0.70	9.5	6.4	0.4	0.2	1.3	8.2	8.6	0.1	0.2	0.28	0.1	b.d.	0.2	83.70
LS31,4	46.9	0.75	*12.3	6.2	0.3	0.3	2.5	11.5	7.1	b.d.	0.4	0.41	0.4	b.d.	0.5	89.54
LS31,5	46.7	*2.36	10.3	*5.2	0.3	0.2	4.0	12.3	6.9	b.d.	b.d.	0.20	0.3	b.d.	0.8	89.65
Average	46.27	0.75	9.66	6.72	0.34	0.23	2.79	10.40	7.54	0.18	0.40	0.34	0.42	0.27	0.52	86.82
STDS	1.04	0.04	0.46	0.48	0.06	0.01	1.01	1.61	0.74	0.10	0.17	0.10	0.26	0.15	0.20	2.53

Sample	SiO2	TiO2	Al2O3	FeO	MnO	MgO	CaO	Na2O	K2O	P2O5	F	Cl	SO3	BaO	SrO	Total
RSD	2%	5%	5%	7%	18%	6%	36%	15%	10%	56%	43%	29%	63%	56%	38%	3%
CP38																
LS38,1	47.3	1.08	15.3	7.7	0.4	0.8	5.8	11.2	5.1	0.3	0.2	0.28	0.6	0.4	0.4	96.69
LS38,2	46.5	1.02	15.3	*8.2	0.4	0.8	6.1	11.4	5.1	0.2	0.1	0.27	0.5	b.d.	0.3	96.22
LS38,3	45.6	1.09	15.3	7.7	0.2	1.0	5.9	11.1	5.1	0.1	0.2	0.35	0.5	0.1	0.2	94.26
LS38,4	47.7	0.95	15.3	7.5	0.2	0.9	6.0	11.0	5.2	0.2	0.2	0.34	0.5	0.2	0.3	96.32
LS38,5	46.7	1.08	15.3	7.6	0.3	0.8	5.8	*10.2	5.1	0.4	0.1	0.29	0.5	0.1	0.4	94.68
Average	46.77	1.04	15.30	7.61	0.27	0.86	5.90	11.16	5.12	0.23	0.17	0.31	0.52	0.18	0.30	95.74
STDS	0.82	0.06	0.03	0.09	0.12	0.06	0.14	0.19	0.06	0.08	0.08	0.04	0.05	0.13	0.10	1.09
RSD	2%	6%	0%	1%	45%	7%	2%	2%	1%	35%	46%	12%	9%	71%	34%	1%
CP40																
LS40,1	49.9	1.00	14.5	9.7	0.3	0.4	4.5	10.7	5.9	.3<	0.4	0.40	0.4	1<	4<	98.10
LS40,2	49.7	1.06	12.6	10.4	0.6	0.5	4.4	9.8	6.1	0.5	0.3	0.49	0.7	0.4	5<	97.64
LS40,3	50.2	1.01	12.8	10.0	0.5	0.4	5.0	9.2	5.9	0.3	0.5	0.44	0.7	0.4	0.8	98.18
LS40,4	50.1	1.09	13.3	10.3	.2<	0.5	3.7	11.2	6.0	0.4	0.4	0.47	0.7	1<	0.8	98.93
LS40,5	*50.8*	*-.08<*	*11.2*	*10.6*	*0.4*	*3.1*	*8.4*	*9.3*	*4.7*	*0.3*	*-.08<*	*0.41*	*0.6*	*2<*	*.3<*	*99.84*
Average first 4	49.98	1.04	13.30	10.10	0.47	0.45	4.40	10.23	5.98	0.40	0.40	0.45	0.63	0.40	0.80	99.01
STDS	0.22	0.04	0.85	0.32	0.15	0.06	0.54	0.90	0.10	0.10	0.08	0.04	0.15	0.00	0.00	0.53
RSD	0%	4%	6%	3%	33%	13%	12%	9%	2%	25%	20%	9%	24%	0%	0%	1%
CP41																
LS41.2	*47.1*	*1.22*	*12.3*	*10.2*	*0.3*	*0.6*	*8.0*	*11.9*	*5.2*	*0.4*	*0.6*	*0.51*	*0.8*	*2<*	*5<*	*99.32*
LS41,1	47.3	1.51	10.9	12.0	0.5	0.9	5.8	11.5	5.6	0.3	0.6	0.60	0.9	-.0<	0.8	99.23
LS41,3	47.0	1.59	10.3	12.3	0.4	0.7	4.1	10.4	5.9	0.5	0.7	0.73	1.0	3<	6<	95.60
LS41,4	47.4	1.60	10.0	12.7	0.5	0.9	4.3	11.3	5.7	0.5	0.7	0.73	1.0	4<	0.8	98.15
LS41,5	47.6	1.49	10.8	11.4	0.5	0.8	4.8	12.9	5.8	0.3	0.8	0.67	0.9	4<	2<	98.70
LS41,6	47.5	1.49	10.4	11.1	0.5	0.9	6.9	11.6	5.4	0.3	0.6	0.64	0.7	3<	0.8	98.94
Average last 5	47.36	1.54	10.48	11.90	0.48	0.84	5.18	11.54	5.68	0.38	0.68	0.67	0.90	b.d.	0.80	98.43
STDS	0.23	0.05	0.37	0.65	0.04	0.09	1.16	0.90	0.19	0.11	0.08	0.06	0.12	n.d.	0.00	1.47
RSD	0%	4%	4%	5%	9%	11%	22%	8%	3%	29%	12%	8%	14%	n.d	0%	1%
CP42																
LS42.1	*47.4*	*1.22*	*7.5*	*8.9*	*0.5*	*0.9*	*15.6*	*8.9*	*4.6*	*0.5*	*0.7*	*0.55*	*0.7*	*4<*	*4<*	*98.00*
LS42,2	45.9	1.40	*10.0	10.0	0.5	1.0	8.8	12.9	5.4	0.5	0.7	0.67	0.9	3<	3<	98.69
LS42,3	46.7	1.51	8.8	11.6	0.6	1.3	6.7	10.5	5.8	0.4	1.0	0.78	1.0	0.6	3<	97.50
LS42,4	*43.9	1.66	8.3	12.0	0.5	1.1	6.0	11.8	5.7	0.7	0.9	0.76	0.9	2<	0.8	94.97
LS42,5	45.1	1.42	8.6	10.5	0.4	0.9	9.2	12.0	5.3	0.6	0.7	0.77	0.9	2<	0.7	97.14
LS42,6	45.1	1.60	8.9	11.1	0.4	1.2	6.2	13.7	5.7	0.8	0.6	0.79	0.9	0.7	0.7	98.36
Average last 5	45.70	1.52	8.65	11.04	0.48	1.10	7.38	12.18	5.58	0.60	0.78	0.75	0.92	0.65	0.73	98.07
STDS	0.77	0.11	0.26	0.81	0.08	0.16	1.51	1.21	0.22	0.16	0.16	0.05	0.04	0.07	0.06	1.46
RSD	2%	7%	3%	7%	17%	14%	20%	10%	4%	26%	21%	6%	5%	11%	8%	1%
CP43																
LS43,1	38.3	1.37	5.0	10.5	0.6	0.9	11.0	17.1	5.4	0.8	1.2	0.59	1.1	4<	0.9	94.75
LS43,2	38.0	1.35	5.2	10.2	0.7	1.2	10.8	17.0	5.2	0.8	1.2	0.55	1.0	4<	1.0	94.21
LS43,3	37.6	1.31	5.1	10.2	0.5	1.1	10.6	17.1	5.5	0.8	*1.5	0.59	1.1	0.5	0.9	94.38
LS43,4	38.7	1.35	5.1	10.7	0.6	1.1	10.8	16.8	5.8	0.8	1.2	0.58	1.1	0.6	1.1	96.44
LS43,5	37.4	1.33	5.0	10.2	0.7	1.0	11.0	16.8	5.2	1.1	1.0	0.59	1.1	0.6	*1.6	94.64
LS43,6	37.0	1.30	5.1	10.1	0.5	0.9	10.7	*16.1	5.1	0.9	1.1	0.57	1.1	0.8	1.2	92.57
LS43,7	37.5	1.28	5.0	10.4	0.5	1.0	11.1	17.4	5.3	0.8	1.2	0.58	1.1	0.8	0.7	94.71
LS43,8	38.1	1.34	5.1	10.5	0.4	1.1	11.0	16.9	5.2	0.9	1.3	0.60	1.0	0.5	1.1	95.14
Average	37.83	1.33	5.08	10.35	0.56	1.04	10.88	17.01	5.34	0.86	1.17	0.58	1.08	0.63	0.99	94.71
STDS	0.55	0.03	0.07	0.21	0.11	0.11	0.18	0.21	0.23	0.11	0.10	0.02	0.05	0.14	0.17	1.07
RSD	1%	2%	1%	2%	19%	10%	2%	1%	4%	12%	8%	3%	4%	22%	17%	1%
CP47																
LS47.1	49.2	1.31	9.1	12.0	0.5	0.3	3.2	2.8	5.6	0.3	0.6	0.56	0.2	3<	0.9	86.65
CP48																
LS48.1	*38.1*	*4.55*	*6.5*	*15.0*	*0.3*	*0.5*	*15.3*	*6.2*	*3.3*	*b.d.*	*b.d.*	*0.25*	*0.2*	*b.d.*	*b.d*	*90.16*
LS48.3	*53.3*	*1.54*	*8.0*	*13.1*	*0.6*	*0.7*	*3.7*	*1.2*	*1.7*	*0.6*	*1.0*	*0.67*	*0.7*	*.3<*	*1.2*	*87.99*
LS48,2	42.4	1.37	6.1	12.5	0.6	0.5	4.3	4.5	6.0	0.3	1.2	0.54	0.5	0.7	0.8	82.24
LS48,4	43.7	1.38	6.3	12.2	0.6	0.6	4.2	5.3	6.1	0.3	1.1	0.59	0.6	0.7	0.6	84.35
Average last 2	43.05	1.38	6.20	12.35	0.60	0.55	4.25	4.90	6.05	0.30	1.15	0.57	0.55	0.70	0.70	83.29
STDS	0.92	0.01	0.14	0.21	0.00	0.07	0.07	0.57	0.07	0.00	0.07	0.04	0.07	0.00	0.14	1.49
RSD	2%	1%	2%	2%	0%	13%	2%	12%	1%	0%	6%	6%	13%	0%	20%	2%
CP52																
LS52.1	*44.0*	*1.74*	*7.1*	*12.6*	*0.6*	*1.1*	*7.6*	*4.9*	*5.2*	*0.9*	*1.2*	*0.61*	*0.3*	*0.5*	*0.8*	*89.07*
LS52,2	42.3	1.64	6.3	12.2	0.5	1.1	7.4	11.2	5.5	1.0	1.2	0.60	0.4	0.6	.4<	91.82
LS52,3	42.4	1.78	5.7	12.2	0.6	1.2	8.9	10.6	5.0	0.8	1.3	0.64	0.5	0.7	0.8	93.02
LS52,4	*44.2	1.79	5.9	12.4	0.5	1.1	6.9	9.1	6.1	0.9	1.1	0.58	0.4	0.7	0.7	92.38
LS52,5	42.9	1.62	6.7	11.8	0.6	1.1	8.0	10.4	5.8	0.8	1.2	0.64	0.3	4<	0.8	92.68
Average last 4	42.53	1.71	6.15	12.15	0.55	1.13	7.80	10.33	5.60	0.88	1.20	0.62	0.40	0.67	0.77	92.46
STDS	0.32	0.09	0.44	0.25	0.06	0.05	0.86	0.88	0.47	0.10	0.08	0.03	0.08	0.06	0.06	0.51
RSD	1%	5%	7%	2%	10%	4%	11%	9%	8%	11%	7%	5%	20%	9%	8%	1%
CP53																
LS53,1	37.0	1.56	5.0	10.9	0.7	0.8	11.1	14.6	5.2	0.5	1.2	0.42	0.2	0.7	0.9	90.81
LS53,2	*38.6	*1.72	4.9	11.3	0.8	0.8	10.5	*12.7	5.6	0.5	1.2	0.45	2<	0.5	0.7	90.30

Sample	SiO2	TiO2	Al2O3	FeO	MnO	MgO	CaO	Na2O	K2O	P2O5	F	Cl	SO3	BaO	SrO	Total
LS53,3	36 8	1.58	4.9	10.6	0.7	0.8	10.9	15.4	4.9	0.7	1.2	0.43	.2<	0.7	1.1	90.82
LS53,4	37.3	1.65	4.1	11.2	0 9	0.7	11.4	14.4	4.8	0.7	1.3	0.43	.2<	0.8	1.0	90.51
LS53,5	37 5	1.64	4 2	10.8	0.8	0.7	10.8	13.7	5.9	0.6	1.1	0.39	.2<	0.4	0.8	89.29
Average	37 15	1 61	4.62	10.96	0.78	0.76	10.94	14.53	5.28	0.60	1.20	0.42	0.20	0.62	0.90	90.57
STDS	0.31	0.04	0.43	0.29	0.08	0.05	0.34	0.70	0.47	0.10	0.07	0.02	n.d.	0.16	0.16	0.63
RSD	1%	3%	9%	3%	11%	7%	3%	5%	9%	17%	6%	5%	n.d.	27%	18%	1%
CP54																
LS54,1	*40.5	0.38	15 6	5.6	.2<	0.2	4.3	9.1	5.4	.2<	0.5	0.35	1<	1<	0<	81.92
LS54,2	*39 5	0.45	13.6	5.9	.2<	0.3	5.3	8.8	5.1	0.7	0.7	0.41	1<	0<	0.6	81.47
LS54,3	*39 5*	*0.88*	*9.2*	*10.2*	*0.5*	*0.5*	*6.1*	*10.4*	*3.3*	*0<*	*0.2*	*0.36*	*1.1*	*1<*	*1<*	*82.26*
Average first 2	n.d.	0.42	14.60	5.75	b.d.	0.25	4.80	8.95	5.25	0.70	0.60	0.38	b.d.	b.d.	0.60	n.d.
STDS	n.d.	0 05	1.41	0.21	n.d.	0.07	0.71	0.21	0.21	n.d.	0.14	0.04	n.d.	n.d.	n.d.	0.32
RSD	n d.	12%	10%	4%	n.d.	28%	15%	2%	4%	n.d.	24%	11%	n.d.	n.d.	n.d.	n.d.
CP55																
LS55,1	*34 0*	*0.49*	*16 2*	*5.4*	*0.3*	*1<*	*2.2*	*9.6*	*4.7*	*0.5*	*08<*	*0.14*	*0 2*	*- 2<*	*5<*	*73.75*
LS55,2	37 6	0.71	13 5	5.7	1<	0.4	5.2	10 8	5.1	0.5	0.7	0 26	1.4	1<	3<	81.87
CP60																
LS60,1	51 2	0 72	13 8	*8.6	0.4	0.2	2.3	11.1	6.9	2<	0.6	0 37	0 6	0.5	5<	97 21
LS60,2	50.4	1 05	12 6	9.3	0.4	0.3	3.0	10.1	6.9	1<	0 6	0.28	0<	0.5	2<	95.24
LS60,3	51 4	0.95	13 3	9.6	0.2	0 2	2.6	9.8	7.3	0.4	0.5	0.29	2<	3<	2<	96.44
LS60,4	52.8	0 81	13 5	9.4	2<	0 3	2.2	*7 5	7.3	2<	0.7	0 30	0<	2<	5<	94.94
Average	51 45	0 88	13.30	9.43	0.33	0.25	2.53	10.33	7 10	0.40	0 60	0 31	0.60	0 50	b.d.	98.02
STDS	1 00	0 15	0 51	0 15	0 12	0.06	0.36	0.68	0 23	n.d.	0 08	0 04	n.d.	0.00	n.d.	1.06
RSD	2%	17%	4%	2%	35%	23%	14%	7%	3%	n.d.	14%	13%	n.d.	0%	n.d.	1%
CP74																
LS74,4	*50.4*	*0.56*	*15.3*	*7.4*	*0 4*	*0 2*	*3.9*	*7 0*	*6.4*	*0 8*	*0.6*	*0 35*	*0 3*	*3<*	*5<*	*93.56*
LS74,1	51 9	0 29	15 6	6.9	0.3	0.3	1.8	5.6	6.7	0.6	0 5	0.32	0.2	- 0<	0.9	91.95
LS74,2	50 9	0.35	15.7	6.8	0.4	.2<	2.5	5.6	7.0	1.4	0 6	0.29	- 1<	3<	0.8	92.33
LS74,3	52.7	0.33	16.1	6.9	0.2	0.2	1.1	5 4	7 4	1<	0 3	0.23	0<	2<	4<	90.91
LS74,5	52.0	0.33	15.8	6.8	.2<	0.4	1 3	5 9	7.1	3<	0 4	0.32	0<	0<	1.1	91.43
Average last 4	51 88	0 37	15 80	6.85	0.30	0.30	1.68	5.63	7.05	1 00	0.45	0.29	0.20	b.d.	0.93	92.72
STDS	0.74	0 03	0 22	0 06	0.10	0.10	0 62	0 21	0.29	0 57	0.13	0 04	n d.	n d.	0.15	0.62
RSD	1%	7%	1%	1%	33%	33%	37%	4%	4%	57%	29%	15%	n d.	n d	16%	1%
CP78																
LS78,1	*44 6*	*2 29*	*5 0*	*13 0*	*0 6*	*1 3*	*5.3*	*9 3*	*6 4*	*0 7*	*1 6*	*0 79*	*1 3*	*0 8*	*0 7*	*93 82*
LS78,2	*49 3*	*2 51*	*5.3*	*14 8*	*0 8*	*1 3*	*6.3*	*4 5*	*4.3*	*0 9*	*1 7*	*0 98*	*1 5*	*0 9*	*1 1*	*96 14*
LS78,4	*47 6*	*1 81*	*4 0*	*11 9*	*0 7*	*3.1*	*11.5*	*10.3*	*4.7*	*1.0*	*1 3*	*0 60*	*0 9*	*0 6*	*1.0*	*100 99*
LS78,3	46 8	2 09	5 2	11 9	0.5	1 3	8 2	12.1	6.1	0.8	1 7	0 81	1 1	1 1	0 7	100 50
LS78,5	45 9	1 90	5 0	11 9	0 6	1.1	9 0	12.7	5 9	0.9	1.4	0.79	1.3	0 7	1.4	100.36
LS78,6	46 5	1 99	5 0	13.0	0.6	1 1	7 5	12.4	6.2	0 7	1 5	0 84	1 2	1 1	1 2	100.75
LS78,7	45 8	2.12	6.2	13.0	0 7	1.3	5.4	12.0	6.5	0 7	1 5	0 89	1.7	0.8	1.1	99.72
Average last 4	46 25	2.03	5 35	12.45	0 60	1 20	7.53	12.30	6 18	0.78	1 53	0 83	1.33	0.93	1 10	100.36
STDS	0 48	0 10	0 57	0.64	0.08	0 12	1.54	0.32	0 25	0.10	0.13	0.04	0.26	0.21	0.29	0 44
RSD	1%	5%	11%	5%	14%	10%	21%	3%	4%	12%	8%	5%	20%	22%	27%	0%
CP89																
LS89,1	*47 3	0 75	12 4	5 3	0 4	b.d.	4.7	6.1	7.7	0.6	0 6	0 45	b.d.	b.d	0.9	87.17
LS89,2	50 5	0 81	13 4	6 5	0 6	0 6	3 0	5 5	7 2	b.d.	0 4	0 33	b.d.	b d.	0.9	89.56
LS89,3	50 9	*0 91	11 8	6 3	0 4	0 4	2 2	*9.6	*8.9	b.d.	0 5	0 29	b.d.	b d.	b.d.	92.18
LS89,4	50 3	0 79	13 1	6 4	0 7	0 6	3 9	5 4	6 4	0 5	0 4	0 41	b d	b d	b.d	88 81
LS89,5	*45 2	0 70	13 4	5 3	0 5	0 5	5 7	7 2	7 4	0 5	0 7	0 40	b d	b d	b d.	87 49
Average	50.56	0 76	12 82	5 94	0.50	0.55	3.90	6.05	7 16	0.51	0.52	0 38	b.d.	b.d.	0.90	90 54
STDS	0 28	0 05	0 72	0 59	0 11	0 08	1 38	0 83	0 56	0 07	0 12	0 06	n d.	n d	0 05	2 01
RSD	1%	6%	6%	10%	21%	14%	35%	14%	8%	14%	23%	17%	n d	n d.	6%	2%
CP91																
LS91,1	43 1	1 41	7 3	10 0	0 6	0.9	8.9	13 1	5.8	0.6	0.9	0.50	0.4	0 5	3<	93 99
LS91,2	*43 9	1 33	8.3	10 3	0.5	0.9	8.1	13.1	5.9	0.6	0.8	0.56	0.5	0.4	.3<	95 06
LS91,3	41.9	1 39	7.7	10.6	0.4	1.0	9.3	14.4	5.3	0 8	0.9	0.61	0.5	0.5	1 0	96.28
LS91,4	41 9	1.32	7.5	10.3	0 6	1.0	9.9	15.4	5.3	0 7	1.1	0.62	0.4	0.6	0.9	97 63
LS91,5	42.3	1.23	7 6	9.9	0.4	1.0	9 1	15.3	5.7	0 6	0.9	0.46	0.3	0.5	0.9	96.34
LS91,6	42.1	1.41	7 7	10.3	0.4	1.1	9.8	14.4	5.2	0.7	1 1	0.57	0.4	3<	1.0	96.22
LS91,7	42.3	1.31	8.0	10.1	0.4	0.9	10.1	14.8	5.2	0.8	0 9	0 53	0.4	3<	0.8	96.60
LS91,8	42.3	1.27	8.5	9.8	0.5	0.9	9.0	14.6	5.3	0.7	0.9	0.43	0.4	3<	5<	94.70
LS91,9	42 2	1.29	8.0	10 2	0.4	1.0	9.2	14.4	5.2	0.7	1.0	0.54	0.4	2<	0.6	95.10
Average	42.26	1 33	7 84	10.17	0.47	0.97	9.27	14.39	5.43	0.69	0 94	0.54	0.41	0.50	0.87	96.07
STDS	0.38	0.06	0.39	0.24	0 09	0.07	0.61	0.82	0.28	0 08	0 10	0 06	0.06	0.07	0.15	1 13
RSD	1%	5%	5%	2%	19%	7%	7%	6%	5%	11%	11%	12%	15%	14%	17%	1%
CP92																
LS92,1	42 1	1 00	12.7	8 4	0.5	0.8	6.9	13.4	5.8	0.4	1.0	0.42	0.3	1<	4<	93 71
LS92,2	43 1	1 03	12.8	8.6	0.4	0.8	7 3	13.1	5.6	1<	0 7	0 43	2<	3<	- 3<	93.85
LS92,3	42.7	0.97	12.7	8.5	0.4	0.8	7 3	13.0	5.5	0.3	1 0	0 37	2<	1<	2<	93.61
LS92,4	42.4	0 98	12.7	8.3	0.4	0.7	7 3	13.0	5.6	2<	0.6	0.40	0.3	2<	3<	92.60
LS92,5	43 2	1 05	13.0	8.5	0.4	0.9	7.2	13.0	5.7	0.4	0.8	0.41	0.2	0.6	3<	95.45
LS92,6	42.9	0.97	12.7	8.6	0.4	0.9	7 3	13.2	5.6	1<	0.8	0.44	0.2	3<	1<	93.95
LS92,7	42.6	0.98	12.7	8.7	0.5	0.7	7.5	12.6	5.5	0.3	0.7	0.40	0.3	3<	2<	93.57

Sample	SiO2	TiO2	Al2O3	FeO	MnO	MgO	CaO	Na2O	K2O	P2O5	F	Cl	SO3	BaO	SrO	Total
LS92,8	43.2	1.00	12.9	8.5	0.4	0.8	7.6	13.0	5.6	0.3	0.6	0.39	0.2	3<	.3<	94.54
LS92,9	42.6	0.97	12.9	8.5	0.4	0.9	7.5	13.2	5.7	0.3	0.7	0.47	0.3	0.4	.3<	94.91
LS92,10	42.5	1.01	12.7	8.3	0.4	0.8	7.7	13.0	5.5	3<	0.9	0.38	0.2	0.5	3<	93.79
Average	42.73	1.00	12.78	8.49	0.42	0.81	7.36	13.05	5.61	0.33	0.78	0.41	0.25	0.50	b.d.	94.52
STDS	0.37	0.03	0.11	0.13	0.04	0.07	0.23	0.21	0.10	0.05	0.15	0.03	0.05	0.10	n.d.	0.79
RSD	1%	3%	1%	2%	10%	9%	3%	2%	2%	15%	19%	7%	21%	20%	n.d.	1%
CP93																
LS93,1	41.1	0.74	12.9	7.2	0.2	0.5	5.7	13.3	6.2	0.4	0.6	0.43	0.3	3<	0.6	90.25
LS93,2	41.3	0.72	13.1	7.1	0.5	0.5	5.8	14.5	5.9	0.4	0.8	0.38	0.2	2<	.5<	91.15
LS93,3	41.3	0.71	12.8	6.9	0.5	0.5	5.6	13.4	6.8	0.3	0.7	0.39	.1<	0.4	.4<	90.43
LS93,4	42.0	0.68	13.1	7.1	0.5	0.5	5.3	12.9	6.8	0.4	0.5	0.37	0.2	3<	.5<	90.41
LS93,5	42.1	0.71	13.3	7.2	0.5	0.6	5.6	12.9	6.2	0.4	0.8	0.37	1<	0.6	0.9	92.05
LS93,6	41.6	0.70	13.0	6.9	0.4	0.5	5.8	12.7	6.2	0.4	0.7	0.41	1<	0.5	1.0	90.76
LS93,7	42.3	0.76	13.2	7.1	0.4	0.4	5.5	13.5	5.9	.3<	0.7	0.43	1<	2<	.5<	90.31
Average	41.67	0.72	13.06	7.07	0.43	0.50	5.61	13.31	6.29	0.38	0.69	0.40	0.23	0.50	0.83	91.69
STDS	0.46	0.03	0.17	0.13	0.11	0.06	0.18	0.60	0.38	0.04	0.11	0.03	0.06	0.10	0.21	0.65
RSD	1%	4%	1%	2%	26%	12%	3%	5%	6%	11%	16%	7%	25%	20%	25%	1%
CP97																
LS97,1	49.9	0.74	13.2	7.4	0.5	0.3	2.2	9.3	7.8	.2<	0.4	*0.21	-.0<	2<	3<	91.97
LS97,2	50.9	0.78	12.7	7.4	0.5	0.3	2.0	8.9	7.7	.0<	0.3	0.28	-.1<	-.1<	-.2<	91.62
LS97,3	49.3	*0.67	12.6	7.4	0.3	0.4	2.3	11.0	6.8	0.3	0.5	0.27	1<	1<	.4<	91.69
LS97,4	49.6	0.78	12.8	7.2	0.3	0.4	2.2	10.9	6.9	.0<	0.4	0.29	0<	3<	2<	91.80
Average	49.93	0.74	12.83	7.35	0.40	0.35	2.18	10.03	7.30	0.30	0.40	0.26	b.d.	b.d.	b.d.	92.07
STDS	0.69	0.02	0.26	0.10	0.12	0.06	0.13	1.08	0.52	n.d.	0.08	0.01	n.d.	n.d.	n.d.	0.15
RSD	1%	3%	2%	1%	29%	16%	6%	11%	7%	n.d.	20%	4%	n.d.	n.d.	n.d.	0%
CP102																
LS102,1	*49.0*	*0.39*	*13.0*	*7.5*	*0.5*	*0.5*	*3.2*	*10.8*	*6.6*	*b.d*	*0.7*	*0.35*	*b.d.*	*b.d*	*0.9*	*93.42*
LS102,2	50.6	0.41	13.6	7.6	0.4	0.5	2.6	8.0	7.2	b.d.	0.6	0.40	b.d.	b.d.	b.d.	91.77
LS102,3	51.4	0.41	13.8	7.5	b.d.	0.6	2.3	7.7	7.3	0.5	0.4	0.32	b.d.	b.d.	1.0	93.12
LS102,4	51.0	0.37	13.8	7.6	0.4	0.6	1.9	8.3	7.4	b.d.	0.4	0.27	b.d.	b.d.	1.1	93.05
LS102,5	50.6	0.41	13.6	7.8	b.d.	0.6	2.2	8.2	7.3	b.d.	0.4	0.23	b.d.	b.d.	b.d.	91.18
LS102,6	51.3	0.43	13.6	7.7	0.4	0.7	2.9	6.3	*6.5	2<	0.6	0.32	1<	2<	4<	90.74
Average last 5	50.98	0.41	13.66	7.63	0.38	0.60	2.37	7.68	7.31	0.46	0.48	0.31	b.d	b.d	1.05	93.29
STDS	0.37	0.02	0.09	0.09	0.03	0.07	0.38	0.81	0.10	n.d	0.11	0.06	n.d	n.d	0.02	1.08
RSD	1%	5%	1%	1%	7%	12%	16%	11%	1%	n.d	23%	21%	n.d	n.d	2%	1%
CP103																
LS103,1	*46.5*	*0.74*	*12.0*	*8.0*	*0.6*	*b.d.*	*6.3*	*8.0*	*8.7*	*b.d.*	*0.4*	*0.26*	*b.d.*	*b.d.*	*b.d.*	*88.41*
LS103,2	45.4	0.76	11.8	8.2	0.3	0.4	3.1	11.9	8.6	b.d.	0.5	0.29	b.d.	b.d.	b.d.	91.25
LS103,3	44.5	*0.67	12.0	8.1	0.4	0.4	3.2	12.1	8.9	b.d.	0.6	0.26	b.d.	b.d.	b.d.	91.10
LS103,4	44.3	0.76	11.0	9.1	0.6	0.6	2.5	11.1	8.8	b.d.	0.4	0.26	b.d.	b.d.	b.d.	89.47
LS103,5	45.3	0.73	11.8	8.1	0.5	0.4	2.9	11.1	9.1	b.d.	0.7	0.30	b.d.	b.d.	b.d.	90.85
Average last 4	44.88	0.75	11.66	8.39	0.44	0.43	2.92	11.56	8.85	b.d.	0.53	0.28	b.d.	b.d.	b.d.	90.68
STDS	0.55	0.02	0.42	0.47	0.10	0.10	0.30	0.51	0.21	n.d.	0.10	0.02	n.d.	n.d.	n.d.	0.82
RSD	1%	2%	4%	6%	22%	23%	10%	4%	2%	n.d.	19%	7%	n.d.	n.d.	n.d.	1%
CP109																
LS109,1	49.4	0.46	15.0	6.5	0.3	2<	1.6	10.7	7.4	-.0<	0.4	0.25	1<	0<	-.2<	92.15
LS109,2	49.9	0.50	14.9	6.7	2<	0.2	1.7	10.4	7.4	1<	0.4	0.28	1<	1<	0<	92.36
LS109,3	49.9	0.52	14.6	7.1	0.4	2<	1.6	10.6	7.2	2<	0.4	0.31	-.0<	1<	0<	92.55
LS109,4	49.3	0.47	14.5	6.9	0.3	2<	1.7	10.7	7.1	2<	1<	0.30	1<	1<	1<	91.30
LS109,5	48.8	0.51	15.5	6.7	0.3	1<	1.4	10.7	7.3	2<	0.4	0.28	0<	-.0<	0.7	92.65
Average	49.46	0.49	14.90	6.78	0.33	0.20	1.60	10.62	7.28	b.d.	0.40	0.28	b.d.	b.d.	0.70	93.04
STDS	0.46	0.03	0.39	0.23	0.05	n.d.	0.12	0.13	0.13	n.d.	0.00	0.02	n.d.	n.d.	n.d.	0.54
RSD	1%	5%	3%	3%	15%	n.d.	8%	1%	2%	n.d.	0%	8%	n.d.	n.d.	n.d	1%
CP110																
LS110,1	48.7	0.86	15.8	8.3	0.3	0.5	4.0	12.3	5.7	0.4	0.5	0.43	0.8	1<	1<	98.53
LS110,2	49.2	0.92	14.6	8.4	2<	0.6	4.7	11.6	5.9	3<	0.3	0.27	0.4	3<	.4<	96.99
LS110,3	48.9	0.99	15.6	8.6	0.2	0.4	4.0	12.1	6.0	-.0<	0.5	0.40	0.5	-.1<	-.6<	98.18
LS110,4	49.3	0.90	15.4	8.1	0.3	0.4	4.4	12.1	6.0	.2<	0.4	0.37	0.5	.3<	1<	98.27
LS110,5	49.1	1.02	14.6	8.5	0.3	0.6	5.0	11.2	5.9	3<	0.4	0.30	0.2	0.4	.0<	97.53
Average	49.04	0.94	15.20	8.38	0.28	0.50	4.42	11.86	5.90	0.40	0.42	0.35	0.48	0.40	b.d.	98.57
STDS	0.24	0.07	0.57	0.19	0.05	0.10	0.44	0.45	0.12	n.d.	0.08	0.07	0.22	n.d.	n.d.	0.63
RSD	0%	7%	4%	2%	18%	20%	10%	4%	2%	n.d.	20%	19%	45%	n.d.	n.d.	1%
CP111																
LS111,1	38.3	1.90	4.0	10.9	1.1	0.8	9.2	14.2	6.7	0.6	1.4	0.44	b.d.	b.d.	1.1	90.60
LS111,2	38.0	1.87	3.7	11.8	1.1	1.0	10.5	12.9	5.9	b.d.	1.4	0.38	b.d.	b.d.	b.d.	88.61
LS111,3	36.7	1.71	3.9	10.7	1.1	0.9	10.1	13.3	6.2	0.6	1.3	0.39	b.d	0.7	1.0	88.51
LS111,4	39.4	1.96	4.0	12.0	1.2	0.8	9.5	10.6	6.5	0.5	1.7	0.38	b.d.	0.7	0.8	90.02
LS111,5	*33.9*	*1.68*	*4.1*	*11.7*	*1.4*	*0.9*	*15.0*	*11.3*	*4.5*	*0.8*	*1.1*	*0.27*	*b.d.*	*0.7*	*1.6*	*88.92*
LS111,6	*38.9*	*1.91*	*4.2*	*11.8*	*1.2*	*1.0*	*10.9*	*7.3*	*5.6*	*0.3*	*1.0*	*0.42*	*0.2*	*0.9*	*1<*	*85.72*
Average first 4	38.09	1.86	3.89	11.35	1.15	0.87	9.83	12.74	6.31	0.55	1.47	0.40	b.d.	0.70	0.99	90.18
STDS	1.13	0.11	0.15	0.66	0.05	0.08	0.60	1.54	0.35	0.06	0.16	0.03	n.d.	0.01	0.14	1.04
RSD	3%	6%	4%	6%	4%	9%	6%	12%	6%	12%	11%	7%	n.d.	2%	14%	1%
CP113																
LS113,1	44.6	1.43	5.9	12.3	0.4	1.4	6.7	12.5	5.7	0.6	1.0	0.59	0.5	0.6	.2<	94.16

Sample	SiO2	TiO2	Al2O3	FeO	MnO	MgO	CaO	Na2O	K2O	P2O5	F	Cl	SO3	BaO	SrO	Total
LS113,2	43.6	1.40	6.0	12.3	0.6	1.3	6.0	14.0	5.7	0.8	1.3	0.56	0.7	0.6	.2<	94.80
LS113,3	42.9	1.43	5.9	11.9	0.6	1.3	5.8	13.7	5.9	0.7	1.1	0.61	0.6	0.7	.4<	93.27
Average	43.70	1.42	5.93	12.17	0.53	1.33	6.17	13.40	5.77	0.70	1.13	0.59	0.60	0.63	b.d.	94.07
STDS	0.85	0.02	0.06	0.23	0.12	0.06	0.47	0.79	0.12	0.10	0.15	0.03	0.10	0.06	n.d.	0.77
RSD	2%	1%	1%	2%	22%	4%	8%	6%	2%	14%	14%	4%	17%	9%	n.d.	1%
CP120																
CP120,1	34.5	1.33	5.0	10.3	0.8	1.1	14.3	15.5	4.4	0.5	1.1	0.38	.1<	0.6	1.2	90.95
CP120,2	33 8	1.32	4.6	10.1	0.9	1.2	15.2	15.9	4.4	0.6	1.2	0.44	0.4	0.9	1.0	92.13
CP120,3	34.4	1.33	4 6	10.9	1.0	1.1	15.4	15.3	4.2	0.7	1 2	0.37	0.2	0.9	1.2	92.71
CP120,4	35.2	1.42	4 5	10.8	0.9	1.2	14.8	15.0	4.6	0.6	1.1	0.32	0.2	0 8	1 0	92.68
CP120,5	34.6	1 41	4 4	10.4	0.9	1.1	14.5	14.8	4.8	0.5	1.2	0.38	0.2	0.9	1.0	91.23
CP120,6	35.5	1.34	5.3	10.9	0.9	0.9	13.4	14.6	5.0	0.3	1.1	0.42	0.2	0.8	-.0<	90.62
CP120,8	32 8	*1.14	4.1	9.1	0.8	0.9	15.4	15.4	3.9	0.5	1.4	0.38	0.4	0.7	0.6	87 44
CP120,9	34.0	1.31	*3.3	9.6	1 0	1.0	15.7	15.9	3.9	0.8	1.5	0.42	0.4	0.8	0.7	90.21
CP120,10	35 8	1.34	5.1	11.2	1.0	1.0	15.6	*10.3	4.0	0.4	0.9	0.34	0.2	0.8	0.9	88.79
CP120,7	*31 0*	*1.26*	*4.4*	*9.2*	*0 7*	*0.8*	*12.1*	*17.5*	*5.6*	*0 6*	*0.9*	*2.50*	*0.4*	*0 7*	*.4<*	*87.84*
Average first 9	34.51	1 35	4 70	10.37	0.91	1.06	14.92	15.30	4.36	0.54	1.19	0.38	0.28	0.80	0.95	91.61
STDS	0 92	0.04	0.40	0.68	0.08	0.11	0.75	0.48	0.39	0.15	0.18	0.04	0.10	0 10	0.21	1 76
RSD	3%	3%	9%	7%	9%	11%	5%	3%	9%	28%	15%	10%	38%	13%	23%	2%
CP121																
LS121,1	38 0	1.39	5.3	10.0	0.6	1.1	12.3	15.2	5.0	0.5	0.9	0.41	0<	0.6	0.7	92.06
LS121,2	38.2	1 45	5 0	9.5	0.7	1.0	10.4	14.6	6.6	0.5	1 1	0.44	0.3	0.6	.4<	90.25
LS121,3	*41.0	1.67	4.4	9.7	0.7	1 2	10.3	*12.5	6.6	0.4	1.0	0.45	0.2	0.4	.5<	90 48
LS121,4	34.5	1.30	*3.4	9.9	0.7	1.1	*16.7	15.1	3.7	0.8	1.4	0.40	0.4	0.7	0.9	90.95
LS121,5	35 5	1.27	4.9	10.6	0 6	1.2	*15.7	14 5	4.1	0.6	1.3	0.35	0.2	0.8	0.8	92.33
LS121,6	38.0	1 60	4.6	10.2	0.9	1.1	11.7	14.8	5.4	.0<	0.9	0 43	0.3	1 0	- 2<	90.79
LS121,7	36 9	1 39	5.4	9.8	0.8	1.2	13.0	14.4	5.0	0.4	1 2	0.35	0.2	0.7	5<	90.84
LS121,8	38 5	1.51	5 1	9.3	0.7	1.0	11 2	14.8	5.3	0 4	1 1	0.34	2<	0.6	1<	89.78
LS121,9	34.4	1.36	5 1	*8 3	0.8	0.8	13.2	14.9	4.3	0.6	1.5	0.43	0.2	0 8	0.5	87.26
LS121,10	34 9	1 22	5 3	9 4	0.7	0.8	13.8	14.1	4.3	0.5	1 4	0.49	0.5	0.7	4<	88.16
LS121,11	*41 6*	*1 56*	*4 7*	*10 3*	*0 9*	*1 1*	*10.5*	*9 2*	*6.5*	*0 3*	*0 9*	*0 43*	*1<*	*.3<*	*0.6*	*88.71*
LS121,12	*42.0*	*1 54*	*4 9*	*10 3*	*0 7*	*1 1*	*10 1*	*9 1*	*6.7*	*0 4*	*1 1*	*0 38*	*0.2*	*0.6*	*0.7*	*89.95*
Average first 10	36 54	1 42	5 01	9 82	0 72	1.05	11.99	14.71	5.03	0.52	1.18	0.41	0.29	0.69	0.73	90.11
STDS	1 71	0 14	0 33	0.41	0 09	0.15	1.31	0.35	0.99	0.13	0.21	0.05	0.11	0 16	0.17	1 57
RSD	5%	10%	7%	4%	13%	14%	11%	2%	20%	25%	18%	12%	39%	23%	24%	2%
CP122																
LS122,1	50 4	0.46	5 9	13 1	1 5	1 7	5.3	3.2	4.7	b.d.	1.5	0.45	b.d.	0.6	b.d.	88 74
LS122,2	49 7	0.48	6 1	13.2	1 4	1.6	5 7	3.7	4.9	0.6	1.0	0.39	b.d.	b.d.	1 1	89 91
LS122,3	*45.4	0.46	5.3	12.2	1 3	1.5	*6.9	5.0	*6.8	0.5	1.5	0 40	b.d.	0 7	1.0	88.91
LS122,4	49.5	0.43	7.4	12.9	1.5	1.5	5.3	4.5	5.4	b.d.	1 5	0.36	b.d.	0.6	b.d.	90.88
LS122,5	*19 8*	*0.43*	*5.1*	*13 7*	*1.5*	*1 6*	*5.7*	*3 5*	*4.9*	*0 6*	*1.6*	*0.40*	*0.3*	*b d*	*b.d.*	*89.05*
Average first 4	49.84	0 46	6 19	12.86	1.43	1 58	5 44	4.10	4 99	0.55	1.38	0.40	b.d.	0.62	1.06	90.88
STDS	0.46	0 02	0.89	0.48	0 09	0.12	0.23	0 82	0.39	0.05	0.23	0 04	n.d.	0.06	0.02	0.99
RSD	1%	5%	14%	4%	6%	7%	4%	20%	8%	9%	17%	9%	n.d.	10%	2%	1%
CP124																
LS124,1	48.17	0 92	5.40	12.76	1.17	1.41	4.61	3 71	5 24	b.d.	1.11	0 39	b.d.	0 77	b.d.	85.66

Note: whole analyses not taken into account in average are in italics, and analyses of individual elements that are rejected from the calculation of the average are indicated by an asterix (*). b.d. below detection

Table A6.3. Major element microprobe analyses of crystals in experiments on the join HOL14/OL5 (in wt. %).

Sample	SiO2	TiO2	Al2O3	FeO	MnO	MgO	CaO	Na2O	K2O	P2O5	F	Cl	SO3	BaO	SrO	TOTAL
CP1																
Nepheline	*42.7*		*30.6*	*1.46*			*0.17*	*18.6*	*6.26*							*99.75*
Nepheline	*41.9*		*31.3*	*1.37*			*0.17*	*16.8*	*5.86*							*97.32*
Nepheline	*41.5*		*29.9*	*1.38*			*0.13*	*17.3*	*6.2*							*96.42*
Nepheline	*41.6*		*32.3*	*0.91*			*0.16*	*16.9*	*6.72*							*98.54*
Nepheline	45.6		30	2.62			0.07	17	6.57							101.84
Nepheline	44.3		31.5	2.29			0.11	16.8	6.27							101.32
Average	44.9		30.7	2.46			0.09	16.9	6.42							101.58
Melanite	*31.9*	*6.09*	*0.85*	*23.4*	*0.78*	*0.56*	*31.1*	*2.53*	*0.21*							*97.45*
Melanite	**30.4**	**11.8**	**0.84**	**21.4**	**0.5**	**0.37**	**30.9**	**0.47**	**0.16**							**96.66**
Wollastonite	**51.04**		**0.02**	**0.70**	**0.47**	**0.19**	**47.40**	**0.19**	**0.08**						**0.34**	**100.43**
Wollastonite	*50.12*		*0.08*	*0.88*	*0.41*	*0.13*	*45.35*	*0.50*	*0.14*						*0.27*	*97.88*
CP2																
Clinopyroxene	**51**	**0.54**	**0.96**	**13.5**	**0.5**	**9.54**	**21.2**	**1.96**								**99.22**
Clinopyroxene	*49.8*	*0.39*	*0.67*	*13.8*	*0.49*	*9.61*	*20.9*	*1.95*								*97.56*
Clinopyroxene	*48.1*	*0.85*	*0.42*	*22.3*	*0.69*	*4.18*	*13.4*	*5.92*								*95.82*
Melanite	**28.5**	**13.1**	**0.88**	**20.7**	**0.39**	**0.56**	**31.9**	**0.58**								**96.63**
Melanite	*30.8*	*10.7*	*0.9*	*21.8*	*0.47*	*0.31*	*31.7*	*0.31*								*96.86*
Nepheline	42.5		31.2	1.69			0.18	16.1	7.08							98.83
Nepheline	43.5		30.7	2.8			0.11	16.3	6.75							100.17
Average	43		31	2.25			0.15	16.2	6.92							99.50
Wollastonite	53.00		0.82	1.56	0.39	0.14	41.71	0.77	0.58						0.50	99.47
Wollastonite	52.42		1.75	1.65	0.35	0.15	41.82	1.33	0.62						0.39	100.48
Average	52.71		1.29	1.61	0.37	0.15	41.77	1.05	0.60						0.45	99.98
Vishnevite	40.4		29.7	2.2			1.29	9.79	2.33		b.d.	2.41	5.25	0.29	0.1	93.72
Vishnevite	40.4		29.2	1.81			1.38	11.4	2.81		b.d.	2.72	4.08	0.29	0.15	94.26
Average	40.4		29.4	2.01			1.34	10.6	2.57		b.d.	2.57	4.67	0.29	0.13	94.01
CP5																
Nepheline	*41.8*		*30*	*1.26*			*0.13*	*16.7*	*6.17*							*95.97*
Nepheline	**43.4**		**32.2**	**1.69**			**0.2**	**17.6**	**6.67**							**101.67**
Clinopyroxene	**49.9**	**0.45**	**0.82**	**16.3**	**0.61**	**7.63**	**19.9**	**3.8**								**99.37**
Clinopyroxene	*49.9*	*0.52*	*1.13*	*18.9*	*0.82*	*6.14*	*19.6*	*2.44*								*99.50*
Clinopyroxene	*52*	*0.57*	*0.84*	*11.7*	*0.39*	*11.2*	*22.5*	*1.39*								*100.61*
Clinopyroxene	*50.7*	*0.56*	*1.09*	*14.9*	*0.51*	*8.63*	*21*	*2.03*								*99.32*
Wollastonite	*50.58*		*1.86*	*1.78*	*0.47*	*0.18*	*41.78*	*0.44*	*0.87*						*0.54*	*98.50*
Wollastonite	*52.07*		*0.07*	*1.23*	*0.38*	*0.16*	*47.42*	*b.d.*	*0.10*						*0.16*	*101.59*
Wollastonite	**51.50**		**0.24**	**1.76**	**0.60**	**0.16**	**46.49**	**0.04**	**0.24**						**0.14**	**100.17**
CP7																
Melanite	29.1	12.7	0.65	21.5	0.3	0.64	32	1.07								98.14
Melanite	29.3	12.5	1.14	21.4	0.34	0.59	32.6	0.48								98.60
Melanite	29.8	13	1.18	21.1	0.4	0.58	31.6	0.48								98.60
Average	29.4	12.7	0.99	21.4	0.35	0.6	32	0.68								98.45
Nepheline	*41.9*		*32.2*	*1.17*			*0.2*	*17.4*	*6.45*							*99.32*
Nepheline	*42.4*		*31.7*	*1.82*			*0.15*	*17.4*	*6.83*							*100.27*
Clinopyroxene	*51*	*0.99*	*1.14*	*8.93*	*0.46*	*12.6*	*22.7*	*1.88*								*99.74*
Clinopyroxene	*48.9*	*0.45*	*1.19*	*16.5*	*0.54*	*7.18*	*20.1*	*3.24*								*98.07*
Clinopyroxene	*51.4*	*0.47*	*0.96*	*15.4*	*0.54*	*9.06*	*21.3*	*2.19*								*101.33*
Clinopyroxene	51.6	0.43	0.88	14.5	0.65	9.02	21.2	2.32								100.51
Clinopyroxene	51.5	0.87	1.57	12.9	0.32	10.3	21.7	1.6								100.78
Clinopyroxene	50.9	0.53	0.95	14.2	0.36	9.83	21.5	1.97								100.26
Average without first	51.34	0.61	1.13	13.87	0.44	9.71	21.44	1.96								100.52
Apatite	0.69			0.21	0.01	b.d.	53.1	0.45	0.08	38.9	2.02	0.02		0.04	1.62	97.14

Sample	SiO2	TiO2	Al2O3	FeO	MnO	MgO	CaO	Na2O	K2O	P2O5	F	Cl	SO3	BaO	SrO	TOTAL
CP8																
Clinopyroxene	49.7	1 23	2.23	13.6	0.3	9.37	21.7	1.66								99.78
Clinopyroxene	49.6	0.73	1.59	16.5	0.48	7.39	20.4	2.2								98.94
Clinopyroxene	51.4	0.51	0.94	14.5	0.22	8.98	21.3	2.09								99.86
Clinopyroxene	*49.8*	*0.51*	*0.92*	*15.8*	*0.39*	*7.86*	*20.1*	*2.44*								*97 74*
Clinopyroxene	*47.8*	*0.55*	*3.19*	*19.3*	*0.64*	*3.64*	*13.5*	*8.83*								*97 46*
Average first 3	50.24	0.82	1.59	14.87	0.33	8.58	21.11	1.98								99.53
Melanite	*31.6*	*9.94*	*0.83*	*21 5*	*0.41*	*0.29*	*32.2*	*0.35*	*0.06*							*97 14*
Melanite	29.8	12.8	0.76	20.6	0.31	0.58	31.1	0.97	0.09							96.98
Melanite	30.8	11.9	0 89	21.4	0.37	0.51	30.9	0.34	b.d.							97 14
Average last 2	30.30	12.34	0.83	21 00	0.34	0.55	31.03	0.66	0.09							97 06
Nepheline	*44 2*		*31 5*	*2.11*			*0 19*	*16.8*	*6.64*							*101 40*
Nepheline	43 2		31 8	1 78			0.17	16.7	6.56							100.16
Nepheline	43.4		31 3	1 52			0.13	16.8	6.54							99.69
Nepheline	43		31 6	1.99			0.19	16.7	6.64							100.15
Average last 3	43 22		31 59	1 76			0.16	16.69	6.58							100 00
Wollastonite	50 95		0 06	1 36	0 47	0.07	46.08	0 12	0 17							99.64
Wollastonite	51 87		0.05	0 58	1.00	0.08	46.07	0.25	0.06							100.30
Average	51 41		0 06	0.97	0 74	0.08	46.08	0.19	0.12							99.97
K-Feldspar	63.7	0 06	17 9	1.18	0.08	0 03	0.18	1.75	14.3					2.33	0.02	101.51
K-Feldspar	64 1	0.09	17 9	0.94	0.05	b.d.	0.03	1.57	14.6					1	b.d.	100.26
K-Feldspar	*61 3*	*0 36*	*16.2*	*3.64*	*0 23*	*0.09*	*1.13*	*2.72*	*12.1*					*1 33*	*0 17*	*99.29*
Average first 2	63.9	0 08	17 87	1 06	0.07	0 03	0 11	1 66	14.49					1.67	0.02	100.89
Na-poor vishnevite	*40 4*		*27 5*	*1 83*			*1.36*	*13 6*	*1.6*		*b d.*	*0 96*	*5 12*	*b d*	*0 39*	*92.78*
Vishnevite	**41**		**27.1**	**3.03**			**1.33**	**17.2**	**2.94**		**b.d.**	**0.75**	**3.06**	**0.25**	**0.26**	**96.91**
CP10																
Melanite	*30*	*12 1*	*1 96*	*20 1*	*0 46*	*0.42*	*28.7*	*5.41*	*0.43*							*99 48*
Melanite	*29 5*	*13.3*	*1 01*	*21*	*0.45*	*0.58*	*31.7*	*1 97*	*0.05*							*99.51*
Melanite	*27 9*	*15.7*	*1 24*	*19 6*	*0.32*	*0.86*	*31 2*	*1*	*0.08*							*97 91*
Melanite	*29 9*	*13.9*	*0 98*	*20.2*	*0.13*	*0.71*	*31.5*	*0 41*	*0.08*							*97 79*
Melanite	30 6	12 4	0.87	21.6	0.21	0 6	32.6	0.4	0 01							99.32
Melanite	31 2	10.6	0 96	21.3	0 21	0.43	31 4	0.35	0 09							96.39
Average last 2	30.91	11.47	0 92	21 45	0.21	0.52	31 97	0.38	0.05							97 86
Clinopyroxene	*50 5*	*0.25*	*0.91*	*19 3*	*0.47*	*6*	*17 3*	*4.48*								*99 24*
Clinopyroxene	*50 7*	*0 82*	*0 41*	*23.2*	*0.52*	*3.16*	*11 1*	*8 36*								*98.24*
Clinopyroxene	*50 7*	*1 39*	*0 8*	*22 1*	*0 56*	*3.89*	*12.4*	*8.12*								*99 89*
Clinopyroxene	*50 9*	*0 32*	*0.87*	*18.7*	*0.63*	*6.13*	*18.2*	*4.08*								*99.88*
Clinopyroxene	*50 2*	*0.71*	*1 04*	*13 7*	*0 37*	*9 49*	*21 3*	*3.91*								*100 66*
Clinopyroxene	51 7	0 79	0 85	14.7	0.51	8.72	19.5	3.1								99.85
Clinopyroxene	49 7	0.65	1 16	14 1	0 45	8.91	21 2	2.8								98.91
Clinopyroxene	51 8	0 5	0.72	11	0.26	12	22.6	1.34								100.18
Clinopyroxene	51 5	0.78	0.93	14.4	0.5	9.16	21.5	2.13								100.88
Average last 4	51 16	0 68	0.92	13.54	0 43	9.69	21.20	2.34								99.96
Nepheline	*39 7*		*27.1*	*3.18*			*1.39*	*17 4*	*6.02*							*94 76*
Nepheline	*42 7*		*30.8*	*1 82*			*0.12*	*17 4*	*6.78*							*99.69*
Nepheline	43 3		30 4	2.19			0.13	16.4	6.62							99 07
Nepheline	43 5		32.2	0.98			0.11	16.4	6.97							100.17
Nepheline	44.1		31.3	1.33			0.17	16.2	7.03							100.09
Average last 3	43 62		31.30	1 50			0.14	16.34	6.87							99.78
Wollastonite	51.53		0.06	1.22	0.62	0.14	46.55	0.20	0.17						0.25	100.74
Wollastonite	50 20		0 14	1 76	0 90	0.05	45.50	0.36	0.42						0 38	99.71
Wollastonite	*49.41*		*0.96*	*2.60*	*0.72*	*0.14*	*42.25*	*2.48*	*1.33*						*0.36*	*100.25*
Average first 2	50.87		0 10	1.49	0.76	0.10	46.03	0.28	0.30						0.32	100.23
Titanite	30.5	38.3	0.53	1.75	0.25	b.d.	27 7	0.33	0.14		0.22					99.72
CP11																
Clinopyroxene	*50 1*	*0.7*	*1.78*	*17.9*	*0.56*	*6.09*	*16.4*	*4.42*								*97.90*
Clinopyroxene	*49.9*	*0 47*	*0.34*	*20.5*	*0.42*	*5.23*	*15.2*	*5.12*								*97 18*
Clinopyroxene	*48.9*	*0.44*	*1 19*	*21*	*0.93*	*4.2*	*17.6*	*3.65*								*97 89*
Clinopyroxene	*49.9*	*0.33*	*1.11*	*20 3*	*0.9*	*4.63*	*17.6*	*3.48*								*98.20*

Sample	SiO2	TiO2	Al2O3	FeO	MnO	MgO	CaO	Na2O	K2O	P2O5	F	Cl	SO3	BaO	SrO	TOTAL
Clinopyroxene	*52.5*	*1.04*	*0 48*	*24.4*	*0.48*	*2.83*	*9.45*	*8.26*								*99.43*
Clinopyroxene	50 9	0.6	1 06	13.3	0.35	10.1	20.3	2.79								99.33
Clinopyroxene	51.9	0.54	0 86	15.6	0.58	8.01	20.2	2.52								100.16
Clinopyroxene	50.6	0.67	1.3	13	0.53	10.1	22	1.42								99.54
Average last 3	51.1	0.6	1.07	13 9	0.49	9.38	20.9	2.24								99.68
Melanite	**29.5**	**13.4**	**0.67**	**20.9**	**0.36**	**0.55**	**32**	**0.33**	**0.16**							**97.78**
Melanite	*31.3*	*9*	*0 5*	*23.1*	*0.47*	*0.37*	*32.1*	*0.3*	*0.12*							*97 29*
Wollastonite	51.78		0 01	1 30	0.32	0.12	46.10	0.32	0 14						0.14	100.23
Wollastonite	51.23		0 04	1 06	0.39	0.11	46.98	b.d.	0.21						0.34	100.36
Average	51.51		0.03	1 18	0.36	0.12	46.54	0.32	0.18						0.24	100.30
Nepheline	**43.2**		**32.4**	**1.85**			**0.16**	**16.4**	**7**							**100.97**
Nepheline	*42.9*		*32 7*	*1 29*			*0.12*	*16.8*	*7 38*							*101.13*
Nepheline	*43 8*		*32.3*	*1.49*			*0.17*	*16 4*	*7.34*							*101 53*
Titanite	31	39 3	0 22	1 68	b.d.	b.d.	28.1	0.31	0.05		0 34					100.96
CP13																
Nepheline	*43 6*		*32 7*	*1 78*			*0 17*	*17 5*	*6 72*							*102.47*
Nepheline	*43 7*		*32.6*	*1 55*			*0.09*	*17.5*	*6.59*							*101 92*
Nepheline	*43 3*		*31 5*	*2.31*			*0 12*	*17 1*	*6.63*							*100.87*
Nepheline	43 6		32.6	1 22			0.14	16.7	6.27							100 49
Nepheline	44 1		31 7	1.73			0.83	16.5	6.25							101 12
Average last 2	43 87		32.12	1.48			0.49	16.60	6.26							100.81
CP14																
Melilite	*42*		*9 74*	*8 48*	*0 4*	*3 13*	*23.3*	*7 78*	*1.69*						*2.23*	*98.68*
Melilite	41 7		6 51	9 61	0 42	3.62	27.9	6.04	0.3						2.42	98 59
Melilite	41 2		6 59	8 2	0.37	3.71	28.6	5.9	0.16						2.54	97 25
Melilite	41 7		5 87	9.29	0 55	3.72	28.2	5 79	0.19						2.68	98.00
Melilite	42 7		6 61	9 41	0 5	3.45	27 5	6 51	0.21						3 1	99 97
Melilite	42 1		6 28	9 36	0.31	3.75	28.5	5.76	0.2						2.35	98 53
Melilite	42 7		6 31	8 88	0.48	3.08	29.3	5.75	0.32						2.41	99.27
Melilite	42.1		6 36	9 25	0 51	3.63	28	6 43	0 13						2.4	98 73
Average without first	42		6 36	9 14	0 45	3 57	28 3	6 03	0 22						2.56	98 63
Nepheline	*42.3*		*29 2*	*1 97*			*1 24*	*17*	*6.5*							*98 23*
Nepheline	*40 7*		*29 5*	*1 52*			*0 19*	*16.6*	*6.32*							*94 78*
Nepheline	43 1		31 3	1 88			0 05	16 5	7 39							100 21
Melanite	*32.8*	*5 51*	*0.5*	*24 1*	*0.42*	*0 4*	*32.3*	*0.87*	*0 05*							*96 93*
Melanite	*33 2*	*7 69*	*0 84*	*23.2*	*0.43*	*0 17*	*31 6*	*0.44*	*0 06*							*97 56*
Melanite	29 2	14 6	1.21	19.1	0.4	0.8	32.5	1 04	0.05							98 95
Melanite	29 7	13 4	0 88	20.9	0.22	0.57	31 4	0 82	0.13							97 98
Average last 2	29 45	14.03	1 05	20.00	0.31	0 69	31 93	0 93	0.09							98.47
Wollastonite	52.21		0 05	1 37	0.35	0.18	46.51	0.51	0 15						0.29	101.62
Wollastonite	52.54		0 02	0 61	0 31	0 03	48 09	0.12	0.21						0.07	102.00
Average	52.38		0 04	0 99	0.33	0 11	47 30	0.32	0.18						0 18	101 81
CP15																
Melanite	30.1	12.4	0 59	21.2	0 49	0.53	31 8	0 44	b d							97 47
Melanite	30.5	12.4	0 76	21.8	0.35	0.48	31.2	0.34	0.03							97 93
Average	30 3	12.4	0.68	21 5	0.42	0.51	31 5	0.39	0.03							97 73
Vishnevite	**39.7**		**29.3**	**2.12**			**1.44**	**12.1**	**3.09**		**b.d.**	**2.82**	**4.33**	**0.21**	**0.13**	**96.30**
Vishnevite	*41 2*		*22.2*	*3 27*			*6.5*	*13.4*	*3.34*		*b d*	*2.08*	*4.51*	*0 21*	*0.23*	*96.90*
Nepheline	43 2		32.3	1 36			0 09	16.5	7 19							100 67
Clinopyroxene	52	0.45	0 93	13.8	0 55	9.31	20.7	1 79								99.41
Clinopyroxene	51 7	0 71	1 02	11.9	0.48	10.9	21.9	1.46								100.13
Average	51 8	0 58	0 98	12.8	0.52	10.1	21.3	1.63								99 77
Wollastonite	*52.12*		*0.11*	*1.05*	*0.44*	*0.13*	*47.40*	*0.05*	*0.22*						*0.50*	*102.02*
Wollastonite	**51.36**		**0.29**	**1.41**	**0.48**	**0.20**	**45.68**	**0.29**	**0.39**						**0.29**	**100.39**
CP16																
Combeite	*47 5*			*0 87*	*0.63*	*0.05*	*24.9*	*19.4*	*0.18*						*0.17*	*93.64*

Sample	SiO2	TiO2	Al2O3	FeO	MnO	MgO	CaO	Na2O	K2O	P2O5	F	Cl	SO3	BaO	SrO	TOTAL
Combeite	*48.6*			*0.93*	*0.47*	*0.08*	*25.5*	*19.6*	*0.11*						*0.85*	*96.04*
Combeite	50.1			1	0.63	0.08	27.5	19.4	0.14						0.23	99.03
Combeite	49.7			0.97	0.6	0.07	27.1	19.3	0.1						0.21	98.13
Combeite	50.4			1.53	0.6	0.06	27.7	18.8	0.27						0.61	99.99
Average without first	50.1			1.17	0.61	0.07	27.4	19.2	0.17						0.35	99.05
Nepheline	*41.9*		*32.7*	*1.21*			*0.32*	*16*	*7.73*							*99.89*
Nepheline	43.2		31.3	1.49			0.08	16.5	7.29							99.74
Nepheline	42.4		31.9	1.21			0.18	16	7.41							99.03
Nepheline	42.5		30.1	2.1			0.46	15.9	7.33							98.35
Average last 3	42.68		31.06	1.60			0.24	16.11	7.34							99.04
Melanite	**29.1**	**14**	**0.61**	**20.4**	**0.31**	**0.76**	**32**	**0.6**	**0.04**							**97.77**
Melanite	*32.9*	*5.69*	*0.3*	*23.5*	*0.78*	*0.51*	*31.9*	*0.39*	*0.04*							*96.01*
Melanite	*32*	*7.14*	*0.51*	*23.7*	*0.44*	*0.24*	*32.1*	*0.41*	*0.08*							*96.58*
Clinopyroxene	*50.4*	*0.5*	*0.97*	*18*	*0.68*	*6.67*	*19.3*	*3.2*								*99.70*
Clinopyroxene	*50.5*	*0.62*	*1*	*12.4*	*0.36*	*10.3*	*21.1*	*2.32*								*98.67*
Clinopyroxene	50.9	0.6	1.03	13.9	0.54	9.24	20.9	2.29								99.40
Clinopyroxene	50.6	0.39	0.82	16.5	0.42	7.98	20.2	2.42								99.34
Average last 2	50.76	0.50	0.93	15.22	0.48	8.61	20.54	2.36								99.37
Wollastonite	*49.65*		*0.12*	*1.25*	*0.48*	*0.12*	*45.96*	*0.72*	*0.27*						*0.16*	*98.73*
Wollastonite	*50.34*		*0.04*	*0.96*	*0.36*	*0.15*	*47.26*	*0.52*	*0.11*						*0.16*	*99.90*
CP17																
Nepheline	*42.2*		*32.2*	*1.69*			*0.16*	*16.4*	*7.81*							*100.54*
Nepheline	**43**		**31.9**	**1.27**			**0.32**	**16.2**	**7.61**							**100.13**
Melanite	29.7	13.1	0.92	21	0.58	0.6	31.6	0.87	0.09							98.47
Melanite	30.7	11.7	0.74	21.2	0.31	0.45	31.6	0.33	0.01							96.99
Average	30.2	12.4	0.83	21.1	0.45	0.53	31.6	0.6	0.05							97.76
Clinopyroxene	**49.7**	**0.83**	**1.69**	**16.9**	**0.53**	**7.31**	**20.2**	**2.23**								**99.31**
Clinopyroxene	*51*	*0.43*	*1.32*	*17.6*	*0.62*	*5.99*	*17.9*	*3.39*								*98.27*
Wollastonite	51.33		1.27	2.50	0.65	0.06	42.86	1.12	1.03						0.70	101.52
Wollastonite	52.05		1.69	2.82	0.82	0.13	37.94	1.07	1.28						0.73	98.53
Average	51.69		1.48	2.66	0.74	0.10	40.40	1.10	1.16						0.72	100.03
CP18																
Nepheline	*42.8*		*31.9*	*1.08*			*0.1*	*17*	*6.67*							*99.50*
Nepheline	*44.1*		*31.8*	*1.63*			*0.12*	*16.7*	*6.66*							*101.00*
Nepheline	43.6		30.8	2.68			0.27	16.6	6.46							100.37
Nepheline	43.1		31.9	1.68			0.19	16.6	6.75							100.23
Nepheline	43		30.8	2.4			0.12	16.5	6.61							99.38
Nepheline	44.1		31.4	1.54			0.13	16.7	6.58							100.49
Average last 4	43.45		31.23	2.08			0.18	16.59	6.60							100.12
CP19																
Nepheline	*43.1*		*31.3*	*1.93*			*0.24*	*16.7*	*7.01*							*100.28*
Nepheline	43.1		30.3	2.4			0.19	16.4	6.77							99.13
Nepheline	44.1		31.1	1.62			0.17	16.7	6.37							100.09
Nepheline	43.6		32	1.35			0.2	16.6	6.96							100.69
Average last 3	43.60		31.12	1.79			0.19	16.58	6.70							99.97
Wollastonite	49.72		0.49	1.17	0.58	0.13	45.93	0.31	0.34						0.07	98.74
Wollastonite	50.04		0.62	0.92	0.39	0.24	45.89	0.19	0.37						0.41	99.07
Average	49.88		0.56	1.05	0.49	0.19	45.91	0.25	0.36						0.24	98.91
Vishnevite	38.2		29.8	1.84			2.44	12.7	2.85		b.d.	2.23	5.26	0.29	0.15	95.74
Vishnevite	38.9		29.1	2.03			2.68	10.1	2.5		b.d.	2.28	5.67	b.d.	b.d.	93.22
Vishnevite	38.2		28.7	1.56			2.23	8.63	1.88		0.01	2.18	6.39	0.12	0.13	90.05
Average	38.4		29.2	1.81			2.45	10.5	2.41		0.01	2.23	5.77	0.21	0.14	93.13
Apatite	*0.55*			*0.42*	*0.06*	*b.d.*	*52.6*	*0.03*	*0.29*	*39.1*	*3.41*	*0.05*		*0.13*	*5.59*	*102.20*
Apatite	**0.72**			**0.5**	**0.04**	**b.d.**	**54.9**	**0.17**	**0.22**	**38.5**	**2.11**	**0.06**		**b.d.**	**0.98**	**98.18**
Melilite	*43.6*		*8.1*	*7.8*	*0.2*	*4*	*30.7*	*5.8*	*1<*						*1.9*	*102.10*
Melilite	*43.4*		*7.9*	*8*	*0.3*	*4.1*	*30.5*	*6*	*0.1*						*2.2*	*102.50*
Melilite	*43.2*		*7.4*	*8.4*	*2<*	*4.1*	*30.4*	*5.5*	*0.2*						*1.9*	*101.10*

Sample	SiO2	TiO2	Al2O3	FeO	MnO	MgO	CaO	Na2O	K2O	P2O5	F	Cl	SO3	BaO	SrO	TOTAL
Melilite	*44.1*		*8.2*	*7.7*	*.2<*	*3.9*	*30.3*	*6.3*	*0.1*						*1.9*	*102.50*
Melilite	*44.2*		*7.7*	*8.2*	*1<*	*4.3*	*30.7*	*5.8*	*0.2*						*1.6*	*102.70*
Melilite	*43.8*		*8*	*8*	*0.4*	*3.8*	*30.1*	*6*	*0.1*						*1.9*	*102.10*
Melilite	*43.9*		*7.4*	*8.5*	*0.2*	*4*	*30.6*	*5.7*	*0.1*						*1.6*	*102.00*
Melilite	*43.7*		*8.1*	*7.6*	*0.3*	*4.1*	*30.3*	*6*	*0.2*						*2*	*102.30*
Melilite	**43.4**		**7.7**	**8**	**0.4**	**3.7**	**30.3**	**5.7**	**.1<**						**1.6**	**100.80**
CP20																
Nepheline	*42.7*		*30.6*	*1.44*			*0.15*	*16.9*	*5.49*							*97.24*
Nepheline	*44.1*		*31.5*	*1.77*			*0.12*	*16.7*	*6.09*							*100.27*
Nepheline	42.7		31.9	1.45			0.13	17.1	6.32							99.57
Nepheline	42.6		32.5	1.1			0.19	17.3	6.04							99.69
Nepheline	42.4		31.3	1.56			0.18	16.7	6.16							98.30
Average last 3	42.59		31.88	1.37			0.17	17.01	6.17							99.19
CP21																
Nepheline	*43.7*		*32*	*2.57*			*0.32*	*14.5*	*6.45*							*99.56*
Nepheline	*44.2*		*30.2*	*3.01*			*0.31*	*16.3*	*6.25*							*100.33*
Nepheline	*43.9*		*33*	*1.89*			*0.33*	*15.9*	*7.05*							*102.02*
Nepheline	43.4		31.6	2.05			0.18	16.7	6.65							100.57
Nepheline	43.5		31.5	2.13			0.25	16.9	6.59							100.85
Average last 2	43.44		31.55	2.09			0.22	16.80	6.62							100.71
Na-poor vishnevite	*39.7*		*29.6*	*1.42*			*3.24*	*3.75*	*1.3*		*b.d.*	*1.49*	*7.01*	*0.58*	*0.2*	*88.28*
Vishnevite	*40.9*		*20.3*	*4.96*			*5.51*	*14.5*	*4.06*		*0.18*	*1.21*	*2.36*	*0.16*	*0.17*	*94.31*
Vishnevite	**38.5**		**28.8**	**0.98**			**3.46**	**11.8**	**2.4**		**b.d.**	**1.78**	**5.46**	**0.04**	**0.23**	**93.43**
Melanite	28.9	15.1	1.01	20.3	0.42	0.77	31.7	0.21	0.02							98.35
Melanite	30.2	12.7	0.96	20	0.52	0.63	31.7	0.26	0.13							97.04
Average	29.6	13.9	0.99	20.1	0.47	0.7	31.7	0.24	0.08							97.71
Apatite	0.49			0.19	0.12	b.d.	54	0.06	0.18	39.5	3.43	0.04		b.d.	1.74	99.71
CP22																
Nepheline	*41.2*		*29*	*1.63*			*0.08*	*17*	*6.6*							*95.57*
Nepheline	*42.8*		*31.4*	*2.48*			*0.27*	*16.5*	*7.3*							*100.65*
Nepheline	*44*		*31*	*2.27*			*0.27*	*16.3*	*6.92*							*100.68*
Nepheline	*41.9*		*32.1*	*1.59*			*0.14*	*16*	*7.4*							*99.09*
Nepheline	*43.9*		*32.6*	*1.37*			*0.1*	*16.7*	*7.01*							*101.70*
Nepheline	42.4		31.7	1.75			0.2	16.4	7.42							99.86
Nepheline	43.4		31.1	1.91			0.16	16.7	7.02							100.25
Nepheline	43.7		31.3	1.33			0.47	16.2	7.03							100.05
Average last 3	43.16		31.39	1.66			0.28	16.40	7.16							100.05
Melilite	*41.1*		*6.49*	*7.31*	*0.47*	*3.66*	*28.1*	*5.68*	*0.28*						*2.18*	*95.21*
Melilite	*42.4*		*6.96*	*9.6*	*0.5*	*3.55*	*28.7*	*5.75*	*0.17*						*1.66*	*99.29*
Melilite	*43.2*		*6.8*	*8.33*	*0.39*	*4.18*	*29.4*	*5.35*	*0.18*						*2.57*	*100.33*
Melilite	41.8		7.12	8	0.4	4	29.1	5.66	0.24						2.81	99.03
Melilite	42.6		7.12	7.75	0.38	4.01	29.2	5.71	0.21						2.33	99.37
Melilite	42.6		6.99	7.74	0.45	3.84	29.6	5.82	0.24						2.43	99.70
Melilite	42.6		7.18	7.54	0.44	3.95	29.4	5.67	0.22						1.72	98.76
Melilite	43.6		7.81	7.36	0.31	3.72	28.8	6.1	0.21						1.93	99.86
Average last 5	42.64		7.24	7.68	0.40	3.90	29.22	5.79	0.22						2.24	99.34
CP23																
Nepheline	**43.2**		**32.4**	**2.14**			**0.17**	**16.4**	**6.99**							**101.30**
Nepheline	*42.8*		*31.7*	*1.8*			*0.34*	*16.1*	*7.51*							*100.29*
Wollastonite	52.16		0.50	1.26	0.27	0.23	46.34	0.22	0.38						0.18	101.54
Wollastonite	52.53		0.37	1.13	0.41	0.11	46.25	0.30	0.46						0.41	101.97
Average	52.35		0.44	1.20	0.34	0.17	46.30	0.26	0.42						0.30	101.76
Vishnevite	**40.6**		**29.6**	**2**			**2.26**	**11**	**2.67**		**b.d.**	**2.77**	**5.81**	**0.33**	**0.16**	**97.18**
Vishnevite	*40.8*		*23.1*	*3.33*			*4.18*	*10.6*	*3.54*		*0.11*	*1.88*	*3.94*	*0.7*	*0.23*	*92.46*
Apatite	2.49			0.52	0.07	b.d.	51	0.59	0.25	38.4	3.14	0.01		b.d.	3.69	100.14
Melanite	*29.6*	*13.3*	*0.85*	*20.7*	*0.4*	*0.61*	*32.3*	*0.26*	*0.13*							*98.04*
Melilite	*43*		*7.6*	*7.8*	*0.47*	*3.78*	*29.3*	*5.78*	*0.31*						*1.65*	*99.64*

Sample	SiO2	TiO2	Al2O3	FeO	MnO	MgO	CaO	Na2O	K2O	P2O5	F	Cl	SO3	BaO	SrO	TOTAL
Melilite	43.2		6.58	8.75	0.31	4.08	29.9	5.35	0.14						1.48	99.75
Melilite	43		7.04	8.57	0.22	3.89	29.2	5.42	0.15						1.46	98.96
Average last 2	43.11		6.81	8.66	0.27	3.99	29.53	5.39	0.15						1.47	99.36
CP27																
Wollastonite	51.13		0.18	1.39	0.55	0.07	45.59	0.14	0.24						0.50	99.79
Sodalite	38.8		30.4	0.53			0.14	21.8	3.13		0.04	6.28	0.92	b.d.	0.26	102.31
Sodalite	38.5		30.6	0.82			0.12	21.3	3.68		0.06	6.35	0.99	b.d.	0.08	102.51
Average	38.6		30.5	0.68			0.13	21.6	3.41		0.05	6.32	0.96	b.d.	0.17	102.44
Nepheline	*44.6*		*31.9*	*1.72*			*0.11*	*16.3*	*7.09*							*101.74*
Nepheline	**43.9**		**32.5**	**1.42**			**0.19**	**16.6**	**7.36**							**101.90**
Apatite	0.88			0.19	0.02	b.d.	54.1	0.23	0.25	38.6	2.78	b.d.		b.d.	1.63	98.63
CP31																
Clinopyroxene	*50.4*	*0.87*	*1.34*	*20.3*	*0.73*	*4.86*	*17.2*	*3.88*								*99.62*
Clinopyroxene	*50.1*	*0.69*	*1.21*	*22.3*	*0.81*	*3.33*	*17.4*	*3.43*								*99.27*
Clinopyroxene	*50.6*	*1.3*	*2.04*	*10.2*	*0.4*	*12*	*23.3*	*0.72*								*100.49*
Clinopyroxene	*51.5*	*0.47*	*0.89*	*16.6*	*0.67*	*7.78*	*20.7*	*2.27*								*100.78*
Clinopyroxene	*50.9*	*0.52*	*0.57*	*21.3*	*0.88*	*4.18*	*19.5*	*2.54*								*100.39*
Clinopyroxene	50.6	0.6	1.06	18	0.61	6.97	19.4	2.53								99.70
Clinopyroxene	51.4	0.44	1.15	18.4	0.67	6.17	19.3	2.78								100.33
Clinopyroxene	50.5	0.51	1.06	16.3	0.67	7.81	20.3	2.35								99.49
Average last 3	50.84	0.52	1.09	17.55	0.65	6.98	19.66	2.55								99.84
Apatite	0.55			0.1	0.08	b.d.	55	0.18	0.01	39	2.21	0.03		b.d.	0.91	98.13
Pyrrhotite	**0.08**	**0.12**	**0.03**	**60.9**	**0.06**	**b.d.**	**0.11**	**b.d.**	**0.09**	**b.d.**	**b.d.**	**b.d.**	**33.8**	**b.d.**	**b.d.**	
Pyrrhotite	*3.12*	*0.17*	*0.53*	*75.3*	*0.12*	*0.04*	*0.31*	*1.34*	*0.62*	*0.13*	*b.d.*	*0.05*	*76.8*	*0.08*	*0.24*	
Wollastonite	**52.90**		**b.d.**	**0.84**	**0.45**	**0.06**	**46.51**	**0.01**	**0.05**						**0.16**	**100.98**
Wollastonite	*51.06*		*3.01*	*1.24*	*0.39*	*0.04*	*43.38*	*1.10*	*1.02*						*0.14*	*101.38*
Nepheline	*44.1*		*31.7*	*1.5*			*0.12*	*16.5*	*6.7*							*100.61*
Nepheline	**43.3**		**32.6**	**1.4**			**0.11**	**16.7**	**7.02**							**101.00**
CP38																
Clinopyroxene	*48.3*	*0.39*	*0.7*	*19.8*	*0.5*	*4.9*	*18.4*	*3.1*								*96.09*
Clinopyroxene	*49.6*	*0.51*	*0.5*	*18.7*	*0.7*	*6*	*18.5*	*3*								*97.51*
Clinopyroxene	*48.8*	*0.42*	*0.8*	*13.7*	*0.5*	*8.4*	*20.8*	*2.1*								*95.52*
Clinopyroxene	*50.2*	*0.43*	*0.8*	*14.2*	*0.4*	*8.6*	*20.7*	*2.1*								*97.43*
Clinopyroxene	50.9	0.45	0.7	13.5	0.6	9.3	21.5	2								98.95
Wollastonite	50.00		1<	1.00	0.30	0<	45.90	1<	0.10						4<	97.30
Apatite	0.4			0.6	0<	-0<	54	2<	0.1	41.2	4	02<		0<	1	101.30
Apatite	0.4			0.4	0<	1<	54.4	2<	0.1	40.9	2.9	04<		-0<	1.3	100.40
Apatite	0.3			0.3	0<	1<	53.8	0<	0.1	40.7	4	00<		-2<	1.5	100.70
Average	0.37			0.43	b.d.	b.d.	54.1	b.d.	0.1	40.9	3.63	b.d.		b.d.	1.27	100.8
CP40																
Nepheline	43.9		32.7	2.04			0.19	17	5.84							101.59
Nepheline	43.4		33.1	1.75			0.38	17	5.65							101.20
Nepheline	44.2		32.5	1.94			0.28	16.9	5.55							101.29
Average	43.8		32.8	1.91			0.28	16.9	5.68							101.36
Melanite	30.3	10.7	0.88	22.1	0.29	0.49	30.8	0.48	0.09							96.09
Melanite	30.9	11.9	0.97	21.4	0.39	0.69	31.3	0.39	0.09							97.93
Melanite	30.4	12.1	1.07	21	0.29	0.59	30.8	0.39	0.19							96.78
Average	30.5	11.6	0.97	21.5	0.32	0.59	30.9	0.42	0.13							96.94
Clinopyroxene	**50.1**	**1.02**	**1.96**	**17.9**	**0.68**	**6.62**	**19.5**	**2.51**								**100.07**
Clinopyroxene	*53.7*	*0.5*	*0.68*	*12.2*	*0.48*	*10.9*	*21.7*	*1.83*								*101.91*
Clinopyroxene	*52.5*	*0.62*	*1.07*	*17.2*	*0.48*	*7.9*	*19.3*	*2.99*								*102.04*
CP41																
Nepheline	44.3		33	1.46			0.09	16.8	5.93							101.49
Nepheline	44.1		32.8	1.84			0.19	16.6	6.02							101.47

Sample	SiO2	TiO2	Al2O3	FeO	MnO	MgO	CaO	Na2O	K2O	P2O5	F	Cl	SO3	BaO	SrO	TOTAL
Nepheline	43.4		32.7	1.94			0.19	16.8	6.21							101.17
Average	43.9		32 8	1.75			0.16	16.7	6.06							101.38
Clinopyroxene	52.1	0.58	1.36	16.1	0.68	8.99	20.4	2.31								102.58
CP42																
Nepheline	43.5		30 8	2.62			0.19	16.1	6 02							99.25
Nepheline	43 3		31	2.72			0.09	15.8	6.12							99.05
Nepheline	44.8		32.2	2.23			b.d.	16.9	6.31							102.36
Average	43 9		31 4	2.52			0.14	16.3	6.15							100.22
Wollastonite	50 00		1.40	1.50	1<	0.20	41.80	0.70	0.80						4<	96.40
CP43																
Nepheline	*43.6*		*32.6*	*1.84*			*b.d.*	*16.1*	*7.15*							*101.25*
Nepheline	42.7		33	1.36			0.19	16.4	6.87							100.48
Nepheline	43.3		33.1	1.36			0.19	16.3	6.87							101.06
Average	43.00		33.03	1.36			0.19	16.33	6.87							100.77
Wollastonite	52.40		0.19	0.49	b.d.	b.d.	46.40	b.d.	b.d.						b.d.	99.48
Wollastonite	52.50		b.d.	0.87	0.48	b.d.	46.03	b.d.	b.d.						0.58	100.46
Average	52 5		0 19	0.68	0.48	b.d.	46.2	b.d.	b d.						0.58	99.97
Melilite	44		7 78	7 57	0.39	4 05	28.4	5.68	0 19						2 33	100 40
Melilite	43 8		7 49	8 16	0 29	4.25	28.6	5.59	b.d.						2 52	100 69
Melilite	43 7		7 3	8 35	0 39	3 95	28.7	5.4	0.09						2 72	100.59
Melilite	43 9		7 88	7 57	b d	3.95	28.6	5.88	0.09						2.62	100.48
Average	43 8		7 61	7 91	0 35	4 05	28 6	5.64	0 13						2.55	100.66
CP46																
Melanite	*29 1*	*14 2*	*0 68*	*20 1*	*0.39*	*0 79*	*30.8*	*0.29*	*b.d.*							*96.29*
Melanite	30 6	11.4	1 07	21.6	b.d.	0.69	30.6	0.48	0.19							96.49
Melanite	29 7	11 8	0.97	21.1	0.29	0.49	30.4	0 48	0.09							95 31
Melanite	29 6	11.5	0 88	21.2	0.29	0.69	30.9	0.39	b.d.							95.33
Average last 3	29 94	11 55	0.97	21.26	0.29	0.62	30.62	0.45	0.14							95.71
Clinopyroxene	51 8	0 47	0 88	15 6	0.68	8.2	20.1	2.22								100 03
Clinopyroxene	51 3	0 51	0 97	16.6	0.58	7 61	19.5	2.6								99.67
Average	51 6	0 49	0 93	16 1	0.63	7 91	19.8	2.41								99.85
Clinopyroxene	*54*	*0 31*	*0 39*	*11 8*	*0 48*	*11 6*	*22*	*1 83*								*102.41*
Nepheline	44 2		32 3	1 6			1<	16 6	6 1							100 80
Nepheline	41 9		32.7	1 9			1<	16.1	6.8							99.40
Average	43 1		32.5	1.75			b.d.	16.4	6.45							100.10
K-Feldspar	**62.1**	**0.12**	**17.7**	**2.7**	**.1<**	**.1<**	**0.4**	**2.2**	**10.4**					**1.2**	**.0<**	**96.82**
K-Feldspar	*56*	*- 01<*	*21.5*	*2.5*	*- 0<*	*- 1<*	*0<*	*2<*	*14.7*					*1<*	*- 1<*	*94.70*
Wollastonite	50 50		0.20	1.50	0.60	1<	46.80	1<	0.10						.2<	99.70
Titanite	*30.1*	*34.5*	*0.49*	*2.14*			*27.2*				*0.19*					*94.56*
CP48																
Melanite	33	10.8	0.78	21 4	0.39	0.4	30	0.48	0.09							97 32
Melanite	32.3	11 6	0 78	21 7	0.29	0.59	31.4	0.58	b.d.							99.20
Average	32 7	11 2	0 78	21 5	0.34	0.49	30.7	0.53	0.09							98.29
Clinopyroxene	*49.4*	*0.44*	*0 3*	*21.7*	*0.6*	*4.7*	*14.9*	*4.6*								*96.64*
Clinopyroxene	**51.6**	**0.43**	**0.49**	**19.2**	**0.77**	**6.12**	**17.4**	**3.86**								**99.72**
Wollastonite	52 80		1<	1.10	0.30	1<	48.30	2<	0.20						5<	102.70
Nepheline	44.3		32.9	1.65			b.d.	16.9	6.4							102.06
Vishnevite	*44.8*		*23.4*	*5.5*			*1.8*	*4.8*	*2.1*			*1.9*	*5*			*89.30*
CP50																
Fe-Ti-spinel	0.98	1.86	0.19	88	0.77	0.49	0.28	0.58								93.11
Fe-Ti-spinel	3 04	2.01	0.58	84.5	1.06	0.49	0.66	1.16								93.47

Sample	SiO2	TiO2	Al2O3	FeO	MnO	MgO	CaO	Na2O	K2O	P2O5	F	Cl	SO3	BaO	SrO	TOTAL
Average	2.01	1.94	0.39	86.2	0.92	0.49	0.47	0.87								93.30
Clinopyroxene	*55*	*1.34*	*0.78*	*17.9*	*0.68*	*8.79*	*15.3*	*5.49*								*105.32*
Clinopyroxene	*53.2*	*0.65*	*1.07*	*18*	*0.68*	*9.68*	*18.2*	*3.56*								*104.95*
Clinopyroxene	*53.7*	*0.46*	*0.78*	*12.9*	*0.48*	*10.8*	*21.7*	*1.93*								*102.65*
Clinopyroxene	49.9	0.58	1.17	18.5	0.58	6.03	18.8	2.7								98.28
Clinopyroxene	51 8	0.59	0.58	15.2	0.68	8.3	19.1	2.6								98.82
Average last 2	50.83	0.59	0 88	16.85	0.63	7 17	18.97	2.65								98.55
Wollastonite	*52 69*		*b.d*	*0.58*	*0.48*	*b.d.*	*45.84*	*b.d.*	*b.d.*						*b.d*	*99.59*
Melanite	**29.4**	**12.9**	**1.07**	**21.3**	**0.29**	**0.49**	**30.8**	**0.48**	**b.d.**							**96.66**
Melanite	*30.3*	*11.2*	*2.04*	*20.4*	*0.48*	*0.49*	*28.8*	*1.45*	*0.56*							*95.64*
CP52																
Nepheline	44		32.3	1.75			b.d.	16	6.59							100.61
Nepheline	43.3		32.3	2.62			0.19	16	6.78							101 17
Average	43.6		32.3	2.18			0.19	16	6.68							100.89
Melilite	43.9		7 78	7 96	0.39	3.85	28.4	5.78	0.19							98.26
Melilite	43 4		6.71	9.22	b.d.	3.85	28.6	5.68	0.19							97 65
Average	43 6		7 25	8.59	0.39	3.85	28.5	5.73	0.19							98.15
CP53																
Wollastonite	51		b.d.	0 97	0 77	b d	45 4	0.29	0.19						b.d.	98 62
Melilite	42 9		6 32	8 74	0 39	3.85	28.3	5.97	0.28							96 78
Melilite	43		6 61	8 64	0 48	4.05	28 4	5.4	0.19							96.80
Average	43		6 47	8 69	0 43	3 95	28 4	5 68	0 24							96 79
Nepheline	*40 8*		*31 7*	*2 91*			*b.d.*	*15.5*	*7 15*							*98 12*
Nepheline	**42.6**		**30.6**	**2.52**			**0.19**	**15.6**	**6.59**							**96.06**
CP54																
Clinopyroxene	*51 6*	*0 45*	*0 3*	*23.7*	*0 5*	*4*	*13.7*	*6.1*								*100.35*
Clinopyroxene	*51 5*	*0 66*	*0 5*	*25.1*	*0.6*	*3.2*	*12.1*	*7.1*								*100 76*
Clinopyroxene	*52*	*0 39*	*0 7*	*16.8*	*0 5*	*8*	*20 9*	*2.5*								*101 79*
Clinopyroxene	*50 9*	*0 48*	*0 6*	*19.1*	*0 7*	*6.5*	*20 6*	*2.4*								*101 28*
Clinopyroxene	*51 1*	*0 56*	*1 1*	*18*	*0.6*	*7.1*	*20.7*	*2.6*								*101 76*
Clinopyroxene	51 1	0 51	0 8	16.9	0 5	7 5	20 2	2 8								100 31
Nepheline	*42 5*		*32 7*	*2*			*0.3*	*16.1*	*7.4*							*101 00*
Nepheline	*43 8*		*31 1*	*1 9*			*1<*	*15.7*	*6.7*							*99 20*
Nepheline	43		32 2	2.2			0<	16	7 1							100.50
Nepheline	43 7		31 2	2.8			0<	16.2	7							100 90
Average last 2	43 3		31 8	2 23			0 3	16	7.05							100 70
Melanite	29 9	12.7	0 8	21 7	0.4	0.7	31.9	0 4	0<							98.50
Melanite	30.6	12.1	0 9	22.3	0.4	0.5	31 9	0.5	1<							99.20
Average	30 3	12.4	0 85	22	0 4	0.6	31 9	0.45	b.d.							98.85
Titanite	30 6	37 7	0.5	2	b.d.	b.d.	28 3	b.d.	b.d.		0 3					99.40
CP55																
Clinopyroxene	*50 6*	*0.71*	*0 9*	*23*	*0 6*	*3.5*	*15 4*	*4.5*								*99.21*
Clinopyroxene	*48.9*	*0 55*	*1 2*	*18 9*	*0 8*	*4 9*	*17 9*	*3.1*								*96.25*
Clinopyroxene	*51.2*	*0.63*	*0 4*	*21 4*	*0 6*	*5*	*14 6*	*5.8*								*99.63*
Clinopyroxene	*50 5*	*0 83*	*1*	*11 9*	*0 4*	*9.9*	*21*	*2*								*97 53*
Clinopyroxene	*53 3*	*0 45*	*0 8*	*12 4*	*0 3*	*10.7*	*22.2*	*1 9*								*102.05*
Na-clinopyroxene	*51 5*	*1 86*	*1*	*23 6*	*0.6*	*2.9*	*11 7*	*7*								*100 16*
Clinopyroxene	50.2	0 68	1	19	0 4	6 3	19 5	2.8								99.88
Clinopyroxene	51 9	0 48	0 7	14 6	0.5	8.8	21.2	2.1								100.28
Average last 2	51 05	0 58	0 85	16.80	0.45	7 55	20.35	2.45								100.08
Nepheline	*43.5*		*32.8*	*1.3*			*0.2*	*16.1*	*6.9*							*100.80*
Nepheline	**42.6**		**32.3**	**1.6**			**0.2**	**15.8**	**7.2**							**99.60**
Melanite	30 4	12.9	0.9	22.2	0.4	0.7	31.9	0.5	0.2							100.10
Melanite	30.9	11 4	0.8	22.8	0.3	0.5	32.3	0.5	0.2							99.70
Average	30 7	12.2	0 85	22.5	0 35	0.6	32.1	0 5	0.2							99.90

Sample	SiO2	TiO2	Al2O3	FeO	MnO	MgO	CaO	Na2O	K2O	P2O5	F	Cl	SO3	BaO	SrO	TOTAL
CP60																
Nepheline	42.6		32.3	2			.1<	16.6	6.1							99.60
Nepheline	42.9		32.1	1.9			0.2	16.5	5.9							99.50
Nepheline	42.6		32.5	2.2			0.2	16.4	6.4							100.30
Average	42.7		32.3	2.03			0.2	16.5	6.13							99.80
Clinopyroxene	**52**	**0.6**	**0.8**	**11.7**	**0.5**	**10.9**	**22.9**	**1.3**								**100.70**
Clinopyroxene	*51.2*	*0.45*	*0.7*	*17.7*	*0.6*	*7.4*	*20.3*	*2.6*								*100.95*
Clinopyroxene	*51.3*	*0.46*	*0.3*	*20.9*	*0.7*	*5.3*	*15.5*	*5.1*								*99.56*
Melanite	30.3	11.9	0.6	22.2	0.4	0.6	32	0.5	0<							98.50
Melanite	30.8	11.6	1.1	22.1	0.3	0.6	32.5	0.5	0.1							99.60
Average	30.6	11.8	0.85	22.2	0.35	0.6	32.3	0.5	0.1							99.10
Fe-Ti-spinel	7.8	1.26	3.6	77	0.6	0.4	1.3	3.6								95.56
CP64																
Clinopyroxene	**50.7**	**1.07**	**1.6**	**19.8**	**0.6**	**5.7**	**19.2**	**3**								**101.67**
Clinopyroxene	*52.8*	*0.47*	*0.4*	*14.6*	*0.5*	*9.5*	*21.3*	*2.9*								*102.47*
Nepheline	**43.1**		**32.8**	**1.7**			**0.2**	**16.3**	**7.3**							**101.40**
Nepheline	*42.7*		*31.7*	*3.6*			*1<*	*16.1*	*7.6*							*101.70*
Wollastonite	52.40		1<	0.50	0.30	0<	48.20	1<	-0<						6<	101.40
Titanite	30.5	37.7	0.3	1.8	b.d.	b.d.	28.4	b.d.	b.d.		1<					98.70
Melanite	*30.2*	*13.5*	*0.7*	*21.9*	*0.4*	*0.7*	*32.2*	*0.5*	*0<*							*100.10*
Melanite	**31.2**	**10.8**	**1.1**	**22.3**	**0.4**	**0.5**	**32.3**	**0.4**	**.0<**							**99.00**
Apatite	0.7			2<	-0<	0<	55.2	2<	0.1	40.5	2.2	01<		-1<	1.3	100.00
Apatite	0.5			1<	-1<	-0<	55	-0<	1<	40.5	3.4	-01<		-1<	2.1	101.50
Average	0.6			b.d.	b.d.	b.d.	55.1	b.d.	b.d.	40.5	2.8	b.d.		b.d.	1.7	100.70
CP65																
Combeite	51.7			1.2	0.7	-0<	28	20	1<							101.60
Combeite	51.6			1	0.8	1<	27.7	20	1<							101.10
Combeite	51.6			1.2	0.7	0<	28.1	19.9	0<							101.50
Combeite	51.3			0.9	0.6	0<	28.3	19.7	1<							100.80
Combeite	51.5			1.1	0.8	-0<	28.5	19.5	1<							101.40
Combeite	50.7			0.8	0.7	0.2	26.4	19.8	1<							98.60
Average	51.4			1.03	0.72	0.2	27.8	19.8	b.d.							101.00
Clinopyroxene	51	0.42	0.9	16.9	0.5	7.6	20.1	2.6								100.02
Clinopyroxene	51.4	0.47	0.9	16.9	0.6	7.6	20.2	2.6								100.67
Clinopyroxene	*51.1*	*0.58*	*1*	*18.1*	*0.6*	*6.9*	*19.8*	*3.1*								*101.18*
Clinopyroxene	*51.2*	*0.61*	*1.1*	*15.5*	*0.5*	*8.8*	*21.5*	*2*								*101.21*
Average first 2	51.20	0.45	0.90	16.90	0.55	7.60	20.15	2.60								100.35
Melanite	*31.9*	*11.9*	*4.1*	*19.6*	*0.5*	*0.4*	*28.4*	*3.1*	*0.8*							*100.70*
Melanite	*28.7*	*13.7*	*0.5*	*19.3*	*0.3*	*0.6*	*30.5*	*0.8*	*0<*							*94.40*
Melanite	30.1	12.9	0.9	21.5	0.4	0.5	32.3	0.4	.1<							99.00
Melanite	30.5	13.3	1.1	21.7	2<	0.4	32.4	0.5	0.2							100.10
Average last 2	30.3	13.1	1	21.6	0.2	0.45	32.4	0.45	0.1							99.55
Nepheline	43.4		32.3	2.2			0.2	16.3	7.4							101.80
Nepheline	43.3		32.4	2.2			0.2	16.2	7.5							101.80
Average	43.4		32.4	2.2			0.2	16.3	7.45							
CP66																
Melanite	30.1	12.8	1.1	21.8	0.3	0.6	31.8	0.7	1<							99.20
Melanite	30.6	12.1	1	22.2	2<	0.5	32.2	0.4	0.1							99.10
Melanite	*31*	*11.2*	*0.9*	*23.1*	*0.4*	*0.5*	*32.5*	*0.4*	*0<*							*100.00*
Average first 2	30.35	12.45	1.05	22.00	0.30	0.55	32.00	0.55	0.10							99.15
Nepheline	*42.4*		*34.1*	*1.2*			*0.2*	*16.9*	*6.9*							*101.70*
Nepheline	**43.2**		**32.1**	**2.5**			**0.3**	**16.6**	**6.5**							**101.20**
Na-clinopyroxene	*51.1*	*0.71*	*1.4*	*21.7*	*0.6*	*4.3*	*15.3*	*5.2*								*100.31*

Sample	SiO2	TiO2	Al2O3	FeO	MnO	MgO	CaO	Na2O	K2O	P2O5	F	Cl	SO3	BaO	SrO	TOTAL
Na-clinopyroxene	*50.5*	*0.92*	*1*	*25.7*	*0.5*	*2.3*	*13.2*	*6.2*								*100.32*
Clinopyroxene	52.3	0.71	1.3	13.4	0.5	9.8	21.9	1.7								101.61
Clinopyroxene	52.4	0.54	0.9	15.8	0.5	8.8	20.8	2.4								102.14
Average last 2	52.4	0.63	1.1	14.6	0.5	9.3	21.4	2.05								101.88
Wollastonite	52.30		1<	1.60	0.70	.0<	46.70	1.00	0.30						0<	102.60
CP67																
Na-clinopyroxene	*52*	*1.23*	*0.6*	*23*	*0.4*	*4.2*	*12.9*	*6.5*								*100.83*
Na-clinopyroxene	*51.4*	*0.77*	*1.4*	*18.2*	*0.7*	*6.5*	*18*	*4.2*								*101.17*
Clinopyroxene	52.2	0.6	0.9	13.9	0.6	9.6	21.7	2.2								101.70
Clinopyroxene	52.5	0.52	0.7	13.7	0.4	10	21.8	2								101.62
Average last 2	52.4	0.56	0.8	13.8	0.5	9.8	21.8	2.1								101.66
Nepheline	**42.6**		**32.3**	**2.1**			**0.2**	**16.6**	**6.4**							**100.20**
Nepheline	*45.1*		*31.7*	*2*			*0.4*	*16.6*	*5.9*							*101.70*
Melanite	*32.5*	*8.9*	*0.7*	*24*	*.1<*	*0.3*	*32.3*	*0.6*	*0<*							*99.30*
Melanite	30.2	13	0.8	21.5	0.4	0.6	32.1	0.6	1<							99.20
Melanite	31	11.7	0.6	22	0.4	0.4	32.3	0.4	1<							98.80
Average last 2	30.60	12.35	0.70	21.75	0.40	0.50	32.20	0.50	b.d.							99.00
alkali Feldspar	*50.8*	*0.21*	*24.2*	*3.4*	*0.2*	*1<*	*0.9*	*11.5*	*9.2*					*3<*	*- 2<*	*100.41*
CP68																
Wollastonite	51.60		0<	1.20	0.30	0.30	47.40	1<	0<						2<	100.80
Clinopyroxene	*53*	*0.46*	*0.9*	*12.9*	*0.4*	*10.7*	*22.2*	*2*								*102.56*
Clinopyroxene	**52.2**	**0.55**	**0.7**	**13.8**	**0.6**	**9.6**	**21.9**	**1.7**								**101.06**
Nepheline	*43.4*		*32.6*	*2*			*0<*	*16.8*	*6.8*							*101.6*
Nepheline	**43.1**		**33.2**	**1.6**			**.0<**	**16.2**	**7.1**							**101.2**
Melanite	*29.6*	*13.7*	*0.9*	*22*	*0.5*	*0.6*	*32*	*0.6*	*1<*							*99.90*
Melanite	**30.8**	**11.6**	**0.8**	**22.4**	**0.4**	**0.5**	**32**	**.3<**	**.1<**							**98.60**
CP69																
Clinopyroxene	*51.1*	*0.45*	*0.8*	*20.8*	*0.8*	*5.4*	*19.3*	*3*								*101.65*
Clinopyroxene	**51.2**	**0.61**	**1.2**	**19.9**	**0.6**	**5.3**	**16.5**	**4.6**								**99.91**
Melanite	**30.5**	**12.3**	**0.9**	**21.9**	**0.3**	**0.6**	**31.9**	**0.4**	**0.1**							**98.90**
Melanite	*29.8*	*13.9*	*0.8*	*21.7*	*0.5*	*0.5*	*31.9*	*0.4*	*0.1*							*99.60*
Nepheline	**43.5**		**32.7**	**1.8**			**0.2**	**16**	**6.9**							**101.1**
Nepheline	*42.9*		*33.1*	*1.8*			*1<*	*16.6*	*7.2*							*101.6*
CP72																
Nepheline	*43.6*		*32.7*	*2*			*1<*	*17.1*	*6.5*							*101.9*
Nepheline	**43.9**		**31**	**2.9**			**.1<**	**16.8**	**6.2**							**100.8**
Melanite	31.9	11.4	1	21.2	0.4	0.4	31.4	0.7	1<							98.40
Melanite	31.7	10.7	0.7	22.5	0.3	0.3	31.4	0.7	0<							98.30
Average	31.8	11.1	0.85	21.9	0.35	0.35	31.4	0.7	b.d.							98.35
Clinopyroxene	*51.9*	*0.86*	*0.6*	*24.2*	*0.4*	*3.1*	*10.9*	*7.9*								*99.86*
Clinopyroxene	*51.7*	*1.18*	*0.4*	*24.1*	*0.5*	*3.2*	*11.4*	*7.5*								*99.98*
Clinopyroxene	*51.9*	*0.57*	*1*	*17.3*	*0.7*	*7.3*	*19.7*	*2.7*								*101.17*
Clinopyroxene	*51.2*	*0.65*	*1.2*	*19.4*	*0.6*	*6.2*	*19.3*	*2.8*								*101.35*
Clinopyroxene	52.6	0.62	1	13.2	0.5	10	21.8	1.8								101.52
Clinopyroxene	52.2	0.82	1	11.3	0.5	11.1	22.9	1.3								101.12
Average last 2	52.40	0.72	1.00	12.25	0.50	10.55	22.35	1.55								101.32
CP74																
Clinopyroxene	*52.2*	*0.76*	*0.5*	*22.1*	*0.5*	*4.6*	*13.9*	*6*								*100.56*
Clinopyroxene	*51.5*	*0.59*	*0.4*	*23*	*0.6*	*4.4*	*13*	*6.3*								*99.79*
Clinopyroxene	*49.9*	*0.68*	*1.1*	*19.7*	*0.5*	*5.7*	*19.4*	*2.6*								*99.58*
Clinopyroxene	51	0.5	1.1	17.8	0.6	7.1	19.5	2.6								100.20
Clinopyroxene	51.2	0.5	0.9	18.1	0.4	7.2	19.5	2.6								100.40
Average last 2	51.10	0.50	1.00	17.95	0.50	7.15	19.50	2.60								100.30

Sample	SiO2	TiO2	Al2O3	FeO	MnO	MgO	CaO	Na2O	K2O	P2O5	F	Cl	SO3	BaO	SrO	TOTAL
Nepheline	*44.5*		*32.2*	*2.1*			*0<*	*17.2*	*5.8*							*101.8*
Nepheline	**43.5**		**32.8**	**1.8**			**0.1**	**17**	**6**							**101.2**
Melanite	**31.1**	**11.9**	**0.9**	**22**	**0.3**	**0.4**	**31.4**	**0.4**	**.0<**							**98.40**
Melanite	*29.3*	*14.4*	*0.6*	*21.1*	*0.4*	*0.7*	*30.9*	*0.7*	*.0<*							*98.10*
Fe-spinel	2.3	0.56	1.1	88.1	0.7	0.5	0.6	0.6								94.46
CP78																
Pyrrhotite				89.4									90.9			
Nepheline	*42.3*		*33.2*	*2*			*0.2*	*16*	*8.7*							*102.4*
Nepheline	**43.2**		**31.9**	**2.1**			**0.2**	**16.2**	**8.2**							**101.8**
Combeite	51 3			1 7	0.3	0 3	27.9	18.6	0.2							100.30
Combeite	51 1			1 4	0.4	0 3	27.8	19	0.1							100 10
Average	51.2			1.55	0.35	0.3	27.9	18.8	0.15							100.20
Clinopyroxene	50 6	0 52	1	18.2	0.7	6.5	19.7	2.6								99.82
CP81																
Melilite	*44*		*7 2*	*7 5*	*0.6*	*4.6*	*28.7*	*6.3*	*0.1*						*2 9*	*101.90*
Melilite	**43.7**		**6.9**	**7.4**	**0.8**	**4.2**	**28.6**	**6.9**	**.1<**						**2.5**	**100.00**
Nepheline	*43 6*		*32 4*	*1 7*			*1<*	*17*	*6.9*							*101 6*
Nepheline	43 1		32 8	1 8			1<	16.6	6.9							101 2
Nepheline	43 7		32 7	1 1			0 2	16.6	6.7							101
Nepheline	43 1		31 2	2.1			0.2	16	6.7							99.3
Average last 3	43 30		32.23	1 67			0 20	16.40	6.77							100 50
Wollastonite	52.30		0 20	0 40	0.50	1<	47 30	- 0<	1<						3<	100.70
Melanite	30.2	11 1	0 4	19	0 5	0.8	31 1	1 2	0.3							94 60
Fe-Mn-Ti-spinel	0 6	3 72	0 3	86 1	2.4	0 8	0.3	0.3								94 52
Fe-Mn-Ti-spinel	0 4	3 9	1<	84 6	2.7	0.7	0 4	0 5								93.20
Fe-Mn-Ti-spinel	0.4	2.71	0.2	86	2.4	0.8	0 3	3<								92.81
Fe-Mn-Ti-spinel	1 1	3.55	2<	85.7	2.1	0.7	0.4	0 8								94 35
Average	0 63	3 47	0.25	85 60	2.40	0 75	0 35	0 53								93.98
CP82																
Melilite	43 3		7 8	7 6	0 8	3 6	29 2	5.6	0.2						2 7	100.80
Melilite	43 2		7 7	7 8	0 7	3.5	29.1	6	0.2						2.7	100.90
Average	43 3		7 75	7 7	0.75	3.55	29 2	5.8	0.2						2.7	100.85
Nepheline	43		33 3	1 6			0.2	16.7	6.6							101.4
Nepheline	42.8		32.6	1 7			0.2	16.7	6.7							100 7
Average	42.9		33	1 65			0.2	16 7	6 65							101 05
CP89																
Nepheline	*42.8*		*31 2*	*2*			*1<*	*16.4*	*5 8*							*98.2*
Nepheline	42.9		32.1	1 7			1<	16 8	5 9							99.4
Nepheline	42.8		32.7	1 2			0.2	16.7	6							99.6
Nepheline	42.7		32.3	1 9			1<	17	5.8							99.7
Average last 3	42.80		32 37	1.60			0.20	16.83	5.90							99 57
CP91																
Melilite	44.1		7 4	8.2	0.3	4.1	29.4	5.9	1<							99.40
Melilite	43.8		8	7 6	2<	4.1	29.7	6	0.1							99.30
Average	44		7 7	7 9	0.3	4.1	29.6	5.95	0.1							99.55
Nepheline	**43.3**		**32.4**	**1.9**			**.1<**	**16.1**	**7**							**100.7**
Nepheline	*43 9*		*29.1*	*3.6*			*1.2*	*16.2*	*6.5*							*100 5*
Wollastonite	52.10		- 0<	1 30	0.50	1<	47 00	1<	1<						- 1<	100.90
CP92																
Vishnevite	36 4		29 4	1			2 8	18.1	2.6		1<	1.69	4.4	- 1<	3<	96.39
Vishnevite	36.6		29 4	1.2			2.8	18.3	2.4		- 0<	1 64	5.1	- 0<	2<	97 44
Vishnevite	36.3		29.2	1 2			2.8	18.4	2.3		1<	1 53	5.2	0<	4<	96.93

Sample	SiO2	TiO2	Al2O3	FeO	MnO	MgO	CaO	Na2O	K2O	P2O5	F	Cl	SO3	BaO	SrO	TOTAL
Vishnevite	36.1		29	1.4			2.9	18.3	2.4		0<	1.45	5.9	- 0<	.5<	97.45
Average	36.4		29.3	1.2			2.83	18.3	2.43		b.d.	1.58	5.15	b.d.	b.d.	97.07
Nepheline	*43.8*		*31.4*	*2.5*			*0.2*	*16.9*	*6*							*100.8*
Nepheline	43.9		32.1	2.4			0.2	16.7	6.1							101.4
Nepheline	43.2		32.7	2.4			0.3	17.2	6.3							102.1
Nepheline	43.7		32	2.5			1<	16.8	6.1							101.1
Nepheline	44.4		32	2.6			0.2	17	6.2							102.4
Average last 4	43.80		32.20	2.48			0.23	16.93	6.18							101.75
CP93																
Nepheline	43.2		31.7	2.7			.1<	16.9	5.7							100.2
Nepheline	42.8		31.3	2.4			1<	16.7	5.9							99.1
Average	43		31.5	2.55			b.d.	16.8	5.8							99.65
CP97																
Melanite	29.7	13.1	0.7	21.5	.2<	0.8	32	0.4	- 0<							98.20
Melanite	29.5	13.9	1	21.4	0.3	0.6	31.3	0.6	1<							98.60
Melanite	*28.8*	*15.5*	*0.5*	*20.5*	*0.3*	*0.8*	*31.5*	*0.6*	*- 0<*							*98.50*
Average first 2	29.60	13.50	0.85	21.45	0.30	0.70	31.65	0.50	b.d.							98.40
Nepheline	**43.4**		**32.8**	**1.4**			**.1<**	**16.6**	**6**							**100.2**
Nepheline	*43.5*		*32.3*	*2.1*			*0.1*	*16.9*	*6.4*							*101.3*
Clinopyroxene	53.6	0.66	0.5	10.1	0.5	12.3	23.3	1.1								102.06
Clinopyroxene	52.1	0.39	0.6	15.8	0.4	8.6	21.3	2.3								101.49
Average	52.9	0.53	0.55	13	0.45	10.5	22.3	1.7								101.78
CP102																
Clinopyroxene	**52.5**	**0.46**	**0.6**	**16.9**	**0.5**	**7.5**	**18.7**	**3.2**								**100.36**
Clinopyroxene	*51.9*	*0.59*	*0.33*	*22.6*	*0.88*	*4.98*	*15.6*	*5.31*								*102.15*
Melanite	*28.2*	*16.8*	*1.4*	*19.3*	*0.2*	*1.1*	*31.2*	*0.8*	*0.2*							*99.20*
Melanite	*30.2*	*13.8*	*1.1*	*21.6*	*0.3*	*0.6*	*31.9*	*.3<*	*1<*							*99.50*
Melanite	*30.7*	*12.3*	*1*	*22.1*	*2<*	*0.8*	*31.5*	*0.5*	*0<*							*98.90*
Melanite	28.7	14.5	0.9	21.7	2<	0.8	31.4	2<	1<							98.00
Melanite	29.3	14.5	0.5	21.4	0.5	0.8	31.2	0.7	0<							98.90
Average last 2	29.00	14.50	0.70	21.55	0.50	0.80	31.30	0.70	b.d.							98.45
Nepheline	**42.5**		**33.7**	**1.4**			**b.d.**	**17**	**6.59**							**101.18**
Nepheline	*43.3*		*33.4*	*1.96*			*b.d.*	*17.2*	*6.31*							*102.07*
CP103																
Nepheline	43.2		32.3	2			0.1	16.6	6.3							100.5
CP109																
Melanite	*30.3*	*13.4*	*0.8*	*21.8*	*0.4*	*0.6*	*31.5*	*0.8*	*- 0<*							*99.60*
Melanite	30.8	11.4	0.8	21.9	0.4	0.5	31.6	0.4	1<							97.80
Melanite	30.6	12.4	0.8	22.2	0.4	0.5	31.6	0.5	- 0<							99.00
Average last 2	30.70	11.90	0.80	22.05	0.40	0.50	31.60	0.45	b.d.							98.40
Nepheline	44.9		31.4	2			1<	17.4	5.5							101.2
Nepheline	43.7		30.7	3.6			0.1	17.3	5.8							101.2
Average	44.3		31.1	2.8			0.1	17.4	5.65							101.20
Clinopyroxene	*51.7*	*0.95*	*0.3*	*22.1*	*0.6*	*4.4*	*14.4*	*5.8*								*100.25*
Clinopyroxene	*52.9*	*0.35*	*0.3*	*17.1*	*0.7*	*7.7*	*16.9*	*4.6*								*100.55*
Clinopyroxene	*52.1*	*0.42*	*0.4*	*20.1*	*0.8*	*5.9*	*18.2*	*3.6*								*101.52*
Clinopyroxene	52.5	0.52	0.7	16.7	0.4	8.3	19.5	2.9								101.52
Clinopyroxene	52.8	0.47	1.1	14.4	0.4	9.7	21.6	1.8								102.27
Clinopyroxene	51.7	0.59	1	17.3	0.6	7.8	20.3	2.8								102.09
Clinopyroxene	51.6	0.73	1.6	15.6	0.6	8.6	21.2	2								101.93
Clinopyroxene	52	0.8	1.6	13.7	0.5	9.5	21.7	2								101.80
Clinopyroxene	50.9	1.01	1.8	13	0.4	9.8	22.3	1.5								100.71
Average last 6	51.9	0.69	1.3	15.1	0.48	8.95	21.1	2.17								101.72
CP110																
Melanite	30.8	11.5	0.6	22.5	0.5	0.5	31.5	0.5	0<							98.40
Melanite	31.5	10.3	0.7	22.9	0.3	0.5	31.7	0.5	1<							98.40
Average	31.2	10.9	0.65	22.7	0.4	0.5	31.6	0.5	b.d.							98.40

Sample	SiO2	TiO2	Al2O3	FeO	MnO	MgO	CaO	Na2O	K2O	P2O5	F	Cl	SO3	BaO	SrO	TOTAL
Nepheline	43.6		32.4	2			0.3	17.1	5.9							101.3
Nepheline	43.8		32.2	2			0.4	17.1	5.8							101.3
Average	43.7		32.3	2			0.35	17.1	5.85							101.30
Clinopyroxene	50.9	0.89	2.4	11.8	0.3	11	23.4	0.9								101.59
Clinopyroxene	52.8	0.71	0.9	11.9	0.5	11.1	22.2	1.6								101.71
Average	51.9	0.8	1.65	11.9	0.4	11.1	22.8	1.25								101.65
Wollastonite	51.90		-0<	1.50	0.30	0.20	46.70	1<	.1<						-4<	100.60
CP111																
Nepheline	43.2		32.8	1.4			0.1	16.7	6.5							100.7
Nepheline	42.9		32.4	1.3			0.2	16.5	6.7							100
Average	43.1		32.6	1.35			0.15	16.6	6.6							100.35
Melilite	**42.9**		**7.2**	**8.6**	**0.8**	**3.4**	**28.9**	**5.8**	**0.3**						**2.1**	**99.90**
Melilite	*43.2*		*6*	*11.2*	*0.7*	*3*	*28.8*	*5.6*	*0.2*						*1.7*	*100.40*
CP113																
Wollastonite	52.19		b.d.	0.93	b.d.	b.d.	47.25	b.d.	b.d.						b.d.	100.37
Melilite	43.7		6.4	9.6	0.2	3.9	28	6.1	0.2						3.1	101.20
Melilite	43		6.5	9.2	2<	4	27.9	6.1	0.1						3.4	100.20
Average	43.4		6.45	9.4	0.2	3.95	28	6.1	0.15						3.25	100.80
Melanite	31.2	11.1	0.9	22.4	0.3	0.4	31.8	0.6	1<							98.70
Melanite	30.7	10.7	0.7	22.3	0.3	0.6	31.7	0.5	1<							97.50
Average	31	10.9	0.8	22.4	0.3	0.5	31.8	0.55	b.d							98.10
Nepheline	**43.4**		**32.3**	**2.2**			**.1<**	**16.5**	**6.8**							**101.2**
Nepheline	*42.4*		*32.9*	*1.8*			*1<*	*16.6*	*7.4*							*101.1*
CP114																
Wollastonite	*48.50*		*-.1<*	*0.50*	*0.40*	*0.20*	*44.50*	*0.50*	*0.20*						*-.8<*	*94.80*
Wollastonite	*50.55*		*b.d*	*0.78*	*0.63*	*b.d*	*46.00*	*b.d*	*b.d.*						*1.09*	*99.05*
Wollastonite	*52.02*		*b.d*	*1.38*	*0.86*	*0.37*	*46.06*	*b.d.*	*b.d.*						*b.d*	*100.69*
Wollastonite	*51.30*		*0.20*	*1.70*	*1.20*	*0.20*	*44.30*	*1.30*	*0.30*						*3<*	*100.50*
Wollastonite	*52.10*		*2<*	*0.50*	*0.30*	*1<*	*47.90*	*2<*	*0<*						*4<*	*100.80*
Average without first	*51.49*		*0.20*	*1.09*	*0.75*	*0.29*	*46.07*	*1.30*	*0.30*						*1.09*	*100.26*
Nepheline	42.3		33.1	1.75			b.d.	16.6	7.34							101.03
Nepheline	42.9		31.5	1.96			0.43	16.6	6.94							100.29
Nepheline	*43.3*		*32.8*	*2.1*			*0.2*	*16.8*	*7.1*							*102.3*
Nepheline	*42.9*		*31.1*	*2*			*0<*	*16.3*	*6.8*							*99.1*
Average first 2	42.59		32.28	1.86			0.43	16.59	7.14							100.66
Melilite	43.3		6.7	8.7	0.7	3.7	28.4	6	0.1						2.9	100.50
Melanite	*27.7*	*16.8*	*1.5*	*19.9*	*2<*	*1*	*31.1*	*0.4*	*1<*							*98.40*
Melanite	**29.2**	**13.7**	**1.1**	**20.8**	**0.4**	**0.9**	**32.2**	**0.4**	**.0<**							**98.70**
CP115																
Wollastonite	*52.14*		*b.d.*	*0.43*	*0.52*	*b.d.*	*47.68*	*b.d.*	*0.20*						*b.d.*	*100.97*
Wollastonite	*51.90*		*1.40*	*0.60*	*0.40*	*1<*	*45.60*	*0.80*	*0.50*						*-.2<*	*101.20*
Wollastonite	*52.30*		*0<*	*1.00*	*0.90*	*1<*	*46.70*	*1<*	*0.20*						*-.5<*	*101.10*
Wollastonite	*52.30*		*0<*	*0.40*	*0.50*	*1<*	*47.80*	*-.0<*	*0<*						*-.1<*	*101.00*
Wollastonite	*52.70*		*0<*	*0.90*	*0.50*	*0.30*	*47.50*	*1<*	*1<*						*-.2<*	*101.90*
Average	*52.27*		*1.40*	*0.67*	*0.56*	*0.30*	*47.06*	*0.80*	*0.30*							*101.23*
Melanite	29.2	14.7	1.21	20.5	0.37	0.75	31.6	b.d.	b.d.							98.37
Nepheline	*43.8*		*32.9*	*1.8*			*0.2*	*17.1*	*7.2*							*103*
Nepheline	*41.5*		*31.7*	*3.1*			*1.1*	*16.6*	*7.8*							*101.8*
Nepheline	43.4		33	1.7			0.2	16.7	7.1							102.1
Melilite	43.2		6.34	8.71	0.58	4.17	28.9	5.54	0.2						3.37	100.99
CP117																
Nepheline	*43.2*		*33.1*	*2.3*			*0.4*	*17.1*	*7*							*103.1*

Sample	SiO2	TiO2	Al2O3	FeO	MnO	MgO	CaO	Na2O	K2O	P2O5	F	Cl	SO3	BaO	SrO	TOTAL
Nepheline	*44.3*		*32.6*	*2.1*			*0.2*	*17.3*	*6.6*							*103.1*
Nepheline	*44.4*		*32.7*	*2*			*.1<*	*17.3*	*6.5*							*102.9*
Nepheline	*44.1*		*33.3*	*1.4*			*0.4*	*17.1*	*6.5*							*102.8*
Nepheline	*44.1*		*33.2*	*1.4*			*0.2*	*17.4*	*6.6*							*102.9*
Nepheline	*43.7*		*32*	*2.09*			*b.d.*	*16.8*	*6.42*							*100.95*
Nepheline	*44.1*		*32.2*	*2.2*			*0.2*	*16.5*	*6.5*							*101.7*
Nepheline	43		32.6	1.6			0.2	16.6	6.6							100.6
Nepheline	42.8		33.2	1.3			1<	16.7	6.9							100.9
Average last 2	42.90		32.90	1.45			0.20	16.65	6.75							100.75
Clinopyroxene (2)	51.3	0.89	0.6	22.7	1.3	3.9	12.9	6.2								99.79
Clinopyroxene (1)	*50.6*	*1.76*	*2.97*	*8.39*	*b.d.*	*12.6*	*23.6*	*1.34*								*101.29*
Clinopyroxene (2)	*50.3*	*1.59*	*1.1*	*22.6*	*0.7*	*3.8*	*11.1*	*7.4*								*98.59*
Clinopyroxene (2)	*51.3*	*1.67*	*1.1*	*22.8*	*0.7*	*3.6*	*10.7*	*8.3*								*100.17*
Melanite	30.6	12.5	0.93	21.7	b.d.	0.58	31.7	0.5	b.d.							98.57
Melanite	30.2	13.2	0.8	20.8	0.3	0.6	31.9	0.6	0<							98.40
Melanite	*30.4*	*12.5*	*1.6*	*21.4*	*2<*	*0.8*	*31.4*	*0.5*	*0.2*							*98.80*
Melanite	*31.7*	*9.6*	*0.6*	*23.9*	*0.5*	*0.2*	*32*	*0.4*	*0<*							*98.90*
Average first 2	30.41	12.84	0.87	21.27	0.30	0.59	31.82	0.55	b.d.							98.49
CP120																
Melilite	*41.8*		*4.3*	*12.8*	*0.8*	*3.5*	*29.8*	*4.6*	*0.2*						*3.2*	*101.00*
Melilite	*41.2*		*3.3*	*13.5*	*0.9*	*3.5*	*29.8*	*4.4*	*0.2*						*3.6*	*100.40*
Average	*41.5*		*3.8*	*13.2*	*0.85*	*3.5*	*29.8*	*4.5*	*0.2*						*3.4*	*100.70*
Nepheline	**43.8**		**32.3**	**2.1**			**.1<**	**16.8**	**6.7**							**101.7**
Nepheline	*42.4*		*33.4*	*1.5*			*0.2*	*16.9*	*6.9*							*101.3*
CP121																
Nepheline	44		31.5	2.8			1<	17.1	6.6							102
Nepheline	43.9		32.9	1.4			0.2	16.9	6.8							102.1
Average	44		32.2	2.1			0.2	17	6.7							102.05
Melilite	**43.1**		**6.82**	**8.46**	**0.49**	**3.83**	**29.1**	**5.65**	**b.d.**						**2.04**	**99.37**
Melilite	*43.7*		*7.49*	*7.92*	*0.41*	*4.31*	*29.7*	*6.17*	*0.22*						*2.13*	*102.01*
CP122																
Melilite	*43.6*		*6.49*	*9.67*	*0.53*	*3.63*	*27.2*	*7.01*	*0.17*						*2.97*	*101.31*
Melilite	*42.7*		*6.6*	*8.34*	*b.d*	*3.98*	*26.2*	*6.58*	*0.31*						*3.21*	*97.86*
Melilite	43.8		6.5	9.6	0.5	3.6	27.1	6.7	0.2						2.7	100.70
Melilite	43.4		5.27	9.4	b.d	3.43	28.6	6.25	0.2						3.26	99.77
Melilite	42.7		5.87	10.4	0.41	3.41	26.7	6.89	0.33						3.53	100.21
Melilite	43.6		6.57	9.6	0.57	3.67	27.3	6.62	b.d.						3.21	101.15
Average	43.37		6.05	9.74	0.49	3.53	27.43	6.62	0.24						3.18	100.46
Nepheline	**43.6**		**32.6**	**1.83**			**b.d.**	**16.3**	**7.1**							**101.23**
Nepheline	*43.1*		*29.8*	*3.8*			*b.d.*	*16.7*	*7.18*							*100.57*
Melanite	29.4	13.5	0.75	21.7	b.d.	0.73	31.7	b.d.	b.d.							97.76
Combeite	51.2			0.61	0.41	b.d.	28.9	18.8	b.d.							99.91
Combeite	51.2			0.6	0.53	b.d.	29.2	18.6	b.d.							100.11
Combeite	51.7			0.75	0.52	b.d.	29.5	19	b.d							101.50
Combeite	51.4			0.5	0.6	1<	29.1	18.9	0.1							100.60
Combeite	51.8			0.5	0.5	0.3	29.6	18.7	0.2							101.60
Combeite	51.4			0.6	0.6	0.2	29.3	18.7	1<							100.80
Combeite	51.4			0.5	0.5	0.4	28.9	18.8	1<							100.50
Combeite	52.1			0.7	0.7	0.2	29.4	19.1	1<							102.20
Combeite	51.8			0.8	0.5	0.3	29.3	19.1	1<							101.80
Average	51.6			0.62	0.54	0.28	29.2	18.9	0.15							101.25
CP123																
Nepheline	42.5		32.4	1.78			b.d.	16.2	7.27							100.15
Nepheline	43.3		31.9	1.83			b.d.	16.7	6.89							100.53
Average	42.9		32.1	1.8			b.d.	16.4	7.08							100.34
Melanite	*27.9*	*12.2*	*0.88*	*17.8*	*0.36*	*0.73*	*28.3*	*0.45*	*b.d.*							*88.51*
Melanite	30.4	11.8	0.66	22.8	b.d.	0.72	31.9	0.62	b.d.							98.92
Melanite	30.2	13.2	0.9	21.4	2<	0.7	32	0.5	0<							98.90

Sample	SiO2	TiO2	Al2O3	FeO	MnO	MgO	CaO	Na2O	K2O	P2O5	F	Cl	SO3	BaO	SrO	TOTAL
Melanite	31	12.6	0.8	21.8	0.4	0.5	31.5	0.6	-.0<							99.20
Melanite	30.8	11.3	0.76	23.4	b.d.	0.58	31.9	0.49	b.d.							99.26
Average last 4	30.6	12.2	0.78	22.3	0.4	0.62	31.8	0.55	b.d.							99.36
Melilite	*39.7*		*6.13*	*6.97*	*0.59*	*3.39*	*23.5*	*6.33*	*b.d.*						*3.04*	*89.68*
Melilite	*35*		*4.56*	*5.18*	*0.45*	*3.55*	*18.9*	*5.98*	*b.d.*						*2.48*	*76.16*
Melilite	*41.9*		*6.32*	*8.64*	*0.5*	*3.47*	*26*	*6.63*	*b.d.*						*3.3*	*96.80*
Melilite	43.1		6.2	9.2	0.5	3.9	27.8	6.3	0.2						3.1	100.30
Melilite	43.5		6.7	9.3	0.7	3.6	27.2	6.7	0.2						2.9	100.80
Melilite	43		6.2	9.6	0.4	3.8	27.7	6.4	0.3						2.9	100.30
Melilite	43.3		6.1	10	0.4	3.3	28.2	6.2	.0<						3.1	100.60
Average last 4	43.2		6.3	9.53	0.5	3.65	27.7	6.4	0.23						3	100.57
Combeite	51.6			0.56	0.5	b.d.	29.3	18.9	b.d.							100.89
Combeite	51.6			0.5	0.58	b.d.	29.6	19.1	0.18							101.59
Combeite	52			0.5	0.6	1<	29.6	19.3	0.1							102.10
Combeite	51.4			0.5	0.5	0.4	29.8	18.6	.1<							101.20
Combeite	52			0.5	0.6	0.2	30	18.8	1<							102.10
Average	51.7			0.51	0.56	0.3	29.7	18.9	0.14							101.84
CP124																
Nepheline	42.4		32.1	1.53			b.d.	16.2	7.24							99.48
Combeite	51.7			0.8	0.61	b.d	28	19.5	b.d.							100.67
Combeite	51.2			0.85	0.62	b.d.	28.8	19	b.d.							100.51
Combeite	51.2			0.8	0.7	0.2	28.3	19.1	0.1							100.40
Average	51.4			0.82	0.64	0.2	28.4	19.2	0.1							100.72
Clinopyroxene	*50.8*	*0.42*	*0.8*	*19.1*	*0.6*	*5.3*	*16.8*	*3.89*								*97.66*
Clinopyroxene	**51.6**	**0.51**	**1.13**	**14.7**	**0.57**	**8.77**	**20.9**	**1.91**								**100.10**
Melanite	29.5	14.5	0.62	21	b.d.	0.7	31.5	0.74	b.d.							98.51
Wollastonite	52.20		-.1<	0.60	0.60	0.20	47.60	1<	0.10						-.3<	101.30
CP125																
Melanite	29.1	14	0.91	20.9	b.d	0.61	31.6	0.71	b.d.							97.90
Melanite	30.1	13.3	0.83	21.5	0.41	0.59	31.6	0.57	b.d.							98.83
Melanite	*31*	*8.11*	*b.d.*	*24.6*	*0.41*	*0.55*	*31.4*	*0.57*	*b.d*							*96.67*
Average first 2	29.6	13.6	0.87	21.2	0.41	0.6	31.6	0.64	b.d.							98.58
Nepheline	42.7		32.1	2			1<	16.3	7.3							100.4
Nepheline	42.4		32.4	1.32			b.d	16.4	7.05							99.61
Average	42.6		32.2	1.66			b.d.	16.4	7.18							100.01
Wollastonite	*53.83*		*b.d*	*0.80*	*0.49*	*b.d.*	*47.31*	*b.d.*	*b.d.*						*0.98*	*103.41*
Wollastonite	52.02		b.d	b.d.	0.50	b.d.	46.91	b.d.	b.d.						b.d.	99.43
Wollastonite	52.00		b.d.	1.07	0.98	b.d.	46.42	0.45	0.18						b.d.	101.10
Average last 2	52		b.d.	1.07	0.74	b.d.	46.7	0.45	0.18						b.d.	100.27
Combeite	51.5			0.8	0.6	0.3	28.8	19	1<							101.00
Combeite	51.4			0.7	0.7	0.3	28.7	18.9	1<							100.70
Average	51.5			0.75	0.65	0.3	28.8	19	b.d.							100.65
Clinopyroxene	52.5	0.69	0.9	10.8	0.4	11.7	22.4	1.6								100.99
Clinopyroxene	50.5	0.36	0.6	15.9	0.6	8	19.5	2.6								98.06
Average	51.5	0.53	0.75	13.4	0.5	9.85	21	2.1								99.53
CP130																
Wollastonite	51.87		b.d	0.60	0.80	b.d.	46.39	b.d.	b.d.						b.d	99.66
Wollastonite	51.70		-.1<	0.40	0.40	1<	47.60	0.40	0.20						-.6<	100.70
Wollastonite	51.47		b.d.	b.d.	0.40	b.d.	47.25	b.d.	b.d.						b.d.	99.12
Average	51.68		b.d.	0.50	0.53	b.d.	47.08	0.40	0.20						b.d.	99.83
Melilite	43.1		7.3	9.4	0.6	3.2	27.5	6.7	0.2						2.1	100.10
Melilite	43.4		4.7	11.8	1.2	2.8	26.7	6.9	0.4						2.3	100.20
Melilite	*43.9*		*7.87*	*9.05*	*0.74*	*2.9*	*27.2*	*6.96*	*b.d.*						*1.96*	*100.58*
Average first 2	43.25		6.00	10.60	0.90	3.00	27.10	6.80	0.30						2.20	100.15
Nepheline	*41.5*		*31.2*	*4.51*			*b.d.*	*16.9*	*7.46*							*101.54*

Sample	SiO2	TiO2	Al2O3	FeO	MnO	MgO	CaO	Na2O	K2O	P2O5	F	Cl	SO3	BaO	SrO	TOTAL
Nepheline	**43.5**		**32.6**	**1.23**			**b.d.**	**16.8**	**6.73**							**100.87**
Melanite	29.1	14.5	1 23	20.2	b.d.	0.77	31.3	0.6	b.d.							97.68
CP131																
Nepheline	43.1		32.7	1.57			b.d.	16.7	6.71							100.8
Melilite	*43 3*		*7 42*	*8.11*	*0.86*	*3.78*	*28.4*	*6.39*	*0.25*						*2.84*	*101 37*
Melilite	*43 9*		*8.11*	*7 15*	*0.86*	*3.59*	*28.2*	*6.71*	*0.18*						*2.84*	*101.50*
Melilite	43 5		7.66	7 6	0.8	3.73	28.7	6.43	b.d.						2.4	100.81
Melilite	43.3		7 43	7 41	0.93	3.79	28.8	6.21	0.22						2.71	100.76
Average last 2	43.38		7 55	7.51	0.87	3.76	28.75	6.32	0.22						2.56	100.79

Note The data are raw data, i.e., all iron is reported as FeO and the totals are not recalculated to 100 wt. %.
Italics indicate whole analyses rejected, asterixes (*) indicate individual elemental analysis rejected,
and bold font indicates that only one analysis was taken into account. b.d.. below detection.

CALCULATION OF the number of non-bridging oxygens per tetrahedra (NBO/T) in silicate liquid from two-liquid experiments and in groundmass of wollastonite nephelinite HOL14, for all, half and no Fe in the tetrahedral site.

The method for calculating NBO/T has been given in Brooker (1995). The melt compositions have been recalculated on a volatile free basis.

The initial steps are to convert the wt. % oxide values to molecular proportions of oxides and then to calculate the atomic proportions of oxygens from each mole. The number of anions are then recalculated on the basis of 100 oxygens. Once the number of anions per hundred oxygens is known, the anions are divided into network formers and modifiers.

The negative charge on 100 oxygens is 100 x 2 = 200. The positive charge on each tetrahedral cation is 4, so the total positive charge is 4 x the number of T cations. Since bridging oxygens have no charge and non-bridging oxygens have a charge of −1, the excess negative charge per tetrahedral cation is equal to the number of non-bridging oxygens per tetrahedral cation.

$$NBO/T = \frac{200 - (4 \times \text{number of network anions / 100 oxygens})}{\text{number of network anions / 100 oxygens}}$$

The following example of calculation is for the silicate liquid in CP13:

	oxide wt%	/mol wt *Nb of oxygens		atomic prop of oxygens	oxygens in melt *anions per oxygen	anions in melt per 100
SiO2	48.40	/60.09)*2		1.6109	*X*(1/2)	31.7846
TiO2	1.21	/79.90)*2		0.0303	*X*(1/2)	0.5969
Al2O3	11.58	/101.94)*3		0.3407	*X*(2/3)	8.9642
Fe2O3	0.00	/159.70)*3		0.0000	*X*(2/3)	0.0000
FeO	8.40	/71.85)*1		0.1169	*X*(1/1)	4.6140
MgO	0.85	/40.32)*1		0.0211	*X*(1/1)	0.8318
CaO	5.95	/56.08)*1		0.1061	*X*(1/1)	4.1873
Na2O	14.36	/61.98)*1		0.2317	*X*(2/1)	18.2890
K2O	6.41	/94.20)*1		0.0681	*X*(2/1)	5.3740
P2O5	0.23	/141.95)*5		0.0083	*X*(2/5)	0.1304
			total	2.5342		

For 100 oxygens; 100 / 2.5342
X=100/2.5342=39.4609

It is assumed that Si, Al, Ti and P are in tetrahedral positions (although the later two could be disputed). If both Fe^{3+} and Fe^{2+} are in the T site (all Fe = T) then NBO/T is:

$$\underset{Si}{31.7846} + \underset{Ti}{0.5969} + \underset{Al}{8.9642} + \underset{Fe^{3+}}{0} + \underset{Fe^{2+}}{4.6140} + \underset{P}{0.1304} = 46.0902$$

and $NBO/T = \frac{200 - (4 * 46.0902)}{46.0902} = 0.3393$

For only Fe^{3+} in the T site then $NBO/T = \frac{200 - (4 * 43.7832)}{43.7832} = 0.5680$

For no Fe in the T site then $NBO/T = \frac{200 - (4 * 41.4762)}{41.4762} = 0.8220$

For the probe data used in this study, the Fe is all expressed as FeO. Since oxygen fugacity is unknown, it is not possible to determine how much Fe is divalent and how much is trivalent. It is assume that no Fe is present in tetrahedral sites.

Table A6.4: Number of non-bridging oxygens per tetrahedra (NBO/T) in silicate liquid from two-liquid experiments and in groundmass of lava HOL14, for all, half and no Fe in the tetrahedral site.

NBO/T	CP109	CP92	CP20	CP93	CP89	CP102	CP13	CP103	CP97	CP18	CP1
All Fe	0.068	0.329	0.355	0.321	0.087	0.103	0.339	0.204	0.102	0.781	0.354
Half Fe	0.233	0.575	0.594	0.530	0.234	0.288	0.568	0.439	0.284	1.134	0.709
No Fe	0.411	0.851	0.860	0.762	0.391	0.490	0.822	0.702	0.484	1.542	1.127

NBO/T	CP91	CP22	CP120	CP121	CP111	CP43	CP53	CP14	CP122	CP124	HOL14
All Fe	0.518	0.934	0.955	0.802	0.616	0.805	0.698	0.630	0.034	0.004	0.108
Half Fe	0.853	1.323	1.423	1.213	1.060	1.222	1.139	1.063	0.377	0.357	0.352
No Fe	1.241	1.780	1.989	1.700	1.599	1.719	1.670	1.586	0.783	0.777	0.626

Note that for CP102, NBO/T is calculated assuming 4.73 wt. % CaO in the silicate liquid.

Table A6.5: Microprobe analyses of crystal phases and of groundmass in lave HOL14 - individual and average analyses (in wt. %).

Sample	SiO2	TiO2	Al2O3	FeO	MnO	MgO	CaO	Na2O	K2O	P2O5	F	Cl	SO3	BaO	SrO	Total
Groundmass																
Gmass HOL14, 1	*53.2*	*1.4*	*7.7*	*11.3*	*0.5*	*0.5*	*3.3*	*4.9*	*5.8*		*0.7*	*0.3*	*1.1*	*0.6*		*91.29*
Gmass HOL14, 2	*54.6*	*1.4*	*9.5*	*12.0*	*0.6*	*0.4*	*2.0*	*2.2*	*4.0*		*0.8*	*0.4*	*1.2*	*0.7*		*89.82*
Gmass HOL14, 3	*47.0*	*0.1*	*1.4*	*2.4*	*0.2*	*1.7*	*23.1*	*1.2*	*1.1*		*0.5*	*.03<*	*1<*	*-.0<*		*78.68*
Gmass HOL14, 4	*55.0*	*1.6*	*7.8*	*12.8*	*0.6*	*0.4*	*2.3*	*1.5*	*4.9*		*0.9*	*0.3*	*1.1*	*4<*		*89.21*
Gmass HOL14, 5	*49.2*	*1.3*	*8.4*	*11.9*	*0.6*	*0.5*	*2.4*	*9.2*	*5.6*		*0.6*	*0.4*	*1.2*	*2<*		*91.31*
Gmass HOL14, 6	*53.9*	*1.29*	*9.2*	*10.9*	*0.4*	*0.4*	*2.7*	*7.6*	*4.9*		*1.20*	*0.33*	*1*	*2<*		*93.82*
Gmass HOL14, 27	*51.7*	*1.2*	**1.2*	*21.9*	*0.6*	**3.3*	*11.7*	**6.7*	*0.7*		*1<*	*.06<*	**0.2*	*-.2<*		*87.83*
Gmass HOL14, 12	*51.7*	*1.4*	**6.1*	**13.5*	*0.5*	**1.4*	**7.2*	*11.6*	*4.6*		*0.8*	*0.3*	*0.9*	*.3<*		*71.76*
Gmass HOL14, 16	*51.5*	*1.3*	*10.8*	*10.3*	*0.5*	*0.3*	*4.3*	**7.0*	*5.7*		**2.7*	*0.3*	*0.9*	*1<*		*85.88*
Gmass HOL14, 7	51.6	1.3	11.6	11.2	0.4	0.5	3.0	10.8	6.1		0.6	0.3	1.0	3<		98.42
Gmass HOL14, 8	48.5	1.1	13.3	9.1	0.5	0.3	2.4	16.9	*4.7		0.6	*2.0	*1.8	2<		92.68
Gmass HOL14, 9	52.6	1.4	8.3	10.8	0.6	0.5	3.6	13.6	6.5		*1.6	0.5	1.1	4<		99.53
Gmass HOL14, 10	51.7	1.3	10.4	11.3	0.3	0.4	2.5	14.3	6.4		0.9	0.4	1.2	0.5		101.60
Gmass HOL14, 11	48.5	0.8	20.6	*7.4	0.4	.2<	*1.1	13.0	5.7		0.4	0.4	0.5	.3<		90.25
Gmass HOL14, 13	48.2	0.7	20.6	*7.6	0.3	.2<	*1.1	16.0	6.2		0.7	0.2	0.5	.2<		93.36
Gmass HOL14, 14	47.6	1.0	14.5	8.5	0.3	0.3	3.2	17.4	*4.6		0.7	*2.4	1.2	2<		94.66
Gmass HOL14, 15	45.6	0.9	14.4	8.8	0.4	0.4	*6.1	10.8	5.7		1.0	0.3	0.7	3<		88.99
Gmass HOL14, 17	51.2	1.4	8.6	11.3	0.5	0.5	3.1	14.9	6.3		1.0	0.4	1.2	2<		100.40
Gmass HOL14, 18	51.6	1.5	8.9	11.6	0.4	0.4	3.1	12.5	6.5		1.1	0.4	1.2	4<		99.22
Gmass HOL14, 19	48.8	0.9	17.9	8.5	0.4	1<	1.6	15.4	6.3		0.6	0.2	0.8	3<		101.45
Gmass HOL14, 20	47.2	1.0	13.0	9.0	0.3	0.2	*6.1	13.2	6.4		1.0	0.3	0.8	3<		92.33
Gmass HOL14, 21	50.8	0.9	13.5	11.3	0.4	*1.0	3.5	9.7	5.0		0.3	0.2	*0.4	3<		95.67
Gmass HOL14, 22	50.6	1.3	12.0	10.4	0.5	0.4	2.6	14.4	6.3		1.0	0.3	1.0	2<		100.76
Gmass HOL14, 23	50.1	1.0	16.3	9.0	0.4	0.3	1.7	10.7	6.2		0.8	0.3	0.7	3<		97.51
Gmass HOL14, 24	50.1	1.2	12.7	10.5	0.4	0.3	2.0	15.7	6.3		0.9	*0.6	1.0	0.6		101.71
Gmass HOL14, 25	51.5	1.5	*7.7	11.4	0.5	0.4	3.1	14.4	6.3		1.1	*0.6	1.3	0.5		92.00
Gmass HOL14, 26	50.0	0.9	17.2	8.6	*0.2	0.2	2.1	12.9	6.1		0.6	0.2	0.8	0.4		100.04
Gmass HOL14, 28	51.1	1.1	10.7	9.9	0.3	0.4	*6.4	11.1	5.9		0.8	0.3	0.9	2<		92.54
Average first 19	49.86	1.12	13.58	10.07	0.41	0.37	2.68	13.56	6.13		0.78	0.31	0.94	0.50		*100.30*
STDS	1.86	0.25	3.76	1.19	0.09	0.10	0.65	2.24	0.38		0.24	0.09	0.25	0.08		
RSD	4%	22%	28%	12%	22%	27%	24%	16%	6%		30%	29%	27%	16%		
Clinopyroxene																
cpx1,core	51.0	0.5	0.6	16.3	0.6	7.9	20.2	2.5								99.6
cpx1,core	51.3	0.4	0.5	16.9	0.5	7.5	20.0	2.9								100.0
cpx1,core	50.8	0.5	0.5	17.4	0.6	7.5	19.7	2.8								99.6
cpx1,core	*50.9*	*0.9*	*0.5*	*21.2*	*b.d.*	*4.9*	*15.1*	*5.5*								*99.0*
average cpx1,core	51.00	0.44	0.55	16.85	0.57	7.64	19.95	2.75								99.75
cpx2,core	50.3	0.4	0.7	17.6	0.7	6.9	19.0	3.3								99.0
cpx2,core	50.7	0.6	0.7	17.3	0.5	7.1	19.2	3.3								99.5
cpx2,core	51.0	0.4	0.5	16.4	0.6	7.7	20.3	2.5								99.3
average cpx2,core	50.69	0.46	0.65	17.10	0.59	7.21	19.50	3.04								99.24
cpx3,core	*51.1*	*0.3*	*0.9*	*15.1*	*0.4*	*8.8*	*21.0*	*2.0*								*99.5*
cpx3,core	50.4	0.4	1.1	18.7	0.7	6.6	18.8	3.2								99.9
cpx3,core	51.1	0.4	0.6	16.1	0.7	8.2	20.1	2.6								99.8
average cpx3,core	50.74	0.38	0.90	17.40	0.70	7.40	19.44	2.91								99.87
cpx4,core	**50.17**	**0.73**	**1.06**	**17.16**	**0.43**	**7.42**	**20.16**	**2.66**								**99.65**
cpx4,core	*50.37*	*0.82*	*0.59*	*20.36*	*0.78*	*5.12*	*17.86*	*3.86*								*99.75*
cpx5,core	*50.93*	*0.39*	*0.40*	*22.32*	*0.66*	*4.54*	*13.88*	*6.25*								*99.37*
inclusion in nepheline	48.29	1.90	2.04	14.11	0.51	9.02	21.02	2.12								99.02
cpx1,nm	51.0	0.8	0.4	25.3	0.5	2.7	9.8	8.7								99.2
cpx1,nm	50.7	1.0	0.5	24.9	b.d.	2.6	9.6	8.7								98.1
cpx1,nm	48.7	2.1	0.4	22.1	0.4	2.2	14.2	8.0								98.0
cpx1,nm	50.8	1.0	0.6	23.0	0.4	3.7	12.0	7.8								99.3
average cpx1,nm	50.29	1.22	0.49	23.84	0.43	2.79	11.40	8.28								98.64
cpx2,nm	50.3	0.5	0.8	17.3	0.8	7.0	21.0	2.1								99.7
cpx2,nm	50.7	0.4	0.3	18.5	0.8	6.5	19.0	3.0								99.3
cpx2,nm	50.5	0.4	0.7	17.8	0.6	6.9	18.5	3.6								99.0
average cpx2,nm	50.50	0.43	0.61	17.85	0.74	6.78	19.51	2.91								99.33
cpx3,nm	50.6	0.6	1.3	17.0	0.7	7.4	20.0	2.5								100.0
cpx3,nm	50.7	0.6	1.1	16.6	0.7	7.6	20.2	2.5								100.0
cpx3,nm	50.3	0.7	0.8	18.3	0.5	6.1	19.4	3.3								99.5
cpx3,nm	49.9	0.8	1.2	20.3	0.5	5.6	19.0	3.0								100.4
average cpx3,nm	50.39	0.66	1.09	18.05	0.60	6.69	19.66	2.84								99.97

Sample	SiO2	TiO2	Al2O3	FeO	MnO	MgO	CaO	Na2O	K2O	P2O5	F	Cl	SO3	BaO	SrO	Total
Melanite garnet																
gt1,core	29.07	14.10	0.85	20.50	0.40	0.62	31.80	b.d.								97.35
gt1,core	29.56	13.40	0.66	20.77	0.40	0.64	31.70	0.59								97.73
gt1,core	*30.32*	*12.24*	*0.95*	*22.11*	*b.d.*	*0.70*	*31.37*	*0.61*								**98.29**
Average last 2	29.32	13.75	0.76	20.64	0.40	0.63	31.75	0.59								97.83
gt2, core	30.56	11.40	1.03	21.96	0.49	0.61	31.68	0.63								98.36
gt1,rim	30.30	11.35	0.98	22.21	b.d.	0.61	31.62	0.44								97.52
gt1,rim	30.70	11.61	0.92	21.28	0.36	0.53	31.69	0.56								97.63
gt1,rim	30.06	11.56	0.90	21.84	0.41	0.58	31.10	0.64								97.09
Titanite																
Titanite 1	29.83	36.94	0.37	1.83	b.d.	b.d.	27.66									96.63
Titanite 2	30.04	37.35	0.39	1.81	b.d.	b.d.	28.13									97.73
Titanite 3	29.95	36.71	0.44	1.69	b.d.	b.d.	28.05									96.84
Titanite 4	30.35	37.85	0.40	1.78	b.d.	b.d.	28.30									98.68
Titanite 5	29.92	37.28	0.41	1.64	b.d.	b.d.	27.97									97.21
Titanite 6	30.10	36.84	0.27	1.83	b.d.	b.d.	27.72									96.76
Average	30.03	37.16	0.38	1.76	b.d.	b.d.	27.97									97.31

Note: the data are raw, i.e., all iron is presented as FeO and totals are not recalculated to 100 wt. %.
Italics indicate whole analyses rejected, asterixes (*) indicate individual elemental analysis rejected,
and bold font indicates that only one analysis was taken into account.
Abbreviations used are: b.d.: below detection; STDS: standard deviation; RSD: relative standard deviation;
gmass: groundmass; Cpx: clinopyroxene; Gt: garnet.

APPENDIX A7

Table A7 1 Trace (and major) element LAM-ICP-MS analyses of carbonate liquid (LC) in the experiments on the join HOL14/OL5 - Individual and average analyses, standard deviation (STDS) and relative standard deviation (RSD)

Sample	MgO wt %	Al2O3 wt %	SiO2 wt %	CaO wt %	CaO wt %	TiO2 wt %	Ba ppm	Sr ppm	Rb ppm	Y ppm	V ppm	La ppm	Ce ppm	Nd ppm	Sm ppm	Eu ppm	Gd ppm	Dy ppm	Er ppm	Yb ppm	Lu ppm	U ppm	Th ppm	Nb ppm	Ta ppm	Zr ppm	Hf ppm
LC1																											
LC1,1	0 85	0 05	2 87	15 03	n d	0 13	12893	16007	94 5	9 83	347	397	436	79 0	6 92	1 57	3 05	1 21	0 53	<0 55	<0 18	*20 9	2 13	76 0	<0 08	2 37	<0 64
LC1,2	0 92	*2 43	9 21	15 03	n d	0 30	10514	11079	77 8	20 0	301	400	440	78 4	5 73	1 58	4 88	2 23	*2 13	*2 81	*0 24	6 10	5 79	94 9	0 52	*210	*3 49
LC1,3	0 82	0 09	2 38	15 03	n d	0 12	8647	12557	63 3	9 93	391	365	400	69 6	*4 90	2 03	3 09	1 52	<0 81	<0 84	<0 11	6 89	1 74	54 3	0 10	7 09	<0 29
LC1,4	1 29	0 05	2 77	15 03	n d	0 16	15857	15104	104	11 0	466	449	484	86 2	6 64	1 49	3 06	1 36	0 79	<0 82	0 10	7 77	2 54	79 1	<0 10	4 06	<0 73
LC1,5	1 16	0 10	4 26	15 03	n d	0 17	24415	16084	118	26 1	508	988	978	181	12 6	2 69	*8 92	3 57	1 48	0 77	<0 16	8 85	3 95	79 2	<0 13	5 29	<0 65
LC1,6	0 74	0 30	2 66	15 03	n d	0 08	18083	15764	81 6	15 4	207	529	642	102	8 21	2 29	3 99	1 85	0 85	0 71	0 11	6 03	3 27	48 6	0 13	11 7	<0 28
LC1,7	*2 43*	*0 63*	*12 0*	*15 03*	*n d*	*0 45*	*11306*	*14171*	*422*	*10 2*	*1271*	*341*	*442*	*81 7*	*7 64*	*2 14*	*3 33*	*2 25*	*0 93*	*0 53*	*0 10*	*16 7*	*4 48*	*205*	*0 37*	*90 0*	*1 45*
Average first 6	0 96	0 12	4 03	15 03	n d	0 16	15068	14433	89 7	15 4	370	525	563	96 1	8 01	1 94	3 61	1 98	0 91	0 74	0 11	7 93	3 24	72 0	0 25	6 11	n d.
STDS	0 21	0 10	2 62	0 00	n d	0 06	5723	2107	19 5	6 57	110	233	220	33 6	2 69	0 48	0 81	0 87	0 40	0 04	0 01	0 71	1 48	17 3	0 23	3 59	n d.
RSD	22%	88%	65%	0%	n d	47%	38%	15%	22%	43%	30%	44%	39%	35%	34%	25%	22%	45%	44%	6%	7%	9%	46%	24%	94%	59%	n d
LC7																											
LC7,1	0 46	0 30	<11 95	20 52	n d	0 44	11921	15194	93 5	39 5	290	608	662	216	24 2	3 78	12 5	11 1	<2 93	<2 84	<1 04	12 5	11 1	198	*1 74	*183	*4 53
LC7,2	0 20	0 34	4 47	20 52	n d	0 22	9570	9975	111	39 2	236	510	612	129	*9 40	3 12	9 15	7 88	2 70	*4 56	0 27	15 6	9 18	161	<0 11	49 6	0 95
LC7,3	<0 21	0 40	<4 02	20 52	n d	0 26	7868	15227	104	29 5	181	380	481	117	14 7	3 19	8 61	4 91	2 40	<1 16	<0 23	12 6	8 31	149	0 43	51 7	<1 55
LC7,4	0 38	0 56	5 36	20 52	n d	0 28	7873	13666	136	37 3	343	502	624	173	16 5	*6 11	*5 32	6 98	3 42	<1 34	0 76	17 7	13 2	216	<0 22	69 4	<1 64
LC7,5	0 34	0 86	6 85	20 52	n d	0 33	10218	14266	158	47 4	337	668	762	166	20 5	5 00	8 85	9 82	5 73	4 64	*0 69	25 9	21 1	278	0 52	122	1 90
LC7,6	0 35	0 38	5 45	20 52	n d	0 26	11713	17258	164	36 9	332	577	694	153	12 5	4 62	11 3	5 86	3 54	3 20	0 39	22 1	11 2	194	0 41	44 2	<0 99
LC7,7	0 36	0 30	4 35	20 52	n d	0 20	10002	15083	135	36 4	295	526	651	137	13 9	4 50	8 76	4 95	2 31	2 94	0 28	16 2	10 3	146	0 32	42 1	0 81
Average	0 35	0 45	5 30	20 52	n d	0 29	9881	14361	129	36 0	288	539	643	156	17 1	4 04	9 86	7 36	3 35	3 59	0 43	17 5	12 1	192	0 42	63 1	1 22
STDS	0 08	0 20	1 00	0 00	n d	0 06	1624	2239	26 9	5 30	60 3	91 9	87 5	33 2	4 44	0 79	1 63	2 41	1 27	0 92	0 23	4 91	4 29	46 4	0 06	30 3	0 59
RSD	24%	45%	19%	0%	n d	20%	16%	16%	21%	14%	21%	17%	14%	21%	26%	20%	17%	33%	38%	25%	54%	28%	36%	24%	20%	48%	48%
LC13																											
LC13,1	1 93	1 08	8 65	19 4	n d	0 67	6133	10455	120	25 1	296	337	381	94 8	10 3	3 15	4 79	4 70	1 89	1 30	0 18	7 31	4 24	172	1 02	90 9	<0 62
LC13,2	2 59	1 13	10 3	19 4	n d	0 90	5824	10788	141	21 6	263	277	322	83 7	9 21	1 87	4 45	3 60	2 01	1 95	0 19	9 01	4 26	218	1 11	83 4	0 92
LC13,3	0 81	0 80	7 43	19 4	n d	0 43	8591	10857	101	33 3	236	442	536	120	14 7	3 70	8 64	6 56	2 91	1 57	0 21	9 37	8 23	132	0 49	84 0	1 14
LC13,4	0 45	1 00	6 40	19 4	n d	0 41	8097	10403	89 6	28 7	139	376	434	86 7	11 2	3 05	6 51	5 08	2 13	*2 53	0 21	8 76	6 33	122	0 89	96 4	1 10
LC13,5	0 89	0 78	8 65	19 4	n d	0 41	10505	13104	85 7	36 6	215	577	648	135	15 5	3 42	7 24	6 21	2 87	*3 46	0 25	8 38	5 64	132	0 52	71 4	1 10
LC13,6	1 26	0 16	5 03	19 4	n d	0 27	6215	9429	116	23 0	382	303	409	103	9 70	2 48	5 51	4 14	1 52	*0 81	<0 19	9 02	*3 09	*52 8	<0 10	*7 03	<1 24
LC13,7	1 05	0 54	5 99	19 4	n d	0 36	*20515	13570	90 9	30 7	379	625	695	127	12 2	4 27	8 81	5 18	1 98	<1 48	0 25	7 28	4 45	111	0 50	49 6	<0 50
Average	1 28	0 78	7 21	19 4	n d	0 49	7561	11230	103	28 4	273	420	489	107	11 8	3 13	6 02	5 06	2 18	1 61	0 22	8 45	5 19	148	0 75	79 3	1 06
STDS	0 74	0 34	1 77	0 00	n d	0 22	1838	1520	23 9	5 52	88 1	136	141	20 3	2 45	0 79	1 10	1 06	0 51	0 33	0 03	0 84	0 99	40 3	0 26	16 8	0 10
RSD	57%	43%	25%	0%	n d	44%	24%	14%	23%	19%	32%	32%	29%	19%	21%	25%	18%	21%	24%	20%	14%	10%	19%	27%	36%	21%	9%
LC14																											
LC14,1	0 55	0 21	4 04	14 80	n d	0 24	10442	10352	101	15 0	309	356	380	82 2	8 97	2 06	3 77	2 12	1 05	*1 75	0 14	6 17	3 29	124	0 58	47 7	0 81
LC14,2	0 36	0 24	5 04	14 80	n d	0 26	7803	9803	133	12 8	*194	254	320	62 4	7 22	1 74	3 22	2 21	1 13	1 15	0 14	7 81	3 11	127	0 61	40 0	0 87
LC14,3	0 74	0 29	5 38	14 80	n d	0 27	11874	11615	123	21 5	395	457	493	97 6	9 15	2 45	5 73	3 13	1 69	1 60	0 17	8 13	3 82	151	0 82	61 7	0 57
LC14,4	0 89	0 14	3 92	14 80	n d	0 20	12030	11748	123	16 0	538	479	496	84 7	9 81	2 13	5 49	*1 49	1 45	<0 85	<0 06	6 35	2 31	111	0 33	*24 0	<0 59
LC14,5	0 65	0 22	4 95	14 80	n d	0 28	11351	11736	117	19 6	293	386	419	88 8	8 28	2 13	4 13	3 09	1 76	*0 67	0 28	8 28	3 86	135	0 44	53 5	<0 41
LC14,6	0 54	<0 10	<2 74	14 80	n d	0 19	12186	11361	104	17 5	374	407	432	74 2	14 0	1 99	4 09	*1 36	1 34	1 22	<0 15	5 93	*1 69	99 0	*0 23	*25 8	<0 93
LC14,7	0 52	0 14	2 99	14 80	n d	0 19	12294	10842	114	11 5	346	285	312	60 3	6 17	1 42	3 09	2 09	0 81	*0 35	0 14	6 04	*2 35	91 9	*0 26	*26 1	<0 44
Average	0 61	0 21	4 39	14 80	n d	0 23	11111	11085	116	16 3	376	372	408	78 6	9 06	1 99	4 22	2 53	1 32	1 32	0 17	6 98	3 28	120	0 52	50 7	0 75
STDS	0 17	0 06	0 80	0 00	n d	0 04	1673	759	11 2	3 57	88 3	83 5	74 6	13 7	2 49	0 33	1 03	0 53	0 35	0 24	0 06	1 06	0 63	20 7	0 13	9 20	0 16
RSD	28%	28%	20%	0%	n d	17%	15%	7%	10%	22%	23%	22%	18%	17%	27%	16%	24%	21%	26%	18%	35%	15%	19%	17%	25%	18%	21%
LC18																											
LC18,1	*<0 84*	*<0 38*	*<14 33*	*20 94*	*n d*	*1 24*	*23927*	*17582*	*1295*	*43 8*	*7501*	*423*	*504*	*128*	*18 7*	*2 98*	*6 41*	*13 4*	*6 53*	*<4 53*	*<1 31*	*30 8*	*9 47*	*123*	*<0 90*	*<7 75*	*<5 32*
LC18,2	0.75	<0 09	<3 55	20 94	n d	0 17	8479	11178	86 2	10 2	291	264	306	56 2	*3 60	1 10	2 73	2 17	2 10	<1 24	0 21	4 07	0 85	52 9	0 19	*4 54	<1 81
LC18,3	1 23	0 40	7 70	20 94	n d	0 33	7768	11869	187	12 9	661	212	248	46 3	5 35	1 84	*1 46	2 36	1 19	1 83	0 31	9 66	2 46	142	0 30	*43 4	<0 80
LC18,4	0 39	<0 04	<1 33	20 94	n d	0 09	6151	*5345	*52 7	7 78	275	161	166	30 5	2 88	0 78	2 06	*0 64	0 70	<0 46	0 10	*1 97	0 62	*20 9	<0 12	*2 01	<0 54
LC18,5	0 48	0 27	4 12	20 94	n d	0 17	6743	11740	99 6	9 58	253	180	210	45 7	5 17	1 43	2 72	1 82	0 89	0 90	<0 09	4 16	1 51	76 3	0 35	31 3	0 59
LC18,6	1.05	0 21	4 26	20 94	n d	0 23	14886	16957	204	23 5	609	445	448	99 3	11 2	1 49	3 37	*5 01	1 89	<1 27	<0 32	7 46	1 67	98 2	<0 74	20 5	<0 72
LC18,7	0 87	0 15	5 60	20 94	n d	0 17	12606	12196	205	17 7	989	376	514	59 0	5 62	*3 45	3 51	2 76	1 37	1 26	0 19	*13 4	1 52	*149	0 33	16 5	0 83

Sample	MgO	Al2O3	SiO2	CaO	CaO	TiO2	Ba	Sr	Rb	Y	V	La	Ce	Nd	Sm	Eu	Gd	Dy	Er	Yb	Lu	U	Th	Nb	Ta	Zr	Hf
Average last 6	0 76	0 26	5 47	20 94	n d	0 19	9442	12788	156	13 6	513	273	315	58 5	6 04	1 32	2 88	2 28	1 36	1 34	0 20	6 34	1 47	92 8	0 29	22 8	0 61
STDS	0 33	0 11	1 67	0 00	n d	0 08	3505	2359	58 8	5 94	294	114	138	23 4	3 07	0 41	0 58	0 39	0 55	0 47	0 09	2 72	0 61	37 5	0 07	7 67	0 03
RSD	43%	42%	31%	0%	n d	42%	37%	18%	37%	44%	57%	42%	44%	41%	51%	31%	20%	17%	41%	35%	43%	43%	41%	40%	24%	34%	5%
LC20																											
LC20,1	0 77	0 72	5 61	22 3	23 5	0 31	7493	13011	101	30 3	222	383	406	91 1	11 3	3 12	6 38	4 07	1 84	1 91	0 34	6 90	3 56	138	0 64	59 5	0 60
LC20,2	0 59	0 39	3 13	22 3	23 2	0 18	7547	12707	77 4	27 2	155	444	444	105	10 4	2 33	7 43	4 65	2 34	*0 95	0 20	*4 01	2 59	85 5	0 54	35 8	0 32
LC20,3	1 23	1 29	8 24	22 3	23 4	0 45	12057	15376	140	42 2	302	609	603	137	15 4	4 04	10 2	6 18	3 18	1 56	0 32	8 57	6 12	197	1 10	*124	*1 90
LC20,4	0 98	0 41	4 56	22 3	23 4	0 36	8090	12859	117	21 8	328	353	385	86 7	11 2	2 41	6 60	4 71	2 36	*0 72	0 19	6 54	2 46	154	0 47	34 9	<0 39
LC20,5	0 58	0 42	3 23	22 3	24 0	0 22	7485	13002	89 7	21 4	189	349	374	98 3	10 6	2 88	6 42	3 60	1 63	1 65	0 19	5 69	2 02	97 4	0 45	39 6	0 45
LC20,6	0 99	0 71	6 28	22 3	23 6	0 36	14880	14872	113	35 9	275	617	635	147	15 6	3 97	9 85	7 06	3 54	1 75	0 26	8 51	4 74	167	0 66	57 9	0 70
LC20,7	2 01	0 38	8 03	22 3	n d	0 55	19571	15092	265	23 1	831	551	814	122	12 3	3 95	7 33	6 19	2 50	2 16	0 27	21 3	5 05	231	0 71	31 1	0 57
LC20,8	1 01	0 61	6 20	22 3	n d	0 48	10158	12265	186	23 1	450	413	501	107	10 7	3 36	6 57	4 88	2 46	2 16	0 27	14 0	4 96	209	0 82	56 6	0 84
LC20,9	1 32	0 70	9 96	22 3	n d	0 94	15036	14710	*484	24 0	828	561	708	131	13 1	4 36	7 87	6 56	3 20	2 84	0 39	*28 1	8 23	*434	1 39	69 1	0 78
LC20,10	*1 00*	*2 13*	*12 0*	*22 3*	*23 7*	*0 63*	*9064*	*12934*	*159*	*41 1*	*364*	*498*	*502*	*110*	*12 8*	*3 67*	*8 14*	*5 74*	*3 42*	*3 46*	*0 37*	*10 0*	*6 78*	*260*	*1 40*	*199*	*2 68*
LC20,11	*1 70*	*0 88*	*10 9*	*22 3*	*n d*	*0 79*	*14002*	*12291*	*246*	*23 1*	*699*	*430*	*669*	*131*	*13 6*	*4 16*	*7 27*	*6 12*	*3 31*	*2 61*	*0 36*	*25 6*	*9 81*	*348*	*1 47*	*75 2*	*1 14*
LC20,12	*1 88*	*1 76*	*13 1*	*22 3*	*n d*	*0 85*	*16170*	*14667*	*308*	*27 9*	*763*	*536*	*724*	*133*	*13 4*	*4 04*	*7 65*	*6 63*	*3 05*	*3 05*	*0 44*	*26 1*	*9 98*	*348*	*1 75*	*154*	*2 21*
LC20,13	*1 87*	*2 77*	*19 4*	*22 3*	*n d*	*0 79*	*8679*	*11249*	*241*	*37 6*	*662*	*331*	*528*	*85 4*	*10 9*	*3 42*	*6 24*	*4 39*	*2 11*	*2 02*	*0 29*	*17 5*	*8 26*	*340*	*1 70*	*203*	*2 98*
LC20,14	*1 62*	*2 31*	*17 3*	*22 3*	*n d.*	*0 89*	*10655*	*13642*	*299*	*28 3*	*628*	*408*	*552*	*109*	*11 4*	*3 26*	*7 05*	*4 77*	*2 32*	*2 63*	*0 34*	*17 5*	*7 71*	*370*	*1 60*	*186*	*1 92*
Average first 9	1 05	0 63	5 92	22 3	23 5	0 43	11369	13744	136	27 7	398	476	541	114	12 3	3 38	7 63	5 32	2 56	2 00	0 27	10 2	4 42	160	0 75	48 1	0 81
STDS	0 44	0 29	2 21	0 00	0 25	0 22	4337	1194	61 8	7 21	259	109	157	21 4	2 00	0 74	1 48	1 20	0 64	0 44	0 07	5 57	1 99	51 8	0 31	14 3	0 18
RSD	42%	46%	37%	0%	1%	52%	38%	9%	45%	26%	65%	23%	29%	19%	16%	22%	19%	23%	25%	22%	26%	55%	45%	32%	41%	30%	30%
LC22																											
LC22,1	*1 10*	*0 70*	*11 7*	*16 13*	*n d*	*0 52*	*9533*	*9741*	*180*	*25 3*	*580*	*317*	*404*	*77 0*	*8 17*	*2 56*	*5 43*	*3 99*	*1 76*	*1 73*	*0 25*	*10 3*	*3 88*	*221*	*1 00*	*114*	*1 24*
LC22,2	0 78	0 14	4 25	16 13	n d	0 24	8171	9343	201	11 0	616	229	328	58 6	4 97	1 22	2 63	1 70	0 82	0 71	0 14	5 35	0 90	83 1	0 24	*12 5	*0 14
LC22,3	1 01	0 48	8 69	16 13	n d	0 42	12226	9529	217	20 0	604	309	425	70 9	6 98	2 36	4 85	3 80	1 41	1 50	0 21	9 14	3 13	171	0 67	80 8	1 06
LC22,4	0 90	0 29	6 11	16 13	n d	0 31	11172	10196	266	19 1	531	335	416	72 2	6 58	2 82	4 00	3 70	1 83	1 45	0 11	8 12	2 16	136	0 55	47 9	0 43
LC22,5	0 53	0 18	3 81	16 13	n d	0 17	11006	10773	173	12 4	451	237	314	58 6	4 75	1 70	2 61	2 12	0 79	0 97	0 06	4 02	1 14	71 1	0 30	22 1	b.d.
LC22,6	0 93	0 21	5 05	16 13	n d	0 22	10743	7476	316	16 6	806	340	368	73 7	6 40	2 13	3 84	2 92	1 42	1 06	0 14	7 01	1 98	103	0 37	37 0	0 70
LC22,7	1 13	0 23	6 61	16 13	n d	0 26	12122	10844	191	16 5	847	319	416	77 0	7 11	2 13	3 99	3 20	1 29	0 98	0 14	7 52	1 94	115	0 47	39 2	b.d.
Average last 6	0 88	0 25	5 75	16 1	n.d.	0 27	10907	9693	228	15 9	642	295	378	66 5	6 46	2 06	3 65	2 91	1 23	1 11	0 14	6 86	1 88	113	0 43	45 4	0 73
STDS	0 21	0 12	1 79	0 00	n d	0 09	1471	1250	54 2	3 59	155	49 3	46 9	7 93	1 43	0 55	0 88	0 85	0 34	0 31	0 04	1 88	0 80	38 5	0 16	21 9	0 32
RSD	24%	49%	31%	0%	n d	32%	13%	13%	24%	23%	24%	17%	13%	12%	22%	27%	24%	29%	28%	28%	32%	27%	42%	32%	37%	48%	43%
LC43																											
LC43,1	0 62	0 76	5 80	15 44	15 4	0 25	12310	12773	146	12 6	758	166	187	39 8	4 34	1 46	2 72	1 78	1 08	*0 88	0 07	3 59	2 52	77 2	0 54	*147	*2 49
LC43,2	0 46	0 14	3 19	15 44	14 1	0 11	13733	11199	220	7 77	1204	135	147	28 3	2 66	0 85	1 36	0 99	0 39	<1 62	0 06	3 18	0 35	46 6	0 13	7 88	0 34
LC43,3	0 38	0 12	1 48	15 44	16 8	0 08	11279	13805	198	4 42	299	77 6	85 7	15 6	1 75	0 63	0 90	0 67	0 30	<0 13	0 02	1 16	0 21	20 8	0 06	4 37	0 05
Average	0 49	0 34	3 49	15 44	15 4	0 14	12441	12526	189	8 34	754	127	140	28 0	2 92	0 98	1 86	1 14	0 59	b.d	0 05	2 64	1 03	46 9	0 24	6 13	0 20
STDS	0 12	0 36	2 16	0 00	1 36	0 10	1232	1222	36 8	4 24	452	45 9	51 2	12 0	1 31	0 43	0 95	0 56	0 43	n d	0 03	1 30	1 30	28 2	0 26	2 48	0 21
RSD	24%	107%	62%	0%	9%	70%	10%	10%	20%	51%	60%	36%	37%	43%	45%	44%	57%	49%	72%	n d	53%	49%	126%	58%	107%	41%	105%
LC50																											
LC50,1	0 57	0 07	2 44	10 31	11 1	0 07	11471	13358	164	9 19	539	426	490	80 9	6 08	1 52	2 64	1 32	0 51	0 44	0 07	6 90	2 52	49 9	0 09	10 4	<0 19
LC50,2	0 39	0 55	4 50	10 31	10 6	0 06	6489	10099	79 3	7 18	101	255	276	44 6	3 25	0 87	1 54	0 80	0 59	0 53	0 14	3 35	1 76	32 6	0 09	43 2	0 79
Average	0 48	0 31	3 47	10 31	10 9	0 07	8980	11728	122	8 19	320	341	383	62 8	4 67	1 20	2 09	1 06	0 55	0 49	0 11	5 13	2 14	41 3	0 09	26 8	0 79
STDS	0 13	0 34	1 46	0 00	0 30	0 01	3523	2304	60 1	1 42	309	121	152	25 7	2 00	0 48	0 78	0 37	0 06	0 06	0 05	2 51	0 54	12 2	0 00	23 2	n d
RSD	27%	109%	42%	0%	3%	11%	39%	20%	49%	17%	97%	35%	40%	41%	43%	38%	37%	35%	10%	13%	47%	49%	25%	30%	0%	86%	n d
LC53																											
LC53,1	0 47	0 13	3 53	11 67	11 5	0 19	8363	7528	197	15 0	400	267	307	55 7	5 80	1 68	3 32	2 33	0 97	0 58	0 10	4 44	1 38	80 0	0 28	*29 4	0 38
LC53,2	0 45	0 08	2 90	11 67	12 0	0 15	9251	7766	218	13 6	392	268	318	57 7	5 80	1 74	3 16	2 07	0 92	0 58	0 08	4 27	1 05	70 8	0 21	15 3	0 38
LC53,3	0 42	0 07	2 67	11 67	12 1	0 15	10163	8080	186	13 6	417	293	343	62 7	6 09	1 71	3 49	2 10	0 91	0 54	0 10	4 56	1 07	74 0	0 20	15 5	0 27
Average	0 45	0 09	3 03	11 67	11 9	0 16	9259	7791	200	14 1	403	276	323	58 7	5 90	1 71	3 32	2 17	0 93	0 57	0 09	4 42	1 17	74 9	0 23	15 4	0 34
STDS	0 03	0 03	0 45	0 00	0 36	0 02	900	277	16 1	0 75	13 0	14 9	18 8	3 83	0 17	0 03	0 17	0 14	0 03	0 02	0 01	0 15	0 19	4 88	0 04	0 17	0 06
RSD	6%	34%	15%	0%	3%	14%	10%	4%	8%	5%	3%	5%	8%	6%	3%	2%	5%	7%	3%	4%	12%	3%	16%	6%	19%	1%	18%
LC65																											
LC65,1	0 38	0 96	10 8	13 4	14 6	0 33	7749	9721	138	9 56	190	383	449	78 9	6 40	1 53	2 81	1 86	0 83	0 63	0 07	14 6	11 9	246	1.05	123	2.23

Sample	MgO	Al2O3	SiO2	CaO	CaO	TiO2	Ba	Sr	Rb	Y	V	La	Ce	Nd	Sm	Eu	Gd	Dy	Er	Yb	Lu	U	Th	Nb	Ta	Zr	Hf
LC91																											
LC91,1	*1 72*	*26 17*	*78 47*	*16 3*	*17 8*	*2 25*	*7634*	*8053*	*248*	*80 8*	*501*	*434*	*519*	*144*	*18 6*	*5 49*	*15 2*	*14 7*	*8 61*	*4 88*	*1 10*	*20 1*	*22 5*	*457*	*4 94*	*2169*	*28 4*
LC91,2	0 78	<0 17	<2 20	16 3	15 7	0 02	6884	5854	18 2	3 06	215	92 9	82 0	14 6	3 05	0 70	0 98	<0 91	<0 48	<1 14	0 02	0 91	0 40	5 70	0 08	2 00	<0 45
LC91,3	0 26	0 35	<1 13	18 3	15 6	0 06	16640	15497	188	14 1	264	157	154	25 5	3 30	1 32	2 09	2 26	<0 96	0 53	0 18	3 30	1 58	10 7	0 18	*24 1	*3 57
Average last 2	0 52	0 35	b d	16 3	15 6	0 04	11762	10675	102	6 60	240	125	118	20 0	3 18	1 01	1 54	2 26	b d	0 53	0 09	2 10	1 00	8 18	0 13	2 00	n d
STDS	0 37	n d	n d	0 00	0 09	0 02	6899	6819	118	7 82	34 6	45 2	51 0	7 71	0 17	0 43	0 78	n d	n d	n d	0 09	1 69	0 84	3 50	0 07	n d	n d
RSD	71%	n d	n d	0%	1%	81%	59%	64%	116%	91%	14%	36%	43%	39%	5%	43%	51%	n d	n d	n d	106%	80%	84%	43%	55%	0%	n d.
LC92																											
LC92,1	0 47	0 66	4 51	25 5	25 6	0 22	5065	9669	103	16 8	239	216	232	58 0	7 51	2 57	4 49	3 62	1 32	1 40	0 11	2.31	1.21	*102	0 33	*62.3	*0 66
LC92,2	0 14	<0 04	0 93	25 5	24 0	0 21	6583	12885	130	11 6	*719	126	196	40 9	4 19	1 45	3 16	2 10	0 98	0 95	0 09	*6 72	1 43	*65 6	0 16	2 37	<0 31
LC92,3	0 21	<0 07	<1 62	25 5	28 8	0 05	4703	12060	95 8	14 2	195	156	231	54 4	5 30	1 79	4 41	2 55	0 91	0 66	<0 05	2 08	0 82	16 8	0.10	1 15	<0 17
LC92,4	0 23	<0 06	<1 34	25 5	27 4	0 05	4578	11499	39 9	14 5	158	187	262	61 9	6 98	2 03	4 48	1 99	0.74	0 50	0 06	2 12	0 59	16 2	<0.03	2 11	0 02
LC92,5	0 33	<0 12	<2 52	25 5	28 5	0 03	3919	10845	34 7	13 5	63 2	165	207	53 9	7 21	2 12	4 48	2 72	0 97	0 64	0 13	0 78	0 30	19 4	<0 09	6.37	0 20
LC92,6	0 15	<0 03	<0 62	25 5	25 2	0 02	2561	8144	30 4	9 32	65 6	116	151	35 2	3 42	1 28	2 40	1 56	0 83	0 73	0 04	0 74	0 17	13 2	<0 01	<0.50	<0.16
LC92,7	0 17	<0 05	<1 02	25 5	27 8	0.04	2075	7630	30 4	10 7	135	116	160	39 2	4 93	1 57	2 60	1 84	0 61	0 49	<0 01	1 14	0 31	16 1	<0.02	<0 66	0 05
LC92,8	*<0 89*	*<0 34*	*<8 36*	*25 5*	*26 5*	*0 39*	*14786*	*13087*	*135*	*26 1*	*1384*	*352*	*493*	*107*	*12 9*	*2 94*	*12 6*	*8 24*	*1 80*	*3 73*	*0 39*	*17 1*	*4 17*	*88 2*	*b d.*	*<5 24*	*<0 83*
LC92,9	**4 40*	*<1 27*	*<27 7*	*25 5*	*17 8*	*0 85*	*22917*	*13456*	*147*	*41 3*	*1071*	*329*	*635*	*102*	*18 4*	*2 41*	*7 11*	*4 92*	*5 77*	*<5 40*	*0 47*	*13 5*	*10 7*	*137*	*<0 93*	*<14 8*	*<2 13*
LC92,10	*2 97*	*58 0*	********	*25 5*	*24 4*	*3 78*	*16736*	*19346*	*910*	*159*	*1167*	*1072*	*1212*	*287*	*38 2*	*12 7*	*26 9*	*24 1*	*10 3*	*15 0*	*1 86*	*44 9*	*60 2*	*1226*	*11 7*	*4230*	*60 4*
Average first 7	0 24	0 86	2 72	25 5	26 8	0 09	4215	10390	66 4	12 9	143	155	206	48 1	5 65	1 83	3 72	2 34	0 91	0 77	0 09	1 52	0 69	16 7	0.20	3.00	0.09
STDS	0 12	n d	2 53	0 00	1 85	0 09	1530	1984	42 0	2 55	70 3	37 5	40 0	10 4	1 60	0 45	0 96	0 69	0 22	0 32	0 04	0 72	0 48	2 35	0 12	2.31	0 10
RSD	48%	n d	93%	0%	7%	101%	36%	19%	63%	20%	49%	24%	19%	21%	28%	24%	26%	30%	25%	41%	46%	48%	70%	14%	59%	77%	109%
LC93																											
LC93,1	0 96	0 57	5 91	16 91	16 5	0 35	11817	12242	169	26 7	437	573	626	140	13 0	3 26	7.29	4 45	2.19	2 31	0 30	16 7	9.48	152	0 54	52.2	0 69
LC93,2	1 00	0 71	6 19	16 91	16 2	0 40	11370	11893	248	24 6	377	662	731	141	13 7	3 36	6 91	3 28	1.72	1 48	0 15	18 4	14 9	197	0.78	90.2	0.78
LC93,3	1 66	2 05	14 5	16 91	16 7	0 62	13741	11800	249	49 0	528	1082	1208	243	23 0	6 02	12 9	7 98	3 58	3 25	0 35	24 9	18 6	278	1.42	219	2.30
LC93,4	1 19	2 08	13 0	16 91	17 0	0 56	10989	11686	179	38 1	264	723	839	174	17 5	4 64	9.71	6 01	2.77	3 09	0 35	20 6	16 1	244	1.43	222	2.81
LC93,5	1 22	2.31	14 1	16 91	16 4	0 60	10632	11028	200	28 1	348	529	597	129	11 7	3 02	6 67	4 25	2.66	3 12	0 35	21 4	17.8	255	1.43	220	2.55
LC93,6	0 79	1 31	7 73	16 91	16 7	0 36	10200	11581	159	26 6	163	565	639	134	13 0	3 45	6 79	4 70	1 95	1 43	0 20	14 4	11 9	153	0 74	125	1.39
LC93,7	0 69	2 08	11 9	16 91	16 4	0 47	10481	11458	166	33 6	185	639	729	157	15 9	4 34	8 66	5 30	2 59	2.33	0 32	16 0	16 6	204	1.32	208	2 59
LC93,8	0 91	1 22	9 37	16 91	16 9	0 44	10625	12509	231	21 8	384	522	607	129	12 4	3 06	8.49	3 40	1 64	1 42	0 31	14 6	12 8	197	0 94	114	1.15
LC93,9	1 25	0 83	10 1	16 91	17 0	0 67	20079	15149	454	38 1	592	1035	1097	204	19 0	4 92	10 3	6 28	2 67	2 29	0 31	18 1	16 9	282	0 92	70 9	0.73
LC93,10	1 06	1.73	11 2	16 91	15 4	0 56	8264	10697	302	16 4	440	380	475	111	9 47	2 60	4 88	2 77	1 29	1 19	0 19	15 4	10 9	241	1.19	173	2 10
LC93,11	1 67	1 21	11 2	16 91	16 7	0 62	15651	14515	256	51 6	625	999	989	213	21 4	5 38	11.2	7 72	4 07	3 79	0 35	25 4	19 9	284	1.16	124	1.17
LC93,12	0 90	0 66	5 89	16 91	16 5	0 35	10703	11818	146	19 9	352	531	589	132	12 1	2 91	5 60	3 44	1 62	1 36	0 15	14 2	9.25	158	0 54	64 4	0 69
Average	1 13	1 40	10 3	16 91	16 5	0 50	12083	12215	230	31 3	389	687	760	159	15 2	3 91	8 11	4 97	2 41	2 26	0 28	18 5	14 8	220	1.04	140	1.56
STDS	0.29	0 83	2 92	.0.00	0 45	0 12	3126	1308	85 3	11 2	146	229	227	41 0	4 21	1.11	2.43	1 73	0 84	0 89	0 09	3 67	3.77	50 3	0 34	65 4	0 83
RSD	26%	45%	29%	0%	3%	23%	26%	11%	37%	36%	37%	33%	30%	26%	28%	28%	30%	35%	35%	39%	29%	21%	25%	23%	33%	47%	53%
LC97																											
LC97,1	0 63	0 36	6 06	18 11	17 5	0 36	8319	11980	184	24 6	285	512	580	122	11 2	2 67	5 83	3 95	1 75	1.22	0 23	12 1	9.79	192	0.50	34.2	0.28
LC97,2	0 85	0 40	6 61	18 11	17 8	0 40	16723	15735	256	18 9	411	751	822	169	14 4	3 52	6 69	4.03	1.70	1 51	0 24	17 9	13 4	195	0 40	36.2	0.36
LC97,3	0 65	0 27	6 36	18 11	16 5	0 46	12845	14017	257	23 8	388	679	752	167	14 5	4 22	7 34	5.09	1 76	1.39	0 26	15 1	11 4	198	0.38	29.2	<0 34
LC97,4	1 06	0 49	8 96	18.11	17.7	0 37	11174	13416	254	29 3	398	685	749	157	15 0	3 85	7 67	4 56	2 15	1.93	0 23	19.8	14.9	217	0.55	48.5	<0.50
LC97,5	1 84	0 53	9 54	18 11	17.5	0 54	21304	16173	245	45 2	665	1027	1126	244	22 4	5 28	11.7	7.22	3 10	3 41	0 44	30 6	20 4	307	0 62	58 4	0.62
LC97,6	2 12	0 61	*12 1	18.11	17 8	0 65	14302	16317	347	37 9	828	832	901	192	20 8	4 51	8 90	5 98	2 70	2.91	0 34	35 2	20 8	375	0 81	53 3	0 57
LC97,7	1 96	0 53	9.88	18 11	18 6	0 59	21241	16480	249	44 9	691	968	1086	240	20 6	5.74	12 5	7.22	3 76	3 05	0 45	32 3	21.9	327	0.71	45 6	0 39
LC97,8	1 14	0 34	5 90	18.11	17.7	0 33	10203	12800	171	23 0	384	569	620	138	13 9	3 29	6 51	3 65	1 76	1 81	0 22	16 2	10 7	190	0.48	33.8	0.44
LC97,9	0 70	0 30	4 80	18 11	17 9	0 24	7761	11781	164	17 5	263	463	499	119	10 8	2 62	5 50	2 82	1 28	1 00	0 12	10 3	6.79	132	0 43	29.9	0.43
LC97,10	0 67	0 42	6 32	18 11	17.2	0 32	9083	11842	197	14 6	270	452	560	119	10 7	2 62	4 61	2 68	1 30	1 28	0 11	13 5	6.70	164	0 56	43 1	0.58
Average	1 16	0 43	6 84	18 11	17.4	0 43	13295	14052	232	28 0	458	694	770	167	15 4	3 83	7 73	4 72	2.12	1.95	0 27	20 3	13 9	232	0 54	41.0	0.46
STDS	0.59	0 11	1 68	0 00	0 51	0.13	5027	1965	55 1	11 1	198	203	217	46 4	4 35	1 09	2 61	1 64	0 61	0 68	0 11	9.03	5.41	77.2	0.14	9.76	0.12
RSD	51%	26%	24%	0%	3%	30%	38%	14%	24%	39%	43%	29%	28%	28%	28%	28%	34%	35%	38%	44%	43%	44%	39%	33%	26%	24%	26%
LC102																											
LC102,1	1 01	0 36	6 80	15 77	16 6	0 15	12207	14824	187	6 92	637	443	487	79 4	5 98	1 36	2 33	1 39	0 81	0 75	0 09	6 06	3.24	131	0.23	20 5	0.48
LC102,2	2 13	0 24	6 31	15 77	17 9	0 16	15951	14869	242	9 77	810	643	678	101	7 62	1 70	2 51	1 80	0 90	0 70	*0 04	*17 5	3.50	*168	*0.30	11.9	0.48
LC102,3	0 67	0 17	3 99	15 77	18 6	0 11	8113	12448	159	5 73	477	315	362	63 0	4 50	1 25	1 54	0 80	0 37	*0.12	0 12	5.72	1.60	111	0.22	7 44	0 22
LC102,4	0 54	0 14	2 11	15 77	17 2	0 07	9071	10430	245	5 19	361	322	414	62 5	4 48	1 01	1 95	1 49	0 48	0 69	<0 07	5 21	1.70	49.6	0 04	6 91	0 21
LC102,5	0 80	0 08	2 67	15 77	15 3	0 12	7676	12793	236	5 47	809	330	385	64 9	5 02	1 16	1 95	0 78	0 32	0.43	0 12	5 09	1.68	76 4	0 04	*3 53	<0 28

Sample	MgO	Al2O3	SiO2	CaO	CaO	TiO2	Ba	Sr	Rb	Y	V	La	Ce	Nd	Sm	Eu	Gd	Dy	Er	Yb	Lu	U	Th	Nb	Ta	Zr	Hf
LC102,6	<0 26	0 23	<2 22	15 77	16 8	0 07	8904	12278	94 7	8 14	366	333	341	61 6	4 41	1 21	1 59	1 37	0 41	<0 40	0 12	3 68	1 70	39 1	0 09	20 3	0 35
LC102,7	<0 24	0 16	<2 23	15 77	17 9	0 05	8469	12046	56 9	7 28	260	381	383	70 3	5 17	1 40	2 17	1 38	*0 31	0 46	<0 07	3 90	1 58	43 2	0 06	13 6	0 42
LC102,8	0 36	<0 09	<2 78	15 77	17 1	0 02	8497	12478	62 2	7 01	233	335	326	62 5	4 44	1 03	1 96	1 17	<0 19	0 28	0 07	2 50	1 24	*8 44	<0 03	<1 03	0 20
LC102,9	<0 33	<0 12	<2 97	15 77	17 2	0 07	8843	12884	101	8 41	375	396	399	62 9	5 16	1 01	1 68	1 34	0 36	<0 34	<0 16	3 47	2 12	58 9	0 05	5 02	<0.31
Average	0 92	0 20	4 38	15 77	17 0	0 09	9746	12783	154	7 10	461	389	417	89 8	5 20	1 24	1 96	1 28	0 52	0 55	0 10	4 73	2 04	72 6	0 10	12 2	0 33
STDS	0 63	0 09	2 11	0 00	0 77	0 05	2662	1372	77 6	1 59	221	104	106	13 1	1 04	0 23	0 33	0 33	0 23	0 19	0 02	1 71	0 79	35 4	0 08	6 30	0 12
RSD	69%	46%	48%	0%	5%	51%	27%	11%	50%	22%	46%	27%	25%	19%	20%	18%	17%	26%	45%	34%	22%	36%	39%	49%	81%	52%	37%
LC103																											
LC103,1	*3 31*	*1.38*	*15 9*	*13 60*	*13 5*	*0 79*	*14481*	*10855*	*395*	*41 4*	*746*	*648*	*747*	*158*	*16 1*	*4 08*	*9 37*	*5 49*	*2 70*	*2 81*	*0 32*	*34 6*	*23 0*	*366*	*1.18*	*164*	*1.68*
LC103,2	*1 30*	*0 85*	*9 11*	*13 60*	*13 0*	*0 45*	*9598*	*8710*	*122*	*38 6*	*255*	*737*	*800*	*162*	*17 6*	*4 07*	*9 00*	*5 39*	*2 41*	*2 33*	*0 26*	*18.1*	*16 9*	*202*	*0 80*	*100*	*1.03*
LC103,3	*1 48*	*0 53*	*7 40*	*13 60*	*12 8*	*0 37*	*16830*	*10894*	*183*	*36 3*	*368*	*953*	*1032*	*194*	*19 1*	*4 70*	*9 50*	*5 22*	*2 37*	*1 87*	*0 24*	*19 9*	*13 6*	*174*	*0 51*	*56 3*	*0 58*
LC103,4	0 73	0 74	6 59	13 60	12 3	0 32	7245	7256	99 3	19 5	138	395	451	91 0	9 11	2 29	4 57	2 89	1 47	1 25	0 18	11 8	13 2	146	0 73	92 4	0.92
LC103,5	0 60	0 43	4 63	13 60	13 2	0 23	5569	8173	167	12 2	232	278	347	76 7	7 06	1 58	3 70	2 26	1 04	0 95	0 11	9 89	8 19	109	0 47	58 7	0 65
LC103,6	0 92	0 94	8 46	13 60	13 3	0 39	8181	9077	183	18 2	389	396	478	103	9 82	2 42	4 54	3 04	1 38	1 15	0 14	14 1	12 4	185	0 95	124	1.23
LC103,7	0 99	0 63	7 02	13 60	13 5	0 35	9782	10132	207	21 2	322	573	634	123	12 3	2 85	6 10	3 13	1 58	1 41	0 16	16 2	13 1	174	0 72	81 4	0 69
LC103,8	1 27	0 47	6 78	13 60	13 6	0 36	8170	9675	264	15 1	469	416	515	105	9 08	2 34	4 75	2 94	1 31	1 37	0 16	19 6	12 5	184	0 60	57 6	0 44
LC103,9	0 87	0 36	5 13	13 60	12 8	0 29	8587	9316	173	19 5	330	487	553	111	11 3	2 49	4 80	2 80	1 14	0 89	0 14	14 6	10 1	138	0 44	44 6	0 46
LC103,10	0 58	0 46	4 47	13 60	13 9	0 23	5970	8746	166	12 0	179	296	342	78 8	7 05	1 91	3 71	2 02	0 92	0 82	0 13	11 2	9 40	110	0 55	60 4	0 60
LC103,11	0 89	0 61	8 27	13 60	13 2	0 31	6872	8697	146	20 2	245	411	463	103	10 2	2 38	5 75	3 42	1 57	1 41	0 16	13 7	12 6	153	0 64	81 8	0 93
Average last 8	0 86	0 58	6 17	13 60	13 2	0 31	7547	8884	176	17 2	288	407	473	99 0	9 46	2 28	4 74	2 81	1 30	1 16	0 15	13 9	11 4	150	0 64	75 0	0 74
STDS	0 22	0 19	1 36	0 00	0 51	0 08	1405	896	47 3	3 65	110	95 0	98 4	15 9	1 64	0 38	0 85	0 46	0 25	0 24	0 02	3 06	1 91	30 2	0 16	25 2	0 27
RSD	26%	33%	22%	0%	4%	19%	19%	10%	27%	21%	38%	23%	21%	16%	19%	17%	18%	16%	19%	21%	15%	22%	17%	20%	26%	34%	36%
LC120																											
LC120,1	*1.57*	*0 88*	*13 6*	*14 45*	*16 2*	*0 64*	*15523*	*10980*	*595*	*51 5*	*1417*	*862*	*1019*	*190*	*19 9*	*5 77*	*11 09*	*6 87*	*2.43*	*2.61*	*0.34*	*19.2*	*7.38*	*278*	*1.20*	*144*	*2 34*
LC120,2	0 69	0 74	9 34	14 45	14 7	0 42	8746	8420	223	26 8	315	519	577	123	12 9	3 34	6 64	4 12	1 75	1 37	0 20	11 4	6 06	175	0 98	122	1.34
LC120,3	0 81	0 98	11 8	14 45	15 8	0 53	9192	8662	251	31 5	398	597	682	139	13 5	3 80	7 70	4 80	2 08	1 76	0 25	14 3	7 56	209	1 21	166	1.94
LC120,4	0 67	0 82	9 13	14 45	14 9	0 44	7504	8624	177	25 0	249	447	523	108	10 5	2 73	6 35	4 39	1 98	1 35	0 22	11 2	6 38	178	1 00	130	1.54
LC120,5	0 94	1 20	12 7	14 45	14 0	0 58	9577	8316	240	34 3	342	594	684	147	15 7	4 37	8 41	5 38	2 50	2 02	0 35	16 0	9 20	223	1 31	189	2.28
LC120,6	0 66	0 68	6 88	14 45	13 8	0 33	8044	7517	201	20 0	290	384	447	90 4	9 28	2 45	4 82	3 42	1 37	1 11	0 17	9 32	4 45	131	0 81	104	1.31
LC120,7	0 88	1 25	10 9	14 45	13 4	0 46	9528	8038	190	27 4	341	472	538	117	11 3	3 19	6 23	4 04	1 92	1 63	0 22	11 3	6 12	166	1 12	210	2.65
LC120,8	0 53	0 44	5 05	14 45	14 0	0 24	8110	8395	134	14 7	247	327	371	77 4	7 43	1 98	3 91	*2 04	*1.07	*0 80	*0 09	6 64	3 26	93 6	*0.38	63 6	0 88
LC120,9	0 57	0 49	5 76	14 45	15 1	0 22	9807	9574	131	14 1	275	330	381	74 0	7 06	1 97	3 62	*2 12	*0 92	*0 50	*0 09	6 26	3 38	95 4	0 60	80 1	1.13
LC120,10	0 83	1 02	11 9	14 45	13 4	0 49	10253	7802	259	26 9	410	558	656	132	12 8	3 86	7 03	4 71	1 84	1 80	0 22	14 8	6 91	186	1 13	155	1.85
Average last 9	0 73	0 85	9 28	14 45	14 3	0 41	8951	8374	201	24 5	319	470	538	112	11 2	3 08	6 08	4 41	1 92	1 61	0 24	11 3	6 15	162	1 02	136	1.66
STDS	0 14	0 29	2 82	0 00	0 81	0 13	906	589	47 4	6 98	59 4	106	119	26 4	2 89	0 85	1 65	0 83	0 34	0 33	0 05	3 44	2 06	46 1	0 23	48.8	0 57
RSD	19%	34%	30%	0%	6%	31%	10%	7%	24%	28%	19%	23%	22%	24%	26%	28%	27%	14%	18%	21%	23%	31%	34%	28%	22%	36%	34%
LC121																											
LC121,1	*0.39*	*0.20*	*9 01*	*14 40*	*14 1*	*0 24*	*8191*	*10057*	*236*	*13 4*	*363*	*233*	*275*	*55 6*	*5 36*	*1 44*	*2 50*	*2 41*	*0 85*	*0 74*	*0 10*	*7.46*	*1.70*	*133*	*0.38*	*26.5*	*<0.56*
LC121,2	1.02	1.52	14.7	14 40	16 2	0 64	9791	8211	328	36 7	433	523	585	123	13 5	4 11	7 69	5 14	2 11	2.20	0 34	14 4	7.34	271	1.20	215	1.74
LC121,3	1.00	1.63	14 4	14 40	13.1	0 62	8837	6818	171	29 5	346	455	495	111	11 5	3 33	7 23	*3 75	2 59	1 44	0 25	12 2	7 08	238	1 48	214	2.80
LC121,4	0 94	0 81	9 59	14 40	12 5	0 42	8450	6792	258	21 4	497	375	428	89 8	8 72	2 16	5 19	2 99	1 89	1 77	0 17	8 55	4 11	159	0 74	108	1.45
LC121,5	0 96	0 61	9 25	14 40	13 0	0 40	6701	7078	176	24 0	334	359	439	92 9	9 25	2 41	5 24	3 43	1 38	1 47	0 19	9 43	4 35	195	0 88	99 9	1.13
LC121,6	1 06	1 54	17 7	14 40	13 7	0 71	8069	7344	196	37 7	298	472	556	120	14 1	3 84	8 43	4 96	2 25	2 54	0 25	14 4	9 03	301	1 59	248	2.95
LC121,7	0 85	0 56	9 58	14 40	12 8	0 38	7488	7466	300	20 3	527	380	446	88 1	9 93	2 46	4 18	3 94	1 35	1 41	0 15	8 95	3 72	160	0 72	89 8	*0.72
LC121,8	1 00	0 33	7 08	14 40	13 0	0 32	9255	8681	396	22 8	871	421	502	99 7	8 75	2 67	4 86	2 80	1 49	1 43	*0 12	8 81	2 27	181	0 44	*40.9	*0.72
LC121,9	0 82	0 85	11 0	14 40	16 3	0 42	8057	9051	280	26 5	270	312	406	78 1	8 74	2 48	4 71	3 81	1 56	1 98	0 21	9 60	5 43	195	1 05	133	1.34
LC121,10	0 71	1 02	12 4	14 40	14 7	0 60	5270	7706	187	26 8	269	273	366	72 8	9 62	2 52	5 27	3 49	1 74	1 69	0 25	14 4	6 47	276	1 35	151	2.09
Average last 9	0 91	0 96	11 7	14 40	13 9	0 50	7991	7683	254	27 3	427	397	469	97 1	10 5	2 89	5 87	3 82	1 82	1 77	0 23	11 2	5 53	217	1 05	157	1.94
STDS	0 15	0 48	3 35	0 00	1 45	0.14	1374	808	78 1	6 30	192	79 3	71 2	17 5	2 10	0 70	1 51	0 85	0 43	0 40	0 06	2 63	2 12	55 5	0 39	80 6	0 74
RSD	17%	48%	28%	0%	10%	29%	17%	11%	31%	23%	45%	20%	15%	18%	20%	24%	26%	22%	24%	23%	25%	24%	38%	28%	37%	39%	38%

Note: italics indicate whole analyses rejected and asterixes (*) indicate individual elemental analysis rejected. b.d. below detection, n.d. not determined.

Table A7 2 Trace (and major) element LAM-ICP-MS analyses of silicate liquid (LS) in the experiments on the join HOL14/OL5 - individual and average analyses, standard deviation (STDS) and relative standard deviation (RSD)

Sample	MgO wt %	Al2O3 wt %	SiO2 wt %	CaO wt %	CaO wt %	TiO2 wt %	Ba ppm	Sr ppm	Rb ppm	Y ppm	V ppm	La ppm	Ce ppm	Nd ppm	Sm ppm	Eu ppm	Gd ppm	Dy ppm	Er ppm	Yb ppm	Lu ppm	U ppm	Th ppm	Nb ppm	Ta ppm	Zr ppm	Hf ppm
LS2																											
LS2,1	*0 21*	*3 86*	*11 8*	*2 92*	*b d*	*0 53*	*932*	*1231*	*33 2*	*16 3*	*64 0*	*51 7*	*85 6*	*24 7*	*4 47*	*1 40*	*2 71*	*3 66*	*1 95*	*1.29*	*0.24*	*2.71*	*3 77*	*106*	*1 29*	*384*	*7.50*
LS2,2	0 55	12 9	30 3	2 92	b d	0 50	2061	2377	65 4	19 1	114	206	128	33 7	4 48	1 34	4 02	3 72	1 54	*2 84	0 36	5 12	7 64	140	1.35	622	9.26
LS2,3	0 63	9 76	28 3	2 92	b d	0 56	2226	2660	71 5	19 0	96 6	110	130	43 1	9 42	2 04	4 31	3 09	*2 97	b.d	*0.60	6 34	6 42	157	1.16	712	13 2
LS2,4	0 65	12 7	44 3	2 92	b d	0 73	3060	4659	179	25 5	223	151	225	58 7	*3 92	b d	4 55	2 41	1 48	1 57	0 17	*15 3	*15 3	252	1 74	1252	19 9
Average last 3	0 61	11 8	34 3	2 92	b d	0 60	2449	3232	105	21 2	144	156	161	44 5	6 95	1 69	4 29	3 07	1 51	1 57	0.27	5 73	7.03	183	1 42	862	14.1
STDS	0 05	1 76	8 73	0 00	n d	0 12	536	1244	64 0	3 69	68 6	47 9	55 5	11 6	3 49	0 49	0 27	0 66	0 04	n d	0 13	0 86	0 86	60 3	0 30	340	5 39
RDS	9%	15%	25%	0%	n d	20%	22%	38%	61%	17%	47%	31%	34%	26%	50%	29%	6%	21%	3%	n d	51%	15%	12%	33%	21%	39%	38%
LS5																											
LS5,1	*0 37*	*7 21*	*25 2*	*4 31*	*n d*	*0 65*	*1594*	*2026*	*58 1*	*21 4*	*111*	*75 8*	*121*	*30 3*	*3 59*	*1 43*	*3 83*	*3 65*	*2 39*	*2 75*	*0 20*	*4 78*	*5 26*	*139*	*1 64*	*575*	*9 90*
LS5,2	0 59	10 2	38 6	4 31	n d	1 19	2427	2923	105	32 9	191	138	188	47 3	*7 25	3 30	8 34	5 34	3 63	4 16	*0 90	9 21	10 5	254	3 19	984	13 4
LS5,3	0 55	10 6	37 0	4 31	n d	1 04	2357	2806	94 8	27 7	164	116	158	46 3	*5 76	2 13	3 96	5 26	2 93	3 22	0 39	6 87	9 07	208	2 40	917	9 77
LS5,4	0 59	11 0	37 9	4 31	n d	1 13	2462	3336	103	31 6	191	133	181	44 3	6 77	2 33	6 28	6 06	2 76	2 85	0 39	7 80	10 2	233	2 56	950	14 9
LS5,5	0 50	11 1	37 2	4 31	n d	0 84	1925	2219	96 8	25 6	146	88 1	136	36 7	*3 68	2 20	5 25	4 72	2 42	2 65	0 33	6 16	7 23	169	1 69	682	11 6
LS5,6	0 53	11.2	38 1	4.31	n d	1 09	2410	3171	105	30 7	167	117	162	46 9	11 2	2 23	5 60	5 40	2 17	1 58	0 35	8.01	8 29	225	2 05	925	13.6
Average first 5	0 55	10 8	37.8	4 31	n d	1 06	2316	2891	101	29 7	172	118	165	44 3	8 98	2 44	5 88	5 35	2 78	2 89	0 38	7 81	9 06	218	2 38	892	12 7
STDS	0 04	0 43	0 66	0 00	n d	0 14	222	429	4 86	2 97	19.1	19 4	20 6	4 42	3 12	0 49	1 61	0 48	0 56	0 93	0 03	1.16	1 35	31.7	0 56	120	1 98
RSD	7%	4%	2%	0%	n d	13%	10%	15%	5%	10%	11%	16%	12%	10%	35%	20%	27%	9%	20%	32%	9%	15%	15%	15%	24%	13%	16%
LS13																											
LS13,1	0 66	*19 4	41 6	5 39	n d	0 87	2481	2842	128	30 3	85 3	216	297	84 5	10 9	2 01	*7 69	4 68	3 15	2 90	0 30	12.7	18 8	198	2 68	1028	16.2
LS13,2	0 82	16 4	40 3	5 39	n d	0 91	2569	3101	112	35 7	95 7	226	324	76 1	9 13	2 96	6 67	6 93	2 79	2 20	0 37	12.4	18 4	188	2 31	1084	15.2
LS13,3	0 82	14 4	42 1	5 39	n d	1 08	2600	2813	153	37 9	112	245	369	85 0	12 1	2 83	6 29	7 20	2 14	*5 03	0 33	15 6	21 4	220	2 67	1277	23.0
LS13,4	0 71	12 2	38 0	5 39	n d	0 93	2205	2655	126	32 7	110	202	306	63 1	*15 1	2 99	5 19	4 22	4 16	2 87	0 21	11 6	16 6	197	2 17	1120	13 8
LS13,5	0 98	11 3	41 3	5 39	n d	0 86	2659	3369	131	35 6	83 1	225	303	83 2	8 73	*1 60	6 64	3 68	3 28	4 07	<0 61	12 9	19 5	189	2 49	1100	21 6
Average	0 80	13 6	40 7	5 39	n d	0 93	2503	2956	130	34 4	97 1	223	320	78 4	10 2	2 70	6 20	5 34	3 10	3 01	0 30	13 1	19 0	198	2 46	1118	18 0
STDS	0 12	2 27	1 64	0 00	n d	0 09	178	281	14 7	2 93	13 4	15 5	28 8	9 26	1 58	0 46	0 69	1 62	0 74	0 78	0 07	1 52	1 66	13 1	0 22	95 6	4 13
RSD	15%	17%	4%	0%	n d	10%	7%	10%	11%	9%	14%	7%	9%	12%	15%	17%	11%	30%	24%	26%	22%	12%	9%	7%	9%	9%	23%
LS18																											
LS18,1	1 08	8 37	35 1	11 77	n d	1.05	4384	5998	125	45 0	145	467	531	129	17 0	4 22	9 81	6 02	3 07	2.6	0 48	13.7	17.8	223	2.34	1191	12.6
LS18,2	0 96	8 96	34 6	11 77	n d	1 03	5282	6022	150	48 1	146	443	559	131	15 7	*2 36	*15 8	4 52	2 30	*5 35	0 62	13 5	18 2	249	2.10	1090	17.7
LS18,3	0 85	*13 2	36 6	11 77	n d	0 91	4783	6539	114	41 1	139	397	483	119	14 2	3 13	*13 6	3 98	2 38	*4 22	<0.18	12 6	17.9	188	2.29	883	20.3
LS18,4	1 02	4 67	30 8	11 77	n d	1 14	4903	6036	82 6	41 5	156	425	577	118	21 0	4 69	8 10	6 33	*8 95	*1.59	0 40	14 5	14 6	240	1.97	875	11.6
LS18,5	1 08	6 92	33 6	11 77	n d	0 87	4237	5927	74 2	42 9	138	374	528	102	14 8	4 74	*4 20	3 39	*5.36	*1.69	0.77	12 0	17.3	178	2.35	859	10.5
LS18,6	1 17	8 48	37.3	11 77	n d	1.05	5750	7755	115	44 9	151	475	617	133	21.1	4 60	10 8	*10 2	3 63	<1.88	<0.49	14 8	16 9	235	2.83	1082	15.8
LS18,7	0 94	9 23	38 5	11 77	n d	0 98	4502	6483	111	48 1	132	422	532	132	15 3	3 98	7 43	*9 69	2 41	*7.56	0 69	11 8	15 8	211	2.21	990	18.6
Average	1 01	7.77	34 9	11 8	n d	1 00	4834	6680	110	44 2	144	429	547	123	17 0	4 26	9 03	4 85	2 76	2.60	0 59	13 3	16.9	217	2.30	998	15 3
STDS	0 11	1 72	2 25	0 00	n d	0 09	535	868	25 5	2 51	8 25	38 1	42 6	11 0	2 87	0 65	1 54	1 28	0 58	n d	0.15	1 16	1.29	27 3	0.27	129	3.75
RSD	11%	22%	6%	0%	n d	9%	11%	13%	23%	6%	6%	8%	8%	9%	17%	15%	17%	26%	21%	n d	26%	9%	8%	13%	12%	13%	25%
LS19																											
LS19,1	0 99	13 0	36 5	6 70	n d	1 14	2053	2754	120	33 2	156	127	162	45 6	10 5	<0 91	6 52	*8 26	2 54	2 63	<0 61	10 2	8 22	206	1.59	1034	22 8
LS19,2	0 78	12 8	41.0	6 70	n d	1 08	2652	2982	111	32 4	187	139	177	*37 0	10 8	*1 80	*5 03	*3 28	4 02	<1.60	0.52	7 13	*15 3	212	2.45	935	12.8
LS19,3	1.06	12 6	39 2	6 70	n d	1 20	3515	3893	105	41 6	220	170	252	68 8	*7.36	3 73	8 82	*4 20	3 89	2 79	0 40	7.02	11 1	225	2.06	1062	20.5
LS19,4	0 90	12 1	39 4	6 70	n d	1 01	2981	3298	112	32 8	191	148	207	39 1	10 1	*1 94	8 45	6 14	*5 36	2 32	*0 77	7 61	10 6	220	1.62	994	15.7
LS19,5	1 77	14 3	40 4	6 70	n d	1 25	3236	3992	102	36 0	205	188	240	*81 2	*15 0	3 47	8 62	6 48	<2 34	<2 91	<0 65	9 79	10 3	236	2 38	1024	11 7
Average	1.10	13 0	39.3	6 70	n d	1 14	2887	3384	110	35 2	192	154	208	51.2	10 4	3 60	8 10	6 31	3 48	2 58	0 48	8 35	10 1	220	2 02	1009	16.7
STDS	0 39	0 82	1 71	0 00	n d	0 10	565	547	6 86	3 87	23 8	24 3	38 6	15 8	0 36	0 18	1 07	0 24	0 82	0 24	0 06	1.53	1.29	11 6	0 41	48.4	4.85
RSD	35%	6%	4%	0%	n d	8%	20%	16%	6%	11%	12%	16%	19%	30%	3%	5%	13%	4%	24%	9%	18%	18%	13%	5%	20%	5%	29%

Sample	MgO	Al2O3	SiO2	CaO	CaO	TiO2	Ba	Sr	Rb	Y	V	La	Ce	Nd	Sm	Eu	Gd	Dy	Er	Yb	Lu	U	Th	Nb	Ta	Zr	Hf
LS20																											
LS20,1	0 62	13 6	41 6	6 29	n d	0 91	2824	3407	136	30 2	108	235	322	77 1	9 13	2 97	6 30	5 16	2 51	2 28	0 33	12 1	17 9	198	2 28	880	13 2
LS20,2	0 66	13 9	41 1	6 29	n d	0 85	2856	3520	138	30 6	109	233	331	73 4	9 29	3 14	6 13	5 30	3 33	1 96	0 36	11.1	15 5	193	1 96	870	14 3
LS20,3	0 58	11 7	38 0	6 29	n d	0 82	2758	3365	129	29 9	104	231	318	75 4	9 17	2 64	6 03	5 57	3 09	2 99	0 33	11 6	16 1	181	2 15	869	13 3
LS20,4	0 68	13 4	40 3	6 29	n d	0 86	2954	3515	133	30 3	109	244	333	75 6	10 1	3 12	5 92	4 67	2 82	2 47	0 39	12 3	17.9	193	2 27	919	13 6
LS20,5	0 64	13 8	40 4	6 29	n d	0 87	2994	3598	137	31 4	112	256	346	81 6	9 36	2 95	6 34	4 94	2 92	3 13	0 38	12 0	17 7	200	2 54	892	14 9
LS20,6	0 67	12 6	40 5	6 29	n d	0 91	2952	3355	142	32 5	110	246	335	79 1	8 94	2 84	6 42	4 98	2 87	2 45	0 41	12 0	17.3	202	2 36	964	15 9
LS20,7	0 44	11 7	44 9	6 29	n d	0 85	2715	3151	109	28 1	99 4	234	305	74 3	7 33	2 40	4 69	5 19	*1 45	1 92	0 42	10 5	14 9	172	2 74	614	16 6
Average	0 61	13 0	41 0	6 29	n d	0 87	2865	3418	132	30 4	107	240	327	76 6	9 04	2 87	5 98	5 12	2 92	2 46	0 37	11.6	16 7	191	2 33	887	14 5
STDS	0 08	0 95	2 08	0 00	0 00	0 03	106	147	11 0	1 36	4 25	9 05	13 4	2 87	0 83	0 27	0 59	0 29	0 27	0 47	0 04	0 63	1.25	11 0	0.25	46 6	1.31
RSD	14%	7%	5%	0%	n d	4%	4%	4%	8%	4%	4%	4%	4%	4%	9%	9%	10%	6%	9%	19%	10%	5%	7%	8%	11%	5%	9%
LS21																											
LS21,1	0 82	14 0	40 5	7 45	n d	0 86	2348	3070	111	32 0	153	132	172	53 0	*6 10	3 02	6 73	6 90	3 58	2 93	*0 23	7 85	9 86	196	2 55	673	12 7
LS21,2	0 72	13 9	42 1	7 45	n d	0 96	2478	3142	117	34 9	169	136	177	46 0	7 30	2 84	7 29	6 44	3 50	2 65	0 50	7 35	9 91	213	1 98	927	13 5
LS21,3	0 87	14.3	44 5	7 45	n d	0 90	2692	3181	116	37 0	146	139	187	54 5	8 09	2 81	6 39	6 34	3 33	4 16	0 46	7 43	10 1	201	2 06	944	19 7
LS21,4	0 75	15 1	41 3	7 45	n d	0 77	2392	3272	98 9	33 4	152	130	170	53 4	10 9	2 43	*4 74	5 35	*2 50	4.17	0 54	7 79	8.51	202	2 61	849	19 9
LS21,5	0 81	13 3	43 4	7 45	n d	0 90	2552	3273	150	38 6	159	139	179	48 1	7 58	2 65	7 91	6 78	3 91	2 36	0 42	7 62	9 86	206	2 22	988	16 3
Average	0 79	14 1	42 4	7 45	n d	0 88	2492	3187	119	35 2	156	135	177	51 0	8 46	2 75	7 08	6 36	3 58	3 25	0 49	7 61	9 66	203	2 28	912	16 5
STDS	0 06	0 69	1 59	0 00	n d	0 07	137	87 3	18 9	2 65	8 73	3 85	6 73	3 72	1 63	0 22	0 67	0 61	0 24	0 86	0 05	0 22	0 65	6.57	0 28	49.7	3 36
RSD	7%	5%	4%	0%	n d	8%	5%	3%	16%	8%	6%	3%	4%	7%	19%	8%	9%	10%	7%	26%	10%	3%	7%	3%	12%	5%	20%
LS22																											
LS22,1	0 66	9 73	33 1	13 27	n d	1 01	6663	6807	165	46 3	176	469	586	129	12 7	3 23	*7 85	7 48	4 19	3 27	0 59	15 8	20.2	252	2 59	994	15 8
LS22,2	0 79	9 39	33 1	13 27	n d	1 18	6037	6050	110	55 2	168	563	738	141	18 8	5 09	10 6	10 2	5 08	4 75	0 74	17 1	24.2	275	2 83	1161	15 9
LS22,3	0 67	10 8	33 2	13 27	n d	0 99	5712	6898	117	41 9	140	492	632	143	16 4	4 22	9 66	9 31	3 82	3 46	0 43	16 2	21.0	220	2.13	981	14 9
LS22,4	0 63	8 47	33 3	13 27	n d	0 98	5431	7100	106	48 2	167	471	613	125	13.0	4 74	11 2	7 70	4 34	5 04	0 49	15 2	19.3	225	2 19	947	15 7
LS22,5	0 63	7 47	34 0	13 27	n d	1 15	5845	6715	162	44 3	146	518	638	147	18 5	5 25	10 5	7 04	*2 64	2 88	*0.30	16 4	21.1	259	2 53	1026	13 2
LS22,6	0 62	7 23	34 8	13 27	n d	1.03	5176	7014	112	48 8	133	505	653	149	14 9	4 62	10 9	7.78	4 01	4 31	0.70	16 9	21.7	253	3 26	1162	16 6
Average	0 67	6 84	33 6	13 27	n d	1 05	5777	6764	129	47 1	155	503	643	139	15 7	4 53	10 6	8 25	4 29	3 95	0 59	16 3	21.2	247	2 59	1042	15 3
STDS	0 06	1.37	0 70	0 00	n d	0 09	521	376	27 2	4 57	17 5	35 2	51 9	9 81	2 64	0 73	0 58	1 22	0.48	0 88	0.13	0 73	1.67	21.0	0.42	98 5	1 19
RSD	10%	15%	2%	0%	n d	9%	9%	6%	21%	10%	11%	7%	8%	7%	17%	16%	5%	15%	11%	22%	22%	4%	8%	9%	16%	9%	8%
LS23																											
LS23,1	*0 88*	*20 1*	*41 5*	*6 81*	*n d*	*1 10*	*3052*	*4134*	*121*	*38 8*	*155*	*161*	*253*	*45 3*	*12 9*	*1 60*	*6 86*	*11 5*	*<4 80*	*8 81*	*1.21*	*8 81*	*20.0*	*264*	*2 37*	*1094*	*27.8*
LS23,2	1 13	13 0	41 1	6 81	n d	1 22	3255	3684	117	38 6	211	166	226	74 6	8 93	3 11	*4 58	6 95	4 30	3 90	0 43	9 98	11 9	236	3 16	1054	18 9
LS23,3	1 06	*21.2	47 3	6 81	n d	1 30	3269	3898	148	47 8	244	176	228	62 5	9 48	*4 05	7 50	*3 42	*6 55	<3.13	*1.76	7 88	*16.1	270	4.13	1193	16 9
LS23,4	1 02	13 2	*35.7	6 81	n d	1.13	3320	3282	113	40 4	202	157	213	62 5	9 41	3 29	6 52	7 23	4 63	4 30	0 43	8 97	11 5	230	3 05	1027	14 2
LS23,5	0 80	14 4	43 9	6 81	n d	1 07	2750	3144	97 5	33 8	168	133	182	50 8	8 01	2 14	6 12	8 37	3 59	*2.63	0 66	8.71	10 2	220	2 11	887	14.7
LS23,6	1 29	13 2	44 6	6 81	n d	1 29	3721	3927	128	37 2	265	171	247	62 2	9 51	2 35	8 65	6 55	3 95	4 56	0 43	10 0	11.2	289	3 16	1138	20 4
Average last 5	1.06	13 5	44 2	6 81	n d	1 20	3263	3587	121	39 6	218	161	219	62 5	9 07	2 72	7 20	6 78	4 12	4 25	0 49	9 12	11.2	249	3 13	1060	17.0
STDS	0 18	0 64	2 52	0 00	n d	0 10	345	357	18 8	5 19	37 7	16 8	24 1	8 42	0 64	0 56	1 13	0 39	0 45	0 33	0 12	0 91	0 71	29.2	0.72	117	2 66
RSD	17%	5%	6%	0%	n d	8%	11%	10%	16%	13%	17%	10%	11%	13%	7%	21%	16%	6%	11%	8%	24%	10%	8%	12%	23%	11%	16%
LS27																											
LS27,1	1.88	12 4	47 0	4 97	n d	1.66	4104	5259	146	40 7	330	208	285	71 3	12 5	*2 06	10.3	7 65	4.64	*7 76	<0 60	16 6	17 7	339	2 89	1570	22 3
LS27,2	1 75	11 6	45 1	4 97	n d	1 66	4278	5596	156	45 6	268	217	303	76 3	19 5	4 28	14 6	7 97	5 15	<3 69	0 81	15.8	13 1	341	3 25	1625	23 2
LS27,3	1 59	10 8	41 4	4 97	n d	1 51	3922	4548	127	58 7	317	195	258	70 2	<2 78	5 51	8 95	8 92	<5 71	<4 64	<0 86	*10 9	17.8	330	3 55	1515	27 6
LS27,4	*0 98*	*14 5*	*37 9*	*4 97*	*n d*	*0 94*	*2589*	*3197*	*89 7*	*30 4*	*215*	*205*	*188*	*45 3*	*10 1*	*1 51*	*8 70*	*<2 86*	*3 41*	*2 39*	*<0 62*	*6 69*	*13 1*	*196*	*3 54*	*1027*	*18.2*
LS27,5	*0 48*	*6 71*	*19 7*	*4 97*	*n d*	*0 44*	*1480*	*1652*	*37 4*	*17 9*	*67 5*	*61 9*	*88 2*	*16 8*	*<2 02*	*1 53*	*5 53*	*3 10*	*2 11*	*1 75*	*<0 24*	*4 31*	*5 75*	*102*	*1 15*	*478*	*4 85*
Average first 3	1 74	11 6	44 5	4 97	n d	1 61	4101	5134	143	48 3	305	207	282	72 6	18 0	4 90	10 6	7 51	4 90	n d	0 81	16 2	16 2	336	3 23	1570	24 4
STDS	0 15	0 79	2 83	0 00	n d	0 09	178	535	14 7	9 29	32 9	11 2	22 7	3 21	4 97	0 87	3 82	0 54	0 36	n d	n d	0 52	2 69	5 92	0 33	54 8	2 82
RSD	8%	7%	6%	0%	n d	5%	4%	10%	10%	19%	11%	5%	8%	4%	31%	18%	36%	7%	7%	n d	n d	3%	17%	2%	10%	3%	12%
LS31																											
LS31,1	0 21	6 54	28 1	2 79	n d	0 45	1945	1884	98 4	29 2	78 0	74 7	125	23 7	4 49	1 44	4 00	4 74	2 51	2 99	0 42	8 96	9 35	140	1 48	784	11 3
LS31,2	0 37	5 69	21 6	2 79	n d	0 41	1701	1101	75 2	20 0	90 3	55 5	117	26 7	<2 99	1 02	5 12	5 76	<1 35	<2.52	<0 38	8.44	7 09	144	1 52	584	11.0
LS31,3	*0 18*	*8 65*	*38 3*	*2 79*	*n d*	*0 58*	*3364*	*4020*	*147*	*33 7*	*<84 6*	*165*	*311*	*42 0*	*12 2*	*2 91*	*6 01*	*6 26*	*2 77*	*2 79*	*0 57*	*16 6*	*16 4*	*200*	*1 42*	*1028*	*17 4*
Average first 2	0 29	6 12	24 8	2 79	n d	0 43	1823	1492	86 8	24 6	84 2	65 1	121	25 2	4 49	1 23	4 56	5 25	2 51	2 99	0 42	8 70	8 22	142	1 50	674	11 1

Sample	MgO	Al2O3	SiO2	CaO	CaO	TiO2	Ba	Sr	Rb	Y	V	La	Ce	Nd	Sm	Eu	Gd	Dy	Er	Yb	Lu	U	Th	Nb	Ta	Zr	Hf
STDS	0 11	0 60	4 61	0 00	n d	0 03	172	554	16 3	8 50	8 66	13 6	5 52	2 10	n d	0 30	0 79	0 72	n d	n d	n d	0 37	1 60	2 98	0 03	156	0 24
RSD	39%	10%	19%	0%	n d	7%	9%	37%	19%	26%	10%	21%	5%	8%	n d	24%	17%	14%	n d	n d	n d	4%	19%	2%	2%	23%	2%
LS43																											
LS43,1	0 94	5 25	29 8	10 88	11 1	1 11	5186	6072	96 0	45 8	198	316	406	96 7	12 9	3 84	9 05	7 61	3 95	3 23	0 45	11 9	14 4	238	2 62	1095	16 5
LS43,2	0 95	5 28	29 7	10 88	11 4	1 11	5416	6273	97 3	47 3	197	332	423	99 4	13 2	4 12	9 55	8 02	3 76	3 56	0 55	12 5	18 4	246	2 66	1121	17 7
LS43,3	0 95	5 36	29 6	10 88	11 1	1 12	5320	6260	93 8	47 2	203	326	416	101	13 1	4 13	9 22	7 78	4 02	3 62	0 57	12 0	16 1	242	2 65	1124	17 4
LS43,4	0 96	5 39	29 7	10 88	11 3	1 12	5332	6177	97 0	47 3	198	331	421	99 6	13 4	3 98	10 1	7 70	4 13	4 25	0 55	12 3	16 2	243	2 74	1141	18 5
LS43,5	0 95	5 42	30 3	10 88	11 3	1 13	5519	6337	101	48 0	207	334	429	103	12 9	4 28	8 73	7 66	4 25	4 04	0 57	13 1	16 3	247	2 81	1149	18 3
Average	0 95	5 34	29 8	10 88	11 2	1 12	5355	6224	97 0	47 1	201	328	419	99 9	13 1	4 07	9 32	7 75	4 02	3 74	0 54	12 4	15 9	243	2 70	1126	17 7
STDS	0 01	0 07	0 29	0 00	0 12	0 01	123	102	2 66	0 83	4 21	7 20	8 94	2 30	0 20	0 17	0 50	0 16	0 19	0 41	0 05	0 47	0 82	3 45	0 08	21 0	0 79
RSD	1%	1%	1%	0%	1%	1%	2%	2%	3%	2%	2%	2%	2%	2%	2%	4%	5%	2%	5%	11%	9%	4%	5%	1%	3%	2%	4%
LS91																											
LS91,1	0 77	19 3	43 9	9 27	9 35	0 98	3300	4171	112	37 3	178	201	238	64 8	8 61	2 83	6 99	5 91	3 22	3 48	0 38	8 42	10 1	209	2 29	950	13 9
LS91,2	0 78	23 8	48 8	9 27	9 07	1 00	3474	4352	123	38 6	191	207	249	66 8	9 85	2 90	7 05	6 09	3 45	3 51	0 42	8 7	10 5	221	2 28	974	13 1
LS91,3	*0 39*	*8 96*	*24 9*	*9 27*	*9 45*	*0 50*	*1667*	*2318*	*49 9*	*23 5*	*90 9*	*103*	*125*	*34 1*	*5 04*	*1 61*	*4 14*	*3 12*	*1 78*	*2 13*	*0 28*	*3 71*	*5 21*	*103*	*0 95*	*476*	*6 92*
Average first 2	0 78	21 6	46 3	9 27	9 21	0 99	3387	4261	117	38 0	184	204	244	65 8	9 23	2 87	7 02	6 00	3 34	3 50	0 40	8 56	10 3	215	2 29	962	13 5
STDS	0 01	3 20	3 42	0 00	0 20	0 01	123	128	7 60	0 93	9 43	4 32	7 27	1 46	0 88	0 05	0 04	0 13	0 16	0 02	0 03	0 20	0 32	8 60	0 01	17 5	0 59
RSD	1%	15%	7%	0%	2%	1%	4%	3%	6%	2%	5%	2%	3%	2%	9%	2%	1%	2%	5%	1%	7%	2%	3%	4%	0%	2%	4%
LS92																											
LS92,1	0 62	12 6	33 0	7 36	7 44	0 78	2680	3413	104	33 4	128	186	233	57 8	8 69	2 68	5 78	5 20	2 65	3 06	0 42	8 48	9 58	188	2 11	759	11 6
LS92,2	0 61	12 9	32 7	7 36	7 67	0 83	2823	3552	101	36 2	134	202	247	60 8	9 41	2 76	6 27	5 72	2 74	2 77	0 42	8 44	10 5	198	2 18	800	12 2
LS92,3	0 64	13 5	34 5	7 36	7 87	0 81	2743	3494	104	34 5	131	192	240	59 9	8 65	2 86	5 79	5 26	2 80	2 73	0 44	8 71	10 5	196	2 13	793	11 8
LS92,4	0 62	12 8	34 1	7 36	7 73	0 79	2536	3249	101	32 8	138	177	219	54 7	8 18	2 77	6 09	5 08	2 51	2 39	0 37	7 54	9 27	189	1 87	746	11 2
LS92,5	0 71	13 0	34 3	7 36	7 88	0 78	2638	3362	102	32 7	132	183	227	58 1	8 07	2 68	6 02	5 05	2 67	2 74	0 39	7 93	9 44	191	1 91	747	11 4
Average	0 64	13 0	33 7	7 36	7 72	0 80	2684	3414	102	33 9	133	188	233	58 2	8 60	2 75	5 99	5 26	2 67	2 74	0 41	8 22	9 86	192	2 04	769	11 6
STDS	0 04	0 32	0 81	0 00	0 18	0 02	108	118	1 39	1 44	3 73	9 71	11 0	2 35	0 53	0 07	0 21	0 27	0 11	0 24	0 03	0 48	0 59	4 36	0 14	25 8	0 40
RSD	6%	3%	2%	0%	2%	3%	4%	3%	1%	4%	3%	5%	5%	4%	6%	3%	3%	5%	4%	9%	7%	6%	6%	2%	7%	3%	3%
LS93																											
LS93,1	0 50	13 3	32 0	5 61	5 81	0 62	2726	3323	117	22 8	59 9	264	354	83 3	8 43	2 45	4 79	3 91	1 64	1 64	0 25	12 9	30 1	137	1 93	1122	16 7
LS93,2	0 51	14 1	34 4	5 61	5 56	0 61	2843	3364	112	23 0	59 3	268	360	82 7	9 07	2 36	5 09	3 49	1 76	2 01	0 24	13 0	30 0	138	1 86	1117	16 9
LS93,3	0 47	13 2	32 2	5 61	5 31	0 58	2774	3233	111	21 7	55 3	260	353	76 5	8 44	2 28	4 81	3 32	1 73	1 83	0 32	11 6	27 7	130	1 70	1089	15 5
LS93,4	0 49	14 0	34 6	5 61	5 63	0 62	3097	3582	128	24 4	63 5	296	402	90 0	9 94	2 72	5 46	3 95	1 85	2 22	0 25	15 0	33 1	148	1 99	1201	18 1
LS93,5	0 48	14 1	34 4	5 61	5 66	0 62	3131	3557	124	24 3	62 9	300	403	89 4	9 85	2 47	5 66	3 94	1 76	1 99	0 26	15 0	33 3	146	2 00	1187	18 0
LS93,6	0 50	13 7	33 9	5 61	5 57	0 63	3102	3529	141	25 2	64 8	304	408	93 1	10 1	2 66	5 84	4 23	2 03	1 93	0 27	15 2	34 2	152	2 08	1208	19 3
LS93,7	0 48	14 0	36 1	5 61	5 60	0 63	3083	3550	121	23 4	62 9	287	393	89 9	9 22	2 59	5 36	3 79	1 72	2 04	0 27	15 1	31 7	147	1 90	1143	17 5
LS93,8	0 49	13 9	33 5	5 61	5 69	0 63	2851	3401	122	23 9	60 5	285	384	86 6	9 15	2 43	5 49	3 54	2 06	2 09	0 30	13 9	31 3	143	1 94	1168	17 2
Average	0 49	13 8	33 9	5 61	5 60	0 62	2951	3442	122	23 6	61 2	283	382	86 4	9 28	2 50	5 31	3 77	1 82	1 97	0 27	14 0	31 4	143	1 93	1152	17 4
STDS	0 01	0 35	1 33	0 00	0 14	0 02	168	130	9 56	1 09	3 03	17 1	22 8	5 37	0 65	0 15	0 38	0 30	0 15	0 17	0 03	1 35	2 15	7 02	0 11	47 8	1 15
RSD	3%	3%	4%	0%	3%	3%	6%	4%	8%	5%	5%	6%	6%	6%	7%	6%	7%	8%	8%	9%	10%	10%	7%	5%	6%	4%	7%
LS97																											
LS97,1	0 28	20 2	43 5	2 18	2 08	0 51	1026	1019	138	15 2	39 7	86 9	132	34 3	3 63	1 12	2 64	2 18	1 30	1.52	0 26	12 7	23 2	159	2 11	916	12 7
LS97,2	0 42	23 0	46 3	2 18	2.11	0 58	1139	1182	170	16 6	45 1	110	160	38 1	5 04	1 37	3 02	2 31	1.56	*1 04	0 22	13 9	31 8	199	2.44	1185	16 0
LS97,3	0 35	18 2	42 1	2 18	2 14	0 56	1040	1051	145	16 8	47 7	98 0	148	39 8	5 39	1 32	3 13	2 45	1 29	1 37	0 21	13 4	27 4	181	2 26	1063	13 9
LS97,4	0 45	21 5	44 8	2 18	2 12	0 45	925	952	136	*12 9	42 0	83 6	123	31 6	3 68	1 04	2 09	2 14	*0 98	1 27	0 17	12 3	23 3	153	1 98	920	12 4
LS97,5	0 40	20 7	45 8	2.18	2 14	0 56	1056	1077	150	16 6	45 3	102	152	37 5	4 63	1 38	2 98	2 47	1 54	1 57	0 22	14 3	27 3	188	2 26	1101	14 6
Average	0 38	20 7	44 5	2.18	2 12	0 53	1037	1056	148	16 3	43 9	96 1	143	38 2	4 47	1 25	2 81	2 31	1 42	1 43	0 22	13 3	26.6	176	2.21	1037	13 9
STDS	0 07	1 75	1 71	0 00	0 02	0 05	78 3	84 3	13 5	0 76	3 11	10 8	15 3	3 29	0 79	0 16	0 42	0 15	0 15	0 14	0 03	0 83	3 56	19 2	0 18	117	1 46
RSD	18%	6%	4%	0%	1%	10%	7%	8%	9%	5%	7%	11%	11%	9%	18%	13%	15%	7%	10%	10%	15%	6%	13%	11%	8%	11%	10%
LS102																											
LS102,1	*0 76*	*34 6*	*89 6*	*4 74*	*5 16*	*0 60*	*2696*	*3122*	*261*	*20 1*	*190*	*234*	*312*	*73 2*	*5 74*	*2 22*	*3 42*	*3 24*	*1 44*	*1 28*	*0 22*	*18 6*	*20 1*	*270*	*1 88*	*1112*	*15 2*
LS102,2	*0 28	6 48	*20 8	4 74	4 42	0 54	*1170	1478	*58 4	23 8	95 0	*81 0	*107	*29 0	4 84	1 80	3 88	3 50	2 06	2 24	0 24	*4 56	*5 28	*119	1 26	*482	*8 84
LS102,3	0 66	19 1	49 0	4 74	4 92	0 56	1806	1929	146	21 8	101	141	195	46 2	5 66	1 82	4 92	2 92	1 18	1 98	*0 12	9 64	11 5	181	1 86	786	9 82
LS102,4	0 54	26 1	54 5	4 74	5 26	0 64	1677	1924	148	24 1	120	134	180	44 9	5 54	1 92	4 20	3 42	1 66	2 14	0 28	8 56	10 3	191	1 58	812	10 8

Sample	MgO	Al2O3	SiO2	CaO	CaO	TiO2	Ba	Sr	Rb	Y	V	La	Ce	Nd	Sm	Eu	Gd	Dy	Er	Yb	Lu	U	Th	Nb	Ta	Zr	Hf
LS102,5	0 60	18 9	47 0	4 74	5 12	0 44	1883	2644	134	17 6	107	142	182	38 6	4 32	1 54	3 02	2 56	1 28	1 36	0 28	8 70	9 90	162	1 28	715	8 88
LS102,6	0 50	12 8	40 0	4 74	4 80	0 46	1886	2110	126	18 1	118	141	185	43 1	4 64	1 68	3 48	2 60	1 26	1 44	0 22	9 10	10 8	163	1 26	686	9 88
Average last 5	0 58	16 7	47 6	4 74	4 90	0 53	1813	2017	138	21 1	108	139	186	43 2	5 00	1 75	3 90	3 00	1 49	1 83	0 26	9 00	10 6	174	1 45	750	9 80
STDS	0 07	7 39	5 98	0 00	0 32	0 08	97 8	421	10 5	3 08	10 7	3 84	7 00	3 34	0 58	0 15	0 72	0 44	0 37	0 41	0 03	0 48	0 67	14 1	0 27	59 1	0 80
RSD	12%	44%	13%	0%	7%	15%	5%	21%	8%	15%	10%	3%	4%	8%	12%	8%	18%	15%	25%	22%	12%	5%	6%	8%	18%	8%	8%
LS103																											
LS103,1	<0 40	11 9	36 5	2 92	2 84	0 53	1524	1811	184	18 8	42 7	160	218	47 0	5 97	1 97	5 05	3 78	*1 28	2 13	<0 21	15 6	44 6	163	2 88	1587	20 5
LS103,2	0 50	10 2	27 2	2 92	2 41	0 51	1466	1432	175	16 2	42 3	149	199	48 8	*4 10	*2 58	*3 31	*2 84	1 83	1 54	0 30	15 0	37 4	148	2 44	1448	28 6
LS103,3	0 41	11 9	35 3	2 92	2 75	0 56	1655	1617	226	18 7	62 2	169	231	54 2	6 66	1 65	4 90	5 38	2 81	2 28	<0 23	16 8	40 4	173	2 72	1616	22 6
LS103,4	0 49	11 8	33 2	2 92	2 77	0 60	1512	1525	203	18 7	50 1	159	217	52 5	*4 77	*1 20	3 98	3 48	1 71	<1 95	0 43	18 5	42 1	170	3 20	1567	25 1
LS103,5	<0 42	12 4	33 4	2 92	3 04	0 56	2056	1906	232	22 5	57 3	193	267	*75 4	7 27	2 09	4 80	4 25	1 94	2 05	0 21	<75 9	45 4	196	3 35	1706	27 9
LS103,6	0 40	11 8	35 2	2 92	2 79	0 57	1715	1793	231	20 4	50 6	174	240	67 3	8 14	1 52	4 12	3 58	2 00	2.31	0 49	19 0	46 7	188	3 36	1768	27 9
LS103,7	0 52	12 9	40 8	2 92	2 96	0 60	1843	1840	262	22 9	54 6	192	267	*75 2	6 95	1 80	4 67	3 91	1 70	1 90	0 28	*24 0	*54 5	218	3 53	1881	32 6
LS103,8	<0 59	11 8	34 6	2 92	2 51	0 61	1652	1699	251	19 5	43 7	173	244	50 9	*10 7	1 57	4 68	4 75	3 01	*3 31	0 25	19 4	42 9	184	4 13	1734	33 7
Average	0 46	11 8	34 5	2 92	2 76	0 57	1678	1703	220	19 7	50 4	171	235	53 5	7 00	1 77	4 60	4 16	2 14	2 04	0 33	17 4	42 8	180	3 20	1683	27 4
STDS	0 06	0 78	3 78	0 00	0 21	0 04	196	168	30 8	2 20	7 32	15 6	24 1	7 2	0 80	0 23	0 40	0 69	0 54	0 29	0 11	1 85	3 19	21 8	0 53	136	4 51
RSD	12%	6%	11%	0%	8%	6%	12%	10%	14%	11%	15%	9%	10%	14%	11%	13%	9%	17%	25%	14%	33%	11%	7%	12%	16%	8%	16%
LS120																											
LS120,1	0 81	5 22	31 6	14 9	15 2	1 22	5513	6786	107	71 7	122	958	1175	281	*31 2	8 97	15 7	10 9	5 36	4.47	0 67	30 5	34 9	371	3 52	973	13 4
LS120,2	0 92	5 87	34 2	14 9	15 6	1 18	5314	6528	109	83 2	113	906	1107	268	25 1	8 50	14 8	10 4	4 99	4 75	0 86	27 7	35 2	353	3 71	1029	12 4
LS120,3	0 92	5 40	36 2	14 9	15 1	1 24	5381	6445	122	76 8	136	888	1090	246	26 0	6 78	16 9	9 65	4 64	5 37	0 78	29 4	33 9	351	3 74	903	12 8
LS120,4	0 82	4 90	28 6	14 9	14.7	1 06	5275	6609	*83 9	62 4	*110	797	976	223	24 8	6 64	14 4	9 61	4 28	4 22	0 58	23 6	30 9	262	2 77	901	12 9
LS120,5	0 75	4 59	26 2	14 9	14 8	1 02	5741	7091	111	58 4	130	765	924	205	23 8	6 59	13 5	9 21	3 98	3 92	0 60	21 2	29 2	248	2 57	859	12 8
Average	0 85	5 20	31.4	14 9	15.1	1 14	5445	6692	112	70 5	125	863	1054	244	24 9	7 50	15 1	9 96	4 65	4 55	0 70	26 5	32 8	317	3 26	933	12 9
STDS	0 08	0 49	4 02	0 00	0 37	0 10	189	256	6 49	10 2	10 3	80 0	102	31.3	0 89	1 15	1 30	0 69	0 55	0 55	0 12	3 94	2 63	57.2	0 55	87.4	0 37
RSD	9%	9%	13%	0%	2%	9%	3%	4%	6%	14%	8%	9%	10%	13%	4%	15%	9%	7%	12%	12%	18%	15%	8%	18%	17%	7%	3%
LS121																											
LS121,1	1.48	6.31	38 7	12 0	11 6	1.48	4341	5098	172	69 3	151	625	762	179	20 7	6 03	12 3	9 40	4 94	5.12	0 85	23 7	23 4	427	4.17	906	11.0
LS121,2	1.04	5 59	29 9	12 0	12 1	1 06	4336	5444	105	52 5	123	554	671	161	18 5	5 03	10 8	8 02	4 03	3.67	0 50	18 4	22.7	280	2 68	836	12.1
LS121,3	0 89	4 31	23 6	12 0	11 4	0 93	4140	4915	95 1	49 8	93 1	511	623	140	*13 4	4 42	9 94	6 75	*2.27	4 35	*0 38	*16 5	*18 3	240	2 83	682	8 98
LS121,4	1 57	5 70	38 1	12 0	13 1	1 58	4960	5607	196	71 9	*195	842	765	194	19 0	6 15	13 1	10 0	3 63	5 22	1.08	27.8	24 6	547	3 97	772	15.7
LS121,5	1.48	5 66	43 4	12 0	12 6	1.78	4893	5436	198	74 6	180	624	779	194	25 2	6 76	16 2	11 2	4 78	*6 72	0 88	31 7	25 8	570	5 09	854	11.2
Average	1.29	5 51	34 7	12 0	12.1	1 36	4534	5300	153	63 6	137	591	720	174	20 9	5 68	12 5	9 08	4.35	4 59	0 83	25.4	24.1	412	3 75	810	11.8
STDS	0.31	0 73	7 90	0 00	0 71	0 36	368	284	50 0	11 6	37 5	56 2	69 2	23 1	3 03	0 94	2 40	1 74	0 62	0 73	0 24	5 71	1.38	150	1.01	86.2	2 46
RSD	24%	13%	23%	0%	6%	26%	8%	5%	33%	18%	27%	10%	10%	13%	15%	17%	19%	19%	14%	16%	30%	22%	8%	36%	27%	11%	21%

Note: italics indicate whole analyses rejected, asterixes (*) indicate individual elemental analysis rejected

Table A7 3 Trace (and major) element LAM-ICP-MS analyses of crystals in the experiments on the join HOL14/OL5 - Individual and average analyses, standard deviation (STDS) and relative standard deviation (RSD)

Comments	MgO wt %	Al2O3 wt %	SiO2 wt %	CaO wt %	CaO wt %	TiO2 wt %	Ba ppm	Sr ppm	Rb ppm	Y ppm	V ppm	La ppm	Ce ppm	Nd ppm	Sm ppm	Eu ppm	Gd ppm	Dy ppm	Er ppm	Yb ppm	Lu ppm	U ppm	Th ppm	Nb ppm	Ta ppm	Zr ppm	Hf ppm
CP1																											
Ne	0 03	30 9	33 9	<0 35	*0 14	0 01	n d	n d	80 4	n d	n d	<0 21	<0 18	n d	n d	n d	n d	n d	n d	<0 60	n d	n d	n d	<0.18	n d	<0.30	n d
Ne	0 04	30 9	30 7	<0 87	*0 17	0 02	n d	n d	77 6	n d	n d	*3 45	*4 57	n d	n d	n d	n d	n d	n d	<1 58	n d	n d	n d	1 83	n d	5 80	n d
Ne	<0 07	30 9	39 6	1 50	1 42	0 01	n d	n d	69 1	n d	n d	*3 55	*5 95	n d	n d	n d	n d	n d	n d	<2 25	n d	n d	n d	1 47	n d	7 54	n d
Average	0 04	30 9	34 7	1 50	1 42	0 01	n d	n d	75 7	n d	n d	n d	n d	n d	n d	n d	n d	n d.	n d	b d	n d	n d.	n d	1 65	n d	6 67	n d.
STDS	0 01	0 00	4 52	n d	n d	0 01			5 88															0 25		1 23	
RSD	20%	0%	13%	n d.	n d	43%			8%															15%		18%	
Mela	*<9 83*	*<6 99*	*<92 1*	*31.0*	*23 6*	*5 74*	*<17 8*	*<623*	*<17 1*	*248*	*1163*	*18 6*	*123*	*161*	*46 4*	*14 2*	*47 3*	*54 4*	*25 6*	*21 7*	*2 25*	*4 35*	*2 76*	*197*	*7 39*	*2024*	*39 5*
Mela	*<26 1*	*<18 1*	*<262*	*<59*	*58 2*	*6 40*	*103*	*<1763*	*<43 3*	*399*	*995*	*1237*	*3527*	*1570*	*247*	*51 9*	*89 4*	*57 9*	*31 4*	*30 7*	*2 66*	*141*	*277*	*2382*	*17 2*	*2251*	*25 0*
Mela	*<15 2*	*<11 2*	*<146*	*311*	*24 5*	*6 11*	*1033*	*1936*	*<38 6*	*265*	*701*	*135*	*352*	*145*	*27 6*	*12 5*	*55 7*	*66 9*	*36 0*	*18 6*	*2 81*	*8 04*	*12 7*	*315*	*5 20*	*2909*	*54 5*
Mela	*<14 2*	*12 1*	*<120*	*<32*	*31 7*	*9 68*	*1333*	*2451*	*62 4*	*256*	*347*	*215*	*429*	*188*	*55 1*	*28 8*	*44 6*	*25 3*	*27 5*	*12 9*	*1 28*	**12 0*	**19 2*	*668*	**17.3*	*4281*	*48 8*
Wo	0.15	0.20	50.7	47.4	46.1	0.04	n.d.	n.d.	n.d.	85.3	n.d.	74.6	188	n.d.	n.d.	n.d.	n.d.	n.d.	n.d.	5.32	n.d.	n.d.	n.d.	n.d.	n.d.	47.2	n.d.
Wo	*0 27*	*1 00*	*50 0*	*47.4*	*43 2*	*0 10*	*nd*	*nd*	*nd*	*95 3*	*nd*	*133*	*278*	*nd*	*nd*	*nd*	*nd*	*nd*	*nd*	*5 58*	*nd*	*nd*	*nd*	*nd*	*nd.*	*131*	*nd*
CP2																											
Ne	<1.50	31.0	38.3	<8.31	<3.86	<0.06	n.d.	n.d.	55.6	n.d.	n.d.	<0.65	<0.56	n.d.	n.d.	n.d.	n.d.	n.d.	n.d.	n.d.	n.d.	n.d.	n.d.	<2.07	n.d.	3.80	n.d.
Ne	*b d*	*31 0*	*51 5*	*b d*	*b d*	*0 48*	*b d*	*b d*	*55 2*	*b d*	*b d.*	*31 2*	*40 5*	*b d*	*b d*	*b d*	*b d.*	*b d*	*b d.*	*b d*	*b d*	*b d.*	*b d*	*64 5*	*b d.*	*256*	*b d.*
Ne	*b d*	*31 0*	*31 4*	*b d.*	*b d*	*0 11*	*b d*	*b d*	*56 6*	*b d*	*b d.*	*13 9*	*18 8*	*b d*	*b d*	*b d*	*b d.*	*b d*	*b d*	*b d*	*b d*	*b d.*	*b d*	*21 1*	*b d.*	*105*	*b d.*
Ne	*<1 81*	*31 0*	*38 8*	*<10 2*	*<3 68*	*0 16*	*nd*	*nd*	*141*	*nd*	*nd*	*48 9*	*69 6*	*nd*	*n d*	*nd*	*nd*	*nd*	*nd*	*nd*	*n d.*	*n d.*	*n d.*	*68 8*	*n d.*	*381*	*n d.*
Cpx	9 27	1 17	53 0	21.0	20 7	0 50	n d	n d	n d	1 95	n d	4.11	10 4	n d	n d	n d.	n d	n d	n d.	1.08	n d.	n d	n d	n d.	n d.	289	n d
Cpx	10 3	1 68	100	<23 2	30 3	1.25	n d	n d	n d	<3 00	n d	9 19	15 9	n d	n d	n d	n d	n d	n d.	<5.72	n d	n d.	n d	n d.	n d.	*954	n d.
Cpx	*6 65*	*1 59*	*50 9*	*21.0*	*21 1*	*1.05*	*n d*	*n d*	*n d*	*8 87*	*n d*	*16 6*	*29 9*	*n d*	*n d*	*n d*	*n d.*	*n d*	*n d.*	*1.70*	*n d*	*n d.*	*n d.*	*n d.*	*n d.*	*600*	*n d.*
Cpx	*8 13*	*2.53*	*74.7*	*21.0*	*19 3*	*0.76*	*n d*	*n d*	*n d*	*7 52*	*n d*	*16 4*	*24 6*	*n d*	*n d*	*n d*	*n d.*	*n d*	*n d.*	**8 17*	*n d*	*n d.*	*n d.*	*n d.*	*n d.*	*554*	*n d.*
Cpx	*6 52*	*14 0*	*62 3*	*21 0*	*12 8*	*1 17*	*n d*	*n d*	*n d*	*46 8*	*n d*	*159*	*199*	*n d*	*n d*	*n d*	*n d*	*n d*	*n d.*	*<5 30*	*n d*	*n d.*	*n d.*	*n d*	*n d.*	*1460*	*n d.*
Cpx	*8 47*	*23 2*	*102*	*<28 5*	*23 7*	*1 13*	*n d*	*n d*	*n d*	*48 9*	*n d*	*172*	*241*	*n d*	*n d*	*n d*	*n d*	*n d*	*n d.*	*<9 43*	*n d*	*n d.*	*n d.*	*n d.*	*n d.*	*1760*	*n d.*
Cpx	*<6 63*	*28 9*	*144*	*<57 3*	*26 7*	*2 27*	*n d*	*n d*	*n d*	*70 9*	*n d.*	*310*	*401*	*n d*	*n d*	*n d*	*n d*	*n d*	*n d.*	*12 7*	*n d*	*n d*	*n d.*	*n d.*	*n d.*	*3430*	*n d.*
Average first 2	9 78	1.43	76 32	21.0	25 5	0 88	n d	n d	n d	1.95	n d	6 65	13 1	n d	n d	n d	n d	n d	n d	1 08	n d	n d	n d	n d.	n d.	289	n d
STDS	0 72	0 36	33 02	n d	6 75	0 53				n d		3 59	3 90							n d						n d.	
RSD	7%	25%	43%	n d	27%	61%				n d		54%	30%							n d						n d	
Mela	*b d*	*4 52*	*35 6*	*31 8*	*26 2*	*9 94*	**655*	**1065*	*21 0.*	*250*	*663*	**82.0*	**270*	**314*	*77 6*	*27 9*	*72 9*	*64 1*	*25 6*	*29.2*	*1 90*	*10 6*	*17 6*	*809*	**38.1*	*2991*	*54 3*
Mela	*b d*	*0 85*	*30 0*	*31 8*	*41 0*	*11 0*	*b d*	*b d*	*b d*	*404*	*1447*	*30 7*	*177*	*216*	*74 1*	*26 8*	*81 6*	*83 0*	*46 5*	*22 2*	*4 49*	**15 4*	**34.7*	*698*	*9 43*	*3123*	*49 2*
Mela	b d	1 44	30 3	31 8	38 2	8 95	11 6	b d	b d	531	1952	11 9	91 2	155	47 5	30 6	105	110	48 2	47 3	3 92	3 41	2 24	163	6.05	3108	44 6
Mela	b d	1 06	36 4	31 8	35 6	12 3	b d	b d	b d	412	1206	21 5	123	137	41 5	23 6	69 3	81 8	43 5	30 2	4.26	3 84	3 40	*303	*14.9	3828	73.1
Mela	b d	1 46	27 0	31 8	37.4	11 0	b d	b d	b d	553	1390	13 1	112	110	67.3	25 9	78 2	123	56.1	47.5	3.98	5 30	b d.	226	8.46	4040	110
Mela	b d	1 48	24 9	31 8	36 5	10 6	4 78	b d	b d	565	1208	18 2	99 0	168	83 5	32 9	123	125	79 4	67.7	5 36	*4 22	*6 02	204	8.61	3241	64 6
Mela	1 08	1 34	29 6	31 8	31 7	13 6	b d	b d	b d	595	1135	20 2	127	150	71 0	31 8	111	139	77 1	63 7	8 39	*7.80	*2 99	299	9.25	4412	113
Mela	0 58	2.02	29 3	31 8	nd	7 25	*70 6	<1940	<16 5	384	1123	20 3	95 1	102	50 5	16 6	54 9	57 6	47.8	40 4	3 11	4.25	2 94	201	6.88	3192	84 4
Mela	0 46	2 84	31 1	31 8	nd	8 14	*103	<969	9 63	437	1573	19 9	87 3	137	49 9	21 6	75 2	79 4	38 5	48 0	4.74	4 98	1.92	157	4.61	2725	58.2
Mela	0 43	2 95	30 4	31 8	nd	9 03	*197	<760	8 73	399	1195	22 1	120	94 3	57 2	24 4	77 6	82 7	54 3	22 9	3 25	4 51	3 34	258	6.31	3038	59 1
Average last 8	0 64	1 82	29 9	31 8	35 9	10 1	8 19	b d	9 28	482	1347	18 4	107	132	58 5	26 0	86 6	99 8	55 6	46 0	4 63	4 38	2 77	215	7.17	3446	75.8
STDS	0 30	0 71	3 36	0 00	2.54	2 15	4 82	n d	0 78	88 5	287	3 85	15 6	26 8	14 2	5 54	23 6	28 3	15.1	15 1	1 69	0 70	0 66	50 5	1 61	578	24.7
RSD	46%	39%	11%	0%	7%	21%	59%	n d	8%	18%	21%	21%	15%	20%	24%	21%	27%	28%	27%	33%	36%	16%	24%	23%	22%	17%	33%
CP5																											
Ne	<16 2	31 1	<124	<35 0	<13 3	<0 38	n d	n d	65 3	n d	n d	<1 35	<1 40	n d	n d	n d	n d	n d	n d	<5 26	n d	n d	n d	<5 05	n d	<11.7	n d
Ne	<11 1	31 1	<68	<19 9	<10 2	<0 17	n d	n d	44 8	n d	n d	*4 47	*4 54	n d	n d	n d	n d	n d	n d	<2 91	n d	n d	n d	*5 26	n d	*21.6	n d
Ne	<11 6	31 1	<79	<21.1	<9 19	<0 13	n d	n d	53 4	n d	n d	<0 46	0 77	n d	n d	n d	n d	n d	n d	<3.58	n d	n d	n d	<1.94	n d	<5 11	n d
Ne	<25 9	*31 1*	*<166*	*<46 7*	*<18 1*	*0 62*	*nd*	*nd*	*212*	*nd*	*nd*	*25 5*	*33 7*	*nd*	*nd*	*nd*	*nd*	*nd*	*nd*	*<2 30*	*nd*	*nd*	*nd*	*49 3*	*nd*	*234*	*nd*
Average first 3	b d	31 1	b d	b d	b d	b d	n d	n d	54 5	n d	n d	n d	0 77	n d	n d	n d	n d	n d	n d	b d	n d	n d	n d	n d.	n d	b d	n d
STDS		0 00							10 4				n d														
RSD		0%							19%				n d														

Comments	MgO	Al2O3	SiO2	CaO	CaO	TiO2	Ba	Sr	Rb	Y	V	La	Ce	Nd	Sm	Eu	Gd	Dy	Er	Yb	Lu	U	Th	Nb	Ta	Zr	Hf
Cpx	12.0	<4.10	<93.0	<26.3	20.7	1.29	n.d.	n.d.	n.d.	<4.42	n.d.	7.15	18.3	n.d.	n.d.	n.d.	n.d	n.d.	n.d.	<4.27	n.d.	n.d.	n.d.	n.d.	n.d.	363	n.d.
Cpx	*<12.7*	*13.3*	*<99.2*	*<32.5*	*20.7*	*1.03*	*nd*	*nd*	*nd*	*4.42*	*nd*	*1.71*	*22.4*	*nd*	*nd*	*nd*	*nd*	*nd*	*nd*	*<3.11*	*nd*	*nd*	*nd*	*nd*	*nd*	*1155*	*nd*
Cpx	*<9.35*	*<4.13*	*<67.0*	*<23.7*	*20.7*	*0.65*	*nd*	*nd*	*nd*	*5.95*	*nd*	*4.96*	*7.90*	*nd*	*nd*	*nd*	*nd*	*nd*	*nd*	*b.d*	*nd*	*nd*	*nd*	*nd*	*nd*	*427*	*n.d*
Cpx	*13.9*	*<5.05*	*<84.9*	*27.4*	*20.7*	*0.55*	*nd*	*nd*	*nd*	*<4.04*	*nd*	*4.39*	*"2.68*	*nd*	*nd*	*nd*	*nd*	*nd*	*nd*	*<5.69*	*nd*	*nd*	*nd*	*nd*	*nd*	*242*	*nd*
Cpx	*<8.43*	*<4.23*	*<70.5*	*24.8*	*20.7*	*0.55*	*nd*	*nd*	*nd*	*8.56*	*nd*	*2.69*	*3.96*	*nd*	*nd*	*nd*	*nd*	*nd*	*nd*	*4.62*	*nd*	*nd*	*nd*	*nd*	*nd*	*419*	*n.d*
Cpx	*<12.5*	*7.79*	*<82.8*	*<28.7*	*20.7*	*0.72*	*nd*	*nd*	*nd*	*"19.2*	*nd*	*7.22*	*"110*	*nd*	*nd*	*nd*	*nd*	*nd*	*nd*	*<3.99*	*nd*	*nd*	*nd*	*nd*	*nd*	*760*	*n.d.*
Cpx	*<11.2*	*4.95*	*<69.1*	*<28.7*	*20.7*	*0.66*	*nd*	*nd*	*nd*	*11.9*	*nd*	*4.82*	*5.05*	*nd*	*nd*	*nd*	*nd*	*nd*	*nd.*	*<3.96*	*nd*	*nd*	*nd*	*nd*	*nd.*	*531*	*nd*
Cpx	*<12.1*	*11.0*	*<109*	*<34.1*	*20.7*	*0.93*	*nd*	*nd*	*nd*	*11.4*	*nd*	*6.33*	*9.47*	*nd*	*nd*	*nd*	*nd*	*nd*	*nd*	*<4.94*	*nd*	*nd*	*nd*	*nd*	*nd*	*662*	*nd*
CP7																											
Ne	<0.03	32.0	34.9	<0.82	0.16	b.d	nd	nd	79.2	nd	nd	<0.33	<0.26	nd	nd	nd	nd	nd	nd	<1.38	nd	nd	nd	<0.38	nd	<0.75	n.d
Ne	0.04	32.0	39.4	<0.84	0.16	0.01	nd	nd	80.4	nd	nd	1.03	2.71	nd	nd	nd	nd	nd	nd	<1.27	nd	nd	nd	2.18	nd	4.72	nd
Ne	<0.06	32.0	37.5	<1.50	<0.20	<0.00	nd	nd	86.2	nd	nd	1.69	1.11	nd	nd	nd	nd	nd	nd	<3.76	nd	nd	nd	<0.61	nd	5.53	nd
Ne	0.06	32.0	34.8	<1.00	0.18	0.01	nd	nd	75.7	nd	nd	1.67	1.17	nd	nd	nd	nd	nd	nd	<1.17	nd	nd	nd	<0.29	nd	1.07	nd
Ne	<0.03	32.0	36.1	<0.66	0.23	0.01	nd	nd	74.8	nd	nd	<0.27	<0.19	nd	nd	nd	nd	nd	nd	<1.50	nd	nd	nd	<0.27	nd	<0.41	nd
Ne	0.10	32.0	36.2	0.53	0.45	0.02	nd	nd	76.3	nd	nd	0.43	0.93	nd	nd	nd	nd	nd	nd	<0.79	nd	nd	nd	0.33	nd.	5.85	nd
Ne	<0.06	32.0	40.5	<2.01	<0.19	<0.01	nd	nd	99.8	nd	nd	<0.43	<0.46	nd	nd	nd	nd	nd	nd.	<3.95	nd.	nd	nd	<0.61	nd.	<1.25	n.d.
Ne	<0.28	32.0	40.1	<4.17	nd	<0.02	<13.24	<945	80.2	<1.55	<10.2	<0.71	b.d	<6.39	<1.85	<1.28	<2.48	<1.92	<3.58	<1.70	0.12	<0.70	<0.86	<1.47	<0.89	2.74	0.65
Ne	*0.68*	*32.0*	*41.0*	*<8.39*	*nd*	*2.38*	*818.45*	*<2736*	*102*	*20.8*	*171*	*28.0*	*54.0*	*15.9*	*<9.14*	*<3.24*	*9.23*	*5.38*	*<4.39*	*<7.34*	*<1.77*	*3.44*	*5.71*	*77.1*	*<0.66*	*414*	*<8.61*
Average first 8	0.07	32.0	37.4	0.53	0.24	0.01	nd	nd	81.8	nd	nd	1.21	1.48	nd	nd	nd	nd	nd	nd	b.d	0.12	nd	nd	1.26	nd	3.94	0.65
STDS	0.03	0.00	2.29	nd	0.12	0.01			8.06			0.60	0.83								nd			1.31		1.98	nd
RSD	48%	0%	6%	nd	50%	40%			10%			50%	56%								nd			104%		50%	n.d
Cpx	13.2	<4.74	<56.6	20.6	21.2	0.28	nd	nd	nd	<1.40	nd	4.16	11.0	nd	nd	nd	nd	nd	nd	<4.60	nd	nd	nd	nd	n.d.	130	n.d.
Cpx	10.2	<2.37	34.2	21.0	21.2	0.53	nd	nd	nd	3.09	nd	6.94	15.2	nd	nd	nd	nd	nd	nd	1.60	nd	nd	nd	n.d.	n.d.	282	n.d.
Cpx	12.4	<5.42	<63.6	21.1	21.2	0.45	nd	nd	nd	2.90	nd	6.11	18.0	nd	nd	nd	nd	nd	nd	<1.30	nd	nd	n.d.	nd	n.d.	237	n.d.
Cpx	9.40	1.00	48.9	21.2	n.d	0.40	<28.1	<1263	<13.0	<3.56	206	3.78	6.60	<11.1	<2.90	<1.67	<3.06	<3.45	<3.80	<4.56	<0.77	<1.09	<1.35	<1.49	<0.41	173	<3.46
Cpx	9.76	1.11	47.0	21.2	nd	0.46	<30.0	<1592	<12.9	3.57	188	8.63	16.6	<8.58	<6.33	<1.18	<3.82	2.23	<4.61	<5.12	0.57	<0.94	<1.33	<2.80	<0.40	233	7.70
Cpx	10.7	1.14	52.8	21.2	n.d.	0.43	9.21	557	<3.93	3.40	237	6.74	20.3	11.59	<2.28	0.54	1.50	<0.93	0.78	<1.11	<0.26	0.32	<0.40	4.51	<0.19	295	4.99
Cpx	*13.2*	*<7.42*	*<87.5*	*22.0*	*21.2*	*0.72*	*nd*	*nd*	*nd*	*7.76*	*nd*	*3.82*	*4.80*	*nd*	*nd*	*nd*	*nd*	*nd.*	*nd.*	*4.03*	*nd*	*nd*	*nd*	*nd.*	*nd.*	*"810*	*nd.*
Cpx	*<15.0*	*<10.6*	*<110*	*<23.8*	*21.2*	*0.43*	*nd*	*nd*	*nd*	*12.3*	*nd.*	*6.37*	*7.78*	*nd*	*nd*	*nd*	*nd*	*nd*	*nd*	*<2.32*	*nd.*	*nd*	*nd*	*nd.*	*nd.*	*471*	*n.d.*
Cpx	*<9.89*	*<7.24*	*<73.0*	*27.2*	*21.2*	*0.84*	*nd*	*nd*	*nd*	*39.2*	*nd*	*"317*	*"370*	*nd*	*nd*	*nd*	*nd*	*nd.*	*nd.*	*<1.97*	*nd.*	*nd.*	*nd*	*n.d.*	*n.d.*	*974*	*n.d.*
Cpx	*<9.21*	*<5.41*	*<69.9*	*17.3*	*21.2*	*0.97*	*nd*	*nd*	*nd*	*25.0*	*nd*	*"216*	*"293*	*nd*	*nd*	*nd*	*nd*	*nd.*	*nd.*	*1.57*	*nd*	*nd*	*nd*	*nd.*	*nd.*	*475*	*n.d.*
Cpx	*11.8*	*4.39*	*84.3*	*21.2*	*nd*	*1.69*	*1477*	*<2314*	*57.1*	*24.4*	*640*	*88.9*	*169*	*28.53*	*5.34*	*4.82*	*<4.63*	*4.82*	*<5.01*	*9.02*	*0.43*	*6.77*	*20.13*	*287*	*2.87*	*795*	*15.8*
Average without last	11.0	1.08	45.7	21.1	21.2	0.43	9.21	557	nd	3.24	210	6.06	15.0	11.6	nd	0.54	1.50	2.23	0.78	1.60	0.57	0.32	nd	4.51	nd.	225	6.95
STDS	1.52	0.07	6.07	0.15	0.00	0.08	nd	nd		0.30	24.9	1.82	4.39	nd		nd	nd	nd	nd	n.d.	nd	nd		nd		63.3	1.92
RSD	14%	7%	18%	1%	0%	20%	nd	nd		9%	12%	30%	29%	nd		nd	nd	nd	nd	n.d	nd	nd		nd		28%	30%
Mela	*<19.4*	*<14.4*	*<184*	*<45.1*	*35.9*	*12.6*	*"336*	*<1291*	*<46.6*	*397*	*919*	*33.4*	*136*	*105*	*33.3*	*26.2*	*74.4*	*77.1*	*36.5*	*24.6*	*6.12*	*11.0*	*9.79*	*320*	*7.37*	*3201*	*59.9*
Mela	*<11.7*	*<6.62*	*<102*	*32.0*	*28.2*	*10.1*	*<10.9*	*<749*	*<20.6*	*695*	*1199*	*29.0*	*186*	*336*	*143*	*41.3*	*133*	*144*	*102*	*46.4*	*8.42*	*5.15*	*4.70*	*252*	*13.9*	*4310*	*47.7*
Mela	*<13.8*	*<8.73*	*<106*	*32.0*	*"48.6*	*12.1*	*14.6*	*<983*	*<26.2*	*501*	*1656*	*37.7*	*264*	*313*	*128*	*54.0*	*126*	*88.6*	*39.9*	*34.3*	*6.62*	*6.38*	*11.6*	*343*	*7.67*	*3323*	*44.0*
Mela	*<10.6*	*<6.17*	*<162*	*32.0*	*36.0*	*11.1*	*"140*	*<741*	*<32.4*	*347*	*639*	*48.4*	*305*	*376*	*119*	*36.3*	*107*	*62.6*	*39.7*	*17.9*	*5.42*	*7.57*	*18.0*	*462*	*30.1*	*3428*	*65.5*
Mela	*<13.7*	*<7.52*	*<119*	*32.0*	*25.4*	*10.6*	*19.1*	*<794*	*<26.2*	*564*	*1184*	*20.8*	*187*	*265*	*86.2*	*48.5*	*127*	*120*	*60.1*	*44.9*	*6.68*	*13.3*	*12.4*	*879*	*17.5*	*3434*	*42.4*
Mela	*0.51*	*1.51*	*31.1*	*32.0*	*nd*	*10.6*	*<11.7*	*<863*	*<7.5*	*633*	*1208*	*25.8*	*141*	*211*	*75.0*	*39.5*	*110*	*108*	*63.7*	*47.5*	*5.86*	*6.65*	*5.23*	*355*	*13.1*	*3199*	*52.7*
Average last 5	0.51	1.51	31.1	32.0	29.9	10.9	16.8	bd	bd	548	1177	32.3	217	300	110	43.9	121	105	61.0	38.2	6.64	8.21	10.4	458	16.5	3539	50.5
STDS	nd	nd	nd	0.00	5.52	0.72	3.13			134	361	10.9	66.7	64.0	28.5	7.18	11.7	30.9	25.3	12.5	1.15	3.08	5.55	247	8.37	441	9.27
RSD	nd	nd	nd	0%	18%	7%	19%			24%	31%	34%	31%	21%	26%	16%	10%	30%	41%	33%	17%	38%	53%	54%	51%	12%	18%
CP8																											
Ne	<0.04	31.6	30.8	<0.92	0.13	0.01	nd	nd	71.01	nd	nd	<0.30	<0.27	nd	nd	nd	nd	nd	nd	<1.80	nd	nd	nd	<0.26	nd	<0.74	nd
Cpx	*<22.2*	*<14.2*	*<151*	*<30.9*	*20.9*	*0.95*	*nd*	*nd*	*nd*	*37.4*	*nd*	*4.88*	*6.28*	*nd*	*nd*	*nd*	*nd*	*nd*	*nd*	*7.05*	*nd*	*nd*	*nd*	*nd*	*nd*	*1036*	*nd*
Cpx	20.0	<13.6	<196	"58.7	<8.17	2.01	nd	nd	nd	13.7	nd	11.4	28.7	nd	nd	nd	nd	nd	nd	<4.76	nd	nd	nd	nd	nd	"980	nd
Cpx	<18.1	<12.6	<139	<27.7	20.9	0.87	nd	nd	nd	14.8	nd	"54.1	"80.0	nd	nd	nd	nd	nd	nd	<2.87	nd	nd	nd	nd	nd	476	nd
Cpx	<35.4	<19.0	<229	<47.6	20.9	0.85	nd	nd	nd	<7.80	nd	4.16	21.7	nd	nd	nd	nd	nd	nd	<4.07	nd	nd	nd	nd	nd	490	nd
Cpx	<106	<76.7	<850	<146	<64.6	<2.03	nd	nd	nd	<34.5	nd	<7.18	<4.71	nd	nd	nd	nd	nd	nd	<21.5	nd	nd	nd	nd	nd	<66.2	nd
Average last 4	20.0	bd	bd	bd	20.9	1.24	nd	nd	nd	14.3	nd	7.77	25.2	nd	nd	nd	nd	nd	nd	b.d	nd	nd	nd	nd	nd	483	nd
STDS	nd				0.00					0.77		5.10	4.95													9.81	
RSD	nd				0%					5%		66%	20%													2%	
Mela	<18.1	<8.64	<161	<36.4	40.0	13.5	<16.40	<999	<29.1	403	"3735	17.4	96.9	133	42.9	32.4	90.3	99.1	59.4	30.8	"7.17	<1.14	<2.11	208	3.74	2874	86.0

Comments	MgO	Al2O3	SiO2	CaO	CaO	TiO2	Ba	Sr	Rb	Y	V	La	Ce	Nd	Sm	Eu	Gd	Dy	Er	Yb	Lu	U	Th	Nb	Ta	Zr	Hf
Mela	<15 1	<7 75	<100	31 4	31 8	9 92	*449	<743	<34 9	316	943	23 3	120	*69 9	58 4	30 2	54 3	63 5	25 6	*16 4	3 16	6 84	2 50	583	9 65	2668	48 1
Mela	<13 0	10 5	<83	31 4	22 1	7 77	*368	<804	*65 4	231	677	40 8	124	*59 9	*29 1	11 8	45 9	39 5	28 5	*12 3	*1 82	7 83	7 23	555	7 58	1874	23 0
Mela	<12 5	<8 88	<110	31 4	45 0	10 8	*261	<828	<26 2	460	1680	32 7	137	170	54 4	19 8	84 4	102	40 9	25 8	4 14	7 31	7 59	548	6 20	3753	86 8
Average	bd	10 5	bd	31 4	34 7	10 5	nd	bd	bd	352	1100	28 5	119	151	51 9	23 8	68 7	76 1	38 6	28 3	3 65	7 33	5 77	468	6 79	2792	56 0
STDS		n d		0 00	10 0	2 38				100	520	10 3	16 9	26 3	8 05	9 56	21 9	30 0	15 4	3 53	0 69	0 50	2 84	173	2 48	772	27 0
RSD		n d		0%	29%	23%				28%	47%	36%	14%	17%	18%	41%	32%	39%	40%	12%	19%	7%	49%	37%	37%	28%	48%
CP10																											
Ne	<1 96	31 2	31 9	<5 66	<2 02	<0 03	n d	n d	n d	<0 87	n d	<0 23	<0 09	n d	n d	n d	n d	n d	n d	<1 11	n d	n d	n d	n d	n d	<1 16	n d
Ne	<13 1	31 2	<81 6	<30 1	<9 95	<0 22	n d	n d	60 0	n d	n d	<0 96	<1 10	n d	n d	n d	n d	n d	n d	<2 21	n d	n d	n d	<1 88	n d	<9 53	n d
Ne	<13 3	31 2	<76 1	<26 2	<9 07	<0 15	n d	n d	66 6	n d	n d	<1 02	<0 44	n d	n d	n d	n d	n d	n d	bd	n d	n d	n d	<2 89	n d	<5 79	n d
Ne	<7 04	31 2	<43 3	<13 3	<5 33	<0 09	n d	n d	82 7	n d	n d	<0 36	<0 37	n d	n d	n d	n d	n d	n d	<1 52	n d	n d	n d	<1 05	n d	<2 45	n d
Ne	<9 04	31 2	<65 5	<21 2	<7 85	<0 10	n d	n d	56 0	n d	n d	bd	<0 50	n d	n d	n d	n d	n d	n d	<2 05	n d	n d	n d	<2 21	n d	<4 70	n d
Ne	<6 52	31 2	<45 9	<12 6	<5 84	<0 03	n d	n d	74 2	n d	n d	<0 38	<0 29	n d	n d	n d	n d	n d	n d	<1 14	n d	n d	n d	<1 07	n d	<3 65	n d
Ne	<12 4	31 2	<80 6	<24 8	<9 31	<0 21	n d	n d	64 2	n d	n d	<0 82	<0 68	n d	n d	n d	n d	n d	n d	<1 46	n d	n d	n d	<3 66	n d	<7 39	n d
Average	bd	31 2	31 9	bd	bd	bd	n d	n d	67 3	n d	n d	bd	bd	n d	n d	n d	n d	n d	n d	bd.	n d	n d	n d	bd	n d	b.d.	n d
STDS		0 00	n d						9 76																		
RSD		0%	n d						15%																		
Cpx	6 12	<1 83	*63 6	22 1	21 2	0 91	n d	n d	n d	10 3	n d	13 6	21 2	n d	n d	n d	n d	n d	n d	<1.76	n d	n d	n d	n d	n d	*1084	n d
Cpx	<9 72	<4 03	<67 6	<29 7	21 2	1 17	n d	n d	n d	<4 60	n d	13 6	28 6	n d	n d	n d	n d	n d	n d.	<5 16	n d	n d.	n d	n d	n d	504	n d
Cpx	*8 49*	*3 83*	*39 54*	*22 6*	*21 2*	*0 87*	*n d*	*n d*	*n d*	*6 25*	*n d*	*82 3*	*530*	*n d*	*n d*	*n d*	*n d*	*n d*	*n d.*	*<1.42*	*n d*	*n d*	*n d*	*n d*	*n d*	*589*	*n d.*
Cpx	*<4 05*	*6 54*	*34 88*	*21 0*	*21 2*	*0 71*	*n d*	*n d*	*n d*	*19 8*	*n d*	*389*	*494*	*n d*	*n d.*	*n d*	*n d*	*n d*	*n d*	*1 85*	*n d*	*n d*	*n d*	*n d*	*n d.*	*387*	*n d.*
Cpx	*<8 11*	**20 6*	*<55 3*	*25 7*	*21 2*	*0 66*	*n d*	*n d*	**49 1*	*n d*	*384*	*491*	*n d*	*n d*	*n d*	*n d*	*n d*	*n d*	*<3 73*	*n d*	*n d*	*n d*	*n d*	*n d*	*549*	*n d.*
Cpx	*<4 53*	*<1 86*	*<35 5*	*20 4*	*21 2*	*0 36*	*n d*	*n d*	*n d*	*28 1*	*n d*	*115*	*200*	*n d*	*n d*	*n d*	*n d*	*n d*	*n d*	*<2.27*	*n d*	*n d.*	*n d.*	*n d*	*n d*	*172*	*n d*
Average first 2	6 12	bd	nd	22 1	21 2	1 04	nd	nd	nd	10 3	nd	13 7	24 9	nd	nd	nd	nd	nd	n d	bd.	nd	nd	nd	nd	n d	504	n d
STDS	nd			nd	0 00	0 18				nd		0 16	5 26													n d.	
RSD	nd			nd	0%	18%				nd		1%	21%													n d.	
Mela	*bd*	*1.50*	*32 1*	*31 7*	*31 2*	*14 4*	*bd*	*bd*	*bd*	*769*	*860*	*41 0*	*225*	*312*	*129*	*51 9*	*150*	*165*	*80 6*	*52 7*	*8 49*	*6 98*	*7.51*	*246*	*16 9*	*5346*	*108*
Mela	bd	bd	bd	31 7	31 3	11 9	bd	bd	bd	606	1194	50 3	263	379	148	34 3	135	145	55 9	32 3	4.17	12 4	9 32	457	22 2	4646	63.1
Mela	0 66	1 32	29 9	31 7	nd	12 1	*324	584	12 0	548	998	66 5	248	297	115	41 6	126	120	59 2	39 9	5 61	9 07	12 5	531	31 6	4302	83.4
Average without first	0 66	1.32	29 9	31 7	31 3	12 0	nd	584	12 0	577	1096	58 4	255	338	132	37 9	130	133	57.5	36.1	4 89	10.75	10 93	494	26 9	4474	73.2
STDS	nd	n.d	nd	0 00	nd	0 06		nd	nd	41 1	139	11 4	11 0	58 1	23 2	5 14	6 58	17 4	2 33	5 32	1 02	2 38	2 27	52 4	6 68	243	14.3
RSD	nd	nd	nd	0%	nd	1%		nd	nd	7%	13%	20%	4%	17%	18%	14%	5%	13%	4%	15%	21%	22%	21%	11%	25%	5%	20%
CP11																											
Cpx	5 14	1.24	40 0	20 9	17 0	0 46	n d	n d	n d	4 77	n d	2 20	9 73	n d.	n d	n d	n d	n d	n d	<1.77	n d	n d	n d	n d	n d	614	n d
Cpx	4 72	<1.45	49 9	<22 4	16 3	0 57	n d	n d	n d	<3 46	n d	<1 43	5 94	n d	n d	n d	n d	n d	n d	<6 99	n d	n d	n d	n d	n d	344	n d.
Cpx	6 87	1 07	48 6	20 9	16 9	0 64	n d	n d	n d	<2 20	n d	1 63	8 52	n d	n d	n d	n d	n d	n d	<3 05	n d.	n d	n d.	n d	n d	288	n d
Cpx	*7 20*	*5 28*	*67 7*	*20 9*	*19 4*	*0 75*	*n d*	*n d*	*n d*	*19 6*	*n d*	*51 8*	*70 8*	*n d*	*n d*	*n d*	*n d*	*n d*	*n d*	*2 24*	*n d.*	*n d*	*n d*	*n d*	*n d*	*689*	*n d*
Cpx	*4 41*	*5 34*	*37 6*	*20 9*	*17 9*	*2 18*	*n d*	*n d*	*n d*	*65 7*	*n d*	**247*	**359*	*n d*	*n d*	*n d*	*n d*	*n d*	*n d*	*8 18*	*n d.*	*n d.*	*n d*	*n d*	*n d*	*839*	*n d.*
Cpx	*7 58*	*3 06*	*59 8*	*20 9*	*18 1*	*0 74*	*n d*	*n d*	*n d*	*10 7*	*n d*	*45 1*	*54 9*	*n d*	*n d*	*n d*	*n d*	*n d*	*n d*	*<5 71*	*n d*	*n d*	*n d*	*n d*	*n d*	*873*	*n d.*
Cpx	*5 08*	**12 8*	**109*	*20 9*	*19 3*	*2 18*	*n d*	*n d*	*n d*	*42 7*	*n d*	**248*	**284*	*n d*	*n d*	*n d*	*n d*	*n d*	*n d*	*3 51*	*n d*	*n d*	*n d*	*n d*	*n d*	**1488*	*n d.*
Cpx	*5 92*	*7 04*	*72 9*	*<25 6*	*20 4*	*0 99*	*n d*	*n d*	*n d*	*25 6*	*n d*	*74 3*	*63 6*	*n d*	*n d*	*n d*	*n d*	*n d*	*n d*	*9 59*	*n d.*	*n d*	*n d*	*n d*	*n d*	*670*	*n d.*
Cpx	*5 98*	*3 39*	*58 9*	*20 9*	*17 5*	*0 83*	*n d*	*n d*	*n d*	*16 7*	*n d*	*38 2*	*51 4*	*n d*	*n d*	*n d*	*n d*	*n d*	*n d*	*4 73*	*n d*	*n d*	*n d*	*n d*	*n d*	*583*	*n d*
Average first 3	6 24	1 16	48 3	20 9	17 4	0 56	nd	nd	nd	4 77	nd	1 92	6 06	nd	nd	nd	nd	nd	nd	bd	nd	nd	nd	nd	nd	408	n d
STDS	2 28	0 12	5 44	0 00	1 39	0 09				nd		0 40	1 94													182	
RSD	37%	10%	12%	0%	8%	16%				nd		21%	24%													45%	
Mela	<1.28	0 85	31 6	32 0	31 7	7 73	107	458	<6 91	331	*2886	*7 76	*62 8	114	54 8	24 2	79 4	72 6	*21 5	19 4	5 05	4 11	<1 13	183	4 85	*1972	*18 3
Mela	<1.18	1 13	25 6	32 0	27 5	8.45	62 0	<238	<8 13	497	1421	19 4	90 6	129	52 4	20 9	77 8	116	71.2	66.1	6 54	7 56	2 06	203	6 20	3140	75 6
Mela	1 09	0 97	31 0	32 0	33 4	10 5	<8 13	<263	<8 04	383	1580	17 5	85 2	120	48 7	22 3	68 1	76 6	45 6	30 9	4 70	2 59	1 33	131	3 60	2971	66 0
Mela	*<17 1*	*<10 6*	*<242*	*<144*	*nd*	*6 40*	*6643*	*53833*	*<421*	*273*	*1045*	*431*	*723*	*632*	*<174*	*18 0*	*<78 5*	*<123*	*<85 4*	*<85 1*	*<34 7*	*36 2*	*76.5*	*393*	*<21.7*	*2514*	*263*
Average first 3	1 09	0 98	29 5	32 0	30 8	8 86	84 4	458	bd	404	1501	18 5	88 0	121	51 9	22 5	75 1	88 5	58 4	38 8	5 43	4 75	1 70	172	4 95	3055	71.9
STDS	nd	0 14	3 19	0 00	3 05	1 42	31 7	nd		85 1	112	1 31	3 94	7 33	3 08	1 64	6 11	24 1	18 0	24 3	0 98	2 55	0 52	37 5	1 20	120	5 54
RSD	nd	14%	11%	0%	10%	16%	38%	nd		21%	7%	7%	4%	6%	6%	7%	8%	27%	31%	63%	18%	54%	30%	22%	24%	4%	8%
Titanite	<1 81	4 48	61 7	32 0	28 1	30 2	809	2446	82 8	100	640	312	694	342	58 9	21 1	57 2	34 3	8 92	3 98	<0 78	24.3	7 29	2409	71.3	2757	64 0
Wo	<5 78	<1 81	66 2	46 5	56 2	0 26	n d	n d	n d	122	n d	76 4	126	n d	n d	n d	n d	n d	n d	16 2	n d	n d	n d	n d	n d	79 1	n d

Comments	MgO	Al2O3	SiO2	CaO	CaO	TiO2	Ba	Sr	Rb	Y	V	La	Ce	Nd	Sm	Eu	Gd	Dy	Er	Yb	Lu	U	Th	Nb	Ta	Zr	Hf
CP13																											
Ne	bd	31 9	bd	bd	bd	bd	bd	bd	59 0	bd	bd	bd	bd	bd	bd	bd	bd	bd	bd	bd	bd.	bd	bd	bd	bd	bd	bd.
Ne	bd	31 9	bd	bd	bd	bd	bd	bd	66 1	bd	bd	bd	bd	bd	bd	bd	bd	bd	bd	bd	bd	bd	bd	bd	bd	bd	bd
Ne	bd	31 9	bd	bd	bd	bd	bd	bd	78 5	bd	bd	bd	bd	bd	bd	bd	bd	bd	bd	bd	bd	bd	bd	bd	bd	bd.	bd.
Average	bd	31 9	bd	bd	bd	bd	bd	bd	67 9	bd	bd	bd	bd	bd	bd	bd	bd	bd	bd	bd	bd	bd	bd	bd	bd	bd	bd
STDS		0 00							9 87																		
RSD		0%							15%																		
CP14																											
Ne	<0.63	30.3	45.5	<7.00	<2.15	<0.07	n.d.	n.d.	67.4	n.d.	n.d	3.72	*10.2	n.d.	n.d.	n.d.	n.d.	n.d.	n.d.	<5.75	n.d.	n.d.	n.d.	<2.71	n.d.	<9.26	n.d.
Ne	<1 08	30 3	33 3	<11 5	<3 51	<0 07	n d	n d	162	n d	n d	4 72	3 66	n d	n d	n d	n d	n d	n d	<18 4	n d	n d	n d	5 97	n d	<15 0	n d.
Ne	<0 60	30 3	42 5	<7 59	<2 02	0 35	n d	n d	83 9	n d	n d	17 1	26 4	n d	n d	n d	n d	n d	n d	<10 8	n d	n d	n d	8 60	n d	97 4	n d
Mela	*2 32*	**21 0*	**95 2*	*31 8*	*30 5*	*4 43*	*n d*	*n d*	*n d*	*196*	*n d*	**1361*	**1880*	*n d*	*n d*	*n d*	*n d*	*n d*	*n d*	*13 8*	*n d*	*n d.*	*n d*	*n d*	*n d*	*4634*	*n d*
Mela	0 96	1 51	33 6	31 8	32 5	12 8	73 6	<633	<14 2	531	852	48 2	226	*296	104	31 3	95 5	130	46 3	38 6	7.31	4.61	15 6	615	29 0	5852	92 4
Mela	0 65	1 25	33 8	31 8	32 0	4 42	*4991	*4321	40 2	433	1412	*192	*385	273	86 0	32 7	78 3	74 3	39 2	34 9	3 02	13 0	32 0	812	13 4	2388	38 6
Mela	<0 34	2 70	38 6	31 8	32 1	7 75	<33 5	<941	<23 1	433	1511	22 5	136	227	33 9	23 8	97 7	105	66 3	22 3	3 79	<8 66	<5 28	180	2 77	3814	95 3
Mela	0 67	1 80	30 7	31 8	30 5	11 2	<44 7	<1116	<23 5	524	769	*71 4	*320	*405	*130	29 2	98 1	106	55 5	53 6	2 72	7 06	30 6	893	43 1	5459	117
Average last 4	0 78	1 82	33 7	31 8	31 8	8 99	73 6	n d	40 2	480	1136	35 3	181	250	74 8	29 2	92 4	104	51 8	37 4	4 21	8 23	26 2	575	22 1	4328	85 9
STDS	0 17	0 63	2 43	0 00	0 86	3 66	n d		n d	54 6	380	16 J	63 5	32 1	36 4	3 92	9 44	22 9	11 7	12 9	2 12	4 33	8 97	294	17 7	1620	33 3
RSD	23%	35%	7%	0%	3%	41%	n d		n d	11%	33%	51%	35%	13%	49%	13%	10%	22%	23%	34%	50%	53%	34%	51%	80%	37%	38%
Wo	<0.75	<0.19	53.4	47.3	45.0	0.11	n.d.	n.d.	n.d.	53.8	n.d.	40.5	122	n.d.	n.d.	n.d.	n.d.	n.d.	n.d.	<18.2	n.d.	n.d.	n.d.	n.d.	n.d.	<8.83	n.d.
Wo	*bd*	*bd*	**32.91*	*47 3*	*bd*	*0 22*	*1187*	*bd*	*bd*	*54.1*	*bd*	*353*	*418*	*bd*	*bd*	*bd*	*bd*	*bd*	*bd*	*bd.*	*bd.*	*b.d*	*bd.*	*67.8*	*bd*	*61.4*	*b.d.*
Melilite	*2 99*	*58 4*	*114*	*28 3*	*33 0*	*0 96*	*4592*	*18806*	*287*	*47.9*	*168*	*708*	*907*	*167*	*16 6*	*3 55*	*15 6*	*<10 6*	*<7 32*	*<17.9*	*<1 52*	*19 4*	*27.3*	*257*	*2.96*	*1216*	*29.1*
Melilite	*1.24*	*11.9*	*42.3*	*28 3*	*n.d*	*1.00*	*12231*	*19852*	*518*	*40 2*	*746*	*639*	*826*	*164*	*17.2*	*3 47*	*10 2*	*5 13*	*3 48*	*4.81*	*0 59*	*27.0*	*20.1*	*464*	*2.16*	*631*	*10.5*
Melilite	*1.99*	*10 2*	*41.3*	*28 3*	*n d*	*0.94*	*12229*	*18627*	*412*	*37.9*	*498*	*763*	*949*	*172*	*16 8*	*5 39*	*11 8*	*8 45*	*2 45*	*<1.54*	*0.51*	*16.0*	*22.1*	*272*	*2.05*	*868*	*9.14*
Melilite	3 91	7.96	42 4	28 3	31.5	0 02	310	21034	<10 5	5 05	<8 36	489	641	126	10 4	<2 77	<5 72	<3 35	<6.39	<11 5	<0 95	<2.84	<3.98	<1.44	<0.69	<2.36	<7.33
Melilite	3 89	7 00	37 6	28 3	28 3	0 01	433	22399	<7.83	5 49	<5 89	400	587	108	6 17	<1 90	<6 77	<4 21	<5.20	<2.45	<1.31	<0 82	<2.31	1.33	<0.92	3.72	<4.61
Melilite	3 08	6 80	44 5	28 3	28 2	0 15	500	12178	<16 4	*20 1	<13 4	305	378	111	<12 2	<4 33	8 66	<8 65	<14 5	<17.5	1.98	<2.85	<8.07	*37.8	<2.35	*37.4	<14.0
Melilite	3 01	6 75	41.5	28 3	28 8	0 04	*3427	18087	45 1	4 86	24 8	346	444	68 0	6 83	1 85	<2 66	1 82	<3.56	<6 27	<0.71	<1.16	1.84	6 24	<0.56	*91.9	<3 66
Melilite	3 92	6 98	45 5	28 3	30 2	0 10	460	24364	<11.9	8 65	<10.4	593	813	157	14 5	3 43	4 79	*8 22	<7.37	<9.34	<1.19	<3.38	<2.98	*30 8	<1.28	*50 93	<11.6
Melilite	4 08	9 53	44 0	28 3	26 0	0 02	578	20400	20 4	3 11	12 3	540	649	140	14 5	<2 72	9 78	<3 25	<7 16	<8.34	<1.28	<2.12	3.46	2 87	<1.40	9.53	<10.6
Melilite	3 05	6 78	31.0	28 3	28.7	0.10	n d	n d	n d	11.7	n d	426	591	n d	n.d	n d	n d	n d	n d	<4 04	n d.	n.d.	n.d.	n d	n d	*75 0	n d.
Melilite	3 42	5 95	37.0	28 3	24 8	0 05	n d	n d	n d	4 14	n d	477	685	n d	n d	n d	n d	n d	n d	<3 83	n d	n.d.	n.d	n d	n d	17.7	n.d.
Melilite	3 78	9 70	42 2	28 3	30 2	0 25	n d	n d	n d	10 2	n d	502	670	n d	n d	n d	n d	n d	n d	<2 34	n d	n d	n d	n d	n d	*131	n d.
Melilite	2 79	5 80	36 4	28 3	28 6	0 02	n d	n d	n d	9 01	n d	259	419	n d	n d	n d	n d	n d	n d	<3 07	n d	n d.	n d.	n d	n d	6 22	n d.
Melilite	2 96	6 27	37 9	28 3	28 7	0 30	n d	n d	n d	10 6	n d	321	405	n d	n d	n d	n d	n d	n.d	<7.79	n d.	n.d.	n.d	n d.	n d	*150	n d.
Melilite	4.25	17 3	46 9	28 3	n d	0 23	*1333	24435	40 8	13 6	*43 2	497	614	180	12.2	3 25	3 76	2 19	<2 04	<2 80	<0 68	2 93	4 64	*38 4	<0 50	*228	3.15
Melilite	2 08	5 92	17.1	28 3	n d	0 15	922	13338	38.0	11 9	*259	282	639	180	<8 28	3 76	<4 16	<5 73	<3 23	<11.5	<1.29	2 26	0.83	16 8	<1.93	*73 7	<5.82
Melilite	3 62	8 62	42 8	28 3	n d	0 33	*3282	23883	47.8	14.7	*85 8	691	828	152	8 24	4 48	7 30	3 31	1.58	<1.84	<0 36	7.72	4.16	*57.9	0.44	*197	4.01
Melilite	2 16	9 66	36 2	28 3	n d	0 29	*5763	18037	*112	*19 0	*135	576	731	120	11.5	2 76	7 15	1 76	<1 22	<1 68	<0 37	4 98	5.76	*59.9	<0.26	*252	4.44
Melilite	2.95	11 6	43 8	28 3	n d	0 26	*7265	16231	*159	9 80	*159	383	605	103	*4.29	1 91	4 61	3 23	<3 17	<2.56	<0 44	4.70	2 89	*53.9	<0.40	*133	2.72
Melilite	3 55	8 31	43 4	28 3	n d	0 11	703	20526	15 7	6 91	13 37	567	716	140	9 06	5 69	3 43	1 99	<4.10	<3 99	<0 35	1.72	2.54	16 2	<0.45	*71 6	2 88
Melilite	3 72	7.19	40 5	28 3	n d	0 08	402	21427	<16 6	5 13	<16 8	492	713	131	11 7	<1 37	3 55	2 35	<4 38	<4 22	<0 51	<2 09	2.79	7.67	<0 91	7.90	<2 81
Melilite	3 38	8 98	38 3	28 3	n d	*0 72	682	15567	29 3	*16 2	<34 1	369	578	131	<9 96	<3 28	5 56	<4 34	*8 00	<10 1	<1 35	4 69	*12.4	*239	2.12	*364	<12 6
Melilite	4 15	8 29	42 1	28 3	n d	<0 02	925	25961	<14 7	4 59	<84 8	500	849	129	15 0	1 76	1 79	1 62	<2 59	<3 55	<0 43	<1.25	1.40	<1 17	<0.55	<4 69	<5.14
Melilite	3 45	7 55	47 2	28 3	n d	0 35	*2221	16571	33 1	*14 8	*42 1	342	470	117	7 21	2 21	9 20	<3 41	<4 05	<3 60	<0 75	3 95	5.35	*68 7	0.62	*244	3.87
Melilite	6 16	10 6	39 5	28 3	n d	0 10	1135	28466	<43 8	8 61	<57 2	515	972	83 0	<15 9	*10 2	<12 4	<12 2	<10 6	<27.9	<3 76	8 74	8 21	*69 2	<1.85	*183	<7.97
Average last 22	3 53	8 44	39 9	28 3	28 3	0 15	641	20289	33 8	8 22	18 8	449	636	128	10 8	3 11	5 82	2 31	1.56	b d	1 98	4 63	3 66	8 88	1.08	9.0	3.48
STDS	0 63	2 51	8 43	0 00	1 95	0 11	260	4448	11 5	3 48	8 93	114	153	30 0	2 95	1 28	2 60	0 63	n d	n d	n d	2 34	2 09	6 49	0 92	5 3	0 68
RSD	24%	30%	18%	0%	7%	77%	41%	22%	34%	42%	41%	25%	24%	23%	27%	41%	45%	27%	n d	n d	n d	51%	57%	73%	87%	59%	19%
CP15																											
Ne	bd	32 2	35 9	bd	bd	bd	bd	bd	63 7	bd	bd	bd	bd	bd	bd	bd	bd	bd	bd	bd	bd	bd	bd	bd	bd	bd.	b.d.
Cpx	9 83	1 26	48 4	21 3	21 4	0 70	n d	n d	n d	9 01	n d	3 93	14 0	n d	n d	n d	n d	n d	n d	<12.7	n d	n d	n d	n d	n d	321	n d
Cpx	7 05	1 31	51 6	21 3	16 4	0 62	n d	n d	n d	3 00	n d	3 81	9 92	n d	n d	n d	n d	n d	n d	<4 12	n d.	n d	n d	n d	n d	316	n d
Cpx	*12 6*	*1 58*	*50 1*	*21 3*	*25 1*	*0 94*	*n d*	*n d*	*n d*	*15 5*	*n d*	**12 5*	**31 4*	*n d*	*n d*	*n d*	*n d*	*n d*	*n d*	*<21.0*	*n d*	*n d*	*n d*	*n d*	*n d*	*457*	*n d*

Comments	MgO	Al2O3	SiO2	CaO	CaO	TrO2	Ba	Sr	Rb	Y	V	La	Ce	Nd	Sm	Eu	Gd	Dy	Er	Yb	Lu	U	Th	Nb	Ta	Zr	Hf
Cpx	*10 5*	*2 63*	*69 3*	*21 3*	*23 5*	*0 79*	*nd*	*nd*	*nd*	*13 4*	*nd*	**40 4*	**73 3*	*nd*	*nd*	*nd*	*nd*	*nd*	*nd*	*<6 87*	*nd*	*nd*	*nd*	*nd*	*nd*	553	*nd*
Average first 2	8 44	1 29	50 0	21 3	18 9	0 66	nd	nd	nd	6 01	nd	3 77	12 0	nd	nd	nd	nd	nd	nd	bd	nd	nd	nd	nd	nd	319	nd
STDS	1 97	0 04	2 22	0 00	3 56	0 06				4 25		0 23	2 88													3 77	
RSD	23%	3%	4%	0%	19%	9%				71%		6%	24%													1%	
Mela	0 62	0 69	30 7	31 5	30 7	10 4	<30 5	<1015	<19 6	335	1460	*9 17	92 1	120	52 8	*11 1	99 1	103	33 0	30 1	6 08	5 65	<5 11	152	<3 61	2899	62 5
Mela	0 76	1 15	30 0	31 5	31 0	10 8	<14 0	<336	<8 91	570	974	39 3	249	346	104	36 8	132	152	66 8	49 6	5 54	10 1	11 3	231	*18 12	*5297	*110
Mela	0 61	3 99	35 8	31 5	31 8	10 4	*292	<794	17 2	511	1412	41 9	133	115	82 1	22 0	88 1	96 6	58 1	42 8	5 48	<5 67	7 08	242	8 65	3856	75 7
Average	0 66	1 94	32 2	31 5	31 2	10 5	nd	bd	17 2	472	1282	40 6	158	194	79 5	29 4	106	117	52 6	40 8	5 70	7 88	9 20	208	8 65	3377	69 1
STDS	0 08	1 79	3 19	0 00	0 55	0 21			nd	122	268	1 80	81 5	132	25 5	10 5	22 8	30 4	17 8	9 89	0 33	3 15	3 00	49 1	nd	677	9 33
RSD	13%	92%	10%	0%	2%	2%			nd	26%	21%	4%	52%	68%	32%	36%	21%	26%	33%	24%	6%	40%	33%	24%	nd	20%	13%
Melilite	1 93	32 3	111	23 7	22 6	2 08	nd	nd	nd	*97 3	nd	304	383	nd	nd	nd	nd	nd	nd	<9 31	nd	nd	nd	nd	nd	*2231	nd
CP16																											
Ne	<0 48	31 5	41 3	<8 01	nd	<0 04	<44 1	<2512	117	<2 83	<29 0	<0 96	<3 74	<33 3	<10 9	<2 31	<5 78	<7 25	<3 68	<7 20	<1 21	<1 99	<2 63	<3 62	<1 33	<5 63	<4.74
Ne	<0 55	31 5	36 1	<10 1	nd	<0 06	*707	<3179	*145	<6 55	<34 9	*24 5	*42 5	<28 7	<6 76	<2 80	<5 78	<7 93	bd	bd	<1 78	<3 56	<2 29	*5 50	<1 89	*10 2	<9.81
Ne	<1 72	31 5	<34 8	<22 9	<7 46	<0 16	nd	nd	<105	nd	nd	<8 40	<4 45	nd	nd	nd	nd	nd	nd	<46 6	nd	nd	nd	<10 10	nd	<34 5	nd
Ne	<0 76	31 5	39 8	<8 68	2 72	0 26	nd	nd	108	nd	nd	*39 5	*53 9	nd	nd	nd	nd	nd	nd	<10 3	nd	nd	nd	*84 4	nd	*2130	nd
Ne	<0 30	31 5	31 8	<3 65	2 44	0 03	nd	nd	129	nd	nd	*84 9	*77 9	nd	nd	nd	nd	nd	nd	<6 39	nd	nd	nd	*14 03	nd	*10 6	na
Ne	<0 22	31 5	33 1	<2 81	<0 59	<0 02	nd	nd	nd	<1 82	nd	<0 50	<0 71	nd	nd	nd	nd	nd	nd	<6 44	nd	nd	nd	nd	nd	<2 36	nd
Average	bd	31 5	36 4	bd	2 58	0 15	bd	nd	118	nd	nd	nd	nd	nd	nd	nd	nd	nd	nd	bd	nd	nd.	nd.	nd	nd	nd.	nd.
STDS		0 00	4 09		0 20	0 16			10 3																		
RSD		0%	11%		8%	112%			9%																		
Cpx	9 77	1 15	46 1	20 4	19 5	0 48	nd	nd	nd	6 11	nd	5 22	17 1	nd	nd	nd	nd	nd	nd	1.41	nd	n.d.	n.d	nd	n.d.	215	n.d.
Cpx	9 52	1 02	42 8	20 4	20 7	0 49	nd	nd	nd	3 49	nd	*16 9	*34 9	nd	nd	nd	nd	nd	nd	1.72	n.d	n.d	n.d	nd	n.d.	226	n.d.
Cpx	9 09	1 08	57 8	20 4	19 2	0 57	nd	nd	nd	3 92	nd	6 65	22 0	nd	nd	nd	nd	nd	nd	<5 32	n.d.	n.d	nd	nd	n.d.	373	n.d.
Cpx	7.58	5 53	54 8	20 4	17.1	0 56	nd	nd	nd	3 52	nd	*1211	*141	nd	nd	nd	nd	nd	nd	<10 8	nd	n.d	nd	nd	nd	315	n.d.
Cpx	8 29	1 11	51 8	20 4	21 4	0 53	nd	nd	nd	10 09	nd	*4 50	*2 61	nd	nd	nd	nd	nd	nd	<13.1	nd.	n.d.	n.d.	nd	nd.	275	n.d.
Cpx	9 13	1 13	48 1	20 4	nd	0 52	<25 0	<1869	<16 0	<2 37	*589	3 13	5 50	<11 0	<7 96	<2 35	<3 14	<5 34	<6 30	<9 81	<0 57	<1.31	<1 52	<2.23	<0.72	428	5.59
Cpx	9 28	0 57	33 8	20 4	nd	0 44	<16 9	<1370	<12 1	4 64	925	7 53	19 6	<10 9	<5 73	<0 78	<3 15	<5.18	<2 46	<6 71	<0 56	<1.20	<0.64	1.29	<0.52	194	<5.68
Cpx	*17.05	3 54	56 2	20 4	nd	0 60	<25 6	<1296	<13 8	10 53	171	8 19	24 2	24 1	<5 07	*2 86	3 55	<3 05	<4 75	<2.74	<0 92	<0.87	<1.69	7.78	<0.81	245	9.97
Cpx	9 89	1 06	47 6	20 4	nd	0 57	<22 5	<1809	<19 7	<3 28	172	10 3	28 1	18 7	6 27	<1.58	<5 01	<5 75	<3.52	<5 97	<1 42	<1.59	<1.56	<3 29	<0 75	357	<7.82
Average	9 07	1 80	48 8	20 4	19 6	0 53	nd	nd	nd	6 04	145	7 17	19 4	21 4	6 27	nd	3 55	nd	nd	1.57	nd	nd	nd	4 54	n.d.	292	7.78
STDS	0 78	1 64	7 50	0 00	1 64	0 05				3 05	45 7	2 58	7 6	3 78	nd		nd			0 22				4 59		80 3	3.10
RSD	9%	91%	15%	0%	8%	10%				50%	31%	36%	40%	18%	nd		nd			14%				101%		28%	40%
Mela	*2 05*	*17.2*	*48 1*	*31 4*	*32 1*	*2 34*	*7094*	*9179*	*241*	*193*	*801*	*542*	*1289*	*567*	*83 3*	*17 8*	*45 0*	*29 8*	*15 6*	*11 6*	*1.50*	*59 5*	*75.2*	*647*	*3.35*	*1840*	*20 6*
Mela	*0 77*	*0 87*	*35 6*	*32 0*	*nd*	*3 18*	*27 9*	*<1393*	*<12 4*	*257*	*1280*	**269*	**1220*	**751*	*100*	*20 1*	**54 5*	**41 4*	**17 7*	**11 6*	**2 12*	**70 4*	**83 7*	*1036*	*3.57*	*1926*	*35.7*
Mela	0 32	0 86	32 8	31 4	30 0	6 44	38 8	<317	<11 1	611	1469	33 8	199	358	122	43 5	133	133	57.3	48 8	<2 04	20 9	29 5	*2343	*27.7	*557	<13 9
Mela	0 76	0 78	31 1	31 4	30 6	11 6	<7.74	<133	<4 29	400	943	41 4	203	242	90 9	30 0	97 8	94 0	52 0	31.4	3 66	6 08	7.53	252	15.1	4100	75.2
Mela	0 63	4 94	37 1	31 4	32 2	10 5	*312	<592	26 9	360	1436	70 2	138	130	63 2	*9 59	108	60 7	31 6	42 3	6 84	4 99	4 25	425	8 65	2937	49 6
Mela	1 29	1 00	35 9	32 0	nd	13 4	*2732	*2920	<22 3	532	*513	203 4	*539	383	155	39 5	154	114	49 1	62 6	7 62	20 1	32 3	*1570	*40.0	4013	45.4
Mela	0 46	1 04	31 6	32 0	nd	6 41	*674	<2084	*54 4	640	1226	*119	*272	273	96 5	31 8	156	165	96 6	54 7	5 96	15 1	31 7	*2236	*21.7	*970	*12.3
Average last 5	0 69	1 72	33 7	31 6	30 9	9 66	38 6	nd	26 9	513	1269	48 4	180	277	106	36 2	130	113	57 3	48 0	6 07	13 4	21 1	338	11.9	3683	56 7
STDS	0 37	1 80	2 65	0 34	1 09	3 14	nd		nd	119	242	19 2	36 6	101	34 6	6 41	26 5	39 4	24 0	12 0	1 78	7.56	13.9	123	4 58	648	18 1
RSD	54%	105%	8%	1%	4%	32%	nd		nd	23%	19%	40%	20%	36%	33%	18%	20%	35%	42%	25%	29%	56%	66%	36%	39%	18%	26%
Wo	<0 37	5 00	*41 6	46 6	41 0	0 10	nd	nd	nd	*15 6	nd	85 5	95 4	nd	nd	nd	nd	nd	nd	<7 75	nd	nd	nd	n.d	n.d	*163	nd
Wo	<0 37	<0 12	51 6	46 6	47 6	<0 04	nd	nd	nd	48 0	nd	18 2	45 9	nd	nd	nd	nd	nd	nd	<8 19	nd	nd	nd	nd	nd	<7 04	nd
Wo	<1 26	<0 56	51 1	46 6	nd	<0 09	<109	<6502	<67 6	74 5	<58 2	15 8	85 2	48 2	<13 6	<4 03	<14 2	<11 5	<17 6	<21 4	<2 96	<8 66	<9 98	<4 80	<1 91	<17 5	<16 3
Wo	<0 29	1 18	51 4	46 6	nd	0 11	147	<1718	<22 3	56 0	<18 0	65 3	108	34 8	7 20	5 13	9 10	5 81	6 06	<3 73	<1 51	<1 19	<1 37	11.7	<1 71	34 0	<5.87
Average	bd	3 08	51 4	46 6	44 3	0 11	147	nd	nd	58 8	nd	45 7	83 6	41 5	7 20	5 13	9 10	5 81	6 06	bd	nd	nd	nd	11 7	nd	34 0	nd
STDS		2 72	0 25	0 00	4 72	0 01	nd			14 5		35 3	26 8	9 50	nd	nd	nd	nd	nd					n.d		nd	
RSD		88%	0%	0%	11%	7%	nd			25%		77%	32%	23%	nd	nd	nd	nd	nd					nd		nd	
Comb	*0 16*	*0 95*	*25 8*	*27 4*	*27 7*	*0 25*	*3032*	*5818*	*120*	*45 4*	*55 8*	*216*	*299*	*86*	*13 6*	*4 14*	*8 26*	*7 55*	*2 95*	*<2 75*	*0 45*	*5.33*	*11 4*	*115*	*1 02*	*205*	*4 78*
Comb	<0 23	1 53	49 0	27 4	26 0	1 12	53 5	3032	<22 1	417	57 8	205	458	400	83 2	19 6	47 4	56 7	38 7	24 5	9 24	6 99	53 2	*148	*5 93	3270	*74 0
Comb	<0 16	<0 03	45 4	27 4	27 6	0 02	98 5	3546	<13 6	334	<7 83	214	509	279	65 1	18 6	44 2	48 0	22 5	25 6	2 63	18 5	48 3	3 83	<0 75	*5818	*65 3
Comb	<0 55	2 48	42 6	27 4	27 5	<0 04	*173	4855	<32 5	198	<30 0	225	559	273	37 9	26 1	46 7	29 7	18 7	21 2	<4 22	*57 1	51 2	4 53	<3 87	2807	*86 3

Comments	MgO	Al2O3	SiO2	CaO	CaO	TiO2	Ba	Sr	Rb	Y	V	La	Ce	Nd	Sm	Eu	Gd	Dy	Er	Yb	Lu	U	Th	Nb	Ta	Zr	Hf
Comb	0 37	0 54	51 0	27 4	26 5	0 16	39 8	3479	<9 81	563	42 0	193	482	244	69 2	21 3	76 2	70 7	34 6	50 1	4 00	13 8	46 5	*33 0	b d	2458	32 9
Comb	<0 25	<0 05	46 0	27 4	25 1	0 03	33 6	2820	<17 3	256	<14 7	167	415	199	49 1	22 2	52 0	36 9	20 2	18 9	3 15	25 9	63 1	2 13	<1 58	4219	57 5
Comb	0 22	*10 7	*66 0	27 4	*16 4	0 23	*435	2416	*92 7	182	26 4	132	365	180	33 9	10 5	26 7	22 2	13 4	14 2	1 51	13 7	*13 6	*73 1	<0 57	1552	16 5
Comb	0 15	5 38	58 2	27 4	26 7	0 20	*180	2485	13 5	211	19 7	172	621	187	41 0	14 2	31 7	26 7	22 4	16 2	<1 60	6 53	27 6	*62 5	<1 10	*655	<8 39
Comb	<0 40	2 96	37 3	27 4	nd	0 14	*2562	5165	<21 5	342	41 0	216	679	183	54 1	19 1	52 7	40 0	12 8	25 2	4 13	*57 4	30 6	*39 7	<0 79	3554	37 7
Comb	0 57	3 14	42 7	27 4	nd	0 23	*690	4916	23 3	279	*112	268	550	246	34 5	13 2	41 3	30 2	9 94	14 0	2 37	19 3	50 1	*57 8	<1 03	3427	49 2
Comb	<0 44	<0 26	32 9	27 4	nd	<0 04	68 9	<2741	<24 4	234	<19 5	140	429	141	53 8	12 9	41 2	26 3	22 0	<20 4	<1 69	2 09	27 1	8 36	<1 53	2488	43 1
Average last 10	0 33	2 67	45 0	27 4	26 5	0 27	58 4	3635	18 4	302	37 4	193	507	231	52 2	17 8	46 0	38 7	21 5	23 3	3 86	13 4	44 2	4 71	n d.	2972	39 5
STDS	0 19	1 64	7 46	0 00	0 96	0 35	25 2	1080	6 99	118	14 9	41 5	97 2	75 4	16 4	4 93	13 4	15 5	9 16	11 0	2 54	7 88	12 7	2 63		822	14 2
RSD	57%	62%	17%	0%	4%	133%	43%	30%	38%	39%	40%	21%	19%	33%	31%	28%	29%	40%	43%	47%	66%	59%	29%	56%		28%	36%
CP17																											
Ne	<0 12	32 0	32 2	<1 52	<0 44	<0 01	n d	n d	71 2	n d	n d	<0 53	<0 62	n d	n d	n d	n d	n d	n.d	<2 85	n d	n d	n d	<0 61	n d	<1 85	n d
Cpx	4 97	0 81	63 6	17 9	16 0	1 57	n d	n d	n d	<3 14	n d	*36 9	*46 3	n d	n d	n d	n d	n d	n d	<11.5	n d	n d	n d	n d	n d	477	n d
Cpx	7.56	2 35	44 7	17 9	16 7	0 59	n d	n d	n d	7 65	n d	*33 4	*44 2	n d	n d	n d	n d	n d	n d	<4 22	n d	n d	n d.	n d	n d	297	n d
Cpx	*4 33*	*5 88*	*59 4*	*17 9*	*20 2*	*0 83*	*n d*	*n d*	*n d*	*23 5*	*n d*	*74 1*	*104*	*n d*	*n d*	*n d*	*n d*	*n d*	*n d*	*<11 6*	*n d.*	*n d.*	*n d.*	*n d.*	*n d.*	*519*	*n d*
Cpx	*7.72*	*4 99*	*50 6*	*17 9*	*18 4*	*0 60*	*n d*	*n d*	*n d*	*21 6*	*n d*	*75 6*	*90 3*	*n d*	*n d*	*n d*	*n d*	*n d*	*n d*	*<11 0*	*n d.*	*n d.*	*n d.*	*n d.*	*n d.*	*465*	*n d*
Cpx	*3 82*	*4 26*	*48 8*	*17 9*	*17 0*	*0 60*	*n d*	*n d*	*n d*	*32 7*	*n d*	*138*	*162*	*n d*	*n d*	*n d*	*n d*	*n d*	*n d*	*<13 7*	*n d*	*n d*	*n d.*	*n d.*	*n d.*	*737*	*n d*
Cpx	*4 62*	*5.91*	*44 2*	*17 9*	*15 4*	*0 51*	*n d.*	*n d*	*n d*	*25 6*	*n d*	*174*	*203*	*n d*	*n d*	*n d*	*n d*	*n d*	*n d*	*<2 38*	*n d*	*n d*	*n d.*	*n d*	*n d.*	*600*	*n d*
Cpx	*4 23*	*3 79*	*41 6*	*17 9*	*17 3*	*0 52*	*n d*	*n d*	*n d*	*24 2*	*n d*	*178*	*206*	*n d*	*n d*	*n d*	*n d*	*n d*	*n d.*	*<6 40*	*n d*	*n d*	*n d.*	*n d*	*n d*	*371*	*n d*
Average first 2	6 27	1.58	54 1	17 9	16 3	1.08	n d	n d	n d	7 65	n d	n d	n d	n d	n d	n d	n d	n d	n d	b d.	n d	n d	n d.	n d.	n d	387	n d.
STDS	1 83	1.09	13 4	0 00	0 47	0 69				n d																127	
RSD	29%	69%	25%	0%	3%	64%				n d																33%	
Mela	*1 64*	*4 76*	*48 9*	*31 6*	*30 6*	*9 26*	*1156*	*1312*	*47.79*	*405*	*935*	*351*	*969*	*553*	*151*	*41 0*	*63 8*	*67 7*	*25 7*	*23 0*	*3 22*	*25 3*	*58 5*	*801*	*21 3*	*2774*	*21 9*
Mela	0 76	2 73	37 2	31 6	31 3	11 4	*866	1042	28 7	444	1077	*102	*340	*358	105	39 2	122	121	46 3	37.7	6.10	*14 8	*17 0	*539	*28 1	3658	95 0
Mela	0 79	1.31	29 1	31 6	29 3	10 3	53 3	b d	b d	469	1280	19 4	70 2	127	64 9	21 9	74 4	141	62 7	56 3	4 30	b d	*4 39	180	4 39	3801	89 3
Mela	0 99	0 73	32 7	31 6	32 0	12 9	b d	b d	b d	470	897	49 0	249	327	101	44 2	129	104	53 7	46 9	2 53	6 06	13 0	*339	*17 7	*5204	*110
Mela	0 36	1 59	32 5	31 6	31 0	6 71	*361	b d	b d	214	*2596	36 7	b d	51 2	33 5	10 3	36 7	66 4	22 2	28 1	b d.	*9 52	*3 61	311	8 95	*1759	*37 3
Mela	0 71	0 71	29 0	31 6	31 6	11 3	b d	b d	b d	396	928	38 5	232	273	121	41 9	112	79 5	53 5	31 9	5 94	4 32	5 36	*279	*11 7	3957	73 2
Mela	0 49	1 50	32 6	31 6	33 1	9 16	b d	b d	b d	582	*2426	13 9	66 1	119	42 9	22 6	71 7	67 3	58 2	66 0	5 55	b d.	*2 40	189	3 43	3481	54 1
Average last 6	0 66	1.43	32.2	31 6	31 4	10 3	53 3	1042	28 66	433	995	31 5	154	179	77 9	30 0	90 9	100	49 4	44 5	4 86	6 19	9 18	227	5 59	3674	77 9
STDS	0 23	0 74	3 02	0 00	1 23	2 15	n d	n d	n d	123	248	14 5	99 9	116	35 9	13 7	35 8	28 0	14 4	14 7	1 49	2 64	5 97	73 2	2 95	202	18 4
RSD	33%	52%	9%	0%	4%	21%	n d	n d	n d	29%	25%	46%	65%	64%	46%	46%	39%	28%	29%	33%	31%	43%	59%	32%	53%	6%	24%
CP18																											
Ne	*0 52*	*31 4*	*46 0*	*. 8 98*	*9 73*	*0 42*	*n d*	*n d*	*126*	*n d*	*n d*	*259*	*332*	*n d*	*n d*	*n d*	*n d*	*n d*	*n d*	*<35 73*	*n d.*	*n d.*	*n d*	*108*	*n d*	*466*	*n d.*
Ne	<0 12	31 4	44 3	<3 24	<0 42	<0 01	n d	n d	50 3	n d	n d	<1 24	<0 77	n d	n d	n d	n d	n d	n d	<2 65	n d.	n d	n d.	<1 35	n d.	<1 08	n d.
Ne	0 04	31 4	35 4	<0 62	0 19	0 01	n d	n d	77 4	n d	n d	0 71	1 47	n d	n d	n d	n d	n d	n d	<1 09	n d	n d	n d.	1 78	n d.	2 87	n d
Ne	<0 08	31 4	32 2	<2 16	0 37	0 02	n d	n d	58 6	n d	n d	*1 44	*3 61	n d	n d	n d	n d	n d	n d	<6 23	n d.	n d	n d	1 60	n d	*4 35	n d
Average last 3	0 04	31 4	37 3	b d	0 28	0 02	n d	n d	62 1	n d	n d	0 71	1 47	n d	n d	n d	n d	n d	n d	b d	n d	n d	n d.	1 69	n d	2 87	n d.
STDS	n d	0 00	6 27		0 13	0 01			13 9			n d	n d											0 13		n d	
RSD	n d	0%	17%		45%	47%			22%			n d	n d											8%		n d.	
CP19																											
Ne	<0 05	31 2	40 4	<1 17	<0 19	<0 01	n d	n d	52 7	n d	n d	<0 33	<0 45	n d	n d	n d	n d	n d	n d	<2 99	n d	n d	n d	<0 57	n d	<1 10	n d
Ne	<0 10	31 2	36 1	<2 19	<0 33	<0 01	n d	n d	*95 5	n d	n d	<0 70	*0 83	n d	n d	n d	n d	n d	n d	<5 24	n d	n d	n d	*1 89	n d	*4 18	n d
Ne	<0 07	31 2	33 6	<1 71	<0 27	<0 01	n d	n d	51 4	n d	n d	<0 50	<0 62	n d	n d	n d	n d	n d	n d	<3 74	n d	n d	n d	<0 74	n d	<1 31	n d
Ne	*<0 11*	*31 2*	*29 9*	*<2 66*	*0 39*	*0 05*	*n d*	*n d*	*67 1*	*n d*	*n d*	*4 00*	*7 64*	*n d*	*n d*	*n d*	*n d*	*n d*	*n d*	*<3 21*	*n d*	*n d*	*n d*	*8 65*	*n d.*	*33 5*	*n d*
Ne	*<0 20*	*31 2*	*43 1*	*<2 88*	*n d*	*0 17*	*428*	*<909*	*77 0*	*5 69*	*47 2*	*18 1*	*31 2*	*10 9*	*<2 74*	*<0 81*	*<3 02*	*<1 38*	*<2 54*	*<4 09*	*<0 25*	*1 53*	*2 11*	*26 1*	*<0 57*	*123*	*<3 19*
Average first 3	b d	31 2	38 7	b d	b d	b d	n d	n d	52 1	n d	n d	b d	n d	n d	n d	n d	n d	n d	n d	b d.	n d	n d	n d	n d	n d	n d.	n d.
STDS		0 00	3 43						0 90																		
RSD		0%	9%						2%																		
Melilite	4 47	10 3	38 6	30 4	35 3	0 10	259	11020	<8 90	9 45	<15 98	69 1	168	<35 9	<8 09	<3 32	<7 58	<7 57	<11 94	<25 7	<2 15	<2 85	<3 94	*15 7	<1 52	*123	6 01
Melilite	5 20	9 62	44 6	30 4	31 8	0 02	*132	13366	<3 40	2 41	<4 51	83 8	102	33 1	4 36	1 31	<3 62	<2 69	<3 96	<4 23	<0 45	<0 83	<3 00	<0 71	b.d.	<1 03	<5 61
Melilite	4 43	10 8	51 1	30 4	36 3	0.07	286	10941	7 56	7 84	14 6	67 6	110	39 6	<10 3	<1 54	<4 92	<154	<8 60	<7 72	<1 70	0 86	<255	8 73	<0 99	*49 0	b d.
Average	4 70	10 3	44 8	30 4	34 5	0 06	272	11776	7 56	6 57	14 8	73 5	127	36 4	4 36	1 31	bd	bd	bd	bd	bd	0 86	bd	8 73	bd	n.d.	8.01
STDS	0 43	0 61	6 23	0 00	2 37	0 04	19 2	1377	n d	3 69	n d	8 93	35 9	4 62	n d	n d						n d		n d			n d	
RSD	9%	6%	14%	0%	7%	64%	7%	12%	n d	56%	n d	12%	28%	13%	n d	n d						n d		n d			n d.	

Comments	MgO	Al2O3	SiO2	CaO	CaO	TiO2	Ba	Sr	Rb	Y	V	La	Ce	Nd	Sm	Eu	Gd	Dy	Er	Yb	Lu	U	Th	Nb	Ta	Zr	Hf
CP20																											
Ne	*<0.20*	*31.8*	*46.6*	*<4.24*	*1.41*	*0.12*	*40.7*	*122*	*47.9*	*nd*	*nd*	*63.0*	*nd*	*nd*	*nd*	*nd*	*nd*	*nd*	*nd*	*<3.62*	*nd*	*nd*	*nd*	*20.0*	*nd*	*nd*	*nd*
Ne	*0.46*	*31.8*	*39.4*	*4.45*	*4.83*	*0.42*	*168*	*546*	*82.3*	*nd*	*nd*	*215*	*nd*	*nd*	*nd*	*nd*	*nd*	*nd*	*nd*	*<3.02*	*nd*	*nd*	*nd*	*96.4*	*nd*	*nd*	*nd*
Ne	<0.08	31.8	31.7	<1.42	<0.22	<0.00	<0.26	<1.13	67.3	nd	nd	<0.41	nd	nd	nd	nd	nd	nd	nd	<2.04	nd	nd	nd	<0.62	nd	nd	nd
Ne	<0.12	31.8	31.9	<2.09	<0.31	<0.01	<0.56	<1.37	85.2	nd	nd	<0.38	nd	nd	nd	nd	nd	nd	nd	<4.43	nd	nd	nd	<0.55	nd	nd	nd
Ne	<0.08	31.8	33.4	<1.68	<0.27	0.01	<0.39	<1.24	53.5	nd	nd	<0.51	nd	nd	nd	nd	nd	nd	nd	<2.53	nd	nd	nd	<0.53	nd	nd	nd
Average last 3	bd	31.8	32.3	bd	bd	0.01	bd	bd	68.6	nd	nd	bd	nd	nd	nd	nd	nd	nd	nd	bd	nd	nd	nd	bd	nd	nd	nd
STDS		0.00	0.92			nd			15.9																		
RSD		0%	3%			nd			23%																		
CP21																											
Mela	<4.09	<1.81	<40.1	36.0	28.5	13.9	<28.7	<613	<26.4	568	1124	23.1	113	132	*81.7	28.3	81.7	107	*86.8	*48.9	4.05	7.18	3.15	200	3.14	4220	*124
CP22																											
Ne	<0.74	31.6	29.3	<4.03	<1.62	<0.02	n.d.	n.d.	66.1	n.d.	n.d.	0.43	1.39	n.d.	n.d.	n.d.	n.d.	n.d.	n.d.	n.d.	n.d.	n.d.	n.d.	1.31	n.d.	3.11	n.d.
Ne	<5.49	31.6	<36.7	<27.4	<9.59	<0.15	nd	nd	31.4	nd	nd	80.9	103	nd	nd	nd	nd	nd	nd	nd	nd	nd	nd	45.6	nd	167	nd
Ne	<2.56	31.6	25.9	<15.3	<6.24	<0.06	nd	nd	98.5	nd	nd	16.3	35.9	nd	nd	nd	nd	nd	nd	nd	nd	nd	nd	10.6	nd	14.6	nd
Ne	<1.71	31.6	30.1	<10.6	<3.54	0.07	nd	nd	64.0	nd	nd	20.0	23.6	nd	nd	nd	nd	nd	n.d.	n.d.	nd	n.d.	nd	4.71	n.d.	23.4	nd
Melilite	*2.74*	*7.60*	*42.2*	*29.2*	*27.1*	*1.17*	*8268*	*13197*	*164*	*57.5*	*185*	*472*	*599*	*134*	*17.4*	*4.70*	*15.3*	*12.2*	*8.13*	*3.73*	*0.44*	*16.8*	*22.7*	*306*	*4.57*	*1535*	*19.8*
Melilite	*2.50*	*11.2*	*47.7*	*29.2*	*27.4*	*0.73*	*3432*	*15743*	*87.7*	*30.6*	*75.6*	*558*	*681*	*222*	*20.0*	*6.44*	*11.1*	*10.5*	*<5.56*	*10.2*	*<1.08*	*12.4*	*10.8*	*168*	*2.77*	*858*	*23.5*
Melilite	4.04	*49.0	*73.7	29.2	29.5	0.09	1014	16249	*186	3.34	*90.5	300	354	80.2	<4.29	2.55	4.20	<2.66	<3.35	<2.80	<0.86	0.63	2.83	10.9	<0.30	10.5	<2.38
Melilite	3.56	7.81	36.3	29.2	28.1	0.06	440	17122	<4.04	2.76	<8.71	279	395	98.8	11.00	3.06	<2.45	<1.19	<2.74	<3.79	<0.44	1.36	2.04	7.32	<0.49	20.2	<2.60
Melilite	3.99	8.28	33.9	29.2	32.7	0.07	606	19659	<10.29	5.15	<24.5	276	393	62.8	3.46	1.47	4.47	<4.83	<3.58	<2.78	<0.97	<1.00	3.02	4.40	<0.86	<4.26	<4.89
Melilite	6.46	11.5	41.4	29.2	31.1	<0.05	359	18266	<11.96	<2.58	<27.1	217	265	114	<5.27	<1.49	1.43	<1.64	<4.33	b.d	<0.91	<0.87	<1.04	<2.62	<0.42	<5.38	<5.21
Melilite	3.31	6.51	37.6	29.2	25.6	<0.04	343	12846	<5.73	7.91	<17.5	146	276	44.1	2.74	1.66	2.62	<1.05	<1.61	<2.56	<0.38	<0.33	<0.93	3.56	<0.66	*81.6	<2.15
Melilite	5.03	8.13	43.3	29.2	32.6	0.21	928	15131	11.9	6.30	25.0	218	348	44.2	3.23	2.15	1.43	<1.81	<1.42	<1.87	<0.52	0.66	3.72	*17.6	0.69	*209	<2.94
Average last 6	4.40	8.44	38.5	29.2	30.0	0.11	615	16546	11.9	5.49	25.0	239	339	74.0	5.11	2.23	2.63	bd	bd	b.d.	bd.	0.95	2.90	8.54	0.69	15.3	bd
STDS	1.17	1.83	3.61	0.00	2.72	0.07	293	2396	n.d	2.55	nd	57.2	56.2	28.9	3.94	0.62	1.46					0.37	0.69	3.29	n.d	6.92	
RSD	27%	22%	10%	0%	9%	65%	48%	14%	n.d	48%	n.d	24%	17%	39%	77%	28%	52%					39%	24%	50%	n.d	45%	
CP23																											
Melilite	3.13	10.7	35.9	<26.3	29.4	<0.11	*122	8673	<21.2	8.07	<38.0	78.1	154	21.2	<8.55	<3.67	<6.36	<4.27	<11.61	<9.58	<1.34	<2.07	<2.71	<5.77	<0.79	9.61	<10.8
Melilite	3.22	6.01	35.0	29.2	24.8	0.03	*177	10533	<5.50	7.75	*37.8	110	137	46.8	3.84	1.34	<1.75	<1.43	<1.29	<2.37	<0.30	<0.45	<0.53	5.27	<0.37	18.9	<1.73
Melilite	4.06	6.22	36.5	29.2	29.9	0.12	251	12250	6.15	6.06	17.76	98.2	136	36.9	8.60	0.86	1.49	<1.58	<1.72	<1.04	<0.19	0.59	0.44	10.12	<0.37	*49.4	<1.81
Melilite	4.82	8.63	42.0	29.2	34.9	<0.04	293	12478	<10.9	3.05	<21.9	106	128	41.0	<2.64	<1.27	bd	<2.25	<3.44	<3.96	<0.70	<1.39	1.57	<2.20	<0.58	23.6	<3.30
Melilite	5.10	7.77	41.6	29.2	31.8	<0.04	260	12694	<8.30	5.81	<18.8	152	213	50.9	<3.15	1.56	<2.48	*3.26	<3.25	*3.64	<0.69	<0.43	<1.06	<2.02	<0.50	<3.17	<2.00
Melilite	3.59	14.8	27.1	29.2	24.4	<0.09	283	8530	<13.6	4.70	<29.4	67.0	87.0	<8.78	<5.95	<1.68	<2.26	1.37	<2.32	bd	<1.50	<1.30	0.62	<10.1	<0.55	*81.0	<8.09
Melilite	4.10	7.55	38.5	29.2	26.6	<0.06	216	15329	<11.5	6.18	<22.9	122	192	39.6	<5.29	1.20	<2.64	<2.03	<8.44	<2.09	<0.73	<0.99	<0.66	<2.01	<0.64	4.85	<3.63
Average	4.01	9.08	36.7	29.2	28.6	0.08	261	11498	6.15	5.94	17.8	105	150	39.4	6.22	1.24	1.49	1.37	bd	bd	bd	0.59	0.88	7.70	bd	14.3	b.d
STDS	0.76	2.60	5.01	0.00	3.60	0.06	30.2	2427	nd	1.72	nd	28.0	42.1	10.3	3.37	0.29	nd	nd				nd	0.61	3.43		8.61	
RSD	19%	31%	14%	0%	13%	85%	12%	21%	nd	29%	nd	27%	28%	26%	54%	24%	nd	nd				nd	69%	45%		60%	
CP27																											
Ne	<1.05	32.2	40.1	<7.15	<1.70	<0.04	n.d.	n.d.	89.6	n.d.	n.d.	<0.61	<0.28	n.d.	n.d.	n.d.	n.d.	n.d.	n.d.	<1.44	n.d.	n.d.	n.d.	<1.34	n.d.	1.71	n.d.
Ne	*<1.72*	*32.2*	*41.3*	*<13.8*	*<2.85*	*<0.05*	*nd*	*nd*	*100*	*nd*	*nd*	*1.52*	*1.88*	*nd*	*nd*	*nd*	*nd*	*nd*	*nd*	*<2.90*	*nd*	*nd*	*nd*	*5.55*	*nd*	*14.3*	*nd*
CP31																											
Ne	<2.77	32.1	44.0	<22.6	<5.47	<0.15	nd	nd	72.4	nd	nd	<2.19	*2.15	nd	nd	nd	nd	nd	nd	<8.06	nd	nd	nd	*8.84	nd	<14.5	nd
Ne	<1.67	32.1	40.7	<14.7	<3.58	<0.10	nd	nd	72.9	nd	nd	<1.56	<0.45	nd	nd	nd	nd	nd	nd	<5.11	nd	nd	nd	<2.98	nd	<4.85	nd
Ne	<1.55	32.1	39.4	<12.8	<2.79	<0.05	nd	nd	44.2	nd	nd	<0.86	<0.49	nd	nd	nd	nd	nd	nd	<3.08	nd	nd	nd	<3.25	nd	<4.86	nd
Ne	<1.14	32.1	24.6	<8.21	<1.99	<0.05	nd	nd	55.4	nd	nd	<0.41	<0.36	nd	nd	nd	nd	nd	nd	<2.82	nd	nd	nd	<1.15	nd	<4.88	nd
Average	bd	32.1	37.2	bd	bd	bd	nd	nd	61.2	nd	nd	bd	nd	nd	nd	nd	nd	nd	nd	bd	nd	nd	nd	nd	nd	bd.	nd
STDS		0.00	8.61						14.0																		
RSD		0%	23%						23%																		
Cpx	*6.52*	*0.91*	*37.4*	*19.8*	*16.6*	*0.41*	*nd*	*nd*	*nd*	*<2.37*	*nd*	*2.01*	*5.80*	*nd*	*nd*	*nd*	*nd*	*nd*	*nd*	*<2.63*	*nd.*	*nd*	*nd*	*nd*	*nd*	*169*	*nd*
Cpx	4.02	1.99	57.5	19.8	20.4	0.73	nd	nd	nd	4.31	nd	5.64	11.8	nd	nd	nd	nd	nd	nd	<3.17	nd	nd	nd	nd	nd	*2879	nd
Cpx	5.48	3.25	53.5	19.8	16.9	0.55	nd	nd	nd	9.47	nd	9.28	18.6	nd	nd	nd	nd	nd	nd	<6.04	nd	nd	nd	nd	nd	517	nd
Cpx	5.12	2.48	51.9	<20.1	22.0	0.95	nd	nd	nd	*18.8	nd	*39.2	*31.0	nd	nd	nd	nd	nd	nd	<10.7	nd	nd	nd	nd	nd	744	nd

Comments	MgO	Al2O3	SiO2	CaO	CaO	TiO2	Ba	Sr	Rb	Y	V	La	Ce	Nd	Sm	Eu	Gd	Dy	Er	Yb	Lu	U	Th	Nb	Ta	Zr	Hf
Cpx	5 86	1 99	45 5	19 8	20 7	0 49	n d	n d	n d	6 57	n d	*24 1	*31 4	n d	n d	n d	n d	n d	n d	<3 66	n d	n d	n d	n d	n d	492	n d
Cpx	6 41	2 71	49 1	19 8	18 2	0 55	n d	n d	n d	6 73	n d	7 05	20 3	n d	n d	n d	n d	n d	n d	<3 78	n d	n d	n d	n d	n d	605	n d
Cpx	5 39	1 82	48 6	19 8	18 3	0 58	n d	n d	n d	9 90	n d	*35 8	*49 0	n d	n d	n d	n d	n d	n d	5 43	n d	n d	n d	n d	n d	608	n d
Average last 6	5 38	2 37	50 7	19 8	19 1	0 64	n d	n d	n d	7 40	n d	7 32	16 9	n d	n d	n d	n d	n d	n d	5 43	n d	n d	n d	n d	n d	593	n d.
STDS	0 80	0 55	4 50	0 00	2 29	0 17				2 30		1 64	4 47							n d						98 9	
RSD	15%	23%	9%	0%	12%	27%				31%		25%	26%							n d						17%	
Wo	<1 29	3 34	49 2	46 5	46 1	0 26	n d	n d	n d	89 4	n d	124	161	n d	n d	n d	n d	n d	n d	7 05	n d	n d	n d	n d	n d	n.d	n d
Apatite	*b d*	*b d*	*b d*	*55 0*	*b d*	*b d*	*2589*	*19814*	*b d*	*166*	*b d*	*2171*	*3607*	*1161*	*134*	*43 7*	*b d*	*48 1*	*b d*	*b d*	*b d*	*b d*	*44 7*	*26 9*	*b d*	*b d*	*b d*
Apatite	b.d.	0.38	1.86	55.0	b.d.	0.03	4063	13712	16.6	125	93.6	1754	4595	1024	95.8	28.3	56.2	21.8	8.70	3.27	0.29	5.63	44.1	8.33	b.d.	19.1	0.84
CP40																											
Mela	0 68	3 69	39 4	30 9	28 3	8 50	*332	517	<31 6	409	1115	35 9	123	126	*49 8	28 5	61 3	65 7	37 5	40 7	4 82	5 88	6 49	186	8 98	3006	68 0
CP54																											
Mela	<1 59	<1 17	<37 4	<33 3	27 1	8 06	2 26	<562	<41 4	274	1332	12 1	74 1	114	*35 2	19 9	49 9	53 4	26 4	*29 0	2 63	4 01	2 65	142	3 67	2869	67 6
CP64																											
Titanite	b d	0 00	0 0	0 0	0 0	0 0	0 0	0	b d	0	0	0	0	0	0 0	0 0	0 0	0 0	0 0	0 00	0 00	0 00	0 00	0	0	0	0
CP65																											
Mela	0 70	0 81	30 0	32 3	32 9	11 9	44 8	<227	<25 3	397	862	50 3	249	335	110	37 0	99 9	92 5	35 0	29 1	3 89	7 42	12 4	488	20 9	3766	75 0
Comb	*0 94*	*1 40*	*67 4*	*27 8*	*32 1*	*2 10*	*1448*	*5255*	*143*	*77 4*	*165*	*314*	*638*	*252*	*41 2*	*11 8*	*21 4*	*14 6*	*7 45*	*6 56*	*1 01*	*22 1*	*60 9*	*620*	*7 06*	*2087*	*29 2*
Comb	0 20	1 82	52 5	27 8	25 2	0 07	58 4	3232	7 04	227	6 97	173	568	255	48 0	15 2	36 9	31 6	16 2	19 6	2 77	24 7	51 3	13 2	0 44	2375	30 3
Comb	<0 38	<0 21	70 6	27 8	28 8	0 16	18 9	3634	<23 4	244	11 4	261	858	270	64 8	22 4	53 9	40 1	33 0	18 6	5 88	29 9	86 7	10 6	<0 84	2176	17 7
Average last 2	0 20	1 82	61 5	27 8	27 0	0 12	38 7	3433	7 04	235	9 17	217	723	263	56 4	18 8	45 4	35 9	25 6	19 1	4 33	27 3	59 0	11 9	0 44	2275	24 0
STDS	n d	n d	12 8	0 00	2 60	0 06	27 9	284	n d	12 2	3 11	62 8	191	11 1	11 9	5 09	12 0	6 02	10 5	0 70	2 20	3 73	10 90	1 83	n.d.	140	8 90
RSD	n d	n d	21%	0%	10%	55%	72%	8%	n d	5%	34%	29%	26%	4%	21%	27%	27%	17%	41%	4%	51%	14%	18%	15%	n.d.	6%	37%
CP66																											
Mela	<0 63	1 17	30 7	32 2	28 6	8 96	24 8	<249	<32 7	421	831	20 5	94 0	140	46 8	23 3	64 5	101.79	*59 31	24 9	3 26	5.71	5.54	947	13.0	2934	68.1
CP67																											
Mela	0 53	1 68	30 9	32 2	34 8	10 8	15 8	<101	<14 3	379	1294	22 1	108	138	56 2	24 4	71 7	74 8	38 6	33 0	4 14	4 64	3 33	389	12 0	3902	77.0
CP68																											
Mela	0 54	1 90	33 1	32 0	30 6	11.2	*468	561	15 3	462	944	39 7	134	167	71 1	30 0	82 0	94 2	54 6	40 5	5 20	5 68	5.80	352	19 0	4066	91 8
CP69																											
Mela	<1 52	1 17	<40 5	<43 6	39 6	13 0	*557	2051	<101	494	1182	*82 5	203	276	96 4	31 7	92 1	105	50 1	42 9	3 12	9 19	8 77	795	21 9	3201	84 9

Note: italics indicate whole analyses rejected, asterixes (*) indicate individual elemental analysis rejected, and bold font indicate that only one analysis was taken into account

Table A7.4: Exchange coefficients between silicate and carbonate liquids from the experiments (labelled CPxx), and between wollastonite nephelinite HOL14 (groundmass) and silicate-bearing natrocarbonatite OL5 (whole rock).

Element pair	CP92	CP20	CP93	CP102	CP13	CP103	CP97	CP18	CP91	CP22	CP120	CP121	CP43	HOL14/OL5
U/Th	0.38	0.30	0.35	0.37	0.42	0.33	0.34	0.18	0.39	0.21	0.44	0.52	0.30	0.73
Nb/Ta	1.12	0.39	0.35	0.17	0.41	0.24	0.19	0.30	1.48	0.37	0.61	0.53	0.45	0.54
Zr/Hf	1.95	0.77	0.75	2.09	0.83	0.60	0.83	1.75	n.d.	1.09	0.89	0.85	2.03	1.04
Lu/La	3.94	2.70	2.36	6.98	2.61	5.26	5.88	1.86	2.74	2.53	1.61	2.42	4.16	10.3

n.d.: not determined.

Table A7.5. Trace (and major) element LAM-ICP-MS analyses of different phases in lava HOL14 - individual and average analyses, standard deviation (STDS) and relative standard deviation (RSD).

Sample	MgO wt. %	Al2O3 wt. %	SiO2 wt. %	CaO wt. %	CaO wt. %	TiO2 wt. %	Ba ppm	Sr ppm	Rb ppm	Y ppm	V ppm	La ppm	Ce ppm	Nd ppm	Sm ppm	Eu ppm	Gd ppm	Dy ppm	Er ppm	Yb ppm	Lu ppm	U ppm	Th ppm	Nb ppm	Ta ppm	Zr ppm	Hf ppm
Nepheline	<0.05	30.8	43.1	<0.32	<0.54	0.01	22.8	109	97.9	<0.07	<2.08	0.70	0.55	<0.55	<0.31	<0.09	b.d.	<0.40	<0.38	<0.63	<0.11	<0.15	<0.10	<0.16	b.d.	0.78	<0.70
Nepheline	<0.02	30.8	40.9	0.16	0.21	0.01	23.0	170	96.0	0.72	14.4	0.61	*0.91	0.51	<0.12	<0.05	<0.11	0.11	<0.12	0.13	<0.06	<0.03	<0.05	*1.13	<0.02	*3.73	<0.11
Nepheline	<0.05	30.8	43.2	<0.43	<0.80	0.01	25.4	147	113	<0.21	<2.01	0.45	0.14	b.d.	<0.38	0.05	b.d.	<0.24	<0.45	b.d.	<0.07	<0.18	<0.17	<0.14	<0.06	0.88	<0.35
Nepheline	<0.04	30.8	39.7	<0.20	<0.53	0.01	19.0	148	124	<0.18	<1.39	0.14	<0.12	<0.43	<0.25	<0.10	<0.22	<0.26	b.d.	<0.42	<0.04	<0.09	<0.10	0.57	<0.05	<0.28	<0.31
Nepheline	<0.11	30.8	45.2	<0.87	<1.35	0.01	17.3	<161	121	<0.29	<4.24	<0.18	0.18	<1.30	b.d.	b.d.	<1.02	<1.03	<0.51	<1.04	b.d.	b.d.	b.d.	<0.44	<0.11	0.77	<0.94
Average	b.d.	30.8	42.4	0.16	0.21	0.01	21.5	144	110	0.72	14.4	0.48	0.29	0.51	b.d.	0.05	b.d.	0.11	b.d.	0.13	b.d.	b.d.	b.d.	0.57	b.d.	0.74	b.d.
STDS	n.d.	0.00	2.13	n.d.	n.d.	0.00	3.28	25.3	12.9	n.d.	n.d.	0.25	0.23	n.d.	n.d.	n.d.	n.d.	n.d.	n.d.	n.d.	n.d.	n.d.	n.d.	n.d.	n.d.	0.08	n.d.
RSD	n.d.	0%	5%	n.d.	n.d.	0%	15%	18%	12%	n.d.	n.d.	52%	78%	n.d.	n.d.	n.d.	n.d.	n.d.	n.d.	n.d.	n.d.	n.d.	n.d.	n.d.	n.d.	7%	n.d.
Clinopyroxene	10.5	1.06	48.6	20.0	20.1	0.47	4.97	458	<0.48	1.78	*137	4.58	12.1	4.57	1.26	0.38	1.00	*0.43	*0.16	0.81	0.12	<0.09	<0.08	*0.76	<0.04	*180	*3.66
Clinopyroxene	8.95	0.62	43.4	20.0	20.6	0.44	4.44	686	<0.35	*6.57	221	4.03	10.7	5.55	1.36	0.48	1.33	1.17	0.90	1.36	0.37	0.10	0.08	3.04	0.17	439	11.6
Clinopyroxene	9.53	0.94	48.1	20.0	20.1	0.49	*2.55	530	<0.26	*4.66	225	3.63	10.3	5.23	1.18	0.33	0.89	0.69	0.57	1.26	0.24	<0.04	0.03	1.39	0.04	364	9.75
Clinopyroxene	4.34	0.76	75.8	20.0	20.1	1.02	*1.26	*1465	<0.53	1.23	*1402	3.60	*6.65	*3.29	*0.58	*0.12	<0.27	<0.11	0.36	0.52	0.14	<0.06	<0.06	3.16	0.09	504	14.0
Average	8.32	0.85	53.5	20.0	20.2	0.61	4.71	558	b.d.	1.51	223	3.98	11.0	5.12	1.27	0.40	1.07	0.93	0.61	0.89	0.22	0.10	0.05	2.54	0.10	436	11.8
STDS	2.72	0.19	15.0	0.00	0.24	0.28	0.37	117	n.d.	0.39	2.83	0.46	0.95	0.50	0.09	0.08	0.23	0.34	0.27	0.39	0.11	n.d.	0.02	1.00	0.07	70.1	2.13
RSD	33%	23%	28%	0%	1%	46%	8%	21%	n.d.	26%	1%	12%	9%	10%	7%	19%	21%	36%	45%	40%	53%	n.d.	47%	39%	69%	16%	18%
Melanite garnet	0.72	1.67	36.5	37.4	38.3	12.0	*237	*330	*12.9	480	1714	33.0	125	158	66.8	27.9	86.0	104	55.8	40.7	5.07	4.91	4.13	251	10.8	3317	73.1
Melanite garnet	0.75	1.10	31.2	33.2	33.3	12.0	1.23	89.1	*0.21	497	1361	23.9	128	178	73.4	30.2	93.2	105	57.9	42.7	5.30	5.52	4.45	301	14.2	4229	94.4
Average	0.74	1.39	33.8	35.3	35.8	12.0	1.23	89.1	n.d.	489	1538	28.5	127	167	70.1	29.1	89.6	105	56.8	41.7	5.19	5.22	4.29	276	12.5	3773	83.8
STDS	0.02	0.40	3.80	2.96	3.56	0.00	n.d.	n.d.	n.d.	12.0	250	6.43	2.12	12.7	4.67	1.63	5.09	0.71	1.63	1.41	0.16	0.43	0.23	35.4	2.40	645	15.1
RSD	3%	29%	11%	8%	10%	0%	n.d.	n.d.	n.d.	2%	16%	23%	2%	8%	7%	6%	6%	1%	3%	3%	3%	8%	5%	13%	19%	17%	18%
Wollastonite	0.13	0.09	43.1	49.5	47.0	0.62	*189	1756	3.27	*62.9	*13.8	21.5	57.2	29.1	6.25	2.61	8.59	9.05	6.47	6.47	0.94	0.23	*0.58	*64.0	*2.28	*81.9	2.39
Wollastonite	0.89	0.07	45.4	47.6	47.0	0.03	72.6	1371	6.09	35.0	3.12	14.0	42.5	20.5	4.89	1.86	4.57	5.64	3.68	3.23	0.52	0.26	0.06	1.31	0.02	6.57	<0.08
Average	0.51	0.08	44.3	48.6	47.0	0.33	72.6	1564	4.68	35.0	3.12	17.7	49.8	24.8	5.57	2.24	6.58	7.35	5.08	4.85	0.73	0.25	0.06	1.31	0.02	6.57	2.39
STDS	0.54	0.01	1.61	1.35	0.00	0.42	n.d.	272	1.99	n.d.	n.d.	5.32	10.4	6.05	0.98	0.53	2.64	2.41	1.97	2.29	0.30	0.02	n.d.	n.d.	n.d.	n.d.	n.d.
RSD	105%	16%	4%	3%	0%	126%	n.d.	0.17	0.43	n.d.	n.d.	0.30	0.21	0.24	0.17	0.24	0.43	0.33	0.39	0.47	0.41	0.09	n.d.	n.d.	n.d.	n.d.	n.d.
Titanite	<0.50	<0.73	25.4	27.9	23.9	26.6	<1.32	677	<1.08	106	483	230	565	302	59.8	19.9	46.8	28.3	9.74	4.39	0.43	2.21	2.13	1924	85.7	2517	75.6
Titanite	<0.95	0.55	26.0	27.9	27.7	30.7	<1.86	1441	<1.55	123	547	385	819	429	77.6	25.5	49.3	36.5	10.5	4.53	0.58	5.53	4.10	4089	168	2822	58.9
Titanite	<0.98	1.53	24.7	27.9	28.2	28.4	151	1211	3.49	180	493	248	508	257	66.1	23.0	62.6	51.4	15.9	8.32	1.10	4.30	3.05	2061	88.8	8288	257
Titanite	<0.62	0.52	28.9	27.9	25.6	27.3	80.0	1157	<1.27	110	458	301	659	341	64.0	19.2	40.4	29.0	9.85	4.56	0.42	5.28	4.69	3132	146	2451	54.4
Titanite	<2.55	1.36	39.9	27.9	30.8	31.3	<5.85	905	<4.32	212	585	282	561	270	72.4	22.8	67.7	50.3	16.5	8.50	1.09	3.90	2.85	2199	72.0	5238	139
Titanite	<4.08	<1.48	23.5	27.9	28.2	29.8	*7.65	1129	*9.58	116	626	191	414	201	45.0	*20.5	39.1	28.5	*5.21	6.78	0.66	<1.80	*1.21	2172	64.7	5597	156
Titanite	<2.47	<0.82	25.6	27.9	27.1	28.3	*2.95*	*766*	<5.30	*51.4*	*496*	*146*	*349*	*169*	*25.9*	*8.06*	*16.4*	*10.7*	*5.11*	*2.66*	*b.d.*	*0.70*	*2.56*	*2381*	*67.1*	*2218*	*55.7*
Average	b.d.	0.99	28.1	27.9	27.4	29.0	116	1087	3.49	141	532	270	587	300	64.2	22.1	51.0	37.0	12.5	6.18	0.71	4.24	3.32	2596	104	4454	123
STDS	n.d.	0.53	6.03	0.00	2.38	1.89	50.2	264	n.d.	44.0	65.2	67.2	139	78.8	11.3	2.55	11.7	11.3	3.40	1.94	0.31	1.32	1.05	848	42.4	2359	77.9
RSD	n.d.	53%	21%	0%	9%	7%	43%	24%	n.d.	31%	12%	25%	24%	26%	18%	12%	23%	30%	27%	31%	43%	31%	32%	33%	41%	53%	63%
Groundmass	0.43	14.1	39.0	2.75	2.03	0.97	2568	2557	101	25.4	207	117	164	38.9	4.95	2.43	4.69	4.24	2.96	2.64	0.25	9.75	12.0	239	1.72	797	12.5
Groundmass	1.17	8.32	34.5	2.47	2.56	0.97	2565	2769	*148	31.8	*405	141	183	54.3	7.52	2.63	6.08	6.24	3.22	2.50	0.28	10.1	13.3	271	2.47	1024	15.5
Groundmass	0.44	12.2	39.1	3.63	3.39	0.97	1820	2253	81.5	22.8	129	87.3	121	30.8	4.30	1.73	3.85	3.81	2.33	2.17	0.26	7.00	8.68	177	1.57	660	9.80
Groundmass	0.37	11.2	38.6	3.08	3.20	0.97	2317	2405	89.8	31.4	131	111	151	42.2	7.57	2.57	5.70	4.86	2.78	2.54	0.36	8.38	10.7	219	1.93	780	10.8
Groundmass	0.39	13.5	46.0	3.00	1.67	0.85	2008	1933	94.7	21.2	119	93.1	130	32.2	5.67	1.70	4.29	3.71	*1.45	*1.45	*0.17	6.60	6.25	202	1.78	618	9.63
Groundmass	0.51	14.0	48.1	3.50	3.84	1.46	3136	3264	114	40.3	166	156	205	57.9	10.2	3.02	7.21	6.75	3.77	3.56	0.41	11.2	15.4	308	2.74	1098	16.6
Average	0.55	11.9	40.6	3.07	2.78	1.03	2402	2530	96.2	28.8	150	118	159	42.7	6.71	2.35	5.30	4.94	3.01	2.68	0.31	8.62	11.4	236	2.04	831	12.4
STDS	0.31	2.96	5.34	0.44	0.64	0.22	468	457	12.1	7.10	38.2	28.9	31.9	11.2	2.18	0.53	1.26	1.28	0.53	0.52	0.07	1.79	2.74	47.6	0.46	193	3.03
RSD	56%	25%	13%	14%	30%	21%	19%	18%	13%	25%	24%	23%	20%	26%	33%	22%	24%	26%	18%	19%	22%	20%	24%	20%	23%	23%	24%